Delphis F. Levia   *Editor*
Darryl Carlyle-Moses
Tadashi Tanaka   *Co-editors*

Forest Hydrology and Biogeochemistry

Synthesis of Past Research and Future Directions

Springer

Ecological Studies, Vol. 216

Analysis and Synthesis

Edited by

M.M. Caldwell, Washington, USA
G. Heldmaier, Marburg, Germany
R.B. Jackson, Durham, USA
O.L. Lange, Würzburg, Germany
H.A. Mooney, Stanford, USA
E.-D. Schulze, Jena, Germany
U. Sommer, Kiel, Germany

Ecological Studies

Further volumes can be found at springer.com

Delphis F. Levia
Editor

Darryl Carlyle-Moses • Tadashi Tanaka
Co-Editors

Forest Hydrology and Biogeochemistry

Synthesis of Past Research
and Future Directions

Springer

Editors
Dr. Delphis F. Levia
University of Delaware
Departments of Geography & Plant
and Soil Science
Newark, DE 19716-2541, USA
dlevia@udel.edu

Dr. Tadashi Tanaka
Department of International Affairs
University of Tsukuba
Ibaraki 305-8577, Japan
tadashi@geoenv.tsukuba.ac.jp

Dr. Darryl Carlyle-Moses
Thompson Rivers University
Department of Geography and Graduate
Program in Environmental Science
900 McGill Road
PO Box 3010
Kamloops, BC, V2C 5N3 Canada
dcarlyle@tru.ca

Foreword

Forest hydrology as a field has evolved greatly since the first paired watershed study was published by Bates (1921) in the *Journal of Forestry*. Bates described his work as the "first serious effort to obtain, under experimental conditions, a quantitative expression of forest influences on snow modeling, streamflow (and thus, by implication, evaporation) and erosion." Since then, many paired watershed studies have been published – with an explosion of such work in the late 1950s and through the 1960s during the First International Hydrological Decade. Despite the appearance of several textbooks in the past decades, the last major benchmarking effort was Sopper and Lull's (1967) edited conference proceedings from the International Symposium on Forest Hydrology, held at Penn State University, USA, in 1965. This was the first and last major synthesis and integration effort for the field in over four decades. Since Sopper and Lull, much has changed in forest hydrology: new instruments, some new theory, new disciplinary additions to forest linkages; most notably biogeochemistry.

Forest Hydrology and Biogeochemistry: *Synthesis of Past Research and Future Directions* is a long anticipated, important addition to the field of forest hydrology. It is, by far, the most comprehensive assemblage of the field to date and written by many of the top researchers in their field. The book reveals for the first time since Sopper and Lull, the current state of the art and where the field is headed – with its many new techniques developed since then (isotopes, fluorescence spectroscopy, remote sensing, numerical models, digital elevation models, etc.) and added issues (fire, insect outbreaks, biogeochemistry, etc.). Levia, Carlyle-Moses, and Tanaka have done a spectacular job of assembling a strong array of authors and chapters. As an associate professor of ecohydrology, Del Levia has a background in water transfers through the forest canopy and biogeochemical transformations in forest systems in American forested watersheds with extensive international experience as well. Darryl Carlyle-Moses is an associate professor of geography with experience in Canadian and Mexican forest systems, focused mostly on water transfers through the forest canopy. Tadashi Tanaka is professor of hydrology at University of Tsukuba in Japan with a long and distinguished career in forest hydrology, from

groundwater studies to tracer studies and water flux measurements in headwater catchments. The geographical teaming of editors is an important element to the work, where the addition of the Japanese perspective (to the more dominant European and North American and Australian perspectives) with many chapters penned by Japanese forest hydrologists adding greatly to the breadth of approaches and examples. Attention to editorial detail is clear; from careful assembly of all the key component areas to an awareness of the benchmark papers in the field and need to include them (even when they fall outside the non-English speaking literature).

Distillation of a large and varied disparate discipline like forest hydrology and biogeochemistry is challenging. The book's organization effectively parses out the many aspects of the field in six useful parts. The first part outlines the historical roots of forest hydrology and biogeochemistry, with special reference to the Hubbard Brook watershed – arguably "Mecca" for the field and the foundation we all now follow in watershed-based coupled hydrobiogeochemical studies. The authors of that chapter are emblematic of the authorship of much of the book, pairing one of the founding fathers of field with one of the most promising young professors in the field. Sampling and novel approaches follow this background setup, with definitive chapters covering the latest in terms of spatial and temporal monitoring. Forest hydrology and biogeochemistry by ecoregion is a part that follows. The ecoregion component is a clever move in the assembly of the material for the book, providing a view into real-world landscapes and how uniqueness of place drives coupled hydrobiogeochemical processes. The editors have gathered authors from Canada, USA, Australia, China, Japan, and over a dozen countries in Europe to produce this range of ecoregion breadth. The three last parts of the book are "hydrologic and biogeochemical fluxes from the canopy to the phreatic surface," "the effects of time, stressors and humans," and finally, "knowledge gaps and research opportunities." Many of the hottest topics in relation to fire, insects, climate change, landuse change are addressed in a thoughtful and stimulating way.

Forest Hydrology and Biogeochemistry: *Synthesis of Past Research and Future Directions* is a celebration of a field. Like Bates' work, it is a serious effort to synthesize quantitative expressions of forest influences on water quantity (and now also water quality). The research pioneers who contributed to Sopper and Lull's major synthesis would be mesmerized by what now is possible and what is defined in this volume in terms of new research directions and opportunities. Reading it will give graduate students and researchers alike, a sense of direction and optimism for this field for many years to come.

Richardson Chair in Watershed Science   Jeffrey J. McDonnell
and Distinguished Professor of Hydrology
College of Forestry, Oregon State University,
Corvallis, OR, USA

Preface

A tremendous amount of work has been conducted in forest hydrology and biogeochemistry since the 1980s, yet there has been no cogent, critical, and compelling synthesis of this work on the whole, although a number of seminal journal review articles have been published on specific aspects of forest hydrology and biogeochemistry, ranging from precipitation partitioning to catchment hydrology and elemental cycling to isotope biogeochemistry (e.g., Bosch and Hewlett 1982; Parker 1983; Buttle 1994; Levia and Frost 2003; Muzylo et al. 2009). The forest hydrology and biogeochemistry volumes published to date have served a different (albeit equally valid) purpose to the current volume, serving as either a reference tool for a particular study site or as a textbook. Over the past 30 years, the Ecological Studies Series has published a number of such volumes, including *Forest Hydrology and Ecology at Coweeta* (1988), *Biogeochemistry of a Subalpine Ecosystem* (1992), and *Functioning and Management of European Beech Ecosystems* (2009). Lee (1980) is one of the last comprehensive forest hydrology texts. Recent published works have focused on climate change and stressors. These books reflect the growing body of research in forest hydrology and biogeochemistry. However, none of these texts were specifically aimed at synthesizing and evaluating research in the field to date. As such, *Forest Hydrology and Biogeochemistry: Synthesis of Past Research and Future Directions* is especially timely, relevant, and arguably necessary as periodic review and self-reflection of a discipline are integral to its progression. Thus, the aim of this international rigorously peer-reviewed volume is to critically synthesize research in forest hydrology and biogeochemistry to date, to identify areas where knowledge is weak or nonexistent, and to chart future research directions. Such a task is critical to the advancement of our discipline and a valuable community building activity. This volume is intended to be a one-stop comprehensive reference tool for researchers looking for the "latest and greatest" in forest hydrology and biogeochemistry. The book also is meant to serve as a graduate level text.

Forest Hydrology and Biogeochemistry: *Synthesis of Past Research and Future Directions* is divided into four primary parts following an introductory chapter (constituting Part I) that traces the historical roots of forest hydrology and biogeochemistry. The introductory chapter employs the Hubbard Brook Experimental Forest as a model to elucidate the merits of watershed scale hydrological and biogeochemical research. The four primary parts of the book are: sampling and methodologies utilized in forest hydrology and biogeochemistry research, forest hydrology and biogeochemistry by ecoregion, hydrological and biogeochemical processes of forests, and the effects of time, stressors, and people on forest hydrology and biogeochemistry. It is important to note that each part examines forest hydrology and biogeochemistry from different perspectives and scales. While overlap among chapters has been kept to a minimum, some overlap is inevitable. One also could argue that some overlap is beneficial given the nature of the book and the fact that most researchers will likely read select chapters of relevance to their research rather than the book in its entirety. The part on sampling and novel approaches is intended to provide researchers and students with a broad cross-section of methodological approaches used by some forest hydrologists and biogeochemists and to foster their wider use by the larger community. As such, these chapters may be used as a primer for one wishing to learn how to utilize various methods to answer questions of importance to forest hydrologists and biogeochemists. The next part adopts a holistic focus on the forest hydrology and biogeochemistry by ecoregion. Specific forest types covered include lowland tropical, montane cloud, temperate, boreal, and urban. These chapters are intended to provide researchers with a concise synthesis of past research in a given forest type and provide future research directions, emphasizing a particular forest type as a whole (i.e., from an ecosystem perspective) rather than hydrological and biogeochemical processes. The following part emphasizes processes regardless of ecoregion and forest type. These chapters begin at the interface of the atmosphere–biosphere with atmospheric deposition and follow the transport of water and elements to the subsurface via routing along roots to surface water–groundwater interactions. Thus, these chapters focus on the hydrology and biogeochemistry of the critical zone. The next part of the book examines the effects of time, people, and stressors on forest hydrology and biogeochemistry, capturing some of the newest thinking on the effects of external stressors, such as ice storms and climate change, on the functional ecology of forests. The final chapter (constituting Part VI) summarizes some of the major findings of the book and is intended to galvanize future research on topics that merit further work by identifying possible research questions and methodologies to move the disciplines of forest hydrology and biogeochemistry forward.

The editors wish to thank all authors for their tremendous work ethic in association with this book. It is clear that chapter authors rose to the occasion and prepared well thought syntheses that will help chart future research directions. The editors also would like to express their gratitude to all of the authors who served as peer reviewers. We were duly impressed with the thorough and thoughtful nature of reviewer comments that undoubtedly improved the quality of the book. The editors also acknowledge the review efforts of those scientists whom were external

to the book itself who provided excellent suggestions for chapter improvement; listed alphabetically, we acknowledge W. Michael Aust, Doug Burns, Sheila Christopher-Gokkaya, Helja-Sisko Helimsaari, April James, Koichiro Kuraji, Daniel Leathers, Myron Mitchell, Aleksandra Muzylo, and Wolfgang Wanek. David Legates is recognized for editorial advice during the project. We also acknowledge Jeff McDonnell for writing the Foreword of the book and the efforts of the Series Editor, E.-D. Schulze. The editors also wish to recognize Dr. Andrea Schlitzberger of Springer's Ecological Studies Series and Project Manager Elumalai Balamurugan for their hard and efficient work on this book. The editors wish to give special thanks and recognition to Springer Geosciences Editor, Robert Doe, and his assistant, Nina Bennink, for their professionalism, timely responses, clear feedback, and generous support as this book evolved through various stages of succession (with a few disturbances along the way) to its climactic completion in the course of 22 months.

It is the sincere hope, belief, and expectation of the editors that this volume will serve as an invaluable resource to many in the forest hydrology and biogeochemistry communities for years to come. We are confident that this volume, composed of the thoughts of some of the very best and talented researchers worldwide, will be a highly cited and impactful book that will catalyze fruitful research that propels our knowledge of forest hydrology and biogeochemistry forward.

Newark, Delaware	Delphis F. Levia
Kamloops, British Columbia	Darryl E. Carlyle-Moses
Tsukuba, Japan	Tadashi Tanaka
March 2011	

References

Baron J (1992) Biogeochemistry of a subalpine ecosystem. Ecological Studies Series, No. 90, Springer, Heidelberg, Germany

Bosch JM, Hewlett JD (1982) A review of catchment experiments to determine the effect of vegetation changes on water yield and evapotranspiration. J Hydrol 55:3–23

Brumme R, Khanna PK (2009) Functioning and management of European beech ecosystems. Ecological studies series, No. 208, Springer, Heidelberg, Germany

Buttle JM (1994) Isotope hydrograph separations and rapid delivery of pre-event water from drainage basins. Prog Phys Geog 18:16–41

Lee R (1980) Forest hydrology. Columbia University Press, New York

Levia DF, Frost EE (2003) A review and evaluation of stemflow literature in the hydrologic and biogeochemical cycles of forested and agricultural ecosystems. J Hydrol 274:1–29

Muzylo A, Llorens P, Valente F et al (2009) A review of rainfall interception modelling. J Hydrol 370:191–206

Parker GG (1983) Throughfall and stemflow in the forest nutrient cycle. Adv Ecol Res 13:57–133

Swank WT, Crossley Jr DA (1988) Forest hydrology and ecology at Coweeta. Ecological studies series, No. 66, Springer, Heidelberg, Germany

Contents

Contributors

Daniel M. Alongi
Australian Institute of Marine Science
D.Alongi@aims.gov.au

Miguel Álvarez-Cobelas
Instituto de Recursos Naturales, IRN – CSIC
malvarez@ccma.csic.es

Sophie Bachmair
Institute of Hydrology, University of Freiburg
sophie.bachmair@hydrology.uni-freiburg.de

Dennis D. Baldocchi
Department of Environmental Science, Policy and Management
University of California, Berkeley
baldocchi@berkeley.edu

Roger C. Bales
Sierra Nevada Research Institute, University of California, Merced
rbales@ucmerced.edu

Maria Victoria R. Ballester
Environmental Analysis and Geoprocessing Laboratory
CENA–University of São Paulo
vicky@cena.usp.br

Sharon A. Billings
Department of Ecology and Evolutionary Biology
Kansas Biological Survey, University of Kansas
sharonb@ku.edu

Peter D. Blanken
Department of Geography, University of Colorado, Boulder
blanken@colorado.edu

Gordon B. Bonan
National Center for Atmospheric Research
bonan@ucar.edu

Elizabeth W. Boyer
School of Forest Resources, The Pennsylvania State University
ewb100@psu.edu

Richard Brinkman
Australian Institute of Marine Science
R.Brinkman@aims.gov.au

James M. Buttle
Department of Geography, Trent University
jbuttle@trentu.ca

Darryl E. Carlyle-Moses
Department of Geography and Graduate Program in
Environmental Science, Thompson Rivers University
dcarlyle@tru.ca

Martha H. Conklin
Sierra Nevada Research Institute, University of California, Merced
mconklin@ucmerced.edu

Rose M. Cory
Department of Environmental Sciences and Engineering
Gillings School of Global Public Health
University of North Carolina, Chapel Hill
rmcory@unc.edu

Irena F. Creed
Department of Biology, The University of Western Ontario
icreed@uwo.ca

Patrick Crill
Department of Geological Sciences, Stockholm University
Patrick.Crill@geo.su.se

Todd E. Dawson
Departments of Integrative Biology and Environmental Science,
Policy and Management and Center for Stable Isotope Biogeochemistry
University of California, Berkeley
tdawson@berkeley.edu

An De Schrijver
Laboratory of Forestry, Ghent University
an.deschrijver@ugent.be

Charles T. Driscoll
Department of Civil and Environmental Engineering
Syracuse University
ctdrisco@syr.edu

Ethan E. Frost
Department of Geography, Colgate University
efrost@colgate.edu

John H.C. Gash
VU University &
Centre for Ecology and Hydrology
jhg@ceh.ac.uk

Gerhard Gerold
Institute of Geography-Department of Landscape Ecology
University of Göttingen
ggerold@gwdg.de

A.M.J. Gerrits
Faculty of Civil Engineering and Geosciences
Delft University of Technology
a.m.j.gerrits@tudelft.nl

Thomas W. Giambelluca
Department of Geography, University of Hawai'i at Manoa
thomas@hawaii.edu

Steven Glaser
Department of Civil and Environmental Engineering
University of California, Berkeley
glaser@ce.berkeley.edu

Douglas Godbold
School of the Environment & Natural Resources
University of Wales
d.l.godbold@bangor.ac.uk

Peter C. Hartsough
Department of Land, Air and Water Resources
University of California, Davis
phartsough@ucdavis.edu

Mathias Herbst
Department of Geography and Geology
University of Copenhagen
mh@geo.ku.dk

Dirk Hölscher
Burckhardt Institute, Tropical Silviculture and Forest Ecology
University of Göttingen
dhoelsc@gwdg.de

Jan W. Hopmans
Department of Land, Air and Water Resources
University of California, Davis
jwhopmans@ucdavis.edu

Benjamin Z. Houlton
Department of Land, Air and Water Resources
University of California, Davis
bzhoulton@ucdavis.edu

Carolyn T. Hunsaker
Pacific Southwest Research Station, U.S. Forest Service
chunsaker@fs.fed.us

Shreeram Inamdar
Department of Bioresources Engineering
University of Delaware
inamdar@udel.edu

Mark S. Johnson
Institute for Resources, Environment and Sustainability
Department of Earth and Ocean Sciences, University of British Columbia
mark.johnson@ubc.ca

Georg Jost
Department of Geography, University of British Columbia
georg.jost@geog.ubc.ca

Richard F. Keim
School of Renewable Natural Resources
Louisiana State University
rkeim@lsu.edu

Branko Kerkez
Department of Civil and Environmental Engineering
University of California, Berkeley
bkerkez@berkeley.edu

Alex V. Krusche
Environmental Analysis and Geoprocessing Laboratory
CENA, University of São Paulo
alex@cena.usp.br

Tomo'omi Kumagai
Hydrospheric Atmospheric Research Center
Nagoya University
tomoomikumagai@gmail.com

Jérôme Latron
Institut de Diagnosi Ambiental i Estudis de l'Aigua
IDÆA – CSIC
jerome.latron@idaea.csic.es

Nei Kavaguichi Leite
Environmental Analysis and Geoprocessing Laboratory
CENA – University of São Paulo
nkleite@gmail.com

Delphis F. Levia
Departments of Geography and Plant & Soil Sciences
University of Delaware
dlevia@udel.edu

Xiao-Yan Li
State Key Laboratory of Earth Surface Processes and Resource Ecology
College of Resources Science and Technology, Beijing Normal University
xyli@bnu.edu.cn

Gene E. Likens
Cary Institute of Ecosystem Studies
likensg@caryinstitute.org

Anders Lindroth
Department of Earth and Ecosystem Science, Lund University
Anders.Lindroth@nateko.lu.se

Timothy E. Link
Department of Forest Resources, University of Idaho
tlink@uidaho.edu

Pilar Llorens
Institut de Diagnosi Ambiental i Estudis de l'Aigua, IDÆA – CSIC
pilar.llorens@idaea.csic.es

Jordi Martínez-Vilalta
Centre de Recerca Ecològica i Aplicacions Forestals, CREAF
Jordi.Martinez.Vilalta@uab.es

William H. McDowell
Department of Natural Resources and the Environment
University of New Hampshire
Bill.McDowell@unh.edu

Kevin J. McGuire
Virginia Water Resources Research Center
Department of Forest Resources & Environmental Conservation
Virginia Polytechnic Institute and State University
kevin09@vt.edu

Diane M. McKnight
Institute of Arctic and Alpine Research
Department of Civil, Environmental and Architectural Engineering
University of Colorado, Boulder
Diane.McKnight@colorado.edu

Matthew Meadows
Sierra Nevada Research Institute, University of California, Merced
mmeadows@ucmerced.edu

Beate Michalzik
Institute of Geography, Department of Soil Science
Friedrich-Schiller-University of Jena
beate.michalzik@uni-jena.de

Panagiotis Michopoulos
Forest Research Institute of Athens
mipa@fria.gr

Noah P. Molotch
Institute of Arctic and Alpine Research and Department of Geography
University of Colorado, Boulder
noah.molotch@colorado.edu

Gerardo Moreno
Deptartment de Biología Vegetal, Ecología y Ciencias de la
Tierra. I.T. Forestal, University of Extremadura
gmoreno@unex.es

Tom Nisbet
Centre for Forestry and Climate Change
tom.nisbet@forestry.gsi.gov.uk

Nobuhito Ohte
Department of Forest Science, Graduate School of Agricultural
and Life Sciences, The University of Tokyo
nobu@fr.a.u-tokyo.ac.jp

Shin-ichi Onodera
Graduate School of Integrated Sciences and Arts, Hiroshima University
sonodera@hiroshima-u.ac.jp

Nathan Phillips
Department of Geography and Environment, Boston University
nathan@bu.edu

Alexandra G. Ponette-González
Department of Geography, University of North Texas
alexandra.ponette@gmail.com

Thomas G. Pypker
School of Forest Resources and Environmental Sciences
Michigan Technological University
tgpypker@mtu.edu

Brian Reynolds
Centre for Ecology and Hydrology
br@ceh.ac.uk

Youngryel Ryu
Department of Environmental Science, Policy and Management
University of California, Berkeley
ryuyr77@gmail.com

Gabor Z. Sass
Department of Biology, The University of Western Ontario
gabor.sass@uwo.ca

H.H.G. Savenije
Faculty of Civil Engineering and Geosciences
Delft University of Technology
h.h.g.savenije@tudelft.nl

Kevin A. Simonin
Faculty of Agriculture, Food and Natural Resources
University of Sydney, Australia
kevin.simonin@sydney.edu.au

Jeroen Staelens
Laboratory of Forestry, Ghent University
jeroen.staelens@ugent.be

Tadashi Tanaka
Department of International Affairs, University of Tsukuba
tadashi@geoenv.tsukuba.ac.jp

Naoko Tokuchi
Field Science Education and Research Center
Kyoto University
tokuchi@kais.kyoto-u.ac.jp

Elena Vanguelova
Centre for Forestry and Climate Change
elena.vanguelova@forestry.gsi.gov.uk

John T. Van Stan II
Department of Geography, University of Delaware
jvanstan@udel.edu

Kathleen C. Weathers
Cary Institute of Ecosystem Studies
weathersk@caryinstitute.org

Markus Weiler
Institute of Hydrology, University of Freiburg
markus.weiler@hydrology.uni-freiburg.de

Part I
Introduction

Chapter 1
Historical Roots of Forest Hydrology and Biogeochemistry

Kevin J. McGuire and Gene E. Likens

1.1 Introduction

The scientific disciplines of forest hydrology and forest biogeochemistry have contributed greatly to our understanding of the natural world even though they are relatively young disciplines. In this chapter, the historical origins, developments, and major advancements of these disciplines will be presented. The Hubbard Brook Ecosystem Study (HBES) will serve as a case study to illustrate the development, integration, and new research directions of these disciplines. Finally, this chapter on the historical roots and evolution of forest hydrology and biogeochemistry sets the stage for the remaining chapters of this volume by providing a conceptual framework in which most hydrological and biogeochemical work is conducted. Excellent reviews on forest hydrology and biogeochemistry are given by Sopper and Lull (1967), Bormann and Likens (1979), Lee (1980), Waring and Schesinger (1985), Likens and Bormann (1995), Schlesinger (1997), Ice and Stednick (2004a), de la Cretaz and Barten (2007), NRC (2008), and DeWalle (2011).

1.2 The Early Foundations of the Influence of Forests on Water

1.2.1 Pre-Twentieth Century

Kittredge (1948), Zon (1912), and Colman (1953) provide the earliest historical perspectives of "forest influences," which Kittredge describes as "including all effects resulting from the presence of forest or brush upon climate, soil water, runoff, stream flow, floods, erosion, and soil productivity." However, the earliest accounts of interactions between forests and water were probably those of Vitruvius (ca. 27–17 BCE) when he recognized that forests played an important role in evaporation. He postulated that in mountainous regions, the loss of water due to evaporation was limited because forests reduced the sun's rays from reaching the surface (Biswas 1970). About 100 years later, Pliny the Elder in *Natural History* (77–79 CE) observed,

"it frequently happens that in spots where forests have been felled, springs of water make their appearance, the supply of which was previously expended in the nutriment of the trees. . .Very often too, after removing the wood which has covered an elevated spot and so served to attract and consume the rains, devastating torrents are formed by the concentration of the waters" (Bostock and Riley 1855).

As Andréassian (2004) notes, Pliny's observations highlight the major concerns of forest cover on water and climate (namely streams and precipitation). These and other observations of forest influences led Medieval and Renaissance governments to establish protection forests (Kittredge 1948). In France, King Philippe Auguste issued a decree in 1219 "of the Waters and Forests" that recognized the close relation between water and forests in forest management (Andréassian 2004). During the mid-nineteenth century in France and Switzerland, debates on the effects of forest clearing emerged partly from recent torrent and avalanche activity that had occurred in the Alps, which formed the beginning of the scientific study on the influence of forests on water (Kittredge 1948). Andréassian (2004) describes several French watershed studies that occurred during this period (Belgrand 1854; Jeandel et al. 1862; Matthieu 1878), which are among the earliest studies to report on measurements of forest influences on hydrology and climate.

Despite the experiences in Europe, national recognition in the USA concerning the role of forests in protecting watersheds did not occur until the late nineteenth century, which essentially ushered in a wave of research on forests and water. During the mid to late nineteenth century, there was much speculation on the role that forests played in climate. The accepted wisdom was that deforestation had caused significant macroscale climate changes, especially higher temperatures and lower precipitation; however, much of that was dismissed when climatic data became available showing that only at the microsite did forests have effects on climate variation (Thompson 1980).

Interests in forest influences in the USA began when conservationists such as George P. Marsh became alarmed by the rate of forest clearing and suggested, after reviewing European findings and observations in the Alps, that forest removal had devastating effects on streamflow (Marsh 1864). The publishing of Marsh's *Man and Nature* followed by several reports on forest influences (e.g., Watson 1865; Hough 1878), eventually led to the 1891 Forest Preservation Act and 1897 Organic Act. These important pieces of legislation both described forest reserves, but the latter also provided a blueprint for their management and for the "purpose of securing favorable conditions of water flows." As Kittredge (1948) noted, the period from 1877 to 1912 might be called the "period of propaganda," when numerous writings and debates occurred concerning issues of forest influences on climate and floods. The importance of forests on flood control was generally accepted by foresters, but it had been challenged by prominent engineers such as Chittenden (1909) of the US Army Corps of Engineers and the Chief of the Weather Bureau, W.L. Moore (1910). With little scientific evidence to resolve the controversy, Raphael Zon, the Chief of Silvics with the USDA Forest Service, proposed the creation of the first experiment stations on the national forests and established the first forest and streamflow experiment at Wagon Wheel Gap, Colorado in 1909.

This study and others (e.g., in New Hampshire, see Federer 1969) helped ensure the passage of the Weeks Act in 1911 that provided "for the protection of watersheds of navigable streams" and the purchase of 9.3 million ha of land for national forests in eastern United States. The following year, Zon (1912) issued a seminal report to Congress on "Forests and water in the light of scientific investigation," which summarized evidence for the influence of forests on floods. This report would become the authoritative reference on the topic for the next several decades.

1.2.2   Early Twentieth Century: Watershed Studies

Disasters in the Alps during the early to mid-nineteenth century when forests were being cleared for pasture land prompted the Swiss to develop the first true watershed study in 1900, in the Emme Valley Emmenthal region (Engler 1919). The study was designed to evaluate the effects of forests on streamflow through comparison of the hydrological response to precipitation of two 0.6 km^2 watersheds, the Sperbelgraben (97% forested) and the Rappengraben (69% pasture and 31% forest) (Colman 1953). However, results from the Emmenthal study were largely qualitative and conclusions were suspect since the watersheds were not first compared under similar forest cover conditions (Bates and Henry 1928), i.e., the experimental design was faulty (Penman 1959; Whitehead and Robinson 1993).

In 1909, the USDA Forest Service began to plan a purposeful experiment on the Rio Grande National Forest, near Wagon Wheel Gap, Colorado with two contiguous watersheds that were similar in topography and forest cover. Observations were made on meteorological characteristics and streamflow under these similar conditions. Then, forest cover was removed from one of the watersheds and measurements continued as before, until the effects of the forest removal had been determined (Bates and Henry 1928). Wagon Wheel Gap was the first true paired-watershed study, which allowed for direct comparison of the timing and amount of streamflow and amount of erosion before and after removal of the forest. The experiment showed that forest removal increased annual water yield compared to the reference watershed, but the increase in water yield lessened over time as vegetation reestablished with essentially no effect after 7 years. This study would set the stage for the development of the paired-watershed approach (Wilm 1944; Hewlett and Pienaar 1973) all across the USA (Fig. 1.1). Although experimental watersheds have been criticized for their lack of representativeness, expense, and difficultly in interpreting results (Hewlett et al. 1969; Ward 1971; Whitehead and Robinson 1993), they have been instrumental to an understanding of forest hydrology.

In 1936, the Omnibus Flood Control Act gave the USDA Forest Service responsibility for flood-control surveys of forested watersheds to determine measures required for retarding runoff and preventing soil erosion and sedimentation (Hornbeck and Kochenderfer 2004). Increased flooding (e.g., Mississippi River in 1927) and concerns over the role of forest harvesting in the next two decades, spawned new USDA Forest Service watershed research at the San Dimas

CALIBRATION PERIOD

TREATMENT PERIOD
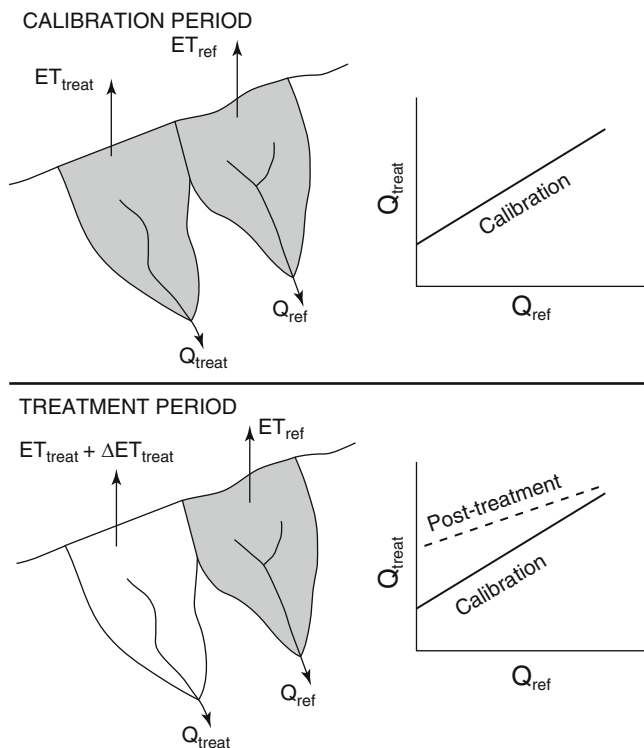
Fig. 1.1 An example of the paired-watershed approach to determine the effect of forest removal on evapotranspiration and water yield (adapted from Hewlett 1982). One watershed is manipulated (treatment, *no* shading) after an initial calibration period of where meteorological and hydrological variables observed to establish a relationship between the two watersheds. Using regression analysis or another statistical approach, differences between the treatment and reference can be established

Experimental Forest in southern California and the Coweeta Hydrologic Laboratory in western North Carolina. Although watershed studies were developed throughout the world, most were located in the USA and included some of the most noteworthy early contributions to forest hydrology (McCulloch and Robinson 1993).

1.2.3 Recognition of a New Discipline: Forest Hydrology

In his book on "forest influences," Kittredge (1948) may be one of the first to use the term "forest hydrology" to describe a new discipline focused on water-related phenomena that are influenced by forest cover. New curricula at universities were developing to provide professional foresters with hydrologic training to deal with watershed management problems (Wilm 1957). In the decades following, there was a proliferation of forest hydrology research and the establishment of numerous experimental watersheds. Many of these experimental watersheds

are now well known (e.g., Fernow, Hubbard Brook, H.J. Andrews); however, of the 150 experimental watersheds that existed by the 1960s in the USA (Anderson et al. 1976), many have since been discontinued. The discipline of forest hydrology was well established by 1965 when the *International Symposium on Forest Hydrology* was held at the Pennsylvania State University (Sopper and Lull 1967). This symposium captured the discipline in reports of findings from studies on the influences of forest cover on water yield, peakflows, and sediment from all over the world. Proceedings from this symposium are one of the most important collections of papers in forest hydrology (Courtney 1981), and at the time, sparked renewed interest in forest hydrology, launching more process-oriented research on how water cycles within forests. Water quality, however, was not given much consideration at the symposium, with the exception of matters related to sediment (McCulloch and Robinson 1993).

1.2.4 The Influence of Forests on Floods and Water Yield: A Summary of Paired-Watershed Results

Initially, experimental watersheds and the paired-watershed approach were primarily used to evaluate the effects of forest management practices on the timing and magnitude of streamflow and sediment load. Many of these studies were used to develop best management practices that are still in use today (e.g., Kochenderfer 1970). The subject of forest management and its influence on flooding has been a recurring scientific, social, and political theme since the mid-nineteenth century (e.g., Eisenbies et al. 2007). Experiments beginning with Wagon Wheel Gap showed that with 100% forest removal, impacts on flooding appear to be minor if soil disturbance is minimized. Generally, complete forest removal increases peakflow and stormflow volume, although results are highly variable and depend on the severity of soil disturbance, storm size, antecedent moisture condition, and precipitation type (Bates and Henry 1928; Hewlett and Hibbert 1961; Lull and Reinhart 1967; Harr and McCorison 1979; Troendle and King 1985). Given that many scientific and legal arguments regarding forests and flooding continue today (e.g., Mortimer and Visser 2004; Alila et al. 2009), we have much to learn from historical studies and could benefit from objectively re-evaluating historical datasets (DeWalle 2003; Ice and Stednick 2004b).

Following initial concerns of flooding and forest cover change, interest began to develop in manipulating forest cover to augment water yields from forested watersheds (Ponce 1983). Thus, the paired-watershed experiments were used to address a different set of questions such as: could streamflow be increased during dry periods? Or could snowpacks be managed to increase streamflow during the summer months? Changes in forest composition, structure, or density that reduce evapotranspiration rates generally increase water yield from watersheds. Paired-watershed studies showed that annual water yield can increase between 15 and 500 mm with forest removal, although these changes are often short lived

(a few years) and depend on climate, soil characteristics, and percentage and type of vegetation removal (Hibbert 1967; Patric and Reinhart 1971; Bosch and Hewlett 1982; Douglass 1983; Hornbeck et al. 1993; Stednick 1996; Brown et al. 2005). The greatest streamflow increases occurred in watersheds with the highest annual precipitation (Bosch and Hewlett 1982), particularly when precipitation was highest during the growing season. Augmenting water yields generally requires that forests cover a significant portion of the watershed, mean annual precipitation exceeds 400 mm, soil depth is greater than about 1 m, and when managed, forest cover is reduced by more than 20% (Chang 2006). At some sites where regrowth species composition differed from that which was present prior to harvesting (e.g., hardwoods to conifer, mature species replaced by early successional species, or forest conversion to grassland), streamflow did not return to pretreatment levels and adjusted to differences in interception (e.g., Swank and Miner 1968) or transpiration losses (e.g., Hornbeck et al. 1997) of the newly established vegetation.

In snow-dominated regions, forest cover alterations can also increase water yield and affect the timing of snowmelt runoff. In a series of experiments at the Fraser Experimental Forest in Colorado (Wilm and Dunford 1948; Hoover and Leaf 1967; Troendle and King 1985), researchers demonstrated that depending on the amount and pattern of forest cutting, water yield could be increased from the net effect of reduced canopy interception loss and losses due to increased evaporation/sublimation (DeWalle and Rango 2008). Changes in the timing and magnitude of peak streamflow will depend on the cutting patterns (slope aspect, size) and the synchronization of melt from cut and uncut areas in a watershed (Troendle 1983).

1.2.5   Process Research in Forest Hydrology

The *International Symposium on Forest Hydrology* in 1965 was the first forum where researchers from experimental watersheds from all over the world came together, exchanged viewpoints, and presented significant results on forest-soil-water relationships and forest watershed behavior. Another objective of this symposium was "to determine the status of research in forest hydrology in order to provide a bench mark which might serve as a point of departure for anticipated research during the [International] Hydrologic[al] Decade" (IAHS 1966). Discussion by prominent hydrologists (e.g., Penman) at the *International Symposium* urged for a more processed-based understanding of hydrological results from watershed experiments (Sopper and Lull 1967). The International Hydrological Decade (IHD) helped expand the scope of research to emphasize the study of hydrologic processes (e.g., streamflow generation processes and evaporation/interception research). In addition, many new "representative" and "experimental" basins were instrumented and monitored as part of the IHD or selected from well-established, existing research watersheds (Toebes and Ouryvaev 1970).

One major outcome of this period was the explosion of research on streamflow generation and hillslope processes as evidenced by the content of the seminal book on

hillslope hydrology by Kirkby (1978). During this period, John Hewlett and colleagues conceptualized the streamflow generation paradigm of forested watersheds that we still work with today – the variable source area concept (Hewlett 1961; Hewlett and Hibbert 1967; Hewlett and Nutter 1970). Building on the earlier work of Hoover and Hursh (1943) at the Coweeta Hydrologic Laboratory, Hewlett suggested that in forested watersheds where infiltration was seldom limiting, interflow delivering water to the base of slopes and the expansion and contraction of the near-stream aquifer created variable sources of streamflow each with different time delays in their contribution. While Hewlett often receives credit for this conceptual model, it was conceived more or less simultaneously in France (Cappus 1960) and Japan (Tsukamoto 1961) and further elaborated on by Dunne and Black (1970a, b) and by Freeze (1972), Hewlett and Troendle (1975), Beven and Kirkby (1979) in the development of simulation models. Other important work related to streamflow generation during the IHD described various pathways by which hillslopes can contribute runoff to streams such as translatory flow (Hewlett and Hibbert 1967), subsurface stormflow (Whipkey 1965), partial-area contributing flow (Ragan 1968), saturated-excess overland flow (Dunne and Black 1970b), and saturated throughflow (Weyman 1973).

At the time of the *International Symposium*, forest hydrology research on interception and evaporation was already well underway. Penman (1963, 1948) had developed his combined energy balance-aerodynamic equation for estimating evaporation, and during the symposium, he made some suggestions on improvements for forest canopies such as obtaining measurements of surface roughness, radiation, and stomatal conductance (Penman 1967). Helvey and Patric (1965) summarized mean throughfall and stemflow equations for the eastern hardwood forest. The equations were surprisingly uniform for throughfall over a wide range of canopy conditions, while stemflow was much more variable. The work of Penman (with Monteith's 1965 modifications) and Helvey and Patric eventually led to models of canopy interception loss (Rutter et al. 1971; Calder 1977; Gash 1979) that form the basis of models used today. By the mid-1970s, there was also general interest in various aspects of water relations in plants and the biophysics of plant physiology and of plant interactions with the environment as noted by seminal works such as Lange et al. (1976), Nobel (1974), and Lee (1978).

1.3 The Emergence of a New Discipline: Forest Biogeochemistry

1.3.1 Origins and Development of Biogeochemistry

Most accounts of the origins of biogeochemistry go back to Vernadsky (1926) where he recognized that all living things had origins from the Earth and that the "biosphere" influences geological processes and vice-versa (Gorham 1991).

Vernadsky also acknowledged the interrelations between the biosphere, lithosphere, hydrosphere, atmosphere, and humanity (i.e., nöosphere) (Vernadsky 1945). However, Hutchinson (e.g., 1943, 1944, 1950) is often credited with outlining the broad scope and principles of biogeochemistry and for introducing the writings of Vernadsky to the English speaking world. Biogeochemistry is a system science that focuses on the cycling (internal to the system) and fluxes (movement to or from a system, i.e., across system boundaries) of elements that mutually interact between the biology and chemistry of the Earth. Scientists of this discipline are quite diverse coming from oceanography, limnology, biology, geology, meteorology, and ecology.

1.3.2   From Forest Nutrition and Management to Ecosystem Science

Forest biogeochemistry, a subdiscipline of biogeochemistry or forest science, also has roots in plant nutrition, ecosystem science, and forest management. The definition of forest biogeochemistry, as the name implies, is the study of the pools and fluxes of nutrients into, within, and from forested ecosystems. Early work in this area sought to understand nutrient cycling as part of effective management strategies for silvicultural systems (Tripler et al. 2006; Van Miegroet and Johnson 2009). The landmark in forest nutrient cycling is Eber-mayer's (1876) *Complete Treatise of Litter and its Importance for the Chemical Stability of Forest Management* (Tamm 1995), where the detrimental effects of litter removal practices on forest productivity were made clear. This work influenced the next generation of nutrient cycling studies in forests such as Mitchell and Chander (1939), Rennie (1955), and Ovington (1959) where comparisons of tree nutrient demands with soil availability began to suggest nutrient limitations and raise concerns about sustainability associated with harvest. However, it was not until the publishing of Odum's second edition of *Fundamentals in Ecology* (1959) that used the ecosystem as the central focus and also emphasized nutrient cycling throughout the text, that forest biogeochemistry began to include more theoretical considerations in addition to the more practical needs of forest management.

The now well-known conceptual box and arrow diagrams of nutrient cycles that connect various aspects of the ecosystem also developed around this time (e.g., Lindeman 1942; Bormann and Likens 1967) (Fig. 1.2). Long-term monitoring of ecosystem processes began with the HBES (see below) and programs such as the International Biological Program (IBP) in the 1960s. The German contribution to the IBP at Solling (ca. 1968) and Hubbard Brook (ca. 1963) are among the longest running records of nutrient and water budgets globally (Bormann and Likens 1967; Likens et al. 1967; Ellenberg 1971; Ulrich et al. 1980; Manderscheid et al. 1995; Likens 2004).
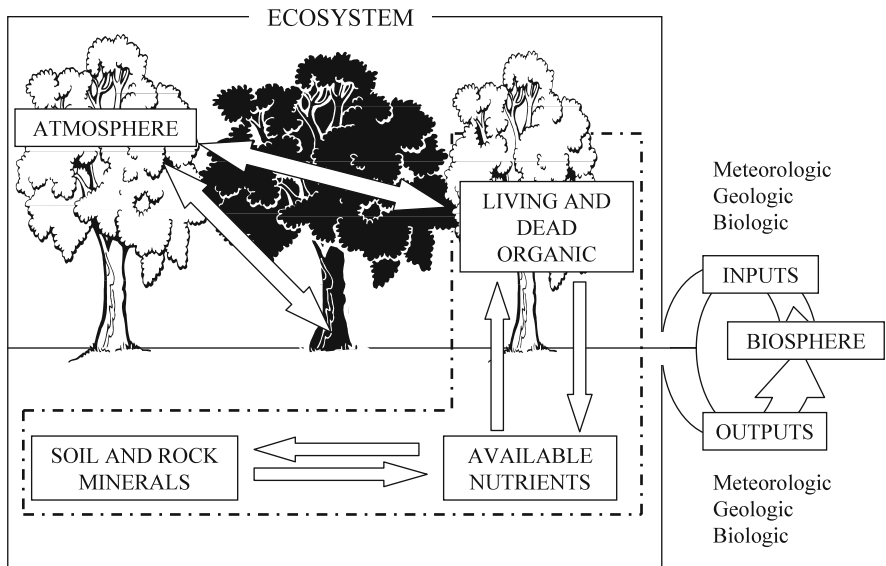
Fig. 1.2 Conceptual model of biogeochemical flux and cycling in a terrestrial ecosystem (redrawn from Bormann and Likens 1967). Inputs to and outputs from the ecosystem occur through meteorologic, geologic, and biotic pathways (Bormann and Likens 1967). Major sites of accumulation and exchange pathways within the ecosystem are shown. Nutrients cycle within the boundaries of the ecosystem among living and dead organic matter and primary and secondary minerals. Fluxes across the boundaries of the ecosystem link individual ecosystems with the rest of the biosphere (adapted from Bormann and Likens 1967 and redrawn from Likens 1992)

1.3.3   A New Paradigm in Biogeochemistry: The Small Watershed Approach

Biogeochemical studies of forest ecosystems must consider boundaries in space and time since ecosystem properties can vary from one plot to another or from month to month. One of the challenges in the study of ecosystems is that of scale and extrapolating information collected by small samples to something representative at a larger scale, for example, a forest stand. In the case of forest biogeochemistry, inputs and outputs of energy and matter are often difficult to estimate at typical field scales (e.g., forest plots or stands). F. Herbert Bormann, a plant ecologist, knew this well. As someone that had been inspired by Odum's book to think about nutrient cycling and after visiting the USDA Forest Service's Coweeta Hydrologic Laboratory and Hubbard Brook Experimental Forest (HBEF) with his classes in the 1950s, he began to think about watersheds as providing topographical and physiological boundaries of ecosystems (Bormann 1996). These Forest Service experimental forests as described above were established to address the effects of forests on components of the hydrologic cycle and erosion. However, in 1960, Bormann would propose in a letter to Robert S. Pierce, Project Leader of the USDA Forest

Service's HBEF, to use the small watersheds at HBEF as intact ecosystems to study element cycling and ecosystem function (Bormann 1996). At the same time, Likens had become enamored with the potential of the ecosystem approach largely through Odum's second edition text (Odum 1959). So, when he joined the faculty of Dartmouth College in 1961, where Bormann was located, they quite naturally began to talk about the potential of a watershed-ecosystem project at HBEF. They combined forces with Pierce and Noye M. Johnson, a young geologist at Dartmouth, to begin the study of the ecology and biogeochemistry of watershed-ecosystems within the HBEF – defining the small watershed approach of ecosystem science into what they called the HBES (Bormann and Likens 1967). Prior to the HBES, little consideration was given to water quality in watershed studies, except in terms of erosion and sedimentation (e.g., see Sopper and Lull 1967).

The hydrologically gauged watersheds at HBEF allowed for direct measurement of linkages among the atmospheric, biotic, hydrologic, and geologic components of the ecosystem. Thus, all chemical inputs and outputs could be quantified and used to calculate nutrient budgets (mass balances) and investigate ecosystem loss or accumulation as well as the vital connection with the rest of the biosphere (Bormann and Likens 1967; Likens et al. 1967, 1970; Lindenmayer and Likens 2010) (Fig. 1.2). When combined with watershed-scale experimental manipulations and long-term data, questions concerning ecosystem function could be addressed quantitatively at the watershed or landscape scale (e.g., Bormann and Likens 1979; Likens 1985, 2004). The small watershed-ecosystem approach provides a means to formulate testable hypotheses about system behavior at the ecosystem scale and perform manipulations to isolate and test-specific processes (Likens 1983, 1985; Carpenter et al. 1995; Hornung and Reynolds 1995). "Watershed manipulation is now a standard part of the biogeochemist's repertoire" (Lewis 2002). As more complex questions concerning forest management and forest ecosystem processes emerged, the small watershed approach became the archetype experimental design for forming a scientific basis to inform policy making (Hornbeck and Swank 1992).

1.4 Case Study: The Hubbard Brook Ecosystem Study as a Lens into the Development of Forest Hydrology and Biogeochemistry

Given the importance of the small watershed approach, it seems appropriate to use the HBES, where the approach was pioneered, as a case study illustrating the history and development of forest hydrology and biogeochemistry. As was discussed earlier, the HBEF was established to address concerns of forest management effects on hydrology (floods, low flows, water yield) and erosion/sedimentation, but this would change when Bormann and Likens would serendipitously become involved in research at the site.

The establishment of the HBEF arose from flood control surveys associated with the 1936 Omnibus Act. For forestlands in New England, the responsibility for conducting flood control surveys fell to the Northeastern Forest Experiment Station of the USDA Forest Service. The Forest Service was frustrated by the lack of guidance on these surveys and expressed the need for "experimental data on the relation of character of vegetative cover to run-off" (Hornbeck 2001). Eventually, with a Congressional appropriation in 1954 to establish watershed management studies in the mountains of New England, the Hubbard Brook Valley was selected as the best suited site for research in the White Mountains and the Experimental Forest was established in 1955 (Hornbeck 2001). Well-known names in forest hydrology were associated with the establishment and early construction of HBEF such as Howard W. Lull, George R. Trimble Jr., Richard S. Sartz, C. Anthony Federer, and Robert S. Pierce. Shortly after the establishment of the HBEF, basic hydrologic characteristics of the northern hardwood forest and the HBEF were assessed such as precipitation (Leonard and Reinhart 1963), snow accumulation/melt (Sartz and Trimble 1956; Federer 1965), soil frost and infiltration (Trimble et al. 1958), canopy interception (Leonard 1961), and streamflow (Hart 1966).

The HBES began in June 1963 when Bormann and Likens had a proposal funded by the National Science Foundation to study "Hydrologic-mineral cycle interaction in a small forested watershed." From the start, collaboration (e.g., with Johnson and Pierce) was seen as an important aspect of success in the HBES. Within two decades, numerous senior investigators, postdoctoral associates and graduate students, and some half-dozen governmental agencies and private foundations supported or participated in the research of the HBES. This level of support, a prolific publication record, the longest running dataset of watershed biogeochemistry (see www.hubbardbrook.org), and a strong international reputation positioned the HBES for National Science Foundation funding in the Long-Term Ecological Research program, which began in 1988 and continues today (Lindenmayer and Likens 2010).

1.4.1 Watershed-Ecosystem Nutrient Budgets

The earliest work to come from the HBES was the study of nutrient budgets for six of the small, south-facing watershed-ecosystems at HBEF (Likens et al. 1967; Bormann and Likens 1967). Although prior to the HBES, there was considerable literature on the chemistry of streams and nutrient cycling on components of ecosystems, this study was the first to estimate nutrient budgets for an entire ecosystem and demonstrate the advantages of the small watershed approach (Fig. 1.2). Likens et al. (1967) found an overall net loss of cations (Ca^{2+}, Mg^{2+}, Na^+, K^+) (i.e., stream water outputs > precipitation inputs) suggesting a contribution of these elements from biogeochemical reactions within the ecosystem, notably chemical weathering. This study suggested that the small-watershed approach

could be used to estimate difficult-to-measure processes, e.g., weathering and evapotranspiration, for an entire watershed through quantitative mass balance analysis (Bormann and Likens 1967). Likewise, the long-term data suggested net retention of some nutrients (NH_4^+, PO_4^{3-}, H^+) or patterns that change over time in others (K^+, NO_3^-, SO_4^{2-}, Cl^-) reflecting the complex interactions between atmospheric inputs, biotic activity, and climate variations (Likens and Bormann 1995; Likens 2004).

1.4.2   Effects of Vegetation on Nutrient Cycling

During the winter of 1965–1966, Bormann, Likens, and colleagues conducted a manipulation experiment on one of the six watersheds at the HBEF (Bormann et al. 1968). The experiment was designed to "test the homeostatic capacity of the ecosystem to adjust to cutting of the vegetation and herbicide treatment" (Likens et al. 1970). In other words, the objective was to maintain the watershed vegetation-free for several years (i.e., 3) to examine the influence of vegetation on water and nutrient flux and cycling. The experiment produced drastic changes in hydrology, nutrient flux, and sedimentation. The primary effect of the experiment was a sharp reduction in transpiration, which translated to increases in streamflow during the critical low flow months of June through September (Hornbeck et al. 1970) (Fig. 1.3). There was also some advance in the timing of snowmelt and observed increases in high flow values (quickflow volumes and instantaneous peaks) during the growing season; however, fall and winter high flows were not significantly affected by the forest clearing (Hornbeck et al. 1970; Hornbeck 1973). These changes in hydrology, mainly during low flows in the summer months, also affected the nutrient flux and cycling.

Nitrogen, which is normally conserved in undisturbed ecosystems (Likens et al. 1969), was rapidly released as nitrate in the cutover watershed (Fig. 1.3). Decomposition and especially nitrification were greatly accelerated with the production of nitrate and hydrogen ion. The increased production of nitrate and the absence of nutrient uptake by vegetation facilitated the loss of nitrate and other nutrients such as Ca^{2+}, Mg^{2+}, Na^+, and K^+ (Bormann et al. 1968; Likens et al. 1969, 1970) (Fig. 1.3). Only sulfate concentrations decreased in stream water of the deforested watershed (Fig. 1.3d). Likens et al. (1969) suggested that dilution from increased streamflow and decreased oxidation of sulfur compounds due to nitrate toxicity of sulfur-oxidizing bacteria might explain the pattern. But Nodvin et al. (1986) showed that increased acidity associated with nitrification could have increased the sulfate adsorption capacity of the soil, thereby reducing stream water concentrations.

At the time of this experiment, the changes in hydrology were expected; however, the changes in microbial activity and nutrient output were not as intuitive. Specifically, the losses of cations were 3–20 times greater than from the comparable undisturbed watershed. Although the experiment was not designed to simulate a
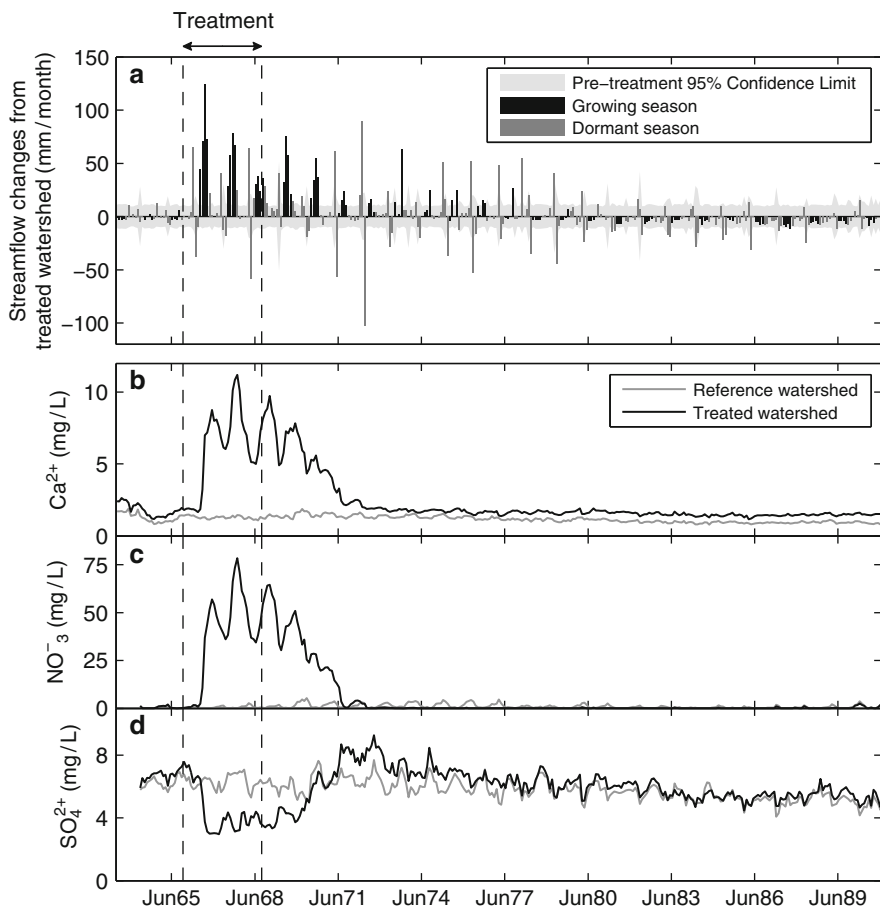
Fig. 1.3 Hydrological (**a**) and biogeochemical (**b–d**) response from the manipulation experiment of the Hubbard Brook Ecosystem Study (Likens et al. 1970; Hornbeck et al. 1970). Vegetation was removed from Watershed 2 (the "treated watershed") in December 1965 and January 1966 and treated with herbicide during the summers of 1966, 1967, and 1968. (**a**) Changes from expected streamflow, based on the monthly regression between reference Watershed 3 and treated Watershed 2 prior to treatment, are most significant during the growing season for approximately 5–6 years. (**b–d**) Major biogeochemical changes (e.g., calcium, nitrate, and sulfate) in the treated watershed, when compared to the reference Watershed 6, also increase for a period of approximately 5–8 years. Chemical concentrations are volume-weighted, mean monthly values

commercial clearcut, the results suggested that the ecosystem had limited capacity to retain nutrients when vegetation is removed, which could have important implications for forest management (Likens et al. 1978). In calcium deficient soils, for example, forest harvest and leaching losses could deplete soil nutrient capital (Federer et al. 1989).

The deforestation experiment at HBEF was followed by commercial harvesting experiments and comparisons to commercial clearcuts in the region (Likens et al. 1978; Hornbeck et al. 1986). These studies showed that the increased concentrations of nutrients in stream water ranged from a few to about 50% of the initial deforestation experiment (Likens et al. 1978). In addition, these studies showed that ecosystem recovery can occur rapidly (Hornbeck et al. 1986). Nutrient fluxes return to predisturbance levels in only a few years even though transpiration may be affected for longer periods (Martin et al. 2000). The time required for ecosystem recovery (hydrologically and biogeochemically) following forest harvest will depend on a number of factors such as type of harvest, severity of disturbance (e.g., size of the cut area, soil and stream channel disturbance), physiography of the site (aspect, slope, etc.), type of vegetation, climate and so forth (Likens et al. 1978; Likens 1985; Martin and Hornbeck 1989; Hornbeck et al. 1997). It was suggested that a site should not be cut more often than 75 years for the forest to be sustainable (Likens et al. 1978). Bormann and Likens (1979) proposed an overall biomass accumulation model for how forested ecosystems develop, and then reorganize and recover from disturbance.

1.4.3 Acid Rain: Transforming Disturbance into Opportunity

The first precipitation sample collected at Hubbard Brook in July of 1963 had a pH of 3.4. It was clear from the beginning of the HBES that the precipitation was acid, but it took several years to discover the cause and nature of its occurrence (Likens et al. 1972; Cogbill and Likens 1974; Likens and Bormann 1974; Likens 1989, 2004, 2010). Acid precipitation had been documented in Europe (e.g., Barret and Brodin 1955), but the first published account of acid precipitation in North America was made at the HBEF (Likens et al. 1972). The small watershed approach and the resulting long-term records on inputs and outputs of chemical constituents of the HBES provided the necessary data to address concerns of acid deposition effects on forested and associated aquatic ecosystems.

These long-term datasets from HBEF were able to show that changes in SO_2 emissions from source areas upwind of HBEF, as a result of federal legislation, were strongly correlated with sulfate concentrations in precipitation and stream water (Likens et al. 2001, 2002). The deposition of NO_3^- was also correlated with increasing NO_x emissions, which could become the dominant acid in precipitation in the future without further controls on emissions (Likens and Lambert 1998). Perhaps, the most surprising result of acid deposition research of HBES was that of soil base cation depletion (Likens et al. 1996). Calcium and other plant nutrients had been depleted in soils due to acid precipitation inputs and as a result of base cation losses, the forest ecosystem is much more sensitive to continuing acid deposition inputs than previously estimated (Likens et al. 1996; Likens 2004). With increased leaching of base cations in low base saturated soils, the mobilization and leaching of inorganic aluminum can occur, which is toxic to terrestrial and

aquatic biota (Cronan and Schofield 1990; Palmer and Driscoll 2002). As much as one half of the pool of exchangeable calcium in the soil at the HBEF has been depleted during the past 50 years by acid deposition (Likens et al. 1996, 1998). To examine the effects of depletion of soil calcium, a new whole-watershed experiment is now underway as part of the HBES in which calcium silicate was added in 1999 to replace the calcium leached from acid deposition (e.g., Peters et al. 2004; Groffman et al. 2006).

The long-term records at the HBEF have made invaluable contributions to the knowledge base for developing policy, federal legislation, and management related to air pollution (Driscoll et al. 2001; Likens 2004, 2010). The complexity of ecosystem response to changes in atmospheric deposition is one example of how, by combining the talents of diverse disciplines, novel scientific approaches (e.g., the small watershed approach, experiment manipulation, modeling, or natural disturbance), and long-term study, critical problems associated with environmental change may be better understood.

1.4.4 Models as Learning and Predictive Tools

The HBES has resulted in one of the most extensive and longest continuous databases on the hydrology, biology, geology, and chemistry of natural ecosystems. Although the strengths of the HBES stem from field-based experiments, ecosystem-scale manipulation, and long-term study, models have been a major part of the research providing additional insight into hydrologic, ecosystem, and biogeochemical trends and processes.

One of the earliest hydrologic simulation models for forested watersheds was the BROOK model that was developed specifically for eastern US watersheds and HBEF (Federer and Lash 1978). The BROOK model (the latest version is BROOK90, Federer 2002) is a parameter-rich, one-dimensional model of soil water movement among multiple soil layers that includes relationships for infiltration processes, energy-based evapotranspiration and snowmelt, and streamflow generation by different flowpaths (e.g., variable source areas) (Federer et al. 2003). It has been used to examine differences in transpiration among hardwood species using data from HBEF and Coweeta Hydrologic Laboratory (Federer and Lash 1978) and to simulate streamflow for cutting experiments when streamflow was not observed (e.g., Hornbeck et al. 1986). Federer and Lash (1978) demonstrated that shifts of 2-week increases or decreases in the timing of senescence or leaf out could cause differences in simulated annual streamflow by ±10–60 mm. When daily transpiration was varied by 20% in the BROOK model as to reflect realistic differences in stomatal conductance among species, differences in simulated streamflow ranged from 15 to 120 mm annually. Today, the results of Federer and Lash can be placed in the context of climate change where observed increases in growing season length have been documented (Huntington et al. 2009).

Ecosystem models have been part of the HBES since the early 1970s. The JABOWA model (Botkin et al. 1972a, b), a forest growth simulator, was the forerunner of many models used today and underpinned the conceptual model development of Bormann and Likens (1979). Another model that has been used extensively in the HBES and at other sites (e.g., Harvard Forest) is the PnET (Photosynthetic/EvapoTranspiration) model (Aber and Federer 1992). The PnET model is essentially a series of simple, lumped-parameter nested models (PnET-II, PnET-Day, PnET-CN) that simulate carbon, water, and nitrogen dynamics for temperate forest ecosystems (Aber et al. 1997). The modules include nutrient allocation, water balance, soil respiration, and canopy photosynthesis that produce a monthly time-step carbon and water model, which is driven by nitrogen availability and cycling within an ecosystem. The PnET-CN model was used to investigate long-term stream water nitrate trends from the reference watershed at HBEF (Aber et al. 2002). Long-term nitrate concentrations in stream water have declined since the mid-1960s, which were unexpected and counter to prevailing theories given a maturing forest and constant atmospheric N deposition (Goodale et al. 2003; Judd et al. 2011). Simulations from PnET-CN suggest that early in the record (1965–1990), temporal variations in stream nitrate concentration at HBEF were largely driven by climatic variation and a series of small disturbances (Aber et al. 2002). They concluded that nitrate losses from the reference watershed were elevated in the 1960s due to a combination of recovery from extreme drought and a significant defoliation event.

Other models that have been important to the HBES include CHESS (Santore and Driscoll 1995) and ALCHEMI (Schecher and Driscoll 1995). These models calculate geochemical equilibria in soils and estimate soil solution chemical concentrations. However, PnET-BGC, is an integrated biogeochemical model incorporating the components of PnET-CN and of major element cycles (i.e., Ca^{2+}, Mg^{2+}, Na^+, K^+, Si, S, P, Al^{3+}, Cl^-, and F^-) in forest and interconnected aquatic ecosystems. The PnET-BGC model simulates the interaction of the processes in soil, vegetation, water, and atmosphere to determine the chemical characteristics of stream water and soil water before emerging as runoff (Gbondo-Tugbawa et al. 2001). This model has been used to assess the long-term effects of air pollution on the Hubbard Brook ecosystem (e.g., Driscoll et al. 2001; Gbondo-Tugbawa et al. 2002).

1.5 Closing Thoughts

This chapter began by introducing the early foundations of forest influences on water and ended by providing examples from the HBES where long-term records, whole-watershed manipulation, field experiments, modeling, and scores of investigators are unraveling the ecological, biogeochemical, and hydrological workings of a forested ecosystem. The HBES is not unique and has served as a model for watershed-based ecosystem studies around the world. Many comprehensive ecosystem studies and individual research efforts worldwide are contributing to the

science of forest hydrology, ecosystem science, and biogeochemistry. Forested landscapes are changing with increased fragmentation, the spread of invasive species and disease, urban/suburban development, forest management for biomass energy, climate and global change, and shifting ownership patterns (NRC 2008). These complex problems will require the development of new approaches for studying complicated ecosystems, but also learning from lessons of past research. Some perspectives from the HBES include:

- Be opportunistic and learn from surprises.
- Focus on linkages, feedbacks, and coupling between ecosystem processes and the interactions of air, land, and water.
- Maintain critical, high-quality, long-term data for understanding patterns and trends in complex ecosystems.
- Develop multidisciplinary, highly collaborative teams, including social sciences, to tackle complex environmental problems.

Forest hydrology and biogeochemistry have evolved and continue to grow as new challenges arise. The remainder of this book aims to synthesize past research and forge future research directions by forest type, process, and stressor. Research topics that are likely to remain high priority in forest hydrology and biogeochemistry are issues related to climate and global change, managing forests for biomass energy feedstocks, and interactions among convergent biogeochemical cycles and between social and biophysical systems. There is also a need for more integration and interpretation of results over large scales (regional to global) and in landscapes where forest land-use/land cover is part of the larger system.

References

Aber JD, Federer CA (1992) A generalized, lumped-parameter model of photosynthesis, evapo-transpiration and net primary production in temperate and boreal forest ecosystems. Oecologia 92:463–474

Aber JD, Ollinger SV, Driscoll CT (1997) Modeling nitrogen saturation in forest ecosystems in response to land use and atmospheric deposition. Ecol Model 101:61–78

Aber JD, Ollinger SV, Driscoll CT et al (2002) Inorganic nitrogen losses from a forested ecosystem in response to physical, chemical, biotic, and climatic perturbations. Ecosystems 5:648–658

Alila Y, Kuraś PK, Schnorbus M et al (2009) Forests and floods: a new paradigm sheds light on age-old controversies. Water Resour Res 45:W08416. doi:10.1029/2008WR007207

Anderson HW, Hoover MD, Reinhart KG (1976) Forests and water: effects of forest management on floods, sedimentation, and water supply. Pacific Southwest Forest and Range Experiment Station, Berkeley

Andréassian V (2004) Waters and forests: from historical controversy to scientific debate. J Hydrol 291:1–27

Barret E, Brodin G (1955) The acidity of Scandinavian precipitation. Tellus 7:251–257

Bates CG, Henry AJ (1928) Forests and streamflow at Wagon Wheel Gap, Colorado. Final report. Monthly Weather Review Supplement 30:1–79

Belgrand E (1854) De l'influence des forêts sur l'écoulement des eaux. Ann Ponts Chaussées 61:1–27

Beven KJ, Kirkby MJ (1979) A physically based, variable contributing area model of basin hydrology. Hydrol Sci Bull 24:43–69

Biswas A (1970) History of hydrology. North-Holland Publishing Company, Amsterdam

Bormann FH (1996) Ecology: a personal history. Annu Rev Energy Environ 21:1–29

Bormann FH, Likens GE (1967) Nutrient cycling. Science 155:424–429

Bormann FH, Likens GE (1979) Pattern and process in a forested ecosystem. Springer, New York

Bormann FH, Likens GE, Fisher DW et al (1968) Nutrient loss accelerated by clear-cutting of a forest ecosystem. Science 159:882–884

Bosch JM, Hewlett JD (1982) A review of catchment experiments to determine the effect of vegetation changes on water yield and evapotranspiration. J Hydrol 55:3–23

Bostock J, Riley HT (1855) The natural history. Pliny the Elder. Taylor and Francis, London

Botkin DB, Janak JF, Wallis JR (1972a) Rationale, limitations, and assumptions of a northeastern forest growth simulator. IBM J Res Dev 16:101–116

Botkin DB, Janak JF, Wallis JR (1972b) Some ecological consequences of a computer model of forest growth. J Ecol 60:849–872

Brown AE, Zhang L, McMahon TA et al (2005) A review of paired catchment studies for determining changes in water yield resulting from alterations in vegetation. J Hydrol 310:28

Calder IR (1977) A model of transpiration and interception loss from spruce forest in Plynlimon, central Wales. J Hydrol 33:247–265

Cappus P (1960) Bassin expérimental d'Alrance – Étude des lois de l'écoulement – Application au calcul et à la prévision des débits. La Houille Blanche A:493–520

Carpenter SR, Chisholm SW, Krebs CJ et al (1995) Ecosystem experiments. Science 269:324–327

Chang M (2006) Forest hydrology: an introduction to water and forests, 2nd edn. CRC Press, Boca Raton

Chittenden HM (1909) Forests and reservoirs in their relation to streamflows, with particular reference to navigable rivers. Am Soc Eng Trans 62:248–318

Cogbill CV, Likens GE (1974) Acid precipitation in the northeastern United States. Water Resour Res 10:1133–1137

Colman EA (1953) Vegetation and watershed management: an appraisal of vegetation management in relation to water supply, flood control, and soil erosion. Ronald Press, New York

Courtney FM (1981) Developments in forest hydrology. Prog Phys Geogr 5:217–241

Cronan CS, Schofield CL (1990) Relationships between aqueous aluminum and acidic deposition in forested watersheds of North America and northern Europe. Environ Sci Technol 24:1100–1105

de la Cretaz AL, Barten PK (2007) Land use effects on streamflow and water quality in the northeastern United States. CRC Press, Boca Raton

DeWalle DR (2003) Forest hydrology revisited. Hydrol Process 17:1255–1256

DeWalle DR (ed) (2011) Forest hydrology. Benchmark papers in hydrology. International Association for Hydrological Sciences, Wallingford (in press) see http://iahs.info/benchmark.htm

DeWalle DR, Rango A (2008) Principles of snow hydrology. Cambridge University Press, Cambridge

Douglass JE (1983) Potential for water yield augmentation from forest management in the eastern United States. Water Resour Bull 19:351–358

Driscoll CT, Lawrence GB, Bulger AJ et al (2001) Acidic deposition in the northeastern United States: sources and inputs, ecosystems effects, and management strategies. BioScience 51:180–198

Dunne T, Black RD (1970a) An experimental investigation of runoff production in permeable soils. Water Resour Res 6:478–490

Dunne T, Black RD (1970b) Partial area contributions to storm runoff in a small New England watershed. Water Resour Res 6:1296–1311

Ebermayer E (1876) Die gesamte Lehre der Waldstreu, mit Rücksicht auf die chemische Statik des Waldbaues. Springer, Berlin

Eisenbies MH, Aust WM, Burger JA et al (2007) Forest operations, extreme flooding events, and considerations for hydrologic modeling in the Appalachians: a review. For Ecol Manage 242:77–98

Ellenberg H (1971) Integrated experimental ecology: methods and results of ecosystem research in the German Solling project, Ecological Studies 2. Springer, Berlin

Engler A (1919) Untersuchungen über den Einfluss des Waldes auf den Stand der Gewasser. Mitt Schweiz Anst Forst Versuchswes 12:1–636

Federer CA (1965) Sustained winter streamflow from groundmelt, Research Note, NE-41. U.S. Forest Service, Northeastern Forest Experiment Station, Upper Darby

Federer CA (1969) New landmark in the White Mountains. Appalachia 12:589–594

Federer CA (2002) BROOK 90: a simulation model for evaporation, soil water, and streamflow. http://home.roadrunner.com/~stfederer/brook/compassb.htm. Accessed Jan 2010

Federer CA, Lash D (1978) Simulated streamflow response to possible differences in transpiration among species of hardwood trees. Water Resour Res 14:1089–1097

Federer CA, Hornbeck JW, Tritton LM et al (1989) Long-term depletion of calcium and other nutrients in eastern US forests. Environ Manage 13:593–601

Federer CA, Vörösmarty CJ, Fekete B (2003) Sensitivity of annual evaporation to soil and root properties in two models of contrasting complexity. J Hydrometeorol 4:1276–1290

Freeze RA (1972) Role of subsurface flow in generating surface runoff 2: upstream source areas. Water Resour Res 8:1272–1283

Gash JHC (1979) An analytical model of rainfall interception by forest. Q J R Meteorol Soc 105:43–55

Gbondo-Tugbawa SS, Driscoll CT, Aber JD et al (2001) Evaluation of an integrated biogeochemical model (PnET-BGC) at a northern hardwood forest ecosystem. Water Resour Res 37:1057–1070

Gbondo-Tugbawa SS, Driscoll CT, Mitchell MJ et al (2002) A model to simulate the response of a northern hardwood forest ecosystem to changes in S deposition. Ecol Appl 12:8–23

Goodale CL, Aber JD, Vitousek PM (2003) An unexpected nitrate decline in New Hampshire streams. Ecosystems 6:75–86

Gorham E (1991) Biogeochemistry: its origins and development. Biogeochemistry 13:199–239

Groffman P, Fisk M, Driscoll C et al (2006) Calcium additions and microbial nitrogen cycle processes in a northern hardwood forest. Ecosystems 9:1289–1305

Harr RD, McCorison FM (1979) Initial effects of clearcut logging on size and timing of peak flows in a small watershed in western Oregon. Water Resour Res 15:90–94

Hart GE Jr (1966) Streamflow characteristics of small, forested watersheds in the White Mountains of New Hampshire. PhD thesis, University of Michigan, Ann Arbor

Helvey JD, Patric JH (1965) Canopy and litter interception of rainfall by hardwoods of eastern United States. Water Resour Res 1:193–206

Hewlett J (1961) Soil moisture as a source of base flow from steep mountain watersheds, Stn. Pap. 132. U.S. Department of Agriculture, Forest Service, Southeastern Forest Experiment Station, Asheville

Hewlett JD (1982) Principles of forest hydrology. University of Georgia Press, Athens

Hewlett JD, Hibbert AR (1961) Increases in water yield after several types of forest cutting. Int Assoc Sci Hydrol Bull 6:5–17

Hewlett JD, Hibbert AR (1967) Factors affecting the response of small watersheds to precipitation in humid areas. In: Sopper WE, Lull HW (eds) International symposium on forest hydrology. Pergamon Press, New York, pp 275–290

Hewlett JD, Nutter WL (1970) Varying source area of streamflow from upland basins. In: Martin GL (ed) Interdisciplinary aspects of watershed management. American Society of Civil Engineers, New York, pp 65–83

Hewlett JD, Pienaar L (1973) Design and analysis of the catchment experiment. In: White EH (ed) Proceedings of a symposium on use of small watersheds in determining effects of forest land use on water quality, University of Kentucky, Lexington, pp 88–106

Hewlett JD, Troendle CA (1975) Non-point and diffused water sources: a variable source area problem. Proceedings, watershed management symposium, American Society of Civil Engineers, New York, 11–13 Aug 1975, pp 21–46

Hewlett JD, Lull HW, Reinhart KG (1969) In defense of experimental watersheds. Water Resour Res 5:306–316

Hibbert AR (1967) Forest treatment effects in water yield. In: Sopper WE, Lull HW (eds) Internation symposium on forest hydrology. Pergamon Press, New York, pp 527–543

Hoover MD, Hursh CR (1943) Influence of topography and soil-depth on runoff from forest land. Trans Am Geophys Union 24:693–698

Hoover MD, Leaf CF (1967) Processes and significance of interception in Colorado subalpine forest. In: Sopper WE, Lull HW (eds) Internation symposium on forest hydrology. Pergamon Press, New York, pp 213–224

Hornbeck JW (1973) Storm flow from hardwood-forested and cleared watersheds in New Hampshire. Water Resour Res 9:346–354

Hornbeck J (2001) Events leading to the establishment of the Hubbard Brook Experimental Forest. http://www.hubbardbrook.org/overview/HBEF_establishment.htm. Accessed Jan 2010

Hornbeck JW, Kochenderfer JN (2004) A century of lessons about water resources in northeastern forests. In: Ice GG, Stednick JD (eds) A century of forest and wildland watershed lessons. Society of American Foresters, Bethesda, pp 19–32

Hornbeck JW, Swank WT (1992) Watershed ecosystem analysis as a basis for multiple-use management of eastern forests. Ecol Appl 2:238–247

Hornbeck JW, Pierce RS, Federer CA (1970) Streamflow changes after forest clearing in New England. Water Resour Res 6:1124–1132

Hornbeck JW, Martin CW, Pierce RS et al (1986) Clearcutting northern hardwoods: effects on hydrologic and nutrient ion budgets. For Sci 32:667–686

Hornbeck JW, Adams MB, Corbett ES et al (1993) Long-term impacts of forest treatments on water yield: a summary for northeastern USA. J Hydrol 150:323–344

Hornbeck JW, Martin CW, Eagar C (1997) Summary of water yield experiments at Hubbard Brook Experimental Forest, New Hampshire. Can J For Res 27:2043–2052

Hornung M, Reynolds B (1995) The effects of natural and anthropogenic environmental changes on ecosystem processes at the catchment scale. Trends Ecol Evol 10:443–449

Hough FB (1878) Connection between forests and climate. In: Report upon forestry. Washington Printing Office, Washington DC

Huntington TG, Richardson AD, McGuire KJ et al (2009) Climate and hydrological changes in the northeastern United States: recent trends and implications for forested and aquatic ecosystems. Can J For Res 39:199–212

Hutchinson GE (1943) The biogeochemistry of aluminum and of certain related elements. Q Rev Biol 18:1–29, 128–153, 242–262, 331–363

Hutchinson GE (1944) Nitrogen in the biogeochemistry of the atmosphere. Am Sci 32:178–195

Hutchinson GE (1950) Survey of the contemporary knowledge of biogeochemistry, III. The biogeochemistry of vertebrate excretion. Bull Amer Mus Nat Hist 96:554

IAHS (1966) International symposium on forest hydrology: final report. Bull Int Assoc Sci Hydrol 11:161–170

Ice GG, Stednick JD (2004a) A century of forest and wildland watershed lessons. Society of American Foresters Press, Loveland

Ice GG, Stednick JD (2004b) Forest watershed research in the United States. Forest History Today Spring/Fall:16–26

Jeandel F, Cantégril JB, Bellaud L (1862) Etudes expérimentales sur les inondations. Bureau des Annales Forestières, Paris

Judd KE, Likens GE, Buso DC et al (2011) Minimal response in watershed nitrate export to severe soil frost raises questions about nutrient dynamics in the Hubbard Brook Experimental Forest. Biogeochemistry doi: 10.1007/s10533-010-9524-4 (in press) see http://www.springerlink.com/content/ww11848367101883/

Kirkby MJ (ed) (1978) Hillslope hydrology. Wiley, New York

Kittredge J (1948) Forest influences. McGraw-Hill, New York

Kochenderfer J (1970) Erosion control on logging roads in the Appalachians, Research Paper NE-158. U.S. Department of Agriculture, Forest Service, Northeastern Forest Experiment Station, Upper Darby

Lange OL, Kappen L, Schulze E-D (1976) Water and plant life: problems and modern approaches. Springer, New York

Lee R (1978) Forest microclimatology. Columbia University Press, New York

Lee R (1980) Forest hydrology. Columbia University Press, New York

Leonard RE (1961) Net precipitation in a northern hardwood forest. J Geophys Res 66:2417–2421

Leonard RE, Reinhart KG (1963) Some observations on precipitation measurement on forested experimental watersheds, Research Note NE-6. U.S. Forest Service, Northeastern Forest Experiment Station, Upper Darby

Lewis W Jr (2002) Message from the president: limnologist makes big splash. Limnol Oceanogr Bull 11:33–35

Likens GE (1983) A priority for ecological research. Bull Ecol Soc Am 64:234–243

Likens GE (1985) An experimental approach for the study of ecosystems. J Ecol 73:381–396

Likens GE (1989) Some aspects of air pollutant effects on terrestrial ecosystems and prospects for the future. Ambio 18:172–178

Likens GE (1992) The ecosystem approach: its use and abuse. Excellence in ecology, vol 3. The Ecology Institute, Oldendorf-Luhe, Germany

Likens GE (2004) Some perspectives on long-term biogeochemical research from the Hubbard Brook Ecosystem study. Ecology 85:2355–2362

Likens GE (2010) The role of science in decision making: does evidence-based science drive environmental policy? Front Ecol Environ 8:e1–e9

Likens GE, Bormann FH (1974) Acid rain: a serious regional environmental problem. Science 184:1176–1179

Likens GE, Bormann FH (1995) Biogeochemistry of a forested ecosystem. Springer, New York

Likens GE, Lambert KF (1998) The importance of long-term data in addressing regional environmental issues. Northeast Nat 5:127–136

Likens GE, Bormann FH, Johnson NM et al (1967) The calcium, magnesium, potassium, and sodium budgets for a small forested ecosystem. Ecology 48:772–785

Likens GE, Bormann FH, Johnson NM (1969) Nitrification: importance to nutrient losses from a cutover forested ecosystem. Science 163:1205–1206

Likens GE, Bormann FH, Johnson NM et al (1970) Effects of forest cutting and herbicide treatment on nutrient budgets in the Hubbard Brook Watershed-ecosystem. Ecol Monogr 40:23–47

Likens GE, Bormann FH, Johnson NM (1972) Acid rain. Environment 14:33–40

Likens GE, Bormann FH, Pierce RS et al (1978) Recovery of a deforested ecosystem. Science 199:492–496

Likens GE, Driscoll CT, Buso DC (1996) Long-term effects of acid rain: response and recovery of a forest ecosystem. Science 77:244–246

Likens GE, Driscoll CT, Buso DC et al (1998) The biogeochemistry of calcium at Hubbard Brook. Biogeochemistry 41:89–173

Likens GE, Butler TJ, Buso DC (2001) Long-and short-term changes in sulfate deposition: effects of the 1990 Clean Air Act Amendments. Biogeochemistry 52:1–11

Likens GE, Driscoll CT, Buso DC et al (2002) The biogeochemistry of sulfur at Hubbard Brook. Biogeochemistry 60:235–316

Lindeman RL (1942) The trophic-dynamic aspect of ecology. Ecology 23:399–418

Lindenmayer DB, Likens GE (2010) Effective ecological monitoring. CSIRO Publishing, Collingwood

Lull HW, Reinhart KG (1967) Increasing water yield in the Northeast by management of forested watersheds, Research Paper NE-66. U.S. Northeastern Forest Experiment Station, Upper Darby

Manderscheid B, Matzner E, Meiwes KJ et al (1995) Long-term development of element budgets in a Norway spruce (*Picea abies* (L.) Karst.) forest of the German Solling area. Water Air Soil Pollut 79:3–18

Marsh GP (1864) Man and nature. Belknap Press of Harvard University Press (reprinted in 1965), Cambridge

Martin CW, Hornbeck JW (1989) Revegetation after strip cutting and block clearcutting in northern hardwoods: a 10-year history, Research Paper NE-625. USDA Forest Service, Northeastern Forest Experiment Station, Broomall

Martin CW, Hornbeck JW, Likens GE et al (2000) Impacts of intensive harvesting on hydrology and nutrient dynamics of northern hardwood forests. Can J Fish Aquat Sci 57:19–29

Matthieu A (1878) Météorologie comparée agricole et forestière. Imprimerie Nationale, Paris

McCulloch JSG, Robinson M (1993) History of forest hydrology. J Hydrol 150:189–216

Mitchell HL, Chander RF (1939) The nitrogen nutrition and growth of certain deciduous trees of northeastern United States. Black Rock Forest Bulletin 11. Harvard University, Cambridge

Monteith JL (ed) (1965) Evaporation and environment. The state and movement of water in living organisms. Cambridge University Press, Cambridge

Moore WL (1910) Report on the infuence of forest on climate and on floods. U.S Weather Bureau, Washington

Mortimer MJ, Visser RJM (2004) Timber harvesting and flooding: emerging legal risks and potential mitigations. South J Appl For 28:69–75

Nobel PS (1974) Introduction to biophysical plant physiology. W.H. Freeman and Company, San Francisco

Nodvin SC, Driscoll CT, Likens GE (1986) The effect of pH on sulfate adsorption by a forest soil. Soil Sci 142:69–75

NRC (2008) Hydrologic effects of a changing forest landscape. National Academies Press, Washington

Odum EP, Odum HT (1959) Fundamentals of ecology, 2nd edn. W.B. Saunders Company, Philadelphia

Ovington JD (1959) The circulation of minerals in plantations of *Pinus sylvestris* L. Ann Bot 23:229–239

Palmer SM, Driscoll CT (2002) Decline in mobilization of toxic aluminum. Nature 417:242–243

Patric J, Reinhart K (1971) Hydrologic effects of deforesting two mountain watersheds in West Virginia. Water Resour Res 7:1182–1188

Penman HL (1948) Natural evaporation from open water, bare soil and grass. Proc R Soc Lond Ser A 193:120–146

Penman HL (1959) Notes on the water balance of the Sperbelgraben and Rappengraben. Eidg Anst Forstl Versuchswes Mitt, Birmensdorf 35:99–109

Penman HL (1963) Vegetation and hydrology. Commonwealth Bureau of Soils, Harpenden

Penman HL (1967) Evaporation from forests: a comparison of theory and observation. In: Sopper WE, Lull HW (eds) Internation symposium on forest hydrology. Pergamon Press, New York, pp 373–380

Peters SC, Blum JD, Driscoll CT et al (2004) Dissolution of wollastonite during the experimental manipulation of Hubbard Brook Watershed 1. Biogeochemistry 67:309–329

Ponce SL (ed) (1983) The potential for water yield augmentation through forest and range management. Water Resour Bull 19:351–419

Ragan RM (1968) An experimental investiagation of partial area contributions. General Assembly of Bern, International Association of Scientific Hydrology, Bern, pp 241–251

Rennie PJ (1955) The uptake of nutrients by mature forest growth. Plant Soil 7:49–95

Rutter AJ, Keshaw KA, Robins PC et al (1971) A predictive model of rainfall interception in forests. I. Derivation of the model from observations in plantation corsican pine. Agric Meteorol 9:367–384

Santore RC, Driscoll CT (1995) The CHESS model for calculations equilibria in soils and solutions. In: Santore RC, Driscoll CT (eds) Chemical equilibrium and reaction models. Soil Science Society of America, Madison, pp 357–375

Sartz RS, Trimble GR (1956) Snow storage and melt in a northern hardwoods forest. J For 54:499–502

Schecher WD, Driscoll CT (1995) ALCHEMI: a chemical equilibrium model to assess the acid-base chemistry and speciation of aluminum in dilute solutions. In: Loeppert R, Schwab AP, Goldberg S (eds) Soil Science Society of America, Special Publication 42, Madison, pp 325–356

Schlesinger WH (1997) Biogeochemistry: an analysis of global change, 2nd edn. Academic Press, San Diego

Sopper WE, Lull HW (eds) (1967) International symposium on forest hydrology. Proceedings of a National Science Foundation advanced science seminar held at the Pennsylvania State University, University Park, Pennsylvania, Aug 29–Sept 10 1965

Stednick JD (1996) Monitoring the effects of timber harvest on annual water yield. J Hydrol 176:79–95

Swank WT, Miner NH (1968) Conversion of hardwood covered watersheds to white pine reduces water yield. Water Resour Res 4:947–954

Tamm CO (1995) Towards an understanding of the relations between tree nutrition, nutrient cycling and environment. Plant Soil 168–169:21–27

Thompson K (1980) Forests and climate change in America: some early views. Climatic Change 3:47–64

Toebes C, Ouryvaev V (1970) Representative and experimental basins, an international guide for research and practice. UNESCO, Paris

Trimble GR, Sartz RS, Pierce RS (1958) How type of soil frost affects infiltration. J Soil Water Conserv 13:81–82

Tripler CE, Kaushal SS, Likens GE et al (2006) Patterns in potassium dynamics in forest ecosystems. Ecol Lett 9:451–466

Troendle CA (1983) The potential for water yield augmentation from forest management in the Rocky Mountain region. Water Resour Bull 19:359–373

Troendle CA, King RM (1985) Effect of timber harvest on the Fool Creek Watershed, 30 years later. Water Resour Res 21:1915–1922

Tsukamoto Y (1961) An experiment on sub-surface flow. J Jpn For Soc 43:62–67

Ulrich B, Mayer R, Khanna PK (1980) Chemical changes due to acid precipitation in a loess-derived soil in central Europe. Soil Sci 130:193–199

Van Miegroet H, Johnson DW (2009) Feedbacks and synergism among biogeochemistry, basic ecology, and forest soil science. For Ecol Manage 258:2214–2223

Vernadsky VI (1926) Biosfera (English translation). Synergetic Press, Oracle

Vernadsky VI (1945) The biosphere and the noosphere. Am Sci 33:1–12

Ward RC (1971) Small watershed experiments: an appraisal of concepts and research developments, Papers in Geography, No. 18. University of Hull, UK

Waring RH, Schesinger WH (1985) Forest ecosystems: concepts and management. Academic Press, San Diego

Watson WC (1865) Forests: their influence, uses and reproduction. Trans N Y State Agric Soc XXV:288–291

Weyman DR (1973) Measurements of the downslope flow of water in a soil. J Hydrol 20:267–288

Whipkey RZ (1965) Subsurface storm flow from forested slopes. Bull Int Assoc Sci Hydrol 2:74–85

Whitehead PG, Robinson M (1993) Experimental basin studies: an international and historical perspective of forest impacts. J Hydrol 145:217–230

Wilm HG (1944) Statistical control of hydrologic data from experimental watersheds. Trans Am Geophys Part 2 2:618–622

Wilm HG (1957) The training of men in forest hydrology and watershed management. J For 55:268–272

Wilm HG, Dunford EG (1948) Effect of timber cutting on water available for streamflow from a lodgepole pine forest. US Dep Agric Tech Bull 968:1–43

Zon R (1912) Forests and water in the light of scientific investigation (Senate Doc. No. 469, 62nd Congress, 2d Session). US Forest Service, Government Printing Office, Washington

Part II
Sampling and Novel Approaches

Chapter 2
Sampling Strategies in Forest Hydrology and Biogeochemistry

Roger C. Bales, Martha H. Conklin, Branko Kerkez, Steven Glaser, Jan W. Hopmans, Carolyn T. Hunsaker, Matt Meadows, and Peter C. Hartsough

2.1 Introduction

Many aspects of forest hydrology have been based on accurate but not necessarily spatially representative measurements, reflecting the measurement capabilities that were traditionally available. Two developments are bringing about fundamental changes in sampling strategies in forest hydrology and biogeochemistry: (a) technical advances in measurement capability, as is evident in embedded sensor networks and remotely sensed measurements and (b) parallel advances in cyberinfrastructure and numerical modeling that can help turn these new data into knowledge. Although these developments will potentially impact much of hydrology, they bring up particular opportunities in forest hydrology (Bales et al. 2006). New sensor technology for most biogeochemical components has lagged that for water and energy, advances in measuring forest–atmosphere exchange of carbon by eddy correlation being an exception.

The availability of accurate, low-cost, low-power sensors for temperature, snowpack, soil moisture, and other components of water and energy balances offers the potential to significantly increase the accuracy of catchment-scale hydrologic measurements by strategically sampling these fluxes and states across heterogeneous landscapes. This is especially important in seasonally snow-covered mountain catchments, where elevation, aspect, and vegetation exert a primary influence on temperature, precipitation state (snow vs. rain), snow accumulation, and energy balance. Topographic patterns are also important, influencing phenomena such as wind patterns and thus cold-air drainage and daytime heating.

Satellites can now routinely provide time series, gridded values across a catchment for snowcover, albedo and snow grain size at a 500-m resolution, but do not give snowpack water content (Rice et al. 2010). It is also well established that operational snow measurements do not provide the representative measurements of snow water equivalent (SWE) needed to blend with satellite data to produce spatial estimates of SWE (Molotch and Bales 2006). However, strategic sampling of snow depth can provide the necessary ground measurements for those interpolations (Rice and Bales 2010). Direct measurements from space of other components of the mountain water balance at similar resolution are not currently in planning;
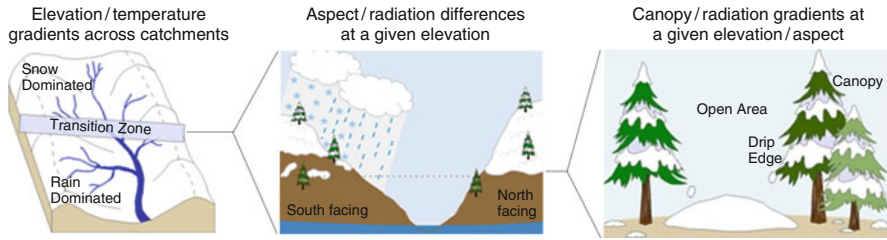
Fig. 2.1 Modeling context for measurements of multiscale heterogeneity in controlling processes, e.g., snow accumulation and melt; which would be lost in a broad regional empirical approach to modeling. Panels from *left* to *right* indicate successively smaller scales. Courtesy: Kyonqho Son

though satellites can provide vegetation information that helps constrain models of hydrologic fluxes and reservoirs. Whole-catchment vegetation characteristics at submeter resolution are being developed using LIDAR (light detection and ranging) (Andersen et al. 2005).

Improvements in cyberinfrastructure enable efficient handling and processing of the larger data streams that result from measurement approaches using dozens to hundreds of sensors, and more computationally intensive simulations. Catchment-scale hydrologic models have also improved, and can take advantage of both spatial data and statistical distributions of data as opposed to a single point value for a time step. That is, models can explicitly account for elevation differences by using either gridded elements or relatively small landscape units; and landscape units can be defined for hillslopes with different aspects, e.g., north vs. south facing, and different vegetation (Tague and Band 2004) (Fig. 2.1). Elevation differences are especially important where winter temperatures are near freezing and some catchments are rain dominated, with other nearby catchments being snow dominated.

The aim of this chapter is to describe how some of these technical advances are being used in the design of measurement systems in seasonally snow-covered, forested catchments, and specifically, how those advances have been applied to sample hydrologic variables in one catchment. The primary emphasis is on water-balance measurements using strategically placed instrument clusters for the mountain water cycle, reviewing results from one instrument cluster that was deployed in the Southern Sierra Nevada of California in 2007. This site represents a synthesis of our knowledge of sampling design. It should be stressed that at this point these systems are experimental, and that design of an instrument cluster is in itself research.

2.2 Science Questions that Build on Recent Advances in Measurement

Several recent reports highlight the need for new water information to enable better decision-making for water resources management, and for the myriad other decisions that are influenced by water (NRC 2008; Dozier et al. 2009). Explosive population

growth and changing climate are combining to create supply-demand mismatches that threaten water supplies across the mountain west. As water becomes a more valuable commodity, more accurate information than is currently available will be needed to support better estimates of natural water reservoirs (e.g., snowpack, groundwater); we will need more complete understanding of water, sediment, and contaminant fluxes (e.g., evapotranspiration [ET], groundwater recharge, erosion, ion fluxes), improved hydrologic modeling (e.g., streamflow forecasting, water quality predictions), and better-informed decision making. The foundation of this new information is an improved program of representative measurements.

Effects on the water cycle are perhaps the most significant impacts of future changes in climate, and the deep uncertainty characterizing climate change require that future water measurements support decision-making under uncertainty (Dozier et al. 2009). For example, an important societal question associated with the mixed rain and snow system that characterizes western mountains is: how do we sustain flood control and ecosystem services when changes in the timing and magnitude of runoff are likely to render existing infrastructure and practices inadequate?

Partitioning rain or snow between ET and runoff is perhaps the most challenging measurement problem in hydrology, especially in mountains, where incoming solar radiation and turbulent mixing cause fine-scale heterogeneity (Dozier et al. 2009). Estimating ET throughout a watershed requires blending multiple sensors: direct measurement with flux towers, along with distributed measurements of sap flow and soil moisture, and models driven by remotely sensed data on soil moisture, surface temperature, and vegetation characteristics.

Four main science questions are driving the measurement program in the Southern Sierra Critical Zone Observatory (CZO): (a) what are the water-balance patterns across rain-dominated vs. snow-dominated forest landscapes, (b) how do snow and soil-moisture patterns control geochemical weathering and transport, (c) what are the primary feedbacks between hydrologic and biogeochemical cycles and landscape evolution, and how are they apparent across the rain-snow transition (d) what are the controlling mechanisms for vegetation, water and nutrient-cycle feedbacks? This chapter places more emphasis on the water-cycle measurements, where advances in measurement technology have been rapid over the past decade.

2.3 Sampling Design Using Embedded Sensors

A prototype water-balance instrument cluster was deployed in the Southern Sierra CZO, which is co-located with the Kings River Experimental Watersheds (KREW), a watershed-level, integrated ecosystem project for long-term research on nested headwater streams in the Southern Sierra Nevada (Fig. 2.2) (Hunsaker et al. 2011). KREW is operated by the Pacific Southwest Research Station of the U.S. Department of Agriculture, which is part of the research and development branch of the Forest Service, under a long-term (50-year) partnership with the Forest Service's Pacific Southwest Region.
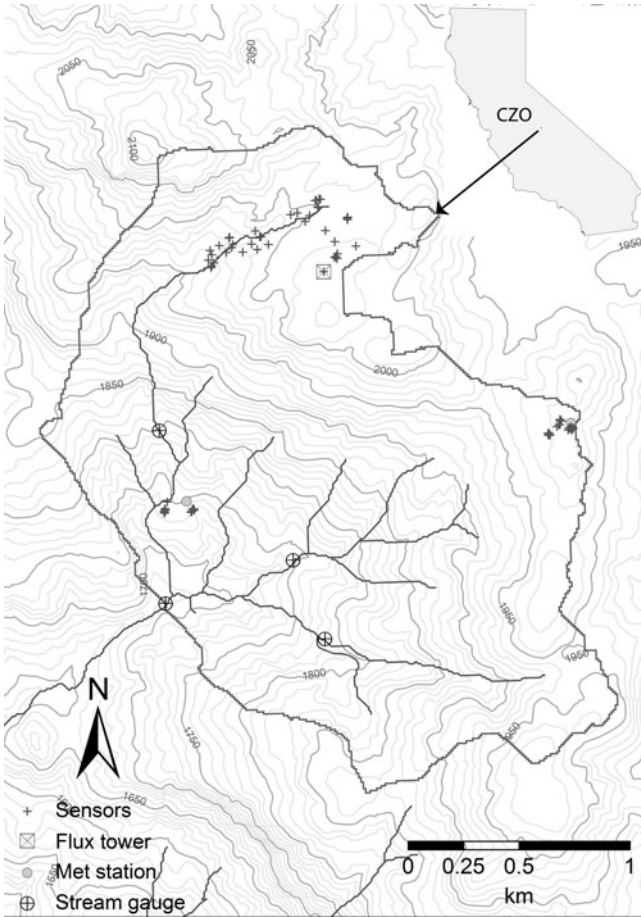
Fig. 2.2 Instrument cluster and location map

One component of the CZO involved developing and deploying a prototype instrument cluster to make comprehensive water-balance measurements across the rain-snow transition, in support of hydrologic and related research by multiple investigators. At the center of the cluster is an eddy-covariance system (flux tower) for measuring water and carbon exchange with the atmosphere. Besides providing measurements of evaporative and turbulent fluxes, the eddy covariance tower serves as the measurement and communications hub of the instrument cluster. Micrometeorological measurements and an embedded sensor network capture the spatial variability of snow depth, soil moisture, air temperature, soil temperature, relative humidity, and solar radiation around the tower.

The instrument cluster was designed to measure snow depth, snow density, soil volumetric water content (VWC), matric potential, and ET. The design of the

instrument cluster was based on placing continuously recording snow-depth, VWC, and temperature sensors to sample end members across the main variables in the catchments. That is, the system was designed to capture landscape variability through stratified rather than random or gridded sampling. Based on the multiple field surveys at different locations and times of year in the Rocky Mountains and Sierra Nevada, it has been determined that five main variables affecting snow distribution are elevation, aspect, slope, canopy cover, and solar radiation (Molotch and Bales 2005; Rice and Bales 2010). Solar radiation is an integrating variable, but was not used in the design as it is redundant with the other variables. It was decided not to sample across different slopes because of shifts in sensor location and possible damage to sensors due to snow creep on steep slopes. Because spatial surveys of soil moisture were not available to guide sensor placement, VWC measurements were co-located with snow sensors. Although it is recognized that soil properties may also be a major determinant of soil-moisture patterns, in snowmelt-dominated catchments it is expected that soil wetting and drying patterns will follow the spatial patterns in snowmelt. It is also recognized that while snowmelt and soil moisture flow in three-dimensional patterns rather than just vertically, co-locating soil moisture sensors with snow sensors provided uniform placement for data analysis and modeling.

Snow density values were available from a co-located snow-depth sensors and snow pillows that measure SWE. Eddy correlation was the main method used to measure ET, supplemented with sap-flow sensors. Groundwater levels were measured at regular intervals along a transect across the main stream channel.

The catchment is southwest facing and has elevations of 1,700–2,100 m, with a mean elevation of 1,917 m (Fig. 2.3). The two meteorological stations, located at elevations of 1,750 and 1,984 m, were put in place by Forest Service scientists prior to deployment of the rest of the instrument cluster, and were located in small clearings. Only the upper meteorological station had a snow pillow. Stream gauging and geochemical sampling using automatic samplers (ISCO) was also in place prior to deployment of the instrument cluster, as were in-stream turbidity and temperature sensors.

Snow-depth and soil-moisture sensors were placed in the vicinity of the two meteorological stations and the flux tower. This was done in part to take advantage of communication links available at these sites. Sensors were then placed under the canopy, at the canopy drip edge and in the open on an east or west trending transect. All sites were located on north/northwest and south/southwest facing slopes. This sampling design was replicated at both elevations, with instruments placed around two to three trees at both north- and south-facing sites; at the higher elevation, a third pair of trees lying on flat ground was instrumented. The five subcluster sites had slopes ranging from 7 to 18°.

Ultrasonic snow sensors (Judd Communications) were mounted on a steel arm extending about 75 cm from a vertical steel pipe that was anchored to a U-channel driven into the ground. Sensors were mounted approximately 3 m above the ground, with extensions available if needed. Pits were excavated and sensors for soil temperature and VWC (Decagon Echo-TM) placed horizontally in the pit walls at depths of 10, 30, 60, and 90 cm. and the cables were routed to avoid preferential
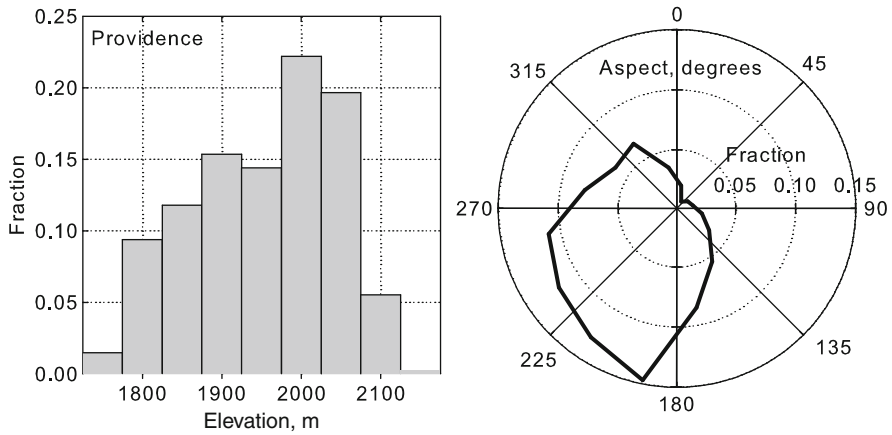
Fig. 2.3 Distribution of elevation and aspect, based on 30-m pixels, for Providence catchments (P300)

flow to sensors. Pits were backfilled and hand compacted to maintain the same horizons and density insofar as possible. Depths were measured from the ground surface, including organic layers, for the examples reported in this chapter. Later deployments measured depths from the top of the mineral soil. In total, 52 snow sensors, 214 EC-TM VWC sensors, and 113 MPS-1 matric potential sensors were deployed. At three locations, it was not possible to reach a depth of 90 cm owing to boulders or lack of soil depth. The EC-TM probes use capacitance to measure the dielectric permittivity of the surrounding medium, which is much more sensitive to the volume of water in the total volume of soil than to the other constituents of the soil. In this method, the sensor probes form a capacitor, with an electromagnetic field produced between the positive and negative plates. The charging of the capacitor is directly related to the dielectric, which depends on VWC (http://www.decagon.com).

A 60-node wireless-sensor network was deployed in 2008 with an additional set of sensors to transmit real-time data collected by the individual sensors to a base station at the eddy flux tower. Deployments of wireless-sensor networks for the purposes of environmental monitoring have been addressed previously (Mainwaring et al. 2002; Hart and Martinez 2006), though the deployment described here addresses performance in remote conditions. *Dust Networks* (2009) developed the underlying ultra low-powered network technology, the core of which relies heavily on network optimization and a randomized channel hopping protocol. These advances allow the network to self-assemble into a redundant mesh, ensuring multiple data paths between any node and the central data aggregation point. Limited acquisition and processing capabilities at each node required the construction of a separate data-manager board to interface with the external sensors. Each wireless node has a 2-year battery life, made possible by an extremely low

duty cycle. For additional reliability, and increased link distance, the stock whip antennas on the network hardware were replaced with 8 dBi omni-directional antennas. Twenty-three nodes were located at snow and soil VWC sensors, while the remaining nodes were used to transfer, or "hop," data, and extend transmission distances.

The hub of the wireless network is composed of a mobile Internet connection, and an embedded computer that actuates sensors inside the network and formats incoming readings. Communication between this computer and the wireless-sensor-network base station is conducted through an Extensible Markup Language (XML) interface over a hard-line Ethernet connection. The XML interface adds an extra layer of reliability by removing the need for low-level programming languages to control network behavior.

Extensive deployments of wireless-sensor networks have been successfully conducted for industrial and indoor monitoring purposes (Howitt et al. 2006; Jang et al. 2008). However, extreme outdoor environmental conditions, such as fluctuations in humidity, temperature, and weather patterns, can have strong effects on overall radio communications (Oestges et al. 2009; Rice and Bales 2010). As such, it becomes important to conduct an analysis of network behavior in outdoor settings to optimize parameters relevant to network performance. Two relevant measures of network performance are known as the received signal strength (RSSI), and the packet delivery ratio (PDR). The RSSI is the physical power present in a received radio signal (usually given in dB or dBm), and is used as an indicator of the quality of radio transmission between two nodes. Increasing the distance between two nodes in the network has an adverse effect on RSSI, as radio signals have to travel further and are thus more susceptible to environmental interference. Critically low RSSI values can cause links within the network to fail, leading to possible isolation of nodes. The PDR is defined as the number of successfully transmitted packets over the total number of transmitted packets, where a packet is the unit of data transmitted within a network. PDR is also a measure of link performance, where values below 100% correspond to the need to retransmit data, thus requiring network hardware to use more energy. As such, desirable RSSI and PDR characteristics are a direct function of proper spacing between network nodes.

It is important to note that our entire instrument cluster is powered by batteries charged by solar panels. Despite canopy closures in the 50–85% range, we have in most cases been able to deploy solar in small clearings and avoid the need to place panels in trees.

2.4 Performance of Sensor Networks

Both snow and soil-moisture sensors were reliable and provided consistent results over the first 2 years of deployment. Minor offsets in the snow-depth measurements from shifts in the mounting hardware were easily corrected at the end of each snow season. Laboratory and field calibration of soil-moisture sensors showed accuracy
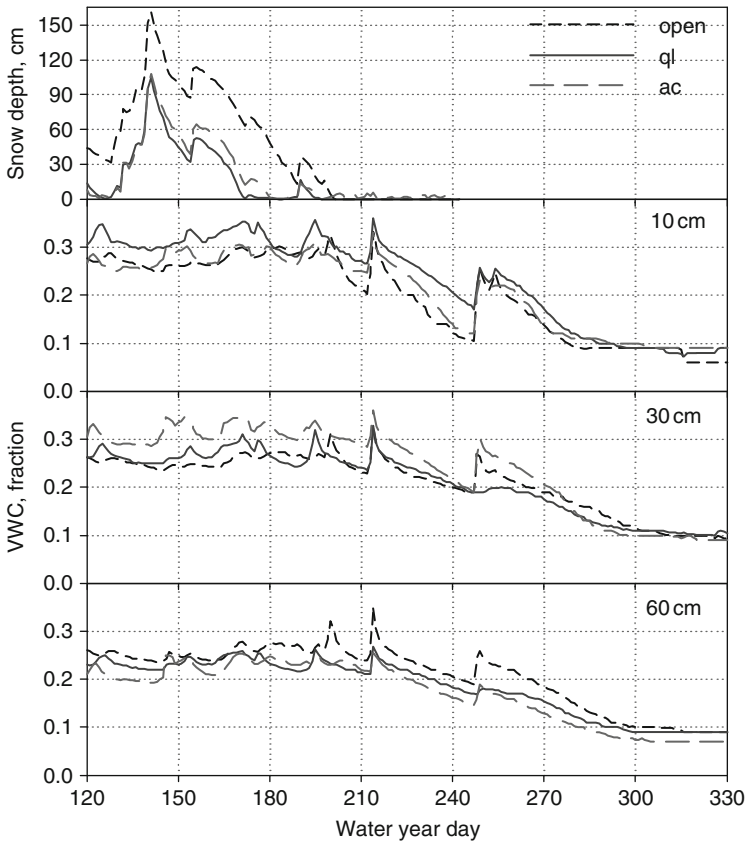
Fig. 2.4 Snow depth and volumetric water content (VWC) for sensors in the open and at the drip edge of *Quercus kelloggii* (California black oak) and *Abies concolor* (white fir), upper met south location. Water year 2009

to ±0.02 fractional VWC. Data from three of the 105 Echo-TM sensors had significant noise, which was attributed to electrical issues associated with splicing cables; however, the VWC signal was still recovered from these sensors by additional data cleaning. Typical data show wet soil while the ground is snow covered, followed by drying in the 1–2 months following depletion of the snow (Fig. 2.4). Sites in the open, i.e., not under the canopy, had on average 25–50 cm deeper snow than those at the drip edge or under tree canopies (Fig. 2.5), though differences in soil moisture were less clear. Sensors at the higher elevation also recorded more snow and later melt out than those at the lower elevation. Soil moisture also showed slightly later drying at the upper location, reflecting longer snowcover.

Across the full instrument cluster, snow-depth values showed consistent decreases during March and April for points with both shallow and deeper snow (Fig. 2.6). Soil-moisture values were slightly less variable than snow depth, and
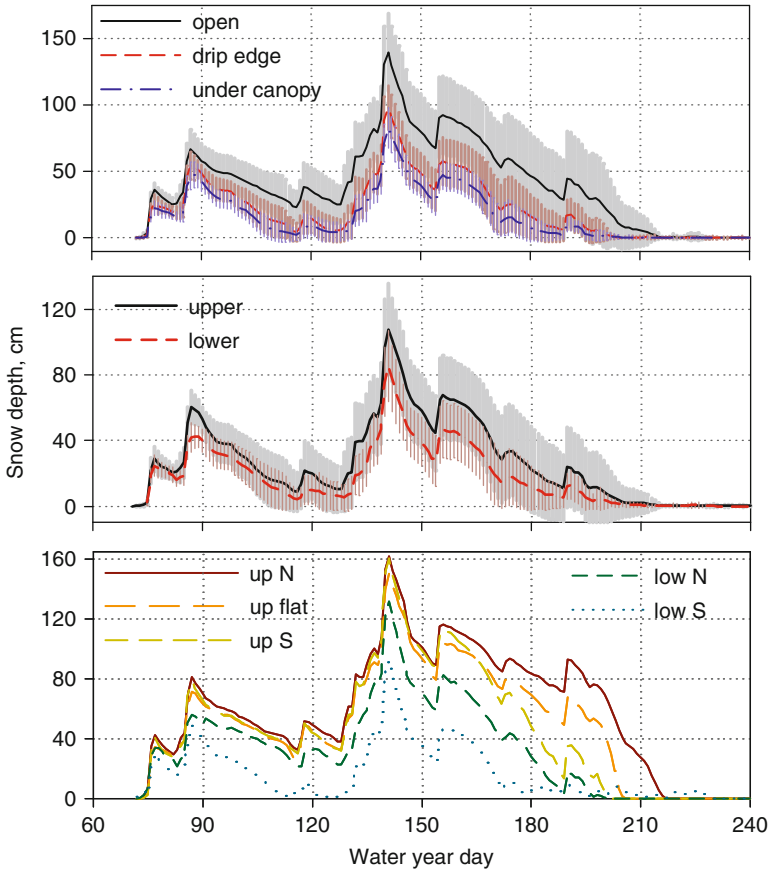
Fig. 2.5 Comparison of snow depths relative to canopy (*upper*), elevation (*middle*), and aspect (*lower*)

showed little change until after the snowpack was depleted. VWC values then decreased from April through September.

Figure 2.7 shows what is known as a *waterfall plot*, displaying network RSSI values against PDR values collected over a 4-week period. For RSSI values of above −78 dBm, PDR remains near 100%, implying that all network data is being transmitted successfully. For RSSI values below this threshold, PDR drops off significantly, requiring numerous retransmissions of the same data. Since lower RSSI values correspond to greater path distance, optimal network performance corresponds to this threshold value, where both PDR and path distance are maximized. Further analysis of RSSI vs. average link distance measures shows this threshold value to correspond to an average path distance of 100 m. Because of the variability of the forest environment, a decision was made to space nodes 50 m apart for further reliability and in anticipation of extreme storm events.
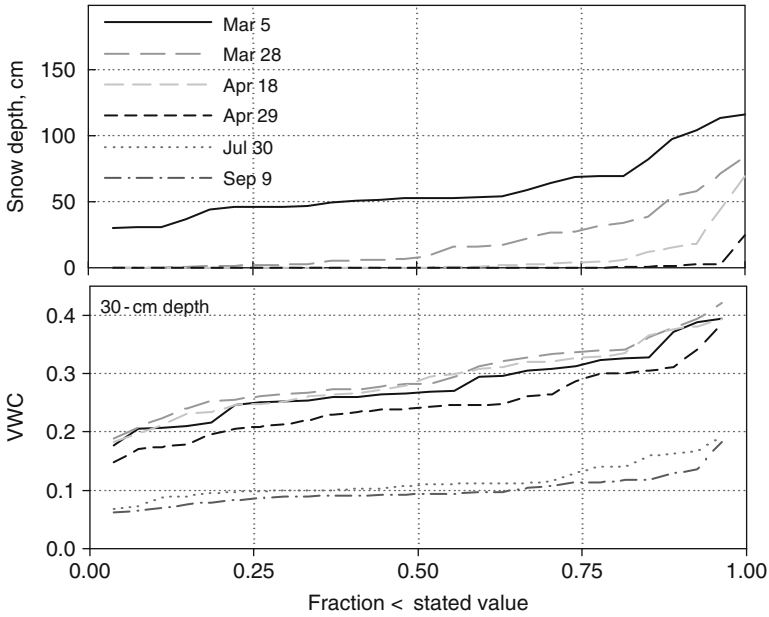
Fig. 2.6 Distribution of snow depth and soil moisture from 27 locations within water-balance instrument cluster
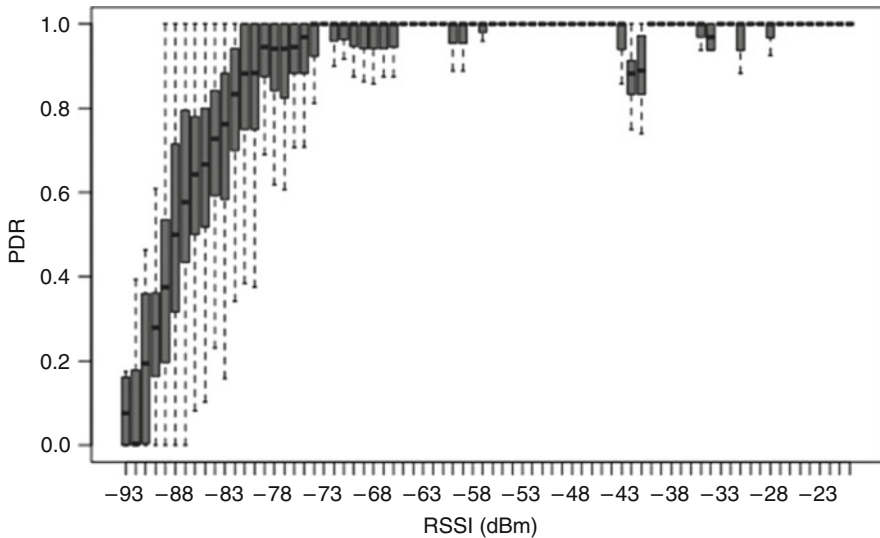
Fig. 2.7 *Waterfall plot* of average network received signal strength indicator against packet delivery ratio, of network data collected over a 4-week span. The *solid boxes* reflect the second and third quartiles around the median, while the *dashed lines* extend to the maximum and minimum measured values

Node-to-node spacing appears to be the best indicator of link performance, while terrain, vegetation, and environmental parameters give little indication as to why some links performed more reliably than others. Until WSN technology adapts to the extreme conditions of outdoor monitoring applications, future WSN deployments will require an iterative deployment process. To achieve optimal network performance (maximizing path distances and battery longevity), site-specific test deployments should be conducted to generate network data which can be used to create analytical tools such as the above *waterfall plot*. Network behavior indicates that 100% of all transmitted packets reach their destination without the need for retransmission as long as RSSI remains above -73 dBm (which corresponds to node-to-node link distance of 100 m and below).

Soil water dynamics can be monitored by either soil water content or soil water matric potential measurements. Soil water content varies between zero and the soil's porosity (at soil saturation). Accurate soil water content measurements provide a measure of soil water storage capacity. Many soil moisture measurement techniques have been developed (Robinson et al. 2008) ranging from small-scale local measurements on the order of centimeters to those that may apply to scales of kilometers (remote sensing). The accurate soil water content range as monitored with Echo-TM sensors is independent of water content, and is about 2% VWC across the complete water content range for the sandy loam soils in the CZO.

In contrast, the range of interest for soil water potential varies from zero (at soil saturation) to potential values of $-1{,}500$ kPa (corresponding to -15 bar) or lower. Soil water matric potential measurements are typically more sensitive to change as small changes in soil water content can cause large changes in soil water matric potential, especially under dry conditions. The typical measurement range for most available sensors though is much smaller. Whereas tensiometers are accurate in the relatively wet range (0–60 kPa), the measurement range for electrical-resistance blocks is typically limited to about 200 kPa. Alternatively, soil water potential can be inferred from the dielectric measurement of a porous block, such as the recently available MPS-1 sensor (Decagon Devices, Pullman, WA), however, also its measurement range is limited to about 400 kPa, and measurement accuracy varies greatly depending on calibration method. For driest conditions, heat-dissipation sensors should be considered. However, at this point they have not been incorporated into our instrument cluster. In general, accurate soil water matric potential measurements are difficult and output values are more an indication of soil water status than the exact measure of soil water matric potential.

Performance of the sensors and radios chosen for this instrument cluster was acceptable, and it is planned to use the same equipment in future deployments. The stratified sampling design that was used did show differences in snowcover, though less so for soil moisture, between the three main variables: elevation, aspect, and location relative to tree canopy. Further evaluation of the adequacy of the design, i.e., number and actual placement of sensors, to capture the variability across this particular basin is pending synoptic surveys and data from the other sensors in the instrument cluster that were deployed in 2009, and modeling to assess the spatial coverage.

2.5   Geochemical Sampling

Geochemical sampling of stream water and watershed reservoirs contributing to streamflow in the Southern Sierra CZO indicates the controls on streamflow generation, and how those controls vary with elevation and snow-rain proportion. Stream samples were collected biweekly at the stream gauge locations, thus defining three subcatchments within the larger catchment (Fig. 2.2). Samples were either grabbed by hand or collected by automated samplers that were triggered when flow exceeded a certain value, providing samples several hours apart during storm events. Soil water samples were collected from soil lysimeters (http://www.prenart.dk). Samples were analyzed for major cations and anions by ion chromatography. Three endmembers contribute to streamflow. Near-surface runoff contributed more than 50% of stream flow in most catchments, though baseflow was important in two that because of topography had more soil storage of water (Liu et al. 2011). Rainstorm runoff on average contributed around 5% of streamflow. These results were developed using diagnostic tools of mixing models to identify conservative tracers and endmember mixing analysis to separate sources of streamflow.

2.6   Satellite Snowcover

Satellite snowcover data were retrieved from NASA's moderate resolution imaging spectroradiometer (MODIS) using a spectral mixing model, in which a set of endmembers (snow, soil, vegetation) in different proportions in each pixel is used to "unmix" a scene on a pixel-by-pixel basis (Dozier and Painter 2004). The algorithm uses the spectral information from MODIS to estimate subpixel snow properties: fractional snow-covered area (SCA), grain size, and albedo (Painter et al. 2009). No correction was made for trees, so the SCA values represent projected snow cover, i.e., snow that the satellite sees. The SCA threshold was set at 0.15, to prevent identification of spurious snow cover, i.e., values below 0.15 were reported as zero.

Basin snowcover for the same time period as shown above for the sensor network peaked during a storm in late February 2009, and declined to near zero by mid April (Fig. 2.8). As is apparent from the figure, part or all of 20 MODIS pixels fall within the basin. The highest snowcover values were in the higher elevations. On-site inspection showed the basin to be nearly completely snow covered on February 24. However, because of heavy forest cover, the satellite values are lower. The complete time series of cloud-free scenes shows that basin-average detectable SCA peaked at just under a fraction of 0.4 (Fig. 2.9). At that time, all 27 snow sensors had at least 60 cm of snow. It can also be seen from the figure that when satellite SCA became zero, the average snow depth from the 27 depth sensors was also near zero. However, snow was not completely absent from the pingers until about 1 month later, at the end of May. At this point, empirical corrections can be
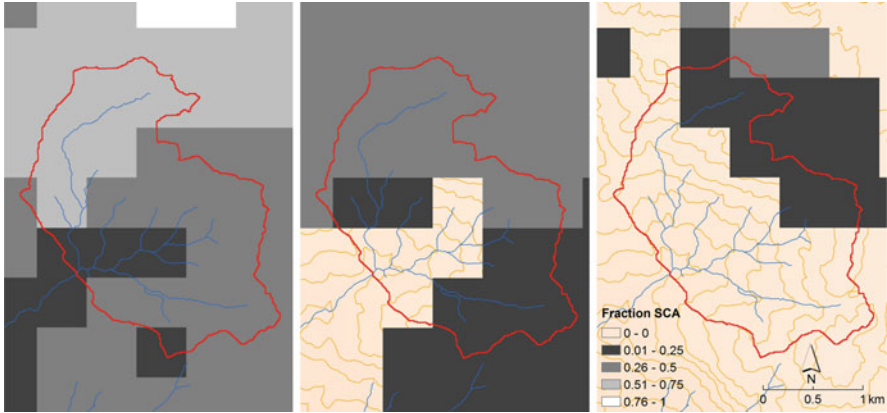
Fig. 2.8 Fractional snow-covered area (SCA) from MODIS for 3 days in 2009. SCA values are binned into four classes for ease of viewing
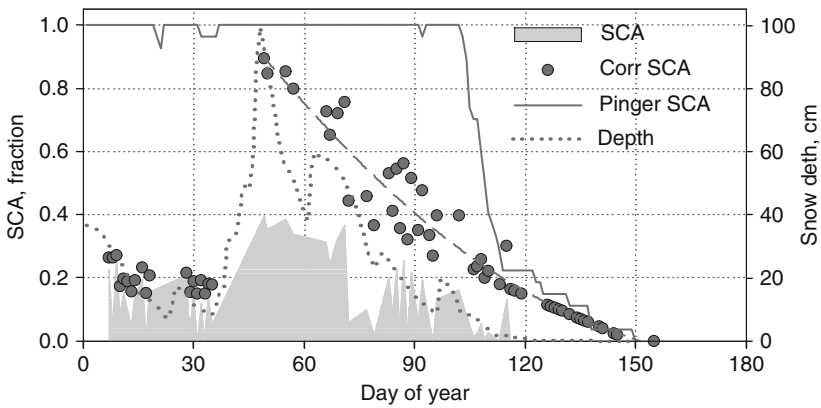
Fig. 2.9 Fractional snow-covered area (SCA) from MODIS, averaged over basin, plus SCA corrected for canopy and threshold effects and fit to corrected SCA for main period of snowmelt. Also shown is the fraction of snow sensors with measurable snow (pinger SCA) and average snow depth for the 27 sensors

made for satellite viewable gap fraction, the result of which is also shown in Fig. 2.9. Based on the field inspections, a correction of 0.5 was assumed for the day of peak snowcover, declining linearly to zero when the snow was melted out at all of the depth sensors. In this case, a detailed, gridded survey (Rice and Bales 2010) was not carried out, but a qualitative assessment was made of the SCA at maximum accumulation. More-involved corrections that make use of detailed vegetation information will be available in the future, pending completion of vegetation and snow mapping by LIDAR for calibration.

2.7 Extensions of Sampling Design

We have recently expanded our original instrument-cluster design, which initially included a single flux tower, to a transect of four towers along an elevation gradient that crosses the rain-snow transition. The transect crosses from a lower-elevation oak-forest ecosystem, where trees cease ET owing to late-summer moisture limitations, through the highly productive conifer forests with almost no shutdown during the year, to a higher-elevation forest ecosystem with subfreezing winter temperatures and cold-limited ET. Integration of sap-flow and flux-tower data is also part of the scaling strategy for water balance in the CZO catchments. The ability to substitute the lower-cost and lower-energy-use soil-moisture sensors for sap flow is also being investigated with ongoing measurements. However, good correlations between sap flow and soil moisture offer the potential to use the lower-cost, lower-power-demanding soil measurements as an index of ET (Bales et al. 2011). Further relating these to the direct eddy-correlation measurements will provide information for scaling soil moisture to regional ET. Flux towers are important components of water-balance measurements, made more valuable when they are part of a network as opposed to being stand alone. It is also expected that embedding them in an instrument cluster with an array of distributed, synergistic measurements such as described here for the CZO will overcome some of the constraints of interpreting eddy correlation data in complex terrain (Brown-Mitic et al. 2007).

It is also important to consider the role of airborne LIDAR data in determining forest and watershed characteristics for scaling and modeling of water and biogeochemical cycles. At the Southern Sierra CZO, understanding the interactions between snow distribution and vegetation, topography, and other meteorological factors has been limited by the lack of spatially distributed and high-definition data. LIDAR measurements of snow depth provide information at spatial scales that are unmatched by any other existing technology, and fill a large data gap for spatial snow depth information. A spatially distributed and high-definition LIDAR dataset from snow on/snow off flights will be combined with the time series of meteorological and snow variables obtained at the instrument clusters to further evaluate the sensor-network sampling strategy. Summer LIDAR data (snow off) characterize spatial patterns of open vs. forest cover and canopy structure that are used in coupled ecohydrologic modeling and scaling of ET and carbon flux.

Geochemical sampling using automatic sensors is generally limited to locations with line power and frequent operator attention. At the Southern Sierra CZO, the emphasis is on use of automatic samplers for collecting stream and soil water, e.g., examining the spatial and temporal patterns of nitrogen concentrations to identify "hot spots" and "hot moments," i.e., links between hydrologic and biogeochemical cycles.

Groundwater-surface water interactions in a stream/meadow complex at the southern Sierra CZO were investigated using a combination of heat and geochemical tracers (Lucas et al. 2008). A distributed temperature system (DTS) with 2-m spatial resolution and 2-min temporal resolution was deployed in the stream,

enabling the capture of diurnal swings in surface water-temperatures over the course of 5 days. Point temperature sensors (Hobo Tidbits) were deployed to assess the vertical temperature profile and stratification within a number of the stream pools. Water samples were collected to determine the activity of radon-222 (3.8 day half-life) as a proxy for groundwater discharge. Temperature and pressure head data were collected from monitoring wells and piezometers. The high spatial and temporal resolution of the DTS enabled locating specific thermal anomalies in the longitudinal stream temperature profile, indicative of groundwater discharge. However, the variable and shallow depth of the stream meant that diel temperature cycles interfered with the groundwater signal. Still the DTS can be a powerful tool for sampling stream, snowpack and air temperature variations (Tyler et al. 2009).

The question of whether precipitation in forested, mountain watersheds falls as snow or rain merits further attention. Current practice relies on calibrated air-temperature relationships to determine precipitation phase, though such relationships are site specific, and highly variable. Measurements in the mountains of Idaho show a strong relationship between dew-point temperature and precipitation phase (Marks and Winstral 2007). Catchment-level measurements of humidity and temperature, supplemented by snow and precipitation along elevation transects can establish this rain-snow partitioning. Because dew point is a property of the air mass, it is less likely to be influenced by site or local conditions, and will be a more stable predictor of precipitation phase than temperature alone. Thus, a combination of regional temperature and humidity profiles, available from twice-daily soundings at a few locations, and local on-the-ground measurements along elevation transects will support estimating rain-snow partitioning of precipitation.

References

Andersen H-E, McGaughey RJ, Reutebuch SE (2005) Estimating forest canopy fuel parameters using LIDAR data. Remote Sens Environ. doi:10.1016/j.rse.2004.10.013

Bales RC, Molotch NP, Painter TH et al (2006) Mountain hydrology of the western United States. Wat Resour Res. doi:10.1029/2005WR004387

Bales RC, Hopmans J, O'Geen T et al (2011) Soil moisture response to snowmelt and rainfall a Sierra Nevada mixed conifer forest (in review/revision)

Brown-Mitic CW, Shuttleworth J, Harlow CH et al (2007) Seasonal water dynamics of a sky island subalpine forest in semi-arid southwestern United States. J Arid Environ 69:237–258

Dozier J, Painter TH (2004) Multispectral and hyperspectral remote sensing of alpine snow properties. Ann Rev Earth Planet Sci. doi:10.1146/annurev.earth.32.101802.120404

Dozier J, Braden JB, Hooper RP et al (2009) Living in the water environment: The WATERS Network Science Plan. doi: 10.4211/sciplan.waters.20090515

Dust Networks (2009) Company website: www.dustnetworks.com. Accessed 22 Feb 2011 2:49 PM

Hart JK, Martinez K (2006) Environmental sensor networks: a revolution in the Earth system science? Earth Sci Rev. doi:10.1016/j.earscirev.2006.05.001

Howitt I, Manges WW, Kuruganti PT et al (2006) Wireless industrial sensor networks: framework for QoS assessment and QoS management. ISA Trans. doi:10.1016/S0019-0578(07)60217-1

Hunsaker CT, Whitaker T, Bales RC (2011) Water yield and runoff timing across the rain-snow transition in California's southern Sierra Nevada (in review/revision)

Jang W-S, Healy WM, Skibniewski MJ (2008) Wireless sensor networks as part of a web-based building environmental monitoring system. Autom Construct. doi:10.1016/j.autcon.2008.02.001

Liu F, Hunsaker CT, Bales RC (2011) Controls of streamflow pathways in small catchments across snow/rain transition in the Southern Sierra Nevada, California (in review)

Lucas RG, Conklin MH, Tyler SW et al (2008) Investigating meadow hydrology and hyporheic exchange. EOS transactions AGU, 89:53, Fall Meeting Supplement, Abstract H21L-06

Mainwaring A, Culler D, Polastre J et al (2002) Wireless sensor networks for habitat monitoring. Proceedings of the 1st ACM international workshop on wireless sensor networks and application WSNA '02. ACM, New York, pp 88–97

Marks DG, Winstral AH (2007) Finding the rain/snow transition elevation during storm events in mountain basins. IUGG 24th general assembly joint symposium JHW001. http://www.iugg2007perugia.it/abstracttype.asp. Accessed 9 June 2010

Molotch NP, Bales RC (2005) Scaling snow observations from the point to the grid element: implications for observation network design. Wat Resour Res. doi:10.1029/2005WR004229

Molotch NP, Bales RC (2006) SNOTEL representativeness in the Rio Grande headwaters on the basis of physiographics and remotely sensed snow cover persistence. Hydrol Process 20:723–739

National Research Council (2008) Integrating multiscale observations of U.S. waters. National Academies Press, Washington

Oestges C, Montenegro-Villacieros B, Vanhoenacker-Janvier D (2009) Radio channel characterization for moderate antenna heights in forest areas. IEEE Trans Veh Technol 58:4031–4035

Painter TH, Rittger K, McKenzie C et al (2009) Retrieval of subpixel snow-covered area, grain size, and albedo from MODIS. Remote Sens Environ. doi:10.1016/j.rse.2009.01.001

Rice R, Bales RC (2010) Embedded sensor network design for snow cover measurements around snow pillow and snow course sites in the Sierra Nevada of California. Wat Resour Res. doi:10.1029/2008WR007318

Rice R, Bales RC, Painter TH, et al (2010) Snow water equivalent along elevation gradients in the Merced and Tuolumne River basins of the Sierra Nevada (in review)

Robinson DA, Campbell CS, Hopmans JW et al (2008) Soil moisture measurement for ecological and hydrological watershed-scale observatories: a review. Vadose Zone J. doi:10.2136/vzj2007.0143

Tague C, Band L (2004) RHESSys: regional hydro-ecologic simulation system: an object-oriented approach to spatially distributed modeling of carbon, water and nutrient cycling. Earth Interact 8(19):1–42

Tyler SW, Selker JS, Hausner MB et al (2009) Environmental temperature sensing using Raman spectra DTS fiber-optic methods. Wat Resour Res. doi:10.1029/2008WR007052

Chapter 3
Bird's-Eye View of Forest Hydrology: Novel Approaches Using Remote Sensing Techniques

Gabor Z. Sass and Irena F. Creed

> *The science of hydrology is on the threshold of major advances, driven by new hydrologic measurements, new methods for analyzing hydrologic data, and new approaches to modeling hydrologic systems ... scientific progress will mostly be achieved through the collision of theory and data*
> ... Kirchner (2006)

3.1 Introduction

Without question, better scientific understanding of hydrological processes in forested environments will be a product of the synergistic play of theory and data. Remote sensing (RS) from satellite and airborne platforms, along with many other sources of hydrological data such as wireless sensor arrays and ground-based radar networks, is playing and will continue to play a vital role in better understanding the hydrosphere by providing the next generation of datasets to the hydrological community. RS systems are planetary macroscopes that allow the study of ecosystems from a completely new vantage point, facilitating a holistic perspective like viewing the Earth does for astronauts.

RS allows us to (1) view large geographic areas instantaneously; (2) spatially integrate over heterogeneous surfaces at a range of resolutions; (3) be totally unobtrusive; and (4) be cost effective compared to ground-based approaches. While there are challenges relating RS data recorded in radiance or backscatter to variables of interest, and RS systems have poor temporal resolution compared to ground-based measurement devices, RS and spatial analytical techniques such as digital terrain analysis and distributed hydrological modeling embedded in Geographical Information Systems (GIS) have allowed hydrologists to better understand the movement of water across a landscape.

This is a synthesis of state-of-the-art research on how RS has informed the study of hydrology, with an explicit focus on forested landscapes. Although there have been other excellent reviews published on RS and other geocomputing approaches for hydrological research, none have focused specifically on forest hydrology

(with the notable exception of Stewart and Finch 1993). In our quest for the Holy Grail of hydrology, we evaluate the ability of RS to provide accurate estimates of various components of the hydrological cycle in forests around the globe. We focus primarily on temperate and boreal forest regions, as it is in these areas that most forestry RS research has been conducted.

The synthesis is framed around the concept of the water budget and how RS techniques can be used to estimate components of the water budget of catchments across a range of scales, from small headwater catchments to larger high-order basins and from hourly to decadal time intervals. Since there are currently no sensors or networks of sensors that can successfully estimate the water budget remotely across this range of spatial and temporal scales, data fusion and data assimilation techniques that exploit synergies of RS and GIS will also be explored. We also illustrate how these novel approaches can be used in forest operations, and outline research needs that will lead to the operational use of RS and related GIS techniques for scientific advancement of forest hydrology.

3.2   A Primer for Forest Hydrologists

RS is the observation of a phenomenon from a distance, using devices that detect electromagnetic (EM) radiation. The use of RS as a tool to understand hydrological phenomena started in the 1970s, but there have been only minor increases in the number of published forest hydrology journal articles that use or refer to RS techniques (Fig. 3.1).
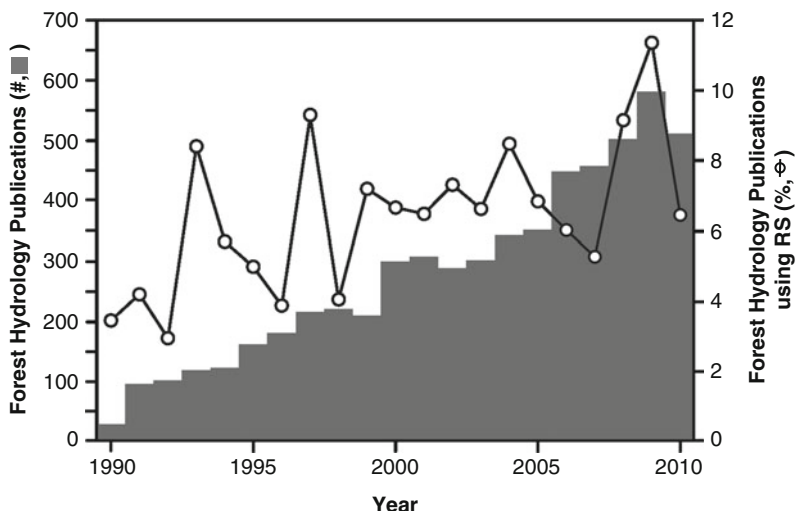
Fig. 3.1 Number of publications per year in forest hydrology (*bars*), with percentage that refer to remote sensing (RS) (*points*), as indicated by ISI Web of Science Citation Index. Search terms: (1) for forest hydrology = forest* AND hydrol*; (2) for RS = "remot* sens*" OR satellite OR airborne OR LiDAR

We hope that this synthesis will give new momentum to the consideration of RS as a worthwhile tool for the study of hydrological phenomena on forested landscapes. Before exploring the potential applications of RS to hydrology, it is important to present some basic RS terminology (Box 3.1) and general observations about the different RS systems applicable for forest hydrological investigations.

There has been a substantial increase in the number of airborne and satellite sensors that cover a large portion of the EM spectrum since 1972 when the first Landsat satellite was launched into orbit (Fig. 3.2). None of these sensors have been designed exclusively for hydrological applications; therefore, their relevance to hydrology in general and forest hydrology in particular needs to be carefully considered and evaluated. Figure 3.2 summarizes the major sensors that we believe have some potential in informing the field of forest hydrology, with detailed

---

Box 3.1 Terms and Terminology

Electromagnetic spectrum (*EM*): Remote sensors measure EM radiation that has been either reflected or emitted from the Earth's surface.

Optical sensors measure shorter wavelengths: visible (0.3–0.7 μm), near-infrared (0.7–1.4 μm), short-wave (1.4–3 μm), and long-wave or thermal infrared (3–15 μm).[1]

Microwave sensors measure longer wavelengths, ranging from 1 to 10 cm.

- *Frequency* is the inverse of wavelength and is the conventional unit for microwave sensors (e.g., C-band is between 4 and 8 GHz, while L-Band is between 1 and 2 GHz).[2]
- *Polarization* is the orientation of the EM radiation wave to the Earth surface (planar = horizontal; perpendicular = vertical). EM radiation waves can be transmitted or received in either horizontal or vertical orientations leading to four common polarizations (HH, VV, HV, and VH).
- *Passive* sensors record microwaves emitted by the surface (also referred to as radiometers).
- *Active* sensors transmit radiation and record the reflected or "backscattered" radiation (also referred to as scatterometers).
- Synthetic aperture radar (SAR) uses the flight path of the sensor platform to simulate an aperture much larger than the platform itself, allowing for high resolution radar imagery. Echo waves received at different positions along the flight path are distinguished to produce a series of observations that can be combined as if they had all been made simultaneously.
- Interferometric SAR (InSAR or IfSAR) uses the difference in phase (period) between transmitted microwave radiation and received backscatter response to estimate distance (elevation). Since phase is influenced by other factors, InSAR techniques use two or more SAR images of the same area and from the same position to reduce noise and ambiguity.

Box 3.1 (continued)

Altimeter: Remote sensors that measure time between the transmission and receipt of radiation pulses. They include as follows:

- Optical altimeters – e.g., Light Detection and Ranging (LiDAR).
- Microwave altimeter – e.g., Shuttle Radar Topography Mission (SRTM).

Data fusion: The combination or integration of RS with other spatial data for analysis and/or visualization.

Data assimilation: The combination or integration of RS into a spatial model for parameterization, and/or validation.

[1]Designated by CIE (Commission internationale de l'éclairage [International Commission on Illumination]).

[2]Designated by IEEE (Institute of Electrical and Electronics Engineers).

characteristics of their wavelengths, spatial resolution, and years of operation. Building on Fig. 3.2, Table 3.1 summarizes the potential of these different parts of the EM spectrum for hydrological applications. Together, these data provide a valuable resource for forest hydrologists wishing to explore the possibilities of using RS techniques.

Optical sensors cannot penetrate vegetation or clouds. For this reason, optical sensors are ideal for monitoring open water areas (lakes and wetlands). Many of the earliest sensors (apart from some of the meteorological satellites) were optical sensors. This means, for example, that in the case of NASA's Landsat program there is a 40-year record of sub-100 m spatial resolution imagery of open water extent, a very good metric of water storage on the landscape. Optical sensors are also used to estimate snow cover and surface temperature, a useful proxy for the delineation of groundwater discharge areas and the determination of evapotranspiration (ET). In tropical regions, cloud-top reflectance and temperature are used to infer precipitation rates although only at coarse temporal resolutions.

In contrast, *microwave* sensors have the ability to penetrate vegetation and can collect data independently of cloud cover and solar illumination. This is important because of the difficulty of acquiring cloud-free imagery during optimal time periods (i.e., when there is a lot of hydrological activity!) using optical sensors. There are two types of microwave sensors: active sensors, which send and receive their own energy, and passive sensors, which detect the microwaves emitted by the Earth's surface. The microwave portion of the EM spectrum is divided into bands where the useful bands for hydrology are K, X, C, and L, ranked in increasing wavelengths. In general, K- and X-bands are useful for detecting surface temperature, snow density, and rainfall rates, whereas C- and L-bands are sensitive to soil moisture.

Although the potential for using microwave sensors for forest hydrology is promising, the technology is relatively new compared to optical sensors
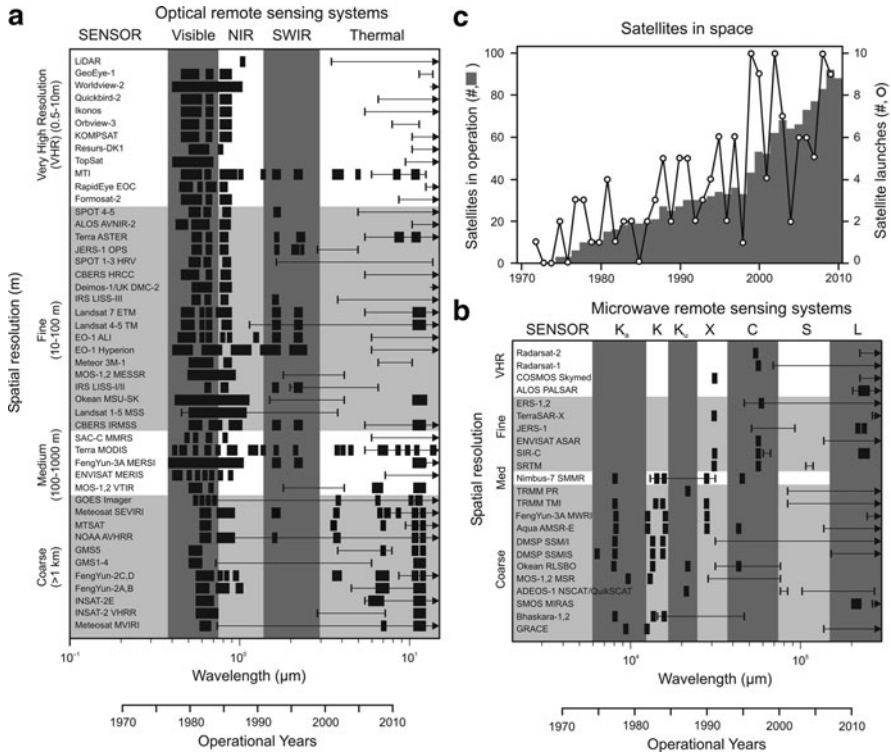
Fig. 3.2 Remote sensors useful for the study of forest hydrology. For each remote sensor, the portions of the electromagnetic spectrum detected (*black bars*) and the period of operation (line, with *arrow* indicating currently operational) are shown for (**a**) optical and (**b**) microwave sensors. The total number of satellites launched (*open circle*) and satellites operating in a given year (*bar*) are shown in (**c**)

(e.g., ERS, the first widely available and fine spatial resolution microwave sensor, was sent to orbit in 1991) and further research is needed to demonstrate their full potential. On the wish list of many hydrologists have been multipolarization and multifrequency sensors since they, much like multispectral optical data, would provide measurements sensitive to different biophysical properties of the surface including vegetation. Multipolarized sensors such as recently launched ALOS-PALSAR and RADARSAT-2 show promise in improved detection of water in forested landscapes (van der Sanden 2004).

While most optical and microwave systems measure reflectance or backscatter, *interferometric* radar (InSAR) and *altimeters* (e.g., Light Detection and Ranging [LiDAR]) measure distances. For example, a space shuttle-based InSAR system (SRTM) was used to derive 90 m spatial resolution digital elevation models (DEMs) for the entire world (van Zyl 2001), which sometimes provides the only source of hydrological data for developing nations. On the other hand, airborne LiDAR systems have been used to derive submeter spatial resolution and centimeter vertical accuracy DEMs, albeit only for smaller regions. Together, InSAR

Table 3.1 Potential application of electromagnetic spectrum to study of forest hydrology

Electromagnetic Spectrum	Water Input			Water Storage						Water Output	
	P	Pl	SC	SD	SW IA	SW SA	SW USA	GW	ET	Q
Visible (0.4-0.7 μm) Reflectance of solar irradiance used to estimate albedo for ET calculations and snow cover area. If cloudy, cloud-top reflectances can be used to infer rainfall rates.	■		■						■	
Near and Shortwave Infrared (NIR, SWIR) (0.7-3.0 μm) Water is a strong absorber of solar irradiance in these wavelengths, making NIR ideal for surface water and plant water mapping.		■	■		■				■	
Thermal Infrared (TIR) (3-15 μm) Emitted thermal radiation from earth's surface used to infer surface temperatures for ET calculations and to differentiate GW recharge/discharge zones. If cloudy, cloud-top temperatures can be used to infer rainfall rates.	■							■	■	
K-bands (K, Ka, Ku) (0.75-2.50 cm or 12-40 GHz) Emitted microwave radiation influenced by surface temperature and snow density. If precipitation is occurring, these microwave frequencies are sensitive to precipitation rates.	■			■						
X-band (2.50-3.75 cm or 8-12 GHz) Microwave radiation influenced by snow depth, soil moisture. Upwelling radiation scattering sensitive to rainfall.	■			■	■	■	■			
C-band (3.75-7.50 cm or 4-8 GHz) Microwave radiation that is highly sensitive to soil moisture, surface roughness and volume scattering within vegetation canopy. Useful for saturated soil estimation under low to medium density canopies, inundation even under dense canopy due to double-bounce off trunks. It is also sensitive to snow density for ripe snow packs.					■	■				
L-band (15-30 cm or 1-2 GHz) Like C-band but longer wavelengths better penetrate vegetation canopies and therefore better detect variations in soil moisture.					■	■	■			

P precipitation; *Pl* plant water; *SC* snow cover; *SD* snow density; *SW* surface water; *IA* inundated areas; *SA* saturated areas; *USA* unsaturated areas; *GW* groundwater; *ET* evapotranspiration; *Q* discharge

systems and altimeters are critical in providing information on surface topography used in understanding water flow and wet area organization, as well as water level dynamics.

A critical component in determining the use of RS imagery is matching the sensor to the "problem," with explicit consideration of spatial and temporal scales. In practice, the selection of sensors is driven by theoretical considerations related to the way radiation interacts with the surface and the atmosphere, scale (resolution and extent) as much as data availability. Many hydrological investigations require long-term datasets; however, only a handful of sensors have a wealth of archival material (e.g., Landsat, ERS, and RADARSAT). Imagery from these sensors has been the mainstay for many long-term hydrological investigations. While it is important to look at the past, current and future monitoring of hydrological trends requires the consideration of some of the exciting new sensors available to the hydrological community. In the following sections, we detail how sensors such as those listed in Fig. 3.2 have been used to detect various components of the water balance in forested landscapes.

3.3 Water Budget

This synthesis highlights the current status and future challenges of applying RS to the study of forest hydrology. We follow a drop of water traveling through a watershed from input, storage, and finally output and assess how RS and associated GIS techniques can be used to track water fluxes and reservoirs. Comprehensive reviews that have been completed for general hydrology and each component of the water budget are listed in Table 3.2. We have used these reviews to evaluate errors in RS-based estimates so that the reader can judge if the errors are in a range that is useful to answer hydrological questions (Table 3.3). While the knowledge presented can be applied to any land cover type, we point out special considerations of using RS technologies and techniques on forested lands.

3.3.1 Water Input

RS can be used to detect rainfall rates, but only at very coarse spatial and temporal scales. Early uses of RS include visible (VIS) and infrared (IR) imagery to estimate precipitation indirectly by inferring rainfall intensity from cloud-top temperatures and reflectance (Petty and Krajewski 1996). This method is most accurate for tropical regions where the cloud-tops of convective cells are much more representative of surface precipitation rates than in more temperate regions (Tang et al. 2009). More recently, microwave sensors have been used to estimate rainfall intensity given their ability to penetrate clouds and directly interact with rain particles (Tang et al. 2009). Unfortunately, the drawback of these sensors (e.g., Advanced Microwave Scanning Radiometer-EOS) is that they capture images at

Table 3.2 Published reviews relevant to remote sensing of forest hydrology

General hydrology	Stewart and Finch (1993),[a] Hall (1996), Kasischke et al. (1997), and Tang et al. (2009)
Water inputs	Petty (1995) and Petty and Krajewski (1996)
Water storage	
Interception	Roth et al. (2007)
Snowpack	Rango (1996)
Open water, inundated, saturated, unsaturated areas	Jackson et al. (1996), Ritchie (1996), Jackson (2002), Moran et al. (2004), Wagner et al. (2007), Vereecken et al. (2008), Verstraeten et al. (2008), and Gao (2009)
Groundwater, recharge vs. discharge areas	Meijerink (1996, 2000), Becker (2006), Entekhabi and Moghaddam (2007), Jha et al. (2007), Ramillien et al. (2008), and Robinson et al. (2008)
Water outputs	
Evapotranspiration	Kustas and Norman (1996), Glenn et al. (2007), Kalma et al. (2008), Verstraeten et al. (2008), and Li et al. (2009b)
Discharge	Schultz (1996) and Smith (1997)
Hydrological modeling	Kite and Pietroniro (1996) and Singh and Woolhiser (2002)

[a] Review specifically focused on remote sensing of forest hydrology

Table 3.3 Relative error of RS-derived water budget components (based on reviews cited in this chapter)

	Units	Relative error (%)
Water inputs		
Precipitation (satellite)	mm/day	60–100
Ground-based radar	mm/day	5–50
Water storage		
Interception	mm	5–15
Snowpack (area)	km^2	1–5 (deciduous)
		10–20 (evergreen)
Snowpack (SWE)	mm	30–50
Open water areas	km^2	1
Saturated areas	km^2	1–10
Soil moisture	m^3/m^3	15–30 (low biomass)
Groundwater, recharge vs. discharge areas	km^2	30–60
Water outputs		
Evapotranspiration	mm/day	15–30
Discharge	mm/s	>50

coarse spatial (4–40 km) and temporal (twice a day) resolutions, and therefore they are only useful for studies of larger watersheds and longer time periods.

In order to improve spatial and temporal resolution, microwave imagery has been combined with VIS/IR products (Hong et al. 2007). There is a new NASA mission with a mandate to achieve the estimation of precipitation on a global scale, which will use multiple VIS, IR, and microwave sensors from the same platform for simultaneous

imaging (Flaming 2005). However, even this system will, at best, only offer an hourly snapshot of precipitation rates. Ground-based radar networks, operated by weather-forecasting agencies, have substantially improved our ability to qualitatively map the spatial structure of precipitation events (rainfall and snowfall intensity). Besides the difficulties in accurately estimating the rainfall rate, the coverage of ground-based radar networks in forested regions is poor. A combination of ground-based radar and rain- and snow-gauge networks with satellite-based products are likely needed to compile continuous yet spatially distributed measurements of precipitation.

3.3.2 Water Storage

3.3.2.1 Interception

Interception of precipitation by forest canopies can be estimated quite accurately using RS approaches. RS helps characterize the physical characteristics of the canopy, but this information must be fed into a hydrological model that estimates actual interception based on both canopy characteristics and antecedent conditions. A simple vegetation index using a combination of red and near-infrared (NIR) bands may be used to estimate canopy interception given the high correlation between vegetation indices and leaf area index (LAI). Typically, the normalized difference vegetation index (NDVI) is used to estimate canopy interception, modified by the inclusion of a middle IR band (Nemani et al. 1993; Hwang et al. 2009). The drawback is that NDVI becomes saturated in dense vegetation conditions when LAI becomes very high. If narrow band hyperspectral data are available, they may improve the estimates derived from NDVI because of greater penetration through the canopy (Bulcock and Jewitt 2010).

However, forests with similar LAI may have different structures, and as a result, different interception rates. Laser altimetry or LiDAR can provide a wealth of data on canopy structure including gaps, depth, bulk density, surface area, and height, thus improving estimates of interception (Roth et al. 2007). Besides the ability to estimate canopy interception, optical and LiDAR data collected to characterize vegetation canopies may also help describe other hydrological processes such as snow accumulation, snow melt, and transpiration from inside the stoma of plants. The importance of including LAI derived from RS in distributed hydro-ecological models cannot be understated and is one of the success stories in the application of RS in forest hydrology (Tague and Band 2004; Hwang et al. 2009).

3.3.2.2 Snowpack

RS of snow cover extent was one of the first hydrological applications that achieved great success. Currently, there are operational systems for snow cover mapping for the entire globe at 0.5–1 km spatial resolution and daily to 8-day composites

(Tang et al. 2009). These systems utilize VIS and NIR sensors from NOAA-AVHRR and MODIS sensors to detect snow cover. Although snow cover extent does not readily convert into snow water equivalent (SWE), which is more important from a water budget perspective, it does provide important information about the surface radiative balance since there is such a big difference between snow-covered and snow-free land areas in terms of net energy due to high reflectance of snow.

Cloud cover is the major limitation of using VIS and NIR bands. It not only prevents sensing the earth, but can also easily confuse the automated systems into classifying cloud-covered areas as snow-covered. The solution to seeing through clouds is to use passive microwave imagery, which is useful for mapping snow cover extent as well as SWE due to its ability to penetrate the snow pack. Unfortunately, current passive microwave configurations provide very coarse imagery at 25 km or poorer resolution and are only useful in flat areas with homogenous land cover such as the Prairies in North America (Tang et al. 2009).

In forested areas, the forest canopy attenuates the microwave signal and as a result the snowpack can be underestimated by as much as 50% (Rango 1996). One way to address this is to use correction factors such as the Normalized Difference Snow Index or NDVI (Klein et al. 1998; Lundberg et al. 2004). However, even modified retrieval methods need local calibration as there can be significant differences between geographic regions due to snow grain size, depth, and subpixel variability with respect to open water areas (Lemmetyinen et al. 2009).

Currently, there are no plans to launch fine spatial resolution passive microwave sensors. Therefore, RS of SWE in heterogeneous environments will remain problematic and require local calibration. The assimilation of either VIS/NIR or passive microwave imagery with snow melt models promises to be a worthwhile pursuit (Klein et al. 1998; Andreadis et al. 2008; Molotch 2009).

3.3.2.3 Surface and Near-Surface Water

Both optical and microwave RS techniques have been used to monitor areal and volumetric measures of surface and near-surface water. Surface water is water stored in lakes and wetlands as inundated land. It may be open to the sky or covered by vegetation. Near-surface water is water held in the soil as pore water (saturated if the pores are full and unsaturated if some pores have air in them). In order to estimate the volume of stored water, it is important to know the depth of water as well as the area of the particular store. In terms of areal estimation of surface water stores, optical RS of open water using short-wave IR sensors, such as Band 5 from Landsat, is one of the most accurate RS techniques, due to the strong absorption of radiation in those wavelengths (Lunetta and Balogh 1999). Unfortunately, short-wave radiation does not penetrate vegetation. One way to get around this limitation is using vegetation vigor to infer the hydrological status of the ground conditions underneath the canopy (Whitcomb et al. 2009). In deciduous forests, leaf-off imagery in combination with summer leaf-on imagery has been useful in detecting

wetlands (Lunetta and Balogh 1999). In general, optical imagery is only useful in mapping open water when there is no vegetation and no clouds present.

Active microwave systems or imaging radars have distinct advantages over optical systems in monitoring the areal distribution of surface water, including (1) penetration of vegetation canopies and sensing both canopy and surface characteristics; (2) penetration of clouds; (3) more frequent data collection due to the active nature of the sensor, which operates during both day and night; and (4) imagery collection from different, programmable angles leading to different modes and very fine spatial resolution (finer than 10 m) over wide swaths (often 50–100 km) (Whitcomb et al. 2009). In general, higher frequency, shorter wavelength radars (e.g., C-band) are more sensitive to hydrological conditions under flooded short vegetation such as fens and bogs, and lower frequency, longer wavelength radars (e.g., L-band) are more sensitive to hydrological conditions under flooded, taller vegetation such as forests and swamps (Kasischke et al. 1997).

Due to the rich archived C-band datasets from ERS and RADARSAT sensors, more publications have used C-band rather than L-band to map soil water and inundated areas in forested environments. The main findings of this research may be summarized as follows: (1) microwaves in C-band are sensitive to soil saturation only in forests with sparse canopies (Sass and Creed 2008; Whitcomb et al. 2009); (2) if the forest floor is flooded, the double-bounce effect produces a strong signal that can be detected even under closed canopies (Townsend 2001); (3) polarization is important, since radiation with horizontal transmit and horizontal receive polarization mode (HH) can penetrate vegetation canopies better than can radiation with vertical transmit and vertical receive polarization mode (VV) (Lang and Kasischke 2008); and (4) time-series analysis of multiple images (e.g., principal component analysis and probability mapping) covering a wide range of hydrological conditions can reveal hydrological patterns of surface water at the landscape scale (Verhoest et al. 1998; Sass and Creed 2008; Clark et al. 2009).

While C-band imagery can detect flooding in forests and saturation under certain circumstances, its performance is inconsistent and inferior to that of L-band. L-band has a longer wavelength (23 cm as compared to 5.6 cm for C-band), allowing it to penetrate much further into the vegetation canopy and detect surface water in forested landscapes (Whitcomb et al. 2009). The next generation of sensors in both C- and L-band (RADARSAT-2 and ALOS-PALSAR) promise a much improved ability to estimate volumetric soil moisture given the multipolarized channels (van der Sanden 2004; Rosenqvist et al. 2007); however, their utility is currently being investigated (e.g., Verhoest et al. 2008).

Besides the necessary advances in sensor technology needed to improve the measurement of vadose zone soil moisture, there are other useful techniques that can be used to estimate the volume of water stored at the surface. One of these techniques uses laser altimeters (i.e., LiDAR systems) to provide bathymetric information for clear water bodies up to 70 m deep (Gao 2009). For smaller, ephemeral water features, LiDAR-derived DEMs of surface topography can be processed using (1) probabilistic approaches to delineate features (e.g., depressions) and the corresponding volumes when water is likely to pond (Creed et al. 2003; Lindsay et al. 2004), and (2) GIS approaches to compute depth to water table

(Murphy et al. 2007). Topographic information may be married with LiDAR intensity information in order to give accurate maps of inundation under forest canopies (Lang and McCarty 2009). The main limitation of airborne LiDAR approaches in mapping surface water is the expense of single, let alone repeat, coverage of large geographic areas. Satellite-based LiDAR systems should alleviate this limitation. Finally, a dynamic approach for estimating surface water volume changes is using interferometric SAR (InSAR) with C- or L-band images to capture a region from two viewing angles and compute surface heights from their combined analysis. Although only applicable for bigger hydrological systems such as large river systems in the Amazon, InSAR is being used to detect water level changes underneath the forest canopy (Alsdorf et al. 2000, 2001; Lu and Kwoun 2008).

In general, the mapping of areal distribution of surface water in forested environments is much further advanced than the mapping of volumetric measurements of near-surface water. Apart from sensor development, the cutting edge of the field is focusing on data fusion, where data from radar, optical, and topographic sources are combined using statistical approaches to downscale coarse spatial resolution imagery of surface saturation and inundation to much finer spatial resolution (Kaheil and Creed 2009), or to extract patterns not observable from single sources of information (Bwangoy et al. 2010). Further integration of data is required where water storage in watersheds can be estimated by assembling information from different sensors detailed here. This could include integrating information on inundated areas from optical sensors, inundated and saturated areas under forest canopies from microwave sensors, water depth from altimeters, and water level changes from InSAR sensors.

3.3.2.4　Groundwater

RS monitoring of groundwater resources is still in its infancy, mostly due to the inability of EM radiation used by current satellite-based sensors to penetrate the ground (Jha et al. 2007). As a result, RS studies to date have used surface information such as topographic, vegetative, geologic, surface temperature, and drainage pattern characteristics of a landscape to give clues to the presence or absence of groundwater recharge or discharge and infer groundwater storages or fluxes (Meijerink 1996; Entekhabi and Moghaddam 2007). At its simplest, images capturing these landscape features can be color coded, and an image interpreter can classify areas as belonging to a certain groundwater class; however, this method is highly dependent on expert knowledge (Meijerink 1996, 2000). More rigorous approaches take NIR and thermal imagery of carefully chosen winter or summer images to map groundwater discharge or recharge zones (Bobba et al. 1992; Batelaan et al. 1993). Similarly, soil moisture and vegetation vigor have been used to infer shallow groundwater tables (Jackson 2002).

Cross-fertilization of technologies is occurring with the introduction of airborne geophysical methods that offer RS of subsurface properties (Robinson et al. 2008). These geophysical methods use radio waves to excite the Earth's subsurface inductively and measure the resulting magnetic field (Robinson et al. 2008).

The resulting resistivity maps can be used to infer groundwater table position and general lithologic information; however, mapping can be done only in flat terrain and at approximately 100 m spatial resolution. Perhaps the most exciting recent development has been the use of microgravity sensors to infer total water storage (Ramillien et al. 2008). Unfortunately, these measurements have been made at the continental scale and are not applicable to headwater catchments. Like most other components of the water balance, groundwater storage and flux estimation are best made with the synergistic use of RS and other geospatial data in groundwater models (Batelaan and De Smedt 2007), which can model not only the flow of water but also associated nutrients and pollutants (Jha et al. 2007).

3.3.3   Water Output

3.3.3.1   Evapotranspiration

RS offers the only way to derive the spatial distribution of ET across forested catchments, albeit still at fairly coarse spatial and temporal resolutions. Although there are no current sensors that measure ET directly (Liu et al. 2003; Min and Lin 2006), satellite-derived vegetation indices, surface temperature, and surface albedo provide inputs into models that can estimate ET. The simplest approach is empirical and makes use of surface temperature and vegetation indices (e.g., NDVI) (Moran et al. 1994). Although this approach is simple with minimal inputs, it does require site-specific calibration. The expanding network of flux towers that estimate ET over a small footprint can be used in combination with this simple approach to accurately map ET over large scales (Yang et al. 2006).

More sophisticated approaches solve for the different components of the surface energy balance, where ET is often calculated as the residual (Bastiaanssen et al. 1998; Wu et al. 2006; Glenn et al. 2007; Mu et al. 2007). These require much more ground-based and satellite-based input data. In general, surface reflectance or albedo derived from visible imagery and surface temperature derived from thermal imagery are used to calculate the short-wave and long-wave portion of net radiation, respectively, and vegetation indices are used to infer stomatal conductance. Important consideration in forested environments must be given to the sunlit and shaded components of canopies, as well as the distribution of leaves (i.e., clumping) (Liu et al. 2003). Direct evaporation from wet leaf surfaces can also be a very important component of ET and requires special consideration in models (Guerschmann et al. 2009).

Operational mapping of ET at medium spatial resolution (i.e., 1 km) and medium temporal resolution (i.e., 1 day) is currently feasible, and many agencies around the world have started to publish such maps (e.g., Liu et al. 2003). However, there is a lot of heterogeneity being masked at these sampling intervals, and the current state of the science aims to improve these maps of ET. One approach is to use fine resolution maps of forest cover (5–10 m range) and interpolate ET measurements associated with each dominant cover type (Goodrich et al. 2000;

Mackay et al. 2002). A more sophisticated statistical approach uses fine resolution imagery with support vector machines to downscale coarse resolution ET maps (Kaheil et al. 2008). This is promising because in frequently cloud-covered regions only passive microwave imagery (at 40 km spatial resolution) can realistically be used to estimate surface temperature and therefore ET (Min and Lin 2006). Improving downscaling techniques is a key research need.

3.3.3.2 Discharge

The use of RS to estimate river discharge is limited to higher order catchments where rivers are wide enough to be detected by sensors (Alsdorf and Lettenmaier 2003). Discharge may be estimated by generating empirical curves relating water surface area to discharge or by using laser or radar altimeters to measure stage variation (Smith 1997). Airborne and space-based altimeters can detect centimeter changes in water levels that can be associated with discharge. Both of these techniques are limited by repeat cycles, spatial resolution in the case of the radar systems, and the fact that water level changes still need to be converted to discharge, which requires ground measurements that can be very difficult to obtain. So far RS of discharge has been most successfully applied in tropical forests where many rivers do not have confined beds and RS imagery is the only way to estimate the flow rates, even if in a crude way (Alsdorf and Lettenmaier 2003). The use of RS snapshots of inundation or stage for larger rivers can be used as input into hydrological models (Vorosmarty et al. 1996). RS also provides important input (such as land cover/land use, LAI, and surface topography) into hydrological models that simulate river discharge (Tague and Band 2004).

3.3.4   An Integrated Approach

As Kirchner (2006) stated, observations will provide direct insights into processes that are crucial to the advancement of forest hydrology. While RS offers the potential for observing hydrological pools and fluxes over a broad range of spatial and temporal scales, this potential has yet to be realized. Current limits of measurable resolutions reveal a trade-off between high temporal resolution but low spatial resolution (e.g., passive microwave) and high spatial resolution but low temporal resolution (e.g., commercial optical sensor such as IKONOS) (Fig. 3.3). Until sensors are developed that can monitor hydrological processes at the necessary time and space scales, data fusion, and data assimilation within statistical and distributed models will provide the way forward.

Distributed hydrological modeling is probably the key area where synergies between RS and GIS can advance the science the most. Distributed hydrological models are critical because they simulate processes at a range of scales from pedons to large drainage basins and they have the ability to forecast (Tague and Band 2004), a very important feature given the uncertainty related to climate change.
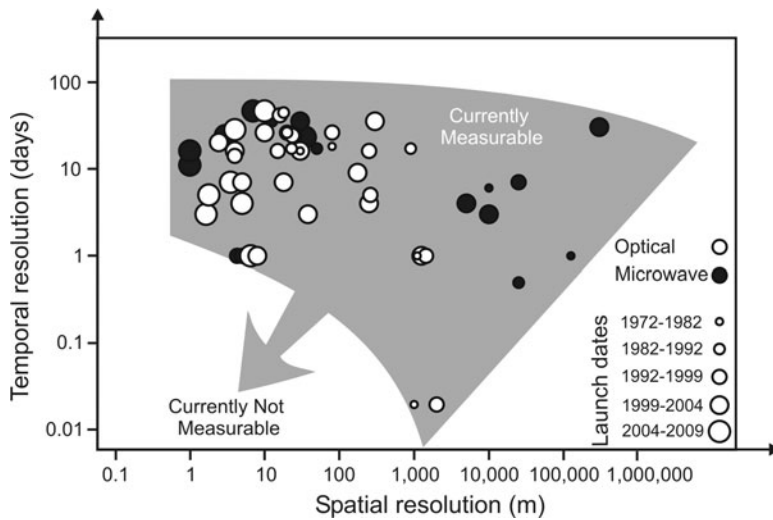
Fig. 3.3 Spatial and temporal resolution of remotely sensed data with a shaded polygon defining limits of currently measurable resolutions. The *arrow* depicts the additional resolutions needed for many forest hydrology applications

Distributed hydrological models, however, have some key shortcomings (Beven 2000), which in part may be answered by the synergistic use of RS and models. Models are plagued by equifinality, the problem of multiple parameter sets that can give the same modeling result, thereby reducing faith in a model's ability to represent real processes. RS imagery may be used as a way to reduce equifinality by providing hydrological information on state variables that can be used to eliminate some of the competing parameter sets (Puech and Gineste 2003). This may be true even if the absolute values of hydrological variables (such as soil moisture) are wrong, but the patterns provide detailed structural information. Another major limitation of hydrological models is the way they deal with water storage, especially in forested wetlands that are not easily identifiable. The power of RS can be harnessed here by mapping the surface or subsurface water reservoirs and including them as spatial objects in the model structure (Creed et al. 2002). Finally, hydrological models need spatially distributed information on initial conditions as well as periodic updates (or checks) of state variables. With the caveats described above, RS imagery may be useful estimates of state variables, including ET, soil moisture, and SWE.

3.4 From Science to Practice

Science-based forest management has been called for by many decision makers; however, implementing science in planning and operational decisions is fraught with difficulty due in part to the wide range of inferences that can be drawn from

scientific findings (Szaro and Peterson 2004). If Kirchner's (2006) call for improved observation to inform theory is true for advancing the hydrological sciences, it applies equally to forest management where better observation will lead to better decisions, provided these data are properly integrated into hydrological process understanding. RS is not a panacea in the provision of data, but it definitely offers spatially explicit datasets, covering large geographies that may inform forest management for tactical and operational planning related to forest hydrology. As an example, we illustrate the use of RS in planning the placement of hydrologically relevant buffer zones.

The primary role of buffer zones around water bodies is to mitigate the adverse effects of land use activities on water, sediment, nutrient, and contaminant fluxes from impacted areas to receiving surface waters. While buffer zones are often required by regulatory agencies to minimize effects on aquatic resources in many jurisdictions, current guidelines for buffer zone width selection have often been established based on best guess, adoption from other forest regions, or political acceptability rather than scientific merit. A fixed buffer width ("one size fits all") is commonly used, but the effectiveness of this approach has been questioned in cases where water bypasses the buffer zone as concentrated flow or as subsurface flow (Buttle 2002). Due to the well-documented strengths of RS in mapping surface hydrological features, RS-derived maps can be used to assess the organization of surface flowpaths prior to the design and placement of buffer strips. These maps may be derived using either static or dynamic approaches, both reliant on RS imagery.

The static approach uses DEMs to map hydrological features. Traditionally, resource agencies derived DEMs and corresponding hydrographic maps using photogrammetry. The inability to see below the canopy meant that many small hydrological features (headwater streams and small wetlands) were inaccurately mapped or missed altogether (Murphy et al. 2007). The recent introduction of LiDAR DEMs in forestry contexts has meant unprecedented realism in the characterization of surficial hydrology compared to the same algorithms applied on existing coarser resolution, photogrammetrically derived datasets. Benefits include better representation of watershed boundaries, location of lower order streams, and more accurate identification of local depressions that form potentially wet areas (Lindsay et al. 2004; Murphy et al. 2007; Remmel et al. 2008). However, in regions with deeper and more complex soils, surface topography may not be the dominant driver of hydrological dynamics. In such cases, static approaches using DEMs may be inappropriate for the prediction of wet areas (Devito et al. 2005). In addition, static approaches do not consider climatic variability, which greatly influences the mapping of hydrological features.

In contrast to static approaches, dynamic approaches use multiple RS imagery to factor in climatic variability on surface hydrological dynamics. As a result, more hydrologically realistic buffers may be designed based on the mapped patterns. For example, Creed et al. (2008) illustrated the use of the return period of saturated and inundated areas derived from a time series of RADARSAT imagery in a boreal landscape to suggest alternatives to fixed-width buffer strip placement. Using this
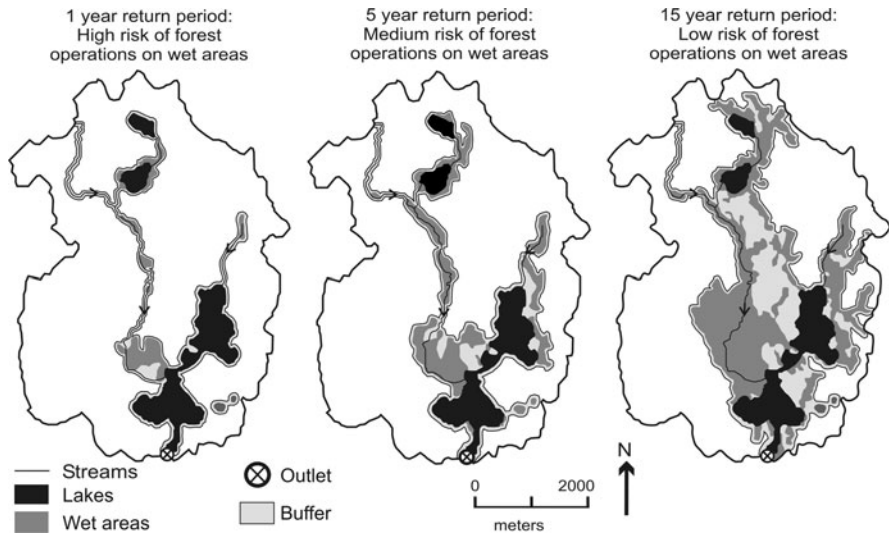
Fig. 3.4 Adaptive-width buffer design. Buffer design is based on hydrological dynamics that consider the return period of a given proportion of a catchment being saturated. If design is based on a 1-year return period, buffers protect a smaller proportion of wet areas, leading to a potentially higher risk of forest operations adversely affecting the hydrological system. If based on a higher return period, larger areas are protected by the buffers, reducing the risk of possible impacts of forest operations on the hydrological system (figure modified from Creed et al. 2008)

probabilistic approach, the amount of area to be retained in buffers is based on the risk tolerance of the forest manager or policy maker. Buffer boundaries may then be prescribed based on the return period of observing a certain proportion of the catchment wetting up, which is in turn related to the magnitude of nutrient and sediment transfer (Fig. 3.4). This exercise is akin to designing bridges and roads to withstand floods of a certain magnitude. However, it is difficult to determine how these return periods are changing in response to climate change and what values society place on maintaining a certain level of water quality.

The incorporation of static or dynamic RS-based hydrological approaches in tactical or operational forestry planning is slowly gaining momentum. While forestry companies have started to use wet area maps in the placement of roads and culverts in an operational sense, the incorporation of RS-derived hydrological information is not routine (Murphy et al. 2008). Unfamiliarity with the strengths and weaknesses of RS technology, high costs of data acquisition, especially for fine resolution datasets such as LiDAR DEMs, and lack of in-house expertise are important obstacles in using RS for tactical and operational forest management planning. This highlights the need for more effective communication of scientific findings to decision makers in policy and management, training of planners and operators in the use of RS techniques, and cooperation between the private sector and government to make RS datasets available at reasonable prices.

3.5   Toward an Operational Bird's-Eye View

There is an urgent need to improve the accuracy and reliability of RS in order to measure fluxes and storages in the hydrological cycle at a range of scales. This will be achieved through innovations in technology, data management, and analytical techniques. More widespread adoption will also result through education and greater sharing of resources. The following recommendations have been echoed by many of the recent review papers in the field of forest hydrology.

3.5.1   Technical Innovation

We need sensors that are designed with the specific purpose of sensing hydrological phenomena. While some of the recently launched and proposed sensors speak to this need (e.g., RADARSAT-2 and SMAP), so far the hydrological community has had to work with products that are not optimized for hydrological purposes. The development of optimal sensors will greatly benefit from the collaboration of ecosystem scientists with design engineers. Key breakthroughs are required in microwave, microgravity, and airborne geophysical sensors. Microwave sensors, especially radar imagers, with multiple polarizations and frequencies are needed in order to better penetrate vegetation canopies to detect soil moisture and to detect SWE. Finer spatial resolution microgravity sensors along the lines of the GRACE sensor, which measures total water content, and airborne geophysical systems, which measure electrical resistivity, will tremendously increase our ability to better characterize the subsurface, still the blackest of the black-boxes for hydrologists. Although airborne geophysical systems are much more expensive (for achieving global coverage) than satellite systems, the slowly changing nature of groundwater systems might make it reasonable to fly such missions.

The synergistic use of satellite RS and airborne geophysical systems would enable powerful imaging of subsurface water systems, since one is strong spatially and the other is strong vertically (Vereecken et al. 2008). Real-time monitoring of the entire hydrological cycle will most likely only occur if the disparate technologies detailed in this chapter are fully integrated into a system, where the strengths of RS, geophysical sensors, distributed wireless sensors on the ground, ground-based radars, and hydrological models are fully exploited and complemented with each other in a GIS setting and broadcast on the internet (e.g., Li et al. 2009a).

3.5.2   Data Archives and Access

There are terabytes of data being processed every day by many sensors; however, much of them are being discarded because there is no mandate or resources to archive all imagery. We need a coordinated public and private effort to archive

imagery acquired by million-dollar sensors. In some instances, imagery has been stored but is locked up in vaults, sometimes in analog format. The opening of the USGS Landsat archives is a boon to scientists, especially ones looking at long-term hydrological trends. Governments around the world need to be encouraged to release their archived RS databases at minimal or no cost (at least to researchers). These programs should be integrated with other long-term monitoring of forest hydrological systems (e.g., monitoring of lake area). It is important that the data made available are in common data formats that can seamlessly interface within GIS.

3.5.3 Data Analytical Techniques

Cross-fertilization of statistical techniques from other fields (such as support vector machines, neural networks, and random forests) has opened up large opportunities for research in applying these methods to hydrological applications. They have already led to breakthroughs in data downscaling (Kaheil et al. 2008). The integration of RS in hydrological models will continue to be a critical research area for years to come. At the minimum, RS products will provide important inputs for parameterization or corroboration such as maps of LAI, land use/land cover, or surface topography. Somewhat more sophisticated is the use of time-series RS imagery as an input, in fashion similar to precipitation. Another novel approach is the identification and input of remotely sensed spatial objects such as wetlands that can inform water redistribution in models. The integration of hydrological models in networks with multiple sensors both on the ground (i.e., wireless sensors, Doppler-radar, and eddy-covariance flux towers) and in the sky can advance the science the most (Chen and Coops 2009). Further integration with spatial decision support systems within GIS will be especially important for managers and other decision makers such as planners.

3.5.4 Interdisciplinary Training

The adoption of RS/GIS techniques by forest hydrologists has been slow. We need transparent and thorough knowledge transfer from product developers and RS scientists to forest hydrologists. Uncertainty, error, and caveats of the latest imaging products need to be well documented; otherwise their use will not be universal. The users of RS imagery will need to learn how to manage and process the raw data, turn it into information, and then transform it into knowledge. The best way for this learning to occur is through the use of Web 2.0 technologies where information flows both ways and "end-users" become "engaged-users" of RS techniques.

3.6 Conclusions

RS of hydrological fluxes and reservoirs at scales relevant to most forest hydrologists is not yet a reality. RS techniques are best suited to observing hydrological storages that cover large areas and change slowly. There are currently operational systems at the global scale that provide daily or weekly updates on the distribution of snow cover, soil moisture, and ET. However, RS of the water budget in headwater catchments on an hourly basis, the main focus for many forest hydrologists, remains problematic. This is related partly to the fact that RS platforms do not continuously observe the same area and therefore do not have the ability to measure continuously key fluxes such as discharge or precipitation. Also, many sensors collect information at spatial scales too coarse for observing hydrological fluxes and storages in low-order catchments. Data fusion and data assimilation of RS imagery within GIS provide ways to improve our ability to monitor low-order catchments. However, the long-term solution is the development of sensors that are being explicitly designed for hydrological applications. This will only occur if hydrologists become more vocal lobbyists in the political arena.

References

Alsdorf DE, Lettenmaier DP (2003) Tracking fresh water from space. Science 301:1491–1494

Alsdorf DE, Melack JM, Dunne T et al (2000) Interferometric radar measurements of water level changes on the Amazon flood plain. Nature 404:174–177

Alsdorf DE, Birkett C, Dunne T et al (2001) Water level changes in a large Amazon lake measured with spaceborne radar interferometry and altimetry. Geophys Res Lett 28:2671–2674

Andreadis KM, Liang D, Tsang L et al (2008) Characterization of errors in a coupled snow hydrology-microwave emission model. J Hydrometeorol 9:149–164

Bastiaanssen W, Menentia M, Feddes R et al (1998) A remote sensing surface energy balance algorithm for land (SEBAL), Part 1: formulation. J Hydrol 212–213:198–212

Batelaan O, De Smedt F (2007) GIS-based recharge estimation by coupling surface-subsurface water balances. J Hydrol 337:337–355

Batelaan O, De Smedt F, Otero Valle MN (1993) Development and application of a groundwater model integrated in the GIS GRASS. HydroGIS 93: application of geographic information systems in hydrology and water resources. In: Proceedings of the Vienna conference. IAHS Publication 211, pp 581–589

Becker MW (2006) Potential for satellite remote sensing of ground water. Ground Water 44:306–318

Beven K (2000) On the future of distributed modelling in hydrology. Hydrol Process 14:3183–3184

Bobba AG, Bukata RP, Jerome JH (1992) Digitally processed satellite data as a tool in detecting potential groundwater flow systems. J Hydrol 131:25–62

Bulcock HH, Jewitt GP (2010) Spatial mapping of leaf area index using hyperspectral remote sensing for hydrological applications with a particular focus on canopy interception. Hydrol Earth Syst Sc 14:383–392

Buttle JM (2002) Rethinking the donut: the case for hydrologically relevant buffer zones. Hydrol Process 16:3093–3096

Bwangoy J-RB, Hansen MC, Roy DP et al (2010) Wetland mapping in the Congo Basin using optical and radar remotely sensed data and derived topographical indices. Remote Sens Environ 114:73–86

Chen BZ, Coops NC (2009) Understanding of coupled terrestrial carbon, nitrogen and water dynamics: an overview. Sensors 9:8624–8657

Clark RB, Creed IF, Sass GZ (2009) Mapping hydrologically sensitive areas on the Boreal Plain: a multitemporal analysis of ERS synthetic aperture radar data. Int J Remote Sens 30:2619–2635

Creed IF, Tague CL, Clark R et al (2002) Modeling hydrologic processes in boreal watersheds: the proof is in the pattern. AGU 83(47) Fall Meeting Supplement, Abstract H61B-0775

Creed IF, Sanford SE, Beall FD et al (2003) Cryptic wetlands: integrating hidden wetlands in regression models of the export of dissolved organic carbon from forested landscapes. Hydrol Process 17:3629–3648

Creed IF, Sass GZ, Wolniewicz MB et al (2008) Incorporating hydrologic dynamics into buffer strip design on the sub-humid Boreal Plain of Alberta. Forest Ecol Manag 256: 1984–1994

Devito KJ, Creed IF, Gan T et al (2005) A framework for broad scale classification of hydrological response units on the Boreal Plain: is topography the last thing to consider? Hydrol Process 19:1705–1714

Entekhabi D, Moghaddam M (2007) Mapping recharge from space: roadmap to meeting the grand challenge. Hydrogeol J 15:105–116

Flaming GM (2005) Global precipitation measurement update. Geoscience and Remote Sensing Symposium, 25–29 July 2005. IGARSS '05. Proceedings. 2005 IEEE International 1:79–82

Gao J (2009) Bathymetric mapping by means of remote sensing: methods, accuracy and limitations. Progr Phys Geog 33:103–116

Glenn EP, Huete AR, Nagler PL et al (2007) Integrating remote sensing and ground methods to estimate evapotranspiration. Crit Rev Plant Sci 26:139–168

Goodrich DC, Scott R, Qi J et al (2000) Seasonal estimates of riparian evapotranspiration using remote and in situ measurements. Agric For Meteorol 105:281–309

Guerschmann JP, Van Dijk AIJM, Mattersdorf G et al (2009) Scaling of potential evapotranspiration with MODIS data reproduces flux observations and catchment water balance observations across Australia. J Hydrol 369:107–119

Hall DK (1996) Remote sensing applications to hydrology: imaging radar. Hydrol Sci J 41:609–624

Hong Y, Gochis D, Cheng JT et al (2007) Evaluation of PERSIANN-CCS rainfall measurement using the NAME Event Rain Gauge Network. J Hydrometeorol 8:469–482

Hwang T, Band L, Hales TC (2009) Ecosystem processes at the watershed scale: Extending optimality theory from plot to catchment. Water Resour Res 45:W11425

Jackson TJ (2002) Remote sensing of soil moisture: implications for groundwater recharge. Hydrogeol J 10:40–51

Jackson TJ, Schmugge J, Engman ET (1996) Remote sensing applications to hydrology: soil moisture. Hydrol Sci J 41:517–530

Jha MK, Chowdhury A, Chowdary VM et al (2007) Groundwater management and development by integrated remote sensing and geographic information systems: prospects and constraints. Water Resour Manag 21:427–467

Kaheil YH, Creed IF (2009) Detecting and downscaling wet areas on boreal landscapes. IEEE Geosci Remote Sens 6:179–183

Kaheil YH, Rosero E, Gill MK et al (2008) Downscaling and forecasting evapotranspiration using a synthetic model of wavelets and support vector machines. IEEE Trans Geosci Remote Sens 46:2692–2707

Kalma JD, McVicar TR, McCabe MF (2008) Estimating land surface evaporation: a review of methods using remotely sensed surface temperature data. Surv Geophys 29:421–469

Kasischke ES, Melack JM, Dobson MC (1997) The use of imaging radars for ecological applications - A review. Remote Sens Environ 59:141–156

Kirchner JW (2006) Getting the right answers for the right reasons: linking measurements, analyses, and models to advance the science of hydrology. Water Resour Res 42:W03S04

Kite GW, Pietroniro A (1996) Remote sensing applications in hydrological modeling. Hydrol Sci J 41:563–591

Klein AG, Hall DK, Riggs GA (1998) Improving snow-cover mapping in forests through the use of a canopy reflectance model. Hydrol Process 12:1723–1744

Kustas WP, Norman JM (1996) Use of remote sensing for evapotranspiration monitoring over land surfaces. Hydrol Sci J 41:495–516

Lang MW, Kasischke ES (2008) Using C-band synthetic aperture radar data to monitor forested wetland hydrology in Maryland's coastal plain, USA. IEEE Trans Geosci Remote Sens 46:535–546

Lang MW, McCarty GW (2009) LiDAR intensity for improved detection of inundation below the forest canopy. Wetlands 29:1166–1178

Lemmetyinen J, Derksen C, Pullianinen J et al (2009) A comparison of airborne microwave brightness temperatures and snowpack properties across the boreal forests of Finland and western Canada. IEEE Trans Geosci Remote Sens 47:965–978

Li X, Li X, Li Z et al (2009a) Watershed allied telemetry experimental research. J Geophys Res 114:D22103

Li ZL, Tang RL, Wan ZM et al (2009b) A review of current methodologies for regional evapotranspiration estimation from remotely sensed data. Sensors 9:3801–3853

Lindsay JB, Creed IF, Beall FD (2004) Drainage basin morphometrics for depressional landscapes. Water Resour Res 40:W09307

Liu J, Chen JM, Cihlar J (2003) Mapping evapotranspiration based on remote sensing: an application to Canada's landmass. Water Resour Res 39:1189

Lu Z, Kwoun O (2008) Radarsat-1 and ERS lnSAR analysis over southeastern coastal Louisiana: implications for mapping water-level changes beneath swamp forest. IEEE Trans Geosci Remote Sens 46:2167–2184

Lundberg A, Nakai Y, Thunehed H et al (2004) Snow accumulation in forests from ground and remote-sensing data. Hydrol Process 18:1941–1955

Lunetta RS, Balogh ME (1999) Application of multi-temporal Landsat 5 TM imagery for wetland identification. Photogram Eng Remote Sens 65:1303–1310

Mackay DS, Ahl DE, Ewers BE et al (2002) Effects of aggregated classifications of forest composition on estimates of evapotranspiration in a northern Wisconsin forest. Global Change Biol 8:1253–1265

Meijerink AMJ (1996) Remote sensing applications to hydrology: groundwater. Hydrol Sci J 41:549–561

Meijerink AMJ (2000) Groundwater. In: Schultz GA, Engman ET (eds) Remote sensing in hydrology and water management. Springer, Berlin, pp 305–325

Min Q, Lin B (2006) Remote sensing of evapotranspiration and carbon uptake at Harvard Forest. Remote Sens Environ 100:379–387

Molotch NP (2009) Reconstructing snow water equivalent in the Rio Grande headwaters using remotely sensed snow cover data and a spatially distributed snowmelt model. Hydrol Process 23:1076–1089

Moran M, Clarke T, Inoue U et al (1994) Estimating crop water deficit using the relation between surface-air temperature and spectral vegetation index. Remote Sens Environ 49:246–263

Moran MS, Peters-Lidard CD, Watts JM et al (2004) Estimating soil moisture at the watershed scale with satellite-based radar and land surface models. Can J Remote Sens 30:805–826

Mu Q, Heinsch FA, Zhao M et al (2007) Development of a global evapotranspiration algorithm based on MODIS and global meteorology data. Remote Sens Environ 111:519–536

Murphy PNC, Ogilvie J, Connor K et al (2007) Mapping wetlands: a comparison of two different approaches for New Brunswick, Canada. Wetlands 27:846–854

Murphy PNC, Ogilvie J, Castonguay M et al (2008) Improving forest operations planning through high-resolution flow-channel and wet-areas mapping. Forest Chron 84:568–574

Nemani R, Pierce L, Running S et al (1993) Forest ecosystem processes at the watershed scale - sensitivity to remotely-sensed leaf-area index estimates. Int J Remote Sens 14:2519–2534

Petty GW (1995) The status of satellite-based rainfall estimation over land. Remote Sens Environ 51:125–137

Petty GW, Krajewski WF (1996) Satellite estimation of precipitation overland. Hydrol Sci J 41:433–451

Puech C, Gineste P (2003) Radar imagery and saturated areas: decreasing model equifinality. Can J Remote Sens 29:729–733

Ramillien G, Famiglietti JS, Wahr J (2008) Detection of continental hydrology and glaciology signals from GRACE: a review. Surv Geophys 29:361–374

Rango A (1996) Spaceborne remote sensing for snow hydrology applications. Hydrol Sci J 41:477–494

Remmel TK, Todd KW, Buttle J (2008) A comparison of existing surficial hydrological data layers in a low-relief forested Ontario landscape with those derived from a LiDAR DEM. Forest Chron 84:850–865

Ritchie JC (1996) Remote sensing applications to hydrology: airborne laser altimeters. Hydrol Sci J 41:625–636

Robinson DA, Binley A, Crook N et al (2008) Advancing process-based watershed hydrological research using near-surface geophysics: a vision for, and review of, electrical and magnetic geophysical methods. Hydrol Process 22:3604–3635

Rosenqvist A, Shimada M, Watanabe M (2007) ALOS PALSAR: a pathfinder mission for global-scale monitoring of the environment. IEEE Trans Geosci Remote Sens 45:3307–3316

Roth BE, Slatton KCS, Cohen MJ (2007) On the potential for high-resolution lidar to improve rainfall interception estimates in forest ecosystems. Front Ecol Environ 5:421–428

Sass GZ, Creed IF (2008) Characterizing hydrodynamics on boreal landscapes using archived synthetic aperture radar imagery. Hydrol Process 22:1687–1699

Schultz GA (1996) Remote sensing applications to hydrology: runoff. Hydrol Sci J 41:453–475

Singh VP, Woolhiser DA (2002) Mathematical modeling of watershed hydrology. J Hydrol Eng 7:270–292

Smith LC (1997) Satellite remote sensing of river inundation area, stage, and discharge: A review. Hydrol Process 11:1427–1439

Stewart JB, Finch JW (1993) Application of remote-sensing to forest hydrology. J Hydrol 150:701–716

Szaro RC, Peterson CE (2004) Evolving approaches toward science-based forest management. For Snow Landsc Res 78(1/2):9–20

Tague CL, Band LE (2004) RHESSys: regional hydro-ecologic simulation system – an object-oriented approach to spatially distributed modeling of carbon, water, and nutrient cycling. Earth Interact 8:1–42

Tang QH, Gao HL, Lu H, Lettenmaier DP (2009) Remote sensing: hydrology. Prog Phys Geog 33:490–509. doi:10.1177/0309133309346650

Townsend PA (2001) Mapping seasonal flooding in forested wetlands using multitemporal Radarsat SAR. Photogram Eng Remote Sens 67:857–864

van der Sanden JJ (2004) Anticipated applications potential of RADARSAT-2 data. Can J Remote Sens 30:369–379

van Zyl JJ (2001) The Shuttle Radar Topography Mission (SRTM): a breakthrough in remote sensing of topography. Acta Astronaut 48:559–565

Vereecken H, Huisman JA, Bogena H et al (2008) On the value of soil moisture measurements in vadose zone hydrology: a review. Water Resour Res 44:W00D06

Verhoest NEC, Lievens H, Matgen P et al (2008) Soil moisture retrieval from ALOS PALSAR in the Alzette (Luxembourg) and Zwalm (Belgium) catchments. The International Workshop on

Microwave Remote Sensing for Land Hydrology Research and Applications. October 20–22, 2008, Oxnard, California, USA

Verhoest NEC, Troch PA, Paniconi C et al (1998) Mapping basin scale variable source areas from multitemporal remotely sensed observations of soil moisture behavior. Water Resour Res 34:3235–3244

Verstraeten WW, Veroustraete F, Feyen J (2008) Assessment of evapotranspiration and soil moisture content across different scales of observation. Sensors 8:70–117

Vorosmarty CJ, Willmott CJ, Choudhury BJ et al (1996) Analyzing the discharge regime of a large tropical river through remote sensing, ground-based climatic data, and modeling. Water Resour Res 32:3137–3150

Wagner W, Bloschl G, Pampaloni P et al (2007) Operational readiness of microwave remote sensing of soil moisture for hydrologic applications. Nord Hydrol 38:1–20

Whitcomb J, Moghaddam M, McDonald K et al (2009) Mapping vegetated wetlands of Alaska using L-band radar satellite imagery. Can J Remote Sens 35:54–72

Wu W, Hall CAS, Scatena FN et al (2006) Spatial modelling of evapotranspiration in the Luquillo experimental forest of Puerto Rico using remotely-sensed data. J Hydrol 328:733–752

Yang F, White MA, Michaelis AR et al (2006) Prediction of continental-scale evapotranspiration by combining MODIS and AmeriFlux data through support vector machine. IEEE Trans Geosci Remote Sens 44:3452–3461

Chapter 4
Digital Terrain Analysis Approaches for Tracking Hydrological and Biogeochemical Pathways and Processes in Forested Landscapes

Irena F. Creed and Gabor Z. Sass

> *We would argue that any mapping or characterization of landscape heterogeneity and process complexity must be driven by a desire to generalize and extrapolate observations from one place to another, or across multiple scales, and must not be allowed to perpetuate the notion of characterization or mapping for its own sake.*
>
> (McDonnell et al. 2007)

4.1 Introduction

Digital terrain analysis (DTA) comprises a set of tools that use digital elevation models (DEMs) to model earth surface processes at a range of scales. DEM and its derivatives are part of a larger set of digital terrain models (DTMs) used in various fields to model the flow of energy and materials across surfaces. The ubiquity of DTMs in the hydrologist's toolkit has led to the widespread use of terrain attributes such as slope and upslope contributing area to characterize the way water and associated nutrients move across landscapes. Algorithms to compute terrain attributes are now programmed into all commercial Geographic Information System (GIS) software (e.g., ArcGIS, Idrisi) and with a push of the button users can map patterns of potential surface hydrological flows. While the derived layers always look visually stimulating, field hydrologists have often raised the question: are DTMs often merely interesting spatial patterns with not much relevance to predicting actual hydrological behavior? This synthesis critically answers this question by discussing the relevance of DTA for practicing forest hydrologists in the twenty-first century.

Topographic information has been exploited to better understand the hydrological functions of catchments since early theories on catchment rainfall-runoff were proposed (Horton 1945; Hewlett and Hibbert 1967). However, prior to desktop computing, catchment scale attributes, such as a catchment's area, length, perimeter and relief ratio (maximum relief divided by longest flow path length), were used to investigate hydrological behavior, because only these attributes could be easily derived from contour maps (Schumm 1956). Although these metrics helped explain differences in water and sediment yields between basins (Garcia-Martinó et al. 1996),

they did little to predict the flow of water within basins. With the advent of the digital age in the 1980s, terrain analysis entered a new era and is now one of the cornerstones of the new computer-enabled toolkit for hydrologists. In many hydrological investigations, it is the first (and sometimes only) step to understanding the way water moves through the landscape since it requires the least data input. New DEM sources, such as laser altimetry, are making it possible to map surface water flow and surface water storage at very fine spatial resolutions and even under dense canopies.

Before pushing any buttons in a terrain analysis system, the hydrologist must consider the physical basis for using topography as the main driver of hydrological flows. Topography controls water flow by directing water from high elevations to low elevations due to the force of gravity and by forcing water to converge or diverge due to the shape of the surface. However, other factors such as climate, geology, soils, and vegetation will also impart some control on the flow of water.

In general, in humid landscapes with shallow soils where the bedrock is impermeable and mimics the surface topography, topography has a strong control on water flow. In these catchments, runoff is first produced in topographically low areas around streams, wetlands and lakes, where the dominant runoff generating mechanism is saturation excess overland flow (Fig. 4.1a). The runoff generating saturated areas vary in size as a function of water input, which results in hydrological behavior that is formally described as variable source area (VSA) dynamics (Hewlett and Hibbert 1967). VSA theory has received considerable experimental support (Dunne et al. 1975) and still lies at the heart of most hydrological models (e.g., Beven and Kirkby 1979; Tague and Band 2004). While providing a good explanation of hydrological behavior in many instances, the list of "exceptions to the rule" has started to increase and many have advocated for a post-VSA hydrological theory (McDonnell et al. 2007). For example, in both subarctic and humid catchments, detailed trenching and tracer work has revealed that flow along the soil–bedrock interface can introduce drainage patterns not well predicted by surface topography (Spence and Woo 2003; Tromp-van Meerveld and McDonnell 2006) (Fig. 4.1b). Interestingly, DTA of bedrock topography has been shown to be useful in explaining the spatial pattern of subsurface flow (Freer et al. 2002). In fact, this type of bedrock driven runoff was also envisaged as part of VSA behavior (Hewlett and Nutter 1970). On the other end of the wetness spectrum, research in subhumid environments with deep surficial deposits has identified runoff to be governed by subsurface high conductivity materials and evapotranspiration by pond side vegetation (Devito et al. 2005) (Fig. 4.1c).

Given these geographic differences in runoff generating mechanisms, users of DTA must carefully decide the physical basis of using DTMs to explain hydrological behavior. Clearly, in geographies where VSA hydrology is dominant, DTA will have a strong conceptual basis. However, hydrologists working in non-VSA dominated terrain might still ask whether analysis of surface topography has some role to play in understanding hydrological behavior. The answer to this question is dependent on spatial and temporal scales. For example, at longer timescales (capturing the full climatic spectrum) and at broader spatial extents (watershed-scale), topography may still be important in predicting the steady-state location of water bodies such as streams and wet areas. Therefore, conceptualization of

Fig. 4.1 Conceptual model of runoff generating mechanisms in three different terrains: (**a**) terrain where water-table mirrors surface topography and runoff may be described by variable source area (VSA) concepts; (**b**) terrain where runoff mechanisms are governed by macropore flow and/or spill and fill subsurface flow along bedrock–soil interface (may be described as a particular case of VSA concept); and (**c**) terrain where subsurface differences in substrate control runoff
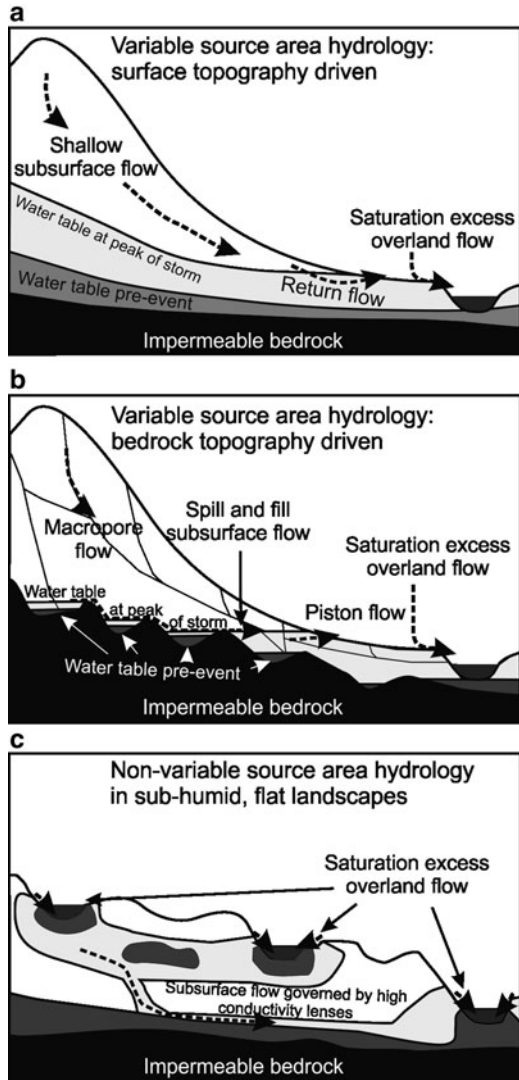
hydrological processes must also consider the scale of analysis when considering the appropriateness of DTA for hydrological investigations.

This chapter is a synthesis of recent advances in DTA techniques and their application to track hydrological and biogeochemical pathways and processes through forested catchments. The discussion is structured to follow the logical evolution of the most relevant and widely used terrain attributes and terrain features that form the basis of analysis in the study of stream initiation, water storage (location and time), and water release (discharge), as well as land-to-atmosphere and land-to-aquatic biogeochemical linkages within different forested landscapes.

Prior to addressing how DTMs have been used in advancing hydrological research, we provide an introduction to the sources of digital elevation data and the basic DTA processing steps required to extract useful hydrological information.

4.2 Digital Terrain Analysis for Forest Hydrologists

4.2.1 Digital Elevation Models

Since DEMs are the ultimate source of all DTMs, their acquisition is the foundation of DTA. DEMs may be derived using three different remote sensing approaches: stereo photogrammetry, radar interferometry, and laser altimetry. Traditionally, stereo pairs of aerial photographs were used to derive DEMs at spatial resolutions of 15–100 m. Canada, USA, and other countries have freely available DEMs, generated using photogrammetry, covering much of their landmass (e.g., http://www.geobase.ca/). The vertical error of these DEMs is in the range of 1–5 m (Natural Resources Canada 2007), with much larger errors over vegetation since the wavelengths used to take the photographs cannot penetrate the vegetation canopy. However, remote areas and poorer jurisdictions have little to no coverage due to the costs associated with flying photogrammetry missions.

Radar interferometric techniques using satellite platforms have been able to provide global coverage of DEMs at 25–100 m spatial resolution, although there is still considerable error in vegetated and mountainous regions (vertical error of 10–20 m) (Bourgine and Baghdadi 2005). Radar interferometry uses two or more radar images to compute the differences in the phase of the waves returning to the satellite. The shuttle radar topography mission (SRTM) provided the first global dataset at sub 100 m resolution for use in DEM development (Farr et al. 2007).

Of the three DEM sources, it is laser altimetry, also known as light detection and ranging (LiDAR) sensors, that has revolutionized the collection of elevation data. LiDAR sensors collect submeter spatial resolution datasets at much higher vertical accuracy (15–30 cm) even in dense vegetation (Reutebuch et al. 2003). The only limitation to LiDAR-derived DEMs is that they are very expensive to acquire from airborne platforms. Future satellite-based LiDAR sensors are needed to allow for imaging of the entire globe at fine spatial resolutions. From the raw elevation points, three main tessellations can be chosen: square grid, triangulated irregular network, and contour-based network (Moore et al. 1991). Of these, the square grid is by far the most common type and this chapter focuses solely on DTMs of this type of tessellation.

4.2.2 Modeling Hydrological Flowpaths

Hydrological flowpaths are modeled using DEMs based on the assumption that water flows along surface or shallow subsurface pathways parallel to the surface. Prior to modeling, the digital surface must be hydrologically conditioned. The first

step of hydrologically conditioning is to "burn" water bodies (streams and lakes) into the DEM to ensure higher order streams and lakes coincide with the digital hydrography derived from aerial photographs whose locations are well accepted by the hydrological community (Hutchinson 1989). It is noteworthy that first- and second-order streams are often not represented in the digital hydrography and are therefore not represented in the DEM. The next step is to ensure that water can "flow" unimpeded from each grid cell to the outlet. In every DEM, there are depressions that terminate the flow of water, usually due to data error, interpolation, and limited horizontal and vertical resolution (Martz and Garbrecht 1998). For this reason, depressions need to be removed and drainage must be enforced across all ambiguous areas including topographic flats and depressions (Martz and Garbrecht 1998). Depressions may be filled by raising the elevation of all depression grid cells or breached by lowering grid cell elevations along a breach channel (Planchon and Darboux 2001). The difference between methods may be substantial; therefore, selective use of either approach is suggested to reduce the overall impact on the DEM modification (Lindsay and Creed 2005). Not all depressions are artifacts and their identification is critical especially in the delineation of biogeochemical source areas to streams. Lindsay and Creed (2006) introduced an innovative probabilistic method of identifying true depressions on the digital landscape.

Once the DEM has been hydrologically conditioned, flow direction can be determined, which is critical for tasks such as delineation of catchment boundaries, stream networks, upslope contributing area, and anything else where flow direction needs to be modeled. Hydrological flow routing is based on the question: which way does a drop of water flow over a surface (Table 4.1)? Given the gridded discretization, there are only eight potential cells water may flow to. The easiest option is directing the flow along the steepest neighboring cells (referred to as the D8 approach) (O'Callaghan and Mark 1984), creating very distinct but often unrealistic linear flow patterns on hillslopes. Paik (2008) improved the realism of flow direction of D8 by allowing for variable neighborhood searches used to determine slopes (GD8). However, more realistic flow dispersal can only be achieved with multiple flow direction algorithms that override the limitation of D8 and GD8 by apportioning flow to more than one downhill cell either by (1) random weighting (Rho8) (Fairfield and Leymarie 1991), (2) weighting by slope gradient and slope length (FD8) (Quinn et al. 1991), (3) fitting a triangular facet (Tarboton 1997), or (4) by a combination of facet fitting and assigning weights by slope (MDinfinity) (Seibert and McGlynn 2007). Perhaps a more accurate approach of multiple flow direction routing, but also more complex and case-specific, is based on flow lines [Digital Elevation Model Networks (DEMON)] (Costa-Cabral and Burges 1994). Recent research in flow routing has advocated the use of "smart routers," where flow on hillslopes is routed using dispersive algorithms and flow focusing routing below channels heads (Lindsay 2003). Investigators comparing these common flow routing algorithms found most algorithms to be efficient in finding channels; however, choice of algorithm strongly affected flow path distributions on hillslopes (e.g., Wolock and McCabe 1995; Desmet and Govers 1996). In summary, differences in flow routing algorithms are least important for finding channels and predicting drainage divides and most important for predicting hillslope distribution of soil moisture.

Table 4.1 Evolution of hydrological flow routing algorithms

Name	Summary	Details	References
D8	Directs flow from each cell to one of the eight nearest neighbors based on slope gradient	Computationally simple, but does not allow for multiple flow directions; bias toward eight cardinal and diagonal directions produces artificial straight lines	O'Callaghan and Mark (1984)
GD8	Directs flow from cells to one of the eight nearest neighbors based on local slope gradient and corrects using higher-order neighborhood searches (up to global search)	Removes accumulated directional error associated with single flowpath algorithms, but does not allow for multiple flow directions	Paik (2008)
Rho8	Random numbers weighted by slope (i.e., flowpaths with steepest gradients have greatest probability) used to direct flow from cells	Removes bias toward eight neighboring directions; degree of randomness breaks up parallel straight flowpaths that D8 tends to produce on flat surfaces, resulting in more realistic-looking networks, but a different network can be produced with each iteration	Fairfield and Leymarie (1991)
FD8	Directs flow to downslope cells weighted by slope gradient, slope length, and directional weights	May produce artificial flow dispersion because flow goes to all downslope grid cells. Multiple flowpaths produce artificial flow dispersion and path crossing on convergent slopes	Quinn et al. (1991)
DEMON	Directs flow from cells using local aspect angle vector calculated from two-dimensional flow strips defined by convergence/ divergence	Produces more realistic flows, but may produce inconsistent results and is computationally complex and may produce inconsistent flowpaths. Computationally complex; two-dimensional planes fit to some elevation combinations leading to inconsistent flow directions	Costa-Cabral and Burges (1994)
ADRA	Directs flow according to slope gradient and prediction of cell's position relative to channel head	Simulates divergence on slopes and convergence in channels	Lindsay (2003)
D∞	Directs flow from cells following path of steepest descent calculated in planar triangular facets between centroids of neighboring cells (infinite angles)	Produces more realistic flows, but may produce unrealistic results in flat areas	Tarboton (1997)
MD∞	Directs multiple flows from cells following path of steepest descent calculated in planar triangular facets between neighboring cell centers (infinite angles) and weighted by slope gradient	Removes dispersion on planar or concave slopes; allows multiple directions on convex slopes	Seibert and McGlynn (2007)

4.2.3   Hydrologically Relevant Terrain Attributes and Terrain Features

At the heart of all DTAs is a set of terrain attributes and terrain features that are used to model hydrological pathways and associated processes. Terrain attributes, on the one hand, are derived from DEMs either by computing surface derivatives or various physical characteristics of flow lines including length, contributing area, and elevation differences. Terrain features, on the other hand, are landform features that share unique physical characteristics defined by various terrain attributes. Terrain attributes can be thought of as continuous grids, whereas terrain features are discontinuous (or discrete) objects.

Although there is a long list of terrain attributes that can be computed from DEMs (e.g., Moore et al. 1991; Wilson and Gallant 2000), only a handful are useful in hydrological or biogeochemical modeling. One of the most important of these attributes is slope, because it is used to approximate the hydraulic gradient, the variable that determines the rate at which water can move through a point (Fig. 4.2). Areas with low slope have a low propensity to transmit water laterally and therefore favor the accumulation of water and the formation of saturated and inundated zones. Upslope contributing area is as important to consider as slope because it provides an approximation of the potential runoff volume that may pass through a point. Valley-bottoms have much larger upslope contributing areas than ridges and are the reason why most saturated or inundated areas are located at the bottom of hillslopes. Combining the concept of hydraulic gradient with potential runoff volume is essential in determining the potential for water accumulation because areas of low slope on higher plateaus or flat ridgelines will not be classified as saturated due to much smaller upslope contributing areas. While slope and upslope contributing area are the two most important terrain attributes for hydrologically or biogeochemically relevant terrain analyses, measures of profile and plan curvature
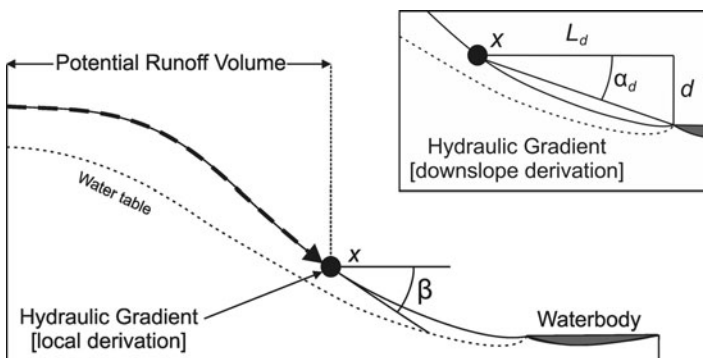
Fig. 4.2 Hydrologically important terrain attributes used in the modeling of water, nutrient, and sediment redistribution along a hillslope

as well as elevational differences between grid cell of interest and local or global elevation minima and maxima are also important for classifying terrain features. Curvature gives an indication of flow divergence or convergence, whereas elevation differences give an indication of hydraulic pressure.

Another way to model spatial variability in the relative importance of hydrological and biogeochemical processes is by classifying catchments into different terrain features, where each unique object class is assumed to behave in a similar fashion with respect to the process being modeled. Such object-oriented analysis overcomes the limitations of looking at individual terrain attributes and instead factors in additional spatial, textural, and contextual information from multiple terrain attributes. Perhaps, the simplest way of classifying landscapes is by differentiating between hillslopes and riparian areas, which has been found to be useful in explaining hillslope coupling to streams (McGlynn and Seibert 2003). More elaborate landscape classification approaches are based on the concept of the catena (Conacher and Dalrymple 1977). These approaches identify terrain features from the top of hillslopes to the bottom, including crest, shoulder, backslope, footslope, toeslope and valley-bottoms, each corresponding to zones of different hydrological, pedological, and biogeochemical processes (Fig. 4.3). From a longitudinal perspective, it is common (and important from a forest management perspective) to differentiate between colluvial and fluvial channel segments, especially in mountainous regions of western North America (Montgomery and Buffington 1997).

The challenge of landscape classification is to find the combinations of terrain attributes that can differentiate between the required terrain features (e.g., riparian zone vs. hillslopes). This is not a trivial process. The most fruitful approaches have involved the application of fuzzy boundaries given the inexact definition of the transition zones (MacMillan et al. 2000). The terrain attributes and heuristic
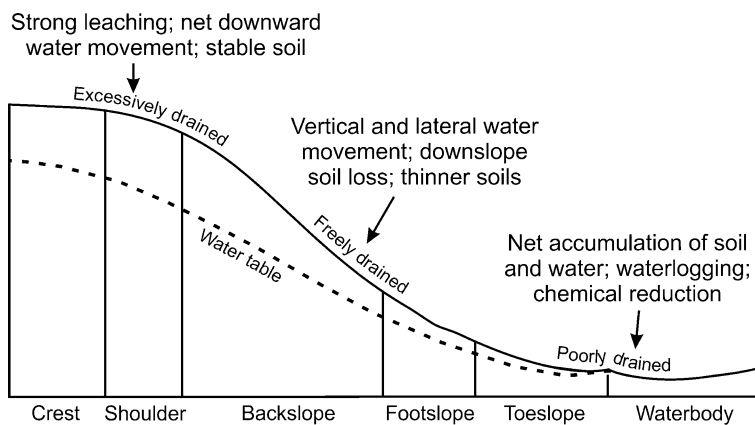
Fig. 4.3 Hydrologically important terrain features used in the modeling of water, nutrient (dissolved and gaseous), and sediment redistribution along a hillslope

classification rules have to be determined for each landscape and often need expert guidance. An alternative classification system fits a mathematical function to the cumulative distribution function of a modified upslope contributing area index (Roberts et al. 1997). It uses derivatives of this function to find breakpoints that are used to create four categories: the combination of ridge tops and upper slopes, midslopes, lower slopes, and in-filled valley/alluvial deposits (Summerell et al. 2005). This approach has successfully delineated major landforms across six catchments with different geologies in Australia but needs to be evaluated on other forested landscapes.

Successful applications of terrain attributes or terrain features in the analysis of hydrological or biogeochemical processes are predicated on the careful consideration of process conceptualization in the selection of proper DTA tools.

4.2.4   Scale Issues

Another important consideration when selecting the most appropriate DTA tools for the process being modeled is scale. One of the central features of DTA is that it is scale dependent (Band and Moore 1995). Although there are different components of scale, such as extent, support and spacing (Blöschl and Sivapalan 1995), the main concern for DTA has been the effect of support or spatial resolution on hydrological modeling. Numerous studies have investigated the effects of DEM spatial resolution on the derivation of terrain attributes and hydrological objects such as stream networks (McMaster 2002; Deng et al. 2007; Sorensen and Seibert 2007). These studies have found that most terrain attributes and features are very sensitive to the spatial resolution at which they are derived (Zhang and Montgomery 1994), and therefore, the hydrological features modeled must be properly matched to the spatial resolution of the DTM.

Beven (1997) suggests that to avoid significant error, terrain attributes should be derived at spatial resolutions well below the average slope lengths of a landscape. However, the reverse is also true where the spatial resolution is too fine to model the hydrological process properly. For instance, due to submeter spatial resolution, laser altimetry derived DEMs may contain too much detail to have hydrological usefulness. This fine spatial resolution may negatively affect the derivation of terrain attributes or require too much computational power because of the large DEM size (Creed et al. 2003). While the optimal grid size needs to be determined for each hydrological process (Zhang and Montgomery 1994), a general rule of thumb is that hillslope-scale features should be modeled with DEM resolutions of 1–5 m, whereas catchment-scale features can be modeled at 5–10 m resolution (e.g., Thompson and Moore 1996).

In the following sections, the potential of some traditional but mostly novel approaches to identify hydrological (Sect. 4.3) and biogeochemical (Sect. 4.4) pathways and associated processes in forested landscapes described in Table 4.2 are illustrated.

Table 4.2 Digital terrain indices used to infer different hydrological and biogeochemical patterns and processes in forested landscapes

Hydrological index	Calculation	Description	References
Drainage network			
Stream initiation	$A_s > C$; where A_s is specific contributing area, and C represents a critical threshold to define the stream channel	Delineates stream network by assuming upslope area controls channelized flow	O'Callaghan and Mark (1984)
Stream initiation	$A_s \tan \beta^{\alpha} > C$; where A_s is specific contributing area, $\tan \beta$ is local slope, α is modifier representing geological differences, and C represents a critical threshold to define the stream channel	Delineates stream network by assuming upslope area is modified by local slope controls channelized flow	Montgomery and Dietrich (1992)
Wet areas			
Local slope index	$\tan \beta < C$; where $\tan \beta$ is computed using finite differences in four cardinal directions, and C represents a critical threshold to define a wet area	Describes wet areas by assuming water accumulation in flat areas is due to local topography	Creed et al. (2003)
Topographic wetness index (TWI)	$\ln(A_s/\tan \beta) > C$; where A_s is specific contributing area, $\tan \beta$ is local slope, and C represents a critical threshold to define a wet area ($\tan \beta$ may be replaced by $\tan \alpha_d$ to consider downslope gradient)	Describes wet areas by assuming water accumulation in float areas is due to upslope and local topography	Beven and Kirkby (1979)
Downslope distance or downslope gradient index	$L_d > C$; where L_d is the downslope distance index defined as the horizontal distance to the point with an elevation d meters below the elevation of the starting cell following the steepest-direction flowpath, and C represents a critical threshold to define a wet area. A modification of this index is $\tan \alpha_d = d/L_d$, where $\tan \alpha_d$ is the downslope gradient index. The d is catchment dependent and needs to be defined for each new locale	Describes wet areas by assuming water accumulation in flat areas is due to upslope, local and downslope topography	Hjerdt et al. (2004)
Hydrogeomorphic terrain feature detection and classification	Terrain features delineated from an edge-enhanced downslope gradient index ($\ln(\tan \alpha_d)$) map	Describes wet areas by hydro-geomorphic features using object-based classification	Richardson et al. (2009)

(continued)

Table 4.2 (continued)

Hydrological index	Calculation	Description	References
Depth-to-water table index	Depth-to-water table is computed in an iterative fashion: (1) cumulate slope values along each flowpath, (2) select least cumulative slope path from source cell to surface water cell, (3) assign cumulated slope value of surface water cell to source cell, (4) take difference of local slope and cumulated slope, and (5) threshold the depth-to-water table index	Describes wet areas by factoring in both the distance from a surface water source and the slope of the land surface between the cell of interest and the surface water source cell	Murphy et al. (2007)
Probability of depression index	$p_{dep} < C$; where p_{dep} is probability of a cell belonging to a topographic flat or depression and C represents critical thresholds to define a wet area. The probability layer is computed Monte Carlo style: (1) add random error term to DEM, (2) extract flats and depressions, and (3) average across all binary realizations	Describes wet areas by assuming all flats and depressions identified by algorithm are areas of water accumulation	Creed et al. (2008)
Hydrological flushing potential			
Variable source area (VSA)	Recursive accumulation of catchment area with normalized TWI $(TWI_n) <$ max catchment TWI_n at stream	Describes hydrologically responsive part of catchments	Creed and Beall (2009)
Effective VSA (*eff*VSA)	Upper quartile of frequency distribution of TWI_n within VSA	Describes hydrological flushing areas, where water table rises to soil surface	Creed and Beall (2009)
Rate of change in flow gradient of VSA	Second derivative of a polynomial equation derived from the frequency distribution of TWI_n within *eff*VSA	Describes potential rate of expansion or contraction of hydrological flushing areas	Creed and Beall (2009)
Hydrologic filtering potential			
Riparian area	Ratio of riparian area to upslope contributing area	Describes riparian buffering capacity of catchments	McGlynn and Seibert (2003)
Riparian curvature	Profile curvature of cells surrounding stream or lake	Describes riparian buffering capacity (via surface vs. subsurface flowpaths) of catchments	Devito et al. (2000)

Table 4.2 (continued)

Hydrological index	Calculation	Description	References
Hydrological connectivity of wet areas to drainage network			
Wet areas connected to surface drainage network or shoreline	Connectivity is defined by the % wet area within upslope contributing area connected to surface waters	Describes hydrological connectivity of wet areas to surface water	Devito et al. (2000) and Sass et al. (2008)
Network index	Connectivity is defined by an analysis of TWI along flowpaths; wet areas contribute to stream discharge only when TWI indicates continuous wetness through the length of a flowpath to the point where the path becomes a stream	Describes hydrological connectivity within drainage network	Lane et al. (2004)
Hydrological residence time			
Median subcatchment area	Median of the subcatchment areas of all stream cells upstream the catchment outlet	Describes catchment-scale differences in drainage structure and residence time	McGlynn et al. (2003)
L/G index	L/G; where L is flowpath distance and G is flowpath gradient	Describes catchment-scale mean water residence time	McGuire et al. (2005)
Compound indices for geographies where topography is not the only dominant control on water flow			
Combined soil-TWI	$\ln(A_s/T \tan \beta)$; where T is lateral transmissivity at saturation of surface soils in the catchment	Modifies TWI by including soil transmissivity as a function of runoff generation (requires knowledge of pattern of hydraulic conductivity and soil depth)	Beven (1986)
Combined climate-soil-TWI	Modifies the size of each cell in the TWI calculation as a function of mean annual water balance relative to catchment average	Modifies TWI to capture the effect of climatic forcing	Güntner et al. (2004)
Hydrogeological index	Index is computed as a function of three factors (Strahler stream order, relative elevation of lake to surrounding landscape, and position of lake within local to regional groundwater flow system), which are combined into an empirical model with weighting of factors calibrated with an independent measure of hydrogeological setting	Describes potential groundwater-lake interactions as recharge vs. discharge areas	Devito et al. (2000)

4.3   Tracking Hydrological Pathways Using Digital Terrain Analysis

4.3.1   Where Do Streams Begin?

Streams begin in the generally uncharted headwaters either within cryptic rivulets and/or wetlands (Creed et al. 2003; Bishop et al. 2008). These hidden source areas of water are not captured on traditional topographic maps; therefore, novel approaches have been sought for their mapping. DTA, especially based on LiDAR-derived DEMs, has significantly improved our ability to map headwater streams in forested environments (Remmel et al. 2008). The difficulty in determining the exact position of stream heads from topographic data alone is that there are additional climatic and geological factors that play a role in stream initiation. Stream networks may be mapped in one of the two ways: (1) analyzing surface morphology and looking for specific patterns such as "v" shapes (Peucker and Douglas 1975), or (2) calculating upslope contributing areas and delineating stream cells based on critical thresholds (O'Callaghan and Mark 1984). Practitioners favor the flow-based method because the morphology-based approaches do not result in a continuous network, something that is critical for topological analysis (Lindsay 2006). The simplest flow-based method classifies stream cells based on specific contributing area alone (O'Callaghan and Mark 1984). The pioneering work of Montgomery and Dietrich (1992) determined that the product of specific catchment area and the square of the local slope can be used to predict the initiation of channelized flow, although with considerable uncertainty (Table 4.2). However, channel initiation thresholds need to be validated in each new locale.

Although the choice for stream initiation thresholds is variable between catchments, the choice of flow routing algorithm is not as critical for stream network delineation because upslope contributing areas derived by different flow algorithms start identifying very similar stream networks in valley bottoms. In fact, single flow algorithms are usually preferred because they identify areas of convergence well, although they may still tend to generate parallel channels in valley bottoms (McGlynn and Seibert 2003). Once the stream network has been extracted, it may serve as the foundation for segmenting the catchment into hillslopes based on stream reaches, defining riparian areas, or extracting physical characteristics of the stream network such as stream order and drainage density. A critical component in many forested landscapes is the presence of wetlands and lakes; however, the incorporation of these open water features is not yet a commonplace feature of most DTA software.

4.3.2   Where is Water Stored?

Water in catchments is held in both surface and subsurface storages. Although subsurface storage of water can be substantially greater than surface storage, surface water storage is particularly important in terms of hydrological response

(rapid water delivery to stream or lake) as well as biogeochemical behavior (e.g., export of nutrients). DTA is particularly well suited to estimate the location and amount of surface water storage. Surface water is stored in depressions or flat areas that inhibit the downhill movement of water. These wet areas may be ephemeral (e.g., small depressions collecting water) or permanent (e.g., bottomland swamps). Wet areas not only store water and therefore retard runoff (if the depression is not at capacity) or enhance runoff (if at capacity), but they may also form critical spots for biogeochemical activity (Agnew et al. 2006).

In many landscapes, topography influences the development of saturated and inundated areas through its effect on the hydraulic gradient. The last three decades have seen many different DTA techniques developed in order to automate the derivation of wet areas (Fig. 4.4). Slope has been a very effective terrain attribute to delineate wet areas (Creed et al. 2003). The shortcoming of using slope
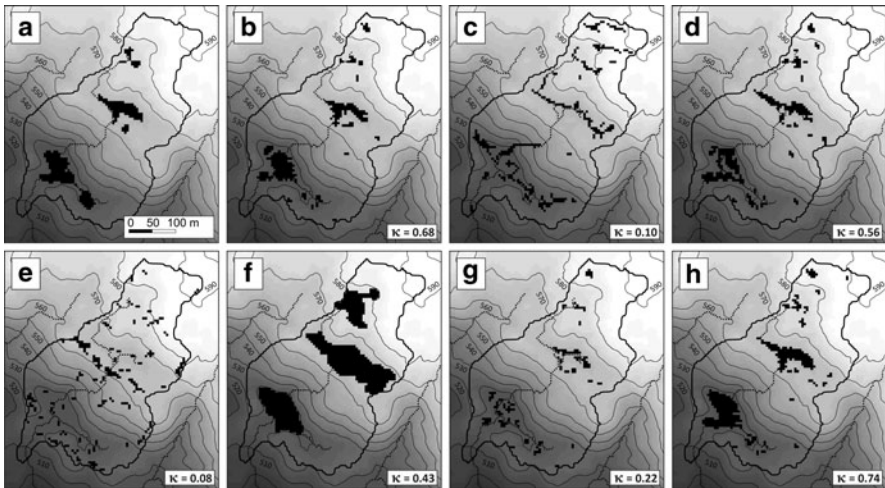
Fig. 4.4 Comparison of digital terrain analysis (DTA) techniques for wet area mapping. Base map is a 5 m LiDAR-derived DEM of catchment (c50) in the Turkey Lakes Watershed in Ontario, Canada. Wet areas were defined by (**a**) ground surveys using a differential global position system to collect geographic coordinates of the boundaries of wet areas; (**b**) local slope, β, $\leq$ critical threshold of $2.7°$ (Creed et al. 2003); (**c**) topographic wetness index, $\ln(A_s/\tan \beta)$, $\geq$ critical threshold of 6.9 (Beven and Kirkby 1979); (**d**) downslope gradient index, $\tan \alpha = d/L_d$, with $d = 2$ m and $\alpha \leq$ critical threshold of $1.7°$ (Hjerdt et al. 2004); (**e**) TWI modified by use of downslope gradient instead of local gradient, $\ln(A_s/\tan \alpha)$, $\leq$ critical threshold of 2.9 (Hjerdt et al. 2004); (**f**) objects classified using downslope gradient index and L/G (Richardson et al. 2009); (**g**) depth-to-water index, where index $\leq$ critical threshold of 1 m (Murphy et al. 2007); and (**h**) probability of depression index, where index $\leq$ critical threshold of 0.3 (Creed et al. 2008). Critical thresholds selected to optimize area to ground-surveyed wet areas. For each map, κ is kappa coefficient showing level of agreement in terms of location and area between DTA-derived map and ground-surveyed map, where 0 is agreement due entirely to chance and 1 is 100% agreement

alone to map wet areas is that there may be low slope areas close to ridgelines (e.g., plateaus) with no water storage observed. The solution to this problem was introduced by the seminal work of Beven and Kirkby (1979), who integrated the concept of runoff volume (using upslope contributing area as a proxy) with hydraulic gradient into a compound index. This topographic wetness index (TWI) has been successfully used around the world to delineate wet areas (Quinn et al. 1995; Güntner et al. 2004), albeit only in humid conditions when surface topography is a reasonable replica of the water table (Western et al. 2001).

One of the limitations of the TWI is that it only takes into account the upslope properties of the hillslope. To incorporate the influence of downslope effects on drainage, Hjerdt et al. (2004) introduced the downslope index, which considers the horizontal distance water would have to travel along a flowpath to drop a given vertical distance (Fig. 4.2). This index is very versatile and has been used in three main ways in identifying wet areas: (1) as a downslope hydraulic gradient; (2) as a new TWI to replace TWI and (3) as a replacement of the local slope term in a modified TWI (Güntner et al. 2004; Hjerdt et al. 2004; Inamder and Mitchell 2006; Sorensen et al. 2006). In terms of approximating the water table gradient, the downslope index greatly improves approximations based on local slope, because local slope is highly sensitive to DEM resolution.

The past decade has seen a number of novel approaches introduced in mapping wet areas that go beyond the traditional approach of identifying a threshold in a terrain attribute (Table 4.2; Fig. 4.1). A recent study used object-based classification to define hydrologically meaningful terrain features using the spatial distribution of downslope gradient as an input (Richardson et al. 2009). The depth-to-water index uses least cost analysis based on a cumulative slope layer from the point of interest to a source cell (stream, lake, or depression) (Murphy et al. 2007). It has been validated in humid catchments on the east coast of Canada and used in forest operations planning (Murphy et al. 2007). Lindsay et al. (2004) identified wet areas based on a probabilistic scheme using Monte Carlo simulation, where a random error term, based on the vertical accuracy of the DEM, was added to the DEM and depressions flagged after each of 1,000 iterations. A layer depicting probability of belonging to a depression was calculated by averaging the individual depression maps, and grid cells above a certain depression probability threshold were identified as a true depression with the potential to saturate or inundate. This method has been very accurate in identifying even cryptic wetlands below dense canopies in forests across eastern Canada (Creed et al. 2003).

It needs to be noted that the source of the input data is critical for each of these techniques. Although there has been some success in DTA modeling of wet areas below canopies using generally available DEMs from provincial or state government agencies (Creed et al. 2008), the best success comes if the DEM is derived from a source that penetrates the canopy (Creed and Beall 2009). Currently, only laser altimetry-based DEMs provide information from below the canopy, emphasizing the need to provide global coverage using this technology.

4.3.3   How Are Water Source Areas Connected
to Surface Waters?

Hydrological response to rainfall at the outlet of catchments is highly dependent on the ability of water source areas to connect to surface waters such as streams and lakes. The basic premise is that saturated areas are prone to the generation of lateral flow leading to quick runoff at the catchment outlet only if they are connected to the stream network of the catchment. Although substantial foundational work on hydrological connectivity has been done, the incorporation of the concept of connectivity into a coherent hydrological framework is only now being undertaken (Bracken and Croke 2007).

A simple measure of connectivity that has been applied in a broad range of forested landscapes is the percent cover of all wet areas that are contiguous and connected to the stream network (e.g., Devito et al. 2000; Creed et al. 2003; Creed and Beall 2009). Another measure of connectivity is based on TWI values along a flowpath; if all upslope cell values are above a given TWI threshold, then all upslope cells are assumed to contribute to stream flow. Using this approach, a large proportion of saturated sources areas were found to be disconnected from the streams, which otherwise would have been assumed to be connected and contribute to stream flow (Lane et al. 2004).

Jencso et al. (2009) strengthened the case for the need to consider both topography and topology (the spatial relationship between terrain attributes) as first-order controls on stream flow response in steep and humid catchments. They found that upslope contributing area explained 91% of the variability in the longevity of the water table connection among hillslope, riparian zone, and stream sequences. The analysis of hydrological connectivity has greatly benefited from ideas infused by geostatistics (Western et al. 2001) and percolation theory (Lehmann et al. 2007). Although much ground-breaking work has been done in exploring hydrological connectivity with DTA, fully integrating this concept into the analysis of catchment hydrology has been slow. As a result, there is great potential for new discoveries and understanding, especially related to the nonlinear behavior of stream flow response.

4.3.4   How Long is Water Stored?

Knowing the length of time a water droplet resides in a catchment is important because the longer a water droplet is in contact with the substrate of a catchment, the greater chance it has to undergo and facilitate biogeochemical reactions (Burns et al. 2003). The residence time of all of the droplets is a fundamental catchment descriptor called the mean residence time (MRT), which can reveal important information on storage, flowpaths, and sources of water (McGuire and McDonnell 2006). MRT can be modeled using a residence time model with stable isotopes of oxygen and hydrogen as inputs (McGuire et al. 2005). However, given

the usefulness of this catchment-wide descriptor, recent studies have focused on investigating the relationship between MRT and catchment characteristics, in order to facilitate automated computation for ungauged catchments.

Contrary to the expectation that catchment size would explain variation in MRT among catchments, MRT was instead correlated to catchment terrain attributes such as median subcatchment area (McGlynn et al. 2003) as well as median flowpath distance and flowpath gradient to the stream network in humid catchments (McGuire et al. 2005). MRT was negatively related to flowpath gradient (shorter MRT with steeper flowpath gradient) and positively related to median flowpath length and median subcatchment areas (longer MRT with longer flowpath length), reflecting the expected relation between hydraulic gradients and water flow. It is interesting to note that although hillslope-scale runoff production in these humid catchments is influenced by subsurface macropore and bedrock flowpaths, surface topographic properties explain the majority of the variation in MRT, which is strongly influenced by the substrate. Perhaps, this provides evidence for the fact that topography is a reflection of climatic forcing on geological substrates. The ratio of flowpath length to flowpath gradient was a weaker predictor in Scottish catchments but still able to explain 44% of the variation in MRT (Tetzlaff et al. 2009).

4.3.5 How Does Topography Influence Flow Response at the Catchment Outlet?

DTA's strength has been at explaining inter-catchment variability in discharge. In general, DTA provides metrics on capturing spatial differences in storage of water and the efficiency of water transfer through a catchment (Table 4.2). Although more traditional attributes such as catchment area, slope, and drainage density are still useful today, especially in studies where only coarser resolution DEMs are available (Garcia-Martinó et al. 1996), newer techniques in combination with newer DEM sources provide the next generation of tools.

For example, the importance of delineating cryptic wetlands under a forest canopy in order to understand stream response was highlighted by Lindsay et al. (2004), who were able to predict both runoff timing and runoff magnitude using wetland metrics from a LiDAR-derived DEM. The performance of the different wetland metrics (e.g., total area of bottomland wetlands, depression volume of wetlands) depended on hydroclimatic conditions. During dry and mesic conditions, wetland metrics explained a higher proportion of the variation of runoff *timing*, whereas during wet conditions, wetland metrics explained a higher proportion of variation of runoff *magnitude* (Lindsay et al. 2004). Along similar lines, Laudon et al. (2007) were able to explain a significant proportion of the variation in event and pre-event partitioning using median subcatchment area, which is another measure of stream network organization. Interestingly, median subcatchment area was useful to predict the pre-event/event ratio at peak flood and on the hydrograph's falling limb, but on the rising limb percent wetland area was the significant factor (Laudon et al. 2007). There is also

evidence that the effectiveness of terrain attributes to explain hydrological response depends not only on hydroclimatic conditions but also on catchment size. Sanford et al. (2007) reported on the existence of a catchment area threshold for low flow conditions, where low flow hydrograph metrics were successfully predicted by the proportion of near stream riparian area within catchments less than 600 ha in size. These examples point to the ability of DTA to capture hydrological source areas, storages, and connectivity with the ability to predict flow response related to catchment size and hydroclimatic conditions.

4.3.6   Digital Terrain Analysis Beyond Topography

Clearly, topography is not a first-order control in every catchment. Consequently, the future of DTA lies in its ability to fuse data and approaches that incorporate other dominant controls on hydrological processes including climate, geology, and soils (Table 4.2). For example, Güntner et al. (2004) proposed factoring in climate patterns in the TWI. Studying catchment-scale differences in hydrological and biogeochemical response, Devito et al. (2000) proposed a hydrogeologic index that incorporated the concepts of stream ordering, relative relief, and recharge vs. discharge nature of lakes, all estimated by proxies derived from topography. In another study, Baker et al. (2003) developed a DTA technique that approximated the regional hydraulic gradient and integrated this information with hydraulic conductivity estimated from surficial geologic maps. Beven (1986) introduced soil transmissivity in the calculation of TWI to account for changes in soil hydraulic conductivity within catchments. In landscapes where depressions on the bedrock surface control fill-and-spill flow (Spence and Woo 2003; Tromp-van Meerveld and McDonnell 2006), it is not so much the DTA techniques that need to be modified but that a DEM is needed of the bedrock surface (Freer et al. 2002; Lehmann et al. 2007). Unfortunately, wide-scale application of these integrative approaches is hindered by the lack of bedrock DEMs as well as other spatially distributed information on climate, geology, and soils.

4.4   Tracking Biogeochemical Pathways Using Digital Terrain Analysis

Hydrology influences biogeochemical cycling through its control on the conditions of chemical reactions (e.g., temperature, moisture, dissolved oxygen) and by facilitating the transport of key reactants. Because water and reactants are not uniformly distributed across landscapes, the rate of biogeochemical activity is also very heterogeneous. Disproportionately high reaction rates are observed in hot spots that occur, where hydrological flowpaths converge with substrates or other flowpaths containing

complementary or missing reactants creating the ideal environmental conditions for biogeochemical processing. Similarly, high reaction rates are observed during hot moments that occur when episodic hydrological flowpaths activate processes and/or mobilize accumulated reactants (McClain et al. 2003). In general, biogeochemical hot spots and hot moments often occur at hydrological transition zones (between terrestrial and aquatic interfaces) along ephemeral and permanent streams, wetlands and lakes (Yarrow and Marin 2007). Below we explore how DTA can be used to identify hydrological controls on the formation of biogeochemical pools and then explore how and where the transfer of water and nutrients creates biogeochemical hot spots and hot moments with respect to land–atmosphere and land–water linkages in forested landscapes.

4.4.1   Soil Biogeochemical Pools

The pioneering work of Geoffrey Milne identified topography as the master variable with which to determine soil properties along a hillslope. Milne (1935) used the concept of the *catena* (Latin for chain) as the fundamental soil-topography land unit that repeats sequentially across the landscape, therefore allowing the systematic mapping of soils across landscapes (Milne 1935).

Catenas form due to the interplay of static and dynamic factors resulting in soils of different properties. Static factors are controlled by terrain attributes such as slope, aspect, and elevation that influence the moisture, temperature, and solar radiation at a site. Dynamic factors are controlled by the relative position of the site within the catena, which influences the transport of particulate and dissolved materials downslope (Young 1972, 1976). Soils formed in a single material (geology) differ because of hydrological processes that result in differential drainage, leaching, translocation, and redeposition of soluble materials (Hall and Olson 1991). Therefore, in general we can expect drier, nutrient-poor conditions at the top and moister, nutrient-rich conditions at the bottom of a slope (Fig. 4.3). The essence of DTA is to take advantage of this predictable heterogeneity of physical and chemical properties of soils, including the precursors (reactants) and products of the transformation of biologically important nutrients, and use it to model biogeochemical activity over entire catchments.

Previous studies that report topographic controls on distribution of soil nutrient pools span over 50 years and cover forested landscapes ranging from gentle to steep relief in forests across major biomes (cf., Creed et al. 2008). The degree of heterogeneity that exists within soils places limits on the ability to predict the distribution of soil nutrient pools. We compared DTA approaches to general purpose soil surveys, where <10% of the heterogeneity in nutrients can be explained (Webster 1977), hence predictions >10% would be an improvement. Creed et al. (2002) found that slope, aspect, and elevation explained 38% of the variation in carbon and nitrogen in the forest floor but none of the variation within the soil profile. Soil sampling schemes based on random or equal spacing such as

those used by Creed et al. (2002) capture the most common topographic features on a landscape but underestimate the rare features. Rare features, although occupying a small proportion of the landscape, may be hot spots with disproportionately higher rates of biogeochemical cycling than other areas.

To detect these small but potentially important features, Webster et al. (2011) combined expert knowledge and a probabilistic classification approach to design a topographic template *sensu* Conacher and Dalrymple (1977) (Fig. 4.3) for the same sugar maple forest studied by Creed et al. (2002). While the carbon in canopy foliage was homogeneous, there was significant heterogeneity in soil carbon pools among the terrain objects, reflecting the importance of topographic templates for detecting, sampling, and mapping carbon pools on the landscape.

It is likely that topographic templates would be applicable to most low-order catchments with minor adjustments, however, estimating topographic controls on the distribution of soil nutrients at larger scales requires nested sampling (and modeling) strategies that incorporate the multiple scales of factors that influence soil development. For example, dominant topographic factors at the hillslope or catchment scale are those that affect dynamic factors of soil development. These include drainage conditions, transport and deposition of suspended materials and/or leaching, translocation and redeposition of soluble materials (modeled by wetness index, planar and profile curvature). However, at a regional scale, the dominant topographic factors are those that affect the static factors of soil development. These are topographic factors, modeled by slope, aspect, and elevation that influence external inputs such as solar radiation, temperature, moisture, and nutrient loadings. Scalable methods that consider heterogeneity and uncertainty in carbon pools will become increasingly important as national and international policies for reporting changes in carbon pools that accompany changes in land cover and land-use are implemented.

4.4.2 Land–Atmosphere Biogeochemical Linkages

Forest soils are significant terrestrial reservoirs of carbon and nitrogen and have a crucial role in the global budgets of the main greenhouse gases (GHGs): carbon dioxide (CO_2), methane (CH_4), and nitrous oxide (N_2O). As countries implement strategies to reduce GHG emissions, detailed information to inform policy making and guide mitigation measures is required on the fluxes of all GHGs from forested areas as well as the accompanying tools that can be used to predict GHG fluxes across landscapes and under different climates (Watson et al. 2000). Many forests are found in complex landscapes with intricate assemblages of substrates and environmental controls of GHG fluxes. Predominant among the controllers of GHG fluxes are those related to hydrology (e.g., the spatial and temporal distribution of soil properties, soil environment, and movement of the substrates for GHG production). We need to develop methods for accurate accounting of GHG fluxes in forests with complex terrain.

The use of DTA to understand land–atmosphere interactions in forests has revealed that topography is an important control on soil CO_2 efflux in both relatively arid and humid forests. In *softwood* forests, such as lodgepole pine in semiarid subalpine ecosystems, upslope contributing area (a proxy for lateral redistribution of water) was positively correlated with seasonal soil CO_2 efflux, where the highest soil CO_2 efflux rates were observed in areas with persistently high soil moisture in riparian lowlands (Riveros-Iregui and McGlynn 2009). In *hardwood forests*, such as sugar maple in humid ecosystems, Webster et al. (2008a) used topographic features to estimate soil CO_2 efflux (Fig. 4.3). The study revealed that transiently wet areas adjacent to wetlands (i.e., footslopes and toeslopes) yield significantly larger CO_2 efflux than the adjacent upland or wetland portions of the catchment. The follow-up study by Webster et al. (2008b) explored sensitivity of catchment-aggregated soil CO_2 efflux to different spatial partitioning schemes and found a minimum of three features (upland, critical transition zone, and wetland) was needed for accurate catchment-averaged estimates, especially under climate scenarios that became warmer and drier. Even in forests with heterogeneous cover, where species composition and site history impart important controls on soil processes, spatial variation of soil CO_2 efflux was attributed to topographically induced hydrological patterns on soil properties, root production, and soil CO_2 efflux (Martin et al. 2009).

These results underscore the importance of considering the relationships between topography and land–atmosphere GHG exchanges. We clearly need much more work especially in understanding efflux of trace gases, such as CH_4 and N_2O, which have much higher global warming potential than CO_2. Furthermore, static DTAs will need to be combined with dynamic approaches such as remote sensing and distributed simulation modeling to capture the roaming nature of hot spots and hot moments across the landscape.

4.4.3   Land–Water Biogeochemical Linkages

Forest soils are also sources of nutrients to surface waters, with important downstream water quality implications for different biota including human uses. DTA can be used to track the movement of nutrients from terrestrial source areas to streams and lakes in both fluvial and lacustrine forested landscapes. Given the interrelated nature of water and nutrient movement, most of the approaches to tracking water pathways noted earlier (Sect. 4.3) are also applicable to tracking nutrients (Table 4.2).

In *VSA-controlled landscapes* (Fig. 4.1a), as the groundwater table rises toward the surface after a drier period and intersects surface soils that have accumulated nutrients in the intervening dry period, nutrients are mobilized and flushed to receiving waters resulting in the export of carbon (Hornberger et al. 1994); nitrogen (Creed et al. 1996), or phosphorus (Evans et al. 2000). Topography influences the hydrological flushing of nutrients in various ways. It affects (a) the generation of nutrient supply (e.g., nutrient-poor areas develop if soil conditions are too dry or too wet);

(b) potential expansion vs. contraction rates of the VSAs (e.g., catchments with a greater potential for lateral expansion of source areas will have longer flushing times and higher rates of nutrients export, while catchments with less potential for lateral expansion of source areas will have shorter flushing times and lower rates of nutrient export); and (c) the transport of flushable nutrients to surface waters, which is a function of both the size and spatial organization of the VSA (e.g., catchments with larger, hydrologically connected VSAs will have larger nutrient export, whereas catchments with smaller or hydrologically disconnected VSAs will have lower nutrient export or more leaching to groundwater).

To date, most studies have assumed that the simple metric of proportion of near-saturated and saturated area within a catchment provides a good assessment of the magnitude of its VSA. This simple approach has been very successful in predicting the export of nutrients, including dissolved organic carbon (Creed et al. 2003; Richardson et al. 2009), dissolved organic nitrogen (Creed and Beall 2009), and total dissolved phosphorus (Creed unpublished data) to streams, explaining up to 90% of the variation in nutrient export. A true test of the strength of this empirical modeling approach is that using DTA on generally available data provided from government agencies across a large geographic area covering diverse climates, forest types, and forest soils explained almost 70% of the variation in DOC export (Creed et al. 2008). Not only is wetland cover highly correlated with nutrient exports to streams, but it is also highly correlated with the nutrient status of lakes (D'Arcy and Carignan 1997; Gergel et al. 1999; O'Connor et al. 2009; Winn et al. 2009). A key finding of many of these studies is that the source of the DEM used to delineate wetlands is very important and consideration of both open canopy and closed canopy wetlands is critical in estimating nutrient export from forested catchments (Creed et al. 2003).

The proportion of wetlands within a catchment has been an effective way to characterize the size of the VSA in relatively humid catchments with shallow soils, where topography is a good approximation for the water table. However, even in VSA-type landscapes (Fig. 4.1a), it is worth investigating whether all of the wetlands are contributing to runoff and whether the potential dynamics (expansion and contraction) of wetlands may be captured by DTA techniques. These were the objectives of Creed and Beall (2009), who used DTA techniques to derive indices of hydrological flushing potential and tested them against stream nutrient export.

Creed and Beall (2009) found that catchments with small nitrate-N export (but considerable DON export) were characterized by catchments with small contiguous source areas connected to the stream (*effective* VSA [*eff*VSA]) that had a small potential for expansion as the catchment wets up and/or a large proportion of wetlands. In contrast, catchments with large nitrate-N export were characterized by large source areas, with greater potential for expansion as the catchment wets up and/or few-to-no wetlands (Table 4.2). These indices explained 85% of the variance in nitrate-N export from topographically varying catchments in a sugar maple forest, which improved the traditional "wetland proportion" index by 18% (Creed and Beall 2009). These results demonstrate that hydrological connectivity is important to assess even in humid catchments. They also show that DTA techniques
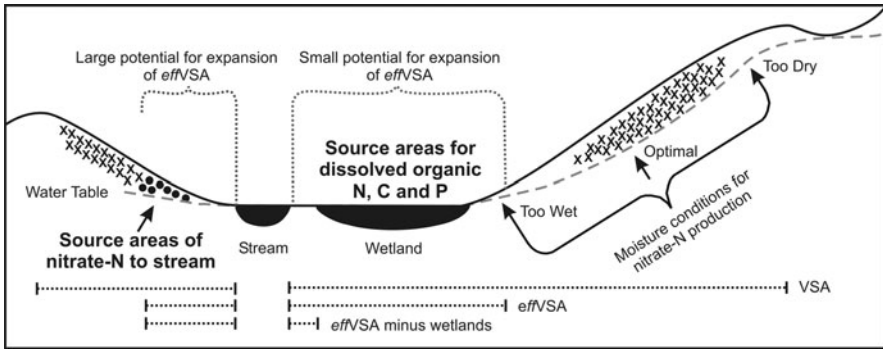
Fig. 4.5 Conceptual model of water and nutrient source areas in VSA-dominated landscapes (adapted from Creed and Beall 2009)

may capture the dynamic concept of hydrological flushing by estimating the potential for expansion of the VSA (Fig. 4.5).

Future work needs to focus on the effectiveness of these topographic indicators in scaling nutrient export from first- to higher-order catchments within a specific forest type and across forested regions with different forest types, forest disturbance histories, and environmental conditions. As VSAs expand and contract with changing climatic conditions, it is also important to consider the changes in magnitude and ratio of C:N:P as it may have consequences for the productivity of downstream aquatic ecosystems.

In *non-VSA-dominated landscapes* (Fig. 4.1c), DTA techniques using surface topography will not suffice in predicting hydrological or biogeochemical pathways. In subhumid catchments, where the characteristics of the deep substrate regulate water and nutrient transfer from land to aquatic systems, terrain indices that capture the spatial pattern of subsurface pathways are needed. A great example of this is a hydrogeological index (Table 4.2) developed using DTA techniques in order to predict total phosphorus (TP) concentration for lakes on the Boreal Plain in Alberta (Devito et al. 2000). The hydrogeology index captured the degree of interaction of lakes with regional, intermediate, and/or local groundwater flow systems by characterizing (a) lake order; (b) elevation of the lake relative to the surrounding landscape; and (c) position of the lake within the local to regional groundwater flow system. Lake order was determined using the ordering method of Mark and Goodchild (1982). The relative elevation of a lake was defined as the ratio of the change in elevation from the lake's surface to the regional low to the change in elevation from the relational low to the regional high. The position of the lake within the potential groundwater flow system was based on a steady-state groundwater model, which predicted whether a lake was in a groundwater recharge or discharge system. The index of hydrogeology was confirmed using an independent chemical measure of groundwater influence (combined concentrations of calcium and magnesium). Devito et al. (2000) combined the hydrogeology index with a hydrological connectivity index (proportion of wetlands connected to the lake) to predict the potential

for TP loading to the lakes. They were able to predict almost 60% of the variation in changes in TP in lakes from a dry to a wet year, reflecting surface and subsurface hydrological controls on TP. In a similar setting, Sass et al. (2008) explained over 70% of the steady-state concentration of chlorophyll *a* in 40 lakes using an index of hydrogeological setting, a proxy for dominant runoff mechanisms (size and organization of wetlands), and lake-to-lake connectivity (presence or absence of contributing lakes).

These studies underscore the value of spatially extensive datasets for developing and testing our understanding of hydrological controls on biogeochemical export to surface waters on forested landscapes and also illustrate that DTA is important in a broad range of hydrogeological contexts (VSA as well as non-VSA dominated) and forest regions. It is noteworthy that comparable amounts of variation in lake nutrient concentrations were explained in both VSA and non-VSA geographies. However, given the different approaches taken, there is a clear need to repeat these studies with standard methods and data to allow for direct intercomparison.

4.5   From Science to Practice

Forest managers aim to minimize adverse impacts of forest operations on water, sediment and nutrient loading to surfaces waters. Although well intended, the management practices used to minimize effects are often borrowed from other jurisdictions, and while based on the best available science may not be wholly applicable to the management locale. Practitioners must recognize the importance of understanding the processes responsible for the movement of water and nutrients across landscapes to predict the effects of forest management strategies on the hydrological and biogeochemical response of surface waters. Echoing the quotation at the beginning of the chapter, we do not need mapping for its own sake but we need process-informed characterization of landscapes to lead to useful generalizations that can be applied in practical contexts.

This chapter has demonstrated that DTA can be used to predict origin, age, pathway, and fate of water and nutrients within a forest. Although our theoretical treatment of DTA techniques has focused on hydrological and biogeochemical studies, there is an increasing body of literature detailing the use of DTA in water-related geomorphic and ecological applications. For example, the susceptibility of landscapes to landslides has been modeled using DTA based on the observation that landslides are partly triggered when soil pore water pressures reach a critical point (Montgomery et al. 2000; Dhakal and Sidle 2004). Depending on the landscape, different terrain attributes have been found to be useful in prediction of areas, where pore water pressures reach critical levels (Montgomery et al. 2000; Gritzner et al. 2001; Borga et al. 2002). An interesting ecological application of the topographic index is the prediction of critical brook trout spawning sites along the margins of forest lakes which in some landscapes occur in topographically convergent zones, where there is discharging groundwater (Borwick et al. 2005).

The transfer of scientific knowledge to practice has been facilitated by different governmental and nongovernmental organizations such as the Sustainable Forest Management Network in Canada. There are now numerous examples of how forest managers have been incorporating the scientific results in best management practices. Forest managers and operators are using DTA to map hydrologically sensitive areas (areas where the water table intersects with the forest floor, such as wetlands and low-order streams), in order to assist in the placement of roads (especially considering water crossings), culverts, as well as cut blocks (Murphy et al. 2007). There is substantial improvement in mapping accuracy when LiDAR-derived DEMs are used to delineate these hydrologically sensitive areas, many of which are often hidden beneath the canopy or are not represented by coarse resolution DEM pixels in traditional aerial photo-derived DEMs (cf., Remmel et al. 2008). In more mountainous terrain, roads are critical conduits of water and the sediments it carries so that the planning of roads is especially important to reduce these impacts (Megahan and King 2001). Roads and cut-blocks also lead to increased susceptibility to landslides (especially for small and moderate size precipitation events), so that forest management in these mountainous regions also considers landslide susceptibility in their planning (Dhakal and Sidle 2003).

DTA-based characterization together with an enhanced understanding of hydrological processes will assist the conservation of hydrologically sensitive areas and minimize adverse impacts through more effective harvest design and location of roads and riparian buffers. DTA can be a powerful tool for forest managers, especially when combined with remote sensing and distributed simulation modeling, which can be used to predict both the spatial heterogeneity and the temporal variability in hydrological features and land–atmosphere and land–water exchanges of water, nutrients, and pollutants.

4.6 Towards an Operational Digital Terrain Analysis Approach

DTA is poised to become an integral tool in many earth science and ecological fields. It has evolved to the point where it has a strong theoretical basis that captures both hydrological and biogeochemical processes and patterns. To develop an operational approach to DTA for forest hydrologists, the following four recommendations should be implemented.

4.6.1 Improved Characterization of Surface and Subsurface

The next generation of DEMs must achieve <15 cm vertical and <5 m horizontal accuracy across all forest cover types. Ideally, this will be achieved with satellite-based LiDAR systems to provide complete global coverage from taiga to tropical forests. A much greater achievement will be the characterization of bedrock topography, also at a global scale. Geotechnical techniques offer some hope in

mapping subsurface features but the type of precision and accuracy needed is currently still out of reach. These achievements would lead to an integrated terrain analysis framework, where water would be able to be routed along surface and/or subsurface pathways. Until we attain the required integrated flow-path characterization, there is a need for continued ground-based surveys of soils and surficial geology so that in combination with geotechnical methods we will be able to predict bedrock topography in unsurveyed areas. Unfortunately, it is all too tempting in the light of budget constraints to chop ground-surveys in the mistaken belief that DEMs of the surface can model everything.

4.6.2   Classification of Process-Based Terrain Attributes and Features

DEMs and the terrain attributes and terrain features derived from them contain a wealth of information and opportunities, many of which have already between translated from science to practice. However, an operational DTA would benefit enormously from a classification of terrain attributes and terrain features based on process-understanding. This could lead to a common DTA toolkit that would help practitioners match the right tool to the right process at the right place. This toolkit could be customized for each hydrological region, so as to reflect climatic, geological, and soil conditions. A common toolkit would also enable direct comparisons between different hydrological regions. The foundation of such classification would have to be based on ground surveys, providing yet another strong reason for their retention.

4.6.3   Global Benchmark Datasets

We have yet to test the true potential of DTA, as the research community has so far used ad hoc, piecemeal approaches. We need a coordinated comprehensive benchmarking of different procedures and products. Global benchmark datasets consisting of DEMs as well as ground-truthing data would allow the authors of new and improved metrics to weigh in against existing ones using the same datasets. Such comparisons would also aid the classification of the metrics based on hydrological regions.

4.6.4   Integration with Other Digital Data, Tools and Techniques

The future of DTA lies in its integration with field data, remote sensing, and distributed hydrological modeling. These integrated systems could use the static maps of DTA as a basis for dynamic modeling of processes and patterns that are

calibrated by local, ground-based monitoring networks. These catchment-scale analysis systems should be freeware with transparent codes such as the Terrain Analysis System and its successor Whitebox (Lindsay 2005).

4.7   Conclusions

DTA is becoming a ubiquitous tool in the hydrologist's toolbox and can be used to predict hydrological and biogeochemical processes and patterns in different hydrological landscapes. Given the general availability of DEMs and how readily DTMs can be derived, there is a strong temptation to uncritically apply topographic analysis as a first (and sometimes only) step in understanding the hydrological and biogeochemical dynamics of an area. The literature is now replete with examples, especially at headwater catchment scales, where runoff is controlled by nonlinear mechanisms, such as bedrock-controlled subsurface flow and macropore flow. In such regions, DTA will be of limited use, especially in understanding rainfall-runoff mechanisms. However, set in a proper physical context, DTA can be an indispensable tool in modeling flowpaths, surface storages, nutrient source areas, and characterizing landforms. The future of DTA lies in the use of LiDAR-derived DEMs at an optimum spatial resolution and the integration of terrain analysis with remote sensing and hydrological distributed modeling to breathe life into the static patterns created by DTMs. The fusion of modern digital tools with forest managers' innate understanding of their landbase will provide a powerful new approach for implementing sustainable forest management.

References

Agnew LJ, Lyona S, Gerard-Marchantet P et al (2006) Identifying hydrologically sensitive areas: bridging the gap between science and application. J Environ Manag 78:63–76

Baker ME, Wiley MJ, Carlson MI et al (2003) A GIS model of subsurface water potential for aquatic resource inventory, assessment, and environmental management. Environ Manag 32:706–719

Band LE, Moore ID (1995) Scale: landscape attributes and geographical information systems. Hydrol Process 9:401–422

Beven KJ (1986) Runoff production and flood frequency in catchments of order n: an alternative approach. In: Gupta VK, Rodriguez-Iturbe I, Wood EF (eds) Scale problems in hydrology. D. Reidel, Dordrecht, pp 107–131

Beven KJ (1997) Topmodel: a critique. Hydrol Process 11:1069–1085

Beven KJ, Kirkby MJ (1979) A physically based, variable contributing area model of basin hydrology. Hydrol Sci 24:43–69

Bishop K, Buffam I, Erlandsson M et al (2008) Aqua Incognita: the unknown headwaters. Hydrol Process 22:1239–1242

Blöschl G, Sivapalan M (1995) Scale issues in hydrological modeling: a review. Hydrol Process 9:251–290

Borga M, Fontana GD, Cazorzi F (2002) Analysis of topographic and climatic control on rainfall-triggered shallow landsliding using a quasi-dynamic wetness index. J Hydrol 268:56–71

Borwick J, Buttle J, Ridgway MS (2005) A topographic index approach for identifying ground-water habitat of young-of-year brook trout (*Salvelinus fontinalis*) in the land–lake ecotone. Can J Fish Aquat Sci 63:239–253

Bourgine B, Baghdadi N (2005) Assessment of C-band SRTM DEM in a dense equatorial forest zone. Comptes Rendus Geosci 337:1225–1234

Bracken LJ, Croke J (2007) The concept of hydrological connectivity and its contribution to understanding runoff-dominated geomorphic systems. Hydrol Process 21:1749–1763

Burns DA, Plummer NL, McDonnell JJ et al (2003) The geochemical evolution of riparian ground water in a forested piedmont catchment. Ground Water 41:913–925

Conacher AJ, Dalrymple JB (1977) The nine unit landsurface model: an approach to pedo-geomorphic research. Geoderma 18:1–154

Costa-Cabral MC, Burges SJ (1994) Digital elevation model networks (DEMON): a model of flow over hillslopes for computation of contributing and dispersal areas. Water Resour Res 30:1681–1692

Creed IF, Beall FD (2009) Distributed topographic indicators for predicting nitrogen export from headwater catchments. Water Resour Res 45:W10407

Creed IF, Band LE, Foster NW et al (1996) Regulation of nitrate-N release from temperate forests: a test of the N flushing hypothesis. Water Resour Res 32:3337–3354

Creed IF, Trick CG, Band LE et al (2002) Characterizing the spatial pattern of soil carbon and nitrogen pools in the Turkey Lakes Watershed: a comparison of regression techniques. Water Air Soil Poll Focus 2:81–102

Creed IF, Sanford SE, Beall FD et al (2003) Cryptic wetlands: integrating hidden wetlands in regression models of the export of dissolved organic carbon from forested landscapes. Hydrol Process 17:3629–3648

Creed IF, Beall FD, Clair TA et al (2008) Predicting export of dissolved organic carbon from forested catchments in glaciated landscapes with shallow soils. Glob Biogeochem Cycles 22: GB4024

D'Arcy P, Carignan R (1997) Influence of catchment topography on water chemistry in southeastern Québec Shield lakes. Can J Fish Aquat Sci 54:2215–2227

Deng Y, Wilson JP, Bauer BO (2007) DEM resolution dependencies of terrain attributes across a landscape. Int J Geog Inf Sci 21:187–213

Desmet PJJ, Govers G (1996) Comparison of routing algorithms for digital elevation models and their implications for predicting ephemeral gullies. Int J Geog Inf Syst 10:311–331

Devito KJ, Creed IF, Rothwell RL et al (2000) Landscape controls on phosphorus loading to boreal lakes: implications for the potential impacts of forest harvesting. Can J Fish Aquat Sci 57:1977–1984

Devito KJ, Creed IF, Gan T et al (2005) A framework for broad-scale classification of hydrologic response units on the Boreal Plain: is topography the last thing to consider? Hydrol Process 19:1705–1714

Dhakal AS, Sidle RC (2003) Long-term modeling of landslides for different forest management practices. Earth Surf Proc Land 28:853–868

Dhakal AS, Sidle RC (2004) Pore water pressure assessment in a forest watershed: simulations and distributed field measurements related to forest practices. Water Resour Res 40:W02405

Dunne T, Moore TR, Taylor CH (1975) Recognition and prediction of runoff-producing zones in humid regions. Hydrol Sci 20:305–327

Evans JE, Prepas EE, Devito KJ et al (2000) Phosphorus dynamics in shallow subsurface waters in an uncut and cut subscatchment of a lake on the Boreal Plain. Can J Fish Aquat Sci 57:60–72

Fairfield J, Leymarie P (1991) Drainage networks from grid digital elevation models. Water Resour Res 27:709–717

Farr TG, Rosen P, Caro E et al (2007) The shuttle radar topography mission. Rev Geophys 45: RG2004

Freer J, McDonnell JJ, Beven KJ, Peters NE, Burns DA, Hooper RP, Aulenbach B, Kendall C (2002) The role of bedrock topography on subsurface storm flow. Water Resour Res 38: WR000872

Garcia-Martinó AR, Scatena FN, Warner GS et al (1996) Statistical low flow estimation using GIS analysis in humid montane regions in Puerto Rico. Water Resour Bull 32:1259–1271

Gergel SE, Turner MG, Kratz TK (1999) Dissolved organic carbon as an indicator of the scale of watershed influence on lakes and rivers. Ecol Appl 9:1377–1390

Gritzner ML, Marcus WA, Aspinall R, Custer SG (2001) Assessing landslide potential using GIS, soil wetness modeling and topographic attributes, Payette River, Idaho. Geomorphology 37:149–165

Güntner A, Seibert J, Uhlenbrook S (2004) Modeling spatial patterns of saturated areas: an evaluation of different terrain indices. Water Resour Res 40:W05114

Hall GF, Olson CG (1991) Predicting variability of soils from landscape models. In: Manusbach MJ, Wilding LP (eds) Spatial variabilities of soils and landforms, Soil Science Society of America Special Publication, No. 28, Madison, pp 9–24

Hewlett JD, Hibbert AR (1967) Factors affecting the response of small watersheds to precipitation in humid areas. In: Sopper WE, Lull HW (eds) Forest Hydrology. Pergamon Press, New York, pp 275–290

Hewlett JD, Nutter WL (1970) The varying source area of streamflow from upland basins. In: Proceedings of the symposium on interdisciplinary aspects of watershed management. Montana State University, Bozeman, 3–6 Aug 1970, pp 65–83

Hjerdt KN, McDonnell JJ, Seibert J et al (2004) A new topographic index to quantify downslope controls on local drainage. Water Resour Res 40:W05602

Hornberger GM, Bencala KE, McKnight DM (1994) Hydrological controls on dissolved organic carbon during snowmelt in the Snake River near Montezuma, Colorado. Biogeochemistry 25:147–165

Horton RE (1945) Erosional development of streams and their drainage basins. Bull Geo Soc Am 56:275–370

Hutchinson MF (1989) A new procedure for gridding elevation and stream line data with automatic removal of spurious pits. J Hydrol 106:211–232

Inamder SP, Mitchell MJ (2006) Hydrologic and topographic controls on storm-event exports of dissolved organic carbon (DOC) and nitrate across catchment scales. Water Resour Res 42: W03421

Jencso KG, McGlynn BL, Gooseff MN et al (2009) Hydrologic connectivity between landscapes and streams: transferring reach- and plot-scale understanding to the catchment scale. Water Resour Res 45:W04438

Lane SN, Brookes CJ, Kirby MJ et al (2004) A network-index-based version of TOPMODEL for use with high-resolution digital topographic data. Hydrol Process 18:191–201

Laudon H, Sjoblom V, Buffam I et al (2007) The role of catchment scale and landscape characteristics for runoff generation of boreal streams. J Hydrol 344:198–209

Lehmann P, Hinz C, McGrath G et al (2007) Rainfall threshold for hillslope outflow: an emergent property of flowpathway connectivity. Hydrol Earth Syst Sci 11:1047–1063

Lindsay JB (2003) A physically based model for calculating contributing area on hillslopes and along valley bottoms. Water Resour Res 39:1332

Lindsay JB (2005) A terrain analysis system: a tool for hydro-geomorphic applications. Hydrol Process 19:1123–1130

Lindsay JB (2006) Sensitivity of channel mapping techniques to uncertainty in digital elevation data. Int J Geog Inf Sci 20:669–692

Lindsay JB, Creed IF (2005) Removal of article depressions from DEMs: towards a minimum impact approach. Hydrol Process 19:3113–3126

Lindsay JB, Creed IF (2006) Distinguishing actual and artefact depressions in digital elevation data: approaches and Issues. Comput Geosci 32:1192–1204

Lindsay JB, Creed IF, Beall FD (2004) Drainage basin morphometrics for depressional landscapes. Water Resour Res 40:W09307

MacMillan RA, Pettapiece WW, Nolan SC et al (2000) A generic procedure for automatically segmenting landforms into landform elements using DEMs, heuristic rules and fuzzy logic. Fuzzy Set Syst 113:81–109

Mark DM, Goodchild MF (1982) Topologic model for drainage networks with lakes. Water Resour Res 18:275–280

Martin JG, Bolstad PV, Ryu SR et al (2009) Modeling soil respiration based on carbon, nitrogen, and root mass across diverse Great Lake forests. Agric For Meteorol 149:1722–1729

Martz LW, Garbrecht J (1998) The treatment of flat areas and depressions in automated drainage analysis of raster digital elevation models. Hydrol Process 12:843–855

McClain ME, Boyer EW, Dent CL et al (2003) Biogeochemical hot spots and hot moments at the interface of terrestrial and aquatic ecosystems. Ecosystems 6:301–312

McDonnell JJ, Sivapalan M, Vache K et al (2007) Moving beyond heterogeneity and process complexity: a new vision for watershed hydrology. Water Resour Res 43:W07301

McGlynn BL, Seibert J (2003) Distributed assessment of contributing area and riparian buffering along stream networks. Water Resour Res 39:1082

McGlynn BL, McDonnell JJ, Stewart M et al (2003) On the relationships between catchment scale and streamwater mean residence time. Hydrol Process 17:175–181

McGuire KJ, McDonnell JJ (2006) A review and evaluation of catchment transit time modeling. J Hydrol 330:543–563

McGuire KJ, McDonnell JJ, Weiler M et al (2005) The role of topography on catchment-scale water residence time. Water Resour Res 41:W04002

McMaster KJ (2002) Effects of digital elevation model resolution on derived stream network positions. Water Resour Res 28:1042

Megahan WF, King JG (2001) Erosion, sedimentation, and cumulative effects in the northern Rocky Mountains, In: Proceedings of the society of American foresters, Washington, 16–20 Nov 2000, pp 58–63

Milne G (1935) Some suggested units of classification and mapping, particularly for East African soils. Soil Res 3:183–198

Montgomery DR, Buffington JM (1997) Channel-reach morphology in mountain drainage basins. Geol Soc Am Bull 109:596–611

Montgomery DR, Dietrich WE (1992) Channel initiation and the problem of landscape scale. Science 255:826–830

Montgomery DR, Schmidt KM, Greenberg HM et al (2000) Forest clearing and regional landsliding. Geology 28:311–314

Moore ID, Grayson RB, Ladson AR (1991) Digital terrain modeling: a review of hydrological, geomorphological, and biological applications. Hydrol Process 5:3–30

Murphy PNC, Ogilvie J, Connor K et al (2007) Mapping wetlands: a comparison of two different approaches for New Brunswick, Canada. Wetlands 27:846–854

Natural Resources Canada (2007) Canadian digital elevation data, level 1, Product Specifications, Government of Canada, Natural Resources Canada, Centre for Topographic Information

O'Callaghan JF, Mark DM (1984) The extraction of drainage networks from digital elevation data. Comput Vision Graph Image Process 28:323–344

O'Connor EM, Dillon PJ, Molot LA et al (2009) Modeling dissolved organic carbon mass balances for lakes of the Muskoka River Watershed. Hydrol Res 40:273–290

Paik K (2008) Global search algorithm for nondispersive flowpath extraction. J Geophys Res 113: F04001

Peucker TK, Douglas DH (1975) Detection of surface-specific points by local parallel processing of discrete terrain elevation data. Comp Graph Image Proc 4:375–387

Planchon O, Darboux F (2001) A fast, simple and versatile algorithm to fill depressions of digital elevation models. Catena 46:159–176

Quinn P, Beven K, Chevallier P et al (1991) The prediction of hillslope flowpaths for distributed hydrological modeling using digital terrain models. Hydrol Process 5:59–79

Quinn PF, Beven KJ, Lamb R (1995) The ln(a/tanB) index: how to calculate it and how to use it within the TOPMODEL framework. Hydrol Process 9:161–182

Remmel TK, Todd KW, Buttle J (2008) A comparison of existing surficial hydrological data layers in a low-relief forested Ontario landscape with those derived from a LiDAR DEM. Forest Chron 84:850–865

Reutebuch SE, McGaughey RJ, Andersen HE et al (2003) Accuracy of a high-resolution lidar terrain model under a conifer forest canopy. Can J Remote Sens 29:527–535

Richardson MC, Fortin MJ, Branfireun BA (2009) Hydrogeomorphic edge detection and delineation of landscape functional units from lidar digital elevation models. Water Resour Res 45: W10441

Riveros-Iregui DA, McGlynn BL (2009) Landscape structure control on soil CO_2 efflux variability in complex terrain: scaling from point observations to watershed scale fluxes. J Geophys Res Biogeosci 114:G02010

Roberts DW, Dowling TI, Walker J (1997) FLAG: a fuzzy landscape analysis GIS method for dryland salinity assessment, Technical Report 8/97, CSIRO Land and Water, Canberra

Sanford SE, Creed IF, Tague CL et al (2007) Scale-dependence of natural variability of flow regimes in a forested landscape. Water Resour Res 43:W08414

Sass GZ, Creed IF, Devito KJ (2008) Spatial heterogeneity in trophic status of shallow lakes on the Boreal Plain: influence of hydrologic setting. Water Resour Res 44:W08444

Schumm SA (1956) The role of creep and rainwash on the retreat of badland slopes. Am J Sci 254:693–706

Seibert J, McGlynn BL (2007) A new triangular multiple flow direction algorithm for computing upslope areas from gridded digital elevation models. Water Resour Res 43:W04501

Sorensen R, Seibert J (2007) Effects of DEM resolution on the calculation of topographical indices: TWI and its components. J Hydrol 347:79–89

Sorensen R, Zinko U, Seibert J (2006) On the calculation of the topographic wetness index: evaluation of different methods based on field observations. Hydrol Earth Syst Sci 10:101–112

Spence C, Woo M-K (2003) Hydrology of subarctic Canadian shield: soil-filled valleys. J Hydrol 279:151–166

Summerell GK, Vaze J, Tuteja NK et al (2005) Delineating the major landforms of catchments using an objective hydrological terrain analysis method. Water Resour Res 41:W12416

Tague CL, Band LE (2004) RHESSys: regional hydro-ecologic simulation system – an object-oriented approach to spatially distributed modeling of carbon, water, and nutrient cycling. Earth Interact 8:1–19

Tarboton DG (1997) A new method for the determination of flow directions and upslope areas in grid digital elevation models. Water Resour Res 33:309–319

Tetzlaff D, Seibert J, McGuire KJ et al (2009) How does landscape structure influence catchment transit time across different geomorphic provinces? Hydrol Process 23:945–953

Thompson JC, Moore RD (1996) Relations between topography and water table depth in a shallow forest soil. Hydrol Process 10:1513–1525

Tromp-van Meerveld HJ, McDonnell JJ (2006) Threshold relations in subsurface stormflow: 2. The fill and spill hypothesis. Water Resour Res 42:W02411

Watson R, Noble I, Bolin B et al (2000) Summary for policymakers: land-use, land-Use change, and forestry. IPCC Special Report 92-9169-114-3, Geneva

Webster R (1977) Quantitative and numerical methods in soil classification and survey. Clarendon Press, Oxford, p 269

Webster KL, Creed IF, Bourbonniere RA et al (2008a) Controls on the heterogeneity of soil respiration in a tolerant hardwood forest. J Geophys Res Biogeosci 113:G03018

Webster KL, Creed IF, Beall FD et al (2008b) Sensitivity of catchment-aggregated estimates of soil carbon dioxide efflux to topography under different climatic conditions. J Geophys Res Biogeosci 113:G03040

Webster KL, Creed IF, Beall FD et al (2010) A topographic template for estimating soil carbon pools in forested catchments, Geoderma 160:457–467

Western AW, Blöschl GRB (2001) Toward capturing hydrologically significant connectivity in spatial patterns. Water Resour Res 37:2000WR900241

Wilson JP, Gallant JC (2000) Terrain analysis: principles and applications. Wiley, New York

Winn N, Williamson CE, Abbitt R et al (2009) Modeling dissolved organic carbon in subalpine and alpine lakes with GIS and remote sensing. Landscape Ecol 24:807–816

Wolock DM, McCabe GJ (1995) Comparison of single and multiple flow direction algorithms for computing topographic parameters in TOPMODEL. Water Resour Res 31:1315–1324

Yarrow MM, Marin VH (2007) Toward conceptual cohesiveness: a historical analysis of the theory and utility of ecological boundaries and transition zones. Ecosystems 10:462–476

Young A (1972) The soil catena: a systematic approach. In: Adams WP, Helleiner FM (eds) International geography, Vol. 1. International geography congress. University of Toronto Press, Toronto, pp 287–289

Young A (1976) Tropical soils and soil survey. Cambridge University Press, Cambridge

Zhang W, Montgomery DR (1994) Digital elevation model grid size, landscape representation, and hydrologic simulations. Water Resour Res 30:1019–1028

Chapter 5
A Synthesis of Forest Evaporation Fluxes – from Days to Years – as Measured with Eddy Covariance

Dennis D. Baldocchi and Youngryel Ryu

5.1 Introduction and History

The annual water budget of a forested landscape is the sum of precipitation minus the sum of evaporation, runoff, storage, and leakage. The evaporation term, which is the subject of this chapter, comprises the sum of plant transpiration and evaporation from the soil/litter system and rainfall/dew intercepted by the foliage.

The literature on "forest evaporation" is vast; at the time of this writing, it contains over 1,100 references, according to a query of the Web of Science. Most of the long-term measurements (years to decades) on forest evaporation are based on forest catchment studies, which evaluate evaporation as a residual of the water balance (Swank and Douglass 1974; Bosch and Hewlett 1982; Komatsu et al. 2007) or by measuring changes in soil water balance and rain interception (Calder 1998). These budget approaches have merit in evaluating forest evaporation because they are relatively inexpensive and they can evaluate water budgets over long time periods, across large geographic areas, and in complex terrain. On the other hand, evaporation sums derived from hydrological water balances are limited in their ability to extract information on biophysical controls of forest evaporation on hourly and daily timescales. Water balance methods are also unable to provide information on the partitioning of evaporation according to transpiration and soil and re-evaporation of intercepted rainfall and dew.

Another segment of this literature uses micrometeorological techniques to produce direct measurements of forest evaporation. Rapid growth in the application of micrometeorological methods over forests occurred over the past 30 years because of its ability to measure fluxes of water vapor directly, in situ, at the stand scale and with minimal interference. But the majority of these studies and the many fine reviews and syntheses on the topic of "forest evaporation" using "micrometeorological methods" are confined to short campaigns during the heart of the growing season (Jarvis et al. 1976; Jarvis and McNaughton 1986; Black and Kelliher 1989; Kelliher et al. 1993; Komatsu et al. 2007; Tanaka et al. 2008). To our knowledge only the review by Tanaka et al. (2008) focuses on long-term evaporation measurements and it concentrates on evaporation from tropical forests.

The earliest measurements of water vapor exchange between forests and the atmosphere relied on the flux-gradient method (an indirect technique that evaluates flux densities of H_2O as the product of a turbulent diffusivity (K) and the vertical gradient of H_2O concentration, dq/dz), rather than the eddy covariance technique, due to a lacking of fast responding anemometers and H_2O sensors (Denmead 1969; Droppo and Hamilton 1973; Stewart and Thom 1973; Black 1979). Application of flux-gradient theory over tall vegetation was found to be problematic at the onset (Raupach 1979). Over tall forests, vertical gradients of H_2O are small and difficult to resolve because turbulent mixing is vigorous at the canopy–atmosphere interface (Black and McNaughton 1971; Stewart and Thom 1973; Hicks et al. 1975). Secondly, use of Monin–Obukhov similarity theory to calculate eddy exchange coefficients (K) is invalid above forests (Raupach 1979). This occurs because turbulent transport is enhanced in the roughness sublayer over the forest – large shear at the canopy–atmosphere interface causes nonlocal transport to occur (Raupach et al. 1996). By the mid-1970s, additional studies on evaporation over forests would need to wait for technical developments that would permit use of the eddy covariance technique.

The earliest eddy covariance measurements of water vapor exchange over forests occurred between the mid-1970s and early 1980s (Hicks et al. 1975; Spittlehouse and Black 1979; Shuttleworth et al. 1984; Verma et al. 1986). This advance was made possible with a wave of technological improvements that included three-dimensional sonic anemometers, fast-responding ultraviolet hygrometers (krypton and Lyman-alpha) (Buck 1976), infrared spectrometers (Hyson and Hicks 1975; Raupach 1978), and personal computers. The execution of the ABRACOS project in Brazil (Shuttleworth et al. 1984) and the BOREAS project in Canada (Sellers et al. 1995) heralded a new era of routine and long-term measurements of evaporation from forests by eddy covariance. And today eddy covariance measurements of evaporation continue worldwide through various regional networks associated with the FLUXNET project (Baldocchi et al. 2001; Baldocchi 2008).

5.2   Forest Evaporation by the Eddy Covariance Method

The eddy covariance technique measures evaporation by assessing the covariance between fluctuations in vertical velocity (w) and the specific water vapor content ($q = \rho_v/\rho_a$ where ρ_a is dry air density and ρ_v is H_2O density):

$$E = \overline{\rho_a} \cdot \overline{w'q'}. \tag{5.1}$$

In (5.1), the overbars denote time-averaging (e.g., 30–60 min) and primes represent fluctuations from the mean (e.g., $q' = q - \overline{q}$). A positively signed covariance represents net H_2O transfer into the atmosphere and a negative value denotes the reverse.

Many issues remain about the applicability and accuracy of eddy covariance measurements over forests. Of most concern are the many circumstances where investigators fail to close the surface energy balance (Twine et al. 2000; Wilson et al. 2002), which is used as an independent data quality check. Lack of energy balance closure, on the other hand, should not always indict the quality or the accuracy of the evaporation measurements. Mitigating factors include: (1) nonrepresentative measurements of the net radiation balance across the flux footprint; (2) biases in net radiation measurements via improper mounting of the sensor close to a tower; and (3) insufficient sampling of soil heat flux and canopy heat storage across the flux footprint (Meyers and Hollinger 2004; Lindroth et al. 2010). In fact, there is growing body of evidence showing good agreement between long-term evaporation measurements by eddy covariance with independent hydrologically based methods. Three studies report that annual sums of evaporation, based on eddy covariance, agree within 6% of independent assessments of forest evaporation; these have been produced by water budgets from catchments (Wilson et al. 2001; Scott 2010), deep groundwater piezometers (Barr et al. 2000), and changes in soil moisture profiles (Baldocchi et al. 2004; Yaseef et al. 2010). Furthermore, daily and annual integrations of eddy covariance water fluxes do not suffer from the night-time systematic biases that plague CO_2 flux measurements (Moncrieff et al. 1996).

5.3   Evaporation from Forests, Magnitudes, and Variations

Over the past decade, several hundred research teams commenced measuring fluxes of water, carbon dioxide, and energy continuously with the eddy covariance method. So, today, many forest evaporation datasets exist, with measurements accumulated over years to decades. Ironically, a small fraction of these research teams have found the time or inclination to publish their long-term evaporation measurements, compared to the several hundred papers that have been published on ecosystem CO_2 exchange (Baldocchi 2008). Nevertheless, there exists a substantial and growing body of literature on long-term forest evaporation, which we have compiled, that merits scrutiny. For this chapter we compiled and evaluated 185 site-years of forest evaporation measurements, derived with the eddy covariance method. These studies are associated with over 40 forests and include data from tropical evergreen broadleaved, temperate evergreen conifer, deciduous broad-leaved forests, savanna woodlands, and shrublands. Below, we draw upon this compiled database and address the following questions relating to forest evaporation: what is the range of annual evaporation from the World's forests and woodlands? Is there a ranking among annual evaporation rates for different forest types, canopy structure, and climates? And how is the amount of annual evaporation constrained or related to annual precipitation and available energy?

Figure 5.1 summarizes the evaporation database, of 185 site-years, by presenting the probability density distribution of annual evaporation. The mean annual evaporation rate of forests from across the globe (and its standard deviation) is 503 ± 338 mm year^{-1}.
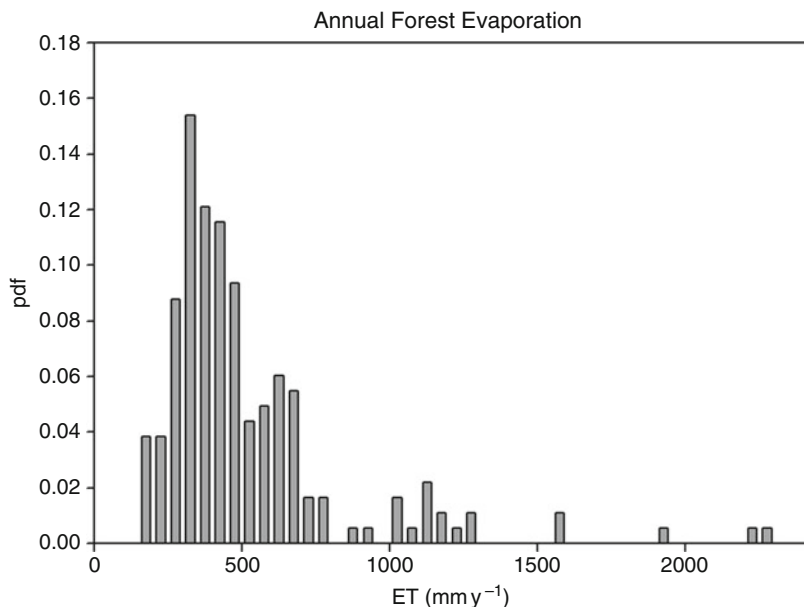
Fig. 5.1 Probability distribution of annual evaporation from forested sites. The probability density function (pdf) is derived from 185 site-years of eddy covariance flux measurements. The mean is 503 ± 338 mm year^{-1} and the median is 408 mm year^{-1}

The probability distribution is positively skewed towards high sums, as annual evaporation from tropical forests can exceed 2,000 mm year^{-1} (Loescher et al. 2005; Fisher et al. 2009). For perspective, these statistical values fall within the range of estimates on land evaporation that are being produced by a new generation of global evaporation models that are being generated using a combination of climate, eddy flux, and remote sensing information; 550 mm year^{-1} (Jung et al. 2010); 539 mm year^{-1} (Zhang et al. 2010); 655 mm year^{-1} (Fisher et al. 2008).

The seasonal pattern of daily evaporation is very distinct for different forest types, distributed across the globe (Fig. 5.2). Tropical forests experience little seasonality in maximum evaporation, which approaches 5 mm day^{-1} (Fig. 5.2a). Most temporal variation occurs on a day-by-day basis and is modulated by cloud cover and daily changes in solar radiation (Vourlitis et al. 2001; Araujo et al. 2002; da Rocha et al. 2004; Loescher et al. 2005; Giambelluca et al. 2009). Deciduous broadleaved forest, in temperate and boreal climates, experience much seasonal variation in daily evaporation (Black et al. 1996; Moore et al. 1996; Lee et al. 1999; Wilson and Baldocchi 2000; Blanken et al. 2001; Oliphant et al. 2004; Barr et al. 2007). During the winter leafless period, daily evaporation fluxes are below 1 mm day^{-1} (Fig. 5.2b). By summer, peak evaporation rates are not dissimilar from those observed over tropical forests. Daily evaporation from savanna woodlands experiences much seasonality (Baldocchi et al. 2004; David et al. 2007; Paço et al. 2009). Highest evaporation rates (~4 mm day^{-1}) occur during the spring,
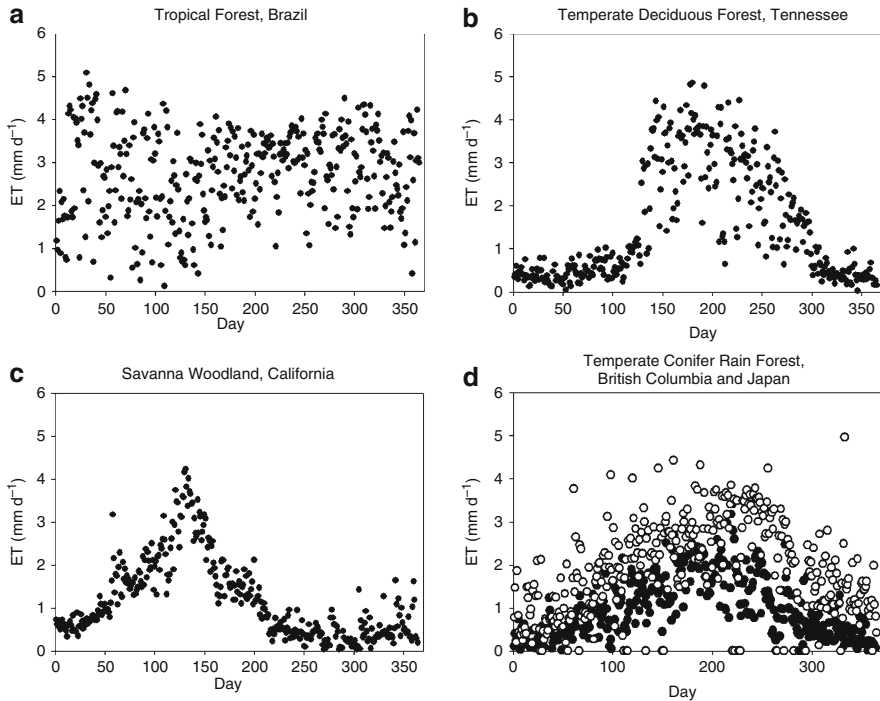
Fig. 5.2 Seasonal variation in daily integrated evaporation from: (**a**) tropical rain forest in Brazil (Araujo et al. 2002); (**b**) a deciduous broadleaved forest in Tennessee (Wilson and Baldocchi 2000); (**c**) a savanna woodland in California (Baldocchi et al. 2004); and (**d**) a temperate conifer rain forest in British Columbia (Humphreys et al. 2003) and a cypress forest in Japan (*open dot*) (Kosugi et al. 2005)

after winter rains have replenished the soil profile. Lack of rain during the summer depletes the soil moisture reservoir, causing stomata to close, transpiration to be restricted, and soil evaporation to be nil (Fig. 5.2c). Evaporation from temperate evergreen, conifer forests occurs year-round and their daily magnitude follows the seasonal course of the sun (Anthoni et al. 2002; Humphreys et al. 2003; Kosugi et al. 2005; Grunwald and Bernhoffer 2007). The maximum rates of daily evaporation from an evergreen, conifer, Douglas fir forest in British Columbia tend to be much smaller (less than 3 mm day^{-1}) than that from a temperate evergreen Cypress forest in Japan (Fig. 5.2d). In contrast, daily evaporation from evergreen boreal conifer forests is highly seasonal and is nil during the winter freezing and snow period (Amiro et al. 2006) (not shown).

Very few longer term evaporation records – a decade and longer – have been collected and reported in the literature based on either the eddy covariance (Grunwald and Bernhoffer 2007; Granier et al. 2008) or flux-gradient (Jaeger and Kessler 1997) methods. In general, no trends in evaporation have been detected or attributed to climate, forest function, and structure or successional stage in these few studies.

The lack of a long-term trend in evaporation contrasts with trends associated with CO_2 exchange and forest age (Urbanski et al. 2007; Stoy et al. 2008); net carbon exchange of a closed canopy is a strong function of stand age. This small sampling of the very long evaporation literature also contrasts with findings reported in a 30-year catchment study in the United Kingdom (Marc and Robinson 2007). Younger forests evaporate more than grasslands, while the opposite is true for older forests (Marc and Robinson 2007). On the other hand, Jung et al. (2010) found no trend in terrestrial evaporation at the global scale between 1998 and 2008; they used a machine learning algorithm based on the flux tower network and remote sensing.

5.4 Forest Evaporation and Hydrology

Forests cannot evaporate more water than is available from precipitation. But the questions we ask here include: What fraction of annual precipitation is lost by annual evaporation? Is the evaporation to precipitation ratio conservative? Or does it vary with climate and forest type? Figure 5.3 shows there is a strong linear relationship between precipitation and annual evaporation from forests distributed across the globe. On average, forest evaporation increases 46 mm for every 100 mm increase in rainfall. Furthermore, variations in annual precipitation explain over 75% of the variance in annual evaporation, a remarkably high r^2 value in our opinion. Surprisingly, few workers have examined or reported a correlation
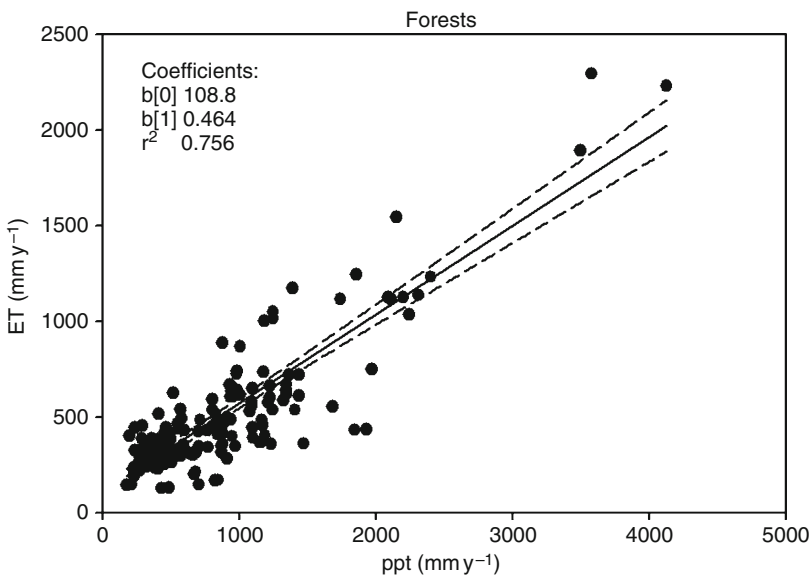
Fig. 5.3 Correlation between annual precipitation (ppt) and annual evaporation (ET) from forests. $N = 165$

between direct measurements of forest evaporation and precipitation at annual timescales, to our knowledge. Albeit indirect correlations are inferred from the Budyko function (Budyko 1974; Donohue et al. 2007). And recently, Alton et al. (2009) evaluated the Marconi version of the FLUXNET database and reported that an ensemble of ecosystems evaporates about 58% of monthly precipitation.

We do not claim that the slope between annual precipitation and forest evaporation (0.46) holds within specific climate spaces, just across the global climate space. For example, in semiarid regions forests tend to evaporate all precipitation (Anthoni et al. 1999; Scott 2010; Yaseef et al. 2010), so the local evaporation–precipitation ratio is near one. In Mediterranean climates, evaporation from evergreen and deciduous oak woodlands is capped below 500 mm year^{-1}, despite interannual variations in rainfall that can range between 600 and 1,200 mm (Joffre and Rambal 1993; Baldocchi et al. 2010).

To investigate the residual sources of variance shown in Fig. 5.3, we plotted annual evaporation (ET) as a function of annual precipitation and net radiation (Fig. 5.4). This surface plot indicates that adding net radiation increases the coefficient of determination (r^2) only slightly, to 0.82. In general, the highest sums of annual evaporation occur where both precipitation and net radiation are high (tropical forests), and the lowest evaporation occurs where annual sums of precipitation and net radiation are low (e.g., boreal forests).

On longer timescales, eco-hydrological factors conspire with one another to limit actual evaporation rates in semiarid regions from meeting extremely high potential evaporation levels ($>1,200$ mm year^{-1}) that are conducive of this region (Rambal 1984; Baldocchi and Xu 2007; Yaseef et al. 2010). In effect, limitations in precipitation and soil moisture limit stand recruitment by modulating sapling and
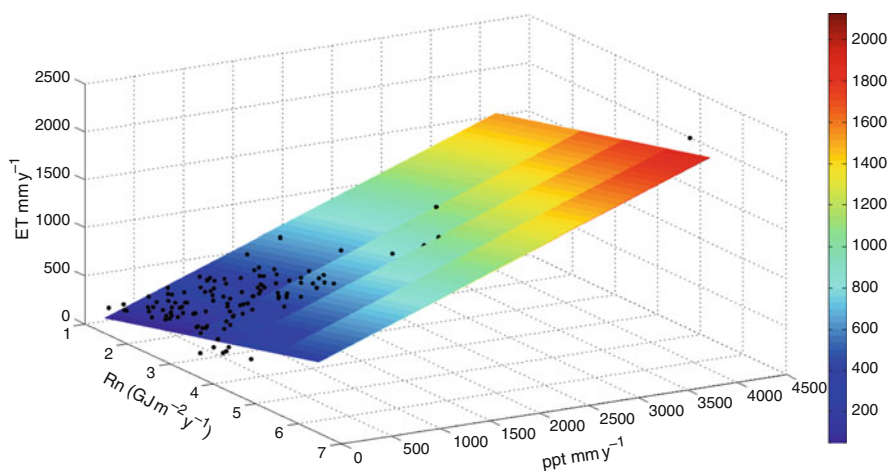
Fig. 5.4 Three-dimensional plot between annual evaporation (ET), net radiation (Rn), and precipitation (ppt). A linear additive model has the following statistics: ET = −141 + 116*Rn + 0.378*ppt, r^2 = 0.819. The *color bar* refers to annual ET

Coefficients:
b[1]-0.773
b[1] 0.936
r^2 0.642
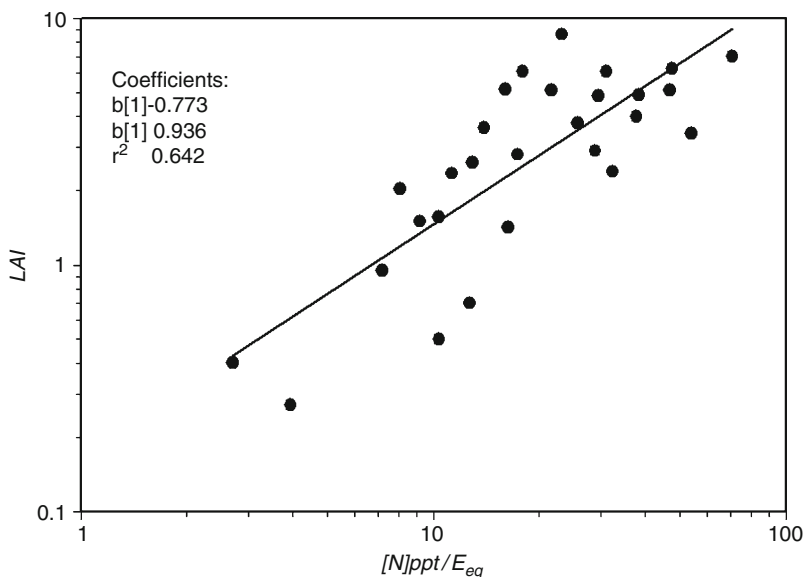
Fig. 5.5 Relation between leaf area index of forests vs. a nondimensional index defined as the product of leaf nitrogen times annual precipitation divided by the annual sum of equilibrium evaporation

seedling mortality. An equilibrium between water use and availability is eventually met to form a canopy with a relatively low tree density and low leaf area index (Eamus and Prior 2001; Baldocchi and Xu 2007; Joffre et al. 2007) (Fig. 5.5).

Another ecological question pertaining to forest evaporation relates to the functional role of broadleaved vs. needleleaved and deciduous vs. evergreen trees on evaporation of forests growing in similar climates. This question was addressed by Komatsu et al (2007) for a number of forest catchments across Japan. They found that evaporation from broadleaved forests was approximately the same for young conifer stands and it was higher than evaporation from old conifer stands. Swank and Douglass (1974), on other hand, found stream flow was reduced by 20% by converting a deciduous forest to conifer forest due to more interception losses by pine. In Mediterranean climates, annual evaporation from deciduous oaks is significantly greater than evaporation from evergreen oaks, by 110 mm year^{-1}, after difference in leaf area index and local climate is considered (Baldocchi et al. 2010).

5.5   Biophysical Controls on Evaporation

The Penman–Monteith equation provides a theoretical framework for quantifying forest evaporation, in terms of latent heat exchange (Monteith and Unsworth 1990), and for diagnosing how evaporation rates will respond to changes in weather and plant variables. For improved diagnostic reasons, the Penman–Monteith equation

has been redefined as the additive combination of equilibrium (E_{eq}) and imposed (E_{imp}) evaporation (Jarvis and McNaughton 1986):

$$E = \Omega \cdot E_{eq} + (1 - \Omega)E_{imp}. \tag{5.2}$$

Equilibrium evaporation is a function of available energy and computed as:

$$E_{eq} = \frac{s}{s + \gamma} \frac{(R_{net} - G - S)}{\lambda}. \tag{5.3}$$

Imposed evaporation is a function of atmospheric demand and physiological supply and is expressed as:

$$E_{imp} = \frac{G_s D}{P}. \tag{5.4}$$

In (5.2) through (5.4), Ω denotes the coupling factor and ranges between zero and one, s is the slope of the saturation vapor pressure–temperature relationship, R_n is the net radiation balance, S is canopy heat storage, G is soil heat storage, D is vapor pressure deficit, γ is the psychrometric constant, ρ is air density, C_p is specific heat of air, λ is the latent heat of evaporation, and G_h and G_s are the canopy-scale conductances for boundary layer and surface.

Forests are aerodynamically rough and tend to be better coupled with their environment, hence they tend to have low omega values (Jarvis and McNaughton 1986; Verma et al. 1986). Despite the theoretical association between forest evaporation with imposed evaporation, a large number of investigators have interpreted their forest evaporation rates as a multiplicative fraction of equilibrium evaporation, α:

$$E = \alpha \frac{s}{s + \gamma}(R_{net} - G - S). \tag{5.5}$$

For short vegetation with adequate soil moisture and extensive fetch, α is about 1.26. But a number of studies show that α deviates from 1.26 for dry (Baldocchi et al. 1997; Komatsu 2005; Baldocchi and Xu 2007) and wet forest canopies (Shuttleworth and Calder 1979). Table 5.1 reproduces a survey of α values for a range of forest types. In general, α values for forests range between 1.09 and 0.53 and rank according to the following: broadleaved deciduous > tropical broadleaved evergreen > temperate conifer > boreal conifer > boreal deciduous conifer. Empirical evidence adds that α increases with decreasing canopy height and increasing leaf area index (Kelliher et al. 1993; Komatsu et al. 2007) and it decreases with progressively drying soils (Kelliher et al. 1993; Baldocchi et al. 2004; Chen et al. 2008). Using a theoretical model, we determined that this ranking depends on leaf area index, photosynthetic capacity, and soil moisture (Baldocchi and Meyers 1998); highest α values are produced by forests with high leaf area

Table 5.1 The ratio between actual and equilibrium evaporation for a number of forest categories, otherwise denoted as the Priestley–Taylor coefficient, α (Komatsu 2005)

Forest type	Mean	Std dev.
Boreal broadleaved, deciduous	1.09	–
Temperate broadleaved deciduous	0.851	0.147
Tropical broadleaved, evergreen	0.824	0.115
Temperate broadleaved evergreen	0.764	0.181
Temperate conifer	0.652	0.249
Boreal conifer, evergreen	0.55	0.102
Boreal conifer, deciduous	0.53	0.084

indices, ample soil water, and high photosynthetic capacity. Conversely, lowest α values are associated with sparse forest canopies with low photosynthetic capacity, low leaf area index, low hydraulic conductivity, and/or soil moisture deficits.

The role of biodiversity on forest evaporation remains unclear. On one hand, Currie and Paquin (1987) reported that tree species richness was positively correlated with an inferred estimate of annual evaporation. It was proposed that forest productivity scales positively with biodiversity, so it was expected that evaporation would scale with increased productivity. On the other hand, one of us (Baldocchi 2005) reported that the alpha coefficient in (5.5) decreased with increasing number of the dominant tree species in deciduous broadleaved forests. In the latter study, it was hypothesized that greater biodiversity increases the diversity of xylem architecture (e.g., ring vs. diffuse porous) and xylem conductivity. Hence, more diverse forests would have a mixture of trees with higher and lower xylem conductivities (Cochard et al. 1996), causing the area integrated hydraulic conductivity of a diverse forest to be less than a less diverse forest. The idea remains contentious and merits further scrutiny as it was derived from a relatively small cross-section of the FLUXNET database.

5.6 Understory Evaporation

Not all water is lost by tree transpiration. Some water is lost by re-evaporation of intercepted rainfall, a second fraction is lost by soil evaporation, and the remainder is transpired by understory vegetation. But until the advent of eddy covariance systems, it was difficult to measure understory evaporation directly, albeit lysimeters and chambers provide useful information on soil evaporation (Black and Kelliher 1989; Yaseef et al. 2010). The tall nature of forests enables investigators to deploy eddy covariance systems in the understory (Baldocchi and Meyers 1991) to measure soil evaporation directly. In general, the fraction of evaporation under forests is significant. It ranges between 10 and 50% of total evaporation and the evaporation ratio tends to increase with decreasing leaf area index as the net radiation flux density at the soil increases (Table 5.2).

Table 5.2 Survey on the fraction of understory evaporation based on eddy covariance measurements made in the forest understory and overstory

Location	ET$_{understory}$/ET (%)	LAI	References
Deciduous forest, Tennessee	10	6	Wilson et al. (2000)
Boreal pine forest, Saskatchewan	20–40	~2	Baldocchi et al. (1997)
Oak savanna, California	<20	0.7	Baldocchi et al. (2004)
Temperate pine, Metolius, OR	<20	1.5	Baldocchi et al. (2000)
Boreal deciduous, broadleaved, Prince Albert, Sask	25	5.6	Blanken et al. (2001)
Semiarid pine, Israel	36	1.5	Yaseef et al. (2010)
Semiarid, woodland, Arizona	30–40		Scott et al. (2003)
Larch, Siberia	51	2.0	Iida et al. (2009)
Larch, Siberia	50		Kelliher et al. (1997)
Boreal pine forest, Sweden	10–15		Constantin et al. (1999)
Larch, Siberia	35	3.7	Ohta et al. (2001)

By being nonintrusive, eddy covariance measurements of soil evaporation have produced an alternative interpretation on the controls of soil evaporation. The timescale for turbulent exchange inside a deep forest is on the order of 2–5 min. This periodic re-flushing of the canopy air space inhibits soil evaporation rates from attaining equilibrium with the net radiation budget, and instead forces soil evaporation to be more closely coupled to their vapor pressure deficit (Baldocchi and Meyers 1991; Baldocchi et al. 2000). A consequence of this finding is the potential to restrict or inhibit soil evaporation by using soil chambers.

5.7 Final Comments and Future Directions

Forests play pivotal, and at times contrarian, roles on the water balance of catchments (Salati and Vose 1984) and the climate system (Bonan 2008; Jackson et al. 2008). If one is managing watersheds to maximize water yield, forested catchments tend to provide less runoff than cleared catchments (Bosch and Hewlett 1982; Marc and Robinson 2007). This finding has important implications on the hydrological cost of sequestering carbon by afforestation and reforestation. In semiarid regions, replacing herbaceous vegetation with forests will increase evaporation because forests are aerodynamically rougher and radiatively darker than herbaceous vegetation (Kelliher et al. 1993; Baldocchi et al. 2004). On the other hand, if one is trying to sustain large-scale precipitation in tropical and temperate humid regions, the presence of forests can generate a positive feedback on the hydrological cycle and promote runoff (Salati and Vose 1984; Bonan 2008; Jackson et al. 2008); trees are effective conduits for transferring soil moisture into the atmosphere, which in turn condenses, forms clouds and rain. Conversely, large-scale tropical deforestation has the potential to break this hydrological cycle because C_4 pastures (that typically replace tropical

forests) evaporate less water due to their lower stomatal and surface conductances (Dickinson and Henderson-Sellers 1988; Vourlitis et al. 2002; Sakai et al. 2004).

We are now at the dawn of a new era with the potential to produce decade long, and longer, data records of direct evaporation rates for a wide range of forests in a changing world. The application of eddy covariance, however, is still restricted to rather ideal and flat terrain. Hence, there is still value to continue studying forest evaporation with gauged watersheds in complex terrain. Research questions that need continued attention include the roles of annual precipitation and biodiversity on forest evaporation and how to upscale tower fluxes across complex landscapes to regional and global scales using remote sensing.

References

Alton P, Fisher R, Los S et al (2009) Simulations of global evapotranspiration using semiempirical and mechanistic schemes of plant hydrology. Glob Biogeochem Cycles 23: doi:10.1029/2009GB003540

Amiro BD, Barr AG, Black TA et al (2006) Carbon, energy and water fluxes at mature and disturbed forest sites, Saskatchewan, Canada. Agric For Meteorol 136:237–251

Anthoni PM, Law BE, Unsworth MH (1999) Carbon and water vapor exchange of an open-canopied ponderosa pine ecosystem. Agric For Meteorol 95:151–168

Anthoni PM, Irvine J, Unsworth MH et al (2002) Seasonal differences in carbon and water vapor exchange in young and old-growth ponderosa pine ecosystems. Agric For Meteorol 111:203–222

Araujo AC, Nobre AD, Kruijt B et al (2002) Comparative measurements of carbon dioxide fluxes from two nearby towers in a central Amazonian rainforest: The Manaus LBA site. J Geophys Res Atmos 107:D20, 8090

Baldocchi DD (2005) The role of biodiversity on evaporation of forests. In: Scherer-Lorenzen M, Koerner C, Schulze E-D (eds) Forest diversity and function. Springer, Berlin, pp 131–148

Baldocchi D (2008) TURNER REVIEW No. 15. "Breathing" of the terrestrial biosphere: lessons learned from a global network of carbon dioxide flux measurement systems. Aust J Bot 56:1–26

Baldocchi DD, Meyers TP (1991) Trace gas exchange at the floor of a deciduous forest: I. Evaporation and CO_2 efflux. J Geophys Res Atmos 96:7271–7285

Baldocchi DD, Meyers T (1998) On using eco-physiological, micrometeorological and biogeochemical theory to evaluate carbon dioxide, water vapor and trace gas fluxes over vegetation: a perspective. Agric For Meteorol 90:1–25

Baldocchi DD, Xu L (2007) What limits evaporation from Mediterranean oak woodlands – The supply of moisture in the soil, physiological control by plants or the demand by the atmosphere? Adv Water Resour 30:2113–2122

Baldocchi DD, Vogel CA, Hall B (1997) Seasonal variation of energy and water vapor exchange rates above and below a boreal jackpine forest. J Geophys Res 102:28939–28952

Baldocchi DD, Law BE, Anthoni PM (2000) On measuring and modeling energy fluxes above the floor of a homogeneous and heterogeneous conifer forest. Agric For Meteorol 102:187–206

Baldocchi DD, Falge E, Gu LH et al (2001) FLUXNET: a new tool to study the temporal and spatial variability of ecosystem-scale carbon dioxide, water vapor, and energy flux densities. Bull Am Meteorol Soc 82:2415–2434

Baldocchi DD, Xu L, Kiang N (2004) How plant functional-type, weather, seasonal drought, and soil physical properties alter water and energy fluxes of an oak-grass savanna and an annual grassland. Agric For Meteorol 123:13–39

Baldocchi D, Ma S, Rambal S et al (2010) On the differential advantages of evergreenness and deciduousness in mediterranean oak woodlands: a flux perspective. Ecol Appl 20(6):1583–1597

Barr AG, Gvd K, Schmidt R et al (2000) Monitoring the moisture balance of a boreal aspen forest using a deep groundwater piezometer. Agric For Meteorol 102:13–24

Barr AG, Black TA, Hogg EH et al (2007) Climatic controls on the carbon and water balances of a boreal aspen forest, 1994–2003. Glob Change Biol 13:561–576

Black TA (1979) Evapotranspiration from Douglas-fir stands exposed to soil-water deficits. Water Resour Res 15:164–170

Black TA, Kelliher FM (1989) Processes controlling understorey evapotranspiration. Philos Trans Roy Soc B 324:207–231

Black TA, McNaughton KG (1971) Psychrometric apparatus for Bowen-ratio determination over forests. Bound-Lay Meteorol 2:246–254

Black T, DenHartog G, Neumann H et al (1996) Annual cycles of water vapour and carbon dioxide fluxes in and above a boreal aspen forest. Glob Change Biol 2:219–229

Blanken PD, Black TA, Neumann HH et al (2001) The seasonal water and energy exchange above and within a boreal aspen forest. J Hydrol 245:118–136

Bonan GB (2008) Forests and climate change: forcings, feedbacks, and the climate benefits of forests. Science 320:1444–1449

Bosch JM, Hewlett JD (1982) A review of catchment experiments to determine the effect of vegetation changes on water yield and evapotranspiration. J Hydrol 55:3–23

Buck AL (1976) Variable-path Lyman-Alpha hygrometer and its operating characteristics. Bull Am Meteorol Soc 57:1113–1118

Budyko MI (1974) Climate and life. Academic Press, New York

Calder IR (1998) Water use by forests, limits and controls. Tree Physiol 18:625–631

Chen XY, Rubin Y, Ma SY et al (2008) Observations and stochastic modeling of soil moisture control on evapotranspiration in a Californian oak savanna. Water Resour Res 44: doi:10.1029/2007WR006646

Cochard H, Breda N, Granier A (1996) Whole tree hydraulic conductance and water loss regulation in Quercus during drought: evidence for stomatal control of embolism? Ann For Sci 53:197–206

Constantin J, Grelle A, Ibrom A et al (1999) Flux partitioning between understorey and overstorey in a boreal spruce/pine forest determined by the eddy covariance method. Agric For Meteorol 98–99:629–643

Currie DJ, Paquin V (1987) Large scale biogeographical patterns of species richness of trees. Nature 329:326–327

da Rocha HR, Goulden ML, Miller SD et al (2004) Seasonality of water and heat fluxes over a tropical forest in eastern Amazonia. Ecol Appl 14:S22–S32

David TS, Henriques MO, Kurz-Besson C et al (2007) Water-use strategies in two co-occurring Mediterranean evergreen oaks: surviving the summer drought. Tree Physiol 27:793–803

Denmead OT (1969) Comparative micrometeorology of a wheat field and a forest of Pinus radiata. Agr Meteorol 6:357–371

Dickinson RE, Henderson-Sellers A (1988) Modeling tropical deforestation – a study of GCM land surface parametrizations. Quart J Roy Meteorol Soc 114:439–462

Donohue RJ, Roderick ML, McVicar TR (2007) On the importance of including vegetation dynamics in Budyko's hydrological model. Hydrol Earth Syst Sci 11:983–995

Droppo J, Hamilton H (1973) Experimental variability in the determination of the energy balance in a deciduous forest. J Appl Meteorol 12:781–791

Eamus D, Prior L (2001) Ecophysiology of trees of seasonally dry tropics: comparisons among phenologies. Adv Ecol Res 32:113–197

Fisher JB, Tu KP, Baldocchi DD (2008) Global estimates of the land-atmosphere water flux based on monthly AVHRR and ISLSCP-II data, validated at 16 FLUXNET sites. Remote Sens Environ 112:901–919

Fisher JB, Malhi Y, Bonal D et al (2009) The land-atmosphere water flux in the tropics. Glob Change Biol 15:2694–2714

Giambelluca TW, Martin RE, Asner GP et al (2009) Evapotranspiration and energy balance of native wet montane cloud forest in Hawaii. Agric For Meteorol 149:230–243

Granier A, Breda N, Longdoz B et al (2008) Ten years of fluxes and stand growth in a young beech forest at Hesse, North-eastern France. Ann For Sci 65: Article No. 704, 10.1051/forest:2008052

Grunwald T, Bernhoffer C (2007) A decade of carbon, water and energy flux measurements of an old spruce forest at the Anchor Station Tharandt. Tellus B 59:387–396

Hicks BB, Hyson P, Moore CJ (1975) Study of eddy fluxes over a forest. J Appl Meteorol 14:58–66

Humphreys ER, Black TA, Ethier GJ et al (2003) Annual and seasonal variability of sensible and latent heat fluxes above a coastal Douglas-fir forest, British Columbia, Canada. Agric For Meteorol 115:109–125

Hyson P, Hicks BB (1975) Single-beam infrared hygrometer for evaporation measurement. J Appl Meteorol 14:301–307

Iida S, Ohta T, Matsumoto K et al (2009) Evapotranspiration from understory vegetation in an eastern Siberian boreal larch forest. Agric For Meteorol 149:1129–1139

Jackson RB, Randerson JT, Canadell JG et al (2008) Protecting climate with forests. Environ Res Lett 3. doi:10.1088/1748-9326/3/4/044006

Jaeger L, Kessler A (1997) Twenty years of heat and water balance climatology at the Hartheim pine forest, Germany. Agric For Meteorol 84:25–36

Jarvis PG, McNaughton KG (1986) Stomatal control of transpiration – scaling up from leaf to region. Adv Ecol Res 15:1–49

Jarvis PG, James GB, Landsberg JJ (1976) Coniferous forest. In: Monteith JL (ed) Vegetation and the atmosphere, vol 2. Academic Press, London, pp 171–240

Joffre R, Rambal S (1993) How tree cover influences the water balance of Mediterranean rangelands. Ecology 74:570–582

Joffre R, Rambal S, Damesin C (2007) Functional attributes in Mediterranean-type ecosystems. In: Pugnaire FI (ed) Functional plant ecology. CRC Press, Boca Raton, pp 285–312

Jung M, Reichstein M, Ciais P et al (2010) Recent decline in the global land evapotranspiration trend due to limited moisture supply. Nature 467:951–954

Kelliher FM, Leuning R, Schulze ED (1993) Evaporation and canopy characteristics of coniferous forests and grasslands. Oecologia 95:153–163

Kelliher FM, Hollinger DY, Schulze E-D et al (1997) Evaporation from an eastern Siberian larch forest. Agric For Meteorol 85:135–147

Komatsu H (2005) Forest categorization according to dry-canopy evaporation rates in the growing season: comparison of the Priestley-Taylor coefficient values from various observation sites. Hydrol Process 19:3873–3896

Komatsu H, Tanaka N, Kume T (2007) Do coniferous forests evaporate more water than broad-leaved forests in Japan? J Hydrol 336:361–375

Kosugi Y, Tanaka H, Takanashi S et al (2005) Three years of carbon and energy fluxes from Japanese evergreen broadleaved forest. Agric For Meteorol 132:329–343

Lee XH, Fuentes JD, Staebler RM et al (1999) Long-term observation of the atmospheric exchange of CO_2 with a temperate deciduous forest in southern Ontario, Canada. J Geophys Res 104:15975–15984

Lindroth A, Molder M, Lagergren F (2010) Heat storage in forest biomass improves energy balance closure. Biogeosciences 7:301–313

Loescher HW, Gholz HL, Jacobs JM et al (2005) Energy dynamics and modeled evapotranspiration from a wet tropical forest in Costa Rica. J Hydrol 315:274–294

Marc V, Robinson M (2007) The long-term water balance (1972–2004) of upland forestry and grassland at Plynlimon, mid-Wales. Hydrol Earth Syst Sci 11:44–60

Meyers TP, Hollinger SE (2004) An assessment of storage terms in the surface energy balance of maize and soybean. Agric For Meteorol 125:105–115

Moncrieff J, Malhi Y, Leuning R (1996) The propagation of errors in long-term measurements of carbon and water. Glob Change Biol 2:231–240

Monteith JL, Unsworth MH (1990) Principles of environmental physics. Edward Arnold, London

Moore KE, Fitzjarrald DR, Sakai RK et al (1996) Seasonal variation in radiative and turbulent exchange at a deciduous forest in central Massachusetts. J Appl Meteorol 35:122–134

Ohta T, Hiyama T, Tanaka H et al (2001) Seasonal variation in the energy and water exchanges above and below a larch forest in eastern Siberia. Hydrol Process 15:1459–1476

Oliphant AJ, Grimmond CSB, Zutter HN et al (2004) Heat storage and energy balance fluxes for a temperate deciduous forest. Agric For Meteorol 126:185–201

Paço TA, David TS, Henriques MO et al (2009) Evapotranspiration from a Mediterranean evergreen oak savannah: the role of trees and pasture. J Hydrol 369:98–106

Rambal S (1984) Water balance and pattern of root water uptake by a Quercus coccifera L. evergreen scrub. Oecologia 62:18–25

Raupach MR (1978) Infrared fluctuation hygrometry in atmospheric surface-layer. Quart J Roy Meteorol Soc 104:309–322

Raupach MR (1979) Anomalies in flux-gradient relationships over forest. Bound-Lay Meteorol 16:467–486

Raupach MR, Finnigan JJ, Brunet Y (1996) Coherent eddies and turbulence in vegetation canopies: the mixing-layer analogy. Bound-Lay Meteorol 78:351–382

Sakai RK, Fitzjarrald DR, Moraes OLL et al (2004) Land-use change effects on local energy, water, and carbon balances in an Amazonian agricultural field. Glob Change Biol 10:895–907

Salati E, Vose PB (1984) Amazon Basin: a system in equilibrium. Science 225:129–138

Scott RL (2010) Using watershed water balance to evaluate the accuracy of eddy covariance evaporation measurements for three semiarid ecosystems. Agric For Meteorol 150(2):219–225

Scott RL, Watts C, Payan JG et al (2003) The understory and overstory partitioning of energy and water fluxes in an open canopy, semiarid woodland. Agric For Meteorol 114:127–139

Sellers PJ, Hall FG, Margolis H et al (1995) Boreal Ecosystem Atmosphere (BOREAS): an overview and early results from the 1994 field year. Bull Am Meteorol Soc 76:1549–1577

Shuttleworth WJ, Calder IR (1979) Has the Priestley-Taylor equation any relevance to forest evaporation? J Appl Meteorol 18:639–646

Shuttleworth WJ, Gash JHC, Lloyd CR et al (1984) Eddy-correlation measurements of energy partition for Amazonian forest. Quart J Roy Meteorol Soc 110:1143–1162

Spittlehouse DL, Black TA (1979) Determination of forest evapotranspiration using Bowen ratio and Eddy correlation-measurements. J Appl Meteorol 18:647–653

Stewart JB, Thom AS (1973) Energy budgets in pine forest. Quart J Roy Meteorol Soc 99:154–170

Stoy PC, Katul GG, Siqueira MS et al (2008) Role of vegetation in determining carbon sequestration along ecological succession in the southeastern United States. Glob Change Biol 14:1409–1427

Swank WT, Douglass JE (1974) Streamflow greatly reduced by converting deciduous hardwood stands to pine. Science 185:857–859

Tanaka N, Kume T, Yoshifuji N et al (2008) A review of evapotranspiration estimates from tropical forests in Thailand and adjacent regions. Agric For Meteorol 148:807–819

Twine TE, Kustas WP, Norman JM et al (2000) Correcting eddy-covariance flux underestimates over a grassland. Agric For Meteorol 103:279–300

Urbanski S, Barford C, Wofsy S et al (2007) Factors controlling CO_2 exchange on timescales from hourly to decadal at Harvard Forest. J Geophys Res 112: doi:10.1029/2006JG000293

Verma SB, Baldocchi DD, Anderson DE et al (1986) Eddy fluxes of CO_2, water vapor and sensible heat over a deciduous forest. Bound-Lay Meteorol 36:71–91

Vourlitis GL, Priante N, Hayashi MMS et al (2001) Seasonal variations in the net ecosystem CO_2 exchange of a mature Amazonian transitional tropical forest (cerradao). Funct Ecol 15:388–395

Vourlitis GL, Priante N, Hayashi MMS et al (2002) Seasonal variations in the evapotranspiration of a transitional tropical forest of Mato Grosso, Brazil. Water Resour Res 38: Art. no. 1094

Wilson KB, Baldocchi DD (2000) Seasonal and interannual variability of energy fluxes over a broadleaved temperate deciduous forest in North America. Agric For Meteorol 100:1–18

Wilson K, Hanson PJ, Baldocchi DD (2000) Evaporation and energy fluxes beneath a temperate deciduous forest in North America. Agric For Meteorol 102:83–103

Wilson KB, Hanson PJ, Mulholland PJ et al (2001) A comparison of methods for determining forest evapotranspiration and its components: sap-flow, soil water budget, eddy covariance and catchment water balance. Agric For Meteorol 106:153–168

Wilson K, Goldstein A, Falge E et al (2002) Energy balance closure at FLUXNET sites. Agric For Meteorol 113:223–243

Yaseef NR, Yakir D, Rotenberg E et al (2010) Ecohydrology of a semi-arid forest: partitioning among water balance components and its implications for predicted precipitation changes. Ecohydrology 3:143–154

Zhang K, Kimball JS, Nemani RR et al (2010) A continuous satellite-derived global record of land surface evapotranspiration from 1983 to 2006. Water Resour Res 46:W09522. doi:10.1029/2009WR008800

Chapter 6
Spectral Methods to Advance Understanding of Dissolved Organic Carbon Dynamics in Forested Catchments

Rose M. Cory, Elizabeth W. Boyer, and Diane M. McKnight

6.1 Introduction

Literally the stuff of life, carbon is ubiquitous in forested catchments and sustains growth of terrestrial and aquatic life. Carbon cycling describes the complex recirculatory processes whereby carbon is transformed from inorganic to organic forms then back again. These processes are strongly influenced by the pervasive feedbacks between hydrology and biogeochemistry, operating at a multiple temporal and spatial scales in catchments. For example, the distribution of vegetation (i.e., organic carbon produced by photosynthesis) and its productivity (which often is limited by nitrogen availability) are related to climatic gradients associated with the distribution of precipitation (i.e., hydrology). In turn, vegetation affects both precipitation and temperature through evapotranspiration and the accumulation of detrital organic matter in the litter layer and soils influences soil moisture. Further, changes in the species, density, and pattern of vegetation in a catchment can have profound impacts on the amount, timing, and quality of water levels and streamflow. Forested catchments play many important roles in the carbon cycle. For example, they store carbon (e.g., for widely varying lengths of time as a function of hydrology and biogeochemistry), they transform carbon (e.g., with sites for terrestrial and aquatic CO_2 removal through photosynthesis), and they transport carbon (e.g., moving organic carbon along surface and ground water flowpaths and stream networks).

Water quality is strongly influenced by the biogeochemical cycles of carbon. Carbon is abundant in the waters issuing from forested catchments and is transported in several forms: (1) dissolved inorganic carbon, such as dissolved carbon dioxide, bicarbonate and carbonate ions; (2) particulate organic carbon, composed of matter such as leaf litter, woody debris, and soil organics; and (3) dissolved organic carbon (DOC), which arises from such processes as decomposition of plant and soil material, and from in-stream primary production. In this chapter, we focus specifically on advances in understanding DOC concentration and composition in surface waters of forested catchments. DOC is a primary measure of the total dissolved organic matter (DOM) present in natural waters (Thurman 1985). Spatial and temporal variation in climatic variables, vegetation, soils, and bedrock will

result in variability in both DOC source areas and in hydrological pathways (Boyer et al. 1997; Mulholland and Hill 1997; McGlynn and McDonnell 2003; Saraceno et al. 2009).

The DOC has long been recognized to be a critical water quality characteristic in forested catchments and is highly relevant to diverse environmental problems (Findlay and Sinsabaugh 2003; Leenheer and Croue 2003). DOC is a major component of the carbon cycle and energy balance in forested catchments (Fisher and Likens 1973; Mulholland 1997). Labile fractions of the DOC pool fuel the food web in aquatic ecosystems (Carpenter et al. 2005). Its key role in metabolism in streams has been demonstrated in environments ranging from the Arctic (Naiman et al. 1987) and temperate forests (Roberts et al. 2007) to southern blackwaters (Meyer and Edwards 1990). The humic fraction of DOC pool can act as an electron shuttle, contributing to energy transfer via hyporheic exchange in streams, for example, Miller et al. (2006). Chromophoric DOC, which includes the humic fractions, acts as a sunscreen for aquatic ecosystems, absorbing visible and ultraviolet radiation. DOC thus mediates photochemical processes, degrading in the presence of sunlight to form various degradation products (Scott et al. 2003; Porcal et al. 2004; Cory et al. 2007; Yoshioka et al. 2007). DOC is associated with the formation of harmful disinfection by-products during standard drinking water treatment of downstream waters (Fuiji et al. 1998; Bergamaschi et al. 1999). Via complexing reactions and by enhancing solubility, humic and other fractions of the DOC pool are significant in the mobilization and transport of trace metals and contaminants (McKnight et al. 1992; Haitzer et al. 2002). Further soluble organic acids comprising DOC can be important in the analytical cation–anion balance, contributing to stream acidity in many forested freshwater environments (Oliver et al. 1983).

The importance of organic carbon on water quality is widely recognized, but challenges remain in quantifying fluxes of DOC in surface waters, and understanding its composition and reactivity. In natural waters, the chemical character of DOM depends on its sources, which include degrading plant and soil material delivered from the watershed and breakdown products of bacterial and algal matter in the water column (Thurman 1985; McKnight et al. 2003). The quantity and quality of DOC in streams is dynamic, exhibiting short-term fluctuation due to diurnal influence from photodegradation (Cory et al. 2007; Spencer et al. 2007) or from storm event driven inputs of DOC (Boyer et al. 2000; Carstea et al. 2009; Fellman et al. 2009b). Changing biogeochemical processes in the watershed over seasonal timescales are also reflected in DOC quality (Fellman et al. 2009b). Long-term patterns of change in response to shifts in climate, land use, or other perturbations in the watershed are also evident as changing quantity or quality of DOC (Monteith et al. 2007; Wilson and Xenopoulos 2009). Because DOC quantity and quality reflect a dynamic interplay between organic matter sources and biogeochemical processes (Jaffe et al. 2008), changes to water resources from climate, land use, and urbanization are expected to be evident in the shifts of the concentration and chemical signatures of DOC.

Classifying DOM to resolve its actual components remains a contemporary research challenge. Although somewhat laborious (Leenheer and Croue 2003),

chemical fractionation methods have been incorporated into monitoring studies in watersheds. Recent studies using fractionation methods have enhanced their effectiveness by concomitant use of spectral methods to characterize the DOC (Hood et al. 2003; Cory et al. 2007; Miller et al. 2009). For example, Hood et al. (2003) studied coupled hydrological and biogeochemical processes in a subalpine watershed containing a sequence of lakes (Fig. 6.1). Peak DOC concentrations at all sites occurred in May and June on the early rising limb of the hydrograph. Using DOC fractionation methods, they showed that the percentage of the DOC in stream water accounted for by fulvic acid (a component of DOC linked in this case to allochthonous or terrestrial sources of organic matter) increased on the rising limb of the hydrograph and decreased after the snowmelt pulse. A simple fluorescence index (FI) developed as an indicator for DOC source in freshwaters was consistent with these data, indicating an increasing contribution of DOM from terrestrial sources during snowmelt when hydrological connectivity between the streams and the landscape was heightened, and indicated an increasing contribution of DOM from phytoplankton growth in the lakes during the summer when hydrological connectivity between the streams and the landscape was minimal. Similarly, Cory et al. (2007) used a combination of DOM fractionation and chemical characterization approaches, including spectral analyses, to demonstrate the interplay between hydrologic transport and biogeochemical alteration on the ultimate fate of DOM in arctic surface waters. The application of recent advances in spectral methods to understand carbon cycling has great potential, keeping in mind that fractionation or other ancillary measurements of DOC character may be warranted to confirm data interpretation.

In this chapter, we review the use of simple spectral methods to quantify DOC composition in forested catchments. We discuss use of absorbance spectroscopy, which has been widely used as a surrogate for DOC concentration and as an indicator of changing DOC composition in waters of forested catchments (e.g., Aiken and Cotsaris 1995; Weishaar et al. 2003). We also discuss use of fluorescence spectroscopy, where spectral analyses of three-dimensional excitation–emission matrices (EEMs) are used to characterize sources of DOC (McKnight et al. 2001). In less than a decade, the FI method first presented by McKnight et al. (2001) has become widely used and refined, as evidenced by the fact that it has already been cited 291 times in the peer-reviewed literature, accessed via Google Scholar, October 25, 2010. Subsequently, others have developed and applied parallel factor analysis (PARAFAC) to further classify the EEMs into components of varying DOC character, which has also become widely used to quantify the character of DOC in freshwater systems (Stedmon et al. 2003; Cory and McKnight 2005; Stedmon and Bro 2008). Due to the relative simplicity of applying absorbance and fluorescence analytical techniques, and to recent rapid advances in their application to freshwater ecosystems in the context of understanding organic matter dynamics, simple spectral methods are now very widely used to determine, as a first approximation, the origins, sources, and magnitude of DOC in fresh waters (Aiken and Cotsaris 1995; McKnight et al. 2001; Leenheer and Croue 2003; Baker and Spencer 2004; Cory and McKnight 2005; Ågren et al. 2008).
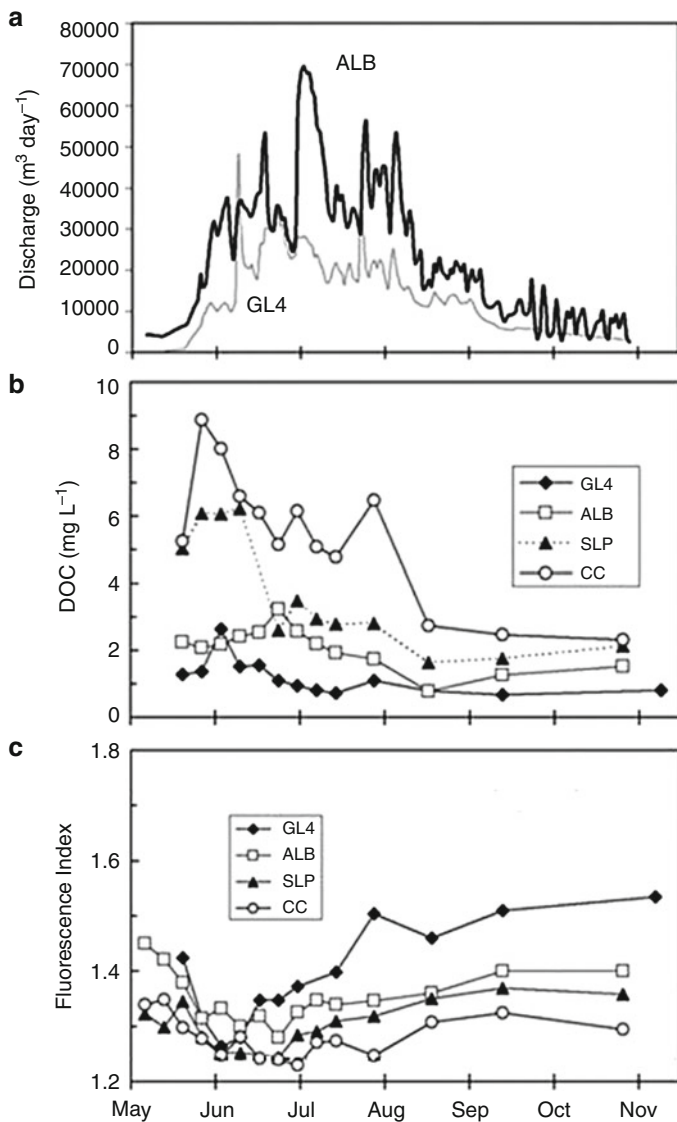
Fig. 6.1 Relationships between hydrology, DOC concentration, and DOM character in the Green Lakes Valley, Colorado Front Range, United States. Modified from Hood et al. (2003). Stream water samples were collected from forested upland catchments at two sites above the tree line (GL4 and ALB) and two sites below the tree line (SLP and CC). Associated with the rising limb of the streamflow hydrograph (**a**), peak DOC concentrations at all sites occurred early in the season in May and June (**b**). A simple fluorescence index (FI) indicated shifting sources of organic matter throughout the year (**c**). These results suggested that DOC was derived primarily from allochthonous precursor material (from terrestrial vegetation and soils) during snowmelt at peak runoff, and was derived primarily from autochthonous precursor material (from algal and microbial biomass within the lakes) during the summer

6.2 Toward Classifying Organic Matter with Simple Methods

6.2.1 DOC Concentration Reflects a Heterogeneous DOM Pool

The DOM is operationally defined as all the naturally occurring organic molecules in water that pass through an average filter with a pore size less than 0.7 μm. (Though the standard classification of dissolved constituents in natural waters is often 0.45 μm, analysis of organic matter typically requires use of a binder-free glass-fiber filter, of which 0.7 μm is the smallest nominal pore size available.) The analytical challenges associated with the characterization of DOM, a complex and polydisperse mixture of compounds ranging in molecular sizes, weights, and reactivities, have long been documented. New insights from ultra-high resolution mass spectrometry approaches (e.g., Kim et al. 2006; Sleighter and Hatcher 2007) confirm that a given DOM sample contains thousands of compounds, which deepens on our understanding of the complexity of the DOM pool. The conceptual pie diagram (Fig. 6.2) illustrates the chemical heterogeneity of DOC of a typical riverine freshwater (modified from McKnight et al. 2003). The pie diagram also illustrates the importance of organic acid fractions in the DOC pool, which reflects the extent to which ionized carboxylic acid functional groups enhances the solubility of organic molecules. The specific chemical classes (or wedges) can be separated based on DOM fractionation techniques (Thurman and Malcolm 1981; Aiken et al. 1992). The different wedges may be derived from different precursor sources of organic material in soils, litter, plankton, suspended organic matter, or sediment (McKnight et al. 2003). The different precursor pools are also subject to different biogeochemical transformation processes (e.g., microbial uptake), which increase the difficulty of establishing a link between a particular precursor pool and a specific chemical class DOM (McKnight et al. 2003). Thus, the complexity of the DOM pie suggests that searching for a meaningful tracer for DOC or DOM as a "whole" may not be fruitful.

Fig. 6.2 Distribution of DOC in a typical river. Each of the humic fractions (fulvic, humic, and transphilic acids) are heterogeneous mixtures of compounds that have similar chemical properties in terms of acidic functionality, hydrophobic character, and molecular weight. Modified from McKnight et al. (2003)
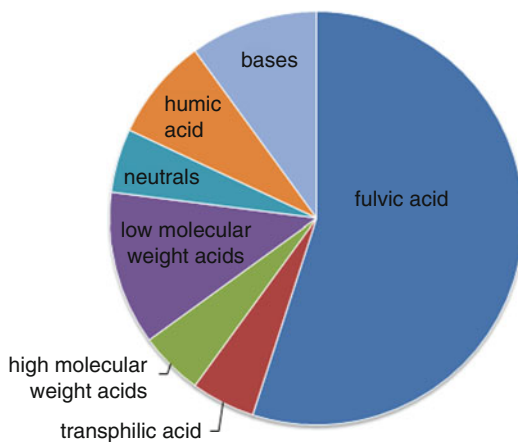
Quantification of the thousands of unknown (unidentified) compounds present in low abundance (e.g., at "background" level compared to conventional analysis of analytes in solution) exceeds current analytical capabilities. Because the organic compounds that comprise the DOM pool are 50% carbon by mass, DOM concentration is measured as DOC by methods that use catalysis, heat, chemical oxidation, ultraviolet radiation, or a combination thereof to quantitatively oxidize the organic carbon to CO_2 (Aiken et al. 2002). DOC concentration is typically measured by either wet oxidation or high temperature combustion methods. Each method can be challenging and calls for great care in analysis (Kaplan 1992). For example, measurements with persulfate oxidation methods can be affected by interferences with chloride (Aiken 1992), while measurements with high-temperature combustion methods can be affected by incomplete combustion (Kaplan 1992). Because DOM contains such a wide-ranging mixture of compounds varying in molecular sizes, weights, and reactivities, problems can arise in the analysis of DOC due to differences in oxidation efficiency among the compounds in the mixture, which can depend on the sample matrix–thus highlighting the need for careful DOC analyses (Aiken et al. 2002). In addition, because DOC analysis detects the sum total of many compounds, each present at low abundance, avoiding sample contamination and obtaining reliable blank water are additional difficulties of the measurement.

6.2.2 DOM Characterization by Absorbance and Fluorescence Spectroscopy

Optical properties of the light absorbing or chromophoric fraction of DOM can provide information on the amount, source, and quality of chemically distinct moieties within the DOM pool. The chromophoric fraction of the DOM generally overlaps with the fulvic and humic acid fractions (see Fig. 6.2), but can include nonhumic and potentially more labile fractions, such as transphilic acids and other nonhumic fractions. Recent research has demonstrated that combining rapid benchtop or in situ measurement of ultraviolet–visible (UV–Vis) or fluorescence spectra with multivariate statistical techniques hold enormous potential to transform our understanding of biogeochemical dynamics in aquatic system (McKnight et al. 2001; Cory and McKnight 2005; Hood et al. 2005; Miller et al. 2006; Fellman et al. 2009a). The UV–Vis absorption spectrum of DOM decreases with increasing wavelength in an approximately exponential fashion across the ultraviolet and visible portions of the spectrum, where the absorbance as a function of wavelength depends on both the quantity and the quality of the light absorbing, or chromophoric, fraction of the DOM pool. The absorbance spectrum of DOM can be modeled using the following exponential equation, as described in (Stedmon and Markager 2001):

$$a_\lambda = a_{\lambda_0} e^{s(\lambda_0 - \lambda)}, \tag{6.1}$$

where a_λ is the Naperian absorption coefficient of a certain wavelength (Hu et al. 2002), a_{λ_0} is the absorption coefficient at a reference wavelength (commonly 400 nm), and S is the spectral slope coefficient that describes the shape of the absorbance curve (Stedmon and Markager 2001). Spectral slope is independent of DOM concentration and is a measure of the average source, quality, and diagenesis of DOM. Lower S values have been observed for terrestrially derived DOM sources and higher values have been observed in systems with greater autochthonous inputs (Stedmon and Markager 2001). In addition, photobleaching of DOM has consistently been reported to result in an increase in spectral slope (Vahatalo and Wetzel 2004; Helms et al. 2008). However, S values depend strongly on the wavelength range and method used for its calculation. To minimize the potential artifacts associated with the spectral slope calculation due to lack of a standard approach for its calculation, a new approach to characterize the spectral slope properties of the DOM absorbance spectrum was recently developed (Helms et al. 2008). Helms et al. (2008) proposed the spectral slope ratio (S_R), which is a dimensionless ratio of the slope of the shorter wavelength region (275–295 nm) divided by the slope of the longer wavelength region (350–400 nm). One advantage of the slope ratio is that it avoids use of spectral data near the detection limit of the instrument (e.g., at long wavelength). Another advantage is that it focuses on the absorbance ranges that have been shown to shift most dramatically as a function of DOM source, quality, and diagenesis (Helms et al. 2008). The slope ratio has been strongly, inversely correlated to the average molecular weight of the DOM (Helms et al. 2008) and as such may be a good proxy for relative differences in molecular weight of the DOM among samples or along a flowpath.

Many other spectral values or absorption ratios have been evaluated and employed as proxies for average DOM characteristics. Probably, the most widely employed approach among freshwater studies is the specific UV absorbance (SUVA; Weishaar et al. 2003). SUVA values are defined as the decadic UV absorbance coefficient at 254 nm in inverse meters (m^{-1}) divided by the DOC concentration measured in mg C L^{-1}. SUVA values for aquatic fulvic acids at neutral pH range from 1 to 6 L mg C^{-1} m^{-1}, whereas SUVA for filtered whole waters are generally lower. SUVA is strongly, positively correlated with the aromatic carbon content of fulvic fraction of DOM acids as measured by ^{13}C-NMR (Weishaar et al. 2003) and many studies have verified that SUVA is an excellent proxy for the aromatic content of DOM (e.g., Cory et al. 2007). SUVA values have been shown to depend on sample pH, and high nitrate and dissolved iron species can interfere with the SUVA measurement and interpretation (Weishaar et al. 2003). For example, the concentration range of ferric iron typical of surface waters, 0–0.5 mg L^{-1}, adds only 0–0.04 cm^{-1} to the absorbance at 254 nm (Weishaar et al. 2003) and thus does not interfere with characterization of DOM with the SUVA measurement. However, in iron-rich waters, the absorbance of ferric and ferrous iron at 254 nm is high enough to interfere with the SUVA measurement (Weishaar et al. 2003). Thus, it is important to compare measured SUVA values to reference humic and fulvic acid samples, as well as to other water samples reported in the literature, especially if it is suspected that interfering species may cause SUVA values of the sample to fall out of the expected range (Weishaar et al. 2003).

A subset of the DOM pool fluoresces in a manner dependent on its concentration and chemical composition, and because characterization of DOM by fluorescence spectroscopy offers some distinct advantages over UV–Vis absorbance spectroscopy, this approach is increasingly employed in field and laboratory studies of DOM and was recently a focus of a Chapman Meeting (Organic Matter Fluorescence, University of Birmingham, Birmingham, UK 2008). A major consideration is that fluorescence is more sensitive compared to absorption spectroscopy (~10–1,000×; Lakowicz 1999).

Furthermore, it is well established that analysis of the fluorescent fraction of DOM provides insight into three types of carbon within the DOM pool, e.g., carbon associated with terrigenous or microbial source material, as well as carbon associated with free or combined fluorescent amino acids, specifically tryptophan, tyrosine, and phenylalanine (Coble et al. 1990). Fluorescence EEMs spectroscopy, which measures DOM fluorescence as topographic surfaces of emitted light as a function of excitation wavelength, is the most widely used approach to study the fluorescent fraction of DOM because it captures how excitation and emission spectra of fluorescing moieties within the DOM pool vary with the composition of DOM (Fig. 6.3; Coble et al. 1990; Coble 1996; Stedmon et al. 2003; Cory and McKnight 2005). The FI is essentially a qualitative measure of the relative
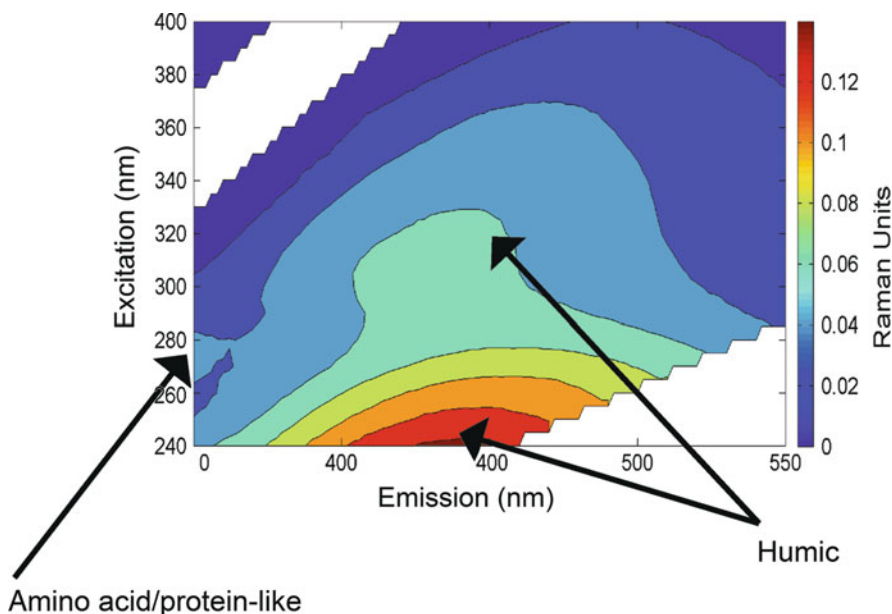
Fig. 6.3 A typical EEM of dissolved organic matter (DOM) showing the three characteristic peak regions related to amino acid/protein-like moieties, as well as peaks associated with humic material derived from microbial and/or terrestrial precursor organic matter. The *color bar* shows the intensity of emission in Raman Units (RU)

proportion of the terrigenous and microbial source of the fluorophores primarily associated with humic DOM fractions and is less resolved than a full EEM. Fluorescence characterization of DOM is relatively rapid, inexpensive, and requires no sample preparation beyond filtration (Cory et al. 2010), although it is critical to properly correct the EEMs for instrument characteristics and to consider inner filter effects as discussed later on in this chapter. These attributes, in addition to the weak dependence of DOM fluorescence on typical fluctuations in natural stream water chemistry (e.g., pH, ionic strength, temperature; Mobed et al. 1996) make fluorescence characterization of DOM well suited to real-time monitoring (Spencer et al. 2007; Carstea et al. 2009).

In addition, understanding of the underlying variability captured in an EEM has been significantly advanced through parallel factor analysis (PARAFAC), a statistical modeling approach that separates a dataset of EEMs into mathematically and chemically independent components (each representing a single fluorophore or a group of strongly covarying fluorophores; Fig. 6.4) multiplied by their excitation and emission spectra (representing either pure or combined spectra). PARAFAC analysis of an EEM dataset results in a reduction of complex, three-dimensional data into several two-dimensional spectra representing chemically independent components that describe the total EEM (Stedmon et al. 2003), and ultimately allows for the identification of patterns in dataset that would otherwise not be
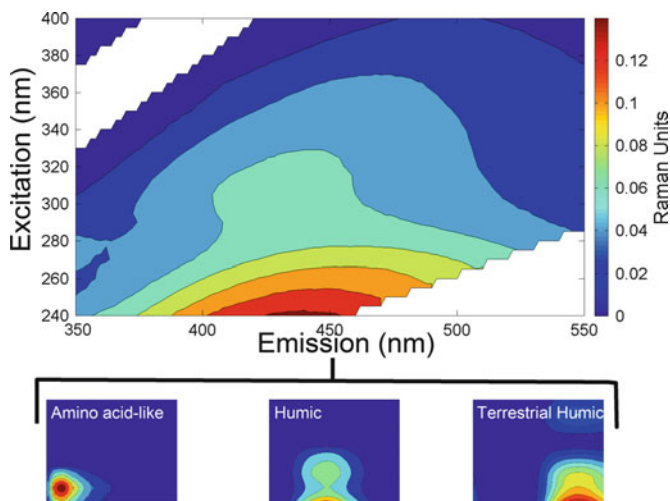
Fig. 6.4 *Top*: DOM fluorescence spectra are commonly evaluated as excitation–emission matrices (EEMs, *top*) that show topographic surfaces of emission (em) spectra collected over a range of excitation (ex) wavelengths where the color is proportional to the intensity of fluorescence (RU). With PARAFAC, EEMs are separated into underlying fluorescent constituents, e.g., groups of similarly fluorescing moieties associated with humic or amino acid groups. Once the fluorescent groups are identified, the relative concentration of each fluorescing group can be quantified in every sample (Stedmon and Bro 2008)

obtained by visual inspection of peak positions. For a review and tutorial of the EEM/PARAFAC approach as applied to DOM, see Stedmon and Bro (2008).

Cory and McKnight (2005) developed a PARAFAC model from a "global" dataset of freshwater samples that identified 13 components representing similarly fluorescing groups, some of which were associated with humic substances which exhibited consistent variation across environmental redox gradients. Given that multiple lines of evidence have suggested a link between fluorescing moieties associated with the humic fraction of DOM and redox reactive moieties in the humic fraction of DOM as measured by electron spin resonance spectroscopy (Scott et al. 1998; Klapper et al. 2002; Fulton et al. 2004; Cory and McKnight 2005; Fimmen et al. 2007), Miller et al. (2006) developed a "redox index" based on a ratio of red-shifted, potentially more reduced fluorescing components to the total humic components obtained from the EEM/PARAFAC approach developed by Cory and McKnight (2005). Miller et al. (2006) then used a conservative tracer approach combined with PARAFAC analysis of DOM fluorescence spectra in an alpine stream/wetland ecosystem to evaluate the energy transfer associated with advection of reduced humics from the anoxic hyporehic zone into oxic surface waters of the stream through hyporheic exchange, which was found to be comparable to the rate of nitrification of ammonium also being advected from the hyporheic zone. Miller et al. (2009) also found that the redox index decreased upon exposure of microbial DOM to sunlight in the alpine lake studied by Hood et al. (2003), whereas similar changes did not occur in adjacent stream system which did not contain lakes. Thus, identification of redox-active fluorescing constituents in DOM may pave the way for researchers to sensitively observe redox processes involving DOM in the environment (Miller et al. 2009).

Recent studies have demonstrated that the three different types of fluorescing DOM (e.g., terrestrial, microbial, and amino) respond in contrasting ways to biogeochemical processes, namely photolysis or biodegradation (Cory et al. 2007). Thus, the EEM/PARAFAC approach is increasingly used to understand how different fractions of DOM change with hydrologic regime, season, or land cover in the watershed (Erlandsson et al. 2008; Fellman et al. 2009a; Williams et al. 2010). For example, fluorescence from amino acid moieties hypothesized to be associated with protein residues in DOM has been positively correlated with biodegradable dissolved organic carbon (BDOC) concentrations (but not with bulk DOC concentrations), and are increasingly used as a strong proxy for the biodegradable DOM pool (Balcarczyk et al. 2009; Fellman et al. 2009b; Hood et al. 2009). In contrast, fluorescent moieties associated with the humic fraction of DOM have been found to correlate with bulk DOC concentrations. Consistently, recent studies have shown that these different groups of fluorescing moieties have dissimilar lability profiles in streams, exhibiting variable uptake rates and temporal dynamics (Fellman et al. 2009c). Together, these studies demonstrate how different fractions of the DOM pool cycle in natural waters. Given that the different fluorescent fractions of DOM have variable relationships to bulk DOC concentration, normalization of fluorescence intensities to bulk DOC concentrations may confound interpretation of EEM/PARAFAC results.

6.2.3 Absorbance and Fluorescence as Proxies for DOM Character

Many recent studies have demonstrated that the data derived from UV–Vis and fluorescence measurements correlate very well with DOM properties measured with more intensive methods (McKnight et al. 2001; Cory et al. 2007; Helms et al. 2008; Spencer et al. 2008). For example, DOC-SUVA at 254 nm is an established proxy for DOM aromaticity and spectral slope is proxy for DOM molecular weight (Weishaar et al. 2003; Helms et al. 2008), which in turn have generally been inversely correlated with DOM bioavailability (Kujawinski et al. 2004; Kim et al. 2006).

Relationships between signals in an EEM and DOM composition have been inferred from strong correlations, consistent across different aquatic and marine systems, that relate features observed in EEMs to average or bulk characteristics of the carbon in the DOM sample, such as aromatic carbon content, relative contribution from terrestrial or microbial precursor material (McKnight et al. 2001; Cory and McKnight 2005; Cory et al. 2007), free or combined amino acids (Yamashita and Tanoue 2003), or C/N ratio and isotopic signature of the organic nitrogen within the DOM sample (Cory et al. 2007). These relationships lend weight to the hypothesis that, despite the fact that all water samples show the same three classes of organic matter represented by three characteristic peak regions in an EEM, there is underlying variability in the specific EEM features related to molecular level variability in DOM composition.

6.2.4 Challenges to DOM Characterization by Fluorescence Spectroscopy

Typically an analytical chemist has the objective to quantify an unknown amount of a known (molecularly identified) analyte of interest, and its measurement is then based on the response of an unknown amount of the analyte in solution in comparison to a calibration curve generated with known amounts of the analyte. This approach, although susceptible to interference from sample matrix effects, particularly for complex environmental samples, allows for any response from the instrument used to be effectively "canceled out" via comparison to the calibration curve. Similarly, absorbance spectra of DOM are measured relative to a reference (e.g., deionized water), and thus absorbance spectra do not depend on the instrument employed. However, in contrast, for DOM fluorescence, we are not measuring identified compounds, but instead are looking at the relative abundance of groups of compounds that behave similarly based on their absolute (not relative) fluorescent properties, e.g., shapes of excitation and emission spectra. In addition, fluorescence spectra are not measured against a blank, e.g., water does not fluoresce. Thus, fluorescence spectra of DOM are strongly dependent on the instrument employed

for the analysis (Cory et al. 2010). The wavelength dependencies of spectrofluorometer instrument components are large, and so the characteristics of a fluorometer are superimposed on sample spectra. Thus, for accurate intensity or peak position comparison, sample spectra are commonly corrected for variation in lamp profile as a function of wavelength, lamp decay over time, as well as performance in the gratings or emission detector as a function of wavelength.

Because the chemical character of DOM depends on the dynamic interplay between DOM sources and biochemical reactions (e.g., Jaffe et al. 2008), the fluorescence signature of DOM is increasingly used as a proxy measurement to assess shifts in DOM composition occurring in response to changes in the watershed (Huang and Chen 2009). To implement this approach most effectively, and potentially for monitoring of in situ variation in DOM quality over long time periods, it is necessary to obtain fluorescence spectra of DOM that are independent of instrument, analyst, or laboratory or instrument performance over time (Coble et al. 1993; Holbrook et al. 2006; Cory et al. 2010). Although details of fluorescence correction procedures as applied to DOM EEMs have been described in Cory et al. (2010), given the widespread application of the FI developed by McKnight et al. (2001) to assess DOM source, it is worth noting here that correction procedures have a significant impact on the absolute value and range of the FI, as described in detail in Cory et al. (2010). An effect of correction on the FI emission spectra was a red shift in the peak position compared with the uncorrected spectra presented in the McKnight et al. (2001) study. In the McKnight et al. (2001) study, the FI was calculated as the ratio of intensities at 450 to 500 nm, corresponding to the slope of the observed (uncorrected) emission peak, at an excitation wavelength of 370 nm. Therefore, to evaluate the same slope as the McKnight et al. (2001) study, the FI obtained from corrected spectra from each fluorometer was shifted to the ratio of intensities at 470 to 520 nm (Cory et al. 2010). Therefore, as recommended in the Cory et al. (2010) study, the FI values obtained from corrected emission spectra should be evaluated as the ratio of emission intensities at 470 to 520 nm. It is also critical to consistently correct for the inner filter effect and for analysis based on EEMs to avoid making measurements in samples with a maximum absorbance greater than 0.3 (Miller et al. 2010).

6.3 Future Needs in Fluorescence Biogeochemistry

6.3.1 Role of Dissolved and Particulate Organic Carbon

Although only 1% of the DOM pool is thought to be fluorescent, characterization of DOM via its fluorescent fingerprint is an approach that is widely applied to understand DOM biogeochemistry in natural waters. Variation in fluorescence from humic-like and protein-like groups, the two general types of fluorescing DOM, can provide information on DOM source and its roles in biogeochemical

processes. For example, amino acid-like fluorescence attributed to DOM has been positively correlated with increased biological activity and the BDOC content of DOM (Hudson et al. 2008; Fellman et al. 2009c), and is therefore increasingly accepted as a proxy for the fraction of DOM bioavailable to microorganisms.

However, protein fluorescence has also been observed from the particulate organic matter (POM) pool (Baker et al. 2007). In some systems, the POM pool can be dominated by bacterial cells (Cotner et al. 2004) which are well known to exhibit intrinsic (endogenous) fluorescence from tryptophan, tyrosine, and phenylalanine residues associated with proteins. It follows that sources of protein fluorescence observed in natural waters may include proteinaceous matter associated with colloids or intact bacterial cells in addition to DOM. The extent to which POM is separated from DOM during filtration likely influences the potential contribution of particulate protein-like fluorescence from a water sample.

It is possible that the conventional approach to separate DOM from POM has led to increased influence of POM in the fluorescence signature attributed to DOM. Although the operational distinction of DOM and POM is based on a 0.2–0.45 μm pore size cut-off, in practice this separation is commonly carried out with carbon-free glass fiber filters (GF/F) that have a nominal pore-size cut-off of 0.7 μm. GF/F filters are widely preferred to separate DOM from POM because they are easy to clean and do not add any contamination to the sample. However, some colloids (0.001–1 μm) and particles such as small bacteria and viruses pass through GF/F filters (Hedges 2002). Given that the amount of carbon in the DOM pool is typically tenfold greater than the carbon concentration in the POM pool in most natural waters (Meybeck 1982), the fact that GF/F filtration allows some POM to pass through the filter has been considered a minor source of error in studies focusing on the quantity and quality of the bulk-carbon content in each pool. From an ecological perspective, this method of separation is also effective in distinguishing the carbon pool that can be taken up by filter feeding aquatic organisms compared to the fraction taken up by microbes.

Although POM may contribute only a small fraction of the carbon concentration relative to DOM in a GF/F filtered sample, the influence of POM on the measured fluorescence signal depends on the amount and nature of the fluorescent material in the DOM and POM pools, which are poorly understood. Indirect evidence suggesting that particulate matter may contribute to protein-like fluorescence typically attributed to DOM has resulted from comparison of water samples after filtration through filters with increasingly smaller pore sizes ranging from 1.2 to 0.2 μm. Significant loss of protein-like fluorescence intensity from a water sample has been observed upon removal of particulate matter larger than 1.2 and 0.45 μm (Baker et al. 2007). In contrast, no significant change in humic fluorescence is observed upon filtration (Baker et al. 2007). Similar results are shown here for comparison of 0.7 μm (GF/F) and 0.2 μm filtered water (Fig. 6.5). Quantitative analysis of the differences between the filtered fractions of Lake Superior water demonstrated that humic fluorescence did not vary between the filtered fractions, but protein fluorescence was significantly greater in the 0.7 μm filtered water compared to the 0.2 μm filtered fraction. The latter results support previous reports in the literature that some protein fluorescence may not be associated with operationally defined DOM.

Fig. 6.5 Effect of filtration on amino acid/protein-like and humic fluorescence in EEMs of DOM. (**a**) 0.7 μm filtered water sample. (**b**) 0.2 μm filtered fraction of the same water sample. Intensities in (**a**) and (**b**) are plotted on difference scales, based on the maximum fluorescence intensity in each EEM. Humic peaks in (**a**) and (**b**) show similar intensities, while fluorescence from the amino acid/protein-like groups is higher in (**a**) compared to (**b**)
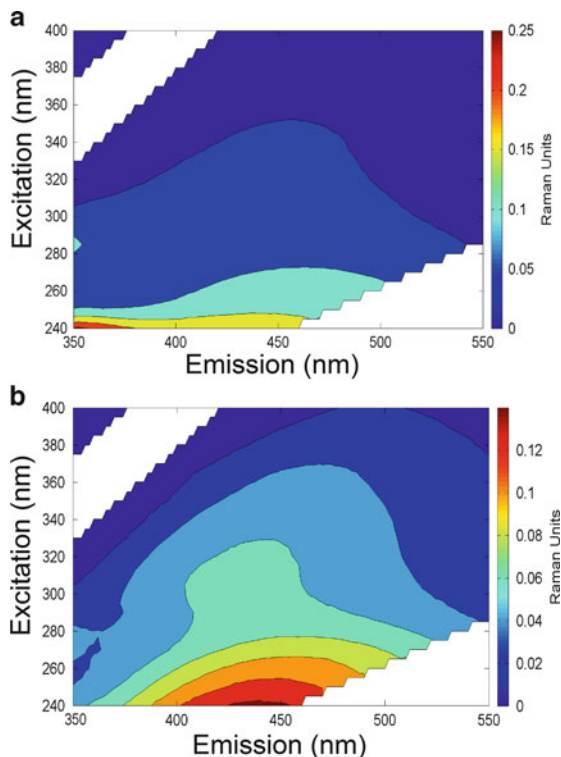
Despite evidence for a contribution from fluorescent POM, most studies interpret the fluorescence signature of GF/F filtered water as due entirely to DOM, which could lead to misinterpretations of important biogeochemical processes involving DOM. Because there is so much information to be gained from the fluorescence signature of natural waters, it is important to know what types of organic matter actually contribute to the observed fluorescence signals, and future work should be directed in this area.

6.3.2 How Much Carbon Is Fluorescent?

EEMs have high potential to capture DOM dynamics in situ. We already know that we can detect large changes in the fluorescent fraction of DOM as a function of time and space in the environment, and we are increasingly able to relate those changes to the likely controlling biogeochemical processes, which are providing information on how compartments of the DOC pool may be cycling in the environment. The limitation is that we currently cannot relate EEM signals to DOC concentrations, e.g., we do not know what fraction of the DOM pool we "see" in the EEM signals. Since fluorescing entities within the DOM pool must necessarily be part of

the aromatic carbon pool, an upper limit on fluorescing carbon may be ~12–30% of the carbon, since we know from ^{13}C-NMR and FT-ICR MS that this is the range of aromatic carbon for DOM (e.g., McKnight et al. 1997; Hockaday et al. 2009). It is very unlikely that all aromatic moieties contribute to the observed fluorescence, so we are probably looking at only a small fraction of the 12–30% of the aromatic carbon pool. A common assumption is that 1% of the DOC pool is fluorescent. Although this is a small fraction of the DOC pool, the working hypothesis is that fluorescent moieties behave similarly to (biogeo) chemically similar nonfluorescing moieties, such that the fluorescing moieties are a proxy for the wider nonfluorescent carbon pool for a given type/source of carbon.

Most studies to date show that some fluorescence signals, meaning some fluorescing moieties, are strongly, positively correlated to DOC concentrations (Stedmon et al. 2003; Stedmon and Markager 2005; Huang and Chen. 2009). Typically fluorescence signals associated with terrestrial-humic moieties most strongly correlate with bulk DOC concentrations, while in contrast fluorescence signals from amino acids do not. Studies have also demonstrated that although fluorescence from terrestrial components is generally correlated with DOC concentrations, the slope of this relationship varies between and among systems (with space and time), which suggests that there are differences in the amount of fluorescence per carbon among systems. A goal is to use this variability in order to understand the relationships between EEM signals and carbon composition and concentration. We can only push the EEM capability further, to get more out of these measurements, by conducting concurrent analyses on DOM composition and developing relationships between these analyses.

References

Ågren A, Buffam I, Berggren M et al (2008) Dissolved organic carbon characteristics in boreal streams in a forest-wetland gradient during the transition between winter and summer. J Geophys Res 113:G03031. doi:10.1029/2007JG000674

Aiken GR (1992) Chloride interference in the analysis of dissolved organic carbon by the wet oxidation method. Environ Sci Technol 26:2435–2439

Aiken G, Cotsaris E (1995) Soil and hydrology – their effect on NOM. J Am Water Works Assoc 87:36–45

Aiken GR, McKnight DM, Thorn KA, Thurman EM (1992) Isolation of hydrophilic organic acids from water using nonionic macroporous resins. Org Geochem 18:567–573

Aiken G, Kaplan LA, Weishaar J (2002) Assessment of relative accuracy in the determination of organic matter concentrations in aquatic systems. J Environ Monitor 4:70–74. doi:10.1039/b107322m

Baker A, Spencer RGM (2004) Characterization of dissolved organic matter from source to sea using fluorescence and absorbance spectroscopy. Sci Total Environ 333:217–232

Baker A, Elliott S, Lead JR (2007) Effects of filtration and pH perturbation on freshwater organic matter fluorescence. Chemosphere 67:2035–2043

Balcarczyk KL, Jones JB Jr, Jaffe R et al (2009) Stream dissolved organic matter bioavailability and composition in watersheds underlain with discontinuous permafrost. Biogeochemistry 94:255–270. doi:10.1007/s10533-009-9324-x

Bergamaschi BA, Fram MS, Kendall C et al (1999) Carbon isotopic constraints on the contribution of plant material to the natural precursors of trihalomethanes. Org Geochem 30:835–842

Boyer EW, Hornberger GM, Bencala KE et al (1997) Response characteristics of DOC flushing in an alpine catchment. Hydrol Process 11:1635–1647

Boyer EW, Hornberger GM, Bencala KE et al (2000) Effects of asynchronous snowmelt on flushing of dissolved organic carbon: a mixing model approach. Hydrol Process 14:3291–3308

Carpenter SR, Cole JJ, Pace ML et al (2005) Ecosystems subsidies: terrestrial support of aquatic food webs from ^{13}C addition to contrasting lakes. Ecology 86:2737–2750. doi:10.1890/04-1282

Carstea EM, Baker A, Pavelescu G et al (2009) Continuous fluorescence assessment of organic matter variability on the Bournbrook River, Birmingham, UK. Hydrol Process 23:1937–1946. doi:10.1002/hyp. 7335

Coble PG (1996) Characterization of marine and terrestrial DOM in seawater using excitation emission matrix spectroscopy. Mar Chem 51:325–346

Coble PG, Green SA, Blough NV et al (1990) Characterization of dissolved organic-matter in the Black-Sea by fluorescence spectroscopy. Nature 348:432–435

Coble PG, Schultz CA, Mopper K (1993) Fluorescence contouring analysis of DOC intercalibration experiment samples – a comparison of techniques. Mar Chem 41:173–178

Cory RM, McKnight DM (2005) Fluorescence spectroscopy reveals ubiquitous presence of oxidized and reduced quinones in dissolved organic matter. Environ Sci Technol 39:8142–8149

Cory RM, McKnight DM, Chin YP et al (2007) Chemical characteristics of fulvic acids from Arctic surface waters: microbial contributions and photochemical transformations. J Geophys Res 112:G04S51, doi:10.1029/2006JG000343

Cory RM, Miller MP, McKnight DM et al (2010) Effect of instrument-specific response on the analysis of fulvic acid fluorescence spectra. Limnol Oceanogr Meth 8:67–78

Cotner JB, Biddanda BA, Makino W et al (2004) Organic carbon biogeochemistry of Lake Superior. Aquat Ecosyst Health 7:451–464

Erlandsson M, Buffam I, Folster J et al (2008) Thirty-five years of synchrony in the organic matter concentrations of Swedish rivers explained by variation in flow and sulphate. Global Change Biol 14:1191–1198. doi:10.1111/j.1365-2486.2008.01551.x

Fellman JB, Hood E, Edwards RT et al (2009a) Changes in the concentration, biodegradability, and fluorescent properties of dissolved organic matter during stormflows in coastal temperate watersheds. J Geophys Res 114:G01021. doi:10.1029/2008JG000790

Fellman JB, Hood E, Edwards RT et al (2009b) Uptake of allochthonous dissolved organic matter from soil and salmon in coastal temperate rainforest streams. Ecosystems 12:747–759. doi:10.1007/s10021-009-9254-4

Fellman JB, Hood E, D'Amore DV et al (2009c) Seasonal changes in the chemical quality and biodegradability of dissolved organic matter exported from soils to streams in coastal temperate rainforest watersheds. Biogeochemistry 95:277–293. doi:10.1007/s10533-009-9336-6

Fimmen RL, Cory RM, Chin YP et al (2007) Probing the oxidation-reduction properties of terrestrially and microbially derived dissolved organic matter. Geochim Cosmochim Acta 71:3003–3015

Findlay SEG, Sinsabaugh RL (eds) (2003) Aquatic ecosystems: interactivity of dissolved organic matter. Academic Press, San Diego

Fisher SG, Likens GE (1973) Energy flow in Bear Brook, New Hampshire: an integrative approach to stream ecosystem metabolism. Ecol Monogr 43:421–439. doi:10.2307/1942301

Fuiji R, Ranalli AJ, Aiken GR et al (1998) Dissolved organic carbon concentrations and compositions, and trihalomethane formation potentials in waters from agricultural peat soils, Sacramento-San Joaquin Delta, California: implications for drinking-water quality. Water Resources Investigations Report WRIR-98-4147

Fulton JR, McKnight DM, Foreman CM et al (2004) Changes in fulvic acid redox state through the oxycline of a permanently ice-covered Antarctic lake. Aquat Sci 66:27–46

Haitzer M, Aiken GR, Ryan JN (2002) Binding of mercury (II) to aquatic humic substances: the role of the mercury-to-DOM concentration ratio. Environ Sci Technol 36:3564–3570

Hedges JI (2002) Why dissolved organic matter? In: Hansell D, Carlson CA (eds) Biogeochemistry of marine dissolved organic matter. Academic Press, Amsterdam, pp 1–34

Helms JR, Stubbins A, Ritchie JD et al (2008) Absorption spectral slopes and slope ratios as indicators of molecular weight, source, and photobleaching of chromophoric dissolved organic matter. Limnol Oceanogr 53:955–969

Hockaday WC, Purcell JM, Marshall AG et al (2009) Electrospray and photoionization mass spectrometry for the characterization of organic matter in natural waters: a qualitative assessment. Limnol Oceanogr Meth 7:81–95

Holbrook RD, DeRose PC, Leigh DS et al (2006) Excitation–emission matrix fluorescence spectroscopy for natural organic matter characterization: a quantitative evaluation of calibration and spectral correction procedures. Appl Spectrosc 60:791–799

Hood E, McKnight DM, Williams MW (2003) Sources and chemical quality of dissolved organic carbon (DOC) across and alpine/subalpine ecotone, Green Lakes Valley, Colorado Front Range, USA. Water Resour Res 39:1188. doi:10.1029/2002WR001738

Hood E, Williams MW, Mcknight DM (2005) Sources of dissolved organic matter (DOM) in a Rocky Mountain stream using chemical fractionation and stable isotopes. Biogeochemistry 74:231–255

Hood E, Fellman J, Spencer RGM et al (2009) Glaciers as a source of ancient and labile organic matter to the marine environment. Nature 462:1044–1047. doi:10.1038/nature08580

Hu CM, Muller-Karger FE, Zepp RG (2002) Absorbance, absorption coefficient, and apparent quantum yield: a comment on common ambiguity in the use of these optical concepts. Limnol Oceanogr 47:1261–1267

Huang W, Chen RF (2009) Sources and transformations of chromophoric dissolved organic matter in the Neponset River Watershed. J Geophys Res 114:G00F05, doi:10.1029/2009JG000976

Hudson N, Baker A, Ward D et al (2008) Can fluorescence spectrometry be used as a surrogate for the biochemical oxygen demand (BOD) test in water quality assessment? An example from South West England. Sci Total Environ 391:149–158. doi:10.1016/j.scitotenv.2007.10.054

Jaffe R, McKnight DM, Maie N et al (2008) Spatial and temporal variations in DOM composition in ecosystems: the importance of long-term monitoring of optical properties. J Geophys Res 113: doi:10.1029/2008JG000683

Kaplan LA (1992) Comparison of high-temperature and persulfate oxidation methods for determination of dissolved organic carbon in freshwaters. Limnol Oceanogr 37(5):1119–1125

Kim S, Kaplan LA, Hatcher PG (2006) Biodegradable dissolved organic matter in a temperate and a tropical stream determined from ultra-high resolution mass spectrometry. Limnol Oceanogr 51:1054–1063

Klapper L, McKnight DM, Fulton JR et al (2002) Fulvic acid oxidation state detection using fluorescence spectroscopy. Environ Sci Technol 36:3170–3175

Kujawinski EB, Del Vecchio R, Blough NV et al (2004) Probing molecular-level transformations of dissolved organic matter: insights on photochemical degradation and protozoan modification of DOM from electrospray ionization Fourier transform ion cyclotron resonance mass spectrometry. Mar Chem 92:23–37

Lakowicz JR (1999) Principles of fluorescence spectroscopy, 2nd edn. Springer, Heidelberg

Leenheer JA, Croue JP (2003) Characterizing aquatic dissolved organic matter. Environ Sci Technol 37:18–26

McGlynn BL, McDonnell JJ (2003) Role of discrete landscape units in controlling catchment dissolved organic carbon dynamics. Water Resour Res 39:1090. doi:10.1029/2002WR001525

McKnight DM, Bencala KE, Zellweger GW et al (1992) Sorption of dissolved organic carbon by hydrous aluminum and iron oxides occurring at the confluence of Deer Creek with the Snake River, Summit Country, Colorado. Environ Sci Technol 26:1388–1396

McKnight DM, Harnish R, Wershaw RL et al (1997) Chemical characteristics of particulate, colloidal, and dissolved organic material in Loch Vale Watershed, Rocky Mountain National Park. Biogeochemistry 36:99–124

McKnight DM, Boyer EW, Westerhoff PK et al (2001) Spectrofluorometric characterization of dissolved organic matter for indication of precursor organic material and aromaticity. Limnol Oceanogr 46:38–48

McKnight DM, Hood E, Klapper L (2003) Trace organic moieties in dissolved organic matter in natural waters. In: Findlay SEG, Sinsabaugh RL (eds) Interactivity of dissolved organic matter. Academic Press, San Diego, pp 71–93

Meybeck M (1982) Carbon, nitrogen, and phosphorus transport by world rivers. Am J Sci 282:401–450

Meyer JL, Edwards RT (1990) Ecosystem metabolism and turnover of organic carbon along a blackwater river continuum. Ecology 71:668–677

Miller MP, McKnight DM, Cory RM et al (2006) Hyporheic exchange and fulvic acid redox reactions in an alpine stream. Environ Sci Technol 40:5943–5949

Miller MP, McKnight DM, Chapra SC (2009) A model of degradation and production of three pools of dissolved organic matter in an alpine lake. Limnol Oceanogr 54:2213–2227

Miller M, Simone BE, McKnight DM et al (2010) New light on a dark subject: comment. Aquat Sci 72:269–275. doi:10.1007/s00027-010-0130-2

Mobed JJ, Hemmingsen SL, Autry JA (1996) Fluorescence characterization of IHSS humic substances: total luminescence spectra with absorbance correction. Environ Sci Technol 30:3061–3065

Monteith DT, Stoddard JL, Evans CD et al (2007) Dissolved organic carbon trends resulting from changes in atmospheric deposition chemistry. Nature 450:537–539. doi:10.1038/nature06316

Mulholland PJ (1997) Dissolved organic matter concentration and flux in streams. J North Am Benthol Soc 16:131–141

Mulholland PJ, Hill WR (1997) Seasonal patterns in streamwater nutrient and dissolved organic carbon concentrations: separating catchment flow path and in-stream effects. Water Resour Res 33:1297–1306

Naiman RJ, Melillo JR, Lock MA et al (1987) Longitudinal patterns of ecosystem processes and community structure in a subarctic river continuum. Ecology 68:1139–1156

Oliver BG, Thurman EM, Malcolm RL (1983) The contribution of humic substances to the acidity of colored natural waters. Geochim Cosmochim Acta 47:2031–2035. doi:10.1016/0016-7037 (83)90218-1

Porcal P, Hejzlar J, Kopáček J (2004) Seasonal and photochemical changes of DOM in an acidified forest lake and its tributaries. Aquat Sci 66:211–222. doi:10.1007/s00027-004-0701-1

Roberts BJ, Mulholland PJ, Hill WR (2007) Multiple scales of temporal variability in ecosystem metabolism rates: results from two years of continuous monitoring in a forested headwater stream. Ecosystems 10:588–606. doi:10.1007/s10021-007-9059-2

Saraceno JF, Pellerin BA, Downing BD et al (2009) High-frequency in situ optical measurements during a storm event: assessing relationships between dissolved organic matter, sediment concentrations, and hydrologic processes. J Geophys Res 114:G00F09, doi:10.1029/ 2009JG000989

Scott DT, McKnight DM, Blunt-Harris EL et al (1998) Quinone moieties act as electron acceptors in the reduction of humic substances by humics-reducing microorganisms. Environ Sci Technol 32:2984–2989

Scott DT, Runkel RL, McKnight DM et al (2003) Transport and cycling of iron and hydrogen peroxide in a freshwater stream: influence of organic acids. Water Resour Res 39:1308

Sleighter RL, Hatcher PG (2007) The application of electrospray ionization coupled to ultrahigh resolution mass spectrometry for the molecular characterization of natural organic matter. J Mass Spectr 42:559–574

Spencer RGM, Pellerin BA, Bergamaschi BA et al (2007) Diurnal variability in riverine dissolved organic matter composition determined by in situ optical measurement in the San Joaquin River (California, USA). Hydrol Process 21:3181–3189. doi:10.1002/hyp. 6887

Spencer RGM, Aiken GR, Wickland KP et al (2008) Seasonal and spatial variability in dissolved organic matter quantity and composition from the Yukon River basin, Alaska. Glob Biogeochem Cycles 22:GB4002, doi:10.1029/2008GB003231

Stedmon CA, Bro R (2008) Characterizing dissolved organic matter fluorescence with parallel factor analysis: a tutorial. Limnol Oceanogr Meth 6:572–579

Stedmon C, Markager S (2001) The optics of chromophoric dissolved organic matter (CDOM) in the Greenland Sea: an algorithm for differentiation between marine and terrestrially derived organic matter. Limnol Oceanogr 46:2087–2093

Stedmon CA, Markager S (2005) Tracing the production and degradation of autochthonous fractions of dissolved organic matter by fluorescence analysis. Limnol Oceanogr 50:1415–1426

Stedmon CA, Markager S, Bro R (2003) Tracing dissolved organic matter in aquatic environments using a new approach to fluorescence spectroscopy. Mar Chem 82:239–254

Thurman EM (1985) Organic geochemistry of natural waters. Nijhoff/Junk Publishers, Boston

Thurman EM, Malcolm RI (1981) Preparative isolation of aquatic humic substances. Environ Sci Technol 15:463–466

Vahatalo AV, Wetzel RG (2004) Photochemical and microbial decomposition of chromophoric dissolved organic matter during long (months-years) exposures. Mar Chem 89:313–326. doi:10.1016/j.marchem.2004.03.010

Weishaar JL, Aiken GR, Bergamaschi BA et al (2003) Evaluation of specific ultraviolet absorbance as an indicator of the chemical composition and reactivity of dissolved organic carbon. Environ Sci Technol 37:4702–4708

Williams CJ, Yamashita Y, Wilson HF et al (2010) Unraveling the role of land use and microbial activity in shaping dissolved organic matter characteristics in stream ecosystems. Limnol Oceanogr 55:1159–1171. doi:10.4319/lo.2010.55.3.1159

Wilson HF, Xenopoulos MA (2009) Effects of agricultural land use on the composition of fluvial dissolved organic matter. Nat Geosci 2:37–41. doi:10.1038/NGEO391

Yamashita Y, Tanoue E (2003) Chemical characterization of protein-like fluorophores in DOM in relation to aromatic amino acids. Mar Chem 82:255–271

Yoshioka T, Mostofa KMG, Konohira E et al (2007) Distribution and characteristics of molecular size fractions of freshwater dissolved organic matter in watershed environments: its implication to degradation. Limnology 8:29–44

Chapter 7
The Roles of Stable Isotopes in Forest Hydrology and Biogeochemistry

Todd E. Dawson and Kevin A. Simonin

7.1 Introduction

Forests cover approximately one third of the terrestrial land surfaces (Hansen et al. 2000) and are arguably the most important biome type on Earth for acquiring, transforming, and recycling major and limiting biogeochemical resources such as water, carbon, and many mineral elements such as nitrogen or phosphorous; well-documented drivers of global biogeochemical cycles. Studying the processes that govern the manner and magnitude of biogeochemical cycling through forest systems with their enormous stature, age, complexity, diversity, and spatiotemporal heterogeneity and that are rarely ever in steady-state possess real and mind-boggling challenges for forest scientists. These challenges may cause some to abandon efforts to understand the complex nature of forests biogeochemical systems altogether. However, in recent years, the application of stable isotope methods, at both natural abundance levels and through targeted experiments using enriched isotopes have revolutionized our capacity to explore a wide range of biogeochemical processes in forests. In this regard, stable isotopes are now known to provide new and important insights from *tracing* the origin and movements of key elements and substances through the Earth–plant–atmosphere continuum (Gat 1996; Dawson et al. 1998, 2002; Fry 2006; Sharp 2007), to *indicating* the presence and the magnitude of key Earth system processes (Holton et al. 2006; Bowling et al. 2008), to *integrating* various biogeochemical processes in both space and time (Bowen et al. 2009; Craine et al. 2009; West et al. 2010b), to also *recording* biological responses to the Earth's changing environmental conditions (McCarroll and Loader 2004; Augusti et al. 2006; Dawson and Siegwolf 2007; Sternberg 2009).

In this chapter, we review recent advances in the areas of forest ecohydrology and biogeochemical research in forested systems that have made use of isotope methods. Given limited space, we cannot provide a comprehensive review or treatment of these issues and methods, so instead we focus our attention on examples of water and carbon cycling research in forests and how isotope methods have helped advance our understanding of these cycles. In the discussions that follow we also advocate an approach that has only recently been embraced by these

communities of scientists; to employ whenever possible more than one isotope as well as accompanying and complimentary data. With modern advance in both isotope methods and the theory that underlies isotope variation in nature as well as in other areas or methods development and modeling, we can now and should use multiple isotopes because we know that they provide better constraints on the processes that lead to the patterns we observe in forested ecosystems and catchments (see chapters in Kendall and McDonnell 1998). Moreover, we feel that it is far more powerful and insightful when complimentary, nonisotope methods, are used because they can extend, independently validate, and very much deepen or understanding of both pattern and process and drivers that impact both. Advances in quantifying water movement through streams, in the subsurface and through the vegetation as well as real-time quantification of water vapor exchange via eddy-flux or Bowen-ratio methods between vegetated surfaces and the atmosphere have matured and when used in combination with H and O stable isotope analyses are providing new insights into the water cycling as discussed below. In addition, the application of geographically based and often remotely sensed information, the quantification of elemental fluxes, the probing of molecular-level variation and the development and use of process-based models are all powerful ways to extend what isotope information may not or cannot. As such, we see some of the most fruitful future advances in the areas of forest hydrology and biogeochemical research being intimately linked with the application of multiple isotopes, and these types of complimentary methods as well. As climate and land-use continue to change, sometimes unabated, this may be the only way to not only track and quantify these changes but also then discover the reasons for the changes.

7.2   Why Isotopes?

The analysis of the stable isotope composition of the light elements began in the disciplines of chemistry and geochemistry (Faure 1986; Hoefs 1997; Criss 1999; Sharp 2007) and later in biogeochemistry (Boutton and Tamasaki 1996; Clark and Fritz 1997; Griffiths 1998; Kendall and McDonnell 1998; Flanagan et al. 2005) and ecology (Rundel et al. 1989; Ehleringer et al. 1993; Unkovich et al. 2001; Dawson et al. 2002; Fry 2007; Dawson and Siegwolf 2007; Lajtha and Michener 1994; West et al. 2010a, b). The information garnered from isotope analyses has revolutionized our ability to understand both pattern and process in terrestrial, aquatic, marine, and atmospheric systems. Since about the 1980s, a wide range of investigations in the broad areas of hydrology and biogeochemistry have addressed many types of questions using stable isotope information. This information has in turn helped develop and expand cutting-edge methodology that included the use of continuous-flow isotope analyses pioneered by John Hayes (Hayes et al. 1990; Hayes 2004). The range of investigations that has emerged since these early evaluations have significantly impacted the fields of hydrology and biogeochemistry across a wide range of temporal and spatial scales.

Using stable isotope data requires a grasp of some fundamental principles of isotope behavior and the underlying basis of observed variation in the isotope composition of different "ecological" materials. The fundamentals of how stable isotopes behave in all types of reactions are well understood owing to the pioneering work in the 1930s by physical scientists such as Alfred Nier, Harold Urey, Malcolm Dole, Samuel Epstein, and Harmon Craig to mention some of the leaders (see Sharp 2007 for a brief history of how stable isotope science developed). Of particular relevance to hydrologists and biogeochemists is how the ratios of the lighter isotopes of H, C, N, O, and S as well as Sr vary and are measured using mass spectrometers and modern laser-based spectroscopic techniques. These stable isotopes show some of the greatest variation on Earth, constitute the bulk of all living matter, and are arguably the most effective tool for revealing changes in the Earth's biogeochemical cycles. Our goal therefore for this chapter is to demonstrate how stable isotope of the water (H, D and ^{16}O, ^{18}O) and carbon (^{12}C, ^{13}C) inform our understanding of the hydrological and carbon cycles that drive and sustain the Earth's forests.

7.3 Stable Isotope Notation

Nearly all of the elements used by forest ecohydrologists and biogeochemists are composed of at least two different stable isotopes (Table 7.1), one at a high relative abundance, and most often the lighter isotope, and the other(s) at a very low relative abundance(s). The ratio of the rare-to-common (or heavy-to-light) stable isotope in any material contains valuable information about both processes and sources. In addition, because of the very small absolute abundances of each isotope in any material, by convention the stable isotope composition is expressed as the difference in isotope abundances in a sample relative to an international standard. Relative abundances are then used to discuss particular issues of interest, and this is done more easily than with absolute isotope abundance or ratios, which only vary in the third decimal place. This has led to the use of the widely accepted (δ) notation (see McKinney et al. 1950), where the isotope ratio of your unknown sample (SA) is expressed relative to an internationally accepted standard (STD; Table 7.1) as,

$$\delta^{XX}E = (R_{SA}/R_{STD} - 1) \times 1,000, \tag{7.1}$$

where E is the element of interest (H, C, N, O, S), "XX" is the atomic mass of the heaviest isotope in the ratio, R is the absolute ratio of the element of interest (e.g., ^{18}O/^{16}O in H_2O), and the subscripts SA and STD are as noted above. Because the isotope abundances are very small, the δ value is multiplied by 1,000 to allow the expression of small differences in units that are convenient to use, parts per thousand (ppt), or the commonly used "per mil" notation represented by the symbol, ‰. By definition, the accepted standard (STD) has a δ value of 0‰.

Table 7.1 Abundance, ratios, and reference standards for selected stable isotopes

Element	Isotope	Abundance	Ratio measured	Reference standard
Hydrogen	^{1}H	99.984	^{2}H/^{1}H (D/H)	VSMOW[a]
	^{2}H (D)[b]	0.0156		
Carbon	^{12}C	98.982	^{13}C/^{12}C	PDB[c]
	^{13}C	1.108		
Nitrogen	^{14}N	99.630	^{15}N/^{14}N	N$_2$-atm.[d]
	^{15}N	0.366		
Oxygen	^{16}O	99.763	^{18}O/^{16}O	VSMOW, PDB[e]
	^{17}O	0.0375	^{18}O/^{17}O[f]	VSMOW
	^{18}O	0.1995		
Sulfur	^{32}S	95.02	^{34}S/^{32}S	CDT[g]
	^{33}S	0.756		
	^{34}S	4.210		
	^{36}S	0.014		
Strontium	^{84}Sr	0.560	^{87}Sr/^{86}Sr	NBS-987[h]
	^{86}Sr	9.860		
	^{87}Sr	7.020		
	^{88}Sr	82.56		

[a] The original standard SMOW, or standard mean ocean water is no longer available, so the International Atomic Energy Agency or IAEA (http://www.iaea.org/) makes (mixes) an equivalent water sample in Vienna of a similar isotope value now known as VSMOW

[b] Correct notation for the heavy isotope of hydrogen is ^{2}H though another convention used is "D" standing for the hydrogen isotope with mass 2 called "deuterium"

[c] The original carbon isotope standard, the fossil belemnite from the PeeDee geological formation is no longer available and instead the IAEA "builds" an equivalent carbon standard in Vienna of a similar isotope value (VPDB) though for carbon isotope analyses it is still referred to as PDB

[d] The IAEA standard is N_2 gas in the atmosphere; because N_2 comprises ~78% of the Earth's atmosphere, and there is no known additional source of N_2 of significance to dilute this atmospheric source it is assumed that N$_2$-atm is not changing enough to warrant developing a different standard

[e] In the case where investigators desire to know the ™^{13}C of a carbonate the standard VPDB is used instead of VSMOW

[f] The 17-O composition of air or water is also referenced to VSMOW

[g] Sulfur isotope values are expressed relative to the FeS in a meteoritic troilite from Meteor Crater in Arizona (USA) known as the Cañon Diablo Troilite or CDT

[h] A widely used standard for strontium isotope analyses is the National Bureau of Standards #987 (now called the National Institute of Standards and Technology, NIST; http://www.nist.gov/), a carbonate power. ^{87}Sr/^{86}Sr and ^{86}Sr/^{88}Sr ratios are determined with a thermal-ionization mass spectrometer (TIMS) and unlike the other light isotopes the ratio measured is not expressed as the rare-to-abundant ratio (or heavy-to-light ratio) but as the ratio of the two isotopes that are most easily measured, ^{87}Sr/^{86}Sr. Commonly, ^{87}Sr/^{86}Sr values are normalized with the ^{86}Sr/^{88}Sr (the light-to-heavy ratio of 0.1194) present in seawater because of fractionations that can occur during thermal ionization

This permits us to easily see that any substance with a positive δ value has a ratio of the heavy-to-light isotope that is higher than the standard. In contrast, a negative δ value has the opposite meaning. Substances with positive δ values are commonly said to be "heavier" or "enriched" relative to the standard, although this convention can often lead to confusion or errors if not expressed carefully (e.g., heavier or

lighter relative to what?). Sharp (2007) provides some discussion of this issue and the various errors commonly made when using delta notation or when expressing isotope language.

The reason for the different abundances between the heavier and lighter isotopes is that heavier atoms have a lower vibration frequency than lighter ones. Therefore, heavier atoms or molecules react more slowly than their lighter counterparts, largely because the bond strengths to the heavier isotopes in any substance is greater and more energy is required to break the bonds than if they contained lighter isotopes. This is because the potential energy (E_H) for the heavier isotope is lower than for the lighter isotope (E_L). The result is a lower rate of turnover when a substance carrying the heavier isotope is involved. This eventually leads to uneven isotope distributions between the reactant and the product that is called *fractionation*. Isotope fractionation can occur during a chemical reaction or during simple diffusion of a substance along a concentration gradient. The result is that the abundance of the heavy isotopes in the *substrate* is greater than the abundance of the heavy isotopes in the *product* that is defined by a fractionation factor, α, for that reaction as,

$$\alpha_{A-B} = R_A/R_B, \tag{7.2}$$

where R_A and R_B are the isotope ratio of the two substances involved in the reaction like a substrate (A) and the product (B) it forms. For most isotope fractionating processes, we can distinguish between those that occur in one direction (with no back reactions), termed "kinetic" fractionation from those that are reversible, termed "equilibrium" fractionation (e.g., diffusion or dissociation of CO_2 in water). For biological systems, kinetic fractionation is almost always associated with enzyme-mediated processes (e.g., photosynthesis or biosynthesis), and this is generally referred to as isotope discrimination. Kinetic or equilibrium characteristics of different isotopes involved in physicochemical or biologically mediated (enzymatic discrimination) reactions is what leads to the changes in the isotope abundances we measure. And while in absolute terms such changes are only on the order of a few percent, in relative, or "delta" terms, some of these changes are very specific and quite large and can therefore be used to track process, determine source, and therefore record change. Below we use these facts in examples and case studies to show just how informative they can be for forest hydrological and biogeochemical investigations.

7.4 The Water Cycle

As noted, forests and woodlands occupy a significant fraction of terrestrial surfaces and represent a pivotal component of most major terrestrial headwaters. The stable isotopes in water (H, D, ^{16}O and ^{18}O) can and have been used to characterize the water pools and flux pathways through these wooded landscapes and have allowed

scientists to track water entering forests as precipitation to where it is eventually returned to the atmosphere from soils, streams, and groundwater aquifers via evaporation or transpiration by plants. Stable H and O isotopes also allow hydrologists to trace surface waters into runoff or groundwater recharge components (Fig. 7.1a). The distribution of D and ^{18}O water isotopes varies in predictable
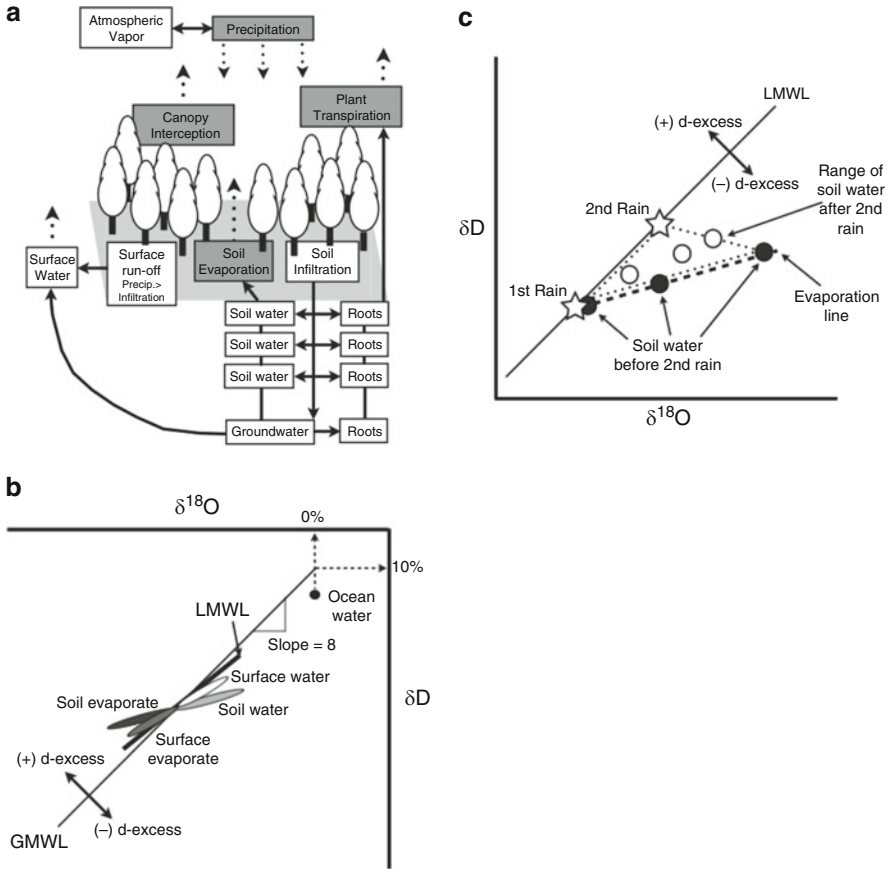
Fig. 7.1 (**a**) As water moves through forested ecosystems, the distribution of D and 18-O water isotopes vary in predictable ways through the process of equilibrium and kinetic fractionation events (*gray boxes*) and the mixing of isotopically distinct water reservoirs (*white boxes*) through advection and redistribution by plant roots. (**b**) The covariation of δD and δ^{18}O in global precipitation (*Global Meteoric Water Line*) as described by the linear model $\delta D = 8 \times \delta^{18}O + 10$. After a rain event, the δD and δ^{18}O of surface and soil waters will increase, and the *d*-excess will decrease, as the lighter water isotopes are preferentially converted from liquid to vapor. (**c**) The mixing of residual soil water (*filled circles*) and precipitation (*open stars*) is dependent upon soil physical properties and rain intensity. In the example shown here, the isotope composition of soil water with depth after a rain event is represented by the *open circles*. The potential range of soil water isotopes after the second rain event is bound by the *dotted lines*

ways as water is subdivided into these flux pathways through the process of equilibrium and kinetic fractionation events (e.g., see gray boxes in Fig. 7.1a), the mixing of precipitation events in the unsaturated zone, and from the selective utilization and redistribution of water by plants (Gat and Tzur 1967; Dawson et al. 1998; Gat and Airey 2006). In the following sections, we review the processes driving variation in the distribution of H and O isotopes in forest waters. We discuss how the use of stable water isotopes, when combined with other measures of forest hydrology (e.g., soil water content, rain intensity) and meteorology (e.g., air temperature, relative humidity) have been used to better understand environmental and biological controls over forest hydrology and water balance; specifically, those studies which used both δD and $\delta^{18}O$, that is, a dual isotope approach.

7.4.1 Precipitation

The isotope composition of precipitation entering forest landscapes can vary greatly throughout a given year or between years. The greatest environmental driver for variation in the stable water isotope composition of precipitation is condensation temperature (Dansgaard 1964). This is because the equilibrium fractionation factor describing the redistribution of stable water isotopes between the liquid and vapor phase, denoted as α_{l-v}, is extremely temperature sensitive. As such, the δD and $\delta^{18}O$ of precipitation varies predictably with changes in air temperature, specifically air temperature at the cloud base as reflected in α_{l-v} (Dansgaard 1964; Rozanski et al. 1992, 1993; Criss 1999). The general trend is that precipitation in cold regions tends to be isotopically depleted in D and ^{18}O relative to precipitation in warmer regions. Additionally, as ocean derived water vapor moves inland and condenses to fall as rain the remaining atmospheric water vapor becomes progressively depleted in D and ^{18}O. The distillation of an air mass through progressive rain events follows a predictable pattern commonly referred to as Rayleigh distillation. For further details on Rayleigh distillation in the hydrological context, see Kendall and Caldwell (1998).

Despite the fact that α_{l-v} is extremely temperature sensitive, the ratio of α_{l-v} D to α_{l-v} ^{18}O is relatively constant at 8.1 ± 0.2 (Criss 1999). This ratio is reflected in precipitation globally as first recognized by Craig (1961) and was expressed graphically as the covariation between δD and $\delta^{18}O$ in precipitation that has not experienced evaporation. The δD vs. $\delta^{18}O$ plot of precipitation is then best described as a linear function with a slope of ~8 and an average offset of 10‰; $\delta D = 8 \times \delta^{18}O + 10$ (Fig. 7.1b). It is important to note that ocean water, the source for ~90% of the atmospheric water vapor globally (Chahine 1992), does not fall on the global meteoric water line (GMWL). This is because ocean evaporate (vapor) is rarely ever in equilibrium with the liquid phase. Evaporation from the ocean surface into a well-mixed troposphere, by definition, occurs at less than saturating conditions and this results in an additional nonequilibrium isotope

effect (i.e., a diffusive or kinetic fractionation effect) between vapor and liquid as water vapor is transported away from the liquid–vapor interface (near the ocean surface). This kinetic fractionation effect increases as relative humidity in the air above the ocean surface decreases as described by Craig and Gordon (1965) and later by Gat (1996). The average relative humidity above the ocean surface is ~81% and as water evaporates into this unsaturated air the outcome is the 10‰ offset in δD (enrichment) commonly referred to as d-excess (Fig. 7.1a). The d-excess of any given meteoric water reservoir is defined as, d-excess = $\delta D - 8 \times \delta^{18}O$. An increase in the d-excess of atmospheric water vapor and/or precipitation suggests a greater influence of nonequilibrium effects that occur in air at lower relative humidity's that in turn change (lower) diffusion resistance for the lighter isotopologue of water, $H_2^{16}O$, to move into the atmosphere. Using d-excess to characterize the stable isotope composition of precipitation, forest waters (e.g., subsurface water, plant xylem water) can provide insight into a number of forest hydrologic processes and will be discussed in more detail in the following sections.

As rainfall reaches forest canopies we must recognize that the stable H and O isotope composition of this precipitation that enters the forest may also be modified by canopy interception and reevaporation (Gat and Airey 2006; Wenjie et al. 2006). Commonly, rain water that comes into contact with the forest canopy and moves through tree crowns to the forest floor, called throughfall precipitation, can be isotopically enriched in D and ^{18}O and posses a lower d-excess value relative to precipitation collected above the forest canopy or in the open. When rain is intercepted by forest canopies, the film of water that is held on leaf surfaces is subject to reevaporation. During the process of evaporation, the lighter water isotopes (H and ^{16}O) are preferentially lost to the vapor phase resulting in an increase in the concentration of heavy water isotopes (D and ^{18}O) in the liquid phase (discussed in greater detail in Sect. 7.4.2). Subsequent rain events that interact and mix with this enriched D and ^{18}O water pool result in throughfall that is potentially distinct in its δD and $\delta^{18}O$ from rain. The difference between the isotopic composition of rain and throughfall is ultimately dependent upon the amount of water held in the forest canopy (its capacity), rain intensity, the duration of time between rain events, and the windspeed and relative humidity during the rain-free period that all impact mixing dynamics, and the magnitude of fractionation. For example, in a seasonal tropical rain-forest (~1,600 mm of rain per year) dominated by broadleaved evergreen angiosperm species (*Pomentia tomentosa* and *Terminalia myriocarpa*) Wenjie et al. (2006) found throughfall to be relatively enriched in D (e.g., up to 4‰ greater in δD) and 18-O (e.g., up to 0.7‰ greater in $\delta^{18}O$) compared to precipitation collected above the forest. In contrast, within a temperate mixed conifer forest that receives ~2,100 mm rain annually over a 4- to 6-month period and dominated by an evergreen gymnosperm species (*Pseudotsuga menziesii*) little difference was observed in the stable water isotope composition of throughfall compared with the rain meaning that the linear models describing covariation between δD and $\delta^{18}O$ of throughfall and rain were relatively indistinguishable (Simonin and Dawson, unpublished data).

7.4.2 Soil Hydrology: Evaporation and Infiltration

In between precipitation events, surface evaporation from soil will decrease the water content of the unsaturated zone resulting in a progressive enrichment of D and ^{18}O in the residual soil water until steady-state evaporation is achieved (Allison et al. 1983; Dawson et al. 1998). The effect of surface evaporation on the δD and δ^{18}O of residual soil water generally decreases with depth along a mixing gradient defined by the diffusion kinetics of the heavier isotopologues of water away from the liquid–vapor interface against the transport of water from deeper soil horizons by capillary action (Zimmermann et al. 1967; Allison et al. 1983; Barnes and Allison 1983; Gat 1996; Kendall and Caldwell 1998). The result of these two opposing fluxes is an exponential decrease in δD and δ^{18}O with depth. If, however, the mixing gradient of heavier water is solely defined by the process of diffusion, then a near-linear model best describes the decrease in δD and δ^{18}O with depth (Barnes and Turner 1998).

Covariation between δD and δ^{18}O of residual soil water caused by surface evaporation can be described by a well-known "soil evaporation line" (Fig. 7.1c). Similar to the linear model describing covariation between δD and δ^{18}O in atmospheric water vapor and precipitation (i.e., the GMWL; Fig. 7.1a), the linear model describing the soil evaporation line is directly related to the ratio of α_{l-v} D to α_{l-v} ^{18}O. However, the slope of any soil evaporation line is always less than the slope of the linear model describing the isotope composition of atmospheric water vapor and precipitation (i.e., <8; Fig. 7.1b, c). The lower slope of evaporation lines is the result of kinetic isotope effects (α_K) associated with the transport of lighter isotopologues of water away from the liquid–vapor interface (e.g., $H_2^{16}O >$ $HD^{16}O > H_2^{18}O$). This transport or kinetic isotope effect, $\alpha_{K,}$ increases as the relative humidity above the liquid–vapor interface decreases. The linear slope, S, describing the covariation of δD and δ^{18}O along an evaporation line is described as: $S = [a_{l-v} + a_K + h(d_a - d_w)]a_{l-v} + a_K + h(d_a - d_w)]_{18-O}$; where δ_a and δ_w are the stable isotope composition of atmospheric water vapor and soil water, and h is the atmospheric relative humidity the water is evaporating into (Kendall and Caldwell 1998). The end result of surface evaporation is an overall decrease in the d-excess of residual soil water and an increase in the d-excess of water in the soil evaporate (vapor leaving the soil surface), relative to the d-excess of precipitation (Fig. 7.1b). Therefore, decreases in soil water content due to evaporation are expected to increase the difference between the d-excess of precipitation and residual soil water (Fig. 7.1c). If a decrease in soil water content occurs in the absence of changes in d-excess, then the loss of water from the unsaturated zone is due to a forest hydrologic process that does not result in fractionation and/or the mixing of isotopically distinct water pools in the unsaturated zone. One such process is root water uptake (Fig. 7.1a), a nonfractionating process that will be discussed in Sect. 7.4.3.

Natural variation in δD, δ^{18}O, and d-excess, of soil water, groundwater, and precipitation (e.g., Fig. 7.1c) when combined with evaluations of soil water content

and/or water potential, can be used in unsaturated flow models to calculate the mean residence time (MRT) of water in the unsaturated zone, and the transport processes directly contributing to groundwater recharge (Mathieu and Bariac 1996; Dewalle et al. 1997; Asano et al. 2002; Gazis and Feng 2004; Kabeya et al. 2007; Lee et al. 2007; Brooks et al. 2010). This is because water held in the unsaturated zone is often a mixture of many precipitation events, each with their own unique stable water isotope composition (see discussion above and Fig. 7.1b). How a particular rain event mixes with residual soil water is strongly influenced by the physical properties of the unsaturated zone and of course by the precipitation events themselves (intensity, duration, temperature). For example, on any given site, a new precipitation event may act to physically push all residual water down a hydraulic gradient (i.e., commonly referred to as piston flow). And even though there is water displacement, water is adhesive and so some mixing of waters with different isotopes compositions with depth can occur (Zimmermann et al. 1967). At the opposite extreme, one might expect that a very large fraction of precipitation could pass through upper soil layers via macropores and large fractures resulting in minimal contact with bulk soil water held in the soil pore spaces (i.e., commonly referred to as preferential flow; e.g., Mathieu and Bariac 1996). These complexities result in variation in the stable water isotope composition of the unsaturated zone and groundwater that is a function of: (1) the δD and $\delta^{18}O$ of precipitation, (2) the fractionation that occurs when water is lost through the process of evaporation, and (3) the mixing ratio of precipitation and residual water as determined by soil physical properties and rain intensity (Henderson-Sellers et al. 2006). Plant root water update and releases may also complicate this picture as in the case of hydraulic lift seen in trees (Dawson 1993; Caldwell et al. 1998).

To date the majority of water transport studies in the unsaturated zone have focused on the use of a single stable isotope (H or O but not both). However, recent research suggests that d-excess is a better tracer of water transport in the unsaturated zone than either δD or $\delta^{18}O$ because natural variation in the d-excess of forest waters is often many times greater than either δD or $\delta^{18}O$ alone (Lee et al. 2007). This is because soil water and precipitation may be identical when assessed on an individual isotope basis (i.e., δD or $\delta^{18}O$) yet, possess drastically different d-excess (Fig. 7.1c). How can this happen? Because, the d-excess reflects isotopic changes associated with kinetic fractionation events and thus acts as an indicator of evaporation. As such, we recommend a dual-isotope approach relying on d-excess values for understanding water transport in the unsaturated zone. For example, Lee et al. (2007) predicted the MRT of water in the unsaturated zone of volcanic derived by monitoring variation in the δD, $\delta^{18}O$ and d-excess of precipitation and soil water at three depths over the course of a year. Model results showed that the use of d-excess values provide the best estimate of the MRT of water in the unsaturated zone.

Additionally, when applying natural variation in the distribution of stable water isotopes to transport processes in the unsaturated zone it is important to consider the field methods used to sample soil water. This is because soil water resides in a variety of pore sizes, which directly influences water mobility and thus our ability to extract a particular water reservoir for stable isotope analysis. For example, soil

water obtained using tension lysimeters will only remove the very mobile water fraction that resides in soil macropores or fractures with relatively high hydraulic conductivity (Burns et al. 2001). In contrast, soil water extracted using cryogenic vacuum distillation represent a mixture of more immobile and mobile water pools (Ehleringer et al. 2000). Therefore, the use of *both* lysimeter and vacuum distillation methods to sample subsurface water is likely to provide a more detailed picture of the spectrum of bound and unbound pools of water within and outside (below) the unsaturated zone. This may facilitate better quantification of the transport processes contributing to groundwater recharge and to transient water pools that trees may use.

7.4.3   Water Use by Trees

The major factors controlling tree water use can be subdivided into physical factors associated with soil and subsurface water transport and availability, biophysical factors associated with variation in plant hydraulic traits, and meteorological factors (Lambers et al. 1998). Stable isotopes are a useful tool for understanding the relative contribution of these different abiotic and biotic controls on tree water use (Dawson and Ehleringer 1998). For example, measurements of the *d*-excess determined from a plant xylem water sample and subsurface water samples form different depths can be used with isotope mass balance models to trace where trees and understory plants are obtaining water (Phillips and Gregg 2003; Ogle et al. 2004; Romero-Saltos et al. 2005). This is because transpiration decreases soil water content without changing the stable isotope composition of bulk soil water (Wershaw et al. 1970; White et al. 1985). Since evaporation of subsurface water results in the progressive decrease in *d*-excess with depth (see Sect. 7.4.2), the difference between the *d*-excess of trees and mean annual precipitation (i.e., *d*-excess of *L*ocal *M*eteoric *W*ater *L*ine – *d*-excess of plants) is expected to decrease with increasing rooting depth. Put another way, within a particular environment the difference in *d*-excess between precipitation and tree xylem water is expected to change in predictable ways with variation in plant water use strategy.

It is important to note that not all water taken up by plant roots is directly transported to leaves. A fraction of subsurface water extracted by roots can be redistributed within the unsaturated zone through a process commonly referred to as "hydraulic lift or redistribution" (Dawson 1993; Burgess et al. 1998; Caldwell et al. 1998). The redistribution of subsurface water has important implications for rhizosphere water content and thus total forest evaporation and transpiration (Dawson 1993; Caldwell et al. 1998; Lee et al. 2005a; Brooks et al. 2006). It may also impact nutrient cycling locally (Caldwell et al. 1998). This is because hydraulic redistribution can replace a large fraction of the water removed by trees each day (Emmerman and Dawson 1996; Lee et al. 2005a). Since root water uptake does not result in water isotope fractionation, hydraulic redistribution has the potential to mix isotopically distinct subsurface water pools on a daily time step. This isotope mixing effect has been used to evaluate lateral and vertical redistribution of water

in the unsaturated zone and the contribution of this redistributed water to both understory plant water use (e.g., Dawson 1993; Brooks et al. 2006) and stand transpiration (Dawson 1996).

7.4.4 Forest Water Balance

As described in the previous sections, characterizing the distribution of stable water isotopes between water reservoirs in a forest can provide insight into many aspects of forest hydrology. Here, we discuss how natural variability in the D and ^{18}O isotope composition of water in soils, trees, and the atmosphere can be used to estimate the relative contribution of tree transpiration and soil evaporation to forest stand water balance (Walker and Brunel 1990; Moreira et al. 1997; Wang and Yakir 2000; Yepez et al. 2003; Williams et al. 2004). In general, the hydrogen and oxygen isotope composition of water vapor in forests is the product of three major sources: (1) water vapor from the troposphere, (2) surface evaporation from soils, and (3) plant transpiration. In order for natural variation in stable water isotopes to be an effective tool for partitioning the relative contribution of soil evaporation (E) and transpiration (T) to total forest water use (ET), soil evaporate and tree transpiration must be isotopically distinct. Additionally, partitioning is made easier if the isotope composition of the "background vapor" (i.e., water vapor from the troposphere) is relatively constant or alternatively well defined by high frequency measurements. If these conditions are met, then changes in the isotope composition of atmospheric water vapor, throughout the day as ambient humidity changes, is considered to be due to the addition of two distinct sources of water vapor, soil evaporate, and plant transpiration. The mixture of these vapor sources can be partitioned using what is commonly referred to as "Keeling plots" (Keeling 1961; Yakir and Sternberg 2000; Dawson et al. 2002). Keeling plots, first developed for carbon isotopes in CO_2 (see Sect. 7.5), identify δ_{ET} based on mass balance mixing relationships where the isotopic values of air, collected at different heights above the ground are plotted against the inverse of the concentration of water vapor. The y-intercept of Keeling plots reflects the isotope composition of the ET flux (Dawson et al. 2002; Yepez et al. 2003). The validity of the Keeling plot relies on the assumption that: (1) the isotope composition of the background atmosphere that E and T are mixing into is relatively constant and (2) no water is lost from the atmosphere due to condensation.

To interpret δ_{ET} derived from Keeling plots, we will calculate the fractional contribution of transpiration (F_T) to the evapotranspiration flux as (Yakir and Sternberg 2000):

$$F_T = \frac{\delta_{ET} - \delta_E}{\delta_T - \delta_E} \times 100, \qquad (7.3)$$

where δ_E is the isotopic composition of evaporated soil water and δ_T is the isotopic composition of transpired water. The isotope composition of these sources could be

expressed as δD, $\delta^{18}O$ or even as d-excess. The spatial resolution of δ_{ET} derived form Keeling plots depends on the height from which the samples are taken and the surface roughness of the forest canopy (Yepez et al. 2003). Collection from different heights may allow for separate isotopic analysis of particular vegetation layers (i.e., understory and overstory canopies). In ecosystems with a distinct overstory and understory component and poor mixing conditions, Keeling plots near the ground surface will provide an integrated measure of soil evaporation and understory evapotranspiration. Keeling plots from higher profiles will integrate the isotopic flux from all ecosystem sources. Therefore, the fractional contribution of transpiration can also be calculated for understory fluxes.

The δ_E and δ_T values used in the isotope mixing model described above are derived from the isotope composition of the ambient atmosphere (δ_a), tree xylem water (δ_x), soil surface water (δ_s), and basic meteorological measurements (e.g., soil temperature, air temperature, and relative humidity). The Craig and Gordon (1965) model describes the isotope fractionation events that occur during evaporation and can be used to predict δ_E if air temperature, soil temperature, δ_s and relative humidity (h) are known, as described by Wang and Yakir (2000):

$$\delta_E = \frac{\alpha^* \times \delta_s - h \times \delta_a - \varepsilon_{eq} - (1 - h) \times \varepsilon_k}{(1 - h) + (1 + h) \times \varepsilon_k / 1,000}, \tag{7.4}$$

where α^* is the liquid–vapor equilibrium fractionation factor and can be expressed in "delta units" as ε_{eq}. Similarly ε_k is the kinetic fractionation factor an h is the humidity of the ambient air normalized to soil temperature. When leaf water enrichment is at steady state, the δ_x is equal to the isotope composition of xylem water, and thus the average δD and $\delta^{18}O$ of water uptake by roots. Thus, during steady-state evaporation, δ_x is generally enriched in δD and $\delta^{18}O$ relative to δ_s. However, it is important to note that steady-state transpiration often times only occurs during a narrow window of time on a diurnal cycle; often at mid-day when h is relatively stable (Harwood et al. 1998). Further previous research has shown that the isotope composition of the "background air" that surface evaporation and tree transpiration are mixing into can be extremely variable depending on meteorological conditions (Lee et al. 2005a, b). As such, the Keeling plot technique is limited to meteorologically favorable conditions.

7.4.5   Water Provenance and Hydrograph Separation

One final application for stable isotopes in forested watersheds is their use in quantifying the provenance of the water in the runoff and within the groundwater in a particular watershed, where the hydrograph is also being measured. When precipitation falls into the watershed and impacts runoff and aquifer recharge dynamics, we expect the waters in the various pools to possess different δD and $\delta^{18}O$. This occurs because of differences in pool sizes, mixing dynamics, and the

relative importance of processes such as evaporation that can all impact the δD and $\delta^{18}O$ of the runoff, the groundwater, the soil water, and the plant available water. In well-constrained watersheds, the isotope composition of water in the underlying aquifer can deviate quite significantly from the annual precipitation δD and $\delta^{18}O$ indicating not only that mixing has occurred but also can be used to determine residence times as well (Fetter 1994). When the stream flow, precipitation amounts, groundwater discharge, evaporation, and all of the respective isotope changes in the waters associated with these process are known, one can determine the dominate provenance (winter snowmelt, summer showers, fall rainfall) that contribute to the runoff and recharge in the system (Kendall et al. 2001). In addition, following storm events and changes in the stream hydrograph (discharge at some set point), one can use the δD or $\delta^{18}O$ of the groundwater and the precipitation (storm event) to separate base flow from storm flow. This is best achieved when the hydrograph is composed of only two components (storm runoff in the stream and groundwater flow). If there are additional components to discharge such as deep groundwater flow, shallow groundwater, or porous soil flow, in addition to storm flow, then other chemical tracers can be used (e.g., natural SiO_2 or artificially applied SF6, Bromide; Fig. 7.2). Using end-member mixing analyses that make use of the isotope values, the chemical tracers and the hydrograph one can provide estimates of the relative contributions of say storm flow, base flow from groundwater, and percolation flow through soils to total flow from the watershed (Clark and Fritz 1997; Burns et al. 2001).

7.5   The Carbon Cycle

The vast majority of carbon that cycles through the Earth's ecosystems begins with CO_2 fixation by autotrophic organisms and for the vast majority of forest tree species this means plants that possess what is called the C3 photosynthetic pathway. During C3 photosynthesis, there are two processes that cause isotopic variation in the carbon molecules fixed. The first process is differential diffusion of $^{13}CO_2$ and $^{12}CO_2$ through the stomatal pores and the second comes about when the carboxylating enzyme, Rubisco (ribulose bisphosphate carboxylase-oxygenase), discriminates against the "heavier" carbon isotope within the isotopologue of carbon dioxide, $^{13}CO_2$ and this results in the products of photosynthesis being relatively depleted in their carbon isotope ratio, $\delta^{13}C$. The degree of ^{13}C depletion in the carbon products produced by trees ultimately depends on the ratio of availability of $^{12}CO_2$ and $^{13}CO_2$ at the site, where CO_2 is assimilated relative to the external atmosphere (c_a); the so-called c_i/c_a or c_c/c_a ratio (referred to as either c_i or c_c for the leaf internal or chloroplast carbon dioxide concentrations, respectively; Farquhar et al. 1989; Flexas et al. 2007). As the c_i/c_a or c_c/c_a ratio declines Rubisco ends up discriminating less and less against $^{13}CO_2$ and the subsequent carbon isotope ratio increases. For example, at a c_i/c_a of 0.9 theory shows that the $\delta^{13}C$ of photosynthetic products should be $-31.6‰$ compared to a c_i/c_a of 0.7, where the calculated $\delta^{13}C$
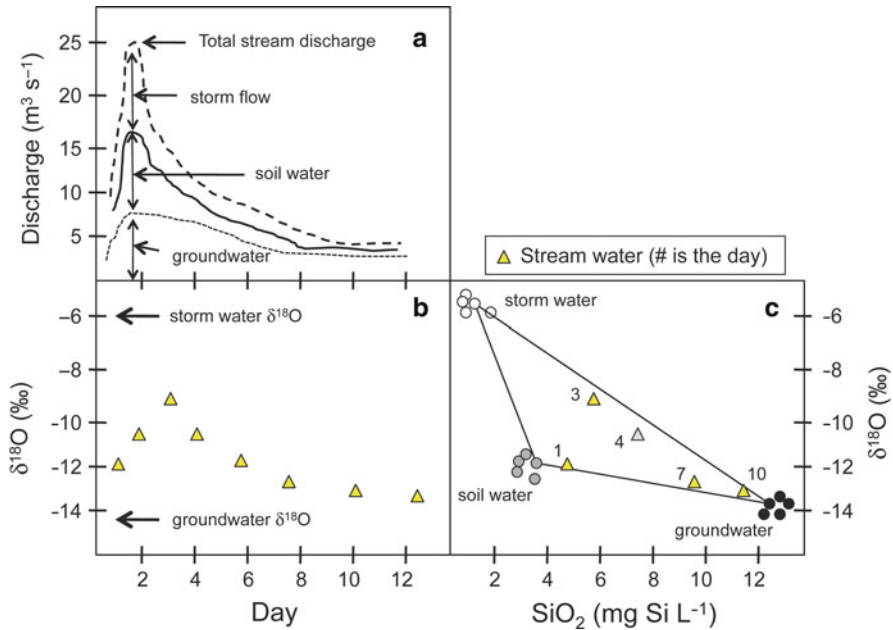
Fig. 7.2 Three-way analysis of a rain storm's impact on the discharge dynamics of the total stream water hydrograph (*dashed line*) and its relative contributions to discharge in the ground water, soil water, and storm flow (runoff) (**a**), the oxygen stable isotope ratio ($\delta^{18}O$) of stream water samples (*triangles*) taken at various times (days) after the storm event (**b**), and the bivariate plot of the SiO_2 vs. $\delta^{18}O$ in storm water (*open circles*), soil water (*gray circles*), and ground water (*filled circles*) samples collected at the same site over the 12-day event (**c**). The *triangles* in plot (**c**) show the SiO_2 and $\delta^{18}O$ values for storm water collected on a particular day (the day is number shown next to the symbol) that are the same data shown in plot (**b**). The initial $\delta^{18}O$ for the storm water and groundwater are shown with *arrows* in plot (**b**) (adapted from Clark and Fritz 1997)

would be much heavier or −24.6‰. The factors that cause variation in either c_i/c_a or c_c/c_a are therefore of two general types – those that impact the *supply* of CO_2 (mostly commonly through the stomatal pores and therefore by the stomatal apertures that ultimately affect the rate of conductance, g_c) and the *demand* for CO_2 by Rubisco. The relative importance of CO_2 supply vs. the demand for this C-substrate in determining the c_i/c_a is in turn determined by a suite of environmental (light, evaporative conditions at the leaf surface, soil water availability, plant available nitrogen in soils, etc.) and physiological (degree of plant water stress, allocation of nitrogen to enzymes vs. other functions, leaf energy balance, etc.) factors (Dawson et al. 2002). We do not have space in this chapter to explore the manner and importance of all of these factors. For our purposes here, it is most important to keep in mind that these factors ultimately determine the ^{13}C isotope composition of organic compounds in leaf litter, woody debris, or various other carbon-based compounds that in turn serve as the substrates for the oxidation of carbon via respiration. In fact, it is the respired $\delta^{13}CO_2$ from forested ecosystems

that can be used to track and quantify a wide range of carbon cycling questions at the stand or ecosystem scale (Pataki et al. 2003). Therefore, for the remainder of this chapter we focus on research that has used measurements of the $\delta^{13}CO_2$ of respiration and the concentration of the CO_2 in this efflux to inform forest C-cycling research. We also briefly highlight the use of ^{14}C methods and how they can provide additional information that ^{13}C may or may not (also see Trumbore 2006 for review on the uses of the ^{14}C method in ecosystem science).

7.5.1 Ecosystem Respiration

The measurement of the C-isotope composition of air sampled from plant parts such as roots, leaves, or entire crowns and from soils provides valuable information about forest carbon cycling. In particular and as noted above, the C-isotope composition of respired CO_2 from these sources (an others) provides insights into the controls, the flows and the sources of C in forest ecosystems. Moreover, tracking the isotope composition and sources of respiratory CO_2 fluxes provides an opportunity to understand the processes of C-isotope fractionation and the "routing" of carbon in forested ecosystems. A valuable method that is aimed at drawing many of these elements together and that extracts the C-isotope composition of different CO_2 sources (e.g., respired CO_2 from plant, soil, autotrophic, heterotrophic sources) from the bulk or background air in a quantitative manner was first developed by Charles D. (Dave) (Keeling 1958, 1961) and is now known as the "Keeling plot."

The establishment of the Keeling plot method that employs the simultaneous measurements of carbon dioxide concentration and the $\delta^{13}C$ of CO_2 samples collected has proven to be a robust approach for quantifying the source(s) of respired CO_2 from a range of ecosystems, including forests. Samples are generally collected at night from multiple heights across a gradient of CO_2 concentrations (C_{air}) that are very often observed when samples from the surface of the soil upward through the canopy into the background atmosphere (ambient air) or from soil-surface chambers over time. The data obtained from these plant and soil respiration samples are plotted with the $\delta^{13}C$ of each CO_2 sample as our dependent variable on the vertical-axis against the inverse of the carbon dioxide concentration (e.g., $1/[CO_2]$) on the horizontal axis (Fig. 7.3a) as the independent variable described by the equation

$$\delta^{13}C_{sample}C_{sample} = \delta^{13}C_{air}C_{air} + \delta^{13}C_RC_R, \qquad (7.5)$$

where C is the concentration (mole fraction) of CO_2 in dry air, the subscripts "sample," "air" and "R" represent the total CO_2 in each sample, the background CO_2 in ambient air from that particular ecosystem, and the respired sources of CO_2 from the ecosystem of interest, respectively. Of course, the $\delta^{13}C$ of the "sample," "air" and "R" represent the carbon isotope ratio ($^{13}C/^{12}C$) of each relative to the
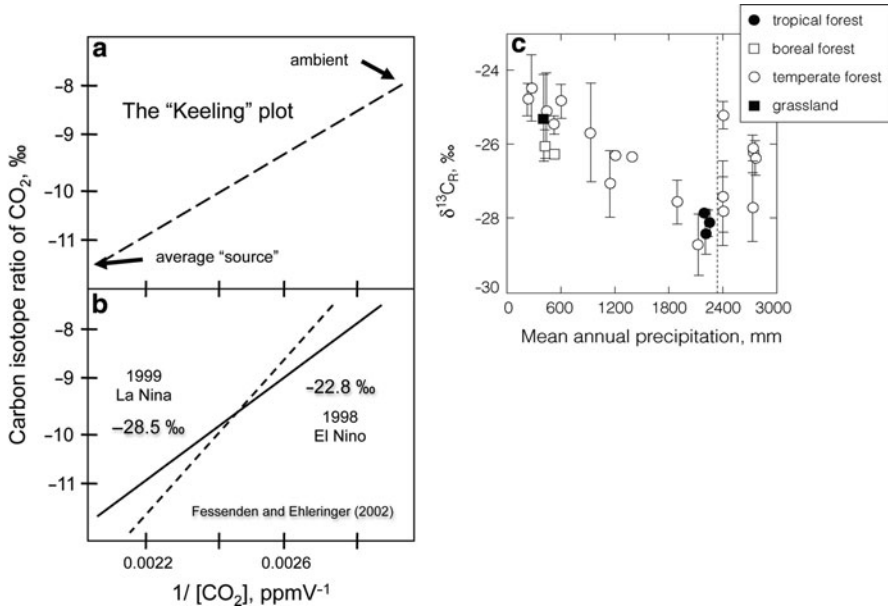
Fig. 7.3 (**a**) The "Keeling Pot" for ecosystem respiration (C_R), where the inverse of the carbon dioxide (CO_2) concentration (*x*-axis) is plotted against the stable carbon isotope composition (^{TM13}C) of a set of samples through which a linear regression (*dashed line*) is fit. The *y*-axis intercept of the *regression line* represents the average ^{TM13}C of ecosystem C_R, or $^{TM13}C_R$. (**b**) Example of how Fessenden and Ehleringer (2002) used the Keeling Plot method in a Pacific Northwestern conifer forest to investigate the impacts of a drier than normal El Niño year in 1998 compared with a wet La Niña year in 1999 on the Keeling Plot intercept, or $^{TM13}C_R$ (in 1998 $^{TM13}C_R = -22.8$‰ and in 1999 $^{TM13}C_R = -28.5$‰). (**c**) The $^{TM13}C_R$ obtained for a range of field sites (North and South America) in relation to mean annual precipitation (MAP) (from Pataki et al. 2003; reproduced with permission of the American Geophysical Union). *Error bars* are standard errors for all of the observation obtained at that site. In general, as MAP declined $^{TM13}C_R$ increased. At a coniferous forest site from the Northwestern United States, when MAP exceeded 2,400 mm year^{-1} (*vertical dotted line* at *right*), $^{TM13}C_R$ increases again

standard as described above. If C_R as $C_{sample} - C_{air}$ is substituted into the equation above, then

$$\delta^{13}C_{sample} = [C_{air}(\delta^{13}C_{air} - \delta^{13}C_R)/C_{sample}] + \delta^{13}C_R. \qquad (7.6)$$

A Model II linear regression is fit to the data and at the intersection of regression line with the *y*-axis the average $\delta^{13}C$ of ecosystem respiration, $\delta^{13}C_R$ (the source of the CO_2) is obtained. The method is based on the principle that at the *y*-intercept there is a hypothetically infinite source of CO_2 largely from biological activity (e.g., plant, bacterial, and fungal respiration) while at the opposite end of the regression line (upper right) is the ambient atmosphere. Recent efforts that have employed the Keeling plot method have used it to investigate interannual variation in the primary source of ecosystem respiration (Flanagan et al. 1996; Bowling et al. 2001, 2002)

and how significant changes in the magnitude of either soil water deficit (from precipitation changes; Fessenden and Ehleringer 2003; Scartazza 2004; Lai et al. 2005) or forest tree response to atmospheric demand (Bowling et al. 2002) may impact the δ^{13}C of this CO_2 source. For example, Fessenden and Ehleringer (2002) showed that in a coniferous forest during wet El Niño vs. drier La Niña conditions the intercept of the Keeling plot changed by nearly 6‰ (Fig. 7.3b). The interpretation for such a shift in this case was that under drier La Nina conditions, the forest trees that were believed to be the primary source of ecosystem respiration down-regulated their water use via stomatal closure that in turn changed (lowered) carbon isotope discrimination and therefore the relative amounts of ^{13}C and ^{12}C they assimilate. If trees discriminated less against ^{13}C, this would increase the δ^{13}C of the carbon they fixed; it is this carbon, by inference, that was the primary source of respiration (i.e., it determined the Keeling plot intercept). Keeling plots have also been used to follow how ecosystem respiration changes under varying conditions within a single season or across a wide range of ecosystem types that are exposed to large variations in site precipitation inputs (Fig. 7.2c; Buchmann et al. 1997; Harwood et al. 1999; Pataki et al. 2003).

7.5.2 Respiration Partitioning

Most recently, investigators using the Keeling plot method have begun to ask the question, what are the sources of respiration that contribute to a single plot intercept? Posing this question has in turn led investigators to conduct detailed partitioning studies aimed at deconvoluting the potentially complex set of respiration sources and then separating their relative contributions. This requires being able to identify the diversity of biological sources of respired CO_2 such as roots, leaves, tree boles, soils, etc. and further divide these into their respective autotrophic or heterotrophic origins (Fig. 7.4; Tu and Dawson 2005). It also seems possible that biogenic sources could be separated from possible geochemical sources of carbon dioxide (Tu and Dawson in review). A recent review by Bowling et al. (2008) highlights the power and promise of using the Keeling plot approach as well as other carbon isotope measurements in terrestrial ecosystem such as forest for deepening our understanding of what underlies the patterns as well as the processes governing ecosystem-scale carbon cycling. Additionally, recent literature that use carbon isotope data, including Keeling plots, reveals that when this information is linked with other forest metrics (e.g., stand age, basal area, species composition or other stand properties), site characteristics (e.g., slope exposure, soil moisture, evaporative demand for water from the vegetation by the atmosphere) as well as other knowledge about tree physiology (e.g., photosynthetic production and limitation, water use) and the ecology of the forested stand (e.g., disturbance regime and history, levels of competition within and among species, species or functional type diversity), new insights into the forest C-cycle and the physical and biological controls that impact it are beginning to emerge.
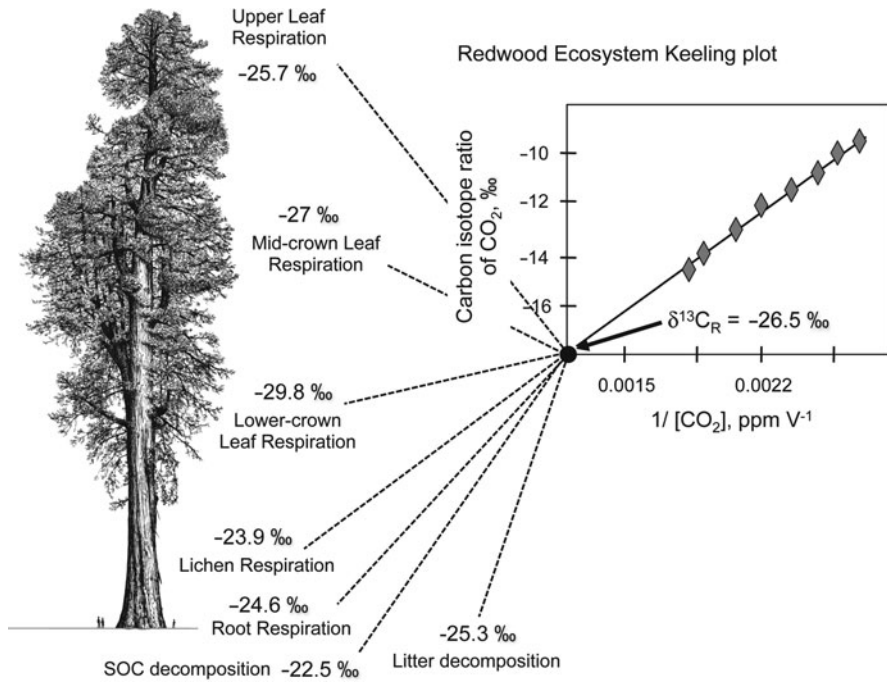
Fig. 7.4 Example of a deconvolution (partitioning) attempt where the various $\delta^{13}C$ values from different ecosystem compartments that are respiring are measured separately (the values at *left* side of the figure and at the end of each *dashed line* are each individual respired $\delta^{13}CO_2$ value obtained from that tissue type, compartment or pool) that make a possible contribution to the single $\delta^{13}CR$ (Keeling Plot intercept $= -26.5''$) value. Data were obtained from a central California Coastal Redwood Forest site (adapted from Tu and Dawson 2005; tree drawing by Robert Van Pelt from "Forest Giants of the Pacific Coast," University of Washington Press, reproduced with permission)

7.5.3 Radio Carbon

While the focus of this chapter is on "stable" isotopes, it is worth pointing out that the use of ^{14}C radiocarbon methods have also been a very powerful approach in forest carbon cycling research and particularly for aging soil organic matter (Horwath et al. 1994; Trumbore 2006) as well as roots (Gaudinski et al. 2001, 2009), for partitioning the gaseous fluxes out of forest soils (Hanson et al. 2000; Trumbore et al. 2006) or entire stands into their autotrophic and heterotrophic components (Hahn et al. 2006; Shuur and Trumbore 2006; Subke et al. 2006; Carbone et al. 2007) or from different species (Carbone and Trumbore 2007) and for tracking changes in the sources of soil respiration following catastrophic disturbances such as fire (Czimczik et al. 2006). It is likely that future research aimed at identifying and partitioning different sources of ecosystem respiration will very much benefit from using both ^{13}C and ^{14}C methods in combination not unlike using D and ^{18}O together for hydrological research highlighted above.

7.6 Future Directions

As advocated at the beginning of this chapter, we feel that the real advances will
come about in future of stable isotope investigations in forest hydrology and biogeo-
chemistry when multiple isotopes and numerous and complimentary methods are
applied. What has yet to be truly achieved with isotope methods is a comprehensive
investigation of the coupling of the water and carbon cycles in a forested system.
It is likely that now such study has yet to be done because of the expense and the
relative limitations of obtaining data at the right spatial and temporal scales.
And even though a variety of stable isotopes techniques have become more com-
monly used by forest hydrologists and biogeochemists, the availability of fully
automated analytical systems that can enhance the frequency of sampling has only
recently been achieved. For example, the development of a new generation of field-
deployable, optically based stable isotope analyzers (called tunable-diode, cavity
ring-down and quantum cascade lasers) is now permitting the analysis of fine-scale
changes in the isotope composition of meteoric waters (vapor and liquid; Welp et al.
2006) and atmospheric CO_2 at high-frequencies (e.g., Bowling et al. 2003; Kerstel
2004; Kerstel and Gianfrani 2008; Berman et al. 2009). These new instruments are
smaller, less expensive than modern mass spectrometers, can be powered using
portable battery banks, generators or solar arrays and thus can be deployed in the
field. They are also providing real-time data with very high precision and therefore
have the potential to revolutionize our ability to characterize carbon and water
pools and fluxes using isotopes in ways that have never been achievable. Many
challenges still remain in designing robust sampling schemes and rapid methods of
data analysis using these new techniques. Moreover, stable isotope analyses for a
wide range of sample types such as plant and soil extracts are currently posing
a challenge because organic substances in the water extracts are creating an optical
interference and therefore produce erroneous results (e.g., see Brand et al. 2009;
West et al. 2010a, b showing discrepancies between the isotope data generated by
laser and mass spectrometer). Despite the current challenges and limitations, the
use of these new optically based instruments will soon be overcome and inform forest
process studies in new ways and generate a new set of questions we never knew
to ask. Finally, new instruments and the data they can generate should have the
capacity to extend stand- and watershed-level investigations more rigorously to entire
regions so as to provide new perspectives on manner and magnitude of carbon and
water balance exchange under a diversity of biome- and land-use types such as those
proposed by the National Ecological Observatory Network, or NEON (see Ehleringer
and Dawson 2007; Bowen et al. 2009; West et al. 2010a, b).

References

Allison GB, Barnes CJ, Hughes MW (1983) The distribution of deuterium and ^{18}O in dry soils 2. Experimental. J Hydrol 64:377–397

Asano Y, Uchida T, Ohte N (2002) Residence times and flow paths of water in steep unchannelled catchments, Tanakami, Japan. J Hydrol 261:173–192

Augusti A, Betson TR, Schleucher J (2006) Hydrogen exchange during cellulose synthesis distinguishes climatic and biochemical isotope fractionations in tree rings. New Phytol 172:490–499

Barnes CJ, Allison GB (1983) The distribution of deuterium and ^{18}O in dry soils 1. Theory. J Hydrol 60:141–156

Barnes CJ, Turner JV (1998) Isotopic exchange in soil water. In: Kendall C, McDonnell JJ (eds) Isotope tracers in catchment hydrology. Elsevier, New York, pp 137–163

Berman ESF, Gupta M, Gabrielli C et al (2009) High-frequency field-deployable isotope analyzer for hydrological applications. Water Resour Res 45:W10201

Boutton TW, Tamasaki S-I (eds) (1996) Mass spectrometry of soils. Marcel Dekker, New York

Bowen GJ, West JB, Hoogewerff J (2009) Isoscapes: isotope mapping and its applications. J Geochem Explor 102:103–186

Bowling DR, Tans PP, Monson RK (2001) Partitioning net ecosystem carbon exchange with isotopic fluxes of CO_2. Glob Change Biol 7:127–145

Bowling DR, McDowell NG, Bond BJ et al (2002) ^{13}C content of ecosystem respiration is linked to precipitation and vapor pressure deficit. Oecologia 131:113–124

Bowling DR, Sargent SD, Tanner BD et al (2003) Tunable diode laser absorption spectroscopy for stable isotope studies of ecosystem-atmosphere CO_2 exchange. Agric For Meteorol 118:1–19

Bowling DR, Pataki DE, Randerson JT (2008) Carbon isotopes in terrestrial ecosystem pools and CO_2 fluxes. New Phytol 178:24–40

Brand WA, Geilmann H, Crosson ER et al (2009) Cavity ring-down spectroscopy versus high-temperature conversion isotope ratio mass spectrometry; a case study on δ^2H and δ^{18}O of pure water samples and alcohol/water mixtures. Rapid Comm Mass Spectrom 23:1879–1984

Brooks JR, Meinzer FC, Warren JM et al (2006) Hydraulic redistribution in a Douglas-fir forest: lessons from system manipulations. Plant Cell Environ 29:138–150

Brooks JR, Barnard HR, Coulombe R et al (2010) Ecohydrologic separation of water between trees and streams in a Mediterranean climate. Nat Geosci 3:100–104

Buchmann N, Guehl J-M, Barigah TS et al (1997) Interseasonal comparison of CO_2 concentrations, isotopic composition, and carbon dynamics in an Amazonian rainforest (French Guiana). Oecologia 110:120–131

Burgess SSO, Adams MA, Turner NC et al (1998) The redistribution of soil water by tree root systems. Oecologia 115:306–311

Burns DA, McDonnell JJ, Hooper RP et al (2001) Quantifying contributions to storm runoff through end-member mixing analysis and hydrologic measurements at Panola Mountain Research Watershed (Georgia, USA). Hydrol Process 15:1903–1924

Caldwell MM, Dawson TE, Richards JH (1998) Hydraulic lift: consequences of water efflux from the roots of plants. Oecologia 113:151–161

Carbone MS, Trumbore SE (2007) Contribution of new photosynthetic assimilates to respiration by perennial grasses and shrubs: residence times and allocation patterns. New Phytol. doi:10.1111/j.1469-8137.2007.02153x

Carbone MS, Czimczik CI, McDuffee KE et al (2007) Allocation and residence time of photosynthetic products in a boreal forest using a low-level ^{14}C pulse-chase labeling technique. Glob Change Biol 13:466–477

Chahine MT (1992) The hydrological cycle and its influence on climate. Nature 359:373–380

Clark ID, Fritz P (1997) Environmental isotopes in hydrogeology. CRC Press, Boca Raton

Craig H (1961) Isotopic variations in meteoric waters. Science 133:1702–1703

Craig H, Gordon L (1965) Deuterium and oxygen-18 in the ocean and marine atmosphere. In: Tongiorgi E (ed) Stable isotopes in oceanographic studies and paleotemperatures. Consiglio, Spaleto, pp 9–130

Craine JM, Elmore AJ, Aidar MPM et al (2009) Global patterns of foliar nitrogen isotopes and their relationships with climate, mycorrhizal fungi, foliar nutrient concentrations, and nitrogen availability. New Phytol 183:980–992

Criss RE (1999) Principles of stable isotope distribution. Oxford University Press, New York

Czimczik CI, Trumbore SE, Carbone MS et al (2006) Changing sources of soil respiration with time since fire in a boreal forest. Glob Change Biol 12:957–971

Dansgaard W (1964) Stable isotopes in precipitation. Tellus 16:436–468

Dawson TE (1993) Hydraulic lift and water use by plants: implications for water balance, performance and plant-plant interactions. Oecologia 95:565–574

Dawson TE (1996) Determining water use by trees and forests from isotopic, energy balance and transpiration analyses: the roles of tree size and hydraulic lift. Tree Physiology 16:263–272

Dawson TE, Ehleringer JR (1998) Plants, isotopes, and water use: a catchment-level perspective. In: Kendall C, McDonnell JJ (eds) Isotope tracers in catchment hydrology. Elsevier, Amsterdam, pp 165–202

Dawson TE, Siegwolf RTW (2007) Stable isotopes as indicators of ecological change. Academic Press, San Diego

Dawson TE, Pausch RC, Parker HM (1998) The role of hydrogen and oxygen stable isotopes in understanding water movement along the soil-plant-atmospheric continuum. In: Griffiths H (ed) Stable isotopes and the integration of biological, ecological and geochemical processes. BIOS Scientific Publishers, London, pp 169–183

Dawson TE, Mambelli S, Plamboeck AH et al (2002) Stable isotopes in plant ecology. Annu Rev Ecol Syst 33:507–559

Dewalle DR, Edwards PJ, Swistock BR et al (1997) Seasonal isotope hydrology of three Appalachian forest catchments. Hydrol Process 11:1895–1906

Ehleringer JR, Dawson TE (2007) Stable isotopes record ecological change, but a sampling network will be critical. In: Dawson TE, Siegwolf RTW (eds) Stable isotopes as indicators of ecological change. Academic Press, San Diego, pp 19–24

Ehleringer JR, Hall AE, Farquhar GD (1993) Stable isotopes and plant carbon-water relations. Academic Press, San Diego

Ehleringer JR, Roden J, Dawson TE (2000) Assessing ecosystem-level water relations through stable isotope analyses. In: Sala OE, Jackson RB, Mooney HA, Howarth RW (eds) Methods in ecosystem science. Springer, New York, pp 181–198

Emmerman SH, Dawson TE (1996) Hydraulic lift and its influence on the water content of the rhizosphere: an example from sugar maple, *Acer saccharum*. Oecologia 108:273–278

Farquhar GD, Ehleringer JR, Hubick KT (1989) Carbon isotope discrimination and photosynthesis. Ann Rev Plant Physiol Plant Mol Biol 40:503–537

Faure G (1986) Principles of isotope geology, 2nd edn. Wiley, New York

Fessenden JE, Ehleringer JR (2002) Age-related variations in ^{13}C of ecosystem respiration across a coniferous forest chronosequence in the Pacific Northwest. Tree Physiol 22:159–167

Fessenden JE, Ehleringer JR (2003) Temporal variation in delta C-13 of ecosystem respiration in the Pacific Northwest: links to moisture stress. Oecologia 136:129–136

Fetter CW (1994) Applied hydrogeology. Prentice-Hall, New Jersey

Flanagan LB, Brooks JR, Varney GT et al (1996) Carbon isotope discrimination during photosynthesis and the isotope ratio of respired CO_2 in boreal forest ecosystems. Glob Biogeochem Cycles 10:629–640

Flanagan LB, Ehleringer JR, Pataki DE (eds) (2005) Stable isotopes and biosphere-atmosphere interactions: processes and biological controls. Academic Press, New York

Flexas J, Ribas-Carbó M, Diaz-Espejo A et al (2007) Mesophyll conductance to CO2: current knowledge and future prospects. Plant Cell Environ 31:602–621

Fry B (2007) Stable isotope ecology. Springer

Gat JR (1996) Oxygen and hydrogen isotopes in the hydrologic cycle. Annu Rev Earth Planet Sci 24:225–262

Gat JR, Airey PL (2006) Stable water isotopes in the atmosphere/biosphere/lithosphere interface: scaling-up from the local to continental scale, under humid and dry conditions. Global Planet Change 51:25–33

Gat JR, Tzur Y (1967) Modification of the isotopic composition of rainwater by processes which occur before groundwater recharge. In: Proceedings of the symposium on isotopes in hydrology, Rep. IAEA-SM-83. International Atomic Energy Agency, Vienna, pp 49–60

Gaudinski JB, Trumbore SE, Davidson EA et al (2001) The age of fine root carbon in three forests of the eastern United States measured by radiocarbon. Oecologia 129:420–429

Gaudinski JB, Torn MS, Riley WJ et al (2009) Use of stored carbon reserves in growth of temperate tree roots and leaf buds: analyses using radiocarbon measurements and modeling. Glob Change Biol 15:992–1014

Gazis C, Feng X (2004) A stable isotope study of soil water: evidence for mixing and preferential flow paths. Geoderma 119:97–111

Griffiths H (ed) (1998) Stable isotopes: integration of biological, ecological and geochemical processes. BIOS Scientific Publishers, Oxford

Hahn V, Högberg P, Buchmann N (2006) ^{14}C – a tool for separation of autotrophic and heterotrophic soil respiration. Glob Change Biol 12:972–982

Hansen MC, Defries RS, Townsend JRG et al (2000) Global land cover classification at 1km spatial resolution using a classification tree approach. Int J Remote Sens 21:1331–1364

Hanson PJ, Edwards NT, Garten CT et al (2000) Separating root and soil microbial contributions to soil respiration: a review of methods and observations. Biogeochemistry 48:115–146

Harwood KG, Gillon JS, Griffiths H, Broadmeadow MSJ (1998) Diurnal variation of $\Delta^{13}CO_2$, $\Delta C^{18}O^{16}O$ and evaporative site enrichment of $\delta H_2^{18}O$ in *Piper aduncum* under field conditions in Trinidad. Plant Cell and Environment 21:269–283

Harwood KG, Gillon JS, Roberts A et al (1999) Determinants of isotopic coupling of CO_2 and water vapour within a *Quercus petraea* forests canopy. Oecologia 119:109–119

Hayes JM (2004) Isotopic order, biogeochemical processes, and earth history [publication version of Goldschmidt lecture, 2002]. Geochim Cosmochim Acta 68:1691–1700

Hayes JM, Freeman KH, Popp BN et al (1990) Compound-Specific isotopic analyses: a novel tool for reconstruction of ancient biogeochemical processes. Org Geochem 16:1115–1128

Henderson-Sellers A, Fischer M, Aleinov I et al (2006) Stable water isotope simulation by current land-surface schemes: results of iPILPS phase 1. Glob Planet Change 51:34–58

Hoefs J (1997) Stable isotope geochemistry. Springer, Berlin

Holton BZ, Sigman DM, Hedin LO (2006) Isotopic evidence for large gaseous nitrogen losses from tropical rainforests. Proc Natl Acad Sci U S A 103:8745–8750

Horwath WR, Pregitzer KS, Paul EA (1994) C-14 allocation in tree soil systems. Tree Physiol 14:1163–1176

Kabeya N, Katsuyama M, Kawasaki M et al (2007) Estimation of mean residence times of subsurface waters using seasonal variation in deuterium excess in a small head water catchment in Japan. Hydrol Process 21:308–322

Keeling CD (1958) The concentration and isotopic abundances of atmospheric carbon dioxide in rural areas. Geochim Cosmochim Acta 13:322–334

Keeling CD (1961) The concentration and isotopic abundance of carbon dioxide in rural and marine air. Geochim Cosmochim Acta 24:277–298

Kendall C, Caldwell EA (1998) Fundamentals of isotope geochemistry. In: Kendall C, McDonnell JJ (eds) Isotope tracers in catchment hydrology. Elsevier, New York, pp 51–86

Kendall C, McDonnell JJ (1998) Isotope tracers in catchment hydrology. Elsevier, Amsterdam

Kendall C, McDonnell JJ, Gu W (2001) A look inside "black box" hydrograph separation models: a study at the Hydrohill catchment. Hydrol Process 15:1877–1902

Kerstel E (2004) Isotope ratio infrared spectrometry. In: de Groot P (ed) Handbook of stable isotope analytical techniques. Academic Press, San Diego, pp 759–787

Kerstel E, Gianfrani L (2008) Advances in laser-based isotope ratio measurements: selected applications. Appl Phys B 92:439–449

Lai C-T, Ehleringer JR, Schauer AJ et al (2005) Canopy-scale ™13C of photosynthetic and respiratory CO₂ fluxes: observations of forest biomes across the United States. Glob Change Biol 11:633–643

Lajtha K, Michener RH (1994) Stable isotopes in ecology and environmental science. Blackwell, Oxford

Lambers H, Chapin FS III, Pons TJ (1998) Plant physiological ecology. Springer, New York

Lee J-E, Oliveira RS, Dawson TE et al (2005a) Root functioning modifies seasonal climate. Proc Natl Acad Sci U S A 102:17576–17581

Lee X, Sargent S, Smith R et al (2005b) In situ measurement of the water vapor $^{18}O/^{16}O$ isotope ratio for atmospheric and ecological applications. J Atmos Ocean Technol 22:555–565

Lee K-S, Kim J-M, Lee D-R et al (2007) Analysis of water movement through an unsaturated soil zone in Jeju Island, Korea using stable oxygen and hydrogen isotopes. J Hydrol 345:199–211

Mathieu R, Bariac T (1996) An isotopic study (^2H and ^{18}O) of water movements in clayey soils under a semiarid climate. Water Resour Res 32:779–789

McCarroll D, Loader NJ (2004) Stable isotopes in tree rings. Quat Sci Rev 23:771–801

McKinney CR, McCrea JM, Epstein S et al (1950) Improvements in mass spectrometers for the measurement of small differences in isotope abundance ratios. Rev Sci Instrum 21:724–730

Moreira MZ, Sternberg LDSL, Martinelli LS et al (1997) Contribution of transpiration to forest ambient vapour based on isotopic measurements. Glob Change Biol 3:439–450

Ogle K, Wolpert RL, Reynolds JF (2004) Reconstructing plant root area and water uptake profiles. Ecology 85:1967–1978

Pataki DE, Ehleringer JR, Flanagan LB et al (2003) The application and interpretation of Keeling plots in terrestrial carbon cycle research. Glob Biogeochem Cycles 17:1022

Phillips DL, Gregg JW (2003) Source partitioning using stable isotopes: coping with too many sources. Oecologia 136:261–269

Romero-Saltos H, Sternberg LDSL, Moreira MZ et al (2005) Rainfall exclusion in an eastern amazonian forest alters soil water movement and depth of water uptake. Am J Bot 92:443–455

Rozanski K, Araguás-Araguás L, Gonfiantini R (1992) Relation between long-term trends of Oxygen-18 isotope composition of precipitation and climate. Science 258:981–985

Rozanski K, Araguás-Araguás L, Gonfiantini R (1993) Isotopic patterns in modern global precipitation. Geophys Monogr 78:1–36

Rundel PW, Ehleringer JR, Nagy KA (eds) (1989) Stable isotopes in ecological research. Ecological studies, vol 68. Springer, Heidelberg

Scartazza A (2004) Comparisons of delta C-13 of photosynthetic products and ecosystem respiratory CO2 and their response to seasonal climate variability. Oecologia 140:340–351

Sharp Z (2007) Principles of stable isotope geochemistry. Prentice-Hall, New Jersey

Shuur EA, Trumbore SE (2006) Partitioning sources of soil respiration in boreal black spruce forests using radiocarbon. Glob Change Biol 12:165–176

Sternberg LSO (2009) Oxygen stable isotope ratios of tree-ring cellulose: the next phase of understanding. New Phytol 174:553–562

Subke J-E, Inglima I, Cotrufo F (2006) Trends and methodological impacts in soil CO₂ efflux partitioning: a metaanalytical review. Glob Change Biol 12:921–943

Trumbore S (2006) Carbon respired by terrestrial ecosystems – recent progress and challenges. Glob Change Biol 12:141–153

Trumbore SE, Da Costa ES, Nepstad DC et al (2006) Dynamics of fine root carbon in Amazonian tropical ecosystems and the contribution of roots to soil respiration. Glob Change Biol 12:217–229

Tu KP, Dawson TE (2011) Partitioning ecosystem respiration between plant and microbial sources using natural abundance stable carbon isotopes: a study of four California ecosystems (in review)

Tu K, Dawson T (2005) Partitioning ecosystem respiration using stable carbon isotope analyses of CO_2. In: Flanagan LB, Ehleringer JR, Pataki DE (eds) Stable isotopes and biosphere-atmosphere interactions: processes and biological controls. Academic Press, San Diego, pp 125–153

Unkovich M, McNeill A, Pate J et al (2001) The application of stable isotope techniques to study biological processes and the functioning of ecosystems. Kluwer Academic Press, Boston

Walker CD, Brunel J-P (1990) Examining evapotranspiration in a semi-arid region using stable isotopes of hydrogen and oxygen. J Hydrol 118:55–75

Wang X, Yakir D (2000) using stable isotopes of water in evapotranspiration studies. Hydrol Process 14:107–1421

Welp LR, Randerson JT, Liu H (2006) The effects of stand age on seasonal exchange of CO_2 and δ18O-CO_2 in boreal forest ecosystems of interior Alaska. J Geophys Res 111:G03007

Wenjie L, Pengju L, Hongmei L et al (2006) Estimation of evaporation rate from soil surface using stable isotopic composition of throughfall and stream water in a tropical seasonal rain forest of Xishuangbanna, Southwest China. Acta Ecol Sinica 26:1303–1311

Wershaw RL, Friedman I, Heller SJ et al (1970) Hydrogen isotopic fractionation of water passing through trees. In: Hobson GD (ed) Advanced in organic geochemistry. Pergamon Press, Oxford, pp 55–67

West AG, Goldsmith GR, Brooks PD, Dawson TE (2010a) Discrepancies between isotope ratio infrared spectroscopy and isotope ratio mass spectrometry for the stable isotope analysis of plant and soil waters. Rapid Comm Mass Spectrom 24(14):1948–1954

West JB, Bowen GJ, Dawson TE et al (eds) (2010b) Isoscapes – understanding movement, pattern, and process on Earth through isotope mapping. Springer, Berlin

White JWC, Cook ER, Lawrence JR et al (1985) The d/h ratios of sap in trees – implications for water sources and tree-ring d/h ratios. Geochim Cosmochim Acta 49:237–246

Williams DG, Cable W, Hultine K et al (2004) Evapotranspiration components determined by stable isotope, sap flow and eddy covariance techniques. Agric For Meteorol 125:241–258

Yakir D, Sternberg LDSL (2000) The use of stable isotopes to study ecosystem gas exchange. Oecologia 123:297–311

Yepez EA, Williams DG, Scott RL et al (2003) Partitioning overstory and understory evapotranspiration in a semiarid savanna woodland from the isotopic composition of water vapor. Agric For Meteorol 119:53–68

Zimmermann U, Ehhalt D, Münnich KO (1967) Soil water movement and evapotranspiration: changes in the isotopic composition of the water. In: Proceedings of the symposium on isotopes in hydrology, Rep. IAEA-SM-83. International Atomic Energy Agency, Vienna, pp 49–60

Chapter 8
The Use of Geochemical Mixing Models to Derive Runoff Sources and Hydrologic Flow Paths

Shreeram Inamdar

8.1 Introduction

Mixing models have long been used in catchment studies to partition streamflow runoff into individual source components and characterize hydrologic flow paths (Pinder and Jones 1969; Sklash and Farvolden 1979; Bazemore et al. 1994; Buttle 1994). These models assume that catchment runoff is a mixture of unique runoff sources whose contributions can be determined using tracers that behave conservatively. The key benefit of using these models is that they describe the integrated catchment response as opposed to point-specific information provided by, for example, groundwater wells. These models are especially valuable for understanding watershed behavior when used in conjunction with hydrometric data (Bonell 1998; Buttle 2005). The use of mixing models in catchment hydrology has evolved over time with a focus on different types of runoff components, changes in computational methods, and a greater recognition of the limitations and benefits of these models.

The use of mixing models started in earnest in the 1970s when they were implemented to determine the "new" (event) and "old" (pre-event) components of runoff (Sklash and Farvolden 1979). The new and old water components can be referred to as *time-source* (Sklash et al. 1976) components since they characterize the temporal origins of runoff. Identification of these runoff components was achieved through the use of stable isotopes of water like oxygen-18 (^{18}O) and deuterium (^2H or D) and thus these models were also referred to as isotope hydrograph separations (IHSs) (Buttle 1994, 2005). Subsequently, storm runoff was partitioned into sources such as "surface runoff" and/or "groundwater" using solutes like silica (Si) and chloride (Cl^-) (Genereux and Hooper 1998). These mixing models can be referred to as geochemical hydrograph separations (GHSs) since they utilized geochemical tracers. The intent of these models was not necessarily to characterize the temporal origins of runoff (event vs. pre-event waters), but rather to determine the *geographic sources* of water in the catchment (Genereux and Hooper 1998). The assumption was that runoff waters flowing through various watershed compartments (or geographic sources) acquired unique chemical signatures (solute concentrations) representative of the geochemistry of those compartments and that these distinct chemical signatures could be used to determine the runoff contributions from the sources. While GHSs have also been

indirectly assumed to infer the flowpaths taken by runoff waters, our current understanding is that GHSs may provide only an idea of the last geographic source that runoff waters have been in contact with and not necessarily the complete flowpath taken by water since its origin (Hooper 2001; Katsuyama et al. 2009).

An important observation from these early studies of IHS and GHS was that catchment runoff, especially, in humid, temperate, watersheds was predominantly composed of pre-event or groundwater and surface runoff or event water constituted only a small fraction (Buttle 1994). This was a revolutionary finding in hydrology at that time because it refuted the predominant perceptual model of Horton (1933) that infiltration-excess overland flow was the dominant source of runoff during storms. Subsequent studies in the late 1980s and early 1990s suggested that surface runoff and groundwater alone could not explain the runoff chemistry and a third component "soil water" was needed to reconcile the runoff observations (Dewalle et al. 1988; Kennedy et al. 1986; Bazemore et al. 1994). More recently, the interest in geographic sources of runoff has become even more explicit, with the identification of watershed sources such as riparian groundwater, wetland and hillslope waters, O-horizon water and throughfall (Brown et al. 1999; Burns et al. 2001; Hooper 2001; McHale et al. 2002; McGlynn and McDonnell 2003; James and Roulet 2006; Inamdar and Mitchell 2007).

Early applications of mixing models solved mass balance equations for a minimum number of tracers (often just one or two stable isotopes or solutes) required to identify the likely runoff components (Sklash and Farvolden 1979; Dewalle et al. 1988; Bazemore et al. 1994). In the 1990s however, Christopherson and Hooper (1992) and Hooper et al. (1990) introduced multivariate statistical analyses that used a suite of tracers (e.g., cations, anions, and silica) for mixing models. This methodology was referred to as end-member mixing analysis (EMMA) since the key geographic sources of runoff were labeled as "end-members."

Since the introduction of EMMA, the interest in using geochemical mixing models as an investigative tool to identify runoff sources has increased dramatically. While some of these studies have confirmed our conceptual models of watershed hydrologic behavior, others have raised new questions and even challenged the existing paradigms of watershed response (e.g., Robson et al. 1992; Hooper 2001). The use of EMMA and mixing models, however, is based on assumptions which more often than not are violated under typical watershed conditions. The "failure" of mixing models due to violation of these assumptions, can nevertheless, provide as much (or more) insight into catchment processes as a "successful" application (Hooper 2001, 2003). The following discussion highlights the key lessons learned from GHS and EMMA applications, provides guidance for future applications, and explores the new opportunities that lie ahead. This article does not address IHSs, since excellent reviews by Buttle (1994, 2005) and Genereux and Hooper (1998) have already covered this topic in detail. Specific topics that will be covered in this article are:

- The theory, assumptions and procedures for geochemical mixing models and/or EMMA.
- Applications of geochemical mixing models in watershed studies and the important insights that have been derived from these applications.

- Pitfalls associated with geochemical mixing models and ways we can avoid them.
- Future challenges and opportunities for geochemical mixing models.

8.2 Equations, Assumptions, and Procedures for Geochemical Mixing Models and EMMA

Geochemical mixing models rely on the solution of simple mass balance equations for water and the chosen tracers and can be given by:

$$Q_t = \sum_{i=1}^{n} Q_i,$$

$$Q_t C_t{}^j = \sum_{i=1}^{n} Q_i C_i{}^j \quad \text{where } j = 1, \ldots, (n-1), \tag{8.1}$$

where Q_t is the catchment outflow or streamflow, Q_i is the contribution from the end-member or runoff component i, and $C_i{}^j$ is the concentration of tracer j for end-member i. In the absence of hydrometric data, the solution of these equations for n end-members requires a minimum of $n-1$ tracers. The key assumptions for geochemical mixing models are:

1. The tracers behave conservatively, i.e., the tracer concentrations do not change due to biogeochemical processes over the time-scale considered by the mixing model.
2. The mixing process is linear.
3. The chemical composition of end-members (tracer concentrations) does not change over the time-scale considered by the mixing model (time invariance).
4. The chemical composition of end-members (tracer concentrations) does not change with space (space invariance).

In the simplest form, the contributions of end-members can be computed by directly solving the mass balance equations for the selected tracers or solutes given the observed concentrations for both the stream outflow and the potential end-members (e.g., Sklash and Farvolden 1979; Dewalle et al. 1988; Bazemore et al. 1994). This simple approach, however, does not constitute EMMA, as has been incorrectly assumed by a few studies in literature. EMMA, as described by Christopherson and Hooper (1992) and Hooper et al. (1990), involves the use of a large number of tracers (more than the minimum required to identify potential end-members and solve the mass balance equations) within a principal component analysis (PCA) framework. The PCA is used to reduce the dimensionality of the data set with the selected principal components (e.g., first two components for a three end-member model) being used to solve the mass balance equations. The use of additional tracers increases the information content of the data set and thus the

reliability and confidence in the mixing model. Christopherson and Hooper (1992) and Hooper et al. (1990) further suggested that the number and identity of the potential end-members could be determined by plotting the end-members in the PCA mixing space defined by stream chemistry and determining which end-members bounded the stream chemistry. More recently, Hooper (2003) suggested that the number (or rank) of the end-members can also be independently determined from stream chemistry data alone (i.e., without knowledge of end-member chemistry). In addition, Hooper (2003) also presented specific tests to evaluate if the tracers behaved conservatively and if the mixing proportions varied along the drainage path. These two approaches (Christopherson and Hooper 1992; Hooper 2003) are not mutually exclusive and ideally should be combined. These methods are characterized through four key steps in the description below. For a complete description of the theory and mathematical treatment of EMMA, the readers are referred to Christopherson and Hooper (1992) and Hooper (2003).

8.2.1 Evaluation and Selection of Tracers

Tracers that behave conservatively are vital for a successful application of EMMA. Hooper (2003) suggested that assumptions of linearity of mixing and conservative behavior of tracers can be evaluated using bivariate scatter plots and residuals derived from the selected model. Bivariate scatter plots should be developed for all potential combination of available solutes (e.g., see Fig. 8.1). While Hooper (2003) suggested that a collinear structure in the bivariate plots could be used to infer conservative behavior, it does not necessarily confirm or prove conservative behavior of the solutes (Hooper, personal communication). A more objective method to evaluate the linearity of solute mixing, however, is still lacking.
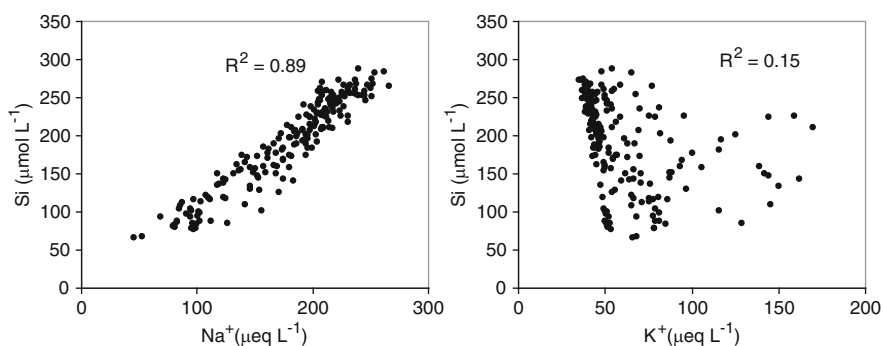
Fig. 8.1 Bivariate solute plots to investigate linear mixing and conservative behavior of potential tracers. The plot on the *left* (Si-Na$^+$) indicates a strong linear mixing trend whereas the one on the *right* (Si-K$^+$) indicates a weak trend. This analysis suggests that Si and Na$^+$ can be retained as potential tracers whereas K$^+$ should be discarded. Data from a 12 ha forested catchment in Maryland, USA (Inamdar, unpublished data)

8.2.2 Determination of the Number of End-Members from Stream Chemistry Data Alone

Following the selection of tracers, the stream or runoff concentrations should be normalized by subtracting the mean for each solute and by dividing by its standard deviation. This standardization prevents any particular solute with greater variation from exerting more influence on the model (Burns et al. 2001). These data are then used to develop a correlation matrix followed by PCA to determine eigenvectors and eigenvalues. The standardized stream data can then be projected into PCA space (or U-space) by multiplying it with the eigenvectors. At this stage, the numbers of eigenvectors (or the potential end-members) that need to be retained can be determined from stream data alone following the procedures of Hooper (2003). The standardized stream data are multiplied with incremental addition of eigenvectors and the residuals computed for each additional set. The minimum number of eigenvectors required to yield a random structure in the residuals and to satisfy the "rule of 1" (Hooper 2003; James and Roulet 2006) indicates the rank (potential end-members = rank of eigenvectors + 1) of the data set.

8.2.3 Identification of Potential End-Members for Stream Chemistry

If two eigenvectors are adequate (indicating three potential end-members) from the assessment in Sect. 8.2.2; the stream chemistry can be plotted in two-dimensional mixing space by using the first two principal components (e.g., PC1 and PC2 in Fig. 8.2) of the model. To project the potential end-members in this mixing subspace, the tracer concentrations for all potential end-members should be normalized to the stream water by using the mean and standard deviation of the stream solutes. The standardized end-member values can then be projected into the stream U-space by multiplying with the two principal components or eigenvectors. Subsequently, the selection of the three key end-members is made based on their ability to enclose the stream concentrations in U-space. Following the selection of the end-members, the chosen EMMA model is used to back-calculate the standardized stream water values. The standardized values are de-standardized by multiplying by the standard deviation of each solute and adding the corresponding mean concentration to yield the predicted value of solute concentration.

8.2.4 Validity of the EMMA Model

Following model development, residuals (difference between predicted and observed tracer concentrations) should be plotted against the observed sample (e.g., Fig. 2
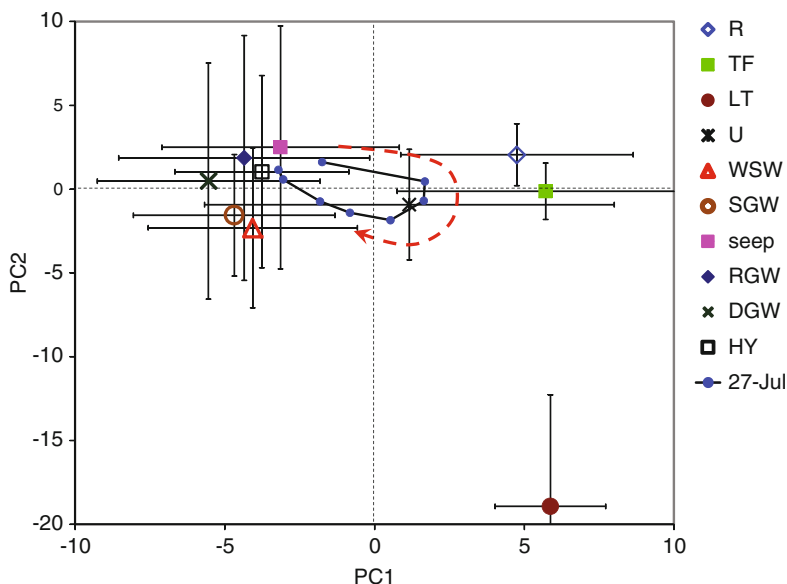
Fig. 8.2 A principal component analysis (PCA) mixing diagram illustrating the evolution of stream chemistry during a storm event. PC1 and PC2 are the first two principal components. Data are for an intense summer rainfall event (July 27, 2008) at the outlet of a 12-ha forested catchment in Maryland, USA (Inamdar, unpublished data). Potential end-members include: rainfall (R), throughfall (TF), litter leachate (LT), unsaturated soil water (U), wetland soil water (WSW), shallow ground water (SGW), GW seep (seep), riparian ground water (RGW), deep ground water (DGW), and hyporheic zone water (HY). The stream chemistry displayed a clockwise hysteresis loop with stream concentrations moving from seep toward TF and returning back to seep groundwater. If three end-members were to be chosen, they could include seep, TF, and WSW. End-member concentrations were determined using the mean of sample concentrations collected before and after the storm event. Error bars are computed from 1 standard deviation of the tracer concentrations. Selected tracers for this EMMA were: sodium, magnesium, calcium, silica, dissolved organic carbon (DOC) and UV absorption coefficient at 254 nm (a_{254})

in Hooper 2003). A random pattern of the residuals indicates a conservative mixing subspace while a structure in the residuals can be attributed to a nonconservative behavior or poor selection of end-members (Hooper 2003). In addition, the validity of the EMMA model can also be evaluated by determining the difference between the predicted and observed streamwater solute concentrations. Mathematical indices such as root mean square error (RMSE), relative bias (BIAS), and standard correlation coefficient (R) can be used to quantify the difference in predicted and observed concentrations (Hooper 2003; Inamdar and Mitchell 2007; Jung et al. 2009). In addition to these comparisons, it is highly recommended that EMMA predictions be evaluated using independently-measured hydrometric data and solutes that have not been used in model development. The value and importance of such additional comparisons cannot be emphasized enough and are highlighted in the discussions below.

8.3   Lessons from Applications of Geochemical Mixing Models in Watershed Studies

The introduction of geochemical mixing models and EMMA in watershed studies has no doubt furthered catchment science and our understanding of catchment-scale hydrologic and biogeochemical processes. It is highly unlikely that such insights into watershed behavior could have been gained through the use of hydrometric data alone. A selection of EMMA applications from around the world and spanning the last 15 years is summarized in Table 8.1 highlighting the tracers used and the runoff end-members identified. While three end-members have been found to be adequate for explaining catchment stormflow in most applications, some recent studies have proposed a larger number of end-members (e.g., Morel et al. 2009).

8.3.1   Runoff End-Members and the Importance of Riparian Water

Although a variety of end-members have been identified by GHS and EMMA (Table 8.1), one common theme that emerges from these studies is the importance of the riparian zone or the alluvial aquifer in affecting stormflow chemistry. In most of the investigations, the riparian aquifer has been found to exert a substantial control on storm runoff (Durand and Torres 1996; Burns et al. 2001; Hangen et al. 2001; Hooper 2001; McGlynn and McDonnell 2003; Soulsby et al. 2003; Subagyono et al. 2005; Inamdar and Mitchell 2007). Hooper (2001) found that runoff contributions from different parts of the riparian zone influenced stream chemistry during storm events but chemical contributions from the hillslope which constituted the largest fraction of catchment area were absent. This finding led Hooper (2001) to question the generally accepted paradigm that stream water represented an integrated chemical signature of *all* parts of the catchment.

   In comparison to riparian groundwater, the expression of hillslope runoff or other upland water sources (e.g., bedrock outcrop runoff in Burns et al. 2001) in streamflow has been found to be generally small with the exception of large storm events. During large events or events following wet antecedent moisture conditions, upland contributions have been observed to increase dramatically (Burns et al. 2001; McGlynn and McDonnell 2003). Some researchers have hypothesized that there may be volumetric moisture "thresholds" associated with upland and riparian aquifers which, when exceeded, may result in a sudden shift in relative contributions from these water sources (Burns et al. 2001; McGlynn and McDonnell 2003). Such studies highlight the need to determine the volumetric riparian storage vis-à-vis upland or hillslope fluxes so as to better quantify the threshold storage beyond which upland runoff contributions are observed in catchment stormflow.

   While other studies have also concurred about the importance of riparian zone for runoff generation, they also suggest that the riparian aquifer is not a single, well-mixed

Table 8.1 A selection of recent EMMA studies from around the world highlighting the tracers used and the end-members identified

References	Location	Site description	Tracers used	End-members	Additional observations
Jung et al. (2009)	Southern California, USA	690 and 1,400 ha catchments; semi-arid climate	Ca^{2+}, Mg^{2+}, K^+, Na^+, SO_4^{2-}	Groundwater (GW), overland flow, shallow subsurface flow	Early postfire storm events generated larger amounts of overland flow. The fire effect on runoff was more pronounced at the smaller catchment scale.
Katsuyama et al. (2009)	Shiga Prefecture, Japan	0.68 ha catchment; humid climate	SiO_2, Na^+, Mg^{2+}, Cl^-, NO_3^-, and SO_4^{2-}	Rainfall, hillslope GW and riparian GW	Riparian GW was not homogenous but contained waters of different ages.
Morel et al. (2009)	Central Brittany, France	500 ha agricultural watershed; humid climate	DOC, SO_4^{2-}, NO_3^-, Cl^-	Wetland soil water, shallow GW, deep GW, rain	Wetland soil water was the largest contributor. A systematic sequence in end-member contributions was observed.
Verseveld et al. (2008)	Cascade Mountains, Oregon, USA	10.2 ha forested watershed; Mediterranean climate	DOC, SO_4^{2-}, SUVA, Cl^-	Throughfall, organic horizon, deep GW, transient GW	EMMA performed for hillslope and catchment runoff. Deep soil and GW contributions higher during hydrograph recession.
Inamdar and Mitchell (2007)	Western New York, USA	1.6–696 ha catchments; forested, glaciated; humid climate	Si, Mg^{2+}, DOC	Throughfall, seep (springs) GW and riparian water	Throughfall contributions were elevated on the hydrograph rising limb while riparian water contributions increased on the recession limb
James and Roulet (2006)	Quebec, Canada	7–147 ha catchments; glaciated; humid climate	Na^+, Mg^{2+}, Ca^{2+}, EC, alkalinity	GW, perched water and throughfall	Mixing proportions for solutes varied across the catchments.
Bernal et al. (2006)	Northeastern Spain	1,050 ha forested catchment; Mediterranean climate	Cl^-, SO_4^{2-}, and DOC	Event water, hillslope GW and riparian GW	Riparian and hillslope GW's were the primary runoff sources. No clear relationship between hillslope GW contributions and catchment wetness.

Reference	Location	Catchment	Tracers	Sources	Findings
Subagyano et al. (2005)	Central Japan	5.2 ha forested catchment	Ca^{2+} and Si	Near-surface riparian, hillslope soil water and deep riparian GW	Near-surface riparian GW was the largest contributor during events. In contrast, contributions from the deep riparian GW were minimal.
Wenninger et al. (2004)	Blackforest, Germany	4,000 ha forested, glaciated catchment; humid climate	Si, deuterium, and sum of cations	Precipitation and GW	Near-stream GW contributed significantly during events.
McGlynn and McDonnell (2003)	Maimai, South Island, New Zealand	2.6 ha forested catchment; humid climate	Si and ^{18}O	New water, hillslope runoff and riparian GW	While riparian water was important, hillslope runoff contributions increased for large events
Soulsby et al. (2003)	Northeast Scotland, UK	100–23,300 ha catchments; humid climate	Gran alkalinity	GW and acidic overland flow	GW contribution increased with increasing catchment scale
McHale et al. (2002)	Adirondack Mountains, New York, USA	135 ha forested, glaciated catchment; humid climate	Na^+, Ca^{2+}, Mg^{2+}, SO_4^{2-}	Soil water, wetland GW, deeper till GW (springs)	Soil water and till GW were the dominant contributors to streamflow
Hooper (2001)	Panola Mountain, Southeast USA	41 ha forested catchment; humid subtropical climate	Ca^{2+}, Mg^{2+}, Na^+, SO_4^{2-}, Si, alkalinity	Floodplain GW, upper GW, and A horizon soil water	Riparian waters (floodplain and upper GW) were the significant contributors to runoff. A-horizon water changed over an 8-year period
Hangen et al. (2001)	Black Forest, Germany	9.3 ha basin	^{18}O and Si	Direct runoff, soil water and GW	Rapid response from saturation overland flow and near-channel reservoir.
Burns et al. (2001)	Panola Mountain, Southeast USA	10 ha subcatchment with a third occupied by bedrock outcrop	Ca^{2+}, Mg^{2+}, Na^+, Si, Cl^-, SO_4^{2-}	Riparian GW, hillslope runoff and rock outcrop runoff	Outcrop runoff (event water) was high during large events and peak discharge. Riparian GW contributed during baseflow and storm recession.

(continued)

Table 8.1 (continued)

References	Location	Site description	Tracers used	End-members	Additional observations
Brown et al. (1999)	New York State, USA	8–161 ha multiple forested catchments; humid temperate climate	DOC, Cl^-, SO_4^{2-}, and ^{18}O	Throughfall, O horizon soil water, and GW	GW was the dominant contributor but a clear sequencing of end-member contributions was observed. GW contributions increased with catchment size.
Rice and Hornberger (1998)	Mid-Atlantic USA	98 ha forested catchment; humid temperate climate	Deuterium, ^{18}O, Cl^-, Si, Na^+	Throughfall, soil water and GW	Reliability of various tracer combinations was investigated. GW contributions were highest.
Durand and Torres (1996)	Central Brittany, France	500 ha agricultural catchment	NO_3^-, Si, SO_4^{2-}, alkalinity	GW, rainwater, riparian zone water, and hillslope water	Riparian zone water was the largest contributor to storm runoff, while GW was high during baseflow.
Elsenbeer et al. (1994)	Queensland, Australia	25.7 ha rain-forest catchment	ANC and K^+	Saturation overland flow, soil water, and hillslope GW	Overland flow contributions were high during high-intensity event while soil water was the main contributor for low-intensity event.

reservoir, but rather, is composed of multiple, stratified layers with waters of varying ages and/or residence times (Subagyono et al. 2005; Katsuyama et al. 2009). Observations from these studies suggest that it is only the shallow or "newer" portion of riparian water that is preferentially displaced into the stream during storm events. In contrast, the deeper riparian waters are discharged slowly during baseflow. Thus, only a small portion of the riparian or alluvial aquifer may be "mobilized" or "activated" during storm events (Katsuyama et al. 2009). Elevated hydraulic gradients associated with rapid, shallow hillslope interflows and high transmissivity of near-surface riparian soils are some of the possible mechanisms that may be responsible for displacing near-surface riparian waters into the stream (Hangen et al. 2001; Wenninger et al. 2004; Subagyono et al. 2005; Inamdar and Mitchell 2007).

8.3.2 Temporal Pattern of End-Member Contributions and the Influence of Event Size and Antecedent Moisture Conditions

EMMA has provided valuable insights into the temporal patterns of the end-member contributions during and between storm events (Burns et al. 2001; McHale et al. 2002; McGlynn and McDonnell 2003; Inamdar and Mitchell 2007; Verseveld et al. 2008; Morel et al. 2009). For example, in many studies riparian water contributions have been observed to peak at or after discharge and continue through hydrograph recession (Durand and Torres 1996; Inamdar and Mitchell 2007; Morel et al. 2009). Temporal patterns of contributions from other end-members have also been characterized (Burns et al. 2001; Verseveld et al. 2008). This temporal information along with other hydrometric data (e.g., groundwater elevations, soil matric potential) has been especially valuable for developing conceptual models that describe how various parts of the catchment contribute to runoff generation during and between storm events (Hangen et al. 2001; Wenninger et al. 2004; Subagyono et al. 2005; Inamdar and Mitchell 2007; Verseveld et al. 2008).

The application of mixing models for multiple storm events and across contrasting antecedent moisture conditions has also been insightful (Burns et al. 2001; Bernal et al. 2006; Inamdar and Mitchell 2007; Hooper and Rudolph 2009; Morel et al. 2009). These studies imply that not only do the relative amounts of end-member contributions vary with event size and antecedent moisture conditions, but the controlling end-members could also change with events (Katsuyama et al. 2001; Verseveld et al. 2008). However, there is no universal consensus on whether particular events (large or small) favor enhanced contributions from any specific catchment source or end-member. While some studies have reported increased runoff from the riparian zone during large storm events (Inamdar and Mitchell 2007) others have found that large events triggered greater contributions from hillslope or upland sources (Burns et al. 2001; McGlynn and McDonnell 2003). Thus, the amounts of contributions from various end-members appear to be influenced by site-specific catchment conditions.

EMMA mixing diagrams (e.g., Fig. 8.2) have been observed to vary for storm events following wet or dry antecedent moisture conditions. Events following wet antecedent moisture conditions have yielded "clean" or "well-defined" mixing diagrams (Rice and Hornberger 1998; Inamdar and Mitchell 2007) whereas those following the dry antecedent moisture conditions have yielded "poor" mixing patterns (Bernal et al. 2006). This would suggest that the runoff was "well-mixed" and the watershed compartments "primed" to contribute to runoff for wet event conditions, as opposed to events following dry conditions. It is possible that dry catchment conditions or hydrophobic soil conditions encourage poor runoff mixing and a greater opportunity for preferential, "bypass," or "fingered" flow mechanisms (Burch et al. 1989; Dekker and Ritsema 1994). It is also likely that dry conditions may promote nonconservative solute behavior (Borken and Matzner 2008) and thus violate one of the key assumptions for these models.

8.3.3   End-Member Contributions with Catchment Scale

Understanding whether the choice of end-members varies with catchment scale or whether the relative contributions of end-members change with catchment scale is a topic of considerable interest. Surprisingly, however, very few studies have explored this aspect in detail (Soulsby et al. 2003; James and Roulet 2006; Inamdar and Mitchell 2007). The extensive work at Panola Mountain research watershed in Georgia (USA) revealed that end-members identified for runoff at one scale may not necessarily influence runoff at another scale (Burns et al. 2001; Hooper 2001). The bedrock outcrop which occupied one-third of the 10 ha catchment and was an important runoff contributor (Burns et al. 2001) was not seen to influence runoff at the larger 41 ha catchment scale (Hooper 2001). In peatland catchments of Scotland (Soulsby et al. 2003), groundwater contributions were reported to increase with increasing catchment size from 100 to 23,300 ha because of the relative importance of freely draining soils and an increase in the size of alluvial aquifers. In a western New York catchment, the runoff contribution from the riparian zone was highest at the largest 696 ha catchment scale (Inamdar and Mitchell 2007) and was attributed to the larger alluvial/riparian aquifer at this scale.

8.4   Critical Considerations While Using Geochemical Mixing Models

While geochemical mixing models have provided valuable insights into catchment processes, their results need to be interpreted with caution because in most EMMA applications the model assumptions are likely to be violated. Some of the challenges we face in model implementation and how these pitfalls can be avoided are described below.

8.4.1   Choice of Solutes as Tracers

The choice of tracers for implementing EMMA is one of the foremost challenges. EMMA assumes that the tracers behave conservatively and that the mixing is a linear process (Hooper 2001, 2003). Among the many solutes that have been used (see Table 8.1) for EMMA, NO_3^- and SO_4^{2-} are the redox-sensitive species (Bernal et al. 2006; Verseveld et al. 2008; Katsuyama et al. 2009). While these solutes may display conservative behavior for short-duration events (maybe a few hours), it is highly unlikely that this behavior will extend to long duration events (e.g., note change in SO_4^{2-} for a long duration rain event, Inamdar et al. 2009) or for baseflow conditions. Elsewhere, Hooper (2001) and Lovett et al. (2005) have shown that Cl^- may not always behave conservatively and this has led to some researchers excluding Cl^- from their EMMA models (Jung et al. 2009). Similarly, while the use of dissolved organic carbon (DOC) has been fairly popular for its ability to characterize near-surface sources of runoff (Brown et al. 1999; Inamdar and Mitchell 2007; Verseveld et al. 2008; Morel et al 2009), it is also a highly reactive solute (Aitkenhead-Peterson et al. 2003). Furthermore, solutes suitable as tracers at one site may not necessarily be appropriate for other watershed locations. Thus, it is highly recommended that site-specific evaluations of tracers be performed for every EMMA application (e.g., through the use of bivariate plots or residuals, Fig. 8.1). In addition, tracers that display the largest separation in concentrations among potential end-members should be preferred since they will likely provide the best test of the selected model. Solutes that yield small differences in concentrations among end-members cannot provide a reliable assessment of the model. Finally, if multiple solutes are available, it is preferable that model predictions be verified using tracers that have not been used in model development.

8.4.2   Spatial and Temporal Variability in Tracer Concentrations

Numerous studies have indicated that solute concentrations vary spatially across catchments (Katsuyama et al. 2001; Kendall et al. 2001; Rademacher et al. 2005; James and Roulet 2006). This observation directly contradicts the assumption of spatial invariance in EMMA. Variation in geologic strata or bedrock and the differences in contact or residence times of runoff waters may contribute to these spatial differences (James and Roulet 2006). Spatial variation in groundwater solute concentrations is likely the norm rather than the exception for most natural ecosystems (Rademacher et al. 2005). Large variability in SiO_2 and Cl^- tracers in groundwater was reported even for a small (490 m^2) artificial grassland catchment in China (Kendall et al. 2001). Spatial variation in solute concentrations is also likely an important reason why mixing proportions of tracers change with catchment scale (Hooper 2003; James and Roulet 2006; Jung et al. 2009). This shift in mixing proportions has important implications for how we use tracers in EMMA to

assess the relative contributions of end-members with catchment scale. A change in mixing proportions of the solutes is likely to invalidate their use for comparison of end-member contributions across scale and thus should be verified beforehand (following procedures of Hooper 2003; James and Roulet 2006).

Changes in end-member concentrations have also been observed to occur temporally, both over the short- (Durand and Torress 1996; Rice and Hornberger 1998; Inamdar and Mitchell 2007; Verseveld et al. 2008) as well as the long-term (Hooper 2001) and thus violating the time-invariance assumption for EMMA. A multi-year investigation by Hooper (2001, 2003) revealed that SO_4^{2-} and Ca^{2+} concentrations in the A-horizon end-member decreased by 50% from 1988 to 1991. This decrease was also followed by a simultaneous change in stream chemistry values indicating the importance of temporal variability in end-member concentrations for watershed runoff. Such observations especially highlight the value of long-term watershed studies and also that EMMA interpretations for a site may have to be revised periodically over time.

Solute concentrations also vary seasonally (Rice and Hornberger 1998; Rademacher et al. 2005) and this may have important implications if the storm-event end-member contributions are being compared across seasons (e.g., Bernal et al. 2006; Inamdar and Mitchell 2007). One of the ways that investigators have addressed this problem is by using end-member solute concentrations in the immediate temporal vicinity of the storm event (samples collected prior to or after the storm event) (Rice and Hornberger 1998; Burns et al. 2001; Inamdar and Mitchell 2007) and not using the annual or seasonally averaged concentrations. Others have found that end-member contributions may also vary within the time-scale of storm events (Katsuyama et al. 2009). Such rapid changes in end-member concentrations may have serious consequences for EMMA results if they are not accounted for appropriately.

8.4.3 Selection of Potential End-Members

For EMMA, end-members controlling stream chemistry are typically identified by plotting all potential sources in the EMMA space and by identifying the end-members that enclose the stream chemistry completely (Christopherson and Hooper 1992; Burns et al. 2001; Hooper 2001; McHale et al. 2002; Inamdar and Mitchell 2007). In another approach, researchers have made an a priori selection of end-members using a perceptual model of the catchment and then verified the choice through EMMA (Durand and Torres 1996; Morel et al. 2009). In yet another approach, Hooper (2003) proposed that the number of end-members (or rank) could also be identified using stream chemistry data alone. Ideally, all of these approaches should be used in concert to identify the end-members. The methods of Hooper (2003) could be implemented initially to determine the rank of end-members followed by the identity of the end-members from EMMA space and any available perceptual models of the catchment. Greater attention should also be paid

to the directional shift and hysteresis of runoff chemistry in EMMA space. The directional shift and hysteresis of runoff waters can provide important information on the relative influence of end-members on stream chemistry. Lastly, it needs to be emphasized that precise end-member proportions or contributions may not necessarily be that important or even reliable, but the overall trends (relative contributions and the temporal sequencing of end-members) may be more helpful in furthering our understanding of catchment response (Hooper and Rudolph 2009, unpublished manuscript).

For characterizing runoff end-members, all potential sources should preferably be sampled across the full range of hydrologic conditions in the watershed. The work of Katsuyama et al. (2001) highlighted how new end-members (e.g., transient groundwater) were "activated" as the catchment progressively wetted-up during a sequence of three storm events. Watershed monitoring needs to be relatively intensive, and EMMA application sufficiently flexible to accommodate such dynamic changes. The sampling protocol (sampling device and collection procedure) for potential end-members should be described explicitly. Water chemistry can vary significantly with sampling device; for example, soil waters from zero- and tension-lysimeters can differ considerably (Weihermüller et al. 2007). In addition, it is best if potential end-members are measured individually and independently and not derived from stream chemistry (Hooper and Rudolph 2009, unpublished manuscript). Scanlon et al. (2001) found that groundwater discharge can be progressively underestimated if the prestorm baseflow is assumed to be groundwater. Other studies have shown that the chemistry of groundwaters can be considerably different from stream baseflow (Inamdar and Mitchell 2007). This suggests that stream baseflow itself is often a mixture of a unique set of end-members (e.g., deep groundwater from fractured bedrock which is not frequently sampled in many watershed studies).

Another challenge is the use of inconsistent terminology that has been used to characterize potential end-members. This is especially highlighted in Table 8.1 where end-members are described using terms such as deep, shallow, and/or perched groundwaters; organic horizon and forest floor; shallow subsurface and soil water. How do we distinguish between perched, shallow or deep groundwaters; or, shallow subsurface and soil waters? This can be especially confusing when comparisons of EMMA are made across study sites. Clearly, a more precise approach to defining watershed runoff sources is needed which could facilitate EMMA comparisons across sites.

8.4.4   Uncertainty in EMMA Predictions

Uncertainty in EMMA predictions stem from the spatial and temporal variability of tracers, laboratory analytical uncertainty for the solutes, and uncertainty associated with model assumptions or hypotheses (Joerin et al. 2002). Uncertainty evaluations for geochemical mixing models have primarily been performed using two separate approaches: the first-order Taylor series expansion method (Genereux 1998;

Brown et al. 1999; Burns et al. 2001) and the Monte-Carlo approach (Bazemore et al. 1994; Durand and Torress 1996; Rice and Hornberger 1998; Joerin et al. 2002). Except for Joerin et al. (2002) who also addressed model uncertainty (e.g., uncertainty in model assumptions), all other applications have been limited to addressing statistical uncertainty (uncertainty in tracers due to spatial and temporal variation and laboratory analytical errors). While the procedures have differed, all of these analyses clearly show that there can be significant uncertainty in model predictions. The choice of end-members may not necessarily be negated by this uncertainty, but the calculated end-member contributions could differ considerably (Rice and Hornberger 1998). Rice and Hornberger (1998) implemented seven mixing-model combinations for a three-component model using five tracers and found that while hydrograph separations could be performed for most storm events, the results were not always meaningful. Error analysis using Monte Carlo simulations indicated that none of the tracer pairs were immune to serious error in hydrograph separations (Rice and Hornberger 1998). These results underscore the need for some type of uncertainty analyses to be included in all EMMA applications. The Monte-Carlo approach is best suited for uncertainty analyses where the tracer concentrations are used in the mass balance equations (as opposed to the use of EMMA-derived principal components) since the process can be conveniently automated or programmed for multiple simulations. The first-order Taylor series expansion approach is more amenable for the use with PCA.

8.4.5 Verification of EMMA Predictions Using Hydrometric Data

Studies that have provided the most insights into watershed response have been the ones in which mixing model results have been used in conjunction with independent hydrometric data (Elsenbeer et al. 1994; Burns et al. 2001; Hangen et al. 2001; Wenninger et al. 2004; Subagyono et al. 2005; Inamdar and Mitchell 2007; Verseveld et al. 2008; Katsuyama et al. 2009). Burns et al. (2001) used three different hydrometric measurements – rainfall intensity, hillslope trench outflow, and riparian groundwater elevations – to evaluate the contributions from the three selected end-members. While these data had certain limitations, they still corroborated the choice and the relative contributions of the end-members. Similarly, Inamdar and Mitchell (2007) found that the rise and peak in riparian groundwater elevations during storm events matched the temporal expression of riparian water in streamflow and thus validated its choice and contribution as an end-member. Other types of data that have been used include matric potential and soil moisture from various soil depths (Verseveld et al. 2008). Simultaneous use of hydrometric data and EMMA has allowed us to not only verify mixing models, but also develop mechanistic models describing the flowpaths taken by runoff in the catchment (Hangen et al. 2001; Wenninger et al. 2004; Subagyono et al. 2005; Inamdar and

Mitchell 2007; Verseveld et al. 2008). Thus, it is imperative that geochemical mixing models be used in combination with additional hydrometric data.

8.5 Future Challenges and Opportunities

While mixing models have been used for many years now in catchment hydrology, the use of innovative tools like EMMA is still in its infancy. EMMA is not routinely implemented in many catchment studies and there is much to learn about how runoff sources vary across different watershed and climate conditions. Furthermore, with the improvement in sampling technology and the advent of high-frequency, in situ, water-quality sensors (e.g., Saraceno et al. 2009) the types of data that could be available for EMMA are likely to increase dramatically.

One of the most obvious opportunities for geochemical mixing models that have surprisingly not been utilized as often is its use in evaluation and development of numerical watershed models. The work of Hooper (2001) clearly demonstrated how parameters for the MAGIC model could be constrained using EMMA. Knowledge of geographic sources of runoff could also be extremely valuable for testing spatially-distributed models. Furthermore, one would assume that information such as the relative contributions of riparian and hillslope units to runoff and the changes in these contributions with event size would be extremely valuable for developing watershed models. However, again, very few studies have used such information for model development. Clearly, much work still needs to be done.

The large increase in upland and hillslope contributions during large events or antecedent moisture conditions suggests a threshold-driven, nonlinear hydrologic response (McDonnell 2003). However, we know very little about the mechanisms or controls responsible for this type of behavior. Especially interesting would be to investigate if there are any threshold-driven, nonlinear relationships between the physical size and geometry of the riparian and hillslope reservoirs (or other watershed compartments) and the relative fluxes from these units.

The relative sizes of watershed units are likely to change with watershed scale and this may have implications for end-member contributions (Brown et al. 1999; Soulsby et al. 2003). Landscape analysis (e.g., McGlynn and Seibert 2003) is a tool that could be used in conjunction with EMMA to investigate the change in size and geometry of the watershed compartments and the impacts this may have on end-member contributions. Hydrologic connectivity (Jencso et al. 2009) of landscape units could also significantly influence the runoff contributions from various watershed units. Insights into such relationships would be extremely valuable in quantifying watershed response with catchment scale. Such evaluations could also be performed through intercomparison of catchments with similar or dissimilar hydrologic and biogeochemical characteristics.

Buttle (2005) has already highlighted the questions and challenges associated with in-stream processes for IHSs. We believe many of these challenges may be

even more pertinent for GHSs. DOC is one of the important tracers that has been used in GHS and EMMA and which can be influenced by instream processes (Aitkenhead-Peterson et al. 2003). The key issue would be to investigate if the changes in DOC concentrations due to instream processes are significant at the time-scale of events and/or the travel-time in the drainage network. The amount and chemistry of runoff water (storage) in the drainage network (stream) is also often neglected in EMMA models and we need to investigate if this storage has a significant impact, especially, at the larger catchment scales.

As noted above, the use of hydrometric data with EMMA has been extremely beneficial. Other innovative tools such as mean residence time (MRT) analysis can associate the age of water with the spatial sources of runoff. The value of this tool has been highlighted in the recent work by Katsuyama et al. (2009) who showed that not all riparian water is of the same age. MRT procedures can help relate the geographic source components to the time source components in a more precise manner than the isotope-based classification of simply new and old water components. Similar to MRT, advances in analytical technology have opened up potentially new tracers such as spectrofluorometric indices (Hood et al. 2006; McKnight et al. 2001) that can be used to characterize the quality of DOC (e.g., specific ultraviolet absorbance or SUVA). Such tracers can be used in conjunction with DOC concentrations to provide additional insights into the sources of runoff (e.g., Katsuyama and Ohte 2002; Verseveld et al. 2008).

In contrast to the observations from humid, temperate locations, the work of Elsenbeer et al. (1994) in a tropical rain forest environment provided new insights into the significance of overland flow for runoff generation (Bonell 1998). Such studies underscore the need for conducting research in diverse climate and geologic settings and especially in arid and/or tropical climates where a different set of hydrologic processes may be dominant. The need for conducting research in arid or tropical climates is especially pressing considering the large-scale changes in landuse occurring in these geographic regions (e.g., the clear-cutting or burning of Amazonian rainforests for agriculture). The recent application of EMMA by Jung et al. (2009) in an arid setting to understand postfire runoff dynamics underscores the value of EMMA to address such changes. Similarly, future climate change scenarios suggest that storm events are likely to become more intense with longer and drier intervening periods (Knapp et al. 2008; USGCRP 2000). As noted earlier, storm events following dry conditions yielded "poor" mixing diagrams (Rice and Hornberger 1998) and were indicative of nonuniform runoff mixing and resulted in considerable uncertainty in mixing model predictions. Despite the increased uncertainty associated with complex and extreme storm events, understanding runoff sources for these events will be critical to provide meaningful management options to mitigate the impact of climate and land use change.

References

Aitkenhead-Peterson JA, McDowell WH, Neff JC (2003) Sources, production, and regulation of allochthonous dissolved organic matter inputs to surface waters. In: Findlay S, Sinsabaugh R (eds) Aquatic ecosystems: interactivity of dissolved organic matter. Elsevier, New York, pp 25–70

Bazemore DE, Eshleman K, Hollenbeck KJ (1994) The role of soil water in stormflow generation in a forested headwater catchment: synthesis of natural tracer and hydrometric evidence. J Hydrol 162:47–75

Bernal S, Butturini A, Sabater F (2006) Inferring nitrate sources through end member mixing analysis in an intermittent Mediterranean stream. Biogeochemistry 81(3):269–289

Bonell M (1998) Selected challenges in runoff generation research in forests from hillslope to headwater drainage basin scale. J Am Water Resour Assn 34(4):765–785

Borken W, Matzner E (2008) Reappraisal of drying and wetting effects on C and N mineralization and fluxes in soils. Glob Change Biol 14:1–17

Brown VA, McDonnell JJ, Burns DA et al (1999) The role of event water a rapid shallow flow component and catchment size in summer stormflow. J Hydrol 217:171–190

Burch GJ, Moore ID, Burns J (1989) Soil hydrophobic effects on infiltration and catchment runoff. Hydrol Process 3(3):211–222

Burns DA, McDonnell JJ, Hooper RP et al (2001) Quantifying contributions to storm runoff through end-member mixing analysis and hydrologic measurements at the Panola Mountain Research Watershed (Georgia, USA). Hydrol Process 15:1903–1924

Buttle JM (1994) Isotope hydrograph separations and rapid delivery of pre-event water from drainage basins. Prog Phys Geogr 18:16–41

Buttle JM (2005) Isotope hydrograph separation of runoff sources. In: Anderson MG (ed) Encyclopedia of hydrological sciences. New York, Wiley, pp 1763–1744

Christopherson N, Hooper RP (1992) Multivariate analysis of stream water chemical data: the use of principal component analysis for the end-member mixing problem. Water Resour Res 28:99–107

Dekker LW, Ritsema CJ (1994) Fingered flow – the creator of sand columns in dune and beach sands. Earth Surf Proc Land 19:153–164

Dewalle DR, Swistock BR, Sharpe WR (1988) Three component tracer model for stormflow on a small Appalachian forested catchment. J Hydrol 104:301–310

Durand P, Torres JLJ (1996) Solute transfer in agricultural catchments: the interest and limits of mixing models. J Hydrol 181:1–22

Elsenbeer H, West A, Bonell M (1994) Hydrologic pathways and stormflow hydrochemistry at South Creek, northeast Queensland. J Hydrol 162:1–21

Genereux DP (1998) Quantifying uncertainty in tracer-based hydrograph separations. Water Resour Res 34:915–919

Genereux DP, Hooper RP (1998) Oxygen and hydrogen isotopes in rainfall-runoff studies. In: Kendall C, McDonnell JJ (eds) Isotope tracers in catchment hydrology. Elsevier, Amsterdam, pp 319–346

Hangen E, Lindenlaub M, Leibundgut C et al (2001) Investigating mechanisms of stormflow generation by natural tracers and hydrometric data: a small catchment study in the Black Forest, Germany. Hydrol Process 15:183–199

Hood E, Gooseff MN, Johnson SL (2006) Changes in the character of stream water dissolved organic carbon during flushing in three small watersheds, Oregon. J Geophys Res 111:G01007

Hooper RP (2001) Applying the scientific method to small catchment studies: a review of the Panola Mountain experience. Hydrol Process 15(10):2039–2050

Hooper RP (2003) Diagnostic tools for mixing models of stream water chemistry. Water Resour Res 39(3):1055

Hooper RP, Rudolph B (2009) Interpreting hysteresis in concentration-discharge models using mixing approach. Unpublished manuscript

Hooper RP, Christopherson N, Peters J (1990) End-member mixing analysis (EMMA): an analytical framework for the interpretation of streamwater chemistry. J Hydrol 116:321–345

Horton RE (1933) The role of infiltration in the hydrologic cycle. Trans Am Geophys Union 14:446–460

Inamdar SP, Mitchell MJ (2007) Contributions of riparian and hillslope waters to storm runoff across multiple catchments and storm events in a glaciated forested watershed. J Hydrol 341:116–130

Inamdar SP, Rupp J, Mitchell MJ (2009) Groundwater flushing of solutes at wetland and hillslope positions during storm events in a small glaciated catchment in western New York, USA. Hydrol Process 23:1912–1926

James AL, Roulet NT (2006) Investigating the applicability of end-member mixing analysis (EMMA) across scales: a study of small, nested catchments in a temperature forested watershed. Water Resour Res 42:W08434

Jencso KG, McGlynn BL, Gooseff MN et al (2009) Hydrologic connectivity between landscapes and streams: transferring reach- and plot-scale understanding to the catchment scale. Water Resour Res 45:W04428

Joerin C, Beven KJ, Iorgulescu I et al (2002) Uncertainty in hydrograph separations based on geochemical mixing models. J Hydrol 255:90–106

Jung HY, Hogue TS, Rademacher LK et al (2009) Impact of wildfire on source water contributions in Devil Creek, CA: evidence from end-member mixing analysis. Hydrol Process 23:183–200

Katsuyama M, Ohte N, Kobashi S (2001) A three-component end-member analysis of streamwater hydrochemistry in a small Japanese forested headwater catchment. Hydrol Process 15:249–260

Katsuyama M, Ohte N (2002) Determining the sources of stormflow from the fluorescence properties of dissolved organic carbon in a forested headwater catchment. J Hydrol 268:192–202, doi:10.1016/S0022-1694(02)00175-0

Katsuyama M, Kabeya N, Ohte N (2009) Elucidation of the relationship between geographic and time sources of stream water using a tracer approach in a headwater catchment. Water Resour Res 45:W06414

Kendall C, McDonnell JJ, Gu W (2001) A look inside "black box" hydrograph separation models a study at the Hydrohill catchment. Hydrol Process 15:1877–1902

Kennedy VC, Kendall C, Zellweger GW et al (1986) Determination of components of stormflow using water chemistry and environmental isotopes, Mattole river basin, California. J Hydrol 84:107–140

Knapp AK et al (2008) Consequences for more extreme precipitation regimes for terrestrial ecosystems. Bioscience 58(9):811–821

Lovett GM, Likens GE, Buso DC et al (2005) The biogeochemistry of chlorine at Hubbard Brook, New Hampshire, USA. Biogeochemistry 72:191–232

McDonnell JJ (2003) Where does water go when it rains? Moving beyond variable source area concept of rainfall-runoff response. Hydrol Process 17:1869–1875

McGlynn BL, McDonnell JJ (2003) Quantifying the relative contributions of riparian and hillslope zones to catchment runoff. Water Resour Res 39(11):1310

McGlynn BL, Seibert J (2003) Distributed assessment of contributing area and riparian buffering along stream networks. Water Resour Res 39(4):1082

McHale MR, McDonnell JJ, Mitchell MJ et al (2002) A field-based study of soil water and groundwater nitrate release in an Adirondack forested watershed. Water Resour Res 38(4):1–17

McKnight DM, Boyer EW, Westerhoff PK et al (2001) Spectrofluorometric characterization of dissolved organic matter for indication of precursor organic material and aromaticity. Limnol Oceanogr 46(1):38–48

Morel B, Durand P, Jaffrezic A et al (2009) Sources of dissolved organic carbon during stormflow in a headwater agricultural catchment. Hydrol Process 23:2888–2901

Pinder GF, Jones JF (1969) Determination of the ground-water component of peak discharge from the chemistry of total runoff. Water Resour Res 5:438–445

Rademacher LK, Clark JF, Clow DW et al (2005) Old groundwater influence on stream hydrochemistry and catchment response times in a small Sierra Nevada catchment: Sagehen Creek, California. Water Resour Res 41:W02004

Rice KC, Hornberger GM (1998) Comparison of hydrochemical tracers to estimate source contributions to peak flow in a small, forested headwater catchment. Water Resour Res 34:1755–1766

Robson A, Beven KJ, Neal C (1992) Towards identifying sources of subsurface flow: a comparison of components identified by a physically based runoff model and those determined by chemical mixing techniques. Hydrol Process 6:199–214

Saraceno JF, Pellerin BA, Downing BD et al (2009) High frequency in situ optical measurements during a storm event: assessing relationships between dissolved organic matter, sediment concentrations and hydrologic processes. J Geophys Res 114:G00F09

Scanlon TM, Raffensperger JP, Hornberger GM (2001) Modeling the transport of dissolved silica in a forested headwater catchment: Implications for defining the hydrochemical responses of observed flow pathways. Water Resour Res 37(4):1071–1082

Sklash MG, Farvolden RN (1979) The role of groundwater in storm runoff. J Hydrol 43:45–65

Sklash MG, Farvolden RN, Fritz P (1976) A conceptual model of watershed response to rainfall developed through the use of oxygen-18 as a natural tracer. Can J Earth Sci 13:271–283

Soulsby C, Rodgers P, Smart R et al (2003) A tracer-based assessment of hydrological pathways at different spatial scales in a mesoscale Scottish catchment. Hydrol Process 17:759–777

Subagyono K, Tanaka T, Hamada Y et al (2005) Defining hydrochemical evolution of streamflow through flowpath dynamics in Kawakami headwater catchment, Central Japan. Hydrol Process 19(10):1939–1965

USGCRP (United States Global Change Research Program) (2000) Climate change impacts on the United States: the potential consequences of climate variability and change. US Global Change Research Program, Washington. http://www.usgcrp.gov/usgcrp/Library/nationalassessment/overview.htm. Accessed May 2010

Verseveld WJ, McDonnell JJ, Lajtha K (2008) A mechanistic assessment of nutrient flushing at the catchment scale. J Hydrol 358:268–287

Weihermüller L, Sieimens J, Deurer M et al (2007) In situ soil water extraction: a review. J Environ Qual 36:1735–1748

Wenninger J, Uhlenbrook S, Tilch N et al (2004) Experimental evidence of fast groundwater responses in a hillslope/floodplain area in the Black Forest Mountains, Germany. Hydrol Process 18:3305–3322

Part III
Forest Hydrology and Biogeochemistry by Ecoregion and Forest Type

Chapter 9
Hydrology and Biogeochemistry of Terra Firme Lowland Tropical Forests

Alex V. Krusche, Maria Victoria R. Ballester, and Nei Kavaguichi Leite

9.1 Tropical Climatology

Tropical climates are characterized by high temperatures that do not fall below 18°C in the coolest month, according to the Köppen-Geiger climate classification system (Peel et al. 2007). This temperature regime strongly influences hydrology both at the global and local ($10–10^2$ km^2) scales. Globally, irradiance from the sun affects the circulation of air masses and contributes to the formation of the Hadley cells and the associated convergence of trade winds from the intertropical convergence zone (ITCZ) (McGregor and Nieuwolt 1998). The uplift of hot and humid air at the ITCZ results in intense precipitation that, together with high temperatures, characterizes tropical regions. For example, in humid tropical Western Nigeria with convective thunderstorm-type precipitation, rain intensities vary approximately between 13 and 240 mm h^{-1}, whereas in temperate Washington, DC, with predominantly frontal precipitation, intensities typically vary from 0.8 to 51 mm h^{-1} (Jackson 1989).

Regionally, the warming of wet surfaces and evapotranspiration in the tropics produce convective rains that are highly variable both in space and time. In the Amazon, basin wide estimates of evapotranspiration range from 30 to 80% of total precipitation (Marengo and Nobre 2001 and citations therein). As a result of the combination of these processes with other abiotic (e.g., bedrock and soil types, relief) and biotic (e.g., canopy structure, plant species diversity) drivers, tropical forests constitute perhaps the biome with highest biogeochemical heterogeneity on Earth (*sensu* Townsend et al. 2008). Within the Köppen-Geiger classification system, tropical climate is subdivided into rainforest, monsoon and savanna, based on differences in the annual distribution of monthly averaged precipitation depth. Altitude also affects the characteristics of tropical forests, giving rise, in many cases, to montane cloud forests (Hamilton et al. 1995). Each one of these tropical forest types and subdivisions could be the subject of several books and are beyond the scope of this chapter, which deals mostly with examples from Amazonian terra firme lowland tropical forests. For a comprehensive introduction to tropical climate see, for example, McGregor and Nieuwolt (1998).

The amount, frequency, duration and intensity of rainfall at any scale depends greatly on various physical forces acting on the Earth, including gravity, atmospheric pressure, net radiation, atmospheric and oceanic circulation patterns as well as Coriolis, friction and centripetal forces. However, a recent hypothesis proposes that large areas of contiguous forests could control the amount of precipitation in terrestrial ecosystems by acting as "pumps" of moisture (Makarieva and Gorshkov 2007; Sheil and Murdiyarso 2009). Data from the Amazon are used by the authors to corroborate such hypothesis, but several other studies demonstrate strong seasonal and inter annual variations that relate to regional and global climatic conditions (Figueroa and Nobre 1990; Marengo 1992; Marengo and Nobre 2001). Although likely to play some role on large-scale atmospheric water flows, the relative importance of forests compared to physical forcing is still to be demonstrated.

According to Marengo and Nobre (2001) seasonality of precipitation in the Amazon is mainly controlled by solar activity affecting large-scale upper air circulation and, at least indirectly, ocean surface conditions. Together with these large-scale processes, local and regional mechanisms affect rainfall patterns contributing to the observed high variability in precipitation, with different degrees of importance depending on which part of the Amazon they act upon. These mechanisms include diurnal convection (Garreaud and Wallace 1997) in central Amazonia, deep-convection related to the ITCZ (Marengo and Nobre 2001) in the north, formation of squall lines from the mouth of the Amazon river (Cohen et al. 1995) and entrance of frontal systems from the south (Marengo and Nobre 2001).

Figure 9.1 shows the annual distribution of precipitation over the Amazon lowlands. Despite displaying different seasonal patterns, the variation in rainfall patterns over the course of a year is the product of interactions of even more heterogeneous processes occurring at smaller scales. For example, the annual distribution of precipitation in the Ji-Paraná river basin, in southwest Amazon (Fig. 9.2), which covers an area of 75,000 km^2, clearly illustrates how variable the distribution of rain is, especially during the rainy season (December–March), when temperatures are higher and convective rains are more common (Victoria 2004). Even at smaller scales within this basin, data from a single rain gauge in a first-order catchment (Rancho Grande, Rondonia, Table 9.1) demonstrate that precipitation during the rainiest months is not evenly distributed as could be deduced from the analysis of monthly averaged data for the entire basin (Bonilla 2005; Germer et al. 2006, 2007). Hence, spatio-temporal heterogeneous rainfall distribution over tropical rainforests is a major driver of hydrology and biogeochemistry in these systems.

9.2 Hydrology of Terra Firme Lowland Tropical Forests

9.2.1 Precipitation Partitioning

The quantity and quality of water within tropical forests is dependent on the partitioning of rain by the canopy as well as the flowpaths taken by water reaching the forest floor. Interception of rain by the canopy, although a rather complex
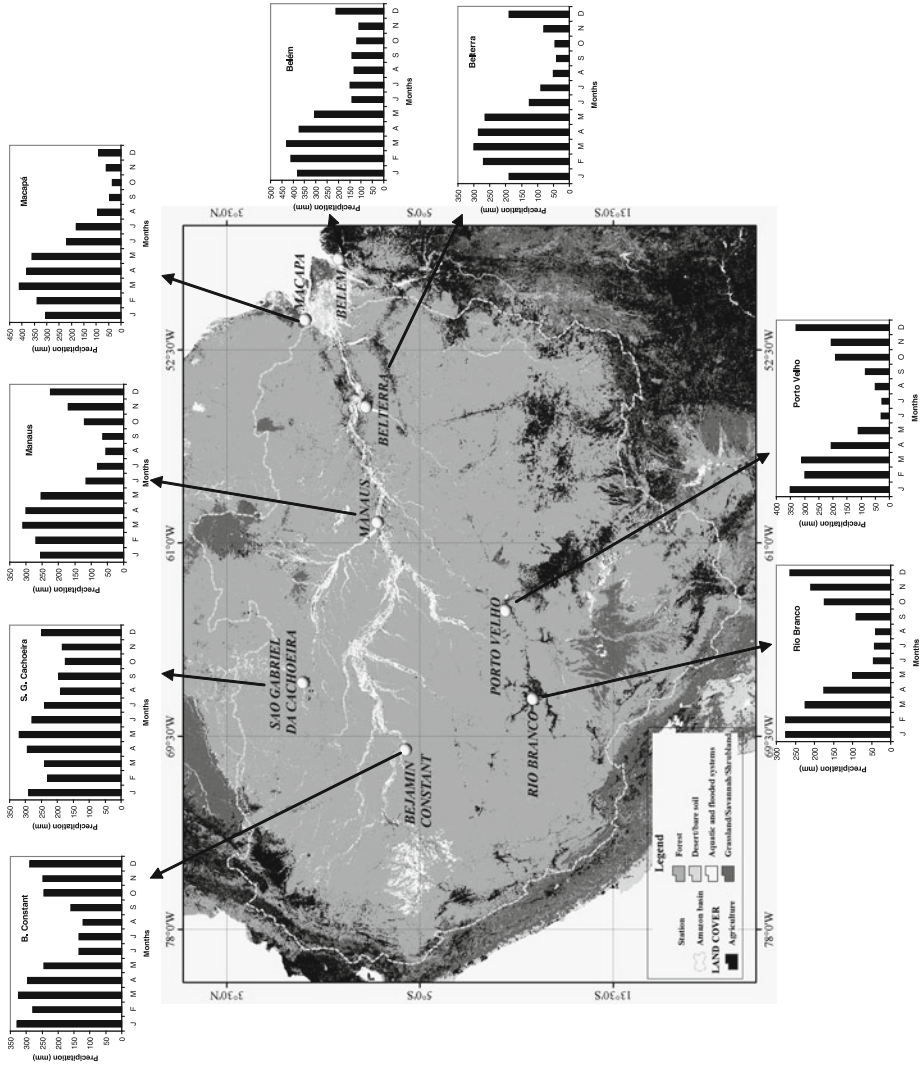
Fig. 9.1 Distribution of rainfall in sites located over the central lowland Amazon (data source: Agencia Nacional de Águas, Brazil)
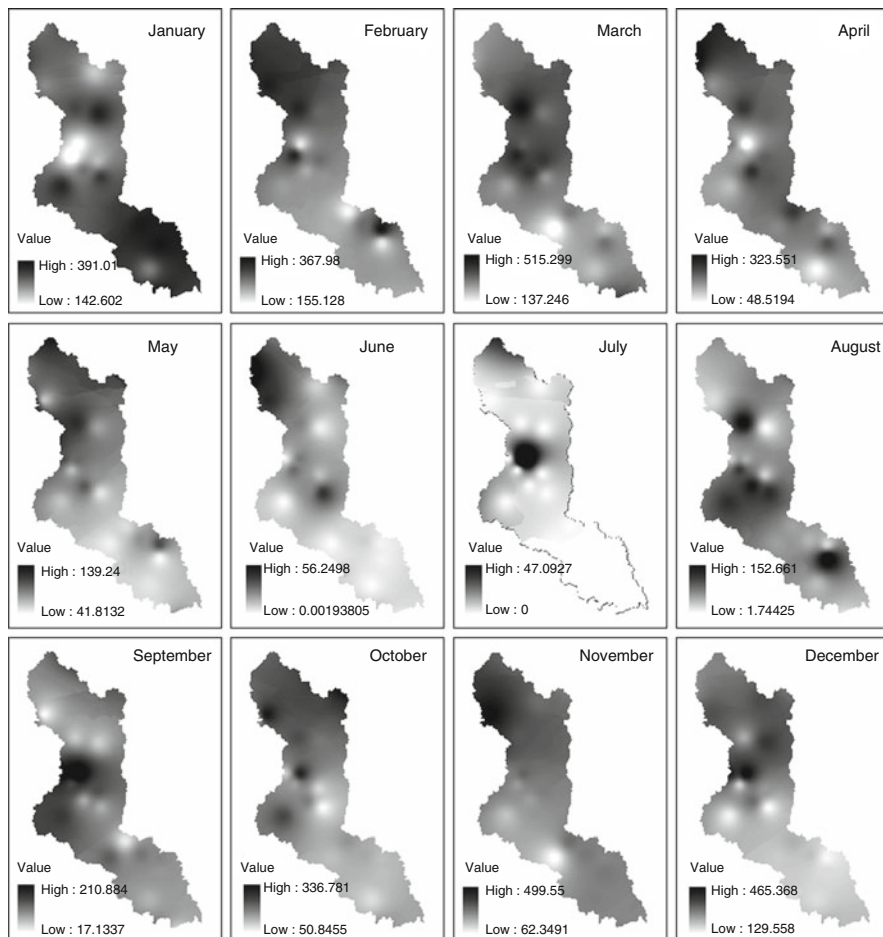
Fig. 9.2 Interpolated maps of monthly average precipitation (mm) in the Ji-Paraná river basin, Rondonia, Brazil (from Victoria 2004, reproduced with permission)

Table 9.1 Volume, duration and intensity of rain during several events at Rancho Grande site, Rondonia, Brazil[a]

Date	Total precipitation (mm)	Duration (min)	Intensity (mm h^{-1})
01/24/2004	22.4	230	5.8
01/27/2004	13.2	20	40
01/31/2004	7.9	30	15.8
02/04/2004	16.8	130	7.7
02/15/2004	9.1	30	18.3
02/17/2004	35.3	285	7.4
02/19/2004	79.5	230	20.7
02/25/2004	47.0	50	56.4
02/27/2004	8.6	35	14.8

[a]Data source: Bonilla (2005)

process (interception models, for example, can require information on up to 39 variables, Muzylo et al. 2009), can be simply described as the difference between gross rainfall and the sum of throughfall and stemflow. Table 9.2 shows a comparison of studies in which all these variables were measured or estimated in tropical forests of the Amazon.

Of gross precipitation, most rain enters the forest as throughfall, with values ranging from 77 to 91% (average = 83 ± 5%). Stemflow accounts for 1.7% (±2.2%) and interception, calculated as the difference between gross rainfall and

Table 9.2 Bulk precipitation and its partition into throughfall, stemflow and canopy interception in several lowland tropical forests

Study site	Gross precipitation (mm)	Throughfall (%)	Stemflow (%)	Interception (%)	Source
Riparian Forest, Rondonia	2069.5	84.0	5.0	11.0	Leite, personal communication
Caxiuanã National Forest, Para	1153.4	76.8	1.7	21.5	Oliveira et al. (2008)
Cuieiras Reserve, Amazonas	3064.2	82.9	0.6	16.5	Cuartas et al. (2007)
Rancho Grande, Rondônia	2286.0	89.9	7.8	2.4	Germer et al. (2006)
ZF2 Reserve, Amazonas	2913.0	80.8	[a]	19.2	Ferreira et al. (2005)
Anavilhanas, Amazonas	2083.0	78.5	[a]	21.0	Filoso et al. (1999)
ZF2 Reserve, Amazonas	3100.0	92.0	2.0	6.0	Cornu et al. (1998)
Rio Doce Biological Reserve, Para	1649.9	86.2	0.8	12.9	Ubarana (1996)
Jaru Biological Reserve, Rondonia	3563.8	87.0	1.4	11.6	Ubarana (1996)
La Cuenca, Peru	2987.0	83.1	[a]	16.9	Elsenbeer et al. (1994)
Ducke Reserve, Amazonas	2721.0	91.1	1.8	7.1	Lloyd and Marques (1988)
Bacia Modelo, ZF2, Amazonas	1705.0	78.4	0.3	21.2	Leopoldo et al. (1987)
Ducke Reserve, Amazonas	2076.0	80.7	0.3	19.0	Leopoldo et al. (1987)
Bacia Modelo, ZF2, Amazonas	2570.4	80.2	[a]	19.8	Franken et al. (1992)
Ducke Reserve, Amazonas	1388.7	76.8	0.3	22.9	Franken et al. (1992)
Middle Caqueta, Colombia	3400.0	85.0	1.0	14.0	Tobón Marin et al. (2000)

[a] Not estimated

throughfall plus stemflow represents, on average, 15.6% ($\pm$6.5). It is worth noting that the largest variations occur in the estimates of stemflow and interception. Although part of this variation could be attributed to methodological bias involved in measuring stemflow (Levia and Frost 2003), it is also reflected in the heterogeneous nature of tropical forest composition. In general, the distribution of throughfall is directly related to the amount of and characteristics of the precipitation input, and, to some degree, forest structure. Stemflow has been found to follow a power relation with precipitation depth (Lloyd and Marques 1988; Tobón Marin et al. 2000; Oliveira et al. 2008).

Of the canopy partitioning of rainfall studies available from the Amazon, Germer et al. (2006) reported that the largest stemflow contribution to the forest floor was 7.8% of gross precipitation and the smallest interception loss was 2.4% of gross precipitation. Their results can be explained by the more open canopy of the study site (compared to the typical "terra firme" forests at ZF2 and Reserva Ducke) combined with a high density of babaçu palms (*Orbignya phalerata*). The morphology of these palms favor funneling of incident rain into the stems and drip points, creating localized and unevenly distributed inputs of water to the forest floor. Germer et al. (2006) conclude that, given the widespread occurrence of babaçu palms in Amazonian forests, their role on rainfall distribution should be given greater consideration in hydrologic studies in the region.

Overall, for the whole Amazon, observational data show that annually about half of gross precipitation (5.8 mm day^{-1}) flows out of the basin as river runoff (2.9 mm day^{-1}), but a much higher fraction than that measured as interception (potential evaporation) at catchment scale studies returns to the atmosphere as evapotranspiration (4.3 mm day^{-1}). At the same time, a substantial amount of water (1.4 mm day^{-1}) moves horizontally within the basin as integrated moisture convergence (Marengo 2006).

9.2.2 Transpiration

Annual transpiration from an Amazonian tropical forest was reported to be 1,030 mm (Shuttleworth 1988). Because soil water deficits are generally unproblematic in the Amazon, a weak relationship was observed between soil moisture deficit and transpiration (Shuttleworth 1988). Daily transpiration rates of tropical trees in the Amazon were similar to that of conifers and deciduous trees in temperate zones at approximately 3.6 mm day^{-1} (Roberts 2000). Similar to their temperate counterparts, tropical trees in the Amazon exhibited strong physiological control over the transpiration stream (Roberts 2000). Depicting the daily stomatal conductance curve (mm s^{-1}) from Shuttleworth (1988) at Reserva Ducke in Manaus, Roberts (2000) showed that stomatal conductance at 06:00 local time was approximately 8 mm s^{-1}, increasing to a daily maximum of around 12 mm s^{-1} between 1100 and 1200 local time, and then dropping to 2 mm s^{-1} at 18:00. These stomatal conductance values differed from those in Thetford Forest in the United Kingdom that began around 11 mm s^{-1} at 06:00 local time and then continually decreased to around 4 mm s^{-1} at 18:00 local time (Roberts 2000).

It is also worth noting that the middle and upper portions of tropical rainforest canopies account for a disproportionately large share of the total transpiration despite a lower proportion of the total leaf area (Roberts 2000). This is likely attributable to increased light levels in the upper canopy that leads to higher rates of stomatal conductance and the more favorable anatomy of upper canopy leaves to conduct photosynthesis compared to shaded lower leaves (Horn 1971). Specifically, leaves at the top of the canopy will have higher densities of chloroplasts and thicker layers of palisade mesophyll than shaded leaves lower in the canopy.

9.2.3 Lateral Flow and Return Flow

The rain that finally reaches the forest floor will flow along several pathways depending on the characteristics of precipitation, forest structure, the terrain, and the soils present. Elsenbeer (2001) proposed a general conceptual framework for the study of hillslope hydrology in the tropics based on changes of soil hydraulic conductivity with depth (or, anisotropy), which seems to fit most of the studies described in the literature (Elsenbeer 2001 and references therein; Bruijnzeel 2004; Tomasella et al. 2009). In general, since hydraulic conductivity decreases slowly with depth in oxisols common within the central Amazon, the results of Nortcliff and Thornes (1989) served as the basis for the generalization that in tropical soils overland flow is insignificant (Elsenbeer 2001). More recent hillslope studies have demonstrated that lateral flow and return flow are also common in the tropics and should be more carefully evaluated (Elsenbeer and Lack 1996; Moraes et al. 2006; Tomasella et al. 2009; Chaves et al. 2009).

Due to shallow soils and a plinthite layer that impedes both vertical and lateral flow, some terra firme lowland tropical forests have relatively high soil water content levels, especially during the wet season. In a terra firme lowland tropical rainforest first-order 0.33 ha catchment with a slope of 0.09, saturated hydraulic conductivity (K_{sat}) was observed to change with soil depth (Moraes et al. 2006). Specifically, median K_{sat} values were approximately 500 mm h^{-1} at a depth of 0.05–0.15 m, decreasing to 30 mm h^{-1} at a depth of 0.2–0.3 m, decreasing further to approximately 8 mm h^{-1} at a depth of 0.4–0.5 m, and then reaching a median minimum of 1 mm h^{-1} at a depth of 0.8–0.9 m (Moraes et al. 2006). The very low K_{sat} values at the plinthite layer would impede vertical and lateral flow and trigger saturated overland flow during discrete rain events and the wet season. In point of fact, Moraes et al. (2006) noted that saturated overland flow occurred with regularity at their experimental research site during the wet season, whereas subsurface shallow flow was relatively minor. Overland flow occurred approximately 60% of days during the wet season with streamflow representing 3.2% of the throughfall input on average (Moraes et al. 2006). They observed that all of the overland flow initiated in saturated areas of the catchment.

9.3 Biogeochemistry of Terra Firme Lowland Tropical Forests

9.3.1 Carbon

Tropical forests contain the largest stock of carbon in terrestrial biomes (340 of a total of 652 Pg C) and are estimated to have a net primary production (NPP) of 20.2 Pg C year^{-1} (Saugier et al. 2001; Sabine et al. 2004). However, at least for the Amazon basin, there is still much controversy on the real role of tropical forests in the global carbon cycle. Estimates of net ecosystem exchange (NEE) for the entire Amazon basin vary from -3 to 0.75 Pg C year^{-1} (Ometto et al. 2005). Despite this uncertainty, considering the fact that on a global scale the difference between fluxes of C in terrestrial NPP and respiration and fires are only on the order of 2.5 Pg C year^{-1} (Sabine et al. 2004), any exact value within this range has potential global influence. For instance, the largest forested biome on Earth, tropical savannas and grasslands, with almost twice the area (27.6 vs. 17.5×10^6 km^2) have an NPP of almost half of that of tropical forests (13.7 Pg C year^{-1}) and a total stock of only 79 Pg C (Saugier et al. 2001; Sabine et al. 2004).

Tropical forests estimated from satellite images look as a continuum of evergreen trees. However, the Amazon landscape is instead dissected by a dense network of small streams (Mayorga et al. 2005a) that forms the largest river in the world. As integral parts of the basin, streams and rivers are usually supersatured in CO_2 in relation to the atmosphere, releasing large amounts of C into the atmospheric reservoir after degassing (Richey et al. 2002). The exact sources of carbon and mechanisms that control these concentrations and fluxes are still poorly understood (Richey et al. 2002; Mayorga et al. 2005b). One known mechanism is the transfer of CO_2-rich soil and groundwater to streams at the smaller orders (Johnson et al. 2006). However, since degassing at these scales occurs within a few meters of the river channel, for larger rivers other CO_2 sources are also likely to play important roles.

In order to obtain more insights into the biogeochemistry of carbon in these tropical forests, several catchment scale studies have been conducted recently, with distinct levels of detailed measurements, ranging from only rain and runoff to throughfall, stemflow, soil water, soil respiration, and evasive fluxes. The more detailed of these studies (Neu 2009) illustrated the fluxes along flowpaths of the major forms of C inside the forest (Table 9.3). Precipitation contained twice as much carbon in its dissolved organic form (DOC) than in its inorganic form (DIC) (82 vs. 38.8 kg C ha^{-1} year^{-1}). While DOC increased in throughfall solution (142.6 kg C ha^{-1} year^{-1}), DIC decreased substantially (18.1 kg C ha^{-1} year^{-1}), and the subsequent flowpaths transported significantly lower amounts of carbon within the forest. Stemflow accounted for 1.5 and 0.1 kg C ha^{-1} year^{-1}, overland flow for 4.5 and 0.5 kg C ha^{-1} year^{-1} and stream export for 1.6 and 0.9 kg C ha^{-1} year^{-1} in the forms of DIC and DOC, respectively. The stream also exported 0.01 kg C ha^{-1} year^{-1} in particulate forms, 48.3 kg C ha^{-1} year^{-1} as evasive fluxes of CO_2 and 7.93 kg C ha^{-1} year^{-1} as CH_4. Soil respiration was the most striking

Table 9.3 Fluxes of dissolved organic and inorganic carbon, CO_2, and CH_4 (kg C ha^{-1} year^{-1}) in a forest in southeastern Amazon[a]

Pathway	Dissolved organic carbon	Dissolved inorganic carbon	CO_2	CH_4
Precipitation	82.3	38.8		
Throughfall	142.6	18.1		
Stemflow	1.5	0.1		
Overland flow	4.5	0.5		
Stream runoff	1.6	0.9		
Stream degassing			4.8	0.7
Soil respiration			6,548	−4.4

[a]Data source: Neu (2009)

pathway of carbon transferred in this forest with an outflux in the form of CO_2 of 6,548 kg C ha^{-1} year^{-1}, although sequestering CH_4 at a rate of 4.37 kg C ha^{-1} year^{-1}. The sum of input-fluxes of the different carbon forms cannot account for these respiration rates, implying that, at least at this study site, forests absorb large quantities of atmospheric CO_2. In fact, although not estimated at this site, in a similar forest of around the same latitude in the state of Rondonia, Grace et al. (1995) found a net carbon gain in the forest of approximately 1 ton C ha^{-1} year^{-1}.

The study by Neu (2009) is perhaps the most detailed for the Amazon, but the study site was located within an area of transition between typical tropical rainforests and the more sparse and open canopy forests of the Brazilian Cerrado. This forest is characterized by a strong hydrological seasonality, with at least 3 months of the year with little or no rain (22 mm accumulated precipitation from May to August during the experiment). In another strongly seasonally affected forest, Markewitz et al. (2004) found an input of 123 kg C ha^{-1} year^{-1} by gross precipitation and an ecosystem export via stream water amounting to 4 kg C ha^{-1} year^{-1}, whereas Gouveia Neto (2006) computed corresponding annual fluxes of DOC of 162.3 kg C ha^{-1} year^{-1} entering the forest ecosystem and an export of 4.4 kg C ha^{-1} year^{-1}. However, in the central part of the basin, where monthly precipitation is greater than 100 mm for most of the year (except for 1 or 2 months), contrasting results were obtained by Waterloo et al. (2006), which exhibited a net export of DOC in a black water stream catchment exceeding the DOC input by bulk deposition. One possible explanation for this discrepancy is the fact that Waterloo et al. (2006) regarded only DOC fluxes with bulk precipitation as C input, while most other studies account for the enrichment in organic carbon as rain passes through the canopy entering the ground as throughfall (Table 9.4). Unfortunately, we know of no other studies similar to that of Neu (2009), in which all forms and pathways of carbon within the forest are considered.

Despite the efforts to understand the biogeochemistry of carbon in tropical forests using biometric assessments (Houghton et al. 2001; Baker et al. 2004; Malhi et al. 2004), eddy covariance estimates of NEE (Grace et al. 1995; Malhi et al. 1998; Araujo et al. 2002; Saleska et al. 2003), input–output studies (Neu 2009) and the analysis of flowpaths (Markewitz et al. 2004; Gouveia Neto 2006), more comprehensive long-term studies in which all these components are measured

Table 9.4 Fluxes of carbon in precipitation and throughfall in several sites in the Amazon

Location	Precipitation C flux (kg ha^{-1} year^{-1})	Throughfall C flux (kg ha^{-1} year^{-1})	References
North Amazon	123.4	149	Markewitz et al. (2004)
Northeast Amazon	133.9	83.1	Tobón Marin et al. (2004)
Central Amazon	27.5	190	Filoso et al. (1999)
Central Amazon	48	159	Williams et al. (1997)
Southwest Amazon	162.3	332.9	Gouveia Neto (2006)
Southeast Amazon	82.3	142.6	Neu (2009)

simultaneously should be coordinated at key experimental sites (for instance, where previous information and infrastructure already exists, such as the ZF2 site near Manaus, Amazonas).

9.3.2 Nitrogen

The cycle of nitrogen in tropical forests is considered to be less conservative than in temperate forests, that is, exporting proportionally more N to adjacent systems (Vitousek and Sanford 1986). Davidson et al. (2004) showed that much more biomass is produced per unit N at the Hubbard Brook forest than at the Paragominas forest in the state of Pará, Brazil, and that the opposite is held true for P. Other results provide evidence for high rates of NO_2 and NO emissions from soils (Verchot et al. 1999; Davidson et al. 2001; Melillo et al. 2001), the predominance of nitrate over ammonium in KCl-extractable soils (Neill et al. 1995; Verchot et al. 1999; Luizão et al. 2004) and higher dissolved inorganic to organic nitrogen ratios in soil solutions (Neill et al. 2001, 2006; Markewitz et al. 2004; Tomasella et al. 2009). However, whole catchment budgets and flowpath analysis of nitrogen cycling are strikingly scarce for tropical forests and if they exist, they do not take all of the required forms and fluxes of nutrients into account.

Lesack and Melack (1996) found modest net gains of N, based on the measurements of N fluxes in soil solution without considering gaseous fluxes from soils, whereas Bonilla (2005) showed high export rates based on the same type of data. The most detailed analysis of N cycling in the Amazon was conducted in the Paragominas forest where Markewitz et al. (2004) found inputs of 4 kg N ha^{-1} year^{-1} with bulk precipitation, increasing to 9.5 kg N ha^{-1} year^{-1} in throughfall solution and 12 kg N ha^{-1} year^{-1} in soil solution. These high concentrations of N in soil solution are consistent with the estimates of gaseous fluxes in the order of 2.9 kg N ha^{-1} year^{-1} (Verchot 1999), which after the addition of a stream export

of 0.9 kg N ha^{-1} year^{-1} indicates net gains of N at this site. Germer et al. (2009) also found a clear sink of N at a catchment study in Rondonia, however, only regarding input–outputs of inorganic N.

9.3.3 Phosphorus

Although considered to be the main limiting factor to plant growth in tropical forests (Vitousek 1984), phosphorus dynamics in Amazonian forests have received little attention thus far. Concentrations of soluble available P are always very low in soil solutions (Lesack and Melack 1996; Markewitz et al. 2004; Neill et al. 2006) and in streams draining forests (Lesack and Melack 1996; Markewitz et al. 2004; Neill et al. 2006; Tomasella et al. 2009). Without gaseous forms, atmospheric P input is also low and believed to originate in part from long distance transport of dust from western Africa (Koren et al. 2006) or from apatite containing bedrock weathering.

Two recent studies, based on budgets of annual inputs and outputs of P, showed a tendency of P accumulation (Lesack and Melack 1996; Markewitz et al. 2004). For the sake of comparison with N fluxes, at the Paragominas forests Markewitz et al. (2004) found inputs of P with bulk precipitation of 0.03 kg P ha^{-1} year^{-1} and a stream export of less than 0.01 kg P ha^{-1} year^{-1}, while for N a net gain of 0.5% of the inputs was observed. Other budgets within central Amazon have shown similar results (Brinkmann 1983, 1985).

9.3.4 The Role of Adventitious and Apogeotropic Roots on Internal Nutrient Cycling

Floristic diversity is at its greatest in tropical forests. Aboveground root systems, including adventitious and apogeotropic roots, have been found on certain lowland tropical forest tree species (Sanford 1987; De Simone et al. 2002). Apogeotropic roots have a detectable effect on the cycling of calcium in tropical forests (Sanford 1987). Because these aboveground root systems acquire extra nutrients beyond those acquired by subterranean roots, both adventitious and apogeotropic roots are believed to be ecological adaptations by tropical forest trees to combat inherently nutrient-poor tropical soils (Sanford 1987). Sanford (1987) hypothesized that stem-flow leachates spawn the growth of apogeotropic roots. Adventitious roots also have been documented to have a significant influence in an Australian montane tropical forest by altering stemflow nutrient inputs to the forest soil (Herwitz 1991). Further work on apogeotropism in the lowland rainforest would yield further insights into the physiological ecology and biogeochemistry of these diverse forests.

9.4   Suggestions for Future Work

Although a vast literature on tropical forests exists, it is striking how limited the information is on the biogeochemistry of Amazonian lowland rainforests. There is only one experimental site where all compartments and fluxes of nutrients have been measured to enable precise forest budgets (Markewitz et al. 2004). Even this single study cannot be used for generalization purposes since it is representative of a region with strong seasonality in which dry periods favor the development of deep root structures in the forests. Nowhere in the central lowland of Amazonia, where a dry season is lacking, have multi-year studies of C, N and P forms and fluxes (*sensu* Hubbard Brook forest) been conducted. Although generalizations about the functioning of tropical forests can be made based on climate and soil similarities, biotic feedbacks on physical drivers can impart site-specific dynamics that can only be understood by field measurements. Following the advice of Townsend et al. (2008), it is possible to employ recent developments in remote sensing, in combination with a coordinated and detailed field campaign, to better understand and model the biogeochemical heterogeneity of tropical forests at multiple spatial scales. As such, we issue a call for action to develop, plan, coordinate, and implement a field and remote sensing campaign that will yield an increased understanding of the hydrology and biogeochemistry of lowland tropical forests.

References

Araujo AC, Nobre AD, Kruijt B et al (2002) Dual tower long term study of carbon dioxide fluxes for a central Amazonian rain forest: the Manaus LBA site. J Geophy Res Atmos 107(D20):8090

Baker TR, Philips OL, Malhi Y et al (2004) Variation in wood density determines spatial patterns in Amazonian forest biomass. Global Change Biol 10:545–562

Bonilla ALC (2005) Balanço de nitrogênio em microbacias pareadas (floresta vs pastagem) no estado de Rondônia. MSc Dissertation Universidade de São Paulo, São Paulo

Brinkmann WLF (1983) Nutrient balance of a central Amazonian rainforest: comparison of natural and man-managed systems. IAHS Publ 140:153–163

Brinkmann WLF (1985) Studies on the hydrobiogeochemistry of a tropical lowland forest system. GeoJournal 11:89–101

Bruijnzeel LA (2004) Hydrological functions of tropical forests: not seeing the soil for the trees? Agr Ecosyst Environ 104:185–228

Chaves J, Neill C, Germer S, Neto SG, Krusche AV, Elsenbeer H (2008) Land management impacts on runoff sources in small Amazon watersheds. Hydrological Processes 22:1766–1775

Cohen JCP, Silva Dias MAF, Nobre CA (1995) Environmental conditions associated with Amazonian squall lines: a case study. Mon Weather Rev 123:3163–3174

Cornu S, Ambrose JP, Lucas Y et al (1998) Origin and behaviour of dissolved chlorine and sodium in a Brazilian rainforest. Water Res 32:1151–1161

Cuartas LA, Tomasella J, Nobre AD et al (2007) Interception water-partitioning dynamics for a pristine rainforest in Central Amazonia: marked differences between normal and dry years. Agr Forest Meteorol 145:69–83

Davidson EA, Bustamante MMC, Pinto AS (2001) Emissions of nitrous oxide and nitric oxide from soils of native and exotic ecosystems of the Amazon and Cerrado regions of Brazil. In: Galloway J, Cowling E, Erisman J et al (eds) Optimizing nitrogen management in food and energy production and environmental protection: proceedings of the 2nd international nitrogen conference on science and policy. AA Balkema Publishers, Lisse, pp 312–319

Davidson EA, Neill C, Krusche AV et al (2004) Loss of nutrients from terrestrial ecosystems to streams and the atmosphere following land use change in Amazonia. In: DeFries R et al (eds) Ecosystems and land use change. American Geophysical Union, Washington, Monograph Series 153, pp 147–158

De Simone O, Muller E, Junk WJ et al (2002) Adaptations of central Amazon tree species to prolonged flooding: root morphology and leaf longevity. Plant Biol 4:515–522

Elsenbeer H (2001) Hydrologic flowpaths in tropical rainforest soilscapes – a review. Hydrol Process 15:1751–1759

Elsenbeer H, Lack A (1996) Hydrometric and hydrochemical evidence for fast flowpaths at La Cuenca, Western Amazonia. J Hydrol 180:237–250

Elsenbeer H, Cassel DK, Zuniga L (1994) Throughfall in terra firme forest of western Amazonia. J Hydrol (NZ) 32:30–44

Ferreira SJF, Luizão FJ, Dallarosa RLG (2005) Precipitação interna e interceptação da chuva em floresta de terra firme submetida à extração seletiva de madeira na Amazônia central. Acta Amazonica 35:55–62

Figueroa NP, Nobre CA (1990) Precipitation distribution over central and western tropical South America. Climanalise 5:36–40

Filoso S, Williams MR, Melack JM (1999) Composition and deposition of throughfall in a flooded forest archipelago (Negro River, Brazil). Biogeochemistry 45:169–195

Franken W, Leopoldo PR, Matsui E, Ribeiro MNG (1992) Estudo da interceptação da água da chuva em cobertura florestal Amazônica do tipo terra firme. Acta Amazonica 12(2):327–331

Garreaud R, Wallace JM (1997) The diurnal march of convective cloudiness over the Americas. Mon Weather Rev 125:3157–3171

Germer SH, Elsenbeer H, Moraes JM (2006) Throughfall and temporal trends of rainfall redistribution in an open tropical rainforest south-western Amazonia (Rondonia, Brazil). Hydrol Earth Syst Sci 10:383–393

Germer SH, Neill C, Krusche AV et al (2007) Seasonal and within-event dynamics of rainfall and throughfall chemistry in an open tropical rainforest in Rondonia, Brazil. Biogeochemistry 86:155–174

Germer SH, Neill C, Vetter T et al (2009) Implications of long-term land-use change for the hydrology and solute budgets of small catchments in Amazonia. J Hydrol 364:349–363

Gouveia Neto S (2006) Concentrações e balanços de carbono orgânico dissolvido em duas bacias do estado de Rondônia: uma comparação entre floresta e pastagem. MSc Dissertation, Universidade de São Paulo, São Paulo

Grace J, Lloyd J, McIntyre J et al (1995) Carbon dioxide uptake by an undisturbed tropical rain forest in Southwestern Amazonia, 1992–1993. Science 270:778–780

Hamilton LS, Juvik JO, Scatena FN (1995) Tropical montane cloud forests. Springer, New York

Herwitz SR (1991) Aboveground adventitious roots and stemflow chemistry of *Ceratopetalum virchowii* in an Australian montane tropical rain forest. Biotropica 23:210–218

Horn HS (1971) The adaptive geometry of trees. Princeton University Press, Princeton

Houghton RA, Lawrence KT, Hackler JL (2001) The spatial distribution of forest biomass in the Brazilian Amazon: a comparison of estimates. Global Change Biol 7:731–746

Jackson IJ (1989) Climate, water and agriculture in the tropics, 2nd edn. Longman, Essex

Johnson MS, Lehmann J, Selva EC et al (2006) Organic carbon fluxes and stream water exports from headwater catchments in the Southern Amazon. Hydrol Process 20:2599–2614

Koren I, Kaufman YJ, Washington R et al (2006) The Bodele depression: a single spot in the Sahara that provides most of the mineral dust to the Amazon forest. Environ Res Lett 1:Art No. 014005

Leopoldo PR, Franken W, Salati E et al (1987) Toward A water balance in the central Amazonian region. Experientia 43:222–233

Lesack LFW, Melack JM (1996) Mass balance of major solutes in a rainforest catchment in the Central Amazon: implications for nutrient budgets in tropical rainforests. Biogeochemistry 32:115–146

Levia DF, Frost EE (2003) A review and evaluation of stemflow literature in the hydrologic and biogeochemical cycles of forested and agricultural ecosystems. J Hydrol 274:1–29

Lloyd CR, Marques AO (1988) Spatial variability of throughfall and stemflow measurements in Amazonian rainforest. Agr Forest Meteorol 42:63–73

Luizão RCC, Luizão FJ, Paiva RQ et al (2004) Variation of carbon and nitrogen cycling processes along a topographic gradient in a central Amazonian forest. Global Change Biol 10:592–600

Makarieva AM, Gorshkov VG (2007) Biotic pump of atmospheric moisture as driver of the hydrological cycle on land. Hydrol Earth Syst Sci 11:1013–1033

Malhi Y, Nobre AD, Grace J et al (1998) Carbon dioxide transfer over a central Amazonian rain forest. J Geophys Res Atmos 103:31593–31612

Malhi Y, Baker T, Philips OL et al (2004) The above-ground wood productivity and net primary production of 100 neotropical forest plots. Global Change Biol 10:563–591

Marengo JA (1992) Interannual variability of surface climate in the Amazon basin. Int J Climatol 12:853–863

Marengo JA (2006) On the hydrological cycle of the Amazon basin: a historical review and current state-of-the-art. Rev Bras Meteorol 21:1–19

Marengo JA, Nobre CA (2001) General characteristics an variability of climate in the Amazon basin and its links to global climate system. In: McClain ME, Victoria RL, Richey JE (eds) The biogeochemistry of the Amazon basin. Oxford University Press, New York, pp 17–41

Markewitz D, Davidson E, Moutinho P et al (2004) Nutrient loss and redistribution after forest clearing on a highly weathered soil in Amazonia. Ecol Appl 14:S177–S199

Mayorga E, Logsdon MG, Ballester MVR et al (2005a) Estimating cell-to-cell land surface drainage paths from digital channel networks, with an application to the Amazon basin. J Hydrol 315:167–182

Mayorga E, Aufdenkampe AK, Masiello CA et al (2005b) Young organic matter as a source of carbon dioxide outgassing from Amazonian rivers. Nature 436:538–541

McGregor GR, Nieuwolt S (1998) Tropical climatology. Wiley, Chichester

Melillo JM, Steudler PA, Feigl BJ et al (2001) Nitrous oxide emissions from forests and pastures of various ages in the Brazilian Amazon. J Geophys Res 106:34,179–34,188

Moraes JM, Schuler A, Dunne T et al (2006) Water storage and runoff processes in linthic soils under forest and pasture in eastern Amazon. Hydrol Process 20:2509–2526

Muzylo A, Llorens P, Valente F et al (2009) A review of rainfall interception modeling. J Hydrol 370:191–2006

Neill C, Piccolo MC, Steudler A et al (1995) Nitrogen dynamics in soils of forests and active pastures in the western Brazilian Amazon Basin. Soil Biol Biochem 27:1167–1175

Neill C, Deegan LA, Thomas SM et al (2001) Deforestation for pasture alters nitrogen and phosphorus in small Amazonian streams. Ecol Appl 11:1817–1828

Neill C, Deegan LA, Thomas SM et al (2006) Deforestation alters the hydraulic and biogeochemical characteristics of small lowland Amazonian streams. Hydrol Process 20:2563–2580

Neu V (2009) O ciclo do carbono na bacia do Alto Xingu: interações entre ambientes terrestre, aquático e atmosférico. PhD Thesis, Universidade de São Paulo, São Paulo

Nortcliff S, Thornes JB (1989) Variations in soil nutrients in relation to soil moisture status in a tropical forested ecosystem. In: Proctor J (ed) Mineral nutrients in tropical forest and savanna ecosystems. Blackwell, Oxford, pp 43–54

Oliveira LL, Costa RF, Souza FA et al (2008) Precipitação efetiva e interceptação em Caxiuanã, na Amazônia Oriental. Acta Amazonica 38:723–732

Ometto JPHB, Nobre AD, Rocha HR et al (2005) Amazonia and the modern carbon cycle: lessons learned. Oecologia 143:483–500

Peel MC, Finlayson BL, McMahon TA (2007) Updated world map of the Köppen-Geiger climate classification. Hydrol Earth Syst Sci 11:1633–1644

Richey JE, Melack JM, Aufdenkampe AK et al (2002) Outgassing from Amazonian rivers and wetlands as a large tropical source of atmospheric CO_2. Nature 416:617–620

Roberts J (2000) The influence of physical and physiological characteristics of vegetation on their hydrological response. Hydrol Process 14:2885–2901

Sabine C, Heimann M, Artaxo P et al (2004) Current status and past trends on the global carbon cycle. SCOPE 62. Island Press, Washington, pp 17–44

Saleska SR, Miller SD, Matross DM et al (2003) Carbon in the Amazon forests: unexpected seasonal fluxes and disturbance-induced losses. Science 302:1554–1557

Sanford RL Jr (1987) Apogeotropic roots in an Amazon rain forest. Science 235:1062–1064

Saugier B, Roy J, Mooney HA (2001) Estimations of global terrestrial productivity: converging toward a single number? In: Saugier B, Mooney HA (eds) Terrestrial global productivity. Academic, San Diego, pp 543–557

Sheil D, Murdiyarso D (2009) How forests attract rain: an examination of a new hypothesis. Bioscience 59:341–347

Shuttleworth WJ (1988) Evaporation from Amazonian rainforest. P Roy Soc B Biol Sci B233:321–346

Tobón Marin C, Bouten W, Sevink J (2000) Gross rainfall and its partitioning into throughfall, stemflow and evaporation of intercepted water in four forest ecosystem in western Amazonia. J Hydrol 237:40–57

Tobón Marin C, Sevink J, Verstraten JM (2004) Solute fluxes in throughfall and stemflow in four forest ecosystems in northwest Amazonia. Biogeochemistry 70:1–25

Tomasella J, Neill C, Figueiredo R, Nobre AD (2009) Water and chemical budgets at the catchment scale including nutrient exports from intact forests and disturbed landscapes. In Keller et al (eds) Amazonia and Climate Change. AGU Geophysical Monograph 186, pp 505–524

Townsend AR, Asner GP, Cleveland CC (2008) The biogeochemical heterogeneity of tropical forests. Trends Ecol Evol 23:424–431

Ubarana VN (1996) Observation and modelling of rainfall interception at two experimental sites in Amazônia. In: Gash JHC, Nobre CA, Roberts JM et al (eds) Amazônian deforestation and climate. Wiley, Chichester, pp 151–162

Verchot LV, Davidson EA, Cattânio JH, Ackerman IL, Erickson HE, Keller M (1999) Land use change and biogeochemical controls of nitrogen oxide emissions from soils in eastern Amazonia. Glob Biogeochem Cycles 13:31–46

Victoria DC (2004) Estimativa da evapotranspiração da bacia do Ji-Paraná (RO) através de técnicas de sensoriamento remoto e geoprocessamento. PhD Thesis, University of São Paulo, São Paulo

Vitousek PM (1984) Litterfall, nutrient cycling, and nutrient limitation in tropical forests. Ecology 65:285–298

Vitousek PM, Sanford RL (1986) Nutrient cycling in moist tropical forests. Ann Rev Ecol Syst 17:137–168

Waterloo MJ, Oliveira SM, Drucker DP et al (2006) Export of organic carbon in runoff from an Amazonian rainforest blackwater catchment. Hydrol Process 20:2581–2598

Williams MR, Fisher TR, Melack JM (1997) Chemical composition and deposition of rain in the central Amazon, Brazil. Atmos Environ 31:207–217

Chapter 10
Hydrology and Biogeochemistry of Mangrove Forests

Daniel M. Alongi and Richard Brinkman

10.1 Introduction

Situated at the interface between land and sea, the structure and function of mangrove forests, perhaps more than any other forest type, are closely linked to hydrology. For a part of every day, tidal waters flood and ebb through these coastal forests of low latitudes, and in most locations are influenced by waves and other circulatory processes. The pantropical distribution of mangroves is delimited by the major ocean currents and the 20°C winter isotherm of seawater. Mangroves are limited globally by temperature but rainfall, tides, waves, and river flow are of fundamental importance at the regional and local scale.

Most mangrove forests represent a continuum of morphological types based on broader geophysical settings such as those dominated by rivers, tides, reef carbonates, and drowned river valleys (Woodroffe 1992). Variations in waves, tides, river flow, and rainfall affect water circulation by generating advective and diffusive processes that operate both longitudinally and laterally within estuaries to mix and trap coastal water (Wolanski 1992). The turbulence induced by temporal and spatial gradients in hydrodynamic processes influences the rate of erosion and deposition of soil on which mangroves colonize and grow.

Mangroves are typically distributed from mean sea-level to highest spring tide with a sequential change in tree species parallel to shore being one of their most conspicuous features. Forest zonation has been overemphasized in mangrove ecology. But gradients in salinity, soil type and chemistry, and nutrient content as regulated by duration of tidal inundation, as well as physiological tolerances, predation, competition, and combinations of these factors (Alongi 2009), are all important in regulating the structure and function of mangroves. Indeed, patterns of nitrogen and phosphorus limitation of mangrove primary production mirror the salinity gradients and gradients of nutrient availability across the intertidal seascape (Feller et al. 2002; McKee et al. 2002), highlighting the complexity of mangrove ecology in relation to nutrient biogeochemistry and environmental gradients (Feller et al. 2010).

Disturbances also play a key role in regulating mangroves; hurricanes, monsoons, and tsunami occur throughout low latitudes and their effects often mask

natural change. Mangroves exhibit considerable resilience to disturbance – an adaptive mechanism to life in a physically demanding environment – undergoing perpetual change in forest and ecosystem development in synchrony with the geomorphological development of shorelines. The end result of these natural and human-induced disturbances and adaptive responses are forest mosaics of arrested or interrupted successional sequences (Berger et al. 2006).

Mangroves are a valuable economic and ecological resource, being important breeding sites for a wide variety of wildlife; a renewable resource of timber; and accumulation sites for sediment, contaminants, carbon, and nutrients. They also offer some protection against coastal erosion, strong waves, high tides, and tsunami. In this chapter, we review and critically assess the role of hydrology in regulating biogeochemical processes in mangroves and the impact that these tidal forests in turn have on coastal hydrology.

10.2 Waterway Circulation and Material Fluxes

Snaking through and bisecting mangrove forests are a wide array of shallow and deep tidal channels. These can range from fairly straight and narrow waterways to complex networks of interconnected channels, creeks, and estuaries. These waterways – another conspicuous feature of mangroves – are conduits by which water, sediments, and nutrients move into and out of the forests by tides, and to a much lesser extent, by waves (Mazda et al. 2007). Tides and waves constitute an auxiliary energy subsidy. Tides do the work of exporting waste products and importing nutrients, oxygenated water, food, and sediments to mangroves and their food webs. This allows tidal forests to store and pass on fixed carbon and benefit organisms adapted to make use of the energy subsidy; animals that do not have to expend their own energy to export wastes and import essential materials can shunt more energy to growth and reproduction (Alongi 2009).

There are biogeochemical consequences of water movements in simple vs. complex waterways. To oversimplify: long, fairly straight waterways can facilitate dispersal and export of dissolved and particulate matter, whereas convoluted waterways can weaken dispersion of water to the extent that the upper reaches of intricate channels can trap material. Nevertheless, in most mangrove waterways, tidal circulation is characterized by a pronounced asymmetry between ebb and flood tides with the ebb tide being shorter, but with stronger current velocity, than the flood tide. This asymmetry results in self-scouring of the bottom of most channels such that channel beds are usually rocky, gravelly, or sandy, with little or no accumulation of fine sediment.

Ecosystem geometry, especially the ratio of forest area to waterway area, and the slope of the forest floor, ultimately determines the velocity of tidal circulation. This areal ratio in most mangroves appears to be in the range of 2–10 (a dimensionless number) with a very small forest slope within the range of $1–4 \times 10^{-3}$ (Wolanski 1992). An increase in the ratio of forest to waterway area thus increases

the tidal prism. Current direction in relation to the forest imparts additional tidal asymmetry; rising tidal waters flow into the forest perpendicular to the banks but ebbing tidal waters are oriented at usually 30–60° to the bank, lengthening the pathway of water at falling tide and thus reducing the chance that materials such as mangrove detritus can escape the forest.

Tidal hydrology is also longitudinally complex. Along the length of a waterway, water velocity decreases from the mouth to the headwaters, and at the headwaters of mangrove creeks and channels where currents are very weak, mixing rates are also very small (Ridd et al. 1990). Cross-channel gradients of longitudinal velocity also exist, due partially to the shear dispersion processes that are magnified by the presence of the forest. Mangrove waterways also exhibit longitudinal salinity gradients which act in concert with gradients of current speed to control the intensity of mixing and trapping of water and materials within the estuary. Trapping occurs when some of the water flowing in and out of an estuary is temporarily retained in the forest by drag forces to be returned later to the main channel. In the dry season with little, if any, freshwater inflow to cause buoyancy-driven circulation, salinity increases landward, driven by evaporation of water and the buildup of salt excluded by trees. Thus, trapping in the headwaters is enhanced. In the wet season, buoyancy effects trap freshwater in the forest at high tide, and at low tide the freshwater is manifest as a low salinity lens or boundary layer hugging the river banks.

Longitudinal gradients of velocity and salinity interact to produce secondary circulation patterns superimposed on the primary tidal circulation. This leads to trapping of floating mangrove detritus in density-driven convergence fronts during a rising tide (Stieglitz and Ridd 2001). On flooding tides, velocity near the river banks is slower than in the center of the estuary due to friction, resulting in water of greater density mid-channel. In the center of the estuary, this more dense water sinks to cause a two-cell circulation pattern with a convergence front approximately midstream. This convergence swiftly breaks down with the onset of ebb tides. There are clear biogeochemical and biological implications in the existence of these cells (Ridd et al. 1998; Stieglitz and Ridd 2001):

- A net upstream movement of floating debris occurs.
- Propagules and other materials are unlikely to enter the forests when the secondary cells are present.
- Propagules and detritus accumulate in large traps upstream from the convergence and upstream from the mangrove fringe.
- Trapping of propagules is not conducive to successful seed dispersal of mangroves.

Trapping of water and waterborne material in mangrove estuaries is also enhanced by tides, onshore winds, and shoreward waves (Kitheka 1996).

All of these hydrological processes translate into residence times that are long, especially in the dry season, and this has direct biogeochemical consequences. For instance, nutrients or contaminants introduced into the head of a mangrove waterway may be retained longer than if they were introduced further downstream.

One often-recurring longitudinal pattern is a link between pH, oxygen, and dissolved organic matter (DOM). Moving upstream, it is common to observe a decline in both pH and oxygen concentrations but an increase in DOM (Boto and Bunt 1981). This pattern can be explained as the lowering of pH and oxygen levels as a result of oxidation of polyphenolic compounds. An alternative explanation is that pelagic respiration increases upstream when water becomes stagnant or experiences long residence time, enabling microbes to concentrate and bloom; respiration lowers oxygen levels and produces carbonic acid which lowers pH.

The low opacity of mangrove waters as a result of fine suspended loads and polyphenolics results in a high ratio of bacterioplankton to phytoplankton production (Alongi 2009). This ratio is a reflection of either comparatively low rates of phytoplankton production due to severe light limitation or the efficiency with which mangrove bacterioplankton convert organic matter into biomass, or both. The high ratio also suggests intense recycling within the microbial web or that organic matter from other sources such as mangrove detritus and benthic algae are fueling bacterial growth. Metadata analysis (Alongi 2009), however, shows that most mangrove waters are net autotrophic, with more carbon being fixed than lost via respiration. The mean ratio of primary to community respiration (P/R) in mangrove waters is 1.8 with a standard deviation of 0.3, substantially higher than the P/R of 0.8–1.0 that has been measured in other estuaries (Alongi 1998; Gattuso et al. 1998).

The metabolic state of mangrove waters is known to change seasonally in some estuaries. For example, in the Mandovi and Zuari estuaries of southwestern India (Ram et al. 2003) waters are net autotrophic in the pre- and post-monsoon months when quiescent conditions maximize water clarity. During the monsoon, waters are very turbid because of sediment resuspension; also, peak loads of land-derived organic matter, low water levels, and salinity lead to a metabolic shift toward net heterotrophy.

The greatest biogeochemical consequence of these complex hydrodynamic processes is the rapid exchange of solids, dissolved materials, and gases among mangroves, adjacent coastal waters, and the atmosphere. The amount of material potentially available for exchange depends on several factors: net forest primary production, tidal range, ratio of mangrove to watershed area, lateral trapping, high salinity plugs, total mangrove area, frequency of storms, amount of rainfall, volume of water exchange, and the extent of biological activity (Wolanski 2007). Each mangrove ecosystem is unique; some mangroves export particulate and dissolved materials and some do not, but all systems exchange a variety of gases with the atmosphere and coastal ocean.

Like other forests, there is a vertical hydrological flux in mangroves via precipitation and throughfall (Twilley and Chen 1998; Wanek et al. 2007). Few studies have examined the significance of vertical flux in terms of water and nutrient budgets, and the results to date are equivocal. A water budget for the mangroves in Rookery Bay, Florida (Twilley and Chen 1998) found that throughfall and stemflow equated to 91% of annual rainfall, with nearly 77% lost as runoff to the bay. The ecological impact was most discernible as dilution of soil salinity in the high intertidal zone. Similar results were obtained in Belizean mangroves

(Wanek et al. 2007) where throughfall represented 84% of precipitation; ammonium and phosphorus were retained in the canopy, whereas nitrate, dissolved organic carbon (DOC), and dissolved organic nitrogen (DON) increased from throughfall. However, at the ecosystem level, vertical fluxes are likely minor compared with horizontal flows. Nitrogen budgets for the mangrove ecosystems of Sawi Bay, Thailand and Hinchinbrook Island, Australia, demonstrate that N-derived from precipitation is in fact small (Alongi et al. 1992, 2002).

Most data on material exchange are estimates of the export of particulate organic carbon (POC), mainly as litter, from mangrove estuaries. Only very recently has the exchange of gases been measured. Estimates of POC export from mangrove estuaries range widely from 5.3 to 27.7 mol C m^{-2} $year^{-1}$, but mangroves account for 10–11% of the total input of terrestrial carbon to the ocean and 12–15% of the total carbon accumulation in sediments along the continental margins (Jennerjahn and Ittekot 2002; Dittmar et al. 2006). On average, the current estimate of global POC export from mangroves is ≈29 Tg $year^{-1}$ (Bouillon et al. 2007; Alongi 2009).

The smallest exports tend to come from microtidal ecosystems while the largest outwelling occurs from mesotidal and macrotidal estuaries, highlighting the importance of tides and the fact that ebb tides are stronger than flood tides. In some mangrove ecosystems, especially in basin forests and in microtidal systems, more carbon is exported in dissolved than in particulate form. Chemically, exported DOC has a strong mangrove stable isotope signature, whereas imported DOC is mainly of marine origin. On average, the current estimate of global DOC export from mangroves is ≈14 Tg $year^{-1}$ (Bouillon et al. 2007; Alongi 2009).

In contrast, there are no universal patterns of dissolved nitrogen and phosphorus exchange between mangroves and adjacent coastal waters. The lack of a consistent pattern may be due to the fact that rates of autotrophic assimilation and microbial uptake vary greatly among ecosystems. Simply, an ecosystem will tend to export nutrients if there are more nutrients than needed for utilization, and conversely, nutrients such as nitrogen will be imported if not available. In many estuaries, some nutrient species are imported, whereas others are exported.

Despite the fact that globally at least 40 Tg $year^{-1}$ of mangrove carbon is exported to the coastal ocean, the influence of this exported carbon on coastal food chains and nutrient cycles is usually restricted to a few kilometers offshore. Several factors account for these spatial limitations:

- Local geomorphology and hydrodynamics of mangrove estuaries mitigate against extensive outwelling of labile material.
- Coastal boundary layers off tropical coasts or the presence of a high salinity plug in the dry season effectively trap litter and suspended particles inshore.
- Most material exported from mangroves is either highly refractory particulate matter or DOC; this material is usually further degraded in the water-column.

As demonstrated by the classic work of Wolanski and his colleagues (Wolanski and Ridd 1986; Wolanski et al. 1990; Mazda et al. 2007), a barotropic coastal boundary layer forms off mangrove estuaries if the coast is straight due to shallow water effects and trapping in mangrove forests, resulting in long-term retention of

water close inshore in calm weather. Waters are continuously exchanged and mixed between the estuary and the adjacent coastal boundary layer, but mixing is restricted between coastal and offshore waters. Mixing, however, does occur and the coastal boundary layer breaks down along rugged coasts and at headlands. What estuarine water does leave the coastal zone does so when tidal jets of coastal water peel off headlands and other salient topography and locally enrich and mix with offshore waters (Wolanski 2007).

Recent studies of CO_2 exchange from mangrove waterways suggest that pelagic respiration and subsequent emission of CO_2 to the atmosphere represents another significant pathway of carbon flux from mangrove forests (Ghosh et al. 1987; Richey et al. 2002; Borges et al. 2003; Ralison et al. 2008). Mangrove waters are oversaturated in CO_2 as a direct result of pelagic mineralization and CO_2 respired by forest soils that is dissolved in the interstitial water and transported laterally by tidal pumping to adjacent waterways. Emission rates vary greatly depending on tidal stage, temperature, and precipitation. Koné and Borges (2008) estimate that CO_2 emissions from mangrove waters correspond to $\approx 7\%$ of the total emission from oceanic waters in subtropical and tropical latitudes. This value is small but nevertheless reflects a disproportionate contribution of dissolved inorganic carbon (DIC) by mangroves to the coastal ocean.

10.3 Facilitation of Water and Material Flows in Relation to Forest Structures Across the Intertidal Zone

Trees, roots, animal burrows and mounds, timber and other vegetation decaying on the forest floor exert drag on the movement of water within a forest. For tidal flows, drag force can be simplified to a balance between the slope of the water surface and the flow resistance due to the vegetation. This flow resistance can be approximated by a drag coefficient which varies in mangrove forests from 0.4 to 10 (Mazda et al. 2005). The drag coefficient decreases with increasing values of the Reynolds number. Biologically, this means that in densely vegetated forests, prop roots, and pneumatophores play an important role in slowing and altering water flow, and enhancing trapping of material within the forest. Currents within the forest are not negligible and secondary circulation patterns are usually present due to the density of the vegetation and overflow of water into the forest at high tide. The magnitude of tidal trapping depends on the drag force due to the vegetation, so the magnitude of dispersion depends ultimately on vegetation density.

Biogenic structures within the forest floor also affect water circulation in mangrove forests, playing a crucial role in soil biogeochemistry by enhancing flushing times and replenishing oxygenated interstitial water (Ridd 1996; Susilo and Ridd 2005). Tidal waters flow through burrows in the same direction as the surface current. The total quantity of water flowing through burrows in a 1 km^2 area of forest can range from 1,000 to 10,000 m^3, representing 0.3–3% of the total water volume moving through a forest. There is also passive irrigation through burrows.

Parts of burrows that are no more than 20 cm apart can reduce the diffusion distances belowground of salt expelled from tree roots. Well-flushed burrows are thus an efficient mechanism by which salt and anoxic metabolites can be transported from the roots, ameliorating salt stresses, and exposure to toxic metabolites such as sulfides. The irrigation of biogenic structures also helps poise soil metabolism to a suboxic redox state, fostering oxidation of sulfides, and other anoxic solutes.

Nitrogen metabolism is also greatly influenced by water flow through biogenic structures, cracks, and fissures within the forest floor. Such processes may favor anaerobic ammonium oxidation (anammox), the anaerobic conversion of nitrite (NO_2^-) to N_2. Although NO_2^- accumulates from both nitrification and nitrate + nitrite reduction, the latter process regulates nitrite availability in suboxic soil layers. Denitrification also provides a substrate for the anammox process, although it appears that N_2 loss via denitrification is of proportionally less significance in mangroves than in other aquatic ecosystems (Alongi 2009). Subsequently, rates of nitrous oxide (N_2O) emissions from mangrove soils are low, N_2O being an intermediate product of nitrification and denitrification. Indeed, in Indian mangroves, emission rates of N_2O are greater from creek waters than from mangrove soils (Barnes et al. 2007; Upstill-Goddard et al. 2007). In short, the unique patterns of water flow through forests and their structures facilitate retention of nitrogen and other nutrients crucial for mangrove growth.

Being located at the land–sea margin, mangroves often have significant groundwater flow. This flow can be an important pathway for removal of subsurface salt and solutes (Ovalle et al. 1990; Sam and Ridd 1998) and is probably interlinked with water flow through crab burrows, cracks, and fissures in the soil. There are three components of mangrove groundwater flow:

- A near-steady flow seawards due to the pressure gradient induced by the height differential between forest and sea.
- A reversing tidal flow with a dampened amplitude and delayed phase toward the forest.
- A residual flow landwards due to the dampened tidal flow. This residual flow reduces the outflow of water from the forest to the sea.

Groundwater-derived nutrients can have a variable impact on nutrient dynamics in mangrove waterways, often linked to seasonal rainfall (Kitheka et al. 1999). In Mida Creek in Kenya, the groundwater flow of silicate through the mangroves was greater in the wet season, although the opposite was true for dissolved nitrogen. Nutrient concentrations were greater in the groundwater than in the creek and except for $NO_2^- + NO_3^-$, greater in the wet season than in the dry months. Groundwater seepage contributed from 8 to 140% of the net dissolved N flux, but <5% of the net silicate flux.

In most other mangroves, a variety of factors determine the relative contribution of groundwater to surface water flow. In river-dominated forests on islands in the Federated States of Micronesia, the average groundwater contribution is 5% but the contribution approaches 20% in forests closer to land (Drexler and DeCarlo 2002).

This pattern is of selective advantage in that greater groundwater flow in more landward forests helps to alleviate salt stress, soil desiccation and anoxia, promoting growth in areas that may be otherwise unsuitable for mangroves.

10.4   Sediment Dynamics and Burial of Carbon and Nitrogen

The attenuation of water flow within mangrove forests facilitates deposition of fine particles. The transport of suspended sediments in mangroves is controlled by several interlinked processes (Wolanski 1995):

- Tidal pumping.
- Baroclinic circulation.
- Trapping of small particles in the turbidity maximum zone.
- Flocculation.
- Physicochemical reactions that destroy cohesive sediment flocs.
- Microbial production of mucus.

In fringing mangroves or in those inhabiting rocky shores, such processes are insignificant. But in most mangroves these processes have a profound impact on sediment transport and deposition, and ultimately, on biogeochemical processes such as rates of element accumulation, burial, and storage.

Most sediment is transported into a forest during the wet season when riverine sediment inflow is at its height. Up estuary, mud banks form as a result of baroclinic circulation and by tidal pumping and trapping especially in the turbidity maximum, a zone formed within an estuary where the residual inward bottom flow meets the outward river flow. This zone is usually located at the most landward point reached by the saline inflow. The biogeochemical implications of these processes is that flocculation of silt and clay particles begins, with flocs colonized by a rich consortium of bacteria, protists, algae, and fungi, and glued together by their extracellular mucus and threads. These attached microbes, in helping to cement flocs, serve as foci for decomposition and respiratory processes in mangrove waters (Ayukai and Wolanski 1996). Within the forest, the settling of flocs occurs when the tides turn from rising to falling and water velocity is minimal. Settling is enhanced by the sticking of mucus and by pelletization of invertebrate excreta.

Mangroves do not just passively import fine particles. By a variety of mechanisms, they actively capture silt, clay, and organic particles. The presence of trees has a profound impact on sedimentation. Large trees with complex root systems (e.g., *Rhizophora*) facilitate particle settling to a greater degree than small trees or those with minimal above-ground root structures (e.g., *Ceriops*). In Coral Creek in northeastern Australia, 80% of particles brought in at spring flood tides are retained within the forest (Furukawa et al. 1997). So despite the fact that turbulent wakes created by tree trunks and roots maintain particles in suspension, high vegetation density inhibits water motion, creating conditions unfavorable for resuspension of particles.

The biogeochemical consequence of facilitated accumulation of fine sediment particles within mangroves is net sediment accretion and burial of carbon and other elements. Sedimentation rates measured by radiotracers and by short-term measurements of changes in topographic height relative to mean sea-level show a pattern of net accumulation in many, but not all, forests. Mass sediment accumulation rates range from <1 mm year^{-1} to >3–5 cm year^{-1}, with highest rates within forests lining high discharge rivers and rivers severely impacted by human activities. Lowest sedimentation rates occur in mangroves fringing open bays and estuaries, especially in the dry tropics. Net deposition cannot continue indefinitely because deposition slows as the forest floor grows over time and is inundated less frequently by tides.

Rates of soil carbon and nitrogen cycling closely depend on rates of sediment accumulation as well as on temperature, rates of bioturbation, quality of deposited organic matter, and the degree of tidal wetting. No one factor regulates soil decomposition rates but clearly, wet, warm, bioturbated soils with high-quality organic matter will have higher rates of diagenesis than other soils. On average only a small proportion (1–5%) of organic carbon and nitrogen is buried in mangrove soils as nearly all labile organic matter is eventually mineralized.

Aerobic respiration and anaerobic sulfate reduction are the main decomposition pathways in mangrove soil. As oxygen penetrates and is depleted within the upper few mm of soil, anaerobic metabolism, especially sulfate reduction, dominates belowground. Iron reduction may be important, but more empirical measurements are needed to assess its relative importance in mangroves. Methanogenesis accounts for only a small fraction (1–10%) of total soil carbon mineralization, but rates are often highly variable. Methane production occurs in and on parts of trees so its significance to total carbon flux is likely underestimated. However, what is puzzling and what in future may turn out to be an important pathway is the lack of agreement between the sum of carbon mineralized by these individual metabolic processes and measurements of DIC and CO_2 emissions across the soil–water/air interface. In aquatic environments, such measurements across the soil surface are thought to represent the sum of carbon mineralization within soils, assuming steady-state conditions. The lack of such agreement in mangroves suggests nonsteady state conditions, which is probable given the number of complex ecological and biogeochemical processes in mangrove soils and the complex hydrology of the forest floor. As we will see later, nonsteady state conditions may have important consequences for carbon balance in mangrove ecosystems, altering our perception of net ecosystem production (NEP) (see Sect. 10.5).

Unlike terrestrial forests, a significant fraction of litter on the forest floor is swept away by tides. Before organic carbon is incorporated into the soil to be decomposed by microbes, nearly 50% of litterfall remaining on the forest floor is initially processed by crabs and other benthic invertebrates. What litter escapes crab processing is usually decomposed further by microbes and meiofauna, and litter shredded, but uneaten, is returned to the soil to also eventually be consumed by microflora. Detritus not processed by crabs and other macroconsumers decomposes into three stages: (1) leaching of soluble compounds; (2) saprophytic decay; and

(3) fragmentation (Robertson et al. 1992; Kristensen et al. 2008). Leaching involves the loss of up to 20–40% of the organic carbon in the litter when submerged for 10–14 days. The bulk of the leachate is labile, mostly sugars, tannins, and other phenolic compounds, and up to 90% of this dissolved material is readily degraded aerobically and incorporated into microbial biomass. The second phase of decomposition occurs when aerobic and anaerobic prokaryotes, and oomycotes, colonize the remaining particulate litter. Unlike terrestrial plant litter, ascomycetes appear to play only a minor role as decomposers of mangrove debris. In fact, it is the oomycotus protoctists, especially *Halophytophthora vesiculara*, that efficiently capture cellulosic compounds via pervasion and digestion. Mangrove litter thus becomes relatively enriched in lignin which decomposes only very slowly. Microbial enrichment over years of decomposition results in a chemical signature reflecting the compositional changes in the colonized microflora. On average there is a decrease in the C:N and C:P ratios of decomposing litter over time. There are some common features of litter decomposition, some of which point to hydrology as an important factor:

- Absolute decay parameters are site- and species-specific.
- Litter decays faster when more frequently immersed and when litter retains its moisture.
- Litter with low tannin content and high initial nitrogen content decomposes faster than litter with higher tannin content, such as *Rhizophora* and *Bruguiera* leaves.
- Litter decomposition of the same species occurs at similar rates in the subtropics and tropics, but decays more slowly in the dry tropics where litter is subject to intense aridity and high salinity.

10.5 The Role of Hydrodynamic Processes in Net Ecosystem Production

The balance between photosynthetic gains by autotrophs and losses by all organisms is reflected in the exchange of carbon between the ecosystem, atmosphere, and the adjacent coastal ocean. This balance is called NEP. As forests are especially important habitats for storage of carbon, reducing the impact of anthropogenic increases in atmospheric CO_2, NEP has become a crucial diagnostic feature for assessing whether or not human impacts have altered ecosystem balance.

At the ecosystem level, determining the carbon balance of mangroves involves summing the carbon inputs from carbon fixation minus losses via respiration and the shedding of litter. Other inputs and outputs need to be accounted for: groundwater, burial within the forest floor, tidal exchanges, river inputs, and respiratory losses by fauna and any other flora. A simple mass balance equation is the basis for these flux calculations:

$$C_i = F_i + \Sigma R_i, \tag{10.1}$$

where C_i is the concentration of element i in mass per unit volume per unit time; F_i is the flux of element i in mass per unit area or volume per unit time and R_i is the rates of physical, chemical or biological processes affecting element i in mass per unit volume or area per unit time. This equation simply represents the difference between what carbon comes in and what carbon goes out. When input exceeds output, NEP is greater than zero and the ecosystem is accumulating carbon. If it roughly equals zero, the ecosystem is at steady-state. If negative, the ecosystem is unsustainable, losing more carbon than it is gaining.

A metadata analysis of six mangrove forest ecosystems (Alongi 2009) worldwide highlights two primary features: (1) mangrove ecosystems are net autotrophic with an average P/R ratio of 1.6 and (2) gross primary production and NEP average 383 and 139 mol C m^{-2} year^{-1}, respectively. A few other important generalizations:

- Mangroves export organic carbon equivalent to 2–25% of mangrove net primary production.
- Canopy respiration equates to 58% of gross primary production, but may be higher as the data account only for leaf respiration, not root and stem respiration.
- Tree production dominates carbon input, but inputs from humans and from rivers and oceans can be substantial in some locations.
- Soil and pelagic respiration losses are minor compared to canopy respiration, but may be larger if "unaccounted for" DIC (see below) is found to be laterally transported from soils.
- Carbon burial equates to only 1–4% of total carbon input into the forest.
- NEP is positive in all six ecosystems, but true NEP is probably lower because CO_2 emissions from the waterways were not measured.

The relationship between tidal range and NEP (Fig. 10.1) suggests that tides play a crucial role in regulating ecosystem production, supporting the tidal subsidy hypothesis proposed by Odum (1968), Odum et al. (1995), and Nixon (1988). In such ecosystems, maximum power is achieved when biological "pulses" are in synchrony with external forces such as tides (Odum et al. 1995). Nixon (1988) moreover suggested that greater fisheries yields, stronger currents, and more vigorous vertical mixing in marine ecosystems compared with lakes, reflects the additional mechanical energy from tides. The positive relationship between mangrove NEP and tidal range may thus be explained by physical forces linked to tides, assisting in maximizing transport of wastes and toxic metabolites, assisting in oxygenating soils that would otherwise be waterlogged, and maintaining an intermediate level of disturbance in breaking down any biophysical and chemical gradients.

A contrary hypothesis is equally compelling. A great deal of DIC produced in mangrove soils as a result of microbial decomposition of organic matter may be unaccounted for, perhaps lost via lateral transport or via groundwater flow. These pathways have not typically been measured in mangroves. For example, the large tides in Darwin Harbour, Australia, may laterally transport great amounts of respired carbon derived from the interstitial water. So what appears to be greater NEP than
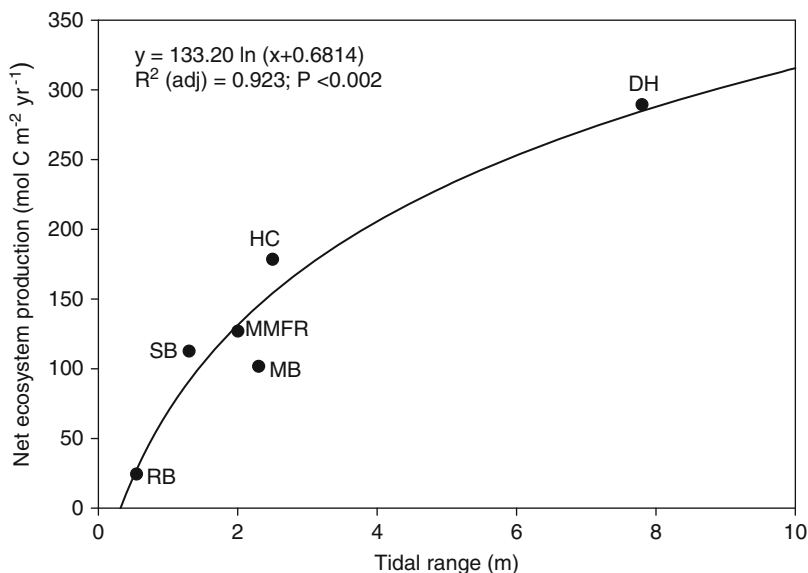
Fig. 10.1 The relationship between tidal range and net ecosystem production in various mangrove estuaries. *DH* Darwin Harbour, Australia; *HC* Hinchinbrook Channel, Australia; *MB* Missionary Bay, Australia; *MMFR* Matang Mangrove Forest Reserve, peninsular Malaysia; *SB* Sawi Bay, Thailand; *RB* Rookery Bay, Florida (from Alongi 2009)

in mangroves with smaller tides (Fig. 10.1) may in fact be a greater proportion of respired carbon lost from the ecosystem as DIC. If true, this means that mangroves are contributing even greater amounts of DIC to the tropical coastal ocean.

The overarching influence of tides on mangrove biogeochemistry can be unambiguously discerned from the mass balance of nitrogen from the mangrove ecosystem on Hinchinbrook Island in northeastern Australia (Alongi et al. 1992; Alongi 2009). The nitrogen budget for this tidally dominated system shows that tidal exchange dominates the flux of nitrogen entering and leaving the ecosystem. Indeed, tidal export as a percentage of total output is greater in this ecosystem than in salt marshes. Physical control by tides therefore dominates the flux of nitrogen possibly to a greater extent than in other aquatic ecosystems, and such may be the case for DIC in mangroves.

10.6   A Global Carbon Model

The biogeochemical importance of mangrove forests have been placed within a global context with the two most recent budgets (Bouillon et al. 2007; Alongi 2009) instructive in pinpointing patterns of flow important to global carbon cycling and where further research should be focused.
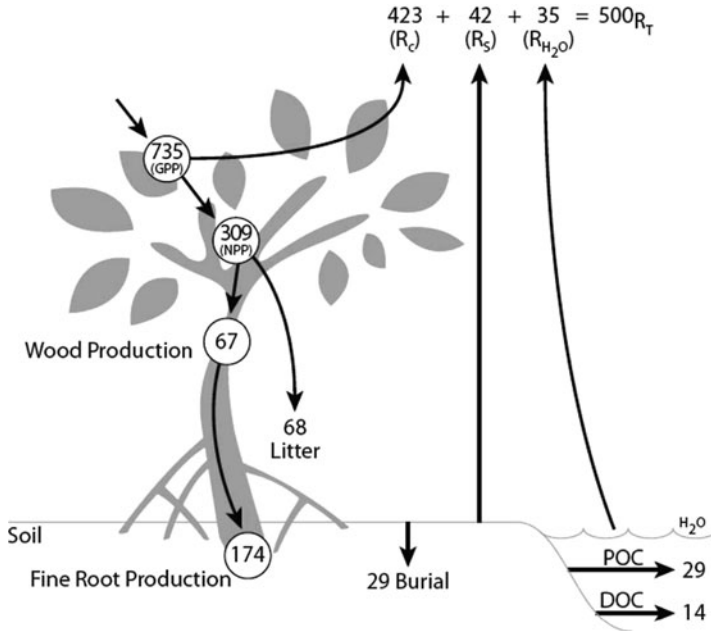
Fig. 10.2 Model of the major carbon fluxes through the world's mangrove forests. Units $=$ Tg C year^{-1}. The budget assumes a global area of 160,000 km^2 (from Alongi 2009). The global area was incorrectly printed in Alongi (2009) as 160,000 ha

Figure 10.2 summarizes the major pathways of carbon flow through the world's mangroves (160,000 km^2) showing that the largest flux is between the trees and the atmosphere as a little more than half of gross primary production is respired by trees. Litterfall (20%), wood production (20%), and fine root production (50%) account for nearly all forest net primary production. Summing canopy respiration, soil respiration, and water-column respiration, total ecosystem respiration equates to 500 Tg C year^{-1} or nearly 70% of forest GPP. Carbon burial averages 29 Tg C year^{-1} or about 10% of forest NPP; export of POC and DOC equates to 43 Tg C year^{-1} which is about 10–15% of forest NPP. Subtracting carbon losses from inputs leaves a NEP estimate of 160 Tg C year^{-1}. This figure is problematical because some unknown portion of this carbon is likely to actually represent lateral loss of DIC from soils. Bouillon et al. (2007) estimated that 112 Tg C year^{-1} is "unaccounted for" mangrove production and similarly suggested that this value may represent possible DIC exported laterally from the world's mangroves.

The idea that a large amount of DIC is transported laterally and lost from the system is supported by a few facts: (1) soil microbes are highly productive to a soil depth of at least 1 m; (2) lateral drainage has been frequently observed, but unquantified, in a number of mangrove systems, and (3) the sum of individual carbon measurements is usually greater than the rate of total C metabolism measured at the soil surface. In macrotidal estuaries, mangroves sit atop highly sloped

escarpments from which a large quantity of interstitial water can alternatively drain and replenish soils via tides (Woodroffe 2003). Obviously, other processes not measured may constrain the amount of carbon that is "unaccounted for" including faunal production and respiration, viral repellents, protective metabolites, or more subtle mechanisms such as symbiotic or mutualistic relationships that may require fixed carbon.

If the large production of fine roots (174 Tg C year^{-1}) is correct, rapid turnover of fine roots would equate closely to the value of the excess carbon (160 Tg C year^{-1}). Strong investment in root production makes sense for mangroves from an evolutionary perspective given that, unlike terrestrial forests, mangrove eco-systems lose large amounts of carbon and nutrients via tides and lateral drainage. The principal pathway to recycle nutrients in a tropical terrestrial forest is via the rapid recycling of litter within a relatively thin layer of soil humus, whereas the main pathway in mangrove forests is via close coupling between soil microbes and roots to deep soil horizons, which serves to lessen the force of tidal drainage, at least to a level that is less than at the surface of the forest floor. Furthermore, many mangrove forests accumulate dead roots in peat which may serve as a reservoir to retain material within the system.

Compared with tropical humid evergreen forests, mangroves invest more energy in roots than in foliage (Table 10.1). Given that mangroves are subjected to intense water circulation, this seems a wise investment. The low rates of heterotrophic respiration in mangrove forests at first seems puzzling considering their life in waterlogged soils, but if "unaccounted for" carbon is considered as soil respiration, the rates of heterotrophic respiration and the ratio of R_e/GPP are equivalent between forest types (0.90 for mangroves, 0.88 for humid terrestrial forests). Mangrove NPP is a greater proportion of GPP than in their terrestrial counterparts (Table 10.1),

Table 10.1 Comparison of major carbon fluxes (g C m^{-2} year^{-1}) through mangrove forests and tropical humid evergreen forests

Process	Mangrove forests	Humid forests
GPP	4,596	3,551
NPP (%GPP)	1,930 (42%)	852 (24%)
fNPP (%total NPP)	425 (22%)	316 (37%)
wNPP	419 (22%)	212 (25%)
rNPP	1,086 (56%)	324 (38%)
NEP	1,018	403
R_e	3,125	3,061
R_a	2,644	2,323
R_h	481	877
R_e/GPP	0.68	0.88
	0.90[a]	

From Alongi (2009)

GPP gross primary production; *NPP* net primary production; *fNPP* foliage net primary production; *wNPP* wood net primary production; *rNPP* root net primary production; *NEP* net ecosystem production; R_e total ecosystem respiration; R_a canopy respiration; R_h heterotrophic respiration
[a]Assumes NEP as DIC export

but given the high level of variability within each dataset, it seems likely that tropical mangrove and humid evergreen forests allocate carbon similarly. Compared with terrestrial forests, however, the life of mangroves at the interface between land and sea comes at considerable energetic expense (Feller et al. 2010).

10.7 Future Research Directions

The biogeochemistry of mangrove forests in relation to coastal hydrology is still in its infancy. Nevertheless, the most urgent research needs can be prioritized on the basis of clarifying the role of mangroves in global change:

- More eddy covariance studies are required to better understand the vertical flow of carbon dioxide and other gases from the soil surface to the top of the canopy, as current data underscores the size and importance of fluxes between forest and atmosphere.
- Studies of the flow of groundwater nutrients is urgently required to understand the magnitude of this pathway in whole-ecosystem scale budgets. Factors regulating the scale of this pathway are unknown and need to be done in collaboration between biogeochemists and hydrologists.
- Nutrient limitation in relation to hydrology and physicochemistry across the intertidal zone needs to be better understood. At present, we know that most mangroves are either N- or P-limited or both, but we do not know why.
- The role of animal burrows and other structures within the forest floor in coastal hydrology and their biogeochemical consequences need to be better quantified. Present information acknowledges the importance of the forest floor in soil biogeochemical processes, but information is still limited, especially for nitrogen and phosphorus cycling.
- Factors affecting mass accumulation (and erosion) rates of mangrove soils are virtually unknown. Despite the fact that there is a fair amount of radiochemical data, regulatory factors affecting the vertical profiles of radionuclides have not been explored.
- Long-term studies to examine decadal changes in mangroves in relation to shoreline development are urgently needed. Few studies have ever attempted to examine the cycle of mangrove succession and shoreline development over sufficient timescales to fully delineate the process.
- Studies continue to be published on the dynamics of litter decomposition, but few are extant on root decomposition and fine root production. Root growth and production estimates are needed to close the budget on carbon allocation by trees.
- Models are needed to quantify the upper limits of sustainable use of mangrove resources, especially wood.
- The mystery of the "unaccounted for" carbon in the global carbon models needs to be solved.

References

Alongi DM (1998) Coastal ecosystem processes. CRC Press, Boca Raton

Alongi DM (2009) The energetics of mangrove forests. Springer, Dordrecht

Alongi DM, Boto KG, Robertson AI (1992) Nitrogen and phosphorus cycles. In: Robertson AI, Alongi DM (eds) Tropical mangrove ecosystems. American Geophysical Union, Washington, pp 251–292

Alongi DM, Trott LA, Wattayakorn G et al (2002) Below-ground nitrogen cycling in relation to net canopy production in mangrove forests for southern Thailand. Mar Biol 140:855–864

Ayukai T, Wolanski E (1996) Importance of biologically-mediated removal of fine particles from the Fly River plume, Papua New Guinea. Est Coast Shelf Sci 44:629–639

Barnes J, Purvaja R, Ramesh R et al (2007) Nitrous oxide fluxes in Indian mangroves: tidal production mechanisms, fluxes and global significance. In: Tateda Y (ed) Greenhouse gas and carbon balances in mangrove coastal ecosystems. Gendai Tosho, Kanagawa, pp 139–151

Berger U, Adams M, Grimm V et al (2006) Modelling secondary succession of neotropical mangroves: causes and consequences of growth reduction in pioneer species. Ecol Model 132:287–302

Borges AV, Djenidi S, Lacroix G et al (2003) Atmospheric CO_2 flux from mangrove surrounding waters. Geophys Res Lett. doi:10.1029/2003GL017143

Boto KG, Bunt JS (1981) Dissolved oxygen and pH relationships in northern Australian mangrove waterways. Limnol Oceanogr 26:1176–1178

Bouillon S, Borges AV, Castañeda-Moya E et al (2007) Mangrove production and carbon sinks: a revision of global budget estimates. Glob Biogeochem Cycles 22:GB2013. doi:10.1029/2007GB003OS2

Dittmar T, Hertkorn N, Kattner G, Lara RJ (2006) Mangroves, a major source of dissolved organic carbon to the oceans. Glob Biogeochem Cycles 20: GB1012. doi:10.1029/2005GB002570

Drexler JZ, DeCarlo EW (2002) Source water partitioning as a means of characterizing hydrologic function in mangroves. Wetlands Ecol Manage 10:103–113

Feller IC, McKee KL, Whigham DF et al (2002) Nitrogen vs phosphorus limitation across an ecotonal gradient in a mangrove forest. Biogeochemistry 62:145–175

Feller IC, Lovelock CE, Berger U et al (2010) Biocomplexity in mangrove ecosystems. Annu Rev Mar Sci 2:395–417

Furukawa K, Wolanski E, Mueller H (1997) Currents and sediment transport in mangrove forests. Est Coastal Shelf Sci 44:301–310

Gattuso J-P, Frankignoulle M, Wollast R (1998) Carbon and carbonate metabolism in coastal aquatic ecosystems. Annu Rev Ecol Syst 29:405–434

Ghosh S, Jana TK, Singh BN et al (1987) Comparative study of carbon dioxide system in virgin and reclaimed mangrove waters of Sunderbans during freshnet. Mahasagar Bull Natl Inst Oceanogr 20:155–161

Jennerjahn TC, Ittekkot V (2002) Relevance of mangroves for the production and deposition of organic matter along tropical continental margins. Naturwissenschaften 89:23–30

Kitheka JU (1996) Water circulation and coastal trapping of brackish water in a tropical mangrove-dominated bay in Kenya. Limnol Oceanogr 41:169–176

Kitheka JU, Mwashote BM, Ohowa BO et al (1999) Water circulation, groundwater outflow and nutrient dynamics in Mida Creek, Kenya. Mangr Salt Marsh 3:135–146

Koné YJ-M, Borges AV (2008) Dissolved inorganic carbon dynamics in the waters surrounding forested mangroves of the Ca Mau Province (Vietnam). Est Coast Shelf Sci 77:409–421

Kristensen E, Bouillon S, Dittmar T et al (2008) Organic carbon dynamics in mangrove ecosystems: a review. Aquat Bot 89:201–219

Mazda Y, Kobashi D, Okada S (2005) Tidal-scale hydrodynamics within mangrove swamps. Wetlands Ecol Manage 13:647–655

Mazda Y, Wolanski E, Ridd PV (2007) The role of physical processes in mangrove environments: manual for the preservation and utilization of mangrove ecosystems. TERRAPUB, Tokyo

McKee KL, Feller IC, Popp M et al (2002) Mangrove isotopic ($^{15}\delta N$ and $^{13}\delta C$) fractionation across a nitrogen vs phosphorus limitation gradient. Ecology 83:1065–1075

Nixon SW (1988) Physical energy inputs and the comparative ecology of lake and marine ecosystems. Limnol Oceanogr 33:1005–1025

Odum EP (1968) A research challenge: evaluating the productivity of coastal and estuarine water. In: Proceedings of the second sea grant congress. University of Rhode Island, Graduate School of Oceanography, Kingston, pp 63–64

Odum WE, Odum EP, Odum HT (1995) Nature's pulsing paradigm. Estuaries 18:547–555

Ovalle ARC, Rezende CE, Lacerda LD et al (1990) Factors affecting the hydrochemistry of a mangrove tidal creek, Sepetiba Bay, Brazil. Est Coast Shelf Sci 31:639–650

Ralison OH, Borges AV, Dehairs F et al (2008) Carbon biogeochemistry of the Betsiboka estuary (north-western Madagascar). Org Geochem 39:137–149

Ram ASP, Nair S, Chandramohan D (2003) Seasonal shift in net ecosystem production in a tropical estuary. Limnol Oceanogr 48:1601–1607

Richey JE, Melack JM, Aufdenkampe AK (2002) Outgassing from Amazonian rivers and wetlands as a large tropical source of atmospheric CO_2. Nature 416:617–620

Ridd PV (1996) Flow through animal burrows in mangrove creeks. Est Coast Shelf Sci 43:617–625

Ridd PV, Wolanski E, Mazda Y (1990) Longitudinal diffusion in mangrove-fringed tidal creeks. Est Coast Shelf Sci 31:541–554

Ridd PV, Steiglitz T, Larcombe P (1998) Density-driven secondary circulation in a tropical mangrove estuary. Est Coast Shelf Sci 47:621–632

Robertson AI, Alongi DM, Boto KG (1992) Food chains and carbon fluxes. In: Robertson AI, Alongi DM (eds) Tropical mangrove ecosystems. American Geophysical Union, Washington, pp 293–326

Sam R, Ridd PV (1998) Spatial variations of groundwater salinity in a mangrove-salt flat system, Cocoa Creek, Australia. Mangr Salt Marsh 2:121–132

Stieglitz T, Ridd PV (2001) Trapping of mangrove propagules due to density-driven secondary circulation in the Normanby River estuary, NE Australia. Mar Ecol Progr Ser 211:131–142

Susilo A, Ridd PV (2005) The bulk hydraulic conductivity of mangrove soil perforated with animal burrows. Wetlands Ecol Manag 13:123–133

Twilley RR, Chen R (1998) A water budget and hydrology model of a basin mangrove forest in Rookery Bay, Florida. Mar Freshwater Res 49:309–323

Upstill-Goddard RC, Barnes J, Ramesh R (2007) Are mangroves a source or sink for greenhouse gases? In: Tateda Y (ed) Greenhouse gas and carbon balances in mangrove coastal ecosystems. Gendai Tosho, Kanagawa, pp 127–138

Wanek W, Hofmann J, Feller IC (2007) Canopy interactions of rainfall in an offshore mangrove ecosystem dominated by Rhizophora mangle (Belize). J Hydrol 345:70–79

Wolanski E (1992) Mangrove hydrodynamics. In: Robertson AI, Alongi DM (eds) Tropical mangrove ecosystems. American Geophysical Union, Washington, pp 43–62

Wolanski E (1995) Transport of sediment in mangrove swamps. Hydrobiologia 295:31–42

Wolanski E (2007) Estuarine ecohydrology. Elsevier, Amsterdam

Wolanski E, Ridd P (1986) Tidal mixing and trapping in mangrove swamps. Est Coast Shelf Sci 23:759–771

Wolanski E, Mazda Y, King B et al (1990) Dynamics, flushing and trapping in Hinchinbrook Channel, a giant mangrove swamp. Est Coast Shelf Sci 31:555–579

Woodroffe C (1992) Mangrove sediments and geomorphology. In: Robertson AI, Alongi DM (eds) Tropical mangrove ecosystems. American Geophysical Union, Washington, pp 7–41

Woodroffe CD (2003) Coasts: form, process and evolution. Cambridge University Press, Cambridge

Chapter 11
Hydrology and Biogeochemistry
of Tropical Montane Cloud Forests

Thomas W. Giambelluca and Gerhard Gerold

11.1 Introduction

Tropical montane cloud forests (TMCFs) are differentiated from other forest types by their frequent immersion in fog. This characteristic implies that TMCFs are unique in their hydrological functioning, as they receive a substantial amount of water input via direct deposition of cloud droplets. Because it is generally associated with reduced solar radiation and increased humidity, frequent fog occurrence can lower evapotranspiration (ET). Many TMCFs also have certain characteristic structural and floristic features, which have further hydrological effects. Cloud water is often chemically different from rain water (Heath 2001; Liang et al. 2009); hence, fog deposition can alter inputs of nutrients and other chemicals into the ecosystem. The hydrological, biological, and chemical characteristics of cloud forests give rise to differences in biogeochemical processes as well.

Cloud forests are valued as reservoirs of biological diversity, are noted for high levels of endemism, and are recognized as critical refugia for many endangered species (Bubb et al. 2004). Meyer (2010) notes that TMCFs are the most diverse plant communities found in French Polynesia, harboring 60% to more than 70% of the archipelago's endemic vascular plant species. Owiunji and Pumptre (2010) concluded that conservation of six cloud forest sites in the Albertine Rift of central Africa would result in protection of 94% of endemic mammals and 95% of endemic birds found in the region. Despite recognition of the biotic richness and importance of these forests, they are among the most threatened terrestrial ecosystems (Scatena et al. 2010). TMCFs are suffering rapid decline in many areas due to clearing for agriculture, alien species invasion, and climate change.

Montane cloud forests are known to occur at higher latitudes (Bruijnzeel et al. 2010); however, most are located within the tropics (Mulligan 2010). The United Nations Environment Programme defines cloud forests as "a type of evergreen mountain forest in tropical areas, where local conditions cause cloud and mist to be frequently in contact with the forest vegetation." (UNEP Tropical Montane Cloud Forests; http://www.unep-wcmc.org/forest/cloudforest/cloudforests.cfm#, accessed 24 May 2010). The elevation at which ground-level clouds are found varies throughout the tropics. Jarvis and Mulligan (2010) examined the locations

and characteristics of 477 cloud forest sites in 62 countries. Of those sites, 83% are located in the northern hemisphere tropics and 85% are found in the 400–2,800 m elevation range, with a mean elevation of 1,687 m. On average, cloud forests are 4.2°C cooler and receive 185 mm more rainfall annually than tropical montane forests in general (Jarvis and Mulligan 2010).

Several different types of TMCFs have been identified (Scatena et al. 2010). Moving up in elevation from lower montane rainforest (LMRF), the transition to lower montane cloud forest (LMCF) is noted by an increase in moss cover on tree stems. This zone generally has trees in the 15–35 m height range and gives way to upper montane cloud forest (UMCF), with lower-statured trees of 2–20 m and greater moss abundance (Scatena et al. 2010). At higher elevations, stunted trees are found with ferns dominating in the understory (Kappelle 1995). This zone is often referred to as elfin cloud forest (ECF) or subalpine cloud forest (SACF).

11.2 TMCF Hydrology

As noted, TMCFs have a unique hydrological regime. In general, the effects of fog presence tend to increase the wetness of these forests by increasing water input and reducing evaporative loss. The effects of fog certainly vary among and within individual cloud forests. However, observations of hydrological processes in TMCFs are relatively sparse, and efforts to model these processes are in the early stages of development. In this section, some of the methods and findings of field observations and modeling of cloud forest hydrology are summarized. Comprehensive summaries of TMCF hydrology have previously been published by Bruijnzeel and Proctor (1995) and Bruijnzeel (2001, 2005).

11.2.1 Cloud Water Interception

Climate and forest structure control partitioning of water in the canopy (Crockford and Richardson 2000). Water input in TMCFs are determined by the amount, intermittency, and duration of rain events, the frequency and duration of fog events, and wind velocity. Vegetation roughness, aboveground biomass distribution, and connectivity affect the capture and redistribution of rain and fog. Net radiation, temperature, humidity, and wind speed influence evaporation from the wet canopy.

Several approaches have been adopted to estimate the amount of water added to cloud forest ecosystems via direct interception of cloud droplets, including basin-scale water balance, passive fog gauge measurements, wet-canopy water balance (WCWB), stable isotope analysis, and eddy covariance measurements. One of the earliest investigations of the hydrological effect of fog in montane forests was done using the basin-scale water balance approach. Working astride the Continental Divide in Costa Rica, Zadroga (1981) showed that streamflow in the foggier

Atlantic watersheds was approximately equal to rainfall, while that of the Pacific watersheds was much lower (34% of rainfall). Zadroga's (1981) conclusion, that unmeasured input of water from fog interception was responsible for the high runoff coefficient in the Atlantic basin, was later supported by Calvo (1986).

11.2.2   Passive Fog Gauges

Until recently, much of the field work on cloud water interception has been carried out using passive fog gauges or "fog catchers" (Bruijnzeel and Proctor 1995). Numerous TMCF sites have been equipped with fog gauges of several different designs. These devices were designed to capture fog droplets when mounted at or above the canopy level. Fog gauges can provide a reliable indication of when fog has occurred and can be used to assess relative degrees of fog exposure for different sites. Although authors have often equated such measurements with cloud water interception by vegetation, this is problematic. For many designs, interpreting measurements is made difficult by the inability to distinguish rainfall from fog. Combining fog and wind-driven rainfall (WDR) under the term horizontal precipitation has been suggested. In addition, the catch efficiency of some gauges is also affected by wind direction (Giambelluca et al. 2010b). Even when these effects are mathematically removed, fog gauges generally do not accurately represent CWI of the natural vegetation (Bruijnzeel 2005). Nonetheless, the value of passive fog gauge measurements as a means of determining spatial patterns in local fog climatology is sufficient that work continues on the appropriateness of different gauge designs. Giambelluca et al. (2010b) found that measurements made with a planar screen gauge were not well correlated with cloud water flux. Comparing the performance of the wire harp, tunnel-type, and cylindrical screen gauges, Frumau et al. (2010) concluded that the Juvik-type gauge was superior to the other designs because its collection efficiency remained near 100% independent of wind speed and direction.

11.2.3   Wet-Canopy Water Balance

In more recent years, much of the cloud forest hydrology research has been based on the WCWB approach, which involves measuring or estimating all the inputs and outputs of water to and from the vegetation canopy (Fig. 11.1). A simple mass balance equation describes the partitioning of water in the canopy:

$$RF + CWI = TF + SF + E_i + \Delta S \tag{11.1}$$

where RF is gross rainfall, usually measured above the canopy or in a nearby clearing, CWI is cloud water interception, TF is throughfall, the water falling freely
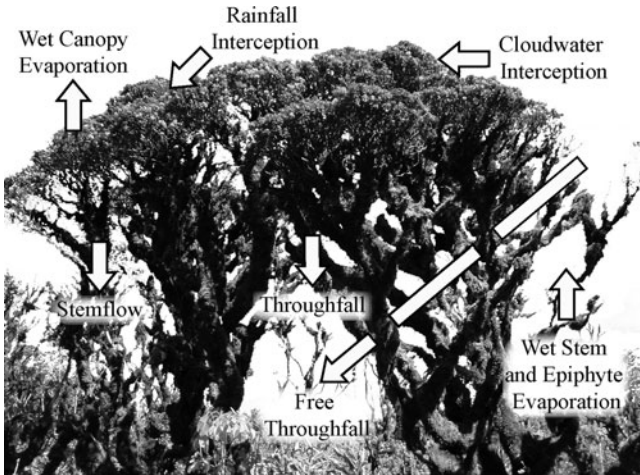
Fig. 11.1 Wet-canopy water flows. All water transfers shown are part of the wet-canopy water balance (after DeLay (2005), reproduced with permission)

through the canopy, splashing off the canopy surfaces, or dripping from leaves, branches, and stems, SF is stemflow, water running down the stems of trees, E_i is interception evaporation, and ΔS is the change in canopy water storage. All terms are in depth units (e.g., mm). With measurements of RF, TF, and SF, and estimates of E_i based on meteorological measurements, CWI can be determined from (11.1) as a residual. In many studies, an alternative approach is used, in which the amount of TF and SF derived from RF is estimated, and the excess of measured over estimated TF plus SF is attributed to CWI. Although this quantity can be used as an approximation of CWI, it does not account for fog deposition evaporated from the canopy. A better term for estimates derived in this fashion is fog drip (FD).

In relation to RF, TF and SF in tropical montane forests vary considerably. Field observations of TF and SF in different types of TMCF complied by Bruijnzeel et al. (2010, Appendix 74.2) based on the work of Gerold et al. (2008), Vis (1986), Fleischbein et al. (2006), Oesker et al. (2010), Häger and Dohrenbusch (2010), Hölscher et al. (2004), Holder (2004), Dietz et al. (2006), Kumaran (2008), Cavelier et al. (1997), Edwards (1982), Gomez-Peralta et al. (2008), and Lundgren and Lundgren (1979). In LMRF, little affected by fog, TF ranged from 62 to 85% (mean of 14 sites: $71 \pm 7\%$) and SF from 0.1 to 2.2% (mean of seven sites: $1.0 \pm 0.8\%$). Exposure to fog generally produced higher amounts of TF and SF in relation to RF in LMCF: TF had a range of 54–106% (mean of 23 sites: $81 \pm 11\%$) and SF ranged from 0.2 to 8.8% (mean of ten sites: $2.5 \pm 2.6\%$). With greater fog exposure in UMCF, TF was 64–179% of RF (mean of 17 sites: $101 \pm 27\%$) and for SF the range was 0.1–30.5% (mean of ten sites: $10 \pm 11\%$). At SACF-ECF sites, the percentages were 75–126% (mean of eight sites: $106 \pm 21\%$, excluding 1 outlier) for TF and 2.8–18% (mean of six sites: $7.2 \pm 5.8\%$) for SF.

Bruijnzeel et al. (2010, Fig. 74.12a and Appendix 74.3) also compiled field-based E_i estimates. Those results show that E_i generally decreases with elevation: LMRF,

665 mm yr^{-1} (32% of RF, $n = 1$); LMCF, 571 ± 201 mm yr^{-1} ($24 \pm 6\%$ of RF, $n = 9$); UMCF, 385 ± 181 mm yr^{-1} ($6.2 \pm 1.7\%$ of RF, $n = 3$); and SACF-ECF, 193 ± 107 mm yr^{-1} ($9.5 \pm 5.0\%$ of RF, $n = 1$).

Using the mean values of each canopy water partitioning component based on Bruijnzeel et al. (2010), summarized above, it is possible to derive estimates of the CWI fraction for each forest type as:

$$\frac{\text{CWI}}{\text{RF}} = \frac{\text{TF}}{\text{RF}} + \frac{\text{SF}}{\text{RF}} + \frac{E_i}{\text{RF}} - 1 \qquad (11.2)$$

Doing so suggests mean CWI fractions of 4.0, 7.5, 17, and 23% of RF for LMRF, LMCF, UMCF, and SACF-ECF, respectively. However, these averages belie the wide range in CWI estimates obtained in various settings. As Bruijnzeel et al. (2010) note, the CWI estimates available so far are not sufficient in number to establish regional patterns. As expected, though, CWI tends to be higher at wetter, windier sites (Bruijnzeel et al. 2010). Two examples illustrate the diversity in observed CWI values. Holwerda et al. (2010b) used the WCWB approach to estimate CWI in mature and secondary LMCF at ~2,100 m elevation in Veracruz, Mexico. They found that CWI contributed only about 0.15 mm day^{-1} (1.7% of RF) and 0.10 mm day^{-1} (1.1% of RF), respectively, at the two sites. In contrast, Takahashi et al. (2010) also utilized the WCWB to estimate CWI for two LMCF sites in Hawai'i, an intact native forest site (1,201 m elevation) and a site invaded by the alien tree *Psidium cattleianum* (1,029 m elevation), finding values of 3.3 mm day^{-1} (37% of RF) and 2.0 mm day^{-1} (20% of RF), respectively. Obviously, differences in climate among sites, especially in fog frequency, liquid water content (LWC), and wind speed play a large role in the wide range of observed CWI amounts.

11.2.4 Eddy Covariance Approach

Over continuous, homogeneous vegetation, interception of fog being transported by wind moving parallel to the canopy surface can be conceptualized as a turbulent transfer process. The terminal velocity of fog droplets is low, and hence, turbulent eddies are the principal means by which fog is transported downward into the canopy, where it way be deposited by impaction on the leaves, branches, and stems of trees and shrubs or on epiphytes, or by reaching a sheltered area where droplets will have time to settle by gravity. Were the movement of all droplets to be strictly parallel to the canopy surface, fog deposition would occur only at exposed forest edges, isolated trees, or along topographic ridges. The continuous turbulence-driven downward transport of fog-rich air is required to maintain cloud water interception over continuous canopy surfaces. With this in mind, attempts have been made to utilize the eddy covariance technique to observe the downward flux of fog droplets over vegetation, as a direct measurement of cloud water interception (Eugster et al. 2006; Schmid et al. 2010). The eddy covariance technique, which is widely used to measure fluxes of energy and trace gases over terrestrial ecosystems,

derives vertical fluxes as a function of the covariance of vertical wind velocity and the concentration (or magnitude) of the appropriate scalar quantity (Baldocchi et al. 1988); in this case, the LWC of the air.

11.2.5 Field Estimates of CWI

Table 11.1 summarizes CWI estimates derived from field observations of WCWB or from direct measurements using eddy covariance at a range of TMCF sites. Among the studies compiled in Table 11.1, CWI averages 2.1 ± 2.1 mm day^{-1} and ranges from 0.1 mm day^{-1} (four sites) to 9.7 mm day^{-1}. Expressed as a percentage of RF, the average is $57 \pm 104\%$ and the range is 1–465%. Subdividing the sites into groups according to exposure – leeward, windward, and ridge (Table 11.1) – provides some explanation of this extreme range. TMCFs are generally found within orographic clouds. While these clouds can form on leeward slopes under some circumstances or can persist as they are advected from windward to leeward exposures, they are much more frequent and often driven by stronger winds on windward slopes. The site grouping in Table 11.1 bears this out, with mean CWI of 0.3 ± 0.2 mm day^{-1} ($19 \pm 8\%$ of RF) for sites with leeward exposures and 1.6 ± 1.4 mm day^{-1} ($16 \pm 15\%$ of RF) for windward sites. In particular, CWI of the ridge-top sites and isolated trees (4.0 ± 2.6 mm day^{-1}; $154 \pm 163\%$ of RF) are clearly extreme. The ridge sites generally experience high wind speeds, and vegetation is fully exposed to the fog-laden air. Exposure of the entire vegetation profile to wind is a characteristic of ridge-top vegetation, isolated trees, and forest edges. These zones are known to be hotspots for CWI. Notable are the Lānaʻihale sites (Table 11.1) near the summit of Lānaʻi Island, Hawaiʻi, where alien *Araucaria* trees were planted decades ago along exposed windward ridgelines to enhance fog and wind-driven rain capture (Juvik et al. 2010). While these highly exposed sites can have spectacular rates of CWI, these estimates obviously cannot be extrapolated onto the adjoining hillslopes. Excluding the ridge sites and isolated trees, among the sites listed in Table 11.1, CWI averages 1.3 ± 1.4 mm day^{-1} ($17 \pm 14\%$ of RF).

11.2.6 Stable Isotope Approach

Stable isotopes of oxygen and hydrogen in water can be used as a tracer to distinguish fog from rain. Fog droplets are isotopically enriched, having higher concentrations of heavy isotopes (^{2}H and ^{18}O) in comparison with rain water (Scholl et al. 2010). This has led several researchers to assess fog input to ecosystems by comparing the isotopic concentrations in water sampled within terrestrial ecosystems (e.g., soil water, stream water, groundwater, and/or plant tissue water) with the relative isotopic compositions of local fog and rain (Ingraham

Table 11.1 Field observations of cloud water interception and fog drip within tropical montane cloud forests

Site	Elev (m)	Exposure	Aspect	Forest type	Long-term mean annual RF (mm day⁻¹)	Study period mean annual RF (mm day⁻¹)	CWI or FD (mm day⁻¹)	CWI/RF or FD/RF (%)	Method	Source
Leeward										
Hawai'i, Auwahi	1,219	Leeward	S	LMCF	2.8	2.6	0.5	20%	WCWB	1
Hawai'i, Kona (North)	1,047	Leeward	W	Degraded LMCF	4.1	0.7	0.1	12%	FD	2
Hawai'i, Kona (South)	962	Leeward	W	LMCF	4.1	1.0	0.3	27%	FD	2
Mean	1,076					1.4	0.3	19%		
Standard deviation	131					1.0	0.2	8%		
Windward										
Australia, N Queensland (ML1)	1,100	Windward	S	LMCF		7.8	0.6	7%	WCWB	3,4,5
Australia, N Queensland (ML2)	1,160	Windward	N	LMCF		7.3	1.1	15%	WCWB	3,4,5
Australia, N Queensland (UB)	1,050	Windward	SE	LMCF		6.6	1.5	23%	WCWB	3,4,5
Costa Rica, San Gerardo	1,460	Windward	NE	LMCF	16.4	7.5	0.3	4%	EC	6
Hawai'i, Waikamoi	1,951	Windward	NE	UMCF	7.4	6.5	3.3	51%	WCWB	1
Hawai'i, Kīlauea (Thurston)	1,201	Windward	NNE	LMCF	6.8	8.9	3.3	37%	WCWB	7
Hawai'i, Kīlauea (Ola'a)	1,029	Windward	E	Invaded LMCF	10.0	10.2	2.0	20%	WCWB	7
Hawai'i, Kohala	1,180	Windward	SE	ECF	11.9	9.0	0.6	7%	FD	8
Mexico, Veracruz (MAT)	2,060	Windward	SSE	LMCF	5.5–8.2	8.7	0.1	2%	WCWB	9
Mexico, Veracruz (SEC)	2,140	Windward	SSW	Secondary LMCF	5.5–8.2	8.7	0.1	1%	WCWB	9
Puerto Rico, Luquillo (Pico del Oeste)	970	Windward	E	ECF	10.9	10.9	1.4	13%	WCWB	10
Puerto Rico, Luquillo (Pico del Este)	1,015	Windward	ENE	ECF	28.0	28.0	4.4	16%	EC	11
Mean	1,360					10.0	1.6	16%		
Standard deviation	437					5.8	1.4	15%		
Ridge/isolated tree										
Australia, N Queensland (BK)	1,560	Ridge		UMCF	22.2	14.5	5.9	41%	WCWB	3,4,5

(continued)

Table 11.1 (continued)

Site	Elev (m)	Exposure	Aspect	Forest type	Long-term mean annual RF (mm day⁻¹)	Study period mean annual RF (mm day⁻¹)	CWI or FD (mm day⁻¹)	CWI/RF or FD/RF (%)	Method	Source
Australia, SE Queensland	1,000	Windward-isolated tree	S	LMCF	3.7	2.7	0.9	35%	FD	12
Hawai'i, Lāna'ihale	838	Ridge-isolated tree		Planted alien tree		3.5	2.1	60%	WCWB	13
Hawai'i, Lāna'ihale	1,021	Ridge-isolated tree		Planted alien tree	2.7	3.0	4.4	147%	FD	14
Hawai'i, Lāna'ihale	921	Ridge-isolated tree		Planted alien tree	2.5	1.7	7.9	465%	FD	14
Hawai'i, Lāna'ihale	765	Ridge-isolated tree		Planted alien tree	2.2	1.4	2.5	179%	FD	14
Mean	1,018					4.5	4.0	154%		
Standard deviation	283					5.0	2.6	163%		
All sites										
Mean	1,221					7.2	2.1	56%		
Standard deviation	392					6.1	2.1	104%		
Nonridge/isolated tree sites										
Mean	1,303					8.3	1.3	17%		
Standard deviation	408					6.3	1.4	14%		

Note: *RF* rainfall, *CWI* cloud water interception, *FD* fog drip (additional throughfall plus stemflow due to fog deposition), *WCWB* wet-canopy water balance method, *EC* eddy covariance method

Sources: (1) Giambelluca et al. (2010a); (2) Brauman et al. (2010); (3) McJannet et al. (2007); (4) McJannet et al. (2010); (5) (McJannet, personal communication 2010); (6) Schmid et al. (2010); (7) Takahashi et al. (2010); (8) DeLay (2005); (9) Holwerda et al. (2010b); (10) Holwerda et al. (2010a); (11) Eugster et al. (2006); (12) Hutley et al. (1997); (13) Ekern (1964); (14) Juvik et al. (2010)

and Mark 2000; Scholl et al. 2007, 2010). On Maui Island, Hawai'i, Scholl et al. (2002) found isotopic enrichment of waters in mountain streams and springs to be high relative to volume-weighted rainfall from different elevations along the mountain slope. They inferred that fog input was contributing a substantial amount of water to the local hydrological cycle. Scholl et al. (2007) later estimated fog input at two Maui cloud forest sites, a wet windward site and a relatively dry leeward site. Using an isotopic mixing model, they estimated 37 and 46% of the total precipitation was derived from cloud water at the windward and leeward sites, respectively. At these same sites, CWI was estimated to be 34 and 16.5% of total water input based on the WCWB approach (Giambelluca et al. 2010a). The poor agreement may be due to errors in the WCWB estimates and/or the indistinct isotopic signatures often found for mountain sites frequently immersed in orographic clouds producing rainfall, including Hawai'i (Scholl et al. 2007).

11.2.7 Modeling CWI

Field measurement of CWI is difficult, expensive, and error prone. The results of any such measurement are valid only at the location of the observations and only for the climate and vegetation conditions during the measurements. It is sometimes desirable to predict the effects of future land cover changes, but this cannot be done using field measurements in the existing vegetation. Also, because of its dependence on climate and vegetation factors, CWI is likely to be highly spatially variable. Hence, the applicability of point measurements is limited. To ascertain the effects of fog input on hydrological and ecological processes, the spatial patterns of CWI must be determined across TMCF landscapes. This clearly points to the need for process-based modeling of CWI. Several researchers have attempted to develop models of cloud water deposition. Lovett (1984) developed a one-dimensional CWI model driven by inputs of wind velocity, LWC of the air, drop size spectrum, and vegetation parameters. Walmsley et al. (1996) and Klemm et al. (2005) have used physically based models with parameterizations of vegetation and, in some cases, topography, and driven by field measurements of wind velocity and LWC or fog interception by a passive fog gauge to derive point estimates or spatial patterns of CWI. Mesoscale meteorological model estimates of cloud water advection can be used to develop spatially dependent input fields for simulating the pattern of CWI.

A notable advance in CWI modeling was initiated when the FIESTA (Fog Interception and Enhanced Streamflow in Tropical Areas) project set out to determine the effects of cloud forest conversion to pasture on hydrological processes in the Tiláran Range of northern Costa Rica (http://www.falw.vu/~fiesta/, accessed 11 June 2011). Clearing of TMCF for pasture in Central America was suspected of causing the observed decline in the discharge of some mountain streams in the region. To address project objectives, a spatially distributed modeling approach was adopted. Much of the model development made use of standard hydrological methods. But, a specialized fog input component had to be developed

(Mulligan and Burke 2005). Models were developed for three different spatial scales, 3–10 ha, 10K ha, and ≥6 Mha. Because of the importance of local-scale wind effects in the high relief areas under investigation, the FIESTA modelers incorporated an algorithm to estimate the spatial distribution of WDR and fog. This feature takes into account topographically induced variations in local wind velocity and direction and the interaction of rainfall- and fog-laden winds with landscape facets of different slope and aspect, and vegetation patches of varying character- istics. These capabilities allow the model to more accurately represent the patterns of rainfall and fog deposition in complex landscapes (Mulligan and Burke 2005). The FIESTA model is now available as a web-based, pan-tropical application for use as a tool in hydrological research or support of policy exercises (http:// www.policysupport.org/cgi-bin/aguaandes/start.cgi?, accessed 11 June 2010).

Fog input estimated by the FIESTA model is low in comparison with many field- based estimates. For most TMCF areas, CWI was estimated to be less than 0.4 mm day^{-1} on a mean annual basis, with highly exposed sites reaching 1.1 mm day^{-1} (Mulligan and Burke 2005). Recall that field-based estimates average 1.3 mm day^{-1} for sites other than exposed ridges and isolated trees and reach as high as 7.9 mm day^{-1} for highly exposed sites (Table 11.1). It is not clear whether inaccuracies in the model or errors in field observations are responsible for this discrepancy. However, it calls attention to the fact that rainfall is likely to be consistently underestimated leading to overestimates of CWI in field studies. First, rainfall under-catch due to turbulence induced by the rain gauge can be significant. This effect can be accounted for if wind velocity measurements and estimates of the drop size spectrum are available. The second effect is that of WDR. Redistribution of rainfall under high wind speeds can be very significant in sloping terrain (Sharon 1980; cf. Blocken et al. 2005) or for stands with irregular crown heights (Herwitz and Slye 1992). Again, this effect can be corrected (e.g., Giambelluca et al. 2010b), but is often ignored. Because wind causes rain to fall diagonally, windward slopes, where most CWI fieldwork has been conducted, actually receive substantially higher amounts of rainfall than indicated by a rain gauge with a horizontal orifice. This consistent bias in the observed rainfall, if not removed in the analysis, produces an overestimate of CWI when estimating with the WCWB approach (11.1). From a hydrologist's perspective, this may be a fine point, as it may not matter whether it is called fog or WDR, it counts as water input over and above the observed rainfall. However, this would be the case with or without the presence of fog. Hence, it is important to make this distinction when assessing the unique hydrological characteristics of cloud forests.

11.2.8 Role of Epiphytes in Hydrology of TMCFs

TMCFs are often most recognizable by the abundance of epiphytes, which, in some cloud forests, cover a large portion of stems and branches of trees (Fig. 11.2). High epiphyte biomass is correlated with stand age (Köhler et al. 2007, 2010) and more

Fig. 11.2 Elfin cloud forest at Alakahi, Hawai'i, showing the characteristic low stature, compact crowns, and abundance of nonvascular epiphytes (photo by John DeLay, Delay (2005), reproduced with permission)

constant fog immersion (Hietz 2010), and favors long-lived trees with high stem surface area (Hofstede et al. 1993). Many studies of the hydrologic role of epiphytes in TMCFs have focused on the "sponge effect" of stem- and branch-covering mats of nonvascular epiphytes (mostly mosses, liverworts, and lichens), which are able to retain large amounts of water (Pocs 1980; Veneklaas et al. 1990). The water storage capacity of mossy epiphytes is typically two to five times their dry weight (Mulligan et al. 2010). Epiphytes water storage capacity is extremely high at some studied sites, up to 5.0 mm in LMCF in Monteverde, Costa Rica (Tobón et al. 2010), 7.2 mm of water at stand level in Columbian UMCF (Veneklaas et al. 1990), and around 8.0 mm at another Costa Rican LMCF site (Clark 1994, reported by Mulligan et al. 2010). Stand-level epiphyte water storage capacity in other cloud forests is generally lower than these values, but still significant in relation to storage capacities of other canopy elements. Mudd (2004) estimated stand level epiphyte water storage capacity to be 1.48 mm in native LMCF in Hawai'i. In a montane rainforest in Costa Rica, Hölscher et al. (2004) found that epiphytes had a maximum water storage capacity of 0.81 mm, a substantial level in comparison with estimated leaf water storage capacity (1.08 mm). Maximum ET rates by epiphytes were estimated to be 0.36 mm d^{-1} (Mudd 2004) and 0.23 mm d^{-1} (Hölscher et al. 2004), representing, respectively, 25 and 28% of epiphyte water storage capacity.

Nonvascular epiphytes are thought to readily capture incident rainfall, fog, and throughfall, in contrast to leaves and bare branches and stems, from which a substantial amount of water from impacting drops is lost by splash (Veneklaas et al. 1990). Water stored by epiphytes tends to drain slowly (Veneklaas et al. 1990) and, as Mudd (2004) showed in Hawai'i, most of the epiphyte biomass is found on the lowest portion of the stems where stored water evaporates more slowly. As a result, epiphyte water content tends to remain high, reducing available epiphytes water storage capacity, thereby minimizing the hydrological effects of epiphytes (Hölscher et al. 2004). Mulligan et al. (2010) found that epiphytes in LMCF at their Tambito, Columbia field site intercepted fog only very slowly

(less than 1% of rainfall), perhaps because of the sheltered location of the epiphyte biomass. Tobón et al. (2010) found higher fog absorption rates by epiphytes in Monteverde LMCF, averaging 49–63 ml h^{-1} per kg dry biomass (dry weight) during fog events.

Clearing (Köhler et al. 2007) and alien tree invasion (Mudd 2004) of TMCF have been shown to have lasting impacts on epiphytic biomass, and hence, on the hydrological effects of epiphytes. Epiphytic biomass was only 5 and 15% of that found in nearby old-growth forest for 10-to-15- and c. 40-year-old, secondary successional stands in Costa Rica, respectively (Köhler et al. 2007). In Hawaiian LMCF, a site invaded by the alien tree *P. cattleianum* had epiphytic biomass of 0.89 t ha^{-1} (of which only 5% was found colonizing the stems of invasive trees) compared with 2.57 t ha^{-1} in undisturbed forest (Mudd 2004). As a result, the epiphyte water storage capacity of the invaded site was reduced by 60%. For the same pair of sites, Takahashi et al. (2010) found that E_i was reduced by about 25% at the invaded site, due in part to the reduced canopy water storage capacity.

11.2.9   *Evapotranspiration in TMCF*

Frequent fog reduces incoming solar radiation and lowers vapor pressure deficit (Letts and Mulligan 2005), resulting in relatively low evaporative demand in TMCF (Bruijnzeel and Veneklaas 1998; McJannet et al. 2010). For example, potential ET was 61% lower in UMCF than in LMF along an elevational transect in the eastern Andes of Bolivia (Schawe et al. 2010). Canopy surfaces, including leaves, are wet during a higher percentage of the time in cloud forests, because of the additional source of water from CWI. Frequent wetting increases the amount of water lost to the atmosphere as wet-canopy evaporation, but may reduce transpiration. Katata et al. (2010) found that for their dry cloud forest study area, fog-wetted leaves led to increased stomatal conductance. But, transpiration was not increased because of compensating reduction in atmospheric demand.

The thin film of water on a wet leaf surface can effectively block gas exchange through the stomata. Wetting the undersides of leaves (abaxial surfaces), which occurs more commonly from fog deposition than from rainfall, is especially important in this regard, because for most TMCF species stomata are concentrated on the abaxial side. Letts and Mulligan (2005), for example, showed that wetted leaves have restricted CO_2 exchange when abaxial leaf surfaces are wetted by fog. This process affects both photosynthesis and transpiration.

High water input and poor soil drainage in some TMCF also lead to reduced transpiration (Santiago et al. 2000; Schawe et al. 2010). Santiago et al. (2000) found that poorly drained sites in LMCF in Hawai'i had significantly reduced transpiration related to lower leaf area.

Despite reduced transpiration, total ET of TMCF can be quite high, due to high interception evaporation rates. McJannet et al. (2010) reported mean annual ET of 1,518 mm at their Upper Barron site in Queensland, Australia.

11.2.10 Climate Change Effects

Bruijnzeel (2005) cited evidence that TMCF and the ecosystem services they provide, such as enhanced water inputs to streams and groundwater, may be negatively impacted by climate change. Lawton et al. (2001) presented evidence that regional climate effects of lowland deforestation in Central America were causing an upward shift in the lifting condensation level (LCL, the height of the orographic cloud base), resulting in a reduction in fog immersion frequency in Costa Rican TMCF. Simulations of doubled atmospheric CO_2 suggest that global warming may produce an upward shift in the LCL in Costa Rica (Still et al. 1999), and perhaps other areas of the tropics, with consequent impacts on TMCF. In many parts of the tropics, the upper limit of the orographic cloud and the upper boundary of TMCF, are defined by the trade-wind inversion (TWI), which caps upward motion in the atmosphere throughout much of the tropics. Cao et al. (2007) have shown evidence of a possible downward shift in the TWI over Hawai'i as a result of recent warming. Increases in the height of the LCL and/or decreases in the TWI level would reduce fog input to existing cloud forests and could also result in higher ET. These changes would cause severe reductions in moisture conditions with devastating ecological impacts, including extinction of species (Williams et al. 2003).

11.3 TMCF Biogeochemistry

As noted previously (see Sect. 11.1), hydrological processes in TMCFs are affected by direct interception of cloud water and reduced ET, which alters inputs of nutrients, the soil water budget, soil nutrient leachates, and nutrient cycling. For the first substantive review on TMCF biogeochemistry, see Bruijnzeel et al. (1995).

Major nutrient input fluxes are throughfall with fog interception, litterfall, the biological fixation of nitrogen, and the turnover of organic matter. Very few studies exist on output fluxes in TMCF with litter and soil leachates and surface runoff (Wilcke et al. 2008b). In this section, the main patterns of nutrient fluxes are summarized with revised field observations and some methods for assessing nutrient limitation. For soil nutrients and global inventory of soil chemistry, see Roman et al. (2010).

11.3.1 Litter Nutrients, Decomposition, and Mineralization

Total leaf litter varies between 2.3 and 5.7 t ha^{-1} year^{-1} (Bruijnzeel et al. 1995). Values for LMCF range between 2.3 and 8.4 (total fine litterfall 3.6–11) t ha^{-1} year^{-1}

and for UMCF between 3.4 and 6.5 (total fine litterfall 4.3–7.4) t ha^{-1} year^{-1} (Hafkenscheid 2000). The fraction of leaf litterfall in total fine litterfall (fine branches, fruits & seeds & others) shows values from 60 to 90%. We focus on leaf litter because of its higher importance for internal nutrient cycling and the comparison with leaf element concentrations.

The mean concentrations of major nutrients (N, P, Ca, K, Mg) in Bolivia lie within the normal global distribution range, but in Ecuador N and P values are higher and K reaches the upper value given by Hafkenscheid (2000) (Schawe 2005; Wilcke et al. 2002). Compared with leaf element contents, retranslocation in leaves seems negligible in LMCF, but in UMCF and SACF retranslocation processes increase (Columbia: 39% N, 45% P). Data from Colombia, Bolivia, and Costa Rica allow only a rough examination of altitudinal effects with a clear decrease of N, P, and K in Colombia, of N in Costa Rica, and significant decrease of all macroelements in Bolivia with increasing altitude (Veneklaas 1991; Nadkarni and Matelson 1992a, b; Schawe 2005).

These findings underline the assumption that uptake of macroelements is affected by soil conditions (acidification, water-logging) and that nutrient cycling slows down with increasing altitude. A further indicator is the decomposition and mineralization rate of surface litter (Oi). We calculate the quotient of mass and nutrient in the Oi-horizon to the annual flux of mass and nutrient by litterfall (k_{Oi}), which is similar to the inverse of the k_L value in literature (Smith et al. 1998), to obtain the mean residence time in the Oi-horizon. In Ecuador, mass k_{Oi} increases from 0.94 to 1.5 years within less than 200 m of increasing altitude, which is at the upper limit for LMCF. In Bolivia, the results are in the lower part of worldwide range of values with a significant increase from 0.47 to 1.35 years (Table 11.2). For all nutrients in the Oi, residence time increases as it does from LMCF to UMCF and SACF in Bolivia (factor 2.5–3.5) with the largest decrease of mineralization rate from LMCF to UMCF! Decomposition of fine woody debris in Oi takes 2.5 times as long on average as leaf litter with less than 25% portion on total litterfall so that annual nutrient release is low. Wilcke et al. (2002) report a contribution of woody debris of 1.5% to the total plant-available nutrients in the forest soil. The mineralization rate of K is highest and of N lowest in relation to other nutrients. Because of general high C/N relationship, the N mineralization rate approaches to the total litter mass mineralization rate. The highest differences in mineralization rate between LMCF and SACF are found for N, P and S (0.7 years).

There was a similar significant decrease with altitude for the main organic-bound nutrients (N, P, K) which we found in the Oi-horizon and in litterfall. For Ca and K, a decrease from LMCF to UMCF exists and is followed by an increase to SACF, which correlates with an increase in base saturation (O- and Ah-horizon) and pH-increase (O-horizon).

Decreasing decomposition with increasing elevation is observed for both litter decomposition and soil organic matter turnover (Bruijnzeel et al. 1993; Kitayama et al. 2000; Leuschner et al. 2007). In forests with lower tree height and basal area litter decomposition, nitrogen mineralization rates tend to be lower (Hafkenscheid 2000). Benner et al. (2010, Fig. 7.2) summarize results for net nitrogen

Table 11.2 Quotients of the storages of mass and nutrients in the Oi-horizon to the annual litterfall (koi) in TMCF of Bolivia and Ecuador

Location	Altitude	Mass [k_oi years]	C	N	P	Ca	K	Mg	Al	S	Fe	Na	Mn	Zn	Authors
Bolivia	1,800	0.47	0.46	0.30	0.36	0.18	0.28	0.51	0.28	0.31	0.64	0.45	0.41	0.42	Schawe (2005)
Bolivia	2,600	1.14	1.02	0.77	0.73	0.49	0.54	0.78	2.38	0.86	1.16	1.28	0.93	1.56	Schawe (2005)
Bolivia	3,050	1.35	1.20	0.98	0.94	0.50	0.64	1.19	1.16	1.01	1.04	1.61	0.96	2.08	Schawe (2005)
Ecuador, MC 1	1,900	0.94	0.95	0.95	0.72	0.89	0.47	0.68	0.84	0.96	1.70	0.14	2.10	1.10	Wilcke et al. (2002)
Ecuador, MC 2/3	2,000	1.50	1.50	1.40	0.72	1.90	0.41	1.50	1.40	1.70	2.30	0.99	2.80	1.30	Wilcke et al. (2002)

mineralization and net nitrification along elevational transects in different TMCFs and show that rates of nitrogen release decreases with increasing elevation. Furthermore, extractable ammonium concentrations are higher than extractable nitrate in TMCF soils.

An intensive field study in the Luquillo Experimental Forest in Puerto Rico along an elevation gradient (350 to 1,050 m a.s.l.) provided estimates of gross and net N mineralization and nitrification rates (Silver et al. 2010). They conclude that mineral nitrogen supply does not result in strong nitrogen limitation of NPP. However, a global meta-analysis of nitrogen additions and litter decomposition (Knorr et al. 2005) shows that adding nitrogen to low-nitrogen litter does not accelerate its decomposition, especially if the lignin content is high. In addition, fertilization experiments must be interpreted carefully, in light of the positive response to nitrogen addition in the short term (e.g., incubation experiments) and the decrease in the decomposition rate in the long term (2 years) (Janssens et al. 2010). This may explain why Soethe et al. (2006) measured no ^{15}N-fertilization effect after 60 days of application in UMCF in Ecuador. Laboratory and field incubations (under the litter layer) show a clear decline for both nitrogen mineralization and nitrification rate (Marrs et al. 1988). There was no significant effect of phosphorus at any altitude. At the highest altitude (UMCF 2,600 m), net immobilization of mineral nitrogen occurs.

For the outer tropics, nitrogen addition reduces decomposition rates in species with more recalcitrant litter (Janssens et al. 2010)! The role of microbial decay and shifts in microbial community with change in abiotic conditions with elevation on mineralization rates for TMCF is poorly understood. The shift to more recalcitrant SOC reduces carbon availability for mineralization in the organic soil layer, followed by further reductions in saprotrophic biomass and increase of net nitrogen mineralization (Janssens et al. 2010).

Studies on phosphorus release are extremely rare. Soil phosphorus fractionation along an elevation gradient at Mount Kinabalu (Kitayama et al. 2000) gives evidence on the importance of primary mineral P pool and altitude. P-use efficiency increases with altitude on ultrabasic bedrock, but not on sedimentary bedrock. The proposed reason is that the P-pool on sedimentary rock was much higher, and therefore the pool of actively cycling P was also higher.

Soil aeration or waterlogging was proposed as a limiting factor. This is in line with extremely low soil oxygen levels ($<3\%$) for longer periods of time in very wet ECF in Puerto Rico (Silver et al. 1999). Accordingly, high soil methane levels were found (up to 24%), indicating strongly reducing soil conditions. This is also in agreement with the large increase in soil water saturation in UMCF and SACF and placic soil horizons in SACF in Bolivia (Gerold et al. 2008). Comparing wet and dry sites on Hawai'i, Schuur and Matson (2001) concluded that anaerobic soils were the primary cause of decreased decomposition at high annual precipitation sites, followed by litter quality. Slower litter decomposition/nitrogen mineralization can be more limited under wetter site conditions and also reduce nutrient uptake by inhibiting root growth (Santiago et al. 2000).

Analyzing the rooting pattern at three altitudes in Ecuador (1,900, 2,400, 3,000 m a.s.l.) and performing ^{15}N fertilization experiments for nutrient uptake, Soethe et al. (2006) assume that with increasing altitude waterlogged conditions and less favorable soil chemical properties reduced root growth.

Wilcke et al. (2008c) performed a principal components analysis for soil properties and tree growth (independent variable). The main positive factor loadings for the organic layer were S and N, P, and the main cations (Ca, Mg, K) and the negative factor loading was given by C:N ratio. But nutrient concentrations only explained a small part of the total variance in tree properties. In Bolivia, the correlation between changing α-diversity with elevation for the studied plant families (Bach 2004) and complex soil factors of podzolization indicates the importance of precipitation excess with elevation, nutrient leaching, hydromorphic and stagnant soil conditions (Gerold et al. 2008).

11.3.2 Altitudinal Change of Soil Nutrient Ratios and Toxic Soil Elements

As mentioned above, it is more likely that nitrogen limitation than phosphorus limitation occurs in UMCF and SCAF, and that the decomposition rates of organic matter decrease with increasing altitude. The C:N, C:P and C:S ratios of the O-layer can be evaluated as an indication of the degree of soil organic matter (SOM) degradation (Fig. 11.3). Wilcke et al. (2008c) showed a significant increase of these ratios with altitude. For Bolivia, the same significant trend exists for C:N and C:S up to SACF, but for C:P it seems that relationship ends in the UMCF belt. In contrast to the decrease of leaf P concentration with increasing altitude (but no data from Bolivia), the P content in the O-layer does not decrease with altitude in Bolivia. No critical ratio values for nutrient uptake limitation are known from the literature, but under consideration of the increasing k_{Oi}-values for N, P, and S (Table 11.2), we assume that mainly organic-bound macronutrients have a limited availability with increasing altitude. This is substantiated by the fact that we found a decrease in throughfall deposition in relation to incident rainfall for total mineralized nitrogen (NO_3–N) and sulfur (SO_4–S) and for PO_4–P in the SACF. Soethe et al. (2008b) found a significant decrease in tree area growth rates with increase of C:N ($r^2 = 0.53$) and C:P ($r^2 = 0.55$) ratios.

High levels of free aluminum and polyphenols are reported in TMCF soils (Roman et al. 2010), and high soil water concentration of polyphenols may influence forest productivity in UMCF (Hafkenscheid 2000). But very few research results exist, and the existing data are contradictory. For example, Northup et al. (1995) found that phenolic compounds produced by the roots in stunted pine forests reduce leaching of scarce nitrogen. No increase in polyphenols and a decrease in VSC lignin concentrations in the O-horizons was reported for a transect in Ecuador (Wilcke et al. 2008c). They conclude that there are no indications for an influence of lignin or polyphenols on the decreasing organic matter turnover rates with increasing altitude.
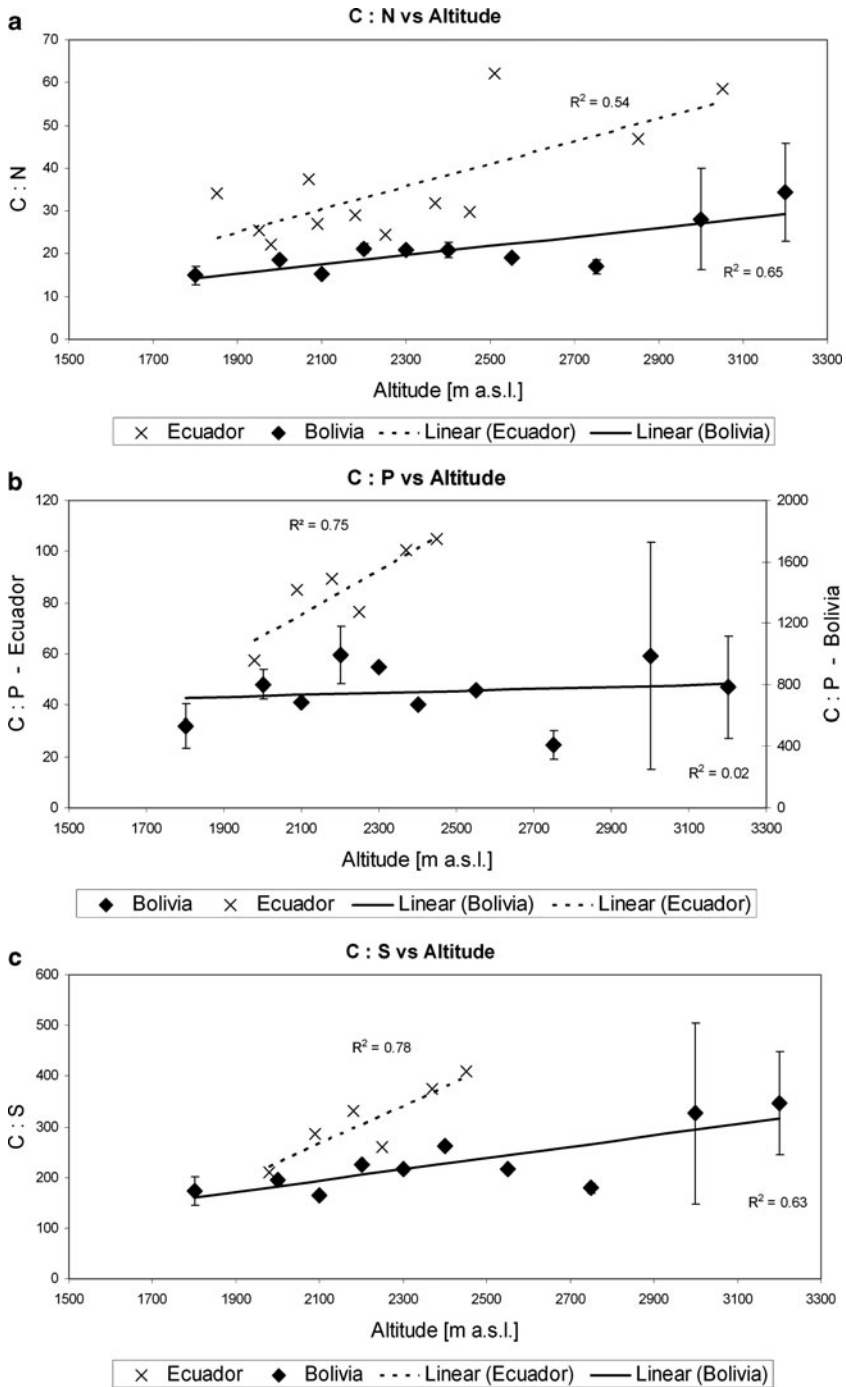
Fig. 11.3 Relationship between altitude and mean C:N, C:P, C:S ratios in the O-layer. *Error bars* indicate standard deviation (*n* = 3). Data after Wilcke (2008a, Ecuador) and own data (Bolivia)

Little is known about soil biological processes to avoid element toxicity with nutrient absorption by roots.

11.3.3   Litterfall and Nutrient Deposition

The total litter input decreases from LMCF to UMCF and SACF (Table 11.3). The annual litterfall in Bolivia and Ecuador in the LMCF is at the upper end of the range for different TMCF (Hafkenscheid 2000). In Ecuador, it did not vary much through the study (Wilcke et al. 2008b). The difference between LMCF and the other two vegetation belts was significant in Bolivia ($p < 0.05$). The leaf litter fraction was 69–71% in all three belts, but seasonal variation differed. Leaf and wood litter reached maximum quantities at the end of the dry season (September/ October, Schawe 2005). The vegetation belt with the highest abundance of epiphytes produced the highest epiphyte litter rates (0.26 t ha^{-1} year^{-1}, Table 11.3), which is lower than reported for Costa Rica (Monteverde 0.5 t ha^{-1} year^{-1}, Bruijn- zeel et al. 1995). For LMCF, high litter input in Bolivia and Ecuador results in relatively high element deposition rates. Because of decreasing litter nutrient concentrations from LMCF to UMCF and SACF (Sect. 11.3.1) with highest decrease for N, K, Mg and S, nutrient input was 3–4 times higher in LMCF than in UMCF and SACF (Table 11.3). Furthermore, large differences between LMCF and SACF (70–90%) exist for N, P, Ca, Mg, K, S, and differences between LMCF and UMCF are much higher in Bolivia than worldwide levels (Hafkenscheid 2000).

11.3.4   Nutrient Enrichment by Throughfall: Canopy Interaction

Nutrient deposition with incident rainfall, cloud or fog precipitation in TMCF depends on regional characteristics, the distance to marine or industrial sources and the origin of air masses. Long-term monitoring of matter deposition by rain and fog in South Ecuador (eastern escarpment of the Andes) with geostatistical modeling of backward-trajectories demonstrates the high influence of pollution sources (Rollenbeck 2010). Elevated values of SO_4 and NO_3 are traced back to biomass burning and industrial emissions. Na, K, SO_4, and Cl are transported by marine aerosols from the pacific (high during dry season) and Ca, Mg, and PO_4 are influenced by air masses from African deserts. Only 35% of the samples (2002–2007) exhibited low ionic concentrations with air masses from continental nonpolluted areas! Comparison of annual deposition for Na, K, and Mg with incident rainfall confirms the significant differences between maritime and more conti- nental research sites. High seawater contribution of ions in rainfall was reported for LMCF in Panama by Cavelier et al. (1997). For fire periods in Amazonia, Boy et al. (2008a) found a significant increase in element concentrations of rainfall for H, N_t, NO_3–N, DON, TOC, and Mn with higher dry deposition of biomass

Table 11.3 Litter input with epiphytes (t ha^{-1} year^{-1}) and nutrient input with annual litterfall in TMCF (kg ha^{-1} year^{-1})

Country	Forest type	Altitude (m a.s.l.)	Litter input (epiphytes) (t ha^{-1} a^{-1})	N	P	K	Ca	Mg	Al	S
Bolivia	LMCF	1,900	12.2(0.12)	218	11.0	48.4	123	46.6	15.5	18.0
Bolivia	UMCF	2,600	5.3(0.26)	57	3.4	14.6	36	12.5	6.9	4.6
Bolivia	SACF	3,050	4.7(0.03)	46	2.7	14.5	39	11.7	4.3	3.9
Venezuela[a]	LMCF-	2,300	7.0	69	4.0	33.1	43	14.2	9.3	–
Ecuador[b]	LMCF-MC1	1,900	8.5–13	165–204	12–20	77–131	154–250	49–57	4.7–12.0	20–23
Ecuador[b]	LMCF-MC2/3	2,000	8.6–13	152–218	11–16	15–108	117–188	37–55		
World[c]	LMCF	610–2,600	3.6–11	23.9–100.5	0.7–7.7	4.6–59.3	16.3–119.2	7.6–25.0		
World[c]	UMCF	1,550–3,370	4.3–7.4	28.9–80.8	1.1–2.9	5.7–33.0	6.7–50.2	6.3–18.2		

[a] Steinhardt (1979)
[b] Yasin (2001), Wilcke et al. (2008a)
[c] Hafkenscheid (2000)

burning-related elements. But nearly twice the quantity of rainfall for "no fire" periods does not result in any significant differences in incident rainfall deposition for these elements between "fire" and "no fire" periods.

The mean rainfall solute concentration varies greatly. Zimmermann et al. (2007) assembled literature data for TMCF in Ecuador, Colombia, Venezuela, Costa Rica, Panama, and Jamaica. For the main macronutrients, the following ranges were given (in µmol l^{-1}): NH$_4$ 2.8–61.7, NO$_3$ 3.6–11.0, PO$_4$ 0.1–0.6, SO$_4$ 4.1–38.6, Cl 0.9–32.2, Na 5.7–78.7, K 2.3–12.2, Ca 4.5–19.8, Mg 0.7–21.1 (see Table 2, Zimmermann et al. 2007).

The chemical quality of throughfall and stemflow is controlled by inter site-specific conditions (topography, canopy structure, and plant species) and rainfall characteristics (rainfall intensity, dry deposition, amount of fog, and cloud stripping). In Table 11.1, the means of cloud water interception or FD by the canopy are +16% (windward sites) and +154% (ridge/isolated trees). In South Ecuador, nearly all throughfall nutrient concentrations exhibit significantly high spatial heterogeneity when ridges and gorges were compared. Combined with different canopy parameters throughfall deposition (Ca, Mg, K) is also approximately two times higher in gorges than on ridges ($p < 0.001$) (Oesker et al. 2008). For the LMCF in South Ecuador (1,950 m a.s.l., 2,200 mm rainfall), the coefficient of variation for nutrient element concentrations (spatial pattern, 22 TF collectors) varies between 28% (Na) and 292% (NO$_3$). Oesker et al. (2010) found strong correlations between element concentrations in throughfall and tree species diversity. Leaf leaching experiments for seven tree species in the TMCF in South Ecuador showed a threefold higher leaching between the lowest and highest quantities of leached potassium.

In addition, weekly nutrient deposition of incident rainfall was highly variable during the measurement periods (Veneklaas 1990; Kellner 2006), and the element concentrations in incident rainfall and throughfall exhibited high standard deviations (Veneklaas 1990; Kellner 2006). In general, nutrient fluxes in throughfall showed the same seasonal pattern as those in incident rainfall, and the net fluxes (throughfall minus incident rainfall quantities) of most elements were proportional to rainfall volumes (Veneklaas 1990). In Ecuador element concentrations in rainfall were not correlated with rainfall volume (Boy et al. 2008a, b).

Most evaluated annual fluxes of nutrients in throughfall from 22 sites are in the worldwide range reported by Hafkenscheid (2000). However, in SACF of Bolivia N, Mg, and K inputs are much lower and P-input in LMCF in Bolivia and Ecuador, much higher than the worldwide data range.

A common method for characterizing site-specific canopy influence on throughfall matter input with the integral of all influencing factors is the comparison of incident rainfall and throughfall (Table 11.4). In general, element concentration in throughfall is greater than in rainfall as a result of leaching from the leaves (TOC, Al, Ca, Mg, K), particulate dry deposition (Cl, NH$_4$–N), and gaseous dry deposition (NO$_3$–N, total N, S). However, Veneklaas (1990), Cavelier et al. (1997) and Gerold (2008) reported negative values for the difference in the annual flux in throughfall and rainfall for total N (Panama, Colombia, Bolivia), NO$_3$–N (Bolivia), S (Panama,

Table 11.4 Throughfall enrichment factors for selected elements in TMCFs as shown by (a) volume-weighted mean concentrations and (b) deposition ratios

Location	Altitude (m a.s.l.)	Precipitation (mm)	Forest type	TOC	Ca	Cl	K	Mg	NH_4^+–N	NO_3^-–N	N	Na	P	S	Author
(a)															
Ecuador	1,900–2,010		LMCF	3.1–3.7	5.3–12.7	1.9–4.5	31.5–74.4	7.4–30.0	2.3–3.6	3.2–7.3	4.7–8.8	1.3–1.8	6.9–23.8	3.0–7.3	Wilcke et al. (2008b)
Bolivia	1,900	2,310	LMCF	2.24	2.86	1.29	23.93	12.57		0.88	2.10	1.33	33.00	1.15	Schawe (2005)
Bolivia	2,600	3,970	UMCF	4.01	1.30	1.10	1.11	2.00		0.30	1.82	1.04	1.09	0.94	Schawe (2005)
Bolivia	3,050	5,150	SACF	3.38	1.35	1.11	1.89	2.71		0.72	1.13	1.16	3.36	1.03	Schawe (2005)
(b)															
Malaysia	870		LMCF		3.0	2.6	5.8	5.8					1.0	1.8	Bruijnzeel et al. (1993)
Jamaica	1,550	2,600	LMCF		2.4		6.0	2.3				1.4			Tanner (1977)
Panama	1,200	3,510	LMCF		1.3	1.4	4.7	1.9			1.0	2.1	3.1	0.5	Cavelier et al. (1997)
New Guinea	2,450	3,800	UMCF		6.3		10.7	9.4			5.6		5.7		Edwards (1982)
Venezuela	2,300	1,576	UMCF		1.2		26.8	0.64			0.9	1.3	1.3	0.0	Steinhardt (1979)
Colombia	2,550	2,115	UMCF		2.7	1.9	12.1	3.3	1.2		1.2	1.1	2.3	1.6	Veneklaas (1990)
Colombia	2,550		UMCF		1.9	1.0	4.2	2.2			0.6	0.6	0.6	3.5	Veneklaas (1990)
Colombia	3,370	1,453	SACF		2.6	1.5	4.8	2.8	1		0.9	0.9	0.8	1.9	Veneklaas (1990)
Ecuador	1,900–2,010		LMCF	1.6–3.0	3.8–7.2	1.3–3.2	20.5–44.9	6.9–17.5	1.0–2.8	1.9–4.0	2.8–5.0	0.5–1.2	6.0–14.0	2.0–6.2	

														References
Bolivia	1,900	LMCF	1.6	2.2	1.1	18.6	11.5	0.8	1.9	1.1	1.8	0.9		Wilcke et al. (2001)
Bolivia	2,600	UMCF	3.4	1.0	1.0	0.9	1.7	0.3	1.7	0.9	1.0	0.8		Gerold (2008)
Bolivia	3,050	SACF	64.3	1.1	0.8	1.2	2.1	0.4	0.9	0.9	0.9	0.8		Gerold (2008)
														Gerold (2008)

Bolivia), and PO_4–P (Colombia, Bolivia – only SACF) (Table 11.4, enrichment factor <1). This suggests that these nutrients are being absorbed by the canopy with foliar uptake and in some cases with uptake and storage by epiphytic biomass (Sect. 11.3.5). Also in a moss-covered montane cloud forest in Costa Rica, Clark et al. (1998) found that the canopy retained H (92%), NO_3 (80%), and NH_4 (61%). From LMCF to UMCF and SACF enrichment factors of main macronutrients decrease to nearly 1 in Bolivia. Despite higher rainfall with altitude Ca, Mg, K, S, Na, and Cl, nutrient deposition with incident rainfall decreases and throughfall deposition of Ca, Mg, K, N, NO_3–N, and P decreases from LMCF to UMCF (Bolivia, Gerold 2008). We assume that higher nutrient retention in the canopy indicates a higher requirement for these nutrients by forest trees and organisms. Net absorption by the canopy was measured for NO_3–N (UMCF with -5.3 kg ha^{-1}, SACF with -4.4 kg ha^{-1}) and SO_4–S on an annual basis in Bolivia (Gerold 2008). The main canopy nitrogen uptake form is nitrate, whereas ammonium and organic nitrogen showed positive net fluxes (Kellner 2006). Studies on sulfur fluxes are rare, and S-deposition in Bolivia TMCF is high, which seems contradictory to depletion via the canopy pathway (Gerold 2008). Enrichment with throughfall at much lower sulfur fluxes is reported by Veneklaas (1990) and Asbury et al. (1994) for Colombia and Puerto Rico. Throughfall in UMCFs and SACFs is often much reduced in nitrate and, in some cases, sulfur and phosphate compared to concentrations in incident rainfall and cloud water. Species diversity and stand structure, as well as epiphyte biomass affect nutrient absorption and release.

11.3.5   *Cloud Water Interception and Role of Epiphytes*

Cloud and fog water input into UMCFs and SACFs is of great importance for the hydrological budget and reaches high values, for example, it averaged 4.4 mm d^{-1} at windward sites in Puerto Rico (see Table 11.1). Depending on origin of air masses, frequency and height of condensation levels, wind velocity at canopy boundary layer, duration of cloud and fog cover, and the throughflow rate of cloud and fog droplets, the quantity and chemical composition of cloud or fog water varies in a wide range. When fog forms, air pollutants are trapped and gases and particles become incorporated in the droplets (Liu et al. 2010). Because of drop size, residence time and less dilution by rainfall, studies on fog- and rainwater chemistry show higher ionic concentrations in fog and cloud deposition than in rainwater (Hafkenscheid 2000; Chang et al. 2010; Rollenbeck et al. 2010). Liu et al. (2010) found increased pH and alkaline ions (mainly K and Mg) in FDs compared to incident fog with an increase of pH from 6.78 to 7.30 (Table 42.1 in Liu et al. 2010). The same processes and influencing factors as for chemical throughfall composition can be related to nutrient enrichment in FDs with wash-off of dry depositions on leaves and leaching of alkaline ions from leaves. The pH increase in cloud- and fog-water induced throughfall and very low H-deposition rates (Fig. 11.4) indicate buffering of acidity by exchange of H with other cations in the canopy (Rao et al. 1995). Where NH_4 inputs are high, enhanced fluxes of Ca and
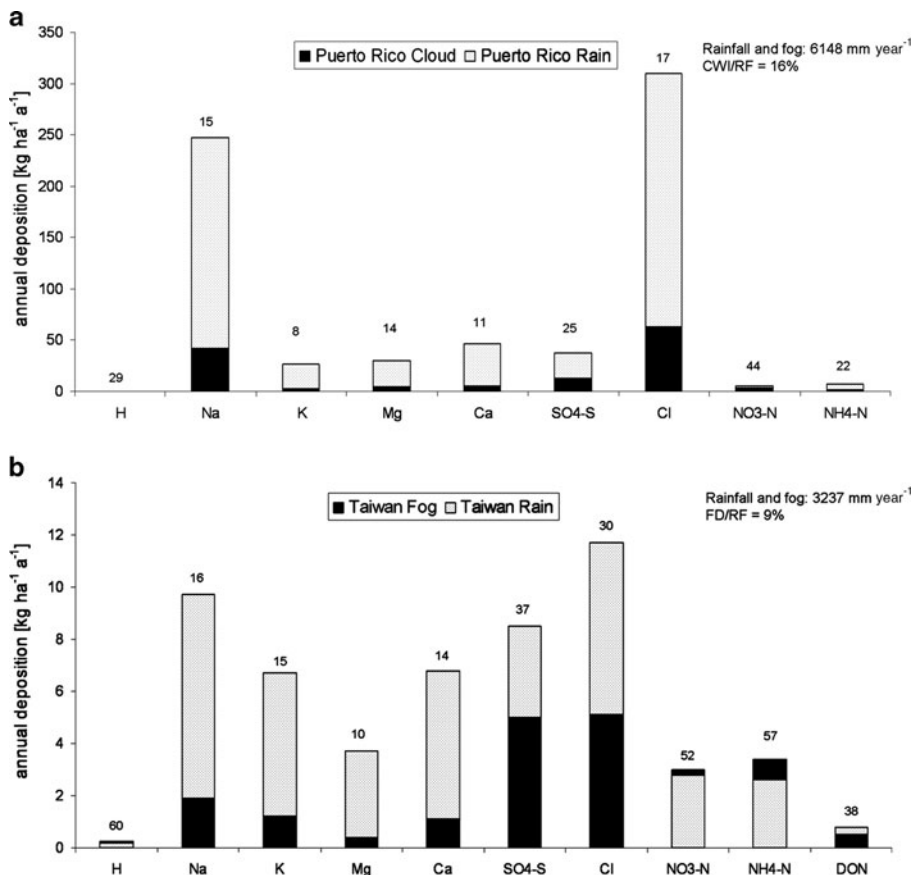
Fig. 11.4 Annual deposition rates in TMCF sites from cloud and fog and rainfall (kg ha^{-1} year^{-1}) and relative contributions by cloud or fog deposition on total rainfall and cloud/fog deposition (%). Data after Asbury et al. (1994) and Chang et al. (2010)

Mg in throughfall due to leaching occurs (Liu et al. 2010). Boy et al. (2008a, b) found that biomass burning in the Amazon with elevated H deposition resulted in elevated base metal loss from the canopy in South Ecuador.

Due to higher nutrient concentrations in fog or cloud water, the ratios of fog/cloud water to total rainwater are high and exceeded the throughfall enrichment ratios mainly for NH_4, Na, Cl, NO_3, and SO_4. Data evaluation from Taiwan (Beiderwieden et al. 2007), SW-China (Liu et al. 2010), Costa Rica (Clark et al. 1998), and Puerto Rico (Asbury et al. 1994) shows enrichment ratios of volume weighted mean ion concentrations for CW/R or F/R with 3–18 (NH_4), 2–53 (Na), 3–15 (Cl), 4–15 (NO_3), 4–14 (SO_4). Beiderwieden et al. (2007) argued that fog water represents lower layers of the atmosphere and are therefore more influenced by continental emissions. Concentrations of H, NH_4, NO_3, and SO_4 are much higher and enriched in fog or cloud water compared to other ions (Asbury et al. 1994; Clark et al. 1998; Beiderwieden

et al. 2007; Liu et al. 2010). As a result of high ion enrichment in fog or cloud water by marine, industrial or biomass burning sources, fog deposition can contribute significantly to total atmospheric nutrient inputs at TMCF sites (Fig. 11.4).

As at other sites (see Sect. 11.3.4), inorganic nitrogen was absorbed by the canopy with net depletion (throughfall–rainfall) (Chang et al. 2010).

We assume that important elements for nutrient cycling are enriched by cloud or fog deposition in TMCF ecosystems, with highest contribution of roughly 50% for NO_3 related to the sum of rainfall and fog/cloud deposition. The consequences for nutrient cycling are not well understood. Studies focusing on nutrient input via fog water deposition are rare because experimental quantification of fog deposition fluxes is still a challenge (see Sect. 11.2 and Beiderwieden et al. 2007), and a combined study of fog/cloud deposition with nutrient fluxes into the soil and nutrient uptake by plants at the same site has not yet been conducted.

Canopy organic matter, composed of epiphyte community and their associated dead organic matter, exist as a complex subsystem in the TMCFs. Quantification for water and nutrient storage is very rare, and researchers have used direct (harvesting all canopy organic matter, Lin Chen et al. 2010) and indirect methods (dry weight-to-substrate surface area ratio with allometric models, Nadkarni et al. 2004). Lin Chen et al. (2010) found that the diameter of the host trees at breast height (DBH) was the best parameter in the estimation of epiphytic biomass. Within the Monteverde UMCF, the fraction of total canopy biomass (33.1 t ha^{-1}) to total aboveground biomass was 6.8% (Nadkarni et al. 2004). But if we compare canopy organic matter to labile nonwoody biomass (7.6 t ha^{-1}), the ratio is very different with 4.3:1! Dead organic matter (crown humus, intercepted litterfall) comprised over 60% of the total epiphytic material, whereas in the drier subtropical UMCF in south-western China canopy organic matter was dominated by bryophytes with 74% (2.3 t ha^{-1} canopy organic matter).

Epiphytic mass varies in a wide range in the canopies of TMCFs. In old growth TMCFs, epiphyte mat weight can reach more than 10 t ha^{-1} with highest values reported from Costa Rica (33 t ha^{-1}) and Colombia (44 t ha^{-1}) (Table 11.5). Epiphytes intercept nutrients from aerosols, litterfall, rainfall, throughfall, and animal droppings. The high contents of nitrogen in Bryophytes and epiphyte leaves may indicate that some epiphyte species can fix nitrogen or harbor nitrogen fixing symbionts, but fluxes are not known (Table 11.5). Dead organic matter, bryophytes, and epiphyte leaves have similar nitrogen and sometimes higher potassium concentrations than tree leaves in LMCFs and UMCFs (Nadkarni et al. 2004). For P, Ca and Mg concentrations in epiphytes and bryophytes are roughly 50% of tree leaf concentration.

Nadkarni's results (1984, 2004) from the Monteverde Cloud Forest Reserve in Costa Rica showed the importance of nutrient capital from canopy organic matter with a portion of 3.7% (K) up to 10.5% (N) of the total aboveground biomass stock. Compared with 438.7 kg ha^{-1} nitrogen, the preliminary estimate of 0.7 kg ha^{-1} N immobilized in microbial tissue in the canopy seems negligible (Bruijnzeel et al. 1995).

Epiphyte litterfall exhibits a high spatial heterogeneity, and field measurements are extremely rare. With a specially designed sampling system, Nadkarni et al. (1992) found that the nutrient quantity in epiphytic litterfall was about 1–8% of

Table 11.5 Nutrient compositions (mg g^{-1}) for canopy organic matter

Components	N		P		Ca		K		Mg		Authors
	Mean (mg g^{-1})	SD	Mean	SD	Mean	SD	Mean	SD	Mean	SD	
DOM	16.0	4.0	0.7	0.1	6.0	2.0	3.0	0.2	1.0	1.0	Nadkarni et al. (2004)
BRY	14.0	2.0	0.8	0.1	5.0	1.0	7.0	1.0	1.0	1.0	
EPST	7.0	1.0	0.6	0.2	9.0	3.0	7.0	8.0	2.0	2.0	
EPLV	14.0	10.0	0.9	1.0	13.0	4.0	16.0	8.0	4.0	4.0	
EPRO	9.0	2.0	0.6	0.1	7.0	2.0	7.0	1.0	2.0	2.0	
EREP	13.0	1.0	1.0	2.0	5.0	1.0	6.0	0.0	1.0	1.0	
FER	12.0	3.0	0.9	0.4	10.0	2.0	17.0	7.0	4.0	4.0	
Lichens	12.3	0.2	1.0	0.0	3.2	0.1	3.6	0.0	0.8	0.0	Lin Chen et al. (2010)
Litterfall	11.9	0.2	0.6	0.0	8.7	0.1	1.4	0.0	1.1	0.0	
Ferns	11.7	0.1	1.2	0.1	5.1	0.2	10.4	0.4	2.4	0.1	
Bryophytes	17.1	0.3	0.8	0.0	4.1	0.0	3.9	0.0	1.1	0.0	
Canopy humus	19.5	0.1	0.9	0.0	3.8	0.0	2.2	0.0	0.9	0.0	
L. pachyphylloides											
Bole	4.8	0.1	0.3	0.0	9.8	0.1	1.2	0.0	0.3	0.0	
Branches	9.1	0.0	1.3	0.0	16.9	0.2	3.8	0.0	1.2	0.0	
Leaves	16.5	0.1	1.2	0.0	5.0	0.0	4.1	0.1	1.0	0.0	

	Epiphyte mass in TMCFs (16 sites, kg ha^{-1}), mean and standard deviation (SD)[a]	
	Altitude (m a.s.l.)	Epiphyte mat weight
LMCF – mean	1,675	106,665
LMCF – SD	387	7,502
UMCF – mean	2,225	8,347
UMCF – SD	813	11,548
SACF – mean	1,669	13,038
SACF – SD	1,178	17,350

DOM dead organic matter, *BRY* bryophytes and lichens, *EPST* epiphyte stems, *EPLV* epiphyte leaves, *EPRO* epiphyte roots, *EPREP* epiphyte reproductive parts(flowers, fruits), *FER* ferns

[a] Data evaluation after: Edwards and Grubb (1977), Pocs (1980), Tanner (1980, 1985), Veneklaas et al. (1990), Hofstede et al. (1993), Weaver (1972), Nadkarni et al. (1984, 2004), Köhler et al. (2007), Hsu et al. (2002), Lin Chen et al. (2010)

corresponding foliar litterfall. With litterfall traps in Bolivia, a fraction of 1% (LMCF, SACF) to 5% (UMCF) was found for epiphyte litter input per year (Table 11.3). If we roughly calculate the annual nutrient input by canopy organic matter from the Monteverde Cloud Forest using 5% for epiphyte litter input, we get hypothetical values of 21.9 kg ha^{-1} for N, 1 kg ha^{-1} for P and 7.6 kg ha^{-1} for K; these values correspond to 38, 31 and 52% of nutrient input with annual litterfall in UMCF. With analysis of δ^{15}N signals for different canopy organic matter compounds in the UMCF at Monteverde, Hietz et al. (2002) found that dead organic matter (canopy soil) is mainly derived from epiphytes. Consequently, atmospheric (dry matter deposition, N_2-fixation by epiphytes and influence of epiphylls on leaves) and throughfall characteristics together with complex tree architecture (Nadkarni et al. 2004) control biogeochemical nutrient storage and fluxes of the

canopy organic matter. The conclusion formulated by Bruijnzeel et al. (1995) is thus still valid, i.e., that fog and cloud water and also epiphytes play an important role in the nutrient cycling of TMCFs and much remains to be discovered.

11.3.6 Element Export with Soil Leachate and Stream Water and Catchment Budget

Frequent increases in rainfall from LMCF to UMCF/SACF and the additional input of cloud- or fog water with a decrease of real ET with altitude result in a high positive water budget for the entire year with a high potential for nutrient leaching in the unsaturated soil compartment and generation of runoff. Bruijnzeel (2004) evaluated post-1993 water budget studies in TMCFs, where the water output with runoff (based on the yearly water balance) ranges between 815 mm (Venezuela) and 4,015 mm (Puerto Rico). Detailed ecophysiological measurements on stand structure, stand transpiration, and the energy balance parameters were performed by Küppers et al. (2008) in the LMCF (1,975 m a.s.l.) in South Ecuador. With this microclimatic approach, they found a real annual ET of 561 mm, which consumed only 22–25% of the annual precipitation. In Bolivia, annual potential ET decreases by 60–70% from LMCF to UMCF/SACF (400–460 mm), with the result of a high water surplus when the high yearly rainfall of 3,970 mm (UMCF) up to 5,150 mm (SACF) is taken into consideration (Gerold et al. 2008).

Nutrient enrichment via the canopy rainfall pathway (see throughfall 11.3.4) and the additional nutrient input by cloud or fog water, relative high nutrient stocks in the organic layer, less deeply weathered soils, and high leaching potential with leachate might lead us to believe that nutrient concentrations in runoff are not low. Bruijnzeel (1998) has reviewed inputs and outputs of nutrients via water pathways in rainforests and discussed the limitations of methods to evaluate nutrient losses via leaching at plot and catchment scale (Proctor 2005). There are only very few studies within intact TMCFs, which combine research on input and output water pathways with nutrient budgets. In the scope of the long-term inter-disciplinary research project in South Ecuador (Beck et al. 2008), measurements over several years for three microcatchments in the LMCF (1,900–2,100 m a.s.l.) enable a comparison of the main nutrient fluxes (Wilcke et al. 2008a). For Jamaica, Hafkenscheid (2000) depicted annual fluxes of nutrients in litter percolate and drainage water (Table 7.9 in Hafkenscheid 2000) and estimated the different annual nutrient fluxes for the Mull- and Mor forest (see Hafkenscheid 2000, Tables 7.10 and 7.11).

Water chemistry analysis by Bücker et al. (2010) showed very low content of soluble elements with electrical conductivity of 5–15 $\mu S\ cm^{-1}$ for baseflow conditions for the cloud forest subcatchments without actual anthropogenic influence. The main ions in decreasing order were $NO_3 > SO_4 > Na > K > Ca$ and Mg. The mean concentrations of K, Ca, and Mg are in the same range as reported by

Wilcke et al. (2008a) for the microcatchments (10 ha), but the nitrate concentration double. Proctor (2005) pointed out the problems caused by organically bound nutrients (e.g., N) in the measurement of nutrient losses from forests at the catchment scale, because soils in the riparian zone or even the organic matter in the stream (e.g., litterfall) can have a dominant influence on stream water composition.

For the microcatchments in Ecuador, the main nutrient status and fluxes from incident rainfall to stream water were analyzed. The slightly acidic rainfall (mean pH 5.3) is buffered by complex canopy interactions, so that throughfall pH was 6.1–6.7. With zero-tension lysimeters, the soil solution was collected below the organic layer (litter leachate) and at 0.15 m and 0.30 m depth in the mineral soil (Wilcke et al. 2001). The median of the pH of litter leachate was 4.8–6.8, which indicates an input of additional acidic components of dissolved organic matter from the organic layer. Also, it must be considered that measurements with throughfall collectors does not depict acid fog and cloud input. With increasing acidity of the organic layer, nutrient concentrations decreased in litter leachate, reflecting different exchangeable nutrients status and decreasing biological turnover. Litter leachate had the highest concentrations of macronutrients of all ecosystem fluxes. Under consideration of the most acidic transect of the microcatchments (MC2/1 Wilcke et al. 2001), which are similar to the site characteristics in Jamaica (Hafkenscheid 2000), the concentrations of all nutrients (N, P, K, Ca, Mg) strongly decreased from the O-layer to the mineral horizon (0.15 and 0.30 m depth). A further decrease from the mineral soil solution (0.30 cm depth) to the runoff only occurred for N and P, whereas cations had higher concentrations in stream water output. The element concentrations observed in runoff were much lower than those found in litter leachates. As pointed out by Bruijnzeel (2004), nutrient losses via drainage (streamflow) primarily reflect the fertility of the substrate and the amount of runoff.

We conclude that the major proportion of the nutrients were retained in the organic layer, and that root distribution as well as distribution of nutrient stocks show that main nutrient uptake occurs in the O-layer (Soethe et al. 2008a). Wilcke et al. (2001) found that concentrations of Ca and Mg in litter leachate and throughfall correlated significantly with those in the soil in Ecuador, but not with runoff concentrations. Storm-flow events showed increasing N and P concentrations in stream water (no dilution), which was related to high fraction of subsurface flow with higher export of DOC and DON. Boy et al. (2008a, b) summarize that the concentrations of most elements increased in the order rainfall < throughfall < litter leachate. A large decrease of concentration and deposition in throughfall was measured for UMCF and SACF in Bolivia.

Based on the findings by Wilcke et al. (2008b) and Hafkenscheid (2000), the main input and output fluxes and the external element budget for the MC2 catchment and Mull-UMCF was calculated (Table 11.6). The catchment budget was calculated as the difference between measured rainfall and calculated dry deposition and output with runoff, respectively, between rainfall and cloud water minus drainage in Jamaica. The stemflow contribution was < 5% of the throughflow deposition rates and is therefore neglected. In addition, gaseous N losses were not

Table 11.6 Catchment budget of main nutrient elements in LMCF in South Ecuador with ranges of annual deposition rates in incident rainfall, throughfall, dry deposition, litterfall, and surface flow export based on volume-weighted mean concentrations and mass-weighted mean concentration and annual water fluxes (microcatchment MC2 1998–2003, Wilcke et al. 2008b), and annual nutrient fluxes in the Mull-UMCF in Jamaica, estimated by Hafkenscheid (2000)

Water/litter flux Ecuador	N $kg\ ha^{-1}\ year^{-1}$	P	K	Ca	Mg
Incident rainfall	9.3–9.8	0.21–1.4	3.6–16	2.4–16	0.86–6.7
Dry deposition	6.7–19	0.15–2.7	3.0–12	1.7–12	0.6–5.2
Throughfall	16–17	0.96–2.0	65–157	5.6–24	3.6–9.0
Litterfall	173–225	10–14	65–112	103–126	31–43
Runoff	3.0–4.9	0.02–1.6	2.2–6.1	3.7–12.0	4.2–6.0
Jamaica	$kg\ ha^{-1}\ a^{-1}$				
Rainfall + cloud water	5.9[a]	0.14[a]	8.5	9.6	2.2
Throughfall + stemflow	5.4[a]	0.18[a]	44.0	13.2	5.9
Litterfall	52.9	2.9	11.4[b]	50.2	13.2
Loss via drainage	8.0	0.24	9.1	7.7	8.6
Jamaica: external budget (rainfall + cloud water – drainage)	−1.1[a]	0.06[a]	−0.6	1.9	−6.4
Ecuador: external budget (rainfall + dry deposition – runoff)	13–23.9	0.34–2.5	4.4–21.9	0.4–16	−2.7–5.9

[a] Mineral forms only
[b] Seriously underestimated

considered. External budget (net ecosystem gain or loss) in Jamaica was negative for N and Mg. Hafkenscheid (2000) calculated the net uptake (via nutrient immobilization in stems) of Ca, Mg, K, and N, which represents only 1.7% (Mg) until 8% (N) of litter percolate (readily available nutrients)!

Close correlation was found between annual total deposition and nutrient export with runoff ($r > 0.6$). Net budgets among hydrological years varied to a great degree (1998–2003, Fig. 13.3 in Wilcke et al. 2008b). Base metals varied most, and for 2 years Ca and Mg were depleted. In years with high atmospheric base metal input, increased metal accumulation was observed in the vegetation and organic layer compartment. The minimum and maximum values of the external budget for Ca and Mg indicate high influence of interannual variation in deposition rates (Table 11.6). It is remarkable that those years with net-negative budgets (1998/1999, 2002/2003) for Ca and Mg were influenced by higher dryness in Amazonia with higher biomass burning (El Nino year 1998) and the air masses that passed the erupted volcanoes El Reventador (November 2002) (Rollenbeck et al. 2006).

With biomass burning, significantly elevated H, N, and Mn depositions occurred in South Ecuador. Elevated H input during the burning season in Amazonia resulted in elevated base metal loss from the canopy and organic horizon and in deterioration of the already low base metal supply of the vegetation (Boy et al. 2008a, b). Boy et al. (2008a, b) conclude that related increase of acid deposition impoverishes base-metal-scarce ecosystems.

For internal nutrient cycling, high nutrient inputs via throughfall and litterfall exist. The sum of throughfall and litterfall in Ecuador are similar to LMCF in

Bolivia for N, Ca, and Mg, but lower for P and much higher for K (Table 7 in Gerold 2008). The main contribution to nutrient input in TMCFs is provided by cycling of litter. Transect studies in Bolivia (Gerold 2008) showed that litter input is about 70% higher in LMCF than in UMCF and SACF, mainly due to three to four times higher litterfall rates. The depletion of nitrogen and sulfur in throughfall in UMCF and SACF, which is influenced by the high epiphytic biomass ("nutrient capacitor", Sect. 11.3.5) and high decrease in litter nutrient input (only 25–30% compared to LMCF) indicates a decreasing availability of these nutrients with altitude (Gerold 2008).

It appears that nutrient fluxes in TMCF ecosystems (throughfall, litterfall, litter leachate, soil solution) possess a high variation linked with altitudinal changes, intersite variation in the same altitudinal belt (topography and soil, e.g., LMCF in South Ecuador, SACF in Puerto Rico) and external factors such as source and element composition of air masses, which determine rainfall-, cloud-, and fog deposition.

11.4 Future Research Directions

Much work remains to be done to better understand the hydrological functioning of TMCFs, particularly the spatial distributions of water inputs, both CWI and WDR. Process-based modeling (e.g., Mulligan and Burke 2005) offers the best solution in this regard. Field measurements can never be numerous enough to represent the complex spatial patterns in CWI and WDR. But, high-quality observations are badly needed to help validate and refine models. Future field-based research should focus on addressing the challenges of accurately measuring rainfall in the presence of high winds and in areas of high topographic relief (Bruijnzeel et al. 2010). In addition, water use in TMCF has not received sufficient attention. Only a small proportion of field studies have quantified wet canopy evaporation and very few have given estimates of transpiration (Bruijnzeel et al. 2010, Appendix 74.3).

The hydrological effects of conversion of TMCFs to other land covers is another major concern, and studies done thus far have not yielded generalizable results. Additional work is needed to understand how and under what conditions stream discharge is affected by conversion of TMCFs (Bruijnzeel et al. 2010). With global warming and corresponding changes in cloud frequency, height, and LWC, much more needs to be known about the resulting effects on TMCF hydrology.

A review of the literature shows that the net annual nutrient flux with throughfall decreases from LMCF to UMCF and SACF. The net absorption by the canopy was measured for NO_3–N and SO_4–S in Bolivia, NO_3–N and NH_4–N in Costa Rica, NO_3–N in Jamaica. Studies on the function of sulfur in ecosystem fluxes are rare. Fog and cloud water are mainly enriched by H, NH_4, Na, Cl, NO_3, and SO_4; this reflects maritime impacts and the influence of industrial or biomass burning sources. Fog or clouds contribute up to 50% of the NO_3–N to the sum of rainfall

and fog/cloud deposition. Fog and cloud water as well as epiphytes play an important role in nutrient cycling in TMCFs and must be more intensively studied.

Climate change with increasingly drier years in Amazonia and widespread deforestation, logging, and human settlements can cause substantial changes in atmospheric deposition, with higher inputs by H, NH_4, NO_3, SO_4 for the humid eastern escarpment of the tropical Andes (Mahowald et al. 2005; Rollenbeck 2010). As a consequence, complex ecological interactions (see Sect. 11.3.6) can result in elevated nutrient loss (depletion of base metals) and decreasing decomposition rates, which may be in conflict with the predicted shift of timber line in tropical mountains, and may increase stress for nutrient supply in the future. Future research should investigate the influence of climate change on TMCF.

Several knowledge gaps exist on biogeochemical processes in TMCFs, so that coupling of hydrologic modeling with matter modeling is still a great challenge. We recommend future research to enable coupling hydrologic and biogeochemical modeling in TMCF. Open questions are (1) how is nutrient enrichment by throughfall related to forest structure; (2) can fog and cloud water interception (water flux) with averaged nutrient concentration be used for the calculation of nutrient input by throughfall; (3) can submodules of C-modeling be used for better analysis and simulation of litter decomposition and nutrient release; (4) how can ^{15}N-fertilization experiments be used for nutrient uptake modeling; and (5) are conceptual storage models adequate to simulate soil nutrient leachate and water nutrient output?

References

Asbury CE, McDowell WH, Trinidad-Pizarro R et al (1994) Solute deposition from cloud water to the canopy of a Puerto Rican montane forest. Atmos Environ 28:1773–1780

Bach K (2004) Vegetationskundliche Untersuchungen zur Höhenzonierung tropischer Bergregenwälder in den Anden Boliviens. Diss, Marburg, 123

Baldocchi D, Hicks B, Meyers T (1988) Measuring biosphere-atmosphere exchanges of biologically related gases with micrometeorological methods. Ecology 69:1331–1340

Beck E, Bendix J, Kottke I et al (2008) Gradients in a tropical mountain ecosystem of Ecuador, Ecol Stud 198. Springer, New York

Beiderwieden E, Schmidt A, Hsia YJ et al (2007) Nutrient input through occult and wet deposition into a subtropical montane cloud forest. Water Air Soil Pollut 186:273–288

Benner J, Vitousek PM, Ostertag R (2010) Nutrient cycling and nutrient limitation in tropical montane cloud forests. In: Bruijnzeel LA, Scatena FN, Hamilton LS (eds) Tropical montane cloud forests. Science for conservation and management. Cambridge University Press, Cambridge, pp 90–100

Blocken B, Carmeliet J, Poesen J (2005) Numerical simulation of the wind-driven rainfall distribution over small-scale topography in space and time. J Hydrol 315:252–273

Boy J, Rollenbeck R, Valarezo C et al (2008a) Amazonian biomass burning-derived acid and nutrient deposition in the north Andean montane forest of Ecuador. Glob Biogeochem Cycles 22:1–16

Boy J, Valarezo C, Wilcke W (2008b) Water flow paths in soil control element exports in an Andean tropical montane forest. Eur J Soil Sci 59:1209–1227

Brauman KA, Freyberg DL, Daily GC (2010) Forest structure influences on rainfall partitioning and cloud interception: a comparison of native forest sites in Kona, Hawai'i. Agric For Meteorol 150:265–275

Bruijnzeel LA (2001) Hydrology of tropical montane cloud forests: a reassessment. Land Use Water Resour Res 1:1–18

Bruijnzeel LA (2004) Hydrological functions of tropical forests: not seeing the soil for the trees? Agric Ecosys Environ 104:185–228

Bruijnzeel LA (2005) Tropical montane cloud forests: a unique hydrological case. In: Bonell M, Bruijnzeel LA (eds) Forests, water, and people in the humid tropics. Cambridge University Press, Cambridge, pp 462–483

Bruijnzeel LA, Proctor J (1995) Hydrology and biogeochemistry of TMCF: What do we really know? In: Hamilton LS, Juvik J, Scatena FN (eds) Tropical montane cloud forests. Ecological studies 110. Springer, New York, pp 38–78

Bruijnzeel LA, Veneklaas EJ (1998) Climatic conditions and tropical montane forest productivity: the fog has not lifted yet. Ecology 79:3–9

Bruijnzeel LA, Waterloo MJ, Proctor J et al (1993) Hydrological observations in montane rain forests on Gunung Silam, Sabah, Malaysia, with special reference to the 'Massenerhebung' effect. J Ecol 81:145–167

Bruijnzeel LA, Kappelle M, Mulligan M, Scatena FN (2010) Tropical montane cloud forests: state of knowledge and sustainability perspectives in a changing world. In: Bruijnzeel LA, Scatena FN, Hamilton LS (eds) Tropical montane cloud forests. Science for conservation and management. Cambridge University Press, Cambridge, pp 691–740

Bubb P, May I, Miles L et al (2004) Cloud forest agenda. Cambridge, UK: UNEPWCMC. Online at: http://sea.unep-wcmc.org/forest/cloudforest/index.cfm

Bücker A, Crespo P, Frede HG et al (2010) Identifying controls on water chemistry of tropical cloud forest catchments: combining descriptive approaches and multivariate analysis. Aquat Geochem 16:127–149

Calvo JC (1986) An evaluation of Thornthwaite's water balance technique in predicting stream runoff in Costa Rica. Hydrol Sci J 31:51–60

Cao G, Giambelluca TW, Stevens D et al (2007) Inversion variability in the Hawaiian trade wind regime. J Clim 20:1145–1160

Cavelier J, Jaramillo M, Solis D et al (1997) Water balance and nutrient inputs in bulk precipitation in tropical montane cloud forest in Panama. J Hydrol 193:83–96

Chang SC, Yeh CF, Wu MJ et al (2010) Fog deposition and chemistry in a sub-tropical montane cloud forest in Taiwan. In: Bruijnzeel LA, Scatena FN, Hamilton LS (eds) Tropical montane cloud forests. Science for conservation and management. Cambridge University Press, Cambridge, pp 378–386

Chen L, Liu WY, Wang GS (2010) Estimation of epiphytic biomass and nutrient pools in the subtropical montane cloud forest in the Ailao Mountains, south-western China. Ecol Res 25:315–325

Clark KL (1994) The role of epiphytic bryophytes in the net accumulation and cycling of nitrogen in a tropical montane cloud forest. PhD dissertation, University of Florida, Gainesville, FL, pp 271

Clark KL, Nadkarni NM, Schaefers D et al (1998) Cloud water and precipitation chemistry in a tropical montane forest, Monteverde, Costa Rica. Atmos Environ 32:1595–1603

Crockford RH, Richardson DP (2000) Partitioning of rainfall into throughfall, stemflow and interception: effect of forest type, ground cover and climate. Hydrol Process 14:2903–2920

DeLay J (2005) Canopy water balance of an elfin cloud forest at Alakahi, Hawai'i. Master's thesis, Geography, University of Hawai'i at Mānoa, Honolulu, USA

Dietz J, Hölscher D, Leuschner C et al (2006) Rainfall partitioning in relation to forest structure in differently managed montane forest stands in Central Sulawesi, Indonesia. For Ecol Manage 237:170–178

Edwards PJ (1982) Studies of mineral cycling in a montane rain forest in New Guinea. V. Rates of cycling in throughfall and litter fall. J Ecol 70:807–827

Edwards PJ, Grubb PJ (1977) Studies of mineral cycling in a montane rain forest in New Guinea. I. The distribution of organic matter in the vegetation and soil. J Ecol 65:943–969

Ekern PC (1964) Direct interception of cloud water on Lāna'ihale, Hawai'i. Soil Sci Soc Am Proc 28:419–421

Eugster W, Burkard R, Holwerda F et al (2006) Characteristics of fog and fogwater fluxes in a Puerto Rican elfin cloud forest. Agric For Meteorol 139:288–306

Fleischbein K, Wilcke W, Valarezo C et al (2006) Water budgets of three small catchments under montane forest in Ecuador: experimental and modeling approach. Hydrol Process 20:2491–2507

Frumau KFA, Burkard R, Schmid S et al (2010) Fog gauge performance under conditions of fog and wind-driven rain. In: Bruijnzeel LA, Scatena FN, Hamilton LS (eds) Tropical montane cloud forests. Science for conservation and management. Cambridge University Press, Cambridge, pp 293–301

Gerold G (2008) Soil, climate and vegetation in tropical montane forests – a case study from the Yungas, Bolivia. In: Gradstein SR, Homeier J, Gansert D (eds) The tropical mountain forest. Biodiversity and ecology series 2. University Of Akron Press, Göttingen, pp 137–162

Gerold G, Schawe M, Bach K (2008) Hydrometeorologic, pedologic and vegetation patterns along an elevational transect in the montane forest of the Bolivian Yungas. DIE ERDE 139:141–168

Giambelluca TW, DeLay JK, Nullet MA, et al (2010a) Canopy water balance of windward and leeward Hawaiian cloud forests on Haleakalā, Maui, Hawai'i. Hydrol Process 25:438–447

Giambelluca TW, DeLay JK, Nullet MA et al (2010b) Interpreting canopy water balance and fog screen observations: separating cloud water from wind-blown rainfall at two contrasting forest sites in Hawai'i. In: Bruijnzeel LA, Scatena FN, Hamilton LS (eds) Tropical montane cloud forests. Science for conservation and management. Cambridge University Press, Cambridge, pp 342–351

Gomez-Peralta D, Oberbauer SF, McClain ME et al (2008) Rainfall and cloudwater interception in tropical montane forests in the eastern Andes of Central Peru. For Ecol Manage 255:1315–1325

Häger A, Dohrenbusch A (2010) Structure and dynamics of tropical montane cloud forests under contrasting biophysical conditions in north-western Costa Rica. In: Bruijnzeel LA, Scatena FN, Hamilton LS (eds) Tropical montane cloud forests. Science for conservation and management. Cambridge University Press, Cambridge, pp 208–216

Hafkenscheid RLLJ (2000) Hydrology and biogeochemistry of tropical montane rain forests of contrasting stature in the Blue Mountains, Jamaica. PhD Thesis, VU University Amsterdam, Amsterdam, The Netherlands. (http://dare.ubvu.vu.nl/bitstream/1871/12734/1/texst.pdf)

Heath JA (2001) Atmospheric nutrient deposition in Hawai'i: methods, rates and sources. PhD Thesis, Oceanography, University of Hawai'i at Mānoa, Honolulu, USA

Herwitz SR, Slye RE (1992) Spatial variation in the interception of inclined rainfall by a tropical rainforest canopy. Selbyana 13:62–71

Hietz P (2010) Ecology and ecophysiology of epiphytes in tropical montane cloud forests. In: Bruijnzeel LA, Scatena FN, Hamilton LS (eds) Tropical montane cloud forests. Science for conservation and management. Cambridge University Press, Cambridge, pp 67–76

Hietz P, Wanek W, Wania R et al (2002) Nitrogen-15 natural abundance in a montane cloud forest canopy as an indicator of nitrogen cycling and epiphyte nutrition. Oecologia 131:350–355

Hofstede RGM, Wolf J, Benzing DH (1993) Epiphytic biomasss and nutrient status of a Colombian upper montane rain forest. Selbyana 14:37–45

Holder CD (2004) Rainfall interception and fog precipitation in a tropical montane cloud forest of Guatemala. For Ecol Manage 190:373–384

Hölscher D, Köhler L, Van Dijk AIJM et al (2004) The importance of epiphytes to total rainfall interception by a tropical montane rain forest in Costa Rica. J Hydrol 292:308–322

Holwerda F, Bruijnzeel LA, Muñoz-Villers LE et al (2010a) Rainfall and cloud water interception in mature and secondary lower montane cloud forests of central Veracruz, Mexico. J Hydrol 384:84–96

Holwerda F, Bruijnzeel LA, Oord AL et al (2010b) Fog interception in a Puerto Rican elfin cloud forest: a wet-canopy water budget approach. In: Bruijnzeel LA, Scatena FN, Hamilton LS (eds) Tropical montane cloud forests. Science for conservation and management. Cambridge University Press, Cambridge, pp 282–292

Hsu CC, Horng FE, Kuo CM (2002) Epiphyte biomass and nutrient capital of a moist subtropical forest in north-eastern Taiwan. J Trop Ecol 18:659–670

Hutley LB, Doley D, Yate DJ et al (1997) Water balance of an Australian subtropical rainforest at altitude: the ecological and physiological significance of intercepted cloud and fog. Aust J Bot 45:311–329

Ingraham NL, Mark AF (2000) Isotopic assessment of the hydrologic importance of fog deposition on tall snow tussock grass on southern New Zealand uplands. Austral Ecol 25:402–408

Janssens IA, Dieleman W, Luyssaert S et al (2010) Reduction of forest soil respiration in response to nitrogen deposition. Nat Geosci 3:315–322

Jarvis A, Mulligan M (2010) The climate of cloud forests. In: Bruijnzeel LA, Scatena FN, Hamilton LS (eds) Tropical montane cloud forests. Science for conservation and management. Cambridge University Press, Cambridge, pp 39–56

Juvik JO, DeLay JK, Kinney KM, et al (2010) A 50th anniversary reassessment of the seminal "Lāna'i fog drip study" in Hawai'i. Hydrol Process 25:402–410

Kappelle M (1995) Ecology of mature and recovering Talamancan montane *Quercus* forests, Costa Rica. PhD dissertation, University of Amsterdam, Amsterdam, The Netherlands

Katata G, Nagai H, Kajino M et al (2010) Numerical study of fog deposition on vegetation for atmosphere–land interactions in semi-arid and arid regions. Agric For Meteorol 150:340–353

Kellner T (2006) Niederschlagsnährstoffeinträge im Bergregenwaldökosystem der Yungas (Bolivien). Diplomarbeit Göttingen

Kitayama K, Majalap-Lee N, Aiba S (2000) Soil phosphorus fractionation and phosphorus use efficiencies of tropical rainforests along altitudinal gradients of Mount Kinabalu, Borneo. Oecologia 123:342–349

Klemm O, Wrzesinsky T, Scheer C (2005) Fog water flux at a canopy top: direct measurement versus one-dimensional model. Atmos Environ 39:5375–5386

Knorr M, Frey SD, Curtis PS (2005) Nitrogen additions and litter decomposition: a meta-analysis. Ecology 86:3252–3257

Köhler L, Arnoud Frumau KF et al (2007) Biomass and water storage dynamics of epiphytes in old-growth and secondary montane cloud forest stands in Costa Rica. Plant Ecol 193:171–184

Köhler L, Hölscher D, Bruijnzeel LA et al (2010) Epiphyte biomass in Costa Rican old-growth and secondary montane rain forests and its hydrologic significance. In: Bruijnzeel LA, Scatena FN, Hamilton LS (eds) Tropical montane cloud forests. Science for conservation and management. Cambridge University Press, Cambridge, pp 268–274

Kumaran S (2008) Hydrometeorology of tropical montane rain forests of Gunung Brinchang, Pahang Darul Makmur, Malaysia. PhD dissertation, University Putra Malaysia, Serdang, Malaysia

Küppers M, Motzer T, Schmitt D et al (2008) Stand structure, transpiration responses in trees and vines and stand transpiration of different forest types within the mountain rainforest. In: Beck E, Bendix J, Kottke I et al (eds) Gradients in a tropical mountain ecosystem of Ecuador. Ecological studies 198. Springer, Berlin, pp 243–258

Lawton RO, Nair US, Pielke RA Sr et al (2001) Climatic impact of tropical lowland deforestation on nearby montane cloud forests. Science 294:584–587

Letts MG, Mulligan M (2005) The impact of light quality and leaf wetness on photosynthesis in north-west Andean tropical montane cloud forest. J Trop Ecol 21:549–557

Leuschner C, Moser G, Bertsch C et al (2007) Large altitudinal increase in tree root/shoot ratio in tropical montain forests in Ecuador. Basic Appl Ecol 8:219–230

Liang YL, Lin TC, Hwong JL et al (2009) Fog and precipitation chemistry at a mid-land forest in central Taiwan. J Environ Qual 38:627–636

Liu WY, Li HM, Zhang YP et al (2010) Fog- and rain water chemistry in the seasonal tropical rain forest of Xishuangbanna, South-west China. In: Bruijnzeel LA, Scatena FN, Hamilton LS (eds) Tropical montane cloud forests. Science for conservation and management. Cambridge University Press, Cambridge, pp 387–392

Lovett G (1984) Rates and mechanisms of cloud water deposition to a subalpine balsam fir forest. Atmos Environ 18:361–371

Lundgren L, Lundgren B (1979) Rainfall, interception and evaporation in the Mazumbai forest reserve, West Usambara Mts., Tanzania and their importance in the assessment of land potential. Geogr Ann A 61:157–178

Mahowald NM, Artaxo P, Baker AR et al (2005) Impacts of biomass burning emissions and land use change on Amazonian atmospheric phosphorus cycling and deposition. Glob Biogeochem Cycles 19(GB4030):S1–S15

Marrs R, Proctor J, Heaney A et al (1988) Changes in soil nitrogen mineralization and nitrification along an altitudinal transect in tropical rain forest in Costa Rica. J Ecol 76:466–482

McJannet D, Wallace J, Reddell P (2007) Precipitation interception in Australian tropical rain-forests: II. Altitudinal gradient of cloud interception, stemflow, throughfall and interception. Hydrol Process 21:1703–1718

McJannet D, Wallace J, Reddell P (2010) Comparative water budgets of a lower and an upper montane cloud forest in the wet tropics of northern Australia. In: Bruijnzeel LA, Scatena FN, Hamilton LS (eds) Tropical montane cloud forests. Science for conservation and management. Cambridge University Press, Cambridge, pp 479–490

Meyer J-Y (2010) montane cloud forest in remote tropical islands of Oceania: the example of French Polynesia (South Pacific Ocean). In: Bruijnzeel LA, Scatena FN, Hamilton LS (eds) Tropical montane cloud forests. Science for conservation and management. Cambridge University Press, Cambridge, pp 121–129

Mudd R (2004) Significance of the epiphyte layer to stem water storage in native and invaded tropical montane cloud forests in Hawaiʻi. Bachelor of Science thesis, Global Environmental Science Program, University of Hawaiʻi at Mānoa, Honolulu, Hawaiʻi

Mulligan M (2010) Modelling the tropics-wide extent and distribution of cloud forest and cloud forest loss, with implications for conservation priority. In: Bruijnzeel LA, Scatena FN, Hamilton LS (eds) Tropical montane cloud forests. Science for conservation and management. Cambridge University Press, Cambridge, pp 14–38

Mulligan M, Burke SM (2005) FIESTA Fog Interception for the enhancement of streamflow in tropical areas. Final Technical Report for AMBIOTEK contribution to DfID FRP R7991

Mulligan M, Jarvis A, González J et al (2010) Using "biosensors" to elucidate rates and mechanisms of cloud water interception by epiphytes, leaves and branches in a sheltered Colombian cloud forest. In: Bruijnzeel LA, Scatena FN, Hamilton LS (eds) Tropical montane cloud forests. Science for conservation and management. Cambridge University Press, Cambridge, pp 249–260

Nadkarni N (1984) Epiphyte biomass and nutrient capital of a neotropical elfin forest. Biotropica 16:249–256

Nadkarni NM, Matelson TJ (1992a) Biomass and nutrient dynamics of fine litter of terrestrially rooted material in a Neotropical montane forest, Costa Rica. Biotropica 24:113–120

Nadkarni NM, Matelson TJ (1992b) Biomass and nutrient dynamics of epiphytic litterfall in a neotropical montane forest, Costa Rica. Biotropica 24:24–30

Nadkarni NM, Schaefer D, Matelson TJ et al (2004) Biomass and nutrient pools of canopy and terrestrial components in a primary and a secondary montane cloud forest, Costa Rica. For Ecol Manage 198:223–236

Northup R, Yu Z, Dahlgren RA et al (1995) Polyphenol control of nitrogen release from pine litter. Nature 377:227–229

Oesker M, Dalitz H, Günter S et al (2008) Spatial heterogeneity patterns – a comparison between gorges and ridges in the upper part of an evergreen lower montane forest. In: Beck E,

Bendix J, Kottke I et al (eds) Gradients in a tropical mountain ecosystem of Ecuador, Ecological studies, 198. Springer, Berlin, pp 267–274

Oesker M, Homeier J, Dalitz H et al (2010) Spatial heterogeneity of throughfall quantity and quality in tropical monatne forests in southern Ecuador. In: Bruijnzeel LA, Scatena FN, Hamilton LS (eds) Tropical montane cloud forests. Science for conservation and management. Cambridge University Press, Cambridge, pp 393–401

Owiunji I, Pumptre A (2010) The importance of cloud forest sites in the conservation of endemic and threatened species of the Albertine Rift. In: Bruijnzeel LA, Scatena FN, Hamilton LS (eds) Tropical montane cloud forests. Science for conservation and management. Cambridge University Press, Cambridge, pp 164–171

Pocs T (1980) The epiphytic biomass and its effect on the water balance of two rain forest types in the Uliguru Mountains (Tanzania, East Africa). Acta Bot Hung 26:143–167

Proctor J (2005) Rainforest mineral nutrition: the "black box" and a glimpse inside it. In: Bonell M, Bruijnzeel LA (eds) Forests, water, and people in the humid tropics. Cambridge University Press, Cambridge, pp 422–446

Rao PSP, Momin GA, Safai PD et al (1995) Rain water and throughfall chemistry in the Silent Valley forest in South India. Atmos Environ 29:2025–2029

Rollenbeck R (2010) Global sources – local impacts: natural and anthropogenic matter deposition in the Andes of Ecuador. GEO-ÖKÖ 31:5–27

Rollenbeck R, Fabian P, Bendix J (2006) Precipitation dynamics and chemical properties in tropical mountain forests of Ecuador. Adv Geosci 6:73–76

Rollenbeck R, Fabian P, Bendix J (2010) Temporal heterogeneities – matter deposition from remote areas. In: Beck E, Bendix J, Kottke I et al (eds) Gradients in a tropical mountain ecosystem of Ecuador. Ecological studies 198. Springer, Berlin, pp 303–310

Roman L, Scatena FN, Bruijnzeel LA (2010) Global and local variations in tropical montane cloud forest soils. In: Bruijnzeel LA, Scatena FN, Hamilton LS (eds) Tropical montane cloud forests. Science for conservation and management. Cambridge University Press, Cambridge, pp 77–89

Santiago L, Goldstein G, Meinzer F et al (2000) Transpiration and forest structure in relation to soil waterlogging in a Haiwaiian montane cloud forest. Tree Physiol 20:673–681

Scatena FN, Bruijnzeel LA, Bubb P et al (2010) Setting the stage. In: Bruijnzeel LA, Scatena FN, Hamilton LS (eds) Tropical montane cloud forests. Science for conservation and management. Cambridge University Press, Cambridge, pp 3–13

Schawe M (2005) Hypsometrischer Klima- und Bodenwandel in Bergregenwaldökosystemen Boliviens. Diss. Göttingen, 126

Schawe M, Gerold G, Bach K et al (2010) Hydrometeorological patterns in relation to montane forest types along an elevational gradient in the Yungas of Bolivia. In: Bruijnzeel LA, Scatena FN, Hamilton LS (eds) Tropical montane cloud forests. Science for conservation and management. Cambridge University Press, Cambridge, pp 199–207

Schmid S, Burkard R, Frumau KFA et al (2010) The wet-canopy water balance of a Costa Rican cloud forest during the dry season. In: Bruijnzeel LA, Scatena FN, Hamilton LS (eds) Tropical montane cloud forests. Science for conservation and management. Cambridge University Press, Cambridge, pp 302–308

Scholl M, Gingerich SB, Tribble G (2002) The influence of microclimates and fog on stable isotope signatures used in the interpretation of regional hydrology: East Maui, Hawai'i. J Hydrol 264:170–184

Scholl MA, Giambelluca TW, Gingerich SB et al (2007) Cloud water in windward and leeward mountain forests: the stable isotope signature of orographic cloud water. Water Resour Res 43: W12411. doi:10.1029/2007WR006011

Scholl M, Eugster W, Burkard R (2010) Understanding the role of fog in forest hydrology: stable isotopes as tools for determining input and partitioning of cloud water in montane forests. In: Bruijnzeel LA, Scatena FN, Hamilton LS (eds) Tropical montane cloud forests. Science for conservation and management. Cambridge University Press, Cambridge, pp 228–241

Schuur EAG, Matson PA (2001) Net primary productivity and nutrient cycling across a mesic to wet precipitation gradient in Hawaiian montane forest. Oecologia 128:431–442

Sharon D (1980) The distribution of effective rainfall incident on sloping ground. J Hydrol 46:165–188

Silver WL, Lugo AE, Keller M (1999) Soil oxygen availability and biogeochemistry along rainfall and topographic gradients in upland wet tropical forest soils. Biogeochemistry 44:301–328

Silver WL, Thompson AW, Herman DJ et al (2010) Is there evidence for limitations to nitrogen mineralization in upper montane tropical forests? In: Bruijnzeel LA, Scatena FN, Hamilton LS (eds) Tropical montane cloud forests. Science for conservation and management. Cambridge University Press, Cambridge, pp 418–427

Smith K, Gholz HL, Oliveira FA (1998) Litterfall and nitrogen-use efficiency of plantations and primary forest in eastern Brazilian Amazon. For Ecol Manage 109:209–220

Soethe N, Lehmann J, Engels C (2006) The Vertical pattern of rooting and nutrient uptake at different altitudes of a south Ecuadorian montane forest. PlantSoil 286:S287–S299

Soethe N, Lehmann J, Engels C (2008a) Nutrient availability at different altitudes in a tropical montane forest in Ecuador. J Trop Ecol 24:397–440

Soethe N, Wilcke W, Hohmeier J et al (2008b) Plant growth along the altitudinal gradient – Role of plant nutritional status, fine root activity, and soil properties. In: Beck E, Bendix J, Kottke I et al (eds) Gradients in a tropical mountain ecosystem of Ecuador. Ecological studies 198. Springer, Berlin, pp 259–266

Steinhardt U (1979) Untersuchungen über den Wasser- und Nährstoffhaushalt eines andinen Wolkenwaldes in Venezuela. Göttinger Bodenkundliche Berichte 56:1–185

Still CJ, Foster PN, Schneider SH (1999) Simulating the effects of climate change on tropical montane cloud forests. Nature 398:608–610

Takahashi M, Giambelluca TW, Mudd RG et al (2010) Rainfall partitioning and cloud water interception in native forest and invaded forest in Hawai'i Volcanoes National Park. Hydrol Process 25:448–464

Tanner EVJ (1977) Mineral cycling in montane rain forests in Jamaica. PhD thesis, University of Cambridge

Tanner EVJ (1980) Litterfall in montane rain forests of Jamaica and its relation to climate. J Ecol 68:833–848

Tanner EVJ (1985) Jamaican montane forests: nutrient capital and cost of growth. J Ecol 73:553–568

Tobón C, Köhler L, Frumau KFA et al (2010) Water dynamics of epiphytic vegetation in a lower montane cloud forest: fog interception, storage and evaporation. In: Bruijnzeel LA, Scatena FN, Hamilton LS (eds) Tropical montane cloud forests. Science for conservation and management. Cambridge University Press, Cambridge, pp 261–267

Veneklaas EJ (1990) Nutrient fluxes in bulk precipitation and throughfall in two montane tropical rain forests, Colombia. J Ecol 78:974–992

Veneklaas EJ (1991) Litterfall and nutrient fluxes in two montane tropical rain forests, Colombia. J Trop Ecol 7:319–336

Veneklaas EJ, Zagt RJ, van Leerdam A et al (1990) Hydrological properties of the epiphyte mass of a montane tropical rain forest, Colombia. Vegetation 89:183–192

Vis M (1986) Interception, drop size distributions and rainfall kinetic energy in four Colombian forest ecosystems. Earth Surf Proc Land 11:591–570

Walmsley JL, Schemenauer RS, Bridgman HA (1996) A method for estimating the hydrological input from fog in mountainous terrain. J Appl Meteorol 35:2237–2249

Weaver PL (1972) Cloud moisture interception in the Luquillo Mountains of Puerto Rico. Carribbean J Sci 12:129–144

Wilcke W, Yasin S, Abramowski U et al (2001) Change in water quality during the passage through a tropical montane rain forest in Ecuador. Biogeochemistry 55:45–72

Wilcke W, Yasin S, Abramowski U et al (2002) Nutrient storage and turnover in organic layers under tropical montane rain forest in Ecuador. Eur J Soil Sci 53:15–27

Wilcke E, Yasin S, Schmitt A et al (2008a) Soils along the altitudinal transect and in catchments. In: Beck E, Bendix J, Kottke I et al (eds) Gradients in a tropical mountain ecosystem of Ecuador. Ecological studies 198. Springer, Berlin, pp 75–85

Wilcke W, Yasin S, Fleischbein K et al (2008b) Nutrient status and fluxes at the field and catchment scale. In: Beck E, Bendix J, Kottke I et al (eds) Gradients in a tropical mountain ecosystem of Ecuador. Ecological studies 198. Springer, Berlin, pp 203–215

Wilcke W, Oelmann Y, Schmitt A et al (2008c) Soil properties and tree growth along an altitudinal transect in Ecuadorian tropical montane forest. J Plant Nutr Soil Sci 171:220–230

Williams S, Bolitho E, Fox S (2003) Climate change in Australian tropical rainforests: an impending environmental catastrophe. P Roy Soc Lond B Biol Sci 270:1887–1893

Yasin S (2001) Water and nutrient dynamics in microcatchments under montane forest in the south Ecuadorian Andes. (Bayreuther Bodenkundliche Berichte 73) University of Bayreuth, Bayreuth

Zadroga F (1981) The hydrological importance of a montane cloud forest area of Costa Rica. In: Lal R, Russell EW (eds) Tropical agricultural hydrology. Wiley, New York, pp 59–73

Zimmermann A, Wilcke W, Elsenbeer H (2007) Spatial and temporal patterns of throughfall quantity and quality in a tropical montane forest in Ecuador. J Hydrol 343:80–96

Chapter 12
Hydrology and Biogeochemistry of Temperate Forests

Nobuhito Ohte and Naoko Tokuchi

12.1   Introduction

Temperate forests are distributed extensively in middle latitude regions, where the mean annual temperature range is 3–18°C and the mean annual precipitation range is 500–3,300 mm (for cooler region 500–2,000 mm; warmer season 500–3,300 mm). The total area and biomass of the world's temperate forests are slightly less than those of tropical and boreal forests; their net productivity is second to that of tropical wet and moist forests, and is greater than that of boreal forests (Table 12.1).

Whittaker's biome classification scheme is the commonly accepted method for defining biomes; it subdivides temperate forests into three major forest types (Whittaker 1975). The first type is the temperate rain forest, which occurs in regions with the greatest precipitation and consists of evergreen coniferous or evergreen broadleaf trees. Its distribution is limited compared with the distributions of other types of temperate forests. Most temperate rain forests occur in the oceanic-moist climates of western North America, southwestern South America (southern Chile and adjacent Argentina), northwestern Europe (southern Norway to northern Spain), southeastern Australia (Tasmania and Victoria), New Zealand (South Island's west coast), eastern Taiwan's Pacific coast, and southwestern Japan. The rainy season varies by region; it is represented by the monsoon system in summer in the Asian rain forest, and occurs in winter along the west coast of North America. Species diversity of the temperate rain forest is relatively low.

The second type of temperate forest, the temperate deciduous forest, is the dominant temperate forest type. It occurs mostly in continental regions that are moderately humid, with sufficient summer rain and markedly cool or cold winters. Temperate deciduous forest is found in the eastern and western United States, Canada, central Mexico, South America, Europe, China, Japan, North Korea, South Korea, and parts of Russia. The third type of temperate forest is the temperate evergreen forest. This forest type comprises a great variety of plant life, depending on the climate. In the dry summer Mediterranean climate of the southern west coast of the US and southern Australia, the evergreen forest is dominated by small-leaved evergreen trees. In the continental climate of the western US, there are large-scale evergreen coniferous

Table 12.1 Comparison of primary production and biomass estimates for temperate, tropical, and boreal forests[a]

Forest	Area (10^{12} m^2)	Mean plant biomass (kg C m^{-2})	Carbon in vegetation (10^{15} g)	Mean net primary production (g C m^{-2} year^{-1})	Net primary production (10^{15} g year^{-1})
Tropical wet and moist forest	10.4	15	156.0	800	8.3
Tropical dry forest	7.7	6.5	49.7	620	4.8
Temperate forest	9.2	8	73.3	650	6.0
Boreal forest	15.0	9.5	143.0	430	6.4

[a] From Houghton and Skole (1990) and Schlesinger (1997)

forests. In southern China and Japan, where the climate is dominated by the East Asian summer monsoon, there are broadleaf evergreen forests.

Temperate forests are dominated by a large variety of community structures, relatively high biodiversity, and complex nutrient cycles consisting of numerous biogeochemical reactions (e.g., Odum 1963; Likens et al. 1977; Matzner 2004). It is common in temperate regions for forests to be the dominant landscape feature in the mountainous headwaters of river catchments, often including river sources. Therefore, studies of forest hydrology have investigated "catchment" hydrology, targeting landscapes of hillslopes and valleys (Kirkby 1978).

Seasonal variations in air temperature are greater in the temperate ecoregion than in tropical regions, and evapotranspiration has clear seasonality in temperate regions. There are also seasonal patterns of precipitation, such as a summer or winter rainy season, and the amplitudes of the seasonal variations in amount and type of precipitation are larger in temperate forests than in boreal forests. The combination of seasonal patterns of precipitation and evapotranspiration contributes to complex variations in catchment hydrological conditions, including soil wetness, groundwater level, and discharge. Even with equal amounts of annual precipitation, the dryness and hydrological conditions of forested catchments can vary by region among summer rainy climates (humid subtropical climate in the southeastern US, east coast of Eurasia, southeastern Africa, and the east coast of Australia), winter rainy climates (Mediterranean climate in southern Europe and the southwest coast of North American), and climates with less seasonality in precipitation (maritime temperate climate in Europe, except the Mediterranean and Scandinavian regions, and the northwest coast of North American). Consequently, the wetness or dryness of a forested catchment influenced by climatic characteristics affects the biogeochemical dynamics of the ecosystem. Apart from its effects on plant physiological activities, hydrological seasonal variation adds seasonality to the biogeochemical dynamics driven by soil microbes.

Since the 1930s, many studies have examined forest hydrology, mainly in temperate regions. Enormous amounts of data and knowledge regarding hydrological and biogeochemical processes have been archived. Kirkby (1978) reviewed and summarized the scientific essence of hillslope hydrology studies until the 1970s. A milestone study of forest ecosystem biogeochemistry conducted in the Hubbard

Brook Experimental Forest in New Hampshire, United States, identified the biogeo-chemical cycles operating in forested catchments and developed methodologies for examining the mechanisms governing these cycles (Likens et al. 1977; Bormann and Likens 1979). These works have influenced many forest ecosystem ecologists.

In this chapter, we review the cutting-edge work in forest hydrology and biogeo-chemistry undertaken in the last three decades. We also attempt to identify important advances in temperate forest ecosystem studies that are likely to be addressed in the coming decade, including the influence of climatic variation on the biogeochemical dynamics of temperate ecosystems under various seasonal precipitation regimes.

Gas exchange between forests and the atmosphere is not considered in this chapter. Interested readers are referred to Chap. 5 and the comprehensive synthesis of Valentini (2003). Details of the physical aspects of hillslope hydrological processes are described in Chap. 23.

12.2 Hydrology and Biogeochemistry of Temperate Forests

12.2.1 Hydrological Characteristics

As for forests in other climate regions, the most critical climatic factor characteriz-ing temperate regions is temperature. Under given air temperatures, certain levels of evapotranspiration are caused by the amount of radiative energy, controlling the water budgets of forested catchments.

Figure 12.1 shows the relationship between annual precipitation and discharge for various forested catchments in temperate and tropical forests (Tables 12.2 and 12.3, respectively). Annual precipitation ranges from 990 to 3,673 mm for temperate forests and from 1,851 to 5,795 mm for tropical forests. The slope of the regression line for each forest is approximately 1. This indicates that there is smaller variability in annual loss than in annual precipitation, and that this relationship is fairly constant within regions with variable precipitation, in both temperate and tropical forests. Namely, annual runoff rate mainly depends on the precipitation amount of each forest catch-ment. Furthermore, annual evapotranspiration rates assumed from loss (precipitation – evapotranspiration) in temperate forests (average, 710.8 mm) are lower than those in tropical forests (average, 1,502.2 mm).

For the boreal or taiga forests, catchment studies have been conducted mainly in Scandinavia and Eastern Canada (e.g., Grip and Bishop 1991; Buttle et al. 2000). In the NOPEX (Northern hemisphere climate-process land-surface experiment) proj-ect conducted in the boreal forest of southern Sweden (Halldin et al. 1999), Seibert (1994) estimated the annual average (1981–1990) water balance; the mean annual precipitation, evaporation, and runoff were 730, 470, and 270 mm, respectively. Observations of evapotranspiration by flux techniques are common in boreal regions. In the taiga forest of eastern Siberia, near Yakutsk, annual evapotranspiration was estimated at 151 mm, and was 73% of the total water input (211 mm; precipitation,

Fig. 12.1 Relationship between the annual precipitation and discharge of forested catchments in temperate (*open circle*) and tropical (*closed circle*) forests (sites are listed in Tables 12.2 and 12.3). Slopes and intercepts of the regression lines, respectively: temperate forests, 0.982 and −679.2 mm; tropical forests, 1.020 and −1,528.9 mm. Both correlations are significant ($p < 0.001$)
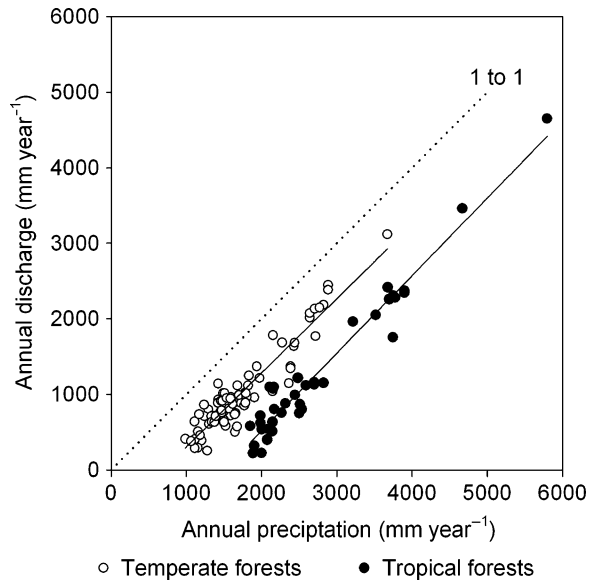
106 mm; snow melt water, 105 mm) between April 2 and September 7, 1998 (Ohta et al. 2001). In the taiga forest of central Siberia, estimates of the mean annual precipitation and evapotranspiration were 600 and 265 mm, respectively, during the growing season (Kelliher et al. 1998). For some BOREAS (Boreal Ecosystem-Atmosphere Study) sites in central Canada, mean annual precipitation rates were estimated at 421–447 mm and simulated evapotranspiration rates were 197–271 mm (Kimball et al. 1997).

These data indicate that the most important hydroclimatic characteristics of temperate forests are moderate evapotranspiration rates and moderate ranges of annual precipitation. Evapotranspiration rates in temperate forests are about half of those in tropical moist forests and 1.5–2 times of those in boreal forests.

As mentioned in the introduction of this chapter, the majority of forest hydrology studies have been conducted in temperate regions. It is not an exaggeration to state that the principles of the physical hydrology of forested catchments have been established in temperate regions. The reasons for this involve the presence of complex hydrological processes consisting of the multiple physical and biological processes associated with perennial stream flow throughout the year and the highly dynamic flow variation that occurs with storm events. These are exciting targets from a scientific standpoint. The practical importance of these systems has also long been recognized, as forest headwaters have frequently provided water resources for populated downstream areas in temperate regions. The provision of high quantities and quality of water, and the prevention of flood and debris-flow disasters are some of the most important issues for governments. The quality of stream water in water resource regions has traditionally been studied alongside biogeochemical investigations of forest ecosystems, as in the experiments in the Hubbard Brook Experimental Forest (Likens et al. 1977) and the

Table 12.2 Forest type, annual rainfall, annual runoff, and annual evapotranspiration (loss) of catchments in temperate regions

Catchment	Forest type[a]	Annual rainfall (mm year^{-1})	Annual runoff (mm year^{-1})	Annual loss (mm year^{-1})	Notes
Japan					
Watarasegawa (Japan)	CE (planted)	2,430	1,638	792	b
Tsukuba (Japan)	CE (planted)	1,587	720	867	b
Takayama A (Japan)	CE (planted)	2,439	1,683	756	b
Takayama B (Japan)	CE (planted)	2,439	1,683	756	b
Asiu Kamitani (Japan)	BD	2,885	2,448	437	b
Asiu Yusentani (Japan)	BD	2,885	2,385	500	b
Ryuouzan (Japan)	CE (planted)	2,273	1,686	587	b
Kiryu (Japan)	CE (planted), BD	1,672	936	736	b
Hieizan S. (Japan)	CE (planted)	1,976	1,215	761	b
Hieizan H. (Japan)	CE (planted)	1,976	1,215	761	b
Kagawa 24 (Japan)	CE (planted), BD (planted)	1,202	390	812	b
Kagawa 25 (Japan)	CE (planted), BD	1,202	390	812	b
Kagawa 26 (Japan)	BE, BD	1,202	390	812	b
Kagawa 32 (Japan)	BE	1,202	390	812	b
Jiuriansan (China)	BE	1,906	958	948	b
Kamabuchi 1 (Japan)	BD, CE (planted)	2,641	2,016	625	c
Kamabuchi 2 (Japan)	BD, CE (planted)	2,641	2,075	566	c
Takaragawa H. (Japan)	BD, CE	3,673	3,117	556	c
Takaragawa S. (Japan)	BD, CE	2,153	1,783	370	c
Hitachi Ohta B. (Japan)	BD, CE	1,567	916	651	c
Hitachi Ohta C. (Japan)	CE (planted), BD	1,654	752	902	c
Hitachi Ohta Y. (Japan)	CE (planted)	1,666	905	761	c
Kasama B. (Japan)	BD	1,646	504	1,142	c
Kasama C. (Japan)	CE (planted)	1,674	574	1,100	c
Ashio (Japan)	BD	2,363	1,148	1,215	c
Tatsunokuchi S. (Japan)	CE, CE (planted)	1,153	293	860	c
Tatsunokuchi N. (Japan)	CE	1,113	290	823	c
Ananomiya (Japan)	CE, BD	1,478	913	565	c

(*continued*)

Table 12.2 (continued)

Catchment	Forest type[a]	Annual rainfall (mm year^{-1})	Annual runoff (mm year^{-1})	Annual loss (mm year^{-1})	Notes
Kazunari (Japan)	CE, BD	1,468	829	639	c
Higashiyama (Japan)	CE, BD	1,782	1,022	760	c
Shirasaka (Japan)	CE, BD	1,724	886	838	c
North America					
Coweeta WS2 (USA)	CE, BD	1,772	854	918	b
Hubbard Brook (USA)	BD, CE	1,295	800	495	b
Bear Brook (USA)	BD, CE	1,422	930	492	c
Catskill (USA)	BD, CE	1,679	1,118	561	c
Huntington Forest (USA)	BD, CE	1,112	639	473	c
White Oak Run (USA)	BD	990	413	577	b
Walker Branch (USA)	BD	1,368	713	655	b
Sugar Cove Creek (USA)	BD	1,480	813	668	b
Hall Creek (USA)	CE, BD	1,452	762	690	b
Puncheon Creek (USA)	BD	1,158	508	650	b
Chestnut Flats Branch (USA)	BD	1,301	610	691	b
Cosby Creek (USA)	BD, CE	1,240	711	529	b
Roaring Fork (USA)	BD	1,115	406	709	b
False Gap Prong (USA)	CE, BD	1,335	711	624	b
Correll Branch (USA)	BD, CE	1,170	737	434	b
Little Sandymush Creek (USA)	BD	1,063	381	682	b
Eagle Creek (USA)	CE, BD	1,459	889	570	b
Forney Creek (USA)	BD	1,422	1,143	279	b
Grassy Creek (USA)	BD, CE	1,337	635	702	b
Brush Creek (USA)	BD, CE	1,419	889	530	b
Henderson Creek (USA)	CE, BD	1,375	635	740	b
Welch Mill Creek (USA)	CE, BD	1,525	838	686	b
White Oak Creek (USA)	BD	1,534	864	671	b
Catheys Creek (USA)	BD	1,820	1,118	702	b

(*continued*)

Table 12.2 (continued)

Catchment	Forest type[a]	Annual rainfall (mm year^{-1})	Annual runoff (mm year^{-1})	Annual loss (mm year^{-1})	Notes
Mud Creek (USA)	BD, CE	1,618	914	704	[b]
Allison Creek (USA)	BD	1,593	965	628	[b]
Brush Creek (USA)	BD, CE	1,702	991	711	[b]
Middle Saluda River (USA)	BD	1,802	965	836	[b]
Little Branch Creek (USA)	BD	1,238	864	374	[b]
Perry Creek Tributary (USA)	CE, BD	1,391	711	680	[b]
Dunn Mill Creek (USA)	CE, BD	1,488	1,016	472	[b]
Owenby Creek (USA)	BD, CE	1,462	914	548	[b]
Bear Creek (USA)	BD, CE	1,493	762	731	[b]
Weaver Creek (USA)	BD, CE	1,509	1,016	493	[b]
Kiutuestia Creek Tributary (USA)	CE, BD	1,479	914	565	[b]
White Path Creek (USA)	CE, BD	1,564	813	751	[b]
Bryant Creek (USA)	CE, BD	1,597	940	657	[b]
Hinton Creek (USA)	CE	1,496	635	861	[b]
Persimmon Creek (USA)	BD, CE	1,791	1,016	775	[b]
She Creek (USA)	CE, BD	1,785	889	896	[b]
Deep Creek (USA)	CE, BD	1,644	737	908	[b]
Fernow 1 (USA)	BD	1,524	584	940	[c]
Fernow 2 (USA)	BD	1,500	660	840	[c]
Fernow 5 (USA)	BD	1,473	762	711	[c]
Fernow 3 (USA)	BD	1,500	635	865	[c]
Fernow 7 (USA)	BD	1,469	788	681	[c]
H.J. Andrews 1 (USA)	CE	2,388	1,372	1,016	[c]
H.J. Andrews 3 (USA)	CE	2,388	1,346	1,042	[c]
Pine Tree Branch (USA)	BD	1,280	255	1,025	[c]
White Hollow (USA)	CE, BD	1,184	460	724	[c]
Hany (Canada)	CE	2,146	1,040	1,106	[b]
Europe					
Mont Lozere B. (France)	BD	1,831	1,251	580	[b]

Table 12.2 (continued)

Catchment	Forest type[a]	Annual rainfall (mm year^{-1})	Annual runoff (mm year^{-1})	Annual loss (mm year^{-1})	Notes
Mont Lozere S. (France)	CE	1,936	1,370	566	[b]
White Laggan (UK)	CE (planted)	2,822	2,185	637	[b]
Green Burn (UK)	CE	2,707	2,135	572	[b]
Monachyle (UK)	HE, GR	2,770	2,149	621	[b]
Beddgelert Forest (UK)	CE (planted)	2,717	1,770	948	[b]
Villingen (Germany)	CE (planted)	1,616	874	742	[b]
Emmental Rappengraben (Swiss)	CE, BD	1,536	952	584	[c]
Sperbel-Graben (Swiss)	CE, BD	1,589	942	647	[c]

[a] Forest types: *BD* broadleaf and deciduous; *BE* broadleaf and evergreen; *CE* coniferous and evergreen; *HE* heath; *GR* grassland
[b] Original references are listed in Ohte and Tokuchi (1999)
[c] Listed in Nakano (1976), reproduced with permission

Table 12.3 Forest type, annual rainfall, annual runoff, and annual loss of catchments in tropical regions[a]

Catchment	Forest type[b]	Annual rainfall (mm year^{-1})	Annual runoff (mm year^{-1})	Annual loss (mm year^{-1})	Notes
Asia-Pacific					
Babinda south (Australia)	N	3,899	2,372	1,502	
Babinda north (Australia)	N	3,899	2,344	1,501	
Mondo (Indonesia)	S	4,668	3,460	1,217	
Sungai Bedup (Malaysia)	N	3,516	2,050	1,466	
Ulu Gombak (Malaysia)	N	2,500	750	1,750	
Sungai Langat (Malaysia)	N	2,823	1,152	1,670	
Sungai Gombak (Malaysia)	N	2,588	1,120	1,468	
Ulu Langat (Malaysia)	N	2,483	1,219	1,263	
Sungai Lui 1 (Malaysia)	N	2,156	1,077	1,079	Year: 1968–1969
Sungai Lui 2 (Malaysia)	N	2,109	1,100	1,009	Year: 1968–1969
Sungai Lui 3 (Malaysia)	N	2,162	1,100	1,062	Year: 1968–1969

Table 12.3 (continued)

Catchment	Forest type[b]	Annual rainfall (mm year^{-1})	Annual runoff (mm year^{-1})	Annual loss (mm year^{-1})	Notes
Sungai Lui 1 (Malaysia)	N	2,537	803	1,734	Year: 1972–1974
Sungai Lui 1 (Malaysia)	N	2,266	757	1,509	Year: 1988
Sungai Tekam C (Malaysia)	N	1,902	322	1,580	
Sungai Tekam sub B (Malaysia)	S	2,148	634	1,514	
Sungai Tekam A (Malaysia)	S	2,171	804	1,368	
Berembun C1 (Malaysia)	N	1,884	223	1,661	
Berembun C3 (Malaysia)	N	2,003	225	1,778	
Mendolong W3 (Malaysia)	S	3,215	1,962	1,253	
Bukit Tarek C1 (Malaysia)	N	2,700	1,160	1,540	
Bukit Tarek C2 (Malaysia)	N	2,700	1,132	1,568	
Sapulut (Malaysia)	N	2,318	880	1,450	
Ulu Kalungpan (Malaysia)	S	1,851	581	1,206	
Watawala (Sri Lanka)	N	3,777	2,282	2,495	
Africa					
Tai 1 (Ivory Coast)	N	2,003	538	1,465	
Tai 2 (Ivory Coast)	N	1,986	623	1,363	
Guma (Sierra Leone)	N	5,795	4,649	1,146	
Central and South America					
Sierra Nevada (Colombia)	N	1,983	718	1,265	
Barro Branco (Brazil)	N	2,076	400	1,675	Year: 1976–1977
Barro Branco (Brazil)	N	2,510	868	1,642	Year: 1981–1982
Bacio Modelo (Brazil)	N	2,089	541	1,548	
Gregoire 1 (French Guiana)	N	3,676	2,418	1,528	
Gregoire 2 (French Guiana)	N	3,697	2,260	1,437	
Gregoire 3 (French Guiana)	N	3,751	2,307	1,444	
Mt. Airy (Jamaica)	S	3,233	1,375	1,850	Elevation: 617–794

(*continued*)

Table 12.3 (continued)

Catchment	Forest type[b]	Annual rainfall (mm year^{-1})	Annual runoff (mm year^{-1})	Annual loss (mm year^{-1})	Notes
Mt. Airy (Jamaica)	N	3,746	1,753	1,998	Elevation: 777–1,265
Barro Colorado (Panama)	N	2,444	992	1,452	
Tonka (Slinam)	N	2,143	513	1,630	

[a] All data are cited from Kuraji (1996), with exception of those for high-altitude and small (<5 ha) catchments
[b] Forest types are categorized according to Kuraji (1996): *N* natural growth; *S* secondary stands that had clear-cut logging within the past 10 years. Natural forests were classified as broadleaf evergreen forests

Coweeta Hydrologic Laboratory (North Carolina, USA; Swank and Crossley 1988), which were conducted to elucidate the ecosystem functions controlling water and biogeochemical cycles in forests. Disaster prevention has also motivated hydrological studies alongside geomorphological examinations of mountainous regions (e.g., Okunishi et al. 1987; McDonnell 1990; Montgomery and Dietrich 1994; Okunishi 1994).

12.2.2 Milestone Studies in Physical Hydrology

Studies of the physical processes of hillslope hydrology began with the discovery of overland flow and descriptions of its function by Horton (1933) in the 1930s. Although the details are described in Chap. 23, here we present the characteristics of studies of physical processes of forest hydrology in temperate regions. Generally, in temperate forest regions, researchers should consider the effects of evapotranspiration and runoff processes simultaneously when discussing catchment wetness, because the combination of seasonal variations in these two factors can influence the seasonal patterns of catchment wetness. In other words, we can estimate and evaluate seasonal variations in both evapotranspiration and runoff rates by analyzing the temporal variation in one of these. For example, short-term water budget calculations can estimate the seasonal variation in the evapotranspiration rate based on the effects of evapotranspiration on the recession pattern of the runoff rate after a storm event (e.g., Suzuki 1980; Kosugi and Katsuyama 2007).

This phenomenon may be especially relevant in regions with summer rainy climates, because when summer precipitation is low, the seasonal pattern of the runoff rate is regulated mainly by evapotranspiration intensity, and not by precipitation. This mechanism is relatively simple compared with that in regions with high summer precipitation. In regions with rainy summers, the relative intensities of precipitation and evapotranspiration control catchment hydrological factors such as soil wetness, groundwater level, and discharge rate. Consequently, the hydrological response to
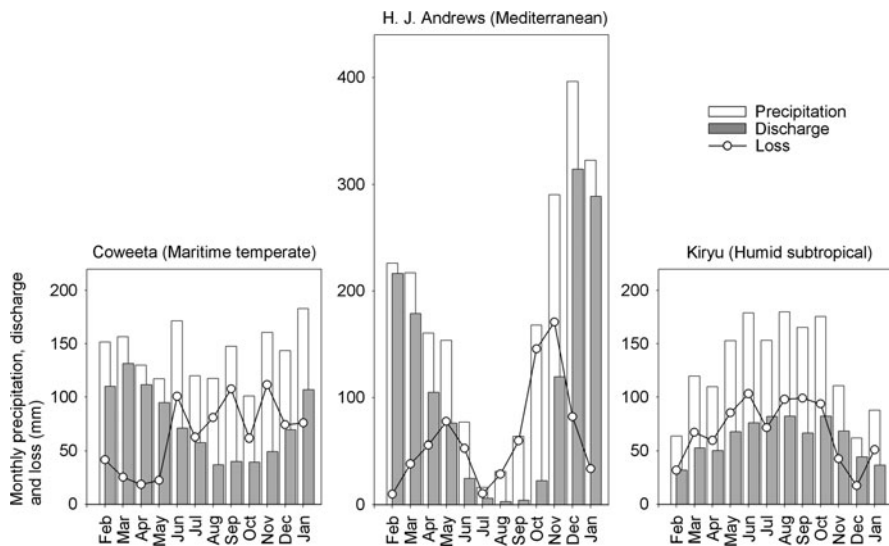
Fig. 12.2 Seasonal variations in precipitation, discharge, and evapotranspiration (ET) (estimated by subtracting discharge from precipitation) in three different temperate forest catchments: Coweeta's broadleaf deciduous forest under a maritime temperate climate (Coweeta Long Term Ecological Research 2010, http://coweeta.uga.edu/results_catalog_b.php); H.J. Andrews' evergreen coniferous forest under a Mediterranean climate (Andrews Experimental Forest Long Term Ecological Research 2010, http://andrewsforest.oregonstate.edu/data/mastercatalog.cfm?topnav=97); and Kiryu's evergreen coniferous forest under a humid subtropical climate (adapted from Kosugi and Katsuyama 2007). In maritime temperate and Mediterranean climatic regions, discharge usually decreases in summer, and the catchment becomes dry due to water loss by ET. In the forest in the humid subtropical climate, the seasonal pattern of discharge depends upon the balance between precipitation and ET, especially in summer. In eastern Asia under this climate, the discharge peak occurs during the rainy summer

storm events is rather complex in summer. Thus, seasonal patterns in precipitation have important influences on the seasonality of hydrological conditions, even among temperate regions with common temperature seasonality and total annual precipitation levels (Fig. 12.2).

In the last three decades, several cutting-edge theoretical and experimental studies have been conducted on rainfall-runoff processes in forested catchments. For example, end-member mixing analysis (Christophersen et al. 1990; Hooper et al. 1990) has become an indispensable technique for the quantitative analysis of discharge components. The concepts behind TOPMODEL (Beven and Moore 1993) have also continued to influence modeling studies of headwater catchments. TOPMODEL has even been applied to describe the biogeochemical responses of forested catchments (e.g., Tague and Band 2004). Isotope tracer techniques are the most advanced and valuable methods used in field observations and in hydrological and biogeochemical experiments in forested ecosystems. Stewart and McDonnell (1991) proposed techniques for estimating the mean residence time of stream water using temporal variations in water isotope compositions,

and other studies used these techniques to make similar estimations in several different forested catchments (e.g., Vitvar and Balderer 1997; Asano et al. 2002; Kabeya et al. 2007).

12.2.3 Biogeochemical Characteristics and Studies

Biogeochemical studies of forested ecosystems have addressed the coupled aspects of determining the mechanisms of nutrient cycling and ecosystem dynamics and identifying the factors that control water chemistry. Motivated primarily by reports of heavy acid deposition in surface waters, the pioneering studies at Hubbard Brook, which started in the 1950s, aimed to elucidate the mechanisms of pH decline in stream waters in affected forests (Likens et al. 1977). Acid rain issues spurred further biogeochemical studies in northeastern US and European forested regions (Likens and Bormann 1974; Likens et al. 1976; Wright and Gjessing 1976; Reuss and Johnson 1986; Reuss et al. 1987). One major finding was the significant occurrence of freshwater acidification, especially in forests situated in areas characterized by carbonate-free and highly siliceous bedrock, overburden, and soils. Freshwater in these areas was poorly buffered and had low ionic strength. A number of papers presented theoretical discussions on the mechanisms of acidification (Van Breemen et al. 1984; Ulrich and Matzner 1986; Reuss et al. 1987). Several process-based models were developed based on this experimental and theoretical knowledge, with the aim of predicting the impacts of acid deposition on soil and stream water chemistry (e.g., Cosby et al. 1985; Alcamo et al. 1987; Wolford et al. 1996).

Such studies identified sulfate (SO_4^{2-}) as the major contributor to acid deposition. In the latter half of the 1970s, governments in Europe, North America, and Japan instituted measures to control SO_2 emissions by heavy industry and to reduce the impacts of acid deposition. These countermeasures effectively reduced SO_2 emission rates, and several subsequent studies have examined the recovery process of soil environments damaged by acid deposition (e.g., Church 1989; Driscoll et al. 1998).

Nihlgård (1985) presented an alternative hypothesis for forest decline in northern Europe, which had previously been ascribed to acid deposition. He stressed the importance of excess inputs of ammonium (NH_4^+) as a causative factor. Based on the NH_4^+ hypothesis, many forest biogeochemists have examined the influences of heavy atmospheric nitrogen input into forest ecosystems.

Since the late 1980s, American and European researchers have noted that human activities have markedly changed the nitrogen cycles of terrestrial and aquatic ecosystems, both regionally and globally. This has occurred mainly in temperate regions, especially since the rapid rise of industrialization in the nineteenth century (Kinzig and Socolow 1994; Galloway et al. 1995; Vitousek et al. 1997). Anthropogenic nitrogen supply to natural ecosystems has increased the nitrogen loads of many rivers (e.g., Paces 1982; Turner and Rabalais 1991; Goolsby 2000;

Rabalais 2002). Atmospheric deposition is a major pathway of anthropogenic inorganic nitrogen loading into terrestrial ecosystems (Galloway et al. 1995; Galloway and Cowling 2002).

Excess inorganic nitrogen deposition causes not only soil and freshwater acidification (Murdoch and Stoddard 1992) but also severe disturbances of nitrogen dynamics, which play an essential role in biogeochemical cycling in forest ecosystems (Stoddard 1994). As a primary example, investigations of the mature forest at Hubbard Brook in the 1960s showed that the flux of internal nitrogen cycling was much greater than the input of reactive nitrogen derived from atmospheric deposition (Bormann et al. 1977). It has also been recognized in the European forests (Nihlgård and Lindgren 1977; Schulze 2000). However, recent heavy atmospheric nitrogen input has caused nitrogen saturation and high NO_3^- concentrations in forest streams in the northeastern US and Europe (Ågren and Bosatta 1988; Aber et al. 1989).

Nitrogen saturation has ecosystemic effects, as biomes are freed from nitrogen limitation by excess nitrogen input from sources such as atmospheric deposition. Depending on its ecological functions and structures, a nitrogen-saturated ecosystem has been variously defined as: (1) an ecosystem in which primary production does not increase with additional nitrogen input (Nilsson 1986); (2) an ecosystem in which nitrogen output is the same as or greater than nitrogen input (Ågren and Bosatta 1988); and (3) an ecosystem in which biologically available nitrogen supplies exceed the demands of the ecosystem's plants and microbes (Aber et al. 1989).

Stoddard (1994) proposed a conceptual model to explain the changes in seasonal patterns of nitrogen (mainly nitrate) discharge from forested catchments in the northeastern US and Europe, along with the progression of nitrogen saturation. The model suggests that the inorganic nitrogen pool, which is normally depleted during the growing season, is sustained by atmospheric nitrogen input and exceeds the demands of the plants and microbes drawing from it. Consequently, nitrate discharges chronically into streams. Aber et al. (1998) suggested the importance of microbial and mycorrhizal inorganic nitrogen immobilization as a mechanism for the gradual response (discharge of excess nitrogen) to increases in atmospheric nitrogen input. Many case studies have been conducted, mainly in the northeastern US (e.g., Stoddard 1994; Lovett et al. 2000), Europe (e.g., Nilsson 1986; Ågren and Bosatta 1988; Matzner 2004), and Japan (Ohrui and Mitchell 1997; Ohte et al. 2001).

12.3 Subjects and Issues

12.3.1 Climatic Variations Affect Catchment Characteristics

In discussing future directions of forest hydrology and biogeochemistry, we must note that most hydrological and biogeochemical studies in forested headwaters have focused on limited regions of the temperate zone, such as the northeastern US and northern Europe. However, as mentioned above, even within temperate
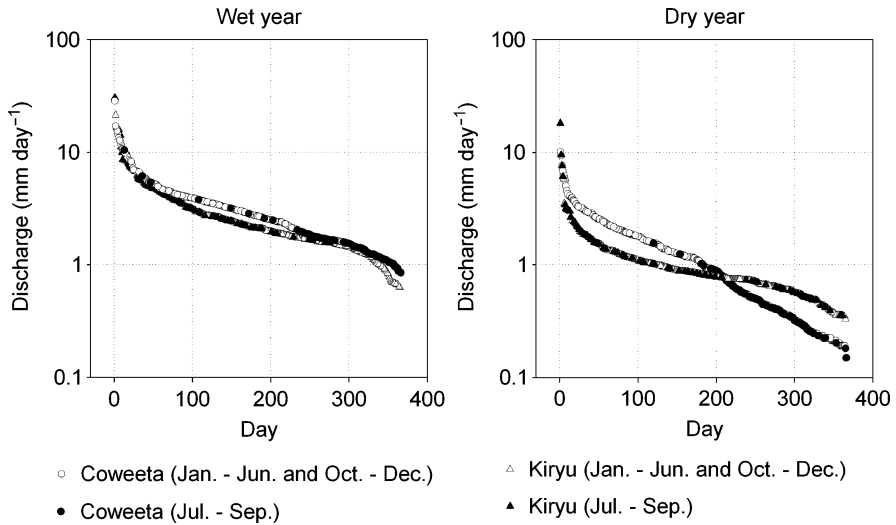
Fig. 12.3 Flow duration curves for the Coweeta Hydrologic Laboratory (CWT/W18, 12.5 ha) under a maritime temperate climate and the Kiryu Experimental Watershed (KEW, 6.0 ha) under a humid subtropical climate. CWT data were obtained from Coweeta Long Term Ecological Research (2010). KEW data were obtained from Katsuyama, personal communication, and used with permission

climatic regions, the amount and seasonal patterns of precipitation vary significantly by climatic subcategory. For example, Fig. 12.3 shows flow duration curves for the Coweeta Hydrologic Laboratory (CWT/W18, 12.5 ha) under a maritime temperate climate and for the Kiryu Experimental Watershed in Japan (KEW, 6.0 ha) under a humid subtropical climate. Both sites have similar annual precipitation and annual mean air temperatures; however, CWT has no significant seasonality in precipitation, whereas KEW has a significant summer rainy season caused by the Asian monsoon. Although there was no remarkable difference in the flow duration characteristics of wet years, the seasons of low and high flow were opposite, with summer (July, August, and September) being the high-flow season at KEW and the low-flow season at CWT. In summers of dry years, there was a decrease in the highest flow rate at KEW and the lowest flow rate at CWT; consequently, the catchment-scale summer drought was more severe in CWT than in KEW.

Variations in seasonal precipitation patterns generate remarkable differences in hydrological conditions such as soil wetness, and potentially affect the biogeochemical reactions of the forest ecosystem during the growing season. In this section, we describe the important influence of climatic differences on hydrology, biogeochemistry, and their interaction in forested ecosystems. To discuss this issue, we focus especially on nitrate export from forested catchments. We chose this focus because nutrient discharge from forested ecosystems typically requires both hydrological and biogeochemical insights, and it continues to be a vital topic in environmental science and ecosystem ecology.

12.3.2 Nitrogen Export from Forested Catchments

Many previous studies have reported that nitrate concentrations in stream water show typical seasonal variation, with higher concentrations in the dormant season, a concentration peak at snowmelt, and lower concentrations during the growing season. This seasonal pattern has been observed in the Rocky Mountains (e.g., Baron and Campbell 1997; Sickman and Melack 1998), eastern Canada (e.g., Spoelstra et al. 2001; Watmough et al. 2004), northeastern US (e.g., Mitchell et al. 1996; Goodale et al. 2000; Driscoll et al. 2003; Sebestyen et al. 2008), Scandinavia (e.g., Wright et al. 1999; de Wit et al. 2008), Great Britain (e.g., Curtis et al. 2005; Davies et al. 2005), the Czech Republic (e.g., Veselý et al. 2002), and a mountainous region of Italy (Rogora 2007). Commonly, these studies have found that the amounts and seasonal patterns of stream NO_3^- concentrations vary inversely with the demands of the plants and soil microbes in each forest ecosystem. Goodale et al. (2009) referred to this seasonal pattern as a "conventional" pattern.

On the other hand, Goodale et al. (2009) also reported an "unusual" seasonal pattern with a summer peak in the Susquehanna River basin in the northeastern US. A seasonal pattern with a summer peak has been reported previously in the US, including at the Coweeta Hydrologic Laboratory (Swank and Vose 1997), the Pond Branch catchment in Baltimore (Band et al. 2001), and the Oak Ridge National Environmental Research Park (Mulholland and Hill 1997) in the Appalachian Mountains of the southeastern US. These cases were from two different regions of the US (northeastern and southeastern US) and had different factors controlling the unusual NO_3^- seasonality. For the Susquehanna River, Goodale et al. (2009) proposed that the likely factor driving the summer NO_3^- peak was the high net nitrification rate, whereas Mulholland and Hill (1997) concluded that the peak was attributable to an increased relative contribution of groundwater discharge, which contained high NO_3^- concentrations, during the low-flow conditions in summer. Several other studies have also reported on hydrological effects causing seasonal variations in stream NO_3^- concentration (e.g., Burns and Kendall 2002). Consequently, Goodale et al. (2009) concluded that the unusual NO_3^- seasonality pattern recorded at their northeastern US study site could be regulated by variations in NO_3^- production, retention, and transport, rather than by plant and soil microbe demands.

Mulholland and Hill (1997) also pointed out that in-stream nutrient uptake in spring and fall altered the seasonal patterns of stream NO_3^- concentration. Other studies by Mulholland and colleagues have also emphasized the importance of in-stream processes as controlling factors in the seasonal variations in stream nutrient concentrations (Mulholland 1992, 2004; Mulholland et al. 2008).

However, we believe that an additional influential factor has not been fully considered, namely the climatic condition. Figure 12.4 depicts the climatic seasonality (monthly mean air temperature and monthly precipitation) of typical sites with conventional seasonal patterns of stream NO_3^- concentrations in the northeastern US, and of sites with unusual patterns in Japan (Ohte et al. 2001). The differences in seasonal precipitation variations are remarkable. For all cases in the northeastern US,
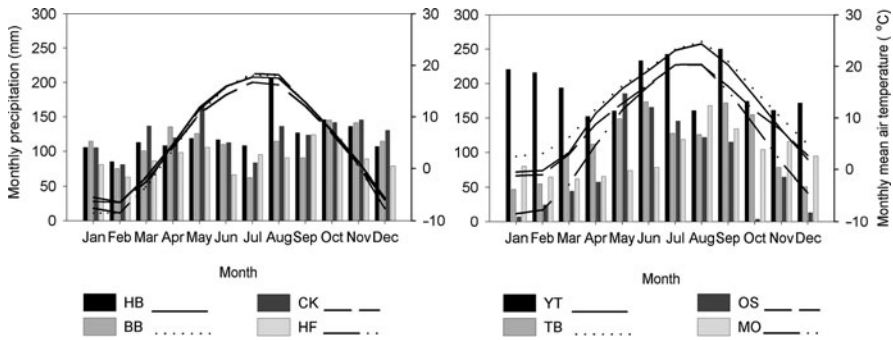
Fig. 12.4 Monthly precipitation (*columns*) and mean air temperatures (*lines*) at the sites (from Ohte et al. 2001). *Left*: Sites shown are in the northeast US (*HB* Hubbard Brook; *CK* Catskill; *BB* Bear Brook; *HF* Huntington Forest). *Right*: Sites shown are in Japan (*YT* Yanagatani; *OS* Ohyasan; *TB* Tsukuba; *MO* Moshiri). See Ohte et al. (2001) for site descriptions and original references

monthly precipitation is almost constant throughout the year. In contrast, in the Japanese catchments, precipitation shows a significant summer peak attributable to the strong influence of typical Asian monsoon systems and typhoons, which usually bring a heavy rainy season to eastern temperate Asia during summer. The sites in the US as well as in Europe with conventional seasonal patterns of stream NO_3^- concentration exhibit typically similar seasonal variations (no or less seasonal fluctuation) in precipitation, or high precipitation in fall and winter. None of the conventional sites has a summer peak in precipitation. The climate conditions of these regions cause the soil moisture content and groundwater table to decrease during summer due to water uptake by plants; consequently, the transport of nitrate and other nutrients from soil profiles to streams declines.

The above case studies were conducted mainly in regions with maritime temperate and continental humid temperate climates. It is easy to speculate that the conventional seasonal patterns in stream NO_3^- are influenced by a climate with a flat seasonal precipitation distribution such as that found commonly in the northeastern US, and northern and western Europe. This precipitation pattern leads to significantly dry conditions in summer. Moreover, the phase of this hydrological seasonal pattern (high flow in winter to early spring, with low flow in the summer growing season) corresponds to that of the biological seasonality in NO_3^- pool size, with a high NO_3^- pool in winter to early spring and a reduced pool in the summer growing season. Owing to this synchronicity, it is difficult to separate the relative contributions of hydrological and biological controls to seasonal variations in stream NO_3^- concentration in regions with conventional seasonal patterns.

Ohte et al. (2001) examined the differences in seasonal patterns of stream NO_3^- concentration between the northeastern US and Japan (Fig. 12.5). They found a distinct difference: in Japanese watersheds, marked decreases in NO_3^- concentrations in stream waters during the summer growing season were not observed, and NO_3^- concentration peaked in summer, especially at sites with high NO_3^- discharge. These Japanese cases were cited as examples of an unusual seasonal pattern
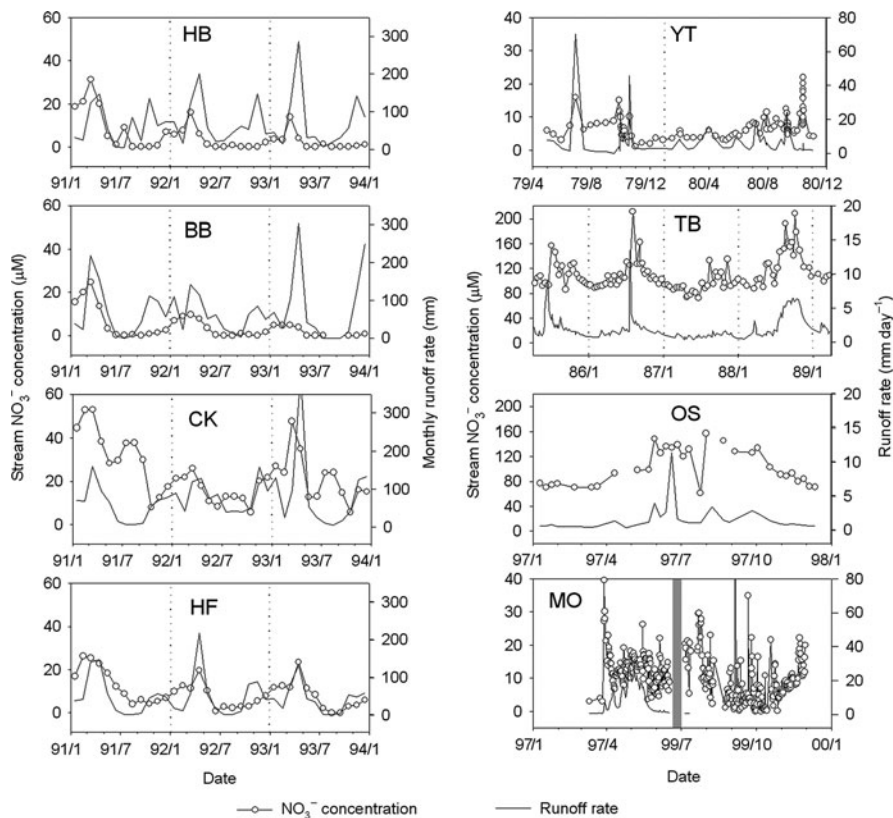
Fig. 12.5 Seasonal variations in NO_3^- concentrations and runoff rates (from Ohte et al. 2001). Abbreviations of site names are as shown in Fig. 12.4. See Ohte et al. (2001) for site descriptions and original references

by Goodale et al. (2009). Ohte et al. (2001) suggested that one possible cause of the summer peak was a high net nitrification rate due to the warm humid summer of the Asian monsoon climate. However, we believe emphasis should be placed on differences in seasonal precipitation patterns between the northeastern US and Japan, namely the different hydrological conditions. Ohte et al. (2006) also reported the seasonal variations in soil NO_3^- pool size and NO_3^- discharge in a forested catchment in central Japan. The phase of seasonal variation in the soil NO_3^- pool peaked in late fall, unlike the stream NO_3^- concentration, which peaked in summer. The seasonality of stream NO_3^- concentrations did not correspond with the changes in soil NO_3^- pool size, but rather with changes in the water discharge rate. The mechanism of this particular phenomenon was explained as a disconnection between the processes generating soil NO_3^- seasonality and those generating groundwater NO_3^- seasonality.

Ohte et al. (2003) showed a disconnection in the system that regulates NO_3^- concentration between the unsaturated soil profile (vadose zone) and the

groundwater zone. Where the soil was sufficiently deep, seasonal variations in the relatively shallow soil horizon (<100 cm) became unclear or disappeared during vertical soil water infiltration, owing to dispersion, while changes in the groundwater level could generate seasonality in discharge NO_3^- concentration because of differences in the NO_3^- concentrations between shallow and deep groundwater bodies. Thus, where the soil water contribution from shallow soil horizons to stream water generation is high, the seasonal variation in NO_3^- pool size, controlled by soil nitrogen dynamics, can strongly reflect stream water NO_3^- concentrations. In contrast, where the water contribution from the groundwater zone, which is substantially deeper than the biologically active zone (root zone), is significant, seasonal variations in NO_3^- concentration can be controlled by hydrological conditions such as changes in the groundwater level.

In temperate East Asia under the Asian monsoon climate, which is characterized by a distinct rainy season in summer, warm and humid conditions are generally favorable for nitrogen mineralization and nitrification during the growing season. High precipitation also provides hydrologically active conditions for nutrient export from the soil profile to streams. It is possible that hydrological transportation is more important than soil nitrogen dynamics in regulating the seasonal variation of NO_3^- export from forested catchments in these regions.

12.3.3   Catchment-Scale and Contributing Processes

Many studies have emphasized the importance of in-stream processes to the spatio-temporal variations in nutrient concentrations (Mulholland 1992, 2004; Mulholland and Hill 1997; Bernhardt et al. 2005; Mulholland et al. 2008). This is a natural occurrence in a relatively large stream, because the spatial importance of the hyporheic zone in streambed and riparian zones generally increases with stream scale. Thus, the relative contributions of biogeochemical processes in hillslopes and streams should change with catchment or stream scale, with greater hillslope influences on small streams in the upper reaches, and greater in-stream effects on larger streams.

We should also note the geographical variations in the relationship between stream order and catchment scale. For example, in the Susquehanna River in the northeastern US, Goodale et al. (2009) established observation sites in first- and second-order headwater catchments, with catchment scales ranging from 43 to 266 ha. In contrast, the scales of first- and second-order catchments in many Japanese headwaters range from 1 to 10 ha (e.g., Asano et al. 2002; Ohte et al. 2003; Oda et al. 2009). This difference in geographical scale may cause further differences among these sites in the relationship between stream scale and the relative contribution of in-stream processes. Moreover, differences in stream-scale regulation originate from not only differences in geological or geomorphological settings but also climatic conditions. The minimum scale of a catchment that can sustain a perennial stream is regulated by the amount of dischargeable water in the catchment during the driest season. As shown in Fig. 12.3, minimum discharge

occurs during the dry summer in nonmonsoon regions (maritime temperate and Mediterranean climates), including most of the US and Europe, whereas minimum discharge occurs during the winter in regions with markedly rainy summer seasons, as in monsoon Asia. Thus, the minimum catchment scale required to provide a perennial stream in dry summer regions is larger than that in wet summer regions.

12.4 Future Research Directions for Temperate Forests

Coordinated research efforts in various climate regions are required to provide a more universal understanding of the mechanisms behind the seasonal variations in both hydrological and biogeochemical conditions, including the mechanisms controlling seasonal variations in stream NO_3^- concentrations. More data must be collected and compiled from study sites with various climate, hydrology, and vegetation conditions. In particular, more hydrological and biogeochemical data are required from regions with high precipitation and flow in summer, such as temperate and subtropical East Asia. Process-based quantitative evaluations of nitrogen dynamics in soils and streams are also needed, as wet summer conditions may provide unique nitrogen dynamics compared with regions with dry summers. For this type of meta-analysis, we must extensively survey previously published literature as well as conventional and project-based databases such as the United States Long Term Ecological Research Network (US Long Term Ecological Research Network 2010) and the NITREX/EXMAN database (European Community ecosystem manipulation projects; Tietema and Beier 1995). One hypothesis may be that nutrient loss through streams is increased in ecosystems with high summer precipitation relative to ecosystems with dry summers. Moreover, to maintain the same level of plant growth and nutrient availability in soils in dry summer regions, ecosystems with rainy summers may have a higher gross nutrient supply due to higher mineralization and nitrification rates. These hypothetical discussions were previously presented by Ohrui and Mitchell (1997) and Ohte et al. (2001).

Multi-scale investigations are needed to evaluate the relative contributions of hillslope biogeochemical effects and in-stream biological activities. A number of studies of in-stream biogeochemical processes have previously been conducted in the US (e.g., Mulholland and Hill 1997; Mulholland et al. 2008); however, investigations in different climatic regions are critically limited. Assessment of the contributions of scale effects to the hillslope and in-stream biogeochemical processes in regions under various climatic conditions is also required.

References

Aber J, Nadelhoffer K, Steudler P et al (1989) Nitrogen saturation in northern forest ecosystems. Bioscience 39:378–386
Aber J, McDowell W, Nadelhoffer K et al (1998) Nitrogen saturation in temperate forest ecosystems. Bioscience 48:921–934

Ågren GI, Bosatta E (1988) Nitrogen saturation of terrestrial ecosystems. Environ Pollut 54:185–197

Alcamo J, Amann M, Hettelingh J-P et al (1987) Acidification in Europe: a simulation model for evaluating control strategies. Ambio 16:232–245

Andrews Experimental Forest Long-Term Ecological Research (2010) Master data catalog. http://andrewsforest.oregonstate.edu/data/mastercatalog.cfm. Accessed 20 June 2010

Asano Y, Uchida T, Ohte N (2002) Residence times and flow paths of water in steep unchanneled catchments, Tanakami, Japan. J Hydrol 261:173–192

Band LE, Tague CL, Groffman P et al (2001) Forest ecosystem processes at the watershed scale: hydrological and ecological controls of nitrogen export. Hydrol Process 15:2013–2028

Baron JS, Campbell DH (1997) Nitrogen fluxes in a high elevation Colorado Rocky Mountain basin. Hydrol Process 11:783–799

Bernhardt ES, Likens GE, Hall RO et al (2005) Can't see the forest for the stream? In-stream processing and terrestrial nitrogen exports. Bioscience 55:219–230

Beven KJ, Moore ID (1993) Terrain analysis and distributed modeling in hydrology. Wiley, Chichester

Bormann FH, Likens GE (1979) Pattern and process in a forested ecosystem: disturbance, development, and the steady state based on the Hubbard Brook Ecosystem Study. Springer, New York

Bormann FH, Likens GE, Melillo JM (1977) Nitrogen budget for an aggrading northern hardwood forest ecosystem. Science 196:981–983

Burns DA, Kendall C (2002) Analysis of d15N and d18O to differentiate NO_3^- sources in runoff at two watersheds in the Catskill Mountains of New York. Water Resour Res 38:1051. doi:1010.1029/2001WR000292

Buttle JM, Creed IF, Pomeroy JW (2000) Advances in Canadian forest hydrology, 1995–1998. Hydrol Process 14:1551–1578

Christophersen NC, Neal RP, Hooper RD et al (1990) Modeling stream water chemistry as a mixture of soil water end-members – a step towards second-generation acidification models. J Hydrol 116:307–320

Church MR (1989) Direct/delayed response project; predicting future long-term effects of acidic deposition on surface water chemistry. Eos Trans AGU 70:801

Cosby B, Hornberger G, Galloway J et al (1985) Modeling the effects of acid deposition: assessment of a lumped parameter model of soil water and streamwater chemistry. Water Resour Res 21:51–63

Coweeta Long Term Ecological Research (2010) Coweeta LTER data catalog. http://coweeta.uga.edu/results_catalog_b.php. Accessed 20 June 2010

Curtis CJ, Evans CD, Helliwell RC et al (2005) Nitrate leaching as a confounding factor in chemical recovery from acidification in UK upland waters. Environ Pollut 137:73–82

Davies JJL, Jenkins A, Monteith DT et al (2005) Trends in surface water chemistry of acidified UK freshwaters, 1988–2002. Environ Pollut 137:27–39

de Wit HA, Hindar A, Hole L (2008) Winter climate affects long-term trends in stream water nitrate in acid-sensitive catchments in southern Norway. Hydrol Earth Syst Sci 12:393–403

Driscoll CT, Likens GE, Church MR (1998) Recovery of surface waters in the northeastern U.S. from decreases in atmospheric deposition of sulfur. Water Air Soil Pollut 105:319–329

Driscoll CT, Driscoll KM, Roy KM et al (2003) Chemical response of lakes in the Adirondack region of New York to declines in acidic deposition. Environ Sci Technol 37:2036–2042

Galloway JN, Cowling EB (2002) Reactive nitrogen and the world: 200 years of change. Ambio 31:64–71

Galloway JN, Schlesinger WH, Levy H II et al (1995) Nitrogen fixation: anthropogenic enhancement-environmental response. Glob Biogeochem Cycles 9:227–234

Goodale CL, Aber JD, McDowell WH (2000) The long-term effects of disturbance on organic and inorganic nitrogen export in the White Mountains, New Hampshire. Ecosystems 3:433–450

Goodale C, Thomas S, Fredriksen G et al (2009) Unusual seasonal patterns and inferred processes of nitrogen retention in forested headwaters of the Upper Susquehanna River. Biogeochemistry 93:197–218

Goolsby DA (2000) Mississippi basin nitrogen flux believed to cause Gulf hypoxia. Eos Trans AGU 81:321–327

Grip H, Bishop K (1991) Chemical dynamics of an acid stream rich in dissolved organics. In: Mason BJ (ed) The surface water acidification program. Cambridge University Press, London, pp 75–84

Halldin S, Gryning SE, Gottschalk L et al (1999) Energy, water, and carbon exchange in a boreal forest landscape – NOPEX experiences. Agr Forest Meteorol 98–99:5–29

Hooper RP, Christophersen N, Peters NE (1990) Modeling stream water chemistry as a mixture of soil water end-members – an application to the Panola Mountain catchment, Georgia, U.S.A. J Hydrol 116:321–343

Horton RE (1933) The role of infiltration in the hydrologic cycle. Trans Am Geophys Union 14:446–460

Houghton RA, Skole DL (1990) Carbon. In: Turner BL II et al (eds) The earth as transformed by human action. Cambridge University Press, Cambridge, pp 393–408

Kabeya N, Katsuyama M, Kawasaki M et al (2007) Estimation of mean residence times of subsurface waters using seasonal variation in deuterium excess in a small headwater catchment in Japan. Hydrol Process 21:308–322

Kelliher FM, Lloyd J, Arneth A et al (1998) Evaporation from a central Siberian pine forest. J Hydrol 205:279–296

Kimball JS, White MA, Running SW (1997) BIOME-BGC simulations of stand hydrologic processes for BOREAS. J Geophys Res 102:29043–29051

Kinzig AP, Socolow RH (1994) Human impacts on the nitrogen cycle. Phys Today 47(11):24–31

Kirkby MJ (1978) Hillslope hydrology. Wiley, New York

Kosugi Y, Katsuyama M (2007) Evapotranspiration over a Japanese cypress forest. II. Comparison of the eddy covariance and water budget methods. J Hydrol 334:305–311

Kuraji K (1996) Water balance studies in moist tropical forested catchments. J Jpn For Soc 78:89–99 (in Japanese)

Likens GE, Bormann FH (1974) Acid rain: a serious regional environmental problem. Science 184:1176–1179

Likens GE, Johnson NM, Galloway JN et al (1976) Acid precipitation: strong and weak acids. Science 194:643–645

Likens GE, Bormann FH, Pierce RS et al (1977) Biogeochemistry of a forested ecosystem. Springer, New York

Lovett GM, Weathers KC, Sobczak WV (2000) Nitrogen saturation and retention in forested watersheds of the Catskill Mountains, New York. Ecol Appl 10:73–84

Matzner E (2004) Biogeochemistry of forested catchments in a changing environment. Ecology studies series, vol 172. Springer, New York

McDonnell JJ (1990) The influence of macropores on debris flow initiation. Q J Eng Geol Hydrogeol 23:325–331

Mitchell MJ, Driscoll CT, Kahl JS et al (1996) Climatic control of nitrate loss from forested watersheds in the northeast United States. Environ Sci Technol 30:2609–2612

Montgomery DR, Dietrich WE (1994) A physically based model for the topographic control on shallow landsliding. Water Resour Res 30:1153–1171

Mulholland PJ (1992) Regulation of nutrient concentrations in a temperate forest stream – roles of upland, riparian, and instream processes. Limnol Oceanogr 37:1512–1526

Mulholland PJ (2004) The importance of in-stream uptake for regulating stream concentrations and outputs of N and P from a forested watershed: evidence from long-term chemistry records for Walker Branch Watershed. Biogeochemistry 70:403–426

Mulholland PJ, Hill WR (1997) Seasonal patterns in streamwater nutrient and dissolved organic carbon concentrations: separating catchment flow path and in-stream effects. Water Resour Res 33:1297–1306

Mulholland PJ, Helton AM, Poole GC (2008) Stream denitrification across biomes and its response to anthropogenic nitrate loading. Nature 452:202–205

Murdoch PS, Stoddard JL (1992) The role of nitrate in the acidification of streams in the Catskill Mountains of New York. Water Resour Res 28:2707–2720

Nakano H (1976) Forest hydrology. Kyoritsu, Tokyo (in Japanese)

Nihlgård B (1985) The ammonium hypothesis: an additional explanation to the forest dieback in Europe. Ambio 14:2–8

Nihlgård B, Lindgren L (1977) Plant biomass, primary production and bioelements of three mature beech forests in south Sweden. Oikos 28:95–104

Nilsson SI (1986) Limits for the nitrogen deposition to forest soils. In: Nilsson J (ed) Critical loads for nitrogen and sulphur. Nordic council of ministers report 11, Copenhagen, pp 211–221

Oda T, Asano Y, Suzuki M (2009) Transit time evaluation using a chloride concentration input step shift after forest cutting in a Japanese headwater catchment. Hydrol Process 23:2705–2713

Odum EP (1963) Ecology. Holt, Rinehart and Winston, New York

Ohrui K, Mitchell MJ (1997) Nitrogen saturation in Japanese forested watersheds. Ecol Appl 7:391–401

Ohta T, Hiyama T, Tanaka H et al (2001) Seasonal variation in the energy and water exchanges above and below a larch forest in eastern Siberia. Hydrol Process 15:1459–1476

Ohte N, Tokuchi N (1999) Geographical variation of the acid buffering of vegetated catchments: factors determining the bicarbonate leaching. Glob Biogeochem Cycles 13:969–996

Ohte N, Mitchell M, Shibata H et al (2001) Comparative evaluation on nitrogen saturation of forest catchments in Japan and northeastern United States. Water Air Soil Pollut 130:649–654

Ohte N, Tokuchi N, Katsuyama M et al (2003) Episodic increases in nitrate concentrations in streamwater due to the partial dieback of a pine forest in Japan: runoff generation processes control seasonality. Hydrol Process 17:237–249

Ohte N, Fujimoto M, Mimasu Y (2006) Information behind the seasonal variation in nitrate discharge from the forested catchment. Eos transactions AGU: 87, fall meeting supplement, Abstract H13A-1345

Okunishi K (1994) Concept and methodology of hydrogeomorphology. Trans Jpn Geomorph Union 15A:5–18

Okunishi K, Okuda S, Suwa H (1987) A large-scale debris avalanche as an episode in slope-channel processes. IAHS Publ 165:225–232

Paces T (1982) Natural and anthropogenic fluxes of major elements from central Europe. Ambio 11:206–208

Rabalais NN (2002) Nitrogen in aquatic ecosystems. Ambio 31:102–112

Reuss JO, Johnson DW (1986) Acid deposition and the acidification of soils and waters. Springer, New York

Reuss JO, Cosby BJ, Wright RF (1987) Chemical processes governing soil and water acidification. Nature 329:27–32

Rogora M (2007) Synchronous trends in N-NO$_3$ export from N-saturated river catchments in relation to climate. Biogeochemistry 86:251–268

Schlesinger WH (1997) Biogeochemistry: an analysis of global change. Academic Press, San Diego

Schulze E-D (2000) Carbon and nitrogen cycling in European forest ecosystems. Springer, Heidelberg

Sebestyen SD, Boyer EW, Shanley JB et al (2008) Sources, transformations, and hydrological processes that control stream nitrate and dissolved organic matter concentrations during snowmelt in an upland forest. Water Resour Res 44: doi: 10.1029/102008WR006983

Seibert P (1994) Hydrological characteristics of the NOPEX research area. Thesis paper, Uppsala University, Institute of Earth Science, Uppsala, Sweden

Sickman J, Melack J (1998) Nitrogen and sulfate export from high elevation catchments of the Sierra Nevada, California. Water Air Soil Pollut 105:217–226

Spoelstra J, Schiff SL, Elgood RJ et al (2001) Tracing the sources of exported nitrate in the Turkey Lakes watershed using 15N/14N and 18O/16O isotopic ratios. Ecosystems 4:536–544

Stewart MK, McDonnell JJ (1991) Modeling base flow soil water residence times from deuterium concentrations. Water Resour Res 27:2681–2693

Stoddard JL (1994) Long-term changes in watershed retention of nitrogen. In: Baker LA (ed) Environmental chemistry of lakes and reservoirs, Advances in chemistry series. American Chemical Society, Washington, pp 223–284

Suzuki M (1980) Evapotranspiration from a small catchment in hilly mountains (I): spatial variations in evapotranspiration, rainfall interception and transpiration. J Jpn For Soc 62:46–53

Swank WT, Crossley JDA (1988) Forest hydrology and ecology at Coweeta. Springer, New York

Swank WT, Vose JM (1997) Long-term nitrogen dynamics of Coweeta forested watersheds in the southeastern United States of America. Glob Biogeochem Cycles 11:657–671

Tague CL, Band LE (2004) RHESSys: Regional Hydro-Ecologic Simulation System: an object-oriented approach to spatially distributed modeling of carbon, water, and nutrient cycling. Earth Interact 8:1–42

Tietema A, Beier C (1995) A correlative evaluation of nitrogen cycling in the forest ecosystems of the EC projects NITREX and EXMAN. Forest Ecol Manag 71:143–151

Turner RE, Rabalais NN (1991) Changes in Mississippi River water quality this century. Bioscience 41:140–147

Ulrich B, Matzner E (1986) Anthropogenic and natural acidification in terrestrial ecosystems. Cell Mol Life Sci 42:344–350

US Long Term Ecological Research Network (2010) The US long term ecological research network data portal. http://metacat.lternet.edu/das/lter/index.jsp. Accessed 29 March 2010

Valentini R (2003) Fluxes of carbon, water and energy of European forests. Ecology studies series, vol 163. Springer, New York

Van Breemen N, Driscoll CT, Mulder J (1984) Acidic deposition and internal proton sources in acidification of soils and waters. Nature 307:599–604

Veselý J, Majer V, Norton SA (2002) Heterogeneous response of central European streams to decreased acidic atmospheric deposition. Environ Pollut 120:275–281

Vitousek PM, Aber JD, Howarth RW et al (1997) Human alteration of the global nitrogen cycle: sources and consequences. Ecol Appl 7:737–750

Vitvar T, Balderer W (1997) Estimation of mean water residence times and runoff generation by180 measurements in a pre-Alpine catchment (Rietholzbach, eastern Switzerland). Appl Geochem 12:787–796

Watmough SA, Eimers MC, Aherne J et al (2004) Climate effects on stream nitrate concentrations at 16 forested catchments in south central Ontario. Environ Sci Technol 38:2383–2388

Whittaker RH (1975) Communities and ecosystems. Macmillan, New York

Wolford RA, Bales RC, Sorooshian S (1996) Development of a hydrochemical model for seasonally snow-covered alpine watersheds: application to Emerald Lake watershed, Sierra Nevada, California. Water Resour Res 32:1061–1074

Wright RF, Gjessing ET (1976) Acid precipitation: changes in the chemical composition of lakes. Ambio 5:219–223

Wright RF, Alewell C, Cullen JM et al (1999) Trends in nitrogen deposition and leaching in acid-sensitive streams in Europe. Hydrol Earth Syst Sci 5:299–310

Chapter 13
Hydrology and Biogeochemistry of Semiarid and Arid Regions

Xiao-Yan Li

13.1 Introduction

Arid and semi-arid areas with more than 30% of the world's land surface are characterized by low and sporadic moisture availability and sparse or discontinuous vegetation, both spatially and temporally. Vegetation, water, and nutrients are intimately coupled in the arid environments with strong feedbacks and interactions occurring across fine to coarse scales. This chapter reviews and synthesizes recent advances in ecohydrology and biogeochemistry in arid and semiarid regions and discusses future research needs and directions. Four connections are needed in future studies: (1) connecting hydrology and biogeochemistry with other two new emerging interdisciplinary fields of hydropedology and ecohydrology to understand a complex network of interaction and feedbacks between vegetation, hydrology, and biogeochemical cycling; (2) connecting aboveground and belowground processes to investigate how canopies redistribute rainfall and nutrient and their impact on subsurface flow, and to integrate landscape connectivity through recharge and discharge dynamics; (3) connecting individual plant, patch, slope and watershed scales to identify key variables, nonlinearities and linkages for interacting hydrological and biogeochemical processes between different spatial scales; (4) connecting vegetation perturbation (degradation) and recovery to understand how anthropogenic changes in landscape heterogeneity and watershed processes alter the dynamic regimes of the coupled hydrological-biogeochemical systems at different scales.

13.2 Influence of Rainfall Partitioning by Vegetation on Hydrology and Biogeochemistry at the Individual Plant Scale

13.2.1 Hydrological Partitioning Processes

Vegetation canopies can affect spatial heterogeneity of the rainwater input process within individual plant community. Precipitation intercepted by the canopy is

partitioned into throughfall and stemflow, as diffuse input and point input, respectively (Liang et al. 2007, 2009). The partitioning of rainfall into interception, throughfall and stemflow is affected by various factors such as rainfall characteristics (the amount, intensity and duration of rainfall and the temporal distribution of rain events), meteorological conditions (wind speed, air humidity deficit, net radiation) and vegetation (type, canopy height, canopy area, basal area, branch angle, leaf area index, bark roughness, leafed or leafless) (Crockford and Richardson 2000; Levia and Frost 2003). Pressland (1973) reported that the important factors affecting interception in arid woodland were the duration of the rainfall event and the occurrence of short rainless periods during an individual event, large percentage of rainfall interception usually occur during small rain events. Many studies indicated that throughfall, stemflow and interception were positive and linearly correlated with incident gross rainfall amount (Pressland 1973, 1976; Carlyle-Moses 2004; Owens et al. 2006; Li et al. 2008b, 2009); however, the percentages of throughfall, stemflow and interception could be represented by power (Domingo et al. 1998), curvilinear (Carlyle-Moses 2004) and logarithmic functions (Liu and Zhao 2009). Percentage of interception decreased with increasing rainfall amount. Rainfall intensity generally has a poor relationship with interception, throughfall and stemflow, partly due to the counteracting effects between rainfall amount and intensity.

The proportions of interception, throughfall and stemflow to incident gross precipitation are highly variable between and within vegetation species, as well as ecoregions (Levia and Frost 2003). Previous studies mainly focus on tropical and temperate forests; in contrast, relatively few studies were conducted in the tree, shrub and grass communities of drylands (Dunkerley 2000a; Carlyle-Moses 2004). Dunkerley (2000a) reported that interception losses from forests are greater in absolute volume than those from dryland communities, because of the more extensive plant canopy and the higher frequency of rain events. However, on a percentage basis, drylands lose considerably more water via interception than do more humid environments (Wilcox et al. 2003a). In general, the evaporation of intercepted rainfall by plant canopies typically accounts for 10–30% of the gross rainfall (Zinke 1967). Llorens and Domingo (2007) reviewed that for an annual rainfall of 200–1,600 mm, mean relative throughfall was about 79% with a variation coefficient of about 9% under Mediterranean conditions. For shrubs and bushes in semiarid environments, however, the mean relative throughfall was about 49% with a coefficient of variation of about 32% under an annual rainfall range of 90–800 mm (Llorens and Domingo 2007). Levia and Frost (2003) reported that the mean maximum stemflow values, expressed as a percentage of the incident gross precipitation, were approximately 3.5, 11.3, and 19% for tropical, temperate, and semiarid regions, respectively. Johnson and Lehmann (2006) found that stemflow can vary by more than three orders of magnitude, from 0.07 to 22% of incident rainfall, under a wide range of precipitation regimes (600–7,100 mm year^{-1}). Llorens and Domingo (2007) found although stemflow averaged 3% of incident precipitation under Mediterranean conditions, there was an associated coefficient of variation of 111%.

I summarized previous publications (41 papers) concerning rainfall partition by tree, shrub and grass in arid and semiarid zone (mean annual precipitation less than 600 mm year^{-1}) during the last 60 years. Many studies focused on rainfall interception by vegetation, there is a general paucity of information on stemflow and throughfall and factors affecting it in desert and rangeland shrub species. Quantitative information on stemflow and throughfall processes, and the final fate of this redistributed water in the soil is still sparse (Martinez-Meza 1994). Considering tree, shrub and grass as a whole, we found that percentage of interception, throughfall and stemflow of the incident gross precipitation averaged 26.9 ± 18.7, 65.2 ± 15.5, and $11.5 \pm 11.9\%$, respectively, under mean annual precipitation from 117 to 570 mm year^{-1}. Grass had a higher mean value of interception ($38.4 \pm 32.3\%$) than tree ($23.6 \pm 14.9\%$) and shrub ($24.8 \pm 12.9\%$), whereas no significant differences in interception, throughfall and stemflow were found between tree and shrubs. Carlyle-Moses (2004) had reported that shrubs in semi-arid systems intercepted from 13 to 40% of bulk rainfall, deciduous trees from 9 to 20% and coniferous trees from 20 to 48%. Stemflow showed much greater variability (coefficient of variation is larger than 100%) than throughfall (coefficient of variation is less than 30%) and interception (coefficient of variation is less than 60%). Shrub systems tend to have higher stemflow ($12.1 \pm 12.4\%$) than those dominated by trees ($10.3 \pm 11.6\%$), perhaps attributed to the fact that the threshold at which rainfall produces stemflow in shrubs is normally very low, 1–3 mm for different species. In contrast, tree-dominated systems have a relatively high threshold of 4–30 mm for stemflow generation (Llorens and Domingo 2007).

13.2.2 Chemical Partitioning Processes

Vegetation plays an important role in transferring the input of chemical solutes from aboveground vegetative surfaces to the soil via throughfall and stemflow. The chemistry of throughfall and stemflow mainly results from the chemical interaction among rainfall, dry deposition, sticky exudations and canopy leaching, and is influenced by canopy characteristics (species, age, branch angle, bark roughness and water repellency) and climate factors (rainfall amount and intensity, season, wind speed, lag time between rains) (Levia and Frost 2003; Johnson and Lehmann 2006). Previous studies concerning chemical composition of rainfall, throughfall and stemflow mainly focus on canopies of temperate and tropical forests; however, very few works were reported in the arid and semiarid regions, particularly for the shrub type vegetation (Návar et al. 2009). One known study by Whitford et al. (1997) reported that the concentration of NH_4-N, NO_3-N and PO_4-P, total N, Ca, Mg; Na and K were significantly higher in stemflow than in the bulk precipitation for creosote bush in the northern Chihuahuan Desert, while no significant differences in the concentration of ions were found between throughfall and precipitation except for SO_4, K and total nitrogen. They also found that increases in nitrogen in stemflow water may be due to biological activity of

stem crust micro-organisms in addition to dry-fall and concluded that the nutrient enrichment in stemflow may contribute to the development of "fertile island" under shrubs (Schlesinger and Reynolds 1990; Schlesinger and Pilmanis 1998). In another study of the concentration of eight chemical solutes (Ca, Mg, K, Na, Cu, Mn, Zn and Fe) in gross rainfall and throughfall for four shrub species (*Acacia rigidula* Benth., *Acacia berlandieri* Benth., *Pithecellobium ebano* C.H. Mull. and *Pithecellobium pallens*) in northeastern Mexico, Návar et al. (2009) reported that average throughfall (37.8 kg ha^{-1} year^{-1}) almost doubled the flux of solutes compared to rainfall (24.1 kg ha^{-1} year^{-1}). Calcium was the dominant cation with 48% and 52% of the total constituent flux for rainfall and throughfall, respectively. However, K, Mg and Cu approximately doubled in throughfall in contrast to gross rainfall.

13.2.3 Knowledge Gaps and Research Needs for Rainfall Partitioning in Drylands

Despite recognition of the potentially large effect of rainfall partition and associated processes on the hydrologic budget, few studies have quantitatively evaluated the multiple components simultaneously in arid and semiarid areas, nor have the effects of rainfall intensity within storms been rigorously evaluated (Owens et al. 2006). The separate effects of rainfall amount and intensity on rainfall partitioning by vegetation need further investigation under arid conditions (Li et al. 2009). Vertical fluxes redistributed by aboveground shrub stems and belowground roots with stemflow and preferential flow, respectively, were also not well understood, although stemflow was considered an important source of soil moisture in arid and semiarid lands (Pressland 1973; Tromble 1987; Li et al. 2008b). Water utilization by plants is controlled by many factors including vegetation type, soil moisture storage and redistribution, depth of root and bedrock, and frequency of rainfall events, as a result, the extent and importance of stemflow used by plants needs further experimental investigations. Integrated observations during long period (such as a series of successive years) and with wide range (different vegetation types) are also needed to investigate spatio-temporal variability of rainfall partitioning by canopy and water flow in the soil as well as their controlling factors, thus providing parameters associated with the processes for modelling.

Spatial pattern of nutrients due to chemical partitioning processes by virtue of physical vegetation presence and concomitant influences is very important for arid ecosystem sustainability, therefore understanding these processes will help us develop much greater predictive capability for dryland productivity. Future studies need to quantitatively investigate chemical partitioning processes of more vegetation types and their priming effect on the associated soil in arid and semiarid areas, and also examine how meteorological conditions and seasonality (including winter) may affect nutrient leaching. No known studies have specifically examined intraspecific differences in stemflow chemistry at the species level are needed. Further work should also be directed to stemflow nutrient transfers from standing dead trees (Levia and Frost 2003).

13.3 Patchy Vegetation and its Response to Hydrology and Biogeochemistry at Patch and Slope Scales

13.3.1 Redistribution of Flows and Nutrients at Patch Scale

The vegetation of arid and semiarid regions is usually patterned, consisting of patches with high plant cover interspersed in a low-cover or bare soil matrix (Aguiar and Sala 1999). The self-organized patchiness differs in scale and shape. Patterns reported include gaps, labyrinths, stripes ("tiger bush") and spots ("leopard bush"), which occur in semiarid and arid regions of Africa, Asia, Australia and North America (Aguiar and Sala 1999; Rietkerk et al. 2004). Vegetated patches and bare ground couple together in a landscape mosaic of sources and sinks of water, sediments and nutrients (Reynolds et al. 1999; Wilcox et al. 2003b). Vegetated patches are characterized by greater water storage capacity, increased soil organic carbon, larger nutrient inputs, greater soil biological activity and higher net primary productivity than adjacent inter-canopy area (Puigdefábregas 2005), leading to the so-called "fertility islands" (Schlesinger and Pilmanis 1998), "resource islands" (Reynolds et al. 1999) and "hydrologic islands" (Rango et al. 2006). Dunkerley (2000b) reported that the water uptake rate within shrub patch is at least 10% greater than the shrub interspace. Galle et al. (2001) estimated that rainfall concentration factor (infiltration in the vegetated band divided by rainfall) was up to approximately 1.4 for *A. aneura* in Australia, 2–4 for tiger bush in Mexico and Niger. The enhanced infiltration rates under vegetated patches are due to improved soil aggregation and macroporosity related to biological activity (e.g., termites, ants, and earthworms are very active in arid areas) and vegetation roots (Ludwig et al. 2005). Li et al. (2008a) reported that a spot-structured shrub patch in the Tengger Desert of China could trap 55% of the runoff from the crust patches, and therefore more than 75% of the sediments, 63% soil carbon, 74% nitrogen and 45–73% dissolved nutrients triggered by runoff from crust patches were delivered to shrub patches. Bisigato et al. (2009) reviewed that soil of vegetation patches showed 1.23–3.70 times more organic matter, 1.25–5.00 times more nitrogen and 1.10–1.66 times more phosphorus than the soil of interpatch areas in Monte Desert. Different mechanisms have been proposed for higher concentrations of nutrients under plant cover: litterfall and death of roots of plants present in the patch, deposition of wind-blown soil and organic matter, washing of dust and nutrients deposited in the canopies by rain, and/or nutrient losses by erosion in the interpatch areas. However, the relative importance of these mechanisms has not been evaluated.

13.3.2 Spatial Redistribution of Flows and Nutrients at Slope Scale

Spatial redistribution of flows and nutrients at the slope scale is regulated by the connectivity among plant islands and interspace patches and the patterning of soil

water, which is influenced by the characteristics of rainfall, interspaces, plant community structure, topography and ground cover (Imeson and Prinsen 2004; Puigdefabregas 2005). Rainfall intensity and infiltration rate on the individual patch (interspace or plant island) determine whether materials are absorbed by the receiving patch or transferred downslope (Belnap et al. 2005). When rainfall rates exceed interspace or plant-island infiltration rates, the resultant overland flow horizontally redistributes water, sediment and nutrients. Overland flow, evapotranspiration and leaching all result in water and nutrient loss from the hillslope, and nutrient losses from a given patch can serve as a resource subsidy for receiving patches or be lost from the system to downslope intermittent washes (Belnap et al. 2005). Usually at the slope scale, more organic matter, nutrients and microbial biomass accumulate in topographic depressions or valley bottoms. Very few studies have attempted to describe how naturally produced runoff and erosion at the vegetation patch scale relate to those same processes at the hillslope scale (Wilcox et al. 2003b). A study by Wilcox et al. (2003b) examined the effects of spatial scale (the intercanopy unit, the patch and the hillslope) on runoff and erosion, and concluded that unit-area runoff and erosion decrease dramatically and non-linearly from the patch to the hillslope scale, more than a 50-fold decrease in cumulative runoff and more than a 150-fold decrease in cumulative erosion from the bare microplots to the hillslope. These findings suggest that scale-dependent runoff–runon processes exert much more control over runoff from a hillslope than does the spatial variability of point infiltration. Moreover, disturbances can modify the effects of scale on runoff and erosion, both directly and via the modification of vegetation patterns, which can produce an increase in erosion rates leading to the creation of gullies and can result in irreversible degradation (Wilcox et al. 2003b).

13.3.3 Knowledge Gaps and Research Needs for the Effect of Patchy Vegetation on Hydrology and Biogeochemistry

Although vegetation self-organizing in spatial patterns has been considered as an optimized response to climatic and landscape conditions, the effects of scale and spatial complexity on hydrological and biogeochemical process have yet to be fully elucidated (Newman et al. 2006). Interactions between spatial (e.g., surface type) and temporal (e.g., soil moisture) variation in hydrological control factors can be expected in semiarid patchy landscapes; however, there still is an important knowledge gap about the relative importance and the interaction of these factors as determinants of the hydrological response of semiarid soils (Mayor et al. 2009). Therefore, quantifications of spatial and temporal interactions and feedback among vegetation patches and hydrologic elements (i.e., rainfall, topography, soils) across scales are needed in future research. The challenge remains to characterize connectivity and identify indicators as well as thresholds of spatio-temporal hydrological and biogeochemical process (Michaelides and Chappell 2009). Moreover, preferential flow is known to influence hillslope hydrology and biogeochemistry in many

areas around the world; however, most research has been performed in temperate regions. Preferential infiltration has also been found in semiarid regions, but its impact on the hydrology and biogeochemistry of these regions is poorly known (van Schaik et al. 2008). There is a need to quantify the influence of preferential flow networks on the hillslope hydrology at different spatial scales. Linking self-organized patchiness with catastrophic shift (e.g., critical transition from a self-organized patchy state to a barren state) by the resource concentration mechanism deserve great attention, which would help to bridge the present gaps among theory, observation and management (Rietkerk et al. 2004; Scheffer et al. 2009).

13.4 Impact of Vegetation Change on Hydrology and Biogeochemistry at the Watershed Scale

13.4.1 Impact of Vegetation Change on Water Yield

The influence of vegetation change on water quantity and quality in the watershed has long been a concerned subject worldwide. Deforestation, shifting cultivation and conversions of land covers such as from forest or brushlands to croplands or pastures are examples of changes that can alter streamflow response (Brooks et al. 1991). The hydrologic implications of extensive and long-term changes in vegetation cover are controversial. A large number of studies have been conducted to ascertain the effect of forest on streamflow throughout the world (Bosch and Hewlett 1982; Stoneman 1993; Scott et al. 1998; Zhang et al. 2001; Andreassian 2004; Brown et al. 2005). An international review by Bosch and Hewlett (1982) found that reducing forest cover causes an increase in water yield, increasing forest cover causes a decrease in water yield. A 10% change in cover in humid evergreen (e.g., eucalypt, pine) forests results in a 30–40 mm change in streamflow. The corresponding changes for deciduous hardwood (poplar, oak) and scrub were ±25 and 10 mm, respectively. Zhang et al. (2001) modelled that mean annual stream flow had responses to the changes in vegetation at the precipitation gradients. When grassland changes to permanent forests, the absolute reduction in mean annual water yield in a high rainfall region is much greater than that in a low rainfall region, while the proportional reduction is reversed. Relative losses in stream flow appear to increase linearly with increasing aridity; however, the level of annual precipitation at which the linear relationship breaks down is uncertain (Jackson et al. 2009).

In arid and semiarid regions, systematic studies concerning vegetation changes and their effects on hydrology are comparatively scarce and mainly focus on forested uplands, rangelands and riparian communities at the small scale (Brooks et al. 1991; Wilcox et al. 2008). The effect of woody plants changes on streamflow in drylands has been still a subject of debate. For rangelands, relatively few studies have shown that streamflow can be increased by reducing the cover of woody plants (Wilcox et al. 2006); however, in the upland areas where conditions allow for some

deep drainage and riparian areas dominated by invasive phreatophytes, there is an increase in water yield by reducing woody plant cover (Wilcox et al. 2006). The close coupling between vegetation and runoff has been repeatedly demonstrated at small scales, but very rarely at larger scales. Wilcox et al. (2008) ascertained streamflow changes on rangelands in response to degradation and recovery at the watershed scale in central Texas, and found that there was no indication that the decline in streamflow was related to diminished groundwater flows caused by extraction of subsurface water by woody plants, suggesting that declines in streamflow are a signal of hydrological recovery rather than the usurping of subsurface water by woody plants.

Riparian ecosystems occupy very small portions of the landscape in arid regions, yet they exert substantial influence on hydrologic, geomorphic, and ecological processes (Shaw and Cooper 2008). Riparian vegetation species are usually phreatophytes. Grass and shrub communities generally prevail among riparian floodplain species and their zonation along valley floors can vary considerably. Analyses of the sources of water used by these species carried out in the San Pedro River (Arizona, USA) show that grasslands basically rely on recent precipitation, whereas mesquite shrubs obtain water from deeper zones in the soil profile and are therefore more sensitive to groundwater changes (Scott et al. 2000; Camporeale et al. 2006). Woody plants have the deepest root systems and are capable of extracting large volumes of water from depths of 10 m or more. In South Africa, the impacts of vegetation changes on baseflow or groundwater have been documented in both humid and sub-humid catchments but the greatest changes in groundwater levels have followed type conversions in semiarid savanna. Transpiration of water by plants accounts for about half of the largest changes in the water balance associated with vegetation-type conversions (Maitre et al. 1999). Hancock et al. (1996) argued that arid catchments exhibited riparian vegetation with more complex structure, survival ability and competitive strategy than upland vegetation which is instead more inclined to tolerate water stress. The dynamics of riparian vegetation in drylands seems to be predominantly influenced by the competition (or cooperation) between different communities classified as native dominant, pioneering, invader or opportunistic (Camporeale et al. 2006). Existing knowledge of riparian ecosystems is derived almost exclusively from plot- or habitat-scale (e.g., floodplains and streambanks) studies, and focuses largely on perennial rivers while relatively little is known about the factors controlling the distribution of riparian vegetation in ephemeral stream networks (Shaw and Cooper 2008).

13.4.2 Impact of Vegetation Change on Biogeochemistry

Vegetation or land use changes can affect ionic balance on upland watersheds and the streamflow originating from them. The dissolved chemical load of stream after various forest disturbances such as timber harvesting or fire are largely a function of biotic and abiotic processes (Brooks et al. 1991). Investigations of the effects of

deforestation on soil and stream biogeochemistry have focused on changes observed in soil and stream chemistry during forest clearing and regrowth, often modelled on small watershed studies (Biggs et al. 2006). Regional surveys of stream biogeochemistry in forested and pasture areas of the Amazon basin show that streams draining pastures have higher concentrations and fluxes of Na, Cl, and K than streams draining forests in both wet and dry seasons (Biggs et al. 2002), and increased concentrations of nitrogen and phosphorus in the dry season (Biggs et al. 2004, 2006).

The conversion of grassland to shrubland or woody plant expansion in semiarid and arid ecosystem is a global phenomenon with important hydrological and biogeochemical consequences. The causes of shrub or woody plant encroachment in semiarid grasslands throughout the world have been much debated. Most often cited as reasons are climate change, chronic high levels of herbivory, change in fire frequency, changes in grass competitive ability, spread of seed by livestock, small mammal populations, elevated levels of CO_2 and combinations of these factors (Briggs et al. 2005). Previous studies suggest increases in woody plant abundance in dryland ecosystems may alter biogeochemical processes and influence atmospheric chemistry and climate (Schlesinger and Reynolds 1990). Transitions between grass and woody plant-dominated ecosystems can affect rates of soil respiration (Raich and Schlesinger 1992). Replacement of grassland by shrubland is thought to lock up considerable amounts of carbon (Goodale and Davidson 2002). Jackson et al. (2002) reported that woody plant invasion increased contents of soil organic carbon and soil organic nitrogen at the drier area, and decreased them at the wetter area. However, these assessments are characterized by a high degree of uncertainty. In addition, soils associated with woody plants may accumulate more carbon than those associated with herbaceous vegetation, but here too, results are controversial (Goodale and Davidson 2002; Jackson et al. 2002).

13.4.3 Knowledge Gaps and Research Needs for the Effect of Vegetation Change on Hydrology and Biogeochemistry
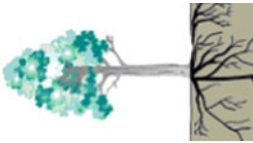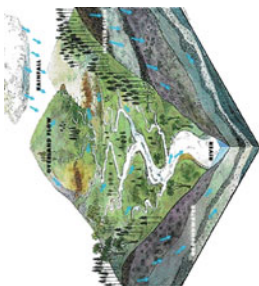
An integrated understanding of feedback loops between vegetation change and steamflow at the watershed scale is an important scientific challenge. Scaling the results to larger catchments is still a major problem because areas subject to vegetation change are likely to be patchy and relatively small compared to the overall catchment size. Moreover, how individual land use practices aggregate to a watershed scale response remains unanswered. Another key issue in the study of the long-term effects of rehabilitation or degeneration of vegetation is the soil vegetation relationship, we need to identify the respective roles of plant and soils in vegetation influence, systematic and long-term research is needed to document the recovery process of soil hydrologic properties along with changes of plant water use during the entire life cycle of plantation. Concerning interaction between riparian

vegetation and hydrology, the contribution of fine vegetation structures to land-scape hydrological roughness needs to be considered in relation to the spatial complexity (patchiness, vertical stratification, rhizosphere) and temporal variability (phenology, succession) of plant communities (Tabacchi et al. 2000). Moreover, with the exception of some woody species, the uptake, storage and return of water to the atmosphere is poorly known for riparian communities, and therefore the assessment of the regional hydrological importance of the riparian corridor remains difficult to estimate. Future studies also need to focus on linking hydrology and biogeochemistry in complex landscapes to understand the stocks, processes and fluxes of dissolved and particulate organic matter, nutrients and trace gases from the uplands across riparian zones and floodplains and down the channels of river corridors. The critical near-stream zone deserves great attention. It is necessary to understand the development of saturated conditions within the near-stream zone to identify biogeochemical "hot spots" that exhibit disproportionately high reaction rates relative to surrounding areas and, as such, can significantly affect the quality of stream water particularly, to understand the development of saturated conditions within the near-stream zone (Burt and Pinay 2005).

13.5 General Future Research Needs and Directions for Hydrology and Biogeochemistry in Semiarid and Arid Regions

The characteristics of hydrological and biogeochemical processes at different spatial scales in semiarid and arid regions are summarized in Table 13.1. We still need "4 connections" in future studies of hydrology and biogeochemistry in semi-arid and arid regions. First, connecting hydrology and biogeochemistry with other two new emerging interdisciplinary fields of hydropedology and ecohydrology to understand a complex network of interaction and feedbacks between vegetation, hydrology and biogeochemical cycling (Lin 2003; Newman et al. 2006; Li et al. 2009). Second, connecting aboveground and belowground processes to investigate how canopies redistribute rainfall and nutrient and their impact on subsurface flow, and to integrate landscape connectivity through recharge and discharge dynamics (Jackson et al. 2009). Third, connecting individual plant, patch, slope and water-shed scales to identify key variables, nonlinearities and linkages for interacting hydrological and biogeochemical processes between different spatial scales. This would help to understand self-organized complexity (such as patchy vegetation and preferential flow networks) and representative processes of hydrology and biogeo-chemistry. Scale transfer or multi-scale bridging issue remains a challenging problem in hydrology and biogeochemistry. Fourth, connecting vegetation pertur-bation (degradation) and recovery to understand how anthropogenic changes in landscape heterogeneity and watershed processes alter the dynamic regimes of the coupled hydrological-biogeochemical systems at different scales and explore underlying mechanism for ecosystem dynamics and health.

Table 13.1 Characteristics of hydrological and biogeochemical processes at different spatial scales in semiarid and arid regions

Attributes	Individual plant scale	Patch and slope scale	Watershed scale
Hydrological characteristics	Rainfall partition by canopy affects heterogeneity of the rainwater input and soil water content. Canopy interception, throughfall and stemflow average 27, 65 and 12% of the incident gross precipitation, respectively, which are highly variable between and within vegetation species. Stemflow has greater variability than throughfall and interception. Shrub tends to have higher stemflow than tree.	Vegetated patches and bare ground couple together in arid landscape. High runoff rate on bare inter-canopy patch, enhanced infiltration rates and greater water storage capacity under vegetated patches. Spatial redistribution of flows at the slope scale is regulated by the connectivity among plant islands and interspace patches and the patterning of soil water.	Soil water, ground water and stream water interact in complex nonlinear ways at watershed scale. The effect of vegetation changes on streamflow in drylands has still been a subject of debate. Riparian ecosystems exert substantial influence on hydrologic, geomorphic and ecological processes in arid regions.

Table 13.1 (continued)

Attributes	Individual plant scale	Patch and slope scale	Watershed scale
Biogeochemical characteristics	Plant transfers the input of chemical solutes from the aboveground vegetative surfaces to the soil via throughfall and stemflow. The chemistry of throughfall and stemflow mainly results from the chemical interaction among rainfall, dry deposition, sticky exudations and canopy leaching. High concentration of chemical solutes in stemflow and throughfall as compared with rainfall.	Increased soil organic carbon, larger nutrient inputs, greater soil biological activity and higher net primary productivity under canopy than adjacent inter-canopy area; more organic matter, nutrients, and microbial biomass accumulate in topographic depressions or valley bottoms	Vegetation or land use changes affect ionic balance. Increases in woody plant abundance alter biogeochemical processes and influence atmospheric chemistry and climate. Hot spots and moments of biogeochemical processes existed in riparian ecosystems.
Interactive controls	Canopy characteristics (species, age, branch angle, bark roughness, leafed or leafless, water repellency), climate factors (rainfall amount and intensity, season, wind speed, lag time between rains).	Rainfall characteristics, vegetation type and patterns, plant community structure and roots, soil structure and fertility, biological activity, topography, ground cover, disturbances	Land use and cover, soil and vegetation pattern, climate factors, hydrological connectivity, topography, surface and subsurface flow networks, human activity

Other critical need includes a network of well-designed long-term monitoring within a spatially nested design framework in the context of arid and semiarid ecosystem across a wide range of geographic regions; we need to consider the episodic nature of water availability and heterogeneous soil surface and temporal–spatial scale effects. An effort must be made to provide guidelines for all the measurements to be made, systematic field data collections must contribute to enhanced understanding at a variety of scales and to the advancement of quantitative modelling and prediction.

References

Aguiar MR, Sala OE (1999) Patch structure, dynamics and implications for the functioning of arid ecosystems. Tree 14(7):273–277

Andreassian V (2004) Waters and forests: from historical controversy to scientific debate. J Hydrol 291:1–27

Belnap J, Welter JR, Grimm NB et al (2005) Linkages between microbial and hydrologic processes in arid and semiarid watersheds. Ecology 86(2):298–307

Biggs TW, Dunne T, Domingues TF et al (2002) The relative influence of natural watershed properties and human disturbance on stream solute concentrations in the southwestern Brazilian Amazon basin. Water Resour Res. doi:10.1029/2001WR000271

Biggs TW, Dunne T, Martinelli LA (2004) Natural controls and human impacts on stream nutrient concentrations in a deforested region of the Brazilian Amazon basin. Biogeochemistry 68:227–257

Biggs TW, Dunne T, Murakowa T (2006) Transport of water, solutes and nutrients from a pasture hillslope, southwestern Brazilian Amazon. Hydrol Process 20:2527–2547

Bisigato AJ, Villagra PE, Ares JO et al (2009) Vegetation heterogeneity in Monte Desert ecosystems: a multi-scale approach linking patterns and processes. J Arid Environ 73:182–191

Bosch JM, Hewlett JD (1982) A review of catchment experiments to determine the effect of vegetation changes on water yield and evapotranspiration. J Hydrol 55(1):3–23

Briggs JM, Knapp AK, Blair JM (2005) An ecosystem in transition: causes and consequences of the conversion of Mesic Grassland to Shrubland. BioScience 55:243–254

Brooks KN, Ffoiliott PF, Gregersen HM et al (1991) Hydrology and the management of watersheds. Iowa State University Press, Ames

Brown AE, Zhang L, McMahon TA (2005) A review of paired catchment studies for determining changes in water yield resulting from alterations in vegetation. J Hydrol 310:28–61

Burt TP, Pinay G (2005) Linking hydrology and biogeochemistry in complex landscapes. Prog Phys Geogr 29(3):297–316

Camporeale C, Perona P, Ridolfi L (2006) Hydrological and geomorphological significance of riparian vegetation in drylands. In: D'Odorico P, Porporato A (eds) Dryland ecohydrology. Springer, New York, pp 161–180

Carlyle-Moses DE (2004) Throughfall, stemflow, and canopy interception loss fluxes in a semi-arid sierra madre oriental matorral community. J Arid Environ 58:180–201

Crockford RH, Richardson DP (2000) Partitioning of rainfall into throughfall, stemflow and interception: effect of forest type, ground cover and climate. Hydrol Process 14:2903–2920

Domingo F, Sanchez G, Moro MJ et al (1998) Measurement and modelling of rainfall interception by three semi-arid canopies. Agric For Meteorol 91(3–4):275–292

Dunkerley D (2000a) Measuring interception loss and canopy storage in dryland vegetation: a brief review and evaluation of available research strategies. Hydrol Process 14:669–678

Dunkerley D (2000b) Hydrologic effects of dryland shrubs: defining the spatial extent of modified soil water uptake rates at an Australian desert site. J Arid Environ 45:159–172

Galle S, Brouwer J, Delhoume JP (2001) Soil water balance. In: Tongway DJ, Valentin C, Seghieri J (eds) Band vegetation patterning in arid and semiarid environments. Ecological studies, vol 149. Springer, New York, pp 77–104

Goodale CL, Davidson EA (2002) Uncertain sinks in the shrubs. Nature 418:593–594

Hancock CN, Ladd PG, Froend RH (1996) Biodiversity and management of riparian vegetation in Western Australia. For Ecol Manage 85:239–250

Imeson AC, Prinsen HAM (2004) Vegetation patterns as biological indicators for identifying runoff and sediment source and sink areas for semi-arid landscapes in Spain. J Agric Ecosyst Environ 104:333–342

Jackson RB, Banner JB, Jobbagy EG et al (2002) Ecosystem carbon loss with woody plant invasion of grasslands. Nature 418:623–626

Jackson RB, Jobbagy EG, Nosetto MD (2009) Ecohydrology in a human-dominated landscape. Ecohydrology 2:383–389

Johnson MS, Lehmann J (2006) Double-funneling of trees: stemflow and root-induced preferential flow. Ecoscience 13(3):324–333

Levia DF, Frost EE (2003) A review and evaluation of stemflow literature in the hydrologic and biogeochemical cycles of forested and agricultural ecosystems. J Hydrol 274:1–29

Li XJ, Li XR, Song WM et al (2008a) Effects of crust and shrub patches on runoff, sedimentation, and related nutrient (C, N) redistribution in the desertified steppe zone of the Tengger Desert, Northern China. Geomorphology 96:221–232

Li XY, Liu LY, Gao SY et al (2008b) Stemflow in three shrubs and its effect on soil water enhancement in semiarid loess region of China. Agric For Meteorol 148:1501–1507

Li XY, Yang ZP, Li YT et al (2009) Connecting ecohydrology and hydropedology in desert shrubs: stemflow as a source of preferential flow in soils. Hydrol Earth Syst Sci 13:1133–1144

Liang WL, Kosugi K, Mizuyama T (2007) Heterogeneous soil water dynamics around a tree growing on a steep hillslope. Vadose Zone J 6(4):879–889

Liang WL, Kosugi K, Mizuyama T (2009) A three-dimensional model of the effect of stemflow on soil water dynamics around a tree on a hillslope. J Hydrol 366:62–75

Lin H (2003) Hydropedology: bridging disciplines, scales, and data. Vadose Zone J 2:1–11

Liu B, Zhao WZ (2009) Rainfall partitioning by desert shrubs in arid regions. Sci Cold Arid Reg 1(3):215–229

Llorens P, Domingo F (2007) Rainfall partitioning by vegetation under Mediterranean conditions. A review of studies in Europe. J Hydrol 335:37–54

Ludwig JA, Wilcox BP, Breshears DD et al (2005) Vegetation patches and runoff-erosion as interacting ecohydrological processes in semiarid landscapes. Ecology 86(2):288–297

Maitre DCL, Scott DF, Colvin C (1999) A review of information on interactions between vegetation and groundwater. Water SA 25(2):137–152

Martinez-Meza E (1994) Stemflow, throughfall and root water channelization by three arid land shrubs in southern New Mexico. PhD thesis, New Mexico State University, Las Cruces, New Mexico

Mayor AG, Bautista S, Bellot J (2009) Factors and interactions controlling infiltration, runoff, and soil loss at the microscale in a patchy Mediterranean semiarid landscape. Earth Surf Process Landforms 34:1702–1711

Michaelides K, Chappell A (2009) Connectivity as a concept for characterising hydrological behaviour. Hydrol Process 23:517–522

Návar J, González JM, Gonzalez H (2009) Gross precipitation and throughfall chemistry in legume species planted in Northeastern México. Plant Soil 318:15–26

Newman BD, Wilcox BP, Archer SR et al (2006) Ecohydrology of water-limited environments: a scientific vision. Water Resour Res 42:W06302. doi:10.1029/2005WR004141

Noy-Meir I (1973) Desert ecosystems: environment and producers. Annu Rev Ecol Syst 4:25–51

Owens MK, Lyons RK, Alejandro CL (2006) Rainfall partitioning within semiarid juniper communities: effects of event size and canopy cover. Hydrol Process 20:3179–3189

Pressland AJ (1973) Rainfall partitioning by an arid woodland (Acacia aneura F. Muell.) in south-western Queensland. Aust J Bot 21:235–245

Pressland AJ (1976) Soil moisture redistribution as affected by throughfall and stemflow in an arid zone shrub community. Aust J Bot 24:641–649

Puigdefábregas J (2005) The role of vegetation patterns in structuring runoff and sediment fluxes in drylands. Earth Surf Process Landforms 30:133–147

Raich JW, Schlesinger WH (1992) The global carbon dioxide flux in soil respiration and its relationship to vegetation and climate. Tellus 44B:81–89

Rango A, Tartowski SL, Laliberte A et al (2006) Island of hydrologically enhanced biotic productivity in natural and managed arid ecosystems. J Arid Environ 65:235–252

Reynolds JF, Virginia RA, Kemp PA et al (1999) Impact of drought on desert shrubs: effects of seasonality and degree of resource island development. Ecol Monogr 69:69–106

Rietkerk M, Dekker SC, de Ruiter PC et al (2004) Self-organized patchiness and catastrophic shifts in ecosystems. Science 305:1926–1929

Sala OE, Lauenroth WK, Golluscio RA (1997) Plant functional types in temperate semi-arid regions. In: Smith TM, Shugart HH, Woodward FI (eds) Plant functional types, International geosphere-biosphere programme book series 1, Cambridge University Press, Cambridge, pp 217–233

Scheffer M, Bascompte J, Brock WA et al (2009) Early-warning signals for critical transitions. Nature 461:53–59

Schlesinger WH, Pilmanis AM (1998) Plant-soil interactions in deserts. Biogeochemistry 42:169–187

Schlesinger WH, Reynolds JF (1990) Biological feedbacks in global desertification. Science 247:1043–1048

Scott DF, Le Maitre DC, Fairbanks DHK (1998) Forestry and streamflow reductions in South Africa: a reference system for assessing extent and distribution. Water SA 24(3):187–200

Scott RL, Shuttleworth WJ, Goodrich DC, Maddock T III (2000) The water use of two dominant vegetation communities in a semiarid riparian ecosystem. Agric For Meteorol 105:241–256

Shaw JR, Cooper DJ (2008) Linkages among watersheds, stream reaches, and riparian vegetation in dryland ephemeral stream networks. J Hydrol 350:68–82

Stoneman GL (1993) Hydrological response to thinning a small jarrah (Eucalyptus marginata) forest catchment. J Hydrol 150(2/4):393–407

Tabacchi E, Lambs L, Guilloy H (2000) Impacts of riparian vegetation on hydrological processes. Hydrol Process 14:2959–2976

Tromble JM (1987) Water interception by two arid land shrubs. J Arid Environ 15:65–70

Van Schaik NLMB, Schnabel S, Jetten VG (2008) The influence of preferential flow on hillslope hydrology in a semi-arid watershed (in the Spanish Dehesas). Hydrol Process 22:3844–3855

Whitford WG, Anderson J, Rice PM (1997) Stemflow contribution to the "fertile island" effect in creosote bush, Larrea tridentata. J Arid Environ 35:451–457

Wilcox BP, Breshears DD, Seyfried MS (2003a) Water balance on rangelands. In: Stewart BA, Seyfried MS (eds) Encyclopedia of water science. Marcel Dekker, New York, pp 791–794

Wilcox BP, Breshears DD, Allen CD (2003b) Ecohydrology of a resource-conserving semiarid woodland: temporal and spatial scaling and disturbance. Ecol Monogr 73:223–239

Wilcox BP, Owens MK, Dugas WA et al (2006) Shrubs, streamflow, and the paradox of scale. Hydrol Process 20:3245–3259

Wilcox BP, Huang Y, Walker JW (2008) Long-term trends in streamflow from semiarid range-lands: uncovering drivers of change. Glob Change Biol 14:1676–1689. doi:10.1111/j.1365-2486.2008.01578.x

Zhang L, Dawes WR, Walker GR (2001) Response of mean annual evapotranspiration to vegetation changes at catchment scale. Water Resour Res 37(3):701–708

Zinke P (1967) Forest interception studies in the United States. In: Sopper W, Lull H (eds) International symposium on forest hydrology. Pergamon, Oxford, pp 137–161

Chapter 14
Hydrology and Biogeochemistry of Mediterranean Forests

**Pilar Llorens, Jérôme Latron, Miguel Álvarez-Cobelas,
Jordi Martínez-Vilalta, and Gerardo Moreno**

14.1   Introduction

The Mediterranean climate is characterized by a regime of hot summer droughts and winter rains in the mid-latitudes, roughly between 30° and 45° North and South of the equator. The main area lying within the Mediterranean climate is the Mediterranean basin, but this climate also occurs in coastal areas of California, South America, South Africa and South and Western Australia.

Mediterranean climate regions occupy less than 5% of the Earth's surface but have more than 20% of the whole vascular plant species of the world (Cowling et al. 1996), forming a very diverse mosaic of communities, from sparse shrubs in dry and degraded areas, through oak woodland savannahs, to dense forests in the wetter areas.

The aim of this chapter is to synthesize current knowledge on hydrology and biogeochemistry of Mediterranean forests highlighting both common features and main differences with respect to other climate-type forests. The chapter also aims to identify poorly understood issues and to suggest future research directions.

14.2   Mediterranean Forest Rainfall Partitioning

Throughfall and stemflow, by modifying the spatial distribution of the water reaching the soil, have significant hydrological and ecological impacts, especially in areas, like the Mediterranean, with periods of water scarcity.

14.2.1   Throughfall and Stemflow Rates in Mediterranean Areas

An exhaustive review of rainfall partitioning by Mediterranean vegetation in Europe (Llorens and Domingo 2007) indicates that mean forest relative throughfall was about 79% (CV = 9%), a similar rate to that observed in temperate conditions. Low relative throughfall observed in the characteristic Mediterranean species

Quercus ilex (ca. $72 \pm 3\%$) in the studies reviewed is also confirmed recently (e.g., David et al. 2006; Limousin et al. 2008; Pereira et al. 2009a). Additionally, similar results were obtained for *Quercus suber* by Xiao et al. (2000). For shrubs, their mean relative throughfall was about 49% (CV = 32%) (Llorens and Domingo 2007). Studies of rainfall partitioning of shrubs and bushes are scarce and, moreover, throughfall rates of shrubs growing in dry environments are highly variable (Dunkerley 2000). For these reasons, it is difficult to compare results in Mediterranean environments with results obtained in other environments.

As stated by Levia and Frost (2003), compared to throughfall, stemflow is under-represented in literature, and Mediterranean vegetation also has this drawback. Trees mean relative stemflow was about 3% (CV = 111%), while, in shrubs, it was 19% (Llorens and Domingo 2007). High stemflow percentages observed in some shrub species may be explained by their aerial structure and a very low rainfall threshold (1–3 mm) for starting stemflow (e.g., Navar 1993).

14.2.2 Specific Factors Affecting Rainfall Interception in Mediterranean Conditions

The elevated inter-event variability of the relationship between bulk rainfall and interception loss described by several authors for different Mediterranean ecosystems (Llorens et al. 1997; Xiao et al. 2000; David et al. 2006; Limousin et al. 2008; Sraj et al. 2008) is attributable to the characteristics of the Mediterranean rainfall regime, which includes frontal rainfall events and short convective storms (Fig. 14.1). The sequence rainfall events with small rainfall depth and intensity (with rainfall breaks in between), which promote larger interception losses, could be considered an important factor for explaining larger interception losses in Mediterranean areas during frontal rainfall events (e.g., Llorens et al. 1997; Limousin et al. 2008). Yet, these higher interception rates are counterbalanced by lower rates observed during large and intense storms that also characterize the Mediterranean rainfall regime (e.g., Llorens et al. 1997; David et al. 2006).

In the Mediterranean climate rainfall rates are variable between seasons, while mean evaporation rates for a wet canopy is a more conservative parameter world wide (David et al. 2005). However, mean wet evaporation rates observed in Mediterranean conditions, ranging between 0.20 mm h^{-1} (Valente et al. 1997) and about 0.46 mm h^{-1} (Llorens 1997; Limousin et al. 2008) are in the higher range of those observed in temperate climate where a number of studies indicate mean wet evaporation rates lower than 0.20 mm h^{-1} (e.g., Gash et al. 1995; Herbst et al. 2008).

Mediterranean areas are frequently covered by open woodlands, savannah-type ecosystems, isolated trees or shrub formations, but, there is less knowledge on the rainfall partitioning process in these covers compared to closed forests (Llorens and Domingo 2007). The latest research on single trees (Xiao et al. 2000; Gomez et al. 2001; David et al. 2006) agree that a correct representation of interception losses when the tree cover is sparse is obtained by measuring the interception loss of individual trees. However, the methodology is still being discussed. Frequently, studies in individuals
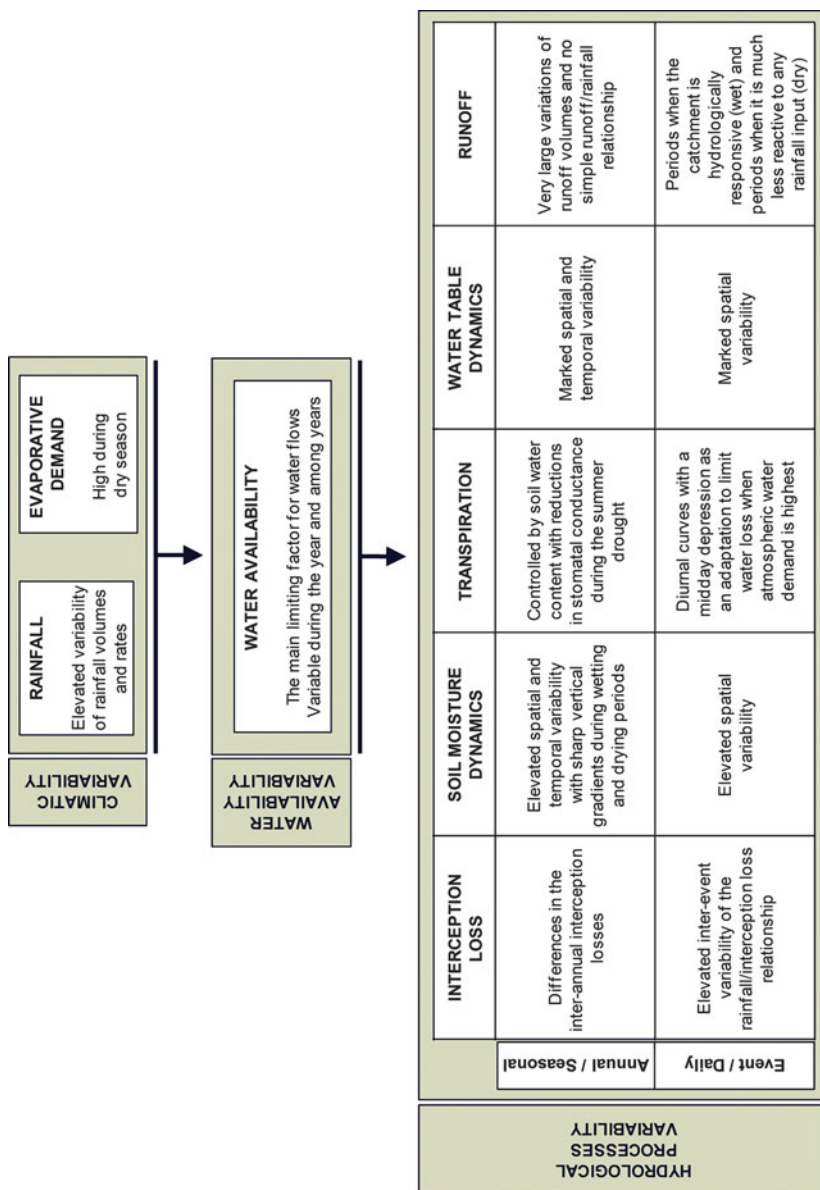
Fig. 14.1 Effect of climatic variability on water availability and hydrological processes under Mediterranean conditions

used standard rainfall gauges located beneath the crown. To avoid the difficulty of using this methodology designed for continuous forest, a device consisting of a collecting surface beneath an individual plant was designed (Belmonte and Romero 1998; Xiao et al. 2000). However, both methodologies are debated because the results obtained are not reasonable during wind-driven rainfall (Dunkerley 2000; David et al. 2006).

14.2.3 Rainfall Interception Modeling in Mediterranean Conditions

The sparse versions of Rutter and Gash models (Gash et al. 1995; Valente et al. 1997) formulated to better represent open forest stands were an important step for a more accurate modeling of the sparse Mediterranean forests as corroborated by recent studies (David et al. 2006; Limousin et al. 2008). The sparse versions, as well as the original ones, have been applied in Mediterranean conditions (e.g., Llorens 1997; Valente et al. 1997; Domingo et al. 1998; Limousin et al. 2008; Sraj et al. 2008) giving efficiencies that are not far from those obtained in other climates. However, a recent review of rainfall interception modeling (Muzylo et al. 2009) indicated that more effort should be devoted to answering some questions that arise from the modeling of very sparse forest (or individuals), such as the validity of one-dimensional equations (i.e., Penman-Monteith) to calculate evaporation and the effect of turbulence enhancement in sparse canopies.

An interesting proposal for the estimation of interception losses by single trees is presented by Pereira et al. (2009b), who corroborate with experimental measurements that a totally saturated single tree crown behaves like a wet bulb. This allows for the calculation of crown evaporation by using a simple diffusion equation. Moreover, a physically based modeling approach at the tree scale based on the former work, with limited data requirements, was performed correctly in the savannah-type woodlands tested (Pereira et al. 2009a).

From the sensitivity analysis of the sparse version of the Gash et al. (1995) analytical model, Limousin et al. (2008) found an inverse sensitivity of a similar magnitude of the evaporation rate and the rainfall rate. Similar results were obtained by Llorens (1997) using the original version of Gash's (1979) model. Limousin et al. (2008) attributed this fact to the seasonality of the Mediterranean climate, along with a high evaporative demand favoring interception losses with high rainfall intensity events reducing those losses throughout the year.

14.3 Mediterranean Forest Transpiration

In Mediterranean forests, water flows are generally limited by water availability as opposed to available energy. At the same time, however, Mediterranean forests tend to be very efficient in using available water. As a result, water balance in

Mediterranean catchments tends to be dominated by forest transpiration, and actual evapotranspiration tends to increase linearly with rainfall.

14.3.1 Controls of Water-Use in Mediterranean Forests

Leaf area index (LAI) is related to site water balance, being a positive function of water availability in Mediterranean ecosystems (Specht and Specht 1989; Hoff and Rambal 2003). For natural eucalypt forests in Southern Australia, for example, LAI ranges from 0.5 where P/ET $\approx$ 0.2–4.5 where P/ET $\approx$ 1.5 (Eamus et al. 2006). In terms of transpiration rates per unit of LAI, Mediterranean ecosystems range between 100 mm in relatively humid forests with LAI of 4–6 and 200 mm in shrublands with lower LAI (Joffre and Rambal 2002). LAI is normally the main component of water use regulation in Mediterranean ecosystems across sites and over long time scales. In Mediterranean shrublands, the regulation of leaf area is a major component of the adjustment of vegetation to changes in water availability (Poole and Miller 1981; Joffre et al. 2007). In the case of Mediterranean forests, the regulation within a site (and over relatively short time scales) is achieved mostly via stomatal control. In Mediterranean plants, as leaves tend to be small, stomatal resistance tends to dominate over boundary layer resistance (e.g., Infante et al. 1997).

Mediterranean species tend to show relatively low values of maximum stomatal conductance, but they also have a tendency to maintain stomatal conductance for longer periods under moderate water stress (e.g., Acherar and Rambal 1992). Although this conservative water-use strategy relies on a relatively rapid and efficient stomatal closure, in reality a continuum of stomatal responses is observed in Mediterranean plants (cf., Joffre et al. 2007), even within a single site (e.g., Martinez-Vilalta et al. 2003). At the species level, stomatal behavior tends to be associated with other plant traits, such as rooting depth or vulnerability to xylem embolism (Davis et al. 1998; Martínez-Vilalta et al. 2002a). In general, Mediterranean species showing a less strict stomatal control tend to operate under more negative water potentials and be more resistant to xylem embolism (e.g., Martinez-Vilalta et al. 2003; Jacobsen et al. 2007).

Another characteristic of Mediterranean plants, including many *Eucalyptus* and *Quercus* species, is the ability to grow very deep root systems. In this way, they are able to access additional ground water resources which allow them to continue transpiration and carbon assimilation during the dry season (Dawson and Pate 1996). Additionally, many Mediterranean plants have dimorphic root systems, which explain why hydraulic lift is particularly common in Mediterranean ecosystems (Jackson et al. 2000). Plants from Mediterranean communities are, on average, more resistant to xylem embolism than those from any other biome, including deserts. This has important implications for drought resistance, as safety margins from hydraulic failure seem to be wider in Mediterranean plants than in species from more arid climates (cf. Jacobsen et al. 2007).

14.3.2 Dynamics of Transpiration in Mediterranean Forests

Diurnal curves of stomatal conductance in Mediterranean plants frequently show a characteristic pattern with two maxima, one in the morning and another one in the afternoon, separated by a midday depression. This drop has been interpreted as an adaptation to limit water loss when atmospheric water demand is highest (Joffre et al. 2007). Similar adjustments have been reported on a seasonal base, with reductions in stomatal conductance during the summer drought (Fig. 14.1). This reduction is caused by the decline in stomatal conductance with vapor pressure deficit (VPD), but also by changes in the functional response of stomata to VPD, probably due to xylem embolism or to changes in the root–soil interface (Martinez-Vilalta et al. 2003). There is some evidence that stomatal behavior of Mediterranean species is optimal in the sense that it allows for maximizing the ratio of carbon gain to water loss throughout the season (Xu and Baldocchi 2003).

At an inter-annual time scale, water use by Mediterranean forests is controlled by water availability and, in particular, by soil water content (e.g., Reichstein et al. 2002; Rambal et al. 2003; Poyatos et al. 2008). As a result, Mediterranean ecosystems are particularly vulnerable to climate change. Several experimental simulations conducted under field conditions have shown that water use in Mediterranean forests is sensitive to reductions in precipitation (Cinnirella et al. 2002; Martinez-Vilalta et al. 2003; Limousin et al. 2009).

14.4 Mediterranean Streamflow Hydrology

The relatively limited number of studies related with the streamflow hydrology of Mediterranean areas has sometimes resulted in the unverified extrapolation of findings obtained in other climatic areas. However, in Mediterranean areas, results obtained in humid regions may only be suitable for short wet periods of the year. Indeed, streamflow hydrology of Mediterranean areas shares hydrological processes of both wet and dry environments (Gallart et al. 1997, 2002). Results obtained on the streamflow hydrology of Mediterranean areas in the last decades correspond mainly to studies performed at the small research catchment scale (less than 10 km^2) in Europe and in the USA. They show (see Latron et al. 2009 and references therein) that the succession of dry and wet periods and the characteristic occurrence of a wetting-up transition between both increases the complexity of the rainfall–streamflow relationship.

14.4.1 Soil Moisture and Water Table Dynamics

The seasonality of the Mediterranean climate has a strong influence on the spatio-temporal dynamics of soil moisture (Fig. 14.1). In the periods when precipitation

exceeds evapotranspiration, catchment shifts into a wet state and soil moisture patterns are generally controlled by factors related to the general catchment topography, with upslope contributing areas as the most relevant feature. Under such conditions, spatial soil moisture patterns are weakly heterogeneous and downslope areas are generally wetter than upslope ones. Examples of time periods with nonlocal controls dominating soil moisture spatial dynamics have been reported in Mediterranean catchments during relatively wet conditions. Contrarily, when the catchment is in a dry state, soil moisture distribution depends mainly on local controls. Among these, vegetation cover, aspect and soil characteristics have been described as the most relevant for Mediterranean catchments (Gómez-Plaza et al. 2001). Soil moisture patterns observed in dry conditions are much more irregular and are very heterogeneous, because sub-surface water redistribution is no longer active. This switching behavior enhances the spatio-temporal dynamics of soil moisture in Mediterranean mountain catchments, in comparison with drier or wetter areas.

The marked seasonality of water table dynamics, as well as its high spatial variability has often been reported for Mediterranean catchments (e.g., Grésillon and Taha 1998). Results obtained recently (Lana-Renault et al. 2007; Latron and Gallart 2008) on the effect of water table dynamics on streamflow response of Mediterranean catchments show that water table dynamics is highly seasonal and that, when the water table is close to the surface, the extent of saturated areas increases, as is often found in more humid areas. The water table does not show a similar response to rainfall throughout the year. This varies from no response in dry conditions to very rapid response in wet conditions. During wetting-up periods, characteristic slow and delayed water table responses are often observed. Finally, and similarly to soil moisture, spatial variations in water table levels are much higher during wetting-up periods than in dry or wet conditions.

14.4.2 Rainfall–Runoff Relationships and Streamflow Generation Processes

In Mediterranean regions, the combination of high seasonality of the climate and the generally high spatial heterogeneity of the landscape increases the nonlinearity of the rainfall–runoff relationship. The highly variable rainfall dynamics have direct consequences on the annual streamflow response of Mediterranean catchments. Indeed, annual rainfall depth, as well as its distribution within the year, strongly affects the streamflow response and very large variations in the annual runoff/rainfall ratio have often been reported (Latron et al. 2009). At the seasonal and monthly scale, no simple relationship between rainfall and runoff depths is generally found (Ceballos and Schnabel 1998), even for the rainiest months. The existence of a threshold in the relationship between rainfall and runoff depths has been identified sometimes (Latron et al. 2008). This threshold distinguishes lower or higher hydrological responses than those usually observed in more humid catchments. At the event scale, the seasonality of the hydrological response of

Mediterranean catchments has also been reported (e.g., Llorens and Gallart 1992; García-Ruiz et al. 2008), with a predominant alternation between a wet period, when the catchment is hydrologically responsive, and a dry period, mainly in the summer, when the catchment is much less reactive to any rainfall input (Fig. 14.1).

In Mediterranean catchments, the relationship between rainfall and stream-flow is strongly dependent on the position of the water table, even if the relationship between streamflow and the depth of the water table is much more scattered than under more humid conditions (Latron and Gallart 2008). However, observed water table variations are not always in phase with streamflow changes. Findings obtained in Mediterranean catchments (Cosandey et al. 2005; Latron et al. 2008) show that streamflow generation processes are widely variable in time and space during the year in relation to the seasonality of catchment water reserves and to rainfall characteristics (intensity, duration, etc.). As a result, runoff events in dry, wetting-up and wet conditions commonly have different characteristics and they are associated with dominating runoff generation processes changing from season to season. For short (and often intense) rainfall events occurring in dry conditions, infiltration excess runoff has been reported as the dominant streamflow process. During wetting-up transitions the steady saturation of the catchment favors an increasing contribution of saturation excess runoff, which leads to a larger hydrological response. Lastly, during wet conditions, the extensive surface saturation within the catchment is generally favorable to saturation excess runoff generation (Latron and Gallart 2007), even if significant contributions of sub-surface runoff processes have been identified in forested catchments (e.g., Marc et al. 2001).

14.5 Mediterranean Forest Biogeochemistry

The biogeochemistry of Mediterranean forests has received little attention. This is evidenced by the low data availability in pan-European databases (Dise et al. 2009 and references therein). Mediterranean forests show many biogeochemistry features common to other climate-type forests, but elevated temperatures determine an intense biogeochemical cycling and a short mean residence time for elements in Mediterranean forest floor. Hence, Mediterranean forest soils have thin litter floors and low contents of organic matter, N and P, compared to other world soils (Day 1983). In addition, nutrients accumulate mostly in the aboveground biomass, in comparison to northern forests (Rodà et al. 1999 and references therein).

14.5.1 Deposition and Nutrient Cycling in Mediterranean Forests

Atmospheric depositions in the Mediterranean basin are frequently alkaline, partly because the influence of Saharan dust (red rains) and other calcareous and salt containing particles (e.g., Löye-Pilot et al. 1986). Except some mountainous forests

in California (Fenn and Poth 1999), Mediterranean forests receive low N deposition, with 5–10 kg N ha^{-1} year^{-1} for Mediterranean basin and South California, 0.1–0.5 kg N ha^{-1} year^{-1} in North Africa, Chile and South Africa, and even less in SW Australia (Galloway 2005).

Accordingly, net canopy depositions reported for Mediterranean forests are generally very low (e.g., Bellot et al. 1999; Michopoulos et al. 2001). In nutrient-limited Mediterranean forests, trees minimize canopy cations and P leaching, even if trees take up of N and S from the atmosphere, as a conservative mechanism of self-regulation (e.g., Moreno et al. 2001). N is retained usually as NH_4^+ but, in very N-limited forests, it can occur also as NO_3^- in the growing season (Moreno et al. 2001).

The asynchrony between availability and plant demand of nutrients makes Mediterranean forests very prone to nutrient loss from soils, which occur at moments of high biological activity that coincides with the movement of leaching waters and gas emission (Fenn et al. 1998; Butturini and Sabater 2002).

Litter decomposition peaks occur with wetting episodes at mild and high temperatures. Nitrification is very efficient, even during a summer drought (Andersen and Gundersen 2000). These conditions promote nutrient mobility and loss, especially with storms occurring after dry antecedent conditions (Àvila et al. 2002; Ahearn et al. 2004; Bernal et al. 2005). These storms promote preferential flows reaching the streams quickly, and leaching the forest floor with an important amount of mineral nutrients (Àvila et al. 2002) and dissolved organic nutrients, as DON (Cortina et al. 1995) and DOP (Butturini and Sabater 2000).

The nutrients exportation in Mediterranean deciduous oak forests, mostly throughout the dormant season (net lost of 3.7 kg ha^{-1} year^{-1} of N reported by Moreno and Gallardo 2002b) is about 100 times greater than in evergreen oak forests (a net export of 0.05 kg N ha^{-1} year^{-1} is reported by Àvila et al. 2002).

Nutrient balances have revealed a net accumulation in most Mediterranean forest soils, with low nutrient output compensated by atmospheric inputs (Moreno and Gallardo 2002b; Rodà et al. 2002). In this way, the slow-growing Mediterranean forests satisfy their nutrient requirements with atmospheric depositions to a large extent (Rodà et al. 1999; Moreno and Gallardo 2002a).

Forest decline or decreased productivity is unlikely in Mediterranean forests, even with high N deposition and active nitrification, because soils have high base saturation and are not prone to severe acidification or Al mobilization. However, forest decline may occur if elevated N concentration hampers mycorrhizal development, or predisposes tree to drought stress, ozone injury, disease or insect infestation (Fenn et al. 1998 and references therein).

14.5.2 Biogeochemistry of Mediterranean Streams

The biogeochemistry of Mediterranean forest streams does not cover all the issues tackled in running waters of other forest types (i.e., deciduous and coniferous cold-temperate streams). With the exception of recent investigations in NE Spain, little work has been done in other Mediterranean forested areas.

Most efforts have been devoted to organic carbon and nitrate transformations, performing studies on mass balances (Williams and Melack 1997; Àvila et al. 2002; Bernal et al. 2006) and nutrient retention and export (Martí and Sabater 1996; Lewis 2002), chemical seasonality (Ahearn et al. 2004; Bernal et al. 2005), exchanges between hyporheic and in-stream waters (Butturini and Sabater 1999), the responses to storms (Bernal et al. 2002; Butturini et al. 2006) and nitrate (Rusjan et al. 2008) and DOC export seasonality (Butturini and Sabater 2000; Butturini et al. 2008). Phosphorus metabolism, however, has not been studied as yet.

Organismic metabolism has been another fruitful approach. Carbon fixation by algal communities and heterotrophic metabolism by bacteria have been addressed by Sabater and Romaní (1996), Romaní et al. (1998), and Romaní and Sabater (2001) in intermittent streams of deciduous forests. Nitrification by biofilms was measured by Butturini et al. (2000), whereas denitrification rates were provided by Merseburger et al. (2006), who also developed a conceptual model for nitrogen metabolism (Merseburger 2006). Organic matter decomposition has also been studied (Artigas et al. 2004), flow and benthic organic carbon being the shaping factors of Mediterranean forest stream metabolism (Acuña et al. 2004).

The biogeochemistry of Mediterranean riparian forests has also deserved scrutiny, Sabater et al. (2000) addressed the effect of riparian vegetation removal on nutrient retention; Romaní et al. (2006) linked biogeochemistry of riparian and in-stream environments.

Available data on annual nutrient export from Mediterranean forest streams are still scant. Measured DOC flux in catchments with deciduous forests (Butturini and Sabater 2000; Bernal et al. 2002) are in the low range of what has been measured world wide (Alvarez-Cobelas et al. in press). Likewise, the total nitrogen export in pristine Mediterranean catchments, covered by different forest species (Àvila et al. 2002; Lewis 2002) is also in the low range in comparison to word wide observations (Alvarez-Cobelas et al. 2008).

The single datum reported on soluble phosphorus export is recorded in the coniferous Tharp's creek catchment (California, 6 kg P km^{-2} $year^{-1}$; Williams and Melack 1997), and is well within world ranges (Alvarez-Cobelas et al. 2009).

Biogeochemistry is reasonably well understood, whereas ecological structure is less known. Therefore, the identification of community elements playing a role in biogeochemistry of Mediterranean forest streams is still poor. Despite the great amount of work on cyanobacterial populations (Sabater 1989, 2000; Sabater et al. 2003), algal groups are not so well known. The identity of heterotrophic bacteria and fungi acting on chemical transformations are also unknown in Mediterranean forested catchments, but some efforts are ongoing using novel DNA technologies (Romaní et al. 2009).

14.5.3 Mediterranean Forests' Vulnerability to Climate Change

As water use by Mediterranean forest is controlled by water availability, Mediterranean ecosystems are particularly vulnerable to climate change, as most models predict both a significant temperature increase and a noticeable decline in precipitation, which

would result in a large reduction of water availability during the summer (cf. Gao and Giorgi 2008 for the Mediterranean Basin). This scenario is particularly critical if one considers that the current aridity levels in the Mediterranean Basin, seem already to be unprecedented in, at least, the previous 500 years (Nicault et al. 2008).

Moreover, a potential decrease of annual runoff in the near future as a consequence of climate change would threaten the tight water balance of Mediterranean catchments, characterized by a strong seasonal rainfall variability and a high and growing demand of water by population.

The tight nutrient cycling of Mediterranean forests could nevertheless change with time, provided that depositions are still increasing, and many aggrading Mediterranean forests promptly reach a steady state, decreasing, thus, the capacity to absorb the depositions (Rodà et al. 2002). Indeed, some N saturated Mediterranean forests in California exhibit the highest stream water nitrate concentration for wildlands in North America (Fenn et al. 1998). Under current and predictable scenarios, most of the Mediterranean forests show a risk of eutrophication (de Vries 2007), with some level of exceedance of N deposition. This could be increasing the frequency of P limited ecosystems (Herut et al. 1999).

Moreover, any increase in temperature would likely increase SOM mineralization (Casals et al. 2000), by contrast a reduction in mineralization rates by slowdown of microbial activity (Gorissen et al. 2004) and by changes in humus quality (Bussotti et al. 2002) could be a result of an increase of droughts in Mediterranean forests. Drought could also diminish plant uptake of P and K and lead to greater recalcitrance of these nutrients in soil (Sardans and Peñuelas 2007).

14.6 Future Prospects

Despite the effort devoted to the study the hydrology and biogeochemistry of Mediterranean environments, there are several aspects that are still poorly understood. In this sense, several aspects should be considered for future work.

14.6.1 Hydrology

The rainfall interception process by some characteristic Mediterranean species has either been poorly studied or never studied at all in particular shrub species, and there is a need for better representation of the rainfall range between 600 and 800 mm year^{-1} (Llorens and Domingo 2007).

For its hydrological and ecological relevance, the effect of stemflow as a source of water concentration and soil preferential flow under isolated shrubs or trees, as well as the role of rainfall interception under these plants need to be deeply analyzed, because some discrepancies are observed in Mediterranean oak savannahs (Joffre and Rambal 1993; Cubera and Moreno 2007).

Moreover, as the seasonality of the Mediterranean climate is expected to be enhanced due to anthropogenic climate change, the occurrence of rainfall events with larger rainfall intensities will increase in frequency (Giorgi and Lionello 2008). Consequently, a model representing rainfall interception processes under Mediterranean climate should be adapted to those changes, considering explicitly the observed rainfall seasonality while keeping in mind the drawbacks observed in interception loss modeling, such as the inadequate validation of the models and the evaluation of input data and the parameters' uncertainty (Muzylo et al. 2009).

In terms of predicting the response of Mediterranean ecosystems and their water flows to predicted climate change, one issue that remains to be solved is the inclusion of water limitations in large-scale vegetation models. The explicit incorporation of plant hydraulic architecture in such models is a promising avenue. In that respect, the use of a species-specific critical water potential representing the limit conditions for stomatal opening (cf. SPA: Williams et al. 1996; HYDRALL: Magnani et al. 2004) seems a simple and effective way of including hydraulic limitations. However, this is unlikely to be sufficient, as some recent studies indicate that models such as SPA perform better under well-watered conditions than under drought conditions (e.g., Hernandez-Santana et al. 2009).

Changes in species composition, or species shifts, are also likely to be critical in the scaling up of the eco-hydrological response of Mediterranean ecosystems to climate change. Despite important efforts (Martínez-Vilalta et al. 2002b; McDowell et al. 2008), the physiological mechanisms underlying tree drought survival are poorly known. Additionally, the effects of other interacting drivers, such as management-driven modifications in forest structure (cf. Palahí et al. 2008) and forest fires (e.g., Tague et al. 2009) should be also taken into account. There is also a lack of studies on the long-term effects of forest fire in nutrient content, availability and relative abundance (Hungate et al. 2003). Research should be devoted to understanding how the short-term nutrient loss influences the function and structure of terrestrial ecosystems (Wan et al. 2001).

The spatial and temporal nonlinearity of the rainfall–runoff relationship severely complicates the modeling of Mediterranean catchments (Gan et al. 1997; Piñol et al. 1997; Beven 2002; Medici et al. 2008), for which model improvements are required (Anderton et al. 2002; Latron et al. 2003; Moussa et al. 2007), and uncertainty in model parameter evaluation needs to be reduced (Lukey et al. 2000; Gallart et al. 2007).

At present, more process-orientated research is needed, using complementary approaches (e.g., hydrometry, environmental tracing, modeling) to improve a perceptual model of the hydrological functioning of Mediterranean catchments. Research should focus mainly on the wetting-up sequence and should be oriented toward the characterization of the spatial variability of saturated and unsaturated stores within the catchment. More flexible process-based modeling structures are also needed that can capture the strong seasonality of Mediterranean catchments' hydrology. At the same time, relatively simple procedures (such as in Gallart et al. 2008) should be developed to constrain model parameter distributions for the simulation of Mediterranean catchments.

14.6.2 Biogeochemistry

Improving our understanding of nutrient cycling in Mediterranean forest is still needed (see Dise et al. 2009 and references therein), and particularly stressed under new scenarios of climate and atmospheric composition changes. Serious gaps in knowledge exist in the critical loads of N and other pollutants (de Vries et al. 2007). A great challenge for Mediterranean forests is to understand the mechanisms by which large amounts of N are incorporated into forest soils, and to develop a method for predicting retention capacity (Meixner and Fenn 2004). Information concerning NO_x gases exchanges is still very scarce (Butterbach-Bahl et al. 2009) and it is necessary to discern whether Mediterranean Forests are emitting or sequestering NO_x gases, which mechanisms govern the processes and how they are affected by climate change.

Long-term studies of Mediterranean catchments nutrients' export and retention along with global change evolvement are also needed. Data on retention is practically nonexistent because, until now, Mediterranean forest biogeochemical processes have seldom been related with stream export. Regarding flux and export, there are no data on total carbon, particulate carbon, total phosphorus or phosphorus fractions other than soluble reactive phosphorus.

The interchange between forest, epi and hyporheic waters fluxes and the changing role of different flow paths and their associated biogeochemical fluxes over time are still understudied.

Finally, there is a need of increasing attention to the chemical characterization of carbon and nitrogen organic compounds and their transformations (i.e., DOC, POC, DON, PON), in addition to other elements currently overlooked in Mediterranean forest streams, such as sulfur, calcium, silicon, and the effects of acid deposition on Mediterranean forested catchments.

References

Acherar M, Rambal S (1992) Comparative water relations of four Mediterranean oak species. Plant Ecol 99(100):177–184

Acuña V, Giorgi A, Muñoz I et al (2004) Flow extremes and benthic organic matter shape the metabolism of a headwater Mediterranean stream. Freshwater Biol 49:960–971

Ahearn DS, Sheibley RW, Dahlgren RA et al (2004) Temporal dynamics of stream water chemistry in the last free-flowing draining the western Sierra Nevada, California. J Hydrol 295:47–63

Alvarez-Cobelas M, Angeler DG, Sánchez-Carrillo S (2008) Export of nitrogen from catchments: a world-wide analysis. Environ Pollut 156:261–269

Alvarez-Cobelas M, Sánchez-Carrillo S, Angeler DG et al (2009) Phosphorus export from catchments: a global view. J N Am Benthol Soc 28:805–820

Alvarez-Cobelas M, Angeler D, Sánchez-Carrillo S, Almendros G (2010) A worldwide view of organic carbon export from catchments. Biogeochemistry. doi: 10.1007/s10533-010-9553-z

Andersen BR, Gundersen P (2000) Nitrogen and carbon interactions of forest soil water. In: Schulze ED (ed) Carbon and nitrogen cycling in European forest ecosystems, ecological studies. Springer, Berlin, pp 332–340

Anderton SP, Latron J, White SM, Llorens P et al (2002) Internal evaluation of a physically-based distributed model using data from a Mediterranean mountain catchment. Hydrol Earth Syst Sci 6:67–83

Artigas J, Romaní AM, Sabater S (2004) Organic matter decomposition by fungi in a Mediterranean forested stream: contribution of streambed substrata. Ann Limnol 40:269–277

Àvila A, Rodrigo A, Rodà F (2002) Nitrogen circulation in a Mediterranean holm oak forest, La Castanya, Montseny, northeastern Spain. Hydrol Earth Syst Sci 6:551–557

Bellot J, Àvila A, Rodrigo A (1999) Throughfall and stemflow. In: Rodà F, Retana J, Gracia CA, Bellot J (eds) Ecology of Mediterranean evergreen oak forests. Springer, Berlin, pp 209–222

Belmonte F, Romero M (1998) A simple technique for measuring rainfall interception by small scrubs "interception flow collection box". Hydrol Process 12:471–481

Bernal S, Butturini A, Sabater F (2002) Variability of DOC and nitrate responses to storms in a small Mediterranean forested catchment. Hydrol Earth Syst Sci 6:1031–1041

Bernal S, Butturini A, Sabater F (2005) Seasonal variations of dissolved nitrogen and DOC:DON ratios in an intermittent Mediterranean stream. Biogeochemistry 75:351–372

Bernal S, Butturini A, Sabater F (2006) Inferring nitrate sources through end member mixing analysis in an intermittent Mediterranean stream. Biogeochemistry 81:269–289

Beven K (2002) Runoff generation in semi-arid areas. In: Bull LJ, Kirkby MJ (eds) Dryland rivers: hydrology and geomorphology of semi-arid channels. Wiley, London, pp 57–105

Bussotti F, Bettini D, Grossoni P et al (2002) Structural and functional traits of Quercus ilex in response to water availability. Environ Exp Bot 47:11–23

Butterbach-Bahl K, Kahl M, Mykhayliv L et al (2009) A European-wide inventory of soil NO emissions using the biogeochemical models DNDC/Forest-DNDC. Atmos Environ 43:1392–1402

Butturini A, Sabater F (1999) Importance of transient storage zones for ammonium and phosphate retention in a sandy-bottom Mediterranean stream. Freshwater Biol 41:593–603

Butturini A, Sabater F (2000) Seasonal variability of dissolved organic carbon in a Mediterranean stream. Biogeochemistry 51:303–321

Butturini A, Sabater F (2002) Nitrogen concentrations in a small Mediterranean stream: 1. Nitrate 2. Ammonium. Hydrol Earth Syst Sci 6:539–550

Butturini A, Battin TM, Sabater F (2000) Nitrification in stream sediment biofilms: the role of ammonium concentration and DOC quality. Water Res 34:629–639

Butturini A, Gallart F, Latron J et al (2006) Cross-site comparison of variability of DOC and nitrate c-q hysteresis during the autumn-winter period in three Mediterranean headwater streams: a synthetic approach. Biogeochemistry 77:327–349

Butturini A, Álvarez M, Bernal S et al (2008) Diversity and temporal sequences of forms of DOC and NO3-discharge responses in an intermittent stream: predictable or random succession? J Geophys. doi:10.1029/2008JG000721

Casals P, Romanyà J, Cortina J et al (2000) CO2 efflux from a Mediterranean semi-arid forest soil. I. Seasonality and effects of stoniness. Biogeochemistry 48:261–281

Ceballos A, Schnabel S (1998) Hydrological behaviour of a small catchment in the dehesa landuse system (Extremadura, SW Spain). J Hydrol 210:146–160

Cinnirella S, Magnani F, Saracino A et al (2002) Response of a mature Pinus laricio plantation to a three-year restriction of water supply: structural and functional acclimatation to drought. Tree Physiol 22:21–30

Cortina J, Romanya J, Vallejo VR (1995) Nitrogen and phosphorus leaching from the forest floor of a mature Pinus radiata stand. Geoderma 66:321–330

Cosandey C, Andreassian V, Martin C et al (2005) The hydrological impact of the mediterranean forest: a review of French research. J Hydrol 301:235–249

Cowling RM, Rundel PW, Lamont BB et al (1996) Plant diversity in Mediterranean-climate regions trends in ecology. Evolution 11(9):362–366

Cubera E, Moreno G (2007) Effect of land-use on soil water dynamic in dehesas of Central–Western Spain. Catena 71:298–308

David TS, Gash JHC, Valente F (2005) Evaporation of intercepted rainfall. In: Anderson M (ed) Encyclopedia of hydrological sciences. Wiley, Chichester, pp 627–634

David TS, Gash JHC, Valente F et al (2006) Rainfall interception by an isolated evergreen oak tree in a Mediterranean savannah. Hydrol Process 20:2713–2726

Davis SD, Kolb KJ, Barton KP (1998) Ecophysiological processes and demographic patterns in the structuring of California chaparral. In: Rundel PW, Montenegro G, Jaksic F (eds) Landscape disturbance and biodiversity in mediterranean-type ecosystems. Springer, Berlin, pp 297–310

Dawson TE, Pate JS (1996) Seasonal water uptake and movement in root systems of Australian phraeatophytic plants of dimorphic root morphology: a stable isotope investigation. Oecologia 107:13–20

Day JA (1983) Mineral nutrients in Mediterranean ecosystems. South African national Scientific Programmes Report No 71. Pretoria, South Africa

de Vries W, Van der Salm C, Reinds GJ et al (2007) Element fluxes through intensively monitored forest ecosystems in Europe and their relationships with stand and site characteristics. Environ Pollut 148(2):501–513

Dise NB, Rothwell JJ, Gauci V et al (2009) Predicting dissolved inorganic nitrogen leaching in European forests using two independent databases. Sci Total Environ 407:1798–1808

Domingo F, Sanchez G, Moro MJ et al (1998) Measurement and modelling of rainfall interception by three semi-arid canopies. Agric Forest Meteorol 91:275–292

Dunkerley D (2000) Measuring interception loss and canopy storage in dryland vegetation: a brief review and evaluation of available research strategies. Hydrol Process 14:669–678

Eamus D, Hatton T, Cook P et al (2006) Ecohydrology: vegetation function, water and resource management. CSIRO Publishing, Canberra

Fenn ME, Poth MA (1999) Nitrogen deposition and cycling in Mediterranean forests: the new paradigm of nitrogen excess. In: Miller PR, McBride JR (eds) Oxidant air pollution impacts in the montane forests of southern California: a case study of the San Bernardino Mountains. Springer, New York, pp 288–314

Fenn ME, Poth MA, Aber JD et al (1998) Nitrogen excess in North America Ecosystems: predisposing factors, ecosystems responses, and management strategies. Ecol Appl 8:706–733

Gan TY, Dlamini EM, Biftu GF (1997) Effects of model complexity and structure, data quality, and objective functions on hydrologic modeling. J Hydrol 192:81–103

Gallart F, Latron J, Llorens P et al (1997) Hydrological functioning of Mediterranean mountain basins in Vallcebre, Catalonia: some challenges for hydrological modelling. Hydrol Process 11:1263–1272

Gallart F, Llorens P, Latron J et al (2002) Hydrological processes and their seasonal controls in a small Mediterranean mountain catchment in the Pyrenees. Hydrol Earth Syst Sci 6:527–537

Gallart F, Latron J, Llorens P et al (2007) Using internal catchment information to reduce the uncertainty of discharge and baseflow predictions. Adv Water Resour 30:808–823

Gallart F, Latron J, Llorens P, Beven KJ (2008) Upscaling discrete internal observations for obtaining catchment-averaged TOPMODEL parameters in a small Mediterranean mountain basin. Phys Chem Earth 33(17–18):1090–1094

Galloway NJ (2005) The global nitrogen cycle. In: Schlesinger WH (ed) Biogeochemistry, Vol. 8, treatise on geochemistry. Elsevier, Oxford, pp 557–583

Gao X, Giorgi F (2008) Increased aridity in the Mediterranean region under greenhouse gas forcing estimated from high resolution simulations with a regional climate model. Global Planet Change 62:195–209

García-Ruiz JM, Regüés D, Alvera B et al (2008) Flood generation and sediment transport in experimental catchments affected by land use changes in the central Pyrenees. J Hydrol 356:245–260

Gash JHC (1979) Analytical model of rainfall interception by forests. Quart J Roy Meteorol Soc 105:43–55

Gash JHC, Lloyd CR, Lachaud G (1995) Estimating sparse forest rainfall interception with an analytical model. J Hydrol 170:79–86

Giorgi F, Lionello P (2008) Climate change projections for the Mediterranean region. Global Planet Change 63:90–104

Gomez JA, Giraldez JV, Fereres E (2001) Rainfall interception by olive trees in relation to leaf area. Agric Water Manag 49:65–76

Gómez-Plaza A, Martínez-Mena M, Albaladejo J et al (2001) Factors regulating spatial distribution of soil water content in small semiarid catchments. J Hydrol 253:211–226

Gorissen A, Tietema A, Joosten NN et al (2004) Climate change effects carbon allocation to the soil in shrublands. Ecosystems 7:650–661

Grésillon JM, Taha A (1998) Saturated contributive areas in Mediterranean catchments: condition for appearance and consequent floods. Hydrolog Sci J 43:267–282

Herbst M, Rosier PTW, McNeil DD et al (2008) Seasonal variability of interception evaporation from the canopy of a mixed deciduous forest. Agric Forest Meteorol 148:1655–1667

Hernandez-Santana V, Martínez-Vilalta J, Martínez-Fernandez J et al (2009) Evaluating the effect of drier and warmer conditions on water use by *Quercus pyrenaica*. For Ecol Manag 258:1719–1730

Herut B, Krom MD, Pan G et al (1999) Atmospheric input of nitrogen and phosphorous to the southeast Mediterranean: sources, fluxes, and possible impact. Limnol Oceanogr 44:1683–1692

Hoff C, Rambal S (2003) An examination of the interaction between climate, soil and leaf area index in a *Quercus ilex* ecosystem. Ann For Sci 60:153–161

Hungate BA, Naiman RJ, Apps M et al (2003) Disturbance and element interactions. In: Melillo JM, Field CB, Moldan B (eds) Interactions of the major biogeochemical cycles, global change and human impacts. Island, Washington, pp 47–62

Infante JM, Rambal S, Joffre R (1997) Modelling transpiration in holm-oak savannah: scaling up from the leaf to the tree scale. Agric For Meteorol 87:273–289

Jackson RB, Sperry JS, Dawson TE (2000) Root water uptake and transport: using physiological processes in global predictions. Trends Plant Sci 5:482–488

Jacobsen AL, Pratt BR, Davis SD et al (2007) Cavitation resistance and seasonal hydraulics differ among three arid Californian plant communities. Plant Cell Environ 30:1599–1609

Joffre R, Rambal S (1993) How tree cover influences the water balance of Mediterranean rangelands. Ecology 74:570–582

Joffre R, Rambal S (2002) Mediterranean ecosystems. In: Encyclopaedia of life sciences. Wiley, Chichester. doi: 10.1038/npg.els.0003196

Joffre R, Rambal S, Damesin C (2007) Functional attributes in Mediterranean-type ecosystems. In: Pugnaire FI, Valladares F (eds) Functional plant ecology, 2nd edn. CRC Press, Boca Raton, pp 285–312

Lana-Renault N, Latron J, Regüés D (2007) Streamflow response and water-table dynamics in a sub-Mediterranean research catchment (Central Pyrenees). J Hydrol 347:497–507

Latron J, Gallart F (2007) Seasonal dynamics of runoff-contributing areas in a small Mediterranean research catchment (Vallcebre, Eastern Pyrenees). J Hydrol 335:194–206

Latron J, Gallart F (2008) Runoff generation processes in a small Mediterranean research catchment (Vallcebre, Eastern Pyrenees). J Hydrol 358:206–220

Latron J, Soler M, Llorens P et al (2008) Spatial and temporal variability of the hydrological response in a small Mediterranean research catchment (Vallcebre, Eastern Pyrenees). Hydrol Process 22:775–787

Latron J, Anderton S, White S, Llorens P, Gallart F (2003) Seasonal characteristics of the hydrological response in a Mediterranean mountain research catchment (Vallcebre, Catalan Pyrenees): field investigations and modelling. Hydrology of Mediterranean and Semiarid Regions. IAHS Publ. no. 278:106–110

Latron J, Llorens P, Gallart F (2009) The hydrology of Mediterranean mountain areas. Geography Compass 3:2045–2064

Levia DF, Frost EE (2003) A review and evaluation of stemflow literature in the hydrologic and biogeochemical cycles of forested and agricultural ecosystems. J Hydrol 274:1–29

Lewis WM Jr (2002) Yield of nitrogen from minimally disturbed watersheds of the United States. Biogeochemistry 57(58):375–385

Limousin JM, Rambal S, Ourcival JM et al (2008) Modelling rainfall interception in a Mediterranean Quercus ilex ecosystem: lesson from a throughfall exclusion experiment. J Hydrol 357:57–66

Limousin JM, Rambal S, Ourcival JM et al (2009) Long-term transpiration change with rainfall decline in a Mediterranean *Quercus ilex* forest. Glob Change Biol 15:2163–2175

Llorens P (1997) Rainfall interception by a Pinus sylvestris forest patch overgrown in a Mediterranean mountainous abandoned area.2. Assessment of the applicability of Gash's analytical model. J Hydrol 199:346–359

Llorens P, Domingo F (2007) Rainfall partitioning by vegetation under Mediterranean conditions. A review of studies in Europe. J Hydrol 335:37–54

Llorens P, Gallart F (1992) Small basin response in a Mediterranean mountainous abandoned farming area – research design and preliminary-results. Catena 19:309–320

Llorens P, Poch R, Latron J et al (1997) Rainfall interception by a Pinus sylvestris forest patch overgrown in a Mediterranean mountainous abandoned area.1. Monitoring design and results down to the event scale. J Hydrol 199:331–345

Löye-Pilot MD, Martin JM, Morelli J (1986) Influence of Saharan dust on the rain acidity and atmospheric input to the Mediterranean. Nature 321:427–428

Lukey BT, Sheffield J, Bathurst JC et al (2000) Test of the SHETRAN technology for modelling the impact of reforestation on badlands runoff and sediment yield at Draix, France. J Hydrol 235:44–62

Magnani F, Consiglio L, Erhard M et al (2004) Growth patterns and carbon balance of *Pinus radiata* and *Pseudotsuga menziesii* plantations under climate change scenarios in Italy. For Ecol Manag 202:93–105

Marc V, Didon-Lescot JF, Michael C (2001) Investigation of the hydrological processes using chemical and isotopic tracers in a small Mediterranean forested catchment during autumn recharge. J Hydrol 247:215–229

Martí E, Sabater F (1996) High variability in temporal and spatial nutrient retention in Mediterranean streams. Ecology 77:854–869

Martínez-Vilalta J, Prat E, Oliveras I et al (2002a) Xylem hydraulic properties of roots and stems of nine Mediterranean woody species. Oecologia 133(1):9–29

Martínez-Vilalta J, Piñol J, Beven K (2002b) A hydraulic model to predict drought-induced mortality in woody plants: an application to climate change in the Mediterranean. Ecol Model 155:127–147

Martinez-Vilalta J, Mangiron M, Ogaya R et al (2003) Sap flow of three co-occurring Mediterranean woody species under varying atmospheric and soil water conditions. Tree Physiol 23:747–758

McDowell N, Pockman WT, Allen CD et al (2008) Mechanisms of plant survival and mortality during drought: why do some plants survive while others succumb to drought? New Phytol 178:719–739

Medici C, Butturini A, Bernal S (2008) Modelling the non-linear hydrological behaviour of a small Mediterranean forested catchment. Hydrol Process 22:3814–3828

Meixner T, Fenn M (2004) Biogeochemical budgets in a Mediterranean catchment with high rates of atmospheric N deposition – importance of scale and temporal asynchrony. Biogeochemistry 70:331–356

Merseburger GC (2006) Nutrient dynamics and metabolism in Mediterranean streams affected by nutrient inputs from human activities. PhD thesis, University of Barcelona

Merseburger GC, Martí E, Sabater F (2006) Net changes in nutrient concentrations below a point source input in two streams draining catchments with contrasting land uses. Sci Total Environ 347:217–229

Michopoulos P, Baloutsos G, Nakos G et al (2001) Effects of bulk precipitation pH and growth period on cation enrichment in precipitation beneath the canopy of a beech (Fagus *moesiaca*) forest stand. Sci Total Environ 281:79–85

Moreno G, Gallardo JF (2002a) Atmospheric deposition in oligotrophic *Quercus pyrenaica* forests: implications for forest nutrition. For Ecol Manag 171:17–29

Moreno G, Gallardo JF (2002b) H+ budget in oligotrophic *Quercus pyrenaica* forests. Atmospheric and management-induced soil acidification? Plant Soil 243:11–22

Moreno G, Gallardo JF, Bussotti F (2001) Canopy modification of atmospheric deposition in oligotrophic Quercus pyrenaica forests of an unpolluted region (CW Spain). For Ecol Manag 149:47–60

Moussa R, Chahinian N, Bocquillon C (2007) Distributed hydrological modelling of a Mediterranean mountainous catchment – model construction and multi-site validation. J Hydrol 337:35–51

Muzylo A, Llorens P, Valente F et al (2009) A review of rainfall interception modelling. J Hydrol 370:191–206

Navar J (1993) The causes of stemflow variation in three semiarid growing species of Northeastern Mexico. J Hydrol 145:175–190

Nicault A, Alleaume S, Brewer S et al (2008) Mediterranean drought fluctuation during the last 500 years based on tree-ring data. Clim Dyn 31:227–245

Palahí M, Mavsar R, Gracia C et al (2008) Mediterranean forests under focus. Int Forest Rev 10:676–688

Pereira FL, Gash JHC, David JS et al (2009a) Modelling interception loss from evergreen oak Mediterranean savannas: application of a tree-based modelling approach. Agric Forest Meteorol 149:680–688

Pereira FL, Gash JHC, David JS et al (2009b) Evaporation of intercepted rainfall from isolated evergreen oak trees: do the crowns behave as wet bulbs? Agric Forest Meteorol 149:667–679

Piñol J, Beven K, Freer J (1997) Modelling the hydrological response of Mediterranean catchments, Prades, Catalonia. The use of distributed models as aids to hypothesis formulation. Hydrol Process 11:1287–1306

Poole DK, Miller PC (1981) The distribution of plant water stress and vegetation characteristics in Southern California Chaparral. Am Midl Nat 105:32–43

Poyatos R, Llorens P, Pinol J, Rubio C (2008) Response of Scots pine (*Pinus sylvestris* L.) and pubescent oak (Quercus pubescens Willd.) to soil and atmospheric water deficits under Mediterranean mountain climate. Ann For Sci 65. doi: 10.1051/forest:2008003

Rambal S, Ourcival JM, Joffre R et al (2003) Drought controls over conductance and assimilation of a Mediterranean evergreen ecosystem: scaling from leaf to canopy. Glob Change Biol 9:1813–1824

Reichstein M, Tenhunen JD, Roupsard O et al (2002) Severe drought effects on ecosystem CO2 and H2O fluxes at three Mediterranean evergreen sites: revision of current hypotheses? Glob Change Biol 8:999–1017

Rodà F, Retana J, Gracia C et al (eds) (1999) Ecology of Mediterranean evergreen oak forests. Springer, Berlin

Rodà F, Àvila A, Rodrigo A (2002) Nitrogen deposition in Mediterranean forests. Environ Pollut 118:205–213

Romaní AM, Sabater S (2001) Structure and activity of rock and sand biofilms in a Mediterranean stream. Ecology 82:3232–3245

Romaní AM, Butturini A, Sabater F et al (1998) Heterotrophic metabolism in a forest stream sediment: surface versus subsurface zones. Aquat Microb Ecol 16:143–151

Romaní AM, Vázquez E, Butturini A (2006) Microbial availability and size fractionation of dissolved organic carbon after drought in an intermittent stream: biogeochemical link across the stream-riparian interface. Microb Ecol 52:501–512

Romaní AM, Artigas J, Camacho A et al (2009) La biota de los ríos: los microorganismos heterótrofos. In: Elósegui A, Sabater S (eds) Conceptos y técnicas en ecología fluvial. Fundación BBVA, Bilbao

Rusjan S, Brilly M, Mikoš M (2008) Flushing of nitrate from a forested watershed: an insight into hydrological nitrate mobilization mechanisms through seasonal high-frequency stream nitrate dynamics. J Hydrol 354:187–202

Sabater S (1989) Encrusting algal assemblages in a Mediterranean river basin. Arch Hydrobiol 114:555–573

Sabater S (2000) Structure and architecture of a stromatolite from a Mediterranean stream. Aquat Microb Ecol 21:161–168

Sabater S, Romaní AM (1996) Metabolic changes associated with biofilm formation in an undisturbed Mediterranean stream. Hydrobiologia 335:107–113

Sabater F, Butturini A, Martí E et al (2000) Effects of riparian vegetation removal on nutrient retention in a Mediterranean stream. J N Am Benthol Soc 19:609–620

Sabater S, Vilalta E, Gaudes A et al (2003) Ecological implications of mass growth of benthic cyanobacteria in rivers. Aquat Microb Ecol 32:175–184

Sardans J, Peñuelas J (2007) Drought changes phosphorus and potassium accumulation patterns in an evergreen Mediterranean forest. Funct Ecol 21:191–201

Specht RL, Specht A (1989) Canopy structure in eucalyptus-dominated communities in Australia along climatic gradients. Acta Oecol 10:191–213

Sraj M, Brilly M, Mikos M (2008) Rainfall interception by two deciduous Mediterranean forests of contrasting stature in Slovenia. Agric Forest Meteorol 148:121–134

Tague C, Seaby L, Hope A (2009) Modeling the eco-hydrologic response of a Mediterranean type ecosystem to the combined impacts of projected climate change and altered fire frequencies. Climatic Change 93:137–155

Valente F, David JS, Gash JHC (1997) Modelling interception loss for two sparse eucalypt and pine forests in central Portugal using reformulated Rutter and Gash analytical models. J Hydrol 190:141–162

Wan S, Hui D, Luo Y (2001) Fire effects on nitrogen pools and dynamics in terrestrial ecosystems: a meta-analysis. Ecol Appl 11:1349–1365

Williams MR, Melack JM (1997) Atmospheric deposition, mass balances, and processes regulating streamwater solute concentrations in mixed-conifer catchments of the Sierra Nevada, California. Biogeochemistry 37:111–144

Williams M, Rastetter EB, Fernandes DN et al (1996) Modelling the soil-plant-atmosphere continuum in a Quercus–Acer stand at Harvard Forest: the regulation of stomatal conductance by light, nitrogen and soil/plant hydraulic properties. Plant Cell Environ 19:911–927

Xiao QF, McPherson EG, Ustin SL et al (2000) Winter rainfall interception by two mature open-grown trees in Davis, California. Hydrol Process 14:763–784

Xu L, Baldocchi DD (2003) Seasonal trends in photosynthetic parameters and stomatal conductance of blue oak (Quercus douglasii) under prolonged summer drought and high temperature. Tree Physiol 23:865–877

Chapter 15
Hydrology and Biogeochemistry
of Boreal Forests

Anders Lindroth and Patrick Crill

15.1 Introduction

The boreal or taiga forest cover 16% of the terrestrial landarea and contains 27% of the biomass carbon in a circumpolar belt across Eurasia and North America (e.g., McGuire et al. 2002). It contains greater than 30% of the world's soil C (>300 Pg, Dixon et al. 1994; Tarnocai et al. 2009). The soil types vary but a major part grows on nutrient poor, heavily podzolized Spodosols. The boreal forest is bordered by treeless tundra on the north and mixed forests on the south (in oceanic influenced climates) and arid steppe or semi-desert (in mid-continental climate regions).

The dominant needle leaf coniferous tree genera in North America are *Abies*, *Picea* and *Pinus* and the deciduous *Larix* (Breckle et al. 2002). The most common broadleaf tree genera are *Alnus*, *Betula* and *Populus*. The large species diversity of North America is in strong contrast to the boreal forests of Europe which are dominated by only two species; *Pinus sylvestris* and *Picea abies*. Moving eastward, *Picea* become less abundant and in continental Siberia *Larix* and *Pinus* are the dominant genera.

The climate of the boreal zone is characterized by a long cold season and a short growing season between 30 and 150 days with air temperatures above 10°C. Winter temperatures frequently drop below −20°C over large areas of the boreal. There are large variations within the zone. Cold oceanic climates have a relatively small annual amplitude in temperature compared to cold continental climates. The continental interior can have a 50°C difference between the coldest and the warmest days within a year. Permafrost occurs in the northern boreal. Precipitation is moderate over most of the area ranging between 250 and 1,000 mm (Leemans and Cramer 1991) with most precipitation occurring in narrow bands along the coastal zones of North America. The lowest rates occur in the interior of Eastern Siberia.

During the last two decades, the development of eddy covariance methods to continuously measure energy and mass exchange between ecosystems and the atmosphere over multiple years has led to a wealth of new information on hydrology and biogeochemistry of boreal ecosystems. Most of our synthesis below is based on such measurements, complemented with smaller scale measurements, e.g., using chamber techniques and sap flow methods, to partition the flux components.

15.2 Hydrology

The hydrological cycle of most forests is dominated by two vertical flows; precipitation (P) and ecosystem evaporation (E_e). The term evaporation is used here irrespectively of the pathway of the water that is evaporated. The difference between P and E_e, if any, generates a lateral flow, runoff (Q), after modification by change in soil water content (ΔS):

$$P = E_e + \Delta S + Q. \tag{15.1}$$

Evaporation is driven by weather and modified by vegetation and soil. Total evaporation from the forest is the sum of transpiration by trees and other plants, evaporation of intercepted water or snow and soil evaporation. A boreal forest is mostly composed of a distinct overstory and an understory. Because it is difficult to separate the water fluxes from the soil and the understory plants, they are often lumped together into understory evaporation (E_u). The Penman-Monteith equation is useful when interpreting evaporation measurements since it identifies the key abiotic and biotic factors that control evaporation:

$$E_e = \frac{\Delta \cdot A + \rho \cdot c_p \cdot \delta e \cdot G_a}{\Delta + \gamma(1 + G_a/G_s)}, \tag{15.2}$$

where Δ is the slope of the saturation vapor pressure curve, A is available energy (net radiation minus storage and soil heat flux), ρ is air density, c_p is specific heat of air, δe is saturation vapor pressure, G_a is the bulk aerodynamic conductance, γ is the psychrometric constant and G_s is the surface conductance of the ecosystem. Vegetation properties have a major impact on the conductances, G_a and G_s, respectively. The ratio, G_a/G_s, will determine how well coupled a specific forest is to the atmosphere (McNaughton and Jarvis 1983). The term "coupling," introduced by McNaughton and Jarvis (1983), describe which of the environmental drivers radiation or ventilation that are the dominant controls of the evaporation of a specific ecosystem. In a well coupled system, the ventilation term, i.e., wind and saturation vapor pressure deficit, constitute the main driver and vice versa in a decoupled system. A large G_a/G_s ratio implies that the forest is well coupled to the atmosphere with air humidity as the major control while the radiation term is less important.

15.2.1 Evaporation and Surface Conductance

Evaporation data from thirteen different boreal forests show that maximum daily rates vary between 2.2 and 7.0 mm day^{-1} (Table 15.1). The highest was found in a deciduous aspen forest in Canada and the lowest in a larch/pine forest in Siberia.

Table 15.1 Evaporation and surface conductance of different boreal forests

References	Location MAT, AnnP	Species LAI, Age	E_{max} (mm) (wet/dry)	E_{mean} (mm) (period)	G_{smax} (mm s^{-1}) (restriction)	G_{srange} (mm s^{-1}) (at $\delta e = 1$ kPa)
Arain et al. (2003)	53.98°N, 105.12°W 1.0°C, 400 mm	*Pinus banksiana* 4.5, 120 years	3.5	1.0 (2 years)	15 (PPFD > 200)	1.9–10.3
Baldocchi et al. (1997)	53.9°N, 104.68°W 0.1°C, 398 mm	*Pinus banksiana* 2, 70 years	3.0 (wet) 2.5 (dry)	1.6 (DOY 140–260)	5 (daily average)	Na
Humphreys et al. (2003)	49.87°N, 125.3°W 8.4°C, 1,409 mm	*Pseudotsuga menziesii* Na, 50 years	3.7	1.2 (2 years)	14	1.9–10.0
Blanken et al. (1997)	53.63°N, 106.2°W −0.2°C, 463 mm	*Populus tremuloides/ Corylus cornuta* Max 5.6, 70 years	7.0	3.8 (June–Aug)	52 (PPFD > 1,400)	3.4–21.0
Pejam et al. (2006)	48.2°N, 82.16°W 1.3°C, 831 mm	*Populus tremuloides/ Picea mariana/ Picea glauca/ Betula papyrifera* Na, 74 years	4–5 (dry)	1.3 (1 year)	25 (PPFD > 200; June–Sep)	4.5–10.0 (PPFD > 200; June–Sep)
Jarvis et al. (1997)	53.98°N, 105.12°W Na, Na	*Picea mariana* 4.5, 115 years	3.5	2.0 (DOY 143–264)	–	–
Matsumoto et al. (2008)	62.25°N, 129.62°E −10.0°C, 237 mm	*Larix cajanderi* 1.6, 170 years	2.6	1.8 (July–Aug)	–	–
Kelliher et al. (1997)	61°N, 128°E Na, Na	*Larix gmelinii* 1.5, 130 years	2.2	–	8 (PPFD > 600)	1.6–7.3
Ohta et al. (2001)	62.25°N, 129.62°E Na, Na	*Larix gmelinii* 2, Na	2.9	1.5 (July–Aug)	13	1.1–5.3
Matsumoto et al. (2008)	62.23°N, 129.65°E −10.0°C, 237 mm	*Pinus sylvestris* 1.1, 130 years	2.2	1.4 (July–Aug)	–	–
Kelliher et al. (1998)	61°N, 89°E −3.8°C, 597 mm	*Pinus sylvestris* 1.5, 215 years	2.3	1.2 (8–25 July)	7	–

(continued)

Table 15.1 (continued)

References	Location MAT, AnnP	Species LAI, Age	E_{max} (mm) (wet/dry)	E_{mean} (mm) (period)	G_{smax} (mm s^{-1}) (restriction)	G_{srange} (mm s^{-1}) (at δe = 1 kPa)
Rannik et al. (2002)	61.85°N, 24.28°E 3.0°C, 700 mm	*Pinus sylvestris* 3.0, 38 years	–	1.0 (July–Aug)	–	–
Wang et al. (2004)	62.85°N, 30.67°E Na, 724 mm	*Pinus sylvestris* 2, 50 years	3.5	1.0 (DOY 120–270)	–	–
Grelle et al. (1999)	60.08°N, 17.47°E 5.5°C, 527 mm	*Pinus sylvestris/Picea abies* 4.5, 100 years	4.0	1.0 (2 years)	16	1.5–13

The values in the table have either been quoted directly from the source or it has been computed from graphs or tables

MAT long term mean annual temperature (or the current year(s)); *AnnP* long term annual precipitation; *LAI* projected leaf area index; E_{max} maximum daily ecosystem evaporation during study period; E_{mean} average daily ecosystem evaporation during study period; G_{smax} maximum surface conductance under certain restricted conditions; G_{srange} range (ca. 90%) of surface conductance at a saturation vapor pressure deficit (δe) of 1 kPa; *PPFD* photosynthetic photon flux density (μmol m^{-2} s^{-1})

Fig. 15.1 Maximum
evaporation rates against leaf
area index for boreal forests
in North America and Euro-
Siberia
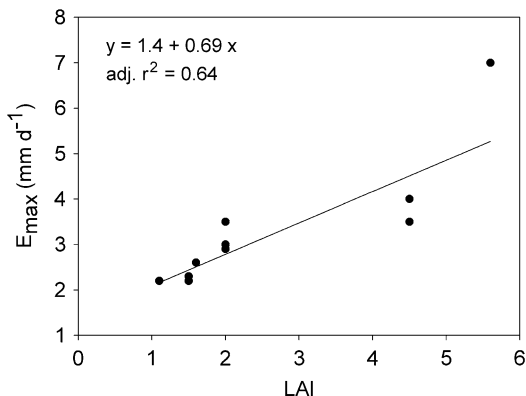
The median of these maximum rates is between 3.0 and 3.5 mm day^{-1} (ca. 0.5 mm day^{-1} higher than reported by Baldocchi et al. 2000). The maximum rates are correlated with the leaf area index (LAI) of forests (Fig. 15.1). A doubling of LAI from 2 to 4 increases the evaporation rate by 1.4 mm day^{-1}. The regression indicates that the ordinate intercept is positive. This is because the LAI values refer only to the tree canopy and exclude ground vegetation.

The mean daily rates (Table 15.1) are more difficult to compare because they represent different periods. Only four sites report annual values and the range was narrow with mean rates between 1.0 and 1.3 mm day^{-1}. The mean rates for these sites were 25–32% of the maximum rates. The calculated runoff would range from 35 to 971 mm year^{-1} by comparing the mean annual rates with the annual precipitation.

As expected, the maximum G_s of the forests were in good correspondence with the maximum evaporation rates (Table 15.1). All sites where G_s and δe were calculated showed a strongly decreasing conductance with increasing δe. There are also other factors that affect G_s, e.g., temperature, solar radiation, soil moisture and leaf area. This makes it difficult to compare G_a of different forests if not all data are available. A first order comparison of G_a at a δe of 1 kPa was calculated for sites where data were available (Table 15.1). A δe of 1 kPa is typical for summer conditions at noon under dry canopy conditions. Three distinct groups could be identified upper ranges of 5–7 mm s^{-1}, of 10–13 mm s^{-1} and of 21 mm s^{-1}. Considering that G_a is typically on the order of 60–200 mm s^{-1} (corresponding to an above canopy wind speed of ca. 1 and 3 m s^{-1}, respectively), the decoupling factor omega (McNaughton and Jarvis 1983) would be 0.08–0.24, 0.11–0.35 and 0.22–0.48 for the three different groups, respectively. The omega factor varies between 0 and 1. A low value indicates the stand is well coupled to the atmosphere and a high value indicates it is decoupled. Considering that the calculations of omega factor were based on the upper range of G_s, all of these forests must be considered well coupled to the atmosphere and mainly controlled by the air humidity. G_s is proportional to LAI for a specific stand (Blanken et al. 1997) and

because boreal forests generally have low LAI, this induces small G_s. This in turn results in low omega values and explains the strong apparent coupling to the atmosphere.

15.2.2 Understory Evaporation

The sparse canopies of most boreal forests make understory vegetation development possible. An interesting question is the understory contribution to the total evaporation. We have found nine boreal forests where both total ecosystem evaporation, E_e and evaporation from the understory, E_u were measured (Table 15.2). The maximum E_u ranged between 0.7 and 3.0 mm day^{-1} which is surprisingly high when compared to maximum rates for whole ecosystems. The site with the highest E_u was a deciduous aspen (*Populus tremuloides*) forest in North America growing on a fertile soil. This site showed the highest evaporation rate of all sites in this study. The fraction of E_u relative to E_e averaged over the growing season, varied between 0.17 and 0.57 (Table 15.2). The lowest fraction occurred in a mixed *P. sylvestri*/*P. abies* stand in Fenoscandia with very low ground coverage (27%) of transpiring *Vaccinium myrtillus*, the rest being mosses and lichens. The highest fraction, 0.92, was found in a *P. sylvestris* site in Siberia (Kelliher et al. 1998). The measurements at this site were only during a short period in the summer which did not allow an estimate of the seasonal average.

It is obvious that understory plays an important role in the water cycle of boreal forests. The understory is less well coupled to the atmosphere because the aerodynamic conductance is lower compared to the whole forest. This means that available energy at the understory level will be more important than the air humidity for control of evaporation. Changes in climate might have different impacts on overstory and understory evaporation.

15.2.3 Drought Effects on Evaporation

Besides the meteorological drivers of evaporation, drought is the most important factor affecting the evaporation rates. However, it is not easy to compare the results from the few studies that have been made on the effect of drought on evaporation (or transpiration) from boreal forests because dependencies can be expressed in many different ways. The same holds true for the dependent variable, soil moisture. Different methods have to be applied in order to eliminate the confounding effects of the variation in all other variables affecting evaporation. In some studies, a certain threshold can be identified below which the soil moisture is affecting the evaporation and in other, no such threshold can be found. Lagergren and Lindroth (2002) found that when the relative amount of extractable water (θ_r) fell below ca. 20%, the canopy conductance of *P. sylvestris* and *P. abies* began to decrease.

Table 15.2 Understory evaporation

References	Location MAT, AnnP	Overstory sp. LAI	Understory sp. LAI	E_{umax} (mm)	E_u/E_e (period)
Lida et al. (2009)	62.25°N, 129.23°E −10.4°C, 259 mm	Larix cajanderii 1.6–2.0	Vaccinium vitis-idaea 2.1	2.0	0.55–0.57 (gr. season)
Blanken et al. (2001)	53.6°N, 106.2°W −0.2°C, 463 mm	Populus tremuloides Max 3.3	Corylus cornuta Max 2.3	3.0	0.17–0.57 (leaf period)
Wang et al. (2004)	62.85°N, 30.67°E Na, 724 mm	Pinus silvestris 2	Lichen (65% coverage)	1.1	0.29–0.36 (3 gr. seasons)
Baldocchi et al. (1997)	53.9°N, 104.68°W 0.1°C, 398 mm	Pinus banksiana 2	Arctostaphylos uvaursi/Vaccinium vitisideae/Cladina spp. (100% coverage)	0.7	0.20–0.29 (DOY 140–260)
Kelliher et al. (1997)	61°N, 128°E −9.6°C, 233 mm (Hollinger et al. 1998)	Larix gmelinii 1.5	Vaccinium/Arctostaphylos spp 1	1.1	0.38–0.5 (15–25 July)
Kelliher et al. (1998)	61°N, 89°E −3.8°C, 619 mm	Pinus sylvestris 1.5	Cladonia/Cladina spp. (65% coverage)	1.6	0.33–0.92 (8–25 July)
Ohta et al. (2001)	62.25°N, 129.62°E Na, Na	Larix gmelinii 2	Vactinium spp.	1.8	0.35 (June–Aug)
Hamada et al. (2004)	62.23°N, 129.65°E −10.2°C, 188 mm	Pinus sylvestris –	Vaccinium uva ursi 2.5	1.6	0.25–0.5 (May–Sep)
Grelle et al. (1997)	60.08°N, 17.47°E 5.5°C, 527 mm	Pinus sylvestris/Picea abies 4.5	Vaccinium myrtillus (27%)/mosses and lichens (78%) (Lagergren 2010, personal communication)	0.8	0.17 (May–Oct)

Same symbols as in Table 15.1 except; E_{umax} maximum daily evaporation from understory including soil evaporation; E_u daily evaporation from understory; E_e daily evaporation from ecosystem

Bernier et al. (2006), which also used θ_r as dependent variable, found that the evaporation of *Pinus banksiana* decreased more or less linearly with decreasing θ_r and that *Picea mariana* started to be affected already at a threshold of ca. 70%. Betts et al. (1999) found very small effects of soil moisture on evaporation in a *P. banksiana* dominated forest where the soil moisture varied between 38 and 75%. Data from Wang et al. (2004) show that the surface conductance of a *P. sylvestris* forest starts to decrease when volumetric soil moisture falls below ca. 30%. There are too few studies available to allow any definitive conclusions to be drawn about the effects of soil moisture on evaporation.

15.2.4 Interception and Interception Evaporation

There are surprisingly few studies of rain interception processes in boreal forests considering that interception evaporation can constitute a large fraction of the total evaporation. Grelle et al. (1997) found that interception was on average 23% of total evaporation in a mixed *P. sylvestris*/*P. abies* forest during the growing period. Ohta et al. (2001) found interception to be only 10% of total evaporation in a *Larix gmelinii* forest during the growing season. The reason for this difference can be found as a difference in weather conditions driving the evaporation (cf. 15.2), the precipitation distribution and intensity or it can be the difference in the water storage capacity of the canopies. It is probably the latter process that is most responsible for the difference. The *Larix* stand had less than half the LAI of the *Pinus*/*Picea* stand and, therefore, probably a much smaller interception storage capacity. Grelle et al. (1997) also estimated the saturated storage capacity of their forest and found it to average 1.5 mm based on throughfall and gross precipitation measurements. Lankreijer et al. (1999) analyzed the same data using a combination of measured throughfall and inverse modeling and found much higher saturated storage capacity, on the order of 2.5 mm.

   More studies of snow interception, evaporation and sublimation have been made. The measurement of snow interception is complicated (Lundberg and Halldin 2001). Surprisingly high evaporation/sublimation rates have been reported considering the usually low evaporative demand in winter. Lundberg and Halldin (1994) found 3.3 mm day^{-1} calculated per unit of vertically projected crown area of *P. abies* in northern Sweden, Harding and Pomeroy (1996) found up to 4.0 mm per a 36 h period in *P. banksiana* stand in Canada in northern Sweden and Grelle et al. (1997) found 1.3 mm day^{-1} in a mixed *P. sylvestris*/*P. abies* stand in central Sweden. Nakai et al. (1999) measured energy exchange over snow covered and snow free canopy over a mixed *Picea* and *Abies* stand in northern Japan and found that the latent heat flux constituted about 80% of the net radiation for snow covered conditions in strong contrast to 10% during snow free conditions. Average evaporation during their 60 days long study period was 0.6 mm day^{-1}. One possible explanation is that the snow storage capacity, expresses as snow water equivalent, can be an order of magnitude larger for snow compared to rain therefore much more water is available for

evaporation at the canopy level where the vapor transport is very efficient. Hedstrom and Pomeroy (1998) reported snow interception in the order of 6 mm for a *Picea mariana* stand and up to 9 mm for a *P. banksiana* stand in Canada. Based on the relatively few studies of both rain and snow interception, snow interception is the more important process which also is reasonable given the long boreal winter period.

15.3   Biogeochemistry

Boreal forests play a significant role in the earth's climate not only because of the direct energy effects considered above but also because of their role in biogeochemical feedbacks mediated through trace gas dynamics. The most important radiatively active gases in boreal forest dynamics, after water vapor, are CO_2, N_2O and CH_4. There are other compounds that play a role in local oxidation chemistry, e.g. VOC's, NMHC's, CO, O_3 and NO, that will affect the local scale atmospheric dynamics of greenhouse gases. We will consider CO_2, N_2O and CH_4 in this discussion. The absolute quantities of N_2O and CH_4 that are exchanged are small compared to the amount of CO_2 but their impact on climate and potential feedbacks is enhanced because of their increased efficiencies in absorbing long wavelength radiation compared to CO_2.

As discussed above, the landscape of the boreal forest biome is diverse and consists of a mixture of forests, wetlands and lakes. Most northern wetlands are peatlands but beaver ponds, a particular type of shallow open water wetland can account for up to 5–10% of the wetlands in boreal Canada (Roulet et al. 1992). A recent assessment indicates larger (0.1–50 km^2) lakes north of ~$45°$N are most abundant in glaciated permafrost peatlands and less in unglaciated permafrost free terrain (Smith et al. 2007). Even though our focus is on forests, spruce and larch biomes can occur on peatlands and lakes and wetlands can be important in the landscape or regional carbon balance of forests when carbon is exported from forested areas. Fire and drainage class or moisture availability determines the dominant growth strategy whether it is semi-arid evergreen dominated by *P. banksiana*/lichen on well drained sandy soils, deciduous humid dominated by aspen or birch broadleaf forests on mixed drainage or spruce or larch on poorly drained soils (Harden et al. 2000).

15.3.1   Components of the CO_2 Exchange in Boreal Forests: Productivity Terms

The two most important and linked chemical equations of the carbon cycle are C fixation and the subsequent oxidation of that fixed C.

$$CO_2 + H_2O + hv \Rightarrow C(H_2O) + O_2, \tag{15.3}$$

$$C(H_2O) + O_2 \Rightarrow CO_2 + H_2O + energy, \qquad (15.4)$$
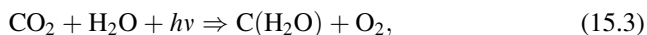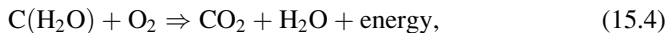
hv is the photon energy where h is Planck's constant and v is the frequency, $C(H_2O)$ is a general representation of C at a representative oxidation state for organic matter. The energy released during biological respiration is available for metabolic processes.

Terminology for the component C fluxes discussed below follow the recommendations of Chapin et al. (2006). The gross uptake of CO_2 during photosynthesis is gross primary productivity (GPP). Some of this stored chemical energy is required for the metabolic processes of the autotroph. This is autotrophic respiration (R_A). The difference is the net primary productivity (NPP):

$$GPP = NPP + R_A. \qquad (15.5)$$

GPP is directly dependent on climatic conditions and growth strategy (evergreen or deciduous). It is often a derived quantity from comparisons of direct measurements of net ecosystem exchange (NEE) (see below) during night and day. A recent analysis of 513 datasets by Luyssaert et al. (2007) allowed them to compare 96 humid and 38 semi-arid boreal sites. Mean GPP varied by a factor of 1.5 for the three boreal forest types (Table 15.3). NPP is the sum of net productivity of a number of components within the system, some more easily measured than others. Components include foliar production (fNPP), aboveground woody growth increment (wNPP), belowground root production (rNPP) and other components of NPP (oNPP) that at the ecosystem level include understory production, reproductive tissue growth, herbivory losses, direct VOC emissions and OC that is exuded from roots or transferred to mycorrhizae:

$$NPP = fNPP + wNPP + rNPP + oNPP. \qquad (15.6)$$

Table 15.3 Mean carbon fluxes, NPP components and their standard deviation for different boreal biomes

	Humid	Semi-arid	
	Evergreen	Evergreen	Deciduous
GPP	973 ± 83	773 ± 35	$1,201 \pm 23$
NPP	271 ± 17	334 ± 55	539 ± 73
fNPP	73 ± 9	47 ± 5	109 ± 11
wNPP	205 ± 28	110 ± 20	304 ± 36
rNPP	69 ± 9	157 ± 31	112 ± 22
NEP	131 ± 79	40 ± 30	$178 \pm NA$
R_E	824 ± 112	734 ± 37	$1,029 \pm NA$
R_A	489 ± 83	541 ± 35	755 ± 31
R_H	381 ± 40	247 ± 26	275 ± 31
CUE	0.36	0.38	0.42

The SD refer to the variability surrounding the mean values (from Luyssaert et al. 2007). Abbreviations are explained in the text. CUE is carbon use efficiency and is the ratio of NPP to NPP plus R_A. Values have units of g C m^{-2} $year^{-1}$ except CUE

The relative contribution of each component of net productivity is the result of specific growth strategies of different forest types in direct response to climatic conditions. Given a sufficient amount of precipitation, GPP and NPP are strongly temperature correlated between 5 and 15°C. However, boreal forests which are adapted to low mean annual temperatures <5°C and low precipitation of <800 mm year^{-1} do not appear to respond strongly to increases in mean annual temperature and precipitation (Luyssaert et al. 2007).

The C fixed into the different components of the ecosystem needs a broad range of times to remineralize or decompose, from centuries (wood) to annual to daily times for labile litter and root exudates of recent photosynthate. Woody production in boreal forests appears to exceed net ecosystem respiration (NEP) (Table 15.3) which suggests greater contribution of historical carbon to decomposition processes and a system adapted to perturbation such as fire.

15.3.2   Components of the CO_2 Exchange in Boreal Forests: Respiration Terms

Decomposition of C pools is mediated mostly by microbial processes known as heterotrophic respiration (R_H). Total ecosystem respiration (R_E) is the sum of autotrophic and heterotrophic decomposition.

$$R_E = R_H + R_A. \tag{15.7}$$

NEP is the difference between NPP and R_H. It is the difference between gross production (GPP) and the sum of respiratory processes.

$$GPP = NPP + R_A = NEP + R_A + R_H = NEP + R_E. \tag{15.8}$$

Autotrophic respiration (R_A) can be a substantial loss of the C fixed by photosynthesis and often exceeds 50% of GPP. A direct evaluation of the cost of R_A is the carbon use efficiency (CUE) of a forest. Deciduous boreal forests are more efficient in fixing C than evergreen stands (Table 15.3). Direct observations using chamber fluxes from different biomes indicate losses of 54–71% to R_A in Canadian forests (Ryan et al. 1997) that are consistent with the 58–65% from Luyssaert et al. (2007) analysis of stand level fluxes. The CUE was similar for similar species from across the range of boreal climate but differed between evergreen and deciduous species. The implication is that the strong link between R_A and production will produce offsetting responses to changing climate. If temperature increases, with enough available moisture, then R_A will increase even as GPP does.

Heterotrophic respiration (R_H) is the sum of the respiratory processes of all the heterotrophic organisms. These processes are generally operative over a broader range of time scales than R_A. R_A is controlled by amount of living biomass,

nutrients (esp. N), cellular activity and temperature (Ryan 1991). R_H is controlled by substrate quality (esp. lignin and litter N), moisture and temperature (Mellilo et al. 1982). Because of differences in controls it is important to distinguish the rates of these processes in order to properly model them. R_E is the sum of autotrophic and heterotrophic respiratory fluxes within an ecosystem and often estimated using night time eddy correlation measurements or using opaque (dark) enclosures.

15.3.3 Components of the CO_2 Exchange in Boreal Forests: Measurement Terms

CO_2 fluxes over ecosystems are now commonly measured with eddy correlation methods or, at local scales, under clear chambers during daylight. Both techniques give a measure of the NEE. NEE is a direct measure of a gross ecosystem exchange (GEE) of CO_2 and the R_E flux especially over short time scales (half hourly to decadal: Wofsy et al. 1993). The overall response of NEE of a boreal forest to weather has been shown to be described by a set of equations that describe the average forest photosynthesis to light and temperature and of the response of R_E to temperature. The small difference between large rates of GEE and R_E imply that the boreal forest would be sensitive to climate changes.

15.3.4 Components of the CO_2 Exchange in Boreal Forests: Other CO_2 Exchanges

There is a basic difference between NEE and NEP. NEP includes the production components of wood, foliage, etc. that are not captured by a simple measure of the gas flux. Chapin et al. (2006) recommend that NEP refer only to the difference between GPP and R_E. Immediate measures of CO_2 exchange, even when combined with growth increment measurements, can differ from the long term carbon balance of the system due to nonrespiratory CO_2 losses and non-CO_2 losses that includes C that is imported from or to nearby ecosystems. Non-CO_2 fluxes can occur at rapid time scales when a portion of the GPP is converted to volatile organic compounds or organic matter is photo oxidized to CO that escape to the atmosphere. Over longer time scales, some portion of GPP is used to produce CH_4 or is laterally transported as dissolved inorganic carbon (DIC) or as dissolved organic carbon (DOC) from the soil and litter.

DIC and DOC are the predominant carbon input to most lakes, followed by particulate organic carbon (POC) and particulate inorganic carbon. Tranvik et al. (2009) point out that the relative importance of the inputs varies with lake location and hydrology. In boreal forests in carbonate terrain, DIC is the dominate form of aquatic C (Finlay et al. 2009) due to high soil respiration, carbonate weathering and groundwater flow. DOC dominates in the humid tropics and in noncarbonate boreal forest (Tranvik et al. 2009).

Nonrespiratory CO_2 fluxes of accumulated NEP occur as fires, harvest loss or mobilization of POC. Chapin et al. (2006) have also defined the net ecosystem carbon balance (NECB) as the total rate of carbon gain or loss from the ecosystem to represent the overall C loss or gain from the ecosystem. It is related to NEP:

$$NECB = \partial C/\partial t = NEP + \sum (\text{non-respiratory } CO_2 \text{ fluxes}) + \sum (\text{non-}CO_2 \text{ fluxes}).$$

(15.9)

15.3.5   Components of the CO_2 Exchange in Boreal Forests: Net Balance Terms

The net components of the carbon balance (NPP, NEP, NECB) can be either sources or sinks of carbon. GPP is always a sink and in boreal forest systems ranges from 773 to 1,201 g m^{-2} year^{-1} (Luyssaert et al. 2007) which is generally less than lower latitude forests. R_E is always a source and, again, is generally lower than lower latitude forests both presumably because of lower annual temperatures and shorter growing seasons. GPP and R_E are the processes that consume or produce most of the inorganic CO_2 within an ecosystem. GPP is highly variable and the rate of which depends on more or less rapidly changing variables such as PAR, temperature and water and nutrient availability. Therefore GPP can only be maintained for short periods of time whereas NECB is the long term carbon balance of ecosystems. The balance of GPP and R_E are two of the key processes that drive NECB, and NEE often approximates NEP and NECB in many ecosystems (Baldocchi 2003). However, an important difference is that NEE measurements can rarely integrate long term effects of disturbance. For example it is very difficult to distinguish the R_H from organic material killed during the last major disturbance and microbial respiration of recently derived root and leaf litter (Harden et al. 2000)

NECB is the net accumulation or loss of C and, when integrated over time and area, it equals the net biome production (NBP; Schulze et al. 1999). NBP is a concept that is reflected in the atmospheric carbon balances and which also recognizes that small incremental accumulation of NEP in northern systems is offset by large episodic losses especially fire and insect outbreaks in boreal forests. However, NBP cannot be practically distinguished from NEP at usual scales of measurement.

15.3.6   Fire and C Exchange in Boreal Forests

Fire and harvest are the dominating disturbance factors in forests (Schulze 2006) and here we focus on fire since it is the disturbance factor which is the most important one on a global scale. The sites of most R_H or other decomposition

processes are the soil, peat and sediments. We will only consider soil processes. However, fire has an important role in how much of the NPP of boreal systems accumulates as organic C in the vast regions of boreal wetlands and forests. Most fires in North America and western Russia are crown fires (Stocks 1991) which have high intensity and severity and may be related to the large fuel loads that accumulate in the moss-rich forest floor. Between 41 and 840 Tg C is emitted by boreal forest fires every year (Harden et al. 2000). Lower amounts are emitted from fires on boreal wetlands. Spruce and larch forests on poorly drained soils are at the low end of the range and deciduous broadleaf forests on mixed drainage are the largest emitters. In their study area between 10 and 30% of the NPP is emitted as fire, 40–80% is released in decomposition and export processes and another 8–30% enters the soil carbon pool (Harden et al. 2000).

Soil drainage is susceptible to changes due to permafrost degradation (thermokarst) and aggradation which are sometimes related to the occurrence of fires. In uplands, the soils are usually drained and well aerated and do not accumulate C in the shallow layers of the soil. In mixed to humid drainage classes the soils develop deeper layers of organic carbon which plays an important role in how NPP is further decomposed. Poorly drained upland sites, which have higher C storage in moss layers owing to greater moss NPP but lower tree NPP (Harden et al. 1997), have plenty of fuel for combustion but deep C storage varies twofold according to the severity of burning. The occurrence of discontinuous permafrost, fires and thermokarst wetlands are due to the interaction of climate, fire disturbance, hydrology and ecosystem structure.

Permafrost and surface hydrology determine the trace gas dynamics of the soils. NPP is the source of nearly all the C that accumulates in these systems. It is the drainage and fire frequency that determines how C is decomposed in boreal soils. Poor drainage and colder temperatures result is a higher ratio of NEP to GPP and thus to accumulation in soils and peats.

15.3.7 CH_4 and N_2O Exchange in Boreal Forests

Soil drainage, structure and productivity of overlying biome affect trace gases from the soils of an ecosystem. In boreal soils, CH_4 emissions represent the difference between anaerobic CH_4 production and oxidation by aerobic microbes in the soil profile determined by redox conditions and transport mechanism (e.g., ebullition or plant transport; e.g., Bubier et al. 1995). The balance between production and oxidation is determined by soil temperature, depth of the aerobic zone in the soil determined by site hydrology (water table and active layer depths) and the populations of methanogens and methanotrophs.

In wetlands, soils are water saturated and organic rich, the resulting anaerobicity slows decomposition processes and allows the accumulation of peats. Boreal wetlands become strong CH_4 producers emitting up to 60% of the global wetland source (Bartlett and Harriss 1993) even though they cover only about 8% of the boreal forest area (Harden et al. 2000).

Drained upland forested sites have usually been observed to be weak sinks of atmospheric CH_4 (Crill 1991; Smith et al. 2000). There is a high degree of variability at the landscape level that is correlated to topography and water level. Moosavi and Crill (1997) observed CH_4 effluxes at all sites along a transect within a boreal forest which extended from dry upland soils to inundated wetlands near a beaver pond and an inundated site within a black spruce forest. Fluxes along this transect varied by 4 orders of magnitude with the drier sites having fluxes close to or below the detection limit. In a broader seasonal survey of CO_2 and CH_4 within the same region of central Manitoba, fluxes were measured in upland boreal forest soils. Most sites consumed atmospheric CH_4 at rates of $+0.6$ to -2.6 mg CH_4 m^{-2} day^{-1}, and emitted CO_2 at rates between 0.2 and 26.8 g CO_2 m^{-2} day^{-1}.

Savage et al. (1997) observed two distinct groups. There were sites from which both CO_2 and CH_4 exchange were strong (mean 5.2 g CO_2 m^{-2} day^{-1}, <-1.0 mg CH_4 m^{-2} day^{-1}); and those which had a weak exchange of both gases (mean 2.5 g CO_2 m^{-2} day^{-1}, -0.2 mg CH_4 m^{-2} day^{-1}). The presence of black spruce, a *Sphagnum* cover and a thick organic layer (20–50 cm) characterized the weak exchange group. These characteristics indicate colder, wetter conditions with longer path lengths to the zone of CH_4 oxidation. The strong flux group had either aspen, jack pine, or birch trees, a vascular plant cover and a thin organic layer (1–5 cm). These characteristics were indicative of warmer, drier conditions and shorter path lengths to the zone of CH_4 oxidation. This is consistent with the observations of Smith et al. (2000) that CH_4 oxidation is most rapid in coarse textured soils with well developed soil structure and a surface organic layer through which gases can readily diffuse. Diffusion characteristics of the soil structure and even transient effects such as water filling pore space can affect CH_4 uptake rates (Ball et al. 1997). Upland sites may become sources of CH_4 when soils become saturated following precipitation events (e.g., Savage et al. 1997).

CH_4 uptake rates have been observed to have only a weak response to rising temperatures (e.g., Born et al. 1990; Crill 1991). This is, in part, due to CH_4 oxidizing activity being found not at the surface of the soil column but rather at the top of the mineral layer or the base of an overlying organic layer in the soil (Crill 1991; Amaral and Knowles 1997) and the weaker temperature effect on diffusion than on biological processes. This may be due to nitrogen interactions suppressing CH_4 oxidizing activity. N additions to forested drained peatland soils from Finland inhibited CH_4 uptake (Crill et al. 1994).

N_2O is produced by both nitrification and denitrification reactions. The former, thought to be the major source of N_2O in aerobic soils (Bremner and Blackmer 1978), is associated with aerobic conditions and the latter with marginally anaerobic. Generally, boreal forest soils and peatlands are not thought to be major sources of N_2O to the atmosphere (Martikainen et al. 1993) though recent discoveries of high rates of N_2O efflux from cryoturbated permafrost soils are challenging that view (Repo et al. 2009).

Simpson et al. (1997) measured CH_4 and N_2O fluxes above an aspen stand using a tunable diode laser. Small emissions of both gases were observed, around 1.9–2.5 ng m^{-2} s^{-1} for N_2O and 21–28 ng m^{-2} s^{-1} for CH_4. The authors correlated

the above canopy measurements with below canopy chamber measurements to conclude that CH_4 emission from scattered anoxic patches in the aspen forest overwhelmed the slow rates of CH_4 uptake that occur across the larger, drier areas. This result is consistent with the discussion above. Their work shows that upland sites might be converted from net sinks to net sources by minor changes in water table; emissions from small wetland regions (e.g., "hotspots," Moosavi et al. 1996) within forested areas have been shown to overwhelm the low-level regional uptake of CH_4. Therefore establishing the contribution from small wetland areas within a mixed forest can be essential in assessing the total CH_4 budget of a given region (Simpson et al. 1997).

15.4 Future Directions

Considering the vast areas covered by boreal forests comparatively little research has been done on both hydrology and biogeochemistry of the different component eco-systems of the biome. The largest changes in climate are expected to take place at latitudes where boreal forests are located and these changes will have significant impacts on hydrology, energy exchange and biogeochemistry. Most significant effects can be expected to occur at the seasonal transition periods from winter to spring and from autumn to winter. Thawing permafrost, longer growing seasons where changing climate leads to shorter snow covered periods or, perhaps counter-intuitively, shorter growing seasons in those areas where shifting precipitation patterns lead to more and longer lasting snow cover with implication for energy exchange. Shifting patterns of temperature and precipitation will lead to changes in fire frequency and intensity and will have consequences for drought frequency/water logging. All are examples of events that have important implication for both hydrological and biogeochemical cycles and their respective feedbacks to the climate system. This, in turn, will have implications for the living conditions in these areas and on earth. These are not decoupled systems. We emphasize that future studies of these regions consider the links between hydrological, energy and biogeochemical processes.

References

Amaral JA, Knowles R (1997) Localization of methane consumption and nitrification activities in some boreal forest soils and the stability of methane consumption on storage and disturbance. J Geophys Res 102:29255–29260

Arain MA, Black TA, Barr AG et al (2003) Year-around observations of the energy and water vapour fluxes above a boreal black spruce forest. Hydrol Process 17:3581–3600

Baldocchi DD (2003) Assessing the eddy covariance technique for evaluating carbon dioxide exchange rates of ecosystems: past, present and future. Global Change Biol 9:479–492

Baldocchi DD, Vogel CA, Hall B (1997) Seasonal variation of energy and water vapour exchange above and below a boreal jack pine forest canopy. J Geophys Res 102:28939–28951

Baldocchi DD, Kelliher FM, Black TA et al (2000) Climate and vegetation controls on boreal zone energy exchange. Global Change Biol 6:69–83

Ball BC, Smith KA, Klemedtsson L et al (1997) The influence of soil gas transport properties on methane oxidation in a selection of northern European soils. J Geophys Res 102:23309–23317

Bartlett KB, Harriss RC (1993) Review and assessment of methane emissions from wetlands. Chemosphere 26:261–320

Bernier PY, Bartlett P, Black TA (2006) Drought constraints on transpiration and canopy conductance in mature aspen and jack pine stands. Agric For Meteorol 140:64–78

Betts AK, Goulden M, Wofsy S (1999) Controls on evaporation in a boreal spruce forest. J Clim 12:1601–1618

Blanken PD, Black TA, Yang PC et al (1997) Energy balance and canopy conductance of a boreal aspen forest: partitioning overstory and understory components. J Geophys Res 102:28915–28927

Blanken PD, Black TA, Neumann HH et al (2001) The seasonal water and energy exchange above and within a boreal aspen forest. J Hydrol 245:118–136

Born M, Dörr H, Levin I (1990) Methane consumption in aerated soils of the temperate zone. Tellus 42B:2–8

Breckle S-W, Walter H, Lawlor G (2002) Walter's vegetation of Earth: the ecological systems of the geo-biosphere. Springer, Berlin

Bremner JM, Blackmer AM (1978) Nitrous oxide: Emission from soils during nitrification of fertilizer nitrogen. Science 199:295–296

Bubier JL, Moore TR, Bellisario L et al (1995) Ecological controls on methane emissions from a northern peatland complex in the zone of discontinuous permafrost, Manitoba, Canada. Glob Biogeochem Cycles 9:455–470

Chapin FS, Woodwell GM, Randerson JT et al (2006) Reconciling carbon-cycling concepts, terminology and methods. Ecosystems 9:1041–1050

Crill PM (1991) Seasonal patterns of methane uptake and carbon dioxide release by a temperate woodland soil. Glob Biogeochem Cycles 5:319–334

Crill PM, Martikainen PJ, Nykänen H et al (1994) Temperature and N fertilization effects on methane oxidation in a drained peatland soil. Soil Biol Biochem 26:1331–1339

Dixon RK, Brown S, Houghton RA et al (1994) Carbon pools and flux of global forest ecosystems. Science 263:185–190

Finlay K, Leavitt P, Wissel B et al (2009) Regulation of spatial and temporal variability of carbon flux in six hard-water lakes of the northern Great Plains. Limnol Oceanogr 54:2553–2564

Grelle A, Lundberg A, Lindroth A et al (1997) Evaporation components of a boreal forest: Variations during the growing season. J Hydrol 197:70–87

Grelle A, Lindroth A, Mölder M (1999) Seasonal variation of boreal forest surface conductance and evaporation. Agric For Meteorol 98–99:563–578

Hamada S, Ohta T, Hiyama T et al (2004) Hydrometeorological behaviour of pine and larch forests in eastern Siberia. Hydrol Process 18:23–39

Harden JW, O'Neill KP, Trumbore SE et al (1997) Moss and soil contributions to the annual net carbon flux of a maturing boreal forest. J Geophys Res 102:28805–28816

Harden JW, Trumbore SE, Stocks BJ et al (2000) The role of fire in the boreal carbon budget. Global Change Biol 6:174–184

Harding RJ, Pomeroy JW (1996) The energy balance of a winter boreal landscape. J Clim 9:2778–2787

Hedstrom NR, Pomeroy JW (1998) Measurements and modeling of snow interception in the boreal forest. Hydrol Process 12:1611–1625

Hollinger DY, Kelliher FM, Schulze E-D et al (1998) Forest-atmosphere carbon dioxide exchange in eastern Siberia. Agric For Meteorol 90:291–306

Humphreys ER, Black TA, Ethier GJ et al (2003) Annual and seasonal variability of sensible and latent heat fluxes above a coastal Douglas-fir forest, British Columbia, Canada. Agric For Meteorol 115:109–125

Jarvis PG, Massheder JM, Hale SE et al (1997) Seasonal variation of carbon dioxide, water vapour, and energy exchange of a boreal black spruce forest. J Geophys Res 102:28953–28966

Kelliher FM, Hollinger DY, Schulze E-D et al (1997) Evaporation from an eastern Siberian larch forest. Agric For Meteorol 85:135–147

Kelliher FM, Lloyd J, Arneth A et al (1998) Evapotranspiration from a central Siberian pine forest. J Hydrol 205:279–296

Lagergren F, Lindroth A (2002) Transpiration response to soil moisture in pine and spruce trees in Sweden. Agric For Meteorol 112:67–85

Lankreijer H, Lundberg A, Grelle A et al (1999) Evaporation and storage of intercepted rain analysed by comparing two models applied to a boreal forest. Agric For Meteorol 98–99:595–604

Leemans R, Cramer W (1991) The IIASA database for mean monthly values of temperature, precipitation and cloudiness on a global terrestrial grid. Research Report RR-91-18, Nov 1991. International Institute of Applied Systems Analyses, Laxenburg

Lida S, Ohta T, Matsumoto K et al (2009) Evapotranspiration from understory vegetation in an eastern Siberian boreal larch forest. Agric For Meteorol 149:1129–1139

Lundberg A, Halldin S (1994) Evaporation of intercepted snow: analyses of governing factors. Water Resour Res 30:2587–2598

Lundberg A, Halldin S (2001) Snow interception evaporation: Review of measurement techniques, processes, and models. Theor Appl Climatol 70:117–133

Luyssaert S, Inglima I, Jung M et al (2007) CO_2 balance of boreal, temperate, and tropical forests derived from a global database. Global Change Biol 13:2509–2537

Martikainen PJ, Nykänen H, Crill P et al (1993) Effect of a lowered water table on nitrous oxide fluxes from northern peatlands. Nature 366:51–53

Matsumoto K, Ohta T, Nakai T et al (2008) Energy consumption and evapotranspiration at several boreal and temperate forests in the Far East. Agric For Meteorol 148:1978–1989

McGuire AD, Wirth C, Apps M et al (2002) Environmental variation, vegetation distribution, carbon dynamics and water/energy exchange at high latitudes. J Veg Sci 13:301–314

McNaughton KG, Jarvis PG (1983) Predicting effects of vegetation changes on transpiration and evaporation. In: Kozlowski TT (ed) Water deficits and plant growth, vol 5. Academic Press, New York, pp 1–47

Mellilo JM, Aber JD, Muratore JF (1982) Nitrogen and lignin control of hardwood leaf litter decomposition dynamics. Ecology 63:621–626

Moosavi SC, Crill PM (1997) Controls on CH_4 and CO_2 emissions along two moisture gradients in the Canadian boreal zone. J Geophys Res 102:29261–29277

Moosavi SC, Crill PM, Pullman ER et al (1996) Control of CH_4 flux from an Alaska boreal wetland. Glob Biogeochem Cycles 10:287–296

Nakai Y, Sakamoto T, Terajima T et al (1999) Energy balance above a boreal coniferous forest: a difference in turbulent fluxes between snow-covered and snow-free canopies. Hydrol Process 13:515–529

Ohta T, Hiyama T, Tanaka H et al (2001) Seasonal variation in the energy and water exchanges above and below a larch forest in eastern Siberia. Hydrol Process 15:1459–1476

Pejam MR, Arain MA, McCaughey JH (2006) Energy and water vapour exchanges over a mixedwood boreal forest in Ontario, Canada. Hydrol Process 20:3709–3724

Rannik Ü, Altimir N, Raittila J et al (2002) Fluxes of carbon dioxide and water vapour over a Scots pine forest and clearing. Agric For Meteorol 111:187–202

Repo ME, Susiluoto S, Lind SE et al (2009) Large N_2O emissions from cryoturbated peat soil in tundra. Nat Geosci. doi:doi: 10.1038/NGEO434

Roulet NT, Ash R, Moore TR (1992) Low boreal wetlands as a source of atmospheric methane. J Geophys Res 97:3739–3749

Ryan MG (1991) The effect of climate change on plant respiration. Ecol Appl 1:157–167

Ryan MG, Lavigne MB, Gower ST (1997) Annual cost of autotrophic respiration in boreal forest ecosystems in relation to species and climate. J Geophys Res 102:28871–28883

Savage K, Moore TR, Crill PM (1997) Methane and carbon dioxide exchanges between the atmosphere and northern boreal forest soils. J Geophys Res 102:29279–29287

Schulze E-D (2006) Biological control of the terrestrial carbon sink. Biogeosciences 3:147–166

Schulze E-D, Lloyd J, Kelliher FM et al (1999) Productivity of forests in the Eurosiberian boreal region and their potential to act as a carbon sink – a synthesis. Global Change Biol 5:703–722

Simpson IJ, Edwards GC, Thurtell GW et al (1997) Micrometeorological measurements of methane and nitrous oxide exchange above a boreal forest. J Geophys Res 102:29331–29341

Smith KA, Dobbie KE, Ball BC et al (2000) Oxidation of atmospheric methane in Northern European soils, comparison with other ecosystems, and uncertainties in the global terrestrial sink. Global Change Biol 6:791–803

Smith LC, Sheng Y, MacDonald GM (2007) A first pan-arctic assessment of the influence of glaciation, permafrost, topography and peatlands on northern hemisphere lake distribution. Permafrost Periglac Process 18:201–208

Stocks BJ (1991) The extent and impact of forest fires in northern circumpolar countries. In: Levine J (ed) Global biomass burning. MIT Press, Cambridge, pp 197–202

Tarnocai C, Canadell JG, Schuur EAG et al (2009) Soil organic carbon pools in the northern circumpolar permafrost region. Glob Biogeochem Cycles 23:GB2023. doi:10.1029/2008GB003327

Tranvik LJ, Downing JA, Cotner JB et al (2009) Lakes and reservoirs as regulators of carbon cycling and climate. Limnol Oceanogr 54:2298–2314

Wang K-Y, Kellomäki S, Zha T et al (2004) Seasonal variation in energy and water fluxes in a pine forest: an analysis based on eddy covariance and an integrated model. Ecol Model 179:259–279

Wofsy SC, Goulden ML, Munger JW et al (1993) Net exchange of CO_2 in a mid latitude forest. Science 260:1314–1316

Chapter 16
Biogeochemistry of Urban Forests

Panagiotis Michopoulos

16.1   Introduction

Green spaces are beneficial to inhabitants of cities, providing a pleasant reprieve from masonry, concrete, and asphalt that comprise much of the urban landscape. Urban trees remove large amounts of air pollutants and consequently improve urban air quality. They also provide a variety of other values and services, including energy savings, esthetics, health benefits, habitat for birds and other wildlife, and recreation enhancement. Nowadays trees are recognized as an important component of urban landscapes. These factors are reflected in higher real estate prices, lower energy bills, and greater attraction to tourists and businesses (Zhu and Zhang 2008) in area with urban trees.

In temperate regions of the world, it is likely that 60–80% of a city's area supports enough trees to meet conventional definitions of "forest" (Rowntree 1984). If urban forests proved to be so valuable, how could man preserve them? In managed natural forests, the science of ecology provides the answers based on the concept of sustainability. But can the ecology of a natural forest be applied to urban forests? The answer is not simple. Both types of forests share common attributes such as sufficient areal extent and biomass. They both exert influence on climate and water regime to a large or small extent and can be both managed albeit for different purposes. Their origin is different, however. Natural forests have evolved through adaptation and natural selection, whereas urban forests are heavily influenced by man. The urban forest is a mosaic of trees and other vegetation, some of which are managed intensively by different agencies or people, and others (Zipperer et al. 1997). Trees can be removed or replanted. An abandoned urban area can be reforested if the authorities decide to do so. Some common features must exist so that the science of ecology can be applied.

The central concept of ecology is that of the ecosystem. According to Kimmins (1996), the ecosystem concept has five major attributes: structure, function, complexion, interaction, and temporal change. An urban forest the structure of which is not interrupted by man (uprooting, replanting) will sooner or later come to equilibrium with its environment and develop ecosystem attributes. Still some differences exist between urban and natural forests. For example, natural disasters such as fires and wind uprootings are not so common in urban forests. In contrast, human influences such as pollution and degraded soils adversely affect urban forests. Coincidentally, air pollution also

threatens natural forests but urban forests are very close to pollution sources. In order to find out the future course of an urban forest, in other words the temporal change, forest science researchers must start monitoring activities. During the past decades, natural forests have been monitored because of the transboundary air pollution threats materialized in acid rain, nitrogen saturation, and recently the greenhouse effect. A question that arises is what is to be monitored when determining quantitative value of natural vs. urban forest? One approach is to consider entire ecological systems as single interacting units instead of limiting studies to only a few components of the system (Likens and Bormann 1995). In this respect, the exchange of matter and energy within an ecosystem and between ecosystems is measurable. The paths of matter and energy exchange are the biogeochemical cycles. By monitoring the biogeochemical cycles of an urban forest and comparing these cycles with those of a natural forest, some conclusions can be drawn on the course of an urban forest ecosystem.

16.1.1   How to Study the Biogeochemistry of Urban Forests?

Very often old natural forests are surrounded by the urban environment. Such forests are called embedded forests. Groffman et al. (2006) suggested that these forests are a useful venue for investigating the effects of multiple factors such as climate change and altered disturbance regimes. Some researchers have compared the biogeochemistry of adjacent rural and urban forests along a transect (McDonnel and Pickett 1990). Kaye et al. (2006) argued that existing biogeochemical models, developed primarily in unmanaged ecosystems, work poorly in urban ecosystems because they do not include human biogeochemical controls, such as impervious surface proliferation, landscape choices, and human demographic trends. Before we draw conclusions on the best method of studying urban forests, it would be useful to review the knowledge on urban forest biogeochemical cycles. In this review we will follow the classical methods used in rural forests, so nutrient inputs and outputs will be taken into account. Inputs contain the fluxes of nutrients through precipitation and nutrients released through weathering. The outputs refer to nutrient losses due to two causes, through the soil solution beyond the rooting depth and through the removal of biomass. The nutrient cycling within an urban forest will be examined using the following equations derived from Cole and Rapp (1981):

1. Nutrient uptake = annual element increment associated with bole and branch wood plus annual loss through litterfall, leaf wash, and stemflow.
2. Nutrient requirement = annual elemental increment associated with bole and branch wood plus the current foliage production.
3. Recycling = requirement minus uptake.

The water path is essential for transferring nutrients to forest floors and exporting nutrients from a forest. Soil moisture also is essential to forest site productivity. Thus, a brief introduction of urban forest hydrology is included below to contextualize the biogeochemistry of urban forests.

16.1.2   Brief Overview of Urban Forest Hydrology

One of the intensive problems of urban catchments is the runoff generated, especially by intense rainfall. This problem is exacerbated by the compacted soils in urban areas. A lot of urban forests have very compacted soils. This situation has resulted from the removal of vegetation and the erosion that followed. Sometimes trees are plentiful but the soil lacks the protective forest floor. Berthier et al. (2004) found that soil contributed 14% of the total runoff per event of rainfall in a small urban catchment. The interception of precipitation by urban vegetation plays an important role in moderating surface runoff. Sanders (1986) found that tree canopy cover in an urban area lowered the potential runoff resulted from an intensive storm by 12%. If the storm was gentle, runoff was reduced even further. Due to anthropogenic conditions in urban zones, rainfall patterns have been modified by global climatic change, urban development, as well as by the greater variation in vegetation and atmospheric conditions that exist in nature (Shepherd 2006). The rainfall interception capacity of an urban forest is strongly influenced by forest structure (species, dimensions, and stocking levels), tree architecture (foliation period, leaf and surface areas, gap fraction, surface detention storage capacity), and meteorological factors (Xiao et al. 2000). Xiao and McPherson (2002) developed a model to simulate rainfall interception processes in urban parks of Santa Monica, California. Their model was based on summing up the individual trees water storing capacity. The logic was that urban trees are open-grown and isolated. A major characteristic of urban forests is the mixture of various species some of which are invasive. Huber and Irume (2001) determined interception losses in a wide range of rainfall zones, forest types, species ages, and densities in Chile. They found that age increases interception losses in conifers due to the horizontal spreading of branches, which in turn decreases stemflow. They also concluded that the final effect of the replacement of native species by exotic ones upon water yield does not only depend on interception losses but also on transpiration and other evaporation losses. Thus, the hydrological properties of the candidate for planting species have to be taken into account.

16.2   Inputs and Losses of Nutrients in Urban Forests

16.2.1   Precipitation Inputs

The geochemical inputs in an urban forest are intimately associated with dry deposition pertaining to the urban environment. The dry deposition consists of gases and particulate matter. Gaseous deposition originates from various sources. Sulfur dioxide is a primary product of the combustion of sulfur containing fossil fuels, whereas nitrogen oxides are by-products of combustion resulted from the thermally induced combination of atmospheric nitrogen and oxygen. The burning of fuels also gives rise to a series of hydrocarbon gases, carbon monoxides, sulfur dioxide, and nitrogen oxides (Fitter and Hay 1987). The inorganic particulates are

salts of sulfates, nitrates, and chlorides. Anatolaki and Tsitouridou (2007) studied the dry to wet deposition fluxes ratio of particulate nitrates, sulfates, and chlorides in the city of Thessaloniki in Greece. They found that the contribution of dry deposition to the total (wet + dry) was at the level of 60–70% for sulfur and nitrogen, whereas for chloride it was 35%. In the urban atmosphere, ammonium forms salts of nitrates and sulfates in aerosols, whereas nitrates can also combine with sodium and calcium (Michopoulos et al. 2004; Anatolaki and Tsitouridou 2007). One would expect that the presence of acid anions would lower the pH of precipitation above a city. However, this is not always so. The suspension of carbonate salts in the atmosphere strongly influences the precipitation pH. Lee (1993) found that the $CaCO_3$ particles were responsible for special variability of the rain pH in the area of Manchester, UK. When the alkaline particles are removed through the process of wash off, the rain pH can have low values.

Research was done with regard to the organic nature of particulates in cities. In the town of Aveiro, Portugal, the organic composition of air particulate matter was identified as alkanes, polycyclic aromatic hydrocarbons, ketones, aldehydes, alcohols, and fatty acids (Alves et al. 1999). The importance of these compounds to the biogeochemistry of the essential nutrients is not clear. The availability of carbon or nitrogen in these compounds to soil microorganisms is probably an important criterion.

Wet deposition can also be significant in an urban environment. The major mechanism for wet deposition is the formation of cloud condensation nuclei. Sulfur and nitrogen containing aerosols take part in the production of cloud water droplets as they form a dominant fraction of the particles suitable for condensation of water vapor (Fowler 1980). This fact can be important to cities where precipitation is high. Since the cloud condensation nuclei pathway dominates wet removal, the more rain that falls the more sulfur and nitrogen are deposited.

The throughfall chemistry of an urban forest mostly reflects the difference between urban and rural environments. Tree foliage is a very good collector of dry deposition and, for this reason, foliar rinsing is often used to analyze and measure dry deposition (Hanson and Linberg 1991). It must be pointed out that not the whole quantity of dry deposition in precipitation ends up as throughfall. A large proportion of gases are absorbed by the stomata in leaf surfaces. The gases must be dissolved in water films surrounding foliage and then washed off in order to reach the forest floor. Particulates with a diameter exceeding 1.0 μm can penetrate the thin air layer (laminar boundary layer) encircling tree needles or leaves and be trapped by foliage. Later they are washed off with rain water. The atmosphere of a city contains particulates of various diameters. Salts of base soil cations are suspended in the air due to building activities, road trafficking, and other works. In remote forests, the traveling of small particulates (<0.1 μm diameter) is more important (Fowler 1980). The deposition of base cations in urban areas can become very important to semiarid environments with carbon and nutrient poor soils (Lohse et al. 2008).

A main attribute of throughfall fluxes in urban forest is the high ion enrichment measured by the ratio of ion concentrations in throughfall and bulk deposition. This ratio is higher than that in remote forests. This fact is exclusively due to dry deposition. Michopoulos et al. (2007a) compared the enrichment ratios of some

Table 16.1 Elemental throughfall fluxes (kg ha^{-1} year^{-1}) in remote and urban forests

Forest type	Ca	Mg	K	NH$_4$-N	NO$_3$-N	SO$_4$-S
Remote fir forest (central Greece)[a]	34.8	6.30	68	4.9	2.6	27
Urban pine forest (Athens, Greece)[a]	63.9	6.72	24.4	10.0	9.18	30.5
Remote forest (Brazil)[b]	12	6.4	115	5.5	2.04	10.1
Urban forest (Sao Paolo, Brazil)[b]	16.8	5.34	48.9	9.7	10.7	19.6
					Inorganic N	SO$_4$-S
Remote forest (Japan)[c, d]					3.3	1.8
Urban forest (Gokurakuji, Japan)[c]					8.4	2.8

[a] Michopoulos et al. (2007a, b)
[b] Forti et al. (2007)
[c] Chiwa et al. (2003)
[d] Dry deposition only

elements in throughfall for an urban, a suburban, and a remote forest. They found significant higher values for ammonium and nitrate in the urban and suburban forests. The amount of water in bulk deposition and throughfall in urban areas is usually lower than those in remote forests. So, despite the high concentrations of solutes in bulk and throughfall deposition in urban forests, remote forests compensate for this with high solute fluxes. When, however, the rain amount in urban areas is high the amounts of elements transferred to the forest floor are also high. In an urban pine forest in Athens, Greece, the usual amount of rain is 400 mm/year. In terms of nutrient inputs to an urban ecosystem, the total deposition of nutrients is the most important. However, it is not easy to calculate this parameter for all elements. Apart from sulfate for which leaching from leaf surfaces is very small (Lindberg et al. 1986) the other solutes are subjected to both wash off and leaching. For this reason, researchers have developed models to distinguish fluxes of base cations due to dry deposition and leaching (Bredemeier 1988). In any case throughfall is considered to be a measure of dry deposition.

Some researchers have compared elemental deposition fluxes of urban forest with natural forests in the same country. Table 16.1 contains three cases of this comparison for throughfall deposition.

16.2.2   Inputs Due to Weathering

Kolka et al. (1996) made an excellent review on the methods applied to measure weathering rates in forest soils. So far none of them has been applied to urban forests. If some methods are to be applied the peculiarities of urban forest, key differences between natural and urban forests should be taken into account. Some urban soils are compacted, others have human made profiles. In general, laboratory methods are not very suitable because the actual weathering rates depend on ecosystem type, climate, and parent material. Mathematical models using soil physical and chemical properties as well as climatic and plant properties can be

tried. Such a model, PROFILE, was developed by Warfvinge and Sverdrup (1992). The results can be compared with those derived from input–output balance studies adapted to forest stand rather to watershed scale.

16.2.3 Nutrient Losses in Soil Solution

There is no data in literature with regard to nutrient losses in soil solution. In order to have the nutrient output, zero tension lysimeters must be installed at rooting depth. This is not always easy especially for urban soils which are often stony and compacted. If lysimeters cannot be installed soil sampling has to take place and soil solution can be extracted either with centrifuging or saturation paste. Then chemical analysis can be done. The volume of water lost from the rooting zone can be calculated from models if soil physical properties are measured.

For intensively managed forests throughout Europe, in a variety of settings, Salm et al. (2007) used a model based on Darcy's law to calculate hydrological fluxes for 245 forest plots. Mean leachate fluxes were found to be 150 mm year^{-1} (Salm et al. 2007).

16.2.4 Nutrient Losses Due to Harvesting

There is not intensive harvesting in urban forests. However, some removal of biomass does take place. Old trees are often cut down. Windstorms can uproot trees. Whether such biomass removals affect an urban ecosystem status depends on the nutrient replenishment through precipitation and weathering (Dyck and Bow 1992). Tree uprooting can cause not only reduction of site productivity but also change of water infiltration rates. This means that biogeochemical cycles change and therefore monitoring is essential to document these changes.

16.3 Nutrient Cycling Within an Urban Forest

16.3.1 Litterfall

There is little information on litterfall fluxes in urban forests. Michopoulos et al. (2007b) calculated the litterfall flux in an urban Aleppo pine forest in the city of Athens in Greece. It was found 3.8 Mg ha^{-1} year^{-1}. This flux is considered lower than those of rural pine stands in respective climates. According to Kimmins (1996), forest litterfall is generally higher in fertile sites. The soil in that area of Athens is shallow and therefore fertility is low. However, the authors found that the

understory vegetation proved valuable in enriching the inorganic soil with N, K, and P. Groffman et al. (2006) also found that litterfall productivity in urban and rural forests of oak and tulip poplar in the Baltimore area varied more with soil type than proximity to urban land use. The urban sites of low soil fertility had approximately the same litterfall production with the low fertility sites of rural forests ($4.7 \text{ Mg ha}^{-1} \text{ year}^{-1}$).

Unfortunately, in many cases urban forest soils are degraded. Compacted soils do not allow the products of litterfall decomposition to mingle with inorganic soil material. These soils are also a barrier to ground vegetation which forms a valuable source of litterfall. In some urban forests, litterfall is collected and discarded. Gradually, tree condition deteriorates as soil is deprived from nutrients.

The removal of trees in an urban forest can affect litterfall production. The information is derived from rural forests since such research has never been conducted for urban forests. Hence, litterfall reduction has been reported in pine forests with different thinning types (Harrington and Edwards 1999).

Water availability generally increases litterfall production as it promotes soil fertility. However, this is not always the case. Ogaya and Peñuelas (2006) found that under drought stress, holm oak in northeast Spain decreased litterfall production, whereas *Phillyrea latifolia* increased it. So each species has its own tactics to cope with adverse conditions.

Another aspect for which there is no information at all is the production of the so-called below ground litterfall. Kimmins (1996) quoted data for some rural forests concerning the fine root litterfall production. The fine root litterfall can be double or four times greater than the above ground litterfall. Fluctuations in the fine root production can serve as an indicator of stress. According to Vogt et al. (1993) the fine root production responds to environmental perturbation faster than the aboveground biomass. As the measurement of that kind of litter involves destructive sampling and laborious work in permanent experimental plots, researchers are reluctant or do not acquire the necessary funding to do it. However, if such information does not exist, the real nutrient take up cannot be calculated.

16.3.2 Litter Decomposition

Litter decomposition integrates the effects of resource quality, environmental factors, and activities of decomposer organisms on nutrient cycling, thereby serving as an easily measured indicator of the impact of urbanization on an important ecosystem function. When comparing litter decomposition rates in urban and rural forest the usual hypothesis is that the rural forest will have higher rates. This holds true for some studies. Pavao-Zuckerman and Colemman (2005) found that decomposition rates for reference litter at urban sites were slower than those of litter placed in rural environment around the area of Asheville. Soil moisture, soil organic matter, and soil C/N ratio played a crucial role. Also reductions in fungal dominance in the soil food web have been hypothesized to decrease decomposition

rates in urban soils (Pouyat et al. 1994). However, this is not always the case. Much research on forest ecological functions was carried out on rural-to-urban gradients on a 140-km transect running from highly urbanized New York to rural areas of Connecticut (McDonnel and Pickett 1990; Zhu and Carreiro 2004). Contrary to expectations, results revealed that decomposition rates were higher in forests at the urban end of the transect (Pouyat et al. 1997). This effect was largely driven by the presence of large numbers of earthworms that stimulated decomposition and N cycling despite lower litter quality in the urban sites. Steinberg et al. (1997) attributed the abundance of earthworms in urban forests to the introduction of peregrine species of earthworms. Through the introduction of European and Asian plants and soils to New York, the exotic earthworm population proliferated in gardens and soon migrated to urban forests (Gates 1976).

It is not always the earthworm's activity that brings about decomposition. Very often urban soils have high concentrations of heavy metals. Tyler et al. (1989) reported that a Pb concentration of 36 mg kg^{-1} adversely affects soil invertebrates. Cotrufo et al. (1995) found that high concentrations of heavy metals in the city of Naples slowed down decomposition rates of leaves. A factor that accelerates litter decomposition in urban forests is the higher temperature with respect to rural forests. Michopoulos et al. (2005) did not find any visible trace of earthworm activity in the soil of an urban Aleppo pine stand which had an average Pb concentration of 92 mg kg^{-1} in the forest floor and 82 mg kg^{-1} in the A horizon. Still decomposition was intense as the forest floor layer was very thin. The climatic conditions of the Mediterranean area are ideal for litter decomposition. Cole and Rapp (1981) also found that among a lot of forest types the Mediterranean forest litter had the highest decomposition rates.

Intense air pollution in industrial areas can slow down decomposition as was found by Singh et al. (2004) in a tropical deciduous forest in India. However, high fluxes of N deposition in cities can accelerate litter decomposition rates by narrowing the ratio of C/N by increasing N uptake in leaves (Vestgarden 2001). This can be important to urban forests which have low litter quality.

16.3.3 Mineralization of Nutrients in Forest Floors and Soils of Urban Forests

Of all elements, N has been studied most. White and McDonnel (1988) compared N mineralization in an urban forest in the city of New York with that in a rural forest 117 km north of New York. They found that the net mineralization rates in forest floor and A horizon samples from a hemlock stand within the urban forest were 81% and 53% lower than respective samples from a comparable rural stand. They argued that hydrocarbons, trampling, and heavy metals may have a synergistic effect to reduce net N mineralization rates. In the New York to Connecticut transect, Steinberg et al. (1997) found that earthworm activity played a crucial

Table 16.2 Nutrient residence times (years) in forest floors for three types of forests

Forest type	N	K	Ca	Mg	P
Temperate coniferous[a]	17.9	2.2	5.9	12.9	15.3
Temperate deciduous[a]	5.5	1.3	3.0	3.4	5.8
Urban pine forest, Greece[b]	6.7	2.1	17.4	13.8	8.5

[a] Cole and Rapp (1981)
[b] Michopoulos et al. (2007b)

role in N mineralization and nitrification. The rural forest with earthworm activity had significant higher values of N mineralization than the urban forest also with earthworm activity, but surprisingly nitrification rates were high in the urban forest given the relatively low litter quality and rates of N mineralization rates. They suggested that in urban soils earthworms may be altering competitive interactions for NH_4^+ by creating microsites in soil where plant and heterotrophic microbial demand for NH_4^+ is low. The other suggestion was the existence of high population of nitrifying bacteria in urban soils due to N deposition. In the same transect, Baxter et al. (2002) did not find any significant difference between urban and rural forests with regard to net N mineralization rates but they found a fivefold increase in net nitrification in urban compared to rural soils. This subject needs further research.

Another method connected with nutrient mineralization rates is the finding of the mean residence time of nutrients in forest floors. This method was first used by Gosz et al. (1976) for the Hubbard Brook forest. Michopoulos et al. (2007b) applied this method for an urban pine forest in Athens. According to this method, the mean residence time for an element in a forest floor is equal to H/L, where H is the amount of an element in the forest floor and L is the input of the element. The input is the litterfall and the throughfall deposition.

Table 16.2 shows some nutrient residence times for three types of forests. In comparison with the temperate coniferous forest, the urban forest in Athens (also coniferous) had significantly lower residence times for N and P, the two elements related with organic matter decomposition. It is obvious that the Mediterranean climate plays a decisive role in mineralization rates. The temperate deciduous forest had the lowest times for these elements, an indication of the labile nature of deciduous litter. The base cations in the urban forest had the longest residence times because of the type of soil parent material (calcareous schist) in that forest. The presupposition to apply this equation is the steady state of the forest ecosystems so young forest stands should be dealt with reservation.

16.3.4 Nutrient Storage in Urban Forest Biomass

Unfortunately, there is little data on nutrient storage in the various components of urban forests. The biomass of tree trunks has to be found in consecutive years so that increments can be calculated. The question that arises is if the equations of rural

Table 16.3 Amounts of some nutrients (kg ha^{-1}) in the soil of an urban forest in Athens, Greece

Soil layer	Ca	Mg	K	N	P
Forest floor	2,502	163	128	497	35.3
Mineral soil	166×10^3	10.7×10^3	10.1×10^3	1,700	724

forests can be used in urban forests. McHale et al. (2009) made a review on the urban forest biomass estimates. They found that when comparing biomass estimates between cities the differences were a function of variability rather than urban forest structure and function. Since variability was so great (60%), it is important to construct special allometric equations for urban forests.

Foliage is another storage component. Current foliage is used to calculate nutrient requirement according to the equations of Cole and Rapp (1981). In order to have the amount of nutrients in foliage, two things are required: nutrient concentrations and foliage biomass. Foliage biomass can be calculated from leaf area of litterfall and the mass of a certain amount of leaves in the dormant period. For deciduous species this is easy to accomplish. For evergreen species, however, the litterfall consists of old leaves which cannot represent the total current leaf production. Models can be developed to relate tree heights and diameters with current year leaf production.

16.3.5 *Nutrient Storage in Soils of Urban Forests*

The nutrient amounts in soils must also be calculated. This is especially important for N and C. Michopoulos et al. (2007b) calculated the amounts of elements in an urban Aleppo pine forest soil in Athens, Greece (Table 16.3). They found that due to the shallow soil of the forest the elements amounts were much less than those reported in literature. Shallow soils are frequent among urban forests so the vegetation biomass is an important factor in the total ecosystem biomass.

16.4 Conclusions and Future Directions

After reviewing the literature on urban forest biogeochemistry, the following conclusions can be drawn and suggestions made for future research:

1. In literature there is information on bulk and throughfall deposition fluxes, litter decomposition, and N mineralization rates. All other information with regard to element dynamics is sparse or missing. Thus, further work needs to be conducted on elemental flux of urban forests.
2. As is the case of rural forests, the estimation of belowground litterfall is necessary in order to assess real values of nutrient take-up. There is some data for rural forests but none for urban ones.

3. Hydrological data concerning water percolation rates do not exist and therefore nutrient fluxes in soil solution cannot be calculated. This is particularly important for the compacted urban forest soils.

4. Weathering rates have to be calculated through models and verified with input–output balance equations. So far no such calculations exist for urban forests.

5. Successive estimations of tree biomass at regular intervals are necessary in order to calculate growth increments in urban forests. In this way, the effects of urban environment on tree biomass will be made evident in time. Foliage biomass must also be estimated to draw conclusions on nutrient requirements.

6. The comparisons of urban and rural forests have the advantage of acquiring results in short time. However, the comparison is often made between forests of different soil fertility, which may mask the effects of urban environment. Experimental plots should be established in urban forests for long-term monitoring with regard to biogeochemistry. Forests with compacted soils must be included in these plots.

References

Alves C, Pio C, Duarte A (1999) The organic composition of air particulate matter from rural and urban Portuguese area. Phys Chem Earth B 6:705–709

Anatolaki C, Tsitouridou R (2007) Atmospheric deposition of nitrogen, sulphur and chloride in Thessaloniki, Greece. Atmos Res 85:413–428

Baxter J, Pickett STA, Dighton J et al (2002) Nitrogen and phosphorus availability in oak forest stands exposed to contrasting anthropogenic impacts. Soil Biol Biochem 34:623–633

Berthier E, Andrieu H, Creutin JD (2004) The role of soil in the generation of urban runoff: development and evaluation of a 2D model. J Hydrol 299:252–266

Bredemeier M (1988) Forest canopy transformation of atmospheric deposition. Water Air Soil Pollut 40:121–138

Chiwa M, Oshiro N, Miyake T et al (2003) Dry deposition wash off and dew on the surfaces of pine foliage on the urban- and mountain-facing sides of Mt. Gokurakuji, western Japan. Atmos Environ 37:327–337

Cole DW, Rapp M (1981) Elemental cycling in forest ecosystems. In: Reichle DE (ed) Dynamic properties of forest ecosystems. Cambridge University Press, London, pp 381–409

Cotrufo MF, De Santo AV, Alfani A et al (1995) Effects of urban heavy metal pollution on organic matter decomposition in *Quercus ilex* L. woods. Environ Pollut 89:81–87

Dyck WJ, Bow CA (1992) Environmental impacts of harvesting. Biomass Bioenergy 2:173–191

Fitter AH, Hay RKM (1987) Environmental physiology of plants. Academic Press, New York

Forti MC, Bourotte C, Cicco V et al (2007) Fluxes of solutes in two catchments with contrasting deposition loads in Atlantic Forest (Serra do Mar /SP-Brazil). Appl Geochem 22:1149–1156

Fowler D (1980) Removal of sulphur and nitrogen compounds from the atmosphere in rain and by dry deposition. In: Drabløs D, Tollan A (eds) Ecological impact of acid precipitation. SNSF Project, Oslo, pp 22–32

Gates GE (1976) More on oligochaete distribution in North America. Megadrilogica 2:1–8

Gosz JR, Likens GE, Bormann FH (1976) Organic matter and nutrient dynamics of the forest and forest floor in the Hubbard Brook forest. Oecologia 22:305–320

Groffman PM, Pouyat RV, Cadenasso ML et al (2006) Land use context and natural soil controls on plant community composition and soil nitrogen and carbon dynamics in urban and rural forests. For Ecol Manage 236:177–192

Hanson PJ, Linberg SE (1991) Dry deposition of reactive nitrogen compounds. Atmos Environ 25A:1615–1634

Harrington TB, Edwards MB (1999) Understory vegetation, resource availability, and litterfall responses to pine thinning and woody vegetation control in longleaf pine plantation. Can J For Res 29:1055–1064

Huber A, Irume A (2001) Variability of annual rainfall partitioning for different sites and forest covers in Chile. J Hydrol 248:78–92

Kaye JP, Groffman PM, Grimm NB et al (2006) A distinct urban biogeochemistry? Trends Ecol Evol 21:192–199

Kimmins JP (1996) Forest ecology. A foundation for sustainable management. Prentice-Hall, New Jersey

Kolka RK, Grigal DF, Natter EA (1996) Forest soil mineral weathering rates: use of multiple approaches. Geoderma 73:1–21

Lee DS (1993) Spatial variability of urban precipitation chemistry and deposition: statistical associations between constituents and potential removal processes of precursor species. Atmos Environ 27B:321–337

Likens GE, Bormann FH (1995) Biogeochemistry of a forested ecosystem, 2nd edn. Springer, New York

Lindberg SE, Lovett GM, Richter DD et al (1986) Atmospheric deposition and canopy interactions for conifer of major ions in a forest. Science 231:141–145

Lohse KA, Hope D, Sponseller R et al (2008) Atmospheric deposition of carbon and nutrients across an arid metropolitan area. Sci Tot Environ 402:95–105

McDonnel MJ, Pickett STA (1990) The study of ecosystem structure and function along urban-rural gradients: an unexploited opportunity for ecology. Ecology 71:1231–1237

McHale MR, Burke IC, Lefscy MA et al (2009) Urban forest biomass estimates: is it important to use allometric relationships developed specifically for urban trees? Urban Ecosyst 12:95–113

Michopoulos P, Baloutsos G, Economou A et al (2004) Effects of nitrogen deposition on nitrogen cycling in an Aleppo pine stand in Athens, Greece. Sci Tot Environ 323:211–218

Michopoulos P, Baloutsos G, Economou A et al (2005) Biogeochemistry of lead in an urban forest in Athens, Greece. Biogeochemistry 73:345–357

Michopoulos P, Baloutsos G, Economou A et al (2007a) Bulk and throughfall deposition chemistry in three different forest ecosystems. Fres Environ Bulletin 16:91–98

Michopoulos P, Baloutsos G, Economou A et al (2007b) Nutrient cycling and foliar status in an urban pine forest in Athens, Greece. Plant Soil 294:31–39

Ogaya R, Peñuelas J (2006) Contrasting foliar responses to drought in *Quercus ilex* and *Phillyrea latifolia*. Biol Plantar 50:373–382

Pavao-Zuckerman MA, Colemann DC (2005) Decomposition of chestnut oak (*Quercus prinus*) leaves and nitrogen mineralization in an urban environment. Biol Fertil Soils 41:343–349

Pouyat RV, Parmelee RW, Carreiro MM (1994) Environmental effects of forest soil-invertebrate and fungal densities in oak stands along an urban-rural land use gradient. Pedobiologia 38:385–399

Pouyat RV, McDonnell MJ, Pickett STA (1997) Litter decomposition and nitrogen mineralization in oak stands along an urban-rural land use gradient. Urban Ecosyst 1:117–131

Rowntree RA (1984) Ecology of the urban forest – introduction to Part I. Urban Ecol 8:1–11

Salm C, Reinds GJ, de Vries W (2007) Water balances in intensively monitored forest ecosystems in Europe. Environ Pollut 148:201–212

Sanders RA (1986) Urban vegetation impacts on the hydrology of Dayton, Ohio. Urban Ecol 9:361–376

Shepherd JM (2006) Evidence of urban-induced precipitation variability in arid climate. J Arid Environ 67:607–628

Singh RK, Dutta RK, Agrawal M (2004) Litter decomposition and nutrient release in relation to atmospheric deposition of S and N in a dry tropical region. Pedobiologia 48:305–311

Steinberg DA, Pouyat RV, Parmelee RW et al (1997) Earthworm abundance and nitrogen mineralization rates along an urban-rural land use gradient. Soil Biol Biochem 29:427–430

Tyler G, Påhlsson MB, Bengstsson G et al (1989) Heavy metal ecology of terrestrial plants, microorganisms and invertebrates. Water Air Soil Pollut 49:189–215

Vestgarden LS (2001) Carbon and nitrogen turnover in the early stage of Scots pine (Pinus silvestris L.) needle litter decomposition effects of internal and external nitrogen. Soil Biol Biochem 37:63–75

Vogt KA, Publicvover DA, Bloomfield J et al (1993) Belowground responses as indicators of environmental change. Environ Exp Bot 33:189–205

Warfvinge P, Sverdrup H (1992) Calculating critical loads of acid deposition with PROFILE – a steady state soil chemistry model. Water Air Soil Pollut 63:119–143

White CS, McDonnel MJ (1988) Nitrogen cycling processes and soil characteristics in an urban versus rural forest. Biogeochemistry 5:243–262

Xiao QF, McPherson EG (2002) Rainfall interception by Santa Monica's municipal urban forest. Urban Ecosyst 291:291–302

Xiao QF, McPherson EG, Ustin SL et al (2000) A new approach to modelling tree rainfall interception. J Geophys Res 105:29173–29188

Zhu WX, Carreiro MM (2004) Temporal and spatial variations in nitrogen transformations in deciduous forest ecosystem along an urban-rural gradient. Soil Biol Biochem 36:267–278

Zhu P, Zhang Y (2008) Demand for urban forests in United States cities. Landscape Urban Plan 84:293–300

Zipperer WC, Foresman TW, Sisinni SM et al (1997) Urban tree cover: an ecological perspective. Urban Ecosyst 1:229–246

Part IV
Hydrologic and Biogeochemical Fluxes from the Canopy to the Phreatic Surface

Chapter 17
Atmospheric Deposition

Kathleen C. Weathers and Alexandra G. Ponette-González*

17.1   Introduction

Atmospheric deposition plays a key role in the biogeochemistry of temperate, tropical, and boreal forests. Many essential macro- and micronutrients as well as pollutants are delivered from the atmosphere to forest ecosystems: (1) dissolved in rain and snow (wet deposition); (2) directly as particles and gases (dry deposition); and (3) dissolved in cloud droplets (cloud, occult, or fog deposition, hereafter referred to as cloud). Here we refer to total atmospheric deposition as the sum of wet, dry, and for some ecosystems, cloud inputs. Substances deposited to forests in any of these three forms can add to soil element pools, while many are immediately labile and thus can be taken up by forest vegetation. Therefore, inputs from the atmosphere can be quantitatively significant relative to the annual nutrient demand for forest growth (Schlesinger 1997), and to watershed input–output budgets (Weathers and Lovett 1998). Conversely, nutrients and pollutants supplied in excess of forest requirements can have adverse ecological effects on sensitive species, soils, and surface waters draining forest watersheds (Likens et al. 1996).

Where do nutrients and pollutants in the atmosphere originate? What are the mechanisms that determine where and how much of an element is deposited to the land surface? What are some of the beneficial and detrimental ecological effects of atmospheric deposition on forest ecosystems? In this chapter, we briefly examine these questions and offer suggestions for future directions in atmospheric deposition research. While many elements are critically important in forest biogeochemistry, our examples largely involve sulfur and nitrogen. Sulfur and nitrogen are essential plant nutrients, but in many places are regarded as air pollutants of concern (Weathers et al. 2006a; Galloway et al. 2008). As such, there is much scientific research on the cycling of these elements in forest ecosystems (Rodhe and Herrera 1988; Johnson and Lindberg 1992; Likens and Bormann 1995; Weathers and Lovett 1998; Likens et al. 2002). In this chapter, we draw examples from

---

*We make no distinction between first and second authors.

primarily temperate, but also tropical forests, because nutrient and pollutant sources, distributions, and effects often differ between these ecosystem types (Matson et al. 2002).

17.2 Sources of Atmospheric Nutrients and Pollutants

Nutrients and pollutants in the atmosphere have diverse natural and anthropogenic sources. The old adage "what goes up, must come down" is apt for atmospheric deposition, and understanding in what form, where, how, and when is the subject of active research. Nitrogen (N), one of the most common limiting nutrients in temperate terrestrial ecosystems, constitutes ~78% of the Earth's atmosphere, where it is found as N_2, dinitrogen, a form that is unavailable to most organisms. Natural phenomena such as lightning, forest fires, and lava flows convert some atmospheric nitrogen into nitric oxide (NO), a highly reactive gas that can undergo numerous transformations in the atmosphere before being deposited to forests in different forms of N (e.g., nitrate – NO_3^-). In contrast to nitrogen, phosphorus (P), magnesium (Mg), calcium (Ca), potassium (K), and iron (Fe) do not exist in gaseous form and are largely derived from mineral weathering (Table 17.1). It is through wind erosion that these rock-derived elements are introduced into the atmosphere. Sea water represents another major source of ions to the atmosphere, including chloride (Cl), sodium (Na), sulfate (SO_4^{2-}), and Ca and Mg, which, as a result of wave action, are suspended in air and deposited downwind to adjacent terrestrial ecosystems (Art et al. 1974). Additional biogenic sources of gases and particles are volcanoes, fires, and trace gas emissions from soils (e.g., organic matter mineralization), vegetation (e.g., volatile organic compounds), and oceans (e.g., dimethyl sulfide production).

In industrialized regions, human emissions dwarf many of these natural sources. In the US, coal and oil combustion for electricity generation, industrial and manufacturing processes, and transportation are the principal anthropogenic sources of sulfur dioxide (SO_2) and NO_x (NO and nitrogen dioxide (NO_2)) – and constitute roughly 90% of these emissions (Weathers et al. 2006a) – to the

Table 17.1 Element inputs (%) to Hubbard Brook Experimental Forest from atmospheric and geologic sources

Element	Atmosphere	Weathering	Taken up as
N	100	0	NO_3^-, NH_4^+
S	96	4	SO_4^{2-}
P	1	99	HPO_4^{2-}, $H_2PO_4^-$
Ca	9	91	Ca^{2+}
K	11	89	K^+
Mg	15	85	Mg^{2+}
Cl	100	0	Cl^-
Fe	0	100	Fe^{2+}
Na	22	78	Na^+

Data from Likens et al. (1981)
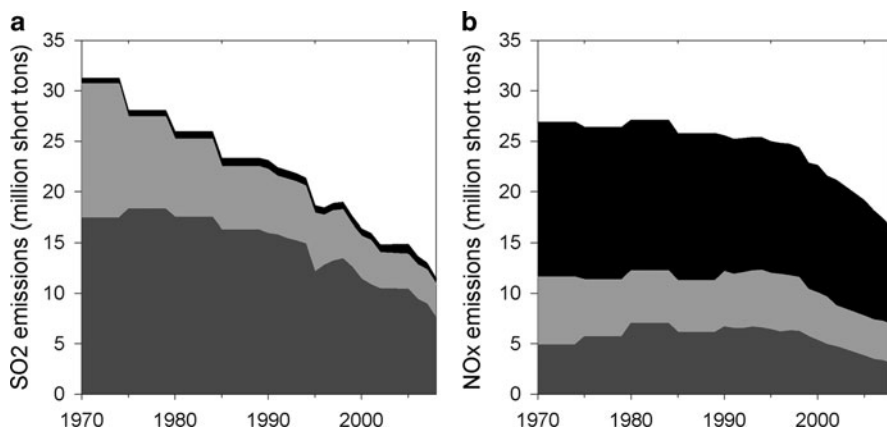
Fig. 17.1 (**a**) SO_2 and (**b**) NO_x emissions in the US from 1970 to 2008. Categories include mobile (*black* = highway and off-highway vehicles) and industrial sources (*light gray* = fuel combustion, waste disposal, and manufacturing and processing by products), and fuel combustion for electric utilities (*dark gray*). Data downloaded on 17 November 2009 from the National Emissions Inventory (http://www.epa.gov/ttn/chief/trends/index.html)

atmosphere (Fig. 17.1). SO_2 and NO_x are precursors of sulfuric and nitric acid, the main components of acid rain, as well as sulfate and nitrate aerosols. In the tropics, biomass burning is the main anthropogenic source of these compounds (Rodhe and Herrera 1988). Additionally, biomass burning releases large quantities of potent greenhouse (e.g., nitrous oxide (N_2O)) and ozone-depleting gases (e.g., methyl chloride (CH_3Cl); Crutzen et al. 1979) as well as aerosols into the atmosphere (Da Rocha et al. 2005). Globally, agriculture and livestock production also alter the chemical composition of the atmosphere. Ammonia (NH_3) volatilization and soil particle suspension from cultivated fields, grazing lands, and intensive livestock operations are significant sources of atmospheric N as well as P (Graham and Duce 1979; Vitousek et al. 1997).

17.3 Geography of Atmospheric Deposition

Clearly, the atmosphere is a major source of many elements to forest ecosystems (Table 17.1), yet there is significant geographic variation in rates of deposition to the land surface. Research conducted as part of the Global Precipitation Chemistry Project (GCPC) demonstrated that differences in anthropogenic emissions contribute to much of this variation at a global scale. For example, sites in eastern North America were found to have significantly higher concentrations of hydrogen ion (H^+), nitrate (NO_3^-), and sulfate (SO_4^{2-}) in precipitation compared with sites distant from industrial sources (Galloway et al. 1984; Weathers et al. 2006a). Today, wet N and S deposition in the eastern US are several times greater than the background deposition of 1–3 kg S ha^{-1} $year^{-1}$ (Rodhe et al. 1995) and
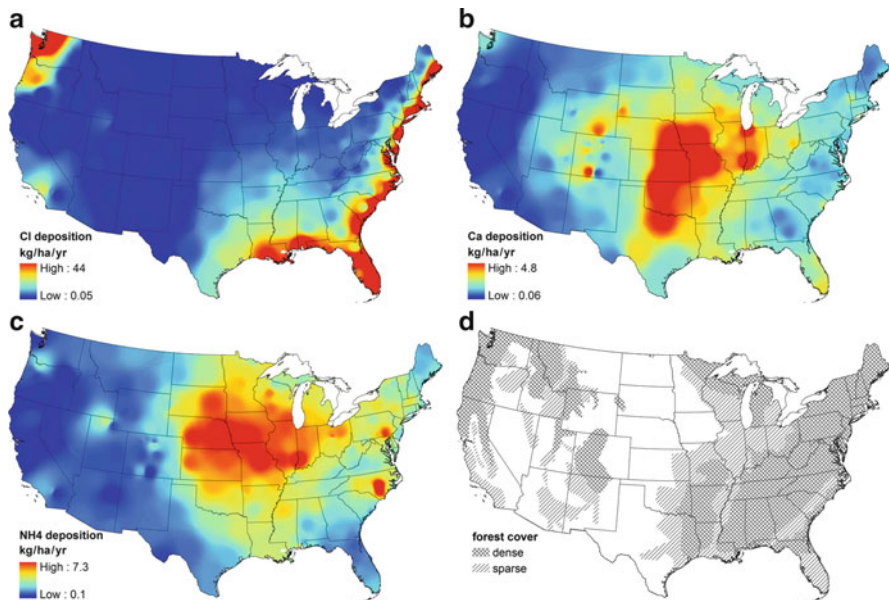
Fig. 17.2 Annual wet (**a**) chloride (Cl⁻), (**b**) calcium (Ca²⁺), and (**c**) ammonium (NH₄⁺) deposition (kg ha⁻¹) across the United States for 2008, and (**d**) dense (cross hatching) and sparse (simple hatching) forest cover. Data from the National Atmospheric Deposition Monitoring Program/National Trends Network (http://nadp.sws.uiuc.edu/). Forest cover is stylized after GLCC v.2 (http://edc2.usgs.gov/glcc/globe_int.php)

0.5 kg N ha⁻¹ year⁻¹ (Galloway et al. 2008) estimated for remote and relatively unpolluted areas. This and other research also has shown that pollutants emitted from industrial source areas can travel long distances in the atmosphere before being washed out in precipitation over remote regions (e.g., Weathers and Likens 1997).

Examination of atmospheric wet (rain + snow) deposition maps for the continental US (National Atmospheric Deposition Program, NADP 2009) similarly reveals the effects both of source areas and prevailing wind trajectories (roughly from west to east) on regional deposition patterns (Fig. 17.2). Chloride, sodium, and magnesium inputs tend to be greater in coastal compared to inland areas due to the generation and subsequent deposition of sea-spray aerosols along the coast. For dust-derived elements, such as calcium and magnesium, aeolian erosion contributes to enhanced deposition downwind from arid and semiarid zones and agricultural fields located predominantly in the middle of the country. Ammonia emissions from agricultural and animal feeding operations result in elevated wet ammonium inputs downwind, especially in the Midwestern and southeastern US.

Determining rates of atmospheric deposition to forest ecosystems is of particular importance, because forests cover ~30% of the Earth's land surface (Fig. 17.3) and supply numerous goods and services essential for human well-being. Data collected through several long-term networks in the Northern Hemisphere (Fig. 17.3) indicate considerable heterogeneity in deposition patterns across forested landscapes as well.

global monitoring sites
- air chemistry
- precipitation chemistry
- air and precipitation chemistry

forest cover type
- deciduous broadleaf
- deciduous needleleaf
- evergreen broadleaf
- evergreen needleleaf
- mixed forest
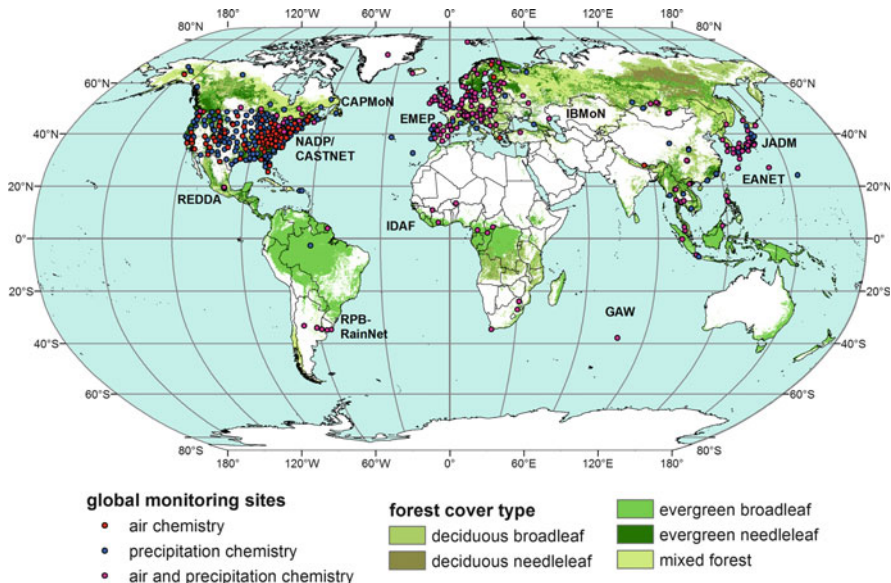
Fig. 17.3 Map of global forest cover (Global Land Cover Characteristics Data Base version 2.0., GLCC, http://edc2.usgs.gov/glcc/globe_int.php) and national atmospheric deposition monitoring networks actively sampling wet deposition (*blue dots*), dry deposition (*red dots*), and wet and dry deposition (*purple dots*). Networks include: National Atmospheric Deposition Program (NADP, USA); Clear Air Status and Trends Network (CASTNET, USA); Atmospheric Deposition Network (REDDA, Mexico City); Canadian Air and Precipitation Monitoring Network (CAPMoN); European Monitoring and Evaluation Programme (EMEP); Integrated Background Monitoring Network (IBMoN, former USSR); Acid Deposition Monitoring over Japan (JADM); Acid Deposition Monitoring Network in East Asia (EANET); IGAC Debits Africa (IDAF); Río de la Plata Atmospheric Deposition Network (RP-RainNet, Argentina); and Global Atmosphere Watch (GAW)

While this variability complicates the task of identifying those forests most vulnerable to elevated deposition, comparisons of deposition fluxes to distinct forest types indicate that contrasts in leaf type and habit are salient features of forest canopies that strongly influence dry and fog deposition (de Schrijver et al. 2008). For example, dry and fog inputs are generally greater to needleleaved than to broadleaved tree species and to evergreen than to deciduous stands (Weathers et al. 2000b, 2006b; see below). Similar variability in deposition rates can be expected in tropical and boreal forest landscapes, which encompass 46 and 29% of global forest cover, respectively (Fig. 17.3). However, we still know comparatively little about which forested areas within these biomes receive high and low deposition fluxes.

In addition, many monitoring networks estimate only wet deposition (Fig. 17.3), which is based on the product of precipitation amount and chemical concentration of rain or snow measurements (e.g., NADP). In the US, there also exists the Clean Air Status and Trends Network (CASTNET), which measures air concentrations and models dry deposition, but estimates of dry deposition to forests remain uncertain because of model limitations (see Sect. 17.6). As dry inputs can
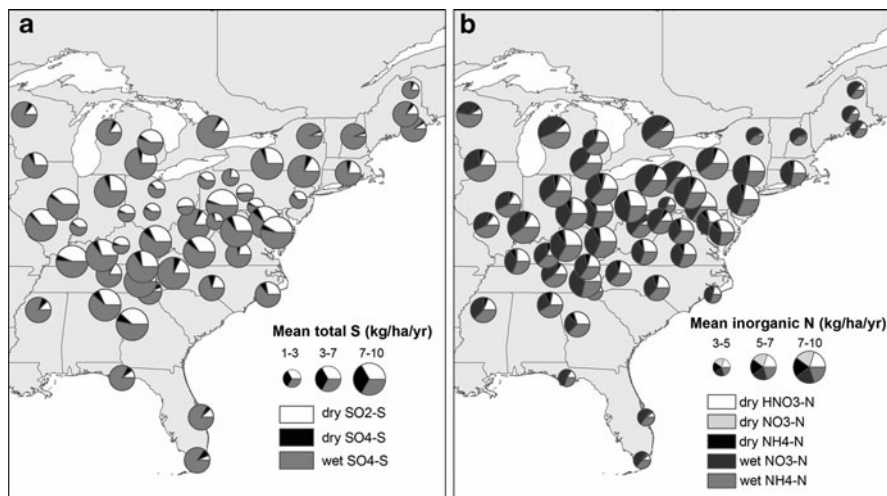
Fig. 17.4 Annual mean wet and dry (**a**) sulfur and (**b**) nitrogen deposition (kg ha^{-1}) to CASTNET monitoring sites in the eastern US for 2004–2008. *Color shading* indicates the proportion of deposition for each measured species. Pie sizes correspond to rates of total deposition. Data downloaded on 9 October 2009 from the National Atmospheric Deposition Monitoring Program/National Trends Network (http://nadp.sws.uiuc.edu/) and the Clear Air Status and Trends Network (http://www.epa.gov/castnet/data.html)

comprise a significant fraction of the total material delivered from the atmosphere to ecosystems (Lovett 1994), measurement of wet deposition only can significantly underestimate total atmospheric deposition to forests (Fig. 17.4). For example, between 2004 and 2008, mean annual dry deposition to US CASTNET monitoring sites was 7–54% of total sulfur and 6–39% of total nitrogen deposition (Fig. 17.4). Cloudwater deposition is also rarely quantified but can be the dominant vector of nutrient and pollutant deposition to forests in montane and coastal regions (Weathers et al. 1986, 1988; Weathers and Likens 1997; Anderson et al. 1999).

17.4 Controls on Atmospheric Deposition: Rates and Patterns

17.4.1 Emissions and Proximity to Source Areas

As noted above, emissions and proximity to source areas influence the magnitude and spatial patterning of atmospheric deposition at regional (1,000s of km) scales (Fig. 17.2). Long-term data from Hubbard Brook Experimental Forest show that SO_2 and NO_x emissions are strongly and positively related to concentrations of SO_4^{2-} and NO_3^- in precipitation (Likens et al. 2005). In addition, both wet and dry deposition tend to decrease with distance from natural (e.g., volcanoes, Delmelle et al. 2001) and industrial emission sources (e.g., northeastern US; Fig. 17.4) due to the gradual removal of chemical substances from air masses.

17.4.2 Meteorology and Climate

The total amount of nutrients and pollutants delivered to forest ecosystems is also dependent on meteorology and climate. All else equal (i.e., precipitation concentrations), higher rainfall (or snowfall) results in greater wet deposition. For example, wet chloride deposition to forests in Puerto Rico was found to be substantially higher than to nearby forest sites with similar concentrations of Cl^- in precipitation but lower annual rainfall (McDowell et al. 1990). Compared with wet deposition, dry and cloud deposition exhibit remarkable spatiotemporal variability, largely as a result of the combination of factors that affect their deposition. Deposition for particles and gases can be estimated by:

$$V_d * [conc] = flux, \tag{17.1}$$

where V_d is the deposition velocity of the particle or gas, [conc] is the chemical concentration in the atmosphere, and flux is the delivery of a chemical in units such as $kg\ ha^{-1}$, $eq\ ha^{-1}$ or $mol(c)\ ha^{-1}$, often expressed as per unit time. Meteorological conditions are important in determining deposition velocities for different canopy types and chemical species, and hence in driving dry deposition rates. Dry inputs typically increase with wind speed due to enhanced turbulent transfer of gases and particles to forest canopies (Fowler et al. 1989), while some particles and water-soluble gases such as SO_2, O_3, and NH_3 deposit more readily under humid than dry conditions (Burkhardt and Eiden 1994). Cloud deposition (the product of cloud water amount and chemical concentration) to forest canopies is directly proportional to cloud frequency and duration and wind speed (Bruijnzeel and Proctor 1995); where cloud immersion is frequent, cloud deposition may greatly enhance total deposition (Lovett and Kinsman 1990). Challenges involved in modeling these parameters have hindered accurate estimation of fog and dry inputs.

17.4.3 Vegetation and Topography

Both land cover (vegetation, in this case) and topography have strong influences on rates and patterns of atmospheric deposition (Lovett and Kinsman 1990; Weathers et al. 2000b, 2006b) across forest landscapes (10s–100s of km). Dry and cloud deposition are partially controlled by vegetation surfaces in contrast to wet deposition (rain, especially), which is influenced less by vegetation than by orographic effects. Forest canopies tend to be efficient scavengers of dry and cloud-deposited nutrients and pollutants relative to ecosystems with more homogeneous surfaces (e.g., cropland, grassland; Fig. 17.5), because turbulent exchange at the atmosphere–vegetation interface increases with surface roughness (Fowler et al. 1999), and because total surface area is likely to be greater in forests than in unforested locations.
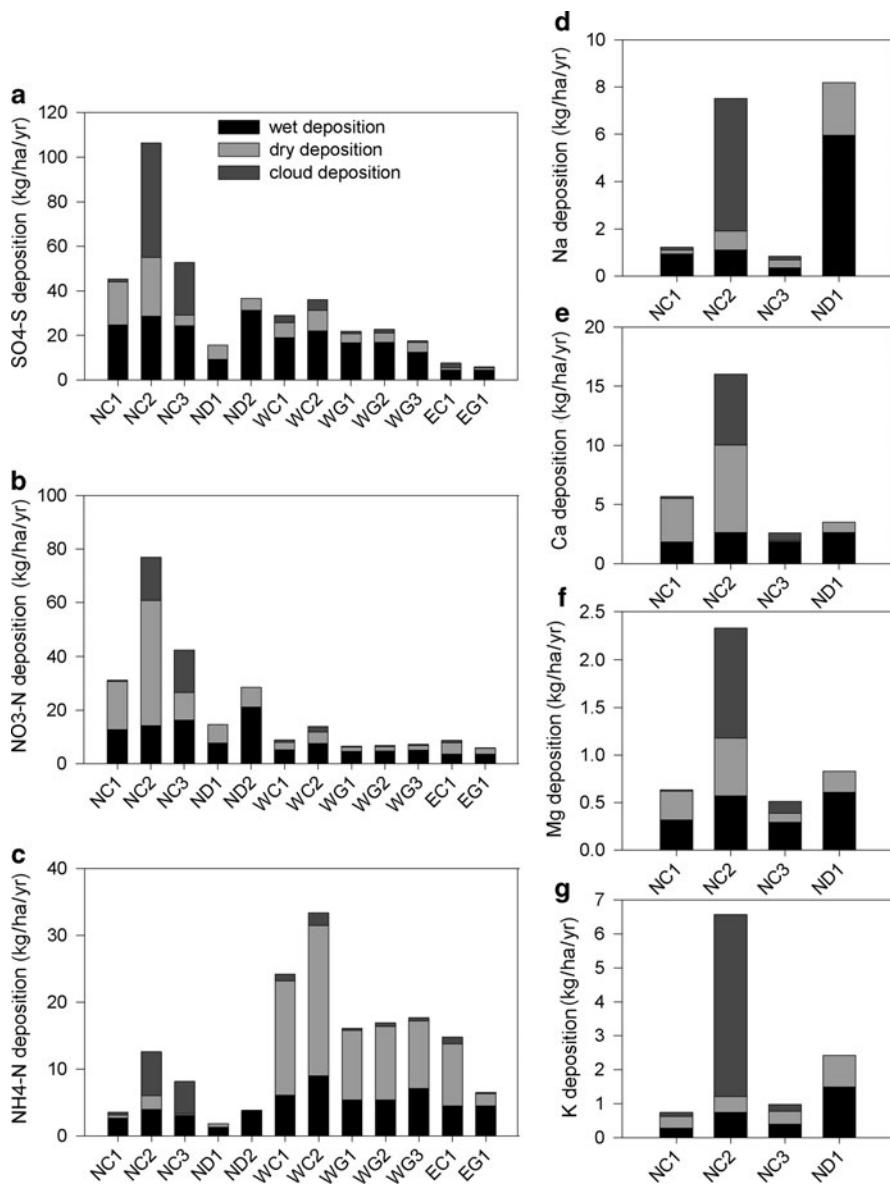
Fig. 17.5 Wet, dry, and cloud deposition of (**a**) SO_4^{2-}-S, (**b**) NO_3^--N, and (**c**) NH_4^+-N to coniferous forest ("C"), deciduous forest ("D"), and grassland ("G") ecosystems in North America ("N"), northern England ("E"), and Wales ("W"), and (**d**) Na, (**e**) Ca, (**f**) Mg, and (**g**) K to four Integrated Forest Study sites (data from Johnson and Lindberg 1992). Sites include Oak Ridge, TN (NC1), Great Smoky Mountain National Park, NC (NC2), Whiteface Mountain, NY (NC3), Cedar River, WA (ND1), Ontario, Canada (ND2), Plynlimon (WC1, WG1, WG2) and Brianne (WC2, WG3), Wales (Reynolds et al. 1997), and Kielder Forest (EC1, EG1), England (Fowler et al. 1989)

Vegetation factors that govern deposition operate on leaf, stand, and landscape scales. At the leaf level, for example, the complex structure of conifer needles is thought to increase both particle and cloud droplet deposition to needleleaved relative to broadleaved tree species (Burkhardt and Eiden 1994; Beckett et al. 2000). In addition, canopy and stand characteristics play an important role in altering dry and fog inputs (e.g., Ewing et al. 2009). In temperate and tropical rainforests, epiphytes can strongly modify atmospheric inputs directly through interception of particles, gases, and cloud droplets, and indirectly by increasing the total capturing surface area of forest canopies (Nadkarni 1984). Deposition is also generally lower in deciduous compared with evergreen stands regardless of leaf type, due to year round collection of atmospheric substances by evergreen trees (Weathers et al. 2000b, 2006b).

The sensitivity of dry and fog deposition to forest attributes indicates that changes in forest structure and composition may have profound effects on atmospheric inputs, and hence on watershed outputs. In Wales and England, afforestation of upland areas has contributed to substantial increases in sulfur and nitrogen inputs to catchments (Fowler et al. 1989; Reynolds et al. 1997; Fig. 17.5). A recent study found that total sulfur deposition increases with Leaf Area Index (leaf surface area per unit ground area) along a tropical grassland–agroforest–forest continuum in eastern Mexico (Ponette-González et al. 2010). Similar enhancements in deposition are likely to occur as areas cleared for cultivation or grazing regenerate back to forest. Elevation, aspect, and forest edges also have been shown to modify deposition fluxes in complex landscapes (Weathers et al. 2000b, 2006b). In fact, empirical models of deposition illustrate that forest stands downwind from pollution sources, exposed to cloudwater input, with large canopy surface area, and at high elevation are likely deposition hotspots within forested landscapes (Weathers et al. 2006b; e.g., site NC2, Fig. 17.5).

17.5 Nutrient Enrichment and Pollution Effects

The ecological effects of atmospheric deposition on forest ecosystems often are complex and difficult to discern. First, there are multiple factors that can determine whether these effects are ecologically beneficial or detrimental, including the nature of the substance deposited, the rate of deposition, plant species composition, soil characteristics, and land-use history (Driscoll et al. 2001). Second, interactions among nutrients and pollutants within ecosystems may serve to produce, enhance, or offset certain ecological effects (Weathers et al. 2006a). Third, ecosystem response times to nutrient and pollutant inputs can be slow, modified, and/or lagged due to the long life span of trees, making it difficult to readily observe many of the direct and indirect effects of deposition on forest ecosystem processes (Lovett et al. 2009).

Deleterious ecological effects notwithstanding, atmospheric inputs are the primary source of elements to some nutrient-limited ecosystems. For example, Chadwick et al. (1999) employed isotopic tracers to resolve the contribution of

atmospheric deposition and rock weathering in the supply of nutrient cations to forests along a substrate-age gradient in Hawai'i. Their study revealed that after 150,000 years of forest succession, rain, cloud, and dry deposition supply sufficient phosphorus, calcium, and magnesium to maintain ecosystem productivity on highly weathered tropical soils. Weathers and Likens (1997) and Weathers et al. (2000a) analyzed cloudwater chemistry in southern Chile and estimated that cloudwater could contribute up to eight times the amount (1–8 kg ha^{-1} year^{-1}) of nitrogen to unpolluted temperate rainforests than wet deposition (i.e., $\leq$1 kg ha^{-1} year^{-1}); their results suggest that N deposited in cloudwater may subsidize these N-limited ecosystems.

In polluted regions of the Northern Hemisphere, where temperate and boreal forests are typically limited by nitrogen, increased rates of anthropogenic N deposition have resulted in a "fertilization" effect (Fenn et al. 1998). However, chronic nitrogen additions eventually can move some forests towards a stage of N saturation, where nitrogen inputs exceed requirements for growth resulting in enhanced nitrification, base cation and nitrate leaching losses, increased levels of nitrate in streamwater as well as a net decrease in forest productivity (Aber et al. 1998). There is now also growing concern over the potential effects of N pollution in tropical and subtropical regions, where many forest soils (e.g., Andosols) may not be N-limited (Matson et al. 1999, 2002).

17.6   Future Research Directions

After decades of intensive research, the significance of atmospheric deposition in forest biogeochemical cycles has been established. Yet, many gaps persist in our current knowledge of this process: from the complex interactions occurring in the atmosphere to the ecological importance of deposition for ecosystems and their functioning.

The atmosphere is a chemical soup. Gases and aerosols emitted to the atmosphere can and often do react with other chemicals (including water), causing changes in the quantity and distribution of atmospheric constituents. What goes up, eventually comes down, either close to the source of emission (e.g., NH_3), or downwind considerable distances (e.g., S) – and across political and geographic lines – before being deposited as rain, snow, dry, or cloud deposition. The role of NO_x in tropospheric ozone ("bad ozone") formation (O_3) is a classic example of the chemical soup phenomenon, and of general air pollution problems affecting forests. Nitrogen emissions to the atmosphere, whether from the burning of fossil fuels, or from denitrification in forest soils, further contribute to such problems as acid rain and "bad" ozone, greenhouse gases, and nitrogen deposition. In North America and Europe, high tropospheric ozone levels cause injury to forests (Taylor et al. 1994), while N deposition can have cascading, sometimes enhancing effects on forest ecosystems (Galloway et al. 2008). At present, many atmospheric and forest element interactions are not known or well understood, making this an area ripe for further research.

There also remain many forests in the world for which estimates of total atmospheric deposition (wet, dry, and cloud) do no exist. Although rain deposition is relatively simple to estimate, accurate quantification of dry, fog, and snow inputs, or of rain inputs to topographically complex terrain, is still lacking. In addition, not all elements of interest are monitored (e.g., dry deposition of Ca). Furthermore, there is currently no atmospheric deposition monitoring across vast tracts of tropical and boreal forest in Asia, Africa, and Latin America (Fig. 17.2). In some of these regions, air-pollution impacts on vegetation already have been documented (Emberson et al. 2001), and acidic deposition is projected to increase in coming decades (Kuylenstierna et al. 2001).

Whether due to measurement problems or monitoring gaps, lack of deposition estimates limits our ability to predict how deposition inputs affect ecosystem processes, such as nutrient cycling, carbon sequestration (but see Thomas et al. 2010), and acidification. In the eastern US, Lovett et al. (2009) have identified two major research needs in regard to the effects of atmospheric deposition. First, continued efforts must be made to discern the effects of N and S on forest species composition and diversity. Second, more research is required to improve understanding of pollutants that have major animal health implications, such as mercury deposition, and their effects on forested watersheds.

Understanding how sources, trends, patterns, and effects of atmospheric deposition are changing in response to global environmental change is another pressing research need. Rapid urbanization coupled with industrialization in emerging nations is leading to dramatic shifts in source areas for atmospheric nutrients and pollutants. In parts of North America and Europe, SO_2 and NO_x emissions are declining (Fig. 17.6), while in Asia emissions of these pollutants are increasing.
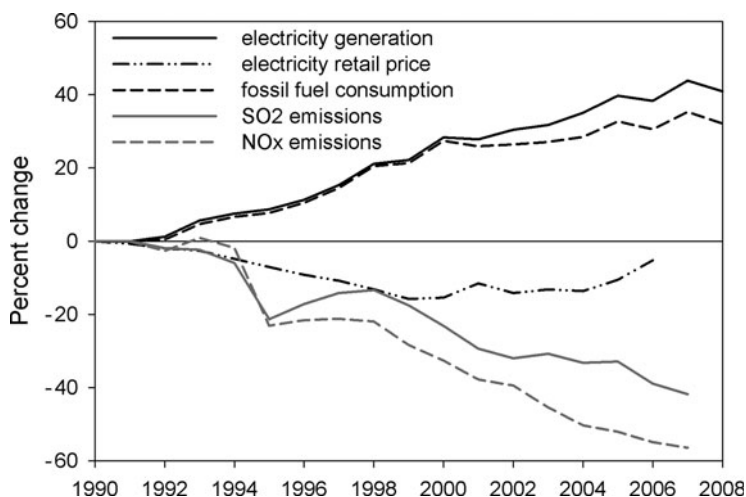
Fig. 17.6 SO_2 and NO_x emissions, electricity generation and retail price and fossil fuel consumption in the United States from 1990–2008 relative to 1990 levels after the Acid Rain and Related Programs 2007 Progress Report. Data from the Annual Energy Review (Energy Information Administration, US Department of Energy, 2008)

Climate warming induced changes in precipitation amount and distribution, the frequency of extreme events, and "cloud lifting" may also affect deposition fluxes (Kelly et al. 2009). Finally, accelerating land-cover change will further modify biogeochemical inputs to ecosystems and watersheds, primarily by altering dry and cloud deposition across forested landscapes (Ponette-González et al. 2010).

Atmospheric deposition is the source of both nutrients and pollutants to forest ecosystems. Although scientists have known this for quite some time, future research should focus on quantifying actual deposition loads to forests, while also investigating the complex transformations occurring within and effects upon forest ecosystems, particularly in light of global change.

References

Aber J, McDowell W, Nadelhoffer K et al (1998) Nitrogen saturation in temperate forest ecosystems: hypotheses revisited. Bioscience 48:921–934

Anderson JB, Baumgardner RE, Volker A et al (1999) Cloud chemistry in the eastern United States, as sampled from three high-elevation sites along the Appalachian Mountains. Atmos Environ 33:5105–5114

Art HW, Bormann FH, Voigt GK et al (1974) Barrier Island forest ecosystem: role of meteorologic nutrient inputs. Science 184:60–62

Beckett KP, Freer-Smith PH, Taylor G (2000) Particulate pollution capture by urban trees: effect of species and windspeed. Glob Change Biol 6:995–1003

Bruijnzeel LA, Proctor J (1995) Hydrology and biogeochemistry of tropical montane cloud forests: what do we really know? In: Churchill SP, Blaslev H, Forero E, Luteyn JL (eds) Tropical montane cloud forests. Springer, New York, pp 38–78

Burkhardt J, Eiden R (1994) Thin water films on coniferous needles. Atmos Environ 28:2001–2017

Chadwick OA, Derry LA, Vitousek PM et al (1999) Changing sources of nutrients during four million years of ecosystem development. Nature 397:491–497

Crutzen PJ, Heidt LE, Krasnec JP et al (1979) Biomass burning as a source of atmospheric gases CO, H_2, N_2O, NO, CH_3Cl and COS. Nature 282:253–256

Da Rocha GO, Allen AG, Cardoso AA (2005) Influence of agricultural biomass burning on aerosol size distribution and dry deposition in southeastern Brazil. Environ Sci Technol 39:5293–5301

De Schrijver A, Staelens J, Wuyts K et al (2008) Effect of vegetation type on throughfall deposition and seepage flux. Environ Pollut 153:295–303

Delmelle P, Stix J, Bourque CPA et al (2001) Dry deposition and heavy acid loading in the vicinity of Masaya volcano, a major sulfur and chlorine source in Nicaragua. Environ Sci Technol 35:1289–1293

Driscoll CT, Lawrence GB, Bulger AJ et al (2001) Acidic deposition in the northeastern United States: sources and inputs, ecosystem effects, and management strategies. Bioscience 51:180–198

Emberson LD, Ashmore MR, Murray F et al (2001) Impacts of air pollutants on vegetation in developing countries. Water Air Soil Pollut 130:107–118

Ewing HA, Weathers KC, Templer PH et al (2009) Fog water and ecosystem function: heterogeneity in a California redwood forest. Ecosystems 12:417–433

Fenn ME, Poth MA, Aber JD et al (1998) Nitrogen excess in North American ecosystems: predisposing factors, ecosystem responses, and management strategies. Ecol Appl 8:706–733

Fowler D, Cape JN, Unsworth MH (1989) Deposition of atmospheric pollutants on forests. Philos Trans Roy Soc B 324:247–265

Fowler D, Cape JN, Coyle M et al (1999) The global exposure of forests to air pollutants. Water Air Soil Pollut 116:5–32

Galloway JN, Likens GE, Hawley ME (1984) Acid precipitation: natural versus anthropogenic components. Science 226:829–831

Galloway JN, Townsend AR, Erisman JW et al (2008) Transformation of the nitrogen cycle: recent trends, questions, and potential solutions. Science 320:889–892

Graham WF, Duce RA (1979) Atmospheric pathways of the phosphorus cycle. Geochim Cosmochim Acta 43:1195–1208

Johnson DW, Lindberg SE (1992) Atmospheric deposition and nutrient cycling in forest ecosystems: a synthesis of the Integrated Forest Study. Springer, New York

Kelly VR, Weathers KC, Lovett GM et al (2009) Effect of climate change between 1984 and 2007 on precipitation chemistry at a site in northeastern USA. Environ Sci Technol 43:3461–3466

Kuylenstierna JCI, Rodhe H, Cinderby S et al (2001) Acidification in developing countries: ecosystem sensitivity and the critical load approach on a global scale. Ambio 30:20–28

Likens GE, Bormann FH (1995) Biogeochemistry of a forested ecosystem. Springer, New York

Likens GE, Bormann FH, Johnson NM (1981) Interactions between major biogeochemical cycles in terrestrial ecosystems. In: Likens GE (ed) Some perspectives of the major biogeochemical cycles. Wiley, New York, pp 93–112

Likens GE, Driscoll CT, Buso DC (1996) Long-term effects of acid rain: response and recovery of a forest ecosystem. Science 272:244–246

Likens GE, Driscoll CT, Buso DC et al (2002) The biogeochemistry of sulfur at Hubbard Brook. Biogeochemistry 60:235–316

Likens GE, Buso DC, Butler TJ (2005) Long-term relationships between SO_2 and NO_X emissions and SO_4^{2-} and NO_3^- concentration in bulk deposition at the Hubbard Brook Experimental Forest, New Hampshire. J Environ Monitor 7:964–968

Lovett GM (1994) Atmospheric deposition of nutrients and pollutants in North America: an ecological perspective. Ecol Appl 4:629–650

Lovett GM, Kinsman JD (1990) Atmospheric pollutant deposition to high-elevation ecosystems. Atmos Environ 24:2767–2786

Lovett GM, Tear TH, Evers DC et al (2009) Effects of air pollution on ecosystems and biological diversity in the eastern United States. Ann N Y Acad Sci 1162:99–135

Matson PA, McDowell WH, Townsend AR et al (1999) The globalization of N deposition: ecosystem consequences in tropical environments. Biogeochemistry 46:67–83

Matson P, Lohse KA, Hall SJ (2002) The globalization of nitrogen deposition: consequences for terrestrial ecosystems. Ambio 31:113–119

McDowell WH, Sanchez CG, Asbury CE et al (1990) Influence of sea salt aerosols and long range transport on precipitation chemistry at El Verde, Puerto Rico. Atmos Environ A 24:2813–2821

Nadkarni NM (1984) Epiphyte biomass and nutrient capital of a Neotropical elfin forest. Biotropica 16:249–256

National Atmospheric Deposition Program (NRSP-3) (2007) NADP program office. Illinois State Water Survey, Champaign

National Atmospheric Deposition Program (2009) NADP program office. Illinois State Water Survey, Champaign

Ponette-González AG, Weathers KC, Curran LM (2010) Tropical land-cover change alters biogeochemical inputs to ecosystems in a Mexican montane landscape. Ecol Appl 20 (7):1820–1837

Reynolds B, Fowler D, Smith RI et al (1997) Atmospheric inputs and catchment solute fluxes for major ions in five Welsh upland catchments. J Hydrol 194:305–329

Rodhe H, Herrera R (1988) Acidification in tropical countries. Wiley, New York

Rodhe H, Langner J, Gallardo L et al (1995) Global scale transport of acidifying pollutants. Water Air Soil Pollut 85:37–50

Schlesinger WH (1997) Biogeochemistry: an analysis of global change, 2nd edn. Academic Press, San Diego

Taylor GE Jr, Johnson DW, Andersen CP (1994) Air pollution and forest ecosystems: a regional to global perspective. Ecol Appl 4:662–689

Thomas RQ, Canham CD, Weathers KC et al (2010) Increased tree carbon storage in response to nitrogen deposition in the US. Nat Geosci 3:3–17

Vitousek PM, Aber JD, Howarth RW et al (1997) Human alteration of the global nitrogen cycle: sources and consequences. Ecol Appl 7:737–750

Weathers KC, Likens GE (1997) Clouds in southern Chile: an important source of nitrogen to nitrogen-limited ecosystems? Environ Sci Technol 31:210–213

Weathers KC, Lovett GM (1998) Acid deposition research and ecosystem science: synergistic successes. In: Pace ML, Groffman PM (eds) Successes, limitations, and frontiers in ecosystem science. Springer, New York, pp 195–219

Weathers KC, Likens GE, Bormann FH et al (1986) A regional acidic cloud/fog water event in the eastern United States. Nature 319:657–658

Weathers KC, Likens GE, Bormann FH et al (1988) Cloudwater chemistry from ten sites in North America. Environ Sci Technol 22:1018–1026

Weathers KC, Lovett GM, Likens GE et al (2000a) Cloudwater inputs of nitrogen to forest ecosystems in southern Chile: forms, fluxes, and sources. Ecosystems 3:590–595

Weathers KC, Lovett GM, Likens GE et al (2000b) The effect of landscape features on deposition to Hunter Mountain, Catskill Mountains, New York. Ecol Appl 10:528–540

Weathers KC, Likens GE, Butler TJ (2006a) Acid rain. In: Rom WN (ed) Environmental and occupational medicine, 4th edn. Lippincott Williams & Wilkins, Philadelphia, pp 1507–1522

Weathers KC, Simkin SM, Lovett GM et al (2006b) Empirical modeling of atmospheric deposition in mountainous landscapes. Ecol Appl 16:1590–1607

Chapter 18
Canopy Structure in Relation to Hydrological and Biogeochemical Fluxes

Thomas G. Pypker, Delphis F. Levia, Jeroen Staelens, and John T. Van Stan II

18.1 Introduction

The structure of forest canopies is highly heterogeneous at multiple scales. Leaves, twigs, and stems are not organized uniformly in space. For example, some plants have highly clustered leaves (e.g., conifers) while others are less clustered (e.g., Kira et al. 1969). Forest canopies contain gaps, but the size and distribution of these gaps is highly variable and forest/disturbance-dependent (e.g., Yavitt et al. 1995; Asner et al. 2004). Leaf area and woody biomass are not evenly distributed along the vertical axis, with some forests having a larger proportion of the leaf area closer to the forest floor, whilst other forests have most of their foliage near the top (e.g., Parker et al. 2004b). How these elements are organized and connected in space can have profound influences on ecosystem process such as hydrological and biogeochemical fluxes.

The canopy affects hydrological and biogeochemical fluxes because, prior to reaching the forest floor, the water must first pass through the forest canopy. Because of the canopy's complexity, the path of water and other chemicals are not well understood. Historically, researchers have treated the canopy as a black box. They determined the effect of the canopy on hydrology/chemistry by quantifying the total amount of a given element that enters the top of the canopy and compared the value to the average amount exiting the bottom (e.g., Zinke 1967). The canopy, combined with micrometeorological conditions, is then assumed to have caused the difference between the two values. In the past two decades, researchers have tried to better understand the mechanisms that control the transfer of water and other chemicals out of the forest canopy by investigating how the vertical and horizontal distribution of the different canopy components affect the hydrology and biogeochemistry. The goal of this chapter is to review our current knowledge of how changes in canopy structure influences hydrological and biogeochemical fluxes (see Chap. 26 for a discussion of the effect of seasonality). After discussing the effect of canopy structure on hydrology and biogeochemical cycles, we propose areas that require further research.

18.2 Canopy Structure and Hydrology

18.2.1 Leaf Shape and Distribution

Leaf shape and configuration affects water storage (Horton 1919). Some leaves only store water as a thin coating whilst others also store water in capillary spaces between leaves. For this reason, flat leaves (i.e., many of the deciduous species) store less than trees that have clumped leaf patterns (i.e., trees with needles) (Keim et al. 2006a). However, other elements, such as the presence of leaf hairs or "cup-shaped" leaves (e.g., Grah and Wilson 1944), must also be considered as these characteristics can also alter the storage ability of the leaf.

In addition to the individual leaf shape, the distribution of the leaves is also important. In forests, the vertical leaf distribution can depend on both forest type and forest age. For example, young temperate forests typically have their foliage located near the top of the forest canopy because each tree is competing for light, while older forests may develop uneven age structure, thereby redistributing their leaf area. This can be clearly seen in the Douglas-fir forests of the Pacific Northwest of the USA. The LAI of young Douglas-fir forests is primarily at the top of the canopy whereas, older forest have a significant portion of the foliage lower in the forest canopy (e.g., Parker et al. 2004b). This occurs because old Douglas-fir trees produce epicormic branches lower on their boles and shade-tolerant trees emerge from the forest floor in this ecosystem (Franklin et al. 2002). Surfaces lower in the canopy experience decreased rates of evaporation because of reduced solar radiation, wind speed, and vapor pressure deficits (Pypker et al. 2005).

18.2.2 Epiphytes

Epiphytes are common in many forest communities and their hydrological effects are poorly understood. Vascular epiphytes effectively increase the surface area within the forest canopy, thereby increasing water storage. Nonvascular epiphytes have the potential to alter canopy water storage even further. In both tropical and temperate forests, lichen and bryophyte biomass has been found to well exceed $2,000 \, kg \, ha^{-1}$ (e.g., Nadkarni 1984; McCune 1993). Lichens and bryophytes rely on intercepted water for biophysical processes and therefore, have very large water holding capacities (Blum 1973; Proctor 2000). Recent studies have shown that epiphytic bryophytes can store greater than 400% of dry weight in some tropical forests (e.g., Hölscher et al. 2004; Köhler et al. 2008) and in excess of 1,000% of dry weight in temperate forests (Pypker et al. 2006a). While this dramatically increases the canopy water storage of a forest, the maximum amount is rarely

Table 18.1 Canopy water storage as related to components of canopy structure

Functional group	Water storage
Whole canopy water storage	
Mature deciduous forest	
With leaves	0.2–2 mm (Leyton et al. 1967; André et al. 2008c)
Without leaves	0.03–0.8 mm (Leyton et al. 1967)
Mature coniferous forest	0.1–4.3 mm (Link et al. 2004; Llorens and Gallart 2000)
Canopy components	
Whole branches	
Still air	0.112–0.8 mm (Llorens and Gallart 2000; Keim et al. 2006a)
Windy	0.017–0.058 mm (Llorens and Gallart 2000)
Epiphytes	2–10 $g_{water}/g_{dry\ weight}$ (Hölscher et al. 2004; Pypker et al. 2006a; Köhler et al. 2007)
Bark	1.3–5.9 mm (Herwitz 1985)
Deadwood/organic matter	~20 $g_{water}/g_{dry\ weight}$ (Pypker et al. 2006a; Ingram and Nadkarni 1993)

Water storage values for the whole canopy are reported in mm of water storage ($l\,m^{-2}_{ground\ surface\ area}$) for whole canopies in zero evaporation conditions after rainfall has ceased (Gash and Morton 1978). For canopy components, water storage is defined as $g_{water}/g_{dry\ weight}$ of epiphyte or deadwood/organic matter and liters of water per m^{-2} (mm) of branch surface or bark surface. The estimate for dead wood/organic matter is not well defined in the literature and should be used with caution

realized for an individual storm event because of the distribution and physical properties of the epiphyte communities (e.g., Hölscher et al. 2004; Köhler et al. 2008). Table 18.1 summarizes some canopy water storages value for epiphytes.

Epiphytes are not evenly distributed throughout the forest canopy. In tropical and temperate regions, both the vertical and horizontal distribution of vascular and nonvascular epiphytes varies dramatically (e.g., van Leerdam et al. 1990; McCune et al. 1997). For example, in the Pacific Northwest, lichens dominate the upper portions of the forest canopy, whereas bryophytes dominate the lower portions (e.g., McCune et al. 1997). The different distributions in old-growth Douglas-fir forests and other forests will likely affect the wetting and drying of the forest canopy. Both Hölscher et al. (2004) and Pypker et al. (2006b) found that while bryophytes in a tropical and temperate forest, respectively, had the potential to store large volumes of water, their effect on canopy water storage on a per storm basis was limited because they did not dry between storms. Furthermore, Pypker et al. (2006a) suggest that epiphyte-laden branches require significant amounts of water to saturate because of preferential flow routes through the branches. The likely occurrence of preferential flow, combined with large water holding capacities, delayed the saturation of a single epiphyte-laden branch for several hours under intense rainfalls (>20 mm h^{-1}). This suggests that forest canopies that contain large bryophyte populations may not saturate in one storm event and may require extended periods between storm events to dry, thereby complicating our understanding of the residence time of water in the forest canopy.

18.2.3 Wood Storage and Organic Matter

18.2.3.1 Dead Wood and Organic Matter

Dead wood and organic matter in the forest canopy offer both surface storage and internal water storage (Table 18.1). Temperate and tropical forest canopies can contain in excess of 500 kg ha^{-1} of dead wood and debris in the canopy that may store greater than 10,000 kg ha^{-1} of water, change water flow paths and alter timing of canopy drying (Ingram and Nadkarni 1993; Pypker et al. 2006a). Just as with soils at the forest floor, water flowing through organic debris may experience preferential flow and the dead branches may slowly absorb water. Furthermore, the organic debris and dead branches may be lower in the canopy and therefore may dry slowly because the dead branches/organic debris are insulated from solar radiation and wind (Köhler et al. 2007).

18.2.3.2 Bark Water Storage

Bark water storage capacity and its role in the hydrology of forest ecosystems have been generally under-appreciated and under-studied, despite its importance on hydrologic fluxes from the canopy to the forest floor (e.g., Levia and Herwitz 2005). For selected tropical rainforest species, Herwitz (1985) found that bark water storage ranged from 1.3 to 5.9 L m^{-2} bark surface (Table 18.1). Recent work reported that forests literally store tens of thousands of liters in bark during precipitation events (Levia and Herwitz 2005).

A key control of bark water storage capacity is bark morphology. The term bark morphology refers to the physical properties of the bark surface, such as thickness, texture, and microrelief, which change with time and along the vertical profile of the bole as a tree ages (Levia and Wubbena 2006). Bark morphology dictates the geometric shape of intercepted water and its routing to the forest floor. Compared to the typical flat or convex shape of detained water on foliar surfaces, water detained on bark surfaces adopts a concave form that increases surface tension, limits evaporation loss, and maximizes residence time with the woody surface. In point of fact, Herwitz (1987) observed that intercepted water on the branches and trunk were less likely to be released to the forest floor as throughfall with increasing wind speeds, providing increased contact time with the bark of the tree and promoting stemflow production.

18.2.4 Canopy Spacing and Forest Management

Rainfall interception loss changes as a result of alterations in canopy water storage, direct throughfall fraction and evaporation during the storm event (e.g., Rutter et al. 1971). Removal of trees will decrease canopy water storage and also decrease the

area readily available for evaporation (Gash et al. 1995). However, by thinning the canopy, foliage lower in the canopy is exposed to greater windspeeds, thereby decreasing the aerodynamic resistance of the canopy and promoting evaporation (Teklehaimanot et al. 1991). Hence, reductions in leaf area, because of stand development, disturbance or harvesting, will likely decrease interception loss, but the change will be moderated by the change in canopy aerodynamic resistance that will help facilitate evaporation.

Conversion of forests from one type to another can also alter rainfall amount of canopy water storage (Table 18.1) and interception loss. For example, Swank and Douglass (1974) report that the conversion from deciduous forests to coniferous forests reduced stemflow and streamflow. In this case, the more erectophile leaf orientation of deciduous trees may have reduced interception relative to the more planophile needles of pine trees. Furthermore, the more vertical branch structure of deciduous trees likely altered the amount of rainfall that is converted into stemflow (see Sect. 18.3.2).

18.3 Canopy Structure and Net Precipitation Distribution

18.3.1 Throughfall

Forest canopies modify both the amount and the horizontal distribution of net precipitation (throughfall and stemflow). As a result of this redistribution, the input of water to the forest floor is characterized by large spatial variability. By the nature of the throughfall process, its spatial variation is explicitly linked to canopy structure. Stemflow contributes little to net precipitation, but is a spatially concentrated water flux across a small area around the boles (see Sect. 18.3.2).

Large within-stand variations in throughfall water have been observed in forests (e.g., Staelens et al. 2006b; Wullaert et al. 2009). The degree of spatial variation seems to depend mainly on the canopy complexity and rainfall depth (see Sect. 18.3.3). Locally, throughfall can exceed incoming gross precipitation, while other parts of the forest floor receive considerably less throughfall. Sampling points where throughfall exceeds the precipitation input have most frequently been reported for tropical rain forests (e.g., Lloyd and Marques Filho 1988). Throughfall data often do not correspond to a normal distribution, and hence require nonparametric statistical tests and measures of spatial variation (Zimmermann et al. 2007) and a careful application of geostatistical analyses. Stable spatial throughfall patterns throughout time, as assessed using time-averaged relative differences to the mean, correlation analysis, and geostatistical variograms, have been observed beneath lowland tropical canopies (e.g., Lloyd and Marques Filho 1988; Wullaert et al. 2009), evergreen coniferous canopies (e.g., Beier et al. 1993; Keim et al. 2005) and broadleaved deciduous canopies during the leafed season but not during the leafless season (Keim et al. 2005; Staelens et al. 2006b).

Temporal stability of spatial throughfall patterns indicates that canopy structure is an important controlling factor of these patterns. Direct empirical relationships between spatial throughfall and local canopy structure have less frequently been reported, but an inverse relationship between canopy density or cover and the amount of throughfall at individual soil points has been observed in several forest types (e.g., Loescher et al. 2002; Nadkarni and Sumera 2004). Throughfall has also been related indirectly to canopy architecture by accounting for the gauge position such as distance to the nearest stem (Beier et al. 1993; Robson et al. 1994). Compared to coniferous forests, relatively little is known on the relationship between the small-scale variability of throughfall and canopy structure for deciduous forests. Nevertheless, broadleaved deciduous canopies have been shown to influence throughfall patterns during the leafed season (Keim et al. 2005; Staelens et al. 2006b). Lower throughfall corresponded to higher LAI values in a resprouted holm-oak forest, but the difference between four LAI classes was not significant (Bellot and Escarre 1998). In contrast, throughfall was not related to plant area index ($m^2 \ m^{-2}$) in two red oak forests (Carlyle-Moses et al. 2004). In the tropics, temporal persistence is highly variable, with some forests exhibiting stability for portions of the growing season (e.g., Zimmermann and lsenbeer 2008). The multiple layers within the forest canopy and differences in canopy phenology may complicate throughfall patterns in tropical forests (e.g., Germer et al. 2006; Zimmermann et al. 2009; Zimmermann and lsenbeer 2008).

18.3.2 Stemflow

Canopy structure governs stemflow drainage to a large extent in wooded ecosystems. Canopy structural parameters such as projected crown area, stand density, and basal area have been found to affect stemflow yield (Ford and Deans 1978; Crockford and Richardson 2000; Park and Hattori 2002). Stemflow production was observed to increase with larger projected crown areas for trees in Sitka spruce plantations and laurel forest (Ford and Deans 1978; Aboal et al. 1999). Canopy gaps tend to increase stemflow yield by increasing the exposure of woody surfaces (Crockford and Richardson 2000); in fact, trees overshadowed by neighbors produced significantly less stemflow than those neighboring trees with more prominent canopy positions (Aboal et al. 1999). In Japan, larger trees, with greater basal areas at breast height and projected crown areas, were found to produce more stemflow than smaller trees (Park and Hattori 2002).

The geometric orientation of branches has been found to dramatically alter stemflow yield (Levia and Frost 2003). Tree species with erectophile branching patterns and smooth bark, such as *Fagus sylvatica* L. (European beech), produce much larger stemflow volumes than those with plagiophile branching patterns and rougher bark, such as *Quercus petraea* Liebl (sessile oak) (André et al. 2008a). It has been suggested that the shape of the canopy can control distribution of stemflow around the base of a tree. For example, Liang et al. (2009) found stemflow

Table 18.2 Mean stemflow funneling ratios (±1 std. error) in relation to basal area at two forested sites in Japan and within semiarid thornscrub vegetation in Mexico[a,b]

		Shirasaka	Yamashiro	Návar (1993)
SFW/BA	Mean	61.3	55.6	34.5
	Std. error	23.3	13.2	5.9
BA (m^2)	Mean	0.0159	0.0082	0.0081

[a]Adapted from Park and Hattori (2002)
[b]*SFW* stemflow/gross precipitation and *BA* basal area

to be greatest on the downslope side of tall stewartia (*Stewartia monadelpha*) trees on a hillslope in Japan. Liang et al. (2009) suggest that this resulted from uneven canopy distributions and asymmetrical flow paths down the stem.

Stemflow funneling ratios also have been observed to change dramatically as a function of tree age and branching architecture in *Chamaecyparis obtusa* (Siebold and Zucc.) Endl. (Japanese cypress) stands (Murakami 2009). Stemflow funneling ratios decreased from 81 at age 9 to 30 at age 10 (Murakami 2009). This drastic change in stemflow funneling was attributed to a sudden change in branching architecture as the canopy approached crown closure (Murakami 2009). At the forested site in Shirasaka, mean stemflow funneling ratios and mean tree basal areas were larger than that recorded for Yamashiro (Park and Hattori 2002) (Table 18.2). Comparing the site at Yamashiro with the Mexican site of Návar (1993), it is evident that stemflow funneling ratios were almost double at Yamashiro, despite similar basal areas (Table 18.2). These differences are likely the result of different branching architectures, thereby underscoring the fact that the canopy structural characteristics that affect stemflow yield are complex and polycausal and must be examined holistically.

Orthogonally projected branch area differs from total branch area and has direct implications on stemflow yield. Steeper branch inclination angles may promote stemflow drainage from the crowns of trees but, a tipping-point likely exists at where steeper branch inclination angles result in decreased orthogonally projected branch area and reduced stemflow (Levia and Frost 2003). The tradeoff between capture efficiency and stemflow generation as a function of branch inclination angle, orthogonally projected branch area, and total branch area is not well understood. Experimental work by Herwitz (1987) demonstrated the interplay between branch inclination angle and stemflow production, observing increased splash loss for branches inclined <45° above the horizontal.

Brown and Barker (1970) found that stemflow generation differed from two oaks with differing bark textures [*Quercus velutina* Lam. (black oak) and *Quercus alba* L. (white oak)]. The tight-barked black oak group produced much larger quantities of stemflow than the flaky-barked white oak group. The vast majority of other studies examining differential stemflow yield from smooth- and rough-barked trees also have documented that smooth-barked trees produce larger stemflow yields than rough-barked trees (Levia and Frost 2003). Levia et al. (2010) discovered earlier and more voluminous stemflow generation for smooth-barked *Fagus grandifolia* Ehrh. (American beech) trees than rough-barked *Liriodendron tulipifera* L. (yellow poplar)

trees as a result of lower bark water storage capacities. *F. grandifolia* trees were also more responsive to changes in rainfall intensities (Levia et al. 2010). Because bark morphology also differs intraspecifically, as a function of tree size and age (Van Stan and Levia 2010), and along the vertical profile of individual trees (Levia and Wubbena 2006), stemflow yield has been found to differ along the vertical profile of individual trees (Hutchinson and Roberts 1981; Kuraji et al. 2001). The upper half of the canopy of an experimental conifer was observed to generate 98% of the stemflow (Hutchinson and Roberts 1981). Kuraji et al. (2001) also noted differences between the stemflow yield of the canopy and stem as opposed to just the tree stem.

18.3.3 Rainfall Intensity and Event Size

In addition to the canopy structure, meteorological conditions and precipitation characteristics affect the partitioning and spatial redistribution of rainfall (Keim et al. 2005; Staelens et al. 2006b; Zimmermann et al. 2007). Forest canopies affect the horizontal pattern of net precipitation by spatial variations in water storage and by redistribution processes, which depend also on rainfall intensity and event size. Rainfall interception is relatively largest during small rain events (e.g., Horton 1919) and the variability of throughfall usually declines with increasing rainfall volume until a certain threshold (Levia and Frost 2006; Staelens et al. 2006b). Likewise, the relationship of throughfall with canopy structure can be more pronounced for small rainfall events than for larger events (Staelens et al. 2006b). Once the local water storage capacity of the canopy is saturated, evaporation of temporary intercepted rain water contributes less to spatial throughfall variations. In addition, canopy water storage is likely to be affected by rainfall intensity (Calder et al. 1996; Price and Carlyle-Moses 2003) and wind speed (Hörmann et al. 1996), although the physical interpretation of canopy storage values that are estimated by calibrating interception models has been questioned (Vrugt et al. 2003; Keim 2004).

Methods for directly quantifying canopy water storage using microwaves (Bouten et al. 1991) or gamma rays (Calder and Wright 1986) are available, but the equipment is currently uncommon or expensive. Alternatively, researchers have also quantified canopy water by weighing whole trees (e.g., Aston 1979) or individual branches (e.g., Hancock and Crowther 1979; Pypker et al. 2006b). These methods may help to clarify the accuracy of interception models.

18.4 Canopy Structure and Biogeochemistry

18.4.1 Throughfall

Like the flow of water, matter transport in forests typically shows considerable spatial heterogeneity. In addition to the heterogeneity of stemflow inputs (see

Sect. 4.3), canopy architecture can contribute to a systematic component of the spatial input of dissolved elements via throughfall. Also in mixed-species forest stands, throughfall has been shown to be the main source of heterogeneity in nutrient input (Hojjati et al. 2009). Similar to the water volume, spatial canopy effects on throughfall solute deposition patterns can be assessed indirectly from their temporal persistence. Spatial deposition patterns have also been related to the distance to the nearest tree or directly to measured local canopy characteristics.

The temporal spatial stability of solute inputs via throughfall has been reported, amongst others, for tropical and temperate forest types (e.g., Whelan et al. 1998; Zimmermann et al. 2007). Within coniferous forests, throughfall ion depositions are generally higher close to the stem, which has been explained by higher canopy densities near the stem (Seiler and Matzner 1995). Such a stem-basis-related approach is more useful for trees with approximately circular crown than for more heterogeneous canopy structures. Direct relationships between local canopy architecture and the small-scale chemical composition of throughfall have been reported for *Picea abies* (Karst) L. (Norway spruce) (e.g., Whelan et al. 1998), *Picea mariana* (Mill.) B.S.P. (black spruce) (Carleton and Kavanagh 1990), European beech (Staelens et al. 2006a), and mixed beech-oak stands (André et al. 2008b).

The spatial variation of solute concentrations in throughfall often exceeds that of solute depositions because of the frequent negative correlation between the throughfall volume and solute concentrations that is caused by dilution effects (e.g., Lawrence and Fernandez 1993). In general, the spatial heterogeneity of solute depositions is larger than that of throughfall volume, while its temporal persistence is lower. Two main driving factors that affect the heterogeneity of throughfall composition are wash-off of dry deposition and canopy exchange processes (see Chap. 17). Similar spatial patterns and positive relationships with measures of canopy density have been found for throughfall solutes associated with dry deposition and canopy leaching, as both processes depend on the amount of foliage, branches (Staelens et al. 2006a), and other canopy elements such as epiphytes (see Sect. 18.4.4). In contrast to other ions, the proton flux in throughfall is often negatively correlated with canopy density due to various acid neutralizing processes within the canopy (Staelens et al. 2006a). In leafless deciduous forests, the spatial variation of throughfall deposition is still affected by tree branching structures, and the heterogeneity of the fluxes then may be as large as during leafed canopy conditions (Duijsings et al. 1986; Staelens et al. 2006a).

18.4.2 Forest Edge Effects

The spatial variation of throughfall water and solutes within forest stands has also been related to distance to the forest edge. The edge between a forested and nonforested area can have important effects on microclimate, plant regeneration and biodiversity, and also affects nutrient fluxes. Many nutrients and pollutants are delivered to

ecosystems via atmospheric transport and consequent wet, dry, or occult deposition (see Chap. 17). Because of the steep transition in vegetation height at most forest edges, air flow is disrupted, and canopy wind speed and air turbulence are enhanced at the edge, thus enhancing dry deposition of particles and gases at the forest edge. Consequently, forest edges have been shown to act as "hotspots" of deposition, with up to fourfold increase in the rate of atmospheric delivery compared with nearby areas without edges (e.g., De Schrijver et al. 2007). In contrast, to enhanced dry deposition at edges, edge effects on wet deposition have rarely been observed (e.g., Wuyts et al. 2008). In addition to an increase in dry deposition, edge gradients in forest structure, soil, microclimate, and precipitation can alter nutrient fluxes via throughfall in forest edges as well (e.g., by modifying the ion exchange capacity of the canopy). However, the depth of the forest edge effect on air turbulence and the associated deposition processes generally extends the depth of other edge effects.

18.4.3 Stemflow

The effects of canopy structure on the wash off of dry deposition and leaching by stemflow are poorly understood. In fact, only one known study has linked stemflow leachate chemistry to branch inclination angle. Using a set of experimental branches harvested from recently felled trees, Levia and Herwitz (2002) found that the leaching and total nutrient input of some base cations were larger from branches inclined at $20°$ than at $5°$ or $38°$ above the horizontal. It was surmised that branches inclined at $20°$ achieved an optimal balance between the residence time of the intercepted precipitation on the branch surface and branchflow volume because of: (1) the lengthened contact time of intercepted precipitation with the branch surface vis-à-vis branch inclined at $38°$; (2) a decreased likelihood of branch drip compared to the branches inclined at $5°$; and (3) insignificant differences in branchflow volume generated in comparison with the branches inclined at $38°$ (Levia and Herwitz 2002). Forest stand density (and branch density, presumably) has been found to affect stemflow chemistry in subalpine balsam fir forests. In a study relating stand density to elemental cycling, Olson et al. (1981) found that the stemflow fluxes of NH_4^+, Na^+, SO_4^{2-}, and Cl^- increased with stand density.

Bark roughness also appears to affect the concentration of leachates from bark surfaces of canopy trees. Deciduous tree species with coarse bark texture, such as *Carya glabra* Mill. (pignut hickory), were observed to have larger concentrations of base cation leachates than trees with somewhat smoother bark (Parker 1983; Levia and Herwitz 2000). Tree species with coarser bark textures have higher nutrient-ion concentrations than those with smoother bark textures because of a prolonged contact time of stemflow with the bark surface. Total nutrient flux, however, may be lower from the rougher-barked trees compared to smooth-barked trees because of lower stemflow yields (Levia and Herwitz 2002).

18.4.4   Epiphytes

Epiphytes can store up to 45% of the nutrients in a forested system (e.g., Nadkarni 1984) and therefore they have the potential to alter the flux of nutrients to the forest floor. During precipitation events epiphytes can remove between 50 and 90% of the nitrogen, phosphorus and potassium in the rainfall prior to it reaching the forest floor (e.g., Clark et al. 1998b). Given their ability to both store and alter the flow paths of water, epiphytes likely play a major role in both the spatial distribution and quantity of nutrients reaching the forest floor. To complicate things, epiphytes may also provide nutrients to the forest floor because some lichen species contain blue-green algae that fix atmospheric N_2. There is also evidence that living epiphytes "leak" nutrients after being rehydrated following an extended dry period (Coxson 1991) and dead epiphytes/canopy litter (Clark et al. 1998a) will release nutrients to the forest floor during storm events. Hölscher et al. (2003) found that stemflow K^+ fluxes were larger for mid-successional tropical forests than old-growth tropical forests. They attributed the differences to longer horizontal branches and larger epiphyte loads of the older forests that would have initiated drip and lowered stemflow production and K^+ flux. Hence, the impact of epiphytes on nutrient cycling may be more complex, as they likely alter the quantity, distribution, and timing of nutrient inputs into the forest floor.

18.5   Future Research Needs

18.5.1   Future Needs for Hydrology and Canopy Structure

Local canopy structure has been shown to cause persistent spatial throughfall patterns in different forest types throughout the world. The potential effects of these patterns on ecological processes in the forest floor and beyond (e.g., microbiological processes) have been reported less frequently, and until now, mainly for coniferous forests (e.g., Manderscheid and Matzner 1995). However, a systematic component of spatial throughfall patterns occurs beneath temperate deciduous and tropical canopies as well, and more research is needed to quantify the extent and ecological consequences of time-persistent spatial throughfall patterns in different forest types. Future research on the effect of canopy structure and micrometeorological conditions (wind speed, rainfall intensity, and storm size) on spatial throughfall is also needed (Keim 2004; Staelens et al. 2006b).

The flow paths of rainfall through the forest canopy require further attention. Water likely follows preferential flow paths through the forest canopy. How preferential flow alters the residence time of water in the forest canopy, the timing of canopy saturation, the spatial distribution of canopy drip, or its impact on models that assume complete saturation of the canopy prior to drip is not understood. Furthermore, forest canopies attenuate the rainfall intensity at the forest floor (e.g., Keim et al. 2006b). Further research is needed to understand how changes in forest canopy structure will affect soil stability and erosion.

Examining the spatial relationship between net precipitation and the forest canopy requires reliable measurements of the local canopy structure. One possible parameter is the fraction of ground overlaid by canopy elements (canopy cover) above throughfall sampling points, determined in varying zenith angles, and the local leaf, wood or plant area index. However, these parameters do not incorporate the complex structural arrangement and connectivity of vegetation elements that affect throughfall. Therefore, more detailed measurements of three-dimensional canopy architecture are needed. For example, the use of light ranging and detection (LiDAR) techniques may be fruitful (e.g., Parker et al. 2004a). Alternatively, Nadkarni and Sumera (2004) used vertical canopy cylinder transects to quantify the distribution of canopy elements, but this approach requires direct access to the canopy. Finally, it would be beneficial to build upon current models that describe the effect of canopy structure on rainfall interception (e.g., Davie and Durocher 1997).

Bark morphology has been shown to impact both hydrological and biogeochemical fluxes. The LaserBark™ automated tree measurement system can be employed to characterize bark microrelief at unprecedented scales, yielding submillimeter spatial data of the bark surface (see Van Stan et al. 2010). With this system, Van Stan and Levia (2010) demonstrated that differences in bark microrelief between smooth- and rough-barked tree species and within species had detectable effects on stemflow yield. Future work with the Laserbark™ automated tree measurement system could supply further quantitative insights into the effects of differing bark morphology on lichen and bryophyte distribution and corresponding alterations in canopy and interception storage capacities.

18.5.2 Future Needs for Biogeochemistry and Canopy Structure

Relatively little is known about the effects of three-dimensional forest canopy structure on dry deposition and canopy exchange processes and the intra-system forest biogeochemical cycle. Research must be directed to the improved understanding of branch inclination angle, orthogonally projected surface area, and total surface area of canopy surfaces on the cycling of nutrient ions and pollutants to the forest floor. Anecdotally, one would expect the scavenging efficiency of pollutants to change as a function of season in deciduous forests (see Chap. 26). But what impact does the presence or absence of leaves have on the capture and routing of pollutants to the subcanopy? Does the cycling of dry deposited pollutants differ as a function of branch inclination angle, orthogonally projected surface area, or total surface area of individual trees and/or forest canopies? Do throughfall and stemflow processes consistently deposit pollutants in any particular localized area of the forest floor, or do these subcanopy net precipitation inputs change among discrete storm events as a function of season or meteorological conditions (i.e., wind speed or wind direction)? Do epiphytes decrease the pollutant load to the forest floor? Answers to these questions will yield insights into the effects of

canopy structure on element cycling in forested areas. The increasing presence and areal extent of forest fragments in urbanizing and suburbanizing landscapes makes such investigations timely and of increasing relevance to environmental policy.

The impact and effects of canopy structure on the chemical character of snowmelt is poorly understood (see Chap. 26). The persistence of intercepted snow on trees and forests with markedly different canopy structures presents the scientific community with a set of interesting questions related to the biogeochemical transfer of solutes and particulate matter to the subcanopy via throughfall and stemflow. The effects of throughfall and stemflow on snowpack chemistry are of importance because of the "acid flush" and the fractionation and preferential elution of nutrient ions and organic pollutants from a melting snowpack. An improved process-based understanding of the influence of canopy structure on snowmelt and elemental cycling would improve hydrologic and nutrient cycling models that aim to predict the timing and magnitude of the "acid flush" that corresponds with the melting of seasonal snowpacks.

At the scale of individual tree boles, the alteration of stemflow chemistry along the vertical profile of the bole likely has a detectable and significant effect on the distribution of corticolous lichens and bryophytes that can have a notable impact on forest biogeochemistry (Knops et al. 1996; Hauck et al. 2002; Levia 2002). Further understanding of the spatial distribution of bryophytes on tree surfaces as a function of bark microrelief is of particular importance since lichens are used as indicator organisms for pollutant levels. How does bark microrelief affects the presence and spatial distribution of lichens and bryophytes on tree boles? No known work has coupled precise measurements of bark microrelief with the distribution of bryophytes along the tree bole.

18.6 Conclusions

Though much research has been conducted on rainfall interception and biogeochemical fluxes, we are still unclear of the role of canopy structure on these processes. Past research has demonstrated that changes in leaf shape, forest age, epiphyte load, bark morphology, organic matter, and dead wood are all correlated to changes in water storage capacity and rainfall interception loss. Furthermore, the distribution of rainfall is controlled by factors such as canopy density, branch orientation, bark morphology, rainfall intensity, and forest type. All of these elements change as a forest ages, thereby making rainfall interception dynamic through time. Similar to hydrologic fluxes, biogeochemical fluxes depend on canopy structure. We described how canopy density and forest type, forest edges, stem flow and bark morphology and epiphytes all play a role in the quantity and spatial distribution of biogeochemical fluxes. Perhaps more important, we provide numerous topics that still need to be explored if are to better understand the role of canopy structure in hydrologic and biogeochemical fluxes in forest communities.

References

Aboal JR, Morales D, Hernández M et al (1999) The measurement and modelling of the variation of stemflow in a laurel forest in Tenerife, Canary Islands. J Hydrol 221:161–175

André F, Jonard M, Ponette Q (2008a) Influence of species and rain event characteristics on stemflow volume in a temperate mixed oak-beech stand. Hydrol Process 22:4455–4466

André F, Jonard M, Ponette Q (2008b) Spatial and temporal patterns of throughfall chemistry within a temperate mixed oak-beech stand. Sci Total Environ 397:215–228

André F, Jonard M, Ponette Q (2008c) Precipitation water storage capacity in a temperate mixed oak-beech canopy. Hydrol Proc 22:4130–4141

Asner GP, Keller M, Silva JNM (2004) Spatial and temporal dynamics of forest canopy gaps following selective logging in the eastern Amazon. Glob Change Biol 10:765–783

Aston AR (1979) Rainfall interception by eight small trees. J Hydrol 42:383–396

Beier C, Hansen K, Gundersen P (1993) Spatial variability of throughfall fluxes in a spruce forest. Environ Pollut 81:257–267

Bellot J, Escarre A (1998) Stemflow and throughfall determination in a resprouted Mediterranean holm-oak forest. Ann Sci For 55:847–865

Blum OB (1973) Water relations. In: Ahmadjian V, Hale ME (eds) The lichens. Academic Press, New York, pp 381–400

Bouten W, Swart PJF, DeWater E (1991) Microwave transmission, a new tool in forest hydrological research. J Hydrol 124:119–130

Brown JH, Barker A Jr (1970) An analysis of throughfall and stemflow in mixed oak stands. Water Resour Res 6:316–323

Calder IR, Wright IR (1986) Gamma ray attenuation studies of interception from sitka spruce: some evidence for and additional transport mechanism. Water Resour Res 22:409–417

Calder IR, Hall RL, Rosier PTW et al (1996) Dependence of rainfall interception on drop size: 2. Experimental determination of the wetting functions and two -layer stochastic model parameters for five tropical tree species. J Hydrol 185:379–388

Carleton TJ, Kavanagh T (1990) Influence of stand age and spatial location on throughfall chemistry beneath black spruce. Can J For Res 20:1917–1925

Carlyle-Moses DE, Laureano JSF, Price AG (2004) Throughfall and throughfall spatial variability in Madrean oak forest communities of northeastern Mexico. J Hydrol 297:124–135

Clark DL, Nadkarni NM, Gholz HL (1998a) Growth, net production, litter decomposition, and net nitrogen accumulation by epiphytic bryophytes in a tropical montane forest. Biotropica 30:12–23

Clark KL, Nadkarni NM, Schaefer D et al (1998b) Atmospheric deposition and net retention of ions by the canopy in a tropical montane forest, Monteverde, Costa Rica. J Trop Ecol 14:27–45

Coxson DS (1991) Nutrient release from epiphytic bryophytes in tropical montane rain-forest (Guadeloupe). Can J Bot 69:2122–2129

Crockford RH, Richardson DP (2000) Partitioning of rainfall into throughfall, stemflow and interception: effect of forest type, ground cover and climate. Hydrol Process 14:2903–2920

Davie TJA, Durocher MG (1997) A model to consider the spatial variability of rainfall partitioning within deciduous canopy 1. Model description. Hydrol Process 11:1509–1523

De Schrijver A, Devlaeminck R, Mertens J et al (2007) On the importance of incorporating forest edge deposition for evaluating exceedance of critical pollutant loads. Appl Veg Sci 10:293–298

Duijsings J, Verstraten JM, Bouten W (1986) Spatial variability in nutrient deposition under an oak beech canopy. Z Pflanzenernähr Bodenkd 149:718–727

Ford ED, Deans JD (1978) The effects of canopy structure on stemflow, throughfall and interception loss in a young sitka spruce plantation. J Appl Ecol 15:905–917

Franklin JF, Spies TA, Pelt RV et al (2002) Disturbances and structural development of natural forest ecosystems with silvicultural implications, using Douglas-fir forests as an example. For Ecol Manage 155:399–423

Gash JHC, Morton AJ (1978) An application of the Rutter model to the estimation of the interception loss from Thetford forest. J Hydrol 38:49–58

Gash JHC, Lloyd CR, Lachaud G (1995) Estimating sparse forest rainfall interception with an analytical model. J Hydrol 170:79–86

Germer S, Elsenbeer H, Moraes JM (2006) Throughfall and temporal trends of rainfall redistribution in an open tropical rainforest, south-western Amazonia (Rondonia, Brazil). Hydrol Earth Syst Sci 10:383–393

Grah RF, Wilson CC (1944) Some components of rainfall interception. J For 42:890–898

Hancock NH, Crowther JM (1979) A technique for the direct measurement of water storage on a forest canopy. J Hydrol 41:105–122

Hauck M, Hesse V, Runge M (2002) The significance of stemflow chemistry for epiphytic lichen diversity in a dieback-affected spruce forest on Mt. Brocken, northern Germany. Lichenologist 34:415–427

Herwitz SR (1985) Interception storage capacities of tropical rainforest canopy trees. J Hydrol 77:237–252

Herwitz SR (1987) Raindrop impact and water-flow on the vegetative surfaces of trees and the effects on stemflow and throughfall generation. Earth Surf Proc Landforms 12:425–432

Hojjati S, Hagen-Thorn A, Lamersdorf N (2009) Canopy composition as a measure to identify patterns of nutrient input in a mixed European beech and Norway spruce forest in central Europe. Eur J For Res 128:13–25

Hölscher D, Kohler L, Leuschner C et al (2003) Nutrient fluxes in stemflow and throughfall in three successional stages of an upper montane rain forest in Costa Rica. J Trop Ecol 19:557–565

Hölscher D, Köhler L, van Dijk AIJM et al (2004) The importance of epiphytes to total rainfall interception by a tropical montane rain forest in Costa Rica. J Hydrol 292:308–322

Hörmann G, Branding A, Clemen T et al (1996) Calculation and simulation of wind controlled canopy interception of a beech forest in Northern Germany. Agric For Meteorol 79:131–148

Horton RE (1919) Rainfall interception. Monthly Weather Review 47:603–623

Hutchinson I, Roberts MC (1981) Vertical variation in stemflow generation. J Appl Ecol 18:521–527

Ingram SW, Nadkarni NM (1993) Composition and distribution of epiphytic organic-matter in a neotropical cloud forest, Costa-Rica. Biotropica 25:370–383

Keim RF (2004) Comment on "Measurement and modeling of growing-season canopy water fluxes in a mature mixed deciduous forest stand, southern Ontario, Canada". Agric For Meteorol 124:277–279

Keim RF, Skaugset AE, Weiler M (2005) Temporal persistence of spatial patterns in throughfall. J Hydrol 314:263–274

Keim RF, Skaugset AE, Weiler M (2006a) Storage of water on vegetation under simulated rainfall of varying intensity. Adv Water Res 29:974–986

Keim RF, Tromp-van Meerveld H, McDonnell J (2006b) A virtual experiment on the effects of evaporation and intensity smoothing by canopy interception on subsurface stormflow generation. J Hydrol 327:352–364

Kira T, Schinozaki K, Hozumi K (1969) Structure of forest canopies as related to their primary productivity. Plant Cell Physiol 10:129–142

Knops JMH, Nash TH, Schlesinger WH (1996) The influence of epiphytic lichens on the nutrient cycling of an oak woodland. Ecol Monogr 66:159–179

Köhler L, Tobon C, Frumau KFA et al (2007) Biomass and water storage dynamics of epiphytes in old-growth and secondary montane cloud forest stands in Costa Rica. Plant Ecol 193:171–184

Köhler L, Hölscher D, Leuschner C (2008) High litterfall in old-growth and secondary upper montane forest of Costa Rica. Plant Ecol 199:163–173

Kuraji K, Punyatrong K, Suzuki M (2001) Altitudinal increase in rainfall in the Mae Chaem watershed, Thailand. J Meteorol Soc Jpn 79:353–363

Lawrence GB, Fernandez IJ (1993) A reassessment of areal variability of throughfall deposition measurements. Ecol Appl 3:473–480

Levia DF (2002) Nitrate sequestration by corticolous macrolichens during winter precipitation events. Int J Biometeorol 46:60–65

Levia DF, Frost EE (2003) A review and evaluation of stemflow literature in the hydrologic and biogeochemical cycles of forested and agricultural ecosystems. J Hydrol 274:1–29

Levia DF, Frost EE (2006) Variability of throughfall volume and solute inputs in wooded ecosystems. Prog Phys Geogr 30:605–632

Levia DF, Herwitz SR (2000) Physical properties of water in relation to stemflow leachate dynamics: implications for nutrient cycling. Can J For Res 30:662–666

Levia DF, Herwitz SR (2002) Winter chemical leaching from deciduous tree branches as a function of branch inclination angle in central Massachusetts. Hydrol Process 16:2867–2879

Levia DF, Herwitz SR (2005) Interspecific variation of bark water storage capacity of three deciduous tree species in relation to stemflow yield and solute flux to forest soils. Catena 64:117–137

Levia DF, Wubbena NP (2006) Vertical variation of bark water storage capacity of *Pinus strobus* L. (Eastern white pine) in southern Illinois. Northeast Nat 13:131–137

Levia DF, Van Stan JT, Mage SM et al (2010) Temporal variability of stemflow volume in a beech-yellow poplar forest in relation to tree species and size. J Hydrol 380:112–120

Leyton L, Reynolds ERC, Thompson FB (1967) Rainfall interception in forest and moorland. In: Sopper WE, Lull HW (eds) International symposium on forest hydrology. Pergamon Press, New York, pp 163–178

Liang WL, Kosugi K, Mizuyama T (2009) Characteristics of stemflow for tall stewartia (*Stewartia monadelpha*) growing on a hillslope. J Hydrol 378:168–178

Link TE, Unsworth MH, Marks D (2004) The dynamics of rainfall interception by a seasonal temperate rainforest. Agric For Meteorol 124:171–191

Llorens P, Gallart F (2000) A simplified method for forest water storage capacity measurement. J Hydrol 240:131–144

Lloyd CR, Marques Filho AO (1988) Spatial variability of throughfall and stemflow measurements in Amazonian rainforest. Agric For Meteorol 42:63–72

Loescher HW, Powers JS, Oberbauer SF (2002) Spatial variation of throughfall volume in an old-growth tropical wet forest, Costa Rica. J Trop Ecol 18:397–407

Manderscheid B, Matzner E (1995) Spatial heterogeneity of soil solution chemistry in a mature Norway spruce (*Picea abies* (L) Karst) stand. Water Air Soil Pollut 85:1185–1190

McCune B (1993) Gradients in epiphyte biomass in three *Pseudotsuga-Tsuga* forests of different ages in Western Oregon and Washington. Bryologist 96:405–411

McCune B, Amsberry KA, Camacho FJ et al (1997) Vertical profile of epiphytes in Pacific Northwest old-growth forest. Northwest Sci 71:145–152

Murakami S (2009) Abrupt changes in annual stemflow with growth in a young stand of Japanese cypress. Hydrol Res Lett 3:32–35

Nadkarni NM (1984) Epiphyte biomass and nutrient capital of a neotropical elfin forest. Biotropica 16:249–256

Nadkarni NM, Sumera MM (2004) Old-growth forest canopy structure and its relationship to throughfall interception. For Sci 50:290–298

Návar J (1993) The causes of stemflow variation in 3 semiarid growing species of Northeastern Mexico. J Hydrol 145:175–190

Olson RK, Reiners WA, Cronan CS et al (1981) The chemistry and flux of throughfall and stemflow in subalpine balsam fir forests. Holarct Ecol 4:291–300

Park H, Hattori S (2002) Applicability of stand structural characteristics to stemflow modeling. J For Res 7:91–98

Parker GG (1983) Throughfall and stemflow in the forest nutrient cycle. Adv Ecol Res 13:57–133

Parker GG, Harding DJ, Berger ML (2004a) A portable LIDAR system for rapid determination of forest canopy structure. J Appl Ecol 41:755–767

Parker GG, Harmon ME, Lefsky MA et al (2004b) Three dimensional structure of an old-growth *Pseudosuga-Tsuga* canopy and its implications for radiation balance, microclimate, and atmospheric gas exchange. Ecosystems 7:440–453

Price AG, Carlyle-Moses DE (2003) Measurement and modelling of growing-season canopy water fluxes in a mature mixed deciduous forest stand, southern Ontario, Canada. Agric For Meteorol 119:69–85

Proctor MCF (2000) Physiological ecology. In: Shaw AJ, Goffinet B (eds) Bryophyte biology. Cambridge University Press, Cambridge, pp 225–247

Pypker TG, Bond BJ, Link TE et al (2005) The importance of canopy structure in controlling the interception loss of rainfall: examples from a young and old-growth Douglas-fir forests. Agric For Meteorol 130:113–129

Pypker TG, Unsworth MH, Bond BJ (2006a) The role of epiphytes in rainfall interception by forests in the Pacific Northwest I. Laboratory measurements of water storage. Can J For Res 36:808–818

Pypker TG, Unsworth MH, Bond BJ (2006b) The role of epiphytes in rainfall interception by forests in the Pacific Northwest II. Field measurements at the branch and canopy scale. Can J For Res 36:819–832

Robson AJ, Neal C, Ryland GP et al (1994) Spatial variations in throughfall chemistry at the small plot scale. J Hydrol 158:107–122

Rutter AJ, Kershaw KA, Robins PC et al (1971) A predictive model of rainfall interception in forests I. Derivation of the model from observations in a plantation of corsican pine. Agric Meteorol 9:367–384

Seiler J, Matzner E (1995) Spatial variability of throughfall chemistry and selected soil properties as influenced by stem distance in a mature Norway spruce (*Picea abies*, Karst) stand. Plant Soil 176:139–147

Staelens J, De Schrijver A, Verheyen K et al (2006a) Spatial variability and temporal stability of throughfall deposition under beech (*Fagus sylvatica* L.) in relationship to canopy structure. Environ Pollut 142:254–263

Staelens J, De Schrijver A, Verheyen K et al (2006b) Spatial variability and temporal stability of throughfall water under a dominant beech (*Fagus sylvatica* L.) tree in relationship to canopy cover. J Hydrol 330:651–662

Swank WT, Douglass JE (1974) Streamflow greatly reduced by converting deciduous hardwood stands to white pine. Science 185:857–859

Teklehaimanot Z, Jarvis PG, Ledger DC (1991) Rainfall interception and boundary layer conductance in relation to tree spacing. J Hydrol 123:261–278

van Leerdam A, Zagt RJ, Veneklaas EJ (1990) The distribution of epiphyte growth-forms in the canopy of a Colombian cloud-forest. Vegetations 87:59–71

Van Stan JT, Levia DF (2010) Inter- and intraspecific variation of stemflow production from *Fagus grandifolia* Ehrh. (American beech) and *Liriodendron tulipifera* L. (yellow poplar) in relation to bark microrelief in the eastern United States. Ecohydrology 3:11–19

Van Stan JT, Jarvis MT, Levia DF (2010) An automated instrument for the measurement of bark microrelief. IEEE Trans Instrum Meas 59:491–493

Vrugt JA, Dekker SC, Bouten W (2003) Identification of rainfall interception model parameters from measurements of throughfall and forest canopy storage. Water Resour Res 39:1251

Whelan MJ, Sanger LJ, Baker M et al (1998) Spatial patterns of throughfall and mineral ion deposition in a lowland Norway spruce (*Picea abies*) plantation at the plot scale. Atmos Environ 32:3493–3501

Wullaert H, Pohlert T, Boy J et al (2009) Spatial throughfall heterogeneity in a montane rain forest in Ecuador: extent, temporal stability and drivers. J Hydrol 377:71–79

Wuyts K, De Schrijver A, Staelens J et al (2008) Comparison of forest edge effects on throughfall deposition in different forest types. Environ Pollut 156:854–861

Yavitt JB, Battles JJ, Lang GE et al (1995) The canopy gap regime in a secondary neotropical forest in Panama. J Trop Ecol 11:391–402

Zimmermann BE, lsenbeer H (2008) Spatial and temporal variability of soil saturated hydraulic conductivity in gradients of disturbance. J Hydrol 361:78–95

Zimmermann A, Wilcke W, Elsenbeer H (2007) Spatial and temporal patterns of throughfall quantity and quality in a tropical montane forest in Ecuador. J Hydrol 343:80–96

Zimmermann A, Zimmermann BE, lsenbeer H (2009) Rainfall redistribution in a tropical forest: spatial and temporal patterns. Water Resour Res 45:W11413

Zinke PJ (1967) Forest interception studies in the United States. In: Sopper WE, Lull HW (eds) International symposium on forest hydrology. Pergamon Press, New York, pp 137–161

Chapter 19
Transpiration in Forest Ecosystems

Tomo'omi Kumagai

19.1 Introduction

Water molecules having sufficient kinetic energy escape from the surface of liquid water to the air, while water molecules in vapor form return from the air to a liquid state. When the rates of escaping and returning water molecules are the same, the process is said to be in an equilibrium status with no net evaporation from the water surface. If air flow carries away many of the molecules that escape from the liquid surface and if this rate of loss is greater than the rate of molecules returning to the surface net evaporation occurs.

Ohm's law describes that the electric current in a circuit is directly proportional to the voltage and inversely proportional to the resistance of the circuit. Mass transport between a surface and its surroundings is analogous with Ohm's law, substituting the mass flow and concentration difference for the current and voltage, respectively. The concentration difference is specified as that between the surface and the overlying air, while the resistance represents a force that reduces the rate of mass flow. Here, we consider evaporation rate (E) from the water surface to the air as a mass flow by assuming an equilibrium status in a thin layer adjacent to the water surface, where the water vapor concentration can be described as the saturation value (C_{WS}) at the surface temperature (T_s) to give

$$E = \frac{C_{WS}(T_s) - C_{Wa}}{r_W} = g_W[C_{WS}(T_s) - C_{Wa}], \qquad (19.1)$$

where r_W is the resistance of the evaporation, g_W is the conductance, the reciprocal of the resistance, and C_{Wa} is the water vapor concentration in the air.

When considering transpiration from plant leaves the evaporating sites are found on the surface of leave's mesophyll cells, and the water vapor concentration at the cell surface can be described as $C_{WS}(T_s)$ because the cell surface is thought to be "perfectly wet" (Fig. 19.1). The pathway of transpiration is from the cell surfaces to the atmosphere via a stoma, and thus total resistance, r_W, consists of stomatal (r_S) and boundary layer (r_a) resistances in series. It should be noted that the reciprocal of the total conductance, g_W, is the sum of the reciprocals of the component conductances, i.e., stomatal (g_S) and boundary layer (g_a) conductances:

Fig. 19.1 A pathway of transpiration (E) from mesophyll cell surface to the atmosphere, showing the stomatal (r_S) and boundary layer (r_a) resistances. Note that the total resistance (r_W) is the sum of r_S and r_a resistances
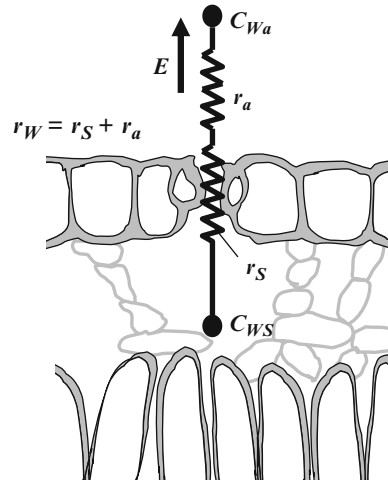
$$\frac{1}{g_W} = \frac{1}{g_S} + \frac{1}{g_a}. \tag{19.2}$$

Equations (19.1) and (19.2) represent the basic formulae of transpiration at both the individual leaf and canopy scales. Thus, determination of g_S and g_a is critical for estimating transpiration at both scales.

19.2 Boundary Layer (g_a) and Stomatal (g_S) Conductance

The velocity of microwind flowing over a leaf decreases toward the leaf surface due to the friction between the surface and the air and the air viscosity. The zone adjacent to the surface, where the airflow is laminar and mass transfer can be described using molecular diffusivity, is referred to as the boundary layer.

The boundary layer conductance of any mass for one surface of a rectangular, flat plate with the downwind width (d_m) was developed using the molecular diffusivity for species j (D_j), Reynolds number, and Schmidt number, and also assuming that wind is naturally turbulent, to give

$$g_a = 0.93 \rho_a D_j^{2/3} v^{1/6} \sqrt{\frac{u}{d_m}}, \tag{19.3}$$

where ρ_a is the air density, v is the kinematic viscosity, and u is the wind velocity of the free stream. Using the molecular diffusivity for water vapor (19.3) becomes the conductance in air for water vapor (mol m^{-2} s^{-1}) (see Campbell and Norman 1998):

$$g_a = 0.147 \sqrt{\frac{u}{d_m}}. \tag{19.4}$$

It should be noted that (19.3) and (19.4) also suggest that the thickness of the boundary layer over the surface decreases in proportion to the increasing square roots of u and $1/d_m$.

Since the water vapor concentration gradient between the stomatal cavity and the air surrounding the leaf is several hundred times greater than the CO_2 concentration gradient, opening stomata for carbon gain is accompanied by much water loss from the plant body via transpiration. Wong et al. (1979) have shown that plants tend to adjust the degree of stomata openness in order to maintain a constant ratio between the intercellular CO_2 concentration (C_{Ci}) and the CO_2 concentration of air inside the leaf boundary layer (C_{Cs}) for a wide range of environmental conditions, but that this relationship varies from species to species. Many researchers have related the net assimilation rate (A) to g_S. One widely used g_S model is the Ball–Berry model (Ball et al. 1987; Collatz et al. 1991), which is given by

$$g_{sC} = m \frac{A h_s}{C_{Cs}} + b, \tag{19.5}$$

where g_{sC} is the stomatal conductance for CO_2 and h_s is the relative humidity of air inside the leaf boundary layer. m and b are, respectively, the slope and intercept obtained by linear regression analysis of data from leaf-level gas exchange measurements, i.e., g_{sC} vs. $A h_s/C_{Cs}$ plots. The stomatal conductance for water vapor is obtained from $g_S = 1.6 g_{sC}$, where 1.6 is the ratio of the diffusivities of CO_2 and water vapor in air.

However, it is widely accepted that stomata respond to the leaf surface humidity deficit (D_s) rather than to h_s. Furthermore, since A approaches zero when C_{Cs} approaches the CO_2 compensation point (Γ), (19.5) cannot describe stomatal behavior at low CO_2 concentrations. Leuning (1995) replaced h_s and C_{Cs} in (19.5) with a vapor pressure deficit correction function $f(D_s)$ and $C_{Cs} - \Gamma$, respectively,

$$g_{sC} = a_{sC} \frac{A f(D_s)}{C_{Cs} - \Gamma} + g_{sC0}, \quad f(D_s) = \left(1 + \frac{D_s}{D_0}\right)^{-1}, \tag{19.6}$$

where g_{sC0} is a residual stomatal conductance (as A approaches zero when light intensity approaches zero), and a_{sC} and D_0 are empirical parameters.

The net assimilation rate, A, can be described as

$$A = g_{sC}(C_{Cs} - C_{Ci}) \tag{19.7}$$

and reduces to

$$C_{Ci} = C_{Cs} - \frac{A}{g_{sC}}. \tag{19.8}$$

Equation (19.8) describes supplying CO_2 to the intracellular photosynthetic site with constraint by stomatal openness (g_{sC}: (19.6)) (Fig. 19.2). On the other hand, A can be described as a function of C_{Ci}. Thus, the intersection of these two function curves gives the "operating point," which denotes that stomata close or open to balance the supply of CO_2 via g_S with the demand of CO_2 by A (Fig. 19.2).
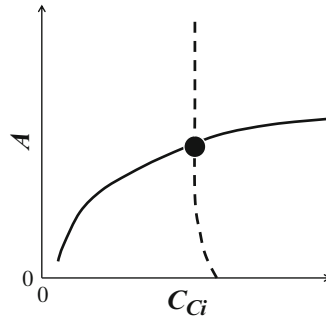
Fig. 19.2 Assimilation rate (A) as a function of intercellular CO_2 concentration (C_{Ci}) at some light and leaf temperature level (*solid line*), showing the photosynthetic demand function. The supply-constraint function (Eq. 19.8) by taking (Eq. 19.6) into consideration (*broken line*) is also shown for some environmental variables and empirical constants. The *solid circle* denotes the "operating point" of the leaf that is given by the intersection of the demand and supply-constraint curves. Note the fundamental concept provided by Leuning (1995)

Equations (19.5) and (19.6) are, in reality, difficult to solve. For example, A as a function of C_{Ci} is dependent on complex biochemical reactions in the intracellular photosynthetic site of the leaf, and intrinsically, A should be determined using a biochemical photosynthesis model (see Box 19.1: Farquhar et al. 1980). Furthermore, it should be noted that (19.4), (19.5), or (19.6), the photosynthesis model, and the leaf energy budget model for determining the leaf surface temperature must be solved simultaneously.

Another method commonly used for analyzing the response of g_S to governing variables is to use the following series of multiplicative functions (Jarvis 1976):

$$g_S = g_{Smax} f_1(Q_0) f_2(D_s) f_3(T_a) \ldots, \tag{19.9}$$

where g_{Smax} is the maximum g_S, Q_0 is the photosynthetic active radiation (PAR), and T_a is the air temperature. Some particularly useful functions for each of f_1, f_2, and f_3 were proposed and parameters contained in each function can be determined by appropriate nonlinear regression analysis. Oren et al. (1999) focused on the relationship between g_S and D_s by relating g_{Smax} to a reference conductance, g_{Sref}, at $D_s = 1$ kPa as follows:

$$g_S = g_{Sref} - \delta \ln D_s, \tag{19.10}$$

where δ is the sensitivity of g_S to D_s (i.e., $-dg_S/d \ln D_s$). Oren et al. (1999) fit (19.10) to literature data from porometry-based leaf-level measurements and regressed with δ and g_{Sref}. As a result, they found that the interspecific response of δ ($= -dg_S/d \ln D_s$) to g_{Sref} was well correlated with a slope of 0.60 (Fig. 19.3). It should be noted that this result generalized the previous findings that the sensitivity of g_S to D_s increased with g_{Sref} regardless of whether the variation in g_{Sref} was related to some other environmental variables.

Box 19.1. Biochemical Model for Leaf Photosynthesis (Farquhar et al. 1980)

Leaf photosynthesis, A, was computed using the biochemical models of Farquhar et al. (1980) and Collatz et al. (1991):

$$A = \min\{J_E, J_C, J_S\} - R_d,$$

where J_E, J_C, and J_S are the gross rates of photosynthesis limited by the rate of ribulose bisphosphate (RuBP) regeneration through electron transport, RuBP carboxylase-oxygenase (Rubisco) activity, and the export rate of synthesized sucrose, respectively, and R_d is the respiration rate during the day but in the absence of photorespiration. The term $\min\{J_E, J_C, J_S\}$ represents the minimum of J_E, J_C, and J_S.

The formulation and parameterization of J_E, J_C, J_S, and R_d as a function of the PAR absorbed by a leaf, C_{Ci}, and leaf temperature are described in Farquhar et al. (1980), Farquhar and Wong (1984), Collatz et al. (1991), and de Pury and Farquhar (1997). The photosynthesis model constants can be determined according to Badger and Collatz (1977), Farquhar et al. (1980), von Caemmerer et al. (1994), and de Pury and Farquhar (1997). The maximum carboxylation rate when RuBP is saturated (V_{cmax}) and the potential rate of whole-chain electron transport (J_{max}) used in these calculations are expressed as nonlinear functions of temperature using their values at 25°C (J_{max_25} and V_{cmax_25}, respectively); the formulations are given in de Pury and Farquhar (1997). In addition, R_d is expressed as a nonlinear function of temperature using R_d at 25°C (R_{d_25}), which was assumed to be linearly related to V_{cmax_25} (e.g., Collatz et al. 1991). Practically, both J_{max_25} and R_{d_25} are related to V_{cmax_25}, and hence, V_{cmax_25} is the key parameter in the leaf photosynthesis model.

19.3 Hydraulic Constraints on Transpiration

The fundamental driving force of water uptake and transportation in the plant is the water potential. The equation of water flow through a water conducting pathway between the roots and leaves also resembles that of electrical flow in a conducting system, i.e., keeping with the Ohm's law analogy:

$$E = K_L[\psi_s - (\psi_L + h\rho_w g)], \tag{19.11}$$

where K_L is the leaf-specific hydraulic conductance between the soil and leaves, ψ_s and ψ_L are the water potential of soil and leaf, respectively, h is the tree height, ρ_w is the density of water, and g is the gravitational constant. Note that E is
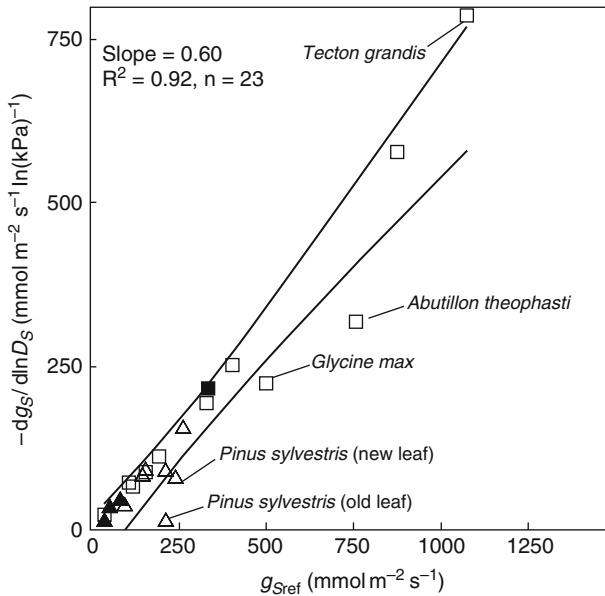
Fig. 19.3 The sensitivity of leaf-level stomatal conductance (g_S) of individual species to increasing vapor pressure deficit at the leaf surface ($-dg_S/d \ln D_s$) as a function of the canopy stomatal conductance at $D_s = 1$ kPa (g_{Sref}). *Lines*: 99% confidence interval. *Symbols*: *triangles*, nonporous; *squares*, diffuse-porous; *full*, boreal species; *shaded*, temperate species; *open*, tropical species. Species outside the confidence interval are shown. From Oren et al. (1999), reproduced with permission

represented as tree transpiration rate per unit leaf area. K_L can be related to sapwood-specific hydraulic conductivity, K_S, as follows:

$$K_L A_L = \frac{1}{h} K_S A_S, \tag{19.12}$$

where A_L and A_S are leaf and sapwood area, respectively. Equation (19.12) denotes that total hydraulic conductance between the roots and leaves increases/decreases with increasing water flow conducting area in the stem cross section, A_S, and soil-to-leaf water flow path length, h, respectively.

The sapwood maintains living cells and can conduct water, while aged xylem changes to the heartwood and loses its water and nutrient transport and storage functions (Fig. 19.4). Anatomically, there are water conducting systems in sapwood (Fig. 19.4) mainly for conifers and broadleaved trees. Conifers have tracheids that serve both mechanical and hydraulic functions, while the broadleaved trees share the role of hydraulic purpose with vessel elements and that of mechanical purpose with fibers. The tracheids are shorter than vessel elements and interlock and exchange water via pits on its side wall. The vessel elements, which are interconnected by simple perforation plates at their ends, are more effective for conducting water.

Fig. 19.4 *Upper*: A cross section of an oak stem showing various anatomical components. *Lower*: Xylem cross sections of (**a**) Japanese cedar (conifer), (**b**) cherry (broadleaved tree: diffuse-porous wood), and (**c**) chestnut (broadleaved tree: ring-porous wood). An *arrow* denotes direction from pith to bark. Courtesy of Drs. Y. Utsumi and T. Umebayashi
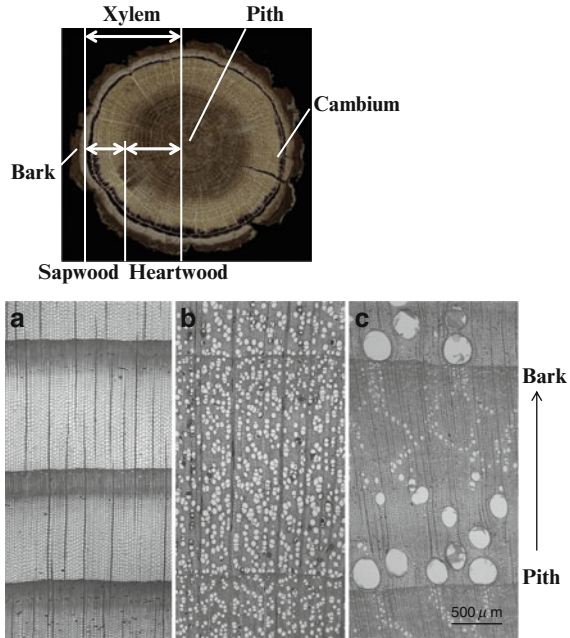
The sapwood of conifers has systematically arranged cuts of cells (Fig. 19.4a). Round openings found in the sapwood of broadleaved trees are the vessels, and fibers fill nonvessel space (Fig. 19.4b, c). Vessel array characteristics for broadleaved trees are broadly classified as diffuse-porous wood with vessels uniformly distributed throughout the entire sapwood (Fig. 19.4b) and ring-porous wood with larger vessels arranged along the boundary of annual rings (Fig. 19.4c). The spatial variation in sapflow in the stem cross section between those vessel arrays needs to be considered. For example, despite the radial variations in sapflow in the stems of conifers and diffuse-porous wood, ring-porous wood trees tend to have biased sapflow distribution and use mainly current and 2-year-old annual rings for conducting water (see Kumagai et al. 2005; Tateishi et al. 2008; Umebayashi et al. 2008).

A water deficit in the leaf caused by the transpiration lowers its water potential, causing water to move from the xylem to the evaporating cells in the leaf. This reduces the tension or pressure in the xylem sap and produces a water potential gradient in the cohesive hydraulic system of the tree. This pressure is transmitted to the root where water uptake occurs. K_S in (19.12) may be expressed in terms of physical properties of the conducting system in sapwood such as size, density, and connectivity of conduits.

Equation (19.1) is coupled to ψ_L using (19.11) and (19.12) to give

$$g_S = K_S \frac{A_S}{A_L} \frac{1}{D} \frac{1}{h} [\psi_s - (\psi_L + h\rho_w g)], \tag{19.13}$$

where D denotes vapor pressure deficit. In fact, the proportionality 0.60 between δ and g_{Sref} in (19.10) (see Fig. 19.3) was predicted from the examination results of (19.13), which suggested that the 0.60 proportionality regulates the minimum ψ_L to prevent excessive xylem cavitation (Oren et al. 1999; Ewers et al. 2005).

19.4 Energy Balance

Radiation incident on the surface (for both of leaf and canopy) is decomposed into solar (short-wave) (R_s) and thermal (long-wave) (R_L) radiation. All surfaces reflect the incident R_s according to the albedo (a_l) of that surface, while the remaining R_s is either absorbed or transmitted through the surface. Also, following the Stefan–Boltzmann law, all surfaces emit long-wave radiation at a rate proportional to the fourth power of the absolute surface temperature (T_s: K). Thus, the total sum of the incident and emitted radiations gives the energy available as net radiation (R_n):

$$R_n = R_{sabs} + R_{Labs} = (1 - a_l)R_s + R_L - \varepsilon\sigma T_s^4 \qquad (19.14)$$

where ε is emissivity compared to a black body, and σ is the Stefan–Boltzmann constant (5.67×10^{-8} W m^{-2} K^{-4}). Intrinsically, the available energy can be represented by the sum of R_s and R_L absorbed in the body (R_{sabs} and R_{Labs}, respectively, in the middle of (19.14)). When considering the upward surface of the body, R_{sabs} and R_{Labs} can be expressed as $(1 - a_l)R_s$ and $R_L - \varepsilon\sigma T_s^4$, respectively, resulting in the right-hand side of (19.14). Because of comparatively low values of a_l and T_s at vegetation surfaces, R_n above forests tends to have higher values compared to other types of surface such as bare lands (Fig. 19.5a).

The surface (also, for both of leaf and canopy) energy balance is expressed by:

$$R_n = H + \lambda E + G, \qquad (19.15)$$

where H and λE are the sensible and latent heat fluxes, respectively, λ is the heat of vaporization of water, and G is the heat storage. It should be noted that when evaporation occurs on the dry leaf or canopy surface, E is the synonym of transpiration. Higher energy partitioning to λE is a characteristic of vegetated surfaces (Fig. 19.5b).

Sensible heat transfer from the leaf surface to the atmosphere is driven by the difference between T_a and T_s and boundary conductance, and thus, leaf-level H is given by:

$$H = c_p g_H(T_s - T_a), \qquad (19.16)$$

where c_p is the specific heat of air at constant pressure, and g_H is the boundary conductance for heat (mol m^{-2} s^{-1}) and can be expressed in the same form as (19.4), but a coefficient of 0.135 is used instead of 0.147. Assuming that G can be considered negligible, the energy balance on a leaf surface as a function of T_s is
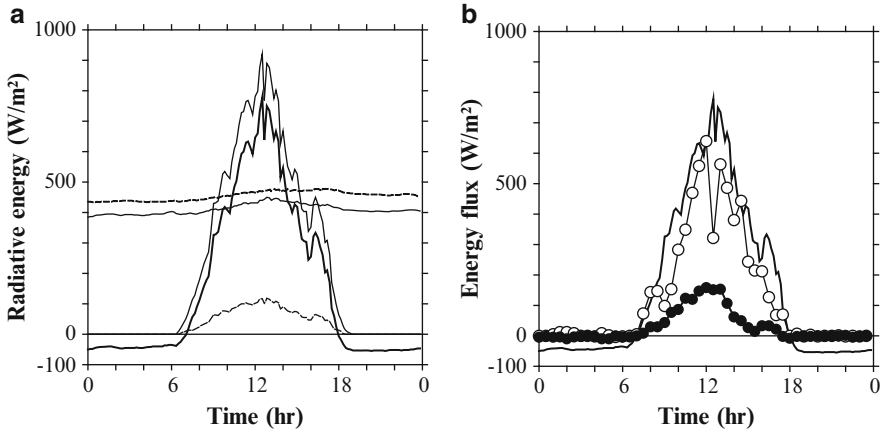
Fig. 19.5 Forest ecosystem energy balance observed in a Bornean tropical rainforest. (**a**) Downward (*thin solid line*) and upward (*thin dashed line*) short-wave radiation, downward (*solid line*) and upward (*dashed line*) long-wave radiation, and the net radiation (*thick solid line*) calculated from balance of those radiation terms. (**b**) Sensible heat flux (*solid circle*), latent heat flux (*open circle*), and the net radiation (*thick solid line*). Note that sensible and latent heat fluxes were measured using the eddy covariance method

described using (19.1) and (19.14) through (19.16). As seen in Box 19.1, T_s is the most critical factor in computing biocatalytic reactions in the photosynthesis model. Thus, it should be noted that while T_s is calculated from the energy balance, T_s simultaneously affects the energy balance via the rate of photosynthesis and the degree of stomatal opening.

When considering the leaf-scale energy balance and photosynthesis within a forest canopy, the radiative transfer through the canopy must be taken into account. Direct beam and diffuse irradiance must, for example, be considered separately due to their different attenuation properties in the canopy. Downward and upward R_L transfer within a canopy follows diffuse irradiance transfer theory, but note that R_L is emitted from any plant body within the canopy. Both direct and diffuse R_s can be further divided into PAR and near-infrared radiation (NIR) according to differential absorption by leaves. Fortunately, approximately half the R_s over the canopy is in the form of PAR, while the other half is in the form of NIR, enabling estimates of R_s penetration inside the canopy. The absorbed PAR or NIR within a canopy layer between z (the height from the ground) and $z + \Delta z$, ΔS, is defined as:

$$\Delta S_b = (1 - \eta - \xi)(1 - P_b)S_b(z + \Delta z), \qquad (19.17)$$

$$\Delta S_d^\downarrow = (1 - \eta - \xi)(1 - P_d)S_d^\downarrow(z + \Delta z), \qquad (19.18)$$

$$\Delta S_d^\uparrow = (1 - \eta - \xi)(1 - P_d)S_d^\uparrow(z), \qquad (19.19)$$

where η and ξ are the leaf transmissivity and reflectivity, respectively, for PAR or NIR, and S is PAR or NIR at the given height, while P is the probability of no

contact with the irradiance within that canopy layer. The subscripts b and d denote direct beam and diffuse irradiation, respectively, and superscript arrows denote the direction of the irradiation. Because P is a complex function of the leaf area density, leaf angle distribution, and foliage clumping factor within a given canopy layer and the solar geometric direction (see Kumagai et al. 2006), (19.17) through (19.19) are not readily solved. The total absorbed solar radiation within the canopy layer is then calculated as the sum of the absorbed PAR and NIR, both of which are calculated by (19.17) through (19.19). Sunlit leaves receive the beam and the upward and downward diffuse radiation, while shaded leaves only receive upward and downward diffuse radiation. Therefore, the irradiance absorption and energy balance need to be computed separately for sunlit and shaded leaves (see Kumagai et al. 2006).

19.5 Canopy Transpiration

19.5.1 Multilayer Approach

Vegetation affects the within-canopy microclimate by intercepting radiation, attenuating wind, and distributing a source/sink of mass and energy to each within-canopy position (Fig. 19.6). These source/sink distributions and canopy turbulence form scalar distributions (i.e., air temperature, humidity, and CO_2 concentration) and above-canopy fluxes such as heat, H_2O, and CO_2. It should be noted that in turn these scalar distributions influence the within-canopy microclimate and scalar source/sink strength.

In reality, forest transpiration or H_2O flux above a forest canopy is formed as a result of the above within-canopy processes. Thus, here we focus on a multilayer canopy approach, which explicitly considers three major within-canopy processes: (1) radiative transfer and leaf-scale energy conservation, (2) leaf-scale
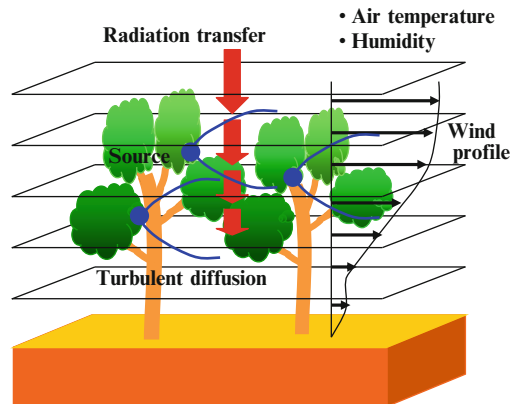
Fig. 19.6 Schematic display of the multilayer Soil–Vegetation–Atmosphere Transfer model for transpiration from a forest ecosystem. Note that the forest canopy is divided into layers for computation of energy and matter exchange between leaves and atmosphere

ecophysiological status for stomatal opening and carbon assimilation, and (3) turbulent diffusion of matter (Baldocchi 1992; Fig. 19.6). For the multilayer approach, the canopy is divided into layers, and all equations describing the within-canopy processes (1–3) (see Kumagai et al. 2006) are solved at each layer. Since the within-canopy processes (1) and (2) have been already introduced, we will proceed to the description of the process (3).

Assuming a steady-state planar-homogeneous and high Reynolds and Peclet numbers flow, and by applying time and horizontal averaging, the scalar continuity and turbulent flux equations for water vapor (q) are (see Katul and Albertson 1999):

$$\frac{\partial \langle \overline{q} \rangle}{\partial t} = 0 = -\frac{\partial \langle \overline{w'q'} \rangle}{\partial z} + S_q, \tag{19.20}$$

$$\frac{\partial \langle \overline{w'q'} \rangle}{\partial t} = 0 = -\langle \overline{w'^2} \rangle \frac{\partial \langle \overline{q} \rangle}{\partial z} - \frac{\partial \langle w'w'q' \rangle}{\partial z} + \left\langle \frac{p'}{\rho_a} \frac{\partial q'}{\partial z} \right\rangle, \tag{19.21}$$

where the overbar and bracket denote time and horizontal averaging, respectively, prime denotes a departure from the temporal averaging operator, w is the instantaneous vertical velocity, $F_q = \langle \overline{w'q'} \rangle$ is the vertical turbulent flux, t is time, z is height from the ground, p is the static pressure, and ρ_a is the density of air. The three terms on the right-hand side of (19.21) represent respectively the production of turbulent flux due to interactions between the turbulent flow and mean concentration gradient, transport of the turbulent flux, and dissipation as a result of the pressure-scalar interaction. S_q is the source term due to mass release (i.e., transpiration) by the ensemble of leaves within the averaging plane and given by:

$$S_q = \frac{1}{\rho_a} (E_{sl}a_{sl} + E_{sh}a_{sh}), \tag{19.22}$$

where E and a denote the leaf-scale transpiration and the leaf area density in a given layer, respectively, and subscripts sl and sh denote sunlit and shaded leaves, respectively. The last two terms on the right-hand side of (19.21) are unknowns requiring closure approximations, as described by Watanabe (1993). To solve (19.20)–(19.22), including these closure approximations, velocity statistics within the canopy need to be computed. Here, the second-order closure model formulated by Wilson and Shaw (1977) may be applied.

The multilayer model introduced here is parameterized by independently collected ecophysiological measurements and is not calibrated or parameterized by canopy-level flux measurements. The outputs from the model are independently validated using a stand-scale sap flow measurement (see Kumagai et al. 2007, 2008) (Fig. 19.7a). After validation, the model can be used to examine how the matter fluxes above the forest ecosystems are generated, for example, how the canopy structure and physiological traits impact H_2O exchange between the canopy and atmosphere (Fig. 19.7b).
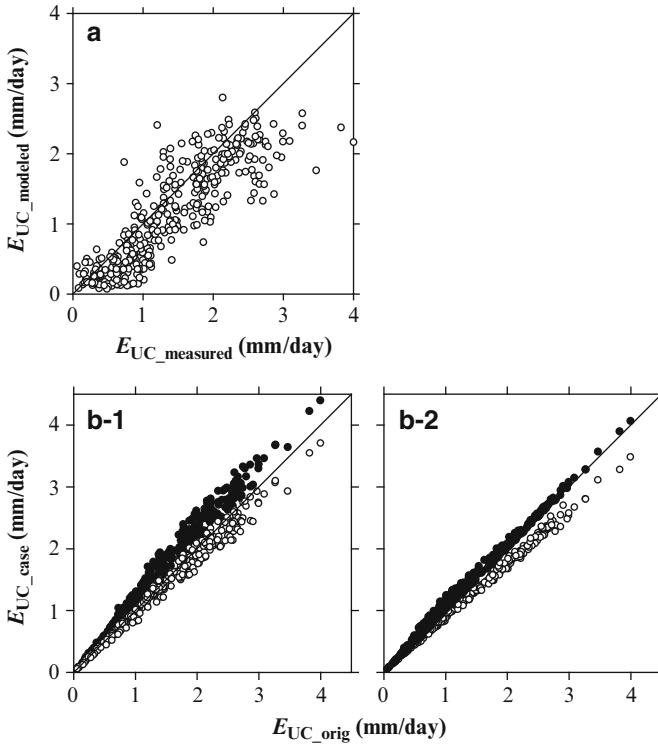
Fig. 19.7 Comparisons (**a**) between measured and modeled (CASE 1) upper-canopy (Japanese cedar trees) transpiration (E_{UC}), and between E_{UC} calculated in CASE 1 (E_{UC_orig}) and in CASEs 2 and 3 (**b-1**) and in CASEs 4 and 5 (**b-2**) (E_{UC_case}). Canopy transpiration was calculated (CASE 1) considering seasonal variations in LAI and the maximum Rubisco catalytic capacity (V_{cmax}), setting LAI as the maximum value (CASE 2: *solid circle*) and the minimum value (CASE 3: *open circle*), and setting V_{cmax} as the maximum value (CASE 4: *solid circle*) and the minimum value (CASE 5: *open circle*) in the study period

19.5.2 Big-Leaf Approach

Assuming that the vegetation in which matter and energy are exchanged can be represented as a single layer, i.e., "big leaf," (19.1) and (19.16) are rearranged using surface or canopy conductance G_S and aerodynamic conductance G_a instead of using g_S and g_a (assuming $= g_H$), respectively.

When leaf area index (LAI) is >3 (see Kelliher et al. 1995) or G_S is derived from transpiration measurement for individual plant, e.g., sap flow measurements, G_S represents mean stomatal conductance within a canopy and is called the canopy conductance. This bulk conductance is usually related to physiological control, and therefore, described using (19.5), (19.6), (19.9), and (19.10), which are the functions for describing leaf-level g_S. At LAI < 3 (see Kelliher et al. 1995) and/or when the water vapor flux is measured above a canopy, e.g., by the eddy covariance method, evaporation from the floor vegetation or the soil surface contributes greatly to G_S.

In case of the "big-leaf" approach, the concept of leaf-level g_a is developed into the conductance between the canopy surface and the atmosphere above the canopy, namely, the aerodynamic conductance G_a. From the equation for wind velocity profile above the canopy under adiabatic condition, G_a can be derived as follows:

$$G_a = \frac{\kappa^2 u}{(\ln(z - d/z_0))^2},\qquad(19.23)$$

where z is the height of wind speed observation, u is the wind speed at z, κ is the von Karman's constant (0.4), d is the zero-plane displacement, and z_0 is the roughness length. For computing G_a, the d and z_0 are usually set as 2/3 and 1/10 of the canopy height, respectively. It should be noted that the G_a represents the conductance of the atmospheric surface layer between a height of $d + z_0$ and z.

Substituting the rearranged (19.1) and (19.16) for the canopy-scale energy balance equation, (19.15), and replacing the surface–air vapor pressure difference by the vapor pressure deficit of the ambient air (D_a), the equation for λE above the canopy, termed the Penman–Monteith (P-M) equation, is given by:

$$\lambda E = \frac{\Delta(R_n - G) + \rho_a c_p G_a D_a}{\Delta + \gamma(1 + (G_a/G_S))},\qquad(19.24)$$

where Δ is the rate of change of saturation water vapor pressure with temperature, and γ is the psychrometric constant (66.5 Pa K^{-1}). Equation (19.24) generally describes the transpiration stream from vegetation to the atmosphere. However, an infinite G_S represents no resistance between the canopy surface and within canopy, allowing (19.24) to derive evaporation from a free water surface, i.e., wet canopy evaporation.

When micrometeorological measurements including a measurement of H_2O exchange between the canopy and atmosphere (see Fig. 19.8a) are conducted, the only unknown variable in (19.24) is G_S. Thus, an inverted operation of (19.24) gives G_S (Fig. 19.8b) and enables us to examine the relationships between the G_S and various environmental factors (D_a in Fig. 19.8c). For example, using an analysis with (19.10) and procedures shown in Ewers et al. (2005) the relationship between the G_S and the D_a in Fig. 19.8c gives us important information on environmental and hydraulic control of G_S (see Fig. 19.3). Note that here G_S was calculated using the simplified form of the P-M equation (Monteith and Unsworth 2008) (detailed later).

19.6   Transpiration: Environmental Controls

When G_a is large enough that it can be assumed to be infinite, the canopy surface is well coupled to the atmosphere and the T_s tends to approach T_a. Then, we can obtain the imposed evaporation rate, E_{imp}, by setting G_a as infinity in (19.24):

$$E_{imp} = \frac{\rho_a c_p}{\lambda \gamma} G_S D_a.\qquad(19.25)$$
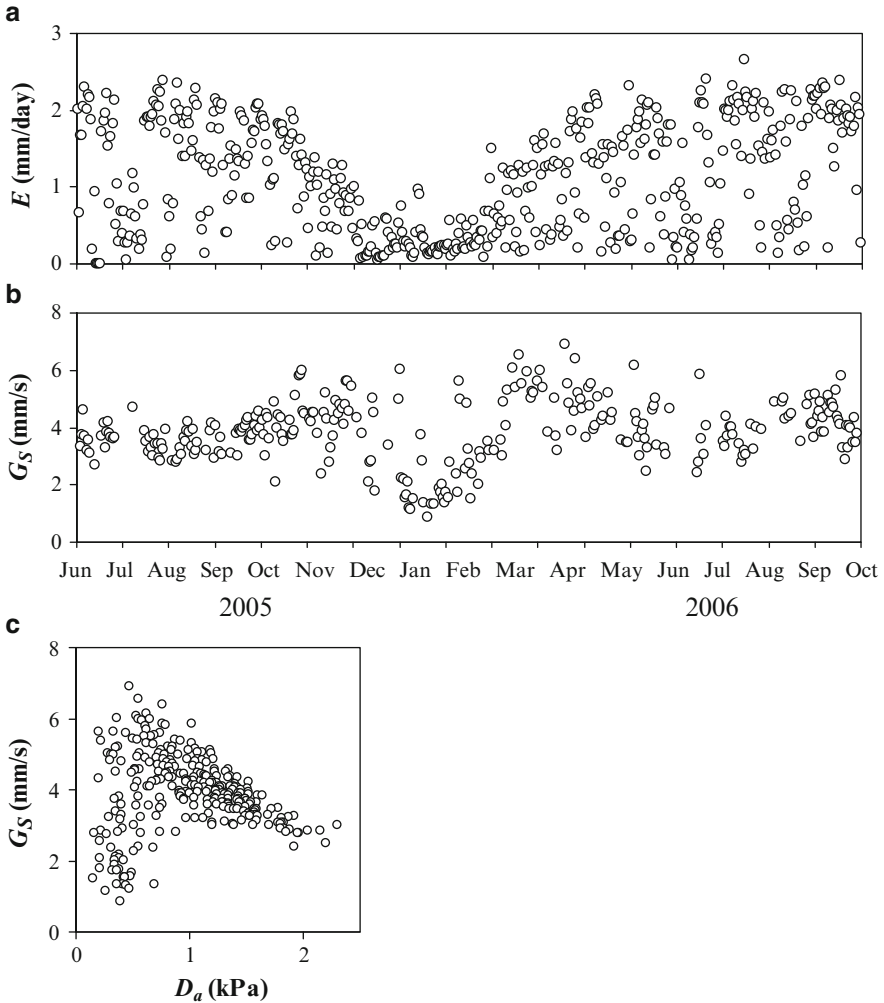
Fig. 19.8 Seasonal patterns of (**a**) daily canopy stand transpiration (*E*) and (**b**) daily canopy conductance (G_S), and (**c**) relationship between the G_S and atmospheric vapor pressure deficit (D_a) in a Japanese cedar forest

In this case, the evaporation is imposed by the atmosphere on the natural canopy surface through the effect of D_a, so that evaporation is proportional to the physiological conductance. Note that (19.25) is the simplified form of the P-M equation for a canopy that is well coupled with the atmosphere (Monteith and Unsworth 2008). On the other hand, when the G_a is very small, the canopy surface is poorly coupled with the atmosphere and evaporation tends to an equilibrium condition. In

this case, E is termed the equilibrium evaporation rate, E_{eq}, which can be obtained by substituting $G_a = 0$ for (19.24):

$$E_{eq} = \frac{\Delta(R_n - G)}{\lambda(\Delta + \gamma)}. \tag{19.26}$$

Equilibrium evaporation, E_{eq}, depends only on the energy supply (radiation) and is obtained over an extensive surface of uniform wetness.

The relative importance of radiative (E_{eq}) and advective (E_{imp}) energy for E (19.24) can be estimated using the equation (McNaughton and Jarvis 1983):

$$E = \Omega E_{eq} + (1 - \Omega)E_{imp}, \tag{19.27}$$

where the decoupling coefficient, Ω, is calculated as follows:

$$\Omega = \frac{\Delta/\gamma + 1}{\Delta/\gamma + 1 + g_a/g_c}. \tag{19.28}$$

The decoupling coefficient, Ω, is a measure of the coupling between conditions at the surface and those in the free air stream and can vary between 0 (for perfect coupling) and 1 (for complete isolation). Stomatal control of transpiration becomes progressively weaker as Ω approaches 1. It is apparent from (19.28) that Ω depends on the ratio between the surface conductance and that of the boundary layer, rather than on their absolute values (Jones 1992).

Observation in a Bornean tropical rainforest showed diurnal variations in E and their environmental control (Kumagai et al. 2004; Fig. 19.9). In this site, E had similar diurnal patterns to R_s, and estimates of Ω ranged from 0.1 to 0.4 and had no clear diurnal cycle.

19.7   Future Research Directions

Vegetation/forests cover a major part of the land surface and promote latent heat exchange as a result of transpiration. How the available energy is partitioned between sensible and latent heat fluxes at the air–land interface is critical for the formation of global and regional climate. In turn, the climatic modifications attendant on the alteration in land surface energy partitioning can impact forest transpiration due to a change in the environmental control. Also, it should be noted that subtracting evaporation from precipitation denotes the upper limit of available water resources for both humans and ecosystems.

The projected growth in atmospheric CO_2 will significantly increase global and regional temperatures with concomitant modifications to various climatic factors such
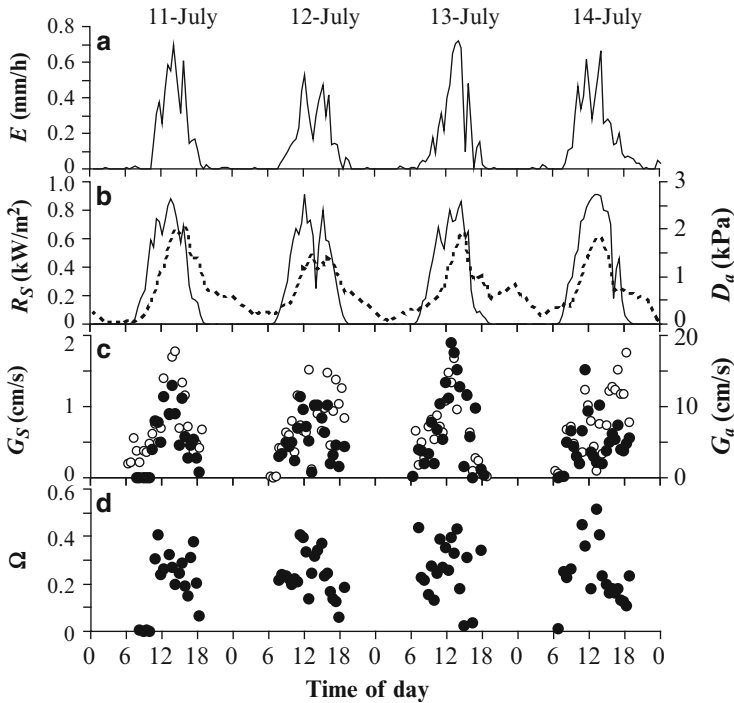
Fig. 19.9 Diurnal variations in (**a**) canopy transpiration (*E*), (**b**) solar radiation (*R*$_s$; *solid line*) and atmospheric vapor pressure deficit (*D*$_a$; *dashed line*), (**c**) canopy conductance (*G*$_S$; *solid circle*) and aerodynamic conductance (*G*$_a$; *open circle*), and (**d**) the decoupling coefficient (Ω; *solid circle*) observed in a Bornean tropical rainforest. From Kumagai et al. (2004), reproduced with permission

as atmospheric evaporative demand and precipitation patterns, and land use change accelerates these impacts. The climate and land use change factors alter forest transpiration by changes in ecophysiological characteristics of assimilation and transpiration as well as by those in the atmospheric evaporative demand. Furthermore, on much longer time scales, both spatial and temporal variations in physiological and morphological characteristics of plant species genotypically and/or phenotypically occur under climate change and could impact the exchange between forests and the atmosphere.

Thus, assessing the potential shifts in forest transpiration from both biological (stomatal opening, photosynthesis, hydraulic restriction in the stem xylem, and their genetic and/or nongenetic acclimation) and physical (surface energy balance, advection, convection, and atmospheric coupling) aspects is necessary for understanding climate change and quantifying local, regional, and global water cycling. Additionally, remote sensing technologies can serve among the most promising tool to investigate spatial impacts of climate and, especially, land use changes on the interaction between forests and the atmosphere.

References

Badger MR, Collatz GJ (1977) Studies on the kinetic machine of ribulose 1,5-bisphosphate carboxylase and oxygenase reaction, with particular reference to the effect of temperature on kinetic parameters. Carnegie Inst Washington Year Book 76:355–361

Baldocchi D (1992) A Lagrangian random-walk model for simulating water vapor, CO2 and sensible heat flux densities and scalar profiles over and within a soybean canopy. Bound Layer Meteorol 61:113–144

Ball JT, Woodrow IE, Berry JA (1987) A model predicting stomatal conductance and its contribution to the control of photosynthesis under different environmental conditions. In: Biggens J (ed) Progress in photosynthesis research. Mirtinus Nijhoff Publishers, The Netherlands, pp 221–224

Campbell GS, Norman JM (1998) An Introduction to Environmental Biophysics. Springer-Verlag, New York

Collatz GJ, Ball JT, Grivet C et al (1991) Regulation of stomatal conductance and transpiration: a physiological model of canopy processes. Agric For Meteorol 54:107–136

de Pury DGG, Farquhar GD (1997) Simple scaling of photosynthesis from leaves to canopies without the errors of big-leaf models. Plant Cell Environ 20:537–557

Ewers BE, Gower ST, Bond-Lamberty B et al (2005) Effects of stand age and tree species on canopy transpiration and average stomatal conductance of boreal forests. Plant Cell Environ 28:660–678

Farquhar GD, Wong SC (1984) An empirical model of stomatal conductance. Aust J Plant Physiol 11:191–210

Farquhar GD, von Caemmerer S, Berry JA (1980) A biochemical model of photosynthetic CO2 assimilation in leaves of C3 species. Planta 149:78–90

Jarvis PG (1976) The interpretation of the variations in leaf water potential and stomatal conductance found in canopies in the field. Philos Trans R Soc Lond Biol 273:593–610

Jones HG (1992) Plants and microclimate, 2nd edn. Cambridge University Press, Cambridge

Katul GG, Albertson JD (1999) Modeling CO_2 sources, sinks, and fluxes within a forest canopy. J Geophys Res 104:6081–6091

Kelliher FM, Luening R, Raupach MR et al (1995) Maximum conductances for evaporation from global vegetation types. Agric For Meteorol 73:1–16

Kumagai T, Saitoh TM, Sato Y et al (2004) Transpiration, canopy conductance and the decoupling coefficient of a lowland mixed dipterocarp forest in Sarawak, Borneo: dry spell effects. J Hydrol 287:237–251

Kumagai T, Aoki S, Nagasawa H et al (2005) Effects of tree-to-tree and radial variations on sap flow estimates of transpiration in Japanese cedar. Agric For Meteorol 135:110–116

Kumagai T, Ichie T, Yoshimura M et al (2006) Modeling CO2 exchange over a Bornean tropical rain forest using measured vertical and horizontal variations in leaf-level physiological parameters and leaf area densities. J Geophys Res. doi:10.1029/2005JD006676

Kumagai T, Aoki S, Shimizu T et al (2007) Sap flow estimates of stand transpiration at two slope positions in a Japanese cedar forest watershed. Tree Physiol 27:161–168

Kumagai T, Aoki S, Shimizu T et al (2008) Transpiration and canopy conductance at two slope positions in a Japanese cedar forest watershed. Agric For Meteorol 148:1444–1455

Leuning R (1995) A critical appraisal of a combined stomatal-photosynthesis model for C3 plants. Plant Cell Environ 18:339–355

McNaughton KG, Jarvis PG (1983) Predicting effects of vegetation changes on transpiration and evaporation. In: Kozlowski TT (ed) Water deficits and plant growth, vol V. Academic Press, New York, pp 1–47

Monteith JL, Unsworth MH (2008) Principles of environmental physics, 3rd edn. Academic Press, Oxford

Oren R, Sperry JS, Katul GG et al (1999) Survey and synthesis of intra- and interspecific variation in stomatal sensitivity to vapour pressure deficit. Plant Cell Environ 22:1515–1526

Tateishi M, Kumagai T, Utsumi Y et al (2008) Spatial variations in xylem sap flux density in evergreen oak trees with radial-porous wood: comparisons with anatomical observations. Trees 23:23–30

Umebayashi T, Utsumi Y, Koga S et al (2008) Conducting pathways in north temperate deciduous broadleaved trees. IAWA J 29:247–263

von Caemmerer S et al (1994) The kinetics of ribulose-1,5-bisphosphate carboxylase/oxygenase in vivo inferred from measurements of photosynthesis in leaves of transgenic tobacco. Planta 195:88–97

Watanabe T (1993) The bulk transfer coefficients over a vegetated surface based on K-theory and 2nd-order closure model. J Meteorol Soc Japan 71:33–42

Wilson NR, Shaw RH (1977) A higher order closure model for canopy flow. J Appl Meteorol 16:1198–1205

Wong SC, Cowan IR, Farquhar GD (1979) Stomatal conductance correlates with photosynthetic capacity. Nature 282:424–426

Chapter 20
Rainfall Interception Loss by Forest Canopies

Darryl E. Carlyle-Moses and John H.C. Gash

20.1 Introduction

When rain falls onto a forest a proportion is intercepted by the canopy and evaporates back into the atmosphere, playing no further part in the terrestrial portion of the hydrologic cycle. This *canopy interception loss*, I_c, can be appreciable (Table 20.1). The first published reports of I_c date from the late nineteenth and early twentieth centuries (Hoppe 1896; Horton 1919; see also Gash and Shuttleworth 2007). Since then numerous studies have been conducted with I_c being found to account for 10–50% of season-long or annual rainfall, P_g, (Roth et al. 2007); varying with both forest characteristics and climate. Because I_c is an important and sometimes dominant component of forest evaporation (David et al. 2005), several models have been developed ranging from simple linear regression (e.g., Helvey and Patric 1965) to physically based numerical (e.g., Rutter et al. 1971, 1975), analytical (e.g., Gash 1979) and stochastic (e.g., Calder 1986) models. Although I_c has been extensively studied by hydrologists, key processes, such as those responsible for the relatively high during-precipitation evaporation rates from forest canopies, E, are still not fully understood (Dunkerley 2009).

The goal of this chapter is to summarize the current state-of-knowledge of the rainfall I_c process, to provide an overview of our understanding of the influence of biotic and abiotic factors on I_c and to discuss the more commonly used I_c models. The chapter will conclude with recommendations as to where hydrologists should direct their future research so that our understanding of I_c as a process can be more fully expanded and our ability to simulate this component of the forest water balance at different spatiotemporal scales can be met with greater success.

Table 20.1 Quantitative importance of canopy interception loss (percentage of precipitation) from different forest types derived from selected recently published studies

Forest type	Location	Season-long or annual I_c (% of rainfall)	References
Coniferous			
Old-growth *Sequoia sempervirens* and *Pseudotsuga menziesii*	Northern California	22.4	Reid and Lewis (2009)
Old-growth >450 yr. old *P. menziesii*	South-Central Washington	25	Link et al. (2004)
25 yr. old *P. menziesii* (assumed no stemflow and 5 % stemflow)	South-Central Washington	21, 16	Pypker et al. (2005)
25 yr. old, dense *Picea abies*	Southern Sweden	45	Alavi et al. (2001)
125 yr. old *Pinus contorta, Picea glauca x engelmanni,* and *Abies lasiocarpa*	Southern British Columbia	31.1	Moore et al. (2008)
Young planted *Chamaecyparis obtuse* stand (annual: year 1, year 2)	Eastern Japan	18.9, 19.1	Murakami (2007)
Hardwood			
Quercus robur, Betula pubescens, Corylus avellana, and *Illex aquifolium* (leafed, leafless periods)	Berkshire, UK	29, 20	Herbst et al. (2008)
Q. rubra , Acer saccharum, Fagus grandifolia, et al. (growing-season)	Southern Ontario	18.8	Price and Carlyle-Moses (2003)
Carpinus orientalis croaticus, Q. pubescentis et al. (annual: north facing, south facing slope)	Slovenia	28.4, 25.4	Šraj et al. (2008)
Fagus silvatica (monospecific plot)	Central Germany	27–40[a]	Krämer and Hölscher (2009)
Mixed			
Q. serrara, et al. (growing, dormant seasons)	Japan	17.6, 14.3	Deguchi et al. (2006)
Pinus pseudostrobus, Q. canbyi, and *Q. laeta*	Northeastern Mexico	15.8	Carlyle-Moses and Price (2007)
Q. alba, Pinus taed, et al.	Georgia, USA	18.6	Bryant et al. (2005)
Tropical Rainforest			
Interior tropical rainforest (normal precipitation year, dry year)	Brazil	13.3, 22.6	Cuartas et al. (2007)
Lowland coastal rainforest	Queensland, Australia	25	Wallace and McJannet (2006)
Lowland tropical rainforest	Indonesia	16.4	Vernimmen et al. (2007)
Heath forest	Indonesia	9.6	Vernimmen et al. (2007)
Monsoon evergreen broadleaf forest	Dinghushan, China	31.8	Yan et al. (2001)
Savanna – Type Woodlands			
Q. suber and *Q. ilex*	Portugal	6.2	Pereira et al. (2009a)

[a]Depending on study period

20.2 The Canopy Interception Loss Process

20.2.1 *Canopy Wetting and Saturation*

Canopy interception loss is composed of evaporation from the forest canopy during a rainfall event, Et, and evaporation from canopy storage once the event has ceased, C_e, (see Klaassen et al. 1998):

$$I_c = Et + C_s \qquad (20.1)$$

For those events in which P_g is sufficiently large to satisfy the canopy storage capacity, S, it is often assumed that $C_e = S$ (e.g., Gash 1979). However, for events in which S is not met, two common approaches exist regarding how the depth of water stored on the canopy, C, changes with increasing P_g.

One approach, termed the "waterbox" concept (Klaassen et al. 1998), suggests that no canopy release, that is drainage, occurs from the canopy until $C = S$. Following the "waterbox" approach the only portion of P_g that reaches the forest floor while $C < S$ is free throughfall, that is throughfall that passes directly through canopy gaps. A second approach suggests that S is reached exponentially and that canopy release occurs before S is satisfied. Klaassen et al. (1998) argued that forest canopies saturate gradually since raindrops splash onto already wetted portions of the canopy (Calder 1986), that bark and the undersides of foliage saturate more slowly (Herwitz 1985), and that foliage in the upper canopy shelters foliage in the lower canopy. The gradual saturation of the canopy may be simulated as (Aston 1979):

$$C = S\{1 - exp(-\tau P_g)\} \qquad (20.2)$$

and τ is a fitting parameter that, theoretically, may be derived as $\tau = (1-p)/S$, and p is the free throughfall coefficient, that is the fraction of P_g that becomes free throughfall (Klaassen et al. 1998).

Determining whether canopies saturate as the "waterbox" approach suggests or they do so gradually, in an exponential manner, may be of significance for estimating I_c in those regions where or during those seasons when a large proportion of P_g falls as a series of small events, particularly if S is relatively large. In addition, accurate derivation of C is a requisite for simulating during-event evaporation as it is generally accepted that (Rutter et al. 1971):

$$E_u = \frac{C}{S} \cdot E \qquad (20.3)$$

where E_u is the evaporation rate from a partially wetted canopy.

Once a canopy becomes saturated $C >$ or $= S$ and E occurs at its maximum rate under the given stand and during-event meteorological conditions. However, if during an event the rainfall intensity, R, is less than E or P_g temporarily ceases then the canopy may start to dry out with $C < S$; E is then reduced to a value given by (20.3) (see Zeng et al. 2000).

20.2.2 Evaporation of Intercepted Rainfall

Like transpiration, I_c is a diffusive process moving water vapor from vegetation canopies into the atmosphere. However, the evaporation of intercepted P_g differs from transpiration in a very important respect. Following the Penman–Monteith equation, transpiration from dry canopies is dependent on two conductances – aerodynamic conductance, g_a, and canopy conductance, g_c, whereas the evaporation of intercepted P_g from a wetted canopy is dependent only on g_a (see Teklehaimanot and Jarvis 1991). Thus, I_c can occur during periods when the stomata of leaves are closed, such as at night for many species or when vegetation is under environmental stress. In addition, I_c not only takes place from foliage, as transpiration does, but also from the woody component of the canopy, the boles of trees, and from lichens and other epiphytes. Thus, I_c occurs throughout the dormant season in the absence of transpiration. As the canopy approaches saturation g_c approaches infinity resulting in higher rates of evaporation of intercepted P_g than transpiration rates under the same environmental conditions. This has been confirmed by field-based measurements (e.g., Stewart 1977). Thus, I_c may, in part at least, be considered a net loss of water from the forest water balance and not an alternative to transpiration as has been found for grass cover (e.g., McMillan and Burgy 1960).

Until recently, the Penman–Monteith equation has been the preferred approach for simulating the evaporation of intercepted P_g (e.g., Rutter et al. 1971; Zeng et al. 2000). The Penman–Monteith equation is the weighted sum of the evaporation rate due to net radiation and the rate due to mass transfer (Dingman 2002):

$$\lambda E = \frac{\Delta(Q_{nst}) + \rho_a c_p g_a \lfloor e^* - e \rfloor}{\rho_w \left[\Delta + \gamma \left(1 + \frac{g_a}{g_c} \right) \right]} \tag{20.4}$$

where λ is the latent heat of vaporization, E is the evaporation rate, Δ is the slope of the saturation vapor pressure vs. temperature curve, Q_{net} is the net radiant energy, ρ_a is the density of air, c_p is the specific heat of air at a constant pressure, ρ_w is the density of water, γ represents the psychrometric constant, and e^*-e is the reference level vapor pressure deficit.

Results from several studies (e.g., Rutter 1967; Stewart 1977; Teklehaimanot et al. 1991) suggest that evaporation from wetted canopies is largely a function of g_a and e^*-e, while Q_{net} plays a minor role. The energy required to sustain E, which typically ranges from 0.07 to 0.70 mm h^{-1} (i.e., ~48–480 W m^{-2}) from forest canopies (Carlyle-Moses and Price 1999), has been attributed to advection energy. Evaporation from a wetted canopy cools the canopy and the surrounding air creating a sensible heat sink (e.g., Rutter 1967; Stewart 1977). Sources of sensible heat that enhance E from the wetted canopy may include air originating from nearby oceans, surrounding dry vegetation, and from within the forest itself (Shuttleworth and Calder 1979; Takanashi et al. 2003; Wallace and McJannet 2006).

With Q_{net} considered a minor component of the overall energy requirements for E and with g_c assumed to be infinite under saturated canopy conditions, Pereira et al. (2009a), following Brutsaert (1991) and Monteith and Unsworth (2008), suggested that E may be derived using a Dalton-type equation:

$$\lambda E = \frac{\rho_a c_p}{\gamma} g_b \left[e_s^* - e_a \right], \tag{20.5}$$

where g_b is the aerodynamic conductance for water vapor integrated over the distance between the surface of the foliage and the adjacent air and $e_s^* - e_a$ represents the vapor pressure deficit between the saturated surface and the overlying air.

Pereira et al. (2009b) found good agreement between observed and simulated I_c at the tree-scale in Mediterranean savannas in southern Portugal using (20.5) by assuming that the temperature of the canopy surface is approximately equal to that of the wet-bulb temperature of the air.

Early I_c studies (e.g., Helvey and Patric 1965) related I_c depth to P_g depth empirically as a simple linear regression equation of the form $I_c = a\ P_g + b$. Gash (1979) showed that the slope, a, represents the ratio between average $\bar{E}$ and the average P_g intensity falling on that canopy, $\bar{R}$, under saturated canopy conditions (i.e., $\bar{E}/\bar{R}$). This relationship suggests that $\bar{E}$ is directly proportional to $\bar{R}$ (i.e., $\bar{E} = a\bar{R}$); however, why this relationship exists is not clear. One possible explanation was put forth by Murakami (2006), who suggested that when a raindrop hits a canopy the resulting splash produces numerous small droplets that are subject to greater evaporation from their surfaces as they fall toward the ground compared to larger raindrops. Smaller drops experience greater evaporation loss since vapor pressures increase over convex surfaces with small radii of curvature and because a larger proportion of the droplet's water volume is exposed to the air. At greater R, raindrops possess greater kinetic energy (see Marshall and Palmer 1948) so that when they strike a canopy the resulting splash produces a larger number of small droplets which in turn results in increased evaporation.

The quantity of small droplets generated by the splashing of a single raindrop may not be inconsequential. Fitt et al. (1982), for example, found that a single large (4–5 mm diameter) simulated raindrop falling 13 m and hitting a rigid surface with a 0.5 mm water film produced >7,000 small droplets ranging in size from 10 to 2,500 μm. Although a drop diameter of 4–5 mm may not be expected under most rainfall conditions, Stow and Stainer (1977) found that splash droplets were produced from raindrops with diameters greater than about ~1.5 mm, or those associated with R values of ~3.4 mm h^{-1} (Dunkerley 2009). This suggests that splash-evaporation may be a common occurrence not only just in the tropics, but also in temperate regions. Dunkerley (2009) provides an extensive review of raindrop – splash drop relationships and the implications of splash drop production for E.

Evaporation not only requires a source of energy, but also a mechanism to transport water vapor from the canopy to the atmosphere. Water vapor, like sensible heat, is transferred by eddy and molecular diffusion, whereas pressure differences govern momentum transfer. Rutter et al. (1975) proposed that the reduction in g_a caused by differences between the transport of momentum and that of scalar quantities is likely balanced by the effects of enhanced turbulence found close to forest canopies. As such, Rutter et al. (1975) suggested that g_a may be calculated using the equation for momentum transfer under near neutral stability:

$$g_a = \left\{ \frac{k}{ln[(z-d)/z_{0,M}]} \right\}^2 u \qquad (20.6)$$

where k is von Kármán's constant, d is the zero plane displacement, $z_{0,M}$ is the roughness length for momentum, and u is wind speed at height z.

Lankreijer et al. (1993) argued that (20.6) should be modified by replacing $z_{0,M}$ with the roughness length for sensible heat and water vapor, $z_{0,H}$, to account for the different transfer mechanisms involved. Lankreijer et al. (1993) found good agreement between simulated and measured I_c in a maritime pine (*Pinus pinaster*) stand in France by estimating E using (20.4) with g_a derived using $z_{0,H}$. However, as Gash et al. (1999) pointed out, canopy cover at the Lankreijer et al. (1993) study stand was 45% and applying (20.4), which assumes complete canopy cover, to sparse stands is not valid (Gash et al. 1995). When wet canopy E rates measured using the eddy correlation/energy balance method were compared to those derived using (20.4) in a maritime pine stand in Portugal, Gash et al. (1999) found that using $z_{0,M}$ and reducing E in proportion to the canopy cover fraction provided much better results than using the methodology of Lankreijer et al. (1993). Thus, the results of Gash et al. (1999) support the continued use of $z_{0,M}$ to estimate E from wetted canopies.

As aforementioned, Rutter et al. (1975) assumed that P_g falls under near-neutral atmospheric stability conditions. Subsequent researchers (e.g., Lankreijer et al. 1993) have also made this supposition eliminating the need for applying stability factor corrections (see Thom 1975) to (20.6). The results of Gash et al. (1999) support this assumption. It should be noted, however, that the use of mean wind speed over the measurement time-step of interest in deriving g_a (20.6) has been questioned. Calder (1990) suggested that wind gusts play an important role in vapor transport from forest canopies, something that (20.6) does not directly take into account. The results of McNaughton and Laubach (1998), which show that vapor transport increases with the increasing standard deviation of wind speed compared to mean wind speed, support the Calder (1990) hypothesis. Additionally, Schellekens et al. (1999) speculated that wind gusts may have been of importance for I_c from a lowland tropical rainforest in northeastern Puerto Rico due to the high E that accompanied P_g events with low mean wind speeds.

20.3 Factors Influencing Canopy Interception Loss

20.3.1 Climate Factors Influencing Canopy Interception Loss

Although forest characteristics influence I_c, increasing evidence suggests that stands with widely differing characteristics may have very similar I_c values under the same P_g regime (e.g., Carlyle-Moses 2002; Krämer and Hölscher 2009). The fraction of P_g that becomes I_c typically decreases asymptotically with P_g depth until reaching a quasi-constant value once a certain threshold P_g has been met (Fig. 20.1).

Thus, in regions where or during seasons when P_g falls as a series of relatively small events, I_c may be relatively large, whereas if the bulk of P_g falls during a few relatively large events, I_c may be comparatively small. Spittlehouse (1998), for example, calculated that annual I_c for the portion of P_g that fell as rain on a coniferous forest in the low rainfall interior of British Columbia, Canada was 24%, but when the rainfall record of the wet British Columbian coast was applied to the interior forest modeled I_c was halved to 12%. Similarly, short duration, high intensity, convective tropical storms generally produce relatively low rates of I_c; for example, in Amazonia I_c is typically 15%, although Cuartas et al. (2007) reported a strong influence of changes in mean storm intensity and duration. The frequency and continuity of events may also influence the magnitude of I_c. If, for example, P_g temporarily ceases during an event or if R becomes lower than E, once saturation has been reached, then, due to evaporation, C will become less than S. This scenario will result in a portion of S being replenished, possibly multiple times during a single event, resulting in larger I_c than that which would occur under continuous P_g (see Zeng et al. 2000).
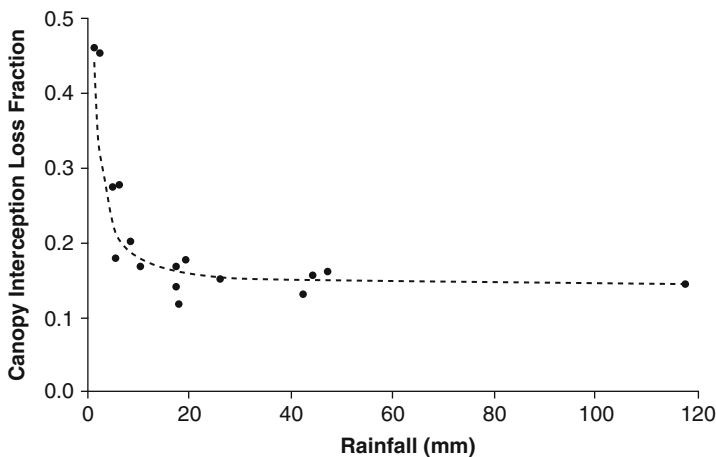
Fig. 20.1 Asymptotic relationship between canopy interception loss fraction and rainfall (mm) for a cedar (*Juniperus flaccida*) – white oak (*Quercus glaucoides*) – ash (*Fraxinus cuspida*) stand in northeastern Mexico. Source: Carlyle-Moses (unpublished data)

An example of the impact that varying P_g characteristics coupled with differing temperature and humidity, and thus vapor pressure deficit conditions, can have on I_c was provided by Llorens et al. (1997). For a Scots pine (*Pinus sylvestris*) forest patch in Spain, it was found that long events with low R and wet atmospheric conditions, and short duration, high R events with dry atmospheric conditions had similar average I_c fractions of 15 and 13% of P_g, respectively. However, medium duration, low R events under dry conditions produced an average I_c fraction of 49% of P_g. The low I_c for the first two types of events were attributed to low vapor pressure deficits and high R, respectively. The large I_c associated with the latter category of events was accredited to high E as a consequence of events being of moderate duration with relatively high vapor pressure deficits.

Wind speed can influence I_c in a number of ways. For example, g_a, and thus E, increases with greater wind speeds, while advection will be greater with higher wind velocities as a constant supply of sensible heat will be ensured. However, if wind speeds are great enough, increased leaf or crown motion may occur that can enlarge canopy release resulting in a decrease in S and possibly I_c (Šraj et al. 2008). Wind direction may also be important in some regions as it may regulate the amount of sensible heat advected toward the wetted forest.

20.3.2   Forest Characteristics Influencing Canopy Interception Loss

Canopy cover fraction exerts an important control on I_c as it represents the proportion of a forested area that contributes to E and S (Gash et al. 1995). Canopy cover fraction, as a measure of canopy sparseness, also influences the magnitude of E in that, all else being equal, sparser stands have greater g_b on a per tree basis, while g_b declines on a per ground-area basis as stands become sparser (Teklehaimanot and Jarvis 1991; Teklehaimanot et al. 1991). With regard to leaf area index (*LAI*), Watanabe and Mizutani (1996) suggested, based on the results of Pitman (1989) and Kondo et al. (1992), that $S = 0.15$ mm $\times$ *LAI* for broadleaved forests and 0.2 mm $\times$ *LAI* for coniferous stands. Although some results agree with this (e.g., Spittlehouse and Black 1981), others have arrived at very different findings. Deguchi et al. (2006), for example, concluded that $S \sim 0.3$ mm $\times$ *LAI* in their deciduous forest study stands in Japan, while Carlyle-Moses and Price (2007) found $S = 0.5 \times$ *LAI* in a pine (*Pinus pseudostrobus*) – oak (*Quercus canbyi* and *Q. laeta*) forest in north-eastern Mexico. Carlyle-Moses and Price (2007) speculated that the relatively high S per *LAI* value derived in their study was probably due to the boles of the oak trees being inclined $\sim 45°$, the rough bark associated with the trees in the stand, and the presence of epiphytes on the branches of the oak and some of the pine trees. Pypker et al. (2005) found that S was higher in an old-growth Douglas fir (*Pseudotsuga menziesii*) forest compared to a young stand, although the two had nearly identical *LAI* values. The authors attributed the larger S in

the old-growth forest to factors such as increased surface area of branches and boles and the occurrence of epiphytes.

Water retention by foliage is governed by the hydrophobicity and microstructure of their surfaces as well as their angle of inclination (Holder 2007). Considerable variability in foliage water retention properties have been found even for foliage of the same form, that is leaf or needle, and may be related to an area's climate. Holder (2007), for example, found that foliage water retention was statistically greater for species in a cloud forest in Guatemala than for species in a Guatemalan dry tropical rainforest and in foot hills/grasslands in Colorado. Holder (2007) suggested that the greater water repellency by trees in dry climates may be a functional adaptation to increase the amount of water reaching the soil for plant growth. In addition, Holder (2007) postulated that leaf trait, for example, deciduous versus evergreen broadleaf, may also influence water retention as leaves may lose their ability to repel water as they become older and weathered.

Differences in I_c between growing and dormant seasons have been shown to be less than expected based on variation in LAI alone (e.g., Deguchi et al. 2006; Herbst et al. 2008). Although the influence of seasonal differences in rainfall characteristics on I_c need to be considered, defoliated stands may have relatively large I_c as a consequence of the relatively large specific storage capacities associated with stems, branches and tree boles – which may be an order of magnitude greater than the specific storage capacities of foliage (e.g., Herwitz 1985). In addition, changes to the aerodynamic properties of the canopy during the leafless dormant season may also maintain relatively high evaporation rates of intercepted P_g (Herbst et al. 2008). Thus, other factors apart from LAI, such as wood area index (WAI), foliage water retention properties, and the presence of epiphytes may have an important control on the magnitude of S and, as consequence, generalizations concerning S, LAI and forest type, for example, coniferous or deciduous, may be subject to considerable error.

An extensive review of P_g partitioning by vegetation communities found in Mediterranean climates in Europe by Llorens and Domingo (2007) concluded that no relationship between stand density and throughfall – and by extension I_c – could be found, in agreement with the conclusions of other studies and reviews (e.g., Llorens and Gallart 2000). Instead, Llorens and Domingo (2007) found that there were statistically significant negative relationships between throughfall and stand basal area (BA), diameter at breast height (DBH), age, and height. These factors suggest that I_c increases as a stand matures and the canopy closes and that tree density may be a poor metric for estimating S and I_c due to forests self-thinning with age.

20.4 Modeling Canopy Interception Loss

A comprehensive review of I_c modeling by Muzylo et al. (2009) identified fifteen physically based I_c models, with ten of these categorized as original approaches and five as significantly improved variants of the original models. Four of the models

dominate the I_c modeling literature – the original Rutter model (Rutter et al. 1971, 1975), the original Gash model (Gash 1979) and their reformulations (Gash et al. 1995; Valente et al. 1997). In addition, complex hydrologic models that include I_c simulation almost always use the Rutter or Gash models and almost all current Global Circulation Model – Soil Vegetation Atmosphere Transfer approaches use an I_c model that is conceptually similar to the Rutter model (Muzylo et al. 2009). Thus, this section will focus on the reformulated Rutter and Gash models.

The revised Rutter model (Valente et al. 1997) is based on a dynamic calculation of the water balance of a forest canopy and trunks, which estimates I_c, as well as throughfall and stemflow, from input P_g and meteorological data. The conceptual framework of the model is shown in Fig. 20.2. The principal difference between the original model and the reformulated model is that the former assumes that evaporation occurs from the whole plot area, while the latter divides the plot into two distinct subareas: an open area with no cover and a covered area comprising the canopy and trunks, with evaporation occurring solely from the covered area. Like the original model, the sparse Rutter model uses the Penman–Monteith equation (20.3) to estimate the evaporation of intercepted P_g from the canopy (Valente et al. 1997):

$$E_c = \begin{cases} (1-\varepsilon)E\dfrac{C_c}{S_c}, C_c < S_c \\ (1-\varepsilon)E, \quad C_c \geq S_c \end{cases} \tag{20.7}$$

and from the trunks:

$$E_{t,c} = \begin{cases} \varepsilon E\dfrac{C_{t,c}}{S_{t,c}}, C_{t,c} < S_{t,c} \\ \varepsilon E, \quad C_{t,c} \geq S_{t,c} \end{cases} \tag{20.8}$$

with I_c from the whole plot area being:

$$I_c = cE_c + cE_{t,c} = E + E_t \tag{20.9}$$

where ε is a constant relating the evaporation rate from the trunks to that from a saturated canopy, c is the canopy cover fraction, and the subscripts "c" and "t" represent per unit of covered area and with reference to the trunks, respectively.

As with the original Rutter model, the sparse version is run with data at time intervals (typically 10 min) using the same numerical integration so that I_c from the whole plot over the duration of the event is calculated as (Valente et al. 1997):

$$I_c = c\left(\int E_c \mathrm{d}t + \int E_{t,c}\mathrm{d}t\right) \tag{20.10}$$

The reformulated Gash model (Gash et al. 1995; Valente et al. 1997) is an analytical simulation tool that combines the conceptual framework of the sparse Rutter model,
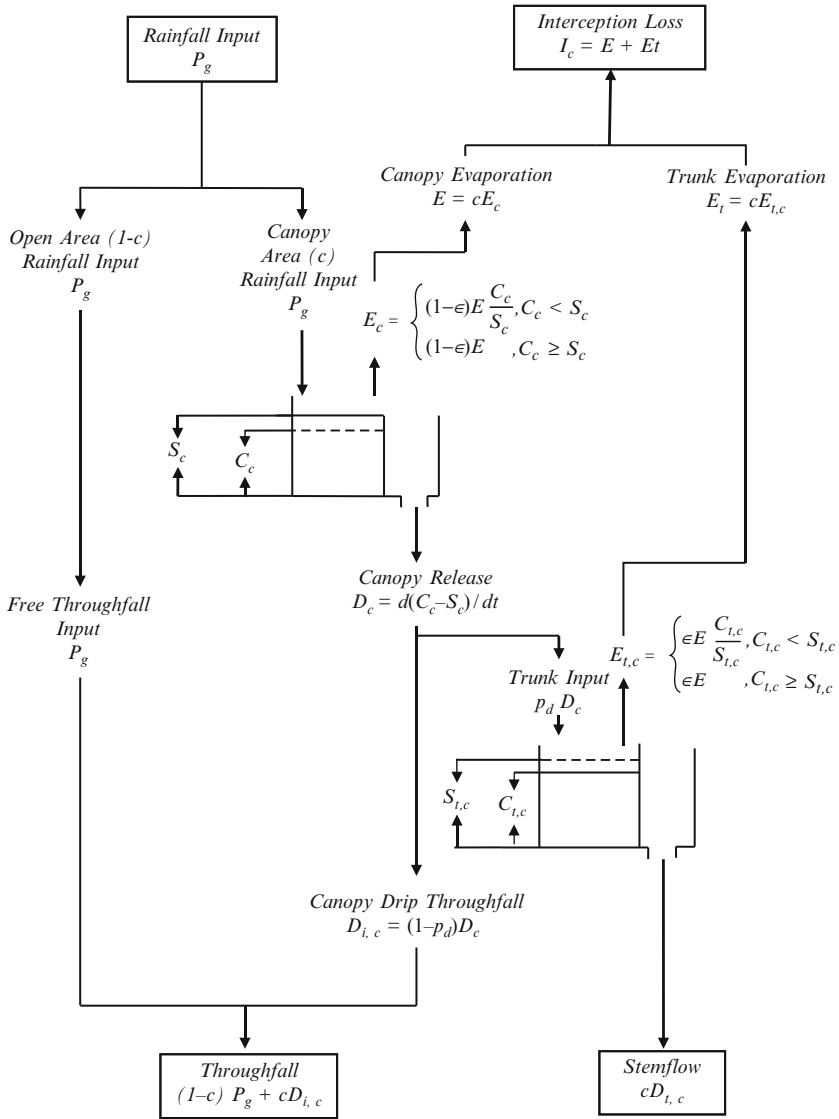
Fig. 20.2 The conceptual framework of the running water balance sparse Rutter model (adapted from Valente et al. 1997). See text and Valente et al. (1997) for details

including the division of a plot area into covered and uncovered subareas, with the ease of empirical equations. The sparse Gash model, like its predecessor, considers that I_c follows three phases for discrete P_g events: (1) the wetting-up of the canopy phase, (2) the saturated canopy phase, and (3) the canopy drying phase. The various components of I_c derived using the sparse Gash model and their

Table 20.2 Components of canopy interception loss in the sparse Gash model (adapted from Valente et al. (1997)

Component of interception loss	Formulation
Amount of incident P_g required to saturate the canopy (P'_g)	$-\frac{\bar{R}}{(1-\varepsilon)\bar{E}_c}\frac{S}{c}ln\left[1-\frac{(1-\varepsilon)\bar{E}_c}{\bar{R}}\right]$
Amount of incident P_g required to saturate the trunks (P''_g)	$\frac{\bar{R}}{\bar{R}-(1-\varepsilon)\bar{E}_c}\frac{S_t}{p_d c} + P'_g$
Interception loss from the canopy for m small storms insufficient to saturate the canopy ($P_g < P'_g$)	$c\sum_{j=1}^{m} P_{g,j}$
And from the canopy for n storms large enough to saturate the canopy ($P_g \geq P'_g$)	$c\left[nP'_g + \frac{(1-\varepsilon)\bar{E}_c}{\bar{R}}\sum_{j=1}^{n}\left(P_{g,j} - P'_g\right)\right]$
Interception loss from the trunks for q storms that saturate the trunks ($P_g \geq P''_g$)	qS_t
And from n-q storms that do not saturate the trunks ($P_g < P''_g$)	$p_d c\left[1-\frac{(1-\varepsilon)\bar{E}_c}{\bar{R}}\right]\sum_{j=1}^{n-q}\left(P_{g,j} - P'_g\right)$

Note: p_d represents the trunk partitioning coefficient. See Valente et al. (1997) for further details

formulation are provided in Table 20.2. It should be noted that when canopy cover is 100% the difference in modeled I_c using the revised Rutter and Gash models should be small compared to the original versions (Valente et al. 1997). For further information concerning model parameterization and the computation of throughfall and stemflow using the sparse models, the reader is directed to Valente et al. (1997).

Muzylo et al. (2009) reported that there has been a steady abandonment of the running water balance approach due, in part at least, to the success of the original and sparse Gash models and the more data-demanding requirements of the Rutter model. Muzylo et al. (2009) also suggested that the analytical approach may be gaining favor since E may be derived using a simple regression of I_c versus P_g, eliminating the need for meteorological measurements at high temporal resolutions.

Although good agreement between observed and measured season-long and annual I_c is generally found using the sparse Rutter and Gash models (Muzylo et al. 2009), certain model assumptions may not be valid. For example, the sparse models follow the "waterbox" approach to canopy saturation and, given the evidence supporting the gradual exponential wetting of forest canopies, may over estimate I_c when C or C_e is $<S$. In addition, Carlyle-Moses and Price (2006) found, using derived stemflow funnelling ratios in a northern hardwood stand in southern Ontario, Canada, that P_g required to saturate the trunks, P''_g, was much greater than that found using the methodology of Valente et al. (1997). However, following the "waterbox" approach to canopy saturation likely has a noticeable impact on small event I_c estimates with little error in seasonal or annual I_c estimates (e.g., Carlyle-Moses and Price 2007). In addition, although P''_g may be underestimated using the methodology outlined by Valente et al. (1997), the resulting error in the I_c estimate is probably minimal. Instead, any large discrepancy between simulated and observed season-long or annual I_c is likely a consequence of the approach used to estimate E. The sparse Rutter model explicitly uses

the Penman–Monteith equation (20.3), while many applications of the sparse Gash model have also used this approach (see Muzylo et al. 2009). Several studies, however, have shown that E inferred from measurements of P_g and understory precipitation is usually higher than that derived using (20.3), especially in maritime climates (e.g., Waterloo et al. 1999), with advection being the likely cause of the enhancement in E. Thus, the use of (20.3) is not valid and other approaches, such as (20.4), should be used.

Evaluation of I_c model performance, including that of the sparse Rutter and Gash models, and comparing the results of different modeling exercises among forests is hampered by the multitude of methods used to derive model parameter estimates. Valente et al. (1997), for example, showed that $\bar{R}$ and $\bar{E}_c$ may vary greatly depending on the time-step and antecedent P_g conditions used in their derivation. In addition, S may be found using a number of direct and indirect methods that can produce very different results for the same forest (see Llorens and Gallart 2000). Muzylo et al. (2009) highlighted some additional drawbacks to I_c model applications. These included inadequate model validation, the dearth of studies that compare different models, and measurement uncertainties.

20.5 Conclusions and Future Research Directions

Canopy interception loss is an important component of the water balance of most forests and, as a consequence, has received considerable study. Although much of this attention has been placed on deriving I_c for a particular forest at the season or annual timestep and expressing its magnitude as a percentage of P_g, important developments in our understanding of the I_c process have been realized. Canopy interception loss is composed of the evaporation from canopy storage during the P_g event as well as after the event has ended. A key reason why I_c from forests is quantitatively important is that E during P_g can be relatively high, often exceeding that possible from Q_{net} alone with E being greater than potential transpiration rates under the same environmental conditions. As such, I_c needs to be modeled separately from transpiration and cannot be simulated by potential evaporation formulae. Advection from air originating over oceans and surrounding dry vegetation, as well as from within forests themselves is thought to be the source of energy responsible for the enhancement of E. The amount of P_g stored on a canopy has been shown to be a function of stand characteristics such as canopy cover fraction, LAI, WAI, BA, tree height, the water retention properties of foliage and the presence of epiphytes. Increasing wind velocities increase E and thus I_c, but wind has also been shown to decrease S and potentially I_c by moving foliage and entire crowns causing stored P_g to be released. By far, the most important factor regulating the magnitude of I_c has been found to be the P_g regime of an area including the depth, duration, frequency, and continuity of the events as well as the during-event vapor pressure deficit characteristics. With regard to I_c models, significant improvements

over empirical regression have been realized with the development of physically based models which, at least at the season-long or annual time scales, have generally provided good agreement with observed I_c. In addition, these I_c models, unlike most hydrologic models, are transferable among forest types and other vegetation cover.

Although important developments in our understanding of the I_c process and our ability to simulate I_c have been made, much has yet to be learned. For example, the cause of the $\bar{E}/\bar{R}$ relationship, especially in areas that do not normally experience high rainfall intensities, remains largely speculative, with the co-relationships among R, event duration, wind speed and vapor pressure needing to be further explored as they relate to E. In addition, which roughness length to use in calculating g_a remains in debate, and the role of wind gusts in transferring water vapor from wetted canopies to the atmosphere is still unexplored in most forest and climate types. Scaling I_c results beyond the plot-scale remains problematic, in part due to difficulties associated with our ability to measure and or estimate model parameter values. Increased I_c model validation exercises and evaluations of differing I_c models in the same forest need to be carried out. Doing so will provide increased insight into our conceptual understanding of the I_c process and allow for the development of better simulation tools. Finally, more study is required to better understand the influence of seasonal change in canopy cover on I_c as well as the impact of climate change and forest disturbances, such as wildfire and pest infestations, on water balance components including I_c.

Opportunities exist to derive new insight into the I_c process, to validate existing models, and to develop new ones using the enormous bank of eddy covariance data available through programs such as Fluxnet (Baldocchi et al. 2001; e.g., Czikowsky and Fitzjarrald 2009). In addition, technologies such as microwave transmission can be used to directly measure C and C_e (e.g., Klaassen et al. 1998), while the high temporal throughfall and stemflow data now being produced (e.g., Pypker et al. 2005) can provide a better perspective into canopy release mechanisms. The role that stand architecture plays in influencing the magnitude of I_c for a given P_g regime needs to be further investigated so that emerging remote sensing technologies such as lidar (light detection and ranging), which can quantify canopy architecture in three dimensions, in conjunction with better estimates of P_g characteristics from radar and satellite-based platforms (e.g., Moges et al. 2007), can be utilized to further our modeling capabilities at the watershed scale and beyond (see Roth et al. 2007). Forest hydrology, including I_c measurement and modeling, will see enormous growth as these technologies and their data products become more readily available to the hydrologic community.

References

Alavi G, Jansson P-E, Hällgren J-E et al (2001) Interception of a dense spruce forest, performance of a simplified canopy water balance model. Nordic Hydrol 32:265–284

Aston AR (1979) Rainfall interception by eight small trees. J Hydrol 42:383–396

Baldocchi D, Falge E, Gu L et al (2001) Fluxnet: A new tool to study the temporal and spatial variability of ecosystem-scale carbon dioxide, water vapor, and energy flux densities. Bull Am Meteorol Soc 82:2415–2434

Brutsaert W (1991) Evaporation into the atmosphere. Environmental fluid mechanics. Kluwer Academic, Dordrecht, The Netherlands

Bryant ML, Bhat S, Jacobs JM (2005) Measurements and modeling of throughfall variability for five forest communities in the southeastern US. J Hydrol 312:95–108

Calder IR (1986) A stochastic model of rainfall interception. J Hydrol 89:65–71

Calder IR (1990) Evaporation in the uplands. Wiley, Chichester, UK

Carlyle-Moses DE (2002) Measurement and modelling of canopy water fluxes in representative forest stands and a matorral community of a small Sierra Madre Oriental watershed, northeastern Mexico. PhD dissertation, University of Toronto, Toronto

Carlyle-Moses DE, Price AG (1999) An evaluation of the Gash interception model in a northern hardwood stand. J Hydrol 214:103–110

Carlyle-Moses DE, Price AG (2006) Growing-season stemflow production within a deciduous forest of southern Ontario. Hydrol Process 20:3651–3663

Carlyle-Moses DE, Price AG (2007) Modelling canopy interception loss from a Madrean pine-oak stand, northeastern Mexico. Hydrol Process 21:2572–2580

Cuartas LA, Tomasella J, Nobre AD et al (2007) Interception water-partitioning dynamics for a pristine rainforest in Central Amazonia: marked differences between normal and dry years. Agric For Meteorol 145:69–83

Czikowsky MJ, Fitzjarrald DR (2009) Detecting rainfall interception in an Amazonian rain forest with eddy flux measurements. J Hydrol 377:92–105

David JS, Valente F, Gash JHC (2005) Evaporation of intercepted rainfall. In: Anderson MG (ed) Encyclopedia of hydrological sciences. Wiley, Chichester, pp 627–634

Deguchi A, Hattori S, Park H-T (2006) The influence of seasonal changes in canopy structure on interception loss: application of the revised Gash model. J Hydrol 318:80–102

Dingman SL (2002) Physical hydrology, 2nd edn. Prentice-Hall, Upper Saddle River, NJ

Dunkerley DL (2009) Evaporation of impact water droplets in interception processes: historical precedence of the hypothesis and a brief literature overview. J Hydrol 376:599–604

Fitt BD, Lysandrou M, Turner RH (1982) Measurement of spore-carrying splash droplets using photographic film and an image-analysing computer. Plant Pathol 31:19–24

Gash JHC (1979) An analytical model of rainfall interception by forests. Quart J R Meteorol Soc 105:43–55

Gash JHC, Shuttleworth WJ (2007) Benchmark papers in hydrology: evaporation. IAHS Press, Wallingford, UK

Gash JHC, Lloyd CR, Lachaud G (1995) Estimating sparse forest rainfall interception with an analytical model. J Hydrol 170:79–86

Gash JHC, Valente F, David JS (1999) Estimates and measurements of evaporation from wet, sparse pine forest in Portugal. Agric For Meteorol 94:149–158

Helvey JD, Patric JH (1965) Canopy and litter interception of rainfall by hardwoods of eastern United States. Water Resour Res 1:193–206

Herbst M, Rosier PTW, McNeil DD et al (2008) Seasonal variability of interception evaporation from the canopy of a mixed deciduous forest. Agric For Meteorol 148:1655–1667

Herwitz SR (1985) Interception storage capacities of tropical rainforest canopy trees. J Hydrol 77:237–252

Holder CD (2007) Leaf water repellency of species in Guatemala and Colorado (USA) and its significance to forest hydrology studies. J Hydrol 336:147–154

Hoppe E (1896) Precipitation measurements under tree crowns. (Transl. Ger. by Krappe AH, Div. of Silv., US For. Serv. 1935, Trans. No. 291)

Horton RE (1919) Rainfall interception. Mon Weather Rev U7:603–623

Klaassen W, Bosveld F, de Water E (1998) Water storage and evaporation as constitutes of rainfall interception. J Hydrol 212–213:36–50

Kondo J, Watanabe T, Nakazono M et al (1992) Estimation of forest rainfall interception (in Japanese). Tenki 39:159–167

Krämer I, Hölscher D (2009) Rainfall partitioning along a tree diversity gradient in a deciduous old- growth forest in Central Germany. Ecohydrol 2:102–114

Lankreijer HJM, Hendriks MJ, Klaassen W (1993) A comparison of models simulating rainfall interception of forests. Agric For Meteorol 64:187–199

Link TE, Unsworth M, Marks D (2004) The dynamics of rainfall interception by a seasonal temperate forest. Agric For Meteorol 124:171–191

Llorens P, Domingo F (2007) Rainfall partitioning under Mediterranean conditions. a review of studies in Europe. J Hydrol 335:37–54

Llorens P, Gallart F (2000) A simplified method for forest water storage capacity measurement. J Hydrol 240:131–144

Llorens P, Poch R, Latron J et al (1997) Rainfall interception by a *Pinus sylvestris* forest patch overgrown in a Mediterranean mountainous abandoned area I. monitoring design and results down to the event scale. J Hydrol 199:331–345

Marshall JS, Palmer WM (1948) The distribution of raindrops with size. J Meteorol 5:165–166

McMillan WD, Burgy RH (1960) Interception loss from grass. J Geophys Res 65:2389–2394

McNaughton KG, Laubach J (1998) Unsteadiness as a cause of non-equality of eddy diffusivities for heat and vapour at the base of an advective inversion. Bound-layer Meteorol 88:479–504

Moges SA, Alemaw BF, Chaoka TR et al (2007) Rainfall interpolation using remote sensing CCD data in a tropical basin – A GIS and geostatistical application. Phys Chem Earth A B 32:976–983

Monteith JL, Unsworth MH (2008) Principles of environmental physics, 3rd edn. Academic Press, London

Moore RD, Winkler RD, Carlyle-Moses DE et al (2008) Watershed response to the McLure forest fire: presentation summaries from the Fishtrap Creek workshop, March 2008. Streamline Watershed Manage Bul 12:1–11

Murakami S (2006) A proposal for a new forest canopy interception mechanism: splash droplet evaporation. J Hydrol 319:72–82

Murakami S (2007) Application of three canopy interception models to a young stand of Japanese cypress and interpretation in terms of interception mechanism. J Hydrol 342:305–319

Muzylo A, Llorens P, Valente F et al (2009) A review of rainfall interception modelling. J Hydrol 370:191–206

Pereira FL, Gash JHC, David JS et al (2009a) Evaporation of intercepted rainfall from isolated evergreen oak trees: do the crowns behave like wet bulbs? Agric For Meteorol 149:667–679

Pereira FL, Gash JHC, David JS et al (2009b) Modelling interception loss from evergreen oak Mediterranean savannas. Application of a tree-based modelling approach. Agric For Meteorol 149:680–688

Pitman JI (1989) Rainfall interception by bracken in open habitat - relations between leaf area canopy storage and drainage rate. J Hydrol 105:317–334

Price AG, Carlyle-Moses DE (2003) Measurement and modelling of growing-season canopy water fluxes in a mature mixed deciduous forest stand, southern Ontario, Canada. Agric For Meteorol 119:69–85

Pypker TG, Bond JB, Link TE et al (2005) The importance of canopy structure in controlling the interception loss of rainfall: Examples from a young and old-growth Douglas-fir forest. Agric For Meteorol 130:113–129

Reid LM, Lewis J (2009) Rates, timing and mechanisms of rainfall interception loss in a coastal redwood forest. J Hydrol 375:459–470

Roth BE, Slatton KC, Cohen MJ (2007) On the potential for high-resolution lidar to improve rainfall interception estimates in forest ecosystems. Front Ecol Environ 5:421–428

Rutter AJ (1967) An analysis of evaporation from a stand of Scots pine. In: Sopper WE, Lull HW (eds) International symposium on forest hydrology. Pergamon Press, Oxford, pp 403–417

Rutter AJ, Kershaw KA, Robins PC et al (1971) A predictive model of rainfall interception in forests I: derivation of the model from observations in a plantation of Corsican pine. Agric Meteorol 9:367–384

Rutter AJ, Morton AJ, Robins PC (1975) A predictive model of rainfall interception in forests II. Generalization of the model and comparison with observations in some coniferous and hardwood stands. J Appl Ecol 12:367–380

Schellekens J, Scatena FN, Bruijnzeel LA et al (1999) Modelling rainfall interception by a lowland tropical rain forest in northeastern Puerto Rico. J Hydrol 225:168–184

Shuttleworth WJ, Calder IR (1979) Has the Priestley-Taylor equation any relevance to forest evaporation? J Appl Meteorol 18:639–646

Spittlehouse DL (1998) Rainfall interception in young and mature conifer forests in British Columbia. In: Proceedings of the 23rd conference on agricultural and forest meteorology, 2–6 Nov 1998, Albuquerque, NM. Am Meteorol Soc, pp 171–174

Spittlehouse DL, Black TA (1981) A growing season water balance model applied to two Douglas fir stands. Water Resour Res 17:1651–1656

Šraj M, Brilly M, Mikoš M (2008) Rainfall interception by two deciduous Mediterranean forests of contrasting stature in Slovenia. Agric For Meteorol 148:121–134

Stewart JB (1977) Evaporation from the wet canopy of a pine forest. Water Resour Res 13:915–921

Stow CD, Stainer RD (1977) The physical products of a splashing water drop. J Meteorol Soc Jpn 55:518–532

Takanashi S, Kosugi Y, Tani M et al (2003) Evapotranspiration from a Japanese Cypress tree during and after rainfall. J Jpn Soc Hydrol Water Res 16:268–283

Teklehaimanot Z, Jarvis PG (1991) Direct measurement of intercepted water from forest canopies. J Appl Ecol 28:603–618

Teklehaimanot Z, Jarvis PG, Ledger DC (1991) Rainfall interception and boundary layer conductance in relation to tree spacing. J Hydrol 123:261–278

Thom AS (1975) Momentum, mass and heat exchange of plant communities. In: Monteith JL (ed) Vegetation and the atmosphere – principles, vol 4. Academic Press, London, pp 57–109

Valente F, David JS, Gash JHC (1997) Modelling interception loss for two sparse eucalypt and pine forests in central Portugal using reformulated Rutter and Gash analytical models. J Hydrol 190:141–162

Vernimmen RRE, Bruijnzeel LA, Romdoni A et al (2007) Rainfall interception in three contrasting lowland rain forest types in Central Kalimantan, Indonesia. J Hydrol 340:217–232

Wallace J, McJannet D (2006) On interception modelling of a lowland tropical rainforest in northern Queensland, Australia. J Hydrol 329:477–488

Watanabe T, Mizutani K (1996) Model study on micrometeorological aspects of rainfall interception over an evergreen broadleaved forest. Agric For Meteorol 80:195–214

Waterloo MJ, Bruijnzeel LA, Vugts HF et al (1999) Evaporation from *Pinus caribaea* plantations on former grassland soils under maritime tropical conditions. Water Resour Res 35:2133–2144

Yan J, Zhou G, Huang Z (2001) Evapotranspiration of the monsoon evergreen broad-leaf forest in Dinghushan. Sci Silvae Sinicae 37:37–45

Zeng N, Shuttleworth JW, Gash JHC (2000) Influence of temporal variability of rainfall on interception loss: part 1: point analysis. J Hydrol 228:228–241

Chapter 21
Throughfall and Stemflow in Wooded Ecosystems

Delphis F. Levia, Richard F. Keim, Darryl E. Carlyle-Moses, and Ethan E. Frost

21.1 Introduction

Incident precipitation is routed to the subcanopy by throughfall and stemflow. Throughfall is defined as the precipitation that passes directly through a canopy or is initially intercepted by aboveground vegetative surfaces and subsequently drips from the canopy, whereas stemflow is the precipitation that drains from outlying leaves and branches and is channeled to the bole (or stem) of plants. Throughfall and stemflow inputs constitute the majority of incident precipitation (Table 21.1) and are of critical importance to wooded ecosystems, ranging from 70 to 90% of incoming precipitation in most cases with the remainder lost to interception (Levia and Frost 2003). The inputs of throughfall and stemflow are highly variable over space and through time with consequent "hot spots" and "hot moments" of water and solute inputs from the canopy to the subcanopy (Stout and McMahon 1961; Levia 2003; Zimmermann et al. 2007). There are marked differences in the routing of intercepted water to the forest floor via throughfall (Keim and Skaugset 2004) and stemflow (Herwitz 1987) in terms of flowpaths and residence times along vegetative surfaces, which result in notable differences in solute concentrations and mass fluxes of canopy leachates (Levia and Frost 2003; Zimmermann et al. 2007). Recent work has documented the demonstrable effects of throughfall and stemflow to the hydrology and biogeochemistry of hillslopes (Keim et al. 2006a; Liang et al. 2009). Liang et al. (2009), for example, have reported that stemflow has led to a root-induced bypass flow infiltration process on hillslopes, a coupled mechanism termed "double-funneling" (Johnson and Lehmann 2006) discussed further in Chap. 24. Stemflow also has been documented to contribute to the enrichment of soils beneath shrubs in semiarid climates, leading to a "fertile island" effect (Whitford et al. 1997), whereas the spatial distribution of fine roots was observed to mirror throughfall inputs (Ford and Deans 1978).

The overarching goal of this chapter is to synthesize and critically assess the current knowledge of the spatiotemporal variability of throughfall and stemflow using abiotic and biotic factors as a unifying theme. Also, we identify knowledge gaps in our current understanding that may direct future research in forest hydrology and biogeochemistry.

Table 21.1 Partitioning of rainfall into throughfall and stemflow from selected studies in deciduous, coniferous, tropical and eucalyptus forest from around the globe

Forest type	Location	Throughfall (%)	Stemflow (%)	Rainfall (mm)	References
Deciduous forests					
Acer spp.	Eastern Canada	77	6	n.a	Mahendrappa (1990)
Fagus sylvatica	NW Italy	73.9	6.4	1,139	Mosello et al. (2002)
Populus gradidentata	Eastern Canada	83	6	n.a	Mahendrappa (1990)
Quercus alba	Georgia, USA	82	0.5	724.8	Bryant et al. (2005)
Quercus ilex	Central Italy	77.8	3.4	861.5	Mosello et al. (2002)
Quercus rubra, Acer saccharum, Fagus grandifolia	Southern Ontario	77.5	3.7	259.3	Price and Carlyle-Moses (2003)
Coniferous forests					
Picea sitchensis	Highland Scotland	69	3	2,130	Johnson (1990)
Pinus contorta, Picea glauca x engelmanni, Abies lasiocarpa	Central British Columbia	71.2	0.2	n.a.	Moore et al. (2008)
Pinus elliotii	Guangzhou, China	74.5	9.5	n.a.	Tang (1996)
Pinus pinaster	Central Portugal	82.6	0.3	528.9	Valente et al. (1997)
Pinus ponderosa	California	84	4	n.a.	Rowe and Hendrix (1951)
Pseudotsuga menziesii (plantation)	Chile	72	6	3,805	Iroumé and Huber (2002)
Pinus sylvestris	NE Spain	73.1	0.8	858	Alvera (1976)
Tsuga canadensis	Connecticut	60.9	5.9		Voigt (1960)
Tropical rainforests					
Amazonian rainforest	Brazil	91	1.8	2,721	Lloyd and Marques (1988)
Amazonian rainforest	Columbia	82–87	1.1	3,121–3,293	Marin et al. (2000)
Lowland rainforest	Indonesia	82.8	0.8		Vernimmen et al. (2007)
Lower montane forest	Ecuador	47–73	0.9–1.0	2,319–2,569	Fleischbein et al. (2005)
Montane forest	Indonesia	70	<1	228	Dietz et al. (2006)
Eucalyptus forests					
Eucalyptus melanophloia	Australia	88	0.6	718	Prebble and Stirk (1980)
Eucalyptus globulus	Central Portugal	87.5	1.7	598.5	Valente et al. (1997)

21.2   Canopy Storage

Canopy storage is generally defined as water on external surfaces of the canopy that subsequently drains to the soil or evaporates during or within a short time (hours) after cessation of rainfall. Canopies are considered saturated to capacity when additional storage does not increase the evaporation rate. The commonly utilized Rutter et al. (1971) canopy interception model assumes that storage may temporarily exceed canopy storage capacity, but some models assume capacity cannot be exceeded (e.g., Mulder 1985; Liu 1997). Confounding factors are rainfall intensity and wind, which affect storage and are sometimes assumed to affect capacity (Calder 1986; Dunkerley 2000). Despite the common modeling assumption that canopies effectively dry within several hours, canopy surfaces may remain moist indefinitely when evaporation is slow and canopy surfaces are geometrically rough (Pypker et al. 2006). Longer-term storage in rough bark or epiphyte mats, and absorption of surface water into plants complicate the concept of canopy storage beyond most canopy storage models.

Several experimental methods have estimated canopy storage in the field during precipitation. There have been a few direct estimates by weighing trees (e.g., Teklahaimanot and Jarvis 1991), though most estimates have been by indirect methods. Measurements of tree deformation under load from water storage have been used to estimate storage on branches (Hancock and Crowther 1979) or entire trees (Friesen et al. 2008). Attenuation of gamma radiation or microwaves also has been used to measure water storage at the canopy scale (Calder and Wright 1986; Bouten et al. 1991). However, the majority of field data used as the basis for modeling has been estimated as the difference between measured rainfall and throughfall, corrected for evaporation during rainfall using measurements (rarely) or estimates of evaporation. Evaporation rates strongly depend on the quantity of canopy storage (Rutter et al. 1971), so the lack of simple methods to measure storage during precipitation and limitations of the estimates made by differencing (Vrugt et al. 2003) have hampered quantitative understanding of canopy interception processes. Although some models have proven useful, their success appears partially due to compensating errors in the modeling assumptions in their adaption of the Penman–Monteith equation (Klaassen 2001).

Laboratory methods to estimate canopy storage dynamics during precipitation have been limited by difficulties in simulating field conditions and in scaling up from the branch scale. The results of rainfall simulation studies depend on the representation of several sources of mass and energy in forests. Drop sizes and velocities, and therefore kinetic energy, of natural rainfall vary by rainfall rate and geographical region (Salles et al. 2002), and strongly affect canopy storage and drip (Calder 1996). Most rainfall simulation experiments have been at high intensities because of difficulties obtaining realistic raindrop sizes for low-intensity rainfall, or because evaporation and sample desiccation are problems for long-duration, lower intensity experiments. Also, rainfall simulations experiments are normally in still air, even though wind affects incidence (Herwitz and Slye 1995) and storage

(Hörmann et al. 1996; Klingaman et al. 2007) of precipitation on canopy surfaces. Estimates of canopy storage obtained by submerging vegetation are usually an order of magnitude lower than those obtained from rainfall simulation (Keim et al. 2006b).

Canopy storage and drip redistribute throughfall in time and space relative to rainfall. Of these two, redistribution in space is relatively well studied, and much less is known about redistribution in time, that is, the effects of the canopy on throughfall intensity. Trimble and Weitzman (1954) first described damping of intensity by canopies, but surprisingly little work has been done to describe or quantify the process since then.

Conservation of momentum dictates that canopies reduce the average downward velocity of water because impingement of rain on canopy surfaces transfers momentum from the rainfall to the trees. When rainfall impinges on surfaces in the canopy, the canopy exerts a force on the rainfall proportional to this loss of velocity according to Newton's second law,

$$dF = \frac{d\bar{v}_r}{dt} dm_r, \tag{21.1}$$

where dF is the force of the canopy acting on dm_r mass of rainfall moving velocity $\bar{v}_r$. This force changes the momentum of the rainfall field, M_r, by

$$\frac{dM_r}{dt} = dt \int_{m_r} \frac{d\bar{v}_r}{dt} dm_r. \tag{21.2}$$

Substituting (21.2) into (21.1) gives

$$\frac{dM_r}{dt} = dt \int_{m_r} dF, \tag{21.3}$$

which describes how the presence of the canopy reduces the momentum of the rainfall field. Conservation of momentum dictates that this momentum must be transferred elsewhere. In this case, it is transferred into the canopy space, thence to the earth or atmosphere. The total momentum within the canopy space, M_c, is

$$M_c = \int_{m_c} \bar{v}_c \, dm_c, \tag{21.4}$$

where $\bar{v}_c$ is the average velocity of all mass elements m_c in the canopy including water, air, and vegetation. Therefore,

$$\frac{dM_c}{dt} = \frac{d}{dt} \int_{m_c} \bar{v}_c \, dm_c \tag{21.5}$$

is the change in the momentum within the canopy space caused by the reduction in mean velocity of the rainfall neglecting dissipation out of the canopy space. By (21.4), M_c is zero before rainfall because $\bar{v}_c = 0$. However, rainfall entering or throughfall leaving the canopy space changes M_c according to (21.5): rainfall adds momentum to the canopy space by (21.2) and throughfall removes it by (21.2). Conservation of momentum dictates that $dM_c = dM_r + dM_{throughfall} + dM_{dissipated}$, so any transfer of momentum from the canopy to the atmosphere or the earth means that $dM_{throughfall} < dM_r$. The decrease in the average velocity of the entire rain field as it moves through the canopy space constitutes a delay, or residence time, in the canopy (Keim and Skaugset 2004); temporary accumulation of water in the canopy is the consequence. Slowing of precipitation by the canopy means that total storage in the canopy increases proportional to rainfall intensity, but deformation of canopy elements due to dissipation of momentum resulting in changes in leaf and branch angles changes the interaction of the canopy with the rainfall so that the relationship is probably more complex. These simple momentum balances neglect wind, which is also an important source of momentum in canopies. Windy conditions often reduce storage (Hörmann et al. 1996) by dislodging water from canopy surfaces. The relative importance of wind compared to incoming rainfall on M_c and canopy storage is unknown, but probably varies with micrometeorological conditions and canopy structure.

Lagging and damping of throughfall intensities compared to rainfall intensities is a consequence of storage; if storage did not temporarily increase during periods of high rainfall intensity, lagging and damping normally observed in the field would not occur. Laboratory experiments with simulated rainfall have sometimes (Keim et al. 2006b), but not always (Calder et al. 1996) found increased storage during higher intensities. The few field measurements of canopy storage during rainfall have generally shown increases during periods of higher intensity (Klaassen et al. 1998).

Despite theoretical and experimental evidence that canopy storage increases with rainfall intensity, optimization of canopy interception models has sometimes led to the conclusion that canopy storage capacity is less for rainstorms with higher average intensity (e.g., Price and Carlyle-Moses 2003). The reason for this apparent conflict is not well understood, but may be related to correlation among event duration, intensity, windspeed, and temperature (Keim 2004), or to systematic differences in canopy wetting that vary by intensity (Hall 2003; Carlyle-Moses 2004) or by timescales of measurement.

The details of specific pathways and residence times of precipitation in the canopy remain poorly understood. Stable isotope tracers reveal relationships more complex than a simple well-mixed canopy (Kendall 1993; DeWalle and Swistock 1994; Broderson et al. 2000); employing these in future research will increase understanding of both hydrological and biogeochemical processes in the canopy.

21.3   Throughfall

21.3.1   Hydrology

The spatial variability of throughfall volume is not inconsequential. Price et al. (1997), for example, found that the spatial variability of throughfall volume, expressed as a coefficient of variation (CV), in a *Picea mariana* (Mill.) B.S.P. (black spruce) stand decreased asymptotically, averaging 60% of rainfall for "small" rain events and remaining appreciable for "large" rainfalls (>10 mm) averaging 24%. Similar results have been found in other forest types (e.g., Bouten et al. 1992; Cantú Silva and Okumura 1996). Intuitively, the spatial variability of throughfall during small rainfalls is relatively large because most, if not all, of the canopy remains unsaturated. Under these canopy wetness conditions, no throughfall originates from areas covered by the canopy, while throughfall will, depending on wind conditions and intensity of the rainfall (Carlyle-Moses and Price 2007), have the potential to be 100% of the rainfall where canopy cover is absent. With greater rainfall inputs, an increasingly larger proportion of the canopy becomes saturated resulting in an increase in release throughfall. At the stand scale, the onset of release throughfall reduces the extreme difference between throughfall inputs beneath areas covered by canopy and those free of cover; however, the lateral movement of water along saturated surfaces within the canopy can result in areas, where relatively large volumes of water coalesce and drip, yielding throughfall inputs that often exceed the incident rainfall input to the canopy (Zimmermann et al. 2009). For relatively large rainfalls, the CV associated with throughfall remains quasiconstant, likely as a result of the entire canopy volume reaching saturation. Carlyle-Moses (2002) found, in a subtemperate oak stand in northeastern Mexico, that under saturated canopy conditions, throughfall spatial variability was not a function of the spatial distribution of canopy storage capacity, but rather was largely dependent on the efficiency and spacing of canopy zones that either shed intercepted rainfall away to other areas of the canopy or concentrated that water into relatively large canopy drip points.

Throughfall has been found to be spatially autocorrelated in some forests. Keim et al. (2005) and Konishi et al. (2006) interpreted the scale of autocorrelation to be related to the size of tree canopies. However, spatial autocorrelation has not been found in all studies; Germer et al. (2006) and Zimmermann et al. (2009) suggested that this may occur when understory vegetation redistributes throughfall patterns inherited from the canopies of overstory trees.

Although the spatial variability of throughfall is a consequence of rainfall interacting with a forest canopy, the interactions that occur and the resulting throughfall spatial pattern, or lack thereof, appear ecosystem dependent. For example, by inference, spatial patterns of throughfall have been related to canopy architecture in forested stands with leaf area index (LAI, $m^2\ m^{-2}$) > 4 (e.g., Nadkarni and Sumera 2004) but weaker (Keim et al. 2005) or nonexistent (e.g., Loustau et al. 1992) in forests where LAI < 4. Carlyle-Moses et al. (2004) evaluated the influence

of canopy and understory cover fraction, vegetation area index (VAI), distance to the nearest tree bole, as well as the basal area and height of that tree on point throughfall input in a subtemperate oak stand. No relationship between throughfall and any of these biotic factors was found for rainfall events >5 mm, while for smaller rainfalls throughfall was related to at least one of these factors.

Abiotic factors, such as rainfall intensity and wind direction, also influence throughfall spatial patterns and variability. Indeed, Zimmermann et al. (2009) found that the relationship between canopy openness and throughfall volume at points of measurement was weaker as storm size increased. Rainfall intensity has been shown to reduce the CV of throughfall (Weiqing et al. 2007), while increasing wind speed may result in increased throughfall spatial variability in certain forests because of the large differences in rainfall delivery between windward and leeward sides of larger tree crowns (Herwitz and Slye 1995).

Although micrometeorological processes controlling spatial patterns in throughfall vary in time, research has generally concluded that spatial patterns persist among storms (Raat et al. 2002). In some cases, patterns vary seasonally in canopies dominated by deciduous trees (Keim et al. 2005; Staelens et al. 2006a), but some canopies retain enough structure during leafed and leafless periods for spatial patterns to persist across seasons (Zimmermann et al. 2009). Even when spatial autocorrelation of throughfall measurements are weak, locations of wet and dry places may persist (Zimmermann et al. 2009) because drip points and sheltered zones are discrete points rather than varying continuously in space (Ziegler et al. 2009). The seasonality of throughfall inputs is discussed fully in Chap. 26.

21.3.2   Biogeochemistry

There are many factors that influence throughfall biogeochemistry in wooded ecosystems (Levia and Frost 2006). Two major factors affecting the spatiality of throughfall chemistry discussed in this chapter are the topographic position and location of a forest with respect to pollution emission sources (Chiwa et al. 2003; Àvila and Rodrigo 2004) and whether the canopy trees are on the edge or in the interior of forests (Devlaeminck et al. 2005).

Throughfall biogeochemistry is markedly different for forests subjected to industrial emissions in comparison with those that are not due to distance, slope position, or local terrain. In Japan, the delivery of SO_4^{2-} and NO_3^- to the forest floor via throughfall was notably higher for slopes facing urbanized locations than slopes oriented toward more rural locations (Chiwa et al. 2003). Marked differences in throughfall chemistry also were observed for two forests in Spain as a result of differential exposure to an industrialized area (Àvila and Rodrigo 2004). Higher trace metal fluxes (i.e., Zn, V, Cu, Cd) in throughfall at Riera de Sant Pere (exposed site) were ascribed to increased atmospheric dryfall in comparison with the more sheltered site at La Castanya (Àvila and Rodrigo 2004).

Spatial variability of throughfall solute flux affects atmospheric loadings to the land surface and their subsequent effects on elemental cycling. In a Belgian *Fagus sylvatica* L. (European beech) forest, Devlaeminck et al. (2005) found that the throughfall inputs of base cations were significantly greater at the forest edge than the forest interior as a result of increased exposure of the aerodynamically rough canopy and consequent increases in the efficient scavenging and capture of dryfall. No striking disparities between the forest edge and interior were detected for SO_4^{2-} throughfall fluxes (Devlaeminck et al. 2005). Interestingly, the canopy leaching of K^+ and Ca^{2+} were markedly lower at the forest edge and to a distance of 30 m inward in comparison with the forest interior (Devlaeminck et al. 2005).

Besides the obvious differences in throughfall chemistry among seasons (Chap. 26), temporal differences in throughfall solute flux exist at shorter time intervals among discrete storms events as a probable result of differences in micrometeorological conditions, such as wind speed and wind direction (André et al. 2008a). Temporal variability of net throughfall ion flux in a mixed deciduous forest was not explained by rain volume and the length of the antecedent dry period between rain events, suggesting that factors such as wind speed and direction are likely to exert a considerable influence on storm-to-storm variations in throughfall chemistry (André et al. 2008a). Over a slightly longer 2-week sampling resolution, Staelens et al. (2006b) reported that the mean CV of throughfall deposition of H^+, K^+, Cl^-, and SO_4^{2-} were greater over the 2-week time intervals compared to leaf and leafless periods. They also demonstrated a very high CV for NO_3^- during leaf burst indicating that phenological development of the canopy has a distinct and detectable effect on throughfall chemistry in mixed deciduous forests. These studies demonstrate the need for further research into the variability of throughfall solute flux across temporal scales.

21.3.3 Throughfall: Future Research Directions

The majority of research into canopy interactions with precipitation has focused on quantifying evaporation and its role in the long-term stand water balance. Fine-scale physical mechanisms controlling retention, evaporation, and spatial redistribution of precipitation by canopies have received lesser attention. The generally good performance of the Penman–Monteith approach to modeling evaporation from wetted canopies has engendered confidence that physical processes in the canopy are correctly represented by the Rutter and Gash models, yet some of the most rudimentary relevant state variables necessary to test these assumptions, such as volume of water in the canopy space, have rarely been measured. There have been attempts to measure storage properties of canopy elements in the laboratory (e.g., Herwitz 1987; André et al. 2008b), although scaling up these measurements is subject to large uncertainties due to the complexity of canopy structure. Innovative ways to measure water in situ in canopies are still needed, especially to understand the poor performance of Rutter–Gash models in some forests (e.g., Calder et al. 1996; Klaassen 2001).

Closing the water balance for canopies is sometimes difficult when woody surfaces and epiphytes are capable of absorbing large quantities of water. Pypker et al. (2006) found that epiphyte mats required >30 mm of rainfall to reach saturation and never dried completely between storm events. These large stores, however, are not always active at the short timescales of individual rain events because of their significant aerodynamic resistance (Hölscher et al. 2004). Thus, understanding the role of canopy storage requires knowledge of structural characteristics in terms of both storage capacities and flux resistance. There are few forest types for which there are detailed understanding of these properties, and almost no research on nested scales of flux resistance within the canopy.

21.4 Stemflow

21.4.1 Hydrology

The stemflow funneling ratio developed by Herwitz (1986) is a useful construct to examine the spatiotemporal variability of stemflow with respect to abiotic and biotic factors. Herwitz (1986) defined the funneling ratio, F, as

$$F = V/(B \times P), \qquad (21.6)$$

where V is stemflow volume, B is trunk basal area, and P is the depth equivalent of incident precipitation. F values >1 indicate that the tree crown is contributing a greater proportion of the stemflow input than what would be expected solely from the trunk basal area, whereas F values <1 indicate that this is not the case, suggesting that the bark water storage capacity may not have been reached during lower magnitude events or that stemflow was diverted as throughfall as a result of canopy structure. Season-long funneling ratios of several deciduous tree species typically ranges from 7 to 26 (Carlyle-Moses and Price 2006); albeit funneling ratios for individual trees may exceed 100 (Herwitz 1986) or be <1 for old growth Douglas-fir (Rothacher 1963).

Abiotic factors that affect stemflow yield over space and through time are related to micrometeorological conditions. Of primary importance with respect to stemflow yield are: precipitation type (rain, snow), storm duration, storm magnitude, storm intensity, wind speed, and wind direction. Most studies have examined stemflow from rain events, rather than stemflow corresponding with snowmelt. Many researchers have observed increased stemflow generation with increased rain amount (e.g., Clements 1972; André et al. 2008c). Stemflow generation corresponding to snowmelt is more complicated with stemflow yields differing greatly as a result of many interacting factors, including the moisture content of snow, energy balance of the intercepted snow mass, and changing albedo and emissivity of the canopy as snowmelt progresses (Levia and Underwood 2004).

On the whole, however, snowmelt induced stemflow volumes tended to be lower than those generated from comparably sized rain events (Levia 2004), possibly attributable to dislodgement and/or sublimation losses of intercepted snow. Herwitz and Levia (1997) found that stemflow amounts originating from snowmelt were the largest when intercepted snow was covered with glaze precipitation, thereby preventing wind from dislodging the intercepted snow mass from the canopy.

Stemflow yield increases with precipitation and, funneling ratios also increase with precipitation until the storage capacity of the stemflow contributing area has been reached. Carlyle-Moses and Price (2006) found that the growing-season geometric mean funneling ratio of eighteen deciduous trees in a forest stand increased with increasing rainfall for events ranging from approximately 4 to 17 mm. For larger events, however, funneling ratios decreased, suggesting that as the canopies and trunks of the trees became saturated the stemflow contributing area increased until a threshold rainfall depth was reached. Once the threshold rainfall depth was exceeded, funneling ratios decreased; possibly as a consequence of changes to flowpath regimes under saturated canopy conditions that result in increased canopy release in the form of throughfall rather than stemflow. Increasing storm intensities have been documented to decrease stemflow yields as preferred flowpaths become overloaded and entrained as throughfall (Levia and Frost 2003). Stepwise linear regression analysis revealed that when rainfall depth was included there was a statistically significant negative correlation between stemflow production and rainfall intensity for *Quercus rubra* L. (red oak), *Acer saccharum* Marsh. (sugar maple) and *Fagus grandifolia* Ehrh. (American beech) (Carlyle-Moses and Price 2006).

Both wind speed and wind direction affect stemflow yield. Some researchers have found that stemflow yield increases with wind speed for isolated trees (Xiao et al. 2000) and trees within forests (Kuraji et al. 2001). It is likely that higher wind speeds wet a greater proportion of the tree crown, which enhances stemflow production. During storm events with strong winds and a single prevailing wind direction, the exposed sides of tree crowns are preferentially wetted and generate stemflow before interception storage capacity is reached. Trees within the lateral rainshadow of taller neighbors and sides of trees opposite to the prevailing wind direction remain sheltered, with no or negligible contributions to stemflow production. A full discussion on the effects of canopy structure and wind on stemflow yields is included in Chap. 18.

Tree species is arguably the most critical biotic factor affecting stemflow yield in wooded ecosystems. Tree species and age often dictate the bark morphology, branching geometry, and potential contributing surface area of trees, all of which have significant influence on stemflow generation (Levia and Frost 2003). Generally, increases in stem diameter and associated increase in crown area and extent have been found to increase stemflow yield (Park and Hattori 2002), but in some stands and species this relationship is not significant (Carlyle-Moses and Price 2006). Considerable influence on stemflow also can be attributed to the morphology

and hydrophobicity of the bark surface. Species exhibiting smooth bark, such as *F. grandifolia* and *F. sylvatica* L. (European beech), can generate stemflow at lower precipitation depth thresholds compared with rougher barked species such *Q. rubra* or *Liriodendron tulipifera* L. (yellow poplar) (Carlyle-Moses and Price 2006; Van Stan and Levia 2010) because of lower water storage capacities and lower resistance to flow along the stem. In smooth-barked species, there is generally a reduced prevalence of potential drip points where stemflow can be lost or converted to near-stem throughfall; however, some smooth-barked eucalypts may divert considerable stemflow to drip points from bark flakes (Crockford and Richardson 2000). The spatial location of these drip points is also of importance as bark or structural changes resulting in drip points further down the stem have greater influence on potential stemflow-to-throughfall conversion due to the cumulative nature of flow along the tree. This may be especially true in forests influenced by disturbances when there is a prevalence of species susceptible to epicormic shoot generation.

Trees with branching geometry consisting of steeper inclination angles have been found to contribute greater stemflow than those with horizontal or subhorizontal architecture (Herwitz 1987), for which intercepted precipitation is more likely to be lost from the surface as release throughfall. This may be one of the main reasons for the significant stemflow generation differences between mature coniferous and deciduous canopy trees, as the near horizontal branch angle in most coniferous tree species are not as conducive to funneling interception precipitation toward the stem (Levia and Frost 2003). Branching angles predominantly vary with species, but considerable intraspecific variation may exist depending on canopy position, age, and competition effects of individual trees. The effects of geometry also extend to foliage, where species exhibiting concave leaves oriented at an angle above the horizontal may effectively funnel precipitation intercepted by the leaf surface to its petiole and ultimately the stem (Crockford and Richardson 2000). This effect can be enhanced with foliage exhibiting a high degree of hydrophobicity, decreasing canopy storage capacity and potentially increasing the available water for stemflow generation.

Stand density can also have a profound effect on stemflow generation. The inclination of incident rainfall in dense stands may produce a significant rain-shadowing effect, subsequently limiting the effective surface area contributing to stemflow generation (Herwitz and Slye 1995). Canopy gaps may also drive stemflow production by allowing greater rainfall penetration into the lower reaches of the canopy, which may be less pronounced in dense plantations with considerable crown overlap (Ford and Deans 1978). The relationship between stemflow generation and biotic factors is a complex interaction among multiple variables, and it may be difficult to isolate individual factors even within species. Due to the significant variation in intraspecific biotic factors that influence stemflow, it should not be assumed that stemflow generation from trees of the same species and size are necessarily equal. The effects of canopy structure on throughfall and stemflow are discussed further in Chap. 18.

21.4.2   Biogeochemistry

Stemflow enrichment ratios are computed by considering the quantity of each canopy leachate draining from the tree in relation to the quantity of each leachate that would be expected in an area equivalent to the tree's trunk basal area. In equation form,

$$E = (C_s \times V)/(C_p \times P \times B), \tag{21.7}$$

where E is the enrichment ratio, C_s is the chemical concentration of a given leachate in stemflow, V is stemflow volume, C_p is the mean chemical concentration of a given leachate in incident precipitation, P is the depth equivalent of incident precipitation, and B is the trunk basal area (Levia and Herwitz 2000). The stemflow enrichment ratio is a useful metric to examine the spatiotemporal variability of stemflow solute inputs as a function of both abiotic and biotic factors.

Relatively little experimental work has investigated the effects of micrometeorological conditions on stemflow leachate chemistry. Tukey (1970) stated that leachate concentrations are lower during high intensity, short duration events than events with prolonged contact time between rainfall and vegetative surfaces. Later work by Crockford et al. (1996) demonstrated that increased rain intensities led to lower stemflow leachate concentrations for eucalypts. The creation of lateral rainshadows also alters the effective crown area of trees, leaving some trees completely or partially dry during a given event and limiting leaching losses. The magnitude, duration, and intensity of a given rain event affect the concentration gradient between the bark surface and intercepted precipitation. Coupled with storm specific characteristics are other abiotic factors – for example, air mass provenance, proximity to the sea, and season – and biotic factors – such as species, tree age and health, and genetics – that govern whether a kinetic solubility gradient or thermodynamic solubility equilibrium is achieved. This complex set of mutually interacting factors ultimately determines stemflow leachate chemistry.

Levia and Herwitz (2000) found that E varies greatly with micrometeorological conditions during winter when temperatures oscillate around the freezing point. For two highly leachable cations, K^+ and Mn^{2+}, E ratios from *Carya glabra* Mill. (pignut hickory) averaged 580 and 1,450, respectively (Levia and Herwitz 2000). E was larger during storm events that transitioned from snow to rain, and there was a crossover from below- to above-freezing air temperatures (Levia and Herwitz 2000). During a rain-on-snow event, with 17 h of light mist following the snow and preceding the rain, E for K^+ and Mn^{2+} were 1,715 and 4,400, respectively (Levia and Herwitz 2000). The larger E ratios during colder and mixed precipitation events were ascribed to the physical properties of water (i.e., viscosity and surface tension) that lengthens the contact time of intercepted precipitation with the bark surface.

Winter stemflow leaching from leafless deciduous trees was affected by precipitation type (Levia 2003). The primary determinants of stemflow enrichment with

regard to precipitation type were interception efficiency and residence time with the bark surface. In essence, contact time with the bark surface enhanced stemflow leaching during snow-to-rain events because the snow kept the rain and meltwater in contact with the bark surface for prolonged periods vis-à-vis stemflow during a rain event (Levia 2003). Moreover, the lower temperatures coincident with the snow-to-rain event, as compared to a rain event, increased the viscosity of stemflow drainage and lengthened the residence time (Levia 2003). Enrichment ratios were least during snow, sleet, and rain shower events because: (1) of the lower interception efficiency from wind displacement of intercepted snow or the bouncing of sleet from the leafless crowns upon impact; and (2) lower bark water storage levels and decreased wetting durations during these types of events (Levia 2003).

Sequential sampling of stemflow chemistry during discrete precipitation events has shed light on the sources the stemflow solute load. Kazda (1990) found that different nutrient-ions had different proportions of their chemistry derived from atmospheric and canopy sources. Roughly, three-fourths of K^+ was derived from canopy leaching, whereas the corresponding percentage for Ca^{2+} was approximately 38% (Kazda 1990).

Intra-storm sequential sampling of variations in stemflow $\delta^{18}O$ revealed mixed results, with some storms exhibiting progressive decreases in $\delta^{18}O$ throughout the event and others exhibiting a decrease and then rapid increase in $\delta^{18}O$ near the end of the discrete storm event (Kubota and Tsuboyama 2003). Stemflow (and throughfall) was more enriched in $\delta^{18}O$ and δD than bulk rainfall 70% of the time (Kubota and Tsuboyama 2003). Chapter 7 discusses isotopes as a tool in forest hydrology and biogeochemistry.

Tree species and characteristics inherent to particular species (e.g., rough bark, branching geometry) have a great impact on stemflow chemistry by affecting stemflow production and altering the residence time of intercepted precipitation on a tree's woody frame. Although it is beyond the scope of this chapter to discuss the myriad ways, species-specific factors could account for variations in stemflow chemistry, some generalizations can be made on the basis of previous work. Similar to effects for stemflow yield, canopy hydrophobicity decreases leachability since detained water has less residence time. Stemflow leachate concentrations have been found to be greater from rougher-barked trees than smoother-barked trees due to increased contact time. Levia and Herwitz (2005) found that rough-barked *C. glabra* had higher stemflow nutrient-ion concentrations than smoother-barked species but lower total nutrient inputs due to lower stemflow volumes as a result of its unique bark morphology that limits stemflow production. Likewise, bark water storage capacity among species affects stemflow solute inputs by affecting how long the bark is wetted and leaching can occur (Levia and Herwitz 2005). Tree species that tend to produce large stemflow volumes as a result of erectophile branching patterns are likely to have greater stemflow inputs than those with plagiophile branching patterns that favor the formation of throughfall.

Tree age and size also have been documented to have a detectable impact on leachability of plants. Older plants were reported to leach larger quantities of nutrient-ions than younger plants (Tukey 1970). André et al. (2008d) reported

that tree size was an important predictor of stemflow chemistry under certain circumstances with larger trees having more leaching than smaller trees. In fact, tree size explained some of the inter-tree variability within a given species (André et al. 2008d). Tree size was more important in the leafless season than during full leaf (André et al. 2008d).

Neary and Gizyn (1994) noted the potential of bark to leach nutrients and found that K^+ concentrations in stemflow were higher in dormancy than the growing season. André et al. (2008d) employed the enrichment ratio to examine the effects of phenological state on stemflow chemistry within a mixed oak-beech forest. In general, E ratios for base cations and some anions (e.g., SO_4^{2-} and Cl^-) were higher in the leafless period than leafed period as a result of higher exchange and dry deposition rates and larger stemflow volumes generated during leafless conditions at this site (André et al. 2008d). NH_4^+ and NO_3^- were notable exceptions with net sequestration by individual trees in the leafless state (André et al. 2008d).

21.4.3   Stemflow: Future Research Directions

In an effort to synthesize the stemflow literature and directly compare results among studies, future work quantifying stemflow inputs must employ both the stemflow funneling and the enrichment ratios. This is critically important since trunk basal area constitutes the area over which stemflow is channeled to the forest soil. Calculations of stemflow inputs based on larger areas (e.g., plot area) probably underestimate the importance of stemflow water and solute fluxes. Such calculations fail to represent stemflow as a spatially localized point input (per unit trunk basal area) commensurate with its importance, often leading to the erroneous conclusion that stemflow is of minor consequence to the hydrology and biogeochemistry of forests.

Future research on stemflow should be directed in four primary directions: (1) investigating stemflow hydrology and leachate chemistry corresponding to snowmelt; (2) quantifying fluctuations in stemflow hydrology and chemistry within discrete precipitation events; (3) measuring stemflow leaching in relation to external stressors; and (4) partitioning and quantifying the contribution of stemflow to streamflow. Further work should examine the volumetric water inputs corresponding with snowmelt-induced stemflow and its chemical character in forests where stemflow production is likely to be significant. Biogeochemical interactions in forests tend to occur in both temporal "hot moments" and spatial "hot spots." Stemflow sequential sampling within particular events is necessary to better understand the effects of stemflow inputs on biogeochemical cycling in forests. The effects of external stressors, such as ice storms and hurricanes, on stemflow leachate chemistry are unknown. Research must examine stemflow leaching in relation to stressors so that the vulnerability and response of forests to a particular stressor can be modeled, predicted, and dealt with proactively. End-member mixing analysis should be employed to determine whether and when stemflow contributes appreciably to streamflow.

References

Alvera B (1976) Contribución al estudio de la interceptación de las precipitaciones atmosféricas en elpinar de San Juan de la Peña. Publ Cent Pir Biol Exp 7:95–100

André F, Jonard M, Ponette Q (2008a) Spatial and temporal patterns of throughfall chemistry within a temperate mixed oak–beech stand. Sci Total Environ 397:215–228

André F, Jonard M, Ponette Q (2008b) Precipitation water storage capacity in a temperate mixed oak-beech canopy. Hydrol Process 22:4130–4141

André F, Jonard M, Ponette Q (2008c) Influence of species and rain event characteristics on stemflow volume in a temperate mixed oak-beech stand. Hydrol Process 22:4455–4466

André F, Jonard M, Ponette Q (2008d) Effects of biological and meteorological factors on stemflow chemistry within a temperate mixed oak–beech stand. Sci Total Environ 393:72–83

Àvila A, Rodrigo A (2004) Trace metal fluxes in bulk deposition, throughfall and stemflow at two evergreen oak stands in NE Spain subject to different exposure to the industrial environment. Atmos Environ 38:171–180

Bouten W, Swart PJF, de Water E (1991) Microwave transmission, a new tool in forest hydrological research. J Hydrol 124:199–230

Bouten W, Heimovaara T, Tiktak A (1992) Spatial pattern of throughfall and soil water dynamics in a Douglas fir stand. Water Resour Res 28:3227–3233

Broderson C, Pohl S, Lindenlaub M et al (2000) Influence of vegetation structure on isotope content of throughfall and soil water. Hydrol Process 14:1439–1448

Bryant ML, Bhat S, Jacobs JM (2005) Measurements and modeling of throughfall variability for five forest communities in the southeastern US. J Hydrol 312:95–108

Calder IR (1986) A stochastic model of rainfall interception. J Hydrol 89:65–71

Calder IR (1996) Dependence of rainfall interception on drop size: 1. Development of the two-layer stochastic model. J Hydrol 185:363–378

Calder IR, Wright IR (1986) Gamma ray attenuation studies of interception from Sitka spruce: some evidence for an additional transport mechanism. Water Resour Res 22:409–417

Calder IR, Hall RL, Rosier PTW et al (1996) Dependence of rainfall interception on drop size: 2. Experimental determination of the wetting functions and two-layer stochastic model parameters for five tropical tree species. J Hydrol 185:379–388

Cantú Silva I, Okumura T (1996) Throughfall, stemflow and interception loss in a mixed white oak forest (*Quercus serrata* Thunb.). J For Res 1:123–129

Carlyle-Moses DE (2002) Measurement and modelling of canopy water fluxes within representative forest stands and a matorral community of a small Sierra Madrea Oriental watershed, northeastern Mexico. PhD Dissertation, University of Toronto

Carlyle-Moses DE (2004) A reply to R. Keim's comment on "Measurement and modelling of growing-season canopy water fluxes in a mature mixed deciduous forest stand, southern Ontario, Canada". Agric For Meteorol 124:281–284

Carlyle-Moses DE, Price AG (2006) Growing-season stemflow production within a deciduous forest of southern Ontario. Hydrol Process 20:3651–3663

Carlyle-Moses DE, Price AG (2007) Modelling canopy interception loss from a Madrean pine-oak stand, northeastern Mexico. Hydrol Process 21:2572–2580

Carlyle-Moses DE, Flores-Laureano JS, Price AG (2004) Throughfall and throughfall spatial variability in Madrean oak forest communities of northeastern Mexico. J Hydrol 297:124–135

Chiwa M, Do Hoon K, Sakugawa H (2003) Rainfall, stemflow, and throughfall chemistry at urban- and mountain-facing sites at Mt. Gokurakuji, Hiroshima, western Japan. Water Air Soil Pollut 146:93–109

Clements JR (1972) Stemflow in a multi-storied aspen community. Can J For Res 2:160–165

Crockford RH, Richardson DP (2000) Partitioning of rainfall into throughfall, stemflow and interception: effect of forest type, ground cover and climate. Hydrol Process 14:2903–2920

Crockford RH, Richardson DP, Sageman R (1996) Chemistry of rainfall, throughfall and stemflow in a eucalypt forest and a pine plantation in south-eastern Australia: 3. Stemflow and total inputs. Hydrol Process 10:25–42

Devlaeminck R, De Schrijver A, Hermy M (2005) Variation in throughfall deposition across a deciduous beech (*Fagus sylvatica* L.) forest edge in Flanders. Sci Total Environ 337:241–252

DeWalle DR, Swistock BR (1994) Differences in O-18 content of throughfall and rainfall in hardwood and coniferous forests. Hydrol Process 8:75–82

Dietz J, Hölscher D, Leuschner C et al (2006) Rainfall partitioning in relation to forest structure in differently managed montane forest stands in Central Sulawesi, Indonesia. For Ecol Manage 237:170–178

Dunkerley D (2000) Measuring interception los and canopy storage in dryland vegetation: a brief review and evaluation of available research strategies. Hydrol Process 14:669–678

Fleischbein K, Wilcke W, Goller R et al (2005) Rainfall interception in a lowland montane forest in Ecuador: effects of canopy properties. Hydrol Process 19:1355–1371

Ford ED, Deans JD (1978) The effects of canopy structure on stemflow, throughfall and interception loss in a young Sitka spruce plantation. J Appl Ecol 15:905–917

Friesen J, van Beek C, Selker J et al (2008) Tree rainfall interception measured by stem compression. Water Resour Res 44:W00D15

Germer S, Elsenbeer H, de Morales JM (2006) Throughfall and temporal trends of rainfall redistribution in an open tropical rainforest in south-western Amazonia (Rondonia, Brazil). Hydrol Earth Syst Sci 10:383–393

Hall RL (2003) Interception loss as a function of rainfall and forest types: stochastic modelling for tropical canopies revisited. J Hydrol 280:1–12

Hancock NH, Crowther JM (1979) A technique for the direct measurement of water storage on a forest canopy. J Hydrol 41:105–122

Herwitz SR (1986) Infiltration-excess caused by stemflow in a cyclone-prone tropical rainforest. Earth Surf Proc Landforms 11:401–412

Herwitz SR (1987) Raindrop impact and water flow on the vegetative surfaces of trees and the effects on stemflow and throughfall generation. Earth Surf Proc Landforms 12:425–432

Herwitz SR, Levia DF (1997) Mid-winter stemflow drainage from bigtooth apsen (*Populus grandidentata* Michx.) in central Massachusetts. Hydrol Process 11:169–175

Herwitz SR, Slye RE (1995) Three-dimensional modeling of canopy tree interception of wind-driven rainfall. J Hydrol 168:205–226

Hölscher D, Köhler L, van Dijk AIJM et al (2004) The importance of epiphytes to total rainfall interception by a tropical montane rain forest in Costa Rica. J Hydrol 292:308–322

Hörmann G, Branding A, Clemen T et al (1996) Calculation and simulation of wind controlled canopy interception of a beech forest in Northern Germany. Agric For Meteorol 179:131–148

Iroumé A, Huber A (2002) Comparison of interception losses in a broadleaved native forest and a *Pseudotsuga menziesii* (Douglas fir) plantation in the Andes Mountains of southern Chile. Hydrol Process 16:2347–2361

Johnson RC (1990) The interception, throughfall and stemflow in a forest in Highland Scotland and the comparison with other upland forests in the U.K. J Hydrol 312:95–108

Johnson MS, Lehmann J (2006) Double-funneling of trees: stemflow and root-induced preferential flow. Ecoscience 13:324–333

Kazda M (1990) Sequential stemflow sampling for estimation of dry deposition and crown leaching in beech stands. In: Harrison AF, Ineson P, Heal OW (eds) Nutrient cycling in terrestrial ecosystems: field methods, applications, and interpretation. Elsevier, Amsterdam, pp 46–55

Keim RF (2004) Comment on "Measurement and modelling of growing-season canopy water fluxes in a mature mixed deciduous forest stand, southern Ontario, Canada". Agric For Meteorol 124:277–279

Keim RF, Skaugset AE (2004) A linear system model of dynamic throughfall rates beneath forest canopies. Water Resour Res 40:W05208

Keim RF, Skaugset AE, Weiler M (2005) Temporal persistence of spatial patterns in throughfall.
  J Hydrol 314:263–274
Keim RF, Tromp-van Meerveld HJ, McDonnell JJ (2006a) A virtual experiment on the effects of
  evaporation and intensity smoothing by canopy interception on subsurface stormflow genera-
  tion. J Hydrol 327:352–364
Keim RF, Skaugset AE, Weiler M (2006b) Storage of water on vegetation under simulated rainfall
  of varying intensity. Adv Water Resour 29:974–986
Kendall C (1993) Impact of isotopic heterogeneity in shallow systems on modeling of stormflow
  generation. PhD Dissertation, University of Maryland
Klaassen W (2001) Evaporation from rain-wetted forest in relation to canopy wetness, canopy
  cover, and net radiation. Water Resour Res 37:3227–3236
Klaassen W, Bosveld F, de Water E (1998) Water storage and evaporation as constituents of
  rainfall interception. J Hydrol 212–213:36–50
Klingaman NP, Levia DF, Frost EE (2007) A comparison of several canopy interception models
  for a leafless mixed deciduous forest stand in the eastern United States. J Hydrometeor
  8:825–836
Konishi S, Tani M, Kosugi Y et al (2006) Characteristics of spatial distribution of throughfall in a
  lowland tropical rainforest, Peninsular Malaysia. Forest Ecol Manag 224:19–25
Kubota T, Tsuboyama Y (2003) Intra- and inter-storm oxygen-18 and deuterium variations of rain,
  throughfall, and stemflow, and two-component hydrograph separation in a small forested
  catchment in Japan. J For Res 8:179–190
Kuraji K, Yuri T, Nobuaki T et al (2001) Generation of stemflow volume and chemistry in a
  mature Japanese cypress forest. Hydrol Process 15:1967–1978
Levia DF (2003) Winter stemflow leaching of nutrient-ions from deciduous canopy trees in
  relation to meteorological conditions. Agric For Meteorol 117:39–51
Levia DF (2004) Differential winter stemflow generation under contrasting storm conditions in a
  southern New England broadleaved deciduous forest. Hydrol Process 18:1105–1112
Levia DF, Frost EE (2003) A review and evaluation of stemflow literature in the hydrologic and
  biogeochemical cycles of forested and agricultural ecosystems. J Hydrol 274:1–29
Levia DF, Frost EE (2006) Variability of throughfall volume and solute inputs in wooded
  ecosystems. Prog Phys Geog 30:605–632
Levia DF, Herwitz SR (2000) Physical properties of stemflow water in relation to leachate
  dynamics: implications for nutrient cycling. Can J For Res 30:662–666
Levia DF, Herwitz SR (2005) Interspecific variation of bark water storage capacity of three
  deciduous tree species in relation to stemflow yield and solute flux to forest soils. Catena
  64:117–137
Levia DF, Underwood SJ (2004) Snowmelt induced stemflow in northern hardwood forests: a
  theoretical explanation on the causation of a neglected hydrological process. Adv Water
  Resour 27:121–128
Liang W-L, Kosugi K, Mizuyama T (2009) A three-dimensional model of the effect of stemflow
  on soil water dynamics around a tree on a hillslope. J Hydrol 366:62–75
Liu S (1997) A new model for the prediction of rainfall interception in forest canopies. Ecol Model
  99:151–159
Lloyd CR, Marques FA (1988) Spatial variability of throughfall and stemflow measurements in
  Amazonian rain forests. Agric For Meteorol 42:63–73
Loustau D, Berbigier P, Granier A et al (1992) Interception loss, throughfall and stemflow in a
  maritime pine stand. I. Variability of throughfall and stemflow beneath the pine canopy.
  J Hydrol 138:449–467
Mahendrappa MK (1990) Partitioning of rainwater and chemicals into throughfall and stemflow in
  different forest stands. For Ecol Manage 30:65–72
Marin CT, Bouten W, Sevink J (2000) Gross rainfall and its partitioning into throughfall, stemflow
  and evaporation of intercepted water in four forest ecosystems in western Amazonia. J Hydrol
  237:40–57

Moore RD, Winkler RD, Carlyle-Moses DE et al (2008) Watershed response to the McLure forest fire: presentation summaries from the Fishtrap Creek workshop, March 2008. Streamline Watershed Manag Bul 12:1–11

Mosello R, Brizzio MC, Kotzias D et al (2002) The chemistry of atmospheric deposition in Italy in the framework of the National Programme for Forest Ecosystems Control (CONECOFOR). J Limnol 61:77–92

Mulder JPM (1985) Simulating interception loss using standard meteorological data. In: Hutchison BA, Hicks BB (eds) The forest-atmosphere interaction. Reidel, Dordrecht, pp 177–196

Nadkarni NM, Sumera MM (2004) Old-growth forest canopy structure and its relationship to throughfall interception. For Sci 50:290–298

Neary AJ, Gizyn WI (1994) Throughfall and stemflow chemistry under deciduous and coniferous forest canopies in south-central Ontario. Can J For Res 24:1089–1100

Park H-T, Hattori S (2002) Applicability of stand structural characteristics to stemflow modelling. J For Res 7:91–98

Prebble RE, Stirk GB (1980) Throughfall and stemflow on silverleaf ironbark (*Eucalyptus melanophloia*) trees. Aust J Ecol 5:419–427

Price AG, Carlyle-Moses DE (2003) Measurement and modelling of growing-season canopy water fluxes in a mature mixed deciduous forest stand, southern Ontario, Canada. Agric For Meteorol 119:69–85

Price AG, Dunham K, Carleton T et al (1997) Variability of water fluxes through the black spruce (*Picea mariana*) canopy and feather moss (*Pleurozium schreberi*) carpet in the boreal forest of northern Manitoba. J Hydrol 196:310–323

Pypker TG, Unsworth MH, Bond BJ (2006) The role of epiphytes in rainfall interception by forests in the Pacific Northwest. II. Field measurements at the branch and canopy scale. Can J For Res 36:819–832

Raat KJ, Draaijers GPJ, Schaap MG et al (2002) Spatial variability of throughfall water and chemistry and forest floor water content in a Douglas fir forest stand. Hydrol Earth Syst Sci 6:363–374

Rothacher J (1963) Net precipitation under a Douglas-fir forest. For Sci 9:423–429

Rowe PB, Hendrix TM (1951) Interception of rain and snow by second growth ponderosa pine. Trans Am Geophys Union 32:903–908

Rutter AJ, Kershaw KA, Robins PC et al (1971) A predictive model of rainfall interception in forests, 1. Derivation of the model from observations in a plantation of Corsican pine. Agric Meteorol 9:367–384

Salles C, Poesen J, Sempere-Torres D (2002) Kinetic energy of rain and its functional relationship with intensity. J Hydrol 257:256–270

Staelens J, De Schrijver A, Verheyen K et al (2006a) Spatial variability and temporal stability of throughfall water under a dominant beech (*Fagus sylvatica* L.) tree in relationship to canopy cover. J Hydrol 330:651–662

Staelens J, De Schrijver A, Verheyen K et al (2006b) Spatial variability and temporal stability of throughfall deposition under beech (*Fagus sylvatica* L.) in relationship to canopy structure. Environ Pollut 142:254–263

Stout BB, McMahon RJ (1961) Throughfall variations under tree crowns. J Geophys Res 66:1839–1843

Tang C (1996) Interception and recharge processes beneath a *Pinus elliotii* forest. Hydrol Process 19:1355–1371

Teklahaimanot Z, Jarvis PG (1991) Direct measurement of evaporation of intercepted water from forest canopies. J Appl Ecol 28:603–618

Trimble GR Jr, Weitzman S (1954) Effect of a hardwood canopy on rainfall intensities. Eos Trans Am Geophys Union 35:226–234

Tukey HB Jr (1970) The leaching of substances from plants. Ann Rev Plant Physiol 21:305–324

Valente F, David JS, Gash JHC (1997) Modelling interception loss for two sparse eucalypt and pine forests in central Portugal using reformulated Rutter and Gash analytical models. J Hydrol 190:141–162

Van Stan JT, Levia DF (2010) Inter- and intraspecific variation of stemflow production from *Fagus grandifolia* Ehrh. (American beech) and *Liriodendron tulipifera* L. (yellow poplar) in relation to bark microrelief in the eastern United States. Ecohydrology 3:11–19

Vernimmen RRE, Bruijnzeel LA, Romdoni A et al (2007) Rainfall interception in three contrasting lowland rain forest types in Central Kalimantan, Indonesia. J Hydrol 340:217–232

Voigt GK (1960) Alteration of the composition of rainwater by trees. Amer Midl Nat 63:321–326

Vrugt JA, Dekker SC, Bouten W (2003) Identification of rainfall interception model parameters from measurements of throughfall and forest canopy storage. Water Resour Res 39:1251. doi:10.1029/2003WR002013

Weiqing Z, Zhiqiang Z, Jun WU et al (2007) Spatial variability of throughfall in a Chinese pine (*Pinus tabulaeformis*) plantation in northern China. Front For China 2:169–173

Whitford WG, Anderson J, Rice PM (1997) Stemflow contribution to the "fertile island" effect in creosotebush, *Larrea tridentata*. J Arid Env 35:451–457

Xiao Q, McPherson EG, Ustin SL, Grismer ME, Simpson JR (2000) Winter rainfall interception by two mature open grown trees in Davis, California. Hydrol Process 14:763–784

Ziegler AD, Giambelluca TW, Nullet MA et al (2009) Throughfall in an evergreen-dominated forest stand in northern Thailand: comparison of mobile and stationary methods. Agric For Meteorol 149:373–384

Zimmermann A, Wilcke W, Elsenbeer H (2007) Spatial and temporal patterns of throughfall quantity and quality in a tropical montane forest in Ecuador. J Hydrol 343:80–96

Zimmermann A, Zimmermann B, Elsenbeer H (2009) Rainfall redistribution in a tropical forest: spatial and temporal patterns. Water Resour Res 45:W11413

Chapter 22
Forest Floor Interception

A.M.J. Gerrits and H.H.G. Savenije

22.1 Introduction

Often it is assumed that throughfall, which is the rainfall that is not intercepted by a canopy, is fully available for infiltration. This is not correct. The forest floor also intercepts rainfall much in the same way as the canopy. The forest floor can temporarily store water on short vegetation, litter, or bare soil. Interception by bare soil seems to have an overlap with soil evaporation, but can be distinguished by the fact that soil evaporation refers to the water that is stored in the root zone (De Groen and Savenije 2006). Whereas interception by bare soil only involves a very thin top layer not accessed by roots, short vegetation is identified as grasses, mosses, small bushes, and creeping vegetation. The litter layer is defined by Hoover and Lunt (1952) as the L & F layers (i.e., leaves, twigs, and small branches).

In general, the interception process (I) can be defined as the sum of the change in interception storage (S_i) and the evaporation from this stock (E_i):

$$I = \frac{dS_i}{dt} + E_i. \tag{22.1}$$

In the case of forest floor interception (I_f), the process can be described as follows:

$$I_f = \frac{dS_f}{dt} + E_{i,f} = T_f - F, \tag{22.2}$$

with S_f [L] the storage on the forest floor, $E_{i,f}$ [L T^{-1}] the evaporation from the forest floor, T_f [LT^{-1}] the throughfall (or net precipitation), and F [L T^{-1}] the infiltration.

Although forest floor interception is often considered a minor process due to lack of radiation under the canopy, research studies show that it can vary between 10 and 50% of the throughfall. In Table 22.1, an overview of past results on forest floor interception is presented.

Table 22.1 Forest floor interception values in the literature, with the water storage capacity $S_{f, max}$ and the interception evaporation $E_{i,f}$ as percentage of net precipitation (i.e., throughfall)

Source	Forest floor type	Location	$S_{f, max}$ [mm]	$E_{i,f}$ [% T_f]
Haynes (1940)	Kentucky bluegrass (*Poa pratensis*)	?		56[a]
Kittredge (1948)	Californian grass (*Avena, Stipa, Lolium,* and *Bromus*)	USA (CA)		26[a]
Beard (1956)	*Themeda* and *Cymbopogon*	South Africa		13[a]
Helvey (1964)	Poplar	USA (NC)		34
Brechtel (1969)	Scot's pine	USA (NY)		21
	Norway spruce	USA (NY)		16
	Beech	USA (NY)		16
	Oak	USA (NY)		11
Pathak et al. (1985)	*Shorea robusta* and *Mallotus phillippensis*	India		11.8
	Pinus roxburghii and *Quercus glauca*	India		7.8
	Pinus roxburghii	India		9.6
	Quercus leucotrichophora and *Pinus roxburghii*	India		10.6
	Quercus floribunda and *Quercus leucotrichophora*	India		11.0
	Quercus lanuginose and *Quercus floribunda*	India		11.3
Clark (1940) in Thurow et al. (1987)	Blue stem *Andropogon gerardi Vitman*	USA (TX)		57–84
Walsh and Voigt (1977)	Pine (*Pinus sylvestris*)	United Kingdom	0.6–1.7	
	Beech (*Fagus sylvaticus*)	United Kingdom	0.9–2.8	
Pitman (1989)	Bracken litter (*Pteridium aquiliunum*)	United Kingdom	1.67	
Miller et al. (1990)	Norway spruce	Scotland		18[a]
	Sitka spruce	Scotland		16[a]
Tamai and Hattori (1993)	Deciduous (*Quercus serrata Murray, Rhododendron reticulatum D. Don, Rhus sylvestris S.* and *Z.*)	Japan		6–18[a]
Thamm and Widmoser (1995)	Beech (*Asperulo-Fagetum*)	Germany	2.5–3.0	12–28
Putuhena and Cordery (1996)	*Pinus radiata*	Australia	2.78	
	Eucalyptus	Australia	1.70	

				0.23 mm d^{-1}
Schaap and Bouten (1997)	Douglas fir	Netherlands		
Li et al. (2000)	Peble mulch (5–9 cm)	China	0.281	11.5[a]
	Peble mulch (2–6 cm)	China	0.526	17.4[a]
Sato et al. (2004)	*Cryptomeria japonica*	Japan	0.27–1.72	
	Lithocarpus edulis	Japan	0.67–3.05	
Guevara-Escobar et al. (2007)	Grass (*Aristida divaricata*)	Mexico	2.5	
	Woodchips (*Pinus*)	Mexico	8	
	Poplar leaves (*Populus nigra*)	Mexico	2.3	
Gerrits et al. (2008)	Mosses and grasses	Netherlands	3–15[b]	52[a]
Gerrits et al. (2010)	Beech (*Fagus sylvatica*)	Luxembourg	1.0–2.8	10–35[a]

[a]Percentage of gross precipitation instead of net precipitation
[b]Also includes soil moisture storage

Special cases are the values from short vegetation where transpiration also occurs. First of all because transpiration and interception are not independent from each other. When it starts raining interception also starts, while transpiration stops because the stomata close (Gerrits et al. 2009a). Only after all the intercepted water has evaporated from the leaves, the stomata will open again and transpiration continues. Second, it is really difficult to separate interception from transpiration, especially for grasses and mosses where it is not possible to measure "throughfall". A way forward to distinguish transpiration from interception can be by isotope fractionation. Since transpiration does not fractionate water and interception evaporation does, this could be a way of separating the two evaporation processes.

A remarkable difference between canopy and forest floor interception is the relatively small interception storage capacity of the canopy compared to the forest floor. On the other hand, the canopy has a larger evaporative potential compared to forest floor (Baird and Wilby 1999). The higher evaporative potential is caused by more turbulent wind fluxes at the canopy level and more available radiation.

Another important difference is the large seasonal influence on canopy interception and the rather constant evaporation rates of the forest floor (e.g., Tamai and Hattori 1993; Gerrits et al. 2010). In summer when the canopy has leaves, the canopy storage capacity is large and the incoming radiation is high, resulting in high evaporation values. In winter, the opposite is true for the canopy. The forest floor, on the other hand, experiences less seasonal variation due to the shading of the canopy. In summer, the canopy reduces radiation reaching the forest floor, while in winter radiation can easily penetrate to the forest floor. As a result, the fluctuation of the total interception is less strong if canopy interception and forest floor interception are considered jointly.

22.2 Influencing Factors for Forest Floor Interception

Generally, interception is determined by vegetation characteristics, rainfall characteristics, and the evaporative demand. This is also the case for forest floor interception. In the following sections, the three main influencing factors are described.

22.2.1 Vegetation Characteristics

As can be seen in Table 22.1, the storage capacity differs per forest floor type. Needles have a different capacity than leaves, although one should be careful to compare the results, because the storage capacity also depends on the layer thickness. A thicker layer can store more water as investigated by Sato et al. (2004) and Guevara-Escobar et al. (2007).

The thickness (or mass) of a forest floor layer can also have a seasonal trend. Often in fall, the thickness increases due to leaf fall and throughout the year the layer becomes thinner by decomposition. Also, snow has an effect on the storage capacity, especially for deciduous floors. After snow, the leaves are flattened and this causes a decrease in the storage capacity (Gerrits et al. 2010).

22.2.2 Precipitation Characteristics

Throughfall characteristics (or precipitation when no canopy is present) have a large influence on the interception process. The throughfall frequency is a major determining factor. It makes a big difference if throughfall falls as one continuous storm or as a sequence of several smaller events with dry spells in between. Even if the total throughfall depth is the same, the last scenario intercepts much more water, because between the events the storage can be (partly) emptied by evaporation and thus more storage is available. Second, the throughfall intensity is important. In Fig. 22.1, the results of a sprinkler experiment on a Cedar needle floor are shown. As can be seen the higher the intensity, the higher the storage capacity.
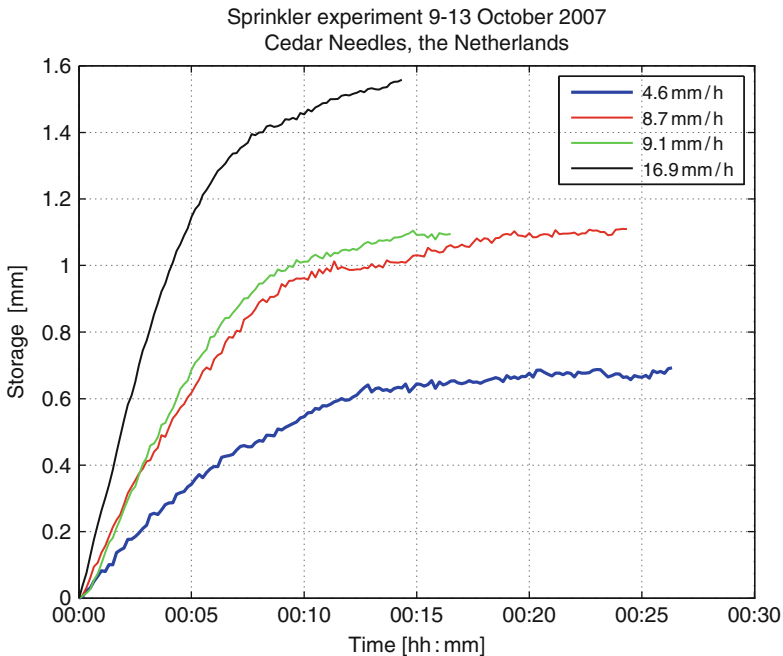
Fig. 22.1 Relation between throughfall intensity and storage capacity of a Cedar needle floor. The sprinkler experiments were carried out with the forest floor device from Gerrits et al. (2007) in the Netherlands (see Fig. 22.2). Special thanks to Anne Ritsema for doing the experiments

Similar results are found by Sato et al. (2004) and Guevara-Escobar et al. (2007). However, Guevara-Escobar et al. found that this was only the case for the dynamic storage (maximum storage during event) and not for the static storage (maximum storage after event ceased). Sato et al. (2004), on the other hand, found that the intensity has a positive relation with both the dynamic and the static storage.

22.2.3 Evaporative Demand

If the potential evaporation (i.e., open water evaporation) is high, the intercepted water can evaporate more easily during and after the event. Wind and radiation are important for evaporation. Although wind plays an important role in removing moisture from the surface providing a higher vapour deficit, wind speed is often low at the forest floor level. Radiation that is able to penetrate the canopy is determined by the Leaf Area Index (LAI), causing in winter more radiation to reach the forest floor than in summer.

Of the above three factors, the throughfall characteristics are dominant. Although the storage capacity (mainly vegetation characteristic) and the available energy form a constraint to the evaporation flux for each event, the number of events is a more important factor. This is confirmed by the sensitivity analysis of Gerrits et al. (2009b).

22.3 Measuring Techniques

Although not much research has been done on forest floor interception, some researchers have tried to quantify it as shown in Table 22.1. Helvey and Patric (1965) divided the applied methods into two categories:

- Lab methods, whereby field samples are taken to the laboratory to carry out the experiments. In this way, the samples are disturbed, but the conditions are completely controlled.
- Field methods, whereby the experiment is executed in the original environment. With field methods, the samples are less disturbed compared to lab experiments.

In the following sections, an overview of these experiments is given.

22.3.1 Lab Methods

The drainage experiment by Helvey (1964) is an example of a lab experiment to determine the maximum water content. When a rainfall event was large enough to saturate the forest floor, Helvey covered the forest floor with an aluminium lid (3 ft^2)

as soon as rainfall ceased. After 24 h when drainage was assumed to have stopped, a 2 ft^2 sample of forest floor was collected and brought to the lab. In the lab, the sample was weighed under wet condition and successively dried in an oven to weigh the sample under dry conditions. Although this is a very simple and cheap method, it disturbs the samples and requires that the field site and the lab are nearby. Furthermore, it only determines the storage capacity and does not give any information on the evaporation. Similar work was done by Beard (1956), Walsh and Voigt (1977), and Sato et al. (2004).

Another lab experiment (also to determine the storage capacity) was carried out by Putuhena and Cordery (1996). They focused on the spatial variability of the storage capacity and collected samples of forest floors in a catchment and mapped them. For each type of forest floor, Putuhena and Cordery (1996) determined the storage capacity with a rainfall simulator. Finally, the spatial map of the forest floor types was combined with the results of the rainfall simulator to obtain an average storage capacity for the catchment. Also, Guevara-Escobar et al. (2007) made use of a rainfall simulator to determine the storage capacity. However, their focus was not the spatial variability, but they investigated the effect of layer thickness on the maximum storage capacity.

22.3.2 Field Methods

Pathak et al. (1985) carried out a similar experiment as Helvey (1964), except that Pathak et al. (1985) measured in the field and weighed before and after every rainfall event. In this way, they also included events that did not saturate the forest floor and thus gave a better approximation of interception evaporation, although they still only measured the storage.

To measure the flux, often lysimeters are used. For example, Schaap and Bouten (1997) developed a weighing concrete lysimeter with a counterbalance. The remaining weight differences were measured with a load cell. Although the applied method is a good way to measure evaporation from the forest floor, the developed lysimeter is quite massive and therefore inflexible and expensive.

The mini-lysimeters of Brechtel (1969) do not have this disadvantage. Brechtel (1969) measured manually the infiltrated water in small pots with a diameter of 15 cm. The advantage of small and cheap lysimeters is that they can easily be used, for example, to investigate the spatial variability. However, manually reading out the mini-lysimeters is labour intensive and due to the small opening size the equipment itself can have an influence on the measurements.

A lysimeter that is in between the concrete and the mini-lysimeter is the set-up of Thamm and Widmoser (1995). They measured forest floor evaporation with suction plates and measured the infiltrated water. Hence, Thamm and Widmoser (1995) measured the sum of the stock and the evaporation flux combined.

The method of Gerrits et al. (2007) enables to measure both the storage and the flux. It consists of two aluminium basins mounted above each other (Fig. 22.2).
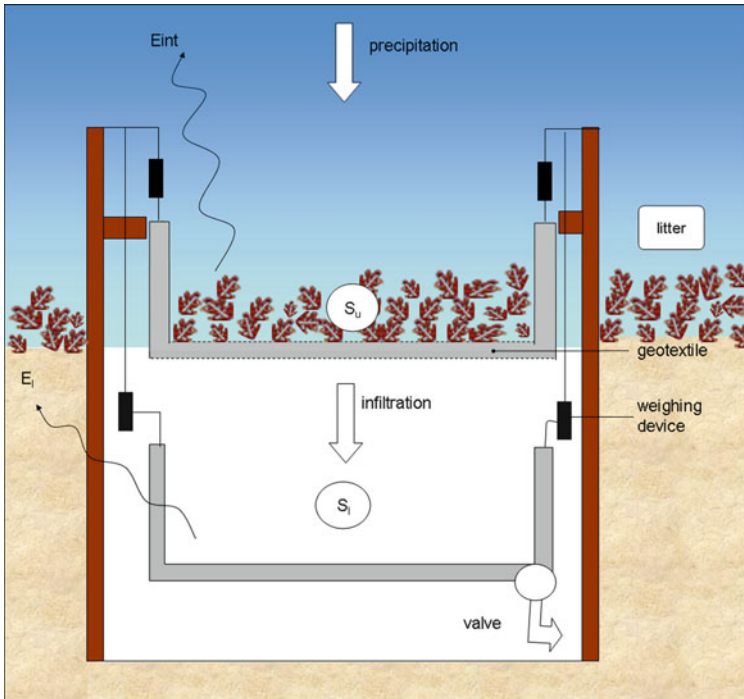
Fig. 22.2 Forest floor interception device (from Gerrits et al. 2007)

The upper basin is permeable and contains the forest floor. Both basins are weighed continuously with strain gauges. By knowing the net rainfall, one can calculate the change in storage in the forest floor and the interception evaporation.

22.4 Concluding Remarks and Future Directions

Although interception is often considered a minor process, it does play an important role in the water balance. Not only the canopy, but also the forest floor can intercept a significant amount of rainfall. Although most surfaces can store only a few millimetres of water, which is often not much in comparison to other stocks in the water balance, the temporal distribution of the rainfall can cause the accumulated effect to be considerable. The impact of interception only becomes evident at longer time scales. Interception storage in itself is small, but the number of times that the storage is filled and depleted can result in a considerable reduction of rainfall recharging soil moisture of producing runoff.

Moreover, canopy and forest floor interception interact and strengthen each other, but this has not been much investigated so far. Generally, the two are considered in

isolation, even where they occur jointly. Where the canopy is dense, less water is available for the forest floor, but also less radiation, while turbulence is reduced. This results in a reduction of forest floor evaporation. On the other hand, in dense forests the forest floor layer is thicker, and thus more water can be intercepted. This feedback interaction should be taken into account in future interception studies and therefore it is recommended to measure canopy and forest floor jointly.

In the past, several methods have been investigated and applied to quantify and study the interception process. Most techniques focused on the determination of the storage capacity, while the evaporation from interception remained underemphasized. Lysimeter set-ups in the field are the best solution to quantify both the flux and the storage. However, they often have problems with the artificial layer underneath the forest floor (so-called interface effect). A way forward could be to measure forest floor evaporation by use of tracers such as stable isotopes. The recent improvement in isotope analysers will push forward this way of determining evaporation, although the challenge remains in figuring out a good (continuous) sampling method. Furthermore, isotope fractionation can also be used to separate interception from transpiration, since interception fractionates, while transpiration does not change the isotopic ratio. This can be helpful for interception studies on small vegetation such as creeping bushes, grasses, and mosses.

Measuring interception evaporation through the energy balance may also overcome the interface effect. Knowing how the available energy is partitioned over the different fluxes and compartments, evaporation by interception can be derived. However, this would require intensive field experiments where both the energy fluxes and the evaporation processes are measured simultaneously. Flux towers will be needed to measure temperature, humidity, and wind profiles under the unstable canopy layer. Although these are complex (and therefore expensive) measurements, the biggest advantage of energy balance measurements is that the forest floor is not disturbed.

In the future, the information on energy partitioning can also be obtained from remote sensing data. Remote sensing could provide the necessary spatial and temporal information; however, it is probably not able to distinguish between canopy and forest floor interception, which for most hydrological applications is not so important. Through a combination of methods interception could be more adequately incorporated in hydrological models.

References

Baird AJ, Wilby RL (1999) Eco-hydrology – Plants and water in terrestrial and aquatic environments. Routledge

Beard JS (1956) Results of the mountain home rainfall interception and infiltration project on black wattle, 1953–1954. J S Afr Forestry 27:72–85

Brechtel HM (1969) Wald und Abfluss-Methoden zur Erforschung der Bedeutung des Waldes fur das Wasserdargebot. Deutsche Gewasserkundliche Mitteilungen 8:24–31

Clark OR (1940) Interception of rainfall by prairie grasses, weeds and certain crop plants. Ecol Monogr 10:243–277

Gerrits AMJ, Savenije HHG, Hoffmann L et al (2007) New technique to measure forest floor interception – an application in a beech forest in Luxembourg. Hydrol Earth Syst Sci 11:695–701

Gerrits AMJ, Savenije HHG, Pfister L (2008) Forest floor interception measurements. IHP-VI Tech Doc Hydrol 81:81–86

Gerrits AMJ, Savenije HHG, Pfister L (2009a) Canopy and forest floor interception and transpiration measurements in a mountainous beech forest in Luxembourg. IAHS Redbook 326:18–24

Gerrits AMJ, Savenije HHG, Veling EJM et al (2009b) Analytical derivation of the budyko curve based on rainfall characteristics and a simple evaporation model. Water Resour Res 45:15

Gerrits AMJ, Pfister L, Savenije HHG (2010) Spatial and temporal variability of canopy and forest floor interception in a beech forest. Hydrol Process 24:3011–3025

De Groen MM, Savenije HHG (2006) A monthly interception equation based on the statistical characteristics of daily rainfall. Water Resour Res 42. doi 10.1029/2006WR005013

Guevara-Escobar A, Gonzalez-Sosa E, Ramos-Salinas M et al (2007) Experimental analysis of drainage and water storage of litter layers. Hydrol Earth Syst Sci 11(5):1703–1716

Haynes JL (1940) Ground rainfall under vegetation canopy of crops. J Am Soc Agr 32:176–184

Helvey JD (1964) Rainfall interception by hardwood forest litter in the southern Appalachians. US For Ser Res Pap SE 8:1–8

Helvey JD, Patric JH (1965) Canopy and litter interception of rainfall by hardwoods of Eastern United States. Water Resour Res 1(2):193–206

Hoover MD, Lunt HA (1952) A key for the classification of forest humus types. Soil Sci Soc Proc 16:368–371

Kittredge J (1948) Forest influences. McGraw-Hill, New York

Li XY, Gong JD, Gao QZ et al (2000) Rainfall interception loss by pebble mulch in the semiarid region of China. J Hydrol 228:165–173

Miller JD, Anderson HA, Ferrier RC et al (1990) Comparison of the hydrological budgets and detailed hydrological responses in two forested catchments. Forestry 63(3):251–269

Pathak PC, Pandey AN, Singh JS (1985) Apportionment of rainfall in central Himalayan forests (India). J Hydrol 76:319–332

Pitman JI (1989) Rainfall interception by bracken litter – relationship between biomass, storage and drainage rate. J Hydrol 111:281–291

Putuhena W, Cordery I (1996) Estimation of interception capacity of the forest floor. J Hydrol 180:283–299

Sato Y, Kumagai T, Kume A et al (2004) Experimental analysis of moisture dynamics of litter layers - the effect of rainfall conditions and leaf shapes. Hydrol Process 18:3007–3018

Schaap MG, Bouten W (1997) Forest floor evaporation in a dense douglas fir stand. J Hydrol 193:97–113

Tamai K, Hattori S (1993) Apportionment of evapotranspiration of a deciduous broadleaved forest in the Yamashiro catchment. IAHS Redbook 212:61–65

Thamm F, Widmoser P (1995) Zur hydrologischen Bedeutung der organischen Auflage im Wald: Untersuchungsmethoden und erste Ergebnisse. Z fur Pflanzenernahrung und Bodenkunde 158:287–292

Thurow TL, Blackburn WH, Warren SD et al (1987) Rainfall interception by midgrass, shortgrass, and live oak mottes. J Range Manage 40(5):455–460

Walsh RPD, Voigt PJ (1977) Vegetation litter: an underestimated variable in hydrology and geomorphology. J Biogr 4:253–274

Chapter 23
New Dimensions of Hillslope Hydrology

Sophie Bachmair and Markus Weiler

23.1 Introduction

Hillslopes are fundamental landscape units that strongly control the processes whereby precipitation or snowmelt is vertically and laterally transported to the streams. They are, in a sense, microcosms of catchments. Understanding and predicting the hillslope response is highly important in terms of flood prediction, transport of nutrients and sediments into surface water bodies, slope stability, and soil-atmosphere-vegetation exchange processes. Through numerous field experiments and numerical studies, much progress has been made in hillslope hydrology in the past decades. However, our ability to extrapolate these findings to ungauged hillslopes and catchments is still very poor (Sivapalan 2005). A common thread that has evolved recently is to search for the underlying principles of hydrological processes instead of characterizing and cataloging the enormous heterogeneity and complexity of rainfall-runoff processes (McDonnell et al. 2007). The aim of this chapter is to provide an overview on today's conceptual models of processes at the hillslope scale and to examine the factors driving these mechanisms. The focus will be on compiling recent findings on the dominant controls of hillslope runoff processes to meet the need of identifying underlying principles. The chapter closes with thoughts on new dimensions and directions of hillslope hydrology and research avenues to follow for the future.

23.2 Conceptual Process Models at the Hillslope Scale

Much of the process understanding in hillslope hydrology in forested landscapes has evolved from only a few intensively studied hillslopes in the Panola Mountain Research Watershed, USA (e.g., Burns et al. 1998; Freer et al. 2002; Tromp-van Meerveld and McDonnell 2006a–c), in Maimai, New Zealand (e.g., Mosley 1979; Sklash et al. 1986; McDonnell 1990; Woods and Rowe 1996), and in the Fudoji catchment, Japan (Asano et al. 2002, 2004; Uchida et al. 2003a, b, 2004). Interestingly, some of the earlier conceptual models derived from these hillslopes were later discarded through novel measurement techniques (McGlynn et al. 2002;

Tromp-van Meerveld et al. 2007). Until today, a number of experimental hillslope studies have been conducted in different environments, leading to an advanced and refined perception of rainfall-runoff processes (e.g., Scherrer et al. 2007; Graham 2008; Kienzler and Naef 2008a, b). Despite the large variety of observed flow processes, one commonality seems to be the strong nonlinearity of hillslope response to rainfall (McDonnell 2003). By definition, a system is nonlinear if the outputs are not proportional to the inputs across the entire range of the inputs (Phillips 2003). Several hillslope studies report on a certain precipitation threshold until significant hillslope outflow is triggered (e.g., Uchida et al. 2005; Tromp-van Meerveld and McDonnell 2006a; Graham 2008). Such a threshold response can be regarded as an extreme form of nonlinearity (Zehe and Sivapalan 2009). To predict this nonlinear system behavior, we need a sound concept of hydrological processes taking place at the hillslope scale.

In general, the hillslope runoff processes can be conceptualized as (1) overland flow (Hortonian and saturation overland flow [SOF]), (2) near-surface flow, (3) subsurface stormflow (SSF), and (4) deep percolation (DP) (see Fig. 23.1) (Scherrer and Naef 2003; Schmocker-Fackel 2004; Sidle et al. 2007). Once precipitation enters the hydrologic system as rainfall or snow, it will be partitioned into different flowpaths depending on the storm and hillslope characteristics.

Hortonian overland flow (HOF), also called infiltration excess overland flow, is lateral flow along the surface when the rainfall intensity exceeds the infiltration capacity of the soil (Horton 1933). Factors fostering HOF are surface sealing and crust building, soil compaction, an abrupt increase of bulk density, topsoil hydrophobicity, and low macroporosity (e.g., Doerr et al. 2000; Scherrer and Naef 2003; Weiler and Naef 2003; Schmocker-Fackel 2004). SOF takes place once the storage capacity of the soil is exceeded and no further infiltration is possible.
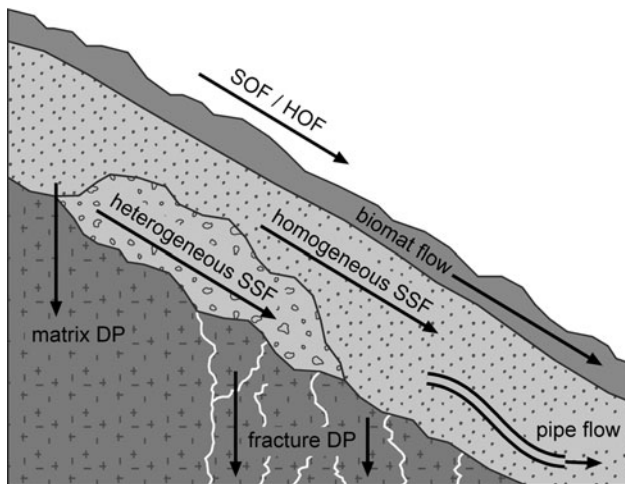
Fig. 23.1 Conceptual process models at the hillslope scale

SOF is thus dependent on antecedent wetness and preferential flow paths, transporting water into deeper soil layers. Once surface flow is established, runoff pathways are influenced by surface roughness (e.g., microrelief, stone and vegetation cover) (Bracken and Croke 2007), reinfiltration and run-on processes (Corradini et al. 1998). True HOF has been rarely observed on forested hillslopes (Sidle et al. 2007), except for HOF generated by disturbed forest soils due to skid roads, trails, and log-landing decks. When overland flow occurs on forest slopes, it is frequently believed to result from return flow (Dunne and Black 1970), which occurs when subsurface water is forced back to the surface (e.g., due to a change in slope or low permeability layers) (Schmocker-Fackel 2004; Sidle et al. 2007), or from saturated areas (Elsenbeer and Vertessy 2000; Godsey et al. 2004). Experimental studies measuring surface runoff via a collection trough, which is usually inserted below the soil surface, often mistakably assume to catch HOF, even though it in fact originates from flow within the forest litter layer (Buttle and Turcotte 1999; Sidle et al. 2007). This near-surface flow phenomenon has been called "organic layer interflow" (Weiler and McDonnell 2004), "biomat flow" (Sidle et al. 2007), "pseudo-overland flow" (McDonnell et al. 1991), and "thatched roof" effect (Ward and Robinson 1990).

The conceptualization of flow processes in the subsurface is more complex. Generally, quickly responding SSF and DP can be discriminated. SSF, also termed subsurface flow, interflow, throughflow, lateral flow, and shallow groundwater flow, is the fast lateral movement of water through the soil matrix or permeable bedrock above a layer of reduced permeability (Dunne 1978; Weiler et al. 2006). DP or groundwater recharge occurs when infiltrated water vertically seeps into the bedrock, thus contributing to slow baseflow (Scherrer et al. 2007). In many early studies on hillslope hydrology, the underlying bedrock was assumed impermeable. However, recently published work showed that both infiltration into the bedrock and exfiltration from the bedrock into the soil can be significant and hence cannot be ignored (e.g., Anderson et al. 1997; Uchida et al. 2002; Kosugi et al. 2006; Tromp-van Meerveld et al. 2007; Graham 2008; Tromp-van Meerveld and Weiler 2008).

The complex nature of SSF formation is subject of ongoing research. A prerequisite for SSF is a transient saturation of parts of the soil matrix (≥ 0 kPa matrix potential) due to a layer of reduced permeability in vertical direction (Weiler et al. 2006). This can be the bedrock or low permeability soil horizons due to a change in soil texture, an increase in bulk density, or a decrease in macroporosity (Weiler et al. 2006). Such low permeability soil horizons develop from different pedogenetic processes (e.g., lixiviation leading to argic horizons), biological processes (reduced earthworm activity or decreasing rooting density), or due to management practices (plough layer, landfill lining). After the soil matrix has reached partial saturation, SSF can take place through high permeability layers of the soil matrix or through soil pipes. High permeability layers are coarse textured and/or have a large pore space. They are often found in talus slopes, landslide debris, periglacial solifluction deposits, or unconsolidated moraine material (Weiler et al. 2006). Soil pipes are defined as lateral voids such as decayed roots, animal burrows, channels due to subsurface hydraulic erosion, and tension cracks (Tsukamoto et al. 1988). They are mostly observed at the soil–bedrock interface (or, more

generally, impeding layer interface), but also within the soil profile and at the organic horizon-mineral soil interface (Sidle et al. 2001; Holden and Burt 2002; Weiler et al. 2006). Soil pipes are mainly short and discontinuous features; however, they were found to form a network of interconnected pipes, which develops parallel to the slope gradient (Terajima et al. 2000; Sidle et al. 2001; Uchida et al. 2001). The interconnection of pipes is facilitated by saturated parts of the soil matrix, high-permeability areas such as pockets of organic material and loose soil, and water emanating from bedrock fractures (Noguchi et al. 1999; Sidle et al. 2001; Anderson et al. 2008). The exact mechanisms of pipe flow activation, pipe flow inter-connection, and exchange processes between pipes and the surrounding soil matrix are still not well known. Nevertheless, the significance of pipe flow making up a large fraction of total SSF was shown by numerous experimental studies (e.g., Jones 1997; Holden and Burt 2002; Uchida et al. 2002, 2005; Kienzler and Naef 2008a; Anderson et al. 2009). Pipe networks effectively drain the hillslope, increasing peak discharge and decreasing peak lag time of the storm hydrograph (Uchida et al. 2001). On the one hand, pipe flow may increase slope stability, counteracting a positive pore water pressure development of the soil matrix. On the other hand, when the capacity of pipe flow exceeded or pipes become clogged, slope failure may be triggered (Uchida et al. 2001).

We propose that SSF predominantly occurs via lateral preferential flow paths as opposed to sheet-like matrix flow, due to the high spatial variability of controlling factors (e.g., bedrock topography, variable soil depth). We define a lateral preferential flow path as either flow through high-permeability areas of the soil matrix or flow through interconnected pipes. This is similar to the concept of vertical flow processes at the plot scale, where a distinction is made between (a) homogeneous matrix flow (homogenous wetting front parallel to the soil surface), (b) heterogeneous matrix flow (preferential flow resulting from instabilities in the wetting front or from funneling due to less permeable zones), and (c) macropore flow (Hendrickx and Flury 2001; Weiler and Flühler 2004). An indication for subsurface flow via lateral preferential flow paths is a hydraulically limited water table response (e.g., Fannin et al. 2000; Anderson 2008). Once the water table rises into a zone where a lateral preferential flow network is present, the hydraulic conductivity significantly increases. After the activation of the preferential flow network, the water table remains relatively constant while the discharge continues to increase (Anderson 2008).

Depending on the pathway incoming precipitation takes (HOF, SOF, biomat flow, SSF, DP) hillslope response parameters such as response time, water transit time and the event to pre-event water ratio will strongly differ (event or "new" water = water from the current rain or snowmelt event; pre-event or "old water" = water that existed in the catchment prior to the current rain or snowmelt event (Sklash 1990); transit time = time between when a water molecule enters the hydrologic system until it exits it). While DP is characterized through mainly pre-event water and long transit times, HOF and SOF have shorter transit times and a high fraction of event water. Due to the heterogeneity of SSF processes (degree of matrix flow vs. pipe flow, timing of pipe network activation, etc.), a diversity of response characteristics for SSF is possible. Recently, Kienzler and Naef (2008a)

showed through an intercomparison study that variations in response time and event to pre-event water ratio can be explained through different degrees of direct or indirect feeding of preferential flow paths: When precipitation feeds directly into preferential flow paths, bypass flow occurs, resulting in a quick SSF response and high event water fractions. In contrast, when preferential pathways are fed indirectly via saturated parts of the soil, SSF response is delayed and contains less event water.

Albeit this progress in generalizable process understanding, predicting the hydrological response of ungauged basins remains anything but trivial. Nonetheless, there have been a few approaches trying to provide a systematic basis for inferring rainfall runoff responses, such as the UK's hydrology of soil type (HOST) classification system (Boorman et al. 1995), the decision tree approach by Scherrer and Naef (2003) to indicate hydrological processes on temperate grassland, or the field instruction for assessing surface runoff coefficients for alpine soil-/vegetation units by Markart et al. (2004). As starting point for new attempts classifying the hillslope response to rainfall, it seems promising to summarize recent findings on the dominant controls of runoff processes.

23.3 Controlling Factors of Flow Processes

Generally, the controlling factors of hillslope response to rainfall or snowmelt can be broken up into static factors, at least in the sense of shorter time scales such as years (parent material, surface and bedrock topography, exposure), also termed the "hillslope configuration" (Hopp and McDonnell 2009), and dynamic factors (precipitation characteristics, soil moisture, vegetation). Despite this division, we discuss the different controlling factors from a top-down perspective, meaning from precipitation entering the system at the upper boundary to the bedrock as lower boundary, thereby highlighting the numerous interrelations among different factors.

23.3.1 Input Characteristics

Input characteristics (amount, intensity, and frequency of storms, characteristics of snow pack and timing of snowmelt) clearly constitute a first-order control on runoff response. Furthermore, the temporal distribution of input and patterns of evapotranspiration strongly influence the soil moisture content, which represents a key factor driving hydrological processes (Sivapalan 1993; Jost et al. 2005; McNamara et al. 2005). Concerning input amount, there seems to be a strong nonlinearity between rainfall or snowmelt input and hillslope response. Several hillslope studies documented that a certain precipitation threshold had to be exceeded until significant hillslope outflow was triggered, e.g., observed precipitation threshold of 55 mm and approx. 23 mm at the trenched Panola and the Maimai hillslope, respectively (Tromp-van Meerveld and McDonnell 2006a; Graham 2008).

The effect of rainfall intensity on runoff generation seems rather complex. Obviously, overland flow is positively correlated with rainfall intensity (Horton 1933). Furthermore, an increase in rainfall intensity enhances macropore flow since the soil water pressure is closer to saturation during rainfall and larger macropores conduct water (Jarvis et al. 2007). Enhanced macropore flow, which channels water to deeper soil layers, leads to the assumption of a positive relation between rainfall intensity and subsurface flow response. This is supported by the finding of SSF velocities being highly correlated with the 1-h rainfall intensity by Anderson et al. (2009). However, Kienzler and Naef (2008b) conclude from sprinkling experiments at three grassland slopes with varying intensity and antecedent wetness that a higher intensity did not increase subsurface flow rates. They explain this with differing flow processes being triggered by rainfall intensity (during low intensity, saturation above the bedrock and thus subsoil SSF was most relevant; during higher intensity, topsoil saturation and overland flow was the dominant runoff process, Kienzler and Naef 2008b). It seems like the effect of rainfall intensity is strongly bound to other interacting factors (e.g., soil hydraulic properties, macroporosity, pipe network, antecedent wetness) and can be both highly relevant and subordinate when buffered by other controls.

23.3.2   Vegetation

The impact of vegetation cover on runoff processes and streamflow has long been a topic of interest, especially with regard to timber harvesting. Several paired catchment studies found that forested catchments are characterized by higher evapotranspiration and lower runoff, delayed peak flow and a longer hydrograph recession time (Schume et al. 2004; Jost et al. 2005). To open the black box of catchment scale processes, vegetation effects at smaller scales need to be examined. Generally, the precipitation signal is heavily modified by the vegetation growing on a slope. Besides an aboveground partitioning of precipitation through overstory and understory vegetation, plants also partition incoming water on the ground and belowground through the litter layer and roots. This "double-funneling" effect (aboveground and belowground) (Johnson and Lehmann 2006) strongly alters hydrologic and nutrient fluxes and leads to heterogeneous soil water dynamics (Johnson and Lehmann 2006; Liang et al. 2007). Preceding and subsequent chapters (Chaps. 18–22 and 24) provide detailed insights into the aspects discussed hereafter.

23.3.2.1   Aboveground Partitioning

Vegetation partitions precipitation into (1) interception (precipitation remaining on the vegetation, which is evaporated after or during rainfall), (2) stemflow (water flowing to the ground via trunks or stems), and (3) throughfall (precipitation falling through the vegetation reaching the ground) (Crockford and Richardson 2000) (see Chaps. 20 and 21). Concentrated water flow along stems and temporary storage on

forest canopies results in evaporative losses and intensity smoothing (Keim et al. 2006), and causes spatially variable patterns of soil moisture and solute deposition (e.g., Johnson and Lehmann 2006; Zimmermann et al. 2008; Levia et al. 2010). This may be highly relevant for runoff generation.

A number of studies documented the importance of stem flow on soil moisture patterns. To highlight some findings, Herwitz (1986) observed that high stem flow fluxes produced localized HOF in a tropical rainforest. Chang and Matzner (2000) found that 13.5% of the annual infiltration in a beech forest occurred within 1 m^2 of the tree base, an area solely representing 3% of the total forest area. More recently, Liang et al. (2007) observed that the pore water pressure at the soil–bedrock interface increased faster and to a greater extent downslope from a tree stem growing on a steep hillslope than upslope (Liang et al. 2007).

Snow accumulation and ablation rates are also strongly influenced by canopies (e.g., López-Moreno and Stähli 2008; Molotch et al. 2009). For instance, Molotch et al. (2009) observed a 29% greater snow accumulation in open-area vs. under-canopy locations. Additionally, snow ablation rates under canopies were reduced by 39%, which extended the duration of snowmelt in some cases (Molotch et al. 2009). The role of interception on soil moisture and runoff was examined by Keim and Skaugset (2003) and Keim et al. (2006). They conducted virtual experiments (numerical experiments driven by collective field intelligence, Weiler and McDonnell 2004) based on data from the Panola hillslope and field-measured throughfall rates. Their virtual experiments revealed that interception delayed the onset of SSF, lowered and delayed stormflow peaks, and decreased total flow and the runoff ratio (Keim et al. 2006). When they used simplified modeled throughfall rates (where they separated the effect of interception into evaporation and intensity smoothing), it became apparent that canopy evaporation was responsible for most of these effects, while intensity smoothing showed measurable differences only in peak SSF rate (Keim et al. 2006). This finding is highly relevant for the calibration of watershed models. "Not only would ignoring interception miss a major effect of vegetation on SSF generation, our work also shows that simply applying some fractional reduction as a scaled input signal (as is customary in watershed modeling studies) may mask important effects on peak flow response in some situations" (Keim et al. 2006). Another set of virtual experiments investigated the effect of rainfall intensity smoothing on soil water pore pressure and slope stability during high-intensity rainfall (Keim and Skaugset 2003). The outcome was that estimates of slope stability were generally greater under forest canopy than for the same hillslope without forest canopy (Keim and Skaugset 2003).

23.3.2.2 Partitioning on the Ground and Belowground

The fraction of rainfall that reaches the surface is further dispersed though funneling on the ground and belowground due to ground vegetation, litter layer coverage, and roots (Buttle and Turcotte 1999; Johnson and Lehmann 2006; Sidle et al. 2007) (see also Chaps. 22 and 24). A widespread feature of wooded ecosystems is a litter

layer covering the soil, consisting of dead leaves, twigs and other fragmented organic material (Sato et al. 2004). The litter layer strongly determines the infiltration capacity of the soil. It may act as barrier to flow, triggering surface runoff, or may favor vertical infiltration and hence SSF or groundwater recharge. Recently, the effects of leaf morphology and rainfall conditions on the moisture dynamics of litter layers were examined for two contrasting litter types (needle-leaf vs. broad-leaf) (Sato et al. 2004). The results showed that the broad-leaf litter intercepted more rainwater than the needle-leaf litter. Additionally, the water moved laterally in the broad-leaf litter layer, whereas it moved vertically down in the needle-leaf litter layer (Sato et al. 2004). However, it has also been observed that dry needle-leaf litter from spruce may exhibit hydrophobic properties and thus hinders vertical infiltration (Schume et al. 2004). Similar effects due to hydrophobicity were also discovered for dry, fur-like root layers in grassland topsoil (Scherrer et al. 2007), alpine mats (Markart et al. 2004), and burned areas (e.g., Doerr et al. 2000). Moreover, seasonal differences in vegetation cover influence the surface roughness and hence runoff production (Bracken and Croke 2007).

Belowground, trees further modify soil moisture and nutrient dynamics through preferential flow along roots (e.g., Bundt et al. 2001; Johnson and Lehmann 2006). These root-derived preferential flow pathways result from localized compaction of soil by roots and the addition of root exudates to adjacent soil (Johnson and Lehmann 2006). The important role of roots during infiltration was early suggested (Beven and Germann 1982). Numerous studies have confirmed the relevance of root induced preferential flow since then (e.g., Bundt et al. 2001; Buttle and McDonald 2002; Bachmair et al. 2009; Lange et al. 2009). As an example, dye tracer experiments in little developed volcanic ash soils documented a straight infiltration front in unvegetated soil; in forested soil, however, water was preferentially channeled (Blume et al. 2008). The effect of different species on water flow in soil has only been recently brought into focus. It is well known that each tree species develops a typical root system. Even though root architecture may differ within species as response to local conditions (soil properties or competition with others), following main root systems can be distinguished: taproot system (one vertically growing taproot dominates); heart-shaped system; sinker root system (shallow, plate-like network of lateral roots with downward sinker roots) (Polomski and Kuhn 1998; Schume et al. 2004). Nordmann et al. (2009) presented remarkable findings on the impact of different root systems on subsurface runoff. They conducted high-intensity rainfall experiments on trenched hillslope segments with similar soil and bedrock but different tree species to assess the water retention capacity of different species. A species-related trend in water retention could be observed: The most favorable retention rates were found in a mixed beech and sycamore maple stand (deep-rooting trees). Stands dominated by spruce showed the lowest retention rates (sinker roots). Nonetheless, the pedologic and geologic properties overcompensated the species effect at one site. Remarkably, subsurface flow paths under spruce mostly occurred on top of the impeding layer, whereas flow paths under beech and sycamore maple also existed within the impeding layer (Nordmann et al. 2009).

Evapotranspiration rates of forests are also linked with root systems (Schume et al. 2004; Schwärzel et al. 2009). Schume et al. (2004), for instance, investigated soil water depletion and recharge patterns in a mixed beech-spruce and a spruce stand by high-resolution time domain reflectometry (TDR) measurements. Maximum differences were observed in periods with high evaporative demand. They state that the overproportionate evapotranspiration of the mixed stand was exclusively attributable to beech, which deepened and intensified its fine-root system in mixture, while spruce rooted shallower. The mixed stand extracted a higher percentage of water from deeper soil layers than the pure stand (Schume et al. 2004).

23.3.3 Topography

As part of the "hillslope configuration," topography undoubtedly represents a major hydrological driver, influencing soil properties, vegetation patterns, and microclimate (Anderson and Burt 1978; Burns et al. 1998; Wagener et al. 2007). Many of the effects topography exerts on hillslope hydrological processes are rather intuitive; nevertheless, a number of studies quantitatively assessed the role of different terrain properties (slope gradient, hillslope geometry, aspect, and microtopography) on runoff generation (e.g., Freer et al. 1997; Burns et al. 1998; Aryal et al. 2002; Troch et al. 2003; Berne et al. 2005; Bogaart and Troch 2006; Lyon and Troch 2007; Fujimoto et al. 2008). Most hillslopes have complex three-dimensional shapes, characterized by their profile curvature (topographic curvature along the flow line: convex, planar, concave) and contour or planform curvature (curvature of contour lines: divergent, parallel, convergent). These attributes significantly control the flow behavior and saturation along hillslopes (Aryal et al. 2002, 2005; Troch et al. 2003). For instance, Troch et al. (2003) conclude from a study, in which they presented a new mathematical formulation of homogeneous subsurface flow along complex hillslopes (hillslope-storage Boussinesq equation), that convergent hillslopes drain much slower than divergent hillslopes, due to the reduced flow domain near the outlet. Furthermore, the accumulation of moisture storage near the outlet of convergent hillslopes results in bell-shaped hydrographs, whereas fast draining divergent hillslopes produce peaked hydrographs (Troch et al. 2003). Field evidence on the effect of hillslope geometry was provided by Fujimoto et al. (2008), who compared the runoff behavior of two contrasting slopes (concave valley-head vs. planar side slope). Besides large-scale hillslope geometry, surface and bedrock microtopography affect the hillslope runoff response (Freer et al. 2002; Tromp-van Meerveld and McDonnell 2006b; Graham 2008). Tromp-van Meerveld and McDonnell (2006b) proposed a "fill-and-spill" mechanism, meaning that during a rainfall event bedrock depressions have to fill up before water spills over the bedrock ridges and contributes to hillslope outflow. An increase in slope angle thus likely decreases the volume of bedrock pools and the height of spilling barriers, thereby changing the balance between fill and spill and the timing and spatial distribution of water flow (Hopp and McDonnell 2009). Clearly, the fill

and spill process solely plays a role if there is an interaction between the bedrock and the overlying soil (e.g., transmissive soil).

Evidence on the coupling of topography and hydrologic response was also reported by Zehe and Flühler (2001), who conducted plot-scale dye tracer experiments at different valley locations. They found that plots located at the bottom of slopes had a greater susceptibility to preferential flow than those in the upper part. An explanation is the presence of deeper, biologically more active, often finer textured soils at the foot slope (Zehe and Flühler 2001). Holden (2009) also investigated the spatial distribution of macropore flow as a proportion of saturated hydraulic conductivity on humid-temperate slopes. He discovered that near-surface macropore flow varied according to slope position, yet spatial patterns differed among hillslopes due to differences in soil type.

An interesting approach linking hydrologic response to geomorphic properties was presented by Broxton et al. (2009). They hypothesized that water transit time is related to aspect (slope direction and exposure), since this determines the amount of energy a particular hillslope receives, which, in turn, affects a variety of factors such as the timing and intensity of snow-melt, evapotranspiration, and vegetation patterns (Broxton et al. 2009). Their experiments conducted in small, snowmelt-dominated mountainous catchments suggested that isotopic variability and estimated transit times were both related to aspect. Despite the observed correlations between hydrologic response and aspect, causality cannot be inferred. Nevertheless, their approach provides insight into the strengths of using aspect as a simple and transferable proxy for energy inputs to capture a variety of factors affecting water fluxes (Broxton et al. 2009).

23.3.4 Soil Properties

Obviously, soil properties strongly control the flowpaths incoming precipitation takes. Depending on the infiltration capacity of the soil, water is split up into surface flow or vertical percolation. The subsurface response is controlled by soil type, soil thickness, drainable porosity, soil pipes, macropores, and moisture content.

23.3.4.1 Soil Type, Soil Thickness, and Drainable Porosity

Generally, the type of soil strongly determines the hydrologic response. Certain pedogenetic processes result in certain properties, which, in turn, predefine hydrologic response (e.g., Luvisols: clay leaching leading to argic horizons, which may act as barrier to flow; Regosols: immature soils, low thickness above bedrock, thus prone to quick saturation) (Boorman et al. 1995; Zech and Hintermaier-Erhard 2002). Thus, information about the spatial distribution of soil types, which is available in many countries, provides a valuable tool for predicting hydrological

processes in ungauged regions (e.g., Tetzlaff et al. 2009). Soil thickness and drainable porosity, which is the pore space between field capacity and saturation, represent first-order controls on SSF (Weiler and McDonnell 2004; Uchida et al. 2006; Hopp and McDonnell 2009). Virtual experiments based on the Panola hillslope revealed that an increase in soil thickness led to a general reduction of the hillslope hydrologic response: SSF started later, the time to peak discharge increased, and peak discharge decreased (Hopp and McDonnell 2009). Another set of virtual experiments investigating the effect of variable soil depth showed that variations in soil thickness not only have a large influence on the spatial variation of subsurface flow but also largely control the total SSF volume (Weiler and McDonnell 2004). Clearly, the vertical travel distance of rainfall from the soil surface to the impeding layer is longer in deeper soils. Thus, the build-up of saturation and the initiation of subsurface flow occur later. Due to the larger total storage volume of deeper soils, incoming precipitation peaks are damped (Hopp and McDonnell 2009). A similar effect emanates from drainable porosity. While a rapid decline in drainable porosity with depth accelerates the development of a transient saturation, a high drainable porosity in combination with high moisture deficits causes a long lag time till SSF is triggered and large event water ratios (Uchida et al. 2004, 2006; Weiler and McDonnell 2004).

23.3.4.2 Soil Pipes and Macropores

Pipe networks seem to be an eminent feature of most hillslopes, as numerous studies suggest (e.g., Jones 1997; Holden and Burt 2002; Uchida et al. 2005; Tromp-van Meerveld and McDonnell 2006a; Graham 2008; Kienzler and Naef 2008a; Anderson et al. 2009). In consequence, the existence and nature of soil pipes, as well as factors influencing the maintenance and interconnection of pipes, govern the subsurface hillslope response to a large extent. Despite this importance, we lack a solid understanding on the controls of pipe flow. The evolution of pipe networks seems to be a complex interaction between mechanical processes (burrowing animals, roots, subsurface erosion), soil, topography, climate, and contributing area (Tsuboyama et al. 1994). Anderson et al. (2009), for instance, observed SSF velocities in a hillslope in coastal British Columbia, Canada, that were among the highest velocities reported in literature. They attribute this to the humid climate (annual precipitation >2,000 mm), shallow soils (often less than 1 m deep), and the lush vegetation, which caused a highly developed preferential flow network. Dye staining experiments and excavations have shown that pipe flow often occurs in decayed root channels (Noguchi et al. 1999; Anderson et al. 2008). Root architecture may thus play a significant role for pipe evolution. Once pipes are formed, subsurface erosion is considered to be highly important for the maintenance and modification of pipes (Uchida et al. 2001; Uchida 2004). Anderson et al. (2008) observed a link between contributing area and distribution of preferential flow features. They showed that the presence of highly developed preferential flow

features corresponded to large surface contributing areas, whereas few preferential flow paths coincided with small contributing areas and relatively flat local topography. This suggests that soils with small contributing area may not receive flow rates large enough to modify and maintain large preferential flow features (Anderson et al. 2008). Moreover, it seems like steeper slopes have better devolved pipes, since higher gradients result in higher energy for pipe erosion. The interconnection of pipes, which strongly increases the effectiveness of hillslope drainage, is assumed to increase with soil moisture (Tsuboyama et al. 1994; Sidle et al. 2000; Uchida et al. 2005; Anderson et al. 2009).

Besides pipe flow, vertical macropores play an important role for hillslope runoff processes, since macropores increase the infiltration capacity and quickly transport precipitation to deeper soil layers. The knowledge on macropore flow is much further advanced than that on pipe flow (for a recent review on controlling factors of macropore flow, see Jarvis et al. (2007)).

23.3.4.3 Soil Moisture

It is self-evident that the hillslope wetness constitutes a first-order control on the timing and the amount of runoff (e.g., Sivapalan 1993; Grayson et al. 1997; Western et al. 2003). However, it is not the soil moisture state alone, it is also the connectedness of saturated soil patches that determines the runoff response (e.g., Stieglitz et al. 2003; Western et al. 2003; McNamara et al. 2005; Tromp-van Meerveld and McDonnell 2006b; James and Roulet 2007). Generally, the wetter the system, the faster and more intense the hydrologic response will be. This applies to both vertical processes such as macropore flow (Weiler 2001), and to lateral processes at the hillslope scale (Kienzler and Naef 2008b). However, Scherrer et al. (2007) inferred from hillslope sprinkling experiments at several different sites that the impact of antecedent soil moisture on runoff volume depends on the runoff process. Kienzler and Naef (2008b) explain the variable influence of antecedent wetness with different mechanisms of SSF initiation (high influence if SSF is initiated via saturated soil patches vs. low influence when SSF is directly fed by preferential pathways).

Soil moisture conditions are characterized by strong seasonality, which not only results from meteorological conditions but also from vegetation dynamics and thus transpiration (e.g., Jackson et al. 2000; Western et al. 2003; Schume et al. 2004; McNamara et al. 2005; Williams et al. 2008; Kim 2009). McNamara et al. (2005) identified five soil moisture states throughout the year governing the runoff response in a snowmelt-driven, semiarid catchment: (1) a summer dry period (soil water depletion due to evaporation exceeding precipitation), (2) a transitional fall wetting period, (3) a winter wet, low-flux period (precipitation falling as snow), (4) a spring wet, high-flux period (snowmelt), and (5) a transitional late-spring drying period. Despite seasonal variations, soil moisture patterns are spatially highly variable, which can be attributed to topography and vegetation effects, as highlighted before.

23.3.5 Geologic Properties

Bedrock topography was already highlighted as a control on runoff generation (fill-and-spill hypothesis by Tromp-van Meerveld and McDonnell 2006b). Evidence supporting this hypothesis was also presented by Graham (2008). During hillslope excavations in the Maimai catchment, he observed that flow paths along the soil-bedrock interface were routed primarily by features such as protruding cobbles and rills on the bedrock surface (Graham 2008). Apart from bedrock topography, the bedrock permeability mainly controls how much water can vertically percolate and laterally redirected, respectively. Tromp-van Meerveld and Weiler (2008) criticize how many experimental hillslope studies and hillslope models assume impermeable bedrock and thus no-flow boundary conditions at the soil–bedrock interface, despite clear evidence of vertical leaching into the bedrock (e.g., Kosugi et al. 2006; Tromp-van Meerveld et al. 2007; Graham 2008; Kosugi et al. 2008b). For instance, a falling head permeability test recently indicated that the bedrock underlying the Maimai hillslope is semipervious (point observation of saturated hydraulic conductivity 2.9×10^{-7} to 8.6×10^{-7} m s^{-1}, Graham 2008). Even higher values of bedrock saturated hydraulic conductivity were observed at the Panola hillslope and in the Fudoji catchment (Uchida et al. 2003a; Tromp-van Meerveld et al. 2007). At the Panola hillslope, at least 20% of the precipitation during large rainstorms infiltrates into the granite bedrock (Tromp-van Meerveld et al. 2007). Kosugi et al. (2006) reported an annual bedrock infiltration ranging from 35 to 55% of the annual precipitation in an unchanneled 0.024-ha catchment near Fudoji (weathered granite). The effect of bedrock leakage on the subsurface flow response at the Panola hillslope was tested through virtual experiments by Tromp-van Meerveld and Weiler (2008). They concluded that bedrock leakage needed to be included to adequately simulate the SSF response to multiple storms. When bedrock leakage was omitted, recessions were too slow and the hillslope stayed too wet in between events, leading to sustained baseflow from the hillslope and an overprediction of simulated subsurface flow responses (Tromp-van Meerveld and Weiler 2008). At the same time, exfiltration from the bedrock into the soil may be a possible process at some hillslopes (Kosugi et al. 2006, 2008b). The soil–bedrock exchange processes are yet not well characterized, even though tracer experiments (Noguchi et al. 1999; Frazier et al. 2002) and bedrock groundwater monitoring documented flow within bedrock fractures (Kosugi et al. 2008a).

23.3.6 Interrelations and Mutual Dependencies

As pointed out in the foregoing summary of controlling factors, there are numerous interrelations among different controls of rainfall-runoff processes at the hillslope scale (e.g., Tromp-van Meerveld and McDonnell 2006c; Hopp and McDonnell 2009).

For instance, the spatial variation of soil moisture is partly due to rainfall partitioning, which is driven by both vegetation and storm characteristics. Furthermore, plant roots alter the soil structure, which, in turn, affects infiltration (Angers and Caron 1998). At the same time, hillslope hydrological processes and its controls are mutually dependent. On the one hand, climate and soil moisture control vegetation dynamics; on the other hand, vegetation controls the hillslope water balance and interacts with the atmosphere (Porporato and Rodriguez-Iturbe 2002). In other words, there is a double feedback between hydrological processes and its controls. Or, as Rodriguez-Iturbe (2000) put it, the spatial distribution of soil moisture (and probably also the saturated zone) and its evolution in time is both cause and consequence of vegetation. This also applies to interactions among hydrology, topography and soil properties. Along a toposequence, soil properties will change due to soil moisture patterns driven by topography (e.g., different weathering rates and biological activity in depressions vs. ridges). Yet, differences in soil properties cause different hydrological processes. This co-evolution of hydrology and landscape (Wagener et al. 2007) adds even more complexity to the system.

As a result of the many interrelations and mutual dependencies, identifying the first-order controls driving the rainfall-runoff response at a specific hillslope is highly challenging, especially since the impact of each control may be temporally variable. Nonetheless, we are confronted with the need to assess the hydrologic behavior of ungauged hillslopes and to develop modeling concepts. Given this nonlinear complex system, what are the hillslope characteristics we have to consider, and how do we pool the many pieces of information to assess its hydrologic response? Generally, the static "hillslope configuration" (geologic, morphologic, and pedologic properties such as soil depth and drainable porosity) determines the predisposition for certain runoff processes. This predisposition is refined through dynamic controls (input characteristics and vegetation dynamics) (e.g., Williams et al. 2008; Hopp and McDonnell 2009). Low-gradient hillslopes with deep soils, for instance, are less prone to fast SSF. There, vegetation effects such as intensity smoothing by canopies and localized stemflow will most likely not strongly modify the overall hydrologic response (Keim et al. 2006). In contrast, at high-gradient hillslopes with shallow soils, such vegetation-induced effects may be highly relevant. However, for less obvious hillslope settings, we still lack the understanding how different static and dynamic hillslope attributes interact in driving the runoff response. We propose that the concept of connectivity provides a viable framework for assessing the underlying controls of the nonlinear rainfall-runoff response at the hillslope scale.

23.3.7   Connectivity as Concept for Assessing the Rainfall-Runoff Response

In recent years, connectivity has emerged to a popular concept (Ali and Roy 2009; Michaelides and Chappell 2009). However, the term "connectivity" was often used ambiguously (e.g., Western et al. 2001; Pringle 2003; Knudby and Carrera 2005;

Bracken and Croke 2007; Lehmann et al. 2007; Michaelides and Chappell 2009), and "there is no consensus among hydrologists about what it is exactly" (Ali and Roy 2009). Similar to the definition by Stieglitz et al. (2003), we understand hydrologic connectivity at the hillslope scale as a system state, in which disconnected "hydrologically-active areas" (Uchida et al. 2001) (areas of surface flow, saturated soil patches, water-channeling subsurface features) interconnect with each other and to the stream, thus significantly contributing to storm runoff.

Many studies have proven that a key factor for surface and subsurface runoff is the connectivity of runoff-producing patches (Stieglitz et al. 2003; McNamara et al. 2005; Lehmann et al. 2007; Gomi et al. 2008). For example, Lehmann et al. (2007) applied percolation theory to the Panola hillslope, and concluded that the rainfall threshold triggering rapid hillslope out-flow seems to be related to the flow path connectivity at the next smaller spatial scale. Recently, Michaelides and Chappell (2009) recommended using connectivity to extract a simplified, universally applicable, quantifiable characteristic that transcends individual hillslope complexity.

Following this incentive, we suggest that the hillslope hydrologic response is determined by the connectivity of hydrologically-active areas on and within the slope. There are three types of hydrologically active areas: (a) areas of surface flow, (b) saturated soil patches, and (c) high-permeability features, which are live and decayed roots, animal burrows, subsurface erosion channels, bedrock fractures, and the soil skeleton. The mechanisms generating areas of surface flow and high-permeability features are straightforward (e.g., rainfall intensity exceeding the infiltration capacity, surface sealing, hydrophobicity, topsoil saturation; presence of structural features and self-reinforcement through subsurface erosion). The mechanisms producing spatially disconnected, saturated soil patches are diverse and can be summarized as follows: (1) variations in surface and bedrock topography, causing saturated conditions preferably in depressions, (2) spatially variable precipitation input due to the double-funneling effect of vegetation aboveground and belowground (interception, throughfall, stemflow, transpiration, litter layer partitioning, preferential flow along roots), and (3) variations in soil depth and drainable porosity (see Fig. 23.2). Once hydrologically active areas are established, they seem to recur during the next event, as observed for finger flow in water-repellent soils (Ritsema and Dekker 2000; Ritsema et al. 1998a, b).

We hypothesize that a significant increase in hillslope outflow is bound to the interconnection of hydrologically active areas; yet, it does not matter what kind of hydrologically active areas interconnect, or by which means they were formed. The fill-and-spill hypothesis (Tromp-van Meerveld and McDonnell 2006b) offers one explanation for the often observed nonlinearity of hillslope runoff response (bedrock depressions have to fill up before a lateral connection to the stream occurs). We believe the interconnection of high-permeability features or saturated soil patches evokes a similar response. The hillslope hydrologic behavior thus relies on the formation of an internal flow network (Tsuboyama et al. 1994; Noguchi et al. 1999; Sidle et al. 2000; Uchida et al. 2001). Such a network presumably consists of different types of hydrologically active areas linked together, e.g., flow in high-permeability features interconnected via saturated soil patches, as observed in a number of
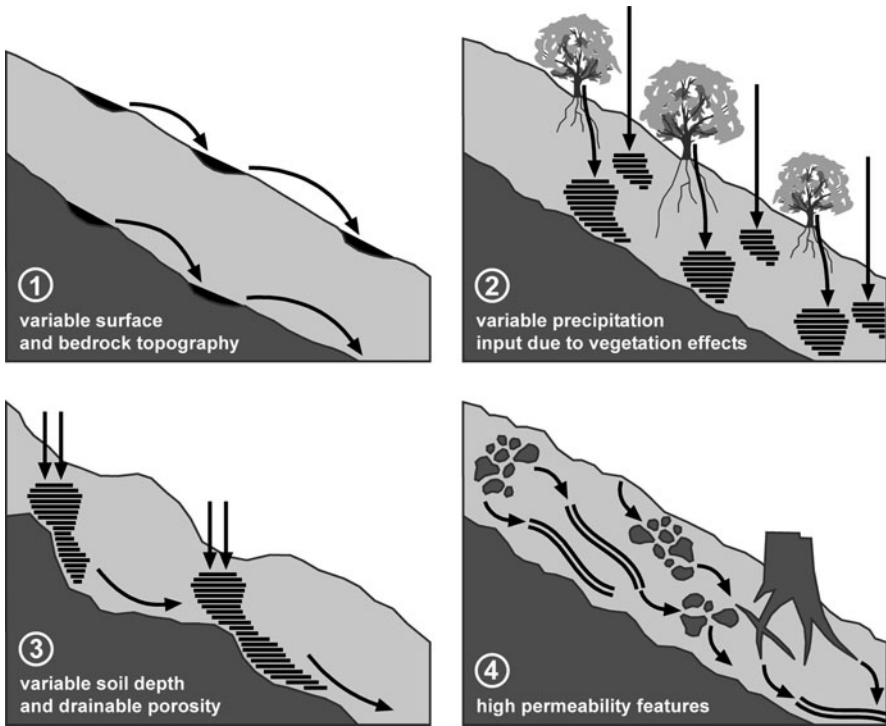
Fig. 23.2 Mechanisms generating and connecting hydrologically-active areas

experimental studies (Noguchi et al. 1999; Sidle et al. 2000; Anderson et al. 2008). In analogy to the fill-and-spill mechanism, we propose a connect-and-react mechanism: only if hydrologically active areas interconnect, a significant reaction (e.g., hillslope outflow or transport of nutrients) is triggered (see Fig. 23.3).

Clearly, this connectivity concept per se does not improve the predictions for ungauged hillslopes (unless we identify certain hillslope attributes as proxies describing the state of the internal network). However, this concept provides a holistic yet simple view on the complex mechanisms operating in and on hillslopes, thereby subsuming the diversity of mechanisms driving hillslope runoff. It could thus serve as a perceptual framework to develop new model structures helping to predict the hydrological behavior of hillslopes.

23.4 New Directions and Research Avenues

The immense heterogeneity and complexity of hydrological processes observed in numerous environments and at different spatial scales represents a great challenge for advances in hydrology (McDonnell et al. 2007). In this context, the call for a
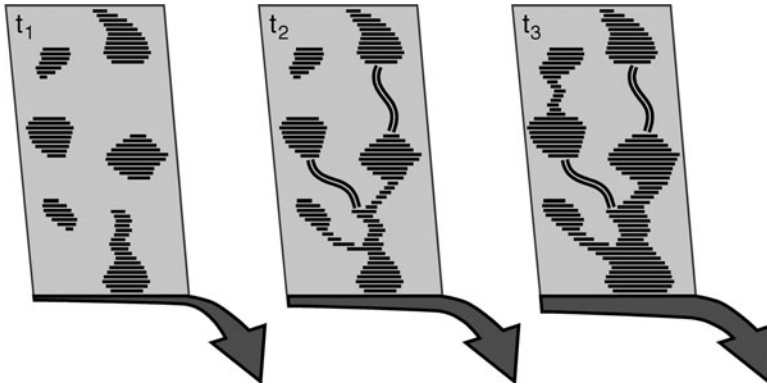
Fig. 23.3 Connect-and-react mechanism: We hypothesize that only if hydrologically active areas interconnect, a significant reaction (e.g., hillslope outflow or transport of nutrients) is triggered; yet, it does not matter what kind of hydrologically active areas interconnect, by which means they were formed, or by which mechanisms they connect

unifying hydrological theory has recently evolved (Sivapalan 2005; McDonnell et al. 2007; Troch et al. 2009). It is stressed to achieve a holistic understanding of the complex hydrologic system and its numerous interaction and feedback processes, thereby explicitly accepting landscape heterogeneity as dominant control. We thus need to systematically examine the first-order controls of hydrological processes rather than focusing on the idiosyncrasies of specific environments (Sivapalan 2005; Uchida et al. 2006; McDonnell et al. 2007; Wagener et al. 2007; Hopp et al. 2009; Troch et al. 2009). Troch et al. (2009) argue that, despite the tremendous heterogeneity of landscape properties, there is structure and organization across spatial and temporal scales. Understanding how and why this heterogeneity occurs may help to improve hydrologic predictability (Troch et al. 2009). In this respect, it was proposed to search for the reasons of heterogeneity and to identify the underlying principles or natural laws governing the hydrologic response (Sivapalan 2005; McDonnell et al. 2007). Regarding hillslope hydrology, what are feasible steps moving towards this great vision?

23.4.1 New Dimensions with Regard to Content

More generally, a holistic understanding of the complex hydrologic system strongly relies on an interdisciplinary perspective. As pointed out before, there are numerous interrelations among different controlling factors driving the hillslope hydrologic response, especially with regard to the soil–plant–atmosphere continuum. Hence, research aimed at identifying underlying principles or natural laws of hydrological processes needs the synergies from many disciplines, such as ecology, biology, biogeochemistry, pedology, geomorphology, and meteorology (Sivapalan 2005;

Lin et al. 2006; Troch et al. 2009). The necessity of interdisciplinary work and its mutual stimulation is expressed by the recent development of conjoined disciplines such as ecohydrology (Rodriguez-Iturbe 2000), hydropedology (Lin 2003), or hydro-geomorphology (Sidle and Onda 2004). We believe that a general process understanding of hillslope hydrology is especially reliant on how vegetation patterns and dynamics influence the hillslope water balance. In this respect, ecohydrology, which "seeks to describe the hydrologic mechanisms that underlie ecologic patterns and processes" (Rodriguez-Iturbe 2000) will play a significant role (e.g., Bond 2003; Hannah et al. 2004; Barnard 2009). As pointed out in the section on vegetation as controlling factor, plants affect hillslope soil moisture patterns and runoff formation in numerous ways. It is interesting though how many experimental and modeling studies neglect these effects. Numerous studies analyzing the hillslope runoff response do not pay special attention to the vegetation growing on the examination area, even if pipe flow is observed (e.g., McDonnell 1990; Woods and Rowe 1996; Kim et al. 2004, 2005; Fujimoto et al. 2008). Then, there are hillslope studies systematically investigating dominant controlling factors by intercomparing slopes differing in certain attributes (soil, bedrock, topography) under varying boundary conditions (rainfall amount and intensity, antecedent wetness); however, only under one type of land use (e.g., Kienzler and Naef 2008a, b), or poorly differentiating between grassland and forest, without specifying what type of forest, grassland, etc. (Scherrer et al. 2007). This shows that vegetation is not thought to be a first-order control. In addition, artificial sprinkling experiments suppress the rainfall partitioning effect of vegetation since water is applied close to the surface and not above the canopy (e.g., Markart et al. 2004; Scherrer et al. 2007; Nordmann et al. 2009). Virtual experiments by Keim et al. (2006), however, showed that the role of interception on SSF may be highly relevant. The influence of different root systems on flow routing in hillslopes has also been rarely considered (e.g., Nordmann et al. 2009), despite growing evidence that preferential flow along roots may override pore-scale controls on infiltration (e.g., Angers and Caron 1998; Bundt et al. 2001; Buttle and McDonald 2002; Bachmair et al. 2009; Lange et al. 2009). In summary, numerous experimental and modeling studies investigating the hillslope runoff response disregard plant effects. At the same time, there are many studies examining how certain tree and stand characteristics influence throughfall or stemflow (see Chap. 21). How this, in turn, affects hillslope runoff is yet seldom inferred, leaving room for interpretations on the actual implications. This gap should be addressed by future ecohydrological hillslope studies.

An idea originating from ecology that has been fruitfully transferred to hydrology is the focus on spatial patterns (Rodriguez-Iturbe 2000). The search for spatial patterns seems promising since it may provide a link to the underlying mechanisms (Rodriguez-Iturbe 2000; Sivapalan 2005). Studies correlating the hydrologic response with quantifiable landscape characteristics (e.g., Broxton et al. 2009) represent valuable attempts in this direction. In this respect, the potential power of optimality principles applied to hydrology shall be pointed out (Reggiani et al. 1998; Kleidon and Schymanski 2008; Schymanski et al. 2008; Rasmussen et al. 2011). Following optimality approaches, which are based on the

principle of maximum entropy production, complex systems far from thermodynamic equilibrium organize in a way that the rate of entropy production is maximized in steady state (Kleidon and Schymanski 2008). Spatial heterogeneity is thus not the result of some random process but the consequence of certain mass and energy fluxes (Schulz et al. 2006; Rasmussen et al. 2011). Further ideas on explaining hydrological patterns in relation to soil and landscape features may come from hydro-pedology (Lin 2003; Lin et al. 2006). According to Troch et al. (2009), identifying ways to quantify the implications of soil development and soil structure on hydrological processes seems promising. In combination with approaches predicting pedogenesis from more readily available information on climate and landscape position, this may be a valuable step toward improving the hydrologic predictability in ungauged regions (Troch et al. 2009).

23.4.2 Research Design

The highlighted new dimensions of hillslope hydrology have several implications for the research design of future hillslope studies. We need a unifying framework for experimental set-ups, analysis strategies and modeling concepts to clear the way for identifying underlying principles of hydrological processes at the hillslope scale.

In general, an improved process conceptualization needed for the development and testing of hydrological models relies on intercomparing processes at different hillslopes to abstract from the ubiquitous spatial and temporal variability. However, there are several obstacles in this respect. First, due to the numerous ways of experimental hillslope set-ups (e.g., trenched vs. nontrenched slopes, different hillslope sizes, artificial sprinkling vs. natural events), examined response metrics (e.g., total hillslope outflow vs. pipe flow, spatiotemporal resolution of internal response characteristics), and measurement techniques (e.g., different types and conditions of tracer application) comparability among different hillslope experiments is not given. Second, many experimental studies operate on rather small hillslope segments; it is questionable whether this size is suitable for deriving general answers (e.g., size of trench or hillslope outflow face: 4 m (Scherrer et al. 2007), 5 m (Kim et al. 2004, 2005), 8 m (Retter 2007; Kienzler and Naef 2008a), 9 m (Anderson et al. 2009), 10 m (McGuire et al. 2007), 16 m (Newman et al. 1998), 20 m (Tromp-van Meerveld and McDonnell 2006a), and 60 m (Woods and Rowe 1996; Graham 2008). Additionally, we need a large number of gauged hillslopes in several contrasting environments to draw meaningful conclusions. Yet, experimental hillslope studies are expensive and labor intensive. We hence need to figure out which response characteristics we have to measure for sufficiently describing the system. This goes hand in hand with the development and application of novel measurement techniques, such as ground penetrating radar or electrical resistance tomography for identifying subsurface structures (Holden et al. 2002; Cassiani et al. 2006; Schulz et al. 2006; Uhlenbrook et al. 2008; Markart et al. 2009),

soil water isotope extractions (Wassenaar et al. 2008), water isotope interactions with vegetation (Barnard 2009), wireless sensor techniques (Trubilowicz et al. 2009), and incremental stream discharge measurements (Szeftel et al. in review). Overall, we have to develop a sort of "minimum requirements" concept for hillslope studies to make them comparable and suitable for model validation and rejection. Furthermore, we should generally aim for intercomparison studies as research design instead of characterizing just one hillslope in detail (Uchida et al. 2005; McDonnell et al. 2007). Such intercomparison studies were successfully applied by a number of authors at the hillslope scale (e.g., Asano et al. 2002, 2004; Scherrer and Naef 2003; Uchida et al. 2004, 2005, 2006; Scherrer et al. 2007; Kienzler and Naef 2008a, b; Nordmann et al. 2009) and catchment scale (e.g., Molenat et al. 2008; Broxton et al. 2009; Hrachowitz et al. 2009; Tetzlaff et al. 2009). However, it is complicated to find natural hillslopes where certain controlling factors can be isolated, and attempts to artificially construct large-scale hillslopes as reported by Hopp et al. (2009) are an exception. Thus, virtual experiments (Weiler and McDonnell 2004) represent an effective framework for advancing our process understanding, as recent studies prove (e.g., Keim et al. 2006; Weiler and McDonnell 2006; Dunn et al. 2007; Tromp-van Meerveld and Weiler 2008; Hopp and McDonnell 2009). Additionally, we should think about ways facilitating data sharing as basis for intercomparison studies, as postulated by Soulsby et al. (2008), which would also benefit model evaluation and improvement.

In conclusion, there have been many attempts to go beyond simply "cataloging" the complexity of rainfall-runoff processes and to develop a more holistic picture of the factors driving the hillslope hydrologic response. Furthermore, the suggested directions regarding research gaps and design of future experimental and modeling studies may be a further step toward the vision of a unified hydrologic theory.

References

Ali G, Roy A (2009) Revisiting hydrologic sampling strategies for an accurate assessment of hydrologic connectivity in humid temperate systems. Geogr Compass 3(1):350–374

Anderson A (2008) Patterns of water table dynamics and subsurface runoff generation in a watershed with preferential flow networks. Dissertation Thesis, University of British Columbia, Vancouver

Anderson MG, Burt TP (1978) The role of topography in controlling throughflow generation. Earth Surf Process 3(4):331–344

Anderson S, Dietrich W, Montgomery D et al (1997) Subsurface flow paths in a steep, unchanneled catchment. Water Resour Res 33(12):2637–2653

Anderson A, Weiler M, Alila Y et al (2008) Dye staining and excavation of a lateral preferential flow network. Hydrol Earth Syst Sci Discuss 5(2):1043–1065

Anderson A, Weiler M, Alila Y et al (2009) Subsurface flow velocities in a hillslope with lateral preferential flow. Water Resour Res 45(11):W11407. doi:10.1029/2008WR007121

Angers D, Caron J (1998) Plant-induced changes in soil structure: processes and feedbacks. Biogeochemistry 42(1):55–72

Aryal S, O'Loughlin E, Mein R (2002) A similarity approach to predict landscape saturation in catchments. Water Resour Res 38(10):1208. doi:10.1029/2001WR000864

Aryal S, O'Loughlin E, Mein R (2005) A similarity approach to determine response times to steady-state saturation in landscapes. Adv Water Resour 28(2):99–115

Asano Y, Uchida T, Ohte N (2002) Residence times and flow paths of water in steep un-channelled catchments, Tanakami, Japan. J Hydrol 261(1–4):173–192

Asano Y, Ohte N, Uchida T (2004) Sources of weathering-derived solutes in two granitic catchments with contrasting forest growth. Hydrol Process 18(4):651–666

Bachmair S, Weiler M, Nützmann G (2009) Controls of land use and soil structure on water movement: lessons for pollutant transfer through the unsaturated zone. J Hydrol 369 (3–4):241–252

Barnard H (2009) Inter-relationships of vegetation, hydrology, and climate in a young Doug-las-fir forest. Dissertation Thesis, Oregon State University

Berne A, Uijlenhoet R, Troch P (2005) Similarity analysis of subsurface flow response of hill-slopes with complex geometry. Water Resour Res 41(9):W09410. doi:10.1029/2004WR003629

Beven K, Germann P (1982) Macropores and water flow in soils. Water Resour Res 18 (5):1311–1325

Blume T, Zehe E, Reusser D et al (2008) Investigation of runoff generation in a pristine, poorly gauged catchment in the Chilean Andes I: a multi-method experimental study. Hydrol Process 22(18):3661–3675

Bogaart P, Troch P (2006) Curvature distribution within hillslopes and catchments and its effect on the hydrological response. Hydrol Earth Syst Sci Discuss 3(3):1071–1104

Bond B (2003) Hydrology and ecology meet-and the meeting is good. Hydrol Process 17 (10):2087–2089

Boorman D, Hollis J, Lilly A (1995) Hydrology of soil types: a hydrologically based classification of the soils of the United Kingdom. IAHS Report 126. IAHS Press, Wallingford

Bracken L, Croke J (2007) The concept of hydrological connectivity and its contribution to understanding runoff-dominated geomorphic systems. Hydrol Process 21(13):1749–1763

Broxton P, Troch P, Lyon S (2009) On the role of aspect to quantify water transit times in small mountainous catchments. Water Resour Res 45(8):W08427. doi:10.1029/2008WR007438

Bundt M, Jaggi M, Blaser P et al (2001) Carbon and nitrogen dynamics in preferential flow paths and matrix of a forest soil. Soil Sci Soc Am J 65(5):1529

Burns D, Hooper R, McDonnell J et al (1998) Base cation concentrations in subsurface flow from a forested hillslope: the role of flushing frequency. Water Resour Res 34(12):3535–3544

Buttle J, McDonald D (2002) Coupled vertical and lateral preferential flow on a forested slope. Water Resour Res 38(5):1060

Buttle J, Turcotte D (1999) Runoff processes on a forested slope on the Canadian shield. Nord Hydrol 30(1):1–20

Cassiani G, Bruno V, Villa A et al (2006) A saline trace test monitored via time-lapse surface electrical resistivity tomography. J Appl Geophys 59(3):244–259

Chang S, Matzner E (2000) The effect of beech stemflow on spatial patterns of soil solution chemistry and seepage fluxes in a mixed beech/oak stand. Hydrol Process 14(1):135–144

Corradini C, Morbidelli R, Melone F (1998) On the interaction between infiltration and Hortonian runoff. J Hydrol 204(1–4):52–67

Crockford R, Richardson D (2000) Partitioning of rainfall into throughfall, stemflow and intercep-tion: effect of forest type, ground cover and climate. Hydrol Process 14(16–17):2903–2920

Doerr SH, Shakesby RA, Walsh RPD (2000) Soil water repellency: its causes, characteristics and hydro-geomorphological significance. Earth Sci Rev 51(1–4):33–65

Dunn S, McDonnell J, Vaché K (2007) Factors influencing the residence time of catchment waters: a virtual experiment approach. Water Resour Res 43(6):W06408

Dunne T (1978) Field studies of hillslope flow processes. In: Kirkby MJ (ed) Hillslope hydrology. Wiley, New York, pp 227–293

Dunne T, Black R (1970) Partial area contributions to storm runoff in a small New England watershed. Water Resour Res 6(5):1296–1311

Elsenbeer H, Vertessy R (2000) Stormflow generation and flowpath characteristics in an Amazonian rainforest catchment. Hydrol Process 14(14):2367–2381

Fannin R, Jaakkola J, Wilkinson J et al (2000) Hydrologic response of soils to precipitation at Carnation Creek, British Columbia, Canada. Water Resour Res 36(6):1481–1494

Frazier C, Graham R, Shouse P et al (2002) A field study of water flow and virus transport in weathered granitic bedrock. Vadose Zone J 1(1):113

Freer J, McDonnell JJ, Beven KJ et al (1997) Hydrological processes – letters. Topographic controls on subsurface storm flow at the hillslope scale for two hydrologically distinct small catchments. Hydrol Process 11(9):1347–1352

Freer J, McDonnell J, Beven K et al (2002) The role of bedrock topography on subsurface storm flow. Water Resour Res 38(12):1269. doi:10.1029/2001WR000872

Fujimoto M, Ohte N, Tani M (2008) Effects of hillslope topography on hydrological responses in a weathered granite mountain, Japan: comparison of the runoff response between the valley-head and the side slope. Hydrol Process 22(14):2581–2594

Godsey S, Elsenbeer H, Stallard R (2004) Overland flow generation in two lithologically distinct rainforest catchments. J Hydrol 295(1–4):276–290

Gomi T, Sidle R, Miyata S et al (2008) Dynamic runoff connectivity of overland flow on steep forested hillslopes: scale effects and runoff transfer. Water Resour Res 44(8):W08411. doi:10.1029/2007WR005894

Graham C (2008) A macroscale measurement and modeling approach to improve understanding of the hydrology of steep, forested hillslopes. PhD dissertation, Oregon State University, Corvallis, Oregon

Grayson R, Western A, Chiew F et al (1997) Preferred states in spatial soil moisture patterns: local and nonlocal controls. Water Resour Res 33(12):2897–2908

Hannah D, Wood P, Sadler J (2004) Ecohydrology and hydroecology: a "new paradigm?". Hydrol Process 18(17):3439–3445

Hendrickx J, Flury M (2001) Uniform and preferential flow mechanisms in the vadose zone. In: Feary DA (ed) Conceptual models of flow and transport in the fractured vadose zone. National Academy Press, Washington, pp 149–187

Herwitz SR (1986) Infiltration-excess caused by stemflow in a cyclone-prone tropical rain-forest. Earth Surf Process Landforms 11(4):401–412

Holden J (2009) Topographic controls upon soil macropore flow. Earth Surf Process Landforms 34 (3):345–351

Holden J, Burt T (2002) Piping and pipeflow in a deep peat catchment. Catena 48(3):163–199

Holden J, Burt TP, Vilas M (2002) Application of ground-penetrating radar to the identification of subsurface piping in blanket peat. Earth Surf Process Landforms 27(3):235–249

Hopp L, McDonnell J (2009) Connectivity at the hillslope scale: identifying interactions between storm size, bedrock permeability, slope angle and soil depth. J Hydrol 376(3–4):378–391

Hopp L, Harman C, Desilets S et al (2009) Hillslope hydrology under glass: confronting fundamental questions of soil-water-biota co-evolution at biosphere 2. Hydrol Earth Syst Sci Discuss 6:4411–4448

Horton R (1933) The role of infiltration in the hydrologic cycle. Trans Am Geophys Union 14:446–460

Hrachowitz M, Soulsby C, Tetzlaff D et al (2009) Using long-term data sets to understand transit times in contrasting headwater catchments. J Hydrol 367(3–4):237–248

Jackson N, Wallace J, Ong C (2000) Tree pruning as a means of controlling water use in an agroforestry system in Kenya. For Ecol Manage 126(2):133–148

James A, Roulet N (2007) Investigating hydrologic connectivity and its association with threshold change in runoff response in a temperate forested watershed. Hydrol Process 21 (25):3391–3408

Jarvis N, Larsbo M, Roulier S et al (2007) The role of soil properties in regulating non-equilibrium macropore flow and solute transport in agricultural topsoils. Eur J Soil Sci 58:282–292

Johnson M, Lehmann J (2006) Double-funneling of trees: stemflow and root-induced preferential flow. Ecoscience 13(3):324–333

Jones JAA (1997) The role of natural pipeflow in hillslope drainage and erosion: extrapolating from the Maesnant data. Phys Chem Earth 22(3–4):303–308

Jost G, Heuvelink G, Papritz A (2005) Analysing the space–time distribution of soil water storage of a forest ecosystem using spatio-temporal kriging. Geoderma 128(3–4):258–273

Keim R, Skaugset A (2003) Modelling effects of forest canopies on slope stability. Hydrol Process 17(7):1457–1467

Keim R, Tromp-van Meerveld H, McDonnell J (2006) A virtual experiment on the effects of evaporation and intensity smoothing by canopy interception on subsurface stormflow generation. J Hydrol 327(3–4):352–364

Kienzler PM, Naef F (2008a) Subsurface storm flow formation at different hillslopes and implications for the "old water paradox". Hydrol Process 22:104–116

Kienzler PM, Naef F (2008b) Temporal variability of subsurface stormflow formation. Hydrol Earth Syst Sci 12:257–265

Kim S (2009) Characterization of soil moisture responses on a hillslope to sequential rainfall events during late autumn and spring. Water Resour Res 45(9):W09425. doi:10.1029/2008WR007239

Kim H, Sidle R, Moore R et al (2004) Throughflow variability during snowmelt in a forested mountain catchment, coastal British Columbia, Canada. Hydrol Process 18(7):1219–1236

Kim HJ, Sidle RC, Moore RD (2005) Shallow lateral flow from a forested hillslope: influence of antecedent wetness. Catena 60(3):293–306

Kleidon A, Schymanski S (2008) Thermodynamics and optimality of the water budget on land: a review. Geophys Res Lett 35(20):L20404

Knudby C, Carrera J (2005) On the relationship between indicators of geostatistical, flow and transport connectivity. Adv Water Resour 28(4):405–421

Kosugi K, Katsura S, Katsuyama M et al (2006) Water flow processes in weathered granitic bedrock and their effects on runoff generation in a small headwater catchment. Water Resour Res 42:W02414. doi:10.1029/2005WR004275

Kosugi K, Katsura S, Fujimoto M et al (2008a) Investigations on hydrological connectivity between soil mantle and weathered bedrock in headwater catchments. AGU fall meeting abstracts, San Francisco, CA

Kosugi K, Katsura S, Mizuyama T et al (2008b) Anomalous behavior of soil mantle groundwater demonstrates the major effects of bedrock groundwater on surface hydrological processes. Water Resour Res 44. doi:10.1029/2006wr005859

Lange B, Lüscher P, Germann P (2009) Significance of tree roots to preferential flow in soil horizons with different degrees of hydromorphy. In: International conference on preferential and unstable flow – from water infiltration to gas injection, Monte Verità, Ascona (Switzerland), pp 1809–1821

Lehmann P, Hinz C, McGrath G et al (2007) Rainfall threshold for hillslope outflow: an emergent property of flow pathway connectivity. Hydrol Earth Syst Sci 11:1047–1063

Levia D, Van Stan J, Mage S et al (2010) Temporal variability of stemflow volume in a beech-yellow poplar forest in relation to tree species and size. J Hydrol 380(1–2):112–120

Liang W, Kosugi K, Mizuyama T (2007) Heterogeneous soil water dynamics around a tree growing on a steep hillslope. Vadose Zone J 6(4):879

Lin H (2003) Hydropedology: bridging disciplines, scales, and data. Vadose Zone J 2(1):1–11

Lin H, Bouma J, Pachepsky Y et al (2006) Hydropedology: synergistic integration of pedology and hydrology. Water Resour Res 42:W05301

López-Moreno J, Stähli M (2008) Statistical analysis of the snow cover variability in a subal-pine watershed: assessing the role of topography and forest interactions. J Hydrol 348 (3–4):379–394

Lyon S, Troch P (2007) Hillslope subsurface flow similarity: real-world tests of the hillslope Péclet number. Water Resour Res 43(7):W07450. doi:10.1029/2006WR005323

Markart G, Kohl B, Sotier B et al (2004) Provisorische Geländeanleitung zur Abschätzung des Oberflächenabflussbeiwertes auf alpinen Boden-/Vegetationseinheiten bei kon-vektiven Starkregen. Schriftenreihe des Bundesamtes und Forschungszentrums für Wald, Wien

Markart G, Bieber G, Römer A et al (2009) Assessment of bandwidths of near surface inter-flow velocities in a high-alpine catchment of Western Austria. In: International conference on preferential and unstable flow – from water infiltration to gas injection. Monte Verita, Ascona, Switzerland, pp 33

McDonnell J (1990) A rationale for old water discharge through macropores in a steep, humid catchment. Water Resour Res 26(11):2821–2832

McDonnell JJ (2003) Where does water go when it rains? Moving beyond the variable source area concept of rainfall-runoff response. Hydrol Process 17:1869–1875

McDonnell J, Owens I, Stewart M (1991) A case study of shallow flow paths in a steep zero-order basin. Water Resour Bull 27(4):679–685

McDonnell JJ, Sivapalan M, Vache K et al (2007) Moving beyond heterogeneity and process complexity: a new vision for watershed hydrology. Water Resour Res 43(7). doi:10.1029/2006wr005467

McGlynn BL, McDonnell JJ, Brammer DD (2002) A review of the evolving perceptual model of hillslope flowpaths at the Maimai catchments. New Zealand J Hydrol 257:1–26

McGuire KJ, Weiler M, McDonnell JJ (2007) Integrating tracer experiments with modeling to assess runoff processes and water transit times. Adv Water Resour 30:824–837

McNamara J, Chandler D, Seyfried M et al (2005) Soil moisture states, lateral flow, and stream-flow generation in a semi-arid, snowmelt-driven catchment. Hydrol Process 19(20):4023–4038

Michaelides K, Chappell A (2009) Connectivity as a concept for characterising hydrological behaviour. Hydrol Process 23(3):517–522

Molenat J, Gascuel-Odoux C, Ruiz L et al (2008) Role of water table dynamics on stream nitrate export and concentration in agricultural headwater catchment (France). J Hydrol 348:363–378

Molotch N, Brooks P, Burns S et al (2009) Ecohydrological controls on snowmelt partitioning in mixed-conifer sub-alpine forests. Ecohydrology 2(2):129–142

Mosley M (1979) Streamflow generation in a forested watershed, New Zealand. Water Resour Res 15(4):795–806

Newman B, Campbell A, Wilcox B (1998) Lateral subsurface flow pathways in a semiarid ponderosa pine hillslope. Water Resour Res 34(12):3485–3496

Noguchi S, Tsuboyama Y, Sidle RC et al (1999) Morphological characteristics of macro-pores and the distribution of preferential flow pathways in a forested slope segment. Soil Sci Soc Am J 63:1413–1423

Nordmann B, Göttlein A, Binder F (2009) Einfluss unterschiedlicher Waldbestockung auf die Abflussbildung – ein Beispiel aus einem Wassereinzugsgebiet im Frankenwald. Hydrol Wasserbewirtsch 53(2):80–95

Phillips J (2003) Sources of nonlinearity and complexity in geomorphic systems. Progr Phys Geogr 27(1):1–23

Polomski J, Kuhn N (1998) Wurzelsysteme. Paul Haupt, Birmensdorf

Porporato A, Rodriguez-Iturbe I (2002) Ecohydrology – a challenging multidisciplinary research perspective. Hydrol Sci J 47(5):811–821

Pringle C (2003) What is hydrologic connectivity and why is it ecologically important? Hydrol Process 17(13):2685–2689

Rasmussen C, Troch PA, Chorover JD et al (2011) An open system framework for integrating critical zone structure and function. Biogeochemistry 102:15–29

Reggiani P, Sivapalan M, Majid Hassanizadeh S (1998) A unifying framework for watershed thermodynamics: balance equations for mass, momentum, energy and entropy, and the second law of thermodynamics. Adv Water Resour 22(4):367–398

Retter M (2007) Subsurface flow formation. Dissertation Thesis, University of Bern, Bern, pp 97

Ritsema CJ, Dekker LW (2000) Preferential flow in water repellent sandy soils: principles and modeling implications. J Hydrol 231–232:308–319

Ritsema C, Nieber J, Dekker L et al (1998a) Stable or unstable wetting fronts in water repellent soils – effect of antecedent soil moisture content. Soil Tillage Res 47(1–2):111–123

Ritsema CJ, Dekker LW, Nieber JL et al (1998b) Modeling and field evidence of finger formation and finger recurrence in a water repellent sandy soil. Water Resour Res 34. doi:10.1029/97wr02407

Rodriguez-Iturbe I (2000) Ecohydrology: a hydrologic perspective of climate-soil-vegetation dynamics. Water Resour Res 36(1):3–9

Sato Y, Kumagai T, Kume A et al (2004) Experimental analysis of moisture dynamics of litter layers – the effects of rainfall conditions and leaf shapes. Hydrol Process 18:3007–3018

Scherrer S, Naef F (2003) A decision scheme to indicate dominant hydrological flow processes on temperate grassland. Hydrol Process 17(2):391–401

Scherrer S, Naef F, Faeh AO et al (2007) Formation of runoff at the hillslope scale during intense precipitation. Hydrol Earth Sci Syst 11:907–922

Schmocker-Fackel P (2004) A method to delineate runoff processes in a catchment and its implications for runoff simulations. Dissertation Thesis, Swiss Federal Institute of Technology Zürich, Zürich

Schulz K, Seppelt R, Zehe E et al (2006) Importance of spatial structures in advancing hydrological sciences. Water Resour Res 42:W0S33

Schume H, Jost G, Hager H (2004) Soil water depletion and recharge patterns in mixed and pure forest stands of European beech and Norway spruce. J Hydrol 289(1–4):258–274

Schwärzel K, Menzer A, Clausnitzer F et al (2009) Soil water content measurements deliver reliable estimates of water fluxes: a comparative study in a beech and a spruce stand in the Tharandt forest (Saxony, Germany). Agric For Meteorol 149(11):1994–2006

Schymanski S, Sivapalan M, Roderick M et al (2008) An optimality-based model of the coupled soil moisture and root dynamics. Hydrol Earth Sci Syst 12(3):913–932

Sidle R, Onda Y (2004) Hydrogeomorphology: overview of an emerging science. Hydrol Process 18(4):597–602

Sidle RC, Tsuboyama Y, Noguchi S et al (2000) Stormflow generation in steep forested headwaters: a linked hydrogeomorphic paradigm. Hydrol Process 14(3):369–385

Sidle RC, Noguchi S, Tsuboyama Y et al (2001) A conceptual model of preferential flow systems in forested hillslopes: evidence of self-organization. Hydrol Process 15(10):1675–1692

Sidle RC, Hirano T, Gomi T et al (2007) Hortonian overland flow from Japanese forest plantations – an aberration, the real thing, or something in between? Hydrol Process 21:3237–3247

Sivapalan M (1993) Linking hydrologic parameterizations across a range of scales: hillslope to catchment to region. Exchange processes at the land surface for a range of space and time scales: proceedings of an international symposium, Yokohama, Japan

Sivapalan M (2005) Pattern, process and function: elements of a unified theory of hydrology at the catchment scale. In: Anderson MG (ed) Encyclopedia of hydrological sciences. Wiley, Chichester, pp 193–219

Sklash M (1990) Environmental isotope studies of storm and snowmelt runoff generation. In: Burt TP, Anderson MG (eds) Process studies in hillslope hydrology. Wiley, Chichester, pp 401–435

Sklash M, Stewart M, Pearce A (1986) Storm runoff generation in humid headwater catchments: 2. A case study of hillslope and low-order stream response. Water Resour Res 22(8):1273–1282

Soulsby C, Neal C, Laudon H et al (2008) Catchment data for process conceptualization: simply not enough? Hydrol Process 22(12):2057–2061

Stieglitz M, Shaman J, McNamara J et al (2003) An approach to understanding hydrologic connectivity on the hillslope and the implications for nutrient transport. Glob Biogeochem Cycles 17:1105. doi:10.1029/2003GB002041

Szeftel P, Moore RD, Weiler M, Alila Y (in review) Controls on water delivery to the stream network in a snowmelt-dominated montane catchment. Hydrol Process

Terajima T, Sakamoto T, Shirai T (2000) Morphology, structure and flow phases in soil pipes developing in forested hillslopes underlain by a quaternary sand-gravel formation, Hokkaido, northern main island in Japan. Hydrol Process 14(4):713–726

Tetzlaff D, Seibert J, Soulsby C et al (2009) Inter-catchment comparison to assess the influence of topography and soils on catchment transit times in a geomorphic province; the Cairngorm mountains, Scotland. Hydrol Process 23(13):1874–1886

Troch P, Paniconi C, Van Loon E (2003) Hillslope-storage Boussinesq model for subsurface flow and variable source areas along complex hillslopes: 1. Formulation and characteristic response. Water Resour Res 39(11):1316

Troch P, Carrillo G, Heidbuechel I et al (2009) Dealing with landscape heterogeneity in watershed hydrology: a review of recent progress toward new hydrological theory. Geogr Compass 3(1):375–392

Tromp-van Meerveld HJ, McDonnell JJ (2006a) Threshold relations in subsurface stormflow: 1. A 147-storm analysis of the Panola hillslope. Water Resour Res 42:W02410. doi:10.1029/2004WR003778

Tromp-van Meerveld HJ, McDonnell JJ (2006b) Threshold relations in subsurface stormflow: 2. The fill and spill hypothesis. Water Resour Res 42:W02411. doi:10.1029/2004WR003800

Tromp-van Meerveld HJ, McDonnell JJ (2006c) On the interrelations between topography, soil depth, soil moisture, transpiration rates and species distribution at the hillslope scale. Adv Water Resour 29:293–310

Tromp-van Meerveld HJ, Weiler M (2008) Hillslope dynamics modeled with increasing complexity. J Hydrol 361:24–40

Tromp-van Meerveld HJ, Peters NE, McDonnell JJ (2007) Effect of bedrock permeability on subsurface stormflow and the water balance of a trenched hillslope at the Panola Mountain Research Watershed, Georgia, USA. Hydrol Process 21:750–769

Trubilowicz J, Cai K, Weiler M (2009) Viability of motes for hydrological measurement. Water Resour Res 45:W00D22. doi:10.1029/2008WR007046

Tsuboyama Y, Sidle RC, Noguchi S et al (1994) Flow and solute transport through the soil matrix and macropores of a hillslope segment. Water Resour Res 30. doi:10.1029/93wr03245

Tsukamoto Y, Minematsu H, Tange I (1988) Pipe development in hillslope soils in humid climate. Rolling Land Res 6:268–280

Uchida T (2004) Clarifying the role of pipe flow on shallow landslide initiation. Hydrol Process 18(2):375–378

Uchida T, Kosugi K, Mizuyama T (2001) Effects of pipeflow on hydrological process and its relation to landslide: a review of pipeflow studies in forested headwater catchments. Hydrol Process 15(11):2151–2174

Uchida T, Kosugi KI, Mizuyama T (2002) Effects of pipe flow and bedrock groundwater on runoff generation in a steep headwater catchment in Ashiu, central Japan. Water Resour Res 38. doi:10.1029/2001WR000261

Uchida T, Asano Y, Ohte N et al (2003a) Seepage area and rate of bedrock groundwater discharge at a granitic unchanneled hillslope. Water Resour Res 39(1):1018

Uchida T, Asano Y, Ohte N et al (2003b) Analysis of flowpath dynamics in a steep unchannelled hollow in the Tanakami Mountains of Japan. Hydrol Process 17(2):417–430

Uchida T, Asano Y, Mizuyama T et al (2004) Role of upslope soil pore pressure on lateral subsurface storm flow dynamics. Water Resour Res 40:W12401. doi:10.1029/2003WR002139

Uchida T, Tromp-van Meerveld HJ, McDonnell JJ (2005) The role of lateral pipe flow in hill-slope runoff response: an intercomparison of non-linear hillslope response. J Hydrol 311:117–133

Uchida T, McDonnell JJ, Asano Y (2006) Functional intercomparison of hillslopes and small catchments by examining water source, flowpath and mean residence time. J Hydrol 327:627–642

Uhlenbrook S, Didszun J, Wenninger J (2008) Source areas and mixing of runoff components at the hillslope scale-a multi-technical approach. Hydrol Sci J 53(4):741–753

Wagener T, Sivapalan M, Troch P et al (2007) Catchment classification and hydrologic similarity. Geogr Compass 1(4):901–931

Ward RC, Robinson M (1990) Principles of hydrology. McGraw-Hill, New York

Wassenaar L, Hendry M, Chostner V et al (2008) High resolution pore water 2H and 18O measurements by H2O (liquid)-H2O (vapor) equilibration laser spectroscopy. Environ Sci Technol 42(24):9262–9267

Weiler M (2001) Mechanisms controlling macropore flow during infiltration. Dissertation Thesis, Swiss Federal Institute of Technology Zürich, Zürich, pp 151

Weiler M, Flühler H (2004) Inferring flow types from dye patterns in macroporous soils. Geoderma 120(1–2):137–153

Weiler M, McDonnell J (2004) Virtual experiments: a new approach for improving process conceptualization in hillslope hydrology. J Hydrol 285(1–4):3–18

Weiler M, McDonnell JJ (2006) Testing nutrient flushing hypotheses at the hillslope scale: a virtual experiment approach. J Hydrol 319:339–356

Weiler M, Naef F (2003) An experimental tracer study of the role of macropores in infiltration in grassland soils. Hydrol Process 17(2):477–493

Weiler M, McDonnel JJ, Tromp-van Meerveld I et al (2006) Subsurface stormflow. In: Anderson MG, McDonnell JJ (eds) Encyclopedia of hydrological sciences, volume 3, part 10. Wiley, New York

Western A, Blöschl G, Grayson R (2001) Toward capturing hydrologically significant connectivity in spatial patterns. Water Resour Res 37(1):83–97

Western A, Grayson R, Blöschl G et al (2003) Spatial variability of soil moisture and its implications for scaling. In: Perchepsky Y, Selim M, Radcliffe D (eds) Scaling methods in soil physics. CRC Press, Boca Raton, pp 120–142

Williams C, McNamara J, Chandler D (2008) Controls on the temporal and spatial variability of soil moisture in a mountainous landscape: the signatures of snow and complex terrain. Hydrol Earth Syst Sci Discuss 5:1927–1966

Woods R, Rowe L (1996) The changing spatial variability of subsurface flow across a hillside. J Hydrol (NZ) 35(1):51–86

Zech W, Hintermaier-Erhard G (2002) Böden der Welt. Spektrum, Heidelberg

Zehe E, Flühler H (2001) Slope scale variation of flow patterns in soil profiles. J Hydrol 247 (1–2):116–132

Zehe E, Sivapalan M (2009) Threshold behaviour in hydrological systems as (human) geo-ecosystems: manifestations, controls, implications. Hydrol Earth Syst Sci 13:1273–1297

Zimmermann A, Germer S, Neill C et al (2008) Spatio-temporal patterns of throughfall and solute deposition in an open tropical rain forest. J Hydrol 360(1–4):87–102

Chapter 24
Ecohydrology and Biogeochemistry of the Rhizosphere in Forested Ecosystems

Mark S. Johnson and Georg Jost

24.1 Introduction

The rhizosphere, defined as the narrow zone within the soil centered on the root–soil interface, has long been recognized as a hotspot for biogeochemical cycling within the soil (Richter et al. 2007). Life on earth is directly dependent upon processes occurring within the small volume of soil surrounding roots (Hinsinger et al. 2009), making the rhizosphere the "epicenter" of the critical zone, where soil weathering, biogeochemical cycling, and root uptake of water and nutrients take place. The physical dimensions of the rhizosphere should be considered in mechanistic rather than in absolute terms, as its width (measured as the distance outward from the center of the root) varies in scale from sub-micron to supra-centimeter depending on the process considered (Hinsinger et al. 2009). For most considerations related to ecohydrology and soil water dynamics, the width of concern for the rhizosphere is on the order of several (<5) centimeters.

The first use of the term "rhizosphere" appeared in the literature over 100 years ago (Hiltner 1904), an occurrence which was commemorated in 2004 with an international conference organized to mark the first century of research explicitly focused on the rhizosphere (Hinsinger and Marschner 2006). The uniqueness of properties and functions of the rhizosphere relative to bulk soil[1] has motivated much of the rhizospheric research to date, which has focused primarily on soil biology and ecology of the rhizosphere (Gregory 2006). Despite the centrality of rhizospheric processes for soil hydrology, hydrologic aspects have received relatively little attention to date in studies of the rhizosphere. For instance, in recent years (e.g., since 2000) there have been an average of 827 papers per year indexed by Web of Science that address some aspect of the rhizosphere. Of these rhizosphere studies, only 2% have appeared in water resources journals. Nevertheless, rhizospheric considerations are central to the study of ecohydrology, particularly within forested ecosystems.

---

[1]In this paper, the term "bulk soil" is used to describe soil in the area outside of the rhizosphere but still within the rooting depth.

Several comprehensive reviews have demonstrated the importance of the rhizosphere to understanding soil biophysical and ecological processes (Gregory 2006; Richter et al. 2007; Hinsinger et al. 2009). In this chapter, we focus on three rhizosphere mechanisms that differentiate the ecohydrological and biogeochemical processes characteristic of the rhizosphere from those of bulk soil. These are (1) double-funneling of stemflow into root-induced preferential flow pathways; (2) hydraulic redistribution (HR) of soil water by roots from wetter to drier soil zones; and (3) CO_2 dynamics of the rhizosphere. We follow with several examples of external influences on the ecohydrology of the rhizosphere. Finally, we present suggestions for future research directions for advancing our understanding of ecohydrology and biogeochemistry of the rhizosphere, and discuss global change issues as they relate to the rhizosphere of forested ecosystems.

24.2 Ecohydrological and Biogeochemical Differences Between Rhizosphere and Bulk Soil

One of the organizing aspects for ecohydrology and biogeochemistry in the rhizosphere is that the transpiration-driven flow of water due to plant water uptake occurs at the interface of roots and soil in the midst of a "central commodities exchange, where organic carbon flux from roots fuels decomposers that, in turn, can make nutrients available to roots" (Cardon and Gage 2006). This makes the rhizosphere a hotspot (*sensu* McClain et al. (2003)) for biogeochemical cycling.

Biogeochemical cycling in the rhizosphere is central to plant nutrient uptake, weathering reactions, and soil respiration of CO_2. Soil microbial populations are concentrated in the rhizosphere (Richter et al. 2007), in part because root exudates provide a principle energetic resource for microbes. Even deep in the soil profile, the few roots present at depth generate a rhizospheric oasis within the ogliotrophic bulk soil, where the rhizosphere hosts microbial populations that are almost undetectable in bulk soil (Richter et al. 2007). The rhizosphere is responsible for a large fraction of weathering (Richter et al. 2007), soil carbon fluxes (Cheng and Gershenson 2007), and plant nutrient availability and uptake through associations with soil mycorrhizas (Hughes et al. 2008). The latter is an underappreciated aspect of the rhizosphere, in that 90% of plant species form symbiotic relationships with mycorrhizal fungi, making the "mycorrhizosphere" the rule rather than the exception (Linderman 1988). The coupled role of the rhizosphere in weathering processes and the global carbon cycle is discussed further in subsequent sections of this chapter.

Ecohydrology of the rhizosphere exhibits large differences in mechanisms and fluxes as compared to bulk soil. For instance, soil water uptake by trees follows an increasingly negative water potential leading from the rhizosphere to the stomata in the leaf. As this uptake follows a diurnal cycle, rhizospheric soil experiences a periodicity in soil water potential dynamics that is not experienced in the bulk soil.

Further, the rhizosphere is an autogenic environment, where the physical space is gained from bulk soil through compressive forces exerted radially by root expansion during plant water uptake as well as axially at the root apex during root elongation (Hinsinger et al. 2009). These rhizopathways are then lined by root exudates and microbial rhizodeposits that are frequently hydrophobic (Jarvis 2007), thus ensuring that water percolation occurs through soil zones most advantageous to the plant.

A significant portion of the water routed through the rhizosphere originates as stemflow and throughfall centered on the trucks of trees. This canopy redistribution of rainfall into heterogeneous distribution of precipitation occurs for most species (Levia and Frost 2003), with the highest relative precipitation rates centered on the trunks of trees. The hydrological continuity between stemflow and root-derived preferential flowpaths belowground has been termed "double-funneling" (Johnson and Lehmann 2006). Stemflow has been found to contribute up to nearly 19% of groundwater recharge (Taniguchi et al. 1996), despite occurring on only a very small fraction of the total forest area. For example, Chang and Matzner (2000) found 13.5% of infiltration to occur over just 3% of the forest floor. Liang et al. (2009) explicitly accounted for double-funneling in a soil moisture model by representing stemflow as a separate soil water input from net precipitation, and were able to obtain much better model representation of soil moisture measurements as a result.

Double-funneling is also important toward understanding nutrient fluxes within the rhizosphere. For instance, De Schrijver et al. (2007) reviewed 20 studies that presented data for both (1) nitrogen deposition rates in throughfall plus stemflow, and (2) seepage rates of inorganic N (NO_3^- + NH_4^+), and found a strong linear relationship ($R_{\text{adj}}^2 = 0.632$, $P < 0.001$) irrespective of forest type (e.g., conifer vs. deciduous forests). While N seepage fluxes were higher under conifer forests, N deposition rates were also higher in throughfall plus stemflow for conifer stands (De Schrijver et al. 2007).

Another key ecohydrological process of the rhizosphere is HR of soil water by roots. During the daytime when leaf stomates are open to allow CO_2 to diffuse into the leaf for photosynthesis, the water potential gradient drives the transpiration stream of water from soil, through the root network, plant stems and leaves and into the atmosphere, which is at a much more negative pressure relative to that of the soil. However, when stomates are closed (e.g., at night or in response to excessive transpirational demands), soil moisture can move through roots from zones of less negative soil water potential (e.g., moister regions of soil) to layers that have more negative soil water potential (e.g., drier regions of soil).

This mechanism, referred to as HR, has been documented for numerous species in ecosystems as diverse as coniferous forests of the Pacific Northwest of North America (Warren et al. 2005), deciduous forests in the Amazon (Oliveira et al. 2005), as well as for trees in arid environments (Hultine et al. 2003). While sometimes referred to as "hydraulic lift," HR results from redistribution of water from wetter to drier areas, and so can transfer water upward or downward relative to the soil surface in response to soil water potential gradients (Baker et al. 2008).

In order for HR to take place, the individual plant must have a dimorphic root distribution consisting of both shallow lateral roots and deeper tap roots (Jackson et al. 2000). For the Amazon forest, HR has been estimated to increase dry-season transpiration by 40% (Lee et al. 2005).

It remains difficult to upscale water redistribution in the rhizosphere to the whole plant level (Darrah et al. 2006). Although the rhizosphere is clearly one of the most complex ecosystems on the planet (Jones and Hinsinger 2008), part of the difficulty in scaling may be due to mycorrhizal associations, which have been found to be involved in the transfer of water and nutrients from mature trees to seedlings (Warren et al. 2008).

Through ecohydrological processes such as double-funneling and HR, the rhizosphere sees water fluxes of a greater magnitude than the bulk soil, and experiences changes in soil water potentials that are much more dynamic than in bulk soil. These processes and other create conditions by which rhizosphere cycling of carbon and nutrients is more pronounced than in bulk soil. The enhanced production of CO_2 within the rhizosphere is one biogeochemical manifestation of the difference between the rhizosphere and bulk soil.

24.3 CO_2 Dynamics in the Rhizosphere

Production of CO_2 within soils occurs predominantly within the rhizosphere, and is controlled in large part by soil moisture dynamics. With this in mind, we present a discussion of the role of the rhizosphere in the global carbon cycle, and on ecohydrological feedbacks on the biogeochemical cycling of carbon within the rhizosphere.

The belowground contribution toward terrestrial carbon fluxes to the atmosphere (e.g., soil CO_2 efflux or soil respiration) is a principle component of the global carbon budget, and is one of the most challenging carbon cycle components to study in detail (Chapin and Ruess 2001). It is also heavily influenced by rhizosphere processes. Hanson et al. (2000) reviewed published studies of the efflux of CO_2 from soil, including 48 field-based studies of forested ecosystems. For the field-based forest studies, the "root" contribution toward total soil respiration was found to represent approximately 50% on average of the total soil respiration in forest ecosystems, and ranges up to 80% of total soil respiration, despite the minor fraction of total soil represented by the rhizosphere. Many of these studies considered autotrophic and heterotrophic respiration within the rhizosphere as an aggregated "rhizosphere respiration" term (Hanson et al. 2000).

The distinction between autotrophic respiration (e.g., respiration by roots and mycorrhizae) and heterotrophic respiration (e.g., microbial respiration) within the rhizosphere is both nontrivial and methodologically challenging from carbon-cycling and ecohydrological perspectives. Autotrophic respiration directly involves the water film at the root interface, and as a product of autotrophic respiration, CO_2 enters the soil in a dissolved form. Heterotrophic respiration under aerobic conditions

also produces CO_2 that is primarily in the dissolved form, as soil bacteria and other microbes live principally within soil water (Hinsinger et al. 2009). Here, we should note that dissolved CO_2 is composed of both "free" CO_2 (e.g., gaseous molecules of CO_2 within a water matrix) and the hydrated form of CO_2 as H_2CO_3 (carbonic acid). At equilibrium conditions, carbonic acid is only a very minor component of dissolved CO_2, as the ratio of free CO_2 to H_2CO_3 is 650 at 25°C (Butler 1982).

Once introduced into the soil environment, rhizosphere-derived dissolved CO_2 is subject to transport with mobile water (including being drawn into plants via root water uptake, Jassal et al. 2004), participation in weathering reactions as carbonic acid, or equilibration with CO_2 concentrations in soil gas. The general assumption that gaseous and liquid phases of CO_2 are in equilibrium concentrations within the soil environment overlooks two key processes: (1) differences in rates of diffusion between liquid and gaseous forms of CO_2, and (2) temperature dependencies on equilibrium conditions between liquid and gaseous forms of CO_2. Diffusion of CO_2 in the aqueous phase is 10,000 times slower than in the gaseous phase. At equilibrium, the partial pressure of CO_2 dissolved in water (e.g., $pCO_2(aq)$) by definition will be equal to the partial pressure of CO_2 in the soil atmosphere. However, the $pCO_2(aq)$ level depends upon Henry's Law, which includes a temperature-dependent component. If $pCO_2(aq)$ remains constant as temperature rises, the result is lower molar concentrations of dissolved CO_2 and higher molar concentrations of gaseous CO_2. Since it is the molecules of dissolved CO_2 that are involved in generating soil acidity and chemical weathering as carbonic acid, this distinction can be significant, particularly in near surface layers where the root length density (km roots m^{-3} soil) is highest, soil microbial populations are highest (Richter and Markewitz 1995), and soil moisture and temperature are most dynamic.

Once produced in the rhizosphere, the CO_2 can be converted to bicarbonate depending on the pH status of the soil environment. In the case that the pH conditions of the soil favors CO_2 in deprotonated forms as bicarbonate (HCO_3^-) or carbonate (CO_3^{2-}), the biogenic (bi)carbonate ions can be involved in other plant–soil reactions or transported by percolating water within the soil. Much of the HCO_3^- transported by rivers originates in the rhizosphere, and represents a "hidden" respiration product that is "masquerading" as the bicarbonate ion (Cole et al. 2007).

Soil moisture dynamics are strongly related to both CO_2 production within soils and the direction of its subsequent transport, making soil CO_2 a key ecohydrological parameter (cf. Johnson et al. 2007). In general, CO_2 production within the rhizosphere increases with soil moisture until conditions become limiting to further production, either due to substrate exhaustion or due to oxygen depletion. Gaseous transport of CO_2 to the soil surface (e.g., soil CO_2 efflux or soil respiration), however, remains inversely related to soil moisture contents across the full range of soil moisture conditions. This is because increasing water content greatly reduces soil diffusivity by reducing the interconnection of air-filled pores, effectively increasing the distance over which CO_2 must travel to reach the soil surface. This is because travel across water-filled pore spaces (or even water films between

air-filled pores) involves gaseous CO_2 entering into and out of solution where the diffusion rate is four orders of magnitude lower than in air-filled pore spaces.

On the one hand, lateral transport of dissolved CO_2 within the vadose zone and eventually to groundwater and streams (Fiedler et al. 2006; Johnson et al. 2008), on the other hand, is enhanced by increasing soil moisture contents. Johnson et al. (2008) compared the lateral transport of dissolved CO_2 to streams with estimates of soil CO_2 efflux, finding that CO_2 drainage was about 50% of the magnitude of soil CO_2 efflux, suggesting that plot-based studies focusing on soil respiration that only consider soil CO_2 efflux systematically underestimate total CO_2 production.

Looking beyond CO_2 to other trace gases in the rhizosphere, it should be noted that heterotrophic respiration by methanogenic microbes, which results in methane (CH_4) as a respiration product, can occur in soil in both water-filled pore space that have become anoxic, as well as in oxygen-depleted air-filed pore spaces. Decreases of pO_2 in the rhizosphere accompany increases in pCO_2, but are sparsely documented in the literature (Hinsinger et al. 2006). Low levels of soil pO_2 result in conditions favorable to methanogenesis (production of CH_4). Given that soils contribute 60% of global CH_4 sources (Conrad and Smith 1995), these dynamics are in need of further study.

24.4 Process-Based Examples of Ecohydrology, Biogeochemistry, and the Rhizosphere

24.4.1 Aboveground and Soil Surface Processes that Influence the Rhizosphere

There are a number of mechanisms by which aboveground and surface mechanisms exhibit functional control over processes within the rhizosphere. Perhaps, foremost among these is the spatial redistribution of incident precipitation into throughfall and stemflow. This redistribution results in a heterogeneous distribution of rainfall with highest relative precipitation rates centered on the trunks of trees for most species (Levia and Frost 2003). Snowfall is also redistributed by forest canopies, with snowmelt-derived stemflow providing a significant water flux centered on the rhizosphere (Levia and Underwood 2004). Further discussion on throughfall and stemflow processes are found in a companion chapter of this volume (Levia et al. 2011, Chap. 21).

A relatively understudied mechanism that influences the fluxes of water and nutrients that enter the rhizosphere is soil water repellency (e.g., soil hydrophobicity). Although there has been a large increase in the number of studies of soil water repellency in recent years (Doerr et al. 2007), few have explicitly considered the spatial coordination of surficial water repellency and belowground wetting patterns. Soil water repellency is known to be spatially heterogeneous and ephemeral. Soil hydrophobicity is most strongly exhibited when soils are dry, and decays slowly

with the progression of the rainy season (Doerr et al. 2000; Wessolek et al. 2008). Repellency at the soil surface influences subsequent routing of soil water through the rhizosphere, which has an added impact on the distribution of nutrients within the soil, particularly since wetting events following dry periods are characterized by the mobilization of high concentrations of solutes that build up on soil and litter layers during dry periods in a process known as the "Birch effect" (Jarvis et al. 2007). Here, we present an example of soil water repellency occurring during the dry season in the Amazon forest that demonstrates the role of surficial processes controlling water fluxes within the rhizosphere.

A water repellent layer at the soil surface soil of an undisturbed primary forest in the seasonal southern Amazon was identified in a study that initially assumed soil water repellency would be negligible in the tropical forest environment (Johnson et al. 2005). Nevertheless, soil at the forest floor was found to exhibit extreme hydrophobicity during the dry season (Johnson et al. 2005). In further study, a manipulative experiment was conducted to evaluate the role of surface repellency on patterns of soil water distribution within the soil. In this experiment, soil on the control plot remained unaltered, while the treatment plot was rendered nonrepellent through application of a soil surfactant (Aquagro-L, Aquatrols Inc., Paulsboro, NJ, USA).

Ammonium carbonate was dissolved in water and applied as a tracer to both the surfactant-treated soil and the hydrophobic control soil for 30 min at a rainfall rate of 50 mm h^{-1} using a mini-rainfall simulator (Ogden et al. 1997). This application rate simulated precipitation events typical of the study area. One hour following tracer application, a trench was excavated centering on the location of simulated rainfall, and a pH indicator was sprayed onto the exposed soil surface within the trench to determine the tracer distribution within the soil profile (Wang et al. 2002).

The experiment demonstrated that the wetting front below the water repellent soil had reached twice the depth of the nonrepellent soil (Fig. 24.1). Further, the wetting front below the water repellent soil exhibited a high degree of preferential
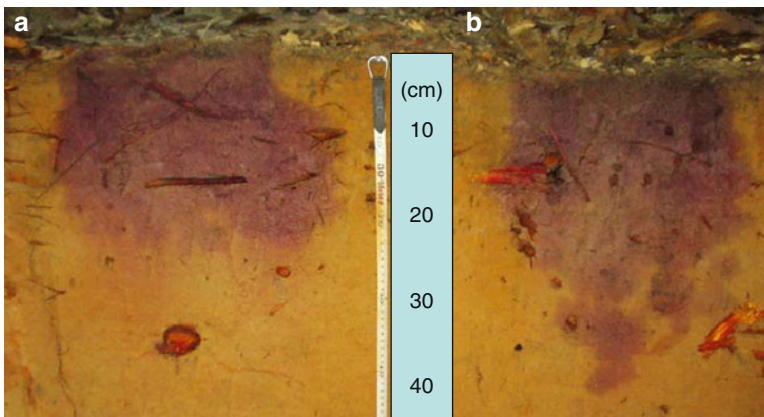
Fig. 24.1 Infiltration patterns for nonrepellent soil (**a**) and soil exhibiting surficial hydrophobicity (**b**)

flow, whereas the infiltration pattern under the nonrepellent soil appeared to be more readily drawn into the bulk soil matrix as evidenced by the pH indicator, which clearly demonstrated where the tracer traveled.

This example is illustrative of the importance of surficial processes on subsurface flow dynamics in the rhizosphere. Wessolek et al. (2008) also found soil water repellency to influence percolation patterns. Due to repellency, a smaller portion of the bulk soil was filled than would be expected in the absence of repellency, which decreased the water storage capacity. This decreased soil water storage capacity, in combination with repellency-induced preferential flow, resulted in a 20-fold increase in the soil water percolation rate (Wessolek et al. 2008). As the repellency was found within the soil profile, and not as a result of burning, it is likely the result of rhizodeposition of microbial and root exudates leading to water repellency of aggregate surfaces and macropore linings, which has been shown to reduce water exchange between macropores and bulk soil (Jarvis 2007).

24.4.2 Species Affects on Soil Moisture Dynamics in the Rhizosphere

Vegetation alters precipitation into spatially variable throughfall, which contributes to persistent patterns of soil moisture in the rhizosphere and bulk soil. Although highly variable in space, throughfall patterns show some stability in time as they are caused by relatively static spatial factors such as canopy density, agglomeration of trees, and species distribution (Jost et al. 2005; Keim et al. 2005). In terms of the rhizosphere, these throughfall patterns contribute toward spatial patterns in soil moisture within the rooting zone. Jost et al. (2005) studied spatial patterns of soil moisture dynamics for a mixed stand of Norway spruce (*Picea abies* (L.) Karst.) and European beech (*Fagus sylvatica* L.) in Kreisbach, Lower Austria, finding that both soil water recharge patterns (Fig. 24.2) and soil water discharge patterns (not shown) closely match patterns of tree species distribution.

These spatial patterns are clearly important considerations for biogeochemical and ecohydrologic processes in the rhizosphere. However, due to the intensity of measurement requirements for adequate spatial representation, it remains an area that should receive additional attention in future research. Some advances have been made in model representation of soil moisture dynamics by explicitly considering spatial throughfall patterns. This approach has shown improved performance over lumped soil moisture representations, because the connectivity between wet patterns can be used to conceptualize lateral flow for moderate rainfall events and improve runoff predictions (Keim et al. 2008).

Antecedent soil moisture determines the capacity of an ecosystem to absorb water and thus to buffer runoff. Due to differences in rates of root water uptake and rooting depths and patterns in the rhizosphere, tree species can enhance or diminish the absorption capacity of a given soil. With a large number of spatially distributed time domain reflectometry (TDR) measurements, Schume et al. (2004) showed how
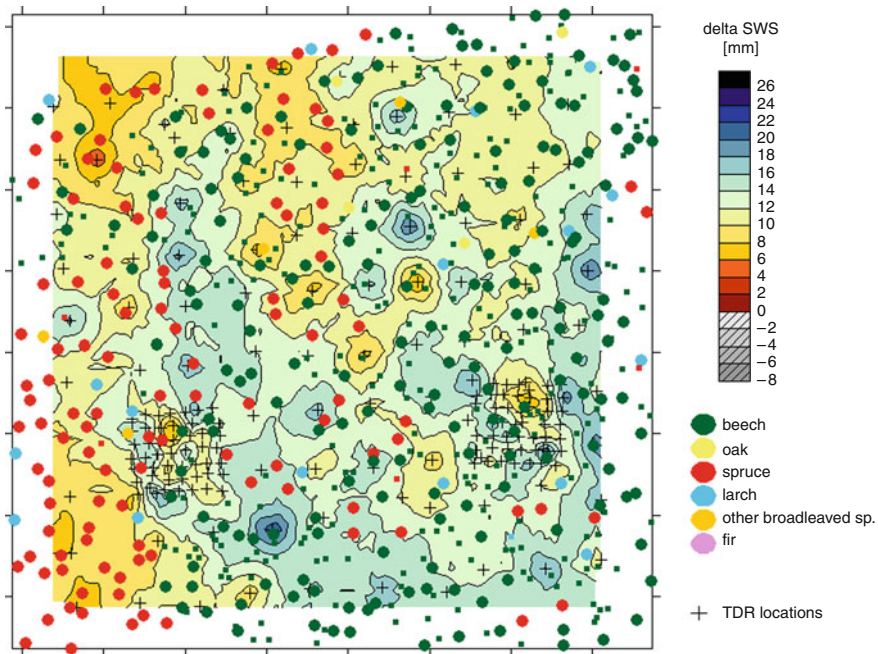
Fig. 24.2 Change in soil water storage (delta SWS) following a 31 mm rainfall in a mixed spruce-beech stand (from Schume et al. 2004)

tree species can alter stand scale hydrology through a combination of processes involving the rhizosphere. In a comparison between spruce and beech forests, the beech stands showed that higher stand precipitation (e.g., throughfall) was compensated by higher transpiration rates and faster soil water depletion in both topsoil and subsoil. As a result, there were higher seasonal fluctuations in soil water content under beech compared to spruce (Fig. 24.3). Throughout the growing season, the soil water content under spruce was generally dryer compared to beech. Tree species effects in the study proved to be nonadditive (a mixed spruce-beech stand behaves very much like a pure beech stand), which suggests that mixed species forests need to be investigated using research methodologies that address the role of individual tree species on the rhizosphere within mixed forest stands.

In this regard, for the same soil type, tree species with different rooting systems and different water consumption can lead to different soil moisture dynamics and lateral flow processes during rainfall and hence to different runoff responses. Soil moisture patterns and interflow were investigated at different soil depths in a Norway spruce (*P. abies* (L.) Karst) forest and in a European beech (*F. sylvatica* L.) forest during sprinkling experiments on two 6×10 m hillslopes with the same soil type (stagnic Cambisol). The deeper rooting system of beech directs more water toward deeper soil horizons, from where the water table rises into the top soil, while the topsoil remains substantially below saturation. Saturation excess overland flow is therefore highly unlikely under beech due to the structure of its rhizosphere.

a

b

c

d
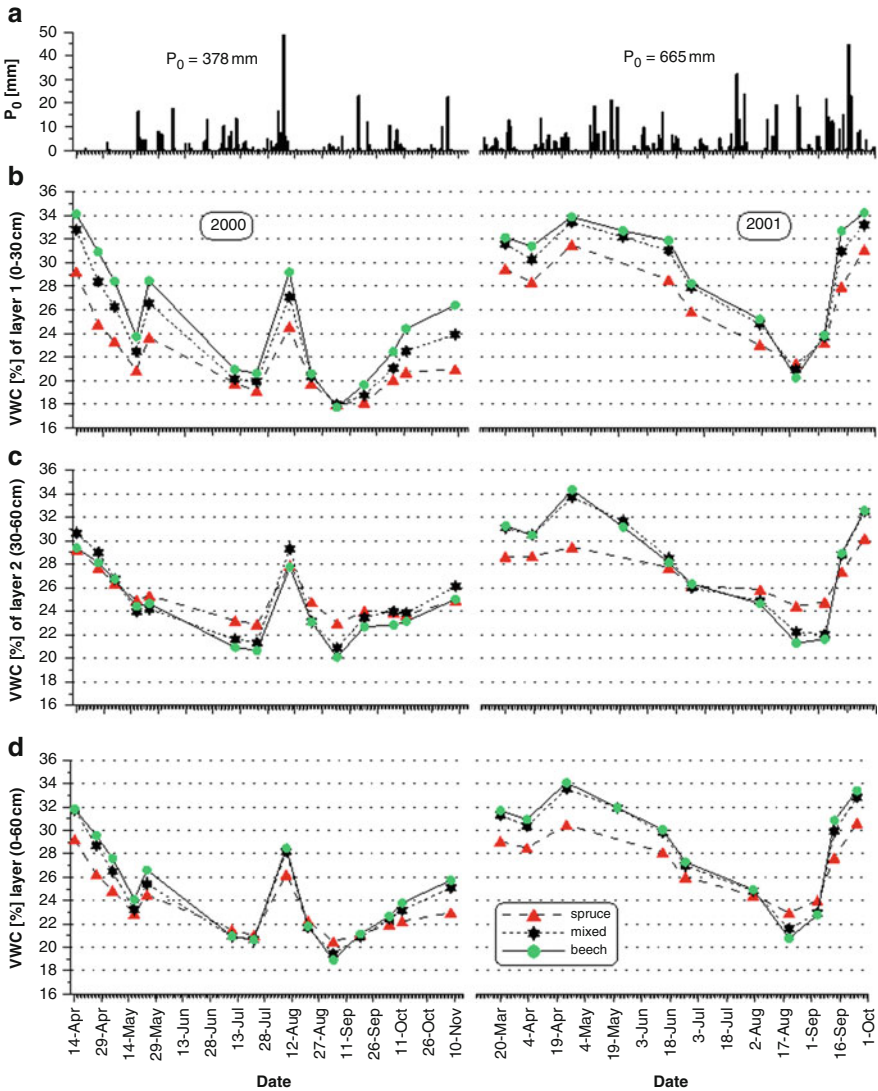
Fig. 24.3 Precipitation (**a**) and seasonal changes of soil water storage in topsoil (**b**), subsoil (**c**), and over soil profile (**d**) under a spruce, a beech, and a mixed spruce-beech stand (from Schume et al. 2004)

Under spruce, the soil water content in the subsoil shows only little changes over time and remains below saturation. However, a perched water table builds at the base of the maximum rooting depth causing near saturated conditions in the topsoil with a higher risk of saturation overland flow. Beech forests contain more macropores because of the more active soil fauna that they recruit (Scheu et al. 2003) and because of the deeper rooting system, which results in higher subsurface flow rates through the rhizosphere relative to surface runoff rates.
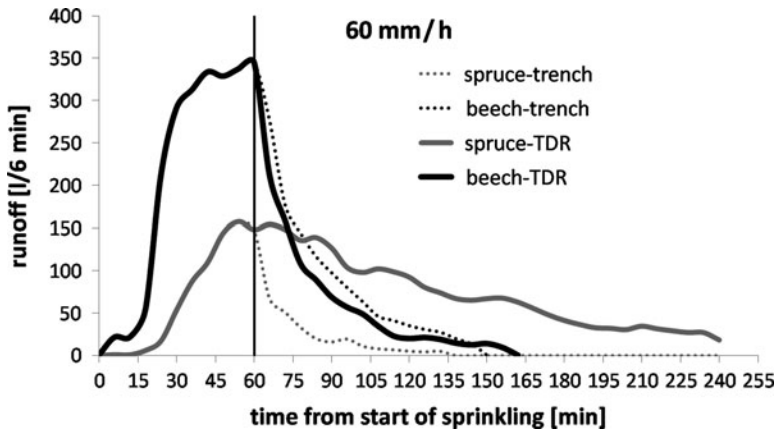
Fig. 24.4 Comparison of runoff responses of spruce and beech in a sprinkling experiment with measured runoff (spruce-trench, beech-trench) and runoff with recession approximated from mean (48 TDRs) decreases of soil water storage (spruce-TDR, beech-TDR) to correct for mass balance errors. The *vertical lines* denote the end of sprinkling (duration = 1 h). *TDR* time domain reflectometry

We see that tree species can lead to different runoff responses for the same soil type. Because of the higher subsurface flow rates, small to moderate rainfall events will cause faster fluxes of water through the rhizosphere and correspondingly higher runoff response in beech forests (Fig. 24.4). For high and extreme rainfall events, however, spruce forests will likely result in faster runoff responses compared to beech, because spruce is more prone to saturation excess overland flow.

24.5 Advancing Ecohydrology and Biogeochemistry in Study of the Rhizosphere

24.5.1 Future Research Directions

One of the key difficulties in advancing ecohydrology and biogeochemistry in study of the rhizosphere and isolating processes occurring within the rhizosphere from those of the bulk soil is the small spatial scale of the phenomena of interest. Thus, identifying effective methodologies for segregating rhizospheric from bulk soil processes is the most important area at present for better understanding ecohydrology and biogeochemistry of the rhizosphere. Field-based research involving tracer applications provides one way forward for distinguishing rhizospheric processes. The advent of increasingly smaller instruments is facilitating advances for in situ measurements of the soil environment, including miniaturized infiltrometers for the determination of rhizosphere hydraulic properties (Hallett et al. 2003).

Micro-tensiometry and miniaturized TDR sensors have also been developed that are appropriate for measurements of moisture conditions at scales relevant for study of the rhizosphere (0.1–10 mm) (Neumann et al. 2009). These will aid in distinguishing the soil water-release characteristics (e.g., soil water characteristic curves or soil moisture retention curves) for rhizosphere vs. bulk soil, which has been demonstrated for agricultural crops (Gregory 2006; Hinsinger et al. 2009) but is not yet well studied in forest soils.

The use of genetically engineered "microbiosensors" has already been applied to the study of the rhizosphere. For example, engineered strains of *Escherichia coli* bacteria have been developed that vary in expression of a green fluorescent protein (GFP) in response to variations in total water potential (Herron et al. 2010). The response of these "microbiosensors" in the form of fluorescence was consistent with rhizosphere theory, with lower water potentials developing away from plant roots in response to transpiration water demand and root water uptake, demonstrating soil water potential gradients at the millimeter scale under laboratory conditions (Herron et al. 2010).

Approaching the study of water in the rhizosphere from a macro-level is also needed. Advances in the use of industrial (rather than medical) computed tomography (CT) scanners are providing both high-resolution and time-series data on soil microstructures, although to date this is only possible on soil columns extracted from the field (Luo et al. 2008). A range of tracer application and other techniques have also proven useful for elucidating preferential flow processes within soil, and were reviewed by Allaire et al. (2009). Many of these techniques can be adapted to focus on rhizosphere vs. bulk soil processes, since rooting networks provide one of the principle conveyances for vertical as well as lateral preferential flow (Weiler and McDonnell 2007).

Modeling approaches that explicitly consider rhizosphere processes in relation to those of the bulk soil represent another research pathway for understanding the rhizospheric components of ecohydrological and biogeochemical processes, particularly when developed and applied in an iterative manner with field-based observations. For example, empirical study has shown rhizosphere soil to be drier than bulk soil at the same matric potential (Whalley et al. 2005). Characterizing these differences within a model structure that extends the mobile-immobile water concept with explicit treatment of mobile and immobile water within both the rhizosphere and bulk soil could be one way forward.

Recent isotopic studies have emphasized that current mobile-immobile conceptualizations are unlikely to capture seasonal variability in bulk soil vs. rhizosphere regimes in soil water recharge and plant transpiration source water dynamics (Renée Brooks et al. 2010). Modelers have had some success incorporating HR into land-surface models used to represent biophysical processes in climate models, but are continuing to work to resolve potential issues of equifinality when HR and other changes are simultaneously incorporated into models (Baker et al. 2008). Future conceptual frameworks and model structures will need to take rhizosphere complexity into account and explicitly address ecohydrological feedbacks between rhizosphere processes and the bulk soil (cf. Domec et al. 2004).

24.5.2   *Global Change and the Rhizosphere*

Empirical CO_2 enrichment studies have identified potential changes in rhizosphere biogeochemistry, including increases in root exudation under high CO_2 treatments (Phillips et al. 2009) and enhanced root respiration relative to root biomass (Cheng 1999). Effects of elevated CO_2 on ecohydrology are perhaps more significant, as the water fluxes through the rhizosphere may significantly increase as a result of reduced plant transpiration due to CO_2-induced stomatal closure (Gedney et al. 2006). While the magnitude of this mechanism for explaining observed changes in global river discharge relative to other drivers is still the subject of debate in the literature (Piao et al. 2007; Gerten et al. 2008), the impacts on the rhizosphere of a CO_2-derived increase in the water flux are essentially unstudied. Further, as the species compositions of entire forested ecosystems appear to be undergoing change due to differential species and genera-level responses to increased atmospheric CO_2 (Laurance et al. 2004), the importance of processes such as rhizosphere respiration, HR, and double-funneling in the tree-rhizosphere continuum is also likely to change. Given the plasticity of responses in rooting patterns due to changes in climate, where an increasingly wet state for a previously dry climate results in deeper roots, and an increasingly wet state for a previously wet climate results in shallower rooting depths (Guswa 2008), there is certain to be another century of study on the rhizosphere.

References

Allaire SE, Roulier S, Cessna AJ (2009) Quantifying preferential flow in soils: a review of different techniques. J Hydrol 378:179–204

Baker IT, Prihodko L, Denning AS et al (2008) Seasonal drought stress in the Amazon: reconciling models and observations. J Geophys Res Biogeosci 113:1. doi:10.1029/2007JG000644

Butler J (1982) Carbon dioxide equilibria and their applications. Addison-Wesley, Reading

Cardon ZG, Gage DJ (2006) Resource exchange in the rhizosphere: molecular tools and the microbial perspective. Ann Rev Ecol Evol Syst 37:459–488

Chang SC, Matzner E (2000) The effect of beech stemflow on spatial patterns of soil solution chemistry and seepage fluxes in a mixed beech/oak stand. Hydrol Process 14:135–144

Chapin FS, Ruess RW (2001) Carbon cycle: the roots of the matter. Nature 411:749–752

Cheng W (1999) Rhizosphere feedbacks in elevated CO_2. Tree Physiol 19:313–320

Cheng W, Gershenson A (2007) Carbon fluxes in the rhizosphere. In: Cardon ZG, Whitbeck JL (eds) The rhizosphere: an ecological perspective. Academic Press, New York, pp 31–56

Cole JJ, Prairie YT, Caraco NF et al (2007) Plumbing the global carbon cycle: integrating inland waters into the terrestrial carbon budget. Ecosystems 10:172–185

Conrad R, Smith KA (1995) Soil microbial processes and the cycling of atmospheric trace gases [and discussion]. Philos Trans Phys Sci Eng 351:219–230

Darrah PR, Jones DL, Kirk GJD, Roose T (2006) Modelling the rhizosphere: a review of methods for 'upscaling' to the whole-plant scale. Euro J Soil Sci 57(1):13–25

De Schrijver A, Geudens G, Augusto L et al (2007) The effect of forest type on throughfall deposition and seepage flux: a review. Oecologia 153:663–674

Doerr SH, Shakesby RA, Walsh RPD (2000) Soil water repellency: its causes, characteristics and hydro-geomorphological significance. Earth Sci Rev 51:33–65

Doerr SH, Ritsema CJ, Dekker LW et al (2007) Water repellence of soils: new insights and emerging research needs. Hydrol Process 21:2223–2228

Domec JC, Warren JM, Meinzer FC et al (2004) Native root xylem embolism and stomatal closure in stands of Douglas-fir and ponderosa pine: mitigation by hydraulic redistribution. Oecologia 141:7–16

Fiedler S, Höll BS, Jungkunst HF (2006) Discovering the importance of the lateral CO_2 transport from a temperate spruce forest. Sci Total Environ 368:909–915

Gedney N, Cox PM, Betts RA et al (2006) Detection of a direct carbon dioxide effect in continental river runoff records. Nature 439:835–838

Gerten D, Rost S, von Bloh W et al (2008) Causes of change in 20th century global river discharge. Geophys Res Lett 35:L20405. doi:10.1029/2008GL035258

Gregory PJ (2006) Roots, rhizosphere and soil: the route to a better understanding of soil science? Euro J Soil Sci 57:2–12

Guswa AJ (2008) The influence of climate on root depth: a carbon cost-benefit analysis. Water Resour Res 44:W02427

Hallett PD, Gordon DC, Bengough AG (2003) Plant influence on rhizosphere hydraulic properties: direct measurements using a miniaturized infiltrometer. New Phytol 157:597–603

Hanson P, Edwards N, Garten CJ et al (2000) Separating root and soil microbial contributions to soil respiration: a review of methods and observations. Biogeochemistry 48:115–146

Herron PM, Gage DJ, Cardon ZG (2010) Micro-scale water potential gradients visualized in soil around plant root tips using microbiosensors. Plant Cell Environ 33:199–210

Hiltner L (1904) Über neuere Erfahrungen und probleme auf dem gebiete der Bodenbakteriologie unter besonderer Berücksichtigung der gründüngung und Brache. Arb Deitsch Landwirtsch Ges 98:59–78

Hinsinger P, Marschner P (2006) Rhizosphere – perspectives and challenges – a tribute to Lorenz Hiltner 12–17 September 2004 – Munich, Germany. Plant Soil 283:vii–viii

Hinsinger P, Plassard C, Jaillard B (2006) Rhizosphere: a new frontier for soil biogeochemistry. J Geochem Explor 88:210–213

Hinsinger P, Bengough AG, Vetterlein D et al (2009) Rhizosphere: biophysics, biogeochemistry and ecological relevance. Plant Soil 321:117–152

Hughes JK, Hodge A, Fitter AH et al (2008) Mycorrhizal respiration: implications for global scaling relationships. Trends Plant Sci 13:583–588

Hultine KR, Williams DG, Burgess SSO et al (2003) Contrasting patterns of hydraulic redistribution in three desert phreatophytes. Oecologia 135:167–175

Jackson RB, Sperry JS, Dawson TE (2000) Root water uptake and transport: using physiological processes in global predictions. Trends Plant Sci 5:482–488

Jarvis NJ (2007) A review of non-equilibrium water flow and solute transport in soil macropores: principles, controlling factors and consequences for water quality. Euro J Soil Sci 58:523–546

Jarvis P, Rey A, Petsikos C et al (2007) Drying and wetting of Mediterranean soils stimulates decomposition and carbon dioxide emission: the "Birch effect". Tree Physiol 27:929–940

Jassal RS, Black TA, Drewitt GB et al (2004) A model of the production and transport of CO_2 in soil: predicting soil CO_2 concentrations and CO_2 efflux from a forest floor. Ag For Meteorol 124:219–236

Johnson MS, Lehmann J (2006) Double-funneling of trees: stemflow and root-induced preferential flow. EcoScience 13:324–333

Johnson MS, Lehmann J, Steenhuis TS et al (2005) Spatial and temporal variability of soil water repellency of Amazonian pastures. Aust J Soil Res 43:319–326

Johnson MS, Weiler M, Couto EG et al (2007) Storm pulses of dissolved CO_2 in a forested headwater Amazonian stream explored using hydrograph separation. Water Resour Res 43:W11201

Johnson MS, Lehmann J, Riha SJ et al (2008) CO_2 efflux from Amazonian headwater streams represents a significant fate for deep soil respiration. Geophys Res Lett 35:L17401

Jones DL, Hinsinger P (2008) The rhizosphere: complex by design. Plant Soil 312:1–6

Jost G, Heuvelink GBM, Papritz A (2005) Analysing the space-time distribution of soil water storage of a forest ecosystem using spatio-temporal kriging. Geoderma 128:258–273

Keim RF, Skaugset AE, Weiler M (2005) Temporal persistence of spatial patterns in throughfall. J Hydrol 314:263–274

Keim RF, Weiler M, Jost G et al (2008) Consequences of spatiotemporal redistribution of precipitation by vegetation for hillslope and runoff processes. Eos transactions AGU 89: Fall meeting supplement, Abstract H14A-03

Laurance W, Oliveira A, Laurance S et al (2004) Pervasive alteration of tree communities in undisturbed Amazonian forests. Nature 428:171–174

Lee JE, Oliveira RS, Dawson TE et al (2005) Root functioning modifies seasonal climate. Proc Natl Acad Sci U S A 102:17576–17581

Levia DF, Frost EE (2003) A review and evaluation of stemflow literature in the hydrologic and biogeochemical cycles of forested and agricultural ecosystems. J Hydrol 274:1–29

Levia DF, Underwood SJ (2004) Snowmelt induced stemflow in northern hardwood forests: a theoretical explanation on the causation of a neglected hydrological process. Adv Water Res 27:121–128

Levia D, Keim RF, Carlyle-Moses DE (2011) Throughfall and stemflow in wooded ecosystems. In: Levia D, Carlyle-Moses D, Tanaka T (eds) Forest hydrology and biogeochemistry: synthesis of research and future directions. Springer, New York

Liang W-L, Ki K, Mizuyama T (2009) A three-dimensional model of the effect of stemflow on soil water dynamics around a tree on a hillslope. J Hydrol 366:62–75

Linderman RG (1988) Mycorrhizal interactions with the rhizosphere microflora – the mycorrhizosphere effect. Phytopathology 78:366–371

Luo LF, Lin H, Halleck P (2008) Quantifying soil structure and preferential flow in intact soil using x-ray computed tomography. Soil Sci Soc Am J 72:1058–1069

McClain ME, Boyer EW, Dent CL et al (2003) Biogeochemical hot spots and hot moments at the interface of terrestrial and aquatic ecosystems. Ecosystems 6:301–312

Neumann G, George T, Plassard C (2009) Strategies and methods for studying the rhizosphere – the plant science toolbox. Plant Soil 321:431–456

Ogden CB, vanEs HM, Schindelbeck RR (1997) Miniature rain simulator for field measurement of soil infiltration. Soil Sci Soc Am J 61:1041–1043

Oliveira RS, Dawson TE, Burgess SSO et al (2005) Hydraulic redistribution in three Amazonian trees. Oecologia 145:354–363

Phillips RP, Bernhardt ES, Schlesinger WH (2009) Elevated CO_2 increases root exudation from loblolly pine (Pinus taeda) seedlings as an N-mediated response. Tree Physiol 29:1513–1523

Piao S, Friedlingstein P, Ciais P et al (2007) Changes in climate and land use have a larger direct impact than rising CO_2 on global river runoff trends. Proc Natl Acad Sci U S A 104:15242–15247

Renée Brooks J, Barnard HR, Coulombe R et al (2010) Ecohydrologic separation of water between trees and streams in a Mediterranean climate. Nat Geosci 3:100–104

Richter DD, Markewitz D (1995) How deep is soil? BioScience 45:600–609

Richter DD, Oh N-H, Fimmen R et al (2007) The rhizosphere and soil formation. In: Cardon ZG, Whitbeck JL (eds) The rhizosphere: an ecological perspective. Academic Press, New York, pp 179–200

Scheu S, Albers D, Alphei J et al (2003) The soil fauna community in pure and mixed stands of beech and spruce of different age: trophic structure and structuring forces. Oikos 101:225–238

Schume H, Jost G, Hager H (2004) Soil water depletion and recharge patterns in mixed and pure forest stands of European beech and Norway spruce. J Hydrol 289:258–274

Taniguchi M, Tsujimura M, Tanaka T (1996) Significance of stemflow in groundwater recharge.1. Evaluation of the stemflow contribution to recharge using a mass balance approach. Hydrol Process 10:71–80

Wang Z, Lu J, Wu L et al (2002) Visualizing preferential flow paths using ammonium carbonate and a pH indicator. Soil Sci Soc Am J 66:347–351

Warren JM, Meinzer FC, Brooks JR et al (2005) Vertical stratification of soil water storage and release dynamics in Pacific Northwest coniferous forests. Ag For Meteorol 130:39–58

Warren JM, Brooks JR, Meinzer FC et al (2008) Hydraulic redistribution of water from Pinus ponderosa trees to seedlings: evidence for an ectomycorrhizal pathway. New Phytol 178:382–394

Weiler M, McDonnell JJ (2007) Conceptualizing lateral preferential flow and flow networks and simulating the effects on gauged and ungauged hillslopes. Water Resour Res 43:W03403. doi:10.1029/2006WR004867

Wessolek G, Schwarzel K, Greiffenhagen A et al (2008) Percolation characteristics of a water-repellent sandy forest soil. Euro J Soil Sci 59:14–23

Whalley WR, Riseley B, Leeds-Harrison PB et al (2005) Structural differences between bulk and rhizosphere soil. Euro J Soil Sci 56:353–360

Chapter 25
Effects of the Canopy Hydrologic Flux on Groundwater

Tadashi Tanaka

25.1 Introduction

At the present, groundwater interactions with forest hydrology fluxes are poorly understood from both physical and biogeochemical perspectives. Our poor understanding of the interactions between canopy and surface fluxes with groundwater from physical and biogeochemical perspectives may be due, in part, to the fact that forest hydrology and groundwater hydrology have developed separately and that relatively little attention has been directed toward the interactions between groundwater and forest hydrology fluxes. Groundwater, however, constitutes a very important component in the hydrological cycle at the watershed scale, connecting precipitation (an input) with surface waters (an output). Hence, further integrated investigations of these groundwater–surface water systems and their interactions are needed to advance our understanding of the connections between surface and groundwater in forested ecosystems. The increasing focus on ecosystems and climate change on hydrological cycles necessitates a much better understanding on the connections and interactions between canopy fluxes and groundwater in forests.

Because the interactions between groundwater and forest hydrology fluxes are broad and complex, operating at multiple temporal and spatial scales, this chapter focuses on the groundwater interactions with selected forest hydrology fluxes, such as stemflow, as one of inputs into forest soils, and evapotranspiration, as one of outputs from the forests or riparian zones. Ordinarily, an investigation of surface and groundwater interactions would include both the physical and chemical aspects; however, this chapter strictly focuses on the hydrological interactions between canopy and groundwater interactions due to the complexity and intricacies of these interactions.

25.2 Groundwater Interaction with Stemflow

25.2.1 Spatial Nature of Stemflow Inputs into Forest Soils

When considering groundwater interactions with forest hydrology fluxes, it is important to evaluate the spatial variability of water inputs into the forest soils.

In a forest, net precipitation is partitioned into throughfall and stemflow before reaching a forest floor. This partitioning means that water reaches the forest floor in two different ways. One is a diffuse input as throughfall and the other is a point source input as stemflow. These two different pathways of water input to the forest floor can lead to spatial variability in physical properties (e.g., Gersper and Holowaychuck 1970a; Ford and Deans 1978; Herwitz 1988; Durocher 1990; Chang and Matzner 2000; Neave and Abrahams 2002; Tanaka et al. 2004, 2008) and chemical properties (e.g., Gersper and Holowaychuck 1970b, 1971; Crabtree and Trudgill 1985; Stevens et al. 1989; Neal et al. 1992; Chang and Matzner 2000; Kakubari 2007; Miyazawa 2009) of the forest soils.

Levia and Frost (2003) conducted a comprehensive review and evaluation on stemflow literature in the hydrological and biogeochemical cycles of forested and agricultural ecosystems. They summarized the selected studies on stemflow quantities expressed as a percentage of the incident gross precipitation. Table 25.1, after Levia and Frost (2003), shows stemflow quantities reported by a number of studies. Although stemflow quantities input into forest and agricultural soils are highly variable between and within types of vegetation cover characteristics (Levia and Frost 2003), in temperate forest watersheds, the ratio of stemflow to net precipitation is very small, usually less than 10% of the net precipitation when the stemflow is evaluated from the collected volume of stemflow water divided by the canopy-projected area, in terms of the total water balance in forested watersheds (e.g., Majima and Tase 1982; Neal et al. 1993; Durocher 1990; Taniguch et al. 1996; Carlyle-Moses and Price 2006). This low value is one of the reasons why little attention has been paid to the effect of stemflow on the groundwater recharge.

During rainfall events, relatively large amounts of intercepted rainfall are funneled down along the stem of canopy trees to produce highly localized input of water at the ground surface (e.g., Voigt 1960; Eschner 1967; Gersper and Holowaychuck 1971; Herwitz 1986a; Tanaka et al. 1991; Chang and Matzner 2000; Levia and Herwitz 2000; Iida et al. 2005a). Voigt (1960) observed that stemflow does not distribute over the entire canopy-projected area but is limited to a restricted area closely adjoining the stem of trees. He reported that the stemflow calculated on the basis of absorption area was larger by 7.4 times for beech, 12.0 times for red pine, and 15.9 times for hemlock than those calculated on the basis of the canopy-projected area. In the context of ecological importance of stemflow and soil moisture patterning, Pressland (1976) observed infiltration phenomena of stemflow during rainfall events of various sizes and intensities, and reported that all stemflow infiltrates into the soil within the area of 50 cm around large trees which circumferences larger than 40 cm and within the area of 30 cm around the smaller trees with circumferences less than 20 cm. He also reported that the stemflow calculated on the basis of infiltration area was 10.0–18.1 larger with mean of 12.7 for *Mulga* than those calculated on the basis of canopy-projected area. More recently, Liang et al. (2007) reported that for a heavy storm event on a steep forested hillslope, the cumulative stemflow per infiltration area along the downslope sides of a tree trunk was 18.9 times the cumulative open-area rainfall.

Table 25.1 Selected stemflow production in percent of incident precipitation

Vegetation type	Stemflow (% of incident precipitation)	References
Tropical montane rainforest	13.6	Herwitz (1986b)
Tropical rainforest	1.8	Lloyd and de Marques (1988)
Cacao plantation	1.99	Opakunle (1989)
Tropical dry forest	0.6–0.9	Kellman and Roulet (1990)
Tropical montane rainforest	<1.0	Veneklaas and Van (1990)
Amazonian lowland tropical forests (a banana-like herb)	24.0–31.0	Holscher et al. (1998)
Tropical rainforest	0.9–1.5	Marin et al. (2000)
Tropical rainforest	2.0–8.0	Dezzeo and Chacon (2006)
Pine-hemlock-beech plots	1.2–9.6	Voigt (1960)
Japanese red pine forest	0.5	Murai (1970)
Subalpine balsam fir forest	3.8–8.0	Olson et al. (1981)
Japanese red pine forest	2.2	Majima and Tase (1982)
Norway spruce	8.6–10.2	Wheater et al. (1987)
Dry sclerophyll forest	4.8	Crockford and Richardson (1990)
Northern red oak plantation	3.8	Durocher (1990)
Pinus radiata plantation	11.2	Crockford and Richardson (1990)
Evergreen-broad leaf forest	14.0–20.0	Masukata et al. (1990)
Beech forest	4.6	Neal et al. (1993)
Slash pine forest	0.94–10.4	Tang (1996)
Japanese red pine forest	0.7–1.7	Taniguch et al. (1996)
Pinus radiata plantation	3.1–3.9	Crockford and Khanna (1997)
Japanese red pine forest	1.2	Iida et al. (2005b)
Japanese red pine and evergreen-broad leaf forest	8.5	Iida et al. (2005b)
Deciduous forest	~2.0	Pryor and Barthelmie (2005)
Mature deciduous beech	8.0	Staelens et al. (2008)
Deciduous old-growth forest	2.0–6.0	Kramer and Holscher (2009)
Eucalypt forest	2.9	Dunin et al. (1988)
Chihuahuan desert shrubs	4.0–45.0	Mauchamp and Janeau (1993)
Semi-arid shrubs	0.76–5.14	Navar (1993)
Chihuahuan desert shrubs	2.0–27.0	Martinez-Meza and Whitford (1996)
Creosotebushes	5.9–26.9	Whitford et al. (1997)
Thornscrub community	3.0	Navar et al. (1999)
Laurel forest	1.2–13.6	Aboal et al. (1999)
Mediterranean holm oak forest	2.6–12.1	Bellot et al. (1999)
Semi-arid mattoral community	8.57 ± 1.9	Carlyle-Moses (2004)

Adapted from Levia and Frost (2003)

Those concentrated inputs of stemflow have been considered as an important source for groundwater recharge (e.g., Durocher 1990; Tanaka et al. 1991; Liang et al. 2007, 2009). As will be mentioned in the subsequent section, however, there are few studies clarifying the contribution of stemflow-induced water quantitatively on the groundwater recharge except for Tanaka et al. (1996) and Taniguch et al. (1996). The main reason is the difficulty to evaluate the infiltration area of stemflow-induced water (A_i), which needed to calculate the groundwater recharge amount as a unit of water column, R_s (i.e., R_s = amount of stemflow water/A_i). Tanaka et al. (1991) evaluated A_i based on the data of infiltration area marks which have the shape similar to a circle, whereas Iida et al. (2005a) evaluated it based on the data of litter marks. It seems that litter marks result from the movement of the litter due to higher intensity of stemflow than infiltration capacity of soil surface (i.e., infiltration excess overland flow). Assuming that the stemflow-induced water percolates in the vertical direction, the infiltration area of stemflow (A_i) can be estimated by the area of infiltration excess overland flow (A_o) (i.e., $A_i = A_o$). Herwitz (1986b) also evaluated A_i from the observed data of stemflow intensity and infiltration capacity of surface soil in a tropical rainforest ($A_i = A_o$ = intensity of stemflow/infiltration capacity). Iida et al. (2005a) reported the relationship between the diameter at the tree base (DTB) and the radius of the litter or infiltration area marks from the center of the stem as shown in Fig. 25.1. The relationship between the DTB and radius of litter or infiltration marks from the center of the stem showed a logarithmic curve as follows,

$$y = 23.36 \ln(x) - 31.53, \quad R^2 = 0.753, \tag{25.1}$$
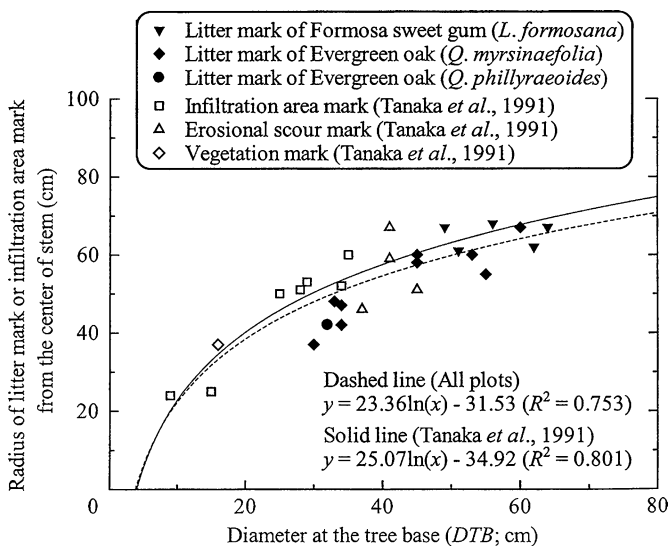
Fig. 25.1 Relationship between the diameter at the tree base and the radius of litter mark or infiltration area mark from the center of the stem (from Iida et al. 2005a, reproduced with permission)

where x is the DTB and y the radius of infiltration area of stemflow inputs and litter marks from the center of the stem (cm). Although the rainfall amount and the intensity are different between Tanaka et al. (1991) and Iida et al. (2005a), the relationship between the DTB and the radius of infiltration area of stemflow-induced water corresponds well between them.

Equation (25.1) indicates that no appreciable stemflow inputs occur close to the base of small diameter trees of approximately 4 cm and that the infiltration area of stemflow inputs does not expand linearly with increasing the diameter of the tree base. The latter fact seems to suggest that there may be a critical range for canopy extent areas, which intercept rainfall, with increasing the diameter of the tree base. Tanaka et al. (1991) reported that the actual infiltrated water of stemflow might reach 10–20% of gross rainfall in a Japanese red pine forest based on the results of applying (25.1) to data obtained during a 1-year period.

Stemflow has a unique form of water input to forest soils and cannot be evaluated by only the water balance consideration of the forest environment. As mentioned by Durocher (1990), Levia and Frost (2003), and Liang et al. (2007, 2009), the modification of water input by stemflow can lead to spatial variability in the physical and chemical properties of forest soils. The effects of stemflow on biogeochemical cycling of nutrients within and through forests and soil solution chemistry have been documented comprehensively by Levia and Frost (2003).

25.2.2   Stemflow Contribution to Groundwater Recharge

Durocher (1990) demonstrated the response of soil water dynamics underneath two large sweet chestnuts during the 7 mm storm event with an array of tensiometer nests. During the event, two trees generated total stemflow of 216.3 and 94.8 mm of water per unit trunk projected area which corresponded 15–30 times the mean throughfall input, respectively. Whilst water potentials between trees have only changed slightly, sharp changes were observed underneath trees and the stemflow caused very rapid water movement generating saturated zones toward the base of the soil profile at nearly 1 m depth. This means that a very small amount of rainfall produces water flow from stemflow inputs down to the bedrock. Similar phenomena recently were observed by Liang et al. (2007) on a steep forested hillslope vegetated by tall stewartia. They reported that the soil water content increased rapidly and greatly in the region downslope of the tree stem due to the occurrence of stemflow-induced bypass flow on the downslope side of the tree trunk, resulting in the development of an asymmetric saturated zone around the tree. The effect of highly localized stemflow inputs on soil water movement and groundwater recharge process has also been reported by Gomez et al. (2002) and Tanaka et al. (2008).

As mentioned in the previous section, there are only few studies to evaluate quantitatively the stemflow contribution to groundwater recharge because it is difficult to collect the data of actual infiltration area of stemflow-induced water (A_i).

To evaluate the stemflow contribution for groundwater recharge quantitatively, Taniguch et al. (1996) applied a mass balance method of chloride within a Japanese red pine forest. Their technique is based on the mass balance of chloride in the forest because chloride transport in the soil is considered only to be influenced by the evapotranspiration rate (ET) which is controlled by the vegetation cover. Because the data requirements for the method are considerably less than those for energy budget methods, many other studies have estimated groundwater recharge rate in forest watersheds using a chloride mass balance method (Claassen et al. 1986; Taniguchi 1991; Thorburn et al. 1991).

Groundwater recharge rate by stemflow was calculated with assumptions that the chloride concentration of soil water at the groundwater level depth is formed from two sources. One is the matrix flow of which the origin is throughfall to give the concentration of soil water at i cm depth and the other is stemflow, the chloride concentration of which has not changed throughout the soil profile. The annual recharge rate by stemflow was calculated by the following equation,

$$R_s = R(C_i - C_g)/(C_i - C_s), \tag{25.2}$$

where R_s is the recharge rate by stemflow, R the total annual groundwater recharge rate, C_i the chloride concentration of soil water at i cm depth, C_g the chloride concentration of soil water at the groundwater level depth, and C_s the chloride concentration of stemflow. They obtained the results that the annual rates recharged by stemflow are calculated to be 62.0 mm at one site and 139.4 mm at the other site and the ratio of recharge rate by stemflow to the total recharge rate is 10.9–19.1%. In the water balance consideration of the experimental pine forest, the ratio of stemflow to bulk precipitation ranged from 0.5 to 1.2%; however, the ratio of the recharge rate by stemflow to the total ratio is relatively large. The results indicate that the effect of stemflow on the groundwater recharge is relatively important even though the ratio of stemflow in the water balance is small.

Considering the nature of stemflow inputs into forest soils, Tanaka et al. (1996) developed a primary model for evaluating the effect of stemflow on groundwater recharge. The model, a cylindrical infiltration model (CI model, Fig. 25.2), is based on the infiltration area of stemflow-induced water instead of canopy-projected area for determining the stemflow inputs to the soil surface. They applied this model to the same experimental Japanese red pine site as Taniguch et al. (1996) mentioned above and evaluated the recharge rate by stemflow to the total recharge rate at two sites. The results indicate that the ratio between rates is 9.1–22.9%. The results indicate that the estimated ratio of recharge rate by stemflow to the total recharge rate using the CI model agrees well with the value obtained from the mass balance method of environmental chloride in subsurface waters. The concept of CI model is based on the evaluation of stemflow in terms of the infiltration area of stemflow-induced water instead of canopy-projected area and the model explains the effect of stemflow on groundwater recharge well regardless whether the ratio of stemflow to net precipitation is small (or not) in the forest water balance.
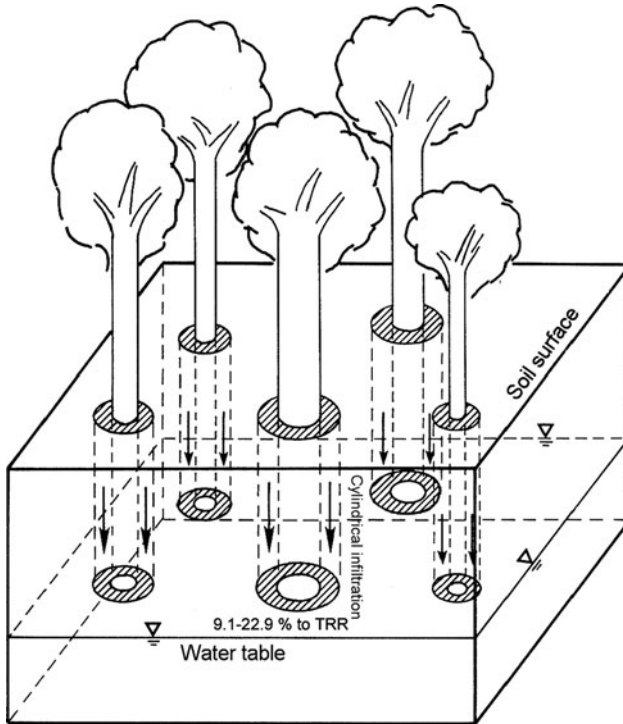
Fig. 25.2 Schematic diagram of CI model for stemflow inputs into the forest soils (from Tanaka et al. 1996). Range of percentage on the figure indicates the evaluated recharge rate by stemflow to the total recharge rate (TRR) using CI model at a Japanese red pine forest

Based on field observations, Tanaka et al. (2004) reported the actual marks of infiltrating water induced by stemflow underneath deciduous oak trees near Tokyo were shaped more like a reverse cone than strictly a cylindrical shape, forming just around the root distribution of the trees. The occurrence of reverse cone-shaped marks of stemflow-induced water underneath trees were reconfirmed with dye tracing experiments conducted in a mixed Japanese red pine and evergreen oak forest by Miyazawa (2009) and Askari (2010). Askari (2010) represented the difference of infiltration process between the CI model and the observed reverse cone shape schematically as shown in Fig. 25.3. Although the cylindrical shape of infiltration due to the stemflow-induced water at the forest floor (surface) may be valid, Hayashi (2010, personal communication) examined the differences of infiltrated water amounts between cylindrical and reverse cone shapes as infiltration water marks underneath a tree with 6 months of data, concluding that the amounts of the latter case are 1.1 times larger than the former case. As such, the difference between the CI model and reverse cone shape appear to be negligible but further research is necessary to confirm whether the conclusions of Hayashi (2010, personal communication) can be confirmed.
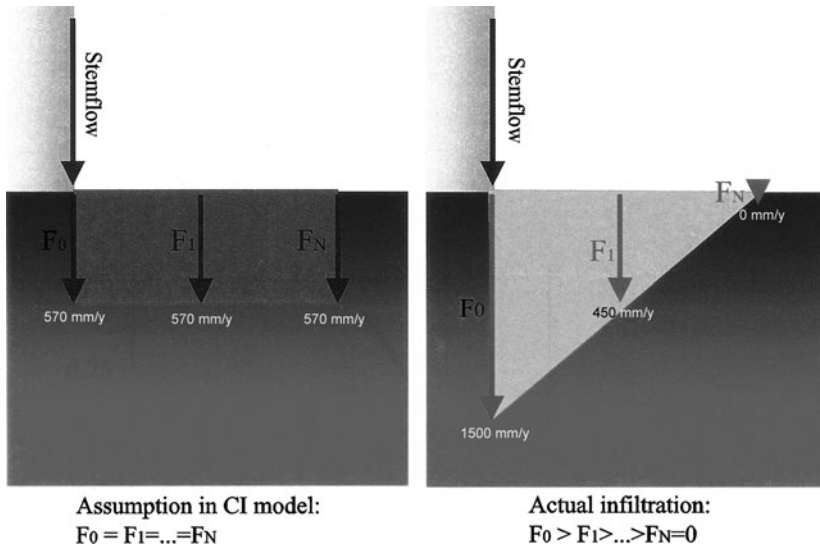
Fig. 25.3 Schematic representation showing the difference of infiltration process between the CI model and the observed reverse cone shape (from Askari 2010, reproduced with permission). Infiltration rates due to stemflow-induced water (mm year^{-1}) indicated on the figure are the round number depending on the actual observed values on broadleaved evergreen oak stands during 1-year period from November 2009 to October 2010 with a total precipitation of 1,236.5 mm year^{-1} (Hayashi 2010, personal communication)

25.2.3 Groundwater Recharge Processes by Stemflow-Induced Water

As mentioned previously, the phenomena of groundwater recharge by stemflow-induced water are very rapid and faster than traditionally believed. Crabtree and Trudgill (1985) suggested the existence of bypassing rapid flow initiated by stemflow in their Whitewell Wood hillslope study. Durocher (1990) also suggested the existence of some sort of bypassing mechanisms, such as flow through macropores (Germann et al. 1986; Germann 1988), for explaining the phenomena of very rapid and deep infiltration generated by stemflow. He verified his assumption using a tension infiltrometer at the study site and obtained the results that a significant proportion of the flow, 33%, occurred through macropores.

The spatial concentration and channelization of stemflow have been reported in arid environment using rhodamine-B dye powder as a tracer (Martinez-Meza and Whitford 1996). They found that stemflow was channeled along preferential flow paths near the roots of *Flourensia cernua*, leading to deep storage of soil water, and hypothesized that the stemflow–root-channelization process of shrubs is an adaptive mechanism to survive seasonal drought in arid environments. This means that the stemflow–root-channelization process is one of the mechanisms for redistribution and movement of stemflow inputs into soils as producing preferential pathways vertically.

Liang et al. (2007, 2009) also reported the existence of stemflow–root-channelization during a heavy storm event on a steep forested hillslope based on high spatial resolution observations of throughfall, stemflow, soil water content, and pore water pressure for 141 storm events. The work of Liang et al. highlights recent advances in our understanding of stemflow-induced preferential infiltration along root pathways.

In general, however, actual infiltration phenomena of spatial and temporal variability due to the stemflow-induced water could not be confirmed directly because the phenomena usually occur underneath the ground. As mentioned before, Tanaka et al. (2004) reported the evidence concerning actual infiltration phenomena due to the stemflow-induced water observed at an outcrop near Tokyo. The outcrop consists of the volcanic ash with a thickness of around 7 m and the observed stands of deciduous oak located on the edge of the outcrop. During 18 days before the field observation, total amount of 136 mm rainfall was recorded with the maximum daily rainfall and rainfall intensity of 42 mm and 9 mm h^{-1}, respectively. On the outcrop, they could observe the infiltration marks due to the stemflow-induced water and the exposed root length of both horizontal and vertical directions. The results indicated that the depth of infiltration marks of stemflow inputs of the stands was 210–230 and 270–300 cm, respectively, and these depths nearly correspond to the exposed vertical root length of each stand of 160 and 380 cm. This finding indicates that the channelization of water flow by roots may occur during the percolation processes of stemflow inputs. They also reported that the radius of infiltration area marks of stemflow inputs of the trees closely corresponded to the horizontal length of exposed surficial root structure, which may be caused by the funneling and concentration of stemflow inputs.

For the modeling of groundwater recharge processes from stemflow-induced water as characterized with root-channelization flow, Liang et al. (2009) incorporated the variable source term in the Richards equation as a new approach and made it possible to represent the root-induced bypass flow process around a tree growing on a steep hillslope. Based on the analysis of the stemflow-sprinkling experiments, they treated stemflow as a source flux term in the soil layers, assigning it to the source term S in the ordinary Richards equation. The source flux at each depth was determined by the increasing ratios of soil water content between the start and end of the stemflow-sprinkling experiment in situ. The model proposed in their study showed adequate spatial and temporal variations in soil water dynamics and closely agreed with observations.

On the other hand, for the modeling of the macropore and/or the root-channelization flow, the concept of bimodality of pore size distribution was introduced by Askari (2010). This concept depends on the result of the formation of secondary pore systems (macroporosity) by soil genetic processes such as soil aggregation or biological soil-forming (Durner 1994; Kosugi et al. 2010). Askari (2010) reported that the bimodal function introduced for simulating the soil water potential changes due to the stemflow-induced root-channelization flow showed rather good results compared to a unimodal function depending on the statistic evaluation analysis. For humid–tropical forest soils, at a depth of <30 cm below the surface,

Kosugi et al. (2010) observed that the soils clearly exhibited retention curves with two inflection points and applied the multi-model function to the observed data for obtaining the soil hydraulic properties and numerical simulations for saturated and unsaturated water flow to analyze and better understand the effects of rain water infiltration on discharge processes. They demonstrated that at the beginning of rainfall event, the discharge with the formations of the secondary pore systems was faster than that of the unimodal pore system formations. Although the study does not directly focus on the infiltration processes due to the stemflow-induced water, it may be one of suggestive lines of research for modeling the macropore flow and/or the root-channelization flow caused by the stemflow-induced water utilizing the concept of the bimodal soil systems.

25.3 Groundwater Interaction with Evapotranspiration

25.3.1 Diurnal Fluctuation in Shallow Groundwater Levels

Diurnal fluctuations of shallow groundwater levels and streamflow rates are well known phenomenon caused by evapotranspiration. Although the diurnal fluctuations of shallow groundwater levels may be caused by several factors, such as alternating processes of freezing and thawing, diurnal cycle of precipitation in the tropics, and/or diurnal cycle of water uptake by vegetation (Gribovszki et al. 2010), in temperate climates, evapotranspiration is the most important factor accounting for alterations in shallow groundwater levels. Gribovszki et al. (2010) provide an excellent review on diurnal fluctuations in shallow groundwater levels and streamflow rates. According to Gribovszki et al. (2010), an historical overview on the topic is summarized as follows in the next paragraph.

In early 1930s, evapotranspiration-induced diurnal signals were observed in streamflow stage and in the groundwater levels in USA, Austria, and the Netherlands (Blaney et al. 1930, 1933; White 1932; Bousek 1933; Thal-Larsen 1934). Among them, White (1932) explained the observed change of groundwater levels more specifically by the water uptake of vegetation and the accompanying transpiration. In this study, he proposed a very simple equation for estimating the daily ET, now referred to as the White-method, depending on the observed groundwater level fluctuations (Fig. 25.4) as follows,

$$\mathrm{ET} = S_y(24r \pm s), \tag{25.3}$$

where S_y is the specific yield of the soil/aquifer system, r the slope of tangential line drawn to the groundwater level curve in the predawn/dawn hours (in Fig. 25.4, from midnight to 4 a.m.), s the difference in the observed groundwater levels over 24-h period.

Troxell (1936) followed the experiments by Blaney et al. (1930, 1933) along the Santa Ana River and observed diurnal fluctuations in streamflow stage and
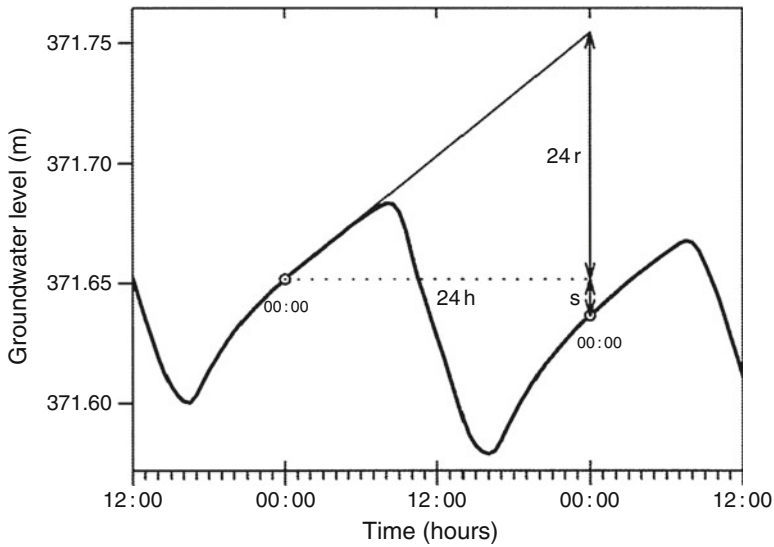
Fig. 25.4 Basic principle of ET estimation by the White-method (from Gribovszki et al. 2010, reproduced with permission)

groundwater levels. He reported that water levels were highest around 10 a.m. and lowest about 6 p.m. regardless of basin area and locations within the basin.

In 1940s–1950s, many observed diurnal alterations of streamflow and groundwater levels (and their consequences) in the several ecoregions (e.g., Wicht 1941, 1942; Dunford and Fletcher 1947; Croft 1948; Haise and Kelley 1950; Rycroft 1955; Kausch 1957). Dunford and Fletcher (1947) analyzed the effect of removal of stream-bank vegetation on water yield at a small watershed in the Coweeta Experimental Forest. The removal of riparian vegetation of 12% area along the stream-bank increased water yield by an average of 12% (Tase et al. 1991). Following treatment, they reported that diurnal fluctuations in streamflow decreased markedly but still existed with little change in fluctuation patterns. They also reported that the fluctuation range caused by evapotranspiration was about 0.1 mm day^{-1} in water depth equivalent. Similar results of fluctuation range with flow rate were reported by Tase et al. (1991) in small two basins in central Japan.

In the 1960s–1970s, research on the groundwater and streamflow interactions exploded, occurring in many different ecoregions worldwide, including Ubell (1961) in Hungary, Heikel (1964) in Thuringer, Tschinkel (1963) in Southern California, Klinker and Hansen (1964) in Germany, Meyboom (1965) in Saskatchewan, Reigner (1966) in Pennsylvania, Hylckama (1968) in Arizona, Turk (1975) in Utah, and Feddes et al. (1976) in Wageningen. Meyboom (1965) formulated a relationship between the diurnal streamflow change and the transpiration rate of the riparian zone for which he estimated by the White-method. For applying the White-method, he used the specific yield (S_y) values in (25.3) of 7.5–11.25% for silty clay and sandy clay soil textures. He also demonstrated a method for riparian

evapotranspiration estimation as the difference between the maximum base flow rate curve and the actual diurnal hydrograph, which corresponds to the missing base flow rate (Gribovszki et al. 2010). Reigner (1966) developed a riparian evapotranspiration estimation method based on the diurnal streamflow signals. He constructed the master streamflow recession curve depending on the maximum record of the streamflow values and calculated the water loss of the riparian zone, meaning the transpiration of riparian vegetation, as the difference between the obtained master recession curve and the actual diurnal hydrograph (Gribovszki et al. 2010). After comparison between the estimated ET from the streamflow hydrograph and the potential ET calculated from the meteorological variables, he reported that the latter indicated the larger values because of the improper determination of the lateral extent of the riparian zone in the latter case of calculation. He mentioned that the riparian zone may shrink and expand dynamically in extent with changes in groundwater levels.

From 1990s to 2000s, less research was conducted on groundwater and streamwater interactions on the whole compared to the 1950s and 1960s, although some work still applied the White-method in estimating ETs (e.g., Gerla 1992; Rosenberry and Winter 1997). Today new measuring techniques and the development of a new method for estimating evapotranspiration, relying on the diurnal fluctuations of groundwater levels and streamflow rates, are making significant progress (Gribovszki et al. 2010).

Koppan et al. (2000) found diurnal fluctuations in xylem-sapflow by measuring the water transport in tree trunks using an Electrical Potential Difference technique of which time series ran parallel to the diurnal streamflow fluctuations. Bauer et al. (2004) introduced a new evapotranspiration estimation method based on numerical solution of the soil moisture dynamics using measured groundwater level fluctuations. Using numerical modeling experiments, Loheide et al. (2005) reported that the ET obtained by the White-method is not influenced perceptibly by the geometry of the vadose zone. Shah et al. (2007) tried to couple dynamics of soil moisture and groundwater numerically and reported that when existing water table was within half a meter of the ground surface nearly all of evapotranspiration comes from groundwater due to the close hydraulic connectivity between the unsaturated and saturated zones. For deep-rooted vegetation, the decoupling of groundwater and the vadose zone dynamics was found to begin at water table depths between 30 and 100 cm depending on soil texture.

Because the White-method depending on the point data influenced local water uptake of vegetation, Engel et al. (2005) modified the White-method by introducing additive constant (ref) into (25.3) as follows,

$$\mathrm{ET} = S_\mathrm{y}(24 \pm s \pm \mathrm{ref}), \tag{25.4}$$

where ref is the groundwater elevation change in a neighboring observation well in an area with natural grass cover as shown in Fig. 25.5. Nosetto et al. (2007), on the Hungarian Great Plains, determined the ref parameter from the neighboring groundwater well data in natural grass cover as the point at which the root system
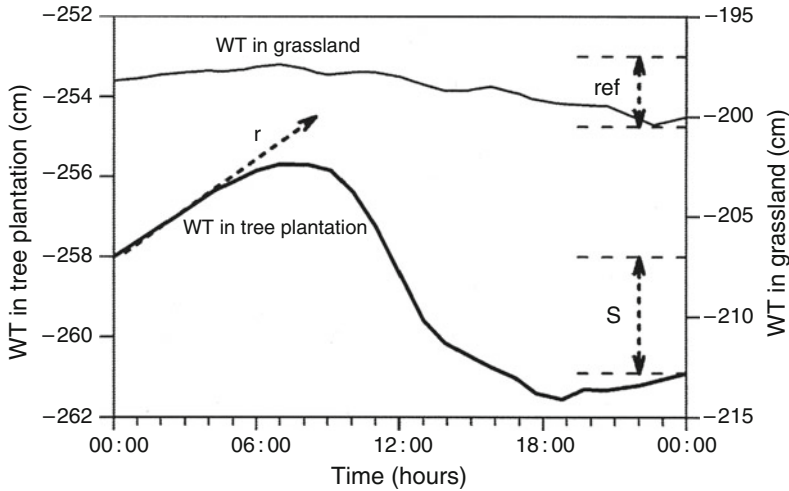
Fig. 25.5 Engel et al. (2005)'s representation of components of diurnal water table fluctuations in tree plantation and surrounding grass land (from Gribovszki et al. 2010, reproduced with permission)

could not significantly tap groundwater, or the capillary fringe for estimating oak forest evapotranspiration from the diurnal groundwater levels. Other modifications of the White-method were reported by Nachabe et al. (2005), Schilling (2007), Loheide (2008), and Gribovszki et al. (2008). Nachabe et al. (2005) adapted the White-method for considering high-frequency soil moisture measurements. Schilling (2007) introduced evapotranspiration estimation method based on an assumed step-like pattern of the groundwater diurnal fluctuations, and Loheide (2008) also introduced the regression-based subdaily evapotranspiration estimation method as an upgrade of the White-method (Gribovszki et al. 2010).

According to the Troxell's (1936) early suggestion that the groundwater supply per unit area, Q_{net}, to the riparian zone is not constant and changes over the course of a day, due to the hydraulic head differences in space, which was against White's (1932) empirical assumption of groundwater supply as $24r$ in (25.3), Gribovszki et al. (2008) upgraded the White-method introducing a hydraulic consideration as follows,

$$ETG = Q_{net} - S_y^* \, dh/dt, \tag{25.5}$$

where ETG is the evapotranspiration from the groundwater, Q_{net} the groundwater supply over the day per unit area obtained from Darcy's equation, S_y^* the readily available specific yield, h the groundwater level, and t the time. They compared the results estimated by the method at the experimental catchment in the Sopron Hills region near the western border of Hungary with the Penman-Monteith estimate on a half-hourly basis and with the early White-method and concluded that two

Table 25.2 Chronological list of the important developments in ET-induced diurnal signal studies (from Gribovszki et al. 2010, reproduced with permission)

References	Basic information on the development
White (1932)	ET estimation based on groundwater level diurnal signal
Troxell (1936)	Suggestions for upgrading the White-method since the rate of groundwater (GW) supply over the day is not a constant
Meyboom (1965)	Riparian ET was calculated as a difference between the maximum base flow rates curve and the actual diurnal hydrograph. Realized that only about 50% of the specific yield value has to be applied in the White-method
Reigner (1966)	Development of diurnal stemflow-signal-based riparian ET estimated method
Bauer et al. (2004)	New ET estimation method based on numerical solution of the soil moisture dynamics using measured GW level fluctuations
Engel et al. (2005)	Upgrading the White-method by introducing an additive constant (represents regional GW level change)
Nachabe et al. (2005)	Adaptation of the White-method for high-frequency soil moisture measurements
Schilling (2007)	ET-estimation method based on an assumed step-like pattern of the GW diurnal signal
Gribovszki et al. (2008)	Subdaily ET estimation by an upgrade of the White method taking into account a diurnal changing GW supply
Loheide (2008)	Regression-based subdaily ET estimation by an upgrade of the White-method

estimates of both the proposed method and the Penman-Monteith method were favorable on a daily basis, but typically 50% higher than those obtained by the original White-method (Gribovszki et al. 2010).

Providing an historical overview of evapotranspiration-induced diurnal signal studies discussed above, Gribovszki et al. (2010) summarized the most important developments as a chronological list (Table 25.2). As argued by Gribovszki et al. (2010), the White-method (White 1932) is a common approach for evapotranspiration estimation of the diurnal fluctuations of groundwater levels and can be readily employed in the study of groundwater interactions with forest hydrology flux studies due to its simplicity, despite the fact it has been modified by many researchers (Table 25.2).

25.4 Conclusions and Future Research Directions

In the chapter, the author examined two topics as a lens to provide insights into the dynamic interactions between surface water and groundwater: stemflow and evapotranspiration. Stemflow often represents only a few percent of the gross or net precipitation in the water balance of the watersheds. This low value, thus, insignificant volumetrically when compared to throughfall, is one of the reasons why little

attention has been paid to the nature of stemflow inputs into the soil surface and to the effect on the groundwater recharge process. However, stemflow, as a locally concentrated point input of water, strongly affects groundwater recharge as described in the chapter. To clarify the process of groundwater interaction with stemflow inputs, it is necessary to reveal the infiltration marks of stemflow-induced water underneath the surface to more precisely evaluate the actual amounts of infiltrated stemflow-induced water. Change in stemflow generation and yield as a result of natural succession, thinning, and/or climate change necessitates further research on the interactions between surface water and groundwater interactions (Iida et al. 2004, 2005b). Some progress has been achieved in explaining the rapid recharge of groundwater by the stemflow-induced water preferential flow mechanism through macropores or via root-channelization. In point of fact, Liang et al. (2009) has incorporated this mechanism into a finite-element model with some success. Further work, however, is required and recommended to incorporate this mechanism into the model more precisely. Modeling and scaling of groundwater interactions with stemflow at the watershed scale is of critical importance for evaluating water resources and its management. In addition to the areal scaling problems, groundwater interactions with stemflow may be affected by variable temporal scales within particular events, across seasons, and annually. Moreover, these interactions may also be affected by watershed conditions, such as antecedent wetness, as seen for other hydrologic and biogeochemical fluxes such as riparian and hillslope water contribution to storm runoff and nitrate transport (e.g., Bernal et al. 2006; Inamdar and Mitchell 2007). Furthermore, groundwater recharge rate caused by stemflow-induced water may be affected by the hydraulic connectivity across and within a watershed as recently espoused by Jencso et al. (2009). Such relationships are poorly understood and deserving of future research.

Research on groundwater interactions with evapotranspiration have been addressed mainly with respect to shallow groundwater level fluctuations and, thus, restricted mostly to and near the riparian zone. Scant attention has been directed to groundwater–evapotranspiration interactions at the watershed scale. As such, further quantitative research should be devoted to the better understanding of the interplay between evapotranspiration and groundwater dynamics and how such interactions change the water balance components at the watershed scale. Such research would be of use to water resource managers. Recently, Hotta et al. (2010) reported that forest harvesting causes changes in groundwater level dynamics and this change causes many watershed problems, such as decreased slope stability, landslides, expansion of saturated areas, and stream water quality changes. These issues should also be approached from the point of view of the groundwater interactions with forest hydrology fluxes, especially alterations in evapotranspiration changes due to forest harvesting.

References

Aboal JR, Morales D, Hernandez M et al (1999) The measurement and modeling of the variation of stemflow in laurel forest in Tenerife, Canary Islands. J Hydrol 221:161–175

Askari M (2010) Infiltration and soil water movement underneath Japanese red pine and oak trees. PhD Thesis, Graduate School of Life and Environmental Sciences, University of Tsukuba

Bauer P, Thabeng G, Stauffer F et al (2004) Estimation of the evapotranspiration rate from diurnal groundwater level fluctuations in the Okavango Delta, Botswana. J Hydrol 288:344–355

Bellot J, Avila A, Rodrigo A (1999) Throughfall and stemflow. In: Roda F, Retana J, Gracia CA, Bellot J (eds) Ecology of Mediterranean evergreen oak forests. Springer, New York, pp 209–222

Bernal S, Butturini A, Sabater F (2006) Inferring nitrate sources through end member mixing analysis in an intermittent Mediterranean stream. Biogeochemistry 81:269–289

Blaney HF, Taylor CA, Yong AA (1930) Rainfall penetration and consumptive use of water in the Santa Ana River Valley and Coastal Plain. California Department of Public Works, Division of Water Resources, Bulletin 33, 162pp

Blaney HF, Taylor CA, Young AA et al (1933) Water losses under natural conditions from wet areas in southern California. California Department of Public Works, Division of Water Resources, Bulletin, 139pp

Bousek R (1933) Das tagliche periodishe steigen und fallen des grundwasserspiegels. Die Wasserwirtschaft 31:427–429

Carlyle-Moses DE (2004) Throughfall, stemflow, and canopy interception loss fluxes in a semi-arid Sierra Madre Priental matorral community. J Arid Environ 58:181–202

Carlyle-Moses DE, Price AG (2006) Growing-season stemflow production within a deciduous forest of southern Ontario. Hydrol Process 20:3651–3663

Chang SC, Matzner E (2000) The effect of beech stemflow on spatial patterns of soil solution chemistry and seepage fluxes in a mixed beech/oak stand. Hydrol Process 14:135–144

Claassen HC, Reddy MM, Halm DR (1986) Use of the chloride ion in determining hydrologic-basin water budgets: a 3-year case study in the San Juan Mountains, Colorado, U.S.A. J Hydrol 85:49–71

Crabtree RW, Trudgill ST (1985) Hillslope hydrochemistry and stream response on a wooded, permeable bedrock: the role of stemflow. J Hydrol 80:161–178

Crockford RH, Khanna PK (1997) Chemistry of throughfall, stemflow and litterfall in fertilized and irrigated *Pinus radiata*. Hydrol Process 11:1493–1507

Crockford RH, Richardson DP (1990) Partitioning of rainfall in eucalypt forest and pine plantation in southern Australia: II. Stemflow and factors affecting stemflow in a dry sclerophyll eucalypt forest and a Pinus radiata plantation. Hydrol Process 4:145–155

Croft AR (1948) Water loss by stream surface evaporation and transpiration by riparian vegetation. Trans Am Geophys Union 29:235–239

Dezzeo N, Chacon N (2006) Nutrient fluxes in incident rainfall, throughfall, and stemflow in adjacent primary and secondary forests of the Gran Sabana, south Venezuela. For Ecol Manag 234:218–226

Dunford AR, Fletcher PW (1947) Effect of removal of streambank vegetation upon water yield. Trans Am Geophys Union 28:105–110

Dunin FX, O'Loughlin EM, Reyenga W (1988) Interception loss from eucalypt forest: lysimeter determination of hourly rates for long term evaluation. Hydrol Process 2:315–329

Durner W (1994) hydraulic conductivity estimation for soils with heterogeneous pore structure. Water Resour Res 30:211–223

Durocher MG (1990) Monitoring spatial variability of forest interception. Hydrol Process 4:215–229

Engel V, Jabbagy EG, Stieglitz M et al (2005) The hydrological consequences of eucalyptus afforestation in the Argentine Pampas. Water Resour Res. doi:10.1029/2004WR 003761

Eschner AR (1967) Interception and soil moisture distribution. In: Sopper WE, Lull HW (eds) Forest hydrology. Pergamon Press, New York, pp 191–200

Feddes RA, Kowalik P, Kolinska-Malinka K et al (1976) Simulation of field water uptake by plants using soil water dependent root extraction function. J Hydrol 31:13–26

Ford ED, Deans JD (1978) The effects of canopy structure on stemflow, throughfall and interception loss in a yang sitka spruce plantation. J Appl Ecol 15:905–917

Gerla PJ (1992) The relationship of water table changes to the capillary fringe, evapotranspiration and precipitation in intermittent wetlands. Wetlands 12:91–98

Germann PF (1988) Approaches to rapid and far-reaching hydrologic processes in the vadose zone. J Contam Hydrol 3:115–127

Germann PF, Pierce RS, Beven KJ (1986) Kinematic wave approximation to the initiation of subsurface storm flow in a sloping forest soils. Adv Water Res 9:70–76

Gersper PL, Holowaychuck N (1970a) Effects of stemflow on a Miami soil under a beech tree: I. Morphological and physical properties. Soil Sci Soc Am Proc 34:779–786

Gersper PL, Holowaychuck N (1970b) Effects of stemflow on a Miami soil under a beech tree: II. Chemical properties. Soil Sci Soc Am Proc 34:786–794

Gersper PL, Holowaychuck N (1971) Some effects of stem flow from forest canopy trees on chemical properties of soils. Ecology 52:691–702

Gomez JA, Vanderlinden K, Giraldez JV et al (2002) Rainfall concentration under olive trees. Agri Water Manage 55:53–70

Gribovszki Z, Kalicz P, Szilagyi J et al (2008) Riparian zone evapotranspiration estimation from diurnal groundwater level fluctuations. J Hydrol 349:6–17

Gribovszki Z, Szilagyi J, Kalicz P (2010) Diurnal fluctuations in shallow groundwater levels and streamflow rates and their interpretation – a review. J Hydrol 385:371–383

Haise HR, Kelley OJ (1950) Causes of diurnal fluctuations of tensiometers. Soil Sci 70:301–313

Heikel W (1964) Zur charakteristik des aflussverhaltens in der thuringer waldflussgebieten des vesser und zahmen gera. Archiv Naturschutz 4:51–82

Herwitz SR (1986a) Episodic stemflow inputs of magnesium and potassium to a tropical forest floor during heavy rainfall events. Oecologia 70:423–425

Herwitz SR (1986b) Infiltration-excess caused by stemflow in a cyclone-prone tropical rainforest. Earth Surf Process Landforms 11:401–412

Herwitz SR (1988) Buttresses of tropical rainforest trees influence hillslope processes. Earth Surf Process Landforms 13:563–567

Holscher D, de A Sa TD, Moller RF et al (1998) Rainfall partitioning and related hydrochemical fluxes in a diverse and in a monospecific (*Phenakospermum guyannense*) secondary vegetation stand in eastern Amazonia. Oecologia 114:251–257

Hotta N, Tanaka N, Sawano S et al (2010) Changes in groundwater level dynamics after low-impact forest harvesting in steep, small watersheds. J Hydrol 385:120–131

Hylckama TEAV (1968) Water level fluctuations in evapotranspirometers. Water Resour Res 4:761–768

Iida S, Tanaka T, Sugita M (2004) Change of stemflow generation due to the succession from Japanese red pine to evergreen oak. Ann Rep Inst Geosci Univ Tsukuba 30:15–20

Iida S, Kakubari J, Tanaka T (2005a) "Litter marks" indicating infiltration area of stemflow-induced water. Tsukuba Geoenviron Sci 1:27–31

Iida S, Tanaka T, Sugita M (2005b) Change of interception process due to the succession from Japanese red pine to evergreen oak. J Hydrol 315:154–166

Inamdar SP, Mitchell MJ (2007) Contribution of riparian and hillslope waters to storm runoff across multiple catchments and storm events in a glaciated forested watershed. J Hydrol 341:116–130

Jencso KG, McGlynn BL, Gooseff MN et al (2009) Hydrologic connectivity between landscapes and streams: transferring reach-and plot-scale understanding to the catchment scale. Water Resour Res. doi:10.1029/2008WR007225

Kakubari J (2007) Effect of vegetation species difference on percolation and soil solution processes. MS Thesis, Graduate School of Life and Environmental Sciences, University of Tsukuba

Kausch W (1957) Die transpiration als ursach fur taglich grundwasser schwankungen. Ber Deut Bot Ges 70:436–444

Kellman M, Roulet N (1990) Stemflow and throughfall in a tropical dry forest. Earth Surf Process Landforms 15:55–61

Klinker L, Hansen H (1964) Bemerkungen zur tagesperiodischen variationen des grundwasser-horizontes und des wasserstandes im kleinen wasserlaufen. Zeitschr Meteor 17:240–245

Koppan A, Wesztergom V, Szarka L (2000) Annual fluctuation in amplitudes of daily variations of electrical signals measured in the trunk of a standing tree. Life Sci 323:559–563

Kosugi K, Hayashi Y, Kato H et al (2010) Effects of soil hydraulic properties on rainwater discharge at the Gunung Walat Educational Forest. Final Report JSPS-DGHE Joint Project, Bull Terre Environ Res Cent Univ Tsukuba 10/Suppl 1:75–84

Kramer I, Holscher D (2009) Rainfall partitioning along a tree diversity gradient in a deciduous old-growth forest in Central Germany. Ecohydrology 2:102–114

Levia DF, Frost EE (2003) A review and evaluation of stemflow literature in the hydrologic and biogeochemical cycles of forested and agricultural ecosystems. J Hydrol 274:1–29

Levia DF, Herwitz SR (2000) Physical properties of water in relation to stemflow leachate dynamics: implications for nutrient cycling. Can J For Res 30:662–666

Liang WL, Kosugi K, Mizuyama T (2007) Heterogeneous soil water dynamics around a tree growing on a steep hillslope. Vadose Zone J 6:879–889

Liang WL, Kosugi K, Mizuyama T (2009) A three-dimensional model of the effect of stemflow on soil water dynamics around a tree on a hillslope. J Hydrol 366:62–75

Lloyd CR, de Marques OFA (1988) Spatial variability of throughfall and stemflow measurements in Amazonian rain-forest. Agric For Meteorol 42:63–73

Loheide SP II (2008) A method for estimating subdaily evapotranspiration of shallow groundwater using diurnal water table fluctuations. Ecohydrology 1:59–66

Loheide SP II, Butler JJ Jr, Gorelick SM (2005) Use of diurnal water table fluctuations to estimate groundwater consumption by phreatophytes: a saturated-unsaturated flow assessment. Water Resour Res. doi:10.1029/2005WR003942

Majima M, Tase N (1982) Spatial variation of rainfall in a red pine forest. Bull Environ Res Cent Univ Tsukuba 6:75–82 (in Japanese)

Marin CT, Bouten W, Sevink J (2000) Gross rainfall and its partitioning into throughfall, stemflow and evaporation of intercepted water in four forest ecosystems in western Amazonia. J Hydrol 237:40–50

Martinez-Meza E, Whitford WG (1996) Stemflow, throughfall and channelization of stemflow by roots in three Chihuahuan desert shrubs. J Arid Environ 32:271–287

Masukata H, Ando M, Ogawa H (1990) Throughfall, stemflow and interception of rainwater in an evergreen broadleaved forest. Ecol Res 5:303–316

Mauchamp A, Janeau JL (1993) Water funneling by the crown of *Flourensia cernua*, a Chihuahuan Desert shrub. J Arid Environ 25:299–306

Meyboom P (1965) Three observations on stream depletion by phreatophytes. J Hydrol 2:248–261

Miyazawa T (2009) Flow pathway of infiltrating water induced by stemflow of different vegetation species. MS Thesis, Graduate School of Life and Environmental Sciences, University of Tsukuba

Murai H (1970) Studies on precipitation interception by forest vegetation. Bull Gov For Exp Stat 232:25–64 (in Japanese with English summary)

Nachabe M, Shah N, Ross M et al (2005) Evapotranspiration of two vegetation covers in a shallow water table environment. Soil Sci Soc Am J 69:492–499

Navar J (1993) The causes of stemflow variation in three semi-arid growing species of northeastern Mexico. J Hydrol 145:175–190

Navar J, Charles F, Jurado E (1999) Spatial variations of interception loss components by Tamaulipan thornscrub in northeastern Mexico. For Ecol Manage 124:231–239

Neal C, Jeffery HA, Conway T et al (1992) Beryllium concentration in rainfall stemflow, throughfall, mist and stream waters for an upland acidified area of mid-Wales. J Hydrol 136:33–49

Neal C, Robson AJ, Bharwaj CL et al (1993) Relationship between precipitation, stemflow and throughfall for a lowland beech plantation, Black Wood, Hampshire, southern England: findings on interception at a forest edge and the effects of storm damage. J Hydrol 146:221–233

Neave M, Abrahams AD (2002) Vegetation influences on water yields from grassland and shrubland ecosystems in the Chihuahuan Desert. Earth Surf Process Landforms 27:1011–1020

Nosetto MD, Jabbagy EG, Toth T et al (2007) The effects of tree establishment on water and salt dynamics in naturally salt-affected grasslands. Oecologia 152:695–705

Olson JS, Reiners WA, Cronan CS et al (1981) The chemistry and flux of throughfall and stemflow in subalpine balsam fir forests. Holarct Ecol 4:291–300

Opakunle JS (1989) Throughfall, stemflow, and rainfall interception in a cacao plantation in south western Nigeria. Trop Ecol 30:244–252

Pressland AJ (1976) Soil moisture redistribution as affected by throughfall and stemflow in an arid zone shrub community. Aus J Bot 24:641–649

Pryor SC, Barthelmie RJ (2005) Liquid and chemical fluxes in precipitation, throughfall and stemflow: observations from a deciduous forest and a red pine plantation in the midwestern U.S.A. Water Air Soil Pollut 163:203–227

Reigner IC (1966) A method for estimating streamflow loss by evapotranspiration from the riparian zone. Fore Sci 12:130–139

Rosenberry DO, Winter TC (1997) Dynamics of water-table fluctuations in an upland between two prairie-pothole wetlands in North Dakota. J Hydrol 191:226–289

Rycroft HB (1955) The effect of riparian vegetation on water-loss from an irrigation furrow at Jonkershoek. J South African Forest Assoc 26:2–9

Schilling KE (2007) Water table fluctuations under three riparian land covers, Iowa, U.S.A. Hydrol Process 21:2415–2424

Shah N, Nachabe M, Ross M (2007) Extinction depth and evapotranspiration from ground water selected land covers. Ground Water 45:329–338

Staelens J, Schrijer AD, Verheyen K et al (2008) Rainfall partitioning into throughfall, stemflow, and interception within a single beech (*Fagus sylvatica* L.) canopy: influence of foliation, rain event characteristics, and meteorology. Hydrol Process 22:33–45

Stevens PA, Hornung M, Hughes S (1989) Solute concentration, fluxes and major nutrient cycles in a mature sitka-spruce plantation in Beddgelert Forest, North Wales. For Ecol Manage 27:1–20

Tanaka T, Tsujimura M, Taniguch M (1991) Infiltration area of stemflow-induced water. Ann Rep Inst Geosci Univ Tsukuba 17:30–32

Tanaka T, Taniguch M, Tsujimura M (1996) Significance of stemflow in groundwater recharge. 2: A cylindrical infiltration model for evaluating the stemflow contribution to groundwater recharge. Hydrol Process 10:81–88

Tanaka T, Iida S, Kakubari J et al (2004) Evidence of infiltration phenomena due to the stemflow-induced water. Ann Rep Inst Geosci Univ Tsukuba 30:9–14

Tanaka T, Iida S, Kakubari J et al (2008) Effect of forest stand succession from conifer trees to broadleaved evergreen trees on infiltration and groundwater recharge process. Int Assoc Hydrol Sci Publ 321:54–60

Tang C (1996) Interception and recharge processes beneath a *Pinus elliotii* forest. Hydrol Process 10:1427–1434

Taniguch M, Tsujimura M, Tanaka T (1996) Significance of stemflow in groundwater recharge. 1: Evaluation of the stemflow contribution to recharge using a mass balance approach. Hydrol Process 10:71–80

Taniguchi M (1991) Groundwater, thermal and solute transport between pine forest and pasture-land. Int Assoc Hydrol Sci Publ 204:425–431

Tase T, Tsujimura M, Tanaka T et al (1991) Diurnal fluctuations in streamflow of the two small basins. Ann Rep Inst Geosci Univ Tsukuba 17:33–35

Thal-Larsen JH (1934) Fluctuations in the level of the phreatic surface with an atmospheric deposit in the form of dew. Bodenkundliche Forschung 4:223–233

Thorburn PJ, Cowie BA, Lawrence PA (1991) Effect of land development on groundwater recharge determined from non-steady chloride profiles. J Hydrol 124:43–58

Troxell HC (1936) The diurnal fluctuation in the ground-water and flow of the Santa Anna River and its meaning. Trans Am Geophys Union 17:496–504

Tschinkel HN (1963) Short-term fluctuation in streamflow as related to evaporation and transpiration. J Geophys Res 68:6459–6469

Turk LJ (1975) Diurnal fluctuation of water tables induced by atmospheric pressure changes. J Hyrdol 26:1–16

Ubell K (1961) Uber die gesetzmassigkeiten des grundwassergangs und des grundwasserhaushalts im flachlandgebieten. Wasserwirtshaft Wasser Technik 11:366–372 (after Gribovszki et al. 2010)

Veneklaas EJ, Van EKR (1990) Rainfall interception in two tropical montane rain forest, Colombia. Hydrol Process 4:311–326

Voigt GK (1960) Distribution of rainfall under forest stands. For Sci 6:2–10

Wheater HS, Langan SJ, Miller JD et al (1987) The determination of hydrological flow paths and associated hydrochemistry in forested catchments in central Scotland. Int Assoc Hydrol Sci Publ 167:433–449

White WN (1932) Method of estimating groundwater supplies based on discharge by plants and evaporation from soil – results of investigation in Escalante valley. US Geol Surv Water Supply Paper 659A:1–105

Whitford WG, Anderson J, Rice PM (1997) Stemflow contribution to the "fertile island" effect in creosotebush, *Larrea tridentata*. J Arid Environ 35:451–457

Wicht CL (1941) Diurnal fluctuation in Jonkershoeck streams due to evaporation and transpiration. J South African Forest Assoc 7:34–49

Wicht CL (1942) Depletion of ground water flow in Jonkershoeck streams. J South African Forest Assoc 8:50–63

Part V
Hydrologic and Biogeochemical Fluxes in Forest Ecosystems: Effects of Time, Stressors, and Humans

Chapter 26
Seasonality of Hydrological and Biogeochemical Fluxes

Jeroen Staelens, Mathias Herbst, Dirk Hölscher, and An De Schrijver

26.1 Introduction

Studies on the hydrology and biogeochemistry of forest ecosystems are often reported at annual timescales. However, seasonal patterns in precipitation or temperature affect ecosystem processes and forest functioning in many regions of the world. Wet tropical forests are considered to experience little seasonal changes but even here small variations in "dry" season conditions may have unexpected large effects on tree performance (Clark et al. 2009). Forests in the subhumid tropics and woodlands in the savannah are exposed to distinct dry and wet seasons, with Mediterranean woodlands experiencing drought in the summer and rainfall in the winter. Woodlands types with wet–dry seasonality are often dominated by evergreen tree species that face a huge variation in hydrological parameters. Summer drought can also influence forest hydrological processes in the temperate zone (Granier et al. 2007), but generally temperate forests are subject to moderately and gradually varying meteorological conditions. Seasonality is here most pronounced in deciduous forests having leaves with a short life span that go through phenological stages within a short time and show plasticity in their response to environmental factors. Forests in the boreal region have a short growing season with an abundance of soil water, which means that seasonality is mainly important in boreal deciduous forests with varying leaf phenology.

It is clear that seasonal changes in water availability strongly influence forest growth and phenology. Inversely, temporal patterns in canopy structure affect forest hydrology and biogeochemistry (see Chap. 18 for spatial effects of canopy structure). In addition, meteorological conditions and atmospheric air concentrations often vary over the year and influence the interaction between the vegetation and the atmosphere as well. Therefore, the aim of this chapter is to summarize current knowledge on the seasonality of hydrological and biogeochemical fluxes in forest ecosystems and to suggest future research directions within this field. The seasonality of streamflow is not discussed here. Other topics that relate to seasonality are discussed elsewhere, e.g., snowfall (Chap. 27), insect infestations (Chap. 28), drought effects (Chap. 29), wild fire (Chap. 30) and ice storms (Chap. 31).

26.2   Seasonality of Hydrological Fluxes

26.2.1   Gross Precipitation

Variation in gross precipitation is creating seasonality in many areas of the world and the annual volume of rainfall and its distribution over the year largely influence composition and productivity of the vegetation. In tropical regions, a dry season is almost absent close to the equator and increases in length and severity north- and southwards from there. In addition to the temporal distribution of precipitation, characteristics such as rainfall intensity and event duration can vary throughout the year and affect rainfall interception and partitioning (Sects. 26.2.2 and 26.2.3).

Forests at high-elevation sites (>600 m a.s.l.) may receive an additional input from clouds or fog (see Chap. 11). In particular in subtropical and Mediterranean regions such as the Canary Islands, characterized by a seasonal precipitation regime with five nearly rainless months, fog input assumes high hydrological importance during the dry summer period (García-Santos and Bruijnzeel in press). Fog precipitation can show seasonality because of seasonally varying meteorological conditions (Brauman et al. 2010).

Not only rainfall in the region of the study forest, but also in other regions may induce seasonality. A prominent example are Amazonian floodplain forests, which grow in areas that are annually flooded by rivers during up to 8 months and at depths of up to 10 m, mainly driven by rainfall seasonality in the headwater of the Amazon watershed in the Andes (Junk et al. 2011).

26.2.2   Canopy Interception and Throughfall

The evaporation of intercepted rain water from the forest canopy depends on meteorological and structural variables. The most important parameters were identified by Horton (1919), on whose comprehensive insight Gash (1979) built his analytical interception model that expresses the essence of the process in a simple formula. According to the review by Muzylo et al. (2009), the Gash model is the most widely used interception model and a revised version (Gash et al. 1995) has made it applicable to even more forest types. The relevant meteorological variables such as rainfall intensity, duration and frequency as well as wind speed and turbulence vary between the seasons and thus cause seasonality in wet canopy evaporation rates and in the fraction of the rainfall that is being intercepted. Such seasonal changes, however, are poorly represented in the Gash model, since it is based on average rainfall and evaporation rates.

The structure of the forest canopy shows the strongest seasonal changes in deciduous forests. Although this would intuitively point towards a particularly strong seasonality of rainfall interception in these forests, several studies have

demonstrated that the rainfall fraction ending up as interception evaporation is often similar between leafed and nonleafed seasons (Dolman et al. 2003). The intercepted fraction of rainfall is particularly larger in foliated conditions for small rainfall events (Staelens et al. 2008). On the one hand, free throughfall and canopy drip are lower in leafed conditions because of the lower gap fraction and the higher surface area from which intercepted rainfall water can evaporate (Link et al. 2004) (Fig. 26.1). Furthermore, evaporation from wetted woody surfaces occurs slower than from wetted foliage because of differences in boundary layer thickness and the development of detained water films in porous bark tissue (Herwitz and Levia 1997). On the other hand, high evaporation rates can be maintained during the
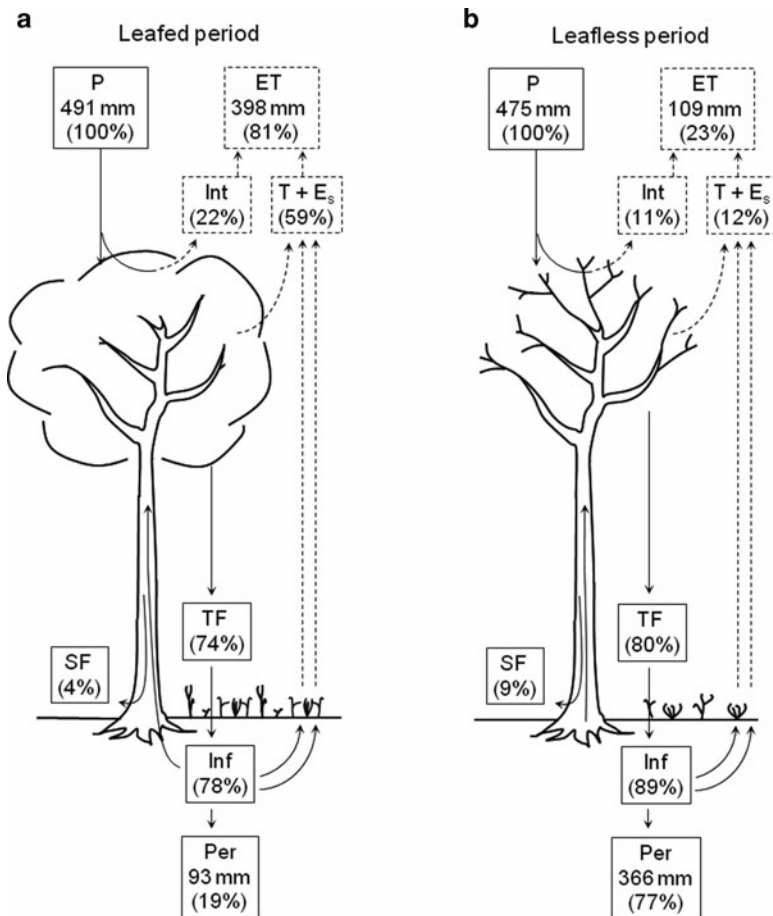
Fig. 26.1 Water balance of a broadleaved deciduous mixed oak forest (Belgium) averaged over four (**a**) leafed and (**b**) leafless periods (modified from Schnock 1971). *P* precipitation; *TF* throughfall; *SF* stemflow; *E* evaporation; *Int* interception evaporation; E_s soil evaporation; *T* transpiration; *ET* evapotranspiration; *Inf* infiltration; *Per* percolation. Seasonal changes in soil and biomass water storage were negligible and therefore not shown

leafless period because of seasonal changes in aerodynamic canopy properties and rainfall characteristics that compensate for the corresponding change in water storage capacity (Herbst et al. 2008b; Krämer and Hölscher 2009).

Because of the higher water storage capacity of leafed canopies, more rainfall is needed to induce throughfall than for leafless canopies. Thus, deciduous canopies have more influence on the spatial redistribution of throughfall water during the leafed season. For example, the spatial variation coefficient of throughfall beneath a European beech (*Fagus sylvatica* L.) canopy was 18 and 8% in the leafed and leafless period, respectively (Staelens et al. 2006), while values of 17 and 12%, respectively, were reported for a mixed deciduous forest (Herbst et al. 2008b).

When using the Gash model in deciduous forests, a separate parameterisation for the leafed and leafless periods is indispensible. Furthermore, an approach that tries to relate structural parameters in the model to the actual leaf area index (Van Dijk and Bruijnzeel 2001) might have the potential to improve the representation of seasonality in interception modelling of deciduous forests, but has not been subject to a wider testing yet. The principal difficulty in modelling rainfall interception in deciduous forests remains the representation of the leafless period, when the heterogeneity of the surfaces contributing to the total evaporation loss is larger than during the leafed period, due to a better coupling of the soil and the trunk space to the atmosphere. More research will be needed to gain a better understanding of the roles of the canopy, the tree trunks, the soil surface and the understory vegetation in the process of rainfall interception by leafless forests. Deciduous forests do not only face a seasonal climate but also seasonality with respect to the within-canopy gradients of the control variables of interception evaporation, which adds to the challenge of developing a physically sound and robust description of the process.

26.2.3 Stemflow

Stemflow of deciduous trees is generally a larger fraction of gross precipitation during the leafless season (Levia and Frost 2003) (Fig. 26.1). Canopy leaves can favour water collection, but also prevent branches from becoming wet and conducting water down the trunk (Herwitz and Levia 1997; Herbst et al. 2008b) and the latter increase of branch exposure to rainfall in leafless conditions appears to be more important. Correspondingly, the rainfall threshold for stemflow generation has been reported to be higher in the leafed period than in the leafless period (André et al. 2008; Staelens et al. 2008). However, greater stemflow generation in the leafed season, e.g., by tall stewartia (*Stewartia monadelpha* Siebold et Zucc.) suggested a positive effect of the presence of leaves on stemflow (Liang et al. 2009). No seasonal variation in stemflow of deciduous trees has been reported either (e.g., Deguchi et al. 2006). This indicates that the impact of seasonal defoliation on stemflow yield depends on corresponding seasonal changes in meteorological conditions, as stemflow generation can be promoted by lower evaporation rates

(Neal et al. 1993), lower rainfall rates (Crockford and Richardson 2000; Staelens et al. 2008) and higher wind speeds (Xiao et al. 2000; André et al. 2008). However, relationships between stemflow and rainfall or meteorological characteristics have not been reported frequently, particularly for species other than temperate oak and beech.

26.2.4 Transpiration

Since the work by Monteith (1965) it is well known that transpiration is influenced by both the available energy and the transport resistances to water vapour between the leaf interior and the atmosphere. Most forests are coupled well to the atmosphere and, as a consequence, their transpiration is controlled to a large extent by stomatal responses to the environment (Jarvis and McNaughton 1986). In other words, radiation, vapour pressure deficit and stomatal conductance (g_s) are the most influential factors for forest transpiration. There is thus an "imposed" seasonal variation in the transpiration rates through the seasonal changes in radiation and vapour pressure deficit. The stomatal conductance responds to these meteorological variables in such a way as it amplifies the influence of radiation (stomata open in the light) and moderates the influence of vapour pressure deficit (stomata close in dry air). The resulting seasonality in forest transpiration is predictable from the meteorological factors involved and well understood.

   In contrast, there is still a large uncertainty about seasonality where it is caused by different responses of the forest canopy and g_s in particular, to the same parameters in different seasons. This difference between seasons can be caused by (1) phenology in terms of differentiation and senescence of leaves, (2) acclimation of the foliage to the prevailing weather patterns and (3) external factors such as drought or defoliation. The relevance of these ubiquitous seasonal effects for the control of transpiration depends on the forest biome and the climatic challenges it faces. Some well-known examples of seasonal plant responses are listed in Table 26.1 and will be explained in the following sub-sections.

Table 26.1 Examples of seasonality in plant physiological control of forest transpiration

Biome	Climatological characteristics	Seasonal plant responses
Tropical and subtropical forests and savannah	Dry and wet seasons	Facultative reduction of leaf area; Osmotic adjustment of roots; Development of deep root systems
Mediterranean woodlands	Dry and hot summer season	Varying stomatal sensitivity to vapour pressure deficit; Development of deep root systems
Temperate and boreal deciduous forests	Short growing season with gradually varying meteorological factors	Leaf differentiation and acclimation; Asynchronous development of over- and understory canopies

26.2.4.1 Tropical and Subtropical Forests

Under seasonal rainfall conditions with extended drought periods trees have to cope with water shortage and thus have developed strategies that are often species specific to adjust at structural, physiological and chemical levels (Baldocchi and Xu 2007; Goldstein et al. 2008). Structural adjustment to dry periods includes reduction of leaf area or development of a deep root system, physiological control is exerted through strong stomatal regulation and roots may respond by the chemical mechanism of osmotic adjustment.

Monsoon forest of Thailand composed of evergreen species experiences a dry season of 5–7 months with a concurrent higher atmospheric evaporative demand. Nevertheless, canopy transpiration was maintained high even during the late dry season (Tanaka et al. 2003). During a more severe dry season in particular small statured trees were affected by the seasonal soil drought and reduced xylem sap flow (Kume et al. 2007) and the soil drought effect was confirmed by sap flow recovery in an irrigation experiment. It was suggested that shallow root systems of small trees and deeper roots of larger trees could be reasons for such differences. As in this study, experimental approaches may help to disentangle environmental drivers of transpiration during seasonal changes. Two stand level throughfall reduction experiments were conducted in Amazonian rainforest. A soil water model applied to the East-Central Amazonian rainforest suggested only a mild transpiration decline after 2 years of throughfall reduction (Belk et al. 2007), while in the Eastern Amazon a strong sap flux decline was found (Fisher et al. 2007). In an Indonesian cacao agroforest, throughfall reduction only moderately reduced tree sap flux rates (Schwendenmann et al. 2010). In contrast to the suggestions based on the monsoon forest in Thailand, here the shallow rooted cacao trees responded less than the deeper rooted shade trees. This may partly be explained by small amounts of throughfall entering gaps in this roof experiments but also by other factors such as osmotic adjustment in cacao roots (Moser et al. 2010).

Seasonal dynamics of tree sap flux and water use were also studied in Panamanian forest plantations (Kunert et al. 2010), where transpiration rates between the dry and wet season differed for six out of nine species. Three species showed 30–110% higher transpiration rates in the dry season than in the wet season, while three other species had 30–60% lower rates in the dry season. In Australian Eucalyptus open-forest, the evergreen tree species also exerted higher transpiration rates during the dry season than during the wet season, which is related to an increased evaporative demand and the use of groundwater (O'Grady et al. 1999).

In Amazonian floodplain forest, most species are evergreen but some shed leaves during the aquatic period. Xylem sap flux and tree water use in the deciduous species follow the seasonality in leaf phenology, whereas evergreens do not show a reduction of sap flux during flooding (Horna et al. 2011).

26.2.4.2 Mediterranean Woodlands

Forests in the Mediterranean climate face the challenge of dry conditions occurring during the period with the highest radiation and temperature, causing a particularly strong evaporative demand of the atmosphere. However, in contrast to other plant

types, many trees manage to maintain transpiration during the summer by use of deep roots (Paço et al. 2009). This means that Mediterranean forests show less seasonality in transpiration than other Mediterranean vegetation does, although a different response of g_s to vapour pressure deficit during the driest periods of the summer season has been reported (Paço et al. 2009). In other cases, rooting depth can completely compensate for the lack of rainfall during the summer, resulting in g_s being only related to irradiance and vapour pressure deficit, but not to moisture content in the top soil (García-Santos et al. 2009). Due to this species-specific ability to access water from deep soil layers, satellite-based data of seasonality in evapo-transpiration can be used to infer rooting depths (Ichii et al. 2009).

Further mechanisms in the response to drought by Mediterranean forest transpiration include hydraulic adjustment and functional changes in trees due to xylem embolism. The evergreen species holm oak (*Quercus ilex* L.) may maintain transpiration during drought at the risk of allowing some embolism (Martinez-Vilalta et al. 2002). High losses of xylem conductivity have also been reported for this species (Tognetti et al. 1998), which can act as a mechanism to save water. In a 4-year throughfall exclusion experiment in southern France, a *Q. ilex* forest reduced water transport capacity jointly with a reduction in leaf transpiring area (Limousin et al. 2009).

26.2.4.3   Temperate Forests

In temperate deciduous forests it has often been observed that g_s responds differently to environmental factors over the course of the season, because leaf area index and even more so physiological leaf differentiation, lack behind the increase in available energy in spring and early summer (Morecroft and Roberts 1999; Morecroft et al. 2003). The speed of leaf differentiation, as well as the time of leaf emergence and senescence, is species specific. In the absence of soil drought, common ash (*Fraxinus excelsior* L.) and pedunculate oak (*Quercus robur* L.) are known to reach their highest g_s late in the growing season (Herbst et al. 2008a) whilst European beech develops the maximum g_s already in the early summer (Kutsch et al. 2001). From further recent studies a tendency appears that diffuse porous trees in general have an earlier seasonal peak in transpiration compared to ring porous trees (Bush et al. 2008; Peters et al. 2010). Since ring porous species are highly vulnerable to xylem cavitation, they often have a more sensitive stomatal regulation as an avoidance strategy (Bush et al. 2008) to reduce transpiration in the early parts of the summer when radiation and vapour pressure deficit are highest. Another aspect of seasonality in the response of g_s is its variation in the dark (Bowden and Bauerle 2008) that influences night-time transpiration. And finally, defoliation by insects (see Chap. 28) can have a substantial effect on the gas exchange of forest canopies (Schäfer et al. 2010) and thus adds to the seasonality of forest transpiration.

According to the widely accepted leaf physiology model by Ball et al. (1987), g_s is closely related to leaf photosynthesis, so that seasonality in the status of the photosynthetic apparatus in the leaves (Misson et al. 2006) can influence g_s and

forest transpiration, too. It is still a matter of debate, to what extent temporal variations in photosynthetic responses to the environment are driven by phenology or by acclimation to mid-term weather patterns, respectively. However, there is growing evidence that acclimation plays an important role for both water and carbon balances of forests (Kutsch et al. 2001; Gunderson et al. 2010).

26.2.4.4 Transpiration from Understory Vegetation

When the forest floor is vegetated, the understory can contribute significantly to forest transpiration. In many situations, the forest floor is decoupled from the atmosphere to a large extent, which leaves the usually small radiation input as the main driving factor. However, the transpiration of the ground vegetation requires sufficient moisture in the top soil, so that in regions with distinct dry and wet seasons the understory transpiration often ceases completely during drought periods (Goldstein et al. 2008; Paço et al. 2009), which alters the seasonality in stand transpiration as predicted from tree physiology only.

A big uncertainty, however, remains for deciduous forests in the temperate and boreal regions. Most species contributing to the ground vegetation in temperate deciduous forests develop their leaves in early spring, well ahead of the onset of budburst in the trees. Due to this phenological specialization the understory can contribute substantially to forest transpiration in the spring and cause an earlier start of the hydrological season than predicted from tree phenology (Roberts et al. 2005). Research in a boreal larch (*Larix cajanderi* Mayr) forest has shown that in this deciduous coniferous forest type the evapotranspiration from the understory is substantial through the whole snow-free period, although its relative contribution to ecosystem evapotranspiration varies seasonally with the development of the overstory canopy (Iida et al. 2009).

26.2.5 Soil Water Uptake and Partitioning

The effect of seasonal or inter-annual drought on ecosystem processes such as transpiration depends on the amount of water stored in the soil profile, the plants' ability to extract this water and their ability to withstand the stress induced as moisture is depleted. During drought in Amazonian forest, deep roots and the uptake of soil water down to great depths contributed significantly to the tree water use (Nepstad et al. 1994; Jipp et al. 1998). In a species-rich Panamanian primary forest, studies based on the natural abundance of hydrogen isotopes pointed to a spatial and temporal partitioning of water resources among tree species (Jackson et al. 1995; Meinzer et al. 1999). During the dry season, evergreen trees were able to exploit progressively deeper sources of soil water and were also able to maintain constant or even increased rates of water use (Meinzer et al. 1999). In a neotropical savanna, large species-specific differences in soil water uptake patterns

were found between deciduous and evergreen trees and among evergreen tree species (Goldstein et al. 2008). Vertical partitioning of water uptake has also been found in an Indonesian agroforestry system. The natural abundance of oxygen and hydrogen isotopes suggested that cacao primarily obtained water from the upper soil profile while the shade trees obtained their water primarily from greater soil depths (Schwendenmann et al. 2010).

To cope with seasonal drought, hydraulic redistribution of soil moisture by plant root systems from relatively wet soil layers to dryer soil layers is an important mechanism. Via hydraulic redistribution water can move passively through the roots upward (hydraulic lift) or downward, whenever a gradient in soil water potential exists among soil layers which is stronger than the overall gradient between soil and atmosphere, e.g., during the night when evaporative demand is low (Burgess et al. 1998; Caldwell et al. 1998). In terms of total evaporation, the contribution of hydrological redistribution is not very high but it can play an important role in maintaining fine root activity under dry conditions. Hydraulically lifted water may not only be beneficial for deep rooting species but may also influence the performance of co-occurring other plant species (Richards and Caldwell 1987; Moreira et al. 2000).

26.2.6 Water Percolation

The amount of water percolating through the forest soil is determined by the net precipitation amount entering the forest floor by throughfall and stemflow, the water stored in the forest floor and the water disappearing by evapotranspiration (Fig. 26.1). During wet seasons, when the water input to the soil surface is high, water percolates generally downward and the rate of infiltration is mainly determined by soil texture and structure. During dry seasons, when there is a net loss of water by evapotranspiration, upward movements may occur (see Sect. 26.2.5).

The forest floor generally has a high moisture-holding capacity and therefore plays an important role for water percolation into the mineral soil. Only water in excess of the water-holding capacity will percolate in the mineral soil. In dry seasons, forest floors can considerably dry out and water repellency is a frequently occurring phenomenon that has been reported in many forest types and regions (Zavala et al. 2009), particularly in Mediterranean soils during and immediately after the dry season. Water repellency strongly declines the water storage capacity of the forest floor and, below a certain moisture threshold, water infiltration into the mineral soil can be considerably impeded, which causes reduced soil percolation rates, enhanced runoff flow and soil erosion (Burch et al. 1989). Frequently, forest floor horizons are neglected in water balance calculations for forest ecosystems, which might be problematic in regions with water repellency problems (Greiffenhagen et al. 2006). Future research is particularly needed for the inverse process of the dynamics of forest floor remoistening.

Another seasonal process affecting water percolation in the mineral soil is the meltdown of snow, which can create considerable amounts of meltwater in a short time span (see Chap. 27). The infiltration of meltwater into the forest floor and mineral soil depends on the ice content of soil pores. When soils are not frozen, large amounts of meltwater will infiltrate and percolate, while in frozen soils, percolation is limited and runoff is generated when the forest floor reaches saturation.

26.3 Seasonality of Biogeochemical Fluxes

26.3.1 Wet and Dry Deposition

Varying seasonal patterns have been reported for the fluxes of major ions in throughfall and stemflow, as a result of seasonal changes in wet deposition, dry deposition and canopy exchange processes. Wet deposition does not depend on the receiving surface area and is consequently not affected by canopy phenology, in contrast to dry deposition. Seasonal variations in the concentration of atmospheric gases and their reaction products can be explained by temporal trends in emissions and meteorological parameters like temperature, humidity and the build-up of inversion layers (Plessow et al. 2005). For example, temporal changes in ambient ammonia concentrations are related to increased emissions by manure spreading in spring and higher temperatures during summer (van Pul et al. 2004). Seasonal trends in both wet and dry deposition also occur as a result of changes in wind speed and direction, which influence the origin of the compounds deposited onto forest canopies. In areas close to the sea, higher wind speeds in winter can enhance sea spray and result in meaningful increases of wet and dry deposited sodium, chlorine and magnesium (Staelens et al. 2007). Seasonal burning of forest and pasture in tropical regions has been reported to strongly influence the time dynamics of dry deposition (Hölscher et al. 1998; Germer et al. 2007). In southern Europe, there is seasonality in dry deposition related to dust intrusions originating from the Sahara and Sahel deserts (Stuut et al. 2009). The temporal distribution of precipitation is important as well, as longer dry periods enhance ion concentrations in throughfall (Lovett et al. 1996; Zhang et al. 2006), particularly at the beginning of a rain event (Hansen et al. 1994). Low rainfall intensities can result in slow and incomplete wash-off of dry deposition (Zimmermann et al. 2007).

Because of seasonal variations in emissions and meteorology, assessing the effects of canopy phenology on dry deposition is not straightforward. The higher collecting surface area of a leafed deciduous canopy can promote the dry deposition of gases and particles. However, other factors affecting turbulent transport such as wind speed and canopy closure are important too, as well as factors that influence the surface conditions like precipitation, relative humidity and net radiation (Erisman and Draaijers 2003). Dry deposition of particles onto leafless canopies can be considerable (Staelens et al. 2007) due to the increased atmospheric

turbulence within defoliated canopies (Beckett et al. 2000) and higher wind speeds in winter. The effect of the branching structure of trees on dry deposition is also indicated by the spatial variation of ion fluxes in the throughfall beneath leafless deciduous canopies, which may be as large as during the leafed period (e.g., Staelens et al. 2006).

26.3.2 Canopy Exchange Processes

26.3.2.1 Canopy Gas Exchange

Leaf and canopy exchange of carbon dioxide (CO_2) depends on assimilation and respiration. Assimilation is strongly dependent on solar radiation as energy input, but it can acclimate to some extent to the prevailing temperature (Gunderson et al. 2010). As a consequence, its seasonal variation often follows the annual course of irradiance and is largest at high latitudes (Falge et al. 2002). In deciduous forests this seasonality is intensified because after leaf emergence it takes time for the photosynthetic apparatus to develop fully. Respiration is mainly controlled by temperature and therefore its seasonal course closely tracks the changes in air temperature whose maximum often occurs later in the season than the radiation maximum. A well-documented example for the resulting effects on leaf and canopy CO_2 exchange is European beech, which has the highest CO_2 uptake early in the summer and the highest respiration rates considerably later (Kutsch et al. 2001; Pilegaard et al. 2001). This means that, in many forest canopies, uptake and release of CO_2 differ in their seasonality. This is important for the analysis and interpretation of the increasing amount of net ecosystem CO_2 exchange data (comprising both assimilation and respiration) from flux towers all around the world (Falge et al. 2002).

Other gases such as oxidized and reduced nitrogen (NH_3, NO, NO_2), sulphur dioxide (SO_2) and ozone (O_3) are also exchanged between the atmosphere and forest canopies and this occurs mainly via the stomata. Dry deposited HNO_3 is thought not be taken up by leaf stomata, but primarily deposited to leaf cuticles (Sparks 2009). Under ambient concentrations, net gas uptake has been reported, except for NH_3, which has a relatively high compensation point (Sparks 2009). The primary control of foliar gas uptake is the size of the stomatal aperture. Consequently, uptake rates depend on g_s as well as on the ambient gas concentration, both of which can have seasonal patterns (see Sects. 26.2.4 and 26.3.1).

26.3.2.2 Canopy Exchange of Dissolved Elements

The exchange of dissolved elements between a forest canopy and passing rainwater includes leaching and retention of ions by foliage, twigs and lichens and is affected by the physiological status of the canopy and by precipitation characteristics.

Canopy leaching of potassium, magnesium, calcium and accompanying weak organic acids (Zhang et al. 2006) is strongly related to tree phenology, as leaching of these elements is generally higher in the growing season compared to the dormant season. Enhanced canopy leaching has been observed for emerging and senescing leaves as well. This is well known for potassium (Lovett et al. 1996) but also holds true for elements such as sodium and chlorine (Staelens et al. 2008; Thimonier et al. 2008), which have often been considered as conservative elements. Also canopy uptake and assimilation of dissolved inorganic nitrogen (ammonium and nitrate) is influenced by leaf phenology (Houle et al. 1999). Buffering of throughfall pH by deciduous forest canopies is most pronounced during the leafed season (Pryor and Barthelmie 2005).

Precipitation characteristics reported to affect ion exchange are event duration, intensity, size and chemical composition. Low intensities increase the contact time between foliage and throughfall (Hansen et al. 1994) while canopy ion pools are emptied more slowly than under heavy intensity rainfall. Seasonal changes in precipitation chemistry can have meaningful effects on canopy leaching of calcium, while leaching of potassium is controlled mainly by the rainfall quantity of an event (e.g., Zhang et al. 2006).

Canopy exchange of dissolved ions is affected by properties of the leaf surface as well, but direct relationships have rarely been reported. Leaf wettability can increase over time due to degradation of the epicuticular wax structure of leaves (Sase et al. 2008) and has been related to accelerated leaching of potassium and magnesium (Bouya et al. 1999) and enhanced canopy uptake of ammonium and nitrate (Sase et al. 2008; Adriaenssens et al. in press). There is a need to relate observations on biogeochemical canopy processes to quantitative leaf traits and canopy characteristics. Studies relating canopy exchange to stomatal characteristics, specific leaf area, wettability, branch angles and bark morphology could help generalizing results obtained for specific tree species and phenological periods.

26.3.3   Soil Nutrient Fluxes

26.3.3.1   Soil Nutrient Uptake

Plant activity and hydrological fluxes are important driving forces of the seasonal dynamics of biogeochemical cycling. Belowground nutrient uptake by plants is determined by the availability and distribution of nutrients in the soil solution and by the amount of water and its transport rate to the roots. Hydraulically lifted water (see Sect. 26.2.5) may promote the activity of mycorrhizas and symbiotic nitrogen fixing bacteria as the bulk soil in the upper portion of the profile dries. Even small amounts of water provided to mycorrhizas by hydraulic redistribution may maintain hyphal viability and facilitate nutrient uptake under drying conditions, which may provide an advantage to seedlings that are hydraulically linked by common mycorrhizal networks to large trees (Warren et al. 2008).

26.3.3.2 Soil Gas Exchange

Emission and uptake of gases by forest soils is affected by seasonal changes in plant productivity and climatic variables. In temperate forests, about 70% of the total ecosystem respiration comes from the soil (Ryan and Law 2005). Soil respiration comprises autotrophic and heterotrophic processes that utilize assimilates allocated to the root zone. Thus, the supply of photosynthetic products is an important control factor and especially the autotrophic component depends on the supply of fresh assimilates which induces seasonality (Högberg et al. 2009). In contrast, heterotrophic respiration in forest soils can utilize carbon much older than 1 year, which rules out seasonality linked to seasonal variations in canopy assimilation (Trumbore 2000). Like leaf respiration, soil CO_2 emission is primarily controlled by temperature (Lloyd and Taylor 1994). However, it is well known that the temperature response is strongly modified by the soil moisture content (Howard and Howard 1993), as both drought and wetness influence heterotrophic respiration. This results in a distinct seasonality of soil respiration and its temperature dependence where soil moisture varies seasonally. Nevertheless, many studies have found that also the temperature response itself changes during the year and acclimates to the prevailing temperatures (Janssens and Pilegaard 2003). The importance of short wetting pulses for seasonality and annual totals of soil respiration has only recently been discussed (Borken and Matzner 2009; Savage et al. 2009) and needs to be investigated further. Freeze–thaw cycles also affect soil CO_2 emission, but there is strong evidence that, at the annual timescale, this has little effect or even reduces soil carbon loss compared to unfrozen conditions (Matzner and Borken 2008). There is a large amount of scientific literature about the variability of soil respiration and we refer to Davidson et al. (2006) for an overview of the current knowledge about seasonality in soil respiration and for future research directions.

While temperature has little effect on the activity of methane (CH_4) consuming soil bacteria, CH_4 uptake by forest soils is negatively correlated with soil moisture under most nondrought conditions (Borken et al. 2006). Emission of nitrogen trace gases (NO, N_2O and N_2) from forest floors and soils mainly depends on microbial denitrification and nitrification processes that are affected by moisture content. However, periods of drought can turn a forest soil from a N_2O source to a transient sink for atmospheric N_2O (Billings 2008; Goldberg and Gebauer 2009). In contrast to CO_2, enhanced emission of N_2O due to freeze–thaw cycles may be relevant for annual nitrogen budgets (Matzner and Borken 2008).

26.3.3.3 Soil Leaching

Rewetting after seasonal droughts can intensify mineralization and nitrification processes in forest ecosystems, with consequently high losses of dissolved carbon and nitrogen. However, there is much controversy on the final result of dry–wet cycles. According to Borken and Matzner (2009), wetting pulses cannot compensate for the smaller mineralization rates during drought periods. For example, in a spruce

forest soil, dry–wet cycles were found to reduce net N mineralization and percolation due to both water stress during the drying phase as well as to incomplete remoistening during the wetting phase because of hydrophobicity of organic layers (Hentschel et al. 2007).

Soil frost may cause increased nitrate leaching from forest soils (Matzner and Borken 2008). Callesen et al. (2007) reported maximum nitrate leaching fluxes in a Norway spruce forest in periods following soil thawing. However, Hentschel et al. (2007) did not find evidence that moderate soil frost triggers leaching losses of nitrogen, carbon and mineral ions from temperate forest soils. In case of enhanced nitrate leaching, also fluxes of potassium, magnesium and calcium might be affected. Overall, the effects of freezing and thawing of forest soils on the turnover and leaching of carbon and nutrients are far from being predictable (Hentschel et al. 2007). Soil conditions are likely to have a strong influence (Matzner and Borken 2008) and generalizations are still hampered by the lack of field experiments on this subject.

26.4   Conclusions and Future Directions

This chapter highlights that seasonality in hydrology and biogeochemistry matters in all forests, including tropical ecosystems. Environmental factors such as precipitation, radiation and air humidity often change simultaneously over time and affect canopy interception and the amount of throughfall and stemflow that replenish soil moisture. Phenological rhythms may go parallel to these seasonal changes, but the response of trees can vary considerably between species. Consequently, future research should not be reduced to global flux networks that average hydrological and biogeochemical fluxes over large areas, but should be complemented with studies at the tree or plot scale. The seasonality of biogeochemical processes is more complex than of hydrological processes and does not necessarily follow the same patterns. To examine the effect of canopy phenology on forest functioning, observational studies need to account for variations in other factors. In addition, experimental approaches such as irrigation, rainfall reduction, fertilization or litter addition may help to improve our understanding of the driving forces of observed changes in vegetation performance and biogeochemical fluxes. With respect to transpiration, stomatal behaviour and CO_2 fluxes from soils and canopies, a stronger focus might be needed on acclimation in data analysis as well as experimental methods in order to use our knowledge about seasonality for predicting global change scenarios. Compared to the comprehension of leafed deciduous forests, there is relatively little information on the interaction between the atmosphere and leafless tree canopies. Finally, seasonal changes in soil processes can affect carbon and nutrient budgets at the annual scale, but are still not yet fully understood.

References

Adriaenssens S, Staelens J, Wuyts K et al (in press) Foliar nitrogen uptake from wet deposition and the relation with leaf wettability and water storage capacity. Water Air Soil Pollut. doi:10.1007/s11270-010-0682-8

André F, Jonard M, Ponette Q (2008) Influence of species and rain event characteristics on stemflow volume in a temperate mixed oak-beech stand. Hydrol Process 22:4455–4466

Baldocchi DD, Xu L (2007) What limits evaporation from Mediterranean oak woodlands – the supply of moisture in the soil, physiological control by plants or the demand by the atmosphere? Adv Water Resour 30:2113–2122

Ball JT, Woodrow IE, Berry JA (1987) A model predicting stomatal conductance and its contribution to the control of photosynthesis under different environmental conditions. In: Biggens J (ed) Progress in photosynthesis research, vol IV. Martinus Nijhoff Publishers, Dordrecht, pp 5.221–5.224

Beckett KP, Freer-Smith PH, Taylor G (2000) Particulate pollution capture by urban trees: effect of species and windspeed. Global Change Biol 6:995–1003

Belk EL, Markewitz D, Rasmussen TC et al (2007) Modeling the effects of throughfall reduction on soil water content in a Brazilian Oxisol under a moist tropical forest. Water Resour Res 43: W08432

Billings SA (2008) Biogeochemistry: nitrous oxide in flux. Nature 456:888–889

Borken W, Matzner E (2009) Reappraisal of drying and wetting effects on C and N mineralization and fluxes in soils. Global Change Biol 15:808–824

Borken W, Davidson EA, Savage K et al (2006) Effect of summer throughfall exclusion, summer drought, and winter snow cover on methane fluxes in a temperate forest soil. Soil Biol Biochem 38:1388–1395

Bouya D, Myttenaere C, Weissen F et al (1999) Needle permeability of Norway spruce (*Picea abies* (L.) Karst.) as influenced by magnesium nutrition. Belg J Bot 132:105–118

Bowden JD, Bauerle WL (2008) Measuring and modeling the variation in species-specific transpiration in temperate deciduous hardwoods. Tree Physiol 28:1675–1683

Brauman KA, Freyberg DL, Daily GC (2010) Forest structure influences on rainfall partitioning and cloud interception: a comparison of native forest sites in Kona, Hawai'i. Agric For Meteorol 150:265–275

Burch GJ, Moore ID, Burns J (1989) Soil hydrophobic effects on infiltration and catchment runoff. Hydrol Process 3:211–222

Burgess SSO, Adams MA, Turner NC et al (1998) The redistribution of soil water by tree root systems. Oecologia 115:306–311

Bush SE, Pataki DE, Holtine KR et al (2008) Wood anatomy constrains stomatal responses to atmospheric vapor pressure deficit in irrigated, urban trees. Oecologia 156:13–20

Caldwell MM, Dawson TE, Richards JH (1998) Hydraulic lift: consequences of water efflux from the roots of plants. Oecologia 113:151–161

Callesen I, Borken W, Kalbitz K et al (2007) Long-term development of nitrogen fluxes in a coniferous ecosystem: does soil freezing trigger nitrate leaching? J Plant Nutr Soil Sci 170:189–196

Clark DB, Clark DA, Oberbauer SF (2009) Annual wood production in a tropical rain forest in NE Costa Rica linked to climatic variation but not to increasing CO_2. Global Change Biol 16:747–759

Crockford RH, Richardson DP (2000) Partitioning of rainfall into throughfall, stemflow and interception: effect of forest type, ground cover and climate. Hydrol Process 14:2903–2920

Davidson EA, Janssens IA, Luo Y (2006) On the variability of respiration in terrestrial ecosystems: moving beyond Q_{10}. Global Change Biol 12:154–164

Deguchi A, Hattori S, Park H-T (2006) The influence of seasonal changes in canopy structure on interception loss: application of the revised Gash model. J Hydrol 318:80–102

Dolman AJ, Moors EJ, Grünwald T et al (2003) Factors controlling forest atmosphere exchange of water, energy, and carbon. In: Valentini R (ed) Fluxes of carbon, water and energy of European forests. Springer, Heidelberg, pp 207–223

Erisman JW, Draaijers G (2003) Deposition to forests in Europe: most important factors influencing dry deposition and models used for generalisation. Environ Pollut 124:379–388

Falge E, Baldocchi D, Tenhunen J et al (2002) Seasonality of ecosystem respiration and gross primary production as derived from FLUXNET measurements. Agric For Meteorol 113:53–74

Fisher RA, Williams M, da Costa AL et al (2007) The response of an eastern Amazonian rain forest to drought stress: results and modelling analyses from a throughfall exclusion experiment. Global Change Biol 13(573):2361–2378

García-Santos G, Bruijnzeel LA (in press) Rainfall, fog and throughfall dynamics in a subtropical ridge-top cloud forest, National Park of Garajonay (La Gomera, Canary Islands, Spain). Hydrol Process. doi:10.1002/hyp.7760

García-Santos G, Bruijnzeel LA, Dolman AJ (2009) Modelling canopy conductance under wet and dry conditions in a subtropical cloud forest. Agric For Meteorol 149:1565–1572

Gash JHC (1979) An analytical model of rainfall interception by forests. Q J R Meteorol Soc 105:43–55

Gash JHC, Lloyd CR, Lachaud G (1995) Estimating sparse forest rainfall interception with an analytical model. J Hydrol 170:79–86

Germer S, Neill C, Krusche AV et al (2007) Seasonal and within-event dynamics of rainfall and throughfall chemistry in an open tropical rainforest in Rondônia, Brazil. Biogeochemistry 86:155–174

Goldberg SD, Gebauer G (2009) Drought turns a Central European Norway spruce forest soil from an N_2O source to a transient N_2O sink. Global Change Biol 15:850–860

Goldstein G, Meinzer FC, Bucci SJ et al (2008) Water economy of neotropical savanna trees: six paradigms revisited. Tree Physiol 28:395–404

Granier A, Reichstein M, Bréda N et al (2007) Evidence for soil water control on carbon and water dynamics in European forests during the extremely dry year: 2003. Agric For Meteorol 143:123–145

Greiffenhagen A, Wessolek G, Facklam M et al (2006) Hydraulic functions and water repellency of forest floor horizons on sandy soils. Geoderma 132:182–195

Gunderson CA, O'Hara KH, Campion CM et al (2010) Thermal plasticity of photosynthesis: the role of acclimation in forest responses to a warming climate. Global Change Biol 16:2272–2286

Hansen K, Draaijers GPJ, Ivens WMPF et al (1994) Concentration variations in rain and canopy throughfall collected sequentially during individual rain events. Atmos Environ 28:3195–3205

Hentschel K, Borken W, Matzner E (2007) Leaching losses of inorganic N and DOC following repeated drying and wetting of a spruce forest soil. Plant Soil 300:21–34

Herbst M, Rosier PTW, McNeil DD et al (2008a) Seasonal variability of interception evaporation from the canopy of a mixed deciduous forest. Agric For Meteorol 148:1655–1667

Herbst M, Rosier PTW, Morecroft MD et al (2008b) Comparative measurements of transpiration and canopy conductance in two mixed deciduous woodlands differing in structure and species composition. Tree Physiol 28:959–970

Herwitz SR, Levia DF (1997) Mid-winter stemflow drainage from bigtooth aspen (*Populus grandidentata* Michx.) in central Massachusetts. Hydrol Process 11:169–175

Högberg P, Bhupinderpal-Singh, Ottosson-Löfvenius M et al (2009) Partitioning soil respiration into its autotrophic and heterotrophic components by means of tree-girdling in old boreal spruce forest. Forest Ecol Manage 257:1764–1767

Hölscher D, De A, Sá TD, Möller RF et al (1998) Rainfall partitioning and related hydrochemical fluxes in a diverse and in a mono specific (*Phenakospermum guyannense*) secondary vegetation stand in eastern Amazonia. Oecologia 114:251–257

Horna V, Zimmermann R, Müller E et al (2011) Sap flux and stem respiration. In: Junk WJ, Piedade MTF et al (eds) Amazonian floodplain forests: ecophysiology, biodiversity and sustainable management. Ecological studies 210, Springer, Heidelberg, pp 223–241

Horton RE (1919) Rainfall interception. Mon Weather Rev 47:603–623

Houle D, Ouimet R, Paquin R et al (1999) Interactions of atmospheric deposition with a mixed hardwood and coniferous forest canopy at the Lake Clair Watershed (Duchesnay, Quebec). Can J For Res 29:1944–1957

Howard DM, Howard PJA (1993) Relationships between CO_2 evolution, moisture content and temperature for a range of soil types. Soil Biol Biochem 25:1537–1546

Ichii K, Wang W, Hashimoto H et al (2009) Refinement of rooting depths using satellite-based evapotranspiration seasonality for ecosystem modelling in California. Agric For Meteorol 149:1907–1918

Iida S, Ohta T, Matsumoto K et al (2009) Evapotranspiration from understory vegetation in an eastern Siberian boreal larch forest. Agric For Meteorol 149:1129–1139

Jackson PC, Cavelier J, Goldstein G et al (1995) Partitioning of water sources among plants of a lowland tropical forest. Oecologia 101:197–203

Janssens IA, Pilegaard K (2003) Large seasonal changes in Q_{10} of soil respiration in a beech forest. Global Change Biol 9:911–918

Jarvis PG, McNaughton KG (1986) Stomatal control of transpiration: scaling up from leaf to region. Adv Ecol Res 15:1–49

Jipp P, Nepstad DC, Cassel K et al (1998) Deep soil moisture storage and transpiration in forests and pastures of seasonally-dry Amazonia. Clim Change 39:395–412

Junk WJ, Piedade MTF, Parolin P et al (eds) (2011) Amazonian floodplain forests: ecophysiology, biodiversity and sustainable management. Ecological studies 210, Springer, Heidelberg

Krämer I, Hölscher D (2009) Rainfall partitioning along a tree diversity gradient in a deciduous old-growth forest in Central Germany. Ecohydrology 2:102–114

Kume T, Takizawac H, Yoshifujib N et al (2007) Impact of soil drought on sap flow and water status of evergreen trees in a tropical monsoon forest in northern Thailand. For Ecol Manage 238:220–230

Kunert N, Schwendenmann L, Hölscher D (2010) Seasonal dynamics of tree sap flux and water use in nine species in Panamanian forest plantations. Agric For Meteorol 150: 411–419

Kutsch WL, Herbst M, Vanselow R et al (2001) Stomatal acclimation influences water and carbon fluxes of a beech canopy in northern Germany. Basic Appl Ecol 2:265–281

Levia DF, Frost EE (2003) A review and evaluation of stemflow literature in the hydrologic and biogeochemical cycles of forested and agricultural ecosystems. J Hydrol 274:1–29

Liang W-L, Kosugi K, Mizuyama T (2009) Characteristics of stemflow for tall stewartia (*Stewartia monadelpha*) growing on a hillslope. J Hydrol 378:168–178

Limousin JM, Rambal S, Ourcival JM et al (2009) Long-term transpiration change with rainfall decline in a Mediterranean *Quercus ilex* forest. Glob Change Biol 15:2163–2175

Link TE, Unsworth M, Marks D (2004) The dynamics of rainfall interception by a seasonal temperate rainforest. Agric For Meteorol 124:171–191

Lloyd J, Taylor JA (1994) On the temperature dependence of soil respiration. Funct Ecol 8:315–323

Lovett GM, Nolan SS, Driscoll CT et al (1996) Factors regulating throughfall flux in a New Hampshire forested landscape. Can J For Res 26:2134–2144

Martinez-Vilalta J, Prat E, Oliveras I et al (2002) Xylem hydraulic properties of roots and stems of nine Mediterranean woody species. Oecologia 133:19–29

Matzner E, Borken W (2008) Do freeze-thaw events enhance C and N losses from soils of different ecosystems? A review. Eur J Soil Sci 59:274–284

Meinzer FC, Andrade JL, Goldstein G et al (1999) Partitioning of soil water among canopy trees in a seasonally dry tropical forest. Oecologia 121:293–301

Misson L, Tu KP, Boniello RA et al (2006) Seasonality of photosynthetic parameters in a multi-specific and vertically complex forest ecosystem in the Sierra Nevada of California. Tree Physiol 26:729–741

Monteith JL (1965) Evaporation and environment. Symp Soc Exp Biol 19:205–234

Morecroft MD, Roberts JM (1999) Photosynthesis and stomatal conductance of mature canopy oak (*Quercus pubescens*) and sycamore (*Acer pseudoplatanus*) trees throughout the growing season. Funct Ecol 13:332–342

Morecroft MD, Stokes VJ, Morison JIL (2003) Seasonal changes in the photosynthetic capacity of canopy oak (*Quercus pubescens*) leaves: the impact of slow development on annual carbon uptake. Int J Biometeorol 47:221–226

Moreira MZ, Sternberg L, da SL, Nepstad DC (2000) Vertical patterns of soil water uptake by plants in a primary forest and an abandoned pasture in the eastern Amazon: an isotopic approach. Plant Soil 222:95–107

Moser G, Leuschner C, Hertel D et al (2010) Response of cocoa trees (*Theobroma cacao*) to a 13-month desiccation period in Sulawesi, Indonesia. Agrofor Syst 79:171–187

Muzylo A, Llorens P, Valente F et al (2009) A review of rainfall interception modelling. J Hydrol 370:191–206

Neal C, Robson AJ, Bhardwaj CL et al (1993) Relationships between precipitation, stemflow and throughfall for a lowland beech plantation, Black Wood, Hampshire, southern England: findings on interception at a forest edge and the effects of storm damage. J Hydrol 146:221–233

Nepstad DC, Carvalho CJR, Davidson EA et al (1994) The role of deep roots in the hydrological and carbon cycles of Amazonian forests and pastures. Nature 372:666–669

O'Grady AP, Eamus D, Hutley LB (1999) Transpiration increases during dry season, patterns of tree water use in eucalypt open-forests of northern Australia. Tree Physiol 19:591–597

Paço TA, David TS, Henriques MO et al (2009) Evapotranspiration from a Mediterranean evergreen oak savannah: the role of trees and pasture. J Hydrol 369:98–106

Peters EB, McFadden JP, Montgomery RA (2010) Biological and environmental controls on tree transpiration in a suburban landscape. J Geophys Res 115:G04006

Pilegaard K, Hummeshoj P, Jensen NO et al (2001) Two years of continuous CO_2 eddy-flux measurements over a Danish beech forest. Agric For Meteorol 107:29–41

Plessow K, Spindler G, Zimmermann F et al (2005) Seasonal variations and interactions of N-containing gases and particles over a coniferous forest, Saxony, Germany. Atmos Environ 39:6995–7007

Pryor SC, Barthelmie RJ (2005) Liquid and chemical fluxes in precipitation, throughfall and stemflow: observations from a deciduous forest and a red pine plantation in the midwestern U. S.A. Water Air Soil Pollut 163:203–227

Richards JH, Caldwell MM (1987) Hydraulic lift – substantial nocturnal water transport between soil layers by *Artemisia tridentata* roots. Oecologia 73:486–489

Roberts JM, Rosier PTW, Smith DM (2005) The impact of broadleaved woodland on water resources in lowland UK: II. A comparison of evaporation estimates made from sensible heat flux measurements over beech woodland and grass on chalk sites in Hampshire. Hydrol Earth Sys Sci 9:607–613

Ryan MG, Law BE (2005) Interpreting, measuring, and modelling soil respiration. Biogeochemistry 73:3–27

Sase H, Takahashi A, Sato M et al (2008) Seasonal variation in the atmospheric deposition of inorganic constituents and canopy interactions in a Japanese cedar forest. Environ Pollut 152:1–10

Savage K, Davidson EA, Richardson AD et al (2009) Three scales of temporal resolution from automated soil respiration measurements. Agric For Meteorol 149:2012–2021

Schäfer KVR, Clark KL, Skowronski N et al (2010) Impact of insect defoliation on forest carbon balance as assessed with a canopy assimilation model. Global Change Biol 16:546–560

Schnock G (1971) Le bilan d'eau dans l'écosystème forêt. Application à une chênaie mélangée de haute Belgique. In: Duvigneaud P (ed) Productivité des écosystèmes forestiers. UNESCO, Paris

Schwendenmann L, Veldkamp E, Moser G et al (2010) Effects of an experimental drought on the functioning of a cacao agroforestry system, Sulawesi, Indonesia. Global Change Biol 16:1515–1530

Sparks JP (2009) Ecological ramifications of the direct foliar uptake of nitrogen. Oecologia 159:1–13

Staelens J, De Schrijver A, Verheyen K et al (2006) Spatial variability and temporal stability of throughfall water under a dominant beech (*Fagus sylvativa* L.) tree in relationship to canopy cover. J Hydrol 330:651–662

Staelens J, De Schrijver A, Verheyen K (2007) Seasonal variation in throughfall and stemflow chemistry beneath a European beech (*Fagus sylvatica*) tree in relation to canopy phenology. Can J For Res 37:1359–1372

Staelens J, De Schrijver A, Verheyen NEC et al (2008) Rainfall partitioning into throughfall, stemflow, and interception within a single beech (*Fagus sylvatica* L.) canopy: influence of foliation, rain event characteristics, and meteorology. Hydrol Process 22:33–45

Stuut J-B, Smalley I, O'Hara-Dhand K (2009) Aelian dust in Europe: African sources and European deposits. Quatern Int 198:234–245

Tanaka K, Takizawa H, Tanaka N et al (2003) Transpiration peak over a hill evergreen forest in northern Thailand in the late dry season: assessing the seasonal changes on evapotranspiration using a multilayer model. J Geophys Res 108:D4533

Thimonier A, Schmitt M, Waldner P et al (2008) Seasonality of the Na/Cl ratio in precipitation and implications of canopy leaching in validating chemical analyses of throughfall samples. Atmos Environ 42:9106–9117

Tognetti R, Longobucco A, Raschi A (1998) Vulnerability of xylem embolism in relation to plant hydraulic resistance in *Quercus pubescens* and *Quercus ilex* co-occurring in a Mediterranean coppice stand in central Italy. New Phytol 139:437–447

Trumbore S (2000) Age of soil organic matter and soil respiration: radiocarbon constraints on belowground dynamics. Ecol Appl 10:399–411

Van Dijk AIJM, Bruijnzeel LA (2001) Modelling rainfall interception by vegetation of variable density using an adapted analytical model. Part 1. Model description. J Hydrol 247:230–238

van Pul A, Van Jaarsveld H, van der Meulen T et al (2004) Ammonia concentrations in the Netherlands: spatially detailed measurements and model calculations. Atmos Environ 38:4045–4055

Warren JM, Brooks JR, Meinzer FC et al (2008) Hydraulic redistribution of water from Pinus ponderosa trees to seedlings: evidence for an ectomycorrhizal pathway. New Phytol 178:382–394

Xiao Q, McPherson EG, Ustin SL et al (2000) Winter rainfall interception by two mature open-grown trees in Davis, California. Hydrol Process 14:763–784

Zavala LM, Gonzales FA, Jordan A (2009) Intensity and persistence of water repellency in relation to vegetation types and soil parameters in Mediterranean SW Spain. Geoderma 152:361–374

Zhang G, Zeng GM, Jiang YM et al (2006) Seasonal dry deposition and canopy leaching of base cations in a subtropical evergreen mixed forest, China. Silva Fenn 40:417–428

Zimmermann A, Wilcke W, Elsenbeer H (2007) Spatial and temporal patterns of throughfall quantity and quality in a tropical montane forest in Ecuador. J Hydrol 343:80–96

Chapter 27
Snow: Hydrological and Ecological Feedbacks in Forests

Noah P. Molotch, Peter D. Blanken, and Timothy E. Link

27.1 Introduction to Snow–Vegetation Interactions

Water inputs to high-elevation and high-latitude ecosystems are often dominated by seasonal snow cover. Several works have investigated the processes controlling ecohydrological impacts on snow accumulation (Golding and Swanson 1978; Pomeroy and Schmidt 1993; Faria et al. 2000; Storck et al. 2002; Gelfan et al. 2004; Musselman et al. 2008), snowmelt (Liston 1999; Woo and Giesbrecht 2000; Sicart et al. 2004), and partitioning of melt into various hydrologic pathways (Molotch et al. 2009). Integrated studies involving direct measurements of governing fluxes and states are rare despite the interconnectedness of the hydrologic system. Developing improved understanding of the coupled ecohydrologic system in mountainous regions is critical as recent studies indicate that seasonal snow accumulation is declining in response to regional increases in spring air temperature (Mote et al. 2005). The impact of these changes on ecological processes remains unknown, although first-order estimates project earlier snowmelt and extended periods of water-related plant stress (Bales et al. 2006). The ecological impacts of these climatic changes may vary considerably across the landscape; e.g., across elevational and latitudinal gradients. Implications of these changes are exacerbated in some instances, particularly as pertaining to the relative contribution of snowmelt vs. rainfall with respect to total annual water availability (Serreze et al. 1999).

In snow-dominated systems, the timing of snowmelt controls the shape of the hydrograph and the input of water to terrestrial ecosystems. Sustained snowmelt infiltration can facilitate significant transpiration rates and carbon uptake late into the growing season (Sacks et al. 2007). The processes controlling the spatiotemporal distribution of snow accumulation and snowmelt are highly complex, varying as a function of the energy balance, and the distribution of vegetation (e.g., Fig. 27.1) and topography (Molotch and Bales 2005). As a result of this complexity, our ability to characterize the distribution of soil moisture (Zehe and Bloschl 2004), and rates of evapotranspiration (Wigmosta et al. 1994) is severely limited.

Variability in forest structure has significant impacts on snow distribution (Faria et al. 2000). Changes in forest structure associated with episodic events such as fire, disease, and drought propagate in time with longer-term impacts on rates of
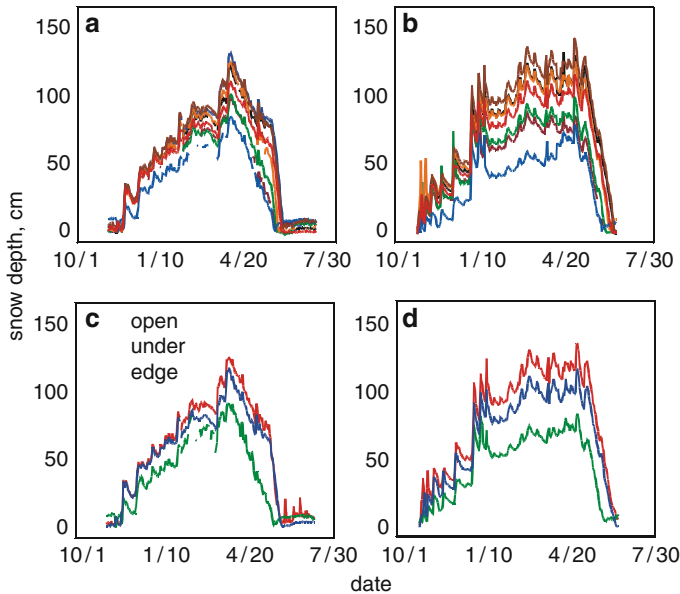
Fig. 27.1 Time series of snow depth in 2005–2006 (**a**) and 2006–2007 (**b**) at Niwot Ridge, Colorado. Snow depth averages for under canopy (*under*), canopy edge (*edge*), and open (*open*) areas are also shown (**c**, **d**) (from Molotch et al. 2009)

sediment transport and water quality. As a result of these longer-term impacts, changes in vegetation structure over time are part of a complex feedback loop that impacts variability in soil moisture availability and therefore forest regeneration and biodiversity (Carignan et al. 2000). Longer-term anthropogenically driven changes in vegetation distribution such as fire suppression (Johnson 1994) have impacts on the cycling of water and nutrients from snow-dominated catchments (Golding and Swanson 1986). To address the impacts of these changes across temporal scales, deterministic models are needed. Such models must be rooted in comprehensive observations of the coupled ecohydrologic system.

Catchment-scale hydrologic response to reductions in forest cover is tightly connected to alterations in snowpack processes as the shape of snowmelt-dominated hydrographs is highly sensitive to changes in forest cover properties (Hibbert 1969). Associated alterations to the timing and flowpaths of snowmelt water are largely responsible for the increased water yield observed after reductions in forest cover (Kattelmann et al. 1983; Stednick 1996). Although this observed increase in water yield is well established, the underlying mechanisms which alter the snowpack energy balance and timing of snowmelt are poorly understood. Radiative and turbulent flux exchange between the snowpack and the atmosphere is well established in forested environments (Price and Dunne 1976; Hardy et al. 1997; Link and Marks 1999a; Woo and Giesbrecht 2000; Gelfan et al. 2004). The influence of vegetation on snow interception and snowpack distribution has also been documented (Golding and Swanson 1978, 1986; Davis et al. 1997; Faria et al. 2000).

Few works, however, have extended these detailed snow-vegetation studies to the feedbacks between water distribution and vegetation response. In this context, numerous studies have established snowmelt controls on water availability, evapo-transpiration, and ecosystem carbon fluxes (Pataki et al. 2000). Closing out the hydroclimatic-ecohydrologic feedback loop are works that have documented the alteration of land–surface–atmosphere energy exchange, the distribution of snow-melt (Faria et al. 2000), soil moisture (Durocher 1990), and the role of vegetation. Direct observations of these feedback mechanisms are lacking and therefore under-standing of the governing processes is limited.

Development of accurate projections of vegetation response to climate change relies on an improved understanding of ecohydrological feedbacks across different biomes. In snow covered systems, however, such improved knowledge is critical given the extreme sensitivity of the magnitude and timing of snowmelt to climate change. Here, snowpack processes may represent one of the most critical components toward understanding the ecohydrologic impacts of climate change and vegetation change; e.g., increased snow interception and decreased subcanopy insolation associated with increased vegetation density (Lopez-Moreno and Latron 2008); increases in regional air temperatures leading to earlier snowmelt (Stewart et al. 2004); and reductions in snow accumulation resulting in increases in soil freezing (Monson et al. 2006). Just these few examples highlight the potential ecohydrological response to shifts in climate and vegetation change. Adequate representation of the myriad of potential changes largely depends on improved under-standing of snowpack processes and the complex interactions between vegetation distribution, snow redistribution, variability in solar irradiance, snowmelt, soil moisture, and soil temperature. These states and fluxes need to be observed directly and continu-ously, from the onset of snow accumulation through to the end of the snowmelt infiltration period – a future direction focus highlighted at the end of this chapter.

As an objective herein, this chapter summarizes a broad swath of literature aimed at understanding the spatial and temporal relationships between snow accumulation and melt distribution, the distribution of soil moisture and temperature, and vegeta-tion structure. In this regard, the following guiding questions scope the problem:

1. How does vegetation structure influence the magnitude and timing of snow accumulation and snowmelt?
2. How does variability in snow accumulation, snowmelt, and snow cover persis-tence influence the temporal variability in soil moisture?
3. How does the timing and magnitude of snowmelt effect vegetation water use and the partitioning of water into different pathways?

27.2 Snow Interception, Sublimation, and Latent Heat Flux

The processes controlling snow sublimation in forested environments are highly complex as sublimation can occur from both intercepted snow, and/or from the subcanopy snowpack. Large quantities of snow are intercepted by coniferous

forests and sublimation from the canopy can be significant. For example, measured seasonal snow sublimation losses were noted to be 32% in a temperate coniferous forest (Packer 1962), and up to 40% for a mature boreal spruce stand (Pomeroy et al. 1998). Subcanopy snow sublimation has been considered largely insignificant in most forests due to the low exposed surface area of the snowpack and low below-canopy wind speeds. Recent studies (e.g., Molotch et al. 2007), however, indicate potentially considerable sublimation losses from the subcanopy snowpack of a subalpine forest. Such losses are consistent with recent indications that large subcanopy longwave radiation fluxes may be present if the canopy above is warm and snow-free, providing significant available energy for subcanopy sublimation or snowmelt (Woo and Giesbrecht 2000). Understanding the processes controlling sublimation from the canopy and the subcanopy snowpack is critical for understanding ecohydrological feedbacks in snow-dominated forests – particularly with regard to understanding the impacts of changes in climate and land use.

Measurement of water vapor fluxes between the ecosystem and the atmosphere using the eddy covariance (EC) method (Goulden et al. 1996; Turnipseed et al. 2002) provide a means to directly estimate snow sublimation. Typically, such calculations during the winter period, when transpiration, melting, and wind-redistribution are negligible, provide a direct measurement of snow sublimation (latent heat flux; λE):

$$\lambda E = L_{\mathrm{v}} \overline{w' \rho_{\mathrm{v}}'}, \tag{27.1}$$

where L_{v} is the combined latent heat of fusion and vaporization (i.e., sublimation), w' is the deviations (primes) of high-frequency (typically 10 Hz) vertical wind speed (w) and water vapor density (ρ_{v}) from the time-averaged means (overbar; typically ½ h). Flux towers are typically deployed in locations with at least 100 m of upwind continuous fetch over relatively homogeneous forest and topography for every 1 m of height above the surface that the flux effectively originates from (the 1:100 rule-of thumb). Once EC measurements have been made, various corrections to the EC data are typically required (e.g., Aubinet et al. 1999; Reba et al. 2009).

Given that snow sublimation can occur from both intercepted snow in the canopy and the subcanopy snowpack, the individual sublimation components can be considered independently:

$$\lambda E_{\mathrm{c,t}} = \lambda E_{\mathrm{c,s}} + \lambda E_{\mathrm{c,i}}, \tag{27.2}$$

where $\lambda E_{\mathrm{c,t}}$ is the total sublimation from the system measured using above-canopy EC instruments and $\lambda E_{\mathrm{c,s}}$ is snowpack sublimation estimated from the subcanopy snowpack; here, subcanopy snowpack sublimation can be estimated using a sub-canopy flux tower (Molotch et al. 2007), using isotopic data (Koeniger et al. 2008; Gustafson et al. 2010), or by tracking changes in subcanopy snowpack mass as observed in snow pits. Sublimation associated with vapor fluxes from intercepted snow, $\lambda E_{\mathrm{c,i}}$ can then be determined by differencing the measured above- and estimated below-canopy fluxes.

Evaluation of the latent heat flux estimates using the EC method is done by quantifying total energy balance closure; the sum of the turbulent fluxes should be equal to the available energy (Blanken et al. 1997; Misson et al. 2007). Turbulent flux footprint estimation methods have been established by Schuepp et al. (1990) and others (see review by Vesala et al. 2008). This calculation estimates the upwind distance that the flux measurements are most sensitive to and represents the effective area where the fluxes originate from. Note that in mountainous environments, the 1:100 upwind fetch criteria can be difficult to satisfy. As a result, often flux tower locations are not representative of the complex topography that typifies mountain environments. Similarly, the deployment of flux towers in complex topography can complicate flux calculations; closure of the energy balance may not be obtained and estimation of the flux footprint may be unreliable.

Sublimation of intercepted snow represents a considerable proportion of the water balance in many snow-dominated forests (Schmidt and Troendle 1992; Lundberg and Halldin 1994; Pomeroy and Gray 1995; Essery et al. 2003). In this regard, canopy interception may constitute about 60% of annual snowfall (Hedstrom and Pomeroy 1998) and subsequent sublimation fluxes to the atmosphere may be greater than 30% of total snowfall (Montesi et al. 2004). Rates of sublimation are dictated by the distribution of radiant and turbulent fluxes. The relative proportion of the different energy fluxes varies considerably with canopy structure as well as climatology (e.g., latitude, elevation, continentality). Interactions that control these fluxes and the resulting sublimation losses of intercepted and subcanopy snow are poorly understood (Bales et al. 2006). Given the complexity of interactions between the snowpack, vegetation, and the surface energy balance, detailed analyses of mass and energy fluxes from observations and models have been developed (Davis et al. 1997; Sicart et al. 2004).

Numerous methods have been applied to estimate sublimation from intercepted snow. Estimating snow sublimation in forested terrain is particularly challenging as above-canopy water vapor fluxes include sublimation losses from both intercepted snow and the snowpack beneath the canopy. Sublimation losses from unforested terrain are well documented (Pomeroy and Essery 1999; Pomeroy and Li 2000; Fassnacht 2004), and recently these techniques have been extended to intercepted snow sublimation (Schmidt and Troendle 1992; Pomeroy and Schmidt 1993; Montesi et al. 2004). In this regard, the distribution of turbulent fluxes within seasonally snow-covered forests has been characterized (Harding and Pomeroy 1996). During the spring transition, notable differences in energy fluxes result as the canopy transitions from snow-covered to snow-free (Nakai et al. 1999). Much of the works documenting these transitions have been developed through the BOREAS project and complementary works conducted in high-latitude boreal forests (Blanken et al. 1997, 1998; Davis et al. 1997; Hardy et al. 1997; Hedstrom and Pomeroy 1998; Link and Marks 1999a, b; Pomeroy et al. 1999; Blanken and Black 2004). Studies focused on above- and below-canopy vapor fluxes are less common – particularly in mountainous regions.

One methodology for observing intercepted snow sublimation is known as the tree-weighting technique (Satterlund and Haupt 1970; Schmidt et al. 1988; Schmidt 1991; Nakai et al. 1994; Storck et al. 2002; Montesi et al. 2004), where a tree(s) are

cut at the trunk but left in place, and their weight is monitored to determine snow interception (gain) and sublimation (loss). Factors leading to errors in this method are numerous. First, small snowfall events can introduce error as these mass inputs can counter sublimation losses and lead to an underestimation of total sublimation losses to the atmosphere. Second, small unloading events can be overlooked, and if not subtracted from sublimation losses, overestimates in sublimation estimates can result. Third, sublimation of unloaded snow may be considerable given the large ice–atmosphere interface surface area as snow falls from the canopy to the ground; underestimates of sublimation may be considerable if the sublimation of this unloaded snow is not considered (Montesi et al. 2004). Furthermore, point-scale sublimation estimates may not transfer linearly to stand-scale sublimation estimates and detailed canopy information is critical for upscaling. Although detailed canopy data sets are increasingly available (e.g., from light detection and ranging [LiDAR]), the lack of canopy structure data limits the utility of distributed models for estimating sublimation losses (Pomeroy and Schmidt 1993; Pomeroy et al. 1998). Although the aforementioned EC approach may have more direct measurement uncertainty than the point-scale methods, the aforementioned scaling limitations in tree-weighting and other point-scale techniques are not inherent to EC method as the latter integrates across (plot) stand-scale water vapor flux.

27.3 Radiation Transfer During Snowmelt

The processes controlling the rates of snow ablation under vegetation canopies remains one of the greatest uncertainties in land surface modeling of snow-dominated forests. Scale-discrepancies between longwave radiative fluxes at the point scale vs. those across the landscape are profound given the complex mosaics of forest cover and topography, which typify mountainous terrain (Molotch and Bales 2005).

Forest, and to a lesser extent, shrub canopies strongly affect the meteorological conditions at the snow surface that concomitantly alter snowcover energetics relative to open locations. One of the most obvious effects is the reduction of shortwave radiation due to canopy shading. Canopy shading is especially pronounced in the winter and on north-facing slopes, due to low sun angles that result in long pathlengths of the solar beam through the forest canopy. The long pathlengths that occur when solar angles are low results in a relatively high degree of shading even in sparse or dead forest stands. Deposition of organic debris within forests, however, leads to lower snowpack albedoes, especially during the melt season, such that the proportion of shortwave radiation absorbed beneath forest canopies is greater than open areas that are typically characterized by higher snowcover albedo (Hardy et al. 2000).

Unlike shortwave radiation, incoming longwave radiation within forest canopies is enhanced relative to open locations. This is primarily due a higher emissivity of the material overlying the snowcover relative to open conditions. This is because

vegetation canopies have an emissivity very close to unity, whereas the atmospheric emissivity ranges from 0.6 for very clear, dry conditions to 1.0 for heavy, low cloud cover. Increased longwave radiation emission in vegetation canopies may also be due to canopy warming during sunny conditions that further enhances thermal emission (Pomeroy et al. 2009). This effect appears to be most pronounced in sparse canopies and canopy discontinuities where solar radiation can directly warm canopy constituents directly above the snow surface.

Although the maximum instantaneous longwave enhancement (50–80 W m^{-2}) is much less than the maximum shortwave reduction (400–600 W m^{-2}) due to shading, when cumulated over an entire day, the differences can be much smaller since the solar effect only occurs during the relatively short winter days, whereas the longwave effect persists for the entire diurnal cycle. The result of the combined shortwave and longwave effects is that longwave radiation dominates the radiative component of the snowcover energy balance in forests, where solar angles are low (i. e., early in the season, at high latitudes and on north-facing slopes), whereas the solar component increases where sun angles are higher (i.e., late in the snow season, at low latitudes on south-facing slopes). The amount of net shortwave radiation decreases rapidly as canopy density increases, whereas the net longwave radiation increases linearly as canopy density increases (Reifsnyder 1971).

Shrubs can either enhance or reduce melt rates relative to open areas depending on the size and density of the vegetation and depth of snow (Pomeroy et al. 2006). Where shrubs are relatively sparse and just protrude above the snow cover they can absorb shortwave radiation thereby warming and increasing longwave emission. Where radiation is able to penetrate the snowcover, shrubs may warm and produce a localized melt hollow within the snowcover. Where shrubs protrude from the snow-cover, they may enhance longwave emission without greatly reducing incoming shortwave radiation, and can increase air temperatures thereby increasing the sensible heat flux relative to open areas. Simulations of the effects of emergent shrubs on regional climate in the arctic suggest an air temperature warming of +2.5°C and acceleration of snow melt rates relative to shrub-free areas (Strack et al. 2007). Where larger and denser shrubs are present over a snowcover, the effect is similar to taller forest vegetation, and can effectively reduce snowmelt rates by reducing net radiation and windspeeds at the snow surface.

Several works have addressed this issue of radiation transfer during snowmelt utilizing arrays of radiometers in combination with detailed canopy energetics models. Development of a canopy energetics conceptual model has been based on observations of a "radiative paradox," in which thermal radiation gains associated with forest emission offset solar reductions leading to higher net radiation in forests depending on solar geometry and snow-surface albedo (Sicart et al. 2004). Within this simple geometric radiative transfer model, two net incoming "radiative paradoxes" can occur within small canopy gaps (Link et al. 2005). A Type I paradox occurs when radiation at the snow surface is greater than radiation in open areas, and will likely produce larger melt rates in canopy gaps, relative to open areas (Fig. 27.2). A Type II paradox is where net radiation at the snow surface is less than under a continuous forest canopy, and will likely produce slower melt rates
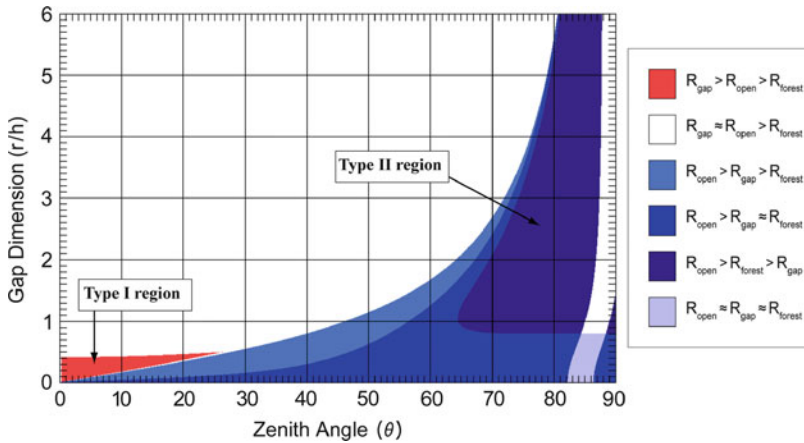
Fig. 27.2 Theoretical model results indicating radiative regimes in the center of a circular canopy gap with dimension of gap radius per surrounding canopy height, over a range of solar zenith angles

than an intact forest. The general relationships described within this model have been developed over a wide range of forest types and across a broad range of latitudes. The model is capable of accounting for nonlinear processes associated with vegetation structure that result in variable patterns of snowcover energetics during melt (Ababou et al. 1994; Link and Marks 1999a, b; Parviainen and Pomeroy 2000; Woo and Giesbrecht 2000). Although there are inherent issues associated with extending this simple canopy energetics model to areas outside the range of conditions in which it was developed, the general relationships provide a means to assess local-scale variability in solar radiation extinction and thermal radiation enhancement and overall net radiation.

In boreal regions, inverse relationships between accumulation and ablation rates have been observed as snow interception reduces accumulation near trees while enhanced longwave radiation emission from the canopy increases snowmelt rates (near the canopy at the ground surface, Faria et al. 2000). However, these relationships are dependent upon canopy density and latitude, both of which dictate the effect of vegetation on net radiation and rates of snowmelt (Sicart et al. 2004). Observations at mid-latitudes indicate that this inverse relationship may not exist as snow ablation rates are often greater in open areas within mid-latitude forests. Furthermore, given that beneath-canopy energy fluxes are lower than open areas in mid-latitude forests, these areas may be less sensitive to mid-winter melt or sublimation, and therefore these areas may be less sensitive to shifts in climate. The implications are extensive with regard to vegetation change associated with fire or beetle infestation as larger proportions of mountainous regions become deforested.

The impacts of vegetation structure on snow cover ablation vary considerably in open, canopy edge, and undercanopy areas. In mid-latitude forests, undercanopy locations may have more persistent snow cover as a result of diminished radiative

fluxes (Sicart et al. 2004). Interrelationships between solar zenith angle (associated with latitude and date) and canopy geometry are evident whereby decreases in canopy gap size with increasing latitude increases overall subcanopy net radiation relative to open areas (Link et al. 2004b). These observations suggest that the geometry of the forest may have large impacts on the water balance during the melt season.

27.4   Snowmelt During Rain-on-Snow and Water Availability

In many areas of the world, flood events are generated during rain-on-snow (ROS) conditions where precipitation and snowmelt combine to produce a large amount of water available for runoff. Snowpack energetics during ROS events are composed of a mix of net radiation, that is dominated by longwave radiation, sensible, latent and advected heat fluxes. For example, during a record flood event characterized by very high windspeeds, warm air temperatures and high vapor pressures, 75–80% of the energy for snowmelt came from turbulent (sensible and latent) energy fluxes (Marks et al. 1998). During this event, the windspeeds beneath a mature forest canopy were found to be about 20% of values at the open sites, and as a result turbulent energy fluxes accounted for approximately 35% for the snowcover energy balance. During this event, differences in net radiation, advected, and ground heat fluxes were very similar between the open and forested sites. Other research across a broader range of ROS events, however, indicated that there was a high degree of interannual variability of energy components, and that net radiation dominated the energy balance, with important contributions from sensible, latent and ground heat fluxes (Mazurkiewicz et al. 2008). The impact of vegetation canopies during ROS conditions will therefore vary depending on specific climate conditions; however, the primary effect in the reduction of windspeeds that consequently causes the magnitudes of the turbulent flux components to be reduced within vegetation canopies.

Spatiotemporal variability in these energy fluxes dictates rates of snowmelt infiltration into subnivean soils. In this regard, the distribution of soil moisture and associated vegetation response is sensitive to two critical transitions in the ecohydrology of these seasonally snow-covered forests. First, the timing of snowmelt infiltration onset and peak soil moisture is largely dependent on winter-season snow accumulation amounts and the average winter air temperature – both of which control the cold content of the snowpack. Second, maximum soil moisture in snow-dominated systems is largely dictated by snowmelt rate and the delivery of water to the subnivean soil. Given that available snowmelt energy increases through the snowmelt season, peak soil moisture often occurs just before the end of the snowmelt season (Molotch et al. 2007). Given that both peak soil moisture and the beginning of the soil dry-down begins just after snow disappearance the sensitivity of forested ecosystems to the timing of snowmelt is considerable. Given that forests in semiarid snow-covered regions are highly sensitive to

maximum water availability, future efforts are needed to identify the impacts of snowmelt timing on evapotranspiration. In this regard, research is needed to identify the impact of earlier snowmelt on net primary productivity (Sacks et al. 2007) and forest fire frequency (Westerling et al. 2006).

27.5 Future Directions

Improving knowledge of the snow-vegetation interactions described above is particularly important since snow-covered systems are highly sensitive to changes in air temperature and to small changes in the flux of energy and water (Williams et al. 2002). Process-level understanding of the hydrology and ecology of snow-covered systems has not translated into knowledge of feedbacks between climate and ecosystem function because coupled hydrological-ecological observations are lacking (Molotch 2009). The problem is urgent, as recent climate analyses have shown widespread declines in the winter snowpack of mountain ecosystems in western North America and Europe that are associated with positive temperature anomalies (Fig. 27.3-left) (Laternser and Schneebeli 2003; Mote et al. 2005).

To date, only statistical inferences have revealed the potential impacts of these climatic shifts on carbon cycling and ecological function. Recent studies have documented an increase in fire intensity associated with earlier onset of snowmelt (Fig. 27.3-middle) (Westerling et al. 2006), and increased tree mortality has been linked with increases in water stress (Fig. 27.3-right). A consistent message has emerged from these studies whereby decreases in water availability over the past half century have profoundly impacted ecological function of subalpine forests.

From these studies (Fig. 27.3), a reasonable hypothesis is that climate-related changes in snow accumulation and snowmelt play a critical role in ecosystem changes across the region as it represents the dominant input of water to these systems. Our ability to evaluate this hypothesis has been limited due to the fact that vegetation structure exerts a strong influence on water and energy fluxes in these systems. For example, forest microstructure impacts interception of snow (Montesi et al. 2004), wind redistribution of snow (Hiemstra et al. 2006), snow sublimation (Montesi et al. 2004), the distribution of thermal and solar radiation (Link and Marks 1999a; Link et al. 2004a), and the timing of snowmelt and soil moisture (Link et al. 2004b; Molotch et al. 2009). In this regard, ecological controls on the hydrology of these systems act as a complex feedback, which complicates our ability to understand climate impacts on ecosystems. Hence, our ability to predict the impact of climate change on ecosystem function is limited. To develop this physical knowledge and improve our ability to predict future changes in ecohydrological processes, future research is needed involving direct observations of these feedbacks across gradients in vegetation community structure, topography, and climatic regime. In parallel, advances in remote sensing and coupled snowpack-biogeochemical modeling approaches are needed. These research needs are not unique to snow-covered systems and hence are a major priority across the ecological and hydrologic communities. Upcoming initiatives in
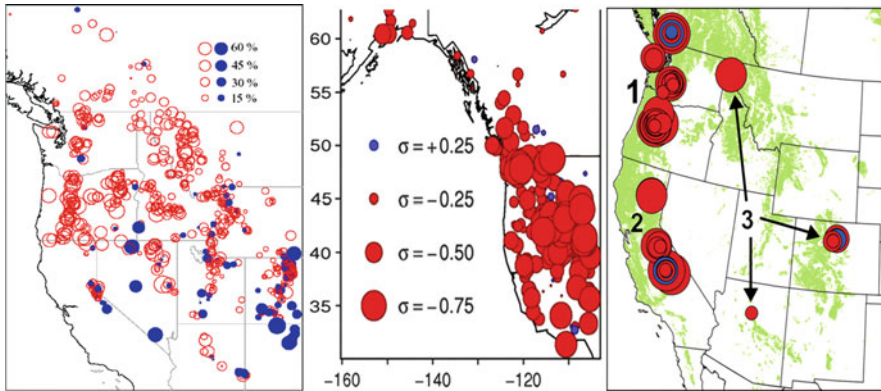
Fig. 27.3 (*Left*) Snow accumulation trends over the last 50 years. *Open/red circles* represent negative trends and *closed/blue* represent positive trends (from Service 2004, after Mote et al. 2004). (*Middle*) Statistical relationship showing between timing of spring snowmelt pulse and frequency of large forest fires; note the strong negative correlation (from Westerling et al. 2006, reproduced with permission). (*Right*) Trends in tree mortality across the Western United States; *red circles* represent increasing mortality rates and the size of the circle corresponds to the magnitude of the trend (from van Mantgem et al. 2009, reproduced with permission)

these areas such as the U.S. National Science Foundation's Critical Zone Exploration Network (http://www.czen.org/), relevant missions in the U.S. National Aeronautics and Space Administration's Decadal Survey such as the Deformation, Ecosystem Structure and Dynamics of Ice (DESDYNI), Soil Moisture Active Passive (SMAP), and the Snow and Cold Lands Processes (SCLP) missions (NRC 2007), spaceborne missions under development by the European Space Agency such as Soil Moisture and Ocean Salinity (SMOS) and the COld REgions Hydrology High-resolution Observatory (CoReH2O), and regional-scale ecological network initiatives such as National Ecological Observatory Network (NEON; http://www.neoninc.org/) provide a means forward for synthesis, integration, and transformative breakthroughs in the research areas described above. Successful integration of new in situ measurement infrastructure with distributed models, supported by new remote sensing capabilities, is critical for extending basic research in these areas to broader science questions at the ecosystem to global scales.

References

Ababou R, Bagtzoglou AC, Wood EF (1994) On the condition number of covariance matrices in kriging, estimation, and simulation of random-fields. Math Geol 26:99–133

Aubinet M, Grelle A, Ibrom A et al (1999) Estimates of the annual net carbon and water exchange of forests: the EUROFLUX methodology. Adv Ecol Res 30:113–175

Bales R, Molotch N, Painter T et al (2006) Mountain hydrology of the western United States. Water Resour Res 42:W08432. doi:08410.01029/02005WR004387

Blanken PD, Black TA (2004) The canopy conductance of a boreal aspen forest, Prince Albert National Park, Canada. Hydrol Process 18:1561–1578

Blanken PD, Black TA, Yang PC et al (1997) Energy balance and canopy conductance of a boreal aspen forest: partitioning overstory and understory components. J Geophys Res Atmos 102 (D24):28915–28927

Blanken PD, Black TA, Neumann HH et al (1998) Turbulent flux measurements above and below the overstory of a boreal aspen forest. Bound Lay Meteorol 89:109–140

Carignan R, D'Arcy P, Lamontagne S (2000) Comparative impacts of fire and forest harvesting on water quality in Boreal Shield lakes. Can J Fish Aquat Sci 57:105–117

Davis RE, Hardy JP, Ni W et al (1997) Variation of snow cover ablation in the boreal forest: a sensitivity study on the effects of conifer canopy. J Geophys Res 102(D24):29389–29395

Durocher MG (1990) Monitoring spatial variability of forest interception. Hydrol Process 4:215–229

Essery R, Pomeroy J, Parviainen J et al (2003) Sublimation of snow from coniferous forests in a climate model. J Clim 16:1855–1864

Faria DA, Pomeroy JW, Essery RLH (2000) Effect of covariance between ablation and snow water equivalent on depletion of snow-covered area in a forest. Hydrol Process 14:2683–2695

Fassnacht SR (2004) Estimating Alter-shielded gauge snowfall undercatch, snowpack sublimation, and blowing snow transport at six sites in the coterminous USA. Hydrol Process 18:3481–3492

Gelfan AN, Pomeroy JW, Kuchment LS (2004) Modeling forest cover influences on snow accumulation, sublimation, and melt. J Hydrometeorol 5:785–803

Golding DL, Swanson RH (1978) Snow accumulation and melt in small forest openings in Alberta. Can J For Res 8:380–388

Golding DL, Swanson RH (1986) Snow distribution patterns in clearings and adjacent forest. Water Resour Res 22:1931–1940

Goulden ML, Munger JW, Fan SM et al (1996) Measurements of carbon sequestration by long-term eddy covariance: methods and a critical evaluation of accuracy. Global Change Biol 2:169–182

Gustafson JR, Brooks PD, Molotch NP et al (2010) Estimating snow sublimation suing natural chemical and isotopic tracers across a gradient of solar radiation. Water Resour Res 46:W12511

Harding RJ, Pomeroy JW (1996) Energy balance of the winter boreal landscape. J Clim 9:2778–2787

Hardy JP, Davis RE, Jordan R et al (1997) Snow ablation modeling at the stand scale in a boreal jack pine forest. J Geophys Res Atmos 102(D24):29397–29405

Hardy JP, Melloh R, Robinson P et al (2000) Incorporating effects of forest litter in a snow process model. Hydrol Process 14:3227–3237

Hedstrom NR, Pomeroy JW (1998) Measurements and modelling of snow interception in the boreal forest. Hydrol Process 12:1611–1625

Hibbert AR (1969) Water yield changes after converting a forested catchment to grass. Water Resour Res 5:634–640

Hiemstra CA, Liston GE, Reiners WA (2006) Observing, modelling, and validating snow redistribution by wind in a Wyoming upper treeline landscape. Ecol Model 197:35–51

Johnson M (1994) Changes in Southwestern forests – stewardship implications. J For 92:16–19

Kattelmann RC, Berg NH, Rector J (1983) The potential for increasing streamflow from Sierra-Nevada watersheds. Water Resour Bull 19:395–402

Koeniger P, Hubbart JA, Link T et al (2008) Isotopic variation of snow cover and streamflow in response to changes in canopy structure in a snow-dominated mountain catchment. Hydrol Process 22:557–566

Laternser M, Schneebeli M (2003) Long-term snow climate trends of the Swiss Alps (1931–1999). Int J Climatol 23:733–750

Link TE, Marks D (1999a) Distributed simulation of snowcover mass- and energy-balance in the boreal forest. Hydrol Process 13:2439–2452

Link TE, Marks D (1999b) Point simulation of seasonal snow cover dynamics beneath boreal forest canopies. J Geophys Res Atmos 104(D22):27841–27857

Link TE, Hardy JP, Marks D (2004a) A deterministic method to characterize canopy radiative transfer properties. Hydrol Process 18:3583–3594

Link TE, Flerchinger GN, Unsworth M et al (2004b) Simulation of water and energy fluxes in an old-growth seasonal temperate rain forest using the simultaneous heat and water (SHAW) model. J Hydrometeorol 5:443–457

Link TE, Reba ML, Essery RLH et al (2005) Small-scale spatial variability of sub-canopy radiant energy during snowmelt in deciduous and coniferous forest patches. Eos, Transactions American Geophysical Union 86: Abstract C21A-1073

Liston GE (1999) Interrelationships among snow distribution, snowmelt, and snow cover depletion: implications for atmospheric, hydrologic, and ecologic modeling. J Appl Meteorol 38:1474–1487

Lopez-Moreno JI, Latron J (2008) Influence of canopy density on snow distribution in a temperate mountain range. Hydrol Process 22:117–126

Lundberg A, Halldin S (1994) Evaporation of intercepted snow: anlaysis of governing factors. Water Resour Res 30:2587–2598

Marks D, Kimball J, Tingey D et al (1998) The sensitivity of snowmelt processes to climate conditions and forest cover during rain-on-snow: a case study of the 1996 Pacific Northwest flood. Hydrol Process 12:1569–1587

Mazurkiewicz AB, Callery DG, McDonnell JJ (2008) Assessing the controls of the snow energy balance and water available for runoff in a rain-on-snow environment. J Hydrol 354:1–14

Misson L, Baldocchi DD, Black TA et al (2007) Partitioning forest carbon fluxes with overstory and understory eddy-covariance measurements: a synthesis based on FLUXNET data. Agric For Meteorol 144:14–31

Molotch NP (2009) Reconstructing snow water equivalent in the Rio Grande headwaters using remotely sensed snow cover data and a spatially distributed snowmelt model. Hydrol Process 23:1076–1089

Molotch N, Bales R (2005) Scaling snow observations from the point to the grid-element: implications for observaiton network design. Water Resour Res 41: doi:10.1029/2005WR004229

Molotch NP, Blanken PD, Williams MW et al (2007) Estimating sublimation of intercepted and sub-canopy snow using eddy covariance systems. Hydrol Process 21:1567–1575

Molotch NP, Brooks PD, Burns SP et al (2009) Ecohydrological controls on snowmelt partitioning in mixed-conifer sub-alpine forests. Ecohydrology 2:129–142

Monson RK, Lipson DL, Burns SP et al (2006) Winter forest soil respiration controlled by climate and microbial community composition. Nature 439:711–714

Montesi J, Elder K, Schmidt RA et al (2004) Sublimation of intercepted snow within a subalpine forest canopy at two elevations. J Hydrometeorol 5:763–773

Mote PW, Clark MP, Hamlet AF (2004) Variability and trends in mountain snowpack in western North America. Presented at 15th symposium on global change and climate variations. American Meteorological Society, Seattle

Mote PW, Hamlet AF, Clark MP et al (2005) Declining mountain snowpack in Western North America. Bull Amer Meteorol Soc 86:39–49

Musselman K, Molotch NP, Brooks PD (2008) Effects of vegetation on snow accumulation and ablation in a mid-latitude sub-alpine forest. Hydrol Process. doi:10.1002/hyp.7050

Nakai Y, Sakamoto T, Terajima T et al (1994) Snow interception by forest canopies: weighing a conifer tree, meteorological observation and analysis by the Penman-Monteith formula. IAHS Publ 223:227–236

Nakai Y, Sakamoto T, Terajima T et al (1999) Energy balance above a boreal coniferous forest: a difference in turbulent fluxes between snow-covered and snow-free canopies. Hydrol Process 13:515–529

National Research Council (2007) Earth science and applications from space: national imperatives for the next decade and beyond. National Academies Press, Washington, DC, 400pp

Packer P (1962) Elevation, aspect, and forest cover effects on maximum snowpack water content in a western white pine forest. For Sci 8:225–235

Parviainen J, Pomeroy JW (2000) Multiple-scale modelling of forest snow sublimation: initial findings. Hydrol Process 14:2669–2681

Pataki DE, Oren R, Smith WK (2000) Sap flux of co-occurring species in a western subalpine forest during seasonal soil drought. Ecology 81:2557–2566

Pomeroy JW, Essery RLH (1999) Turbulent fluxes during blowing snow: field tests of model sublimation predictions. Hydrol Process 13:2963–2975

Pomeroy JW, Gray DM (1995) Snowcover accumulation, relocation and management. NHRI Science Report 7, National Hydrology Research Institute, Environment, Canada, 134pp

Pomeroy JW, Li L (2000) Prairie and arctic areal snow cover mass balance using a blowing snow model. J Geophys Res Atmos 105(D21):26619–26634

Pomeroy JW, Schmidt RA (1993) The use of fractal geometry in modeling intercepted snow accumulation and sublimation. In: Proceedings of the 50th Eastern snow conference, Quebec City, Quebec, Canada, vol 50, pp 1–10

Pomeroy JW, Parviainen N, Hedstrom N et al (1998) Coupled modeling of forest snow interception and sublimation. Hydrol Process 12:2317–2337

Pomeroy JW, Davies TD, Jones HG et al (1999) Transformations of snow chemistry in the boreal forest: accumulation and volatilization. Hydrol Process 13:2257–2273

Pomeroy JW, Bewley DS, Essery RLH et al (2006) Shrub tundra snowmelt. Hydrol Process 20:923–941

Pomeroy JW, Marks D, Link T et al (2009) The impact of coniferous forest temperature on incoming longwave radiation to melting snow. Hydrol Process 23:2513–2525

Price AG, Dunne T (1976) Energy-balance computations of snowmelt in a sub-Arctic area. Water Resour Res 12:686–694

Reba ML, Link TE, Marks D et al (2009) An assessment of corrections for eddy covariance measured turbulent fluxes over snow in mountain environments. Water Resour Res 45: W00D38. doi:10.1029/2008WR007045

Reifsnyder WE (1971) Distribution of radiation in forest. Bull Amer Meteorol Soc 52:207

Sacks WJ, Schimel DS, Monson RK (2007) Coupling between carbon cycling and climate in a high-elevation, subalpine forest: a model-data fusion analysis. Oecologia 151:54–68

Satterlund DR, Haupt HF (1970) Disposition of snow caught by conifer crowns. Water Resour Res 6:649–652

Schmidt RA (1991) Sublimation of snow intercepted by an artificial conifer. Agric For Meteorol 54:1–27

Schmidt RA, Troendle CA (1992) Sublimation of intercepted snow as a global source of water vapor. In: Proceedings of the 60th Western snow conference, Jackson, WY, vol 60, pp 1–9

Schmidt RA, Jairell RL, Pomeroy JW (1988) Measuring snow interception and loss from an artificial conifer. In: Proceedings of the 56th Western snow conference, Kalispell, MT, vol 56, pp 166–169

Schuepp PH, Leclerc MY, Macpherson JI et al (1990) Footprint prediction of scalar fluxes from analytical solutions of the diffusion equation. Bound Lay Meteorol 50:353–373

Serreze MC, Clark MP, Armstrong RL et al (1999) Characteristics of the western United States snowpack from snowpack telemetry (SNOTEL) data. Water Resour Res 35:2145–2160

Service RF (2004) As the West goes dry. Science 303:1124–1127. doi:1110.1126/science.1303.5661.1124

Sicart JE, Pomeroy JW, Essery RLH et al (2004) A sensitivity study of daytime net radiation during snowmelt to forest canopy and atmospheric conditions. J Hydrometeorol 5:774–784

Stednick JD (1996) Monitoring the effects of timber harvest on annual water yield. J Hydrol 176:79–95

Stewart IT, Cayan DR, Dettinger MD (2004) Changes in snowmelt runoff timing in western North America under a "business as usual" climate change scenario. Clim Change 62:217–232

Storck P, Lettenmaier DP, Bolton SM (2002) Measurement of snow interception and canopy effects on snow accumulation and melt in a mountainous maritime climate, Oregon, United States. Water Resour Res 38:1223. doi:10.1029/2002WR001281

Strack JE, Pielke RA, Liston GE (2007) Arctic tundra shrub invasion and soot deposition: consequences for spring snowmelt and near-surface air temperatures. J Geophys Res Biogeosci 112:G04S44. doi:10.1029/2006JG000297

Turnipseed AA, Blanken PD, Anderson DE et al (2002) Energy budget above a high-elevation subalpine forest in complex topography. Agric For Meteorol 110:177–201

van Mantgem PJ, Stephenson SL, Byrne JC et al (2009) Widespread increase of tree mortality rates in the Western United States. Science 323:521–524

Vesala T, Kljun N, Rannik U et al (2008) Flux and concentration footprint modelling: state of the art. Environ Pollut 152:653–666

Westerling AL, Hidalgo HG, Cayan DR et al (2006) Warming and earlier spring increase western US forest wildfire activity. Science 313:940–943

Wigmosta MS, Vail LW, Lettenmaier DP (1994) A distributed hydrology-vegetation model for complex terrain. Water Resour Res 30:1665–1679

Williams MW, Losleben MV, Hamann HB (2002) Alpine areas in the Colorado front range as monitors of climate change and ecosystem response. Geogr Rev 92:180–191

Woo MK, Giesbrecht MA (2000) Simulation of snowmelt in a subarctic spruce woodland: scale considerations. Nord Hydrol 31:301–316

Zehe E, Bloschl G (2004) Predictability of hydrologic response at the plot and catchment scales: role of initial conditions. Water Resour Res 40:W10202. doi:10.1029/2003WR002869

Chapter 28
Insects, Infestations, and Nutrient Fluxes

Beate Michalzik

28.1 Introduction

Forest ecosystems are characterized by a high temporal and spatial variability in the vertical transfer of energy and matter within the canopy and the soil, or, more generally within the above- and below-ground compartments of ecosystems (McDowell and Likens 1988). In temperate forests, the principle flow path of organic matter and associated nutrients from the canopy to the ground is provided by litterfall, amounting to annual fluxes of carbon between 900 and 2,600 kg ha^{-1} year^{-1} and 20–55 kg ha^{-1} year^{-1} for nitrogen (Michalzik et al. 2001). Secondly, organic matter and nutrients are returned to the soil by fluctuating rates of throughfall deposition achieving annual fluxes per hectare between 40 and 160 kg DOC (dissolved organic carbon), 1.2–11.5 kg DON (dissolved organic nitrogen), 0.49–10.4 kg NO_3-N, and 0.28–12.7 kg NH_4-N (Michalzik et al. 2001).

The transfer of organic matter and nutrients between tree canopies and the soil compartment is regarded as an important connective pathway between the above- and below-ground system, exhibiting for example interlinkages between tree species and spatial and temporal patterns of soil acidity and cation cycling in temperate forests (Finzi et al. 1998). Additionally, meta-analyses of literature data supply evidence for the idea that canopy-derived organic matter inputs considerably affect organic matter and nutrient dynamics in the forest floor. For example, Michalzik et al. (2001) found that variations in annual DOC and DON throughfall fluxes explain 46 and 65% of the variability in annual DOC and DON fluxes from the forest floor of temperate forest ecosystems, while water fluxes alone did not explain a significant portion of the variability.

However, the mechanisms and controlling factors behind canopy processes and system-internal transfer dynamics are imperfectly understood at the moment. Seasonal flux diversities and inhomogeneities in throughfall composition have been reported from coniferous (Seiler and Matzner 1995) and deciduous forests (Qualls et al. 1991), and in most cases leaf leaching has been considered as principle driver for differences in the amount and quality of nutrients and organic compounds (Tukey and Morgan 1963).

Since herbivorous insects and the processes they initiate received less attention in the past, ecologists now emphasize the need for linking biological processes occurring in different ecosystem strata to explain rates and variability of nutrient cycling (Bardgett et al. 1998; Wardle et al. 2004). Consequently, herbivore insects in the canopies of forests are increasingly identified to play an important role for the (re)cycling and availability of nutrients, or, more generally, for the functioning of ecosystems not only in outbreak situations but also at endemic (non-outbreak) density levels (Stadler et al. 2001; Hunter et al. 2003).

Before, little attention was paid to insect herbivores when quantifying element and energy fluxes through ecosystems, although the numerous and different functions insects fulfill in ecosystems (e.g., as pollinators, herbivores, or detritivores) were unanimously recognized (Schowalter 2000). Among the reasons for this restraint was the argument that the total biomass of insects tends to be relatively low compared to the biomass of trees or the pool of soil organic matter (Ohmart et al. 1983). A second argument which was put forward to justify the inferior role of insects in nutrient cycling was the supposed low defoliation losses between 5 and 10% of the annual leaf biomass, or net primary production, due to insect herbivory under endemic situations (Larrson and Tenow 1980). Furthermore, practical reasons such as difficulties in accessing the upper canopy area of mature stands (Lowman and Wittman 1996) and methodological obstacles in accurately quantifying and evaluating frass and excretion amounts may have added to the low interest in studying the role of insects in nutrient cycling.

However, at times of insect mass outbreaks with leaf area losses up to 100%, nutrient fluxes are strongly affected at the ecosystem level and consequently attract greater attention (Grace 1986). In this context, mass outbreaks of herbivore insects constitute a class of ecosystem disturbance, which "is any relatively discrete event in time and space that disrupts the structure of populations, communities, and ecosystems and causes changes in resource availability or the physical environment" (Pickett and White 1985). More specifically, insect pests meet the criteria of biogeochemical "hot spots" and "hot moments" (McClain et al. 2003) as they induce temporal–spatial process heterogeneity or changes in biogeochemical reaction rates, but not necessarily changes in the structure of ecosystems or landscapes.

The severity of impacts resulting from disturbance-mediated alterations on forest ecosystems and associated services was recently highlighted by several reviews on forest disturbances within the United States (Ayres and Lombardero 2000; Dale et al. 2001). Among natural disturbances, such as fire, drought, introduced species, hurricanes, windstorms, ice storms, and landslides, which severely affected forested ecosystems, insect and pathogen outbreaks by far captured the largest spatial extent (20.4 million ha, USDA 1997) and caused the highest annual economic costs (1,500 million US Dollars) basically attributed to a decrease in forest productivity (Dale et al. 2001).

Although mass outbreaks of herbivore forest insects are temporally rare events, they can directly and indirectly affect a wide spectrum of ecosystem processes and functions by their leaf and sap-feeding activity (Swank et al. 1981; Ritchie et al. 1998; Chapman et al. 2003). With regard to short- and long-term effects of

herbivory on soil nutrient dynamics, Hunter (2001) suggested seven possible mechanisms encompassing (1) deposition of fecal material (frass), (2) accelerated nutrient release from decomposing insect cadavers, and alterations of (3) through-fall composition, (4) leaf litter quantity and quality, (5) root exudation and symbioses, (6) plant community composition, and (7) soil microclimate shifts due to changes in the canopy cover. The latter two probably affect nutrient dynamics more indirectly following the concept of a "slow cycle" (McNaughton et al. 1988), whereas the first five operate on short temporal scales ("fast cycle", McNaughton et al. 1988), thus directly affecting nutrient cycling. Recent studies additionally emphasize herbivore-mediated alterations in the timing and the quality of organic matter fractions reaching the forest floor and potentially affecting below-ground processes (le Mellec and Michalzik 2008).

To keep the scope of this chapter manageable, the present compilation of insect herbivory effects on nutrient cycling and ecosystem functioning is basically focused on temperate forest ecosystems and on short-term impacts exerted by two focal functional groups of herbivore canopy insects (leaf and sap feeders). In detail, we present research results on effects operating on short temporal scales including (a) alterations in throughfall fluxes encompassing dissolved and particulate organic matter fractions, (b) alterations in the amount, timing, and quality of frass and honeydew deposition, and (c) soil microbial activity and decomposition processes. We also address insect pest-related modifications of abiotic conditions such as changes in the canopy structure and associated alterations in soil temperature and hydrology as well as water uptake and transpiration rates by infested trees.

Finally, the aims of this chapter are to provide a synthesis of past research on herbivore–ecosystem interactions, to exhibit corresponding patterns and mechanisms between biogeochemistry and insect population ecology, to identify gaps in knowledge, and to present future trends in research to evaluate the direction and scale of changing ecosystem properties and functions.

28.2 Spatial–Temporal Population Pattern and Feeding Behavior of Canopy Insects

Insect pests usually exhibit gradient, cyclic, or eruptive population pattern, which, especially under outbreak situations, determines the timing, amount, and quality of nutrients and energy inputs from the canopy to the ground (Stadler et al. 2001). The voluminous literature on insects from varied habitats and their manifold effects on ecological processes dictate a focus on certain functional groups, which have been defined as sets of species showing either similar responses to the environment or similar effects on major ecosystem processes (Gitay and Noble 1997). Consequently, two important functional groups of canopy insects are presented here to allow for comparison of impacts and responses between different ecosystems and to derive more general patterns and regulatory mechanisms of insect-mediated effects on ecosystem functions.

First, we will introduce to the functional group of leaf feeders principally represented by lepidopterous larvae and secondly to the group of sap feeders such as aphids and scale insects (native and invasive ones), exhibiting similar effects on ecosystem key processes, e.g., the release of nutrients from and into the phyllosphere, but substantially differ for example in spatial–temporal population dynamics and feeding behavior.

28.2.1   Leaf Feeders

Several species of *Lepidoptera* are known to develop into mass outbreaks under favorable conditions and have received much attention because of their notable destructive feeding damage sometimes leading to considerable leaf area losses (Schowalter et al. 1986; Lowman 1995). Among the most intensively studied species with regard to population ecology, feeding behavior and regulatory mechanisms are the gypsy (*Lymantria dispar* L.), nun (*L. monacha* L.), winter moth (*Operophtera brumata* L.), and the pine lappet (*Dendrolimus pini* L.) (Carpenter 1940; Liebhold et al. 2000; Visser and Holleman 2001; Allen and Humble 2002; Majunke and Möller 2003). The latter being one of the most important insect pest species on pines in Eurasia and Germany (Majunke et al. 1999).

The excretory activity of the phytophagous larvae becomes notable in the form of magnified frass (insect faeces) and green-fall (green needle debris dropped during herbivory) depositions corresponding with rates of defoliation (Fig. 28.1a–d). The feeding behavior of lepidopterous larvae differs remarkably, especially during outbreak phases. While some species exhibit a polyphagous feeding behavior encompassing different host plants, (e.g., the gypsy moth), others such as the pine lappet commonly feed on coniferous trees (Majunke and Möller 2003). The amount of consumed plant biomass can be enormous. For instance, during its life cycle the pine lappets larvae can pass through up to seven larval stages, exhibiting an 11-fold increase in body length from hatching to pupation and a great increase in the body mass of approximately 900 times. The total feeding demand may amount to 15–20 g of needle biomass of which 90% are consumed by larvae emerging from diapause. The main fraction of needle biomass is consumed 2–3 weeks before pupation, which starts in June/July (Majunke et al. 1999).

As in case of the pine lappet, most of the species produce a single generation per year, often creating regular population cycles, which are recognized as predictable oscillations in mass outbreak numbers normally ranging several years to decades (Hunter et al. 1997). For example, while the western spruce budworm (*Choristoneura occidentalis*) shows outbreak cycles varying from 20 to 33 years (Swetnam and Lynch 1993), others exhibit shorter ones with 7 years of latency and 4–5 years of mass outbreaks like in case of the green oak tortrix (*Tortrix viridana* L.) (Horstmann 2009). Presumably under favorable environmental abiotic (climatic) and biotic (habitat requirements, resource limitations, enemies, and pathogens) conditions, gradual population growth can result in pest outbreaks, which are

Fig. 28.1 Different insect species in temperate forests (**a**) pine lappet (*Dendrolimus pini*) and (**b**) associated frass deposition, (**c**) Mottled umber and winter moth (*Operophtera brumata, Eranis defoliaria*) and (**d**) associated frass and green-fall deposition, (**e**) woolly beech aphid (*Phyllaphis fagi*) and (**f**) honeydew excretions, (**g**) scale insect (*Ultracoelostoma* spp.) and (**h**) honeydew droplets, New Zealand (photos by B. Michalzik)

typified to exceed certain economic threshold levels with peaking insect numbers during culmination, followed by a collapse, which reestablishes endemic or latent density levels (Wallner 1987). Still, the mechanisms that determine the local abundance pattern are under discussion (Royama 1996). However, it appears that most species form "hot spots" of infestations under favorable environmental conditions, which later disperse to neighboring trees.

28.2.2 Sap Feeders

A notable feature of aphids is the excretion of large amounts of honeydew, a sugar-rich solution, which results from their sap-feeding diet. Aphids feed on phloem sap, which is rich in photosynthetically derived carbohydrates. As the insects ingest more carbohydrates than they assimilate, they excrete excess sugar components in large droplets forming crystals on needle and leaf surfaces or glaring coatings as in case of the woolly beech aphid (*Phyllaphis fagi*) (Fig. 28.1e, f). Consequently, aphid honeydew may accumulate on the surface of leaves becoming available as an energy source for the phyllosphere microflora or it may fall directly or as rain washings from the canopy to the soil underneath the host tree (Fig. 28.2). The amounts of honeydew produced in forest ecosystems may yield 400–700 kg fresh weight ha^{-1} $year^{-1}$ (Zoebelein 1954) or 30–60 kg honeydew per tree (Müller 1956).
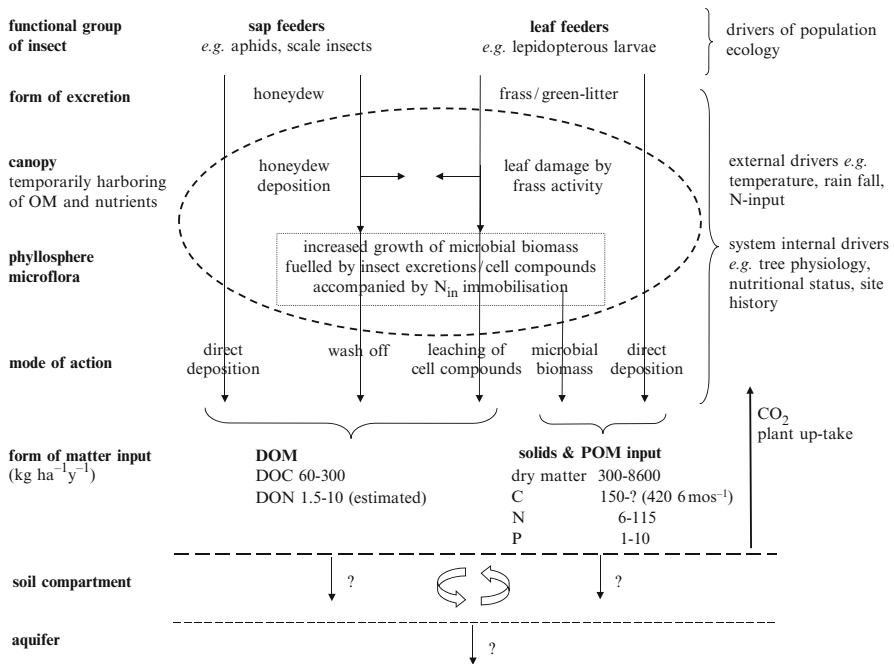
Fig. 28.2 Conceptual sketch on effects of different functional insect groups on OM and nutrient fluxes from the canopy to the ground

The greatest number of species occurs in temperate regions, where few higher plants are free from aphids (Dixon et al. 1987). Most aphid species are monophagous, living on one or a few species of a certain plant genus. In some ecosystems, honeydew represents the key component of energy fluxes, providing an important food source for birds and insects (see Sect. "28.2.3."). In contrast to leptidopters, aphids do not commonly cause notable damages to their host plants; however, they might weaken and thereafter reduce growth in particular of saplings or seedlings.

With regard to population dynamics, changes in the abundance of aphids are usually less predictable, and the numerical response to environmental change is more pronounced. The life cycle of most aphids usually encompasses several asexually reproducing and a single sexual generation with a clustered distribution and highest numbers early in the year (Kidd 1990).

28.2.3   Native and Invasive Scale Insects

In some New Zealand beech forests (*Nothofagus* spp.), the native beech scale insects (*Ultracoelostoma assimile* and *U. brittini* (Hemiptera: Maragodidae)), which colonize the bark of the beech trees, have been assumed to function as keystone species due to the excretion of large amounts of honeydew, which serves as a carbohydrate resource for different species at several trophic levels. Differing from aphids which exhibit a temporally clumped distribution of honeydew excretion, the honeydew of scale insects is produced year round and can achieve substantial amounts of up to $1,930 \, \text{kg ha}^{-1} \, \text{year}^{-1}$, which may represent up to 8% of the net primary productivity (NPP) (Beggs et al. 2005, Table 28.1). Similar to aphids, the beech scale insect feeds on the phloem sap, with the excess sugar being excreted as droplets of honeydew at the end of a long, waxy anal filament (Morales et al. 1988) (Fig. 28.1g, h). The honeydew consists of sucrose, fructose, oligosaccharides, and small quantities of glucose (Grant and Beggs 1989), which is produced by encapsulated second- and third-instar females and second-instar males. Though numbers of individuals can be tremendous ranging from about 10^5 to 2×10^7 scale insects per hectare (Kelly 1990), it is suggested that the beech scale insects do not cause harmful effects to the host trees which encompass different species of *Nothofagus*.

The invasive hemlock woolly adelgid (HWA, *Adelges tsugae*, Annand) is native to Japan and was accidentally introduced to North America in the 1920s, becoming an aphid-like destructive pest of the eastern (*Tsuga Canadensis* L.) and Carolina hemlock (*T. caroliniana* Engelm.). HWA began to cause severe mortality of hemlocks in southern New England in the 1980s. Due to its easy dispersal by wind and animals, HWA continue to move farther north at rates of up to $30 \, \text{km year}^{-1}$ throughout the range of eastern hemlock (McClure 1983, 1991). Adelgids are very host-specific and feed on the xylem ray parenchyma cells by piercing at the base of needles, subsequently causing desiccation and eventual needle loss. Infested hemlock trees usually die within 5–15 years and show only little resistance (Orwig and Foster 1998). Regarding population dynamics, the

Table 28.1 Effects of leaf feeders on nutrient fluxes and soil processes in temperate forests

Insect and infestation level	Study site, type, duration	Flux processes (flux units)	Matter/ nutrients	Fluxes (kg ha^{-1} time^{-1}) Control	Infested	Flux factor (infested/control)	Reference
Leaf feeders		*Above-ground inputs*					
Green oak tortrix (*Tortrix viridana*)	North Lancashire, UK Sessile oak, 40- to 120-year-old Field study plots (1961–1964)	Frass (kg ha^{-1} year^{-1})	Dry matter	28.90	300.00	10.4	Carlisle et al. (1966)
			C	14.25	147.90	10.4	
Moderately severe in 1961, 1962–1964	Outbreak year 1961		N	0.88	6.50	7.4	
low activity	Compared to 1963 (control)		P	0.08	0.81	10.1	
			K	0.34	3.54	10.4	
			Ca	0.16	1.62	10.1	
			Mg	0.04	0.39	9.8	
Gypsy moth (*Lymantria dispar* L.)	Pennsylvania, USA Mixed oak stand 60- to 80-year-old	Leaf fragments (kg ha^{-1} year^{-1})	Dry matter	37.20	918.00	24.7	Grace (1986)
			N	0.97	19.34	19.9	
			P	0.06	1.20	20.3	
Severe infestation	Field study plots (1975–1976)		K	0.12	6.32	52.7	
with heavy	Infested compared to control		Ca	0.20	3.53	17.7	
defoliation			Mg	0.08	1.18	14.8	
	sites	Frass (kg ha^{-1} year^{-1})	Dry matter	–	824.00	–	
			N	–	15.19	–	
			P	–	0.88	–	
			K	–	3.68	–	
			Ca	–	3.16	–	
			Mg	–	1.08	–	
Oak moth (*Phryganidia californica*)	California, USA Mixed oak stand Single study trees of oak	Frass (*Q. agrifolia*) (kg ha^{-1} year^{-1})	Dry matter	870.00	8,630.00	9.9	Hollinger (1986)
			N	13.70	113.70	8.3	
			P	1.10	9.60	8.7	
Severe infestation	(1980–1982)	(*Q. lobata*)	Dry matter	610.00	2,140.00	3.5	
with total	Outbreak year 1981		N	12.20	44.20	3.6	
defoliation	Compared to 1982 (control)		P	0.80	3.10	3.9	

							Reference
Caterpillar, various insects	North Carolina, USA Mixed oak, 70-year-old Field study plots (1985–1986)	Insects (*Q. agrifolia*)	Dry matter	10.00	870.00	87.0	Risley and Crossley (1993)
			N	0.50	89.60	179.2	
			P	0.00	7.20	–	
		(*Q. lobata*)	Dry matter	20.00	350.00	17.5	
			N	2.00	37.60	18.8	
			P	0.10	2.70	27.0	
		Throughfall (*Q. agrifolia*)	N	36.80	22.50	0.6	
			P	3.00	2.20	0.7	
		Throughfall (*Q. lobata*)	N	11.00	13.60	1.2	
			P	3.30	2.40	0.7	
		Greenfall (kg ha⁻¹ year⁻¹)	N	1.00	1.70	1.7	
Winter moth (*Operophthera brumata*), mottled umber (*Erannis defoliaria*) Leaf area loss between 20 and 40%, damaged leaves between 70 and 100%	Bavaria, Germany Mixed beech/oak stands 130-year-old Field study plots (4 months)	Throughfall (kg ha⁻¹ 4 mos⁻¹)	DOC	42.86	44.63	1.0	Stadler et al. (2001), Michalzik (1999) (fluxes)
			Hexose-C	4.80	6.74	1.4	
			DON	2.33	2.85	1.2	
			NH₄-N	2.20	1.37	0.6	
			NO₃-N	2.55	1.40	0.5	
			N_tot	7.08	5.62	0.8	
Pine lappet (*Dendrolimus pini*) Severe infestation up to 60% defoliation	Lower Saxony, Germany Scots pine, 80-year-old Field study plots (6 months) Infested compared to control site	Frass plus green-fall (kg ha⁻¹ 6 mos⁻¹)	Dry matter	–	894.00	–	le Mellec and Michalzik (2008)
			C	–	420.00	–	
			N	–	8.60	–	
		Throughfall (kg ha⁻¹ 6 mos⁻¹)	TOC	81.40	180.40	2.2	
			DOC	67.60	138.00	2.0	
			TN	8.24	14.06	1.7	
			DN	5.99	8.69	1.5	
			NO₃-N	2.35	2.92	1.2	

Table 28.1 (continued)

Insect and infestation level	Study site, type, duration	Flux processes (flux units)	Matter/ nutrients	Fluxes (kg ha^{-1} time^{-1})		Flux factor (infested/control)	Reference
				Control	Infested		
		Soil processes					
Gypsy moth (*Lymantria dispar* L.)	New York, USA Black oak Incubation study (4 months)	Frass addition to soil	Increased growth of microbial biomass Increased N immobilization Increased C mineralization				Lovett and Ruesink (1995)
Walking sticks (*Anisimorpha buprestoides* (Stoll) Forest tent caterpillar (*Malacosoma disstria*)	North Carolina, USA Mixed hardwood, *Q. rubra* Study plots at different elevations levels, 5 months	Frass and throughfall Addition to soil	Inconsistent effects on N and P mineralization No effects on litter decomposition				Reynolds and Hunter (2001)
Gypsy moth (*Lymantria dispar* L.) Simulated 50% defoliation	New York, USA Oak seedlings Field manipulation study 29 months	N^{15}-labeled caterpillar Frass input	Enhanced N mobilization by microbes and direct dissolution Reduced availability to plants				Christenson et al. (2002)
Various herbivore insects at endemic levels	North Carolina, USA Study plots at different elevations levels (4 months)	Frass and throughfall inputs	Less pronounced positive effects on C mineralization and soil N availability				Hunter et al. (2003)
Eastern tent caterpillar (*Malacosoma americanum*) Moderate to endemic levels	Georgia, USA Red oak saplings Pot experiment, 7 months	Frass addition by larvae Feeding, modification of leaf damage	Increased soil respiration Increased C_{mic} Decreased total soil N				Frost and Hunter (2004)

		Ecosystem export				References
Gypsy moth (*Lymantria dispar* L.) 40–100% defoliation	Michigan, USA Hybrid poplars Field study (1996 and 1997)	No significant effects on N losses via NH_3 volatilization, and N_2O gasing and NO_3 leaching No significant effects on N_{mic} and soil inorganic N				Russel et al. (2004)
Fall cankerwurm (*Alsophila pometaria*), outbreak year 1974, 33% defoliation	North Carolina, USA Mixed hardwood Catchment study (1972–1979)	Stream water (kg ha^{-1} year^{-1})	NO_3-N	0.08	0.46	5.5	Swank et al. (1981)
Spruce budworm (*Choristoneura fumiferana*) Severe outbreaks 1981–1984, Endemic levels (1999–2002)	Quebec, Canada Balsam fir, white spruce Approx. 50-year old Field study plots, catchment export (1981–1984) (1999–2002) Outbreak years 1981–1984 Compared to endemic levels (1999–2002)	Soil water (kg ha^{-1} year^{-1})	NH_4-N	0.02	0.11	5.5	Houle et al. (2009)
			NO_3-N	0.28	8.43	30.1	
			K	0.36	2.99	8.3	
			Ca	9.62	24.46	2.5	
			Mg	0.73	1.94	2.7	
		Stream water (kg ha^{-1} year^{-1})	NH_4-N	0.07	0.00	–	
			NO_3-N	0.25	1.05	4.2	
			K	1.29	2.03	1.6	
			Ca	4.61	6.42	1.4	
			Mg	2.67	3.18	1.2	

HWA produces two annual generations including an overwintering one, which deposits eggs into wax-rich woolly egg sacks in spring, from which crawlers hatch in April starting to disperse evenly within the host tree or searching for new suitable sites by wind dispersal. A second generation derived from eggs in June, which were laid by individuals of the first one. Feeding and subsequent maturing of this second generation appear throughout late autumn until February (McClure 1983, 1991).

Differing from aphids, HWA excrete less honeydew, but actively produce wax wool for egg deposition in spring. However, it is assumed that the waxes eventually break down and are washed off with throughfall, providing a low but fairly constant source of energy especially early in the year (Stadler et al. 2005).

28.3 Canopy Herbivory and Effects on Hydrology

The role of forest canopies in ecosystem functioning and services is beyond question. They are of crucial importance for controlling the exchange of carbon, water, and energy between the ecosystem and the atmosphere (Ryan 2002). Within forested ecosystems the canopy has a large influence on nutrient cycling by regulating forest hydrology, microclimatic conditions as well as the chemical quality, and the amount of leaf litter and throughfall inputs to the ground (Prescott 2002).

Outbreaks of defoliating insects temporarily will thin the forest canopy, subsequently promoting different alterations within forest hydrology. In this context, more solar radiation will reach the forest floor (Collins 1961), and the leaf area index (LAI) is lowered which in turn will decrease interception and transpiration rates and increase the amounts of throughfall entering the forest floor, consequently resulting in warmer and moister soil conditions (Classen et al. 2005). These altered soil conditions may stimulate microbial activity including nitrification and litter decomposition (Swank et al. 1981). For example, a study by Cobb et al. (2006) investigating the effects of HWA impacted eastern hemlock (*Tsuga Canadensis* L.) forests on green foliage decomposition exhibits that insect pests significantly alter the forest floor microclimate inducing different soil moisture levels which in turn control decomposition.

Apart from throughfall, stemflow is the second hydrological process being responsible for the transfer of water and solutes from the canopy to the soil. As spatially prominent point input of water and nutrients, it has been shown to significantly alter soil solution chemistry and soil nutrient status as well as soil moisture and groundwater recharge (Levia and Frost 2003). Among meteorological conditions, seasonality, and species-depending traits, the canopy structure was one factor affecting stemflow amounts and composition. The input of easily available carbohydrates and nutrients by stemflow is supposed to be intensified in case of sap feeders. Nevertheless, the role of insect defoliation and excretion and frass activity on altered stemflow production and chemistry is imperfectly understood at the moment.

On a landscape level, persistent infestation and subsequent defoliation, as in case of HWA-damaged hemlock forests, may result in tree health decline, reduced nutrient uptake, and consequently in tree mortality, which clearly provides a severe potential for significant N and nutrient cation losses to soil water. Additionally, reduced vegetation cover promotes the risk for surface runoff and erosion processes especially on steep slopes and during extreme rain events potentially disturbing surface waters.

Global warming is projected to induce changes in the midlatitudes of the Northern Hemisphere, resulting in a warmer and wetter climate, with an increase in extreme weather events such as prolonged summer droughts and heavy rain storms later in the year (IPCC 2007). Some authors suggest that changed environmental conditions will create intensified stressful conditions with regard to tree vigor and resistance and will favor the growth conditions for pest insects (Bale et al. 2002). For instance, a number of extensive insect mass outbreaks were reported following the exceptionally hot and dry summer of 2003 in Europe (Rouault et al. 2006). However, the extent to which biologically governed processes and ecosystem interactions will be affected by climatic and environmental alterations is imperfectly understood (Hunter 2001).

28.4 Linking Herbivore Insects and Biogeochemistry

Figure 28.2 provides an overview of the effects of two functional groups of phytophagous insects on different forms of organic matter and nutrient fluxes cascading downward from the canopy to the ground. While leaf feeders considerably contribute to inputs of solid and particulate organic matter (right-hand side), sap feeders basically affect dissolved organic matter fluxes (left-hand side). The canopy functions as a biochemical reactor harboring manifold processes, which operate in concert with external (abiotic) and internal (biotic) driving variables.

28.4.1 Effects of Insect Herbivory on Canopy Processes

28.4.1.1 Canopy-Derived Organic Matter and Nutrient Fluxes

To explain the varying energy and nutrient transfer patterns with throughfall solution, variable interacting processes such as precipitation patterns (Mercier and Lindow 2000), tree species canopy architecture (Levia and Frost 2006; de Schrijver et al. 2007), atmospheric ecosystem deposition (Lamersdorf and Blank 1995), leaf leaching (Tukey and Morgan 1963), and immobilization processes within the canopy mediated by phyllosphere microorganisms (Stadler and Müller 2000) may be examined. However, few studies on nutrient and energy fluxes through forested

ecosystems have been conducted with a detailed knowledge of the ecology of the
key organisms that affect them.

Table 28.1 elucidates the pronounced differences in above-ground organic
matter and nutrient inputs with throughfall solution or as solids between infested
and noninfested forest sites. For instance, severe infestations of leaf feeders
significantly magnify the nutrient (N, P, K, Ca, and Mg) and organic matter
(C_{org}) transfer to the soil via frass (insect faeces), green-fall (green needle debris
dropped during herbivory), and insect cadavers by a factor of ten or more (Carlisle
et al. 1966; Grace 1986; Hollinger 1986). However, dissolved organic matter
(DOM <0.45 μm) and nutrient fluxes with throughfall solution exhibit less pro-
nounced flux increments under infestation. This is likely due to minor release rates
from feeding-induced leaf damages or to a rapid consumption by microbial miner-
alization and/or immobilization processes within the phyllosphere (see
Sect. 28.4.1.2). Additionally, differences in water fluxes between sites and the
temporal scale of observation might obscure initially significant differences in
element concentrations (Stadler et al. 2001).

To reveal insect–canopy–soil interactions, the accurate determination of input
fluxes to the soil is of central importance. However, since element and nutrient fluxes
are conventionally determined after standard filtration (0.45 μm pore size), the
exclusion of the particulate/unfiltered organic matter fraction (0.45 μm < particulate
organic matter (POM) <500 μm) potentially results in misleading conclusions and
budgeting gaps when studying nutrient and energy fluxes in ecosystems (Michalzik
and Stadler 2005). In this context, le Mellec and Michalzik (2008) report on a
significant contribution of particulate organic N and C providing an extra input
of up to 60% to the dissolved N and up to 30% to the dissolved C fluxes with
throughfall during a mass outbreak of the pine lappet (*Dendrolimus pini*)
(Table 28.1). Furthermore, it appears that particulate organic matter fluxes with
throughfall might serve as an early indicator for leaf feeding activity in the canopies
of trees (le Mellec et al. 2009).

Concerning sap feeders, few studies provide data on throughfall fluxes of matter
and nutrients (Table 28.2). One reason for this might be a more definite statistical
proof of insect-mediated changes of nutrient dynamics when only regarding con-
centrations, while nutrient fluxes exhibit greater fluctuations among replications
(and hence less statistical significance) due to highly varying amounts of water
passing through the system.

The flux data presented here span observation periods between 8 weeks and
1 year and exhibit average increase factors for DOC under infestation between 1
and 2.5. Peak DOC and hexose-C fluxes of 270 and 127 kg C ha^{-1} 10 weeks^{-1},
respectively, were observed under experimental conditions promoting high aphid
infestation levels (flux factors of 30.7 for DOC and 62.4 for hexose-C, respectively;
Table 28.2), which are rarely achieved under field conditions. As in case of Pederson
and Bille-Hansen (1995), larger temporal scales of observation (e.g., on an annual
basis) might level out short-term peak fluxes by temporally dominating periods of
average or low nutrient fluxes.

Table 28.2 Effects of sap feeders on nutrient fluxes in temperate forests

Insect and infestation level	Study site, type, duration	Flux processes (flux units)	Matter/ nutrients	Fluxes (kg ha^{-1} time^{-1})		Flux factor (infested/ control)	Reference
				Control	Infested		
Sap feeders							
Green spruce aphid	Denmark	Ulborg site litterfall	N	34.60	69.70	2.0	Pedersen and
(*Elatobium abietinum*)	Sitka spruce, 30-year old	Throughfall	NO$_3$-N	11.30	10.80	1.0	Bille-Hansen
heavy infestation in	Three field study plots	(kg ha^{-1} year^{-1})	NH$_4$-N	21.60	21.00	1.0	(1995,
1989 and 1993	(1988–1994)		TOC	70.00	66.30	0.9	1999),
	Average annual fluxes of		K	22.20	32.10	1.4	Pedersen
	endemic (control) versus	Lindet site litterfall	N	27.00	54.90	2.0	et al.
	Infestation years	Throughfall	NO$_3$-N	10.80	9.70	0.9	(1995)
		(kg ha^{-1} year^{-1})	NH$_4$-N	14.60	14.50	1.0	
			TOC	61.50	63.50	1.0	
			K	21.00	27.40	1.3	
		Frederiksborg site litterfall	N	29.80	61.40	2.1	
		Throughfall	NO$_3$-N	14.10	12.50	0.9	
		(kg ha^{-1} year^{-1})	NH$_4$-N	11.90	10.10	0.8	
			TOC	51.70	59.90	1.2	
			K	18.30	27.50	1.5	
Spruce aphid (*Cinara	Bavaria, Germany	Throughfall	DOC	12.90	23.70	1.8	Michalzik
pilicornis*)	Norway spruce	(kg ha^{-1} 8 weeks^{-1})	Hexose-C	0.60	9.68	16.1	(1999)
Moderate infestation	10–15-year old		DON	0.62	0.96	1.5	
	Field study plots (8 weeks)		NH$_4$-N	0.98	0.85	0.9	
	Infested compared to		NO$_3$-N	1.34	1.02	0.8	
	control site		N$_{tot}$	2.94	2.83	1.0	
		Forest floor solution	DOC	8.70	15.30	1.8	
		(kg ha^{-1} 8 weeks^{-1})	Hexose-C	0.30	0.43	1.4	
			DON	0.48	1.71	3.6	
			NH$_4$-N	0.47	0.46	1.0	
			NO$_3$-N	0.39	0.81	2.1	
			N$_{tot}$	1.34	2.98	2.2	

Table 28.2 (continued)

Insect and infestation level	Study site, type, duration	Flux processes (flux units)	Matter/nutrients	Fluxes (kg ha⁻¹ time⁻¹)		Flux factor (infested/control)	Reference
				Control	Infested		
Spruce aphid (*Cinara pilicornis*) Heavy infestation	Bavaria, Germany Norway spruce, 10-year old Irrigation pot experiment (10 weeks), infested compared to control site	Throughfall (kg ha⁻¹ 10 weeks⁻¹)	DOC	8.83	271.47	30.7	Michalzik (1999)
			Hexose-C	2.04	127.29	62.4	
			DON	4.26	2.71	0.6	
			NH₄-N	12.40	9.25	0.7	
			NO₃-N	16.91	14.80	0.9	
			N$_{tot}$t	33.57	26.76	0.8	
Scale insect (*Ultracoelostoma* spp.) Different levels of infestation	South Island, New Zealand Southern beech species (*Nothofagus* spp.) Field study (2 years)	Honeydew production (kg ha⁻¹ year⁻¹)	year 1 dry mass	–	3,800.00	–	Beggs et al. (2005)
			C	–	1,600.00	–	
			year 2 dry mass	–	4,600.00	–	
			C	–	1,930.00	–	
Hemlock woolly adelgid (*Adelges tsugae*) Moderate infestation	Connecticut, USA Hemlock, field study plots (15 weeks)	Throughfall (kg ha⁻¹ 15 weeks⁻¹)	DOC	5.84	10.50	1.8	Stadler et al. (2005)
			DON	0.26	0.44	1.7	
			TN	1.00	1.20	1.2	
Spruce aphid (*Cinara pilicornis*) Moderate infestation	Bavaria, Germany Norway spruce, 10-year-old Study plots at 2 sites (12 weeks)	Site 1 throughfall (kg ha⁻¹ 12 weeks⁻¹)	DOC	22.65	51.00	2.3	Mühlenberg and Stadler (2005)(flux data estimated from Fig. 4)
			Hexose-C	1.90	20.75	10.9	
			DON	0.87	1.01	1.2	
			NH₄-N	0.76	0.37	0.5	
			NO₃-N	1.29	0.83	0.6	
			N$_{tot}$	2.92	2.21	0.8	
			K	3.00	5.55	1.9	
		Site 2 throughfall (kg ha⁻¹ 12 weeks⁻¹)	DOC	20.25	47.75	2.4	
			Hexose-C	4.35	23.50	5.4	
			DON	0.73	0.93	1.3	
			NH₄-N	0.39	0.42	1.1	
			NO₃-N	0.95	0.72	0.8	
			N$_{tot}$	2.07	2.07	1.0	
			K	2.40	3.75	1.6	

In general, herbivory can alter the throughfall composition by promoting the fluxes of the organic N (DON) and especially the organic C fraction. However, throughfall fluxes of inorganic N species appear to diminish under heavy infestation showing flux factors <1 (Table 28.2), which might point to microbial immobilization processes within the canopy (see 28.4.1.2).

28.4.1.2 Microbial Phyllosphere Processes

With leaf shooting and increasing temperatures in spring, different groups of sessile and mobile organisms in the canopy such as yeasts, bacteria, filamentous fungi, and epiphytic plants (Kinkel 1997) become active and thus contribute to matter decay, chemical transformation, nutrient immobilization, and release processes into throughfall solutions (Mercier and Lindow 2000). Hence, alterations of the throughfall N composition under herbivory supply evidence for a trophic interaction with phyllosphere microorganisms immobilizing N in the canopy. Diminished fluxes of NO_3-N (and to a lesser extent NH_4-N) during highest insect feeding activity can probably be attributed to an enhanced biomass growth of epiphytic microorganisms (bacteria, yeasts, and filamentous fungi) immobilizing inorganic N in the presence of easily available C compounds released either from honeydew or feeding-damaged needles as observed by Stadler et al. (1998, 2001) and Lovett et al. (2002). Promoted growth of phyllosphere microbial biomass under herbivore infestation likely contributes as well to enhanced flux amounts of particulate organic N and C (le Mellec and Michalzik 2008). Since filtration through a 0.45-μm pore size excludes the majority of microbes (passing through 0.2-μm pore size is defined as "sterile filtration"), it is suggested that the particulate fraction largely represents frass and plant debris, and microbial biomass (Stadler and Müller 2000).

In summary, seasonal patterns of fluctuations in both dissolved and particulate element fluxes with throughfall might be partly explained by the population and feeding activity of different functional groups of canopy insects.

28.4.1.3 Timing and Quality of Nutrient Inputs

Apart from intensified overall organic matter inputs, the form and timing of inputs are remarkably altered especially during mass outbreaks of leaf feeders. In this context, Grace (1986) reported for a 60- to 80-year-old oak stand that 67% of the N, Ca, K, Mg, and P inputs under gypsy moth herbivory already occurred during the growing season compared to only 12% at the control site. Here, the majority (86%) of nutrients returned with litterfall in autumn. This is in accordance with findings by le Mellec and Michalzik (2008) from a pine forest, where the temporal dynamics of organic matter inputs distinctly mirror the life cycle and feeding activity pattern of the pine lappet larvae. As a consequence, peak fluxes occurred within a short period of 4–5 weeks during June/July, where about 80% of the overall inputs under
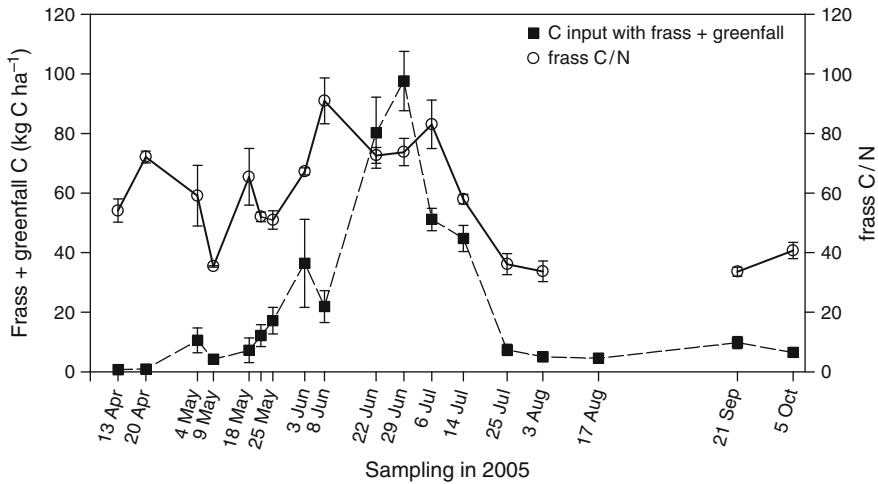
Fig. 28.3 Carbon fluxes with frass and green-fall in kg C ha^{-2} and corresponding C/N ratios in frass material (means $\pm$ S.E.) (adapted from le Mellec and Michalzik 2008)

herbivory enters the ground, pinpointing the enormously altered timing in nutrient cycling (Fig. 28.3).

Besides modified quantities and timing of nutrient inputs, canopy herbivory changes the chemical quality and form of organic compounds as well (Swank et al. 1981). After feeding and digestion, the organic material significantly differs from the chemical composition of the initial plant biomass, exhibiting more nutrients and a higher biological activity, and thus appears to be more readily decomposable by soil microbes (Schowalter et al. 1986; Lovett and Ruesink 1995). In this context, a depletion of N in insect-processed frass material became notable under a heavy pine lappet infestation with highly differing frass C/N of 55 in April/May and up to 90 during peak larval abundance in June/July (Fig. 28.3). In this case, a pronounced assimilation of N by the moth larvae during needle biomass ingestion was assumed, consequently enhancing the C/N ratios by means of a high N utilization efficiency as observed by other authors for the gypsy moth and different food qualities (Lovett et al. 2002).

In contrast to leaf feeders, sap feeders dominantly contribute to the input of readily available dissolved carbon compounds such as hexose-C, representing 40–50% of the DOC (Table 28.2). However, high C input fluxes were only observed for short time periods spanning a few weeks in June/July when aphids are most abundant (Stadler et al. 1998, 2001). In contrast to aphids, the native scale insects in southern *Nothofagus* forests provide honeydew year round, which can achieve substantial amounts of up to 1,930 kg C ha^{-1} year^{-1}, representing up to 8% of the NPP (Table 28.1). While the importance of this carbohydrate resource for different species at several trophic levels is beyond question, the functional relationship between honeydew throughfall and litter decomposition is still under debate (Wardhaugh and Didham 2005).

Nevertheless, the consequences of such insect-mediated "shortcuts" in nutrient cycling with a remarkable and chemically altered loss of canopy biomass during the growing season contrasting the return of nutrients with litterfall in autumn under noninfestation are still imperfectly understood.

28.4.2   Effects of Insect Herbivory on Soil Processes

28.4.2.1   Soil Microbial Activity and Decomposition Processes

Various studies demonstrated that phytophagous insects are capable of transforming needle biomass or leaf constituents into more easily degradable secondary products (e.g., frass, honeydew, and wax wool) (Hunter 2001; Chapman et al. 2003; Stadler et al. 2006). Nevertheless, the outcome of studies testing the effects of insect-promoted input fluxes of organic matter on soil biological processes such as mobilization and mineralization of soil organic matter, priming effects, lignin degradation, and long-term nutrient storage, remains ambiguous as exhibited by Table 28.1. For instance, Swank et al. (1981) reported significantly enhanced nitrate exports from a watershed following insect pest outbreaks, whereas Bormann and Likens (1979) found no such effects in the Hubbard Brook Experimental Forest. Houle et al. (2009) recorded increased soil fluxes of inorganic N and nutrients under budwurm infestation, which were also notable in stream water (Table 28.1). In laboratory experiments, Lovett and Ruesink (1995) observed an immobilization of N after frass material was applied. Decreased inorganic N concentrations in forest floor solution after honeydew addition were also observed by Michalzik and Stadler (2000) during a mesocosm irrigation experiment. No effects of frass/green-fall application on C and N mineralization rates and litter decay were reported by Russel et al. (2004) or by Reynolds and Hunter (2001). On the other hand, Christenson et al. (2002) exhibited an enhanced N mobilization by microbes after frass input. Streminska et al. (2002) recorded changes in the diversity and activity of soil microbes in a pine forest following a heavy mass outbreak of lepitopterous larvae, which caused a 60% defoliation. At the infested site higher numbers of ammonifying and denitrifying bacteria and fungi were found, which were accompanied by enhanced N mineralization rates.

In view of these inconsistent results, it is appropriate to hypothesize whether the spatial and temporal scale of observation is useful to accurately track changes in nutrient fluxes and process rates, thus addressing methodological questions in ecosystem and ecology research. On the other hand, ecosystem state properties such as inherent pools of organic matter and nutrients, atmospheric deposition, and N status or the nutrient demand of the biosphere might govern soil biological processes, hence masking the impact of insect pests. Presumably, there are ecosystem-specific "threshold inputs" of insect-mediated amounts of organic matter, which need to be exceeded to trigger effects on mineralization and mobilization rates.

28.5 Future Directions

The focus of this chapter was on the short-term impacts exerted by two focal functional groups of herbivore canopy insects on nutrient cycling in forest ecosystems. Regarding results from studies operating on short temporal and spatial scales (e.g., several weeks and single trees), patterns of fluctuations in organic matter and nutrient fluxes with throughfall and as solids clearly can be attributed to the population ecology of canopy insects. Therefore, the idea of corresponding patterns and mechanisms between biogeochemistry and insect population ecology appears to be confirmed.

However, on larger temporal and spatial time scales (e.g., annual nutrient fluxes on a plot-level scale) the variability of fluxes caused by phytophagous insects is often filtered in other ecosystem compartments such as the forest floor, or leveled out by temporally dominating periods of average or low nutrient fluxes. Therefore, actual flux amplitudes become largely invisible. Nevertheless, the information on the frequency and magnitude of "hot spots and moments" caused by insect infestations is important, because it is unlikely that ecosystem processes and state properties as, for instance, the establishment or loss of nutrient pools is driven by annual average fluxes but by extreme events and associated peak fluxes. Thus, information on the potential range of variation of matter and energy fluxes on different scales of observation is necessary to understand filter mechanisms and long-term effects caused by varying environmental and presumably warmer conditions within ecosystems.

Studying insect herbivory and ecosystem processes would be also useful in a better understanding of above-ground–soil interactions, which is also one point of interest in Critical Zone (CZ) research (Lin 2009). The CZ refers to top of the vegetation down to the bottom of the aquifer, extending from the near-surface biosphere and atmosphere, through the pedosphere, to the surface and near-surface portion of the hydrosphere and lithosphere. The focus is on water-related research which requires enhanced understanding of processes at environmental interfaces and improved coupling of biological and physical processes (Lin 2009). In this context, insect-mediated inputs of energy and matter to the soil may change biogeochemical process rates, probably functioning as cosubstrates, which in turn trigger enhanced decomposition and destabilizing of previously recalcitrant soil organic matter pools. To date, it is largely unknown how deep and by which mechanisms (e.g., stemflow, preferential flow, rain storms) insect herbivory reaches into the ground and may channel labile carbon into (energy limited) soil horizons or even the aquifer.

Consequently, many areas merit further research, but there are three addressing insect ecology and forest biogeochemistry that deserve special mention: (1) studying insect herbivory and ecosystem processes in a warmer world; (2) examining insect-mediated fluxes in the larger Critical Zone framework; and (3) identifying insect-induced "shortcuts" in nutrient cycling and spatial–temporal bypass flows of water and solutes connecting the soil surface, the deeper ground, and the groundwater.

To answer those questions, integrated research involving different disciplines such as biologists, ecosystem ecologists, foresters, and economists is needed to create a basic knowledge on the interlinkages between insect ecology, vegetation physiology, and biogeochemistry.

References

Allen EA, Humble LM (2002) Nonindigenous species introductions: a threat to Canada's forests and forest economy. Can J Plant Pathol 24:103–110

Ayres MP, Lombardero MJ (2000) Assessing the consequences of global change for forest disturbance from herbivores and pathogens. Sci Total Environ 262:263–286

Bale JS, Masters GJ, Hodkinson ID et al (2002) Herbivory in global change research:direct effects of rising temperatures on insect herbivores. Glob Change Biol 8:1–16

Bardgett RD, Wardle DA, Yeates GW (1998) Linking above-ground and below-ground interactions: how plant responses to foliar herbivory influence soil organisms. Soil Biol Biochem 30:1867–1878

Beggs JR, Karl BJ, Wardle DA et al (2005) Soluble carbon production by honeydew scale insects in a New Zealand beech forest. NZ J Ecol 29:105–115

Bormann FH, Likens GE (1979) Pattern and processes in a forested ecosystem. Springer, Berlin, Heidelberg, New York

Carlisle A, Brown AHF, White EJ (1966) The organic matter and nutrient elements in the precipitation beneath a sessile oak (*Quercus petraea*) canopy. J Ecol 54:87–98

Carpenter JR (1940) Insect Outbreaks in Europe. J Anim Ecol 9:108–147

Chapman SK, Hart SC, Cobb NS et al (2003) Insect herbivory increases litter quality and decomposition: an extension of the acceleration hypothesis. Ecology 84:2867–2876

Christenson LM, Lovett GM, Mitchell MJ et al (2002) The fate of nitrogen in gypsy moth frass deposited to an oak forest floor. Oecologia 131:444–452

Classen AT, Hart SC, Whitman TG et al (2005) Insect Infestations linked to shifts in microclimate: Important climate change implications. Soil Sci Soc Am J 69:2049–2057

Cobb RC, Orwig DA, Currie S (2006) Decomposition of green foliage in eastern hemlock forests of southern New England impacted by hemlock woolly adelgid infestations. Can J For Res 36:1331–1341

Collins S (1961) Benefits to the understory from canopy defoliation by gypsy moth larvae. Ecology 42:836–838

Dale VH, Joyce LA, McNulty S et al (2001) Climate change and forest disturbances. Bioscience 51:723–734

De Schrijver AD, Geudens G, Augusto L et al (2007) The effect of forest type on throughfall deposition and seepage flux: a review. Oecologia 153:663–674

Dixon AFG, Kindlmann P, Lepš J et al (1987) Why there are so few species of aphids, especially in the tropics. Am Nat 129:580–592

Finzi AC, Canham CD, van Breemen N (1998) Canopy tree-soil interactions within temperate forests. Ecol Appl 8:447–454

Frost CJ, Hunter MD (2004) Insect canopy herbivory and subsequent frass deposition influence soil nitrogen and carbon fluxes and nitrogen export in red oak mesocosm. Ecology 85:3335–3347

Gitay H, Noble IR (1997) What are functional types and how should we seek them? In: Smith TM, Shugart HH, Woodward FI (eds) Plant functional types. University Press, Cambridge, pp 3–19

Grace JR (1986) The influence of gypsy moth on the composition and nutrient content of litter fall in a Pennsylvania oak forest. For Sci 2:855–870

Grant WD, Beggs JR (1989) Carbohydrate analysis of beech honeydew. NZ J Ecol 16:283–288

Hollinger DY (1986) Herbivory and the cycling of nitrogen and phosphorus in isolated California oak trees. Oecologia 70:291–297

Horstmann K (2009) Untersuchungen zum Massenwechsel des Eichenwicklers, *Tortrix viridana* L. (Lepidoptera, Tortricidae) in Unterfranken. Z Angew Ent 98:73–95

Houle D, Duchesne L, Boutin R (2009) Effects of a spruce budworm outbreak on element export below the rooting zone: a case study for a balsam fir forest. Ann For Sci 66:707

Hunter MD (2001) Insect population dynamics meets ecosystem ecology: effects of herbivory on soil nutrient dynamics. Agric For Entomol 3:77–84

Hunter MD, Varley GC, Gradwell GR (1997) Estimating the relative roles of top-down and bottom-up forces on insect herbivore populations: a classic study revisited. Proc Natl Acad Sci USA 94:9176–9181

Hunter MD, Linnen CR, Reynolds BC (2003) Effects of endemic densities of canopy herbivores on nutrient dynamics along a gradient in elevation in the southern Appalachians. Pedobiologia 47:231–244

IPCC (2007) Summary for policymakers. In climate change 2007: impacts, adaptation and vulnerability. University Press, Cambridge

Kelly D (1990) Honeydew density in mixed *Nothofagus* forest, Westland, New Zealand. NZ J Bot 28:53–58

Kidd NAC (1990) The population dynamics of the large pine aphid, *Cinara pinea* (Mordv.) II. Simulation of field populations. Res Pop Ecol 32:209–226

Kinkel LL (1997) Microbial population dynamics on leaves. Annu Rev Phytopathol 35:327–347

Lamersdorf NP, Blank K (1995) Evaluation of fine material input with throughfall for a spruce forest in Solling, FRG, by means of a roof construction. In: Jenkings A, Ferrier RC, Kirby C (eds) Ecosystem manipulation experiments: scientific approaches, experimental design and relevant results, Commission of the European Communities, Office for Official Publications of the European Communities, Brussels, Luxembourg. Ecosystem Research Report 20, pp 168–170

Larrson S, Tenow O (1980) Needle-eating insects and grazing dynamics in a mature Scots pine forest in central Sweden. Ecol Bull 32:269–306

le Mellec A, Michalzik B (2008) Impact of a pine lappet (*Dendrolimus pini*) mass outbreak on C and N fluxes to the forest floor and soil microbial properties in a Scots pine forest in Germany. Can J For Res 38:1829–1849

le Mellec A, Habermann M, Michalzik B (2009) Canopy herbivory altering C to N ratios and soil input patterns of different organic matter fractions in a Scots pine forest. Plant Soil 325:255–262

Levia DF, Frost EE (2003) A review and evaluation of stemflow literature in the hydrologic and biogeochemical cycles of forested and agricultural ecosystems. J Hydrol 274:1–29

Levia DF, Frost EE (2006) Variability of throughfall volume and solute inputs in wooded ecosystems. Prog Phys Geog 30:605–632

Liebhold AM, Elkinton JS, Williams D et al (2000) What causes outbreaks of gypsy moth in North America? Popul Ecol 42:257–266

Lin HS (2009) Earth's Critical Zone and hydropedology: concepts, characteristics, and advances. Hydrol Earth Syst Discuss 6:3417–3481

Lovett GM, Ruesink AE (1995) Carbon and nitrogen mineralization from decomposing gypsy moth frass. Oecologica 104:133–138

Lovett G, Christenson LM, Groffman PM et al (2002) Insect defoliation and nitrogen cycling in forests. Bioscience 52:335–341

Lowman MD (1995) Forest canopies. Academic Press, San Diego

Lowman M, Wittman PK (1996) Forest canopies: methods, hypotheses and future directions. Annu Rev Ecol Syst 27:55–81

Majunke C, Möller K (2003) Die Kiefernwälder Brandenburgs – ein Eldorado für Insekten-Großschädlinge. Forst und Holz 20:619–622

Majunke C, Möller K, Walter C (1999) Massenvermehrung des Kiefernspinners im Land Brandenburg. AFZ Der Wald 54:364–367

McClain ME, Boyer EW, Dent CL et al (2003) Biogeochemical hot spots and hot moments at the interface of terrestrial and aquatic ecosystems. Ecosystems 6:301–312

McClure MS (1983) Reproduction and adaptation of exotic hemlock scales (Homoptera, Diaspididae) on their new and native hosts. Environ Entomol 12:1811–1815

McClure MS (1991) Density-dependent feedback and population-cycles in Adelges- Tsugae (Homoptera, Adelgidae) on Tsuga-Canadensis. Environ Entomol 20:258–264

McDowell WH, Likens G (1988) Origin, composition, and flux of dissolved organic carbon in the Hubbard Brook valley. Ecol Monogr 58:177–195

McNaughton SJ, Ruess RW, Seagle SW (1988) Large mammals and process dynamics in African ecosystems. Bioscience 38:794–800

Mercier J, Lindow SE (2000) Role of leaf surface sugars in colonization of plants by bacterial epiphytes. Appl Environ Microbiol 66:369–374

Michalzik B (1999) Flüsse und Dynamik von gelösten organischen Stickstoffverbindungen (DON) in einem Fichtenwaldökosystem. PhD thesis, Dissertation. Bayreuther Forum Ökologie, Bd. 67

Michalzik B, Stadler B (2000) Effects of phytophagous insects on soil solution chemistry: Herbivores as switches for nutrient dynamics in the soil. Basic Appl Ecol 1:117–123

Michalzik B, Stadler B (2005) Importance of canopy herbivores to dissolved and particulate organic matter fluxes to the forest floor. Geoderma 127:227–236

Michalzik M, Kalbitz K, Park JH et al (2001) Fluxes and concentrations of dissolved organic carbon and nitrogen- a synthesis for temperate forests. Biogeochemistry 52:173–205

Morales CF, Hill MG, Walker AK (1988) Life history of the sooty beech scale (*Ultracoelostoma assimile*) (Maskell), (Hemiptera: Margarodidae) in New Zealand *Nothofagus* forests. NZ Entomol 11:24–37

Mühlenberg E, Stadler B (2005) Effects of altitude on aphid-mediated processes in the canopy of Norway spruce. Agric For Entomol 7:133–143

Müller H (1956) Können Honigtau liefernde Baumläuse (*Lachnidae*) ihre Wirtspflanzen schädigen? Z Angew Entomol 39:168–177

Ohmart CP, Stewart LG, Thomas JR (1983) Leaf consumption by insects in three Eucalyptus forest types in southeastern Australia and their role in short-term nutrient cycling. Oecologia 59:322–330

Orwig DA, Foster DR (1998) Forest response to the introduced hemlock woolly adelgid in southern New England, USA. J Torr Bot Soc 125:60–73

Pedersen LB, Bille-Hansen J (1995) Effects of nitrogen load to the forest floor in Sitka spruce stands (*Picea sitchensis*) as affected by difference in deposition and spruce aphid infestations. Water Air Soil Pollut 85:1173–1178

Pedersen LB, Hansen K, Bille-Hansen J et al (1995) Throughfall and canopy buffering in three Sitka spruce stands in Denmark. Water Air Soil Pollut 85:1593–1598

Pickett STA, White PS (1985) Natural disturbance and patch dynamics: an introduction. In: Pickett STA, White PS (eds) The ecology of natural disturbance and patch dynamics. Academic Press, Orlando, pp 3–13

Prescott CE (2002) The influence of forest canopy on nutrient cycling. Tree Physiol 22:1193–1200

Qualls RG, Haines BL, Swank WT (1991) Fluxes of dissolved organic nutrients and humic substances in a deciduous forest. Ecology 72:254–266

Reynolds BC, Hunter MD (2001) Responses of soil respiration, soil nutrients, and litter decomposition to inputs from canopy herbivores. Soil Biol Biochem 33:1641–1652

Risley LS, Crossley DA Jr (1993) Contribution of herbivore-caused greenfall to litterfall nitrogen flux in several southern Appalachian forested watersheds. Am Mid Nat 129:67–74

Ritchie ME, Tilman D, Knops JMH (1998) Herbivore effects on plant and nitrogen dynamics in oak savanna. Ecology 79:165–177

Rouault G, Candau J-N, Lieutier F et al (2006) Effects of drought and heat on forest insect populations in relation to the 2003 drought in Western Europe. Ann For Sci 63:613–624

Royama T (1996) Analytical population dynamics. Chapman & Hall, London

Russel CA, Kosola KR, Paul EA et al (2004) Nitrogen cycling in poplar stands defoliated by insects. Biogeochemistry 68:365–381

Ryan MG (2002) Canopy processes research. Tree Physiol 22:1035–1043

Schowalter TD (2000) Insect ecology. An ecosystem approach. Academic Press, New York

Schowalter TD, Hargrove WW, Crossley DA (1986) Herbivory in forested ecosystems. Ann Rev Entomol 31:177–196

Seiler J, Matzner E (1995) Spatial variability of throughfall chemistry and selected soil properties as influenced by stem distance in a mature Norway spruce (*Picea abies* (L.) Karst.) stand. Plant Soil 176:139–147

Stadler B, Michalzik B (2000) Effects of phytophagous insects on micro-organisms and through-fall chemistry in forest ecosystems: herbivores as switches for nutrient dynamics in the canopy. Basic Appl Ecol 1:109–116

Stadler B, Müller T (2000) Effects of herbivores on epiphytic micro-organisms in canopies of forest trees. Can J For Res 30:631–638

Stadler B, Michalzik B, Müller T (1998) Linking aphid ecology with nutrient fluxes in a coniferous forest. Ecology 79:1514–1525

Stadler B, Solinger S, Michalzik B (2001) Insect herbivores and the nutrient flow from the canopy to the soil. Oecologia 126:104–113

Stadler B, Müller T, Orwig D et al (2005) Hemlock woolly adelgid: canopy impacts transforming ecosystem processes and landscapes in New England forests. Ecosystems 8:233–247

Stadler B, Müller T, Orwig D (2006) The ecology of energy and nutrient fluxes in hemlock forests invaded by hemlock woolly adelgids. Ecology 87:1792–1804

Streminska MA, Blaszczyk M, Sierpinska A et al (2002) Microflora of soils under pine forests area affected by gradation of leaf-eating insects. Acta Microbiol Pol 51:171–182

Swank WT, Waide JB, Crossley DA Jr et al (1981) Insect defoliation enhances nitrate export from forest ecosystems. Oecologia 51:297–299

Swetnam TW, Lynch AM (1993) Multicentury, regional-scale patterns of western spruce bud-worm outbreaks. Ecol Monogr 63:399–424

Tukey HB Jr, Morgan JV (1963) Injury to foliage and its effect upon the leaching of nutrients from above-ground plant parts. Physiol Plant 16:557–564

Visser ME, Holleman LJM (2001) Warmer springs disrupt the synchrony of oak and winter moth phenology. Proc R Soc Lond B 268:289–294

Wallner WE (1987) Factors affecting insect population dynamics: differences between outbreak and non-outbreak species. Ann Rev Entomol 32:317–340

Wardhaugh CW, Didham RK (2005) Preliminary evidence suggests that beech scale insect honeydew has a negative effect on terrestrial litter decomposition rates in *Nothofagus* forests of New Zealand. NZ J Ecol 30:279–284

Wardle DA, Bardgett RD, Klironomos JN et al (2004) Ecological linkages between aboveground and belowground biota. Science 304:1629–1633

Zoebelein G (1954) Versuche zur Feststellung des Honigtauertrages von Fichtenbeständen mit Hilfe von Waldameisen. Z Angew Ent 36:358–362

Chapter 29
Forest Biogeochemistry and Drought

Sharon A. Billings and Nathan Phillips

29.1 Introduction

Soil moisture is a critical regulator of C, water, and nutrients flowing through forests (Kozlowski 1982; Aber et al. 1995; Granier et al. 1999; Kljun et al. 2007; Nepstad et al. 2007; Penuelas et al. 2007; Welp et al. 2007; Johnson et al. 2008; Borken and Matzner 2009), and shortages of moisture thus can have a dramatic influence on forest function and the relationship between forests and surrounding ecosystems and the atmosphere. Drought – defined here as an absence of precipitation sufficient in duration to induce injury to plants – occurs in nearly all forests (Hanson and Weltzin 2000). Although predictions of altered precipitation patterns with climate change typically reflect greater uncertainty than those of future temperature, many climate models forecast longer periods of soil moisture deficit in multiple forested regions of the globe (IPCC 2007). Thus, drought, already identified as an important disturbance in forests (Foster et al. 1997; McDowell et al. 2008), will likely become more frequent with climate change and a more important perturbation to forest biogeochemical cycling in many regions.

Despite the large number of studies exploring soil moisture as a regulator of forest C and nutrient fluxes, the dynamics of biogeochemical fluxes in forests responding to drought are poorly constrained. For example, many studies demonstrate tight linkages between patterns of forest C uptake and release and water availability, but we know little about mechanisms of forest recovery from drought events and the timing of associated C dynamics. We also do not understand how forest soil organic carbon (SOC) responds to drought, and the extent to which soil physical features (e.g., diffusion of substrates to heterotrophic organisms) vs. biological features (e.g., ability of heterotrophic organisms to function in a relatively dry environment) govern reductions in respiration observed during drought events. Further, we do not fully understand the mechanisms behind the apparent influence of drought on the production and consumption of other greenhouse gases such as CH_4 and N_2O. These gases represent key biogeochemical fluxes into and out of forests that are governed, in part, by moisture availability, but developing even conceptual models predicting responses of these fluxes to drought in multiple forest types eludes us.

In this chapter, we review research to date that explores the influence of drought on forest biogeochemistry, and highlight needed research directions. We do not intend this chapter to serve as an exhaustive review on plant or microbial physiological response to drought, as the physiological responses of many organisms to water shortages are well covered in the literature (e.g., Kramer and Boyer 1995; Schimel et al. 2007). Rather, we use this opportunity to summarize knowledge from fields as disparate as plant ecophysiology, dendrochronology, microbial ecology, and soil science to describe responses of above- and belowground forest biogeochemistry to drought, and to specify critical research needs remaining.

29.2 Drought, the Soil–Plant–Atmosphere Continuum, and Canopy Processes

Drought triggers both direct and indirect canopy processes that drive forest biogeochemistry (Breda et al. 2006). In many, but not all cases, the integrative response of these processes to drought is reduced net ecosystem exchange (NEE) between forests and the atmosphere (Schwalm et al. 2010). Extreme drought events may even shift forests to transient net C sources (Ciais et al. 2005). In this section, we summarize responses of tree growth and physiology to drought, and highlight how they underlie whole forest responses to water shortages.

Drought influences a suite of tree tissue maintenance, production and turnover processes, tree net growth (Breda et al. 2006), and tree dieback and mortality (McDowell et al. 2008; Adams et al. 2009). Tree-ring studies form an important body of knowledge about the relationship between tree growth and water availability, and suggest that drought events can negatively influence forest growth decades later (Pedersen 1998; Breda and Badeau 2008; Haavik et al. 2008). This time lag creates challenges when trying to assess the importance of a specific drought event on tree mortality. The stable isotopic composition of tree-rings suggests that declines in growth with drought are associated with reduced discrimination against ^{13}C (Leavitt et al. 2002), but this response is not universal (Haavik et al. 2008), nor does it reveal the extent to which photosynthetic capacity vs. stomatal closure governs growth response (Powers et al. 2009a, b). Recent dendrochronological studies attempt to assess the degree to which hydraulic failure and C starvation induce tree mortality during drought (McDowell et al. 2010), but mechanisms of tree death remain unclear.

Along the soil–plant–atmosphere continuum (SPAC), drought directly impacts soil hydraulic properties, continuity of the soil–root interface, function of the vascular system connecting roots, stems, and leaves, and stomata (Fig. 29.1). In each of these SPAC subsystems, drought affects both the state of water (water potential), and its ability to move against resistance. Both water *state* (Tezara et al. 1999) and *rate* (Hubbard et al. 2001) impact C assimilation. We next describe these impacts, in sequence from soil to leaf.

Drought impacts on canopy processes start in the soil. Soil water potential sets a baseline level of water status, an *a priori* hydraulic "cost" borne by downstream
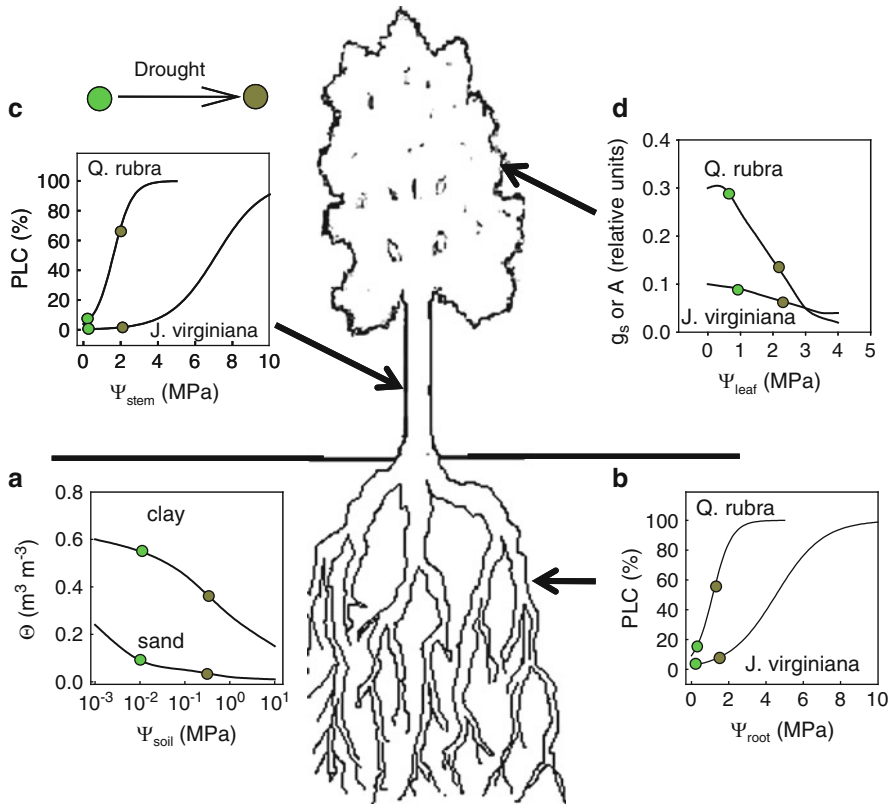
Fig. 29.1 Drought impacts on water potentials (Ψ) of (**a**) soil, (**b**) root, (**c**) stem, and (**d**) foliage; percent loss of hydraulic conductivity (PLC) of root (**b**) and stem (**c**) xylem; and stomatal (g_s) and photosynthetic (*A*) responses of foliage (**d**). Drought progression is indicated by movement along *curves* from *green* to *brown* symbols. Two *curves* in each plot illustrate extremes of soil hydraulic properties and tree cavitation vulnerability (Θ) represents soil volumetric water content

elements of the SPAC. As water moves through distributed frictional resistances, discrete vascular constrictions, and against gravity along its transpiration pathway, the initial hydraulic cost set by soil water availability progressively increases: water potential becomes more negative, and vascular and physiological function, and canopy gas exchange, are generally reduced. Closely associated with soil water potential is hydraulic conductivity; both are highly sensitive to soil water content. Unsaturated conductivity drops rapidly with lower water content in many soils (van Genuchten 1980), increasing resistance to nutrient flow to roots. Drought thus decreases nutrient mobility at the same time that it decreases soil nutrient lability (as discussed below). Decreased uptake of nutrients in turn reduces canopy photosynthesis (Evans 1989), feeding back to reduced SOC supply.

Moving from soil toward the plant, declining bulk soil water content can lead to threshold-type hydraulic discontinuities at the soil–root interface. During drought, soil and roots shrink and can physically separate, increasing hydraulic resistance at

the soil–root interface (Weatherley 1979; Blizzard and Boyer 1980); this process depends on soil texture and porosity (Bristow et al. 1984). Even water that does retain continuity across soil–root interfaces is variably conducted into plants under influence of drought by root aquaporins. Aquaporins, integral membrane water channels, are produced, activated, and/or relocated under water stress, facilitating water uptake (Luu and Maurel 2005). Chemicals involved in gating aquaporins include calcium, protons (Luu and Maurel 2005), and nitrogen (Gloser et al. 2007; Gorska et al. 2008), but little is known about relationships between aquaporin function, root membrane hydraulic function in general, and soil availability of biogeochemicals.

Once water passes from soil through root membranes, its pathway through root, bole, and branch xylem is vulnerable to hydraulic failure. Drought imposes increasingly negative water potentials in xylem of roots to leaves, placing vascular tissues closer to a failure threshold associated with tensile rupturing of liquid water, a phenomena called cavitation. In turn, fewer pathways for water flow in xylem may make remaining xylem even more vulnerable to cavitation (Tyree and Sperry 1988). This illustrates state-rate interdependency. The relationship between degree of cavitation and water tension is called a "cavitation vulnerability curve" (Tyree and Sperry 1989), and is influenced by anatomical and physicochemical properties of xylem conduits. The wide variety of vascular anatomies found among forest trees therefore leads to a diversity of cavitation vulnerabilities. Tree species may "tune" xylem properties and cavitation vulnerability to soil porosity (Hacke et al. 2000). Evidence has accumulated that refilling of embolized (cavitated) vascular material occurs regularly (Zwieniecki et al. 2000; Bucci et al. 2004). This phenomenon occurs when water columns are under tension. A full understanding of how refilling under tension can occur has not yet been developed (Holbrook and Zwieniecki 1999). Little is known about how drought may impact refilling under tension.

Moving from the woody vascular system to the leaf, water transforms from the liquid to gas phase, and here both physics and biochemistry limit exchange of both vapor and CO_2. These two distinct kinds of leaf gas exchange limitations are known as stomatal, or diffusion limitations; and nonstomatal, or biochemical limitations. Because water loss from stomata is a necessary consequence of C uptake in C3 plants, leaves require a constant supply of water from vascular systems when photosynthesizing. Leaf hydraulic resistance is a function of the leaf vascular network (Sack and Holbrook 2006), and can be a dominating control on water supply to the stomatal complex. In addition to water supply rate, leaf water status has biochemical impacts on photosynthesis (Tezara et al. 1999). Operation of the Calvin Cycle or associated processes can be diminished by low (negative) leaf water potential. Finally, leaf expansion is limited by cell turgor, and so the ability for tall trees (or trees in dry soils) to produce photosynthesizing leaf area at their tops can be limited by cell water status (Woodruff et al. 2004).

Importantly, the stable isotopic signature of forest biomass and of CO_2 within forest canopies can help constrain estimates of canopy responses to moisture availability (Bowling et al. 2008). Because drought generally induces more rapid declines in stomatal conductance than photosynthesis, canopy discrimination (Δ) tends to decline with drought (Bowling et al. 2002; Fessenden and Ehleringer 2003). This phenomenon has a negative effect on $\delta^{13}C$ of CO_2 (Randerson 2005),

providing investigators with an important tool for evaluating the extent of forest canopy responses to moisture shortages.

The tight coupling of water and C flows within trees has long been studied, but theories have emerged over the past two decades to explain how such coupling may influence the physical stature of forests (Yoder et al. 1994; Ryan and Yoder 1997; Ryan et al. 2006), their rainfall use efficiency (Huxman et al. 2004), and susceptibility to mortality (McDowell et al. 2008; Adams et al. 2009). These theories, focused on tree processes and ecosystem productivity, have obvious implications for above- and belowground biogeochemistry, but await incorporation into comprehensive forest biogeochemical models.

General patterns have emerged in synthesis studies of canopy processes during drought, and these studies continue to inform theory. Synthesis studies derive from forest sites in the US Long-Term Ecological Research (LTER) Network and FluxNet. Two emerging generalities in forest C response to drought are that canopy photosynthesis is more sensitive to drought than ecosystem respiration (Schwalm et al. 2010); and that, in their driest years, aboveground net primary productivity (ANPP) of forests falls along a line of rain use efficiency (RUE) behavior common to other biomes including deserts (Huxman et al. 2004). These findings represent crucial footholds toward developing general understandings of forest canopy response to drought. However, they also demonstrate that, despite centuries of study, there remain basic unknowns. For example, the remarkable RUE convergence in Huxman et al. (2004), evaluated using ANPP, remains untested using NEE.

Cross-site syntheses permit examination of the limits of generalities. For example, in a FluxNet synthesis that included 128 forest sites, ecosystem C uptake was generally, but not always, reduced by drought (Schwalm et al. 2010). Drought accompanies other environmental changes that impact ecosystem C exchange. For example, tropical drought is associated with greater light availability (e.g., Graham et al. 2003; Hutyra et al. 2007). When forests can access deep stores of soil moisture, higher light supports greater C uptake (Hutyra et al. 2007; Saleska et al. 2007; Bonal et al. 2008). Access to deep soil moisture indicates that generalities about forest drought responses may depend on definitions of drought. An additional interactive influence of drought arises from its common association with higher temperature. Where productivity is temperature limited, the temperature increases associated with drought can enhance C uptake through increased crown photosynthesis or increased growing season (Schwalm et al. 2010). These different drought-associated factors produce regional anomalies (e.g., tropical vs. boreal) in forest C exchange, and demonstrate the need for caution against overgeneralization.

29.3 Litterfall and Its Decomposition

Because mean annual precipitation is positively correlated with forest productivity (Lieth 1975; Schlesinger 1997), litterfall production is typically higher in forests where water is less limiting. However, litterfall production in forests is not necessarily linked with annual or growing season precipitation (Knutson 1997), and can

even exhibit negative correlations with precipitation, reflecting high rates of senescence during severe drought (Beard 2005). The importance of litterfall as a source of nutrient recycling in forests (Singh and Gupta 1977; Aber et al. 1991) is realized, of course, when organic inputs to the soil profile are subject to decomposition – a process strongly linked with water availability. Thus, drought has a large influence on the heterotrophically mediated fate of senesced biomass.

Mean annual precipitation can be an important driver of decomposition rates, given observed links between annual mass loss and actual evapotranspiration (Meentemeyer 1978; Schlesinger 1997). Such observations indicate that drought can impose restrictions on the return of nutrients to available pools from litterfall (Fig. 29.2). This effect may be particularly evident in tropical forests, where precipitation appears to be a more influential driver of decomposition rates than in
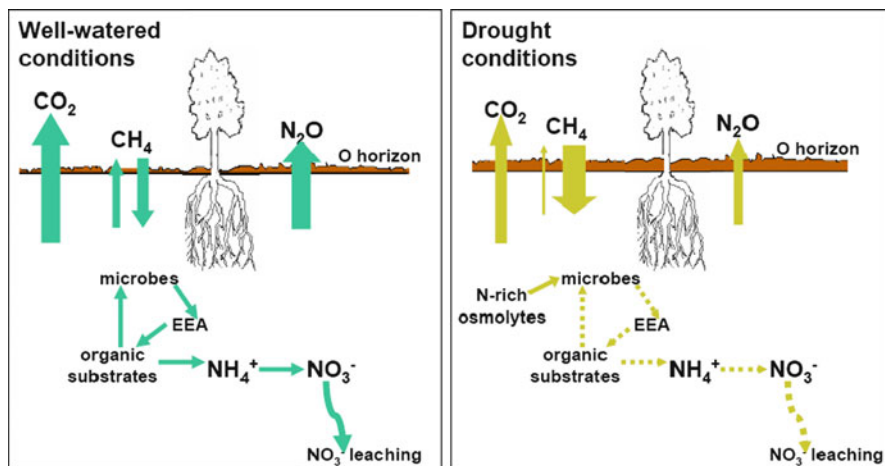
Fig. 29.2 Schematic of hypothetical influences of drought on relative magnitudes of key biogeochemical processes in forest soils, relative to well-watered conditions. Many fluxes depicted have not been measured in situ, such as mass fluxes of exo-enzymes to substrates or substrate flow into microbial communities, or across ecosystems with and without drought. Depicted are gaseous fluxes (CO_2, CH_4, N_2O) via *arrows* of varying width, representing hypothetical relative magnitudes that contrast well-watered (*green*) with drought (*brown*) conditions. Drought conditions generally reduce soil respiration and methanogenesis, and enhance methanotrophy. Production of N_2O declines with drought because anaerobic conditions promote denitrification and associated fluxes of N_2O as a byproduct. Drought can also induce a net N_2O sink in some forests (not depicted here), though the mechanism for this phenomenon remains unclear (see text for details). Relatively short-term drought can enhance litterfall accumulation, represented here as O horizon thickness, though longer-term drought can result in reductions in net primary productivity (NPP) and associated declines in litterfall production. *Dotted arrows* (*brown*) depict enhanced temporal and spatial variability of the activity of some microorganisms belowground with drought, relative to *solid arrows* (*green*) in well-watered conditions, which represent generally larger and more consistent fluxes. Diffusivity of organic substrates to microorganisms is reduced with drought, as is microbial production of many extracellular enzymes. Extracellular enzyme activity (EEA) thus can decline with decreases in microbial functional rates and enzyme diffusivity to substrate reaction sites, with associated declines in organic matter decay and associated NH_4^+ production, nitrification, and NO_3^- leaching. In addition, drought conditions can prompt microbial uptake of solutes to mitigate dessication (not pictured here)

temperate and boreal systems (Berg et al. 1993; Gholz et al. 2000; Trofymow et al. 2002; Powers et al. 2009a, b). The decline in decomposition rates with increasingly limited moisture availability is likely a result of water limitation of decomposer communities (discussed below), but could also result from declines in nutrient concentrations, especially phosphorus, in litterfall with drought (Wood et al. 2005).

Although the influence of drought on decomposition rates and, in some forests, litterfall nutrient concentrations is at least partially characterized, the extent to which these mechanisms negatively influence forest productivity remains unclear. To date, we are unaware of any study that attempts to separate the direct effects of moisture shortages from the indirect effects of drought-imposed nutrient limitation on forest productivity. However, nutrients derived from organic matter decomposition are a significant fraction of those taken up by forest vegetation (Aber et al. 1991), and litterfall accumulation associated with declines in decomposition (Johnson et al. 2002) is linked with nutrient immobilization in litter and reduced cation leaching (Johnson et al. 1998). These phenomena indicate that drought may indirectly influence a forest's ability to assimilate C as the rate of nutrient return to plant-available pools declines. These effects, if present, likely are realized only during drought periods sufficient in duration to impose severe and long-lasting restrictions on litterfall decomposition. Shorter-term drought events, in contrast, can result in transient increases in plant-available pools of nutrients due to inhibited vegetation uptake in some ecosystems (Sardans et al. 2008). The complicated interactions between decomposition dynamics, patterns of plant nutrient uptake, and length and severity of drought inhibit investigators from elucidating the extent to which reduced decomposition rates impose limitations on forest C assimilation. Studies that try to characterize these effects, and the severity of drought required to induce them, remain rare.

29.4 Decomposition Dynamics Within Forest Mineral Soil Profiles

Drought can also be an important determinant of biogeochemical transformations within the mineral soil profile. Perhaps the most critical characteristic of soil profiles experiencing drought with respect to biogeochemical functioning is the decline of diffusion rates of organic and inorganic compounds in soil solution to reaction sites (Fig. 29.2). As a result, substrate availability for many microbially mediated transformations can limit reaction rates. This concept is typically conveyed using Michaelis–Menten kinetics:

$$v = \frac{v_{\mathrm{max}} * S}{K_{\mathrm{m}} + S},\tag{29.1}$$

where v is the reaction rate constant, v_{max} is the maximum reaction rate, S is substrate concentration, and K_{m} is the half-saturation constant. As S declines with moisture availability, v is increasingly influenced by K_{m}, and can be significantly reduced

relative to v_{max}. Michaelis–Menten kinetics thus are an important component for formulating predictions of biogeochemical transformations within soils as they experience moisture fluctuation (Davidson and Janssens 2006; Dalal et al. 2008).

Microbially mediated processes within soil profiles also slow due to microbial physiology and reductions in enzyme diffusivity (Fig. 29.2, Stark and Firestone 1995; Ford et al. 2007; Borken and Matzner 2009). Soil microorganisms either dehydrate and die during periods of low moisture availability, or survive in a state of reduced activity (Killham 1994). Gram-positive bacteria are generally viewed as more drought-resistant than Gram-negative bacteria, due to their thicker cell wall (Schimel et al. 2007), and fungi are thought to be more drought resistant than most bacterial cells (Harris 1981). Surviving microorganisms appear to import solutes for protection from dessication (Harris 1981, discussed in more detail below). Even those organisms well adapted for drought conditions, however, typically experience reduced functioning during times of moisture limitation. The extracellular enzymes produced by still-functioning microorganisms also can experience limited diffusivity. Thus, the transport limitation of substrates, combined with slowed diffusivity of enzymes responsible for their breakdown, result in slower rates of microbially mediated biogeochemical transformations within soils experiencing drought.

The declines in soil microbial activity associated with drought have important biogeochemical consequences. As decomposition slows, microbial respiration declines, consistent with observed declines in soil respiration in multiple forest types with drought (Fig. 29.2, Billings et al. 1998; Sotta et al. 2007), though these measures are confounded with likely declines in autotrophic respiration as well. Laboratory experiments that isolate microbial activity from that of plant roots, however, indicate that microbial respiration is typically negatively affected by water shortages, and that the magnitude of decline depends on nutrient availability, microbial community composition, the time period between wetting events, and the magnitude of the antecedent wetting event (Fierer and Schimel 2003; Schimel et al. 2007; Borken and Matzner 2009). These interacting effects make it difficult to quantifiably predict microbial respiration with drought using empirical data, and reinforce the importance of employing first principles, such as the Michaelis–Menten model discussed above, to model reaction rates. Importantly, because the stable isotopic composition of C substrates varies across soil horizons (Ehleringer et al. 2000; Billings 2006) and can reflect antecedent forest water availability (Balesdent et al. 1993; Bowling et al. 2008), the $\delta^{13}C$ of microbially respired CO_2 can be an important tool for assessing the influence of drought on substrate accessibility and associated soil microbial activity.

29.5 Methane Fluxes and Forest Drought

Of all terrestrial ecosystems, upland forests generally exhibit the highest rates of net soil CH_4 uptake; within forests, net soil CH_4 consumption is greatest in temperate systems (Dalal et al. 2008). These fluxes of CH_4 are influenced by water availability

to a much greater extent than temperature (Castro et al. 1995; Billings et al. 2000). Methanogens transform simple C substrates into CH_4 in anaerobic conditions (Kim and Gadd 2008). Thus, when soil moisture is high and a relatively large number of O_2-depleted soil microsites exist, methanogenesis can represent a significant fraction of CH_4 fluxes within a profile (McLain and Ahmann 2008). In contrast, well-aerated soil profiles support relatively more methanotrophy, the oxidation of CH_4 into CO_2. In such instances, net soil CH_4 consumption is observed at the soil surface (Fig. 29.2). Soil texture and bulk density can be important drivers of CH_4 diffusion into soil (Dorr et al. 1993; Boeckx et al. 1997; Del Grosso et al. 2000), but the influence of moisture availability on air-filled pore space is an additional determinant of CH_4 diffusion into the soil profile and its subsequent oxidation (Dalal et al. 2008). Thus, as moisture declines CH_4 can diffuse more readily into the profile, following the CH_4 concentration gradient maintained by soil methanotrophs (Castro et al. 1995; Whalen and Reeburgh 1996; Billings et al. 2000; Gulledge and Schimel 2000; Le Mer and Roger 2001; Borken et al. 2006).

Studies examining the influence of moisture on forest CH_4 fluxes confirm the potential importance of drought as a determinant of CH_4 biogeochemistry. Davidson et al. (2008) report that rainfall exclusion plots in a tropical forest consistently served as a net CH_4 sink, in contrast with control plots. In a spruce forest in Germany, drought reduced methanogenesis and enhanced methane oxidation (Lamers et al. 2009). Experimentally induced drought in a temperate forest increased soil CH_4 uptake rates, though the effect was small relative to the large change in soil moisture (Borken et al. 2006). Net soil CH_4 uptake was also significantly enhanced with experimental drought in an upland boreal forest in Alaska (Billings et al. 2000). Importantly, however, soil CH_4 uptake declined with drought in a floodplain forest composed of similar vegetation (Billings et al. 2000). These results suggest that factors other than CH_4 diffusivity, such as variation in the composition of CH_4-related microbial communities, may be important influences on soil CH_4 fluxes (Schimel and Gulledge 1998).

Although it remains challenging to quantify predictions of soil surface CH_4 fluxes across multiple moisture scenarios and forest types, recent modeling work suggests that rates of forest soil CH_4 consumption will likely increase with increased drought occurrence and intensity. Curry (2009) predicts that cool temperate and subtropical forest ecosystems will experience the largest absolute increases in soil CH_4 consumption relative to other terrestrial ecosystems by the year 2100, and that boreal forests will be one of the three ecosystems experiencing the largest relative increases in CH_4 consumption. This work, however, neglects methanogenesis, which needs to be incorporated into any future predictions of net forest soil CH_4 fluxes.

29.6   Nitrogen Cycling and Forest Drought

Although the influences of drought on soil N cycling are not well understood, it is generally accepted that soil moisture shortages impose constraints on N availability

via several mechanisms. As discussed above, drought can restrict decomposition rates of litterfall and mineral SOM, reducing the flow of N into the "leaky pipe" (Firestone and Davidson 1989) of soil N cycling with enhanced N immobilization in the O horizon (Johnson et al. 2002, 2008). In addition, drought can impose constraints on N availability due to microbial N immobilization (Fig. 29.2). To survive drought conditions, microorganisms must accumulate osmolytes to reduce their internal water potential (Harris 1981). Although not universally true (Tiemann 2011), osmolytes can be N-rich; for example, bacteria typically employ amino acids for this purpose. Schimel et al. (2007) calculates that the total amount of N in microbial osmolytes can represent between 10 and 40% of annual net N mineralization. Drought, then, can impose N requirements on soil microorganisms that have ecosystem-level implications for N availability.

Drought can also result in reductions in transformation rates of inorganic N (Fig. 29.2). For example, net N mineralization was reduced with drying in soils supporting a Norway spruce forest in Germany (Hentschel et al. 2007). Experimental reductions in throughfall in a temperate deciduous forest also resulted in lower N fluxes through the soil profile (Johnson et al. 2002, 2008). Such effects may result from reductions in microbial population size and activity, and from the declining availability of substrates for enzymatic reaction sites discussed above (Kieft et al. 1987; Franzluebbers et al. 1994; Borken and Matzner 2009). The transformation of ammonium to nitrate by nitrifying bacteria also slows with drought (Tietema et al. 1992). The mechanism governing this effect is unknown, but one study examining the negative effect of drought on nitrifiers indicates that osmotic potentials in the soil below -0.6 MPa induces severe nitrifier dehydration (Stark and Firestone 1995). In contrast, nitrification was inhibited primarily by substrate availability when osmotic potentials were above this threshold (Stark and Firestone 1995). Although drought can promote relative accumulations of inorganic N in soil through reductions in plant uptake of N (Sardans et al. 2008) and nitrate leaching from the soil system (Johnson et al. 2002, 2008; Hong et al. 2005), the negative effects of soil drought on N cycling rates can restrict forest N dynamics.

The evolution of nitrogenous gases from forest soils is also influenced by drought. Because of the acidic nature of forest soils, we do not consider NH_3 volatilization, which tends to occur in soils with pH > 7 (Schlesinger and Peterjohn 1991; Billings et al. 2002). However, forest soils can be significant sources of nitric oxide (NO) and nitrous oxide (N_2O), byproducts of nitrification and denitrification (Fig. 29.2). Nitrogen budgets of multiple ecosystems suggest that significant quantities of N escape via these pathways, but capturing fluxes of these gases sufficient to close N budgets has proven challenging (Schlesinger and Peterjohn 1991; Billings et al. 2002; Groffman et al. 2006), in part because these gases are both produced and consumed by microbial activity within the soil.

Recent work highlights our inability to predict the response of NO and N_2O fluxes from forest soils to drought. For example, soil moisture shortages tend to promote NO emissions relative to N_2O (Firestone and Davidson 1989; Davidson et al. 2000), but some tropical forests require repeated drought years for this effect to be evident, for unknown reasons (Davidson et al. 2008). Moisture availability can

promote N_2O production via enhancement of denitrification and, to a lesser extent, nitrification, but when soil moisture is sufficiently high, this effect is countered by high rates of N_2O consumption (transformation of N_2O into N_2) (Chapuis-Lardy et al. 2007). Paradoxically, Goldberg and Gebauer (2009) report a significant, sustained N_2O sink in a forest soil with experimentally imposed drought, conditions under which we would predict negligible transformation of N_2O into N_2. The mechanism for this unexpected response is not known. Patterns of $\delta^{15}N$ of N_2O throughout the soil profile prompted suggestions of drought resulting in declining in N_2O production, while N_2O consumption was maintained (Goldberg and Gebauer 2009). An alternative explanation for the observed phenomena of drought-influenced soils serving as a net N_2O sink is enhanced rates of N_2O consumption with the maintenance of N_2O production (Billings 2008); this scenario is consistent with the $^{15}N_2O$ profile observed in the German study.

Regardless of the mechanism(s) governing the net N_2O sink in these dry forest soils, Goldberg and Gebauer's work (2009) highlights our lack of understanding of how forest soils can consume N_2O when anaerobic microsites must be relatively rare. Because so few studies report net N_2O consumption at the soil surface, and because those that do tend to dismiss such results merely as evidence of the challenges associated with measuring N_2O fluxes (Chapuis-Lardy et al. 2007), the relationship between moisture availability and forest soil N_2O fluxes remains enigmatic. Although atmospheric N_2O is relatively long lived and well mixed, confounding our ability to use temporal and spatial differences in its isotopic signature to constrain N_2O budgets (Rahn 2005), employing isotopic constraints on N_2O fluxes within the soil profile will be important for future efforts to elucidate drivers of N_2O production and consumption.

29.7   Conclusions

The nature of drought itself – its frequency, severity, and duration – may change as part of climate change (IPCC 2007). Drought can span an almost unlimited spectrum of conditions from the episodic to the chronic, as becomes evident within a few minutes of attempting to design an experiment to explore the influence of drought on forest processes. However, manipulative studies are needed to explore forest responses to previously unobserved regions of the time and frequency domains of drought that may occur in the future. In addition to such studies, cross-ecosystem explorations of forest responses to drought are needed, to permit comparison between forest types and climatic regimes. Such comparisons will augment our understanding of both the diversity and similarities of relationships between forest biogeochemical fluxes and drought. The LTER and FluxNet networks will continue to provide excellent synthesis platforms for such studies. The emerging National Ecological Observatory Network (NEON; Keller et al. 2008), with its unprecedented scope of data monitoring, management, and sharing

capabilities will also serve as a rich source of data for understanding forest responses to drought.

In addition to insights gained from manipulative studies and ecological networks, examination of extreme drought events holds great promise for contributing to general knowledge of forest responses to drought. An emerging body of literature has been built around such extreme events (e.g., Huxman et al. 2004; Ciais et al. 2005; Reichstein et al. 2007; Granier et al. 2007; Saleska et al. 2007; Armone et al. 2008; Marengo et al. 2008; Goldberg and Gebauer 2009). The exceptional events examined in these studies provide crucial tests of emergent general patterns of forest response to drought, and continued examination of extreme events will serve an important role in the developing predictive models of forest responses to drought under climate change scenarios.

The studies described in this chapter also reveal the broad need for a better understanding of how moisture dynamics influence soil microbial activity. Pursuing this wide research area will provide the knowledge needed for developing conceptual and, eventually, more quantitative models of many belowground processes, including decomposition rates, nutrient transformations, and soil production and consumption of multiple gases that influence Earth's climate. The nonlinear and interactive responses to drought of these microbially mediated fluxes (e.g., Schimel et al. 2007; Borken and Matzner 2009; Goldberg and Gebauer 2009) represent an immense and relatively unexplored research frontier. For example, biogeochemical responses to drought severity – as measured by intensity and length – are frequently not linear, likely due to interactions between water availability, microbial functioning, and vegetation physiology, and the multiple timescales at which these factors operate. Complex patterns of responses of these processes within and among varying forest types challenge our efforts to develop predictive models of these fluxes with drought and remain a critical research area for the future.

References

Aber JD, Melillo JM, Nadelhoffer KJ et al (1991) Factors controlling nitrogen cycling and nitrogen saturation in northern temperate forest ecosystems. Ecol Appl 3:303–315

Aber JD, Ollinger SV, Federer CA et al (1995) Predicting the effects of climate change on water yield and forest production in the northeastern United States. Clim Res 5:207–222

Adams HD, Guardiola-Claramontea M, Barron-Gafford GA et al (2009) Temperature sensitivity of drought-induced tree mortality portends increased regional die-off under global-change-type drought. PNAS 106:7063–7066

Armone JA, Verburg PSJ, Johnson DW et al (2008) Prolonged suppression of ecosystem carbon dioxide uptake after an anomalously warm year. Nature 455:383–386

Balesdent J, Girardin A, Mariotti A (1993) Site-related $\delta^{13}C$ of tree leaves and soil organic matter in a temperate forest. Ecology 74:1713–1721

Beard GS (2005) Seasonal climate summary southern hemisphere (summer 2004/05): a neutral ENSO situation with a cooling Pacific. Hot and dry over the western half of Australia. Aust Meteorol Mag 4:347–359

Berg B, Berg MP, Pottner P et al (1993) Litter mass loss rates in pine forests of Europe and Eastern United States: some relationships with climate and litter quality. Biogeochemistry 20:127–159

Billings SA (2006) Soil organic matter dynamics and land use change at a grassland/forest ecotone. Soil Biol Biochem 38:2934–2943

Billings SA (2008) Nitrous oxide in flux. Nature 456:888–889

Billings SA, Richter D, Yarie J (1998) Soil carbon dioxide fluxes and profile concentrations in two boreal forests. Can J For Res 28:1773–1783

Billings SA, Richter DD, Yarie J (2000) Sensitivity of soil methane fluxes to reduced precipitation in boreal forest soils. Soil Biol Biochem 32:1431–1441

Billings S, Schaeffer S, Evans R (2002) Trace N gas losses and N mineralization in Mojave Desert soils exposed to elevated CO_2. Soil Biol Biochem 11:1777–1784

Blizzard WE, Boyer JS (1980) Comparative resistance of the soil and the plant to water transport. Plant Physiol 5:809–814

Boeckx P, VanCleemput O, Villaralvo I (1997) Methane oxidation in soils with different textures and land use. Nutr Cycl Agroecosyst 1–3:91–95

Bonal D, Bosc A, Goret JY et al (2008) The impact of severe dry season on net ecosystem exchange in the neotropical rainforest of French Guiana. Global Change Biol 14:1917–1933

Borken W, Matzner E (2009) Introduction: impact of extreme meteorological events on soils and plants. Global Change Biol 4:781

Borken W, Savage K, Davidson EA et al (2006) Effects of experimental drought on soil respiration and radiocarbon efflux from a temperate forest soil. Global Change Biol 2:177–193

Bowling DR, McDowell NG, Bond BJ et al (2002) ^{13}C content of ecosystem respiration is linked to precipitation and vapor pressure deficit. Oecologia 131:113–124

Bowling DR, Pataki DE, Randerson JT (2008) Carbon isotopes in terrestrial ecosystem pools and CO_2 fluxes. New Phytol. doi:10.1111/j.1469-8137.2007.02342.x

Breda N, Badeau V (2008) Forest tree responses to extreme drought and some biotic events: towards a selection according to hazard tolerance? External Geophys Clim Environ 340:651–662

Breda N, Huc R, Granier A et al (2006) Temperate forest trees and stands under severe drought: a review of ecophysiological responses, adaptation processes and long-term consequences. Ann Sci For 63:625–644

Bristow KL, Campbell GS, Calissendorff C (1984) The effects of texture on the resistance to water movement within the rhizosphere. Soil Sci Soc Am J 48:266–270

Bucci SJ, Scholz FG, Goldstein G et al (2004) Dynamic changes in hydraulic conductivity in petioles of two savanna tree species: factors and mechanisms contributing to the refilling of embolized vessels. Plant Cell Environ 26:1633–1645

Castro M, Steudler P, Melillo J et al (1995) Factors controlling atmospheric methane consumption by temperate forest soils. Glob Biogeochem Cycles 1:1–10

Chapuis-Lardy L, Wrage N, Metay A et al (2007) Soils, a sink for N_2O? A review. Global Change Biol 1:1–17

Ciais P, Reichstein M, Viovy N et al (2005) Europe-wide reduction in primary productivity caused by the heat and drought in 2003. Nature 7058:529–533

Curry CL (2009) The consumption of atmospheric methane by soil in a simulated future climate. Biogeosciences 11:2355–2367

Dalal RC, Allen DE, Livesley SJ et al (2008) Magnitude and biophysical regulators of methane emission and consumption in the Australian agricultural, forest, and submerged landscapes: a review. Plant Soil 1–2:43–76

Davidson E, Janssens IA (2006) Temperature sensitivity of soil carbon decomposition and feedbacks to climate change. Nature 9:165–173

Davidson E, Keller M, Erickson H et al (2000) Testing a conceptual model of soil emissions of nitrous and nitric oxides. Bioscience 8:667–680

Davidson EA, Nepstad DC, Ishida FY et al (2008) Effects of an experimental drought and recovery on soil emissions of carbon dioxide, methane, nitrous oxide, and nitric oxide in a moist tropical forest. Global Change Biol 11:2582–2590

Del Grosso SJ, Parton WJ, Mosier AR et al (2000) General CH_4 oxidation model and comparisons of CH_4 oxidation in natural and managed systems. Glob Biogeochem Cycles 14:999–1019

Dorr H, Katruff L, Levin I (1993) Soil texture parameterization of methane uptake in aerated soils. Chemosphere 26:697–713

Ehleringer JR, Buchmann N, Flanagan JB et al (2000) Carbon isotope ratios in belowground carbon cycle processes. Ecol Appl 10:412–422

Evans JR (1989) Photosynthesis and nitrogen relationships in leaves of C-3 plants. Oecologia 78:9–19

Fessenden JE, Ehleringer JR (2003) Temporal variation in $\delta^{13}C$ of ecosystem respiration in the Pacific Northwest: links to moisture stress. Oecologia 136:129–136

Fierer N, Schimel JP (2003) A proposed mechanism for the pulse in carbon dioxide production commonly observed following the rapid rewetting of a dry soil. Soil Sci Soc Am J 67:798–805

Firestone MK, Davidson EA (1989) Microbiological basis of NO and N_2O production and consumption in soil. In: Andreae MO, Schimel DS (eds) Exchange of trace gases between terrestrial ecosystems and the atmosphere. Wiley, New York, pp 7–21

Ford DJ, Cookson WR, Adams MA et al (2007) Role of soil drying in nitrogen mineralization and microbial community function in semi-arid grasslands of North-West Australia. Soil Biol Biochem 39:1557–1569

Foster DR, Aber JD, Melillo JM et al (1997) Forest response to disturbance and anthropogenic stress: rethinking the 1938 hurricane and the impact of physical disturbance vs chemical and climate stress on forest ecosystems. Bioscience 7:437–445

Franzluebbers K, Weaver RW, Juo ASR et al (1994) Carbon and nitrogen mineralization from cowpea plants decomposing in moist and in repeatedly dried and wetted soil. Soil Biol Biochem 10:1379–1387

Gholz HL, Wedin DA, Smitherman SM et al (2000) Long-term dynamics of pine and hardwood litter in contrasting environments: toward a global model of decomposition. Global Change Biol 6:751–765

Gloser V, Zwieniecki MA, Orians CM et al (2007) Dynamic changes in root hydraulic properties in response to nitrate availability. J Exp Bot 58:2409–2415

Goldberg SD, Gebauer G (2009) Drought turns a Central European Norway spruce forest soil from an N_2O source to a transient N_2O sink. Global Change Biol 15:850–860

Gorska A, Ye Q, Holbrook NM et al (2008) Nitrate control of root hydraulic properties in plants: translating local information to whole plant response. Plant Physiol 148:1159–1167

Graham EA, Mulkey SS, Kitajima K et al (2003) Cloud cover limits net CO_2 uptake and growth of a rainforest tree during tropical rainy seasons. PNAS 100:572–576

Granier A, Breda N, Biron P et al (1999) A lumped water balance model to evaluate duration and intensity of drought constraints in forest stands. Ecol Model 116:269–283

Granier A, Reichstein M, Breda N et al (2007) Evidence for soil water control on carbon and water dynamics in European forests during the extremely dry year: 2003. Agric For Meteorol 143:123–145

Groffman PM, Altabet MA, Bohlke JK et al (2006) Methods for measuring denitrification: diverse approaches to a difficult problem. Ecol Appl 16:2091–2122

Gulledge J, Schimel J (2000) Controls on soil carbon dioxide and methane fluxes in a variety of taiga forest stands in interior Alaska. Ecosystems 3:269–282

Haavik L, Stephen F, Fierke M et al (2008) Dendrochronological parameters of northern red oak (Quercus rubra Fagaceae) infested with red oak borer (Enapholodes rufulus (Haldeman) (Coleoptera: Cerambycidae)). For Ecol Manage 255:1501–1509

Hacke U, Sperry JS, Ewers BE et al (2000) Influence of soil porosity on water use in Pinus taeda. Oecologia 124:495–505

Hanson PJ, Weltzin JF (2000) Drought disturbance from climate change: response of United States forests. Sci Total Environ 3:205–220

Harris RF (1981) Effect of water potential on microbial growth and activity. In: Parr JF, Gardner WR, Elliott LF (eds) Water potential relations in soil microbiology. American Society of Agronomy, Madison, pp 23–95

Hentschel K, Borken W, Matzner E (2007) Leaching losses of inorganic N and DOC following repeated drying and wetting of a spruce forest soil. Plant Soil 1–2:21–34

Holbrook NM, Zwieniecki MA (1999) Embolism repair and xylem tension: do we need a miracle? Plant Physiol 120:7–10

Hong BG, Swaney DP, Woodbury PB et al (2005) Long-term nitrate export pattern from Hubbard Brook watershed 6 driven by climatic variation. Water Air Soil Pollut 160:293–326

Hubbard RM, Stiller V, Ryan MG et al (2001) Stomatal conductance and photosynthesis vary linearly with plant hydraulic conductance in ponderosa pine. Plant Cell Environ 24:113–121

Hutyra LR, Munger JW, Saleska SR et al (2007) Seasonal controls on the exchange of carbon and water in an Amazonian rain forest. J Geophys Res 112:G03008. doi:10.1029/2006JG000365

Huxman T, Smith M, Fay P et al (2004) Convergence across biomes to a common rain-use efficiency. Nature 6992:651–654

IPCC (2007) Climate change 2007: the physical science basis. In: Solomon S, Qin D, Manning M et al (eds) Contribution of working group I to the fourth assessment report of the intergovernmental panel on climate change. Cambridge University Press, Cambridge

Johnson DW, Hanson PJ, Todd DE et al (1998) Precipitation change and soil leaching: field results and simulations from Walker Branch Watershed, Tennessee. Water Air Soil Pollut 1–2:251–262

Johnson DW, Hanson PJ, Todd DE (2002) The effects of throughfall manipulation on soil leaching in a deciduous forest. J Environ Qual 1:204–216

Johnson DW, Todd DE, Hanson PJ (2008) Effects of throughfall manipulation on soil nutrient status: results of 12 years of sustained wet and dry treatments. Global Change Biol 7:1661–1675

Keller M, Schimel DS, Hargrove WW et al (2008) A continental strategy for the National Ecological Observatory Network. Front Ecol Environ 6:282–284

Kieft TL, Soroker E, Firestone MK (1987) Microbial biomass response to a rapid increase in water potential when dry soil is wetted. Soil Biol Biochem 19:119–126

Killham K (1994) Soil ecology. Cambridge University Press, Cambridge

Kim BH, Gadd GM (2008) Bacterial physiology and metabolism. Cambridge University Press, Cambridge

Kljun N, Black TA, Griffis TJ et al (2007) Response of net ecosystem productivity of three boreal forest stands to drought (vol 9, pg 1128, 2006). Ecosystems 6:1039–1055

Knutson RM (1997) An 18-year study of litterfall and litter decomposition in a Northeast Iowa deciduous forest. Am Midl Nat 1:77–83

Kozlowski TT (1982) Water supply and tree growth. II. Flooding. For Abstr 43:145–161

Kramer PJ, Boyer JS (1995) Water relations of plants and soils. Academic Press, San Diego

Lamers M, Fiedler S, Jungkunst HF et al (2009) Impact of the heatwave in 2003 on the summer CH_4 and N_2O budget of a spruce forest ecosystem: a four-year comparison. Geophys Res Abstr 11:EGU2009-3981

Le Mer J, Roger P (2001) Production, oxidation, emission and consumption of methane by soils: a review. Eur J Soil Biol 1:25–50

Leavitt SW, Wright WE, Long A (2002) Spatial expression of ENSO, drought, and summer monsoon in seasonal $\delta^{13}C$ of ponderosa pine tree rings in southern Arizona and New Mexico. J Geophys Res 107. doi:10.1029/2001JD001312

Lieth H (1975) Modeling the primary productivity of the world. In: Lieth H, Whittaker RH (eds) Primary productivity of the biosphere. Springer, New York, pp 237–283

Luu DT, Maurel C (2005) Aquaporins in a challenging environment: molecular gears for adjusting plant water status. Plant Cell Environ 1:85–96

Marengo JA, Nobre CA, Tomaseela J et al (2008) The drought of Amazonia in 2005. J Climatol 21:495–516

McDowell N, Pockman WT, Allen CD et al (2008) Mechanisms of plant survival and mortality during drought: why do some plants survive while others succumb to drought? New Phytol 4:719–739

McDowell N, Allen CD, Marshall L (2010) Growth, carbon-isotope discrimination, and drought-associated mortality across a *Pinus ponderosa* elevational transect. Global Change Biol 16:399–415

McLain JET, Ahmann DM (2008) Increased moisture and methanogenesis contribute to reduced methane oxidation in elevated CO_2 soils. Biol Fertil Soils 4:623–631

Meentemeyer V (1978) Macroclimate and lignin control of litter decomposition rates. Ecology 59:465–472

Nepstad DC, Tohver IM, Ray D et al (2007) Mortality of large trees and lianas following experimental drought in an Amazon forest. Ecology 9:2259–2269

Pedersen BS (1998) The role of stress in the mortality of Midwestern oaks as indicated by growth prior to death. Ecology 79:79–93

Penuelas J, Prieto P, Beier C et al (2007) Response of plant species richness and primary productivity in shrublands along a north-south gradient in Europe to seven years of experimental warming and drought: reductions in primary productivity in the heat and drought year of 2003. Global Change Biol 12:2563–2581

Powers JS, Montgomery RA, Adair EC et al (2009a) Decomposition in tropical forests: a pantropical study of the effects of litter type, litter placement and mesofaunal exclusion across a precipitation gradient. J Ecol 4:801–811

Powers MD, Pregitzer KS, Palik BJ et al (2009b) Wood $\delta^{13}C$, $\delta^{18}O$ and radial growth responses of residual red pin to variable retention harvesting. Tree Physiol. doi:10.1093/treephys/tpp119

Rahn R (2005) Factors influencing the stable isotopic content of atmospheric N_2O. In: Flanagan LB, Ehleringer JR, Pataki DE (eds) Stable isotopes and biosphere-atmosphere interactions. Elsevier, New York, pp 268–287

Randerson JT (2005) Terrestrial ecosystems and interannual variability in the global atmospheric budgets of $^{13}CO_2$ and $^{12}CO_2$. In: Flanagan LB, Ehleringer JR, Pataki DE (eds) Stable isotopes and biosphere-atmosphere interactions. Elsevier, New York, pp 217–234

Reichstein M, Ciais P, Papale D et al (2007) Reduction of ecosystem productivity and respiration during the European summer 2003 climate anomaly: a joint flux tower, remote sensing and modeling analysis. Global Change Biol 13:634–651

Ryan MG, Yoder BJ (1997) Hydraulic limits to tree height and tree growth. Bioscience 4:235–242

Ryan MG, Phillips N, Bond BJ (2006) The hydraulic limitation hypothesis revisited. Plant Cell Environ 3:367–381

Sack L, Holbrook NM (2006) Leaf hydraulics. Ann Rev Plant Biol 57:361–381

Saleska SR, Didan K, Huete AR et al (2007) Amazon forests green-up during 2005 drought. Science 318:612

Sardans J, Penuelas J, Estiarte M et al (2008) Warming and drought alter C and N concentration, allocation and accumulation in a Mediterranean shrubland. Global Change Biol 14:2304–2316

Schimel JP, Gulledge J (1998) Microbial community structure and global trace gases. Global Change Biol 7:745–758

Schimel J, Balser TC, Wallenstein M (2007) Microbial stress-response physiology and its implications for ecosystem function. Ecology 6:1386–1394

Schlesinger WH (1997) Biogeochemistry: an analysis of global change. Academic Press, New York

Schlesinger WH, Peterjohn WT (1991) Processes controlling ammonia volatilization in Chihuahuan Desert soil. Soil Biol Biochem 23:637–642

Schwalm CR, Williams CA, Schaefer K et al (2010) Assimilation exceeds respiration sensitivity to drought: a FLUXNET synthesis. Global Change Biol 16:657–670

Singh JS, Gupta SR (1977) Plant decomposition and soil respiration in terrestrial ecosystems. Bot Rev 43:449–528

Sotta ED, Veldkamp E, Schwendenmann L et al (2007) Effects of an induced drought on soil carbon dioxide (CO_2) efflux and soil CO_2 production in an Eastern Amazonian rainforest, Brazil. Global Change Biol 13:2218–2229

Stark JM, Firestone MK (1995) Mechanisms for soil-moisture effects on activity of nitrifying bacteria. Appl Environ Microbiol 1:218–221

Tezara W, Mitchell VJ, Driscoll SD et al (1999) Water stress inhibits plant photosynthesis by decreasing coupling factor and ATP. Nature 401:914–917

Tiemann LK (2011) Soil microbial community carbon and nitrogen dynamics with altered precipitation regimes and substrate availability. Ph.D. dissertation, University of Kansas

Tietema A, Deboer W, Riemer L et al (1992) Nitrate production in nitrogen-saturated acid forest soils – vertical-distribution and characteristics. Soil Biol Biochem 3:235–240

Trofymow JA, Moore TR, Titus B et al (2002) Rates of litter decomposition over 6 years in Canadian forests: influence of litter quality and climate. Can J For Res 32:789–804

Tyree MT, Sperry JS (1988) Do woody plants operate near the point of catastrophic xylem dysfunction caused by dynamic water stress? Answers from a model. Plant Physiol 88:574–580

Tyree MT, Sperry JS (1989) Vulnerability of xylem to cavitation and embolism. Annu Rev Plant Physiol Mol Biol 40:19–38

Van Genuchten MT (1980) A closed-form equation for predicting the hydraulic conductivity of unsaturated soils. Soil Sci Soc Am J 44:891–898

Weatherley PE (1979) The hydraulic resistance of the soil–root interface – a cause of water stress in plants. In: Harley JL, Scott Russell R (eds) The soil root interface. Academic Press, London, pp 275–286

Welp LR, Randerson JT, Liu HP (2007) The sensitivity of carbon fluxes to spring warming and summer drought depends on plant functional type in boreal forest ecosystems. Agric For Meteorol 3–4:172–185

Whalen S, Reeburgh W (1996) Moisture and temperature sensitivity of CH_4 oxidation in boreal soils. Soil Biol Biochem 10(11):1271–1281

Wood TE, Lawrence D, Clark DA (2005) Variation in leaf litter nutrients of a Costa Rican rain forest is related to precipitation. Biogeochemistry 2:417–437

Woodruff DR, Bond BJ, Meinzer FC (2004) Does turgor limit growth in tall trees? Plant Cell Environ 27:229–236

Yoder BJ, Ryan MG, Waring RH et al (1994) Evidence of reduced photosynthetic rates in old trees. For Sci 3:513–527

Zwieniecki MA, Hutyra R, Thompson MV et al (2000) Dynamic changes in petiole specific conductivity in red maple (*Acer rubrum* L.), tulip tree (*Liriodendron tulipifera* L.) and northern fox grape (*Vitis labrusca* L.). Plant Cell Environ 23:407–414

Chapter 30
Effect of Forest Fires on Hydrology and Biogeochemistry of Watersheds

Shin-ichi Onodera and John T. Van Stan II

30.1 Introduction

Forest fire generally includes both natural wildfire and human-induced fire (e.g., slash-and-burn agriculture and accidental fire). Areas burned by forest fire are relatively widespread across the world (Table 30.1), but vary substantially across continents. For example, burned areas account for about two thirds of the total area in Africa, yet only approximately 1% in North America (Roy et al. 2008). Wildfire occurrence is primarily related to drought intensity, whereas agricultural demands oftentimes drive human-induced fires, particularly slash-and-burn cultivation. Because the controlling factors of both fire types have increased recently, global burned areas have also increased. In the Amazon catchment alone, burned area has expanded to encompass more than ten times its pre-1980 area (Peres et al. 2006). These increases in forest fire frequency and intensity have enhanced its role in, and contribution to, total global deforestation (Roy et al. 2008).

Forest fires have significant impacts on the local watershed and global environments. At the hillslope and catchment scale, forest fire alters hydrological, geomorphological, and biogeochemical processes. At the global scale, forest fires transfer carbon from the forest to the atmosphere, contributing to global warming (Crutzen and Andreae 1990) and other climate forcings (Weber and Flannigan 1997; Siegert et al. 2001; Alencar et al. 2006; Westerling et al. 2006). As a result of these alterations, increases in burned area within a catchment can elevate surface water runoff, soil erosion, and the export of nutrients, ultimately degrading hillslope soils and the downstream aquatic environment (Certini 2005; Shakesby and Doerr 2006; Jung et al. 2009; Noske et al. 2010).

The main objective of this chapter is to review previous research regarding fire-induced alterations of hydrological and biogeochemical processes at the watershed scale, with special attention to the effects of forest fires on the hydrologic cycle, soils, and nutrient (C, N, and P) transport and to highlight future research directions.

Table 30.1 Global distribution of burned area and active fires in each of the six continents as of 2008

Continent	Burned area ($\times 10^5$ km^2)	Active fire area ($\times 10^5$ km^2)	Global burned area per continent (%)	Global active fire area per continent (%)
Africa	25.0	13.7	68.41	49.40
Australia-Oceania	6.32	3.87	17.26	13.94
Northern Eurasia	1.56	2.82	4.26	10.16
Southern Eurasia	1.56	2.14	4.27	7.70
North America	0.40	1.43	1.10	5.17
South America	1.72	3.79	4.70	13.64
Total	36.6	27.8	100	100

Total burned area is defined by the MODIS burned area product (MCD45), and active fire area is defined by the MODIS active fire product (MOD14). (Adapted from Roy et al. 2008)

30.2 Effects of Fire on the Hydrology of Forested Watersheds

30.2.1 Pre- Versus Postfire Hydrological Processes

An undisturbed, forested hillslope intercepts, evapotranspires, and infiltrates incident precipitation efficiently, providing ecosystem services for nearby streams by reducing soil erosion and surface runoff (Fig. 30.1a). After forest fires, drastic changes, such as vegetation loss and production of hydrophobic soil layers, transform the hillslope and alter its hydrological cycling (Fig. 30.1b). Fire, by its very nature, obliterates the plant life responsible for the removal of rainfall via evapotranspiration. The extent of plant death depends on the degree of burn, which directly relates to the magnitude of decrease in evapotranspiration (Montes-Helu et al. 2009; Dore et al. 2010). The relationship between severity of fire and diminished evapotranspiration, however, is underresearched, particularly since the studies known to the authors focus primarily on the ecological succession of burned landscapes (Montes-Helu et al. 2009; Dore et al. 2010). Montes-Helu et al. (2009) more specifically linked the diminished evapotranspiration to burn-related decreases in tree leaf area. But, as burned areas reestablish, predisturbance levels of evapotranspiration can be restored somewhat quickly. For example, Dore et al. (2010) noted that evapotranspiration within an intensely burned ponderosa pine stand rebounded to within 15% of an undisturbed stand in a decade.

Hydrophobic soil layers are more persistent and arguably exert greater influence on downhill and downstream aquatic ecosystems. Water-repellent soil layers are generated by the vaporization of organic compounds in the litter and topsoil during wild and controlled fires, which migrate downward, cool, and condense in underlying soil layers (DeBano 1981, 2000b). Many previous studies have shown that burn-related hydrophobic soil layers can greatly diminish infiltration (Fig. 30.1b) and therefore groundwater recharge (Burch et al. 1989; Robichaud 2000; Wang et al. 2000; Martin and Moody 2001; Lewis et al. 2006). DeBano (2000b) showed that
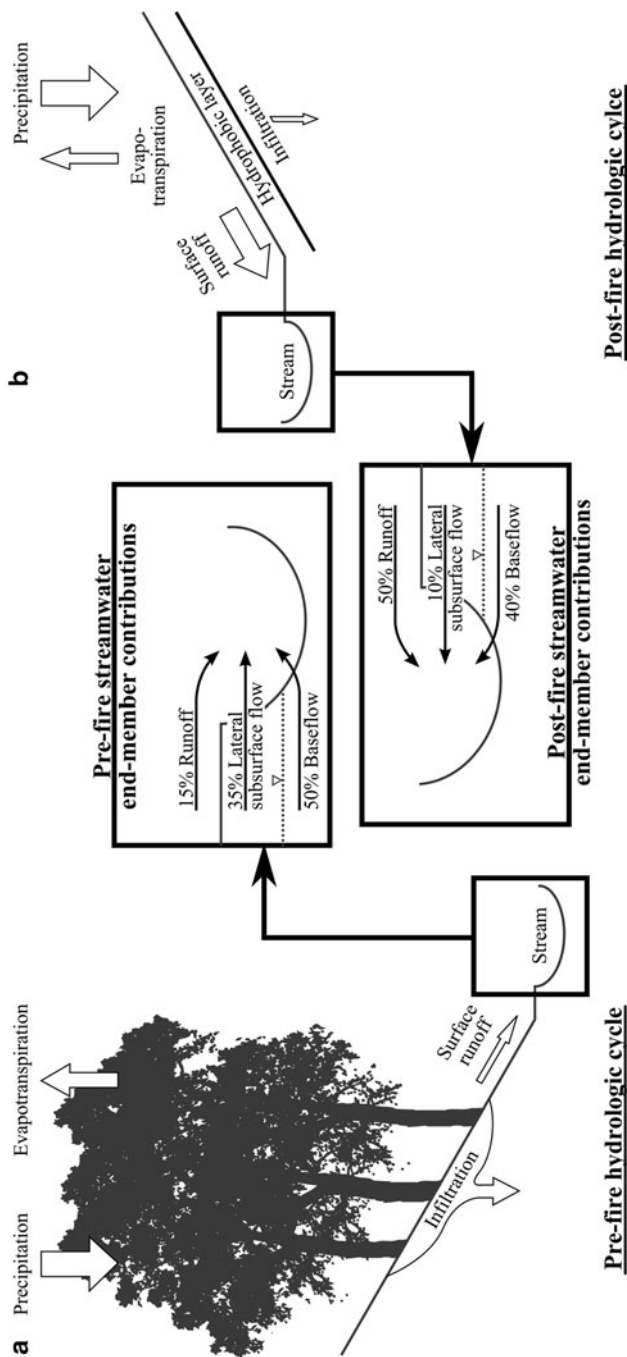
Fig. 30.1 *Impacts of fire on hydrologic cycling and streamwater within forested hillslopes.* Prefire conditions (**a**) efficiently evapotranspire and infiltrate incident precipitation. This diminishes surface runoff contributions to downhill streams, yet increases lateral subsurface flow. Due to the damage, dieback, or absence of vegetation, burned hillslopes (**b**) produce significantly smaller evapotranspiration and infiltration fluxes, reducing baseflow, shrinking contributions from lateral subsurface flow, and tripling runoff contributions to streamwater. Note: Prefire end-member contributions were averaged from previous forested watershed studies (Burns et al. 2001; Katsuyama et al. 2001; Worrall et al. 2003; Bernal et al. 2006; Inamdar and Mitchell 2006; Jung et al. 2009; Harpold et al. 2010). Postfire values were taken from the sole postfire EMMA study known to the authors (Jung et al. 2009)

these burn-related water-repellent sediment layers can form beneath a wettable lens of surface soil. In such cases, infiltration rates are high in the beginning of a storm event, but decrease once the wetting front reaches the hydrophobic sublayer (DeBano 2000b). Since the intensity of water repellency within the hydrophobic soil layer strengthens as soil moisture declines, initial water content can determine infiltration rate through the water-repellent soil (Dekker and Ritsema 1994). Dekker and Ritsema (1994) determined "potential" and "actual" water repellency under lab-based air drying and natural conditions. These properties were shown to control the temporal and seasonal variation of infiltration rates within hydrophobic soil sub-layers. For example, DeBano (2000b) found that dry catchment soil conditions at the start of the rainy season produced high water repellencies and reduced infiltration rate; yet infiltration rate increased with a decrease in water repellency as antecedent soil moisture conditions improved toward the end of the rainy season.

The horizontal and vertical spatial variability of water repellency on hillslopes caused by forest fires is large, simply because the forest floor and soils are naturally highly heterogeneous. Consequently, infiltration rates on a fire-impacted forested hillslope are typically so variable that it prevents uniform infiltration and results in the formation of unstable wetting fronts (Ritsema and Dekker 1994). Ritsema and Dekker (1994) confirmed that wetting fronts within burned soils are likely nonuniform by identifying "finger-like" preferential infiltration pathways through localized, vertical soil profiles of lower water repellency. The average size of these preferential flowpaths was between 10 and 50 cm in diameter (Ritsema and Dekker 1994). Nagahama et al. (2001) also confirmed heterogeneous infiltration processes through burned soils using in situ resistivity experiments. Such preferential infiltration pathways are of particular interest as they can contribute significantly to solute transport.

As infiltration and groundwater recharge within a forested hillslope are impacted by fire, overland flow (surface runoff) fraction tends to increase (Fig. 30.1a,b) (Scott 1997; Jung et al. 2009), which, in turn, enhances peak stream discharge during storm events (Scott 1997; Moody and Martin 2001; Moody et al. 2008). For these same reasons, deforestation by forest fire also lowers evapotranspiration and groundwater levels (Fig. 30.1a,b) and increases soil wetness and total stream discharge (Kusaka et al. 1983; Worrall et al. 2007). These effects are similar to the effects of clear cutting (Bosch and Hewlett 1982), yet typically of higher magnitude due to burn-related soil hydrophobicity. There are few studies comparing these disturbances as it is difficult to monitor all hydrologic variables within storm events across pre- and postfire conditions for a specific watershed (Woodsmith et al. 2004).

Of the few studies, continuous observations by Scott (1997) showed total stream discharge increased by only 12% after a forest fire, but storm runoff swelled by threefold. Petrone et al. (2007) observed similar increases in peak stream discharges and surface runoff volumes for a fire-affected catchment in interior Alaska. End-member mixing analyses conducted by Jung et al. (2009) showed that postfire surface runoff contributions were five times greater than prefire runoff contributions to streamwater. Compared to mean end-member contributions derived for other unburned forested catchments (Burns et al. 2001; Katsuyama et al. 2001;

Worrall et al. 2007; Bernal et al. 2006; Inamdar and Mitchell 2006; Jung et al. 2009; Harpold et al. 2010), Jung et al. (2009) postfire runoff contributions to streamwater were just over three times larger (Fig. 30.1a,b). Postfire baseflow contributions decreased slightly in comparison to the mean baseflow contributions compiled from the unburned forested catchments (Fig. 30.1a,b). Differences in runoff and baseflow contributions between Jung et al. (2009) burned catchment's streamwater and the unburned catchments are likely due to marked decreases in infiltration and groundwater recharge from water-repellent soil layers, lateral subsurface flow, and evapotranspiration (Jung et al. 2009).

30.2.2   Hydrogeomorphology Within Burned Catchments

Mechanisms of water-mediated erosion on hillslopes are highly sensitive to fire-related alterations of land surface properties – particularly those which inflate surface runoff volume and stream discharge (Prosser and Williams 1998; Shakesby et al. 2000; Elliott and Parker 2001; Johansen et al. 2001; Pardini et al. 2004; Leighton-Boyce et al. 2007). Field-based and simulation experiments have linked increases in erosion rate with fire severity (Elliott and Parker 2001; Johansen et al. 2001). Benavides-Solorio and MacDonald (2001) indicated that postfire erosion at high severity plots were 10–26 times greater than unburned and low severity plots, even though runoff was only 15–30% greater. Spigel and Robichaud (2007) confirmed the accelerated erosion processes by overland flow and rain drop.

Many researchers believe that reductions in vegetative cover (Fig. 30.2) play the most critical role in enhancing soil erosion rates on hillslopes devastated by severe fire (White and Wells 1979; Dieckmann et al. 1992; Inbar et al. 1998;

Fig. 30.2 *Post-forest fire catchment within the Rocky Mountains, Colorado, USA.* Note the stark contrast in land surface cover between the *upper* and *lower* portions of the photograph. The combination of vegetation dieback and a soil covered in dark, sooty combustion by-products creates drastically different hydrogeomorphological response. Photo credit: Andrea Holland-Sears, US Forest Service
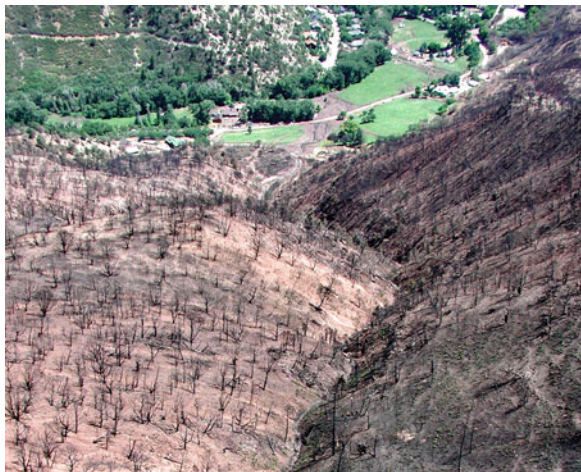
Shakesby and Doerr 2006). In the absence of vegetation, hillslopes lose root masses which act as soil stabilization structures. Burned hillslopes also lack the protection from raindrop impacts that was once provided by litter and canopy cover (Fig. 30.2). Droplet impacts during precipitation are then able to disturb the topsoil matrix and reduce soil water storage capacity (Shakesby and Doerr 2006). Rainsplash-related detachment of soil particles can increase significantly if rainfall is intercepted by the skeletal remains of burnt trees (becoming throughfall) as this increases droplet size and impact (McNabb and Swanson 1990). Throughfall droplet weight is further enhanced by the acquisition of ash particles from singed tree surfaces (McNabb and Swanson 1990). Reductions in vegetative cover also allow for more efficient scouring of hillslope surfaces by sheetwash (Shakesby and Doerr 2006). Depending on the amount of fine sediment particles and the level of water repellency, sheetwash erosion can be quite high (DeBano 2000a,b). This is even more so the case for splash droplet erosion (Terry and Shakesby 1993; Shakesby and Doerr 2006). In fact, lab simulations performed by Terry and Shakesby (1993) showed that fine soils of low hydrophobicity compacted throughout a rain event, eventually sealing and drastically increasing resistance to splash droplet erosion (and potentially sheetwash erosion). Simulated rain events for the more hydrophobic soils resisted water-induced cohesion, allowing erosive forces from droplet splashes and sheetwash to displace particles throughout the event (Terry and Shakesby 1993).

Continuous hydrophobic soil layers promote sheetwash and concentrated channel erosion which, over time, develop rills and gullies (Fig. 30.2). On steep, water-repellent hillslopes sediment is rarely transported in sheetflow, forming concentrated channels that carve extensive rill networks (Doehring 1968; Wells et al. 1987; Shakesby and Doerr 2006). When the wettable surface soil layer becomes saturated, pore pressures increase against the underlying hydrophobic soil and lubricate the interface, causing failure and debris flow (Gabet 2003). As the debris flow moves downgradient, it frees neighboring wettable soil layer water which was previously confined (Shakesby and Doerr 2006). Released water scours the debris flow channel and increases sediment transport into the stream channel via storm runoff (Keller et al. 1997; Kunze and Stednick 2006; Noske et al. 2010).

These debris flows, in conjunction with increased peak stream discharges, increase sediment exports at the watershed scale (Keller et al. 1997; Nishimune et al. 2003; Kunze and Stednick 2006; Desilets et al. 2007; Noske et al. 2010). The extant literature has reported a diverse array of stream channel responses to fire-related increases in sediment load, including channel narrowing, braiding, entrenchment, terracing, channel aggradation, and the formation of alluvial fans (McNabb and Swanson 1990; Meyer and Wells 1997; Moody and Martin 2001; Legleiter et al. 2003; Shakesby and Doerr 2006). These hydrogeomorphological changes can result in the transference of postfire sediments from burnt tributaries to higher order streams (White and Wells 1982; Keller et al. 1997). Keller et al. (1997) even witnessed eroded sediment from a burnt tributary reduce downstream channel cross-sectional area, enhancing flood risk. The hydrophobic organic compounds

within the burnt soils are eventually processed and the burnt hillslope revegetates, diminishing runoff-related suspended sediment contributions to streamwater over time (Desilets et al. 2007). This means sediment yield is typically highest at the first postfire storm event or in the first postfire year due to the abundance of erodible soil and higher water repellency (Desilets et al. 2007; Keller et al. 1997). However, Legleiter et al. (2003) found that postfire erosion effects are not solely restricted to hillslope-related erosion and can be transferred from the hillslope to the stream channel. Legleiter et al. (2003) discovered stream discharge 10 years after the 1988 Yellowstone fire remained elevated, despite a gradual decrease in sediment supply from postfire hillslope erosion. This resulted in a transference of erosion from the postfire hillslope to the stream, inducing a period of channel incision to maintain stream sediment budgets (Legleiter et al. 2003). Researchers are consistently producing surprising results regarding how much the hydrogeomorphological effects of fire alter wooded ecosystems and how far these effects extend beyond the affected area; yet the current studies primarily represent short-term, small-scale observations, leaving many long-term, large-scale fire-related hydrogeomorphological impacts and interactions open for future investigation (Shakesby and Doerr 2006).

30.3 Effects of Fire on Forest Soils

Soils play a critical role in the hydrologic and nutrient cycling of forested ecosystems. Because fire severely degrades soil surfaces, soil-based ecosystem services are greatly diminished in burned areas. In fact, burn-related reduction of soil buffering capacity is rapidly becoming a worldwide concern as the global frequency of forest fire increases (Certini 2005). Forest fire consumes the organic litter layer, the topsoil, and vegetative cover, converting these into CO_2, ash, and char (Ilstedt et al. 2003; Knicker 2007; Kara and Bolat 2009). This results in the death of soil fungi and bacteria (Kara and Bolat 2009) and, correspondingly, a reduction in organic soil matter and organic matter decomposition. The burning of soil organic compounds also changes soil molecular structure (Knicker 2007) and, depending on burn temperature and time, increases soil hydrophobicity (O'Donnell et al. 2009). As the hydrophobic effect of soil generally decreases infiltration rates (Cerda 1998; Martin and Moody 2001), fire can ultimately diminish soil moisture as well.

Fire-related mortality of soil microbe populations reduces soil organic matter and prevents its decomposition (Kara and Bolat 2009; Shakesby and Doerr 2006). Because fungal hyphae stabilize soil matrices and the decomposition process creates cohesive compounds, these phenomena exert significant influence over the erodibility of soils. Beneficial plant–microbe symbioses (mycorrhizae) are also destroyed by extreme heat (Vilariño and Arines 1991; Certini 2005) and the production of combustion-related toxic compounds (Kim et al. 2003). According to phospholipid fatty acid analyses (PFLAs) performed by Bååth et al. (1995), fire-related fungi mortality is much greater than bacteria. In fact, some areas within

burnt catchments contain microbial populations, which are able to persist postfire (Neary et al. 1999; Dragovich and Morris 2002). These localized hot spots of faunal activity can provide preferential subsurface flowpaths by biotransferring easily eroded, hydrophobic sediments from the soil profile and enhancing the vertical infiltration rate (Dragovich and Morris 2002).

The most direct burn-related alteration of a soil's physical properties is the development of the water-repellent soil layer (Dekker and Ritsema 1994; DeBano 2000a; Lewis et al. 2006). When organic material, such as litter on the soil surface, is consumed by fire, volatilized organic compounds intrude into the soil, coating soil particles (DeBano 2000b). This hydrophobic coating specifically reduces infiltration by reducing capillary tension and rejecting the smooth infiltration of water (Letey et al. 2000). Water repellency has generally been determined by water drop penetration time (WDPT) and critical surface tension (CST) (Letey et al. 2000). The WDPT test measures the time required for a water drop to be absorbed into a soil of interest (Letey et al. 2000). If it is longer than 5 s, the soil is considered water repellent (Letey et al. 2000). Fox et al. (2007) measured significantly longer WDPT times for fine soil particles (<2 mm) than for coarse particles (>2 mm). This finding indicates that finer soil particles may be more extensively coated by volatilized organic compounds during fire (Fox et al. 2007). The CST test measures soil–water contact angles by using aqueous ethanol solutions of different concentrations and surface tensions (Letey et al. 2000). The surface tension of the ethanol decreases with increasing concentration (Letey et al. 2000). Using CST tests, Letey et al. (2000) observed that water-repellant soils produce soil water contact angles greater than 90°. Direct contact angles between soil and water, particularly across sharp boundaries of contrasting hydraulic conductivity and pore size, may account for the extended WDPT times described in many studies (Imeson et al. 1992; Everett et al. 1995; Letey et al. 2000; Robichaud 2000; Certini 2005).

The intensity or severity of fire interacts with moisture and particle size distribution to control the intensity and depth of water repellency in soils (Fig. 30.3) (Robichaud 2000; Huffman et al. 2001). When burn temperatures increase, so does the volatilization of organic hydrocarbons and, therefore, the hydrophobicity of burnt soils (DeBano 2000b; Certini 2005). However, when burn temperatures rise above 280°C, the combustion of aliphatic compounds can reduce the VOC-related water repellency (Fig. 30.3). Varela et al. (2005) confirmed this relationship under controlled laboratory conditions, finding increases in water repellency at burn temperatures ranging from 25 to 220°C, peak soil hydrophobicities between 220 and 240°C, and sharp reductions in water repellency above 260–280°C (Fig. 30.3). According to these results, water repellency in burnt surface soils weakens under severe, high intensity forest fires (Fig. 30.3). During conditions of repeated fire, layers of water-repellent soils can alternate sporadically between other horizontal, permeable soil layers (DeBano 2000b; Martin and Moody 2001; Lewis et al. 2006), but rarely do these layers exceeds depths greater than 8 cm (Henderson and Golding 1983; Huffman et al. 2001). The irregular patterning and infiltration effects of alternating burnt soil layers are strongly dependent on the pattern of fire severity
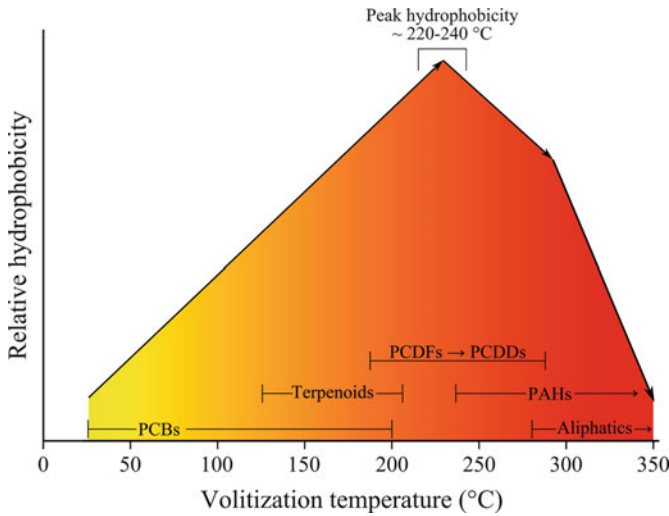
Fig. 30.3 *Volatization temperatures of identified litter-derived organic compounds plotted against laboratory- and field-based temperature trends in soil hydrophobicity.* Fire-related soil temperature increases cause the volatization of various organic compounds that can enhance or diminish water repellency in soils (Nestrick and Lamparski 1982; Coutant et al. 1988; Wunderli et al. 1996; DeBano 2000b; UN-FAO 2000; Isidorov and Jdanova 2002; Kim et al. 2003; Certini 2005; Ramirez et al. 2010)

(Imeson et al. 1992; Certini 2005). Hydrophobic soil layers may persist for 19 months in the soil column, but may weaken somewhat rapidly (within 3 months) after a fire (Huffman et al. 2001).

Although fire tends to reduce the overall structural integrity of soils on hillslopes, some fire-induced hydrophobic films have acted as a surficial bonding agent, holding together soil aggregates (Mataix-Solera and Doerr 2004; Shakesby and Doerr 2006). Burnt aggregates can even become more stable than their original, unburnt states if combustion temperatures are right for the formation of cementing oxides (Giovannini and Lucchessi 1991; Ketterings et al. 2000; Certini 2005). This aggregation effect is oftentimes trumped by reductions in water holding capacity and increased bulk density enhancing the potential for soil erosion (Martin and Moody 2001). Bulk density is increased in burnt soils by a combination of ash clogging soil pores and organomineral aggregate collapse (Durgin and Vogelsang 1984; Giovannini et al. 1988). Oswald et al. (1999) found that soil particle size distribution is not directly influenced by forest fire. Rather, erosion on burnt hillslopes preferentially removes fine particulates from soil surfaces, coarsening postfire hillslope soils over time (Mermut et al. 1997). The effects of soil microbe death, combusted organic matter, enhanced hydrophobicity, and removal of fine particulates within burnt soils combine synergistically to significantly alter catchment hydrologic response and biogeochemistry.

30.4 Effects of Fire on the Biogeochemistry of Forested Watersheds

30.4.1 Nutrient Cycling Within Burnt Watersheds

Most investigations regarding the effects of forest fire on watershed biogeochemistry examine the loss and alteration of soil organic carbon (C) due to combustion (Certini 2005; Shakesby and Doerr 2006; Knicker 2007). Depending on the intensity of a forest fire, subcanopy combustion can consume the entire litter layer (Brais et al. 2000; Simard et al. 2001) and even deplete or eliminate topsoil organic C pools (Knicker 2007). Severe reductions in soil organic C result in long-term modifications to a watershed's humification processes (Ponomarenko and Anderson 2001; Certini 2005; Knicker 2007). Moreover, the remaining soil-based organic C is oftentimes altered during the burn (becoming "pyrogenic" organic C), which exhibits a different molecular structure from biologically generated organic C compounds (González-Pérez et al. 2004; Knicker 2007). During combustion organic C is oxidized by removing external oxygen groups; however, biological oxidation tends to create carboxyl-rich macromolecules (Knicker 2007). These qualitative differences in molecular structure result in diminished solubility for pyrogenic organic C compounds in relation to biogenic C compounds (Knicker and Lüdemann 1995). Previous research has also shown that fire increases the aromatic fraction of organic C and dissolved organic C (DOC) (González-Pérez et al. 2004; Certini 2005; Knicker 2007; Vila-Escalé et al. 2007). Carbon soil solutions with high aromaticity are less efficiently digested by microbes, increasing environmental residence times (Knicker 2007; Vila-Escalé et al. 2007). Aromatic hydrocarbons are also considered contaminants which can be bioaccumulated in fish tissues or interact with other organic compounds to form additional ecologically harmful chemicals, such as trihalomethanes (Imai et al. 2003; Xue and Warshawsky 2005). Further structural differences (as summarized by González-Pérez et al. (2004)) can increase nutrient leaching from soils by modifying sorption properties, enhance erosion and particulate export, and even affect the formation of soil aggregates (Knicker 2007; Noske et al. 2010).

Burn-related changes in the molecular structure of organic C compounds typically combine with enhanced erosion rates and surface runoff to produce greater DOC stream exports (Petrone et al. 2007; Vila-Escalé et al. 2007; Mast and Clow 2008). Vila-Escalé et al. (2007) reported large magnitude increases in postfire DOC stream concentrations (eight times those of similar undisturbed catchments). DOC aromatic content within DOC stream exports also increased, particularly toxic polycyclic aromatic compounds (Vila-Escalé et al. 2007). The presence of these compounds perpetuates microbial die off within aquatic environments and may prevent the reestablishment of microbial populations long after a forest fire subsides (Vila-Escalé et al. 2007). Increases in aromaticity have also been found to affect the redox potential across a watershed's hydrologic compartments, including

biogeochemically important systems such as wetlands and near-stream saturated zones (Mladenov et al. 2008).

The molecular structure and redox potential of organic C compounds link C and N cycling as these properties determine the suitability of organic C compounds to act as electron donors in denitrification (Korom 1992; Lovely et al. 1999). This process, heterotrophic denitrification, has been found to be especially important for NO_3 removal in the near-stream saturated zone and wetlands (Korom 1992; Mohamed et al. 2003). An important by-product of heterotrophic denitrification is HCO_3, which contributes to the pH buffering capacity of streams and lakes (Korom 1992; Mohamed et al. 2003). Many studies have reported elevated stream exports of NO_3 in response to fire (Bayley et al. 1992; Chorover et al. 1994; Williams and Melack 1997; Williams et al. 1997; Gerla and Galloway 1998; Bêche et al. 2005; Lane et al. 2008; Betts and Jones 2009); however, NO_3 is not a direct product of combustion (Certini 2005). NH_4 is the only direct nitrogenous product of vegetative thermal decomposition, indicating that postfire NO_3 exports are likely the result of nitrification processes (Covington and Sackett 1992). High NO_3 streamwater concentrations further imply that the denitrification process is hampered in burnt wetlands and near-stream saturated zones due to the highly aromatic and hydrophobic nature of pyrogenic DOC (González-Pérez et al. 2004; Certini 2005; Knicker 2007). Observations by Mroz et al. (1980) support this, showing that nitrification of NH_4 in soils occurs quite readily unless the NH_4 is fixed to the interlayer of clay minerals. In contrast, NO_3 is not adsorbed to the negatively charged soil particle surfaces and is leached through the soil matrix (Prieto-Fernandez et al. 1993). The fire-generated augmentation of soil NH_4 concentration appears to dissipate after two growing seasons (Grogan et al. 2000). This time scale is synchronous with the return of stream NO_3 exports to undisturbed levels reported by other studies (Bayley et al. 1992; Chorover et al. 1994; Williams and Melack 1997; Williams et al. 1997; Gerla and Galloway 1998; Bêche et al. 2005; Lane et al. 2008).

In addition to NO_3 and an organic C electron donor, heterotrophic denitrification requires adequate concentrations of phosphorous (P). In fact, sufficient N:P ratios are necessary to activate the gene responsible for synthesizing a critical enzyme for denitrification (nitrogenase) in heterotrophic bacteria (Stock et al. 1990). Phosphorous, specifically PO_4, is also a limiting nutrient in plant growth (Marschner 1995). Although many studies show little-to-no increases in postfire total P (TP) or PO_4 exports (e.g., Bayley et al. 1992; Williams et al. 1997; Bêche et al. 2005; Mast and Clow 2008), Noske et al. (2010) found that, when considering coarse matter as well as dissolved and suspended fractions, postfire TP export rates increased to 60 times any values recorded under prefire conditions. Since TP and PO_4 availability limits plant growth and heterotrophic denitrification, high magnitude increases in stream exports could diminish plant succession in the short term and contribute to high postfire NO_3 stream concentrations by preventing denitrification within burnt near-saturated zones and wetlands (Bayley et al. 1992; Chorover et al. 1994; Williams and Melack 1997; Williams et al. 1997; Gerla and Galloway 1998; Bêche et al. 2005; Lane et al. 2008).

30.4.2 Postfire Nutrient Loss by Forest Type

Increases in temperature and wetness postfire drastically change watershed biogeochemical processes across all forest types (Table 30.2), particularly solute chemistries of soil water, groundwater, and streamwater. Burn-related increases in overland flow generally enhance mineralization of litter and vegetation, thereby increasing solute nutrient losses from a catchment (Thomas et al. 2000). Generally, the loss of DOC, NO_3, PO_4, and TP across forest types is great in comparison to preburn, unburnt, or recovered levels (Table 30.2), and the high solute losses continued for 2–3 years (Thomas et al. 2000). On the other hand, most studies observed negligible to no increases in DON and NH_4 losses (Table 30.2), likely due to the aforementioned strong sorption potential for clay minerals (Mroz et al. 1980).

In tropical forests, wildfires have been shown to affect nutrient losses, of both the suspended form in stormflow and the soluble form in baseflow (Malmer 2004; Williams et al. 1997). Suspended nutrient concentrations in burned catchments were tenfold of those in preburned ones (Malmer 2004). Baseflow N concentrations immediately after a fire were three- to fivefold of those after 1 year (Malmer 2004). Postfire DOC, DON, and NH_4 exports also, at a minimum, doubled (Table 30.2). TP and PO4 exports were very low, and sometimes at nondetectable levels, from unburnt and preburn watersheds (Table 30.2). However, catchments affected by fire increased to detectable levels (Table 30.2). Even though postfire TP and PO_4 increases and total exports are small (Table 30.2), many studies assert that ecosystems already limited by P availability may be further stressed by modest P exports (Bayley et al. 1992; Gerla and Galloway 1998; Bêche et al. 2005; Lane et al. 2008; Noske et al. 2010). Enhanced solute concentrations for all nutrients tend to decline the second year after a fire in comparison with those in the first year (Malmer 2004; Williams et al. 1997). Malmer (2004) suggests that the rising of nutrient concentrations during the first year in burnt tropical streams is a result of increased weathering rates and decreased plant uptake. Such plant–soil interactions would also explain the nutrient export reductions during the second year as the nutrient uptake and slope stabilization due to recovered vegetation have been shown to mitigate erosion-related dissolved and particulate nutrient losses (Shakesby and Doerr 2006).

In the boreal and alpine/subalpine forests of colder climate regions, some researchers have reported similar patterns in postfire material transport as what was observed in tropical forests (Bayley et al. 1992; Petrone et al. 2007; Mast and Clow 2008; Betts and Jones 2009). Mast and Clow (2008) monitored stream runoff and solute and suspended sediment (SS) concentrations for 4 years following the fires in glaciated watersheds. They found that nitrate concentrations in a burned catchment increased tenfold of those in the unburned, but only tripled NO_3 exports due to diminished streamflows (Mast and Clow 2008). However, high levels of NO_3 streamwater concentrations continued up to the first postfire snowmelt (Mast and Clow 2008). Postfire responses in NO_3 export were comparable within burnt catchments dominated by boreal forests (Bayley et al. 1992; Petrone et al. 2007; Betts and Jones 2009); yet the magnitude of postfire exports compared to unburnt

Table 30.2 Nutrient loss comparisons between burnt and preburn/unburnt/recovered watersheds from previous studies

Forest type and citation	Nutrient losses (kg ha⁻¹ y⁻¹)											
	DOC		DON		NH₄		NO₃		PO₄		Total P	
	Burnt	Preburn/unburnt/recovered	Burnt	Preburn/unburnt/recovered	Burnt	Preburn/unburnt/recovered	Burnt	Pre-burn/Unburnt/Recovered	Burnt	Pre-burn/Unburnt/Recovered	Burnt	Pre-burn/Unburnt/Recovered
Alpine/subalpine												
Mast and Clow (2008)	33.9–45.1	19.9–26.5	–	–	<1	<1	1.53–3.23	1.01–1.39	–	–	0.018–0.043	0.05–0.102
Boreal												
Betts and Jones (2009)	5.3–12.3	5.7–13.3	0.5–1.3	0.6–1.3	–	–	14.5–33.9	4.8–11.3	–	–	–	–
Petrone et al. (2007)	31.2–43.7	13.9–19.5	3.4–4.8	2.4–3.4	0.05–0.1	0–0.07	9.9–13.8	9.1–12.8	0.2–0.3	0–0.01	–	–
Bayley et al. (1992)	–	–	0.64–1.77	0.62–0.92	0.03–0.11	0.03–0.05	0.04–0.42	0.02–0.06	–	–	0.02–0.13	0.03–0.06
Coniferous												
Bêche et al. (2005)	–	–	–	–	1.6–2.6	1.0–2.8	15.8–26.3	5.9–16	–	–	3.2–5.3	0
Thomas et al. (2000)	–	–	–	–	–	–	1.1	0	0.08	0.0003	–	–
Gerla and Galloway (1998)	–	–	–	–	25.2	22.1	44–257	4–40	–	–	4.4–12.6	0.63–6.3
Chorover et al. (1994)[a] Williams and Melack (1997)[a]	–	–	–	–	<0.1	0.6–1.1	1.4–2.9	0.7–1.4	<0.1	0.3–0.6	–	–
Chorover et al. (1994)[b] Williams and Melack (1997)[b]	–	–	–	–	3.2–6.3	0.9–1.7	52.9–105.8	0.1–0.2	<0.1	<0.1	–	–
Eucalyptus												
Noske et al. (2010)[c]												
Lane et al. (2008)[c]	–	–	1.47	0.35	–	–	2.97 ± 0.16	0.88 ± 0.06	0.01	<0.01	1.03	0.28
Lane et al. (2006)[c]												
Noske et al. (2010)[d]												
Lane et al. (2008)[d]	–	–	2.27	0.27	–	–	2.90 ± 0.17	0.79 ± 0.06	0.06	<0.01	2.14	0.31
Lane et al. (2006)[d]												
Thomas et al. (2000)	–	–	–	–	–	–	1.12	0.06	0.55	0.002	–	–
Tropical												
Malmer (2004)	–	–	–	–	1.3 ± 0.2	<0.006	4.8 ± 0.49	0.33 ± 0.04	0.17 ± 0.009	0.06 ± 0.009	0.048 ± 0.007	<0.006
Williams et al. (1997)	49.9–83.1	23.0–38.4	2.69–4.48	1.55–2.58	0.47–0.79	0.19–0.32	18.9–31.5	13.9–23.1	0.27–0.46	0.17–0.29	0.46–0.76	0.29–0.49

[a]Log Creek catchment
[b]Tharp Creek catchment
[c]Springs Creek catchment
[d]Slippery Rock catchment
Any "–" denotes nutrient comparisons not done in the study

boreal catchments was slightly greater (Table 30.2). Just as reported for tropical forests, increases in TP and PO$_4$ losses due to fire increased from barely detectable to modest levels in colder forested catchments (Table 30.2). Two notable differences in postfire nutrient exports between boreal and alpine/subalpine forested catchments is that (1) flow pathways through boreal systems oftentimes interact with a deeper organic surface soil layer and (2) stream chemistry consists of larger groundwater contributions (Petrone et al. 2007). DOC and DON originated from the organic layer and nutrient contributions from mineral weathering likely explain the differences in the magnitude of nutrient losses between the burnt boreal and alpine/ subalpine forested catchments (Table 30.2).

Reports of enhanced nutrient loss for DON and NO$_3$ from burnt watersheds dominated by eucalyptus forests are larger than those reported for tropical, boreal, alpine, and subalpine environments (Table 30.2). DON exports are 5–9 times higher than observed under pre- and unburnt catchment conditions, and NO$_3$ losses have been recorded at orders of magnitudes above undisturbed levels (Table 30.2). Observed postfire losses of PO$_4$ from eucalyptus forests are generally low, but markedly differ among studies (Table 30.2), likely due to differences in burn intensity. Australian eucalyptus forests for two intensely burnt catchments (Springs and Slippery Rock Creek) produced enhanced PO$_4$ stream exports that were much less enhanced than those recorded from a Portuguese eucalyptus watershed affected by less intense, understory fires (Table 30.2). Watershed losses of TP were comparable to values published in other studies of differing forest types (Table 30.2). Nutrient losses from burnt coniferous forests were among the highest reported and showed the largest increases from preburn or unburnt catchments of similar forest type (Table 30.2). This is particularly noticeable for NO$_3$, NH$_4$, and TP (Table 30.2). In the most affected cases, NO$_3$ exports increased by greater than two orders of magnitude and NH$_4$ by four times after fire (Table 30.2). The greatest observed postfire TP exports were witnessed in a coniferous drainage basin and were six times the next highest value regardless of forest type (Table 30.2).

Studies concerning biogeochemical alterations in burnt, scarcely forested urban watersheds focus more on contaminant and suspended sediment transport – especially in relation to trace metals (Moldan and Cerny 1994; Caldwell et al. 2000; Onodera et al. 2002; DeMarco et al. 2005; Farella et al. 2006). This is because trace metals of many species fall into watersheds as atmospheric pollution and are adsorbed in surface soils and immobilized (Driscoll et al. 1994). Forest fire may release adsorbed trace metals, initiating significant trace metal losses from a hillslope by leaching and/or erosion (Caldwell et al. 2000; DeMarco et al. 2005). The rate of leaching depends on combustion-related alterations of soil organic matter and the availability of adsorbed and mineralized trace metal (Caldwell et al. 2000; DeMarco et al. 2005). Using monthly monitoring data from surface sediment and water chemistries in a reservoir affected by fire, Caldwell et al. (2000) showed that concentrations of toxic monomethylmercury in sediment increased up to 30-fold and the ratio of monomethylmercury to total mercury increased from 5.4 to 33.8%. This indicates that fire altered the chemical species of trace metals (specifically mercury) in surface soils and that these mercury species were transported from the

burnt hillslope to the urban reservoir (Caldwell et al. 2000). Monomethylmercury concentrations of sediments in the reservoir were also distinctly higher than those in the surface soils of the burnt hillslope, suggesting that trace metal losses, likely in soluble form, were not only transported into the reservoir, but were also being magnified over time (Caldwell et al. 2000). Onodera et al. (2002) found that under acid rain conditions, trace metals could become desorbed from surface soil particles and mobilize more easily within runoff. Farella et al. (2006) then found that trace metals desorb under acidic conditions due to the exchange of low pH soluble cations. As forest soil acidification by acid rains common to many areas (Moldan and Cerny 1994), burnt hillslopes near urban water bodies affected by acid rain may exceed the levels of trace metal magnification reported by Caldwell et al. (2000), potentially eliciting drastic changes in water quality.

30.4.3   *Forest Fires and Climate Change*

The amount of wildfires and human-induced fires has increased proportionally with drought and slash-and-burn deforestation (Peres et al. 2006; Roy et al. 2008). Climate change models predict that, should warming occur due to increased C emissions, the temperature and precipitation regime of fire-prone high latitude forests could become hotter and drier (Flannigan et al. 2000). Because such climate changes increase fuel abundance, previous studies have concluded that enhanced anthropogenic C emissions could increase forest fire frequency (Overpeck et al. 1990; IPCC 1996). However, studies relying on global circulation models (GCM) to evaluate the potential for increased forest fire frequency with increased anthropogenic CO_2 emissions have produced conflicting results (e.g., Price and Rind 1994; Tackle et al. 1994; Flannigan et al. 1998; Stocks et al. 1998). Results using doubled atmospheric CO_2 concentrations range from 78% to statistically indistinguishable increases in forest fire frequency (Flannigan et al. 2000). The only similar result across studies was a noticeable increase in the frequency of forest drying – which is a significant factor in the generation of a forest fire (Flannigan et al. 2000). Therefore, it is likely that a climate shift to warmer, drier high latitudes could result in increased forest fire frequency.

Forest fires also contribute to climate change by outputting CO_2 and CH_4 to the atmosphere via combustion of organic material (van der Werf et al. 2009). Carbon output from forest fires was estimated, with high uncertainty, to be between 0.9 and 2.2 Pg C y^{-1} for the 1990s (DeFries et al. 2002; Achard et al. 2004); yet these contributions are difficult to assess simply due to a lack of data with high spatial and temporal resolution (van der Werf et al. 2009). In fact, based on more frequent measurements and higher resolution satellite imagery, van der Werf et al. (2009) determined annual C output from forest fires to be between 70 and 90 Tg C y^{-1}. This accounts for 80–89% of the above-ground living biomass and litter C content within fire-affected areas (van der Werf et al. 2009). Modeling results from van der Werf et al. (2009) indicate that most of the C emissions from Amazonian forest

fires (74%) stem from deforestation activities, with the majority of the remaining emissions resulting from cropland (19%) and pasture (7%) conversion.

Worldwide, total CO_2 emissions from the combustion of vegetative materials equal to just about 50% of anthropogenic fossil-fuel CO_2 emissions (Bowman et al. 2009). As a result, nearly two thirds of the variability in annual CO_2 growth rate during the 1997–2001 El Niño/La Niña period can be explained by biomass burning (van der Werf et al. 2004). Results from van der Werf et al. (2004) further implicate fire-based emissions of CH_4 in nearly all CH_4 anomalies during the 1997–1998 El Niño. The increased radiative forcing from CO_2 produced by deforestation fires alone has been estimated to be as great as 19% since preindustrial times (Bowman et al. 2009). However, long-term positive and negative forcings of CO_2 and CH_4 emissions from natural wildfires are assumed equal and, thus, result in negligible to no global or regional temperature effects (Bowman et al. 2009).

Black carbon aerosols are also produced by fire, which influences climate by changing the surface albedo of burnt landscapes (Bowman et al. 2009). The dark, soot-covered surfaces of burnt landscapes strongly absorb incident solar radiation, producing a secondary warming effect (Bowman et al. 2009). Black carbon is even transmitted in smoke plumes to the troposphere where it has been shown to reduce regional precipitation by inhibiting vertical atmospheric convection and limiting rain cloud formation (Andreae et al. 2004). Depravation of precipitation and increases in regional temperatures can create a positive feedback loop for forest fire, increasing the frequency and geographic extent of burns and their resultant greenhouse gas emissions (Bowman et al. 2009).

30.5 Conclusions and Future Directions

Forest fires are one of the most transformative ecosystem disturbances, producing drastic short- and long-term changes in the physical and chemical properties of soils, which, in turn, affect hydrological and biogeochemical processes. Their increasing global presence makes investigating fire-related alterations critical to our understanding of environmental issues across various scales – from climate change to water quality and sediment transport. While we have a strong body of literature investigating the effects of fire on physical soil/biomass properties and hydrogeomorphology, our understanding is limited by short-term postfire monitoring (1–3 years) and little information regarding alterations at the hydrology–biogeochemistry interface. Future research examining the effects of fire on wooded ecosystems should include:

- Monitoring changes in hydrological and biogeochemical processes for longer periods of time, because the total recovery process in degraded hillslopes and watersheds extends beyond the first few, but dramatic, postfire years to full revegetation
- Determining how far downstream the impacts are transferred, as downstream confluences and even the coastal area may experience postfire alterations

- Reinforcing the call of Levia and Frost (2003), it is suggested that future research seeks to characterize the hydrological and chemical changes in stemflow after fire
- Researching the impact of forest fires on biogeochemical cycling within temperate deciduous forests, as data on burned temperate deciduous hillslopes and/or catchments are (at best) scant
- Investigating changes in pre- and postfire end-member contributions
- The identification of shifts in DOC and DON quality for end members and their relative contributions to stream exports.

References

Achard F, Eva HD, Mayaux P et al (2004) Improved estimates of net carbon emissions from land cover change in the tropics for the 1990s. Glob Biogeochem Cycles 18: doi:10.1029/2003GB002142

Alencar A, Nepstad D, Vera Diaz MC (2006) Forest understory fire in the Brazilian Amazon in ENSO and non-ENSO years: Area burned and committed carbon emissions. Earth Interact 10:1–17

Andreae MO, Rosenfeld D, Artaxo P et al (2004) Smoking rain clouds over the Amazon. Science 303:1337–1342

Bååth E, Frostgård A, Pennanen T et al (1995) Microbial community structure and pH response in relation to soil organic matter quality in wood-ash fertilized, clear-cut or burned coniferous soils. Soil Biol Biochem 27:229–240

Bayley SE, Schindler DW, Beaty KG et al (1992) Effects of multiple fires on nutrient yields from streams draining boreal forest and fen watersheds: nitrogen and phosphorous. Can J Fish Aquat Sci 49:584–596

Bêche LA, Stephens SL, Resh VH (2005) Effects of prescribed fire on a Sierra Nevada (California, USA) stream and its riparian zone. For Ecol Manage 218:37–59

Benavides-Solorio J, MacDonald LH (2001) Post-fire runoff and erosion from simulated rainfall on small plots, Colorado Front Range. Hydrol Process 15:2931–2952

Bernal S, Butturini A, Sabater F (2006) Inferring nitrate sources through end member mixing analysis in an intermittent Mediterranean stream. Biogeochemistry 81:269–289

Betts EF, Jones JB Jr (2009) Impact of wildfire on stream nutrient chemistry and ecosystem metabolism in boreal forest catchments of interior Alaska. Arct Antarct Alp Res 41:407–417

Bosch JM, Hewlett JD (1982) A review of catchment experiments to determine the effect of vegetation changes on water yield and evapotranspiration. J Hydrol 55:3–23

Bowman DMJS, Balch JK, Artaxo P et al (2009) Fire in the earth system. Science 434:481–484

Brais S, David P, Ouimet R (2000) Impacts of wild fire severity and salvage harvesting on the nutrient balance of jack pine and black spruce boreal stands. For Ecol Manage 137:231–243

Burch GJ, Moore ID, Burns J (1989) Soil hydrophobic effects on infiltration and catchment runoff. Hydrol Process 3:211–222

Burns DA, McDonnell JJ, Hooper RP et al (2001) Quantifying contributions to storm runoff through end-member mixing analysis and hydrologic measurements at Panola Mountain Research Watershed (Georgia, USA). Hydrol Process 15:1903–1924

Caldwell C, Canavan C, Bloom N (2000) Potential effects of forest fire and storm flow on total mercury and methylmercury in sediments of an arid-lands reservoir. Sci Total Environ 260:125–133

Cerda A (1998) Changes in overland flow and infiltration after a rangeland fire in a Mediterranean scrubland. Hydrol Process 12:1031–1042

Certini G (2005) Effects of fire on properties of forest soils: a review. Oecologia 143:1–10

Chorover J, Vitousek PM, Everson DA et al (1994) Solution chemistry profiles of mixed-conifer forests before and after fire. Biogeochemistry 26:115–144

Coutant RW, Brown L, Chuang JC et al (1988) Phase distribution and artifact formation in ambient air sampling for polynuclear aromatic hydrocarbons. Atmos Environ 22:403–409

Covington WW, Sackett SS (1992) Soil mineral nitrogen changes following prescribed burning in ponderosa pine. For Ecol Manage 54:175–191

Crutzen PJ, Andreae MO (1990) Biomass burning in the tropics: impact on atmospheric chemistry and biogeochemical cycles. Science 250:1669–1678

DeBano LF (1981) Water repellant soils: A state-of-the-art. USDA Forest Service General Technical Report PS W-46, 21 pp.

DeBano LF (2000a) Water repellency in soils: a historical overview. J Hydrol 231–232:4–32

DeBano LF (2000b) The role of fire and soil heating on water repellency in wildland environments: a review. J Hydrol 231–232:195–206

Dekker LW, Ritsema CJ (1994) How water moves in a water repellent sandy soil 1. Potential and actual water repellency. Water Resour Res 30:2507–2517

DeFries RS, Houghton RA, Hansen MC et al (2002) Carbon emission from tropical deforestation and regrowth based on satellite observations for the 1980s and 1990s. Proc Natl Acad Sci USA 99:14256–14261

DeMarco A, Gentile AE, Arena AA et al (2005) Organic matter, nutrient content, and biological activity in burned and unburned soils of a Mediterranean maquis area of southern Italy. Int J Wildland Fire 14:365–377

Desilets SLE, Nijssen B, Ekwurzel B et al (2007) Post-wildfire changes in suspended sediment rating curves: Sabino Canyon, Arizona. Hydrol Process 21:1413–1423

Dieckmann HH, Motzer H, Harres HP et al (1992) Vegetation and erosion. Investigations on erosion plots in southern Sardinia. Geo-Öko-Plus 3:139–149

Doehring DO (1968) The effect of fire on geomorphic processes in the San Gabriel Mountains, California. In: Parker RB (ed) Contributions to geology. University of Wyoming, Laramie, Wyoming, pp 43–65

Dore S, Kolb TE, Montes-Helu M et al (2010) Carbon and water fluxes from ponderosa pine forests disturbed by wildfire and thinning. Ecol Appl 20:663–683

Dragovich D, Morris R (2002) Fire intensity, slopewash and bio-transfer of sediment in eucalypt forest, Australia. Earth Surf Proc Land 27:1309–1319

Driscoll CT, Otton JK, Iverfeldt A (1994) Trace metals speciation and cycling. In: Moldan B, Cerny J (eds) Biogeochemistry of small catchments. Wiley, Chichester, pp 299–322

Durgin PB, Vogelsang PJ (1984) Dispersion of kaolinite by water extracts of Douglas-fir ash. Can J Soil Sci 64:439–443

Elliott JG, Parker RS (2001) Developing a post-fire flood chronology and recurrence probability from alluvial stratigraphy in the Buffalo Creek watershed, Colorado, USA. Hydrol Process 15:3039–3051

Everett RL, Java-Sharpe BJ, Scherer GR et al (1995) Co-occurrence of hydrophobicity and allelopathy in sand pits under burned slash. Soil Sci Soc Am J 59:1176–1183

Farella N, Lucotte M, Davidson R et al (2006) Mercury release from deforested soils triggered by base cation enrichment. Sci Total Environ 368:19–29

Flannigan MD, Bergeron Y, Engelmark O et al (1998) Future wildfire in circumboreal forests in relation to global warming. J Veg Sci 9:469–476

Flannigan MD, Stocks BJ, Wotton BM (2000) Climate change and forest fires. Sci Total Environ 262:221–229

Fox DM, Darboux F, Carrega P (2007) Effects of fire-induced water repellency on soil aggregate stability, splash erosion, and saturated hydraulic conductivity for different size fraction. Hydrol Process 21:2377–2384

Gabet EJ (2003) Post-fire thin debris flows: sediment transport and numerical modelling. Earth Surf Process Land 28:1341–1348

Gerla PJ, Galloway JM (1998) Water quality of two streams near Yellowstone Park, Wyoming, following the 1988 Clover-Mist wildfire. Environ Geol 36:127–136

Giovannini G, Lucchessi S, Giachetti M (1988) Effects of heating on some physical and chemical parameters related to soil aggregation and erodibility. Soil Sci 146:255–261

Giovannini G, Lucchessi S (1991) Is the vegetation cover the primary factor controlling erosion in burnt soils? In: Sala M, Rubio JL (eds.) Proceedings ESSC conference on soil erosion and degradation as a consequence of forest fire, Sept. 1991, Barcelona and Valencia, Spain, p 16

González-Pérez JA, González-Vila FJ, Almendros G et al (2004) The effect of fire on soil organic matter – a review. Environ Int 30:855–870

Grogan P, Burns TD, Chapin FS III (2000) Fire effects on ecosystem nitrogen cycling in a California bishop pine forest. Oecologia 122:537–544

Harpold AA, Lyon SW, Troch PA et al (2010) The hydrological effects of lateral preferential flow paths in a glaciated watershed in the northeastern USA. Vadose Zone J 9:397–414

Henderson GS, Golding DL (1983) The effect of slash burning on the water repellence of forest soils at Vancouver, British Columbia. Can J For Res 13:353–355

Huffman EL, MacDonald LH, Stednick JD (2001) Strength and persistence of fire-induced soil hydrophobicity under ponderosa and lodgepole pine, Colorado Front Range. Hydrol Process 15:2877–2892

Ilstedt U, Giesler R, Nordgren A et al (2003) Changes in soil chemical and microbial properties after a wildire in a tropical rainforest in Sabar, Malaysia. Soil Biol Biochem 35:1071–1078

Imai A, Matsushige K, Nagai T (2003) Trihalomethane formation potential of dissolved organic matter in a shallow eutrophic lake. Water Res 37:4284–4294

Imeson AC, Verstraten JM, van Mulligen EJ et al (1992) The effects of fire and water repellence on infiltration and runoff under Mediterranean forest type. Catena 19:345–361

Inamdar SP, Mitchell MJ (2006) Hydrologic and topographic controls on the storm-event exports of dissolved organic carbon (DOC) and nitrate across catchment scales. Water Resour Res 42: doi:10.1029/2005WR004212

Inbar M, Tamir M, Wittenberg L (1998) Runoff and erosion processes after a forest fire in Mount Carmel, a Mediterranean area. Geomorphology 24:17–33

IPCC (Intergovernmental Panel on Climate Change) (1996) Climate change 1995 impacts, adaptations and mitigation of climate change: scientific-technical analyses. Cambridge University Press, Cambridge, p 878

Isidorov V, Jdanova M (2002) Volatile organic compounds from leaves litter. Chemosphere 48:975–979

Johansen MP, Hankonson TE, Breshears DD (2001) Post-fire runoff and erosion from rainfall simulation: contrasting forests with shrublands and grasslands. Hydrol Process 15:2953–2965

Jung HY, Hogue TS, Rademacher LK et al (2009) Impact of wildfire on source water contributions in Devil Creek, CA: evidence from end-member mixing analysis. Hydrol Process 23:183–200

Kara O, Bolat I (2009) Short-term effects of wildfire on microbial biomass and abundance in black pine plantation soils in Turkey. Ecol Indic 9:1151–1155

Katsuyama M, Ohte N, Kobashi S (2001) A three-component endmember analysis of streamwater hydrochemistry in a small Japanese forested headwater catchment. Hydrol Process 15:249–260

Keller EA, Valentine DW, Gibbs DR (1997) Hydrological response of small watersheds following the southern California painted cave fire of June 1990. Hydrol Process 11:401–414

Ketterings QM, Bingham JM, Laperche V (2000) Changes in soil mineralogy and texture caused by slash-and-burn fires in Sumatra, Indonesia. Soil Sci Am J 64:1108–1117

Kim EJ, Oh JE, Chang YS (2003) Effects of forest fire on the level and distribution of PCDD/Fs and PAHs in soil. Sci Total Environ 311:177–189

Knicker H, Lüdemann H-D (1995) N-15 and C-13 CPMAS and solution NMR studies of N-15 enriched plant material during 600 days of microbial degradation. Org Geochem 23: 329–341

Knicker H (2007) How does fire affect the nature and stability of soil organic nitrogen and carbon? A review. Biogeochemistry 85:91–118

Korom SF (1992) Natural denitrification in the saturated zone: a review. Water Resour Res 28:1657–1668

Kunze MD, Stednick JD (2006) Streamflow and suspended sediment yield following the 200 Bobcat fire, Colorado. Hydrol Process 20:1661–1681

Kusaka S, Nakane K, Mitsudera M (1983) Effects of fire on water and major nutrient budgets in forest ecosystems 1. water balance. Jap J Ecol 33:323–332

Lane PNJ, Sheridan GJ, Noske PJ et al (2008) Phosphorus and nitrogen exports from SE Australian forests following wildfire. J Hydrol 361:186–198

Lane PNJ, Sheridan GJ, Noske PJ et al (2006) Changes in sediment loads and discharge from small mountain catchments following wildfire in south eastern Australia. J Hydrol 331:495–510

Legleiter CJ, Lawrence RL, Fonstad MA et al (2003) Fluvial response a decade after wildfire in the northern Yellowstone ecosystem: a spatially explicit analysis. Geomorphology 54:119–136

Leighton-Boyce G, Doerr SH, Shakesby RA et al (2007) Quantifying the impact of soil water repellency on overland flow generation and erosion: a new approach using rainfall simulation and wetting agent on in situ soil. Hydrol Process 21:2337–2345

Letey J, Carillo MLK, Pang XP (2000) Review: approaches to characterize the degree of water repellency. J Hydrol 231–232:61–65

Levia DF, Frost EE (2003) A review and evaluation of stemflow literature in the hydrologic and biogeochemical cycles of forested and agricultural ecosystems. J Hydrol 274:1–29

Lewis SA, Wu JQ, Robichaud PR (2006) Assessing burn severity and comparing soil water repellency, Hayman Fire, Colorado. Hydrol Process 20:1–16

Lovely DR, Fraga JL, Coates JD et al (1999) Humics as an electron donor for anaerobic respiration. Environ Microbiol 1:89–98

Malmer A (2004) Streamwater quality as affected by wild fires in natural and manmade vegetation in Malaysian Borneo. Hydrol Process 18:853–864

Marschner H (1995) Mineral nutrition of higher plants. Academic Press, San Diego, CA, USA, p 889

Martin DA, Moody JA (2001) Comparison of soil infiltration rates in burned and unburned mountainous watersheds. Hydrol Process 15:2893–2903

Mast MA, Clow DW (2008) Effects of 2003 wildfires on stream chemistry in Glacier National Park, Montana. Hydrol Process 22:5013–5023

Mataix-Solera J, Doerr SH (2004) Hydrophobicity and aggregate stability in calcareous topsoils from fire-affected pine forests in southeastern Spain. Geoderma 118:77–88

McNabb DH, Swanson FJ (1990) Effects of fire on soil erosion. In: Walstad JD, Radosevich SR, Sandberg DV (eds) Natural and prescribed fire in Pacific Northwest Forest, Oregon State University Press. Corvallis, OR, USA, pp 159–176

Mermut AR, Luk SH, Romkens MJM et al (1997) Soil loss by splash and wash during rainfall from two loess soils. Geoderma 75:203–214

Meyer GA, Wells SG (1997) Fire-related sedimentation events on alluvial fans, Yellowstone National Park, USA. J Sediment Res 67:776–791

Mladenov N, Huntsman-Mapila P, Wolski P et al (2008) Dissolved organic matter accumulations, reactivity, and redox state in ground water of a recharge wetland. Wetlands 28:747–759

Mohamed MAA, Terao H, Suzuki R et al (2003) Natural denitrification in the Kakamingahara groundwater basin, Gifu prefecture, central Japan. Sci Total Environ 307:191–201

Montes-Helu MC, Kolb T, Dore S et al (2009) Persistent effects of fire-induced vegetation change on energy partitioning and evapotranspiration in ponderosa pine forersts. Agric For Meteorol 149:491–500

Moody JA, Martin DA (2001) Post-fire, rainfall intensity- peak discharge relations for three mountainous watersheds in the western USA. Hydrol Process 15:2981–2993

Moody JA, Martin DA, Haire SL et al (2008) Linking runoff response to burn severity after a wildfire. Hydrol Process 22:2063–2074

Moldan B, Cerny J (1994) Biogeochemistry of small catchments. Wiley, Chichester

Mroz GD, Jurgensen MF, Harvey AE et al (1980) Effects of fire on nitrogen in forest floor horizons. Soil Sci Soc Am J 44:395–400

Nagahama N, Onodera S, Kobayashi M et al (2001) Experimental study of the estimation of the infiltration process in water repellent soil, using the electrical exploration. J Jap Soc Hydrol Water Resour 14:27–33

Neary DG, Klopatek CC, DeBano LF et al (1999) Fire effects on belowground sustainability: a review and synthesis. For Ecol Manage 122:51–71

Nestrick TJ, Lamparski LL (1982) Isomer-specific determination of chlorinated dioxins for assessment of formation and potential environmental emission from wood combustion. Anal Chem 54:2292–2299

Nishimune N, Onodera S, Naruoka T et al (2003) Comparative study of bedload sediment yield processes in small mountainous catchments covered by secondary and disturbed forests, western Japan. Hydrobiologia 494:265–270

Noske PJ, Lane PNJ, Sheridan GJ (2010) Stream exports of coarse matter and phosphorus following wildfire in NE Victoria, Australia. Hydrol Process 24:1514–1529

O'Donnell JA, Turetsky MR, Harden JW et al (2009) Interactive effects of fire, soil climate, and moss on CO_2. Ecosystems 12:57–72

Onodera S, Fujisaki C, Naruoka T et al (2002) Metal ion variations from rainfall to stream in a small catchment covered by degraded soil in the Setouchi Rigion. Jap J Limnol 63:21–30

Oswald BP, Davenport D, Neuenschwander LF (1999) Effects of slash pile burning on the physical and chemical soil properties of Vassar soils. J Sustainable For 8:75–86

Overpeck JT, Rind D, Goldberg R (1990) Climate-induced changes in forest disturbance and vegetation. Nature 343:51–53

Pardini G, Gisprt M, Dunjo G (2004) Relative influence of wildfire on soil properties and erosion processes in different Mediterranean environments in NE Spain. Sci Total Environ 328:237–246

Peres CA, Barlow J, Laurance WF (2006) Detecting anthropogenic disturbance in tropical forests. Trends Ecol Evol 21:227–229

Petrone KC, Hinzman LD, Shibata H et al (2007) The influence of fire and permafrost on sub-arctic stream chemistry during storms. Hydrol Process 21:423–434

Ponomarenko EV, Anderson DW (2001) Importance of charred organic matter in black Chernozern soils of Saskatchewan. Can J Soil Sci 81:285–297

Price C, Rind D (1994) The impact of a $2 \times CO_2$ climate on lightning-caused fires. J Clim 7:1484–1494

Prieto-Fernandez A, Villar MC, Carballas M et al (1993) Short-term effects of a wildfire on the nitrogen status and its mineralization kinetics in an Atlantic forest soil. Soil Biol Biochem 25:1657–1664

Prosser IP, Williams L (1998) The effect of wildfire on runoff and erosion in native Eucalyptus forest. Hydrol Process 12:251–265

Ramirez KS, Lauber CL, Fierer N (2010) Microbial consumption and production of volatile organic compounds at the soil-litter interface. Biogeochemistry 99:97–107

Ritsema CJ, Dekker LW (1994) How water moves in a water repellent sandy soil 2. Dynamics of fingered flow. Water Resour Res 30:2519–2531

Robichaud PR (2000) Fire effects on infiltration rates after prescribed fire in northern Rocky Mountain forests, USA. J Hydrol 231–232:220–229

Roy DP, Boschetti L, Justice CO et al (2008) The collection 5 MODIS burned area product – Global evaluation by comparison with the MODIS active fire product. Remote Sens Environ 112:3690–3707

Scott DF (1997) The contrasting effects of wildfire and clearfelling on the hydrology of a small catchment. Hydrol Process 11:543–555

Shakesby RA, Doerr SH (2006) Wildfire as a hydrological and geomorphological agent. Earth-Science Rev 74:269–307

Shakesby RA, Doerr SH, Walsh RPD (2000) The erosional impact of soil hydrophobicity: current problems and future research directions. J Hydrol 231–232:178–191

Siegert F, Ruecker G, Hinrichs A et al (2001) Increased damage from fires in logged forests during droughts caused by El Nino. Nature 414:437–440

Simard DG, Fryles JW, Paré D et al (2001) Impacts of clearcut harvesting and wildfire on soil nutrient status in the Quebec boreal forest. Can J Soil Sci 81:229–237

Spigel KM, Robichaud PR (2007) First-year post-fire erosion rates in Bitterroot National Forest, Montana. Hydrol Process 21:998–1005

Stock WD, Pate JS, Delfs J (1990) Influence of seed size and quality on seedling development under low nutrient concentrations in five Australian and South African members of Proteaceae. J Ecol 78:1005–1020

Stocks BJ, Fosberg MA, Lynham TJ et al (1998) Climate change and forest fire potential in Russian and Canadian boreal forests. Clim Change 38:1–13

Tackle ES, Bramer DJ, Heilman WE et al (1994) A synoptic climatology for forest fires in the NE US and future implications from GCM simulations. Intl J Wildland Fire 4:217–224

Terry JP, Shakesby RA (1993) Soil water repellency effects on rainsplash: simulated rainfall and photographic evidence. Earth Surf Process Land 18:519–525

Thomas AD, Walsh RPD, Shakesby RA (2000) Solutes in overland flow following fire in eucalyptus and pine forests, northern Portugal. Hydrol Process 14:971–985

UN-FAO (Food and Agricultural Organization of the United Nations) (2000) FAO Pesticide disposal series 8: Assessing soil contamination (reference manual). Rome, Italy. http://www.fao.org/docrep/003/x2570e/X2570E00.htm#TOC

van der Werf GR, Morton DC, DeFries RS et al (2009) Estimates of fire emissions from an active deforestation region in the southern Amazon based on satellite data and biogeochemical modeling. Biogeosciences 6:235–249

van der Werf GR, Randerson JT, Collatz GJ et al (2004) Continental-scale partitioning of fire emissions during the 1997 to 2001 el Nino/la Nina period. Science 303:73–76

Varela ME, Benito E, de Blas E (2005) Impact of wildfires on surface water repellency in soils of northwest Spain. Hydrol Process 19:3649–3657

Vila-Escalé M, Vegas-Vilarrúbia T, Prat N (2007) Release of polycyclic aromatic compounds into a Mediterranean creek (Catalonia, NE Spain) after a forest fire. Water Res 41:2171–2179

Vilariño A, Arines J (1991) Numbers and viability of veicular-arbuscular fungal propoagules in field soil samples after wildfire. Soil Biol Biochem 23:1083–1087

Wang Z, Wu QJ, Dekker LW et al (2000) Effects of soil water repellency on infiltration rate and flow instability. J Hydrol 231–232:265–276

Weber MG, Flannigan MD (1997) Canadian boreal forest ecosystem stricter and function in a changing climate: impact on fire regimes. Environ Rev 5:145–166

Wells WG, Wohlgemuth PM, Campbell AG (1987) Post-fire sediment movement by debris flows in the Santa Ynez Mountains, California. In: Erosion and sedimentation in the Pacific Rim, IAHS Press No 165. Institute of Hydrology, Wallingford, UK, pp 275–276

Westerling AL, Hidargo HG, Cayan DR et al (2006) Warming and earlier spring increase western U.S. forest wildfire activity. Science 313:940–943

White WD, Wells SG (1979) Forest fire devegetation and drainage basin adjustments in mountainous terrain. In: Rhodes RD, Williams GP (eds) Adjustments to fluvial systems. Kendall/Hunt Publishers, Dubuque, IA, pp 199–223

White WD, Wells SG (1982) Forest-fire devegetation and drainage basin adjustments in mountainous terrain. In: Rhodes RD, Williams GP (eds) Adjustments of the Fluvial system. Proceedings of the 10th Geomorphology Symposium. Binghamton. Allen and Unwin, New York, pp 199–223

Williams MR, Melack PJ (1997) Effects of prescribed burning and drought on the solute chemistry of mixed-conifer forest streams of the Sierra Nevada, California. Biogeochemistry 389:225–253

Williams MR, Fisher TR, Melack JM (1997) Solute dynamics in soil water and groundwater in a central Amazon catchment undergoing deforestation. Biogeochemistry 38:303–335

Woodsmith RD, Vache KB, McDonnell JJ et al (2004) Entiat experimental forest: before and after a 1970 wildfire. Water Resour Res 40: doi:10.1029/2004WR003296

Worrall F, Armstrong A, Adamson JK (2007) The effects of burning and sheep-grazing on water table depth and soil water quality in a upland peat. J Hydrol 339:1–14

Worrall F, Burt T, Adamson J (2003) Controls on the chemistry of runoff from an upland peat catchment. Hydrol Process 17:2063–2083

Wunderli S, Zennegg M, Dolezal IS et al (1996) Ph levels and congener pattern of PCDD/PCDF in fly and bottom ash from waste wood and natural wood burned in small to medium sized wood firing facilities in Switzerland. Organohalogen Compounds 27:231–236

Xue W, Warshawsky D (2005) Metabolic activation of polycyclic and heterocyclic aromatic hydrocarbons and DNA damage: a review. Toxicol Appl Pharmacol 206:73–93

Chapter 31
The Effects of Ice Storms on the Hydrology and Biogeochemistry of Forests*

Benjamin Z. Houlton and Charles T. Driscoll

31.1 Introduction

A critical challenge of biogeochemical research is to distinguish between the effects of natural and anthropogenic disturbances on nutrient cycles. Natural agents of disturbance – particularly wind and ice storms, insect defoliation episodes, and fire – are stochastic and highly variable; hence, it is difficult to develop broad generalizations about the effects of such exogenous perturbations on ecosystem pattern and process (Waring and Schlesinger 1985). Nonetheless, examples of disturbance effects are apparent (Lemon 1961; Mattson and Addy 1975; Bormann and Likens 1979a; Whitney and Johnson 1984; Bruederle and Stearns 1985), pointing to their importance in the regulation of biogeochemical cycles in general, nitrogen (N) cycles in particular (Swank et al. 1981; Likens and Bormann 1995; Mitchell et al. 1996; Eshleman et al. 1998). Here, we review the impact of ice storms on N cycling in forest ecosystems, also reviewing (and comparing) disturbance effects on N cycling more generally.

Ice storms occur frequently in temperate climates. They form along a narrow band on the cold side of a warm front, where surface temperatures are at or just below freezing (ca. $1°C$); under these conditions, rain becomes super-cooled and freezes upon impact with cold surfaces. This process, in turn, causes ice to accumulate on forest canopies, often resulting in forest damage, tree mortality and changes in structure and succession of land plant communities (Lemon 1961; Whitney and Johnson 1984; Bruederle and Stearns 1985; Rebertus et al. 1997; Warrillow and Mou 1999). Although little is known about their impacts on biogeochemical cycles, there is reason to believe that ice storms can have important effects on the N cycle. Nitrogen is a limiting nutrient in many terrestrial ecosystems; its cycling and availability is tightly regulated by plant–soil–microbe interactions. Following disturbance, this close coupling is disrupted, temporarily increasing N availability and nitrate (NO_3^-) leaching from ecosystems: transiently high rates of N cycling are frequently observed in response to forest harvesting and experimental trenching of stands (Bormann and Likens 1979b; Vitousek et al. 1982).

*Some parts of this chapter are drawn from Houlton et al. (2003) and reused here with permission by Springer.

In January of 1998, a large ice storm affected much of the northeastern United States. Following the storm, forest crown damage was substantial, with areas of 100% canopy loss reported in watersheds in New England (Houlton et al. 2003). In this chapter, we synthesize effects of the 1998 ice storm on forest N cycles in temperate forest ecosystems. We postulated that this disturbance would result in changes to the N cycle similar to those associated with other types of natural disturbances and forest harvesting practices; hence, we review N cycling responses from a variety of agents of disturbance in this chapter as well. We report that a common thread of forest responses to both natural and anthropogenic disturbance is seen in accelerated rates of N cycling and losses, with land use history also playing a vital role in shaping the magnitude and pattern of N export from temperate forests.

31.2   Study Sites in Review Synthesis of Ice Storm Impacts on N Cycling

We summarized N cycling responses of several forest ecosystems to the 1998 ice storm. The Hubbard Brook Experimental Forest (HBEF) is a long-term ecological research site located in the White Mountains of New Hampshire (43°56′N, 71°45′W). Mean annual precipitation at the HBEF is 140 cm, with 25–33% occurring as snow (Federer et al. 1990). Mean temperature varies between 17°C in July and 10°C in January. Soils at the HBEF are mainly well drained, coarse-loamy, mixed frigid Typic Haplorthods developed in shallow glacial till overlying metamorphosed sedimentary and igneous rocks. Organic (Oa, Oe, Oi) and mineral (Bh, Bs, Bs2) soil horizons have a combined average depth of 0.6 m, but this soil depth is highly variable within the experimental watersheds and generally decreases with elevation (Lawrence et al. 1986). The vegetation in W1 and W6 consists of mixed northern hardwood species – yellow birch (*Betula alleghaniensis*), American Beech (*Fagus grandifolia*), and sugar maple (*Acer saccharum*) – at the middle and lower elevations, and stands of conifers – balsam fir (*Abies balsamea*) and red spruce (*Picea rubens*) at upper elevations.

The 607-ha Bowl Natural Area (BNA) is located on the southern slopes of the White Mountains. The valley is bisected by a central ridge (north–south) that rises to an elevation of 1,000 m; this central ridge divides the valley into two major watersheds: the East and West Branches. The 206-ha area located west of the West Branch stream to the top of the ridge connecting Mt. Whiteface with Mt. Passconaway, has been reserved for research by the USDA Forest Service (Lyon and Bormann 1962). Several surveys of the vegetation in the reserved area indicate that this part of the forest has developed with no evidence of logging, agriculture, or extensive fire disturbance (Oosting and Billings 1951). Although much of the East Branch watershed was logged in the 1880s (Harkness 1958), there is no record of the period of logging or the amount of lumber sawed or firewood cut (Martin 1977).

The Bowl is dominated by sugar maple (*A. saccharum*), yellow birch (*B. alleghaniensis*), and beech (*F. grandifolia*) at elevations below 850 m, with balsam fir (*A. balsamea*), red spruce (*P. rubens*), and paper birch (*Betula papyrifera*) at elevations above 850 m.

The BNA is characterized by steep slopes that average 32% but range up to 75% with a total relief of 660 m. The bedrock at the BNA is primarily Passaconaway syenite. Smaller areas near the base of the watershed are underlain by Conway granite. Both of these rocks crystallized from magma emplaced during the Jurassic Period as part of the White Mountains batholith. Exposures of bedrock are frequent along the upper slopes and ridgeline, but they are rare on lower slopes and along the brooks due to relatively thick deposits of glacial till. The dominant soil type under the northern hardwood forest is a Typic Haplorthod in the frigid temperature regime. Textures range from sandy loam to loamy sand, with forest floor depths averaging 10 cm. These soils are acidic (pH 3.5–5.5), well drained and have cation exchange primarily associated with the organic horizon because of low clay content (Martin 1979).

Three small watersheds were surveyed on Tenney Mountain (Grafton County, Newfound Lake quadrangle 6, 71°46′W 43°45′N) located about 25 km southwest of the HBEF. The forests on all three watersheds were dominated by maple-beech-birch forest, with no evidence of agricultural activity. Elevations ranged from 440 to 700 m and slope aspects from ESE to ENE. Second-order streams were sampled draining catchments that ranged in size from about 40 to 70 ha. Two small watersheds were also surveyed on the north slope of Plymouth Mountain (Grafton County, Ashland quadrangle, 71°43′W 43°42′N) located about 5 km southeast of Tenney Mountain. Forest composition was similar to the Tenney Mtn. sites, and no evidence of previous agricultural activity was observed. Elevations range from 290 to 670 m and slope aspects were generally NE. Second-order streams draining catchments were sampled, ranging in watershed area from about 50 to 60 ha.

Three small watersheds with evidence of previous agricultural activity were also sampled as a part of this survey. In particular, pit-and-mound topography was largely absent, and stonewalls were evident across the landscape. The catchment sampled on Pike Hill (Ashland quadrangle, 71°44′W 43°44′N) was directly adjacent to those on Plymouth Mountain. This site ranges in elevation from 260 to 480 m, with an ENE slope aspect. The forest at Pike Hill is dominated by maple, ash and birch, and catchment area was about 30 ha. The catchment on Bridgewater Mountain (Ashland quadrangle, 71°41′W 43°40′N) was about 4 km SSE from Plymouth Mtn., ranged in elevation from 365 to 500 m with ESE slope aspect. The post-agricultural forest on Bridgewater Mtn. was dominated by red maple (*Acer rubrum*) and red oak (*Quercus rubra*), and the catchment area was about 12 ha. Finally, the sample site on Jewell Hill (Newfound Lake quadrangle; 71°51′W 43°44′N) is about 5 km WSW of Tenney Mountain. The watershed ranged in elevation from 335 to 580 m, slope aspect was east and catchment area is about 75 ha. The forest on Jewell Hill was not surveyed quantitatively, but qualitative observations indicated that ice damage was similar to the other severely damaged sample sites.

Six reference watersheds in the same general area as the severely damaged forests were sampled under the assumption that changes in stream chemistry unrelated to the ice storm damage were not occurring. These six watersheds were all located within a few kilometers of the damaged sites, but on west-facing slopes that were not subjected to heavy ice accumulation. Visual inspections indicated minimal ice damage in these reference watersheds, and none appeared to have evidence of previous agricultural history. These catchments ranged in elevation from 290 to 700 m.

31.3 Effects of Ice Storms on Forest Hydrology and Biogeochemistry

31.3.1 Hydrologic Response

Precipitation and streamflow have been monitored in W1 at the HBEF since 1955. Annual stream discharge increases with increasing precipitation (Fig. 31.1). Annual evapotranspiration is calculated as the difference between annual precipitation and streamflow (Likens and Bormann 1995). In the water year following the ice storm (1998–1999), the quantity of precipitation was 1,402 mm and streamflow was 994 mm. (Fig. 31.1). Stream discharge was slightly higher than expected based on the long-term pattern of water yield from these watersheds (Likens and Bormann 1995), but was still within one standard deviation of the historical hydrologic average. Therefore, it does not appear that the ice storm disturbance had measurable short-term effects on hydrology at the HBEF.

31.3.2 Response of Soil Solution Chemistry to the Ice Storm

The biogeochemical effects of the ice storm disturbance were most apparent in changes in patterns of NO_3^- loss to drainage waters. Prior to the disturbance, soil water concentrations of NO_3^- in Oa horizon leachates averaged 23 ± 16 µmol L^{-1} (mean $\pm$ standard deviation) and, in mineral soil solutions averaged 20 ± 9 µmol L^{-1} for the Bh horizon and 18 ± 12 µmol L^{-1} for the Bs horizon across W1. Generally, NO_3^- concentrations in W1 soil water were lowest during the growing season, increased following leaf abscission, and peaked during snow melt.

There was no change in leachate chemistry immediately following the ice storm (Fig. 31.2); the first evidence of a biogeochemical response was an increase in NO_3^- concentrations in Oa horizon leachates in August 1998 (Fig. 31.2). Nitrate concentrations for Oa (490 µmol L^{-1}) and Bh (500 µmol L^{-1}) horizon solutions peaked in September 1998, while concentrations in Bs horizon (300 µmol L^{-1})
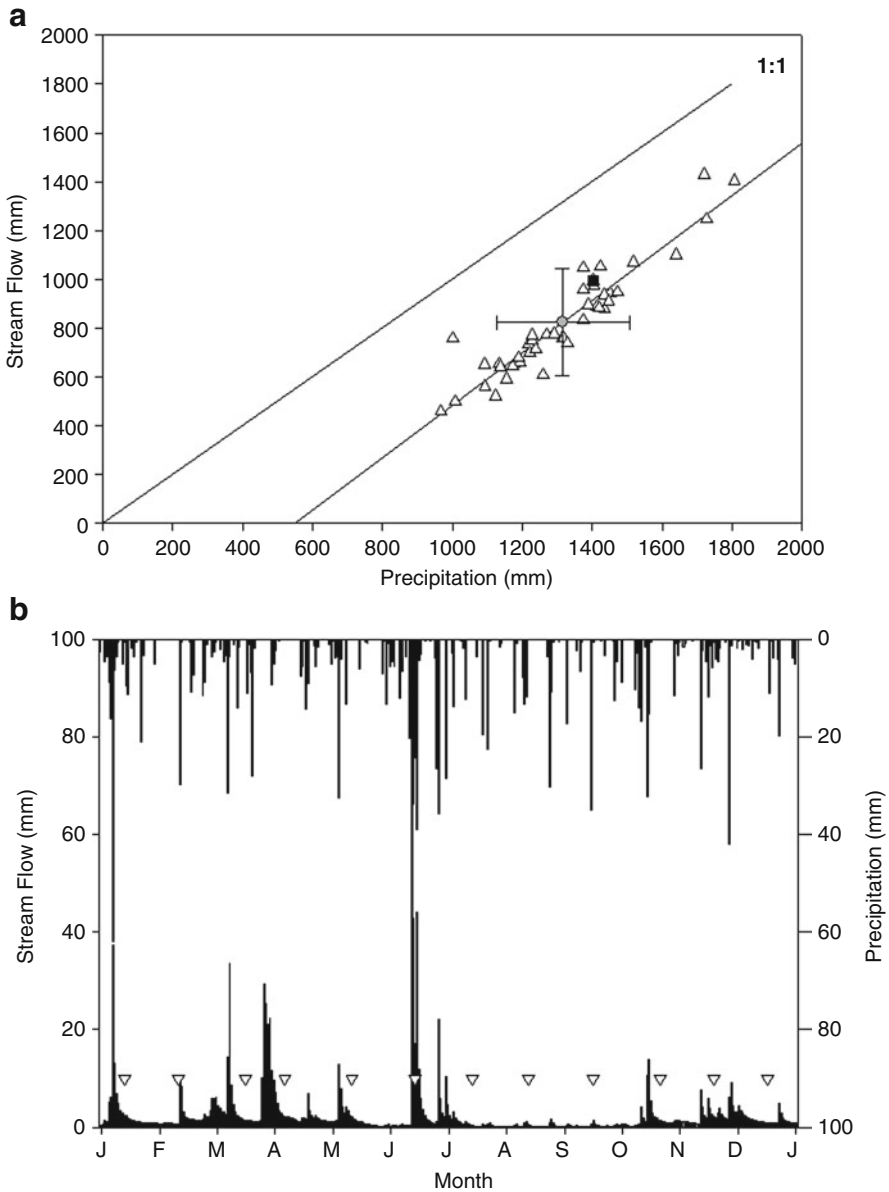
Fig. 31.1 Hydrologic data for W1 at the Hubbard Brook Experimental Forest. (**a**) Relationship between streamflow and precipitation. Water years prior to (*white triangle*) and following the ice storm (1998–1999; *black square*) are shown. The *gray square* represents the average of all years other than 1998–1999 water-year. *Error bars* reflect one unit of standard deviation. (**b**) Temporal pattern of precipitation and streamflow for W1 for 1998–1999. Sampling dates for stream water chemistry are indicated by the *white triangles*
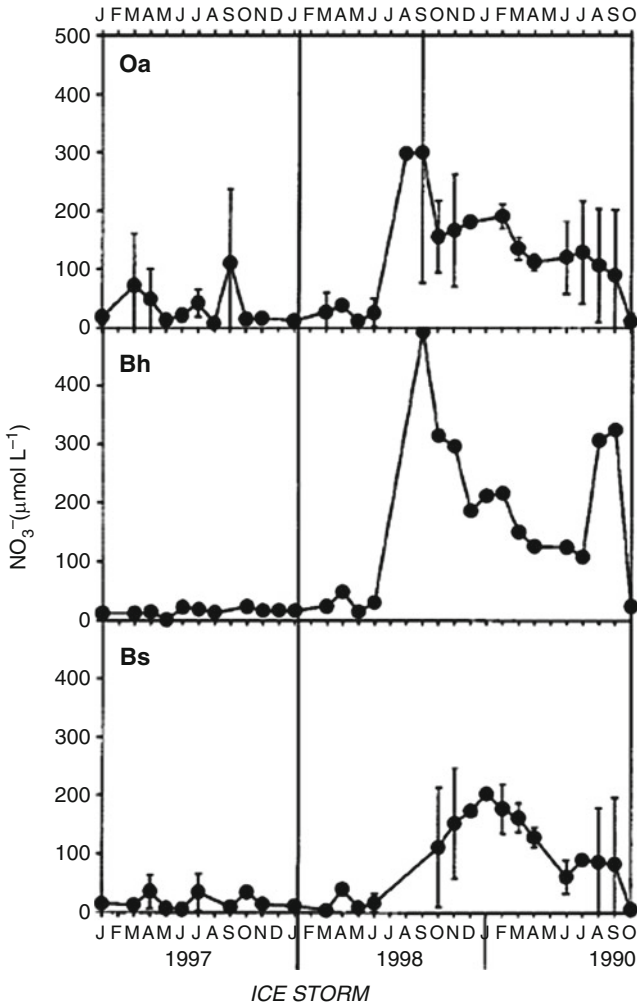
Fig. 31.2 Temporal patterns of soil-solution nitrate concentrations collected from ice-damaged areas in W1 at the Hubbard Brook Experimental Forest. The *error bars* represent one unit of standard deviation (from Houlton et al. 2003)

leachates peaked somewhat later (November 1998; Fig. 31.2). Following this initial response, soil water NO_3^- concentrations remained relatively constant at elevated levels (ca. seven to ten times higher than pre-disturbance) through the winter and spring (Fig. 31.2). The following summer, NO_3^- concentrations increased again with Oa horizon leachates (200 $\mu mol\ L^{-1}$) peaking in July and Bh (300 $\mu mol\ L^{-1}$) and Bs (190 $\mu mol\ L^{-1}$) solutions in September (Fig. 31.2).

In addition to the temporal patterns, distinct spatial patterns of drainage water chemistry following the ice storm were evident in W1 watershed. Prior to the disturbance, there was no distinct spatial pattern for soil water NO_3^- concentrations
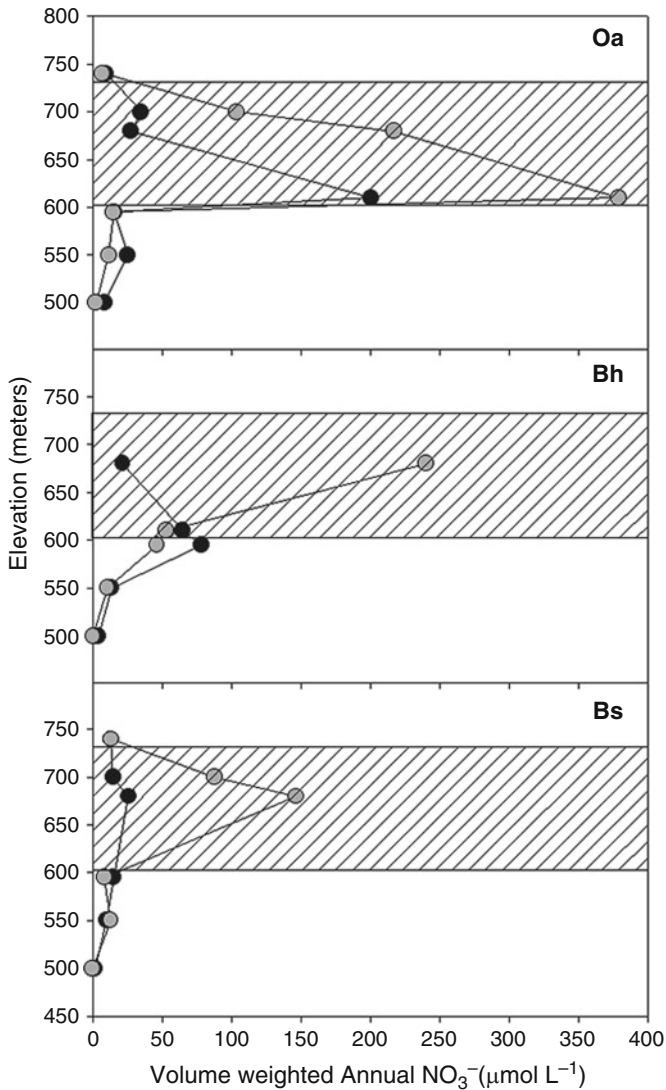
Fig. 31.3 Annual volume-weighted nitrate concentrations in soil waters collected from watershed 1 during 1997–1998 and 1998–1999. The shaded regions represent the approximate location of the extensive crown damage zone (from Houlton et al. 2003)

in W1 (Fig. 31.3). However, the post-disturbance mean NO_3^- concentrations in solutions draining the extensive crown damage zone were significantly higher than the pre-disturbance values (Fig. 31.3). The relatively large standard deviations for NO_3^- concentration means of soil water collected in the disturbance area reflect marked temporal variability (Fig. 31.2). In contrast, soil waters collected outside

the extensive crown damage zone after the ice storm were similar to values prior to the disturbance.

Following the ice storm, there were no significant differences in concentrations or fluxes of ammonium (NH_4^+), dissolved organic nitrogen (DON), and dissolved organic carbon (DOC) in soil waters draining the zone of extensive crown damage with reference to nonimpacted areas in W1 and W6 (data not shown).

31.3.3   Response of Stream Water Chemistry at the HBEF

Stream water chemistry draining W1 and W6 also showed a response to the ice storm in the autumn 1998. Pre-disturbance NO_3^- concentrations in stream water were relatively low along the entire sample reach (Fig. 31.4). In the autumn following the ice storm (September), stream water NO_3^- concentrations increased initially and peaked (150 μmol L^{-1}) at 670 m (Fig. 31.4). Following this initial response, NO_3^- concentrations along the longitudinal stream gradient increased at 610 m, 595 m, and 540 m in September, and at the base of the watershed (495 m, located at the weir) in October (Fig. 31.4). Decreases in NO_3^- concentrations were observed during the high flow period of April and May along the entire stream, but remained elevated at all sites for the duration of this study except for site at the weir, which returned to pre-disturbance levels in May 1999 (Fig. 31.4). This seasonal pattern is in contrast to the pre-disturbance condition in which NO_3^- concentrations generally increased during the high flow conditions in the spring.

Similar to the soil water response in the disturbance area, distinct spatial patterns of NO_3^- losses were evident in stream water following the perturbation (Fig. 31.4). Prior to the ice storm, NO_3^- concentrations were generally uniform along the longitudinal stream gradient. Following the ice storm, NO_3^- concentrations were substantially elevated with reference to pre-disturbance values along the entire stream reach, and showed a general pattern of decreases in concentration with decreasing elevation (Fig. 31.4). Long-term mass fluxes of NO_3^- varied along the stream reach, with the largest values evident at the mid-elevation (110 ± 49 mol ha^{-1} y^{-1}). Nitrate fluxes for the severe crown damage zone increased by as much as a factor of eight in the water-year following the ice storm, and displayed a general pattern of decreasing flux with decreasing elevation (Houlton et al. 2003).

31.3.4   Region-wide Response of Stream Water Chemistry to the Ice Storm

Following the ice storm, a series of streams draining watersheds of various levels of crown damage were surveyed to assess the regional patterns of NO_3^- response (see Houlton et al. 2003 for details). In concordance with results for the HBEF,
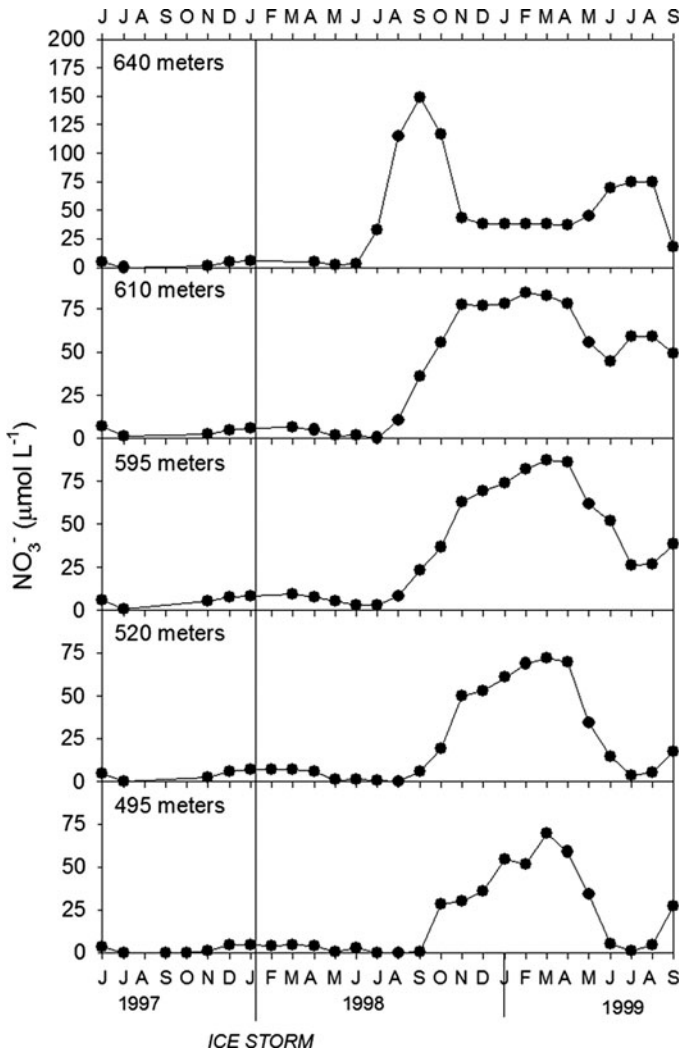
Fig. 31.4 Volume-weighted monthly nitrate concentrations along a longitudinal streamwater gradient in W1 at the Hubbard Brook Experimental Forest (from Houlton et al. 2003)

streams that drained disturbed watersheds at Tenney and Plymouth Mountains showed an initial increase in NO_3^- concentrations during the autumn after the ice storm (Fig. 31.5). Stream NO_3^- concentrations for catchments at Plymouth Mountain peaked in October 1998 (95 ± 35 µmol L^{-1}) and again in January 1999 (80 ± 10 µmol L^{-1}), decreased during spring snowmelt and remained slightly elevated with reference to nonimpacted watersheds (reference) through the spring of 2000. Similarly, NO_3^- concentrations in waters that drained ice storm impacted catchments on Tenney Mountain peaked in January 1999 (150 ± 115 µmol L^{-1}),
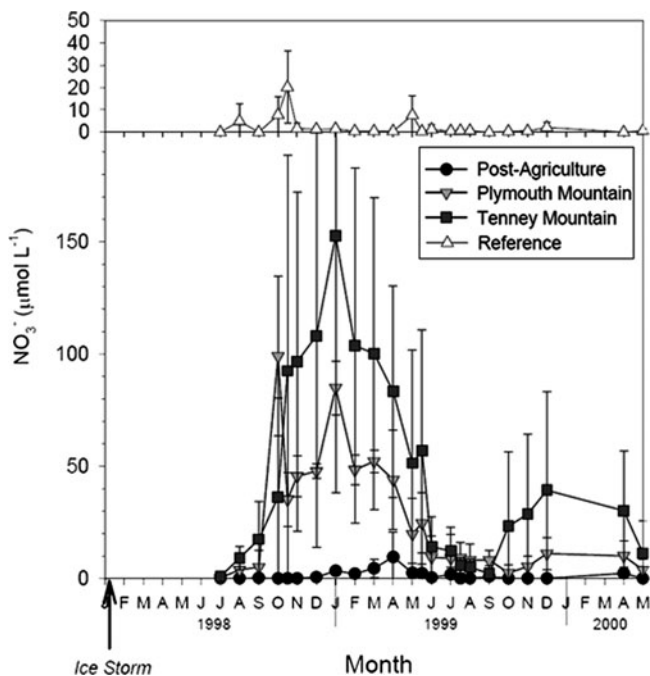
Fig. 31.5 Nitrate concentrations in streams draining watersheds that experienced forest crown damage at Tenney Mountain, Plymouth Mountain, Bridgewater Mountain, Pike Hill, Jewell Hill, and the Bowl Nature Area, and for nonimpacted watersheds (reference) in the Bowl Nature Area and across the southern White Mountain region of New Hampshire (from Houlton et al. 2003)

decreased approaching reference levels during the period of spring snowmelt through the summer growing season, and increased once again during the period of vegetative dormancy. Despite experiencing crown damage comparable to forests at Tenney and Plymouth Mountains, streams that drained secondary forests that were previously in agriculture showed relatively low concentrations of NO_3^- throughout the study period (Fig. 31.5). Note that streams that were previously in agriculture exhibited NO_3^- concentrations similar to values in reference (i.e., undisturbed) watersheds.

Prior to the ice storm, NO_3^- concentrations in stream water draining the lower watershed of the BNA (mature forest) were elevated in comparison with the other study sites. Nitrate concentrations were generally highest during the period of spring snowmelt (25 ± 8 µmol L^{-1}), decreased during the growing-season and increased slightly during the dormant season (Fig. 31.5). However, following the ice storm, NO_3^- concentrations in stream water draining the lower BNA were substantially elevated in comparison with the long-term data (Martin et al. 2000), and unlike the typical seasonal pattern, NO_3^- concentrations in the lower watershed remained relatively constant at elevated levels following the ice storm (Fig. 31.6).
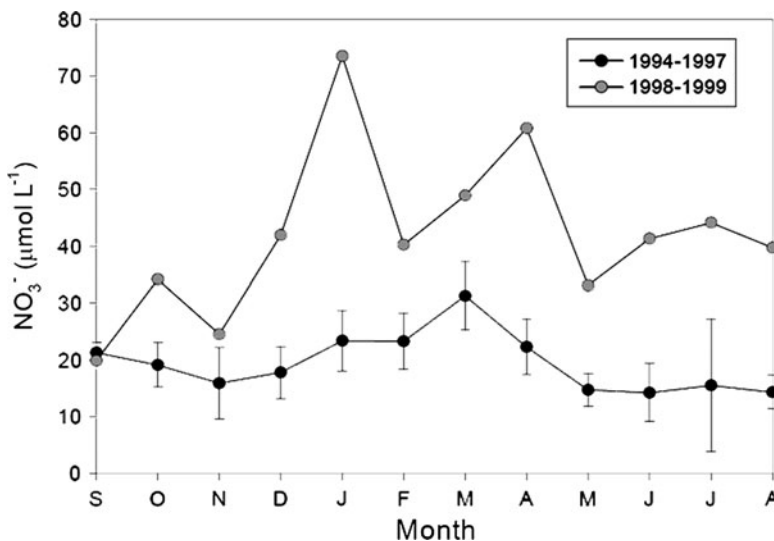
Fig. 31.6 Temporal pattern of stream water nitrate concentrations at the Bowl Nature Area. Data before (*black circles*; 1994–1997) and following (*gray circles*; 1998–1999) the ice storm are shown. *Error bars* reflect standard deviations

31.4   Ice Storms and N Cycling in Forests: Contextualizing the Broader Literature

31.4.1   Spatial Patterns of Ice Storm Damage at the HBEF

The response of drainage water chemistry to the ice storm was isolated to areas of extensive crown damage at the HBEF, which indicated a direct relationship between the magnitude of forest disturbance and ecosystem nutrient losses. Following the perturbation, marked increases in drainage water NO_3^- concentrations were observed in the extensive crown damage zone relative to both nonimpacted areas and pre-disturbance data. This pattern of elevated NO_3^- loss agrees with observations of both natural and anthropogenic disturbances in temperate forest ecosystems (Swank et al. 1981; Pardo et al. 1995; Likens and Bormann 1995; Mitchell et al. 1996; Eshleman et al. 1998; Holmes and Zak 1999). Results for this study have regional implications because the January 1998 ice storm affected a large number of forested areas across the northeastern USA and eastern Canada; elevated NO_3^- loss and associated acidification of surface water likely occurred in many headwater catchments experiencing substantial crown damage as a result of the January 1998 ice storm.

Nitrate concentrations in waters draining the extensive crown damage zone showed a pattern of mobilization from the forest floor and Bh horizon, and

dissipation in the Bs horizon at the HBEF (Fig. 31.3); the upper soil (0–12 cm) was the source of elevated N. Two processes – either separate or in combination – can explain the response (1) enhanced solar radiation to the forest floor (due to newly created gaps in forest over-story) stimulating microbial decomposition (mineralization) and subsequent nitrification; supplying a source of N in excess of biotic requirements, and/or (2) decreased uptake of N.

There was no significant difference in net mineralization, nitrification, soil inorganic N levels (data not presented) or soil moisture (data not presented) in soils from ice-damaged and reference areas either in 1998 (the year just after the storm) or 1999 (Houlton et al. 2003). Denitrification rates increase in the ice-damaged "gap" areas, but the difference was only statistically significant in 1999 (Houlton et al. 2003). As changes in microbial inorganic N production (i.e., mineralization, nitrification) in areas of extensive crown damage were not observed relative to reference areas in the 1998 and 1999 growing-seasons, it is likely that decreased plant uptake was primarily responsible for elevated N loss from the disturbed ecosystem.

Similar to soil solution chemistry, marked increases in stream water NO_3^- concentrations were observed in response to the ice storm disturbance relative to the long-term record at the HBEF. The peak concentration of 150 µmol L^{-1} for the high elevation site in W1 was the highest reported since longitudinal monitoring began in 1991. Nitrate concentrations in W1 stream water showed a general pattern of attenuation with decreasing elevation downstream from the zone of extensive crown damage (Fig. 31.4). Patterns of NO_3^- loss corresponded strongly with crown damage, explaining 85–90% of the longitudinal variations in stream NO_3^- concentrations (Houlton et al. 2003). Thus, the spatial variations in stream water NO_3^- concentrations were clearly controlled by the quantity of crown damage that hydrologic flow paths encountered prior to discharging to streams.

31.4.2 Factors Contributing to the Delay in N Loss at the HBEF

A delay of approximately 7 months elapsed from the timing of the ice storm to the period of elevated NO_3^- concentrations in soil waters draining the extensive crown damage zone in W1. Such delays have been widely reported in previous investigations of perturbations to the N cycle (Bormann and Likens 1979b; Vitousek et al. 1982; Dahlgren and Driscoll 1994; Holmes and Zak 1999). Although the mechanisms for delay in N loss were not investigated as a part of this study, we speculate on the contributing factors.

During the growing-season following the ice storm, it is likely that decreases in plant uptake of N as a result of canopy damage allowed for the accumulation of NO_3^- along the soil water-stream water continuum. Due to the limited quantities of water draining the soil during summer, little leaching of NO_3^- occurred; increased drainage in the late summer and fall allowed for the flushing of NO_3^- from soil to drainage water. The time associated with percolation of water through the soil could

therefore explain the delay. Other mechanisms may also have contributed to the delay in the increase in NO_3^- loss, such as the decomposition of ice storm residues (i.e., branches and twigs), the turnover of fine roots, microbial immobilization, or a delay in the build-up of nitrifier populations (Vitousek et al. 1982).

Once elevated NO_3^- concentrations were supplied to the forest floor, the quantity of water that percolated the soil appeared to control the distribution of NO_3^- in the lower soil profile. Mineral soil lysimeters yielded no water during the late summer collections. When these lysimeters yielded soil water in early fall (September, October), very high concentrations of NO_3^- were observed.

The initial increase in stream water NO_3^- concentrations was observed in September 1998. This observation indicated a relatively rapid flushing (ca. 1 month) of solutes from soil water to stream water. However, detailed evaluation of steam water chemistry data revealed some interesting patterns of solute transport across W1 following the disturbance. Although NO_3^- concentrations showed an initial increase in W1 stream water in September 1998 (Fig. 31.4), Bs lysimeters within the extensive crown damage zone showed no response to the ice storm for this collection period (Fig. 31.2). This finding suggests that at higher elevations of W1, drainage can move laterally through the initial 10 cm of forest soils prior to discharging to the stream. This observation is intriguing because it is generally assumed that hydrologic flow paths move through the deepest soil horizons at the HBEF. This transport phenomenon could also explain the lower NO_3^- concentrations observed for Bs solutions relative to Oa and Bh solutions in the severe crown damage zone at W1 (Fig. 31.2). If the rate of lateral water movement were greater than that of percolation, NO_3^- concentrations would be lower in waters draining Bs horizons.

31.4.3 Regional Pattern of NO_3^- Losses in response to the Ice Storm

The magnitude of disturbance-induced NO_3^- losses to waters draining the disturbed catchments at the Tenney and Plymouth Mountains, and the BNA, was generally greater than NO_3^- loss observed for the HBEF watersheds. In contrast, hydrologic losses of NO_3^- were substantially less for Bridgewater Mountain and Pike Hill catchments (Fig. 31.5). To elucidate controls on the variability observed for these response patterns, the relationship between the extent of forest damage and stream NO_3^- concentrations for the 1998–1999 water-year was evaluated in the surveyed watersheds (Fig. 31.5). One might expect to find a strong linear relationship between the extent of crown damage and the magnitude of stream NO_3^- concentrations, similar to results along the longitudinal stream water gradient in W1 and W6 (Houlton et al. 2003). Instead, however, only a slight correlation ($r^2 = 0.17$) was observed between stream NO_3^- concentrations and forest damage among watersheds surveyed at the regional scale (Fig. 31.7). This interesting
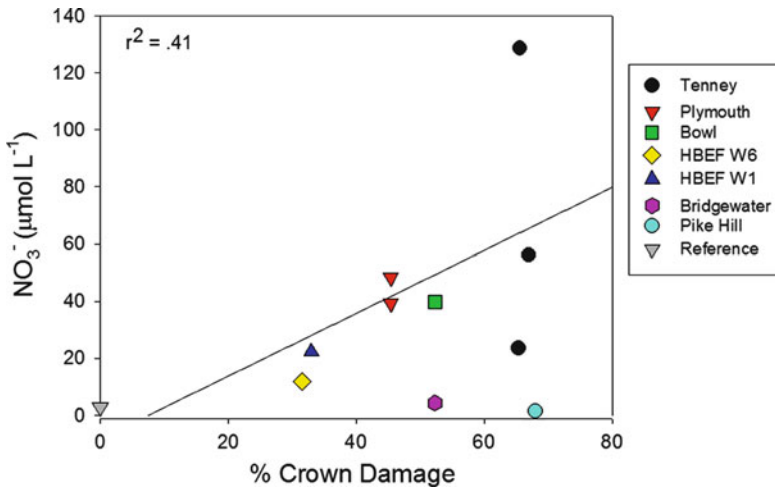
Fig. 31.7 Relationship between average (1998–1999 water-year) nitrate concentrations in streams draining the Southern White Mountain region of New Hampshire and percent crown damage as a result of the 1998 ice storm (see text for site descriptions; from Houlton et al. 2003)

result clearly demonstrates that patterns of N loss in response to perturbations varies widely among Northern Hardwood ecosystems, and that this variability is predominately controlled by watershed characteristics such as, hydrology, geomorphology, soil processes/properties, vegetation, and in-stream processes.

The lack of a NO_3^- response observed for streams draining postagricultural forests that were severely affected by the ice storm suggests that land-use history is a primary control on N cycling. Because agricultural practices extract large quantities of nutrients from soil, it is likely that following the ice storm there was significant retention of N in the post-agricultural secondary forests. (e.g., Aber et al. 1998). Moreover, these results demonstrate the need for improving understanding of the interrelationships between primary and secondary site characteristics for assessing the impacts of chronic deposition of N on northern forest ecosystems. Indeed, previous work has focused on the controls of land use history on dynamics and N losses in temperate forest ecosystems; implicating that previous land use dictates the state of N saturation in Northern Hardwood Forests (Aber and Driscoll 1997; Aber et al. 1998).

Following the ice storm, the losses of NO_3^- observed for the lower watershed at the BNA were prolonged with reference to the impacted secondary forests that were previously logged (withholding post-agricultural sites). This pattern is in general agreement with the N saturation hypothesis, which theorizes that old growth temperate forests should leak N as a result of chronic N-deposition (Aber et al. 1998). However, other factors such as the relatively deep glacial till deposits at the BNA could also have contributed to this prolonged response (i.e., hydrologic residence time; e.g., Martin et al. 2000).

31.5   Comparison of Ice Storms with Other Agents of Disturbance

Broadly, the ice storm of 1998 accelerated losses of NO_3^- to waters draining the severely disturbed forest ecosystems. When compared with the effects of other natural disturbances, such as insect defoliation episodes and soil freezing events, the ice storm disturbance resulted in the greatest flux of NO_3^- loss (Table 31.1). That NO_3^- loss was higher following the 1998 ice storm than soil freezing and insect defoliation events could be due to inherent differences in how these disturbances alter the physical structure of Northern Hardwood ecosystems. For example, while ice storms can cause substantial damage to the stems and branches of trees, insect defoliation episodes are generally exclusive to the loss of leaves from forest over-story, and soil freezing results in enhanced fine root mortality, the physical disruption of soil aggregates, and lysing of microbial cells (Groffman et al. 1999). Moreover, because NO_3^- losses observed for HBEF streams were low in comparison with the other severely damaged forest ecosystems, the NO_3^- flux in Table 31.1 represents a conservative measure and likely underestimates the regional impacts of the 1998 ice storm on patterns of NO_3^- loss.

However, the magnitude of NO_3^- loss associated with the ice storm was markedly less than those observed for forest harvest (Table 31.1). This result is not surprising: forest-harvesting practices are generally more disruptive than natural disturbances to the physical structure (i.e., soil disturbance, complete removal of trees and enhanced runoff) of Northern Forest ecosystems. Among these clear-cutting is the most disruptive, owing to enhanced soil erosion associated with this practice (Bormann and Likens 1979b). At the regional scale, however, the effects of the ice storm on rates of N cycling are substantial, given the spatial extent of this event.

Finally, transiently high losses of N associated with natural and anthropogenic disturbances probably contribute to N limitations of CO_2 uptake in Northern Hardwood ecosystems. Explanations for widespread occurrence of N limitation in temperate ecosystems have focused on fire and harvesting of annual crops (Seastedt et al. 1991),

Table 31.1 Nitrate (NO_3^-) losses (mol $ha^{-1}y^{-1}$) observed for different disturbances to temperate zone forest ecosystems (from Houlton et al. 2003)

Stream flux	Agent of disturbance						
	Exogenous			Anthropogenic			
	Soil freezing[a]	Insect defoliation[b]	Ice storm[c]	Clear-cut		Strip-cut[d]	Whole-tree harvest[d]
				Commercial[e]	Experimental[e]		
NO_3^-	100–450	70–350	349–522	4,100	10,000	1,200	2,000

[a] Mitchell et al. (1996)
[b] Eshleman et al. (1998)
[c] Hubbard Brook experimental forest watershed 1 longitudinal gradient (Houlton et al. 2003)
[d] Pardo et al. (1995)
[e] Likens et al. (1978)

energetic constraints to growth or colonization of N fixers, disproportionate P (or other element) limitation to fixers as opposed to nonfixers, and disproportionately high rates of herbivory on fixers as opposed to nonfixers (Vitousek and Howarth 1991). Other studies have identified the importance of long-term losses of organically bound forms of N, which are generally unavailable to plants (Hedin et al. 1995; Vitousek et al. 1998). Our results clearly demonstrate that ice storms often lead to elevated N export from previously logged secondary forests and mature forest ecosystems. Furthermore, the effects of natural disturbances, such as ice storms, soil freezing events, hurricanes, and insect defoliation episodes, on N availability are often times superimposed upon anthropogenic disturbances (i.e., forest-harvesting, clearing for agriculture, atmospheric deposition) in Northern Forest ecosystems. Thus, anthropogenic and natural disturbances are likely cumulative over long timescales; they contribute synergistically to N-limitation and the subsequent absence of N saturation in northern hardwood forest ecosystems. Because N supply is inherently linked with C storage in temperate forests, knowledge of the roles of natural disturbances in anthropogenically altered landscapes could be important for predicting how these forests will respond to global climate change.

31.6   Future Directions and Concluding Remarks

Our synthesis highlights several future research directions and needs. First, the best-studied cases of ice storm effects on forest N cycles come from ecosystems in temperate forests in New England. Clearly, this is a small area of temperate forest, and at relatively high elevations – yet ice storms occur across large geographic areas of the extra-tropics and from low to high altitudes. Examining impacts of ice storms – when and where they do occur – is a critical research gap. Second, recovery of N cycles following ice storms can occur relatively rapidly, but ultimately the impacts on N limitations are yet to be studied. Follow-up studies – perhaps in combination with remote sensing – of forest growth, community changes, and N fixation inputs are thus warranted. Finally, N is a complex element cycle that entrains many others. For example, accelerated rates of N cycling following disturbances can acidify soils and result in large leaching fluxes of important nutrient-cations such as calcium, magnesium, and potassium. Hence, studying the effects of ice storms on N cycles and associated biogeochemical processes would lead to a clear picture of the extent of such natural disturbance on overall forest ecosystem functioning. Major findings of this work regarding the effects of ice storm on forest biogeochemistry may be summarized as follows:

- Forest crown damage associated with the January 1998 ice storm resulted in accelerated losses of NO_3^- from the disturbed postlogged secondary forests and mature forest ecosystem.
- Following the ice storm, the upper soils (forest floor and upper mineral soil) were the proximate source of elevated NO_3^- loss to waters draining the severe crown damage

zone at the HBEF. This pattern of elevated NO_3^- concentrations was diluted in streams by waters draining nonimpacted areas of W1 and W6 at the HBEF.

- The delay in losses of NO_3^- to waters draining the extensive crown damage zone was likely due to decreased plant uptake in concert with enhanced hydrologic flushing of soils during the autumn. However, other factors such as a lag in the build-up of nitrifier populations, decomposition of ice storm residues, turnover of expendable fine roots and microbial immobilization could also have contributed to this delay.
- Following the ice storm, NO_3^- concentrations were strongly correlated with the forest crown damage along the longitudinal stream water gradient in watershed 1 and watershed 6 at the HBEF.
- Across the lower White Mountains, NO_3^- concentrations were elevated in waters draining both secondary succession and old-growth forests that were affected by the ice storm. In contrast, NO_3^- concentrations remained low in waters draining severely impacted secondary forests that were previously in agriculture. This finding indicated that agricultural land-use history is a primary control of patterns of NO_3^- loss in response to disturbance.
- The ice storm disturbance resulted in the highest efflux of NO_3^- with reference to soil freezing and insect defoliation episodes in northern forest ecosystems; forest-harvesting practices resulted in much higher loss rates of NO_3^- than the ice storm. By accelerating N losses, natural and anthropogenic disturbances contribute to N limitations and delays of N saturation in temperate forest ecosystems.
- Future research should consider ice storm impacts in other extra-tropical sites; forest recovery and N fixation responses to widespread disturbance; and the impact of ice storms on other biogeochemical cycles, especially cation cycles in acid-sensitive ecosystems.

References

Aber JD, Driscoll CT (1997) Effects of land use, climate variation, and N deposition on N cycling and C storage in northern hardwood forests. Glob Biogeochem Cycles 11:639–648

Aber J, Mcdowell W, Nadelhoffer K et al (1998) Nitrogen saturation in temperate forest ecosystems – hypotheses revisited. Bioscience 48:921–934

Bormann FH, Likens GE (1979a) Catastrophic disturbance and the steady-state in northern hardwood forests. Am Sci 67:660–669

Bormann FH, Likens GE (1979b) Patterns and process of a forest ecosystem. Springer, New York, USA

Bruederle LP, Stearns FW (1985) Ice storm damage to a southern Wisconsin mesic forest. Bull Torrey Bot Club 112:167–175

Dahlgren RA, Driscoll CT (1994) The effects of whole-tree clear-cutting on soil process at the Hubbard Brook Experimental Forest, New Hampshire, USA. Plant Soil 158:239–262

Eshleman KN, Morgan RP, Webb JR et al (1998) Temporal patterns of nitrogen leakage from mid-Appalachian forested watersheds: Role of insect defoliation. Water Resour Res 38:2005–2116

Federer CA, Flynn LD, Martin CW et al (1990) Thirty years of hydrometerologic data at the Hubbard Brook Experimental Forest, New Hampshire. U.S.D.A. Forest Service Experiment Station, General Technical Report NE-141. U.S.D.A. Forest Service, Radnor, PA, p 44

Groffman PM, Hardy JP, Nolan S et al (1999) Snow depth, soil frost and nutrient loss in a northern hardwood forest. Hydrol Process 13:2275–2286

Harkness MG (1958) The Tamworth narrative. B. Wheelwright Co., Freeport, Maine, USA

Hedin LO, Armesto JJ, Johnson AH (1995) Patterns of nutrient loss from unpolluted, old-growth temperate forests: evaluation of biogeochemical theory. Ecology 76:493–509

Holmes WE, Zak DR (1999) Soil microbial control of nitrogen loss following clearcut harvest in northern hardwood ecosystems. Eco App 1:202–215

Houlton BZ, Driscoll CT, Fahey TJ et al (2003) Nitrogen dynamics in ice storm-damaged forest ecosystems: Implications for nitrogen limitation theory. Ecosystems 6:431–443

Lawrence GB, Fuller RD, Driscoll CT (1986) Spatial relationships of aluminum chemistry in the streams of the Hubbard Brook Experimental Forest, New Hampshire. Biogeochem 2:115–135

Lemon PC (1961) Forest ecology of ice storms. Bul Torrey Bot Club 88:21–29

Likens GE, Bormann FH (1995) Biogeochemistry of a forest ecosystem, 2nd edn. Springer, New York, USA

Likens GE, Bormann FH, Pierce RS et al (1978) Recovery of a deforested watershed. Science 199:492–496

Lyon CJ, Bormann FH (1962) Natural areas of New Hampshire suitable for ecological research. Dartmouth College, Dep Biol Sci Publ 2: 47

Martin CW (1977) Distribution of tree species in an undisturbed northern hardwood-spruce-fir forest, The Bowl, NH Res Note NE-244. Upper Darby, PA: US Dept Agric, For Serv, Northeast For Expt Sta, p 6

Martin CW (1979) Precipitation and streamwater chemistry in an undisturbed forested watershed in New Hampshire. Ecology 60:36–42

Martin CW, Driscoll CT, Fahey TJ (2000) Changes in streamwater chemistry after 20 years from forested watersheds in New Hampshire. Can J For Res 30:1206–1213

Mattson WH, Addy ND (1975) Phytophagous insects as regulators of forest production. Science 190:515–522

Mitchell MJ, Driscoll CT, Kahl JS et al (1996) Climatic control of nitrate loss from forested watersheds in the northeast united states. Environ Sci Tech 30:2609–2612

Oosting HJ, Billings WD (1951) A comparison of virgin spruce-fir forest in the northern and southern Appalachian system. Ecology 32:84–103

Pardo LH, Driscoll CT, Likens GE (1995) Patterns of nitrate loss from a chronosequence of clear-cut watersheds. Water Air Soil Poll 85:1659–1664

Rebertus AJ, Shifley SR, Richards RH et al (1997) Ice storm damage to an old-growth oak-hickory forest in Missouri. Am Mid Nat 137:48–61

Seastedt TR, Briggs JM, Gibson DJ (1991) Controls of nitrogen limitation in tallgrass prairie. Oecologia 87:72–79

Swank WT, Wade JB, Crossley DA Jr et al (1981) Insect defoliation enhances nitrate export from forest ecosystems. Oecologia 51:2977–2999

Vitousek PM, Howarth RW (1991) Nitrogen limitation on land and in the sea: How can it occur? Biogeochemistry 13:87–115

Vitousek PM, Gosz JR, Grier CC et al (1982) A comparative analysis of potential nitrification and nitrate mobility in forest ecosystems. Ecol Monogr 52:155–177

Vitousek PM, Hedin LO, Matson PA et al (1998) Within-system element cycles, input-output budgets, and nutrient limitation. In: Pace M, Groffman P (eds) Successes limitations and frontiers in ecosystem science. Springer, Berlin, Germany, pp 432–451

Waring RH, Schlesinger WH (1985) Forest ecosystems concepts and management. Academic Press, MO, USA

Warrillow M, Mou P (1999) Ice storm damage to forest tree species in the Ridge and Valley region of southwestern Virginia. J Torrey Bot Soc 126:147–158

Whitney HE, Johnson WC (1984) Ice storms and forest succession in southwestern Virginia. Bul Torrey Bot Club 111:429–437

Chapter 32
Impacts of Hurricanes on Forest Hydrology and Biogeochemistry

William H. McDowell

32.1 Introduction

Hurricanes, typhoons, tropical cyclones, and other tropical storms affect many areas of the globe. Although the names used vary regionally, here I will refer to hurricanes to describe the impacts of these tropical storms globally. The intensity and frequency of hurricanes vary dramatically in different areas of the globe, but their origins are always in warm tropical waters such as the North Atlantic off the African coast, or the central Pacific Ocean. Hurricanes result from the interaction of heated sea water with global wind circulation patterns to create a contained meteorological system with persistent cyclonic circulation rotating around a low-pressure center (Fig. 32.1). Hurricanes initially arise from tropical storms with incomplete circulation, and as they grow in strength the circulation (counterclockwise in the Northern Hemisphere, clockwise in the Southern) closes with an "eye" in the center. Once the circulation is complete, the system is referred to as a hurricane if wind speeds exceed 119 km h^{-1}. Each hurricane has both a speed (the rate at which the storm is moving across the face of the earth) and a strength (the velocity of the cyclonic circulation). The strength of the hurricane changes over time, and usually declines after initial landfall. Damage to forests is typically a function of the hurricane strength, which determines the likelihood of both damage to trees and the storm surges that can occur in low-lying coastal areas. Hurricanes are often associated with high rains, with totals of 25 cm or more.

In the Atlantic and Pacific basins, there is a specific season associated with hurricanes. In the north Atlantic, for example, the hurricane season is specifically designated as June 1 to November 30. Although significant storms with closed circulation can occur outside this time window, those storms are not formally designated as hurricanes. The strength of a hurricane is usually described using the Saffir-Simpson hurricane wind scale, with hurricanes categorized as Category 1–5. The sustained wind strength associated with each hurricane category ranges from 119 km h^{-1} (Category 1) to above 249 km h^{-1} (Category 5). Historic records of hurricane intensity are derived from contemporary accounts of the damage associated with a particular storm. Indexes used include the extent to which materials were embedded in trees, church steeples were toppled, stone buildings were

Fig. 32.1 Closed circulation of Hurricane Hugo as it approaches the U.S. mainland on 21 September 1989. Photo from NOAA archives

Fig. 32.2 Demonstration of the destructive force associated with hurricane winds. Construction timber (5 × 10 cm) impaled in a palm tree, Puerto Rico, September 13 1928. Photo from NOAA archives

damaged, and other measures of destruction. The force of winds impinging on trees during hurricanes can produce rather remarkable effects, such as impalement of trees by flying debris (Fig. 32.2).

In addition to the categorization of a storm by wind speed, individual hurricanes have a trajectory and a forward velocity that is determined by regional meteorological conditions. Although hurricanes in a given region of the world tend to follow a particular track, there is wide variation in the track that will be followed by any particular storm (e.g., Fig. 32.3). Much as a child's spinning top can bounce off obstacles and change its direction, there is a good deal of uncertainty in the direction that a hurricane will take as it heads toward a landfall. Although there have been great improvements in the past few decades in the models used to predict the
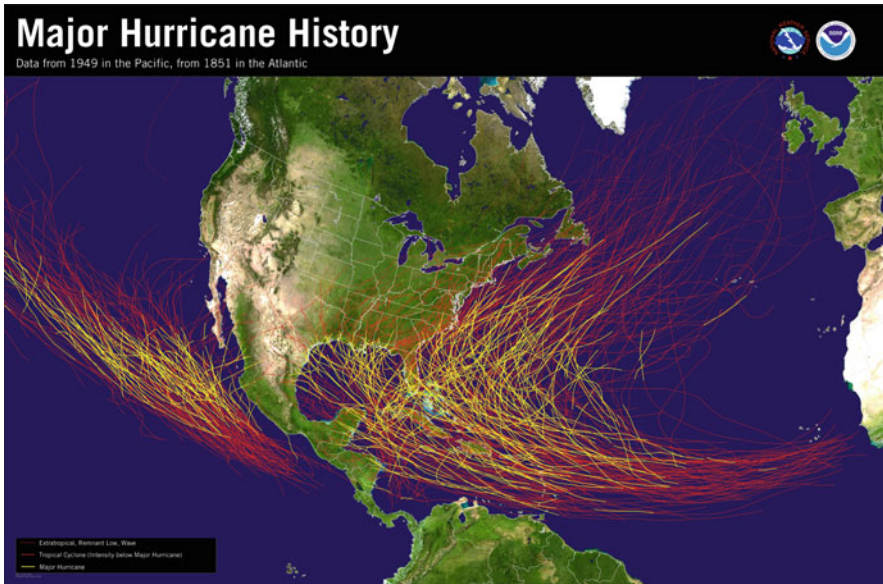
Fig. 32.3 All North Atlantic and Eastern Northern Pacific hurricanes rated at least Category 3 on the Saffir-Simpson scale. Courtesy: NOAA

intensity and track of a given storm, there is still considerable uncertainty associated with both of these predictions. The areas of the globe most susceptible to highly destructive hurricanes are the eastern Caribbean, southeastern US, and Southeast Asia.

32.2 Hurricane Impacts on Forest Hydrology

Hurricane impacts on forest hydrology and biogeochemistry can be categorized as immediate and longer-term. Immediate impacts result from the input of water and nutrients associated with the storm itself. Although hurricanes typically deliver significant amounts of rain, in wetter areas they are not necessarily extraordinary precipitation events. In moist tropical forests such as those of the Luquillo Mountains of Puerto Rico, for example, the most damaging hurricane in the past 70 years was Hurricane Hugo (18 September 1989), with rainfall of 100–339 mm that increased with elevation in the mountains. This represents approximately 5–7% of average annual totals. Rainfall intensity peaked at 34–39 mm h^{-1}, an intensity with an estimated 5-year return interval (Scatena and Larsen 1991). In temperate forests also subject to hurricanes, hurricane rains tend to be proportionally larger. Santee National Forest, near Charleston, South Caroling, received 150–250 mm of rain from Hugo, or 10–20% of average annual rainfall, and hurricanes in coastal South Carolina may account for up to 25% of annual rainfall in a given year (Blood et al. 1991).

Alteration of forest hydrologic function due to canopy damage following hurricanes is not as well documented as rainfall during the storm. Although numerous studies have documented the impacts of hurricanes on forest biomass, stand dynamics, and community structure (summarized by Lugo 2008), few have assessed the hydrologic impacts of these changes in forests. Because forest felling is known to impact both evapotranspiration (ET) and stream runoff in many forests (e.g., Hornbeck et al. 1993; Hubbart et al. 2007), it seems likely that hurricane damage also affects forest hydrology. Patric (1974) concluded that increases in summer runoff of 13 cm could be attributed to the hurricane damage associated with the 1938 hurricane that hit the Connecticut River Valley of the eastern USA, and that no effect remained for 5 years following the hurricane. Similar hydrologic analyses are not available for other hurricanes, in part due to difficulties in establishing the paired basin comparisons that have proven so effective in assessing the impacts of forest harvesting on stream runoff (e.g., Hornbeck et al. 1993). With widespread forest damage in a region hit by a significant hurricane, such comparisons between impacted and unimpacted watersheds are difficult to make. The record of long-term throughfall volumes and interception in the Luquillo Mountains of Puerto Rico provides an example of hydrologic variation associated with hurricanes. For the year prior to Hurricane Hugo, canopy interception of incoming rainfall ranged from 20 to 30% of weekly rainfall. For the year following Hugo, with nearly complete destruction of the canopy, interception loss ranged from 0 to 20%, and averaged only about 10% (Heartsill-Scalley et al. 2007).

The longer-term potential effects of hurricanes on forest hydrology are associated with the trajectory of forest community structure and regrowth. A shift in species composition following extensive hurricane-induced mortality might alter ET, as would the reduction in vegetative biomass following a hurricane and its subsequent regrowth. Such likely changes in forest hydrology following significant hurricanes are not well documented in the literature.

32.3 Hurricane Impacts on Forest Biogeochemistry

32.3.1 Inputs of Marine Salts

One immediate effect of hurricanes on forest biogeochemistry is addition of marine salts to the forest ecosystem through atmospheric deposition or coastal storm surges. Although the impacts of atmospheric deposition on forests are no doubt minor compared to inundation in sea water, there appears to be a strong effect of hurricane winds on rain chemistry. During a typhoon in Japan, Sakihama and Tokuyama (2005) found that Na and Cl content in rainwater increased linearly with mean wind velocity, with a 50-fold increase in Cl content (up to 1,000 μeq l^{-1}) when winds increased from 5 to 30 m s^{-1}. Ammonium and nonsea salt sulfate, however, both showed precipitous declines in concentration with increased wind

speed. Taken together, these results suggest a significant entrainment of marine aerosols and dilution of anthropogenic atmospheric contaminants during hurricanes. Biogeochemical inputs to a forest from atmospheric deposition can thus be profoundly altered during hurricanes.

Sea salts can also be delivered to low-lying coastal forests through the storm surges commonly associated with hurricanes. Perhaps, the best-known examples of the impacts of this storm surge on forest biogeochemistry are found in forests of the barrier islands off the coast of South Carolina, USA, following the passage of Hurricane Hugo in 1989 (Blood et al. 1991; Gardner et al. 1992). A storm surge of up to 9 m swept over coastal South Carolina, with forests in the vicinity of North Inlet receiving 1.5–3.0 m of salt water. The biogeochemical response of soil solution to this inundation was immediate and substantial, with total ionic content (sum of cation and anions) increasing from 1.5 to 143 meq l^{-1} in the OA horizon in the first few months after the hurricane, and the maximum salinity recorded for Bh soil solution was 10 ppt. These dramatic increases in soil solution ionic strength were accompanied by large increases in NH_4 concentrations. In the OA horizon, for example, NH_4 increased from less than 1 to more than 500 µeq l^{-1}. Nitrate concentrations declined from 1 µeq l^{-1} to below detection limits. The appearance of NH_4 in soil solution lagged that of Na in the A horizon (Fig. 32.4), and was attributed to cation exchange by Blood et al. (1991). The lack of NO_3 production following the hurricane, despite the extraordinarily high levels of NH_4, was attributed to inhibition of nitrification by the high salinity (Blood et al. 1991).

Because most forests impacted by hurricanes do not receive a salt water storm surge, the biggest impacts of hurricanes on forest biogeochemistry are associated
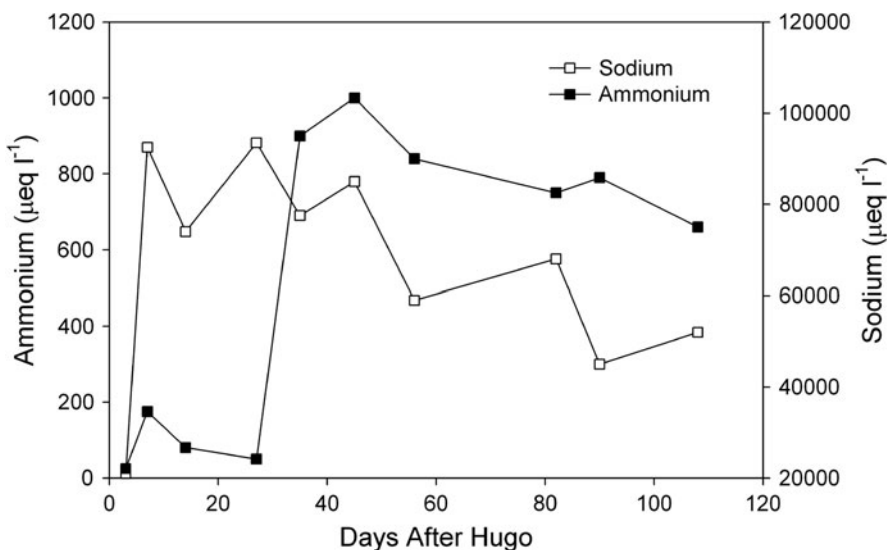
Fig. 32.4 Effects of Hurricane Hugo on forest soil solution collected from the A horizon in a coastal S. Carolina forest, USA. Modified from Blood et al. (1991)

Fig. 32.5 Effects of Hurricane Hugo (September 1989) on a mid-elevation site (Bisley Experimental Watersheds) in the Luquillo Mountains of Puerto Rico. The same site is pictured before (*left*) and after (*right*) the hurricane. Photos by the author

with tree death, tree damage, and the redistribution of living biomass from canopy to forest floor. The strong winds associated with hurricanes can snap boles and branches from large trees and completely strip trees of all their foliage (Fig. 32.5). Because it can be difficult to disentangle the impacts of tree damage and mortality from those associated with the large detrital input to the forest floor, I will not attempt to do so here. Rather, I will focus on the impacts of hurricanes on various aspects of forest biogeochemistry.

32.3.2 *Aboveground Biomass, Litter Inputs, and Decomposition*

The most obvious impact of hurricanes on forest biogeochemistry is the redistribution of biomass and nutrients from the aboveground biomass to the forest floor (Fig. 32.5), and this impact has been carefully assessed in the Luquillo Mountains of Puerto Rico. Heartsill-Scalley et al. (2010) found that following Hurricane Hugo in 1989, aboveground biomass and nutrient content (N, P, K, Ca, and Mg) in the Bisley Experimental Watersheds were only 50% of pre-hurricane values. Despite this massive loss of aboveground biomass, within 5 years both biomass and nutrient content approached pre-hurricane values. Fifteen years after Hurricane Hugo, despite the passage of Hurricane Georges in 1998, aboveground biomass and nutrient content exceeded pre-hurricane values. Thus, it appears that the effects of multiple hurricanes on forest biogeochemistry are not additive; past disturbance regime alters the response of a forest to the latest disturbance (Heartsill-Scalley et al. 2010)

The massive quantities of leaves, wood, and coarse woody debris deposited on the forest floor following a hurricane provide a large pulse of labile and refractory carbon as well as nutrients to the forest floor (Lodge and McDowell 1991). Hurricane litterfall can exceed the litterfall occurring during an entire nonhurricane year, with values of 2 kg m^{-2} total fine litterfall (leaves and small woody stems deposited on the ground and suspended in the canopy) recorded in Puerto Rico following Hurricane Hugo (Lodge et al. 1991), and similar values (1.4 times annual fine litterfall) were obtained in Hawaii following Hurricane Iniki (Herbert et al. 1999). Because hurricane litterfall is green rather than senesced, it also has 10–50% higher N content and 70–330% higher P content than nonhurricane litterfall (Lodge et al. 1991). Despite this increase in N content of fine litter, some components of total biomass deposited on the forest floor (woody boles and large stems) were relatively low in N, and may have immobilized significant amounts of N following Hurricane Hugo. In the Luquillo Mountains of Puerto Rico, Zimmerman et al. (1995) examined the effects of coarse woody debris on soil N availability through field experiments and modeling. They found that following experimental removal of wood following Hurricane Hugo, N availability in soil increased by 40%, and aboveground primary productivity increased. Using the CENTURY model, they concluded that declines in N availability caused by microbial N immobilization during wood decay should decrease primary productivity for 14 years following a hurricane. Direct experimental manipulations of wood at other sites in the Luquillo Mountains have produced conflicting results, however. Wood addition to forest plots resulted in almost a 50% increase in basal area growth rate 9 months after the wood addition, with rates returning to those of control plots within about 18 months of wood addition (Beard et al. 2005). Thus, the extent to which nutrient dynamics during wood decomposition following hurricane felling of trees will hinder or enhance net primary productivity is unclear.

32.3.3   Belowground Processes and Trace Gas Flux

The primary impacts of hurricane damage to upland forests that have been quantified include impacts on root abundance, root decay, and trace gas flux. Following disturbance by Hurricane Hugo in Puerto Rico, fine root biomass decreased by as much as 90%, from approximately 150 to 15 g m^{-2} (Silver and Vogt 1993). Regrowth of roots to pre-disturbance levels following Hugo appeared to take at least a year or more (Parrotta and Lodge 1991). Dead roots in hurricane-damaged plots were slow to decompose, with approximately 65% of initial biomass present 1 year after root death (Silver and Vogt 1993). Extractable nitrogen levels increased in the first few months following the hurricane, with NO_3–N concentrations increasing 6-fold to approximately 12 µg g^{-1} in hurricane-damaged plots (Silver and Vogt 1993). Herbert et al. (1999) observed a similar response in fine roots following Hurrricane Iniki, which struck Hawaii in September 1992. Fine root mortality was 35–48%, and recovery of live fine root biomass to pre-hurricane

levels took 2 years. Hasselquist et al. (2010) examined the response of fine roots to the passage of Hurricane Wilma on the Yucatan peninsula of Mexico in a chronosequence of plots with different ages since burning. They found that in the most mature forest stands, root length density declined from 1.9 to 1.1 cm cm^{-3} post-hurricane and remained depressed for at least 2 years. In soils of earlier seral stages, however, there was no response of root length density to the hurricane. This decline in root density of late seral stage forest was associated with a decline in soil N content from 2.7 to 1.8% of soil dry mass (Hasselquist et al. 2010).

Fluxes of trace gases and CO_2 often respond to the increased availability of organic matter and inorganic nitrogen in forest soils following hurricane disturbance. Steudler et al. (1991) found that N_2O flux was 4- to 10-fold higher in plots receiving extensive damage by Hurricane Hugo in Puerto Rico than in a nearby, relatively undamaged plot that was 80% defoliated and suffered some branch loss. They could not detect an impact of the hurricane on fluxes of CO_2 and CH_4 from soil. Values collected post-hurricane tended to me lower than those collected at a different plot prior to the hurricane, but the differences were not statistically significant (Steudler et al. 1991). Erickson and Ayala (2004) were able to compare 1.5 years of pre-hurricane measurements in Puerto Rico to several years of measurements at the same plots following Hurricane Georges in 1998. They found that hurricane defoliation resulted in increased soil nitrate levels and a 5-fold increase in N_2O flux for the first 7 months following the hurricane. Increases in N_2O flux persisted for at least 2 years (Erickson and Ayala 2004; Fig. 32.6). Vargas and Allen (2008) examined the response of soil CO_2 flux in a seasonally dry tropical forest on the Yucatan peninsula, Mexico to Hurricane Wilma in 2005. Contrary to the results
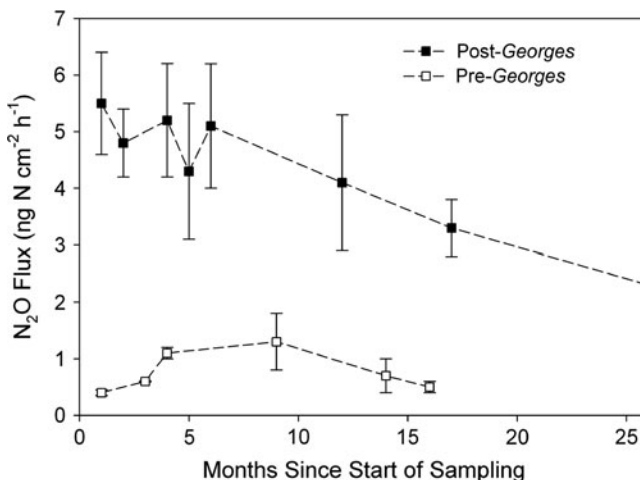
Fig. 32.6 Effects of Hurricane Georges (September 1998) on soil N_2O flux in the Luquillo Mountains of Puerto Rico. Sampling before the hurricane occurred from March 1995 to June 1996; post-hurricane sampling was initiated in November 1998 and continued until December 2000. Modified from Erickson and Ayala (2004)

of Steudler et al. (1991), they observed a doubling of CO_2 flux in the months following the hurricane. Even a year after the hurricane, CO_2 flux was 18% higher than values observed on the same plot prior to the hurricane. They also observed that diel patterns in CO_2 flux were decoupled from temperature following the hurricane, suggesting that the hurricane had long-lasting effects on the biophysical environment of the forest. Vargas et al. (2010) found that Hurricane Wilma also changed belowground carbon cycling, as they documented a decline in sporulation of arbuscular mycorrhizal fungi 3 months after the hurricane. In contrast to the large changes in soil gas fluxes typically observed following hurricanes in tropical forest, responses of temperate forest appear to be muted or absent. Following an experimental toppling of mature trees at the Harvard Forest, Massachusetts, U.S.A. to simulate hurricane blowdown, Bowden et al. (1993) observed no change in CO_2 and CH_4 fluxes, and a decline in N_2O fluxes. They attributed this decline in N_2O fluxes to the low levels of extractable N in the soils even following the modest increase caused by the experimental manipulation. It is unclear whether the response of tropical forests to hurricanes is qualitatively different from that of their temperate counterparts, although differences in N limitation to tree growth (e.g., Matson et al. 1999) might result in different responses to hurricane disturbance among biomes.

32.3.4 Nutrient Fluxes in Throughfall, Groundwater, and Streams

Tracing the fluxes of water and soluble nutrients along hydrologic flow paths can provide considerable insight into biogeochemical conditions and nutrient cycles in forests, and has been used widely to characterize the biogeochemical response of forests to disturbance. Throughfall chemistry provides an integrated signal combining both precipitation inputs and the leaching or washing of materials from leaf surfaces, and is typically a significant input of nutrients and organic matter to the forest floor (e.g., McDowell 1998). With reductions in leaf area index and changes in tree species composition, one might expect that elemental fluxes in throughfall would respond dramatically to the catastrophic disturbance associated with a major hurricane. In contrast, however, throughfall chemistry is remarkably insensitive to the damage associated with major and minor hurricanes over a 15-year period in the Luquillo Mountains of Puerto Rico. Heartsill-Scalley et al. (2007) showed only minor and short-lived changes in the throughfall enrichment ratio (throughfall/precipitation) for the 15-year study period, and concluded that the large changes in forest composition associated with Hurricane Hugo had only a minor effect on throughfall nutrient fluxes.

Unlike throughfall chemistry, groundwater in the Luquillo Mountains of Puerto Rico underwent large increases in nutrient concentration following Hurricane Hugo in 1989, with nitrate and potassium showing the largest changes. In the Bisley Experimental Watersheds, pre-hurricane concentrations of nitrate in groundwater were typically 50–100 μg l^{-1}, and increased to as high as 1 mg l^{-1} post-hurricane.

Similarly, K^+ increased from about 0.4 mg l^{-1} to as much as 13 mg l^{-1} (McDowell et al. 1996). Concentrations of NH_4 and NO_3 peaked sequentially, with most wells showing first a peak in NH_4, and then a subsequent peak in nitrate. This suggests that mineralization of the large amounts of detritus on the forest floor was responsible for the increased nitrogen availability post-hurricane, and that nitrification lagged the production of ammonium.

Stream chemistry integrates the biogeochemical function of an entire basin, and thus has proven to be an extremely useful tool for understanding the integrated response of a forest ecosystem to disturbance (Bormann and Likens 1967). Two detailed studies of stream chemistry provide insight into the immediate effects of hurricanes in forested watersheds. Zhang et al. (2007) describe the impacts of three typhoons that hit Japan in 2004. They observed different responses to the three storms, with few clear patterns emerging. Large increases in concentrations of suspended sediments and particulate nutrients were observed for a few hours at peak stream flow in all the storms (e.g., Fig. 32.7), but the response of dissolved nutrients varied among storms. Nitrate concentrations, for example, were increased during the ascending limb of the hydrograph in one storm, but were unchanged in another (Fig. 32.7). In a similar study of forested watersheds in Taiwan, Tsai et al. (2009) documented differences between native and plantation forests in their response to typhoon rains. They observed that sediment losses were much higher in the plantation forest (reaching 140 mg l^{-1} total suspended solids) than in the native forest (20 mg l^{-1}). Nitrate concentrations increased during the storm in both
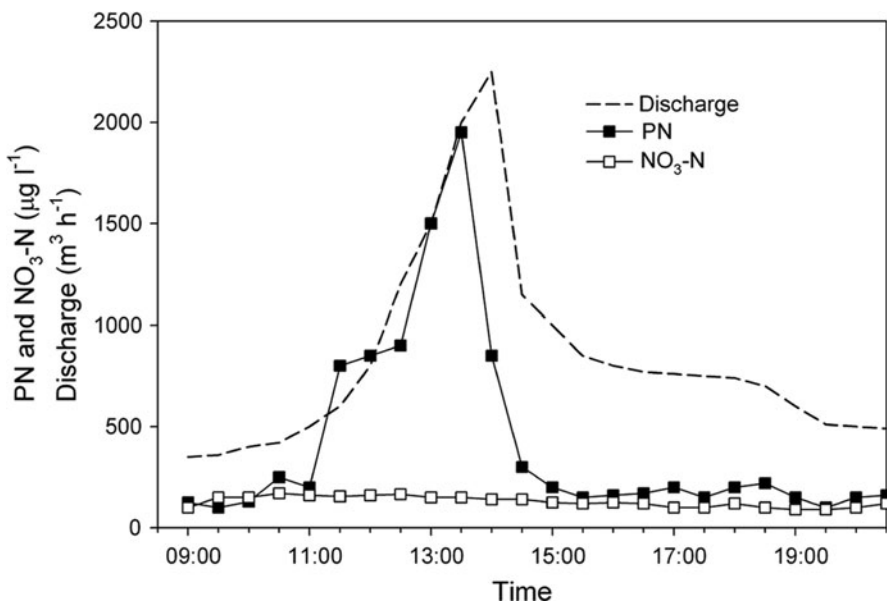
Fig. 32.7 Effects of a typhoon occurring June 21, 2004 on concentrations of particulate nitrogen (PN) and nitrate (NO_3-N) in a headwater stream in central Japan. Modified from Zhang et al. (2007)
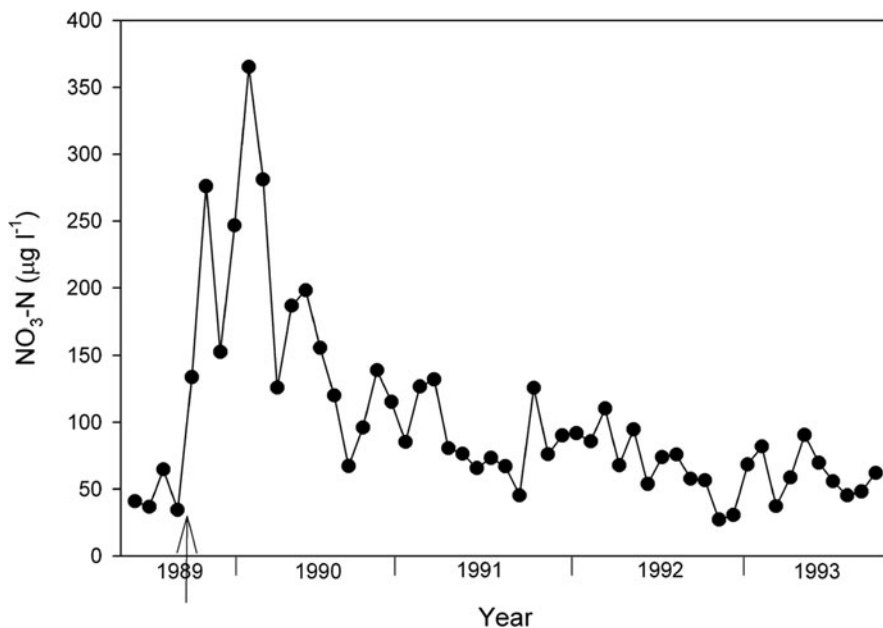
Fig. 32.8 Effects of Hurricane Hugo, September 1989 on monthly average nitrate (NO_3-N) concentrations in Quebrada Prieta, a stream draining the Luquillo Mountains of Puerto Rico. The vertical arrow shows the date of Hurricane Hugo. Modified from McDowell (2001)

watersheds, but reached higher peak values in the native forest (0.7 mg l^{-1} NO_3-N) than in the plantation (0.4 mg l^{-1}). Neither Zhang et al. (2007) nor Tsai et al. (2009) examined the longer-term response of stream chemistry to typhoons.

As is often the case in forest ecosystems, disturbance has the most obvious and long-lasting effects on the nitrogen cycle, which are typically manifested as an increase in stream nitrate concentrations (Fig. 32.8). These increases have been extensively documented in the Luquillo Mountains of Puerto Rico, where 8 watersheds were sampled before and after Hurricane Hugo in September 1989 (Schaefer et al. 2000). In each of the streams, concentrations of nitrate increased in the months following passage of Hurricane Hugo, with monthly average concentrations reaching 350 µg l^{-1}. The average increase in all eight streams was 207% for the year following the hurricane. Annual flux of nitrogen also doubled to approximately 5 kg ha^{-1} yr^{-1} in the year following the hurricane (Schaefer et al. 2000). Potassium concentrations also responded strongly to the hurricane, with increases that averaged 77% in the year following the hurricane.

Riparian zones can reduce the response of stream chemistry to a disturbance, including hurricanes. Because riparian zones are typically redox transition zones, they have the largest impact on transport of redox-sensitive solutes such as nitrogen and sulfur. The best-studied case of hurricane impacts on riparian function in forests is found in the Luquillo Mountains of Puerto Rico. There, McDowell et al. (1996) examined the impacts of Hurricane Hugo on riparian nutrient dynamics in two watersheds with contrasting bedrock and geomorphology. They found that in

Fig. 32.9 Concentrations of dissolved nitrogen in shallow groundwater collected from riparian zone wells in the Luquillo Mountains of Puerto Rico before and after Hurricane Hugo (September 1989). *Upper panel* is dissolved organic nitrogen (DON), *middle panel* is ammonium (NH_4-N) and *lower panel* is nitrate (NO_3-N). From McDowell et al. (1996)
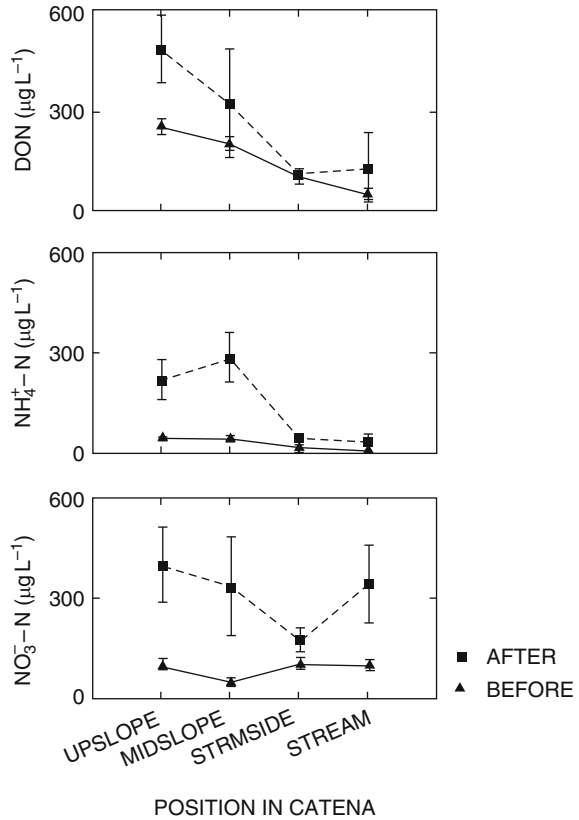
both watersheds, upslope nitrate, ammonium, and dissolved organic nitrogen (DON) concentrations increased following the hurricane, and decreased by up to 90% with passage through the riparian zone (e.g., Fig. 32.9). The effectiveness of the riparian zone in reducing N concentrations was much more evident following hurricane disturbance in the Bisley Experimental Watersheds, when concentrations in upslope groundwater were high enough to detect significant declines when water passed through the riparian zone. In the absence of disturbance, the ability of the riparian zone to reduce N losses is masked by the low upslope concentrations of dissolved nitrogen (McDowell et al. 1996; McDowell 2001).

32.4 Hurricanes and Global Change

Hurricanes have increased in frequency within the last several decades (Goldenberg et al. 2001), and are predicted to increase in frequency and intensity with global climate change (Emanuel 2005; Webster et al. 2005). The impacts of increased

frequency and strength of hurricanes are uncertain. The effects of multiple disturbance might not be additive, as suggested by the work of Heartsill-Scalley et al. (2010), who documented only a minor response in aboveground biomass to the second major hurricane in a decade to hit the Luquillo Experimental Forest. The effects on soil carbon balance and net CO_2 flux are also uncertain, as research to date shows no clear patterns in CO_2 flux following hurricanes. Based on the existing data, however, an increase in N_2O flux with increased hurricane frequency does seem likely. Finally, the impacts of increased hurricane frequency on soil nutrient availability are uncertain. Various observations and manipulations with coarse woody debris have provided conflicting results regarding the likely impact of the increased inputs of coarse woody debris that will be associated with increased hurricane frequency.

32.5   Future Research Directions

Future research needs for forest hydrology and biogeochemistry can be summarized as follows:

1. To what extent is forest hydrology altered by hurricanes globally, and how long do these effects persist following a hurricane?
2. What are the long-term consequences of increased hurricane frequency for forest primary productivity, soil organic matter accumulation, and nitrogen export?
3. Will increased hurricane frequency alter fluxes of greenhouse gases (CO_2, CH_4, and N_2O) fluxes from tropical soils, providing feedbacks to the global climate system?
4. Are changes in regional rainfall patterns following a hurricane similar to those that appear to be associated with anthropogenic deforestation?

References

Beard KH, Vogt KA, Vogt DJ et al (2005) Structural and functional responses of a subtropical forest to 10 years of hurricanes and droughts. Ecol Monogr 75:345–361
Blood ER, Anderson P, Smith PA et al (1991) Effects of Hurricane Hugo on coastal soil solution chemistry in South Carolina. Biotropica 23:348–355
Bormann FH, Likens GE (1967) Nutrient cycling. Science 155:424–429

Bowden RD, Castro MS, Melillo JM et al (1993) Fluxes of greenhouse gases between soils and the atmosphere in a temperate forest following a simulated hurricane blowdown. Biogeochemistry 21:61–71

Emanuel K (2005) Increasing destructiveness of tropical cyclones over the past 30 years. Nature 436:686–688

Erickson HE, Ayala G (2004) Hurricane-induced nitrous oxide fluxes from a wet tropical forest. Glob Change Biol 10:1155–1162

Gardner LR, Michener WK, Williams TM et al (1992) Disturbance effects of Hurricane Hugo on a pristine coastal landscape: North Inlet, South Carolina, USA. Neth J Sea Res 30:249–263

Goldenberg SB, Landsea CW, Mestas-Nuñez AM et al (2001) The recent increase in Atlantic hurricane activity: causes and implications. Science 293:474–479

Hasselquist NJ, Santiago LS, Allen MF (2010) Belowground nitrogen dynamics in relation to hurricane damage along a tropical dry forest chronosequence. Biogeochemistry 98:89–100

Heartsill-Scalley T, Scatena FN, Estrada C et al (2007) Disturbance and long-term patterns of rainfall and throughfall nutrient fluxes in a subtropical wet forest in Puerto Rico. J Hydrol 333:472–485

Heartsill-Scalley T, Scatena FN, Lugo AE et al (2010) Changes in structure, composition, and nutrients during 15 years of hurricane-induced succession in a subtropical wet forest in Puerto Rico. Biotropica 42:455–463

Herbert DA, Fownes JH, Vitousek PM (1999) Hurricane damage to a Hawaiian forest: nutrient supply rate affects resistance and resilience. Ecology 80:908–920

Hornbeck JW, Adams MB, Corbett ES et al (1993) Long-term impacts of forest treatments on water yield: a summary for northeastern USA. J Hydrol 150:323–344

Hubbart JA, Link TE, Gravelle JA et al (2007) Timber harvest impacts on water yield in the continental/maritime hydroclimatic region of the United States. For Sci 53:169–180

Lodge DJ, McDowell WH (1991) Summary of ecosystem-level effects of Caribbean hurricanes. Biotropica 23:373–378

Lodge DJ, Scatena FN, Asbury CE et al (1991) Fine litterfall and related nutrient inputs resulting from Hurricane Hugo in subtropical wet and lower montane rain forests of Puerto Rico. Biotropica 23:336–342

Lugo AE (2008) Visible and invisible effects of hurricanes on forest ecosystems: an international review. Austral Ecol 33:368–398

Matson PA, McDowell WH, Townsend AR et al (1999) The globalization of N deposition: ecosystem consequences in tropical environments. Biogeochemistry 46:67–83

McDowell WH (1998) Internal nutrient fluxes in a tropical rain forest. J Trop Ecol 14:521–536

McDowell WH (2001) Hurricanes, people, and riparian zones: controls on nutrient losses from forested Caribbean watersheds. For Ecol Manage 154:443–451

McDowell WH, McSwiney CP, Bowden WB (1996) Effects of hurricane disturbance on ground-water chemistry and riparian function in a tropical rain forest. Biotropica 28:577–584

Parrotta JA, Lodge DJ (1991) Fine root dynamics in a subtropical wet forest following hurricane disturbance in Puerto Rico. Biotropica 23:343–347

Patric JH (1974) River flow increases in central New England after the hurricane of 1938. J For 72:21–25

Sakihama H, Tokuyama A (2005) Effect of typhoon on chemical composition of rainwater in Okinawa Island, Japan. Atmos Environ 39:2879–2888

Scatena FN, Larsen MC (1991) Physical aspects of Hurricane Hugo in Puerto Rico. Biotropica 23:317–323

Schaefer DA, McDowell WH, Scatena FN et al (2000) Effects of hurricane disturbance on stream water concentrations and fluxes in eight tropical forest watersheds of the Luquillo Experimental Forest. J Trop Ecol 16:189–207

Silver WL, Vogt KA (1993) Fine root dynamics following single and multiple disturbances in a subtropical wet forest ecosystem. J Ecol 81:729–738

Steudler PA, Melillo JM, Bowden RD et al (1991) The effects of natural and human disturbances on soil nitrogen dynamics and trace gas fluxes in a Puerto Rican wet forest. Biotropica 23:356–363

Tsai C-J, Lin T-C, Hwong J-L et al (2009) Typhoon impacts on stream water chemistry in a plantation and an adjacent natural forest in central Taiwan. J Hydrol 378:290–298

Vargas R, Allen MF (2008) Diel patterns of soil respiration in a tropical forest after Hurricane Wilma. J Geophys Res 113:G03021

Vargas R, Hasselquist N, Allen EB et al (2010) Effects of a hurricane disturbance on aboveground forest structure, arbuscular mycorrhizae and belowground carbon in a restored tropical forest. Ecosystems 13:118–128

Webster PJ, Holland GJ, Curry JA et al (2005) Changes in tropical cyclone number, duration, and intensity in a warming environment. Science 309:1844–1846

Zhang Z, Fukushima T, Onda Y et al (2007) Nutrient runoff from forested watersheds in central Japan during typhoon storms: implications for understanding runoff mechanisms during storm events. Hydrol Process 21:1167–1178

Zimmerman JK, Pulliam WM, Lodge DJ et al (1995) Nitrogen immobilization by decomposing woody debris and the recovery of tropical wet forest from hurricane damage. Oikos 72:314–322

Chapter 33
The Effects of Forest Harvesting on Forest Hydrology and Biogeochemistry

James M. Buttle

33.1   Introduction

The hydrological consequences of forest harvesting are arguably the longest-studied aspect of interactions between hydrology and land cover or land use. Chang (2003) notes that increased understanding of interactions between forest management and hydrology led to enactment of forest protection laws in China as early as 300 BC, while the Swiss initiated the establishment of forested watershed reserves in Europe in 1342 (Kittredge 1948). The earliest documented basin-scale comparison of streamflow and erosion from forested and agricultural lands (1902) also comes from Switzerland (Whitehead and Robinson 1993). Numerous studies of forest harvesting effects on various aspects of the hydrological cycle (particularly streamflow) followed, complemented in the past several decades by research on the biogeochemical impacts of forest harvesting. Aspects of this work (particularly related to harvesting effects on streamflow) were summarized in classic reviews by Hibbert (1967), Bosch and Hewlett (1982), and Sahin and Hall (1996). Recent summaries of the hydrologic and biogeochemical impacts of forest harvesting have focused on individual countries (e.g., USA – Stednick 1996, National Research Council 2008; Canada – Buttle et al. 2005, 2009), specific regions (e.g., Pacific Northwest – Moore and Wondzell 2005; Feller 2005), or particular environments (e.g., tropical forests – Bruijnzeel 2004). Rather than restate these reviews, this chapter attempts to synthesize the results of studies of the hydrologic and biogeochemical effects of forest harvesting from a more global perspective. In particular, it focuses on areas of consensus that have arisen from this work, caveats to that consensus that arise from specific environmental conditions or forest management practices, and areas of controversy, both in terms of the results of this research and the methods employed to obtain them. The latter is an important but often overlooked issue in attempts to assess the consequences of forest harvesting, and some of the ongoing debates regarding these outcomes can be linked to the experimental and analytical approaches used in various studies. This assessment of consensus, caveats, and controversies begins with a review of the effects of forest harvesting on hydrological processes and water partitioning, links these effects to harvesting impacts on various aspects of streamflow at the basin scale, and then turns to the biogeochemical

consequences of forest harvesting. The chapter concludes with an outline of major research issues that should be addressed in future work.

33.2   Effects of Forest Harvesting on Hydrologic Processes and Water Partitioning

33.2.1   Precipitation

The question of whether deforestation affects the amount of precipitation at that location is a long-standing one, and some have characterized views on the issue as based on folklore rather than science (Hamilton 1985). Early research (e.g., Pereira 1973) showed little or no relationship between an area's precipitation and whether it was forested or not. However, the topic has received increased interest, partly as a result of concerns regarding the contributions of modifications of Earth's vegetative cover to anthropogenic climate change (Marland et al. 2003). This has been spurred in part by research on precipitation recycling (Vanclay 2009), such as isotopic studies (e.g., Salati et al. 1979) that show that large forest regions, such as Amazonia, can regenerate their own rainfall via evapotranspiration. da Silva and Avissar (2006) note that the effects of forest removal on precipitation may differ depending on the scale of deforestation. Massive deforestation may decrease rainfall due to reduced transpiration and surface roughness combined with increased albedo, as supported by work in Central America (Lawton et al. 2001). However, current levels of deforestation in Amazonia and other tropical regions may enhance convection and promote a transient increase in precipitation (Henderson-Sellers and Pitman 2002; Avissar et al. 2002). Marland et al. (2003) suggest that the scale of deforestation needed to induce a significant change in precipitation patterns depends in part on where such land surface changes occur, with smaller extents of deforestation required in equatorial regions and presumably larger areas needed in other locations.

33.2.2   Interception

It is generally accepted that harvesting increases net precipitation reaching the forest floor as a result of reduced interception losses. The magnitude of this increase can be considerable, given that annual interception can range from 10 to 50% of annual precipitation (Roth et al. 2007). This increase differs depending on the type of forest harvested (e.g., conifers vs. deciduous) and extent of forest removal (clearcutting vs. selection harvesting), and also varies as function of storm size, weather conditions, and canopy characteristics (Van Dijk et al. 2009). The effect of harvesting on net precipitation will vary seasonally for forests that experience a dormant period and will be greatest at the time of maximum leaf area for deciduous forests. While the increase

in net precipitation occurs for both rainfall and snowfall, it is important to note that the significance of forest harvesting for snow interception is strongly linked to regional climate. Thus, work by Pomeroy and colleagues (e.g., Pomeroy et al. 1998, 2002) has demonstrated that most intercepted snowfall in cold, dry boreal forests of central Canada is sublimated back to the atmosphere, such that harvesting can result in a substantial increase in snow accumulation. This increase would be less pronounced in warmer and moisture forest landscapes where sublimation losses of intercepted snow would be reduced. A further caveat is that forest harvesting in some environments can result in a decrease in net precipitation reaching the soil surface. This is attributed to the forest's role in collecting occult precipitation and contributing this water to the soil as fog drip, and has been observed in high-relief coastal forests of the western USA (Harr 1982) as well as maritime forests in eastern Canada (Jewett et al. 1995).

33.2.3   Evaporation/Evapotranspiration

Removal of forest cover produces a dramatic reduction in evaporation and transpiration from the harvested area. This reduction is due to the partial or complete (depending on harvesting intensity) elimination of interception and its subsequent evaporation combined with the cessation of transpiration by the harvested trees (Bosch and Hewlett 1982). Soils in harvested areas generally experience increased solar radiation inputs, turbulent atmospheric fluxes, and soil temperature, which will enhance direct evaporation from the soil surface (Sun et al. 2001). However, this increase only partly counterbalances reduced water loss due to the elimination of transpiration from harvested trees. The reduction in evapotranspiration fluxes is most obvious in clear-cut areas, since the transpiration reduction following partial cuts can be partly compensated for by increased transpiration by the remaining individual trees (Hubbart et al. 2007).

33.2.4   Snow Accumulation and Snowmelt

Harvesting in forested landscapes with seasonal snowcover generally leads to significantly greater snow water equivalents (SWE) in open areas relative to undisturbed forest (e.g., Troendle and Meiman 1984; Gary and Watkins 1985; Stottlemyer and Troendle 1999). This may be partly offset by enhanced sublimation losses as a result of greater wind speeds over the snowpack, as suggested by Stednick (1996) for the Rocky Mountain region and inland intermountain region of Oregon in the USA. Snowmelt rates can increase in harvested areas as a result of increased snowpack exposure to incoming shortwave radiation and turbulent fluxes (Murray and Buttle 2003), and the combination of greater SWE and faster melt rates means that soils in harvested areas receive larger and more intense water inputs during spring snowmelt.

33.2.5 Infiltration

The term "infiltration opportunities" (coined by Bruijnzeel 1988) is a valuable means of conceptualizing the key issues associated with harvesting effects on a soil's ability to infiltrate water. The infiltration capacity of forest soils is generally large and infiltration-excess overland flow is limited, such that most infiltrating water recharges soil water and groundwater stores during wet periods (Bonell 2005). Tree removal by itself does not generally produce significant reductions in infiltration rates unless the harvesting method results in significant soil compaction and reductions in soil hydraulic conductivity and infiltration rate (e.g., Whitson et al. 2003). Nevertheless, if these areas of significant compaction are spatially discontinuous, then any resulting overland flow will likely move laterally to unimpacted sites and have the "opportunity" to infiltrate. Instead, it is specific areas (roads, skidder and tractor tracks, landings) that are associated with a significant reduction in overall basin infiltration rates (Sidle et al. 2004; Waterloo et al. 2007), by virtue of the small infiltration rates for these highly compacted surfaces combined with their spatial connectivity.

33.2.6 Soil Water Storage

The combination of increased net precipitation reaching the soil surface and reduced evapotranspiration losses leads to a general increase in soil water storage in harvested areas (Best et al. 2007; National Research Council 2008). However, increases in soil water content following vegetation removal in the case of partial cuts or canopy thinning may be less than expected due to increased use of available moisture by retained vegetation and vegetation in adjacent uncut areas (Hubbart et al. 2007).

33.2.7 Groundwater Recharge and Discharge

Groundwater recharge generally increases following harvesting (e.g., Cook et al. 1989; Bent 2001), and often results in rising water tables (e.g., Peck and Williamson 1987; Díaz et al. 2007). Implications of increased recharge for groundwater discharge to surface waters will be determined mainly by the travel time of groundwater from the harvested area, such that travel times greatly in excess of the persistence of increased recharge following harvesting likely mean that no significant change in groundwater discharge will be observed immediately after harvesting (Smerdon et al. 2009). This reinforces the need to consider the hydrogeologic setting of a particular forest landscape when considering the hydrologic response to forest harvesting, since harvesting impacts on groundwater discharge

are more likely to manifest themselves for local groundwater flow systems than for larger-scale regional systems (Devito et al. 2000). Nevertheless, the increases in water yields and dry-season low flows that often accompany forest harvesting (see Sect. 33.3.4) indicate that the increased water availability following interception and evapotranspiration reductions due to harvesting is translated into greater groundwater fluxes to surface water bodies.

33.2.8   Changes in Streamflow Generation Processes Following Harvesting

In addition to changes in water flux and partitioning between various hydrologic stores, forest harvesting can lead to significant shifts in the contribution of various runoff-generating mechanisms to streamflow in a drainage basin. As noted previously, infiltration-excess overland flow is rare in undisturbed forest basins, and any overland flow that is observed is generally saturation overland flow (Dunne 1978). Subsurface stormflow is a dominant runoff mechanism in such basins, as saturated layers develop within the soil profile above less-permeable horizons (e.g., Bonell and Gilmour 1978) or at the base of the soil horizon above shallow bedrock (e.g., Peters et al. 1995). Some of this subsurface stormflow may appear as return flow at the soil surface at particular locations (e.g., slope concavities, downslope areas with thinner soil cover). Greater water inputs to the soil surface following harvesting often simply increase subsurface flow discharge to stream channels (Stottlemyer and Troendle 1999), particularly if there has been no significant reduction in infiltration rates. However, overland flow can increase as a result of soil disturbance during forest operations (Waterloo et al. 2007), particularly on roads, skidder trails, and landings. In addition to generating overland flow, roads cut into hillslopes may intercept subsurface water, rerouting it as surface flow along the road and adjacent ditches (Wemple et al. 1996; Hubbart et al. 2007). This interception is maximized when subsurface flow occurs above a hydrologic impeding layer that is exposed at the road cut (Sidle et al. 2006). The potential for such overland flow to contribute to basin streamflow (rather than reinfiltrate into downslope soils) is mediated by the role of hydrologic connectivity within the basin (Stieglitz et al. 2003; Van Miegroet and Johnson 2009), such that water delivery from impacted areas to stream channels depends on the former's position relative to the stream network, downslope vegetative buffers and/or features (e.g., gullies, diversions) that allow surface flow to bypass potential buffers (Sidle et al. 2006). Increased partitioning of water fluxes to overland pathways generated by disturbed areas and the enhanced drainage efficiency provided by roadside ditches and cross drains may be supplemented by more saturation overland flow in harvested basins, since greater soil wetness likely will expand saturated areas within the basin (Waterloo et al. 2007). In addition, groundwater fluxes to streams will generally increase (see Sect. 33.2.7).

33.3   Effects of Forest Harvesting on Streamflow

33.3.1   Approaches Used to Assess Harvesting Impacts on Streamflow

Mallik and Teichert (2009) identified four basin-scale approaches to examine the hydrologic effects of forest harvesting: paired-basin studies (Best et al. 2007); single-basin studies (termed time-trend studies by Bosch and Hewlett 1982); retrospective studies (after-the-fact pairing of harvested and undisturbed basins for which some preharvesting data exist – e.g., Buttle and Metcalfe 2000); and nested basin studies (e.g., Hubbart et al. 2007). Of these approaches, data from paired-basin studies provide the greatest potential to identify any changes in streamflow behavior as a result of forest harvesting, given their greater statistical power (Loftis et al. 2001) when used with multivariate approaches such as analysis of covariance that employ the dummy variable method (e.g., harvested/nonharvested – Scott 1997; Waterloo et al. 2007) to assess harvesting impacts. Nevertheless, the strength of the results of such analyses hinges on the degree to which control and treatment basins are truly similar in terms of geology, soils, topography, and vegetation (Moore and Wondzell 2005), and a sound grasp of the basins' hydrology is needed to distinguish harvesting-related streamflow changes from those due to other factors (Fuller et al. 1988).

33.3.2   Water Yield

Regardless of which experimental or analytical approach is employed, the general finding of studies conducted around the globe indicates that reduced forest cover results in increased water yield (National Research Council 2008). Figure 33.1 shows data from Stednick's (1996) synthesis of paired-basin experiments in the USA, which mirrors findings from studies including results from other countries (e.g., Bosch and Hewlett 1982; Sahin and Hall 1996). Figure 33.1 highlights points that have been raised in previous reviews:

1. Water yield response to harvesting is highly variable. This reflects variations in such factors as climate [e.g., amount and seasonal distribution of precipitation, such that water yield increases tend to be greater in areas of high precipitation (Bosch and Hewlett 1982) and in wetter years (Hubbart et al. 2007)], vegetation type [e.g., greater water yield increases following harvesting of coniferous vs. deciduous forests (Sahin and Hall 1996)] and health prior to harvesting (Waterloo et al. 2007), soils, and geology.
2. Harvesting has to exceed ∼20% of basin area in order to produce a demonstrable increase in water yield.
3. The increase in water yield is inversely related to basin size. This relationship is not apparent when the Stednick basins are standardized according to harvesting
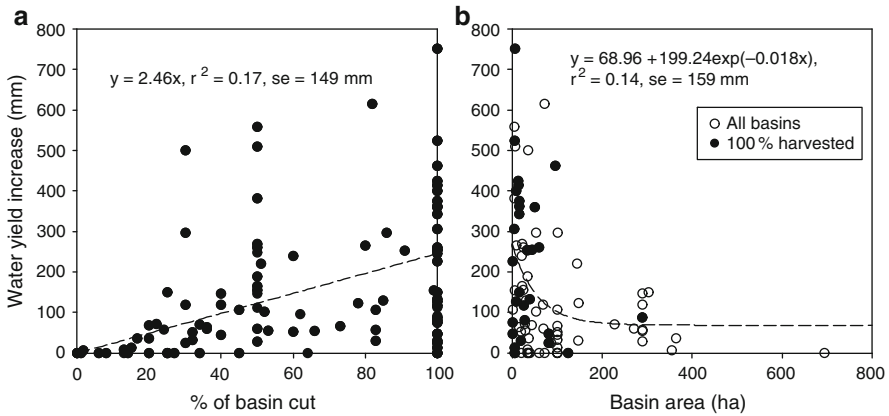
Fig. 33.1 (**a**) Annual water yield increase versus % of basin harvested, based on experimental studies in the USA (data from Stednick 1996); (**b**) annual water increase versus basin area for all basins and basins with 100% of their area harvested (data from Stednick 1996). Lines of best fit are significant at $p = 0.05$; best-fit line in (**b**) is for all basins

magnitude (e.g., 100% harvested), which reflects the greater range of land uses and land covers in large drainage basins (Bruijnzeel 2004).

Best et al. (2007) note that generalizations about annual increases in water yield such as Fig. 33.1 are often based on the maximum change in water yield in the first five years after treatment or first year increases in yield. Permanent land use change experiments indicate that it may take more than five years for the maximum change in water yield to be observed and for a new hydrologic equilibrium to be established, such that summaries such as Fig. 33.1 may underestimate the potential increase in water yield for a given amount of forest removal. Some of the scatter in Fig. 33.1 also reflects variations in experimental design and execution (Adams and Fowler 2006), such as the length of the calibration period, whether regrowth was allowed after harvesting, and the accuracy of the data collected.

33.3.3   Peak Flows

Changes in the relative importance of overland flow pathways to streamflow generation outlined earlier suggest that peak streamflows will increase following harvesting. However, the debate about whether forest harvesting leads to increased peak flows and flooding is one of the most contentious in hydrology (Van Dijk et al. 2009), as illustrated by the controversy regarding whether harvesting changes both frequent as well as infrequent peak flows in a basin. For example, Jones and Grant's (1996) finding that forest operations (forest removal as well as forest roads) in

basins in the Pacific Northwest of the USA increased peak flows for both small and large storms provoked Thomas and Megahan's (1998) reanalysis of the same data and their conclusion that the impact of forest harvesting on peak flows decreases for larger storms. This issue has subsequently been taken up by hydrologists working in other forest landscapes around the world. To some extent, this debate reflects differing opinions regarding the most appropriate statistical approach to use to examine the question (e.g., analysis of variance vs. analysis of covariance). Nevertheless, there appears to be consensus from a process-based perspective that forest harvesting should have a greater proportional effect on small flows compared to larger ones. Thus, Waterloo et al. (2007) found that the largest relative changes in peak discharge and stormflow volume occurred during smaller rainfall events, which was attributed to a shift in the relative importance of runoff-generating mechanisms with storm size. Infiltration-excess overland flow from disturbed surfaces may make a significant contribution to changes in the stormflow hydrograph following harvesting during small storms; however, the effect of harvesting on relative changes in stormflow diminishes with increasing rainfall because runoff contributions from saturated areas and return flow become increasingly more dominant in stormflow generation. Similarly, Van Dijk et al. (2009) contended that the impacts of forest removal on net precipitation delivery to the soil surface and water storage in the soil profile would be minimized for large storm events responsible for generating major peak flows, such that forest harvesting would more likely affect smaller localized floods than extreme, large-scale events.

In order to minimize complications introduced by the influence of storm size on peak flow generation, it is useful to examine harvesting effects on a standardized measure of peak flow, as in Guillemette et al.'s (2005) review of changes in bankfull peak flow from 50 paired-basin studies (Fig. 33.2). Linkage of bankfull flow to stream morphological changes and modifications of aquatic habitat make it a particularly valuable metric to examine in the context of forest disturbance. Figure 33.2 indicates that relative increases in bankfull peak flow increase with the proportion of the basin harvested; however, as with water yield there is substantial variability in response to harvesting, due to such factors as variations in climate, topography, soil characteristics, and species harvested (Guillemette et al. 2005). Several studies show no change in peak flows with harvesting while others show decreases, reinforcing Thomas and Megahan's (1998) observation that previous research provides mixed messages about peak flow response to forest harvesting. Figure 33.2 reveals a tendency for increases in bankfull discharge to decrease with basin size, although unlike the water yield data in Figure 33.1 this trend was not statistically significant. Complete harvesting of basins did not necessarily produce larger percentage increases in bankfull peak flows relative to basins experiencing partial cuts. The data suggest that the smallest proportional increases in bankfull peak flows are in relatively wet landscapes (mean annual precipitation >1,200 mm), likely because such regions experience larger preharvest bankfull flows. Similar to the harvesting threshold noted for water yield increases, Guillemette et al. (2005)
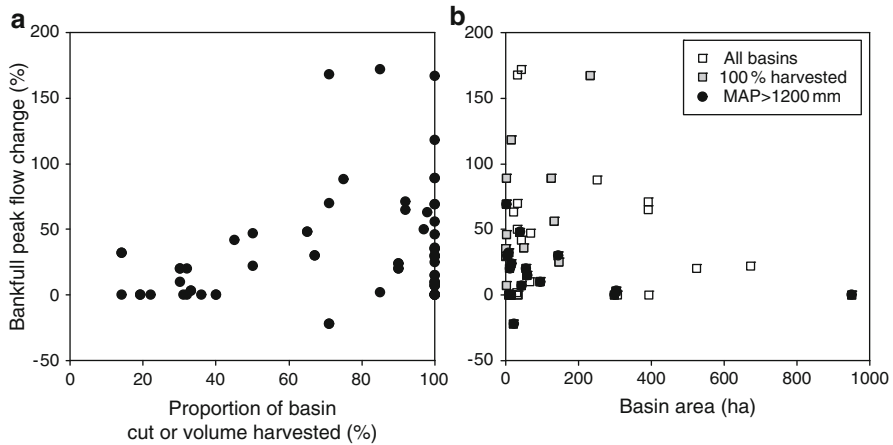
Fig. 33.2 (**a**) % change in bankfull peak flows versus % of basin cut or volume of standing timber harvested, based on experimental studies from around the world (data from Guillemette et al. 2005); (**b**) % change in bankfull peak flows versus basin area for all basins, basins with 100% of their area cut or volume of standing timber cut, and basins where mean annual precipitation (MAP) exceeds 1,200 mm (data from Guillemette et al. 2005)

suggest that harvesting should not exceed 50% of basin area in order to restrict increases in bankfull peak flows to <50% of preharvest values.

33.3.4 Low Flows

There is a general consensus that low flows increase following harvesting, with increased soil and groundwater recharge following forest removal leading to increase in groundwater discharge to streams (Best et al. 2007). Given that increased overland flow contributions to streamflow depend on the degree of compaction within the basin as well as sufficient hydrologic connectivity to allow such runoff to reach stream channels, the general increases in water yield that accompany forest harvesting have been largely been attributed to enhanced low flows (e.g., Hornbeck et al. 1993, 1997). However, Bruijnzeel (2004) sounds a cautionary note that variations in the degree of harvesting impact on soil infiltration properties mean that low flows may not necessarily increase in tropical and semitropical landscapes (particularly in regions with pronounced wet-dry seasonality in precipitation). Impeded infiltration will reduce recharge during the wet season, which in turn may lead to diminished low flows during the dry season relative to an unharvested condition.

The variability in the response of water yield, peak, and low flows (as well as other streamflow metrics not discussed here) to forest harvesting supports the National Research Council's (2008) conclusion: that while forest hydrologists have great confidence in their statements of the general hydrological response to forest harvesting, they cannot predict precisely how harvesting will affect hydrologic processes in areas that have not received intensive study.

33.4 Biogeochemical Aspects of Forest Harvesting

Forest harvesting can affect biogeochemical cycles in a variety of ways, such as through alterations of stream water temperatures, nutrient sinks and sources, soil temperature and humidity, changes in soil structure, and transport of nutrients and dissolved organic carbon (DOC) from organic soil surfaces to receiving waters (Carginan and Steedman 2000). The focus here will be on selected aspects of the water quality of streamflow draining harvested basins, which involves such parameters as temperature, concentrations of suspended sediment, major ions, nutrients such as N and P, cyanobacterial toxins, DOC, and dissolved O_2 (Mallik and Teichert 2009). Attempts to understand the effects of forest harvesting on these parameters must acknowledge their interconnected behavior. For example, water temperatures influence the chemical, biological, and ecological integrity of streams, such as through their control on streamwater dissolved O_2 (Bourque and Pomeroy 2001). These dissolved O_2 levels in turn influence the processing and form of nutrients such as N. It is also important to preface our examination of the biogeochemical aspects of forest harvesting by recognizing that the geologic, geomorphic, pedologic, vegetative, topographic, and management factors that exert a fundamental influence on interbasin differences in water movement will also control the response of a given basin to forest harvesting (Chanasyk et al. 2003; Gravelle et al. 2009).

33.4.1 Water Temperature

Stream water temperatures are influenced by such factors as stream aspect, water surface area, microclimatic conditions at the water surface, surface turbulence, channel morphology, source water temperature, stream water travel time, and upstream land use conditions (Mallik and Teichert 2009). Forest harvesting can impact several of these factors. For example, removal of riparian forest cover can increase solar radiation receipt at the water surface as well as wind speed and exposure to advected energy from nearby harvested areas, thus increasing stream temperatures, particularly in summer (Moore et al. 2005). Harvesting may also impact stream temperatures through increased discharge of groundwater into streams, although the exact nature of this effect depends on such factors as the influence of harvesting on the potential warming of shallow groundwater, and hyporheic exchanges of surface and subsurface waters.

33.4.2 Nutrients and Contaminants

Feller (2005) provides a valuable review of the solution chemistry (nutrients and contaminants) of forested streams (primarily in western North America) that summarizes the major factors controlling this chemistry that likely operate in all forest landscapes: geological weathering, atmospheric deposition and climate; precipitation acidity; terrestrial biological processes; physical/chemical reactions in the soil; and physical, chemical and biological processes within streams. Table 33.1 summarizes the anticipated change in concentrations of a subset of inorganic solutes examined by Feller (2005) resulting from forest harvesting impacts on these controlling factors. For example, the dominant controls on H^+ concentrations in streamflow are precipitation chemistry and physical–chemical reactions in the soil. Forest harvesting will likely lead to an increase in the H^+ concentration in net precipitation due to the reduction or elimination of H^+ exchange with cations on vegetated surfaces, while soil physical–chemical reactions will act to reduce H^+ concentrations after harvesting. As Table 33.1 highlights, the controls on nutrient and contaminant concentrations as well as the influence of harvesting on those controls and the direction of concentration response to harvesting differ between water quality parameters. There is often no consensus regarding how the concentration of a particular nutrient or contaminant will respond to the influence of forest harvesting on a given controlling factor (e.g., the effect of harvesting on the hydrologic factors controlling Al^{3+} concentrations), which partly reflects the variable nature of the controlling factors noted earlier. This also reinforces the need to consider preharvest site conditions when interpreting the biogeochemical response to harvesting (Dise and Gundersen 2004). Thus, McHale et al. (2007) found the response of Al concentrations to harvesting exceeded those reported previously, which they attributed to preceding decades of acid deposition that depleted exchangeable base cations and caused long-term soil acidification.

There is considerable evidence to suggest that there may be a lag between forest harvesting and the biogeochemical response of a particular water quality parameter. Figure 33.3 is adapted from Feller (2005), based on Vitousek and Reiners (1975). Assuming other factors remained the same, chemical fluxes through soils into streams would show an inverse pattern: a decrease after loss of vegetation from an initial value to a minimum (as a result of uptake by forest regrowth) followed by an increase to a dynamic equilibrium in old-growth forests. The magnitude of the minimum concentration attained would depend on whether the chemical was a nonessential, essential, or limiting nutrient. However, the partial picture provided by this ecologically based model of nutrient concentration response to forest harvesting would benefit from consideration of accompanying hydrochemical changes. This is illustrated by the fate of Cl⁻ following harvesting, which is not a limiting nutrient and whose concentrations in streamflow should not change significantly according to Figure 33.3. However, Oda et al. (2009) found that harvesting reduced Cl^- input to a maritime basin in Japan due to reduced dry deposition of Cl^- to vegetation. The resulting step shift in Cl^- inputs led to a

Table 33.1 Major factors governing stream chemistry in forest landscapes and suggested concentration response of selected nutrients and contaminants to harvesting effects on these governing factors (adapted from Feller 2005)

Factor	Al^{3+}	C (CO_3^{2-}, HCO_3^-)	Ca^{2+}	Cl^-	H^+	K^+	N (NO_3^-, NH_4^+)	P (PO_4^{3-}, HPO_4^{2-}, $H_2PO_4^-$)	Trace metals
1. Geological weathering	↑	↑	↑	–	↓	↑	↑–	↑	↑
2. Atmospheric precipitation/ climate									
(a) Precipitation chemistry	↑–	↓–	↑–	–	**↑–**	↑–	**↑–**	↑–	↑–
(b) Hydrologic influences	↑↓	↑↓	↑↓	–	↑↓	↑↓	–	↑↓	**↑↓**
(c) Temperature	↑	↑	↑	↑–	↑↓	↑	↑	↑	↑–
3. Terrestrial biological processes									
(a) Chemical uptake	–	–	↑	↑	↑	↑	**↑**	**↑**	–
(b) Chemical transformations	–	↑↓	–	–	↑↓	–	**↑↓**	–	–
(c) Production of soluble chemicals	–	↑–	↑–	↑	↑–	↑–	↑–	↑–	↑–
4. Physical/chemical reactions in the soil	**–**	↓	–	↓–	**↓–**	–	↓–	↓–	–
5. Processes within aquatic ecosystems	–								
(a) Ion exchange reactions	↑↓	–	↑↓	↑↓	↑↓	↑↓	↑↓	↑↓	**↑↓**
(b) Chemical redox reactions	↑↓	–	–	–	–	–	↑↓	–	↑↓
(c) Evaporation-crystallization									
(d) pH-induced transformations	↑–								
(e) Uptake by primary producers	↓	–	↓–	–	–	↓–	**↓–**	**↓–**	↓–
(f) Microbial transformations	–	–	–	–	–	–	**↑↓**	–	–

↑ harvesting effects on factor lead to an increase in concentration; ↓ harvesting effects on factor lead to a decrease in concentration; – harvesting effects on factor have little to no impact on concentration; bolded symbols indicate that the related factors are the primary and dominant control on concentration

decrease in Cl^- concentrations in streamflow. McHale et al. (2007) stress the importance of considering differences in water residence times for various hydrologic compartments when assessing biogeochemical response to harvesting. Thus, relatively long groundwater residence times mean that the chemical response
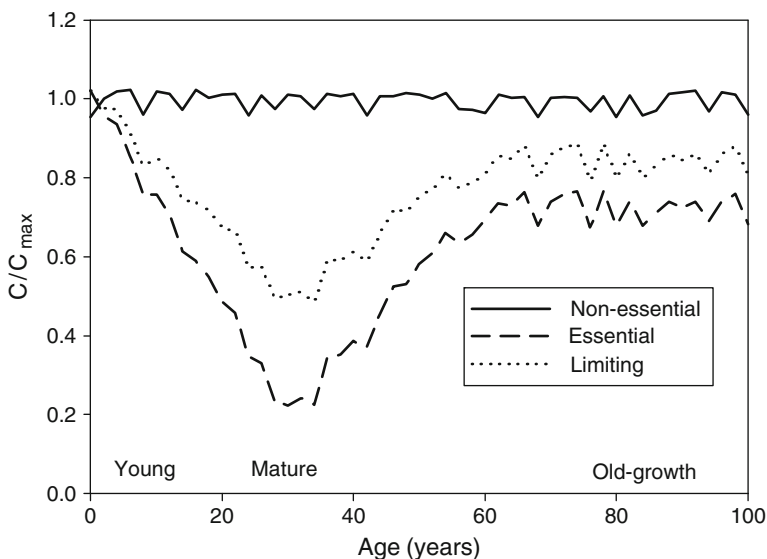
Fig. 33.3 Hypothesized changes in streamflow concentration (*C*) relative to maximum concentration (*C*$_{max}$) for nonessential, essential, and limiting chemicals after forest harvesting and throughout forest regrowth (adapted from Feller 2005)

can lag harvesting by several years while at the same time delaying system recovery, since streams may continue to receive contributions of nutrient-rich groundwater recharged immediately after harvesting while forest regrowth is returning soil water nutrient concentrations to preharvest conditions.

Two water quality parameters that deserve particular attention are N and Hg; N by virtue of its important role as a nutrient and Hg for its potential for accumulation in fish and the resulting implications for human health. Harvesting decreases N uptake by trees and can increase mineralization and nitrification rates, as has been noted elsewhere (e.g., Likens et al. 1969; Reuss et al. 1997). Loss of NO_3-N and other anions by leaching also leads to export of Ca, Mg, and K (Jewett et al. 1995) as well as Al from the basin after the harvest (McHale et al. 2007). However, others have found limited or no effects of harvesting on soil N transformations and litter decomposition (Brais et al. 2002; Westbrook et al. 2006) and have noted that harvesting may lead to reduced NO_3-N leaching (Van Miegroet and Johnson 2009). Conflicting results may be due to differences in such site factors as climate, vegetation, time since harvesting disturbance, type of machinery used for logging, and land use history (Pérez et al. 2009). Thus, Parfitt et al. (2002) found that nitrate-N leaching losses decreased after harvesting, which they attributed to increased weed growth and soil microbial biomass after harvesting that would have removed much of the N from soil solution in the upper soil layers. Microbial processes play a key role in mediating nutrient and element mobility from both harvested and undisturbed forest landscapes (Lindo and Visser 2003), and the effects of harvesting on the soil microbial biomass are often a key element in understanding how

harvesting affects nutrient and contaminant fluxes to streams. This is illustrated by the fate of Hg in harvested basins. Povari et al. (2003) found that clearcutting increased total Hg and methyl Hg (MeHg), partly in response to an increased flux of total organic carbon (TOC) from harvested areas. Hg accumulates in forest soils as a result of atmospheric deposition and Hg methylation may be stimulated by saturation of forest soils due to increased water availability following harvesting. Garcia and Carignan (2000) suggest that harvesting may enhance the transport of toxic MeHg to receiving waters, where it may accumulate in game fish and thus pose a threat to human health.

33.4.3 Sediments

Harvesting impacts on sediment transport to receiving waters must be considered from a biogeochemical as well as a geomorphological perspective, since sediment can be a stressor in its own right (e.g., in terms of its impacts on drinking water quality and its ability to impact fish spawning habitat in streams) and a vector for some contaminants (e.g., metals – Feller 2005) and nutrients (e.g., phosphorus – Gravelle et al. 2009). Sediments can be supplied to streams by surface erosion, mass movements, and bank erosion. It is generally acknowledged that harvesting alone does not substantially contribute to increased sediment fluxes unless severe and widespread disturbance occurs (Sidle et al. 2006). Instead, the primary sediment sources consist of logging roads, road crossings, and skidder trails (Sidle et al. 2004), augmented by such management activities as prescribed burning, scarification (Hetherington 1987), and ditching of forested wetlands for drainage (Prevost et al. 1999).

Sediment yields from harvested basins generally peak shortly after harvesting and decline as forest regrowth proceeds. However, as with nutrient and contaminant fluxes from harvested areas to streams, there may be a lag between harvesting and the period of maximum sediment supply to streams (Bruijnzeel 2004). This is particularly the case if mass movements represent a major vector of sediment transport in a forest landscape. Sidle et al. (2006) cite several studies noting increased landslide erosion roughly 3–15 years after harvesting, which appears to relate to the time required to allow root systems of harvested trees to decay and thus reduce root strength and slope resistance to mass movement. Thus, short-term monitoring of sediment transport after disturbance may give a distorted picture of forest management influences on sediment (Sidle et al. 2006).

33.5 Issues for Future Research

The intention here is not to provide an exhaustive list of issues to be considered in future research dealing with the hydrologic and biogeochemical aspects of forest harvesting, since many research issues raised in previous work are specific to

particular forest landscapes or forest management practices (e.g., the role, dimensions, and function of riparian management practices such as forest buffer zones – Neary et al. 2009). Instead, the goal is to identify common research needs that apply across regional and national scales. Such needs include:

1. Maintaining and expanding the monitoring networks of sites examining the long-term hydrologic and biogeochemical effects of forest harvesting (National Research Council 2008, Neary et al. 2009). Such networks will be of increasing scientific and societal value in the context of a changing climate and associated shifts in the intensity of other impacts on forests (e.g., fire, disease, insect infestations) (National Research Council 2008). A critical element of assessing the hydrologic and biogeochemical effects of harvesting in the context of climate change will require refinement of the "natural range of variability" of water quantity and quality in forest landscapes (Neary et al. 2009), which can be provided by the research results of these networks.

2. As part of (1), promoting mechanistic studies of the internal hydrologic and biogeochemical behavior of forest basins (Hubbart et al. 2007) in a wider range of forest landscapes than has been hitherto examined. The complex interactions between hydrology, chemistry, and ecology ensure that such studies are a vital component of basin studies (Mallik and Teichert 2009), while greater understanding of the role of such factors as climate, geology, and topography on hydrologic and biogeochemical behavior is key to interpreting results from paired-basin studies (Fuller et al. 1988). From a biogeochemical perspective, these mechanistic studies should be extended to include greater consideration of such factors as the effects of harvesting on the geological weathering release of chemicals, the behavior of trace metals, and in-stream processing of nutrients (Feller 2005).

3. Looking beyond harvesting effects on water yield to consider seasonal changes in streamflow and changes in the overall flow regime (Hubbart et al. 2007). Thus, Bruijnzeel (2004) identifies the "low flow problem" as the key research issue for studies of harvesting effects in tropical forests.

4. Assessing how the hydrologic and biogeochemical effects of harvesting change with scale. Sivapalan et al. (2003) note that the processes that dominate basin hydrologic behavior may change with changing scales, while Devito et al. (2005) emphasize that the scale at which dominant processes act to control a basin's hydrologic and biogeochemical behavior must be considered in order to determine the most suitable methodological and modeling strategies to apply to study harvesting impacts in a given region. For example, Sidle et al. (2006) outline the scale issue of sediment delivery from harvested areas: although increases in infiltration opportunities and storage generally lead to reductions in sediment yield with increasing basin size, this may be countered by a change in the dominant sediment delivery process with scale (e.g., gully development, mass wasting) that might produce an increase in yield with scale.

5. Determining the long-term cumulative effects of forest harvesting in the context of other land use/land cover changes. The National Research Council (2008) argues for a landscape-scale approach to relate downstream conditions to

upstream changes in forest conditions, which will require spatially explicit modeling that identifies, connects, and aggregates temporal changes in hydrologic and biogeochemical behavior due to forest disturbance and management at larger spatial scales.

6. Improving our ability to translate the results from experimental basins to other sites within the same forest landscape and between differing landscapes (Best et al. 2007, National Research Council 2008). This will involve an increased integration of stand and paired basin-scale mechanistic studies with modeling of basin hydrologic and biogeochemical response to forest harvesting (Bruijnzeel 2004).

References

Adams KN, Fowler AM (2006) Improving empirical relationships for predicting the effect of vegetation change on annual water yield. J Hydrol 321:90–115

Avissar R, Silva Dias PL, Silva Dias MA et al (2002) The large scale biosphere atmosphere experiment in Amazonia (LBA). Insights and future research needs. J Geophys Res 107:8086. doi:10.129/2002JD002704

Bent GC (2001) Effects of forest-management activities on runoff components and ground-water recharge to Quabbin reservoir, central Massachusetts. For Ecol Manage 143:115–129

Best A, Zhang L, McMahon T, et al (2007) A critical review of paired catchment studies with reference to seasonal flows and climatic variability. Murray Darling Basin Commission Publication 11/03, Murray-Darling Basin Commission, Canberra, ACT, Australia

Bonell M (2005) Runoff generation in tropical forests. In: Bonell M, Bruijnzeel LA (eds) Forests, water and people in the humid tropics. UNESCO Cambridge University Press, Cambridge, UK, pp 314–406

Bonell M, Gilmour DA (1978) The development of overland flow in a tropical rainforest catchment. J Hydrol 39:365–382

Bosch JM, Hewlett JA (1982) A review of catchment experiments to determine the effect of vegetation changes on water yield and evapotranspiration. J Hydrol 55:3–23

Bourque CP-A, Pomeroy JH (2001) Effects of forest harvesting on summer stream temperatures in New Brunswick, Canada: an inter-catchment, multiple-year comparison. Hydrol Earth Syst Sci 5:599–613

Brais S, Paré D, Camiré C et al (2002) Nitrogen net mineralization and dynamics following whole-tree harvesting and winter windrowing on clayed sites in northwestern Quebec. For Ecol Manage 157:119–130

Bruijnzeel LA (1988) (De)forestation and dry season flow in the tropics: a closer look. J Trop For Sci 2:229–243

Bruijnzeel LA (2004) Hydrological functions of tropical forests: not seeing the soil for the trees? Agric Ecosyst Environ 104:185–228

Buttle JM, Metcalfe RA (2000) Boreal forest disturbance and streamflow response, northeastern Ontario. Can J Fish Aquat Sci 57(suppl 2):5–18

Buttle JM, Creed IF, Moore RD (2005) Advances in Canadian forest hydrology, 1999–2003. Hydrol Proc 19:169–200

Buttle JM, Creed IF, Moore RD (2009) Advances in Canadian forest hydrology, 2003–2007. Can Wat Resour J 34:113–126

Carginan R, Steedman RJ (2000) Impacts of major watershed perturbations on aquatic ecosystems. Can J Fish Aquat Sci 57(Suppl 2):1–4

Chanasyk DS, Whitson IR, Mapfumo E et al (2003) The impacts of forest harvest and wildfire on soils and hydrology in temperate forests: a baseline to develop hypotheses for the Boreal Plain. J Environ Eng Sci 2:51–62

Chang M (2003) Forest hydrology: an introduction to water and forests. CRC, Boca Raton, FL

Cook PG, Walker GR, Jolly ID (1989) Spatial variability of groundwater recharge in a semiarid region. J Hydrol 111:195–212

da Silva R, Avissar R (2006) The hydrometeorology of a deforested region of the Amazon basin. J Hydrometeorol 7:1028–1042

Devito KJ, Creed IF, Rothwell RL et al (2000) Landscape controls on phosphorus loading to boreal lakes: implications for the potential impacts of forest harvesting. Can J Fish Aquat Sci 57:1977–1984

Devito K, Creed I, Gan T et al (2005) A frame work for broad-scale classification of hydrologic response units on the boreal plain: is topography the last thing to consider? Hydrol Proc 19:1705–1714

Díaz MF, Bigelow S, Armesto JJ (2007) Alteration of the hydrologic cycle due to forest clearing and its consequences for rainforest succession. For Ecol Manage 244:32–40

Dise NB, Gundersen P (2004) Forest ecosystem responses to atmospheric pollution: linking comparative with experimental studies. Water Air Soil Poll Focus 4:207–220

Dunne T (1978) Field studies of hillslope flow processes. In: Kirkby MJ (ed) Hillslope hydrology. Wiley, Chichester, pp 227–293

Feller MC (2005) Forest harvesting and streamwater inorganic chemistry in western North America: a review. J Am Water Resour Assoc 41:785–811

Fuller RD, Simone DM, Driscoll CT (1988) Forest clearcutting effects on trace metal concentrations: spatial patterns in soil solutions and streams. Water Air Soil Poll 40:185–195

Garcia E, Carignan R (2000) Mercury concentrations in northern pike (*Esox lucius*) from boreal lakes with logged, burned or undisturbed catchments. Can J Fish Aquat Sci 57(Suppl 2):97–104

Gary HL, Watkins RK (1985) Snowpack accumulation before and after thinning a dog-hair stand of Lodgepole pine. U.S. Department of Agriculture Forest Service Resources Note RM-450, Rocky Mountain Forest and Range Experimental Station, Fort Collins, CO

Gravelle JA, Ice G, Link TE et al (2009) Nutrient concentration dynamics in an inland Pacific Northwest watershed before and after timber harvest. For Ecol Manage 257:1663–1675

Guillemette F, Plamondon AP, Prevost M et al (2005) Rainfall generated stormflow response to clearcutting a boreal forest: peak flow comparison with 50 world-wide basin studies. J Hydrol 302:137–153

Hamilton LS (1985) Overcoming myths about soil and water impacts of tropical forest land uses. In: El-Swaify SA, Moldenhauer WC, Lo A (eds) Soil erosion and conservation. Soil Conservation Society of America, Ankey, IA, pp 680–690

Harr RD (1982) Fog drip in the Bull Run Municipal Watershed, Oregon. Water Resour Bull 18:785–789

Henderson-Sellers A, Pitman AJ (2002) Comments on "Suppressing impacts of the Amazonian deforestation by the global circulation change". Bull Am Meteorol Soc 83:1657–1661

Hetherington ED (1987) The importance of forests in the hydrological regime. In: Healy MC, Wallace RR (eds) Canadian aquatic resources, Canadian bulletin of fisheries and aquatic sciences 215. Department of Fisheries and Oceans, Ottawa

Hibbert AR (1967) Forest treatment effects on water yield. In: Sopper WE, Lull HW (eds) Proceedings of international symposium on forest hydrology, Pennsylvania State University, 1965. Pergamon, New York, pp 527–543

Hornbeck JW, Adams MB, Corbett ES et al (1993) Long-term impacts of forest treatments on water yield: a summary for northeastern USA. J Hydrol 150:323–344

Hornbeck JW, Martin CW, Eagar C (1997) Summary of water yield experiments at Hubbard Brook experimental forest, New Hampshire. Can J For Res 27:2043–2052

Hubbart JA, Link TE, Gravelle JA et al (2007) Timber harvest impacts on water yield in the continental/maritime hydroclimatic region of the United States. For Sci 53:169–180

Jewett K, Daugharty D, Krause HH et al (1995) Watershed responses to clear cutting effects on soil solutions and stream water discharge in central New Brunswick. Can J Soil Sci 75:475–490

Jones JA, Grant GE (1996) Peak flow responses to clear-cutting and roads in small and large basins, western Cascades, Oregon. Wat Resour Res 32:959–974

Kittredge J (1948) Forest influences. McGraw Hill, New York

Lawton RO, Nair US, Pielke RA Jr et al (2001) Climatic impact of tropical lowland deforestation on nearby montane cloud forests. Science 294:584–587

Likens GE, Bormann FH, Johnson NM (1969) Nitrification: importance to nutrient losses from a cutover forested ecosystem. Science 163:1205–1206

Lindo Z, Visser S (2003) Microbial biomass, nitrogen and phosphorus mineralization, and meso-fauna in boreal conifer and deciduous forest floors following partial and clear-cut harvesting. Can J For Res 33:1610–1620

Loftis JC, MacDonald LH, Streett S et al (2001) Detecting cumulative watershed effects: the statistical power of pairing. J Hydrol 251:49–64

Mallik A, Teichert S (2009) Effects of forest management on water resources in Canada: a research review. NCASI Technical Bulletin No. 969. December 2009

Marland G, Pielke RA Jr, Apps M et al (2003) The climatic impacts of land surface change and carbon management, and the implications for climate-change mitigation policy. Clim Pol 3:149–157

McHale MR, Burns DA, Lawrence GB et al (2007) Factors controlling soil water and stream water aluminum concentrations after a clearcut in a forested watershed with calcium-poor soils. Biogeochem 84:311–331

Moore RD, Wondzell SM (2005) Physical hydrology and the effects of forest harvesting in the Pacific Northwest: a review. J Am Water Resour Assoc 41:763–784

Moore RD, Spittlehouse DL, Story A (2005) Riparian microclimate and stream temperature response to forest harvesting: a review. J Am Water Resour Assoc 41:813–834

Murray CD, Buttle JM (2003) Impacts of clearcut harvesting on snow accumulation and melt in a northern hardwood forest. J Hydrol 271:197–212

National Research Council of the National Academies (2008) Hydrologic effects of a changing forest landscape. The National Academies Press, Washington, DC

Neary DG, Ice GG, Jackson CR (2009) Linkages between forest soils and water quality and quantity. For Ecol Manage 258:2269–2281

Oda T, Asano Y, Suzuki M (2009) Transit time evaluation using a chloride concentration input step shift after forest cutting in a Japanese headwater catchment. Hydrol Proc 23:2705–2713

Parfitt RL, Salt GJ, Hill LF (2002) Clear-cutting reduces nitrate leaching in a pine plantation of high natural N status. For Ecol Manage 170:45–53

Peck AJ, Williamson DR (1987) Effects of forest clearing on groundwater. J Hydrol 94:47–65

Pereira HC (1973) Land use and water resources in temperate and tropical climates. Cambridge University Press, London

Pérez CA, Carmona MR, Farina JM et al (2009) Selective logging of lowland evergreen rainforests in Chiloé Island, Chile: Effects of changing tree species composition on soil nitrogen trans-formations. For Ecol Manage 258:1660–1668

Peters DL, Buttle JM, Taylor CH et al (1995) Runoff production in a forested, shallow soil Canadian Shield basin. Wat Resour Res 31:1291–1304

Pomeroy JW, Parviainen J, Hedstrom NR et al (1998) Coupled modelling of forest snow intercep-tion and sublimation. Hydrol Proc 12:2317–2337

Pomeroy JW, Gray DM, Hedstrom NR et al (2002) Prediction of seasonal snow accumulation in cold climate forests. Hydrol Proc 16:3543–3558

Povari P, Verta M, Munthe J et al (2003) Forestry practices increase mercury and methyl mercury output from boreal forest catchments. Environ Sci Technol 37:2389–2393

Prevost M, Plamondon AP, Belleau P (1999) Effects of drainage of a forested peatland on water quality and quantity. J Hydrol 214:130–143

Reuss JO, Stottlemeyer R, Troendle CA (1997) Effect of clear cutting on nutrient fluxes in a subalpine forest at Fraser, Colorado. Hydrol Earth Syst Sci 1:333–344

Roth BE, Slatton KC, Cohen MJ (2007) On the potential for high-resolution lidar to improve rainfall interception estimates in forest ecosystems. Front Ecol Environ 5:421–428

Sahin V, Hall MJ (1996) The effects of afforestation and deforestation on water yields. J Hydrol 178:293–309

Salati E, DaU'Olio A, Matsui E et al (1979) Recycling of water in the Amazon Basin: an isotopic study. Water Resour Res 15:1250–1258

Scott DF (1997) The contrasting effects of wildfire and clearfelling on the hydrology of a small catchment. Hydrol Proc 11:543–555

Sidle RC, Sasaki S, Otsuki M et al (2004) Sediment pathways in a tropical forest: effects of logging roads and skid trails. Hydrol Proc 18:703–720

Sidle RC, Ziegler AD, Negishi JN et al (2006) Erosion processes in steep terrain – Truths, myths, and uncertainties related to forest management in Southeast Asia. For Ecol Manage 224:199–225

Sivapalan M, Takeuchi K, Franks SW et al (2003) IAHS Decade on Predictions in Ungauged Basins (PUB), 2003–2012: shaping an exciting future for the hydrological sciences. Hydrol Sci 48:857–880

Smerdon BD, Redding TE, Beckers J (2009) An overview of the effects of forest management on groundwater hydrology. BC J Ecosyst Manage 10:22–44

Stednick JD (1996) Monitoring the effects of timber harvest on annual water yield. J Hydrol 176:79–95

Stieglitz M, Shaman J, McNamara J et al (2003) An approach to understanding hydrologic connectivity on the hillslope and the implications for nutrient transport. Glob Biogeochem Cycles 17:1105. doi:10.1029/2003GB002041

Stottlemyer R, Troendle CA (1999) Effect of subalpine canopy removal on snowpack, soil solution, and nutrient export, Fraser Experimental Forest, CO. Hydrol Proc 13:2287–2299

Sun G, McNulty SG, Shepard JP et al (2001) Effects of timber management on the hydrology of wetland forests in the southern United States. For Ecol Manage 143:227–236

Thomas RB, Megahan WF (1998) Peak flow responses to clear-cutting and roads in small and large basins, western Cascades, Oregon: a second opinion. Water Resour Res 34:3393–3403

Troendle CA, Meiman JR (1984) Options for harvesting timber to control snowpack accumulation. Proc West Snow Conf 52:86–97

Van Dijk AIJ, van Noordwijk M, Calder IR et al (2009) Forest-flood relation still tenuous – comment on 'Global evidence that deforestation amplifies flood risk and severity in the developing world' by C.J.A. Bradshaw, N.S. Sodi, K.S.-H. Peh and B.W. Brook. Glob Change Biol 15:110–115

Van Miegroet H, Johnson DW (2009) Feedbacks and synergism among biogeochemistry, basic ecology, and forest soil science. For Ecol Manage 258:2214–2223

Vanclay JK (2009) Managing water use from forest plantations. For Ecol Manage 257:385–389

Vitousek PM, Reiners WA (1975) Ecosystem succession and nutrient retention: a hypothesis. Bioscience 25:376–381

Waterloo MJ, Schellekens J, Bruijnzeel LA et al (2007) Changes in catchment runoff after harvesting and burning of a *Pinus caribaea* plantation in Viti Levu, Fiji. For Ecol Manage 251:31–44

Wemple BC, Jones JA, Grant GE (1996) Channel network extension by logging roads in two basins, western Cascades, Oregon. Water Resour Bull 32:1195–1207

Westbrook C, Devito KJ, Allan CJ (2006) Soil N cycling in harvested and pristine boreal forests and peatlands. For Ecol Manage 234:227–237

Whitehead PG, Robinson M (1993) Experimental basin studies – an international and historical perspective of forest impacts. J Hydrol 145:217–230

Whitson IR, Chanasyk DS, Prepas EE (2003) Hydraulic properties of Orthic Gray Luvisolic soils and impact of winter logging. J Environ Eng Sci 2:S41–S49

Chapter 34
The Cycling of Pollutants in Nonurban Forested Environments

Elena Vanguelova, Brian Reynolds, Tom Nisbet, and Douglas Godbold

34.1 Introduction

Forests are complex ecosystems which respond to external inputs of pollutants in a variety of ways. Quantifying changes in the storage of pollutants within ecosystem pools and the biogeochemical fluxes between them provides a means of calculating the overall pollutant balance of a forest ecosystem as an indicator of its sustainability and health. This chapter focuses on pollutant cycling in nonurban forest ecosystems with specific attention on quantification of external inputs, pollutant fluxes and pools within forests and exports to adjacent systems (Fig. 34.1). Selected case studies are used to exemplify the approach and illustrate the importance of location, forest type, management practices such as harvesting and soil conditions. Direct pollutant impacts on forest ecosystem functioning, the effects of intensified biomass utilization, and interactions between climate and pollutant cycling are also discussed.

34.2 Pollutants Sources and Trends

Many pollutants, acting alone or in combination, affect forests of which sulfur, nitrogen, and heavy metals are most relevant to impacts on nonurban forest ecosystems. Sulfur and nitrogen are essential nutrients, which only become "pollutants" above a critical concentration or load. Sulfur dioxide is emitted to the atmosphere from combustion of fossil fuels, with the combustion of coal being the dominant source. The main sources of nitrogen oxide emissions are fossil fuel combustion, road transport, and the generation of electricity and heat. Ammonia is primarily emitted to the atmosphere as a result of intensive animal husbandry.

Some heavy metals such as copper (Cu), iron (Fe), manganese (Mn), and zinc (Zn) are essential micronutrients for plant health and have natural and pollution sources, while others such as cadmium (Cd), chromium (Cr), lead (Pb), mercury (Hg), nickel (Ni), silver (Ag), thallium (TI), and vanadium (V) are nonessential and are known to pose a significant risk to forest ecosystem health. Emissions to the atmosphere of heavy metals arise from a wide range of sources. Trace quantities (Hg, V) are found in fossil fuels such as Hg in coal and V in oil,

a

Deposition
5.1 (36)

Translocation
−1.7 (−6)

Foliage
26 (11)

Wood increment
0.06 (1.1)

Litterfall
1.8 (2)

Throughfall + stemflow
7.1 (40)

Stem & bole
47 (130)

Understory
0.6 (6)

Forest floor
59 (251)

Roots
26.1 (13)

Uptake
3.1(10)

Organic sulphur in
mineral soil
1205 (1023)

Mineralisation

Soil solution
31 (132)

Inorganic
sulphate in
mineral soil
197 (219)

Imobilisation

Leaching
4.8 (33)
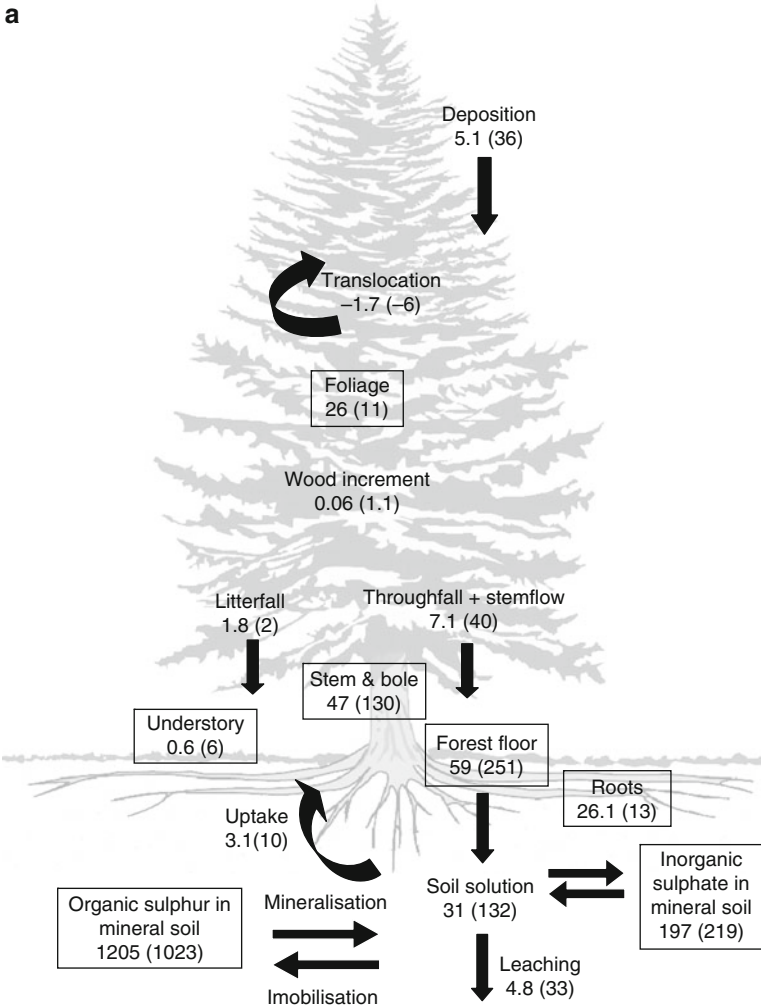
Fig. 34.1 (continued)

while a number of industrial processes emit specific metals, for example, Cd from road transport and Cu, Ni, Pb, and Zn from smelting. The largest source of arsenic (As) is the burning of treated wood.

During the last 3 decades, much attention has been devoted to the ecosystem effects of acid rain arising from the emission of sulfur and nitrogen compounds (SO_2, NOx, and NH_3) into the atmosphere (Schulze et al. 1989; Johnson and Lindberg 1992). The resulting detrimental changes to sensitive terrestrial and freshwater ecosystems led to national and international policies aimed at reducing emissions of acidifying pollutants. For example, in Europe targeted emissions reductions were agreed as part of the Gothenburg Protocol in 1999, (Jenkins and Cullen 2001) and

b

Deposition
4 (28)

Translocation Foliar Uptake
4 (18)   2 (6)

Foliage
271 (120)

Wood in crement
2.5 (2)

Litterfall
17 (8.5)

Throughfall + stemflow
2 (22)

Stem & bole
410 (154)

Understory
8 (85)

Forest floor
525 (2165)

Roots
228 (110)

Uptake
10 (8)

Mineralisation

Soil
6900 (9040)

Imobilisation

Leaching
<1(21)
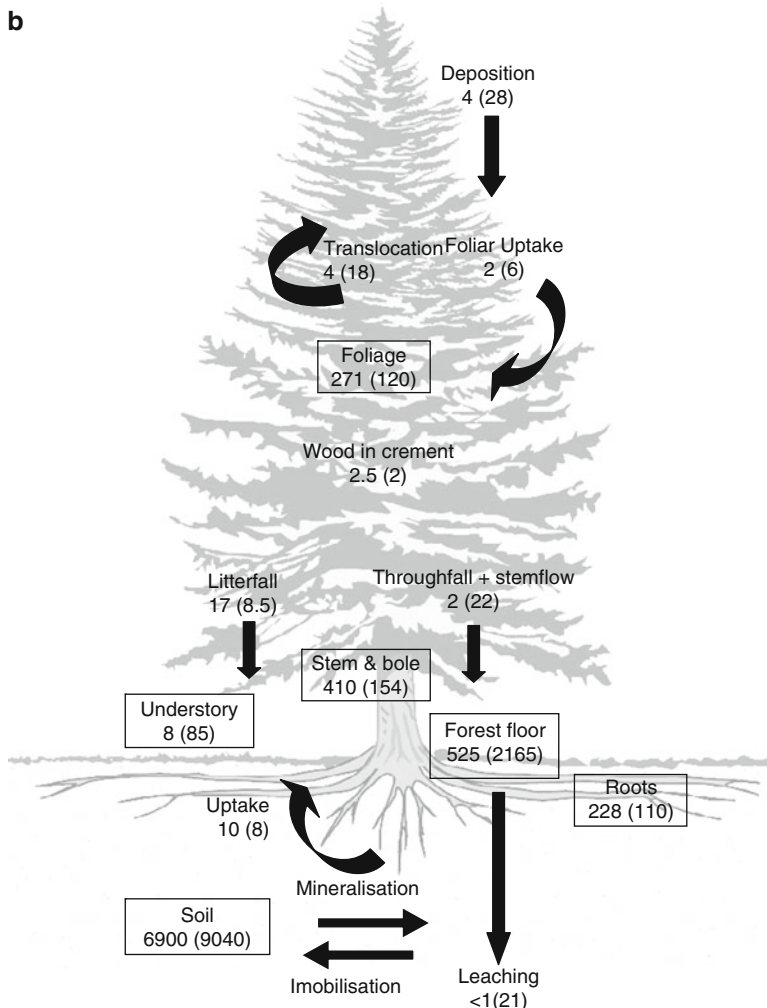
Fig. 34.1 Generalized diagram comparing (**a**) sulfur (S) and (**b**) nitrogen (N) pools and fluxes in *unpolluted* Findley Lake conifer forest site in Washington and *polluted* Smokies Tower conifer forest site at Great Smoky Mountains National Park site (values in *brackets*) [data from Mitchell (1992), Van Miegroet et al. (1992)]. Pools are in *boxes* and in kg S ha^{-1} and kg N ha^{-1} and fluxes are expressed in kg S ha^{-1} y^{-1} and kg N ha^{-1} y^{-1} and flux movement indicated with *arrows*

increasingly policies have adopted a more efficient effect-based approach using steady-state and dynamic acidification and nutrient balance critical loads models (e.g., SMART2, SAFE, MAGIC dynamic models reviewed by de Vries et al. 2010).

Emission control policies adopted under the UN Economic Commission for Europe and the EU have been very successful at reducing European sulfur emissions, which have fallen by 70% since 1981 (ICP report 2009). Emissions are expected to continue to decrease over the next 10–15 years with current policy

agreements and are likely to be less than 10% of 1980 levels by 2020. Nitrogen oxides emissions are decreasing more slowly but by 2010 should be around 70% lower compared to 1990. Ammonia emission reductions have been small to date and expected to fall 40% by 2020.

Evidence for the success of emission control policies is seen at over three-quarters of the European Level II forest intensive monitoring plots (about 500 plots), which now receive inputs of acidity below the critical load. Further progress is dependent on coordinated action to achieve significant reductions in sulfur emissions from shipping (RoTap 2011). In contrast, the deposition of nitrogen has changed little and nutrient critical loads remain exceeded on two-thirds of the monitoring plots (ICP report 2009). In some parts of Europe and North America, emission reductions of oxidized N are contributing to a stabilization or decline in nitrogen deposition, but there is currently limited control of emissions of reduced N (Emmett 2007). Although total deposition is declining linearly in line with emissions, the partitioning between wet and dry deposition is expected to change (Fowler et al. 2005, 2007). This will ensure that N will continue to have a significant impact for some time to come in many regions (Galloway et al. 2003; Vanguelova et al. 2007a) in combination with other pollutants such as tropospheric ozone (Taylor et al. 1994).

A related concern is the significant rise in precipitation and throughfall dissolved organic nitrogen (DON) concentrations observed in the short period between 2000 and 2006 at a number of forest monitoring sites in the UK, further complicating our understanding of nitrogen biogeochemistry in forest ecosystems. The source of DON in precipitation is uncertain (Ham and Tamiya 2007; Vanguelova et al. 2010), and evidence for long-term temporal changes in rainwater organic nitrogen concentrations is ambiguous (Cornell et al. 2003).

For many years, atmospheric inputs of heavy metals resulting from air pollution remained very high and continued to increase until the late 1980s, especially around local point sources (Nriagu 1979; Bergkvist et al. 1989). Within the UK, the National Emissions Inventory, which provides spatially disaggregated emissions data for a large number of metals, has shown significant decreases since 1990 in emissions of Pb, Cd, and Hg in compliance with the 1998 UNECE Protocol on Heavy Metals plus national and local legislation. In Finland between 1985 and 2000, deposition of all heavy metals decreased, with Pb (78%), V (70%), and Cd (67%) showing the strongest reductions, while the concentrations of other heavy metals decreased by 16–34% (Poikolainen et al. 2004).

34.3 Pollutant Cycling in Nonurban Forest Ecosystems

34.3.1 Precipitation, Throughfall, and Stemflow Inputs

The quantity of pollutants deposited from the atmosphere onto rural forests depends on a wide range of factors including distance to local emission sources, amount of precipitation, altitude, and forest type. Geographical region has a dominant influence

Table 34.1 Averaged annual total deposition fluxes of inorganic sulfur and nitrogen in 1997 in different geographical regions (adapted from de Vries et al. 2003)

Region	Total deposition flux (molc ha^{-1} y^{-1})		
	SO$_4$	NO$_3$	NH$_4$
North/Boreal	233	84	156
North/Boreal temperate	399	172	250
South/Mediterranean	562	394	805
West Atlantic	912	431	1104
Central and East	941	757	1101
Region	Total deposition flux (kg ha^{-1} y^{-1})		
	SO$_4$	NO$_3$	NH$_4$
North/Boreal	2.43	1.36	8.64
North/Boreal temperate	4.16	2.78	13.85
South/Mediterranean	5.85	6.36	44.60
West Atlantic	9.50	6.95	61.16
Central and East	9.80	12.21	61.00

Table 34.2 Median hydrological fluxes (mm) calculated for 121 ICP Intensive Forest Monitoring plots in Europe (adapted from van der Salm et al. 2007)

Tree species	Calculated water fluxes (mm)		Transpiration	Soil evaporation	Leaching
	Precipitation	Interception			
Pines	602	152	328	55	17
Spruce	943	303	365	27	192
Oak	777	202	340	99	169
Beech	876	241	358	82	135
Others	1233	437	483	9	218
All	846	247	356	57	136

on the deposition of sulfur and nitrogen in Europe (Table 34.1, de Vries et al. 2003), with a highly significant positive correlation between atmospheric deposition and rainfall amount reflecting the importance of water flux. The generally high water use of trees, mainly due to canopy interception, leads to a marked reduction in water flux and enhanced pollutant concentrations in throughfall (Nisbet 2005). Interception loss varies between forest types and tree species typically ranging between 25 and 45% of annual rainfall for conifers and 10–25% for broadleaves (Calder et al. 2003). Forest transpiration brings about a further reduction in water flux through the soil, and while losses are rather constant among tree species, they significantly differ between climatic zones (Table 34.2, van der Salm et al. 2007).

Pollutant fluxes in throughfall (Fig. 34.1) reflect a mixture of wet, occult, and dry deposition, modified by canopy exchange. Forests are particularly efficient at scavenging pollutants via dry and occult deposition due to their aerodynamically rough canopies (Fowler et al. 1989). Bulk deposition inputs of total N and sulfur are highly positively correlated with throughfall, which is much enriched compared with rainfall (Vanguelova et al. 2010; Fig. 34.2). Sulfate concentrations in throughfall can be two to three times higher than those in rainfall due to canopy
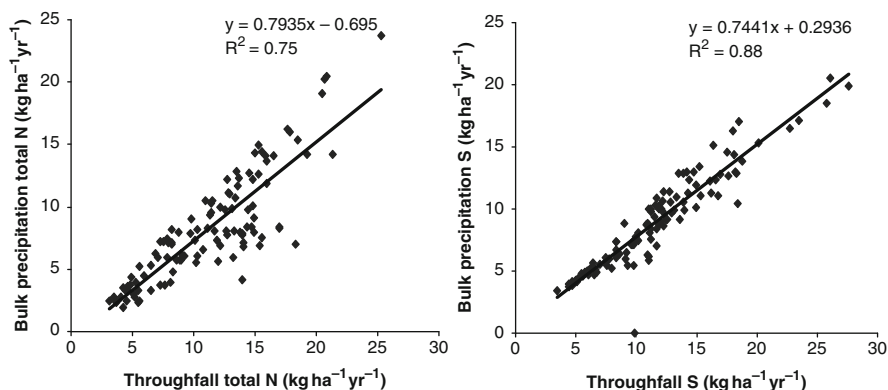
Fig. 34.2 Relationships between throughfall and bulk precipitation total N and S deposition in the UK ICP forest plots (adapted from Vanguelova et al. 2010)

evaporation, pollutant scavenging, and the leaching of internal plant sulfur from foliage (Nyborg et al. 1977; Lindberg and Garten 1988). Ammonia is readily absorbed directly into the foliage and its effect on throughfall nitrogen flux is very marked close to agricultural emission sources. A strong deposition gradient has been observed in a number of studies, with nitrogen fluxes in throughfall decreasing linearly with increasing distance from farm sources, with an edge effect extending to about 200 m (Vanguelova and Pitman 2009). In arid areas such as parts of California, dry N deposition is usually of greater magnitude than wet deposition. Occult deposition can also be marked in areas, where seasonal fogs and N pollution sources coincide. This has resulted in very large nitrogen inputs ($25-45 \, \text{kg ha}^{-1} \, \text{y}^{-1}$) to the most highly exposed forests in the Los Angeles Air Basin (Bytnerowicz and Fenn 1996). Only in very low N deposition areas (e.g., total N deposition of $2-3 \, \text{kg ha}^{-1} \, \text{y}^{-1}$), such as in Finland, do tree canopies tend to retain more N than they capture by dry deposition, due to uptake by epiphytic lichens, microbial immobilization within the canopy, N sorption into foliage and assimilation by leaves and stems (Mustajärvi et al. 2008).

Background deposition of heavy metals tends to be very low (Nriagu 1989; Table 34.3) and assumed to be evenly distributed over the earth's surface (Tipping et al. 2006). In industrialized countries, even in rural areas, metal deposition to forests is above background (Table 34.3) and can be very high closer to urban and industrial centers. Throughfall metal fluxes are generally enhanced compared to bulk precipitation due to a range of processes. For holm oak in NE Spain, canopy leaching was the dominant process for Mn, dry deposition for Cu, Pb, Zn, Cd, and V, and canopy uptake for Cd (Avila and Rodrigo 2004).

Stemflow generally contributes a small, but locally significant, amount to the total volume of water entering the soil profile. Stemflow volume depends on forest age, tree species, and tree spacing. For example, relative stemflow (expressed as a% of gross rainfall) can be as low as 0.1–1.3% in *Quercus* species (Arcangeli 2007) but as high as 14% in 20-year-old *Picea sinthensis* stands (Nisbet and Nisbet 1992).

Table 34.3 Heavy metal deposition values in different regions and levels of pollution

	Total deposition input (g ha^{-1} y^{-1})					References
	Pb	Cd	Ni	Cu	Zn	
Pristine areas (bulk precipitation)	7.6	0.2	1	2.3	23.5	Nriagu (1989)
Urban forestry/close to industry (NE Spain)						
Bulk precipitation	7	nd	nd	6	222	Avila and Rodrigo (2004)
Throughfall	20	nd	nd	32	415	Avila and Rodrigo (2004)
Coniferous forest (Germany)						
Bulk precipitation	nd	nd	nd	nd	140	Herrmann et al. (2006)
Throughfall	nd	nd	nd	nd	290	Herrmann et al. (2006)
Broadleaved forest (Germany)						
Bulk precipitation	nd	nd	nd	nd	140	Herrmann et al. (2006)
Throughfall	nd	nd	nd	nd	580	Herrmann et al. (2006)
Rural broadleaved forest (UK)						
Bulk precipitation	9	1	5	12	146	ICP forest UK[a]
Throughfall	16	1	10	39	247	ICP forest UK[a]
Rural conifer forest (UK)						
Bulk precipitation	14	1	8	16	210	ICP forest UK[a]
Throughfall	19	2	10	35	312	ICP forest UK[a]
Broadleaved forest close to industry (UK)						
Bulk precipitation	20	3	11	17	221	ICP forest UK[a]
Throughfall	31	3	16	43	445	ICP forest UK[a]
Conifer forest close to industry (UK)						
Bulk precipitation	21	1	12	29	308	ICP forest UK[a]
Throughfall	28	2	16	48	467	ICP forest UK[a]

[a]Forest Research – ICP Forest UK (Unpublished data)

Although stemflow volume may be small, fluxes of pollutants can be relatively high due to evaporation concentration, scavenging and leaching effects (Hornung et al. 1987). The localized nature of stemflow inputs at the tree base could also promote rapid routing through the soil and delivery of pollutants to watercourses.

34.3.2   Soil Weathering Inputs

Mineral weathering is considered to be the dominant, long-term, acid-neutralizing process in terrestrial systems and is a central component of steady-state and dynamic models used to determine soil critical loads of acidity and predict the biogeochemical response of forests to acid deposition. Soil weathering rates are mainly governed by geology, soil mineralogy, and climate. Empirical estimates (Table 34.4) are based on the assumption that the weathering rate directly reflects the mix of minerals present in the soil parent material. The evidence supports this case for areas dominated by igneous and metamorphic rocks, where soil mineral suites consist predominantly of primary minerals inherited from the parent material,

Table 34.4 The relationship between parent material and soil weathering rate (adapted from Nilsson and Grennfelt 1988)

Parent Rock	Mineral controlling weathering	eq H^+ ha^{-1} a^{-1}
Granite	Quartz	<200
Quartzite	K-feldspar	
Granite	Muscovite	200–500
Gneiss	Plagioclase	
	Biotite (<5%)	
Granodiorite	Biotite	500–1,000
Greywacke	Amphibole (<5%)	
Schist		
Gabbro		
Gabbro	Pyroxene	1,000–2,000
Basalt	Epidote	
	Olivine (<5%)	
Limestone	Carbonates	>2,000
Marl		
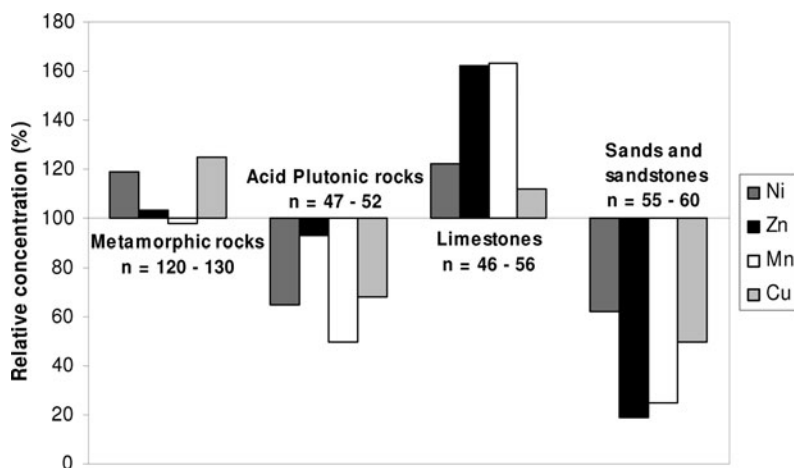
Fig. 34.3 Impacts of parent material on trace metal concentrations in the mineral soil surface layer (average values in mg kg^{-1}, corresponding to 100%, are Ni: 27, Zn: 58, Mn: 638, Cu: 18; n = number of observations) (from Vanmechelen et al. 1997, reproduced with permission)

but is more uncertain in areas dominated by noncalcareous sedimentary parent materials containing a significant proportion of pedogenic clays (Loveland 1993).

Heavy metals are present in all uncontaminated soils as the result of weathering from soil parent material. Metal availability depends on the nature of the parent rock and its ease of weathering (Fig. 34.3). Thus, forests developed on soils derived from sandstones and acid plutonic rocks may exhibit micronutrient deficiencies because of the limited supply of trace elements from weathering. In contrast, Cr and Ni can occur in very large concentrations in some soils derived from

ultrabasic rocks and may in part account for the inherent infertility of these soils (Soon and Abboud 1993). Elements, whose main source in the soil is the parent material, can accumulate to high levels in subsoils, while concentrations in organic matter remain small (Ross 1994). Carbonate minerals are able to adsorb certain heavy metals, such as Zn (Jurinak and Bauer 1956), Mn (McBride 1979), and Cd (McBride 1980). The concentrations of these elements, which are often present in trace quantities in limestone, may be strongly influenced by the high carbonate content (Fig. 34.3). Weathering can be an important process in heavy metal mobilization in boreal ecosystems (Starr et al. 2003), where release rates can be of similar magnitude to deposition, litterfall, and leaching fluxes.

34.3.3   Forests Soils as a Source and Store of Pollutants

Nitrogen in forest soils is found mainly in the organic and surface mineral horizons. Concentrations in the forest floor tend to vary within quite a narrow range, from 5 to 20 g kg^{-1} depending on the amount of mineral material present. The N content of the subsoil decreases with depth from 5.0 g kg^{-1} down to <3 g kg^{-1} (Vanmechelen et al. 1997). Soil nitrogen concentration is highly positively correlated with soil organic matter content, so the amount of carbon is very important in determining the fate of N in soils. Data from 167 forest sites across the UK from the BioSoil survey show that soil C and N content varies with soil type (Fig. 34.4). L and F horizons stored on average 9 and 13 t C ha^{-1}, and 0.3 and 0.6 t N ha^{-1} respectively, adding substantially to the overall soil C and N stocks in forest soils (Vanguelova 2010).

Soil type also determines the leaching or accumulation of different forms of N in the soil. For example, NH$_4^+$ can bind to negatively charged soil particles, be fixed by certain types of clays and be bound firmly and irreversibly between clay layers. Soil texture will therefore influence the fate and leaching of nitrogen compounds and is the key to predicting patterns of N movement and retention.
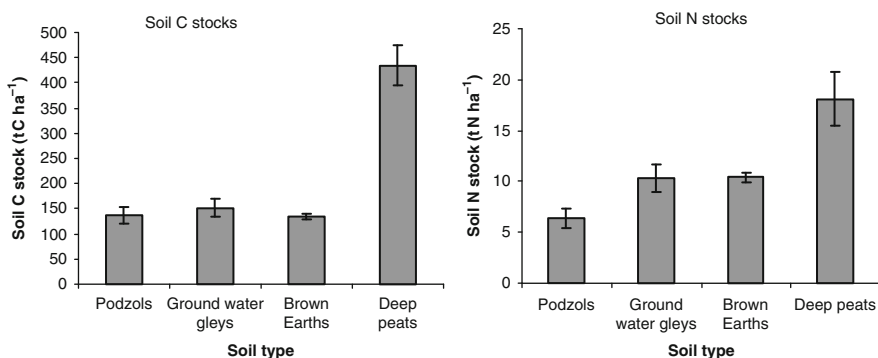
Fig. 34.4   Soil carbon and nitrogen stocks in British forests (from Vanguelova 2010)

The predominant process for the retention of deposited S in forest acid soils is probably adsorption of SO_4^- to sesquioxides and clay minerals (Prietzel et al. 1995). Some authors (Khanna et al. 1987; Courchesne and Hendershot 1990) also suggest that precipitation of Al hydroxy sulfate minerals is of major importance. It is generally assumed that forest ecosystems exposed to elevated S inputs primarily accumulate S as inorganic sulfur in the soil (Johnson et al. 1982; Prietzel et al. 2001). However, organic sulfur constitutes the major proportion of the S pool of most forest soils (David et al. 1982; Mitchell et al. 1992) and atmospheric S may also be immobilized by microbial synthesis of organic S compounds (Freney 1961).

Concentrations of heavy metals such as Fe and Mn vary widely in soils but the range is narrower for Cr, Ni, Zn, Cu, Pb, and Cd. Concentrations can become critical for soil microbiota, especially if enhanced through pollutant deposition (Table 34.5). Concentrations of some heavy metals in mineral soil are directly related to clay content and the importance of soil type in the distribution and the origin of heavy metals in soils has been well documented (Vanmechelen et al. 1997). Acid soils tend to have the lowest metal content, while the highest concentrations occur in calcareous soils and andosols (Vanmechelen et al. 1997). The vertical distribution of metals varies as a function of soil type, pH, iron and aluminum oxide content, clay content, organic matter and cation exchange capacity (Hernandez et al. 2003). In areas with a history of exposure to atmospheric metal deposition, long soil residence times for strongly retained metals such as Co and Pb mean that it may take hundreds of years before a response to recent deposition reductions is noted (RoTAP 2011). Less strongly bound metals, including Ni, Zn, and Cd are expected to decline more rapidly, although current deposition levels of Co, Pb, and Zn still pose a threat to soils in some woodland habitats in the UK (RoTAP 2011).

Table 34.5 Background concentrations of heavy metals in mineral soils and critical concentrations for microbiota in mineral and organic layers (adapted from Vanmechelen et al. 1997)

Metal	Heavy metal content (mg kg^{-1} dry soil)		Organic layer
	Mineral soil		
	Normal range	Critical concentration	Critical concentrations[a]
Fe	200–100,000[b]		
Cr	10–100[c]	75–100[d]	30
Ni	10–100[c]	95[e]	
Mn	20–3,000[b]	1,500–3,000[d]	
Zn	10–300[b]	170[e]	300
Cu	1–50[b]	60[e]	20
Pb	10–100[c]	100–400[d]	500
Cd	<1[c]	3–8[d]	3.5

[a]Tyler (1992)
[b]Barber (1995)
[c]Soon and Abboud (1993)
[d]Kabata-Pendias and Pendias (1984)
[e]Witter (1992)

34.3.4 Above and Belowground Litter: Amounts and Decomposition

Retranslocation, redistribution or resorption of elements from ageing needles and other tree tissues are important processes through which pollutants are cycled in forest ecosystems. For example, in a nonpolluted oak forest, part of the tree S requirements of 3.7 kg ha^{-1} y^{-1} were met by retranslocation of S from senescing leaves just prior to shedding (0.8 kg ha^{-1} y^{-1}) and by canopy absorption (1.0 kg ha^{-1} y^{-1}); the remainder was thought to be supplied by root uptake (Quilchano et al. 2002). Retranslocation of N from senescing needles of *Pinus sylvestris* was between 70 and 85% in study plots in Finland but was not influenced by stand age and fertilization (Helmisaari 1992). N retranslocation has been found to increase linearly with increasing N availability in the soil (Birk and Vitousek 1986), suggesting more rapid N cycling in N-rich systems. Retranslocation of N during autumn senescence is estimated as 58% in Arctic forest, 61% in Boreal forest, 50% in temperate forest, and 45% in Tropical forests (Chapin and Van Cleve 1989).

A significant proportion of terrestrial net primary production is recycled from trees as aboveground litterfall to the forest floor and belowground root litter to the soil. Litterfall is therefore a major pathway through which the pool of pollutants in the soil, depleted by tree uptake and leaching, is replenished. Moreover, litterfall represents one of the primary links between producers and decomposers. Thus, the amount and quality of litterfall provide considerable information about the dynamics of pollutants within forest ecosystems (Ukonmaanaho et al. 2008).

Foliar litter is the dominant component of aboveground litterfall in most European forests ecosystems, although other components such as bark can be important in some forest types, for example, in Eucalyptus plantations (Kimmins 1987). The quantity of litterfall depends on annual climatic variability, tree species, age and stand density, and pollution climate. For example, total annual litterfall of 3.8 t C ha^{-1} y^{-1} measured in Corsican pine in a relatively wet, low N deposition area was approximately half that for the same species in a drier, high N deposition area (8.1 t C ha^{-1} y^{-1}) (Vanguelova and Pitman 2009). Element concentrations in needle litter are affected by several factors, of which tree species, climate, and soil properties are considered to be the most important.

Variable amounts of sulfur can be cycled through litterfall (Pedersen and Bille-Hansen 1999; Quilchano et al. 2002; Ukonmaanaho et al. 2008) depending on the ambient pollution climate (de Vries et al. 2003), but is likely to be much less than that cycled via throughfall (Mitchell 1992; Quilchano et al. 2002). In contrast, litterfall N input to the soil can be up to three times higher than by deposition (Van Miegroet et al. 1992; Blanco et al. 2008) and total litter input (leaf plus woody parts) of N of various broadleaved and coniferous species can reach between 45 and 90 kg N ha^{-1} y^{-1} in Western Atlantic climatic regions (Pedersen and Bille-Hansen 1999; Broadmeadow et al. 2004).

The difference in litterfall quality and quantity influences the decomposition rate and thus the dynamics and incorporation of pollutants into the soil. For broadleaf

species that have sporadic masts (beech and oak) or in good coning years for pines, the annual pollutant input can increase dramatically from dropped seed (Pitman 2004). Leaf litter from broadleaved trees provides organic material that is generally quickly decomposed and incorporated into the upper soil horizon (Drift 1961) and litter N, lignin content, C/N ratio, leaf area, and Ca content are some of the important litter qualities that strongly affect litter decomposition rate (Table 34.6; Vanguelova and Pitman 2011) (Cornelissen 1996; Wedderburn and Carter 1999; Peterken 2001; Reich et al. 2005; Hobbie et al. 2006; Vesterdal et al. 2008). The litter of nondeciduous broadleaves such as *Eucalyptus* species takes longer to decompose (Cornelissen 1996), but will nevertheless be more rapidly decomposed than that of conifers (Wedderburn and Carter 1999). Additional important factors affecting the rate of leaf decomposition are soil pH and soil moisture, with moist, base-rich soils providing conditions for the quickest rate of decomposition (Witkamp and Drift 1961; Pereira et al. 1998; Hunter et al. 2003; Reich et al. 2005). Heavy metal accumulation or release may depend on the gradient of metal concentration between litter and soil, soil pH, and on the capacity of litter to bind the specific metal (De Santo et al. 2002), while metal contamination may slow litter decomposition through adverse impacts on soil microbiota (McEnroe and Helmisaari 2001).

Tree fine roots (<2 mm) are very dynamic and play a key role in forest ecosystem carbon and nutrient turnover and thus in pollutant cycling. Root biomass, distribution, and turnover depend on tree species, soil type, and climatic conditions. Deciduous trees tend to have a higher root biomass than conifers, while for a given species, root biomass is generally greater in the temperate compared to the boreal zone. Nutrient poor forests typically have higher root densities and a strong relationship exists between fine root and aboveground biomass, suggesting that trees regulate proportionally their carbon allocation depending on site conditions (Finér et al. 2007). Estimates of root litter input are often dependent upon the methodology used (Majdi et al. 2005). Root litter inputs were found to be 20% higher in Norway spruce stands on acidified soils compared to base-rich soils (Godbold et al. 2003).

34.3.5   Mineralization and Uptake of Pollutants

Soil N mineralization and nitrification are not only strongly regulated by temperature, but also influenced by soil texture, acidity, and microbial activity. For example, relative nitrification rate in Polar and Upper Alpine climates (annual mean temperature 2–5°C) were only 0.005 kmol m^3 y^{-1} compared to 0.01 kmol m^3 y^{-1} in Boreal and Lower Alpine climates (annual mean temperature 5–8°C) and 0.04 kmol m^3 y^{-1} in Wet Boreal, Atlantic Boreal, and Temperate Continental climates (annual mean temperature of 8–12°C; Nilsson and Grennfelt 1988).

The C/N ratio gives an indication of forest floor nitrogen availability and its rate of decay (Dise et al. 1998a). The majority of forest soils has C/N ratios between 20 and 40 but may frequently exceed this in organic horizons in Northern Europe due

Table 34.6 Estimated/measured litter parameters of different tree species (adapted from Vanguelova and Pitman 2011)

Species	Litter N (%)	Litter SLA (cm² g⁻¹)	Litter BC content[a]	Litter C%	Rate of decomposition	References
Ash	1.24–2.20	180–300	3.83	31.1	Rapid	Cornelissen (1996)
Alder		210			Rapid	Cornelissen (1996)
Sycamore	0.94	(213 fresh) ~250 litter	3.03	46.2	Rapid	Hobbie et al. (2006), Cornelissen (1996)
Hazel	1.34	275–310	2.6	n/a	Rapid	FR[b]
Hornbeam	1.1	210	1.46	46.9	Intermediate-rapid	Hobbie et al. (2006)
Birch	1.0–1.4	170–320	1.31–1.41	47.8–52.8	Intermediate	Cornelissen (1996), Hobbie et al. (2006)
Chestnut	0.98–1.30	~150–200	1.19–1.28	49.7–50.7	Intermediate	FR[b]
S.beech ~N. obliqua	0.6		~0.97		Intermediate	Wigston (1990), Adams and Attiwill (1991)
Willow (S. alba, S. gragilis)		149/160			Intermediate	FR[b]; Cornelissen (1996), Withington et al. (2006)
Poplar (P. trichocarpa), P. tremula/P. nigra		(70–170 fresh) 149–160			Intermediate	FR[b]; Cornelissen (1996), Withington et al. (2006)
Oak	1.0–1.38	165–190	1.83–1.95	36.6–51.1	Intermediate-slow	FR[b]; Hobbie et al. (2006)
Eucalyptus (E. nitens)		61–66			Slow	FR[b]; Wedderburn and Carter (1999)
Eucalyptus (E. gunnii)		57–67			Slow	FR[b]; Adams and Attiwill (1991)

[a] BC base cation Ca+K+Mg% as defined by Cornelissen and Thompson (1997)
[b] FR Forest Research UK (Unpublished data)

mainly to low N inputs and slow decomposition rates. High ratios can occur around the Mediterranean due to the dry climate limiting decomposition, but are rarely found in central Europe, where many forests have organic layers with a C/N ratio approaching 20, caused by high deposition loads (Vanmechelen et al. 1997). In British forest soils, organic layer C/N ratios were found to range between 16 and 42 under conifers and 15–29 under broadleaves (Vanguelova 2010). Sixty percent of conifer plots investigated and nearly 90% of broadleaves had ratios below 25, indicative of N saturation (Emmett 2007). Lower mineralization rates have often been attributed to moder compared to mull forest humus types, although this view has been challenged. In a recent study of 50 beech forests growing on a wide range of soils across northeastern France, high elevation, acidic soils had the highest potential net N mineralization in upper mineral soils, while low elevation, neutral, and calcareous soils had the lowest (Andrianarisoa et al. 2009).

Soil organic sulfur is slowly released by the action of a wide range soil organisms. Unlike nitrogen, little is known about the chemical structure of the sulfur compounds in organic matter, or the specific processes involved in sulfur release. Organic sulfur can be divided into two categories (1) compounds that can be reduced by hydriodic acid to form hydrogen sulfide (H_2S) and (2) those which cannot be reduced by hydriodic acid, a group thought to include all of the sulfur-containing amino acids, such as cysteine and metionine. Degradation is thought to be governed by the action of specific enzymes that are produced by soil microorganisms. Biological S requirements of forests are modest (<5 kg s ha^{-1} y^{-1}) and often exceeded by atmospheric S inputs, even in nonpolluted regions. In polluted forest regions, S inputs may exceed both the requirement for S uptake and the ecosystems ability to accumulate S (Johnson 1984; Mitchell 1992).

More than 90% of certain heavy metals deposited from the atmosphere may not be biologically available due to adsorption or chelation by organic matter, clays and/or hydrous oxides of aluminium, iron or manganese, and complexation with soluble low-molecular-weight organic compounds. Soluble Cd, Cu, and Zn may be chelated in excess of 99%, while up to 80–90% of aluminium in soil solution can be bound by soluble organic compounds (Vanguelova et al. 2007b). Heavy metals may also be precipitated in inorganic compounds of low solubility, such as oxides, phosphates, or sulfates. Adsorption, chelation, and precipitation are strongly regulated by soil pH. As pH decreases and soils become more acid, heavy metals generally become more available for tree uptake.

Soil organic matter decomposition rates can be strongly affected by the presence of heavy metals. A study of Scots pine (*P. silvestris*) stands located at various distances from emission sources in Poland demonstrated a significant decrease in organic matter decomposition rate with increasing heavy metal pollution. The results suggest that after soil carbon, the heavy metal content probably exerts the greatest control on this process in soil profiles affected by metal emissions (Zwolinski 1994).

Rhizosphere processes can transform heavy metals from unavailable to available pools. Typically, rhizosphere soil has lower pH, lower water, osmotic and redox potentials, and higher bulk density than the main soil matrix. These characteristics enable the rhizosphere to dominate regulation of element uptake by tree roots.

Rhizosphere factors that may be particularly important in Pb uptake include pH, organic acid concentration, and phosphate availability. Organic acids are important for complexing and so reducing Co and Zn uptake, while manganese reduction to the divalent form may allow excess uptake of this metal. Complexing agents and reduced rhizosphere pH may also facilitate Cd uptake. Any alteration in rhizosphere processes caused by chemical changes induced by air pollution could easily alter availability and uptake of these potentially toxic elements (Smith 1986).

34.3.6 Soil Leaching and Pollutant Export

For most pollutants, the main export pathway from forest ecosystems is via leaching in drainage water from the rooting zone. Pollutant export depends both on water fluxes through the soil profile, which mainly reflect ambient precipitation (Table 34.2, van der Salm et al. 2007) and on pollutant concentrations in the seepage water. Where forests exhibit minimal net uptake or accumulation of pollutants in biomass as in pristine, old-growth temperate forests, leaching losses should largely equal deposition inputs (Raulund-Rasmussen et al. 2008). Younger growing forests tend to be better at retaining pollutants than older stands, either through greater tree uptake or through accumulation in the soil resulting in lower pollutant leaching losses. Anthropogenic N deposition may lead to either increased retention of nitrogen or leaching of excess inorganic nitrogen (Dise et al. 1998b, 2009). In nitrogen-limited forests leaching of inorganic nitrogen is unlikely, whereas it can be significant in nitrogen-saturated systems (Gundersen et al. 2006). In addition to overall N deposition, tree species and soil type exert important controls on nitrate leaching. For example, in Denmark, higher nitrate leaching rates were found under conifers compared with deciduous trees (Hansen et al. 2009) due to greater pollutant scavenging by evergreen conifer canopies (Rothe et al. 2002). However, the lowest median N leaching fluxes at EU Level II sites are found under pine, partly because of low water fluxes in the drier regions frequented by this forest type (Table 34.7, de Vries et al. 2003; Vanguelova et al. 2010).

In general, median SO_4 leaching fluxes are comparable to SO_4 deposition in European forests, whereas N leaching is usually much lower than N deposition. Sulfate leaching fluxes exceed those of NO_3, although total N deposition is often larger than total S deposition, indicating different retention for N and S in forest ecosystems. Large geographical variation in leaching fluxes reflects that of deposition (Table 34.7, de Vries et al. 2003).

The capacity of soils to export pollutants to water depends on short and long-term soil pollutant buffering capacity, for which the soil volume exploited by roots, and the texture and content of weatherable minerals are major determinants (Raulund-Rasmussen et al. 2008). Fertile soils possess a large pollutant buffer capacity, while poor soils are more sensitive to pollution loading and thus at higher risk of pollutant leaching. The leaching and retention of pollutants is usually determined by the interaction of tree species and soil properties (Bergkvist 1987; de Vries et al. 2003).

Table 34.7 Soil leaching fluxes of SO_4, NO_3, NH_4, DON, and total N (>50 cm soil depth) reported for different deposition, forest ecosystems and regions

Forest type/site name/country	Soil type (FAO)	Precipitation water flux (mm y⁻¹)	Drainage water flux (mm y⁻¹)	Deposition in precipitation		Averaged annual leaching fluxes					Reference
				N	S	SO_4–S	NO_3–N	NH_4–N	DON	Total N	
				kg N ha⁻¹ y⁻¹		kg N ha⁻¹ y⁻¹					
Oak/Alice Holt/UK	Eutric vertisol	800	325	10.9	10.3	20.41	0.18	0.06	1.3	1.55	Vanguelova et al. (2010)
Oak/Savernake/ UK	Eutric vertisol	750	230	13.5	10.4	28.83	4.76	0.08	0	3.65	Vanguelova et al. (2010)
Oak/Grizedale/ UK	Cambic podzol	1,800	1130	14.7	14.2	24.38	0.88	0.38	0.54	1.83	Vanguelova et al. (2010)
Scots pine/ Rannoch/ UK	Gleyic podzol	1,400	465	5	5.9	4.12	0.17	0.09	1.18	1.48	Vanguelova et al. (2010)
Scots pine/ Thetford/ UK	Ferralic arenosol	600	0	14.9	10.9	0.66	2.05	0	0	1.9	Vanguelova et al. (2010)
Scots pine/Lady Bower/UK	Cambic podzol	1,200	365	16.4	17.6	24.41	12.99	0.14	0	9.66	Vanguelova et al. (2010)
Sitka spruce/ Tummel/UK	Ferric podzol	1,100	385	5.3	6.5	6.96	17.5	0.16	7.41	23.95	Vanguelova et al. (2010)
Sitka spruce/ Coalburn/ UK	Umbric gleysol	1,400	420	11.6	10.9	6.89	25.96	1.43	3.41	31.85	Vanguelova et al. (2010)
Sitka spruce/ Llyn Brianne/UK	Umbric gleysol	2,100	950	12.5	20.1	16.86	0.28	0.29	1.41	2.01	Vanguelova et al. (2010)
Pine (EU ICP sites)[a]	Various soil types	642	79	11.9	5.4	2.05	nd	nd	nd	0.50	van der Salm et al. (2007), de Vries et al. (2007)

Spruce (EU ICP sites)[a]	Various soil types	963	205	20.0	7.1	6.14	nd	nd	nd	7.99	van der Salm et al. (2007), de Vries et al. (2007)
Oak (EU ICP sites)[a]	Various soil types	725	123	16.0	6.6	10.67	nd	nd	nd	15.13	van der Salm et al. (2007), de Vries et al. (2007)
Beech (EU ICP sites)[a]	Various soil types	891	138	22.3	6.6	6.29	nd	nd	nd	9.64	van der Salm et al. (2007), de Vries et al. (2007)
Scots pine sites/ Finland[b]	Ferric/haplic podzol	590	215	14	nd	nd	0.4	0.2	1.2	1.4	Mustajärvi et al. (2008)
Norway spruce sites/ Finland[b]	Podzol/ cambisol	575	225	7	nd	nd	0.03	0.1	0.6	0.7	Mustajärvi et al. (2008)
Silver Birch/ Belgium	Podzol	784	281	20.6	nd	nd	7.03	0.53	2.94	10.5	Sleutel et al. (2009)
Corsican pine/ Belgium	Podzol	784	210	20.6	nd	nd	17.17	0.42	3.6	21.2	Sleutel et al. (2009)
Corsican pine/ Belgium	Podzol	792	224	23.5	nd	nd	49.5	0.55	4.95	55	Sleutel et al. (2009)
Norway spruce/ Germany	Cambisol/ cambic podzol	1,100	538	15.7[c]	nd	nd	6.14	0.2	0	6.5	Langusch and Matzner (2002)
Beech/oak/ Germany	Dystric/ vertic cambisol	750	257	21[c]	nd	nd	20.8	0.35	0	21	Langusch and Matzner (2002)

[a]Median water, deposition, and leaching values from number of European ICP forest plots
[b]Averaged values from eight Scots pine sites and eight Norway spruce sites
[c]Throughfall instead of precipitation flux

34.4   Pollutant Impacts on Forest Ecosystems

34.4.1   *Impacts of Pollutants on Forest Soils*

Fluxes of nutrients, contaminants, and other elements within forests are important indicators of ecosystem functioning and stability. Many environmental pollutants (particularly S and N compounds) can affect the functioning of forest ecosystems (Schulze et al. 1989; Luttermann and Freedman 2000). For example, deposition of S and N can cause soil acidification and increased leaching of nitrate and aluminium (Stoddard et al. 1999), leading to surface water acidification (Beier et al. 2001). Atmospheric acid deposition is the main factor underlying widespread soil acidification in Europe (Schulze et al. 1989). Acidified soils affect the rooting systems of trees can impair plant nutrient balance and reduce soil biodiversity. Chronically enhanced $(NH_4)_2SO_4$ deposition may play a major role in controlling soil solution cation concentrations, leading to a "switch" from Ca^{2+} to Al^{3+} and low Ca/Al molar ratios. Soils with low base saturation and a pH in the lower Ca, or Al buffer ranges are the most sensitive to acidification (Carnol et al. 1997).

There is significant potential for heavy metals to interact with other air pollutants affecting forest ecosystems. Acid deposition can alter heavy metal availability by changing soil pH and related chemical parameters. Acid soils can mobilize heavy metals, which have accumulated in the soil due to atmospheric inputs (Tyler 1978; Brümmer and Herms 1983; Verry and Vermette 1992). In acid forest stands, the more mobile metals such as Zn, Mn, and Cd are increasingly taken up by trees (Steinnes 1984; Barlsberg-Påhlsson 1989) and leached to surface and ground waters (Norton and Kahl 1992; de Vries and Bakker 1998). Less mobile metals such as Pb and to a lesser extent Cu accumulate over long time periods in soil organic layers (Siccama and Smith 1978; Friedland 1992; Schulte 1994; Steinnes and Njåstad 1995). Even in regions with decreasing atmospheric inputs (Norton and Kahl 1992), they can still present a potential danger if environmental change promotes their release (Friedland 1992; RoTAP 2011). Unfortunately, insufficient quantitative information is available to rationalize emissions and deposition of heavy metals. Concentrations of Ni, Zn, and Cd in soils have declined, but Cu, Pb, and Hg are unlikely to change for centuries. In many soils, there is a large legacy of historic deposition, much of which is currently not biologically available because of strong binding to soil organic matter. Any decrease in soil organic matter or increase in its decomposition, for example in response to climate change or forest management, would risk releasing this store of metals into the environment in a bioavailable form.

34.4.2   *Impacts of Nitrogen on Tree Growth and Soil Functions*

The availability of N compounds controls many biogeochemical processes and has a strong influence on net primary production in terrestrial ecosystems (Schulze 2000; Pussinen et al. 2002; Hyvönen et al. 2007). Nitrogen deposition increased tree

growth in the four species (European and sessile oak, beech, Scots pine, Norway spruce) studied in 382 European Forest Intensive Monitoring plots (ICP report 2009). The effect was smallest on soils that were already well supplied with nitrogen. Annually nitrogen deposition increased tree growth by ~1%, which corresponds to an average carbon fixation in tree stems of about 20 kg ha^{-1} y^{-1}. Sulfur and acid deposition were found not to have any negative effects on tree growth, possibly due to the counteracting positive effect of nitrogen deposition (ICP report 2009).

Nitrogen enrichment in the soil not only accelerates tree growth, but can also affect the composition of the understory vegetation and the amount of nitrate leaching (Schulze 2000). Over the past few decades, deposition from the air has led to increasing storage of nitrogen in plants and soil. On forest floors that are already nitrogen enriched the soil and the plants can retain little extra nitrogen and so it passes relatively quickly to groundwater. Nitrogen availability influences carbon storage in forest soils through effects on plant growth, litter production, and soil C decomposition and stabilization. Soil C/N ratio and net N-mineralization are commonly reported empirical measures of soil N availability, and changes in these variables due to N inputs may feed back to soil C storage through a variety of biotic and abiotic pathways Nitrogen inputs in northern temperate forests were found to increase soil C (+7.7%) and N mineralization (+62%), and decrease C/N ratio (−4.9%), all depending on mode of N addition, biogeographic factors and time (Nave et al. 2009). Recent analysis of published studies in temperate forest soils suggests that N deposition impedes organic matter decomposition and thus stimulates carbon sequestration, where nitrogen is not limiting microbial growth. Soil carbon sequestration was equivalent in magnitude to the amount of carbon taken up by trees in response to nitrogen fertilization (Janssens et al. 2010).

Atmospheric N deposition can significantly influence soil carbon (C) and nitrogen (N) cycles in natural ecosystems and consequently the production and consumption of the greenhouse gases carbon dioxide (CO_2), nitrous oxide (N_2O), and methane (CH_4), as well as the tropospheric ozone precursor nitric oxide (NO). Pristine forests in areas of low N deposition tend to be N limited and respond to enhanced N deposition (as simulated by short-term field experiments) with increased microbial activity, soil respiration rates, and consequently CO_2 emissions (Bowden et al. 2004). Nitrous oxide emissions are unlikely to be affected, as the N added tends to be immobilized by soil microbes (Skiba et al. 1999). However, continuous N deposition will eventually lead to N saturation and reduced soil respiration rates (Aber and Magill 2004; Janssens et al. 2010). A recent analysis of the net C budgets for European forests has shown a strong correlation between rates of N deposition and C sequestration (Magnani et al. 2007), although there is doubt about the magnitude of this interaction (de Vries et al. 2008). In the long-term, the microorganisms responsible for N_2O and NO production, the nitrifiers and denitrifiers, are expected to successfully compete for the deposited N, and correlations between N deposition rate and N_2O emissions have been demonstrated for a number of forests (Skiba et al. 2004). It is assumed that 1% of the N deposited is emitted as N_2O (IPCC 2006).

Forest ecosystems tend to be net sinks for CH_4. The general view has been that CH_4 oxidation is inhibited by N additions, leading to reduced oxidation rates in

forests (MacDonald et al. 1997; Butterbach-Bahl et al. 2002). Recent publications, however, have shown that N additions can also stimulate CH_4 oxidation (Bodelier and Laanbroek 2004). The source of atmospheric N deposition (wet, dry, reduced, or oxidized) does not appear to influence N_2O and NO emission rates; however, it does have an impact on soil CH_4 fluxes. The N component of atmospheric deposition may inhibit or stimulate CH_4 emissions, whereas the sulfur component inhibits CH_4 emissions (Gauci et al. 2005).

34.4.3   Impacts of Pollutants on Belowground Tree Functioning

Pollutants also threaten the functioning of tree fine roots and ectomycorrhizas, the symbiotic organs of tree roots, which are the main sites of nutrient exchange, with P and N provided by the fungal partner, and C from the host. Emerging from the ectomycorrhizas, fungal hyphae exploit the soil for the mobilization and absorption of water and nutrients. Increased N concentrations in the soil lead to enhanced fungal N uptake and storage, greater N transfer to the host plant, and thus increased aboveground biomass. As a consequence, there is a decrease of C allocation to the plant roots, leading to reduced ectomycorrhization and lower production of external mycelia and fruiting bodies (Brunner 2001). Acid deposition significantly affects fine roots, their length, and biomass (Cudlin et al. 2007). Soil acidification leads to enhanced availability of Al^{3+} and heavy metals, with Al^{3+} toxicity shown to have a significant impact on fine root biomass and Specific Root Length (m g^{-1}) (Ostonen et al. 2007; Vanguelova et al. 2007b). In ectomycorrhizas, the hyphae of the fungal tissues contain vacuolar polyphosphates which have the ability to bind Al^{3+}, heavy metals, and N. These electronegative phosphate polymers represent an effective storage and detoxifying mechanism, which otherwise is lacking in roots. Therefore, ectomycorrhizas have the potential to increase the tolerance of trees to acidifying pollutants and to the increased availability in the soil of toxic elements (Brunner 2001).

34.5   Likely Impacts of Environmental Change and Forest Management on Pollutant Cycling by Nonurban Forest Ecosystems

34.5.1   Climate Change

The impacts of climate change on the sensitivity of forest ecosystems to sulfur and nitrogen deposition have been studied under the EU-funded AIR-CLIM project (Mayerhofer et al. 2001; Alacamo et al. 2002; Posch 2002). One aspect of the study examined the impacts of eight climate scenarios on soil critical loads, acid deposition, and critical load exceedance. For forest soils, all scenarios resulted in a general increase in critical loads across Europe, although with some decreases

noted in mountainous or arid regions. There was a decline in the area of critical load exceedance for all scenarios, leaving only small areas with exceedance for acidity, but substantial areas exceeded for nitrogen. However, achieving nonexceedance of acidity critical loads does not imply immediate recovery of previously exceeded ecosystems (Posch 2002).

It is not possible to review the impacts of climate change on pollutant cycling in forest ecosystems in the absence of a discussion of the effects on both the trees that are supported by forest soils, and the wider land management issues affecting the forest industry. Both climatic warming and rising atmospheric CO_2 levels have the potential to substantially increase tree growth (Norby et al. 2005). Increases in mean temperature also have the potential to increase growth rates in boreal forests, but this may be confounded by an accompanying decrease in precipitation (Lloyd and Fastie 2002). These results exemplify the complexity of predicting changes in forest growth under climate change.

Increased forest net primary productivity under elevated CO_2 does not necessarily mean increased soil carbon storage, despite higher biomass inputs. This is particularly true for mineral soils, although a significant additional carbon sink can be created by the litter layer (Lichter et al. 2005; Hoosbeek and Scarascia-Mugnozza 2009). Where bioturbation rates are high, much of the biomass carbon can be incorporated into the mineral soil creating additional storage in the subsoil (Jastrow et al. 2005). Maintenance of the increase in NPP under elevated CO_2 depends upon adequate supplies of N and other mineral nutrients, which may be partly met by an increase in fine root biomass and depth of rooting (Iversen 2010). The effects of elevated CO_2 would be diminished if wetter and milder winters increase acidification and nutrient leaching, thereby reducing soil nutrient availability. Changes in growth will also affect the amounts and quality of leaf litter inputs to the soil, with consequences for the soil nutrient pool. Rising CO_2 levels have also been shown to alter the C/N ratio of leaf litter (Bradley et al. 2005), which might reduce decomposition rates, although a comprehensive review has concluded that this is not the case (Hyvönen et al. 2007).

If elevated CO_2 affects tree leaf area index, this will have implications for the forest floor microclimate due to changed litter inputs, water and light interception. Changes in both species and growth rates in response to climate change will also affect pollutant uptake by trees. Although this may beneficially increase pollutant sequestration, a recent modeling study suggests only small changes in the uptake and removal of nitrogen for British Forests (RoTAP 2011).

Some insect pests may become more damaging to forest ecosystems as a result of climate change, in part, driven by expectations that more frequent and severe summer droughts will increase the susceptibility of trees to biotic agents (Broadmeadow 2002). There is evidence for insect impacts on the DON, dissolved organic carbon (DOC), and K fluxes in forest ecosystems and their soils in the UK (Pitman et al. 2010). Poor forest crown condition caused either by insect defoliation or by wind damage will influence pollution inputs to forest ecosystems and especially the amount and partitioning of pollutants reaching the forest floor. In contrast, increased winter waterlogging due to higher precipitation coupled with

more frequent storm events may promote soil disturbance resulting from increased tree windthrow, higher pollutant inputs through rainfall and throughfall, and increased release of pollutants from soils to waters (Bradley et al. 2005; Vanguelova et al. 2010).

34.5.2 Biomass Harvesting

Biomass is a significant pollutant pool in forests, which is recycled slowly via decomposition of coarse woody debris (Laiho and Prescott 2004) and other more recalcitrant parts, but relatively quickly through decomposition of litterfall and fine roots (Parton et al. 2007). Harvesting through thinnings and periodic clear-cuts accounts for a large part of the pollutant export in managed forests. Depending on harvesting regime, pollutant export can vary widely reflecting site productivity and biomass utilization (harvesting) intensity. For stem-only harvesting pollutant removal is only slightly influenced by tree species. When logging residues are also removed, pollutant export can be substantially increased but lower for some species such as Scots pine and birch compared to Norway spruce (Fig. 34.5) because of differences in species productivity and crown share (Raulund-Rasmussen et al. 2008). Whole tree harvesting can remove substantial quantities of pollutants but at the same time can increase nitrate leaching and soil water acidification. Significant increases in streamwater concentrations of H^+ and potentially toxic inorganic Al^{3+} can also occur after removal of biomass (Zhang et al. 1999). Nitrogen removal by conventional and whole tree harvesting can range substantially depending on the forest ecosystem, its age and growth, and the climatic conditions (Table 34.8).
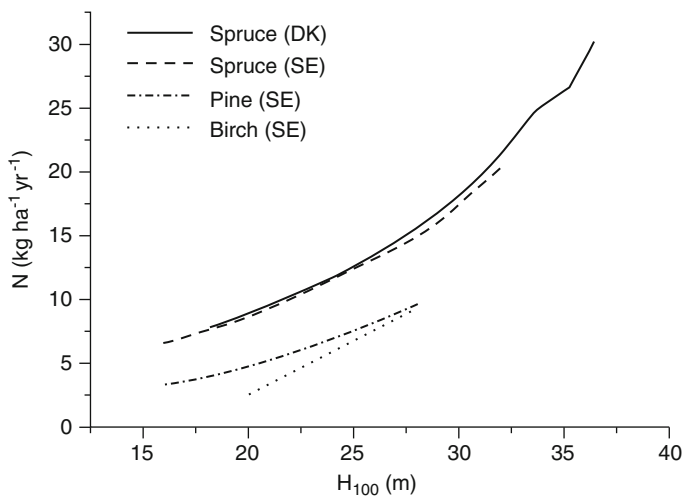
Fig. 34.5 Averaged yearly nitrogen removals for spruce, pine, and birch when all above ground biomass is removed (from Raulund-Rasmussen et al. 2008)

Table 34.8 Comparison of nitrogen removals in harvest and across a range of forest and climatic conditions

Forest/location	Age	Harvesting intensity	N removals kg ha^{-1} (kg ha^{-1} y^{-1})	Reference
Spruce/Sweden	18	Conventional stem harvesting	20 (1.1)	Tamm (1969)
		Whole tree harvesting	163 (9.1)	
	50	Conventional stem harvesting	217 (4.3)	
		Whole tree harvesting	842 (16.8)	
Scots pine/UK	50	Conventional stem harvesting	72 (1.4)	Miller and Miller (1991)
		Whole tree harvesting	248 (5.0)	
Corsican pine/UK	50	Conventional stem harvesting	120	Miller and Miller (1991)
		Whole tree harvesting	290	
Norway and sitka spruce/UK	50	Conventional stem harvesting	145	Miller and Miller (1991)
		Whole tree harvesting	498	
Douglas fir/ Washington	53	Conventional stem harvesting	478 (9.0)	Biggar and Cole (1983)
		Whole tree harvesting	728 (13.7)	
Loblolly pine plantation/ North Carolina	22	Conventional stem harvesting	57.0 (2.5)	Tew et al. (1986)
		Whole tree harvesting	180.4 (8.2)	
Slash longleaf pine/ Florida	40	Conventional stem harvesting	59 (1.5)	Morris et al. (1983)
		Whole tree harvesting	110 (2.8)	
Gmelina/Nigeria	10	Stems/coppices/ standard	384 (38.4)	Nwoboshi (1983)
		Whole tree harvesting	959 (95.9)	
Chestnut/SW France	2	Coppice	92 (46)	Ranger and Belgrand (1996)
Chestnut/SW France	19	Coppice	1596 (84)	Ranger and Belgrand (1996)
Hybrid Aspen/ Estonia	7	Short rotation plantation	31 (4.4)	Tullus et al. (2009)
Sycamore/USA	10	Short rotation plantation	200 (20)	Cobb et al. (2008)
Poplar and Willow/ USA	10	Short rotation plantation	250 (2.5)	Jug et al. (1999)
Eucalyptus globulus/ Australia	8	Short rotation plantation	500 (62.5)	O'Connell and Grove (1999)

In addition, the growth and productivity of the forest and the harvesting rotation length can intensify the removal of N from the ecosystems by several times (Table 34.8).

Mass estimates of phytoaccumulated trace metal contaminants and transfers to soils are necessary to properly evaluate the impact of historic and continued anthropogenic metal deposition to forest ecosystems. An investigation of Cu, Ni, Pb, and Zn mass balances in plant communities subject to metal contamination from smelter emissions in Canada found that accumulation of metals differed significantly among plant vegetation compartments (foliage, fine roots, bark, trunk, and branches). Fine roots were found to dominate annual vegetation transfer of Cu, Ni, and Pb to soils, relative to foliage; fine root mortality played a smaller role than foliage for Zn plant–soil transfer. Plant-associated metal inputs were found to rival or exceed current estimates of atmospheric metal deposition, suggesting that potential benefits of future reductions in emissions to forests need to be evaluated within the context of phytocycling of metals already present (Johnson et al. 2003).

34.6   Conclusions and Future Directions

Forest ecosystems play a crucial role in pollution capture, storage, and cycling. Element concentrations change considerably as bulk precipitation passes through the canopy due to capture of aerosols and gases, absorption, leaching and exchange of elements, and canopy evaporation. Due to their aerodynamic roughness, forest canopies intercept pollutants at much higher rates than shorter vegetation. Organic and mineral forest soils can adsorb and store pollutants acting as buffers to pollutant transfer to the water environment. Tree demand and uptake for macro and micronutrients, including pollutants is much higher than for plants. In this way, trees can remove and store some pollutants either by canopy or by root uptake. However, when the pollution load exceeds the storage capacity of the forest ecosystem, then there is a risk of pollutant loss.

Air pollution is affecting many European, North American, and Asian forests around the globe. In the immediate future, the concern for air pollution effects on forests and associated natural resources will broaden to include interactions with climate change and pollution effects in the world's developing countries. There has been a rapid evolution in air pollution studies in forestry, shifting away from single-factor experimentation toward new ecologically based, multidisciplinary methodologies. This shift recognizes that air pollution is one of the several factors influencing forest productivity, carbon storage and biogeochemistry, and that effects arise through long-term exposure. Little research is available to quantify the feedbacks between pollutant cycling and climate change, although in principle substantial feedbacks are possible since many of the underlying processes are known to be climate sensitive. These interactions are likely to have wide-ranging effects on transboundary air pollution, ranging from emissions, atmospheric transport, and

transformation to environmental impacts. There is increasing interest in the effects of nitrogen deposition on the emissions of greenhouse gases and carbon sequestration by forests and soil. If climate change leads to a reduction in soil organic matter, there is a risk that heavy metals, previously bound to soil organic matter will become bioavailable, increasing the risk of toxicity to organisms and export to water.

The evolution in methodologies will become even more marked in the future as new ecological approaches are adopted and an understanding is developed of how air pollution interacts with changes in climate. One of the most promising methodologies is process level modeling, which utilizes the large databases in tree physiology and forest ecology, watershed chemistry, and atmosphere–forest canopy meteorology, to develop integrated models of tree physiology and soil processes and subsequently scale these investigations to the level of forest landscapes and regions.

References

Aber JD, Magill AH (2004) Chronic nitrogen additions at the Harvard Forest (USA): the first 15 years of a 11 nitrogen saturation experiment. For Ecol Manage 196:1–5

Adams MA, Attiwill PM (1991) Nutrient balance in forests of northern Tasmania. 1. Atmospheric inputs and within-stand cycles. For Ecol Manage 44:93–113

Alacamo J, Mayerhofer P, Guardans R et al (2002) An integrated assessment of regional air pollution and climate change in Europe: findings of the AIR CLIM project. Environ Sci Policy 5:257–272

Andrianarisoa KS, Zeller B, Dopouey JL et al (2009) Comparing indicators of N status of 50 beech stands (*Fagus sylvatica* L.) in northeastern France. For Ecol Manage 257:2241–2253

Arcangeli C, Wilkinson M, Williams M, et al (2007) Modelling rainfall interception. Final Report, Programme No. FF0304UK01 entitled "Forest Focus – UK 2003-2004" Request No. UK7

Avila A, Rodrigo A (2004) Trace metal fluxes in bulk deposition, throughfall and stemflow at two evergreen oak stands in NE Spain subject to different exposure to the industrial environment. Atmos Environ 38:171–180

Barber SA (1995) Soil nutrient bioavailability: a mechanistic approach. Wiley, New York

Barlsberg-Påhlsson A-M (1989) Toxicity of metals (Zn, Cu, Cd, Pb) to vascular plants. A literature review. Water Air Soil Poll 47:287–319

Beier C, Eckersten H, Gundersen P (2001) Nitrogen cycling in a Norway spruce plantation in Denmark – A SOILN model application including organic N uptake. Scientific World 1(S2):394–406

Bergkvist BO (1987) Leaching of metals from forest soils as influenced by tree species and management. For Ecol Manage 22:29–56

Bergkvist B, Folkeson L, Berggren D (1989) Fluxes of Cu, Zn, Pb, Cd, Cr and Ni in temperate forest ecosystems – a literature review. Water Air Soil Poll 47:217–286

Biggar CM, Cole DW (1983) Effects of harvesting intensity on nutrient losses and future productivity in high and low productivity red alder and Douglas-fir stands. In: Ballard R, Gessel SP (eds) I.U.F.R.O. Symp on forest site and continuous productivity. USDA For. Serv. PNW-163 USDA-FS. Portland, OR, pp 167–178

Birk EM, Vitousek PM (1986) Nitrogen availability and nitrogen use efficiency in loblolly pine stands. Ecology 67:69–79

Blanco JA, Imbert JB, Castillo FJ (2008) Nutrient return via litterfall in two contrasting *Pinus sylvestris* forests in the Pyrenees under different thinning intensities. For Ecol Manage 256:1840–1852

Bodelier PLE, Laanbroek HJ (2004) Nitrogen as a regulatory factor of methane oxidation in soils and sediments. FEMS Microbiol Ecol 47:265–277

Bowden RD, Davidson E, Savage K et al (2004) Chronic nitrogen additions reduce total soil 34 respiration and microbial respiration in temperate forest soils at the Harvard Forest. For Ecol Manage 196:43–56

Bradley I, Moffat AJ, Vanguelova E, et al (2005) Impacts of climate change on soil functions. DEFRA project, Report SP0538, London

Broadmeadow MSJ (2002) Climate change: impacts on UK forests. Forestry Commission Bulletin 125. Forestry Commission, Edinburgh

Broadmeadow M, Kennedy F, Vanguelova E, et al (2004) Terrestrial umbrella: eutrophication and acidification of terrestrial ecosystems. Final Report of the Forest Research sub-contract to the Department for Environment, Food and Rural Affairs

Brümmer G, Herms U (1983) Influence of soil reaction and organic matter on the solubility of heavy metals in soils. In: Ulrich B, Pankrath J (eds) Effects of accumulation of air pollutants in forest ecosystems. pp 233–243

Brunner I (2001) Ectomycorrhizas: their role in forest ecosystems under the impact of acidifying pollutants. Perspect Plant Ecol 4:13–27

Butterbach-Bahl K, Breuer L, Gasche R et al (2002) Exchange of trace gases between soils and the atmosphere in Scots pine forest ecosystems of the northeastern German lowlands 1. Fluxes of N_2O, NO/NO_2 and CH_4 at forest sites with different N-deposition. For Ecol Manage 167:123–134

Bytnerowicz A, Fenn ME (1996) Nitrogen deposition in California forests: a review. Environ Pollut 92:127–146

Calder IR, Reid I, Nisbet T et al (2003) Impact of lowland forests in England on water resources – application of the HYLUC model. Water Resour Res 39:1319–1328

Carnol M, Ineson P, Dickinson AL (1997) Soil solution nitrogen and cations influenced by $(NH_4)_2SO_4$ deposition in a coniferous forest. Environ Pollut 97:1–10

Chapin FS, Van Cleve K (1989) Approaches to studying nutrient uptake, use and loss in plants. In: Pearcy RW, Ehleringer J, Mooney HA et al (eds) Plant physiology ecology – field methods and instrumentation. Chapman and Hall, London, pp 187–207

Cobb WR, Will RE, Daniels RF et al (2008) Aboveground biomass and nitrogen in four short-rotation woody crop species growing with different water and nutrient availabilities. For Ecol Manage 255:4032–4039

Cornelissen JHC (1996) An experimental comparison of leaf decomposition rates in a wide range of temperate plant species. J Ecol 84:573–582

Cornelissen JHC, Thompson K (1997) Functional leaf attributes predict litter decomposition rate in herbaceous plants. New Phytologist 135:109–114

Cornell SE, Jickells TD, Cape JN et al (2003) Organic nitrogen deposition on land and coastal environments: a review of methods and data. Atmos Environ 37:2173–2191

Courchesne F, Hendershot WH (1990) The role of basic aluminium sulphate retention in the mineral horizons of two Spodosols. Soil Sci 150:571–578

Cudlin P, Kieliszewska-Rojucka B, Rudawska M et al (2007) Fine roots and ectomycorrhizas as indicators of environmental change. Plant Biosyst 141:406–425

David MB, Mitchell MJ, Nakas JP (1982) Organic and inorganic sulfur constituents of a forest soil and their relationship to microbial activity. Soil Sci Soc Am J 46:847–851

De Santo AV, Fierro A, Berg B et al (2002) Heavy metals and litter decomposition in coniferous forests. Dev Soil Sci 28:63–78

De Vries W, Bakker DJ (1998) Manual for calculating critical loads of heavy metals for terrestrial ecosystems. Guidelines for critical limits, calculation methods and input data. DLO Wienard Staring Centre, Wageningen (The Netherlands), Report 165

De Vries W, Reinds GJ, Vel E (2003) Intensive monitoring of forest ecosystems in Europe 2. Atmospheric deposition and its impacts on soil solution chemistry. For Ecol Manage 174:97–115

De Vries W, van der Salm C, Reinds GJ et al (2007) Element fluxes through European forest ecosystems and their relationships with stand and site characteristics. Environ Pollut 148:501–513

De Vries W, Solberg S, Dobbertin M et al (2008) Ecologically implausible carbon response? Nature 451(7180):E1–E3

De Vries W, Wamelink GWW, van Dobben H et al (2010) Use of dynamic soil-vegetation models to assess impacts of nitrogen deposition on plant species composition: an overview. Ecol Appl 20:69–79

Dise NB, Matzner E, Forsium M (1998a) Evaluation of organic horizon C:N ratio as an indicator of nitrate leaching in conifer forests across Europe. Environ Pollut 102:453–456

Dise NB, Matzner E, Gundersen P (1998b) Synthesis of nitrogen pools and fluxes from European forest ecosystems. Water Air Soil Poll 105:143–154

Dise NB, Rothwell JJ, Gauci V et al (2009) Predicting dissolved inorganic nitrogen leaching in European forests using two independent databases. Sci Total Environ 407:1798–1808

Drift JD (1961) Causes and effects of differences in the soil fauna in different types of oak forest. Ned Bosb Tijdschr 33:90–108

Emmett BA (2007) Nitrogen saturation of terrestrial ecosystems: some recent findings and their implications for our conceptual framework. Water Air Soil Poll Focus 7:99–109

Finér L, Helmisaari H-S, Lõhmus K et al (2007) Variation in fine root biomass of three European tree species: Beech (*Fagus sylvatica* L.), Norway spruce (*Picea abies* L. Karst.), and Scots pine (*Pinus sylvestris* L.). Plant Biosyst 141:394–405

ICP Forests (2009) Executive report (2009) The condition of forests in Europe. European Commission, Environmental Directorate General LIFE Unit. Hamburg and Brussels

Fowler D, Cape JN, Unsworth MH (1989) Deposition of atmospheric pollutants on forests. Philos T Roy Soc B 324:247–265

Fowler D, Smith RA, Muller JBA et al (2005) Changes in atmospheric deposition of acidifying compounds in the UK between 1986 and 2001. Environ Pollut 137:15–25

Fowler D, Smith R, Muller J et al (2007) Long term trends in sulfur and nitrogen deposition in Europe and the cause of non-linearly. Water Air Soil Poll Focus 7:41–47

Freney JR (1961) Some observations on the nature of organic sulfur compounds in soil. Aust J Agr Res 12:424–432

Friedland AJ (1992) The use of organic forest soils as indicators of atmospheric deposition of trace metals. In: Verry ES, Vermette SJ (eds) The deposition and fate of trace metals in our environment. pp 97–104

Galloway JN, Aber JD, Erisman JW et al (2003) The nitrogen cascade. Bioscience 53:341–356

Gauci V, Dise N, Blake S (2005) Long-term suppression of wetland methane flux following a pulse of simulated acid rain. Geophys Res Lett 32:L12804

Godbold DL, Fritz H-W, Jentschke G et al (2003) Root turnover and root necromass accumulation of Norway spruce (*Picea abies*) are affected by soil acidity. Tree Physiol 23:915–921

Gundersen P, Schmidt IK, Raulund-Rasmussen K (2006) Leaching of nitrate from temperate forests – effects of air pollution and forest management. Environ Rev 14:1–57

Ham Y-S, Tamiya S (2007) Contribution of dissolved organic nitrogen deposition to total dissolved nitrogen deposition under intensive agricultural activities. Water Air Soil Poll 178:5–13

Hansen K, Vesterdal L, Schmidt IK et al (2009) Litterfall and nutrient return in five tree species in a common garden experiment. For Ecol Manage 257:2133–2144

Helmisaari H-S (1992) Nutrient retranslocation in three *Pinus sylvestris* stands. For Ecol Manage 51:347–367

Hernandez L, Probst A, Probsta JL et al (2003) Heavy metal distribution in some French forest soils: evidence for atmospheric contamination. Sci Total Environ 312:195–219

Herrmann M, Pust J, Pott R (2006) The chemical composition of throughfall beneath oak, birch and pine canopies in Northwest Germany. Plant Ecol 184:273–285

Hobbie SE, Reich PB, Oleksyn J et al (2006) Tree species effects on decomposition and forest floor dynamics in a common garden. Ecology 87:2288–2297

Hoosbeek MR, Scarascia-Mugnozza GE (2009) Increased litter build up and soil organic matter stabilization in a poplar plantation after 6 years of atmospheric CO_2 enrichment (FACE): Final results of POP-EuroFACE compared to other forest FACE experiments. Ecosystems 12:220–239

Hornung M, Stevens PA, Reynolds B (1987) The effects of forestry on soils, soil water and surface water chemistry. In: Good JEG (ed) Environmental aspects of plantation forestry in Wales. Grange-over-Sands, NERC/ITE, pp 25–36 (ITE Symposium, 22)

Hunter MD, Adl S, Pringle CM et al (2003) Relative effects of macro invertebrates and habitat on the chemistry of litter during decomposition. Pedobiologia 47:101–115

Hyvönen R, Ågren GI, Linder S et al (2007) The Tansley review: the likely impact of elevated (CO_2), nitrogen deposition, increased temperature and management on carbon sequestration in temperate and boreal forest ecosystems: a literature review. New Phytol 173:463–480

IPCC (2006) IPCC Guidelines for National Greenhouse Gas Inventories. In: Eggleston HS, Buendia L, Miwa K, Ngara T, Tanabe K (Eds) Agriculture, forestry and other land use, Vol 4

Iversen CM (2010) Digging deeper: fine-root responses to rising atmospheric CO_2 concentration in forested ecosystems. New Phytol 186:346–357

Janssens IA, Dieleman W, Luyssaert S et al (2010) Reduction of forest soil respiration in response to nitrogen deposition. Nat Geosci 3:315–322

Jastrow JD, Miller RM, Matamala R et al (2005) Elevated atmospheric carbon dioxide increases soil carbon. Glob Change Biol 11:2057–2064

Jenkins A, Cullen JM (2001) An assessment of the potential impact of the Gothenburg protocol on surface water chemistry using the dynamic MAGIC model at acid sensitive sites in the UK. Hydrol Earth Syst Sci 5:529–541

Johnson DW (1984) Sulfur cycling in forests. Biogeochemistry 1:29–43

Johnson DW, Lindberg SE (1992) Atmospheric deposition and forest nutrient cycling. Ecological studies Vol 91. Springer, New York

Johnson DW, Turner J, Kelly JM (1982) The effects of acid rain on forest nutrient status. Water Resour Res 18:449–461

Johnson D, MacDonald D, Hendershot W et al (2003) Metals in northern forest ecosystems: role of vegetation in sequestration and cycling, and implications for ecological risk assessment. Hum Ecol Risk Assess 9:749–766

Jug A, Hofmann-Schielle C, Makeschin F et al (1999) Short-rotation plantations of balsam poplars, aspen and willows on former arable land in the Federal Republic of Germany. II. nutritional status and bioelement export by harvest of shoot axes. For Ecol Manage 121:67–83

Jurinak JJ, Bauer N (1956) Thermodynamics of zinc adsorption on calcite, dolomite and magnesite- type minerals. Soil Sci Soc Am Proc 20:466–471

Kabata-Pendias A, Pendias H (1984) Trace elements in soils and plants. CRC, Boca Raton, FL

Khanna PK, Prenzel J, Meiwes KJ et al (1987) Dynamics of sulphate retention by acid forest soils in an acidic deposition environment. Soil Sci Soc Am J 51:446–452

Kimmins JP (1987) Forest ecology. Macmillan, New York, USA

Laiho R, Prescott CE (2004) Decay and nutrient dynamics of coarse woody debris in northern coniferous forests: a synthesis. Can J For Res 34:763–777

Langusch J-J, Matzner E (2002) N fluxes in two nitrogen saturated forested catchments in Germany: dynamics and modelling with INCA. Hydrol Earth Syst Sci 6:383–394

Lichter J, Barron SH, Bevacqua CE et al (2005) Soil carbon sequestration and turnover in a pine forest after six years of atmospheric CO_2 enrichment. Ecology 86:1835–1847

Lindberg SE, Garten CT (1988) Sources of sulfur in forest canopy throughfall. Nature 336:148–151

Lloyd AH, Fastie CL (2002) Spatial and temporal variability in the growth and climate response of treeline trees in Alaska. Clim Change 52:481–509

Loveland PJ (1993) The classification of the soils of England and Wales on the basis of mineralogy and weathering – the Skokloster approach. In: Hornung M, Skeffington RA (eds) Critical loads: concept and applications. HMSO, London, pp 48–53

Luttermann A, Freedman B (2000) Risks to forests in heavily polluted regions. In: Innes JL, Oleksyn J (eds) Forest dynamics in heavily polluted regions, Report 1 of the IUFRO task force on environmental change. CABI, UK, pp 9–26

MacDonald JA, Skiba U, Sheppard LJ et al (1997) The effect of nitrogen deposition and seasonal variability on methane oxidation and nitrous oxide emission rates in an upland spruce plantation and moorland. Atmos Environ 31:3693–3706

Magnani F, Mencuccini M, Borghetti M et al (2007) The human footprint in the carbon cycle of temperate and boreal forests. Nature 447:848–850

Majdi H, Pregitzer K, More A-S et al (2005) Measuring fine root turnover in forest ecosystems. Plant Soil 276:1–8

Mayerhofer P, Alcamo J, Posch M et al (2001) Regional air pollution and climate change in Europe: an integrated assessment (AIR-CLIM). Water Air Soil Poll 130:1151–1156

McBride MB (1979) Chemisorption and precipitation of Mn^{2+} at $CaCO_3$ surfaces. Soil Sci Soc Am J 43:693–698

McBride MB (1980) Chemisorption of Cd2+ at calcite surfaces. Soil Sci Soc Am J 44:26–28

McEnroe NA, Helmisaari H-S (2001) Decomposition of coniferous forest litter along a heavy metal pollution gradient, south-west Finland. Environ Pollut 113:11–18

Miller HG, Miller JD (1991) Energy forestry – the nutritional equation. In: Aldhous BA (ed) Wood for energy. The implications for harvesting utilisation and marketing. Proceedings Disc. Meet. Edinburgh. Institute of Chartered Forestry, Edinburgh

Mitchell MJ (1992) Analyses of selected sulfur cycles in polluted versus unpolluted environments. In: Johnson DW, Lindberg SE (eds) Atmospheric deposition and forest nutrient cycling, Vol 91. Ecol Stud. Springer, New York, pp 133–137

Mitchell MJ, David MB, Harrison RB (1992) Sulfur dynamics of forest ecosystems. In: Howarth R, Stewart JWB, Ivanov MV (eds) Sulfur cycling on the continents: wetlands, terrestrial ecosystems, and associated water bodies. Wiley, Chichester, pp 215–254

Morris LA, Pritchett WL, Swindel BF (1983) Displacement of site nutrients into windrows during site preparation of a flatwoods forest soil. Soil Sci Soc Am J 47:951–954

Mustajärvi K, Merilä P, Derome J et al (2008) Fluxes of dissolved organic and inorganic nitrogen in relation to stand characteristics and latitude in Scots pine and Norway spruce stands in Finland. Boreal Environ Res 13(suppl B):3–21

Nave LE, Vance ED, Swanston CW et al (2009) Impacts of elevated N inputs on north temperate forest soil C storage, C/N, and net N-mineralization. Geoderma 153:231–240

Nilsson J, Grennfelt P (eds) (1988) Critical loads for sulfur and nitrogen. UN-ECE/Nordic Council Workshop Report, Skoklester, Sweden, Nordic Council Ministers

Nisbet T (2005) Water use by trees. Forest Research Information Note 65, Forestry Commission, Edinburgh

Nisbet AF, Nisbet TR (1992) Interactions between rain, vegetation and soils. In: Howells G, Dalziel TRK (eds) Restoring acid waters: Loch Fleet 1984–1990. Elsevier, New York, pp 135–149

Norby RJ, DeLucia EH, Gielen B et al (2005) Forest response to elevated CO_2 is conserved across a broad range of productivity. Proc Natl Acad Sci USA 102:18052–18056

Norton SA, Kahl JS (1992) Paleolimnological evidence of metal pollution from atmospheric deposition. In: Verry ES, Vermette SJ (eds) The deposition and fate of trace metals in our Environment. pp 85–95

Nriagu JO (1979) Global inventory of natural and anthropogenic emissions of trace metals to the atmosphere. Nature 279:409–411

Nriagu JO (1989) A global assessment of natural sources of atmospheric trace metals. Nature 338:47–49

Nwoboshi LC (1983) Potential impacts of some harvesting options on nutrient budgets of a Gmelina pulpwood plantation ecosystem in Nigeria (*Gmelina arborea*). USDA Forest Service general technical report PNW - United States, Report No. 163: 212–217

Nyborg M, Repin D, Hocking D et al (1977) Effect of sulfur dioxide on precipitation and on the sulfur content and acidity of soils in Alberta, Canada. Water Air Soil Poll 7:439–448

O'Connell AM, Grove TS (1999) Eucalypt plantations in south-western Australia. In: Nambiar EKS, Cossalter C, Tiarks A (eds) Site management and productivity of tropical plantation forests: proceedings of Workshop in South Africa, February 1998. CIFOR, Bogor, pp 53–59

Ostonen I, Püttsepp Ü, Biel C et al (2007) Specific root length as an indicator of environmental change. Plant Biosyst 141:426–442

Parton W, Silver WL, Burke IC et al (2007) Global-scale similarities in nitrogen release patterns during long-term decomposition. Science 315:361–364

Pedersen LB, Bille-Hansen J (1999) A comparison of literfall and element fluxes in even aged Norway spruce, sitka sppruce and beech stands in Denmark. For Ecol Manage 114:55–70

Pereira AP, Graca MAS, Manuel M (1998) Leaf litter decomposition in relation to litter physico-chemical properties, fungal biomass, arthropod colonization, and geographical origin of plant species. Pedobiologia 42:316–327

Peterken GF (2001) Ecological effects of introduced tree species in Britain. For Ecol Manage 141:31–42

Pitman R (2004) Litterfall at the Level II intensive forest monitoring plots in the UK. Report, Forest Research, Forestry Commission

Pitman R, Vanguelova EI, Benham S (2010) Effects of phytophagous insects on the nutrient fluxes through forest stands in the UK Level II network. Submitted to Sci Total Environ 409:169–181

Poikolainen J, Kubin E, Piispanen J et al (2004) Atmospheric heavy metal depositionnext term in Finland during 1985–2000 using mosses as bioindicators. Sci Total Environ 318:171–185

Posch M (2002) Impacts of climate change on critical loads and their exceedances in Europe. Environ Sci Policy 5:307–317

Prietzel J, Majer B, Krouse HR et al (1995) Transformation of simulated wet sulfate deposition in forest soils assessed by a core experiment using stable sulfur isotopes. Water Air Soil Poll 79:243–260

Prietzel J, Weick C, Korintenberg J et al (2001) Effects of repeated $(NH_4)_2SO_4$ application on sulfur pools in soil, soil microbial biomass, and ground vegetation of two watersheds in the Black Forest/Germany. Plant Soil 230:287–305

Pussinen A, Karjalainen T, Makipaa R et al (2002) Forest carbon sequestration and harvests in Scots pine stand under different climate and nitrogen deposition scenarios. For Ecol Manage 158:103–115

Quilchano C, Haneklaus C, Gallardo JF et al (2002) Sulfur balance in a broadleaf, non-polluted, forest ecosystem (central-western Spain). For Ecol Manage 161:205–214

Ranger J, Belgrand CM (1996) Nutrient dynamics of the chestnut tree (*Castanea sativa* Mill) in coppice stands. For Ecol Manage 86:259–277

Raulund-Rasmussen K, Stupak I, Clarke N et al (2008) Effects of very intensive forest biomass harvesting on short and long term site productivity. In: Röser D et al (eds) Use of forest biomass for energy: a synthesis with focus on the Baltic and Nordic region. Springer, Heidelberg, pp 29–78

Reich PB, Oleksyn J, Modrzynski J et al (2005) Linking litter calcium, earthworms and soil properties: a common garden test with 14 tree species. Ecol Lett 8:811–818

Review of Transboundary Air Pollution (RoTAP) (2011) Consultation Draft V1.03

Ross SM (1994) Sources and forms of potentially toxic metals in soil-plant systems. In: Ross SM (ed) Toxic metals in soil-plant systems. Wiley, Chichester, pp 3–26

Rothe A, Huber C, Kreutzer K et al (2002) Deposition and soil leaching in stands of Norway spruce and European beech: results from the Hoglwald research in comparison with other European case studies. Plant Soil 240:33–45

Schulte A (1994) Adsorption density, mobility and limit values of Cd, Zn and Pb in acid soils. Arch Acker-Pfi Boden 38:71–81

Schulze ED (2000) Carbon and nitrogen cycling in European forest ecosystems. Ecol Stud Vol 142. Springer, New York

Schulze ED, Lange OL, Oren R (1989) Air pollution and forest decline: a study of Spruce (*Picea abies*) on acid soils. Ecol Stud Vol 77. Springer, New York, pp 475

Siccama TG, Smith WH (1978) Lead accumulation in a northern hardwood forest. Environ Sci Technol 12:593–594

Skiba U, Sheppard LJ, Pitcairn CER et al (1999) The effect of N deposition on nitrous oxide and nitric oxide emissions from temperate forest soils. Water Air Soil Poll 116:89–98

Skiba U, Pitcairn C, Sheppard L et al (2004) The influence of atmospheric N deposition on nitrous oxide and nitric oxide fluxes and soil ammonium and nitrate concentrations. Water Air Soil Poll Focus 4:37–43

Sleutel S, Vandenbruwane J, Schrijver A et al (2009) Patterns of dissolved organic carbon and nitrogen fluxes in deciduous and coniferous forests under historic high nitrogen deposition. Biogeosciences 6:2743–2758

Smith WH, Siccama TG, Clark SL (1986) Atmospheric deposition of heavy metals and forest health: an overview and a ten-year budget for the input/output of seven heavy metals to a northern hardwood forest. Publication FWS-8702, School of Forestry and Wildlife Resources, Virginia Polytechnic Institute and State University, Blacksburg, USA

Soon YK, Abboud S (1993) Cadmium, chromium, lead, and nickel. In: Carter MR (ed) Soil sampling and methods of analysis. Lewis, Boca Raton, FL, pp 101–108

Starr M, Lindroos A-J, Ukonmaanaho L et al (2003) Weathering release of heavy metals from soil in comparison to deposition, litterfall and leaching fluxes in a remote, boreal coniferous forest. Appl Geochem 18:607–613

Steinnes E (1984) Impact of long – range atmospheric transport of heavy metals to the terrestrial environment in Norway. Scope Workshop on Metal cycling, Toronto, Canada, 2–6 Sep. 1984

Steinnes E, Njåstad O (1995) Enrichment of metals in the organic surface layer of natural soil: identification of contributions from different sources. Analyst 120:1479–1483

Stoddard JL, Jeffries DS, Lukewille A et al (1999) Regional trends in aquatic recovery from acidification in North America and Europe. Nature 401:575–578

Tamm CO (1969) Site damages by thinning due to removal of organic matter and plant nutrients. Thinning and mechanization. In: Proceedings of IUFRO Meeting, Stockholm, pp 175–177

Taylor GE, Johnson DW, Andersen CP (1994) Air pollution and forest ecosystems: a regional to global perspective. Ecol Appl 4:662–689

Tew DT, Morris LA, Allen HL et al (1986) Estimates of nutrient removal, displacement and loss resulting from harvest and site preparation of a *Pinus taeda* plantation in the Piedmont of North Carolina. For Ecol Manage 15:257–267

Tipping E, Lawlor AJ, Lofts S (2006) Simulating the long-term chemistry of an upland UK catchment: major solutes and acidification. Environ Pollut 141:151–166

Tullus A, Tullus H, Soo T et al (2009) Above-ground biomass characteristics of young hybrid aspen (*Populus tremula* L. x *P. tremuloides* Michx.) plantations on former agricultural land in Estonia. Biomass Bioenergy 33:1617–1625

Tyler G (1978) Leaching rates of heavy metal ions in forest soil. Water Air Soil Poll 9:137–148

Tyler G (1992) Critical concentrations of heavy metals in the Mor horizon of Swedish soils. Swedish Environmental Protection Agency, Report 4078

Ukonmaanaho L, Merilä P, Nöjd P et al (2008) Literfall production and nutrient return to forest floor in Scots pine and Norway spruce stands in Finland. Boreal Environ Res 13(suppl B): 67–91

Van der Salm C, Reinds GJ, de Vries W (2007) Water balances in intensive monitored forest ecosystem in Europe. Environ Pollut 148:201–212

Van Miegroet H, Johnson DW, Cole DW (1992) Analysis of N cycles in polluted versus unpolluted environments. In: Johnson DW, Lindberg SE (eds) Atmospheric deposition and forest nutrient cycling. Ecol Stud 91, Springer-Verlag, New York, pp 199–202

Vanguelova EI, Pitman R (2009) Impact of N deposition on soil and tree biochemistry in both broadleaved and coniferous stands in the UK. In: Ukonmaanoho L, Tiina M, Nieminen M, et al (eds) 6th International symposium on ecosystem behaviour BIOGEOMON 2009. ISSN 1795-150X

Vanguelova EI, Barsoum N, Benham S, et al (2007a) Ten years of intensive environmental monitoring of British forests. Forest Research Information Note 88, Forestry Commission, Edinburgh

Vanguelova EI, Hirano Y, Eldhuset TD et al (2007b) Tree fine root Ca/Al molar ratio – indicator of Al and acidity stress. Plant Biosyst 141:460–480

Vanguelova EI, Benham S, Pitman R et al (2010) Chemical fluxes in time through forest ecosystems in the UK – soil response to pollution recovery. Environ Pollut 158:1857–1869

Vanguelova EI (2010) BioSoil case study: Evaluation of the quality and changes in UK forest soils. European Commission. Forest soil and biodiversity monitoring in the EU. Luxembourg: Publications Office of the European Union 2010 – 32 pp; ISBN 978-92-79-14992-4; doi:10.2779/16475

Vanguelova E, Pitman R (2011) Impacts of short rotation forestry on soil sustainability. In: McKay H (ed) Short rotation forestry: review of growth and environmental impacts. Forest Research Monograph 2, Forest Research, Surrey, pp. 212. ISBN 978-0-85538-827-0

Vanmechelen L, Groenemans R, Van Ranst E (1997) Forest soil condition in Europe – results of large-scale soil survey-EU-UN/ECE. In: International co-operative programme on assessment and monitoring of air pollution effects on forests (ICP-Forests)

Verry ES, Vermette SJ (1992) The deposition and fate of trace metals in our environment. USDA-Forest Service, North central Forest Experimental Station

Vesterdal L, Schmidt IK, Calleson I et al (2008) Carbon and nitrogen in forest floor and mineral soil under six common European tree species. For Ecol Manage 255:35–48

Wedderburn ME, Carter J (1999) Litter decomposition by four functional tree types for use in silvopastoral systems. Soil Biol Biochem 31:455–461

Wigston J (1990) Arb J Forest 63:177–196

Withington JM, Reich P, Oleksyn J et al (2006) Comparisons of structure and life span in roots and leaves among temperate trees. Ecol Monogr 76:381–397

Witkamp M, Drift JD (1961) Breakdown of forest litter in relation to environmental factors. Plant Soil 15:295–311

Witter E (1992) Heavy metal concentrations in agricultural soils critical to microorganisms. Swedish Environmental Protection Agency, Report 4079

Zhang Y, Mitchell MJ, Driscoll CT et al (1999) Changes in soil sulfur constituents in a forested watershed 8 years after whole-tree harvesting. Can J For Res 29:356–364

Zwolinski J (1994) Rates of organic matter decomposition in forests polluted with heavy metals. Ecol Eng 3:17–26

Chapter 35
Forests and Global Change

Gordon B. Bonan

35.1 Introduction

Forest ecosystems influence climate through physical, chemical, and biological processes that affect planetary energetics, the hydrologic cycle, and atmospheric composition (Bonan 2008). Physical processes at the intersection of the biosphere and geosphere, commonly referred to as biogeophysics, include momentum transfer and land–atmosphere energy fluxes (absorption and reflection of solar radiation, absorption and emission of longwave radiation, partitioning of net radiation into sensible and latent heat fluxes, and storage of heat in the soil). Hydrologic processes include interception of precipitation, throughfall, stemflow, infiltration, runoff, evapotranspiration, soil water dynamics, and snow melt. Forests additionally influence climate and atmospheric composition through biogeochemical processes including the exchanges of CO_2, CH_4, N_2O, biogenic volatile organic compounds, and aerosols with the atmosphere. Forest ecosystems are now recognized as providing important climate forcing and feedback.

Much of our understanding of how forest ecosystems affect climate comes from numerical models of Earth's climate and their representation of the terrestrial biosphere (Fig. 35.1). These models initially simulated only biogeophysical processes at the land surface. They have since evolved to simulate the hydrologic cycle, biogeochemical cycles, and vegetation dynamics so that the biosphere and atmosphere form a coupled system. The development of numerical parameterizations that represent these processes in global models of Earth's climate is a compelling example of scientific advancement through multidisciplinary research. This interdisciplinary science integrates the numerous climate influences of ecosystems with the impacts of global change to identify and understand ecosystem feedbacks in the Earth system and the potential of ecosystems to mitigate climate change (Bonan 2008).

This chapter provides an overview of the hydrology, biogeochemistry, and ecosystem ecology of climate models. Two ecological processes – the carbon cycle and land cover change – are the focus of much climate change research. In addition, the models are being used to identify ecological mechanisms to mitigate anthropogenic climate change.
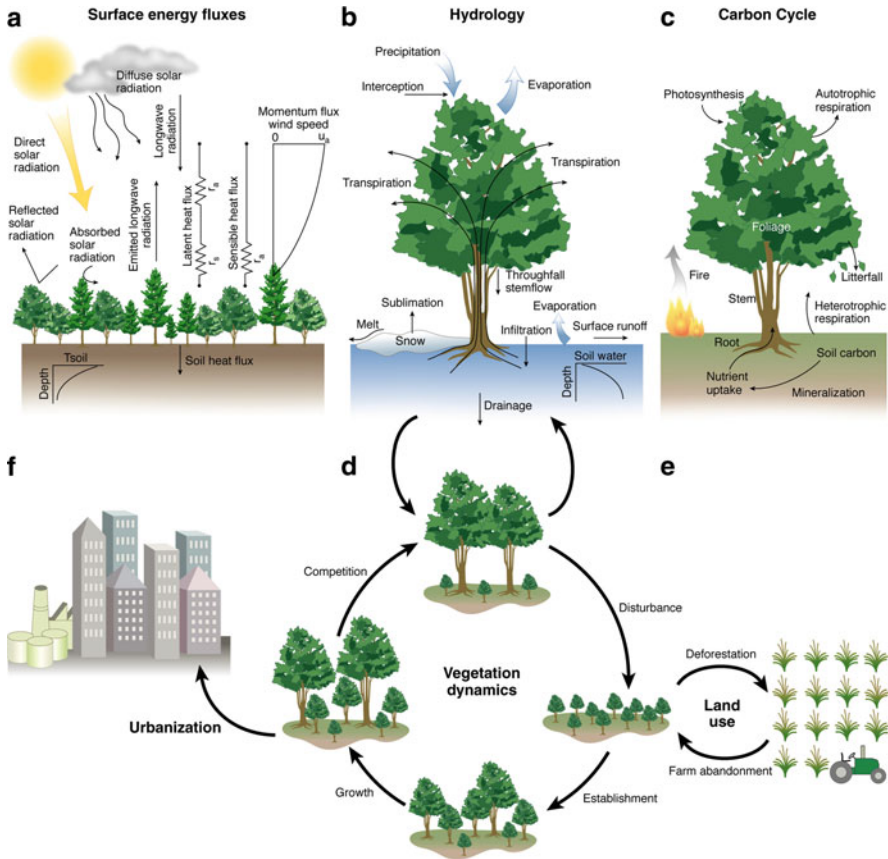
Fig. 35.1 The current generation of climate models treats the biosphere and atmosphere as a coupled system, illustrated here for the National Center for Atmospheric Research Community Land Model. Hydrologic, biogeochemical, and ecosystem processes represented in the model include (**a**) surface energy fluxes, (**b**) the hydrologic cycle, (**c**) the carbon cycle, and (**d**) vegetation dynamics. The model also includes (**e**) land use and (**f**) urbanization to represent human alteration of the biosphere (from Bonan 2008)

35.2 Hydrology, Biogeochemistry, and Ecosystems in Climate Models

The first parameterizations of Earth's land surface in atmospheric models used aerodynamic bulk transfer equations and specified albedo, surface roughness, and soil wetness without explicitly representing vegetation or the hydrologic cycle. The hydrologic cycle, if included, was represented as a "bucket" in which precipitation fills the soil to a specified water-holding capacity, beyond which rainfall runs off (Manabe et al. 1965). Application of these models demonstrated the importance of evapotranspiration in regulating global climate (Shukla and Mintz 1982).

Building upon the pioneering work of Deardorff (1978), model development in the mid-1980s expanded this geophysical representation of the land surface to a biogeophysical paradigm by addressing the full hydrologic cycle and the effects of vegetation on energy and water fluxes (Dickinson et al. 1986, 1993; Sellers et al. 1986). These models represented plant canopies, including radiative transfer, turbulent processes above and within the canopy, and the physical and biological controls of evapotranspiration. The models partitioned evapotranspiration into the separate fluxes of evaporation of intercepted water, soil evaporation, and transpiration. The hydrologic cycle was represented as interception, throughfall, stemflow, infiltration, runoff, soil water, snow, evaporation, and transpiration. Model experiments demonstrated biogeophysical regulation of climate by vegetation, for example, through studies of tropical deforestation (Dickinson and Henderson-Sellers 1988).

In the mid-1990s, representation of the biological control of evapotranspiration was further advanced in a third generation of models that used the theoretical developments of Collatz et al. (1991) to link the biochemistry of photosynthesis with the biophysics of stomatal conductance (Bonan 1995; Sellers et al. 1996a). These models scaled leaf processes to the plant canopy using concepts of sunlit and shaded leaves and optimal allocation of photosynthetic resources. Model experimentation identified the importance of stomata for climate simulations (Sellers et al. 1996b), and the models provided the framework to simulate the effects of the biosphere on atmospheric CO_2 (Denning et al. 1996; Craig et al. 1998).

Formalization of dynamic global vegetation models in the late-1990s (Foley et al. 1996; Sitch et al. 2003), and their coupling to land surface parameterizations (Foley et al. 2000; Bonan et al. 2003), incorporated theoretical advances in biogeochemistry, vegetation dynamics, and biogeography into models of the coupled biosphere–atmosphere system. These models simulate the terrestrial carbon cycle, plant community composition, and vegetation dynamics in relation to climate. Model experiments demonstrated biogeophysical feedbacks from coupled climate–vegetation dynamics in the Arctic, where expansion of trees into tundra decreases surface albedo (Levis et al. 1999, 2000), and in North Africa, where expansion of vegetation into desert similarly lowers albedo (Levis et al. 2004). Other studies demonstrated biogeochemical feedbacks from the carbon cycle (Cox et al. 2000; Friedlingstein et al. 2006).

Development of the current generation of biosphere models for climate simulations continues to incorporate theoretical advances in hydrology, biogeochemistry, and ecology. For example, some carbon cycle parameterizations are built from a biogeochemical modeling heritage and do not represent individual plants, excluding key ecological principles of allometric constraints and age – structure or size – structure that are important determinants of vegetation dynamics. A new class of models better integrates long-term demographic and ecosystem processes with short-term biogeophysical, biogeochemical, and hydrologic processes (Medvigy et al. 2009). Global crop models simulate managed agroecosystems in addition to natural ecosystems (Gervois et al. 2004; Bondeau et al. 2007). New ecological processes added to the models have identified feedbacks from ozone and stomata
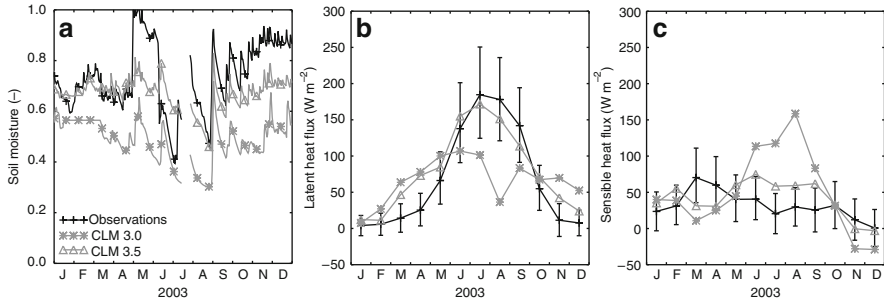
Fig. 35.2 Model simulations (*grey lines*) compared with observations (*black lines*) for Morgan Monroe State Forest, Indiana, during 2003 (**a**) soil moisture relative to saturation at 30 cm depth; (**b**) monthly latent heat flux; and (**c**) monthly sensible heat flux. *Error bars* show estimated uncertainties of observed turbulent fluxes. The *grey lines* show simulations using version 3.0 and version 3.5 of the Community Land Model (from Stöckli et al. 2008)

(Sitch et al. 2007), photosynthetic enhancement by diffuse radiation (Mercado et al. 2009), peatlands and methane (Wania et al. 2009), and carbon–nitrogen biogeochemistry (Sokolov et al. 2008; Thornton et al. 2009; Zaehle et al. 2010).

Scientists have a diverse array of methodologies spanning many spatial and temporal scales with which to test and inform these models. Such data include ecosystem and watershed monitoring (e.g., eddy covariance flux towers, long-term ecological research) and experimental manipulation (e.g., soil warming, free-air CO_2 enrichment), as well as continental- to global-scale coverage from satellite sensors and atmospheric monitoring of CO_2. Such data are routinely used to diagnose and improve deficiencies in the models (Oleson et al. 2008; Stöckli et al. 2008; Randerson et al. 2009).

For example, eddy covariance measurements of sensible and latent heat fluxes identify deficiencies in soil water and surface fluxes, illustrated in Fig. 35.2 for simulations of a temperate deciduous forest using the Community Land Model. Version 3.0 of the model has low soil moisture compared to observations, resulting in low latent heat flux and high sensible heat flux, especially during the growing season. Improvements to the parameterization of infiltration, runoff, soil evaporation, and groundwater in version 3.5 of the model produce wetter soil, higher latent heat flux, and lower sensible heat flux, which better matches observations. Stand–level synthesis of net primary production can be used to test the simulated carbon cycle. For example, Fig. 35.3 compares the simulated net primary production of two different biogeochemical models coupled to the Community Land Model.

35.3 Carbon Cycle–Climate Feedbacks

Undisturbed terrestrial ecosystems absorbed 2.6 Gt C y^{-1} during the 1990s, approximately one-third of the anthropogenic carbon emission from fossil fuel combustion and land use change during the same period (Denman et al. 2007). This carbon sink
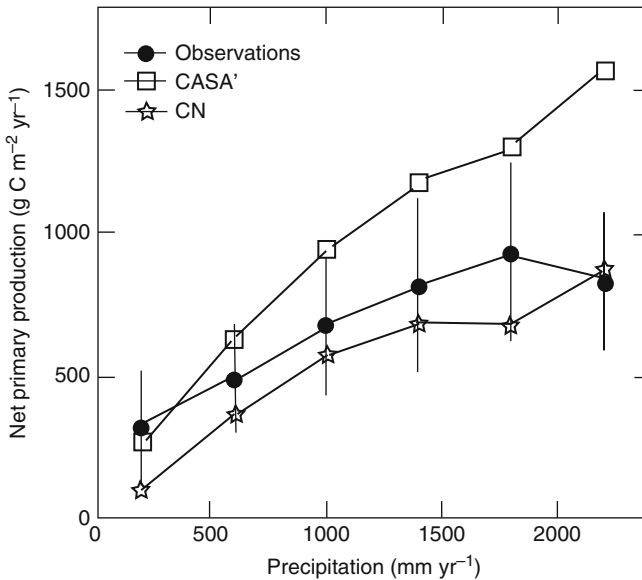
Fig. 35.3 Simulated net primary production for two biogeochemical models (CASA' and CN) coupled to the Community Land Model compared with observations. Net primary production is shown in relation to annual precipitation. *Vertical bars* show observational uncertainty (from Randerson et al. 2009)

is expected to weaken with climate warming. Many climate models now include terrestrial and oceanic carbon fluxes so that atmospheric CO_2 concentration is simulated in response to anthropogenic CO_2 emissions. Coupled carbon cycle–climate simulations find that the capacity of the terrestrial biosphere to store anthropogenic CO_2 emissions decreases over the twenty-first century, providing a positive feedback whereby warming further increases atmospheric CO_2 concentration (Friedlingstein et al. 2006; Plattner et al. 2008).

The overall carbon cycle–climate feedback consists of two distinctly different responses of the terrestrial biosphere to global environmental change. Plants respond to increasing atmospheric CO_2 through photosynthetic enhancement, and increased land carbon uptake through this "CO_2 fertilization" is a negative feedback to higher atmospheric CO_2 concentration. This carbon gain is diminished by net global carbon loss with warming. Respiration loss increases with warming in a positive climate feedback. Warming can enhance photosynthesis (negative feedback) in cold regions, but decrease photosynthesis (positive feedback) in warm regions, where greater evaporative demand dries soil. Model intercomparison finds an overall positive feedback in which carbon cycle processes increase atmospheric CO_2 at the end of the twenty-first century (Friedlingstein et al. 2006; Plattner et al. 2008).

This interpretation of the carbon cycle is formed from models that do not include carbon–nitrogen biogeochemistry. Decomposition of plant litter and soil organic matter produces much of the nitrogen to support plant growth. Biological nitrogen

fixation and anthropogenic nitrogen deposition provide additional inputs. Nitrogen availability limits plant productivity in many ecosystems, and there is insufficient nitrogen available to sustain the CO_2 fertilization simulated by the carbon cycle–climate models (Wang and Houlton 2009). Experimental studies confirm that low nitrogen availability restricts plant productivity gain with CO_2 enrichment (de Graaff et al. 2006). However, soil warming can increase decomposition of organic material and thus nitrogen mineralization, thereby reducing nitrogen limitation (Melillo et al. 2002). These carbon–nitrogen interactions, long included by ecologists in their ecosystem models, are key regulators of ecosystem response to warming and CO_2 enrichment. Two carbon cycle–climate model simulations of future climate change that include carbon–nitrogen biogeochemistry do indeed find that inclusion of the nitrogen cycle decreases carbon uptake from CO_2 fertilization and changes the sign of the warming feedback so that terrestrial ecosystems gain carbon as climate warms (Sokolov et al. 2008; Thornton et al. 2009).

Results of carbon–nitrogen models question the conclusions of carbon-only simulations, but raise new uncertainties. The influence of nitrogen on CO_2 fertilization varies greatly among models (Sokolov et al. 2008; Thornton et al. 2009; Zaehle et al. 2010). Anthropogenic nitrogen deposition can further stimulate plant productivity (Thomas et al. 2009), but progressive nitrogen limitation caused by accumulation of nitrogen in plant biomass and soil organic matter may diminish productivity (de Graaff et al. 2006). Redistribution of plant species in response to climate change alters patterns of nitrogen uptake and mineralization (Pastor and Post 1988). The different results found with carbon–nitrogen models will motivate expansion of carbon cycle–climate models to include the nitrogen cycle, as well as other biogeochemical cycles. However, better understanding of the carbon cycle–climate feedback requires an expansion of model capabilities. The representation of the terrestrial biosphere in climate models has expanded from an initial biogeophysical focus on energy and water to include biogeochemical cycles. The models must be further expanded to represent biogeographical processes such as land use, fire, and postdisturbance vegetation succession. For example, few models currently account for the land use carbon flux directly (Shevliakova et al. 2009).

35.4 Land Cover Change

Human activities have converted large regions of the world from natural forest, grassland, and savanna ecosystems to managed cropland and pastureland (Klein Goldewijk et al. 2007; Ramankutty et al. 2008). Between 1850 and 2005, cropland area increased in much of the world while forest cover decreased (Fig. 35.4). Farm abandonment resulted in an increase in tree cover in eastern United States and Europe. This land cover change produced a net release of carbon to the atmosphere (Denman et al. 2007). It also altered climate through biogeophysical processes at the land surface, including surface albedo, surface roughness, and the partitioning
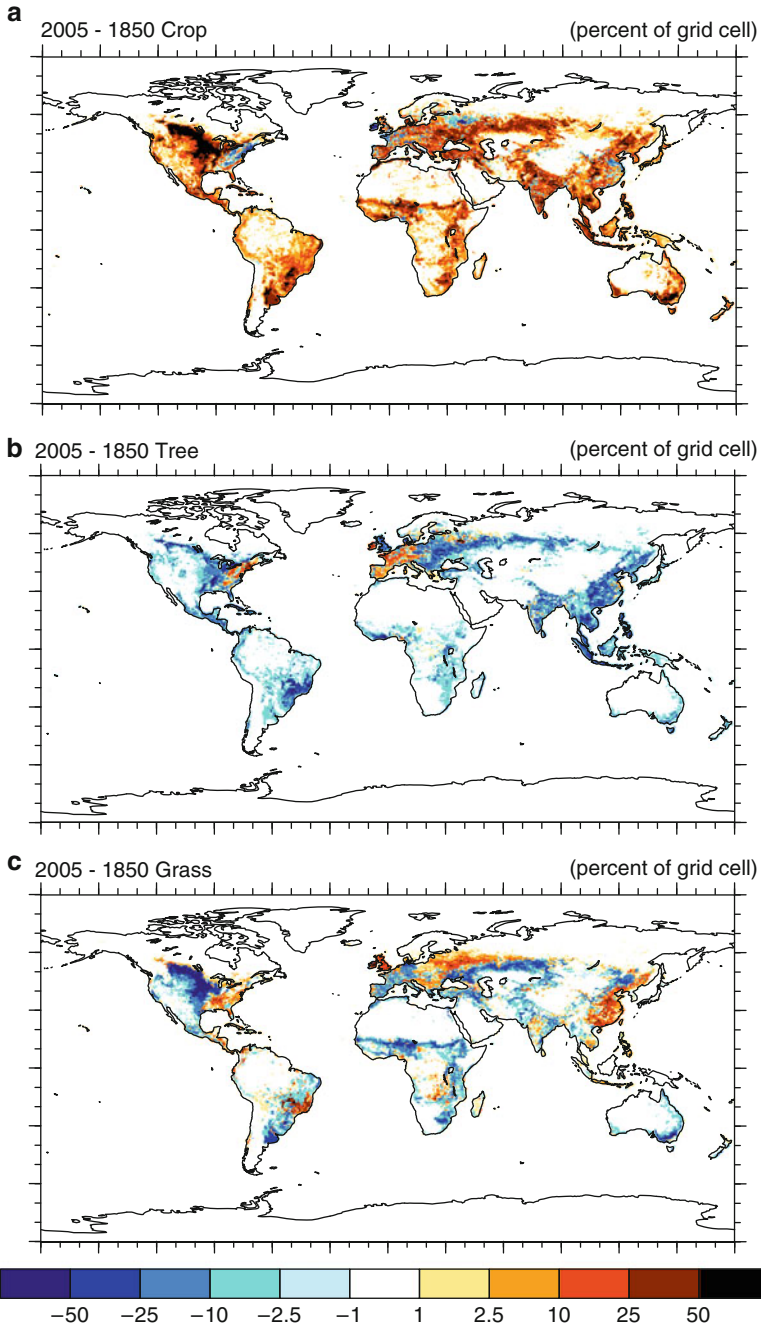
Fig. 35.4 Land cover change represented in the Community Land Model version 4 (CLM4). Shown are the difference in (**a**) crop, (**b**) tree, and (**c**) grass cover (percent of model grid cell) in 2005 compared with 1850

of net radiation into sensible and latent heat fluxes. The biogeophysical effects of historical land cover change are an important climate forcing, especially at regional scales (Pitman et al. 2009).

The climate forcing from land cover change varies among the world's ecosystems (Bonan 2008). Forests generally have a lower albedo than croplands or pasturelands, especially in snow-covered lands. Forests can also sustain high rates of evapotranspiration. Climate model simulations indicate that tropical forests have high rates of evapotranspiration, decrease surface air temperature, and increase precipitation compared with pastureland. Consequently, tropical deforestation is generally accepted to warm climate, because the warming associated with reduced evapotranspiration offsets the cooling from the higher surface albedo of pasturelands. In high latitudes, climate model simulations indicate that the low surface albedo of forests during the snow season warms climate compared to an absence of trees. Consequently, deforestation in northern latitudes is thought to cool climate primarily because of higher surface albedo. In mid-latitudes, higher albedo following conversion of forest to cropland or pastureland leads to cooling, but changes in evapotranspiration can enhance or mitigate this cooling.

The greatest uncertainty in the land cover change forcing is in mid-latitudes and is associated with evapotranspiration (Bonan 2008). Model intercomparison suggests that historical land cover change in mid-latitudes has cooled climate, but the magnitude, and even the sign, of this simulated climate change varies due to model-specific parameterization of albedo, evapotranspiration, and crop phenology (Pitman et al. 2009). Croplands have a higher albedo than forests, and parameterization of surface albedo is a key determinant of the climate forcing. Albedo parameterizations span a range from detailed plant canopy radiative transfer algorithms utilizing leaf optical properties to semiempirical algorithms utilizing prescribed land cover-dependent albedo. Comparison with satellite observations can constrain simulated albedo.

Land cover changes in evapotranspiration are less well known. Our understanding of the effect of land clearing on evapotranspiration is based on the conceptualization that tall, deep-rooted trees have greater rates of evapotranspiration than short, shallow-rooted crops and grasses because of their larger surface roughness and greater pool of soil water to sustain evapotranspiration. Indeed, many land surface components of climate models utilize this paradigm. Such a paradigm is evident in observations. For example, eddy covariance flux tower measurements at the Duke Forest show forests have greater rates of evapotranspiration than adjacent pastureland (Juang et al. 2007). The surface cooling from this higher evapotranspiration offsets the warming due to the lower albedo of forests. In Europe, remote sensing measurements of surface temperature show little difference between forests and crops during a wet summer, but forests are significantly greener (higher normalized difference vegetation index) and cooler than crops during a severe drought (Zaitchik et al. 2006). However, evapotranspiration is the sum of canopy interception, transpiration, and soil evaporation, each of which responds differently to land cover change. Differences among trees, grasses, and crops in stomatal conductance also affect evapotranspiration, as does variation in leaf area index.

The representation of land cover change can affect the climate change signal (Pitman et al. 2009). Some models include parameterizations of crop growth and management to simulate leaf area index; others use prescribed monthly varying leaf area index. Some models allow multiple plant functional types within a model grid cell; others allow only a single dominant land cover type in the grid cell.

35.5 Climate Change Mitigation

An understanding of the combined biogeophysical (albedo and evapotranspiration) and biogeochemical (carbon cycle) effects of ecosystems remains an elusive goal. Through these and other processes, forests can amplify or dampen climate change arising from anthropogenic greenhouse gas emission (Bonan 2008). In tropical forests, the negative climate forcing from strong evaporative cooling augments the negative forcing from high rates of carbon accumulation. The climate forcing of boreal forests is less well known. The positive climate forcing (warming) due to low surface albedo may counter the negative forcing from carbon sequestration so that boreal forests warm global climate. The climate benefit of temperate forests is poorly understood. Reforestation and afforestation may sequester carbon, but the effects of albedo and evapotranspiration are moderate compared with other forests, and forest influences on evapotranspiration are unclear. Warming from the low albedo of forests could offset cooling from carbon sequestration so that the net climatic effect of temperate reforestation and afforestation is negligible, or greater evapotranspiration by trees could augment biogeochemical cooling.

The net climate forcing through historical land use and land cover change is not clear. The dominant competing signals from historical deforestation are an increase in surface albedo countered by carbon emission to the atmosphere. For example, loss of forest increases surface albedo in the eastern United States through the mid-twentieth century until warming reduces snow cover and decreases albedo in the late-twentieth century (Fig. 35.5). Globally, however, loss of forest releases carbon to the atmosphere (Fig. 35.6). Climate warming over the twentieth-century may be less than that expected from greenhouse gases alone, primarily from increased albedo with loss of extratropical forests (Brovkin et al. 2006). Carbon emission from land use dampens this biogeophysical cooling. Biogeophysical cooling may outweigh biogeochemical warming at the global scale (Brovkin et al. 2004) or may only partially offset warming (Matthews et al. 2004; Pongratz et al. 2010). The net effect of these competing processes is small globally, but is large in temperate and high northern latitudes where the cooling due to an increase in surface albedo outweighs the warming due to land use CO_2 emission.

Future trajectories of land use and land cover change over the twenty-first century driven by socioeconomic needs, societal responses to climate change, and policy implementation will also affect climate. The biogeophysical land use forcing of climate may in some regions be of similar magnitude to greenhouse gas climate change (Feddema et al. 2005). For example, one possible socioeconomic trajectory
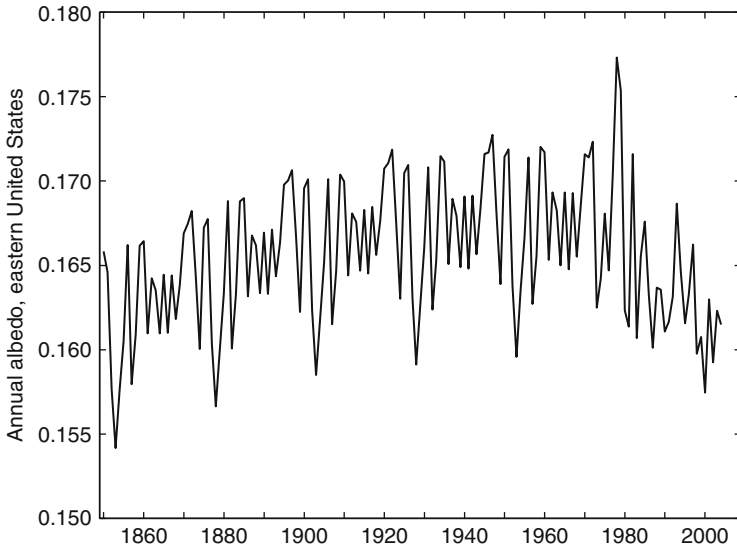
Fig. 35.5 Annual albedo for eastern United States simulated by CLM4 (uncoupled from a climate model) for the period 1850–2005
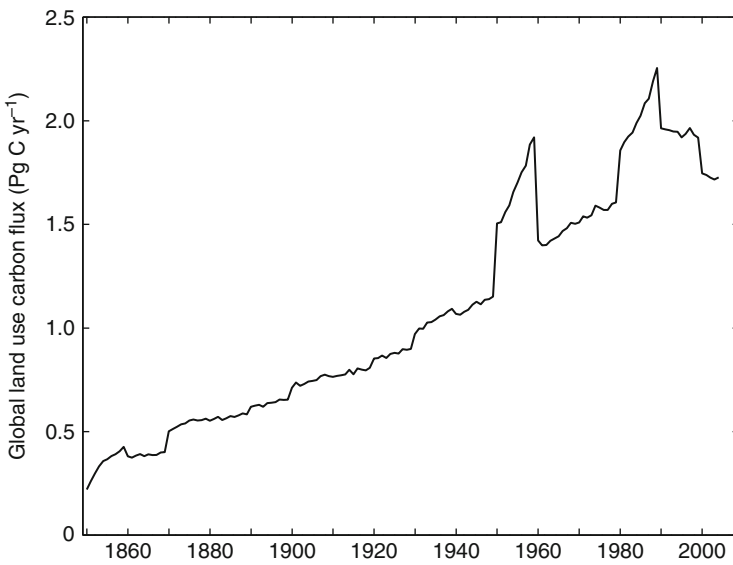
Fig. 35.6 As in Fig. 35.5, but for annual global land use carbon flux simulated by CLM4 for the period 1850–2005

entails high greenhouse gas emission and widespread agricultural expansion with most suitable land used for farming by 2100 to support a large global population. The biogeophysical effects of this forest loss yield warming in Amazonia, but cooling in mid-latitudes. An alternative storyline is low greenhouse gas emission, with temperate reforestation (farm abandonment) and reduced tropical deforestation because of increases in agricultural efficiency and declining global population. Temperate reforestation provides biogeophysical warming, as does tropical deforestation. When the carbon cycle is included, the different storylines yield similar twenty-first century climates despite their different socioeconomic trajectories (Sitch et al. 2005). In both storylines, net carbon loss from deforestation causes biogeochemical warming, greatest in the high growth trajectory with widespread agricultural expansion and weaker in the low growth trajectory with temperate reforestation and reduced tropical deforestation. In the high growth trajectory, widespread agricultural expansion produces strong biogeochemical warming that offsets strong biogeophysical cooling to provide net global warming. The low growth pathway has similar net warming because weak biogeochemical warming augments moderate biogeophysical warming.

As climate models evolve into Earth system models with representation of terrestrial ecosystems and their regulation of hydrological and biogeochemical cycles, they can inform land management practices to mitigate climate change. Reforestation, afforestation, and avoided deforestation are possible such practices. For example, tropical afforestation may help mitigate global warming, while the influence of temperate and boreal afforestation is more complex (Bala et al. 2007). However, the interplay among albedo, evapotranspiration, and the carbon cycle is not well known. These, and other, climate influences of ecosystems need to be better understood to craft strong climate change mitigation science (Bonan 2008). Land use policies must recognize the many forest influences, their competing biogeophysical and biogeochemical effects on climate, and their long-term effectiveness and sustainability in a changing climate.

35.6 Conclusions and Research Needs

The world's forests influence climate through a variety of hydrological, biogeochemical, and ecosystem processes (Bonan 2008). These forest–atmosphere interactions can dampen or amplify anthropogenic climate change. The effects of deforestation on biogeophysical processes (albedo, evapotranspiration) are generally thought to cool mid-latitude climate and warm tropical climate, while biogeochemical processes (carbon) are thought to warm climate globally. The net effect of these and other processes is uncertain and varies among boreal, temperate, and tropical forests. As the climate benefits of forests become better understood, land use policies can be crafted to mitigate climate change. These policies must recognize the many ways in which forests affect climate and their long-term effectiveness and sustainability in a changing climate.

Global models of the biosphere–atmosphere system are still in their infancy, and processes not yet fully understood may initiate unforeseen feedbacks. Key model uncertainties include the interactions of the carbon cycle with other biogeochemical cycles, especially nitrogen and phosphorus; the response to CO_2 fertilization, nitrogen fertilization, and soil warming; and human management of the carbon cycle through land use and land cover change. The overall responses of the hydrologic cycle and biogeochemical cycles to land use and land cover change, and their climate effects are also poorly understood in the models.

Much of our knowledge of forest influences on climate, and our ability to inform climate change mitigation policy, comes from models. Models of climate and the biosphere are abstractions of complex physical, chemical, and biological processes. Extrapolation of process-level understanding of ecosystem functioning gained from laboratory experiments or field studies to large-scale Earth system models remains a challenge. Monitoring studies at the ecosystem and watershed scales and large-scale monitoring from satellite sensors provide important data to test and inform model development. However, model development and validation must better utilize the results of experimental manipulation studies such as soil warming and free-air CO_2 enrichment to test the response of the models to perturbations. In addition, novel model-data fusion techniques allow estimation of model parameters, identify model errors, provide optimal sampling strategies, and improve model simulations (Wang et al. 2009). Comprehensive model-data comparisons are the keys to gaining confidence in the model simulations and their utility for climate change mitigation policy.

References

Bala G, Caldeira K, Wickett M et al (2007) Combined climate and carbon-cycle effects of large-scale deforestation. Proc Natl Acad Sci USA 104:6550–6555

Bonan GB (1995) Land–atmosphere CO_2 exchange simulated by a land surface process model coupled to an atmospheric general circulation model. J Geophys Res 100D:2817–2831

Bonan GB (2008) Forests and climate change: forcings, feedbacks, and the climate benefits of forests. Science 320:1444–1449

Bonan GB, Levis S, Sitch S et al (2003) A dynamic global vegetation model for use with climate models: concepts and description of simulated vegetation dynamics. Glob Change Biol 9:1543–1566

Bondeau A, Smith PC, Zaehle S et al (2007) Modeling the role of agriculture for the 20th century global terrestrial carbon balance. Glob Change Biol 13:679–706

Brovkin V, Sitch S, von Bloh W et al (2004) Role of land cover changes for atmospheric CO_2 increase and climate change during the last 150 years. Glob Change Biol 10:1253–1266

Brovkin V, Claussen M, Driesschaert E et al (2006) Biogeophysical effects of historical land cover changes simulated by six Earth system models of intermediate complexity. Clim Dyn 26:587–600

Collatz GJ, Ball JT, Grivet C et al (1991) Physiological and environmental regulation of stomatal conductance, photosynthesis and transpiration: a model that includes a laminar boundary layer. Agric For Meteorol 54:107–136

Cox PM, Betts RA, Jones CD et al (2000) Acceleration of global warming due to carbon–cycle feedbacks in a coupled climate model. Nature 408:184–187

Craig SG, Holmén KJ, Bonan GB et al (1998) Atmospheric CO_2 simulated by the National Center for Atmospheric Research Community Climate Model. 1. Mean fields and seasonal cycles. J Geophys Res 103D:13213–13235

de Graaff MA, van Groenigen KJ, Six J et al (2006) Interactions between plant growth and soil nutrient cycling under elevated CO_2: A meta-analysis. Glob Change Biol 12: 2077–2091

Deardorff JW (1978) Efficient prediction of ground surface temperature and moisture, with inclusion of a layer of vegetation. J Geophys Res 83C:1889–1903

Denman KL, Brasseur G, Chidthaisong A et al (2007) Couplings between changes in the climate system and biogeochemistry. In: Solomon S, Qin D, Manning M et al (eds) Climate change 2007: the physical science basis. Cambridge University Press, Cambridge, pp 499–587

Denning AS, Randall DA, Collatz GJ et al (1996) Simulations of terrestrial carbon metabolism and atmospheric CO_2 in a general circulation model. Part 2: simulated CO_2 concentrations. Tellus 48B:543–567

Dickinson RE, Henderson-Sellers A (1988) Modeling tropical deforestation: a study of GCM land–surface parameterizations. Q J R Meteorol Soc 114:439–462

Dickinson RE, Henderson-Sellers A, Kennedy PJ et al (1986) Biosphere–Atmosphere Transfer Scheme (BATS) for the NCAR Community Climate Model. NCAR Tech Note NCAR/TN–275 +STR. Natl Cent Atmos Res, Boulder, CO

Dickinson RE, Henderson-Sellers A, Kennedy PJ (1993) Biosphere–Atmosphere Transfer Scheme (BATS) version 1e as coupled to the NCAR Community Climate Model, NCAR Tech Note NCAR/TN–387+STR. Natl Cent Atmos Res, Boulder, CO

Feddema JJ, Oleson KW, Bonan GB et al (2005) The importance of land-cover change in simulating future climates. Science 310:1674–1678

Foley JA, Prentice IC, Ramankutty N et al (1996) An integrated biosphere model of land surface processes, terrestrial carbon balance, and vegetation dynamics. Glob Biogeochem Cycles 10:603–628

Foley JA, Levis S, Costa MH et al (2000) Incorporating dynamic vegetation cover within global climate models. Ecol Appl 10:1620–1632

Friedlingstein P, Cox P, Betts R et al (2006) Climate–carbon cycle feedback analysis: results from the C^4MIP model intercomparison. J Clim 19:3337–3353

Gervois S, de Noblet–Ducoudré N, Viovy N et al (2004) Including croplands in a global biosphere model: methodology and evaluation at specific sites. Earth Interact 8:1–25

Juang JY, Katul G, Siqueira M et al (2007) Separating the effects of albedo from eco-physiological changes on surface temperature along a successional chronosequence in the southeastern United States. Geophys Res Lett. doi:10.1029/2007GL031296

Klein Goldewijk K, Van Drecht G, Bouwman AF (2007) Mapping contemporary global cropland and grassland distributions on a 5×5 minute resolution. J Land Use Sci 2:167–190

Levis S, Foley JA, Pollard D (1999) CO_2, climate, and vegetation feedbacks at the Last Glacial Maximum. J Geophys Res 104D:31191–31198

Levis S, Foley JA, Pollard D (2000) Large-scale vegetation feedbacks on a doubled CO_2 climate. J Clim 13:1313–1325

Levis S, Bonan GB, Bonfils C (2004) Soil feedback drives the mid-Holocene North African monsoon northward in fully coupled CCSM2 simulations with a dynamic vegetation model. Clim Dyn 23:791–802

Manabe S, Smagorinsky J, Strickler RF (1965) Simulated climatology of a general circulation model with a hydrologic cycle. Mon Weather Rev 93:769–798

Matthews HD, Weaver AJ, Meissner KJ et al (2004) Natural and anthropogenic climate change: incorporating historical land cover change, vegetation dynamics and the global carbon cycle. Clim Dyn 22:461–479

Medvigy D, Wofsy SC, Munger JW et al (2009) Mechanistic scaling of ecosystem function and dynamics in space and time: Ecosystem Demography model version 2. J Geophys Res. doi:10.1029/2008JG000812

Melillo JM, Steudler PA, Aber JD et al (2002) Soil warming and carbon–cycle feedbacks to the climate system. Science 298:2173–2176

Mercado LM, Bellouin N, Sitch S et al (2009) Impact of changes in diffuse radiation on the global land carbon sink. Nature 458:1014–1017

Oleson KW, Niu GY, Yang ZL et al (2008) Improvements to the Community Land Model and their impact on the hydrological cycle. J Geophys Res. doi:10.1029/2007JG000563

Pastor J, Post WM (1988) Response of northern forests to CO_2-induced climate change. Nature 334:55–58

Pitman AJ, de Noblet-Ducoudré N, Cruz FT et al (2009) Uncertainties in climate responses to past land cover change: first results from the LUCID intercomparison study. Geophys Res Lett. doi:10.1029/2009GL039076

Plattner GK, Knutti R, Joos F et al (2008) Long-term climate commitments projected with climate-carbon cycle models. J Clim 21:2721–2751

Pongratz J, Reick CH, Raddatz T et al (2010) Biogeophysical versus biogeochemical climate response to historical anthropogenic land cover change. Geophys Res Lett. doi:10.1029/2010GL043010

Ramankutty N, Evan AT, Monfreda C et al (2008) Farming the planet: 1 Geographic distribution of global agricultural lands in the year 2000. Glob Biogeochem Cycles 22:19. doi:10.1029/2007GB002952

Randerson JT, Hoffman FM, Thornton PE et al (2009) Systematic assessment of terrestrial biogeochemistry in coupled climate–carbon models. Glob Change Biol 15:2462–2484

Sellers PJ, Mintz Y, Sud YC et al (1986) A simple biosphere model (SiB) for use within general circulation models. J Atmos Sci 43:505–531

Sellers PJ, Randall DA, Collatz GJ et al (1996a) A revised land surface parameterization (SiB2) for atmospheric GCMs. Part I: Model formulation. J Clim 9:676–705

Sellers PJ, Bounoua L, Collatz GJ et al (1996b) Comparison of radiative and physiological effects of doubled atmospheric CO_2 on climate. Science 271:1402–1406

Shevliakova E, Pacala SW, Malyshev S et al (2009) Carbon cycling under 300 years of land use change: importance of the secondary vegetation sink. Glob Biogeochem Cycles. doi:10.1029/2007GB003176

Shukla J, Mintz Y (1982) Influence of land–surface evapotranspiration on the Earth's climate. Science 215:1498–1501

Sitch S, Smith B, Prentice IC et al (2003) Evaluation of ecosystem dynamics, plant geography and terrestrial carbon cycling in the LPJ dynamic global vegetation model. Glob Change Biol 9:161–185

Sitch S, Brovkin V, von Bloh W et al (2005) Impacts of future land cover changes on atmospheric CO_2 and climate. Glob Biogeochem Cycles. doi:10.1029/2004GB002311

Sitch S, Cox PM, Collins WJ et al (2007) Indirect radiative forcing of climate change through ozone effects on the land–carbon sink. Nature 448:791–794

Sokolov AP, Kicklighter DW, Melillo JM et al (2008) Consequences of considering carbon–nitrogen interactions on the feedbacks between climate and the terrestrial carbon cycle. J Clim 21:3776–3796

Stöckli R, Lawrence DM, Niu GY et al (2008) Use of FLUXNET in the Community Land Model development. J Geophys Res. doi:10.1029/2007JG000562

Thomas RQ, Canham CD, Weathers KC et al (2009) Increased tree carbon storage in response to nitrogen deposition in the US. Nat Geosci 3:13–17

Thornton PE, Doney SC, Lindsay K et al (2009) Carbon–nitrogen interactions regulate climate–-carbon cycle feedbacks: results from an atmosphere–ocean general circulation model. Biogeosci 6:2099–2120

Wang YP, Houlton BZ (2009) Nitrogen constraints on terrestrial carbon uptake: implications for the global carbon–climate feedback. Geophys Res Lett. doi:10.1029/2009GL041009

Wang YP, Trudinger CM, Enting IG (2009) A review of applications of model–data fusion to studies of terrestrial carbon fluxes at different scales. Agric For Meteorol 149:1829–1842

Wania R, Ross I, Prentice IC (2009) Integrating peatlands and permafrost into a dynamic global vegetation model: 1. Evaluation and sensitivity of physical land surface processes. Glob Biogeochem Cycles. doi:10.1029/2008GB003412

Zaehle S, Friedlingstein P, Friend AD (2010) Terrestrial nitrogen feedbacks may accelerate future climate change. Geophys Res Lett. doi:10.1029/2009GL041345

Zaitchik BF, Macalady AK, Bonneau LR et al (2006) Europe's 2003 heat wave: a satellite view of impacts and land–atmosphere feedbacks. Int J Climatol 26:743–769

Part VI
Knowledge Gaps and Research Opportunities

Chapter 36
Reflections on the State of Forest Hydrology and Biogeochemistry

Delphis F. Levia, Darryl E. Carlyle-Moses, and Tadashi Tanaka

36.1   Introduction

There is no question that research conducted by the forest hydrology and biogeochemistry communities over the past several decades has vastly improved our knowledge of the natural world. As reflected in this book, the research output has been both prolific and of high quality, leading to an improved understanding of water and chemical transport within and through forests. The cutting-edge research from Hubbard Brook and other long-term sites has been key in formulating elemental budgets and understanding the effects of stressors, such as acid rain, on forest biogeochemistry. The myriad of more specific process-based studies of forest hydrology and biogeochemistry, in conjunction with these longer term studies, has permitted a wiser management and use of forests. Advances in remote sensing, geographical information science, eddy covariance, fluorescence spectroscopy, isotopes, and solute mixing models have been essential in understanding the transport, modification, and fate of water, carbon, and inorganic solutes through forested ecosystems. While much has been learned to date about the hydrological and biogeochemical processes that cycle water, solutes, particulates, and gases within and through forests that has led to an increased understanding among different ecoregions and forest types, as reviewed and synthesized in this volume, there is still a great deal to learn about the functional ecology, hydrology, and biogeochemistry of forests.

It is beyond the scope of this chapter to highlight all of the theoretical, methodological, and process-based advances that have been made that enhance and amplify our understanding of forest ecosystems. Rather, the intent of this summary chapter is to identify some specific areas where our present knowledge remains particularly weak and to examine and discuss opportunities to address these shortcomings in the near future. Readers seeking detailed synthesis of past research and recommended future directions for a particular method, forest type, process, or stressor are directed to specific chapter(s) of interest.

36.2   Some Weaknesses in Our Current State of Knowledge

As demonstrated in this book, there are a number of research methods that could be and are employed by forest hydrologists and biogeochemists to advance our knowledge of hydrological and biogeochemical cycling in forested ecosystems. A review of the literature shows exemplary examples of the use and application of remote sensing, geographical information science, eddy covariance, fluorescence spectroscopy, isotopes, and solute mixing analyses in forest hydrology and biogeochemistry work. The editors of this volume have specifically included the methods section in the hope that a greater number of forest hydrologists and biogeochemists might integrate these methods into their research as appropriate in the near future. Fluorescence spectroscopy and solute mixing models and analyses, for example, would likely yield new insights into the alteration of stemflow through the canopy and its fate in or through the subsurface. It is likely that a more widespread adoption of cutting edge sensors and the methodological tools covered in this volume (Chaps. 2–8) would generate a more comprehensive and detailed understanding on the cycling of water and solutes within and through forests.

Of all the forest types covered in the volume (Chaps. 9–16), it appears that the lowland tropical rainforest (both *terra firme* [covered in this volume] and seasonally flooded) is the least well understood. This is not to say that high quality work has not been conducted in these forests. Quite the contrary, a number of studies have been conducted that have greatly increased our understanding of these forests, some of which are described in Chap. 9. Our lesser understanding of these forests is partly attributable to their complexity in terms of both species diversity and evolutionary adaptations, such as adventitious and apogeotropic roots, that affect water and biogeochemical cycling but are absent from other forest types as well as the remoteness of many lowland tropical forests. The remoteness of these forests necessitates considerable logistical planning that is very expensive, thereby limiting the length and scope of most field experiments. However, given the vast areal extent and importance of tropical lowland forests on local, regional, and global scales, it is paramount that forest hydrologists and biogeochemists build upon the high quality work to date in an effort to expand our knowledge base of these critically important forest ecosystems.

Table 36.1 lists several topical areas where the editors opine that further research effort be directed. Chapter 18 focuses on the influence of canopy structure on hydrological and biogeochemical fluxes. Canopy structure is complicated. Until very recently, simply characterizing and quantifying canopy structure has been a major challenge. We are now in the position to make significant advances in our understanding on the effects of canopy structure on water and solute flux with the use of high-resolution airborne LiDAR and other instrumental developments (Table 36.1, Chap. 18). Stemflow has been and remains understudied in comparison to other hydrological processes in forests. As described in Chap. 21, many researchers are increasingly acknowledging the importance of stemflow and documenting its notable influence on hillslope hydrology. The use of fluorescence spectroscopy can yield new insights into the importance of stemflow on biogeochemical cycling (Table 36.1). Despite advances in our understanding of the ecohydrology and

Table 36.1 Summary of some key weaknesses in our current state of knowledge posed as possible research questions with some methodological tools to address knowledge gaps[a]

Topic of weakness	Possible research questions and avenues of future research
Canopy structure	How does canopy structure affect biogeochemical flux and cycling? Do total canopy surface area and orthogonally projected canopy area have similar or differential impacts on water and solute flux to the forest floor? To what extent are any effects of these canopy areas overshadowed by canopy texture, bark microrelief, or season? Advances in LiDAR now permit researchers to have unprecedented resolution of forest canopies. Metrics, such as total and projected canopy area, can be calculated for individual trees over large areas. Other laser technologies (Chap. 18) can also be applied to investigate the influence of canopy structure on forest hydrology and biogeochemistry (Chap. 18)
Stemflow	Is stemflow a significant contributor to soil solution or streamflow? At what spatial or temporal scale is stemflow important? How does stemflow chemistry change in response to stressors? What is the quality of stemflow dissolved organic matter? Use of solute mixing models (Chap. 8) and fluorescence spectroscopy (Chap. 6) can permit answers to these questions. Combined with isotopic analyses (Chap. 7), the two above methodologies will yield a clearer picture of the importance of stemflow in forest hydrology and biogeochemistry (Chap. 21)
Rhizosphere hydrology and biogeochemistry	How can we separate the hydrology and biogeochemistry of the rhizosphere from that of the bulk soil? To what extent are roots coupled with the canopy? How will global change affect the rhizosphere? Advances in miniature infiltrometers, microbial biosensors, and computed tomography can shed light on these important questions on hydrologic redistribution by roots and carbon dioxide dynamics in the rhizosphere (Chap. 24). Such instruments will permit better coupling of above- and belowground hydrological and biogeochemical processes and cycling in forested ecosystems (Chap. 24)
Insect stressors	What are the effects of canopy herbivory over the longer term? To what extent is the aboveground flux of particulates and solutes from insect herbivory coupled with belowground cycling? Advances in fluorescence spectroscopy will shed further light on the quality of dissolved organic matter from insect infested forests. Long-term studies should be started that examine the effects of canopy herbivory on forest hydrology and biogeochemistry over years and decades. Ideally, such research would be integrated into LTER and CZO sites (Chap. 28)
Ice storms	How important are ice storms as a forest stressor in deciduous forests? Over the long term across forest types? Ho do ice storms affect N cycling? Do ice storms lead to N limitation? Ice storm studies conducted within LTERs with lengthy and reliable baseline records (and eventually the CZOs as they continue) are a prerequisite to examine the impacts of ice

Table 36.1 (continued)

Topic of weakness	Possible research questions and avenues of future research
	storms on the forest hydrology and biogeochemistry of forests. The use of geospatial technologies that can map the extent and degree of damage (Chaps. 3 and 4) should be coupled with watershed scale experiments and other methods as appropriate to quantify any relationships between the extent of ice storm damage and the hydrological and biogeochemical response over time and space. Research on ice storms is timely as their frequency may very well increase with climate change (Chap. 31)

[a] Some questions and/or methodological recommendations to address them in this table are repeated or derived from respective chapters. Chapter authors are acknowledged for their intellectual contributions and readers are referred to respective chapters for further details and explanation

biogeochemistry of the rhizosphere (Chap. 24), much more work needs to be done to fully comprehend the importance of the rhizosphere on water and biogeochemical cycling. Here again, recent advances in instrumentation and methods (Table 36.1) will yield fruitful insights as to how the rhizosphere modulates the movement of water and solutes in the subsurface. Such work will undoubtedly contribute to our understanding of spatial and temporal heterogeneity of water and biogeochemical flux in forests. Insects are a major stressor of forests. Chapter 28 details the impacts of insects on forest biogeochemistry. The linkages and possible coupling of canopy herbivory with subsurface water and biogeochemical cycling are largely unknown (Table 36.1, Chap. 28). Future work also is needed to examine the long-term effects of insect stressors. Ice storms are relatively frequent in many forested areas yet relatively little is known about the effects of ice storms on forest biogeochemistry (Table 36.1). Chapter 31 discusses some effects of ice storms on N cycling. It is unclear whether ice storms trigger N limitation in forests and their long-term effects.

36.3 Future Opportunities

The above paragraph and Table 36.1 allude to the importance of linking aboveground and belowground processes in order to achieve a fuller understanding of forest hydrology and biogeochemistry. Historically, a number of studies (many reviewed throughout this book) have examined the effects of the forest canopy on the transfer of water and solutes to the forest floor. An increasing number of studies have directly linked the transfer of moisture from the canopy to the subsurface. Chapter 24 specifically discusses a double funneling effect whereby water is preferentially funneled along branches in the canopy and roots in the subsurface. Today, there is a growing interest in hydropedology and linkages between the canopy and subsurface. There is a golden opportunity to capitalize on the emerging interest in hydropedology (as espoused by Lin 2003) and to couple the canopy with the subsurface in a holistic

manner (e.g., Li et al. 2009). Such work may very well adopt the conceptual framework of McClain et al. (2003) and emphasize hot moments and hot spots of water and biogeochemical cycling. Conceptualization of water and biogeochemical cycling in terms of hot moments and hot spots will likely yield invaluable insights into the marked temporal and spatial variability of hydrological and biogeochemical processes. Such thinking will permit innovative experimental designs that should generate significant advances in our knowledge base.

As described in Chap. 2, wireless sensor technology and the rapid development of new sensors will very likely affect future sampling strategies and experimental designs. The number of sensors deployed in future research and the amount of data they collect is likely to increase dramatically in the very near future. Forest hydrologists and biogeochemists should take advantage of these opportunities to answer research questions that may have been unanswerable hitherto. Experiments that seek to better understand hot spots and their effects on biogeochemical cycling will require a large number of sensors that relay data to computers using cellular technologies. The voluminous amounts of data will require standardized QA/QC protocols and a cyberinfrastructure capable of handling multiple data streams. The US National Science Foundation funded Critical Zone Observatories (CZOs) in the United States and Europe are currently involved in standardizing the cyberinfrastructure across all six US CZOs and developing data sharing protocols to ensure widespread dissemination and use of collected data.

Forest hydrologists and biogeochemists should get involved in the CZOs and Long Term Ecological Research sites (LTERs) to the greatest extent possible. These community-based resources can and should be leveraged to further our understanding on the hydrology and biogeochemistry of forests. Hubbard Brook Experimental Forest, a LTER, clearly demonstrates the scientific value of such sites. Involvement in LTERs and CZOs will move the frontiers of knowledge in forest hydrology and biogeochemistry forward. The use of wireless and new sensor technologies will deepen our knowledge and permit better stewardship of forest resources, especially in a changing world where multiple stressors act synergistically at multiple temporal and spatial scales to alter hydrological and biogeochemical cycling in forests.

The editors believe that the knowledge base of forest hydrology and biogeochemistry will be expanded and deepened significantly over the next decade if we avail ourselves to the opportunities described earlier. The synthesis of past research in this volume, together with the future research directions charted in the chapters, should position us well to make the most of these opportunities.

References

Li XY, Yan ZP, Li YT, Lin H (2009) Connecting ecohydrology and hydropedology in desert shrubs: stemflow as a source of preferential flow in soils. Hydrol Earth Syst Sci 13:1133–1144

Lin H (2003) Hydropedology: bridging disciplines, scales, and data. Vadose Zone J 2:1–11

McClain ME, Boyer EW, Dent CL et al (2003) Biogeochemical hot spots and hot moments at the interface of terrestrial and aquatic ecosystems. Ecosystems 6:301–312

Index